A STUDY OF THE MOLECULAR CHEMISTRY OF GLASSES BY INFRARED MICROSPECTROSCOPYAND ITS USE IN FORENSIC GLASS DISCRIMINATION AND CLASSIFICATION

by

BROOKE WEINGER KAMMRATH

VOLUME I

A dissertation submitted to the Graduate Faculty in Criminal Justice in partial fulfillment of the requirements for the degree of Doctor of Philosophy, The City University of New York

2012

© 2012
BROOKE WEINGER KAMMRATH
All Rights Reserved

This manuscript has been read and accepted by the
Graduate Faculty in Criminal Justice in satisfaction of the
Dissertation requirement for the degree of Doctor of Philosophy

Thomas A. Kubic, M.S., J.D., Ph.D.

Date | Chair of Examining Committee

Joshua D. Freilich, J.D., Ph.D.

Date | Executive Officer

John A. Reffner, Ph.D.

Nicholas D.K. Petraco, Ph.D.

Supervisory Committee

THE CITY UNIVERSITY OF NEW YORK

ABSTRACT

A STUDY OF THE MOLECULAR CHEMISTRY OF GLASSES BY INFRARED MICROSPECTROSCOPYAND ITS USE IN FORENSIC GLASS DISCRIMINATION AND CLASSIFICATION

by

BROOKE WEINGER KAMMRATH

Adviser: Thomas A. Kubic, M.S., J.D., Ph.D.

The analysis of the molecular structure of glass is a novel forensic method that provides knowledge about glass chemistry that is not currently employed by forensic scientists as well as improves the discriminatory power within this class of transfer evidence. Infrared (IR) spectra contain extensive information about the molecular structure of the complex silicates in commercial glasses. This research is based on measuring the attenuated total reflection (ATR) mid-IR spectra of soda-lime silicate glasses to detect variations of the molecular structure to assist in the comparison of glass evidence. The use of ATR mid-IR spectra for the discrimination and classification of glasses was investigated. Discrimination error rates of approximately 5% and classification by end-product (window or container) error rates on the order of 2% were achieved with principal component analysis-canonical variate analysis (PCA-CVA) hold-one-out cross validation (HOO-CV) on the first and second derivative spectra of 153 soda-lime silicate glasses.

Silicate glass is a common and valuable class of evidence encountered in criminal and civil litigation. Glass is an excellent source of physical evidence because it is brittle and fractures into fragments that are easily transferred from the source to victim and/or perpetrator.

The challenge to the forensic scientist is to reliably associate these fragments with their source with high probative value. The mid-IR microprobe analysis of glass requires only minimal additional sample preparation to that which is already done for refractive index (RI) analysis and uses IR investigated samples that are the same size and smaller than the ablated hole made in laser ablation-inductively coupled plasma-mass spectrometry (LA-ICP-MS). Thus mid-IR microprobe analysis can be used to provide additional discrimination for glass samples that are indistinguishable by RI and too small for elemental analysis. ATR mid-IR spectral analysis provides information about the molecular structure of soda-lime silicate glass to support other traditional analysis and strengthen the association of this evidence.

.

ACKNOWLEDGEMENTS

Though only my name appears on the cover of this dissertation, a great many people have contributed to its production. I owe my gratitude to all those people who have made this dissertation possible and because of whom my graduate experience has been one that I will cherish forever.

Mentors make a difference! I have been privileged to have three of the very best. They are all quite different, yet the qualities they share have left an indelible mark on me both professionally and personally. Their shared traits are integrity, high performance expectations, passion for forensic science, and a problem-solving attitude. They gave me the freedom to explore on my own, and at the same time the guidance to recover when my steps faltered. Their generosity with their time and knowledge, sense of humor, and encouragement has truly made my graduate education exceptional. These men are Drs. Thomas A. Kubic, John A. Reffner and Nicholas D.K. Petraco. The best way for me to show my appreciation is to commit to pass along their values and teachings to my future students.

I would like to thank my graduate school professors, all of whom have inspired my fascination with forensic science and criminal justice: Dr. Peter De Forest, Nicholas Petraco, Dr. Donald Hoffman, Dr. Richard Stripp, Dr. Margaret Wallace, Dr. Peter Shenkin, Dr. Larry Sullivan, Dr. Richard Culp, and Evan Mandery.

I am indebted to my fellow doctoral students, former and current, for providing a stimulating environment in which to learn and grow. I must specifically mention Dale Purcell and Pauline Leary, both of whom have provided me with encouragement, insightful comments and constructive criticisms at different stages of my research. In addition, I have learned something from every student colleague, all of whom deserve my appreciation: Dr. Michelle

Miranda, Dr. Michelle Boileau, Dr. Kelly Walsh, Dr. Andrew Schweighardt, Thiti Mahacharoen, Peter Valentin, Peter Diaczuk, Ira DuBey, Dr. Rebecca Bucht, and Nikolay Azar.

John Jay College of Criminal Justice is filled with people who have made my time as a graduate student and adjunct lecturer unforgettable, and whom I profusely thank here: Dr. Selman Berger, Dr. Anthony Carpi, Dr. Yi He, Dr. Lawrence Kobilinsky, Dr. Nathan Lentz, Dr. Marcel Roberts, Linda Rourke, Francis Sheehan, Azinia Brooks, and Argeliz Pomales.

I would like to acknowledge Dr. JoAnn Buscaglia, Dr. Robert Koons, Scott Ryland, and Tony Nikischer for their willingness to share their vast knowledge and their glass and/or mineral samples. This research would not have been possible without their generosity. I must also thank Dr. Don Dahlberg for many valuable discussions, his support and his friendship.

I am indebted to the CUNY Graduate Center for providing some financial support for this research through the Doctoral Student Research Grant Program, Competition #5 (2010).

Most importantly, none of this would have been possible without the love of my family. My family has been a constant source of love, encouragement and strength all these years, and I would like to express my heart-felt gratitude to Ben, Ali, Farin, Quinn, JL, Mark, Lara, Barbara, Lucas, and Liana. I wish to thank my best friend and twin sister Lindsey for providing me with love, camaraderie, entertainment, and encouragement every day of my life. I am forever grateful to my mother Shirley and my late father Milton for their emotional and financial support. It was their faith in me that allowed me to be as ambitious as I wanted, and it was under their watchful eye that I gained so much drive and the ability to take a punch.

Lastly, I would like to give my special thanks to my husband Matt whose patient love, infinite generosity, and unparalleled thoughtfulness enabled me to complete this work.

TABLE OF CONTENTS

VOLUME I

LIST OF TABLES…… page xii

LIST OF FIGURES…….. page xxxix

LIST OF ABREVIATIONS……..…….. page lxiv

CHAPTER 1: INTRODUCTION…… page 1

A. Statement of the Problem…… page 1

B. Glass Definitions, Structure and Properties ……... page 2

C. Glass Manufacturing……... page 13

D. Infrared Spectroscopy……. page 19

a. Infrared Theory…….. page 19

b. Attenuated Total Reflection……... page 28

E. Chemometrics…….. page 33

CHAPTER 2: REVIEW OF THE LITERATURE…….. page 36

A. Methods for Forensic Glass Analysis……. page 36

a. Physical Properties……. page 37

i. Optical Properties……. page 45

b. Chemical Composition…….. page 60

B. Discrimination by Combined Analytical Methods……. page 80

C. Mid-IR Spectroscopy of Glass…… page 85

CHAPTER 3: EXPERIMENTAL DESIGN…… page 105

A. Summary……. page 105

B. Hypotheses…….. page 105

C. Sample Collection……... page 106

D. Instrumentation……... page 107

E. Data Collection and Analysis…….. page 117

a. Instrument Validation…… page 117

b. Method Development……..……. page 117

c. Glass Sample Preparation for ATR Mid-IR Microprobe Analysis… page 120

d. Correlation of Mid-IR Spectral Bands with Molecular Structure…. page 124
e. Classification and Discrimination Power……... page 130
i. ATR Mid-IR Spectral Library Searching……. page 134
ii. Comparison of Deconvolved Peaks..……... page 136
iii. Chemometric Analysis……... page 136
f. Mid-IR Microprobe Analysis Compatibility with GRIM…….. page 144
CHAPTER 4: RESULTS…….. page 145
A. Method Development……..…….. page 145
B. Correlation of Mid-IR Spectral Bands with Molecular Structure..... page 180
C. Classification and Discrimination Power…… page 202
a. ATR Mid-IR Spectral Library Searching…….. page 214
b. Comparison of Deconvolved Peaks……... page 217
c. Chemometric Analysis……... page 234
D. Mid-IR Microprobe Analysis Compatibility with GRIM……... page 317
CHAPTER 5: CONCLUSIONS……... page 321
CHAPTER 6: CONTRIBUTIONS TO FORENSIC SCIENCE AND CRIMINAL JUSTICE.…… page 324
CHAPTER 7: FURTHER CONSIDERATIONS……. page 326

VOLUME II

APPENDIX I: DEPTH OF PENETRATION CALCULATIONS AND GRAPHS…….. page 328
APPENDIX II: PERFORMACE VALIDATION REPORTS…….. page 335
APPENDIX III: NIST CERTIFICATES…….. page 395
APPENDIX IV: GLASS SAMPLES…… page 401
APPENDIX V: METHOD DEVELOPMENT PEAK HEIGHTS FOR SRM GLASSES……. page 406
APPENDIX VI: METHOD DEVELOPMENT MID-IR SPECTRAL LIBRARY SEARCH RESULTS....…… page 416
APPENDIX VII: MINERAL SILICATE MID-IR SPECTRA....…… page 546

APPENDIX VIII: DECONVOLUTION DATA…….. page 559

APPENDIX IX: ATR MID-IR SPECTRAL LIBRARY SEARCH RESULTS….. page 573

APPENDIX X: PCA RESULTS FOR CHEMOMETRIC ANALYSIS OF THE FIRST SET OF 30 GLASSES…….. page 589

A. PCA Results for the Unprocessed Spectra…….. page 589

B. PCA Results for the Peak Area Normalized Spectra…….. page 607

C. PCA Results for the Peak Height Normalized Spectra……... page 625

D. PCA Results for the First Derivative Spectra (5-Point Smoothing)….. page 643

E. PCA Results for the First Derivative Spectra (9-Point Smoothing)….. page 661

F. PCA Results for the Second Derivative Spectra (5-Point Smoothing)... page 679

G. PCA Results for the Second Derivative Spectra (9-Point Smoothing)... page 697

VOLUME III

APPENDIX XI: HOO-CV PCA-CVA RESULTS FOR CHEMOMETRIC ANALYSIS OF THE FIRST SET OF 30 GLASSES…….. page 715

A. HOO-CV PCA-CVA Results for the Unprocessed Spectra……... page 715

B. HOO-CV PCA-CVA Results for the Peak Area Normalized Spectra... page 760

C. HOO-CV PCA-CVA Results for the Peak Height Normalized Spectra…….. page 791

D. HOO-CV PCA-CVA Results for the First Derivative Spectra (5-point smoothing)……...……... page 836

E. HOO-CV PCA-CVA Results for the First Derivative Spectra (9-point smoothing)……...……... page 881

F. HOO-CV PCA-CVA Results for the Second Derivative Spectra (5-point smoothing)……...……... page 919

G. HOO-CV PCA-CVA Results for the Second Derivative Spectra (9-point smoothing)……...……... page 964

APPENDIX XII: PCA RESULTS FOR CHEMOMETRIC ANALYSIS OF 153 SODA-LIME SILICATE GLASSES……... page 999

APPENDIX XIII: HOO-CV PCA-CVA RESULTS FOR CHEMOMETRIC ANALYSIS OF 153 SODA-LIME SILICATE GLASSES……. page 1029

APPENDIX XIV: PCA RESULTS FOR CHEMOMETRIC ANALYSIS OF DECONVOLUTION DATA…… page 1044

APPENDIX XV: PCA RESULTS FOR CHEMOMETRIC ANALYSIS OF GLASSES WITH THE SAME RI……..... page 1053

APPENDIX XVI: HOO-CV PCA-CVA RESULTS FOR CHEMOMETRIC ANALYSIS OF GLASSES WITH THE SAME RI……. page 1077

CHAPTER 8: REFERENCES…….. page 1092

LIST OF TABLES

Table 1	Silicate Structures…….	page 5
Table 2	A list of the 30 soda-lime silicate glasses, organized by end-use (architectural, automotive or container)……...	page 127
Table 3	A list of the 153 soda-lime silicate glasses, organized by end-use (architectural, automotive or container)……...	page 131
Table 4	List of the glass samples contained in the 2 glass sets with nominally similar RIs……	page 133
Table 5	RMS noise for the spectra of blanks collected with the 50-µm aperture…….....	page 147
Table 6	Analytical S/N for the spectra of blanks collected with the 50-µm aperture, calculated for the mid-IR region from 1300 – 850 cm^{-1}…...	page 149
Table 7	RMS noise for the spectra of blanks collected with the 25-µm aperture, calculated for the mid-IR region from 1300 – 850 cm^{-1}…...	page 151
Table 8	Analytical S/N for the spectra of blanks collected with the 25-µm aperture, calculated for the mid-IR region from 1300 – 850 cm^{-1}…...	page 153
Table 9	RMS noise for the spectra of blanks collected with the 10-µm aperture, calculated for the mid-IR region from 1300 – 850 cm^{-1}…...	page 154
Table 10	Analytical S/N for the spectra of blanks collected with the 10-µm aperture, calculated for the mid-IR region from 1300 – 850 cm^{-1}…...	page 157
Table 11	Average library search (correlation algorithm) HQI values (and standard deviations) for the SRM 620 glass spectra not used in the making of the mid-IR libraries…….	page 162
Table 12	Average library search (correlation algorithm) HQI values (and standard deviations) for the SRM 620 glass spectra used in the making of the mid-IR libraries…….	page 163
Table 13	Average library search (first derivative correlation algorithm) HQI values (and standard deviations) for the SRM 620 glass spectra not used in the making of the mid-IR libraries……...	page 164
Table 14	Average library search (first derivative correlation algorithm) HQI values (and standard deviations) for the SRM 620 glass spectra used in the making of the mid-IR libraries……...	page 165
Table 15	Average library search (correlation algorithm) HQI values (and standard deviations) for the SRM 621 glass spectra not used in the making of the mid-IR libraries…….	page 166
Table 16	Average library search (correlation algorithm) HQI values (and standard deviations) for the SRM 621 glass spectra used in the making of the mid-IR libraries…….	page 167
Table 17	Average library search (first derivative correlation algorithm) HQI values (and standard deviations) for the SRM 621 glass spectra not used in the making of the mid-IR libraries……...	page 168

Table 18 Average library search (first derivative correlation algorithm) HQI values (and standard deviations) for the SRM 621 glass spectra used in the making of the mid-IR libraries……... page 169
Table 19 Average library search (correlation algorithm) HQI values (and standard deviations) for the SRM 1831 glass spectra not used in the making of the mid-IR libraries.…… page 170
Table 20 Average library search (correlation algorithm) HQI values (and standard deviations) for the SRM 1831 glass spectra used in the making of the mid-IR libraries.…… page 171
Table 21 Average library search (first derivative correlation algorithm) HQI values (and standard deviations) for the SRM 1831 glass spectra not used in the making of the mid-IR libraries…….. page 172
Table 22 Average library search (first derivative correlation algorithm) HQI values (and standard deviations) for the SRM 1831 glass spectra used in the making of the mid-IR libraries…….. page 173
Table 23 Average library search (correlation algorithm) HQI values (and standard deviations) for a 'real world' window glass spectra not used in the making of the mid-IR libraries…….. page 176
Table 24 Average library search (correlation algorithm) HQI values (and standard deviations) for a 'real world' window glass spectra used in the making of the mid-IR libraries…….. page 177
Table 25 Average library search (first derivative correlation algorithm) HQI values (and standard deviations) for a 'real world' window glass spectra not used in the making of the mid-IR libraries…… page 178
Table 26 Average library search (first derivative correlation algorithm) HQI values (and standard deviations) for a 'real world' window glass spectra used in the making of the mid-IR libraries……. page 179
Table 27 Island silicate peak positions (center X, in wavenumbers) for peaks between 1300 – 700 cm^{-1}…… page 183
Table 28 Ring silicate peak position (center X, in wavenumbers) for peaks between 1300 – 700 cm^{-1}…….……... page 183
Table 29 Single chain silicate peak positions (center X, in wavenumbers) for peaks between 1300 – 700 cm^{-1}…….. page 184
Table 30 Double chain silicate peak positions (center X, in wavenumbers) for peaks between 1300 – 700 cm^{-1}…….. page 184
Table 31 Double binary chain silicate peak positions (center X, in wavenumbers) for peaks between 1300 – 700 cm^{-1}……. page 185
Table 32 Double tertiary chain silicate peak positions (center X, in wavenumbers) for peaks between 1300 – 700 cm^{-1}……. page 185
Table 33 Single layer silicate peak positions (center X, in wavenumbers) for peaks between 1300 – 700 cm^{-1}…….. page 185
Table 34 Network silicate peak positions (center X, in wavenumbers) for peaks between 1300 – 700 cm^{-1}……... page 186

Table 35	Results of ANOVA for deconvolved peak 1 position……..	page 190
Table 36	Results of ANOVA for deconvolved peak 2 position……..	page 191
Table 37	Results of ANOVA for deconvolved peak 3 position……..	page 192
Table 38	Results of ANOVA for deconvolved peak 4 position……..	page 193
Table 39	Results of ANOVA for deconvolved peak 5 position……..	page 194
Table 40	Results of ANOVA for deconvolved peak 6 position……..	page 195
Table 41	Results of ANOVA for deconvolved peak 1 area……	page 196
Table 42	Results of ANOVA for deconvolved peak 2 area……...	page 197
Table 43	Results of ANOVA for deconvolved peak 3 area……...	page 198
Table 44	Results of ANOVA for deconvolved peak 4 area……...	page 199
Table 45	Results of ANOVA for deconvolved peak 5 area……...	page 200
Table 46	Results of ANOVA for deconvolved peak 6 area……...	page 201
Table 47	Results of the deconvolved peak position and area comparisons……	page 224
Table 48	Discrimination error rates for HOO-CV PCA-CVA (no pretreatment, centered and autoscaled) and HOO-CV PLS-DA models with varying number of PCs or PLS dimensions for the first set of 30 glass spectra (10 replicates)……..……	page 236
Table 49	Classification (automotive, architectural, or container) error rates for HOO-CV PCA-CVA (no pretreatment, centered and autoscaled) and HOO-CV PLS-DA models with varying number of PCs or PLS dimensions for the first set of 30 glass spectra (10 replicates)…….	page 237
Table 50	Classification (window or container) error rates for HOO-CV PCA-CVA (no pretreatment, centered and autoscaled) and HOO-CV PLS-DA models with varying number of PCs or PLS dimensions for the first set of 30 glass spectra (10 replicates)……...	page 238
Table 51	Discrimination error rates for HOO-CV PCA-CVA (no pretreatment, centered and autoscaled) and HOO-CV PLS-DA models with varying number of PCs or PLS dimensions for the first set of 20 window glass spectra (10 replicates)……	page 239
Table 52	Discrimination error rates for HOO-CV PCA-CVA (no pretreatment, centered and autoscaled) and HOO-CV PLS-DA models with varying number of PCs or PLS dimensions for the first set of 10 container glass spectra (10 replicates)……..	page 239
Table 53	Float classification error rates for HOO-CV PCA-CVA (no pretreatment, centered and autoscaled) and HOO-CV PLS-DA models with varying number of PCs or PLS dimensions for the first set of 20 window glass spectra (10 replicates)……	page 240
Table 54	Tempered classification error rates for HOO-CV PCA-CVA (no pretreatment, centered and autoscaled) and HOO-CV PLS-DA models with varying number of PCs or PLS dimensions for the first set of 20 window glass spectra (10 replicates)……	page 241

Table 55 Discrimination error rates for HOO-CV PCA-CVA (no pretreatment, centered and autoscaled) and HOO-CV PLS-DA models with varying number of PCs or PLS dimensions for the first set of 30 normalized (peak area) glass spectra (10 replicates)……. page 242

Table 56 Classification (automotive, architectural, or container) error rates for HOO-CV PCA-CVA (no pretreatment, centered and autoscaled) and HOO-CV PLS-DA models with varying number of PCs or PLS dimensions for the first set of 30 normalized (peak area) glass spectra (10 replicates)……..……..... page 243

Table 57 Classification (window or container) error rates for HOO-CV PCA-CVA (no pretreatment, centered and autoscaled) and HOO-CV PLS-DA models with varying number of PCs or PLS dimensions for the first set of 30 normalized (peak area) glass spectra (10 replicates)…. page 244

Table 58 Discrimination error rates for HOO-CV PCA-CVA (no pretreatment, centered and autoscaled) and HOO-CV PLS-DA models with varying number of PCs or PLS dimensions for the first set of 20 normalized (peak area) window glass spectra (10 replicates)……. page 245

Table 59 Discrimination error rates for HOO-CV PCA-CVA (no pretreatment, centered and autoscaled) and HOO-CV PLS-DA models with varying number of PCs or PLS dimensions for the first set of 10 normalized (peak area) container glass spectra (10 replicates)……..……..…… page 246

Table 60 Float classification error rates for HOO-CV PCA-CVA (no pretreatment, centered and autoscaled) and HOO-CV PLS-DA models with varying number of PCs or PLS dimensions for the first set of 20 normalized (peak area) window glass spectra (10 replicates)……....……..……..…… page 247

Table 61 Tempered classification error rates for HOO-CV PCA-CVA (no pretreatment, centered and autoscaled) and HOO-CV PLS-DA models with varying number of PCs or PLS dimensions for the first set of 20 normalized (peak area) window glass spectra (10 replicates)……..... page 248

Table 62 Discrimination error rates for HOO-CV PCA-CVA (no pretreatment, centered and autoscaled) and HOO-CV PLS-DA models with varying number of PCs or PLS dimensions for the first set of 30 normalized (peak height) glass spectra (10 replicates)……. page 249

Table 63 Classification (automotive, architectural, or container) error rates for HOO-CV PCA-CVA (no pretreatment, centered and autoscaled) and HOO-CV PLS-DA models with varying number of PCs or PLS dimensions for the first set of 30 normalized (peak height) glass spectra (10 replicates)……..…… page 250

Table 64 Classification (window or container) error rates for HOO-CV PCA-CVA (no pretreatment, centered and autoscaled) and HOO-CV PLS-DA models with varying number of PCs or PLS dimensions for the first set of 30 normalized (peak height) glass spectra (10 replicates)..... page 251
Table 65 Discrimination error rates for HOO-CV PCA-CVA (no pretreatment, centered and autoscaled) and HOO-CV PLS-DA models with varying number of PCs or PLS dimensions for the first set of 20 normalized (peak height) window glass spectra (10 replicates)..... page 252
Table 66 Discrimination error rates for HOO-CV PCA-CVA (no pretreatment, centered and autoscaled) and HOO-CV PLS-DA models with varying number of PCs or PLS dimensions for the first set of 10 normalized (peak height) container glass spectra (10 replicates)..... page 253
Table 67 Float classification error rates for HOO-CV PCA-CVA (no pretreatment, centered and autoscaled) and HOO-CV PLS-DA models with varying number of PCs or PLS dimensions for the first set of 20 normalized (peak height) window glass spectra (10 replicates)..... page 254
Table 68 Tempered classification error rates for HOO-CV PCA-CVA (no pretreatment, centered and autoscaled) and HOO-CV PLS-DA models with varying number of PCs or PLS dimensions for the first set of 20 normalized (peak height) window glass spectra (10 replicates)..... page 255
Table 69 Discrimination error rates for HOO-CV PCA-CVA (no pretreatment, centered and autoscaled) and HOO-CV PLS-DA models with varying number of PCs or PLS dimensions for the first set of 30 glass first derivative (5-point smoothing) spectra (10 replicates)..... page 256
Table 70 Classification (automotive, architectural, or container) error rates for HOO-CV PCA-CVA (no pretreatment, centered and autoscaled) and HOO-CV PLS-DA models with varying number of PCs or PLS dimensions for the first set of 30 glass first derivative (5-point smoothing) spectra (10 replicates)..... page 257
Table 71 Classification (window or container) error rates for HOO-CV PCA-CVA (no pretreatment, centered and autoscaled) and HOO-CV PLS-DA models with varying number of PCs or PLS dimensions for the first set of 30 glass first derivative (5-point smoothing) spectra (10 replicates)..... page 258
Table 72 Discrimination error rates for HOO-CV PCA-CVA (no pretreatment, centered and autoscaled) and HOO-CV PLS-DA models with varying number of PCs or PLS dimensions for the first set of 20 window glass first derivative (5-point smoothing) spectra (10 replicates)..... page 259

Table 73 Discrimination error rates for HOO-CV PCA-CVA (no pretreatment, centered and autoscaled) and HOO-CV PLS-DA models with varying number of PCs or PLS dimensions for the first set of 10 container glass first derivative (5-point smoothing) spectra (10 replicates)…… page 260
Table 74 Float classification error rates for HOO-CV PCA-CVA (no pretreatment, centered and autoscaled) and HOO-CV PLS-DA models with varying number of PCs or PLS dimensions for the first set of 20 window glass first derivative (5-point smoothing) spectra (10 replicates)…… page 261
Table 75 Tempered classification error rates for HOO-CV PCA-CVA (no pretreatment, centered and autoscaled) and HOO-CV PLS-DA models with varying number of PCs or PLS dimensions for the first set of 20 window glass first derivative (5-point smoothing) spectra (10 replicates)…… page 262
Table 76 Discrimination error rates for HOO-CV PCA-CVA (no pretreatment, centered and autoscaled) and HOO-CV PLS-DA models with varying number of PCs or PLS dimensions for the first set of 30 glass first derivative (9-point smoothing) spectra (10 replicates)…… page 263
Table 77 Classification (automotive, architectural, or container) error rates for HOO-CV PCA-CVA (no pretreatment, centered and autoscaled) and HOO-CV PLS-DA models with varying number of PCs or PLS dimensions for the first set of 30 glass first derivative (9-point smoothing) spectra (10 replicates)..... page 264
Table 78 Classification (window or container) error rates for HOO-CV PCA-CVA (no pretreatment, centered and autoscaled) and HOO-CV PLS-DA models with varying number of PCs or PLS dimensions for the first set of 30 glass first derivative (9-point smoothing) spectra (10 replicates)..... page 265
Table 79 Discrimination error rates for HOO-CV PCA-CVA (no pretreatment, centered and autoscaled) and HOO-CV PLS-DA models with varying number of PCs or PLS dimensions for the first set of 20 window glass first derivative (9-point smoothing) spectra (10 replicates)…… page 266
Table 80 Discrimination error rates for HOO-CV PCA-CVA (no pretreatment, centered and autoscaled) and HOO-CV PLS-DA models with varying number of PCs or PLS dimensions for the first set of 10 container glass first derivative (9-point smoothing) spectra (10 replicates)…… page 267
Table 81 Float classification error rates for HOO-CV PCA-CVA (no pretreatment, centered and autoscaled) and HOO-CV PLS-DA models with varying number of PCs or PLS dimensions for the first set of 20 window glass first derivative (9-point smoothing) spectra (10 replicates)…… page 268

Table 82 Tempered classification error rates for HOO-CV PCA-CVA (no pretreatment, centered and autoscaled) and HOO-CV PLS-DA models with varying number of PCs or PLS dimensions for the first set of 20 window glass first derivative (9-point smoothing) spectra (10 replicates)..…… page 269

Table 83 Discrimination error rates for HOO-CV PCA-CVA (no pretreatment, centered and autoscaled) and HOO-CV PLS-DA models with varying number of PCs or PLS dimensions for the first set of 30 glass second derivative (5-point smoothing) spectra (10 replicates)……..…….…… page 270

Table 84 Classification (automotive, architectural, or container) error rates for HOO-CV PCA-CVA (no pretreatment, centered and autoscaled) and HOO-CV PLS-DA models with varying number of PCs or PLS dimensions for the first set of 30 glass second derivative (5-point smoothing) spectra (10 replicates)…….. page 271

Table 85 Classification (window or container) error rates for HOO-CV PCA-CVA (no pretreatment, centered and autoscaled) and HOO-CV PLS-DA models with varying number of PCs or PLS dimensions for the first set of 30 glass second derivative (5-point smoothing) spectra (10 replicates)..……..……..……..… page 272

Table 86 Discrimination error rates for HOO-CV PCA-CVA (no pretreatment, centered and autoscaled) and HOO-CV PLS-DA models with varying number of PCs or PLS dimensions for the first set of 20 window glass second derivative (5-point smoothing) spectra (10 replicates)……..……..……..… page 273

Table 87 Discrimination error rates for HOO-CV PCA-CVA (no pretreatment, centered and autoscaled) and HOO-CV PLS-DA models with varying number of PCs or PLS dimensions for the first set of 10 container glass second derivative (5-point smoothing) spectra (10 replicates)…..……..……... page 274

Table 88 Float classification error rates for HOO-CV PCA-CVA (no pretreatment, centered and autoscaled) and HOO-CV PLS-DA models with varying number of PCs or PLS dimensions for the first set of 20 window glass second derivative (5-point smoothing) spectra (10 replicates)……..……..... page 275

Table 89 Tempered classification error rates for HOO-CV PCA-CVA (no pretreatment, centered and autoscaled) and HOO-CV PLS-DA models with varying number of PCs or PLS dimensions for the first set of 20 window glass second derivative (5-point smoothing) spectra (10 replicates)……..……..….. page 276

Table 90 Discrimination error rates for HOO-CV PCA-CVA (no pretreatment, centered and autoscaled) and HOO-CV PLS-DA models with varying number of PCs or PLS dimensions for the first set of 30 glass second derivative (9-point smoothing) spectra (10 replicates)……..... page 277
Table 91 Classification (automotive, architectural, or container) error rates for HOO-CV PCA-CVA (no pretreatment, centered and autoscaled) and HOO-CV PLS-DA models with varying number of PCs or PLS dimensions for the first set of 30 glass second derivative (9-point smoothing) spectra (10 replicates)……..... page 278
Table 92 Classification (window or container) error rates for HOO-CV PCA-CVA (no pretreatment, centered and autoscaled) and HOO-CV PLS-DA models with varying number of PCs or PLS dimensions for the first set of 30 glass second derivative (9-point smoothing) spectra (10 replicates)……... page 279
Table 93 Discrimination error rates for HOO-CV PCA-CVA (no pretreatment, centered and autoscaled) and HOO-CV PLS-DA models with varying number of PCs or PLS dimensions for the first set of 20 window glass second derivative (9-point smoothing) spectra (10 replicates)……..……..…….. page 280
Table 94 Discrimination error rates for HOO-CV PCA-CVA (no pretreatment, centered and autoscaled) and HOO-CV PLS-DA models with varying number of PCs or PLS dimensions for the first set of 10 container glass second derivative (9-point smoothing) spectra (10 replicates)…..……..……... page 281
Table 95 Float classification error rates for HOO-CV PCA-CVA (no pretreatment, centered and autoscaled) and HOO-CV PLS-DA models with varying number of PCs or PLS dimensions for the first set of 20 window glass second derivative (9-point smoothing) spectra (10 replicates)……..…… page 282
Table 96 Tempered classification error rates for HOO-CV PCA-CVA (no pretreatment, centered and autoscaled) and HOO-CV PLS-DA models with varying number of PCs or PLS dimensions for the first set of 20 window glass second derivative (9-point smoothing) spectra (10 replicates)……..… page 283
Table 97 A summary table of the lowest HOO-CV error rates for each of the chemometric models made with PCA-CVA and PLS-DA…….. page 284
Table 98 Discrimination error rates for HOO-CV PCA-CVA (autoscaled) and HOO-CV PLS-DA models with varying number of PCs or PLS dimensions for all 153 glass first derivative (5-point smoothing) spectra (10 replicates)……..……..... page 288

Table 99 Discrimination error rates for HOO-CV PCA-CVA (autoscaled) and HOO-CV PLS-DA models with varying number of PCs or PLS dimensions for 103 window glass first derivative (5-point smoothing) spectra (10 replicates)..…… page 289

Table 100 Discrimination error rates for HOO-CV PCA-CVA (autoscaled) and HOO-CV PLS-DA models with varying number of PCs or PLS dimensions for 50 container glass first derivative (5-point smoothing) spectra (10 replicates)..…… page 289

Table 101 Classification (window or container) error rates for HOO-CV PCA-CVA (autoscaled) and HOO-CV PLS-DA models with varying number of PCs or PLS dimensions for the all 153 glass first derivative (9-point smoothing) spectra (10 replicates)…… page 290

Table 102 Classification (window or container) error rates for HOO-CV PCA-CVA (autoscaled) and HOO-CV PLS-DA models with varying number of PCs or PLS dimensions for the all 153 glass second derivative (9-point smoothing) spectra (10 replicates)…… page 291

Table 103 Tempered classification error rates for HOO-CV PCA-CVA (autoscaled) and HOO-CV PLS-DA models with varying number of PCs or PLS dimensions for the 103 window glass second derivative (9-point smoothing) spectra (10 replicates)……..... page 291

Table 104 Discrimination error rates for HOO-CV PCA-CVA (no pretreatment, centered and autoscaled) and HOO-CV PLS-DA models with 2 - 12 PCs or PLS dimensions for the first set of 30 glass deconvolution data (10 replicates)……..…….. page 299

Table 105 Classification (automotive, architectural, or container) error rates for HOO-CV PCA-CVA (no pretreatment, centered and autoscaled) and HOO-CV PLS-DA models with 2 - 12 PCs or PLS dimensions for the first set of 30 glass deconvolution data (10 replicates)…….. page 300

Table 106 Classification (window or container) error rates for HOO-CV PCA-CVA (no pretreatment, centered and autoscaled) and HOO-CV PLS-DA models with 2 - 12 PCs or PLS dimensions for the first set of 30 glass deconvolution data (10 replicates)……..... page 300

Table 107 Discrimination error rates for HOO-CV PCA-CVA (no pretreatment, centered and autoscaled) and HOO-CV PLS-DA models with 2 - 12 PCs or PLS dimensions for the first set of 20 window glass deconvolution data (10 replicates)…… page 301

Table 108 Discrimination error rates for HOO-CV PCA-CVA (no pretreatment, centered and autoscaled) and HOO-CV PLS-DA models with 2 - 12 PCs or PLS dimensions for the first set of 10 container glass deconvolution data (10 replicates)…….. page 301

Table 109 Float classification error rates for HOO-CV PCA-CVA (no pretreatment, centered and autoscaled) and HOO-CV PLS-DA models with 2 - 12 PCs or PLS dimensions for the first set of 30 glass deconvolution data (10 replicates)…….. page 302

Table 110 Tempered classification error rates for HOO-CV PCA-CVA (no pretreatment, centered and autoscaled) and HOO-CV PLS-DA models with 2 - 12 PCs or PLS dimensions for the first set of 30 glass deconvolution data (10 replicates)……..... page 302

Table 111 Discrimination error rates for HOO-CV PCA-CVA (autoscaled) and HOO-CV PLS-DA models with varying number of PCs or PLS dimensions for the spectra (10 replicates) of 21 glasses with nominally similar RIs (same RI set 1)……. page 304

Table 112 Discrimination error rates for HOO-CV PCA-CVA (autoscaled) and HOO-CV PLS-DA models with varying number of PCs or PLS dimensions for the spectra (10 replicates) of 30 glasses with nominally similar RIs (same RI set 2)……. page 304

Table 113 Discrimination error rates for HOO-CV PCA-CVA (autoscaled) and HOO-CV PLS-DA models with varying number of PCs or PLS dimensions for the first derivative spectra (5-point smoothing) (10 replicates) of 21 glasses with nominally similar RIs (same RI set 1)…..…..…..…… page 305

Table 114 Discrimination error rates for HOO-CV PCA-CVA (autoscaled) and HOO-CV PLS-DA models with varying number of PCs or PLS dimensions for the first derivative spectra (5-point smoothing) (10 replicates) of 30 glasses with nominally similar RIs (same RI set 2)…..…..…..…… page 305

Table 115 Discrimination error rates for HOO-CV PCA-CVA (autoscaled) and HOO-CV PLS-DA models with varying number of PCs or PLS dimensions for the second derivative spectra (5-point smoothing) (10 replicates) of 21 glasses with nominally similar RIs (same RI set 1)…..…..…..…… page 306

Table 116 Discrimination error rates for HOO-CV PCA-CVA (autoscaled) and HOO-CV PLS-DA models with varying number of PCs or PLS dimensions for the second derivative spectra (5-point smoothing) (10 replicates) of 30 glasses with nominally similar RIs (same RI set 2)…..…..…..…… page 306

Table 117 Confusion matrix for the HOO-CV PCA-CVA results for the first derivative spectra (5-point smoothing, autoscaled) with 94 PCs of same RI set 1……..……..... page 309

Table 118 The HOO-CV PCA-CVA overall statistics for the first derivative spectra (5-point smoothing, autoscaled) with 94 PCs of same RI set 1..…..…..…… page 310

Table 119 Confusion matrix for the HOO-CV PCA-CVA results for the second derivative spectra (5-point smoothing, autoscaled) with 85 PCs of same RI set 1……..…….……..... page 311

Table 120 The HOO-CV PCA-CVA overall statistics for the second derivative spectra (5-point smoothing, autoscaled) with 85 PCs of same RI set 1..…… page 312
Table 121 Confusion matrix for the HOO-CV PCA-CVA results for the first derivative spectra (5-point smoothing, autoscaled) with 107 PCs of same RI set 2…… page 313
Table 122 The HOO-CV PCA-CVA overall statistics for the first derivative spectra (5-point smoothing, autoscaled) with 107 PCs of same RI set 2…….. page 314
Table 123 Confusion matrix for the HOO-CV PCA-CVA results for the second derivative spectra (5-point smoothing, autoscaled) with 98 PCs of same RI set 2…… page 315
Table 124 The HOO-CV PCA-CVA overall statistics for the second derivative spectra (5-point smoothing, autoscaled) with 98 PCs of same RI set 2..…… page 316
Table 125 Depth of penetration variation as a function of the angle of incident calculations……..…….... page 329
Table 126 Depth of penetration variation as a function of the wavelength (or wavenumber) of the incident radiation calculations…… page 333
Table 127 Source information about the glasses analyzed in this research, as well as optical and physical properties……. page 401
Table 128 Peak Heights (in absorbance units) for SRMs 620, 621, 1831 taken with the 50-μm aperture and all 18 combinations of resolution and number of co-added scans (30 replicates)…… page 406
Table 129 Mid-IR spectral library results for SRM 620, correlation search algorithm.……..……..……. page 416
Table 130 Mid-IR spectral library results for SRM 621, correlation search algorithm.……..……..……. page 432
Table 131 Mid-IR spectral library results for SRM 1831, correlation search algorithm……..……..... page 449
Table 132 Mid-IR spectral library results for ‘real world’ window, correlation search algorithm.……..…… page 465
Table 133 Mid-IR spectral library results for SRM 620, first derivative correlation search algorithm……..……... page 481
Table 134 Mid-IR spectral library results for SRM 621, first derivative correlation search algorithm.……..…….. page 497
Table 135 Mid-IR spectral library results for SRM 1831, first derivative correlation search algorithm.……..…….. page 514
Table 136 Mid-IR spectral library results for ‘real world’ window, first derivative correlation search algorithm.……..……. page 530
Table 137 Peak positions (center X, in wavenumbers) from the deconvolution of 30 glass samples (10 replicates) into 6 peaks……. page 559

Table 138 Peak areas (in absorbance units) from the deconvolution of 30 glass samples (10 replicates into 6 peaks.……. page 566
Table 139 ATR mid-IR spectral library search results for 30 glass spectra (5 replicates) using the correlation search algorithm.……... page 573
Table 140 ATR mid-IR spectral library search results for 30 glass spectra (5 replicates) using the first derivative correlation search algorithm…... page 577
Table 141 ATR mid-IR spectral library search results for 30 second derivative glass spectra (5 replicates) using the correlation search algorithm….. page 581
Table 142 ATR mid-IR spectral library search results for 30 second derivative glass spectra (5 replicates) using the first derivative correlation search algorithm.……..……..……..... page 585
Table 143 PCA results for the first set of 30 glass spectra (10 replicates), no data pretreatment.……..……...…… page 589
Table 144 PCA results for the first set of 30 glass spectra (10 replicates), centered.……..……. page 591
Table 145 PCA results for the first set of 30 glass spectra (10 replicates), autoscaled.……...……...…….. page 593
Table 146 PCA results for the first set of 20 window glass spectra (10 replicates), no data pretreatment.……...…….. page 595
Table 147 PCA results for the first set of 20 window glass spectra (10 replicates), centered.……...……...……... page 597
Table 148 PCA results for the first set of 20 window glass spectra (10 replicates), autoscaled.……...……...…….. page 599
Table 149 PCA results for the first set of 10 container glass spectra (10 replicates), no data pretreatment.……...…….. page 601
Table 150 PCA results for the first set of 10 container glass spectra (10 replicates), centered.……...……...……... page 603
Table 151 PCA results for the first set of 10 container glass spectra (10 replicates), autoscaled.……...……...……... page 605
Table 152 PCA results for the first set of 30 normalized (peak area) glass spectra (10 replicates), no data pretreatment.……...…… page 607
Table 153 PCA results for the first set of 30 normalized (peak area) glass spectra (10 replicates), centered.……...……... page 609
Table 154 PCA results for the first set of 30 normalized (peak area) glass spectra (10 replicates), autoscaled.……...…… page 611
Table 155 PCA results for the first set of 20 normalized (peak area) window glass spectra (10 replicates), no data pretreatment.…….. page 613
Table 156 PCA results for the first set of 20 normalized (peak area) window glass spectra (10 replicates), centered.……...…….. page 615
Table 157 PCA results for the first set of 20 normalized (peak area) window glass spectra (10 replicates), autoscaled.……...……... page 617

Table 158 PCA results for the first set of 10 normalized (peak area) container glass spectra (10 replicates), no data pretreatment…….. page 619
Table 159 PCA results for the first set of 10 normalized (peak area) container glass spectra (10 replicates), centered.……...…….. page 621
Table 160 PCA results for the first set of 10 normalized (peak area) container glass spectra (10 replicates), autoscaled.……...……... page 623
Table 161 PCA results for the first set of 30 normalized (peak height) glass spectra (10 replicates), no data pretreatment.……...…… page 625
Table 162 PCA results for the first set of 30 normalized (peak height) glass spectra (10 replicates), centered.……...……... page 627
Table 163 PCA results for the first set of 30 normalized (peak height) glass spectra (10 replicates), autoscaled.……...…… page 629
Table 164 PCA results for the first set of 20 normalized (peak height) window glass spectra (10 replicates), no data pretreatment…….. page 631
Table 165 PCA results for the first set of 20 normalized (peak height) window glass spectra (10 replicates), centered.……...…….. page 633
Table 166 PCA results for the first set of 20 normalized (peak height) window glass spectra (10 replicates), autoscaled.……...……... page 635
Table 167 PCA results for the first set of 10 normalized (peak height) container glass spectra (10 replicates), no data pretreatment…….. page 637
Table 168 PCA results for the first set of 10 normalized (peak height) container glass spectra (10 replicates), centered.……...…….. page 639
Table 169 PCA results for the first set of 10 normalized (peak height) container glass spectra (10 replicates), autoscaled.……...……... page 641
Table 170 PCA results for the first set of 30 glass first derivative (5-point smoothing) spectra (10 replicates), no data pretreatment.……... page 643
Table 171 PCA results for the first set of 30 glass first derivative (5-point smoothing) spectra (10 replicates), centered.……...…… page 645
Table 172 PCA results for the first set of 30 glass first derivative (5-point smoothing) spectra (10 replicates), autoscaled.……...… page 647
Table 173 PCA results for the first set of 20 window glass first derivative (5-point smoothing) spectra (10 replicates), no data pretreatment……... page 649
Table 174 PCA results for the first set of 20 window glass first derivative (5-point smoothing) spectra (10 replicates), centered…….. page 651
Table 175 PCA results for the first set of 20 window glass first derivative (5-point smoothing) spectra (10 replicates), autoscaled…….. page 653
Table 176 PCA results for the first set of 10 container glass first derivative (5-point smoothing) spectra (10 replicates), no data pretreatment……... page 655
Table 177 PCA results for the first set of 10 container glass first derivative (5-point smoothing) spectra (10 replicates), centered…….. page 657
Table 178 PCA results for the first set of 10 container glass first derivative (5-point smoothing) spectra (10 replicates), autoscaled…….. page 659

Table 179 PCA results for the first set of 30 glass first derivative (9-point smoothing) spectra (10 replicates), no data pretreatment..……... page 661
Table 180 PCA results for the first set of 30 glass first derivative (9-point smoothing) spectra (10 replicates), centered..……...…… page 663
Table 181 PCA results for the first set of 30 glass first derivative (9-point smoothing) spectra (10 replicates), autoscaled..……..... page 665
Table 182 PCA results for the first set of 20 window glass first derivative (9-point smoothing) spectra (10 replicates), no data pretreatment……... page 667
Table 183 PCA results for the first set of 20 window glass first derivative (9-point smoothing) spectra (10 replicates), centered..…….. page 669
Table 184 PCA results for the first set of 20 window glass first derivative (9-point smoothing) spectra (10 replicates), autoscaled..…….. page 671
Table 185 PCA results for the first set of 10 container glass first derivative (9-point smoothing) spectra (10 replicates), no data pretreatment……... page 673
Table 186 PCA results for the first set of 10 container glass first derivative (9-point smoothing) spectra (10 replicates), centered..…….. page 675
Table 187 PCA results for the first set of 10 container glass first derivative (9-point smoothing) spectra (10 replicates), autoscaled..…….. page 677
Table 188 PCA results for the first set of 30 glass second derivative (5-point smoothing) spectra (10 replicates), no data pretreatment..……... page 679
Table 189 PCA results for the first set of 30 glass second derivative (5-point smoothing) spectra (10 replicates), centered..……...…… page 681
Table 190 PCA results for the first set of 30 glass second derivative (5-point smoothing) spectra (10 replicates), autoscaled..……..... page 683
Table 191 PCA results for the first set of 20 window glass second derivative (5-point smoothing) spectra (10 replicates), no data pretreatment…... page 685
Table 192 PCA results for the first set of 20 window glass second derivative (5-point smoothing) spectra (10 replicates), centered..……. page 687
Table 193 PCA results for the first set of 20 window glass second derivative (5-point smoothing) spectra (10 replicates), autoscaled..…….. page 689
Table 194 PCA results for the first set of 10 container glass second derivative (5-point smoothing) spectra (10 replicates), no data pretreatment…... page 691
Table 195 PCA results for the first set of 10 container glass second derivative (5-point smoothing) spectra (10 replicates), centered..……. page 693
Table 196 PCA results for the first set of 10 container glass second derivative (5-point smoothing) spectra (10 replicates), autoscaled..…….. page 695
Table 197 PCA results for the first set of 30 glass second derivative (9-point smoothing) spectra (10 replicates), no data pretreatment..……... page 697
Table 198 PCA results for the first set of 30 glass second derivative (9-point smoothing) spectra (10 replicates), centered..……...…… page 699
Table 199 PCA results for the first set of 30 glass second derivative (9-point smoothing) spectra (10 replicates), autoscaled..……..... page 701

Table 200 PCA results for the first set of 20 window glass second derivative (9-point smoothing) spectra (10 replicates), no data pretreatment….. page 703
Table 201 PCA results for the first set of 20 window glass second derivative (9-point smoothing) spectra (10 replicates), centered.……. page 705
Table 202 PCA results for the first set of 20 window glass second derivative (9-point smoothing) spectra (10 replicates), autoscaled.…….. page 707
Table 203 PCA results for the first set of 10 container glass second derivative (9-point smoothing) spectra (10 replicates), no data pretreatment….. page 709
Table 204 PCA results for the first set of 10 container glass second derivative (9-point smoothing) spectra (10 replicates), centered.……. page 711
Table 205 PCA results for the first set of 10 container glass second derivative (9-point smoothing) spectra (10 replicates), autoscaled.…….. page 713
Table 206 Discrimination error rates for HOO-CV with PCA reduced CVA for the first set of 30 glass spectra (10 replicates), no data pretreatment... page 715
Table 207 Discrimination error rates for HOO-CV with PCA reduced CVA for the first set of 30 glass spectra (10 replicates), centered data.……. page 717
Table 208 Discrimination error rates for HOO-CV with PCA reduced CVA for the first set of 30 glass spectra (10 replicates), autoscaled data…….. page 719
Table 209 Classification (automotive, architectural or container) error rates for HOO-CV with PCA reduced CVA for the first set of 30 glass spectra (10 replicates), no data pretreatment.……...…… page 722
Table 210 Classification (automotive, architectural or container) error rates for HOO-CV with PCA reduced CVA for the first set of 30 glass spectra (10 replicates), centered data.……...……... page 724
Table 211 Classification (automotive, architectural or container) error rates for HOO-CV with PCA reduced CVA for the first set of 30 glass spectra (10 replicates), autoscaled data.……...…… page 726
Table 212 Classification (window or container) error rates for HOO-CV with PCA reduced CVA for the first set of 30 glass spectra (10 replicates), no data pretreatment.……...…….. page 729
Table 213 Classification (window or container) error rates for HOO-CV with PCA reduced CVA for the first set of 30 glass spectra (10 replicates), centered data.……...……...….. page 731
Table 214 Classification (window or container) error rates for HOO-CV with PCA reduced CVA for the first set of 30 glass spectra (10 replicates), autoscaled data.……...……...… page 733
Table 215 Discrimination error rates for HOO-CV with PCA reduced CVA for the first set of 20 window glass spectra (10 replicates), no data pretreatment.……...……...……... page 736
Table 216 Discrimination error rates for HOO-CV with PCA reduced CVA for the first set of 20 window glass spectra (10 replicates), centered data.……...……...……...……. page 738

Table 217 Discrimination error rates for HOO-CV with PCA reduced CVA for the first set of 20 window glass spectra (10 replicates), autoscaled data……...……...……...……. page 740
Table 218 Discrimination error rates for HOO-CV with PCA reduced CVA for the first set of 10 container glass spectra (10 replicates), no data pretreatment……...……...……... page 742
Table 219 Discrimination error rates for HOO-CV with PCA reduced CVA for the first set of 10 container glass spectra (10 replicates), centered data……...……...……...…… page 744
Table 220 Discrimination error rates for HOO-CV with PCA reduced CVA for the first set of 10 container glass spectra (10 replicates), autoscaled data……...……...……...……. page 746
Table 221 Float classification error rates for HOO-CV with PCA reduced CVA for the first set of 20 window glass spectra (10 replicates), no data pretreatment……...……...……... page 748
Table 222 Float classification error rates for HOO-CV with PCA reduced CVA for the first set of 20 window glass spectra (10 replicates), centered data……...……...……...……. page 750
Table 223 Float classification error rates for HOO-CV with PCA reduced CVA for the first set of 20 window glass spectra (10 replicates), autoscaled data……...……...…….. page 752
Table 224 Tempered classification error rates for HOO-CV with PCA reduced CVA for the first set of 20 window glass spectra (10 replicates), no data pretreatment……...……...……... page 754
Table 225 Tempered classification error rates for HOO-CV with PCA reduced CVA for the first set of 20 window glass spectra (10 replicates), centered data……...……...…….. page 756
Table 226 Tempered classification error rates for HOO-CV with PCA reduced CVA for the first set of 20 window glass spectra (10 replicates), autoscaled data……...……...…….. page 758
Table 227 Discrimination error rates for HOO-CV with PCA reduced CVA for the first set of 30 normalized (peak area) glass spectra (10 replicates), no data pretreatment……...…….. page 760
Table 228 Discrimination error rates for HOO-CV with PCA reduced CVA for the first set of 30 normalized (peak area) glass spectra (10 replicates), centered data……...……...….. page 761
Table 229 Discrimination error rates for HOO-CV with PCA reduced CVA for the first set of 30 normalized (peak area) glass spectra (10 replicates), autoscaled data……...……...… page 762
Table 230 Classification (automotive, architectural or container) error rates for HOO-CV with PCA reduced CVA for the first set of 30 normalized (peak area) glass spectra (10 replicates), no data pretreatment…… page 765

Table 231 Classification (automotive, architectural or container) error rates for HOO-CV with PCA reduced CVA for the first set of 30 normalized (peak area) glass spectra (10 replicates), centered data..... page 766
Table 232 Classification (automotive, architectural or container) error rates for HOO-CV with PCA reduced CVA for the first set of 30 normalized (peak area) glass spectra (10 replicates), autoscaled data..... page 767
Table 233 Classification (window or container) error rates for HOO-CV with PCA reduced CVA for the first set of 30 normalized (peak area) glass spectra (10 replicates), no data pretreatment..... page 770
Table 234 Classification (window or container) error rates for HOO-CV with PCA reduced CVA for the first set of 30 normalized (peak area) glass spectra (10 replicates), centered..... page 771
Table 235 Classification (window or container) error rates for HOO-CV with PCA reduced CVA for the first set of 30 normalized (peak area) glass spectra (10 replicates), autoscaled data..... page 772
Table 236 Discrimination error rates for HOO-CV with PCA reduced CVA for the first set of 20 window normalized (peak area) glass spectra (10 replicates), no data pretreatment..... page 775
Table 237 Discrimination error rates for HOO-CV with PCA reduced CVA for the first set of 20 window normalized (peak area) glass spectra (10 replicates), centered data..... page 776
Table 238 Discrimination error rates for HOO-CV with PCA reduced CVA for the first set of 20 window normalized (peak area) glass spectra (10 replicates), autoscaled data..... page 777
Table 239 Discrimination error rates for HOO-CV with PCA reduced CVA for the first set of 10 container normalized (peak area) glass spectra (10 replicates), no data pretreatment..... page 779
Table 240 Discrimination error rates for HOO-CV with PCA reduced CVA for the first set of 10 container normalized (peak area) glass spectra (10 replicates), centered data..... page 780
Table 241 Discrimination error rates for HOO-CV with PCA reduced CVA for the first set of 10 container normalized (peak area) glass spectra (10 replicates), autoscaled data..... page 781
Table 242 Float classification error rates for HOO-CV with PCA reduced CVA for the first set of 20 window normalized (peak area) glass spectra (10 replicates), no data pretreatment..... page 783
Table 243 Float classification error rates for HOO-CV with PCA reduced CVA for the first set of 20 window normalized (peak area) glass spectra (10 replicates), centered data..... page 784
Table 244 Float classification error rates for HOO-CV with PCA reduced CVA for the first set of 20 window normalized (peak area) glass spectra (10 replicates), autoscaled data..... page 785

Table 245 Tempered classification error rates for HOO-CV with PCA reduced CVA for the first set of 20 window normalized (peak area) glass spectra (10 replicates), no data pretreatment..…… page 787
Table 246 Tempered classification error rates for HOO-CV with PCA reduced CVA for the first set of 20 window normalized (peak area) glass spectra (10 replicates), centered data.……... page 788
Table 247 Tempered classification error rates for HOO-CV with PCA reduced CVA for the first set of 20 window normalized (peak area) glass spectra (10 replicates), autoscaled data.……... page 789
Table 248 Discrimination error rates for HOO-CV with PCA reduced CVA for the first set of 30 normalized (peak height) glass spectra (10 replicates), no data pretreatment.……... page 791
Table 249 Discrimination error rates for HOO-CV with PCA reduced CVA for the first set of 30 normalized (peak height) glass spectra (10 replicates), centered data.……...……... page 793
Table 250 Discrimination error rates for HOO-CV with PCA reduced CVA for the first set of 30 normalized (peak height) glass spectra (10 replicates), autoscaled data.……..……..... page 795
Table 251 Classification (automotive, architectural or container) error rates for HOO-CV with PCA reduced CVA for the first set of 30 normalized (peak height) glass spectra (10 replicates), no data pretreatment…… page 798
Table 252 Classification (automotive, architectural or container) error rates for HOO-CV with PCA reduced CVA for the first set of 30 normalized (peak height) glass spectra (10 replicates), centered data.……... page 800
Table 253 Classification (automotive, architectural or container) error rates for HOO-CV with PCA reduced CVA for the first set of 30 normalized (peak height) glass spectra (10 replicates), autoscaled data.…… page 802
Table 254 Classification (window or container) error rates for HOO-CV with PCA reduced CVA for the first set of 30 normalized (peak height) glass spectra (10 replicates), no data pretreatment.…….. page 805
Table 255 Classification (window or container) error rates for HOO-CV with PCA reduced CVA for the first set of 30 normalized (peak height) glass spectra (10 replicates), centered data……..... page 807
Table 256 Classification (window or container) error rates for HOO-CV with PCA reduced CVA for the first set of 30 normalized (peak height) glass spectra (10 replicates), autoscaled data.……... page 809
Table 257 Discrimination error rates for HOO-CV with PCA reduced CVA for the first set of 20 window normalized (peak height) glass spectra (10 replicates), no data pretreatment.……... page 812
Table 258 Discrimination error rates for HOO-CV with PCA reduced CVA for the first set of 20 window normalized (peak height) glass spectra (10 replicates), centered data.……...……... page 814

Table 259 Discrimination error rates for HOO-CV with PCA reduced CVA for the first set of 20 window normalized (peak height) glass spectra (10 replicates), autoscaled data..... page 816
Table 260 Discrimination error rates for HOO-CV with PCA reduced CVA for the first set of 10 container normalized (peak height) glass spectra (10 replicates), no data pretreatment..... page 818
Table 261 Discrimination error rates for HOO-CV with PCA reduced CVA for the first set of 10 container normalized (peak height) glass spectra (10 replicates), centered data..... page 820
Table 262 Discrimination error rates for HOO-CV with PCA reduced CVA for the first set of 10 container normalized (peak height) glass spectra (10 replicates), autoscaled data..... page 822
Table 263 Float classification error rates for HOO-CV with PCA reduced CVA for the first set of 20 window normalized (peak height) glass spectra (10 replicates), no data pretreatment..... page 824
Table 264 Float classification error rates for HOO-CV with PCA reduced CVA for the first set of 20 window normalized (peak height) glass spectra (10 replicates), centered data..... page 826
Table 265 Float classification error rates for HOO-CV with PCA reduced CVA for the first set of 20 window normalized (peak height) glass spectra (10 replicates), autoscaled data..... page 828
Table 266 Tempered classification error rates for HOO-CV with PCA reduced CVA for the first set of 20 window normalized (peak height) glass spectra (10 replicates), no data pretreatment..... page 830
Table 267 Tempered classification error rates for HOO-CV with PCA reduced CVA for the first set of 20 window normalized (peak height) glass spectra (10 replicates), centered data..... page 832
Table 268 Tempered classification error rates for HOO-CV with PCA reduced CVA for the first set of 20 window normalized (peak height) glass spectra (10 replicates), autoscaled data..... page 834
Table 269 Discrimination error rates for HOO-CV with PCA reduced CVA for the first set of 30 glass first derivative (5-point smoothing) spectra (10 replicates), no data pretreatment..... page 836
Table 270 Discrimination error rates for HOO-CV with PCA reduced CVA for the first set of 30 glass first derivative (5-point smoothing) spectra (10 replicates), centered data..... page 838
Table 271 Discrimination error rates for HOO-CV with PCA reduced CVA for the first set of 30 glass first derivative (5-point smoothing) spectra (10 replicates), autoscaled data..... page 840
Table 272 Classification (automotive, architectural or container) error rates for HOO-CV with PCA reduced CVA for the first set of 30 glass first derivative (5-point smoothing) spectra (10 replicates), no data pretreatment..... page 843

Table 273 Classification (automotive, architectural or container) error rates for HOO-CV with PCA reduced CVA for the first set of 30 glass first derivative (5-point smoothing) spectra (10 replicates), centered data……..……..... page 845
Table 274 Classification (automotive, architectural or container) error rates for HOO-CV with PCA reduced CVA for the first set of 30 glass first derivative (5-point smoothing) spectra (10 replicates), autoscaled data……..……..……..... page 847
Table 275 Classification (window or container) error rates for HOO-CV with PCA reduced CVA for the first set of 30 glass first derivative (5-point smoothing) spectra (10 replicates), no data pretreatment……... page 850
Table 276 Classification (window or container) error rates for HOO-CV with PCA reduced CVA for the first set of 30 glass first derivative (5-point smoothing) spectra (10 replicates), centered data…….. page 852
Table 277 Classification (window or container) error rates for HOO-CV with PCA reduced CVA for the first set of 30 glass first derivative (5-point smoothing) spectra (10 replicates), autoscaled data……... page 854
Table 278 Discrimination error rates for HOO-CV with PCA reduced CVA for the first set of 20 window glass first derivative (5-point smoothing) spectra (10 replicates), no data pretreatment.……..…… page 857
Table 279 Discrimination error rates for HOO-CV with PCA reduced CVA for the first set of 20 window glass first derivative (5-point smoothing) spectra (10 replicates), centered data.……..……... page 859
Table 280 Discrimination error rates for HOO-CV with PCA reduced CVA for the first set of 20 window glass first derivative (5-point smoothing) spectra (10 replicates), autoscaled data.……..…… page 861
Table 281 Discrimination error rates for HOO-CV with PCA reduced CVA for the first set of 10 container glass first derivative (5-point smoothing) spectra (10 replicates), no data pretreatment.……..... page 863
Table 282 Discrimination error rates for HOO-CV with PCA reduced CVA for the first set of 10 container glass first derivative (5-point smoothing) spectra (10 replicates), centered data.……..……... page 865
Table 283 Discrimination error rates for HOO-CV with PCA reduced CVA for the first set of 10 container glass first derivative (5-point smoothing) spectra (10 replicates), autoscaled data.……..…… page 867
Table 284 Float classification error rates for HOO-CV with PCA reduced CVA for the first set of 20 window glass first derivative (5-point smoothing) spectra (10 replicates), no data pretreatment.……... page 869
Table 285 Float classification error rates for HOO-CV with PCA reduced CVA for the first set of 20 window glass first derivative (5-point smoothing) spectra (10 replicates), centered data.……... page 871

Table 286 Float classification error rates for HOO-CV with PCA reduced CVA for the first set of 20 window glass first derivative (5-point smoothing) spectra (10 replicates), autoscaled data.…… page 873
Table 287 Tempered classification error rates for HOO-CV with PCA reduced CVA for the first set of 20 window glass first derivative (5-point smoothing) spectra (10 replicates), no data pretreatment.……... page 875
Table 288 Tempered classification error rates for HOO-CV with PCA reduced CVA for the first set of 20 window glass first derivative (5-point smoothing) spectra (10 replicates), centered data.……... page 877
Table 289 Tempered classification error rates for HOO-CV with PCA reduced CVA for the first set of 20 window glass first derivative (5-point smoothing) spectra (10 replicates), autoscaled data.…… page 879
Table 290 Discrimination error rates for HOO-CV with PCA reduced CVA for the first set of 30 glass first derivative (9-point smoothing) spectra (10 replicates), no data pretreatment.……...…… page 881
Table 291 Discrimination error rates for HOO-CV with PCA reduced CVA for the first set of 30 glass first derivative (9-point smoothing) spectra (10 replicates), centered data.……...……..... page 883
Table 292 Discrimination error rates for HOO-CV with PCA reduced CVA for the first set of 30 glass first derivative (9-point smoothing) spectra (10 replicates), autoscaled data.……...…… page 884
Table 293 Classification (automotive, architectural or container) error rates for HOO-CV with PCA reduced CVA for the first set of 30 glass first derivative (9-point smoothing) spectra (10 replicates), no data pretreatment.……...……...……... page 887
Table 294 Classification (automotive, architectural or container) error rates for HOO-CV with PCA reduced CVA for the first set of 30 glass first derivative (9-point smoothing) spectra (10 replicates), centered data..……...……...……..... page 889
Table 295 Classification (automotive, architectural or container) error rates for HOO-CV with PCA reduced CVA for the first set of 30 glass first derivative (9-point smoothing) spectra (10 replicates), autoscaled data.……...……...……...……. page 890
Table 296 Classification (window or container) error rates for HOO-CV with PCA reduced CVA for the first set of 30 glass first derivative (9-point smoothing) spectra (10 replicates), no data pretreatment……... page 893
Table 297 Classification (window or container) error rates for HOO-CV with PCA reduced CVA for the first set of 30 glass first derivative (9-point smoothing) spectra (10 replicates), centered data.…….. page 895
Table 298 Classification (window or container) error rates for HOO-CV with PCA reduced CVA for the first set of 30 glass first derivative (9-point smoothing) spectra (10 replicates), autoscaled data.……... page 896

Table 299 Discrimination error rates for HOO-CV with PCA reduced CVA for the first set of 20 window glass first derivative (9-point smoothing) spectra (10 replicates), no data pretreatment..... page 899
Table 300 Discrimination error rates for HOO-CV with PCA reduced CVA for the first set of 20 window glass first derivative (9-point smoothing) spectra (10 replicates), centered data..... page 901
Table 301 Discrimination error rates for HOO-CV with PCA reduced CVA for the first set of 20 window glass first derivative (9-point smoothing) spectra (10 replicates), autoscaled data..... page 902
Table 302 Discrimination error rates for HOO-CV with PCA reduced CVA for the first set of 10 container glass first derivative (9-point smoothing) spectra (10 replicates), no data pretreatment..... page 904
Table 303 Discrimination error rates for HOO-CV with PCA reduced CVA for the first set of 10 container glass first derivative (9-point smoothing) spectra (10 replicates), centered data..... page 906
Table 304 Discrimination error rates for HOO-CV with PCA reduced CVA for the first set of 10 container glass first derivative (9-point smoothing) spectra (10 replicates), autoscaled data..... page 907
Table 305 Float classification error rates for HOO-CV with PCA reduced CVA for the first set of 20 window glass first derivative (9-point smoothing) spectra (10 replicates), no data pretreatment..... page 909
Table 306 Float classification error rates for HOO-CV with PCA reduced CVA for the first set of 20 window glass first derivative (9-point smoothing) spectra (10 replicates), centered data..... page 911
Table 307 Float classification error rates for HOO-CV with PCA reduced CVA for the first set of 20 window glass first derivative (9-point smoothing) spectra (10 replicates), autoscaled data..... page 912
Table 308 Tempered classification error rates for HOO-CV with PCA reduced CVA for the first set of 20 window glass first derivative (9-point smoothing) spectra (10 replicates), no data pretreatment..... page 914
Table 309 Tempered classification error rates for HOO-CV with PCA reduced CVA for the first set of 20 window glass first derivative (9-point smoothing) spectra (10 replicates), centered data..... page 916
Table 310 Tempered classification error rates for HOO-CV with PCA reduced CVA for the first set of 20 window glass first derivative (9-point smoothing) spectra (10 replicates), autoscaled data..... page 917
Table 311 Discrimination error rates for HOO-CV with PCA reduced CVA for the first set of 30 glass second derivative (5-point smoothing) spectra (10 replicates), no data pretreatment..... page 919
Table 312 Discrimination error rates for HOO-CV with PCA reduced CVA for the first set of 30 glass second derivative (5-point smoothing) spectra (10 replicates), centered data..... page 921

Table 313 Discrimination error rates for HOO-CV with PCA reduced CVA for the first set of 30 glass second derivative (5-point smoothing) spectra (10 replicates), autoscaled data.…… page 923
Table 314 Classification (automotive, architectural or container) error rates for HOO-CV with PCA reduced CVA for the first set of 30 glass second derivative (5-point smoothing) spectra (10 replicates), no data pretreatment.…… page 926
Table 315 Classification (automotive, architectural or container) error rates for HOO-CV with PCA reduced CVA for the first set of 30 glass second derivative (5-point smoothing) spectra (10 replicates), centered data.…… page 928
Table 316 Classification (automotive, architectural or container) error rates for HOO-CV with PCA reduced CVA for the first set of 30 glass second derivative (5-point smoothing) spectra (10 replicates), autoscaled data.…… page 930
Table 317 Classification (window or container) error rates for HOO-CV with PCA reduced CVA for the first set of 30 glass second derivative (5-point smoothing) spectra (10 replicates), no data pretreatment…….. page 933
Table 318 Classification (window or container) error rates for HOO-CV with PCA reduced CVA for the first set of 30 glass second derivative (5-point smoothing) spectra (10 replicates), centered data…….. page 935
Table 319 Classification (window or container) error rates for HOO-CV with PCA reduced CVA for the first set of 30 glass second derivative (5-point smoothing) spectra (10 replicates), autoscaled data.…….. page 937
Table 320 Discrimination error rates for HOO-CV with PCA reduced CVA for the first set of 20 window glass second derivative (5-point smoothing) spectra (10 replicates), no data pretreatment.…….. page 940
Table 321 Discrimination error rates for HOO-CV with PCA reduced CVA for the first set of 20 window glass second derivative (5-point smoothing) spectra (10 replicates), centered data.…….. page 942
Table 322 Discrimination error rates for HOO-CV with PCA reduced CVA for the first set of 20 window glass second derivative (5-point smoothing) spectra (10 replicates), autoscaled data.…… page 944
Table 323 Discrimination error rates for HOO-CV with PCA reduced CVA for the first set of 10 container glass second derivative (5-point smoothing) spectra (10 replicates), no data pretreatment.…….. page 946
Table 324 Discrimination error rates for HOO-CV with PCA reduced CVA for the first set of 10 container glass second derivative (5-point smoothing) spectra (10 replicates), centered data.…….. page 948
Table 325 Discrimination error rates for HOO-CV with PCA reduced CVA for the first set of 10 container glass second derivative (5-point smoothing) spectra (10 replicates), autoscaled data.…… page 950

Table 326 Float classification error rates for HOO-CV with PCA reduced CVA for the first set of 20 window glass second derivative (5-point smoothing) spectra (10 replicates), no data pretreatment..……... page 952
Table 327 Float classification error rates for HOO-CV with PCA reduced CVA for the first set of 20 window glass second derivative (5-point smoothing) spectra (10 replicates), centered data.……... page 954
Table 328 Float classification error rates for HOO-CV with PCA reduced CVA for the first set of 20 window glass second derivative (5-point smoothing) spectra (10 replicates), autoscaled data.…… page 956
Table 329 Tempered classification error rates for HOO-CV with PCA reduced CVA for the first set of 20 window glass second derivative (5-point smoothing) spectra (10 replicates), no data pretreatment..……... page 958
Table 330 Tempered classification error rates for HOO-CV with PCA reduced CVA for the first set of 20 window glass second derivative (5-point smoothing) spectra (10 replicates), centered data.……... page 960
Table 331 Tempered classification error rates for HOO-CV with PCA reduced CVA for the first set of 20 window glass second derivative (5-point smoothing) spectra (10 replicates), autoscaled data..……... page 962
Table 332 Discrimination error rates for HOO-CV with PCA reduced CVA for the first set of 30 glass second derivative (9-point smoothing) spectra (10 replicates), no data pretreatment.……...…… page 964
Table 333 Discrimination error rates for HOO-CV with PCA reduced CVA for the first set of 30 glass second derivative (9-point smoothing) spectra (10 replicates), centered data.……...……... page 966
Table 334 Discrimination error rates for HOO-CV with PCA reduced CVA for the first set of 30 glass second derivative (9-point smoothing) spectra (10 replicates), autoscaled data.……...…… page 967
Table 335 Classification (automotive, architectural or container) error rates for HOO-CV with PCA reduced CVA for the first set of 30 glass second derivative (9-point smoothing) spectra (10 replicates), no data pretreatment.……...……...……... page 970
Table 336 Classification (automotive, architectural or container) error rates for HOO-CV with PCA reduced CVA for the first set of 30 glass second derivative (9-point smoothing) spectra (10 replicates), centered data.……...……...…….. page 972
Table 337 Classification (automotive, architectural or container) error rates for HOO-CV with PCA reduced CVA for the first set of 30 glass second derivative (9-point smoothing) spectra (10 replicates), autoscaled data.……...……...…….. page 973
Table 338 Classification (window or container) error rates for HOO-CV with PCA reduced CVA for the first set of 30 glass second derivative (9-point smoothing) spectra (10 replicates), no data pretreatment..…….. page 976

Table 339 Classification (window or container) error rates for HOO-CV with PCA reduced CVA for the first set of 30 glass second derivative (9-point smoothing) spectra (10 replicates), centered data…….. page 978
Table 340 Classification (window or container) error rates for HOO-CV with PCA reduced CVA for the first set of 30 glass second derivative (9-point smoothing) spectra (10 replicates), autoscaled data…….... page 979
Table 341 Discrimination error rates for HOO-CV with PCA reduced CVA for the first set of 20 window glass second derivative (9-point smoothing) spectra (10 replicates), no data pretreatment.……... page 982
Table 342 Discrimination error rates for HOO-CV with PCA reduced CVA for the first set of 20 window glass second derivative (9-point smoothing) spectra (10 replicates), centered data.……... page 983
Table 343 Discrimination error rates for HOO-CV with PCA reduced CVA for the first set of 20 window glass second derivative (9-point smoothing) spectra (10 replicates), autoscaled data.…… page 984
Table 344 Discrimination error rates for HOO-CV with PCA reduced CVA for the first set of 10 container glass second derivative (9-point smoothing) spectra (10 replicates), no data pretreatment.……... page 986
Table 345 Discrimination error rates for HOO-CV with PCA reduced CVA for the first set of 10 container glass second derivative (9-point smoothing) spectra (10 replicates), centered data.……... page 987
Table 346 Discrimination error rates for HOO-CV with PCA reduced CVA for the first set of 10 container glass second derivative (9-point smoothing) spectra (10 replicates), autoscaled data.…… page 988
Table 347 Float classification error rates for HOO-CV with PCA reduced CVA for the first set of 20 window glass second derivative (9-point smoothing) spectra (10 replicates), no data pretreatment.……... page 990
Table 348 Float classification error rates for HOO-CV with PCA reduced CVA for the first set of 20 window glass second derivative (9-point smoothing) spectra (10 replicates), centered data.……... Page 991
Table 349 Float classification error rates for HOO-CV with PCA reduced CVA for the first set of 20 window glass second derivative (9-point smoothing) spectra (10 replicates), autoscaled data.…… page 992
Table 350 Tempered classification error rates for HOO-CV with PCA reduced CVA for the first set of 20 window glass second derivative (9-point smoothing) spectra (10 replicates), no data pretreatment.……... page 994
Table 351 Tempered classification error rates for HOO-CV with PCA reduced CVA for the first set of 20 window glass second derivative (9-point smoothing) spectra (10 replicates), centered data.……... page 996
Table 352 Tempered classification error rates for HOO-CV with PCA reduced CVA for the first set of 20 window glass second derivative (9-point smoothing) spectra (10 replicates), autoscaled data.…… page 997

Table 353 PCA results for the set of 153 glass first derivative (5-point smoothing) spectra (10 replicates), autoscaled……..... page 999
Table 354 PCA results for the set of 103 window glass first derivative (5-point smoothing) spectra (10 replicates), autoscaled……..... page 1004
Table 355 PCA results for the set of 50 container glass first derivative (5-point smoothing) spectra (10 replicates), autoscaled……..... page 1009
Table 356 PCA results for the set of 153 glass first derivative (9-point smoothing) spectra (10 replicates), autoscaled……..... page 1014
Table 357 PCA results for the set of 153 glass second derivative (9-point smoothing) spectra (10 replicates), autoscaled……..... page 1019
Table 358 PCA results for the set of 103 window glass second derivative (9-point smoothing) spectra (10 replicates), autoscaled…….. page 1024
Table 359 Discrimination error rates for HOO-CV with PCA reduced CVA for the set of 153 glass first derivative (5-point smoothing) spectra (10 replicates), autoscaled……...……...……... page 1029
Table 360 Discrimination error rates for HOO-CV with PCA reduced CVA for the set of 103 window glass first derivative (5-point smoothing) spectra (10 replicates), autoscaled……...…… page 1032
Table 361 Discrimination error rates for HOO-CV with PCA reduced CVA for the set of 50 container glass first derivative (5-point smoothing) spectra (10 replicates), autoscaled……...…… page 1035
Table 362 Discrimination error rates for HOO-CV with PCA reduced CVA for the set of 153 glass first derivative (9-point smoothing) spectra (10 replicates), autoscaled……...……...……... page 1038
Table 363 Discrimination error rates for HOO-CV with PCA reduced CVA for the set of 153 glass second derivative (9-point smoothing) spectra (10 replicates), autoscaled……...……...…. page 1040
Table 364 Tempered classification error rates for HOO-CV with PCA reduced CVA for the set of 103 window glass second derivative (9-point smoothing) spectra (10 replicates), autoscaled……..... page 1042
Table 365 PCA results for the first set of 30 glass deconvolution data (10 replicates), no pretreatment……...……..... page 1044
Table 366 PCA results for the first set of 30 glass deconvolution data (10 replicates), centered……...……...……... page 1045
Table 367 PCA results for the first set of 30 glass deconvolution data (10 replicates), autoscaled……...……..... page 1046
Table 368 PCA results for the first set of 20 window glass deconvolution data (10 replicates), no pretreatment……...…… page 1047
Table 369 PCA results for the first set of 20 window glass deconvolution data (10 replicates), centered……...……...……. page 1048
Table 370 PCA results for the first set of 20 window glass deconvolution data (10 replicates), autoscaled……...……..... page 1049

Table 371 PCA results for the first set of 10 container glass deconvolution data (10 replicates), no pretreatment..... page 1050
Table 372 PCA results for the first set of 10 container glass deconvolution data (10 replicates), centered..... page 1051
Table 373 PCA results for the first set of 10 container glass deconvolution data (10 replicates), autoscaled..... page 1052
Table 374 PCA results for the spectra of 21 glasses (10 replicates) with nominally similar RIs (same RI set 1), autoscaled..... page 1053
Table 375 PCA results for the first derivative spectra (5-point smoothing) of 21 glasses (10 replicates) with nominally similar RIs (same RI set 1), autoscaled..... page 1057
Table 376 PCA results for the second derivative spectra (5-point smoothing) of 21 glasses (10 replicates) with nominally similar RIs (same RI set 1), autoscaled..... page 1060
Table 377 PCA results for the spectra of 30 glasses (10 replicates) with nominally similar RIs (same RI set 2), autoscaled..... page 1063
Table 378 PCA results for the first derivative spectra (5-point smoothing) of 30 glasses (10 replicates) with nominally similar RIs (same RI set 2), autoscaled..... page 1068
Table 379 PCA results for the second derivative spectra (5-point smoothing) of 30 glasses (10 replicates) with nominally similar RIs (same RI set 2), autoscaled..... page 1073
Table 380 Discrimination error rates for HOO-CV with PCA reduced CVA for the spectra of 21 glasses (10 replicates) with nominally similar RIs (same RI set 1), autoscaled..... page 1077
Table 381 Discrimination error rates for HOO-CV with PCA reduced CVA for the first derivative spectra (5-point smoothing) of 21 glasses (10 replicates) with nominally similar RIs (same RI set 1), autoscaled.... page 1079
Table 382 Discrimination error rates for HOO-CV with PCA reduced CVA for the second derivative spectra (5-point smoothing) of 21 glasses (10 replicates) with nominally similar RIs (same RI set 1), autoscaled.... page 1081
Table 383 Discrimination error rates for HOO-CV with PCA reduced CVA for the spectra of 30 glasses (10 replicates) with nominally similar RIs (same RI set 2), autoscaled..... page 1083
Table 384 Discrimination error rates for HOO-CV with PCA reduced CVA for the first derivative spectra (5-point smoothing) of 30 glasses (10 replicates) with nominally similar RIs (same RI set 2), autoscaled.... page 1086
Table 385 Discrimination error rates for HOO-CV with PCA reduced CVA for the second derivative spectra (5-point smoothing) of 30 glasses (10 replicates) with nominally similar RIs (same RI set 2), autoscaled.... page 1089

LIST OF FIGURES

Figure 1	SiO_4 tetrahedral structures in crystalline and glassy silicates…….....	page 9
Figure 2	The glass transformation behavior diagram……..	page 10
Figure 3	The Electromagnetic Spectrum…….	page 20
Figure 4	Six types of molecular vibrations.…….....	page 22
Figure 5	The four molecular vibrations of CO_2.…….	page 24
Figure 6	Schematics of IR spectrometer with Michelson interferometer……..	page 27
Figure 7	Refraction of light into a medium of higher RI.……...	page 29
Figure 8	Refraction of light into a medium of lesser RI.…….....	page 29
Figure 9	Photograph of ten different colored glass fragments.……...	page 40
Figure 10	Schematic illustration of the vibrational motions of oxygen atoms with respect to the bridged silicon atoms.…….	page 87
Figure 11	IlluminatIR™ II, from Smiths Detection.…….	page 108
Figure 12	Schematics of IlluminatIR™……...	page 109
Figure 13	Background Spectrum of the IlluminatIR™.…….....	page 109
Figure 14	IlluminatIR™ interferometer layout.…….....	page 110
Figure 15	The ARO and ATR Objectives.…….....	page 111
Figure 16	IR and Visible Light Path through ARO Objective.…….	page 112
Figure 17	Reflection-Absorption IR Pathway.……..	page 113
Figure 18	Specular Reflection IR Pathway……..	page 113
Figure 19	ReflectIR™ IR reflecting glass slide.……...	page 113
Figure 20	IR and Visible Light Path through ATR Objective.…….	page 114
Figure 21	IR Light Path through IRE…….……...	page 115
Figure 22	ATR Objective Modes.…….	page 116
Figure 23	Photomicrograph of a dry mounted glass sample at 400 times magnification, prior to analysis, and a photomicrograph of the same dry mounted glass sample at 36 times magnification after being shattered and scattered by the diamond ATR objective……...	page 120
Figure 24	Photomicrograph of a glass sample in Nujol at 400 times magnification, prior to analysis.……...	page 121
Figure 25	Photomicrographs of a glass sample in Nujol at 360 times magnification using the diamond ATR objective, varied by increasing the contact pressure: after initial contact, after some contact, and after being crushed but not scattered. Below each photomicrograph are their resulting mid-IR spectra…….	page 122
Figure 26	The mid-IR spectra of Figure 25……..	page 122
Figure 27	Photomicrograph of a glass sample in Nujol at 400 times magnification, prior to analysis.……...	page 123

Figure 28	Photomicrographs of a glass sample in Nujol at 360 times magnification using the diamond ATR objective, varied by increasing the contact pressure: after initial contact and after being crushed but not scattered. Below each photomicrograph are their resulting mid-IR spectra.....	page 123
Figure 29	The mid-IR spectra of Figure 28 a-b overlaid.....	page 124
Figure 30	Graph of the RMS noise vs. spectral resolution for the 50-µm aperture.....	page 148
Figure 31	Graph of the RMS noise vs. the number of co-added scans for the 50-µm aperture.....	page 148
Figure 32	Graph of the RMS noise vs. the square root of the number of co-added scans for the 50-µm aperture.....	page 149
Figure 33	Graph of the S/N vs. spectral resolution for the 50-µm aperture.....	page 150
Figure 34	Graph of the S/N vs. the number of co-added scans for the 50-µm aperture.....	page 150
Figure 35	Graph of the S/N vs. the square root of the number of co-added scans for the 50-µm aperture.....	page 150
Figure 36	Graph of the RMS noise vs. spectral resolution for the 25-µm aperture.....	page 152
Figure 37	Graph of the RMS noise vs. the number of co-added scans for the 25-µm aperture.....	page 152
Figure 38	Graph of the RMS noise vs. the square root of the number of co-added scans for the 25-µm aperture.....	page 153
Figure 39	Graph of the S/N vs. spectral resolution for the 50-µm aperture.....	page 154
Figure 40	Graph of the S/N vs. the number of co-added scans for the 50-µm aperture.....	page 154
Figure 41	Graph of the S/N vs. the square root of the number of co-added scans for the 50-µm aperture.....	page 154
Figure 42	Graph of the RMS noise vs. spectral resolution for the 10-µm aperture.....	page 156
Figure 43	Graph of the RMS noise vs. the number of co-added scans for the 10-µm aperture.....	page 156
Figure 44	Graph of the RMS noise vs. the square root of the number of co-added scans for the 10-µm aperture.....	page 157
Figure 45	Graph of the S/N vs. spectral resolution for the 50-µm aperture.....	page 158
Figure 46	Graph of the S/N vs. the number of co-added scans for the 50-µm aperture.....	page 158
Figure 47	Graph of the S/N vs. the square root of the number of co-added scans for the 50-µm aperture.....	page 158
Figure 48	Graph of the HQI (correlation algorithm) from spectra not used to make the mid-IR library vs. the number that was averaged to make each spectrum in the library for SRM 620.....	page 162

Figure 49 Graph of the HQI (correlation algorithm) from spectra used to make the mid-IR library vs. the number that was averaged to make each spectrum in the library for SRM 620…….. page 163
Figure 50 Graphs of the HQI (first derivative correlation algorithm) from spectra not used to make the mid-IR library vs. the number that was averaged to make each spectrum in the library for SRM 620…….. page 164
Figure 51 Graphs of the HQI (first derivative correlation algorithm) from spectra used to make the mid-IR library vs. the number that was averaged to make each spectrum in the library for SRM 620…….. page 165
Figure 52 Graphs of the HQI (correlation algorithm) from spectra not used to make the mid-IR library vs. the number that was averaged to make each spectrum in the library for SRM 621…….. page 166
Figure 53 Graphs of the HQI (correlation algorithm) from spectra used to make the mid-IR library vs. the number that was averaged to make each spectrum in the library for SRM 621…….. page 167
Figure 54 Graphs of the HQI (first derivative correlation algorithm) from spectra not used to make the mid-IR library vs. the number that was averaged to make each spectrum in the library for SRM 621…….. page 168
Figure 55 Graphs of the HQI (first derivative correlation algorithm) from spectra used to make the mid-IR library vs. the number that was averaged to make each spectrum in the library for SRM 621…….. page 169
Figure 56 Graphs of the HQI (correlation algorithm) from spectra not used to make the mid-IR library vs. the number that was averaged to make each spectrum in the library for SRM 1831……. page 170
Figure 57 Graphs of the HQI (correlation algorithm) from spectra used to make the mid-IR library vs. the number that was averaged to make each spectrum in the library for SRM 1831……. page 171
Figure 58 Graphs of the HQI (first derivative correlation algorithm) from spectra not used to make the mid-IR library vs. the number that was averaged to make each spectrum in the library for SRM 1831…… page 172
Figure 59 Graphs of the HQI (first derivative correlation algorithm) from spectra used to make the mid-IR library vs. the number that was averaged to make each spectrum in the library for SRM 1831…… page 173
Figure 60 Graph of the HQI (correlation algorithm) from spectra not used to make the mid-IR library vs. the number that was averaged to make each spectrum in the library for SRM 620, 621 and 1831 (4 cm^{-1} spectral resolution and 256 co-added scans)…….... page 174
Figure 61 Graph of the HQI (correlation algorithm) from spectra used to make the mid-IR library vs. the number that was averaged to make each spectrum in the library for SRM 620, 621 and 1831 (4 cm^{-1} spectral resolution and 256 co-added scans)……. page 174

Figure 62 Graph of the HQI (first derivative correlation algorithm) from spectra not used to make the mid-IR library vs. the number that was averaged to make each spectrum in the library for SRM 620, 621 and 1831 (4 cm^{-1} spectral resolution and 256 co-added scans)…….. page 175

Figure 63 Graph of the HQI (first derivative correlation algorithm) from spectra used to make the mid-IR library vs. the number that was averaged to make each spectrum in the library for SRM 620, 621 and 1831 (4 cm^{-1} spectral resolution and 256 co-added scans)…….. page 175

Figure 64 Graphs of the HQI (correlation algorithm) from spectra not used to make the mid-IR library vs. the number that was averaged to make each spectrum in the library for a 'real world' window…….. page 176

Figure 65 Graphs of the HQI (correlation algorithm) from spectra used to make the mid-IR library vs. the number that was averaged to make each spectrum in the library for a 'real world' window…….. page 177

Figure 66 Graphs of the HQI (first derivative correlation algorithm) from spectra not used to make the mid-IR library vs. the number that was averaged to make each spectrum in the library for a 'real world' window……..…….. page 178

Figure 67 Graphs of the HQI (first derivative correlation algorithm) from spectra used to make the mid-IR library vs. the number that was averaged to make each spectrum in the library for a 'real world' window……..…….. page 179

Figure 68 Results of deconvolution of automotive window glass W10 when using the reference literature values…… page 181

Figure 69 Results of deconvolution of container glass C50 when using the reference literature values……..……. page 182

Figure 70 Results of deconvolution of automotive window glass W10 when using the combined approach to identify the silicate peaks……. page 187

Figure 71 Results of deconvolution of architectural window glass W52 when using the combined approach to identify the silicate peaks……. page 188

Figure 72 Results of deconvolution of container glass C50 when using the combined approach to identify the silicate peaks…….. page 189

Figure 73 The mid-IR spectra, the first derivate spectra (5- and 9-point smoothing), and the second derivative spectra (5- and 9-point smoothing) of automotive glass W10 (10 replicates)…….. page 203

Figure 74 The mid-IR spectra, the first derivate spectra (5- and 9-point smoothing), and the second derivative spectra (5- and 9-point smoothing) of architectural glass W52 (10 replicates)…….. page 205

Figure 75 The mid-IR spectra, the first derivate spectra (5- and 9-point smoothing), and the second derivative spectra (5- and 9-point smoothing) of container glass W50 (10 replicates)……. page 207

Figure 76 The mid-IR spectra, the first derivate spectra (5- and 9-point smoothing), and the second derivative spectra (5- and 9-point smoothing) of automotive glass W10, architectural glass W52, and container glass C50, all overlaid……. page 209

Figure 77 The mid-IR spectra, the first derivate spectra (5- and 9-point smoothing), and the second derivative spectra (5- and 9-point smoothing) of 10 automotive glass averages, 10 architectural glass averages, and 10 container glass averages, all overlaid……... page 212

Figure 78 Histogram of the hit number for the ATR mid-IR spectral library search results for the 30 glass spectra (5 replicates) using the correlation search algorithm.…… page 214

Figure 79 Histogram of the hit number for the ATR mid-IR spectral library search results for the 30 glass spectra (5 replicates) using the first derivative correlation search algorithm.……... page 215

Figure 80 Histogram of the hit number for the ATR mid-IR spectral library search results for the 30 second derivative glass spectra (5 replicates) using the correlation search algorithm.…….. page 215

Figure 81 Histogram of the hit number for the ATR mid-IR spectral library search results for the 30 second derivative glass spectra (5 replicates) using the first derivative correlation search algorithm…... page 216

Figure 82 Graphic comparisons of the peak positions (center X, in wavenumbers) of Peak 1 from the deconvolution of the 30 glass spectra (10 replicates).……..……... page 218

Figure 83 Graphic comparisons of the peak positions (center X, in wavenumbers) of Peak 2 from the deconvolution of the 30 glass spectra (10 replicates).……..……... page 218

Figure 84 Graphic comparisons of the peak positions (center X, in wavenumbers) of Peak 3 from the deconvolution of the 30 glass spectra (10 replicates).……..……... page 219

Figure 85 Graphic comparisons of the peak positions (center X, in wavenumbers) of Peak 4 from the deconvolution of the 30 glass spectra (10 replicates).……..……... page 219

Figure 86 Graphic comparisons of the peak positions (center X, in wavenumbers) of Peak 5 from the deconvolution of the 30 glass spectra (10 replicates).……..……... page 220

Figure 87 Graphic comparisons of the peak positions (center X, in wavenumbers) of Peak 6 from the deconvolution of the 30 glass spectra (10 replicates).……..……... page 220

Figure 88 Graphic comparisons of the peak areas of Peak 1 from the deconvolution of the 30 glass spectra (10 replicates).……. page 221

Figure 89 Graphic comparisons of the peak areas of Peak 2 from the deconvolution of the 30 glass spectra (10 replicates).……. page 221

Figure 90 Graphic comparisons of the peak areas of Peak 3 from the deconvolution of the 30 glass spectra (10 replicates).……. page 222

Figure 91	Graphic comparisons of the peak areas of Peak 4 from the deconvolution of the 30 glass spectra (10 replicates)..……	page 222
Figure 92	Graphic comparisons of the peak areas of Peak 5 from the deconvolution of the 30 glass spectra (10 replicates).…….	page 223
Figure 93	Graphic comparisons of the peak areas of Peak 6 from the deconvolution of the 30 glass spectra (10 replicates).…….	page 223
Figure 94	Graph of the discrimination error rate versus PC dimensions for HOO-CV with PCA reduced CVA for the set of 153 glass first derivative (5-point smoothing) spectra (10 replicates), autoscaled data..……..……..……..……...	page 293
Figure 95	Graph of the discrimination error rate versus PC dimensions for HOO-CV with PCA reduced CVA for the set of 103 window glass first derivative (5-point smoothing) spectra (10 replicates), autoscaled data……..……...……..……..	page 294
Figure 96	Graph of the discrimination error rate versus PC dimensions for HOO-CV with PCA reduced CVA for the set of 50 container glass first derivative (5-point smoothing) spectra (10 replicates), autoscaled data.……..……...……..…….	page 295
Figure 97	Graph of the classification (window or container) error rate versus PC dimensions for HOO-CV with PCA reduced CVA for the set of 103 container glass first derivative (9-point smoothing) spectra (10 replicates), autoscaled data.……..…….....	page 296
Figure 98	Graph of the classification (window or container) error rate versus PC dimensions for HOO-CV with PCA reduced CVA for the set of 103 container glass second derivative (9-point smoothing) spectra (10 replicates), autoscaled data.……..…….....	page 297
Figure 99	Graph of the classification (tempered or non-tempered) error rate versus PC dimensions for HOO-CV with PCA reduced CVA for the set of 103 container glass second derivative (9-point smoothing) spectra (10 replicates), autoscaled data……..……..	page 298
Figure 100	Photomicrograph of a glass sample in silicone oil II at 400 times magnification, prior to analysis.……..…….....	page 318
Figure 101	Photomicrographs of a glass sample in silicone oil II at 360 times magnification using the diamond ATR objective, varied by increasing the contact pressure: after initial contact and after being crushed but not scattered. Below each photomicrograph are their resulting mid-IR spectra.……..…….....	page 318
Figure 102	The mid-IR spectra of Figures 101 d-f overlaid.……..…….....	page 319
Figure 103	The mid-IR spectrum, from 1300-650 cm^{-1}, of the glass sample crushed in silicone oil.……..…….....	page 319
Figure 104	Depth of penetration variation as a function of the angle of incidence, from 0 - 100° and from 39 to 61°.……..……	page 328
Figure 105	Depth of penetration variation as a function of the (a) wavenumber and (b) wavelength of the incident IR radiation.……..	page 332

Figure 106 Mid-IR Spectra of Beryl..... page 546
Figure 107 Mid-IR Spectra of Beryl..... page 546
Figure 108 Mid-IR Spectra of Cristobalite..... page 547
Figure 109 Mid-IR Spectra of Enstatite..... page 547
Figure 110 Mid-IR Spectra of Enstatite..... page 548
Figure 111 Mid-IR Spectra of Forsterite..... page 548
Figure 112 Mid-IR Spectra of Montmorillonite..... page 549
Figure 113 Mid-IR Spectra of Montmorillonite..... page 549
Figure 114 Mid-IR Spectra of Orthoclase..... page 550
Figure 115 Mid-IR Spectra of Orthoclase..... page 550
Figure 116 Mid-IR Spectra of Phenakite..... page 551
Figure 117 Mid-IR Spectra of Quartz..... page 551
Figure 118 Mid-IR Spectra of Quartz..... page 552
Figure 119 Mid-IR Spectra of Sillimanite..... page 552
Figure 120 Mid-IR Spectra of Sillimanite..... page 553
Figure 121 Mid-IR Spectra of Sodic Plagioclase - Albite..... page 553
Figure 122 Mid-IR Spectra of Sodic Plagioclase - Albite..... page 554
Figure 123 Mid-IR Spectra of Spodumene..... page 554
Figure 124 Mid-IR Spectra of Talc..... page 555
Figure 125 Mid-IR Spectra of Talc..... page 555
Figure 126 Mid-IR Spectra of Tremolite..... page 556
Figure 127 Mid-IR Spectra of Tremolite..... page 556
Figure 128 Mid-IR Spectra of Willemite..... page 557
Figure 129 Mid-IR Spectra of Wollastonite..... page 557
Figure 130 Mid-IR Spectra of Wollastonite..... page 558
Figure 131 Mid-IR Spectra of Xonotlite..... page 558
Figure 132 PCA scree plot for the first set of 30 glass spectra (10 replicates), no data pretreatment..... page 590
Figure 133 PCA scree plot for the first set of 30 glass spectra (10 replicates), centered..... page 592
Figure 134 PCA scree plot for the first set of 30 glass spectra (10 replicates), autoscaled..... page 594
Figure 135 PCA scree plot for the first set of 20 window glass spectra (10 replicates), no data pretreatment..... page 596
Figure 136 PCA scree plot for the first set of 20 window glass spectra (10 replicates), centered..... page 598
Figure 137 PCA scree plot for the first set of 20 window glass spectra (10 replicates), autoscaled..... page 600
Figure 138 PCA scree plot for the first set of 10 container glass spectra (10 replicates), no data pretreatment..... page 602
Figure 139 PCA scree plot for the first set of 10 container glass spectra (10 replicates), centered..... page 604

Figure 140 PCA scree plot for the first set of 10 container glass spectra (10 replicates), autoscaled..... page 606
Figure 141 PCA scree plot for the first set of 30 normalized (peak area) glass spectra (10 replicates), no data pretreatment..... page 608
Figure 142 PCA scree plot for the first set of 30 normalized (peak area) glass spectra (10 replicates), centered..... page 610
Figure 143 PCA scree plot for the first set of 30 normalized (peak area) glass spectra (10 replicates), autoscaled..... page 612
Figure 144 PCA scree plot for the first set of 20 normalized (peak area) window glass spectra (10 replicates), no data pretreatment..... page 614
Figure 145 PCA scree plot for the first set of 20 normalized (peak area) window glass spectra (10 replicates), centered..... page 616
Figure 146 PCA scree plot for the first set of 20 normalized (peak area) window glass spectra (10 replicates), autoscaled..... page 618
Figure 147 PCA scree plot for the first set of 10 normalized (peak area) container glass spectra (10 replicates), no data pretreatment..... page 620
Figure 148 PCA scree plot for the first set of 10 normalized (peak area) container glass spectra (10 replicates), centered..... page 622
Figure 149 PCA scree plot for the first set of 10 normalized (peak area) container glass spectra (10 replicates), autoscaled..... page 624
Figure 150 PCA scree plot for the first set of 30 normalized (peak height) glass spectra (10 replicates), no data pretreatment..... page 626
Figure 151 PCA scree plot for the first set of 30 normalized (peak height) glass spectra (10 replicates), centered..... page 628
Figure 152 PCA scree plot for the first set of 30 normalized (peak height) glass spectra (10 replicates), autoscaled..... page 630
Figure 153 PCA scree plot for the first set of 20 normalized (peak height) window glass spectra (10 replicates), no data pretreatment..... page 632
Figure 154 PCA scree plot for the first set of 20 normalized (peak height) window glass spectra (10 replicates), centered..... page 634
Figure 155 PCA scree plot for the first set of 20 normalized (peak height) window glass spectra (10 replicates), autoscaled..... page 636
Figure 156 PCA scree plot for the first set of 10 normalized (peak height) container glass spectra (10 replicates), no data pretreatment..... page 638
Figure 157 PCA scree plot for the first set of 10 normalized (peak height) container glass spectra (10 replicates), centered..... page 640
Figure 158 PCA scree plot for the first set of 10 normalized (peak height) container glass spectra (10 replicates), autoscaled..... page 642
Figure 159 PCA scree plot for the first set of 30 glass first derivative (5-point smoothing) spectra (10 replicates), no data pretreatment..... page 644
Figure 160 PCA scree plot for the first set of 30 glass first derivative (5-point smoothing) spectra (10 replicates), centered..... page 646

Figure 161 PCA scree plot for the first set of 30 glass first derivative (5-point smoothing) spectra (10 replicates), autoscaled.…..……. page 648
Figure 162 PCA scree plot for the first set of 20 window glass first derivative (5-point smoothing) spectra (10 replicates), no data pretreatment….. page 650
Figure 163 PCA scree plot for the first set of 20 window glass first derivative (5-point smoothing) spectra (10 replicates), centered.…..……... page 652
Figure 164 PCA scree plot for the first set of 20 window glass first derivative (5-point smoothing) spectra (10 replicates), autoscaled.…..……... page 654
Figure 165 PCA scree plot for the first set of 10 container glass first derivative (5-point smoothing) spectra (10 replicates), no data pretreatment….. page 656
Figure 166 PCA scree plot for the first set of 10 container glass first derivative (5-point smoothing) spectra (10 replicates), centered…….. page 658
Figure 167 PCA scree plot for the first set of 10 container glass first derivative (5-point smoothing) spectra (10 replicates), autoscaled…….. page 660
Figure 168 PCA scree plot for the first set of 30 glass first derivative (9-point smoothing) spectra (10 replicates), no data pretreatment…… page 662
Figure 169 PCA scree plot for the first set of 30 glass first derivative (9-point smoothing) spectra (10 replicates), centered.…..……..... page 664
Figure 170 PCA scree plot for the first set of 30 glass first derivative (9-point smoothing) spectra (10 replicates), autoscaled.…..……. page 666
Figure 171 PCA scree plot for the first set of 20 window glass first derivative (9-point smoothing) spectra (10 replicates), no data pretreatment….. page 668
Figure 172 PCA scree plot for the first set of 20 window glass first derivative (9-point smoothing) spectra (10 replicates), centered…….. page 670
Figure 173 PCA scree plot for the first set of 20 window glass first derivative (9-point smoothing) spectra (10 replicates), autoscaled.…..……... page 672
Figure 174 PCA scree plot for the first set of 10 container glass first derivative (9-point smoothing) spectra (10 replicates), no data pretreatment….. page 674
Figure 175 PCA scree plot for the first set of 10 container glass first derivative (9-point smoothing) spectra (10 replicates), centered.…..……... page 676
Figure 176 PCA scree plot for the first set of 10 container glass first derivative (9-point smoothing) spectra (10 replicates), autoscaled…….. page 678
Figure 177 PCA scree plot for the first set of 30 glass second derivative (5-point smoothing) spectra (10 replicates), no data pretreatment…… page 680
Figure 178 PCA scree plot for the first set of 30 glass second derivative (5-point smoothing) spectra (10 replicates), centered…… page 682
Figure 179 PCA scree plot for the first set of 30 glass second derivative (5-point smoothing) spectra (10 replicates), autoscaled.…..……. page 684
Figure 180 PCA scree plot for the first set of 20 window glass second derivative (5-point smoothing) spectra (10 replicates), no data pretreatment….. page 686
Figure 181 PCA scree plot for the first set of 20 window glass second derivative (5-point smoothing) spectra (10 replicates), centered.…..……... page 688

Figure 182 PCA scree plot for the first set of 20 window glass second derivative (5-point smoothing) spectra (10 replicates), autoscaled…….. page 690
Figure 183 PCA scree plot for the first set of 10 container glass second derivative (5-point smoothing) spectra (10 replicates), no data pretreatment…..……..…..……... page 692
Figure 184 PCA scree plot for the first set of 10 container glass second derivative (5-point smoothing) spectra (10 replicates), centered……. page 694
Figure 185 PCA scree plot for the first set of 10 container glass second derivative (5-point smoothing) spectra (10 replicates), autoscaled…. page 696
Figure 186 PCA scree plot for the first set of 30 glass second derivative (9-point smoothing) spectra (10 replicates), no data pretreatment…… page 698
Figure 187 PCA scree plot for the first set of 30 glass second derivative (9-point smoothing) spectra (10 replicates), centered…… page 700
Figure 188 PCA scree plot for the first set of 30 glass second derivative (9-point smoothing) spectra (10 replicates), autoscaled…… page 702
Figure 189 PCA scree plot for the first set of 20 window glass second derivative (9-point smoothing) spectra (10 replicates), no data pretreatment….. page 704
Figure 190 PCA scree plot for the first set of 20 window glass second derivative (9-point smoothing) spectra (10 replicates), centered…….. page 706
Figure 191 PCA scree plot for the first set of 20 window glass second derivative (9-point smoothing) spectra (10 replicates), autoscaled…….. page 708
Figure 192 PCA scree plot for the first set of 10 container glass second derivative (9-point smoothing) spectra (10 replicates), no data pretreatment…..……..... page 710
Figure 193 PCA scree plot for the first set of 10 container glass second derivative (9-point smoothing) spectra (10 replicates), centered……. page 712
Figure 194 PCA scree plot for the first set of 10 container glass second derivative (9-point smoothing) spectra (10 replicates), autoscaled…. page 714
Figure 195 Graph of the discrimination error rate versus PC dimensions for HOO-CV with PCA reduced CVA for the first set of 30 glass spectra (10 replicates), no data pretreatment……..... page 716
Figure 196 Graph of the discrimination error rate versus PC dimensions for HOO-CV with PCA reduced CVA for the first set of 30 glass spectra (10 replicates), centered data…..……..... page 718
Figure 197 Graph of the discrimination error rate versus PC dimensions for HOO-CV with PCA reduced CVA for the first set of 30 glass spectra (10 replicates), autoscaled data…..……..... page 721
Figure 198 Graph of the classification (automotive, architectural or container) error rate versus PC dimensions for HOO-CV with PCA reduced CVA for the first set of 30 glass spectra (10 replicates), no data pretreatment…..……..... page 723

Figure 199 Graph of the classification (automotive, architectural or container) error rate versus PC dimensions for HOO-CV with PCA reduced CVA for the first set of 30 glass spectra (10 replicates), centered data……... page 725
Figure 200 Graph of the classification (automotive, architectural or container) error rate versus PC dimensions for HOO-CV with PCA reduced CVA for the first set of 30 glass spectra (10 replicates), autoscaled data……... page 728
Figure 201 Graph of the classification (window or container) error rate versus PC dimensions for HOO-CV with PCA reduced CVA for the first set of 30 glass spectra (10 replicates), no data pretreatment…… page 730
Figure 202 Graph of the classification (window or container) error rate versus PC dimensions for HOO-CV with PCA reduced CVA for the first set of 30 glass spectra (10 replicates), centered data……... page 732
Figure 203 Graph of the classification (window or container) error rate versus PC dimensions for HOO-CV with PCA reduced CVA for the first set of 30 glass spectra (10 replicates), autoscaled data…… page 735
Figure 204 Graph of the discrimination error rate versus PC dimensions for HOO-CV with PCA reduced CVA for the first set of 20 window glass spectra (10 replicates), no data pretreatment…….. page 737
Figure 205 Graph of the discrimination error rate versus PC dimensions for HOO-CV with PCA reduced CVA for the first set of 20 window glass spectra (10 replicates), centered data…….. page 739
Figure 206 Graph of the discrimination error rate versus PC dimensions for HOO-CV with PCA reduced CVA for the first set of 20 window glass spectra (10 replicates), autoscaled data……... page 741
Figure 207 Graph of the discrimination error rate versus PC dimensions for HOO-CV with PCA reduced CVA for the first set of 10 container glass spectra (10 replicates), no data pretreatment……... page 743
Figure 208 Graph of the discrimination error rate versus PC dimensions for HOO-CV with PCA reduced CVA for the first set of 10 container glass spectra (10 replicates), centered data…….. page 745
Figure 209 Graph of the discrimination error rate versus PC dimensions for HOO-CV with PCA reduced CVA for the first set of 10 container glass spectra (10 replicates), autoscaled data……... page 747
Figure 210 Graph of the float classification error rate versus PC dimensions for HOO-CV with PCA reduced CVA for the first set of 20 window glass spectra (10 replicates), no data pretreatment……... page 749
Figure 211 Graph of the float classification error rate versus PC dimensions for HOO-CV with PCA reduced CVA for the first set of 20 window glass spectra (10 replicates), centered data…….. page 751

Figure 212 Graph of the float classification error rate versus PC dimensions for HOO-CV with PCA reduced CVA for the first set of 20 window glass spectra (10 replicates), autoscaled data…….. page 753
Figure 213 Graph of the tempered classification error rate versus PC dimensions for HOO-CV with PCA reduced CVA for the first set of 20 window glass spectra (10 replicates), no data pretreatment…… page 755
Figure 214 Graph of the tempered classification error rate versus PC dimensions for HOO-CV with PCA reduced CVA for the first set of 20 window glass spectra (10 replicates), centered data…….. page 757
Figure 215 Graph of the tempered classification error rate versus PC dimensions for HOO-CV with PCA reduced CVA for the first set of 20 window glass spectra (10 replicates), autoscaled data…… page 759
Figure 216 Graph of the discrimination error rate versus PC dimensions for HOO-CV with PCA reduced CVA for the first set of 30 normalized (peak area) glass spectra (10 replicates), no data pretreatment…… page 760
Figure 217 Graph of the discrimination error rate versus PC dimensions for HOO-CV with PCA reduced CVA for the first set of 30 normalized (peak area) glass spectra (10 replicates), centered data…….. page 761
Figure 218 Graph of the discrimination error rate versus PC dimensions for HOO-CV with PCA reduced CVA for the first set of 30 normalized (peak area) glass spectra (10 replicates), autoscaled data…… page 764
Figure 219 Graph of the classification (automotive, architectural or container) error rate versus PC dimensions for HOO-CV with PCA reduced CVA for the first set of 30 normalized (peak area) glass spectra (10 replicates), no data pretreatment…….. page 765
Figure 220 Graph of the classification (automotive, architectural or container) error rate versus PC dimensions for HOO-CV with PCA reduced CVA for the first set of 30 normalized (peak area) glass spectra (10 replicates), centered data…..……..... page 766
Figure 221 Graph of the classification (automotive, architectural or container) error rate versus PC dimensions for HOO-CV with PCA reduced CVA for the first set of 30 normalized (peak area) glass spectra (10 replicates), autoscaled data…..……..... page 769
Figure 222 Graph of the classification (window or container) error rate versus PC dimensions for HOO-CV with PCA reduced CVA for the first set of 30 normalized (peak area) glass spectra (10 replicates), no data pretreatment…..……..... page 770
Figure 223 Graph of the classification (window or container) error rate versus PC dimensions for HOO-CV with PCA reduced CVA for the first set of 30 normalized (peak area) glass spectra (10 replicates), centered data…..……..... page 771

Figure 224 Graph of the classification (window or container) error rate versus PC dimensions for HOO-CV with PCA reduced CVA for the first set of 30 normalized (peak area) glass spectra (10 replicates), autoscaled data…..……..... page 774
Figure 225 Graph of the discrimination error rate versus PC dimensions for HOO-CV with PCA reduced CVA for the first set of 20 window normalized (peak area) glass spectra (10 replicates), no data pretreatment…..……..... page 775
Figure 226 Graph of the discrimination error rate versus PC dimensions for HOO-CV with PCA reduced CVA for the first set of 20 window normalized (peak area) glass spectra (10 replicates), centered data… page 776
Figure 227 Graph of the discrimination error rate versus PC dimensions for HOO-CV with PCA reduced CVA for the first set of 20 window normalized (peak area) glass spectra (10 replicates), autoscaled data……..... page 778
Figure 228 Graph of the discrimination error rate versus PC dimensions for HOO-CV with PCA reduced CVA for the first set of 10 container normalized (peak area) glass spectra (10 replicates), no data pretreatment……..... page 779
Figure 229 Graph of the discrimination error rate versus PC dimensions for HOO-CV with PCA reduced CVA for the first set of 10 container normalized (peak area) glass spectra (10 replicates), centered data… page 780
Figure 230 Graph of the discrimination error rate versus PC dimensions for HOO-CV with PCA reduced CVA for the first set of 10 container normalized (peak area) glass spectra (10 replicates), autoscaled data……... page 782
Figure 231 Graph of the float classification error rate versus PC dimensions for HOO-CV with PCA reduced CVA for the first set of 20 window normalized (peak area) glass spectra (10 replicates), no data pretreatment……. page 783
Figure 232 Graph of the float classification error rate versus PC dimensions for HOO-CV with PCA reduced CVA for the first set of 20 window normalized (peak area) glass spectra (10 replicates), centered data… page 784
Figure 233 Graph of the float classification error rate versus PC dimensions for HOO-CV with PCA reduced CVA for the first set of 20 window normalized (peak area) glass spectra (10 replicates), autoscaled data……..... page 786
Figure 234 Graph of the tempered classification error rate versus PC dimensions for HOO-CV with PCA reduced CVA for the first set of 20 window normalized (peak area) glass spectra (10 replicates), no data pretreatment…….. page 787
Figure 235 Graph of the tempered classification error rate versus PC dimensions for HOO-CV with PCA reduced CVA for the first set of 20 window normalized (peak area) glass spectra (10 replicates), centered data……..... page 788

Figure 236 Graph of the tempered classification error rate versus PC dimensions for HOO-CV with PCA reduced CVA for the first set of 20 window normalized (peak area) glass spectra (10 replicates), autoscaled data…..……..... page 790
Figure 237 Graph of the discrimination error rate versus PC dimensions for HOO-CV with PCA reduced CVA for the first set of 30 normalized (peak height) glass spectra (10 replicates), no data pretreatment…… page 792
Figure 238 Graph of the discrimination error rate versus PC dimensions for HOO-CV with PCA reduced CVA for the first set of 30 normalized (peak height) glass spectra (10 replicates), centered data…… page 794
Figure 239 Graph of the discrimination error rate versus PC dimensions for HOO-CV with PCA reduced CVA for the first set of 30 normalized (peak height) glass spectra (10 replicates), autoscaled data……. page 797
Figure 240 Graph of the classification (automotive, architectural or container) error rate versus PC dimensions for HOO-CV with PCA reduced CVA for the first set of 30 normalized (peak height) glass spectra (10 replicates), no data pretreatment…..……..... page 799
Figure 241 Graph of the classification (automotive, architectural or container) error rate versus PC dimensions for HOO-CV with PCA reduced CVA for the first set of 30 normalized (peak height) glass spectra (10 replicates), centered data…..……..... page 801
Figure 242 Graph of the classification (automotive, architectural or container) error rate versus PC dimensions for HOO-CV with PCA reduced CVA for the first set of 30 normalized (peak height) glass spectra (10 replicates), autoscaled data…..……..... page 804
Figure 243 Graph of the classification (window or container) error rate versus PC dimensions for HOO-CV with PCA reduced CVA for the first set of 30 normalized (peak height) glass spectra (10 replicates), no data pretreatment…..……..... page 806
Figure 244 Graph of the classification (window or container) error rate versus PC dimensions for HOO-CV with PCA reduced CVA for the first set of 30 normalized (peak height) glass spectra (10 replicates), centered data…..……..... page 808
Figure 245 Graph of the classification (window or container) error rate versus PC dimensions for HOO-CV with PCA reduced CVA for the first set of 30 normalized (peak height) glass spectra (10 replicates), autoscaled data…..……..... page 811
Figure 246 Graph of the discrimination error rate versus PC dimensions for HOO-CV with PCA reduced CVA for the first set of 20 window normalized (peak height) glass spectra (10 replicates), no data pretreatment…..……..... page 813

Figure 247 Graph of the discrimination error rate versus PC dimensions for HOO-CV with PCA reduced CVA for the first set of 20 window normalized (peak height) glass spectra (10 replicates), centered data……..... page 815
Figure 248 Graph of the discrimination error rate versus PC dimensions for HOO-CV with PCA reduced CVA for the first set of 20 window normalized (peak height) glass spectra (10 replicates), autoscaled data……..... page 817
Figure 249 Graph of the discrimination error rate versus PC dimensions for HOO-CV with PCA reduced CVA for the first set of 10 container normalized (peak height) glass spectra (10 replicates), no data pretreatment……..... page 819
Figure 250 Graph of the discrimination error rate versus PC dimensions for HOO-CV with PCA reduced CVA for the first set of 10 container normalized (peak height) glass spectra (10 replicates), centered data……..... page 821
Figure 251 Graph of the discrimination error rate versus PC dimensions for HOO-CV with PCA reduced CVA for the first set of 10 container normalized (peak height) glass spectra (10 replicates), autoscaled data……..... page 823
Figure 252 Graph of the float classification error rate versus PC dimensions for HOO-CV with PCA reduced CVA for the first set of 20 window normalized (peak height) glass spectra (10 replicates), no data pretreatment……..... page 825
Figure 253 Graph of the float classification error rate versus PC dimensions for HOO-CV with PCA reduced CVA for the first set of 20 window normalized (peak height) glass spectra (10 replicates), centered data……..... page 827
Figure 254 Graph of the float classification error rate versus PC dimensions for HOO-CV with PCA reduced CVA for the first set of 20 window normalized (peak height) glass spectra (10 replicates), autoscaled data……..... page 829
Figure 255 Graph of the tempered classification error rate versus PC dimensions for HOO-CV with PCA reduced CVA for the first set of 20 window normalized (peak height) glass spectra (10 replicates), no data pretreatment……..... page 831
Figure 256 Graph of the tempered classification error rate versus PC dimensions for HOO-CV with PCA reduced CVA for the first set of 20 window normalized (peak height) glass spectra (10 replicates), centered data……..... page 833
Figure 257 Graph of the tempered classification error rate versus PC dimensions for HOO-CV with PCA reduced CVA for the first set of 20 window normalized (peak height) glass spectra (10 replicates), autoscaled data……..... page 835

Figure 258 Graph of the discrimination error rate versus PC dimensions for HOO-CV with PCA reduced CVA for the first set of 30 glass first derivative (5-point smoothing) spectra (10 replicates), no data pretreatment……..... page 837
Figure 259 Graph of the discrimination error rate versus PC dimensions for HOO-CV with PCA reduced CVA for the first set of 30 glass first derivative (5-point smoothing) spectra (10 replicates), centered data..……..... page 839
Figure 260 Graph of the discrimination error rate versus PC dimensions for HOO-CV with PCA reduced CVA for the first set of 30 glass first derivative (5-point smoothing) spectra (10 replicates), autoscaled data.……..... page 842
Figure 261 Graph of the classification (automotive, architectural or container) error rate versus PC dimensions for HOO-CV with PCA reduced CVA for the first set of 30 glass first derivative (5-point smoothing) spectra (10 replicates), no data pretreatment..…….. page 844
Figure 262 Graph of the classification (automotive, architectural or container) error rate versus PC dimensions for HOO-CV with PCA reduced CVA for the first set of 30 glass first derivative (5-point smoothing) spectra (10 replicates), centered data.…….. page 846
Figure 263 Graph of the classification (automotive, architectural or container) error rate versus PC dimensions for HOO-CV with PCA reduced CVA for the first set of 30 glass first derivative (5-point smoothing) spectra (10 replicates), autoscaled data.……... page 849
Figure 264 Graph of the classification (window or container) error rate versus PC dimensions for HOO-CV with PCA reduced CVA for the first set of 30 glass first derivative (5-point smoothing) spectra (10 replicates), no data pretreatment.……..... page 851
Figure 265 Graph of the classification (window or container) error rate versus PC dimensions for HOO-CV with PCA reduced CVA for the first set of 30 glass first derivative (5-point smoothing) spectra (10 replicates), centered data.……..... page 853
Figure 266 Graph of the classification (window or container) error rate versus PC dimensions for HOO-CV with PCA reduced CVA for the first set of 30 glass first derivative (5-point smoothing) spectra (10 replicates), autoscaled data.……..... page 856
Figure 267 Graph of the discrimination error rate versus PC dimensions for HOO-CV with PCA reduced CVA for the first set of 20 window glass first derivative (5-point smoothing) spectra (10 replicates), no data pretreatment.……..... page 858
Figure 268 Graph of the discrimination error rate versus PC dimensions for HOO-CV with PCA reduced CVA for the first set of 20 window glass first derivative (5-point smoothing) spectra (10 replicates), centered data.……..... page 860

Figure 269 Graph of the discrimination error rate versus PC dimensions for HOO-CV with PCA reduced CVA for the first set of 20 window glass first derivative (5-point smoothing) spectra (10 replicates), autoscaled data……..... page 862
Figure 270 Graph of the discrimination error rate versus PC dimensions for HOO-CV with PCA reduced CVA for the first set of 10 container glass first derivative (5-point smoothing) spectra (10 replicates), no data pretreatment……..... page 864
Figure 271 Graph of the discrimination error rate versus PC dimensions for HOO-CV with PCA reduced CVA for the first set of 10 container glass first derivative (5-point smoothing) spectra (10 replicates), centered data……..... page 866
Figure 272 Graph of the discrimination error rate versus PC dimensions for HOO-CV with PCA reduced CVA for the first set of 10 container glass first derivative (5-point smoothing) spectra (10 replicates), autoscaled data……..... page 868
Figure 273 Graph of the float classification error rate versus PC dimensions for HOO-CV with PCA reduced CVA for the first set of 20 window glass first derivative (5-point smoothing) spectra (10 replicates), no data pretreatment……..... page 870
Figure 274 Graph of the float classification error rate versus PC dimensions for HOO-CV with PCA reduced CVA for the first set of 20 window glass first derivative (5-point smoothing) spectra (10 replicates), centered data……..... page 872
Figure 275 Graph of the float classification error rate versus PC dimensions for HOO-CV with PCA reduced CVA for the first set of 20 window glass first derivative (5-point smoothing) spectra (10 replicates), autoscaled data……..... page 874
Figure 276 Graph of the tempered classification error rate versus PC dimensions for HOO-CV with PCA reduced CVA for the first set of 20 window glass first derivative (5-point smoothing) spectra (10 replicates), no data pretreatment……..... page 876
Figure 277 Graph of the tempered classification error rate versus PC dimensions for HOO-CV with PCA reduced CVA for the first set of 20 window glass first derivative (5-point smoothing) spectra (10 replicates), centered data……..... page 878
Figure 278 Graph of the tempered classification error rate versus PC dimensions for HOO-CV with PCA reduced CVA for the first set of 20 window glass first derivative (5-point smoothing) spectra (10 replicates), autoscaled data……..... page 880
Figure 279 Graph of the discrimination error rate versus PC dimensions for HOO-CV with PCA reduced CVA for the first set of 30 glass first derivative (9-point smoothing) spectra (10 replicates), no data pretreatment……..... page 882

Figure 280 Graph of the discrimination error rate versus PC dimensions for HOO-CV with PCA reduced CVA for the first set of 30 glass first derivative (9-point smoothing) spectra (10 replicates), centered data..……..... page 883
Figure 281 Graph of the discrimination error rate versus PC dimensions for HOO-CV with PCA reduced CVA for the first set of 30 glass first derivative (9-point smoothing) spectra (10 replicates), autoscaled data.……..... page 886
Figure 282 Graph of the classification (automotive, architectural or container) error rate versus PC dimensions for HOO-CV with PCA reduced CVA for the first set of 30 glass first derivative (9-point smoothing) spectra (10 replicates), no data pretreatment.…… page 888
Figure 283 Graph of the classification (automotive, architectural or container) error rate versus PC dimensions for HOO-CV with PCA reduced CVA for the first set of 30 glass first derivative (9-point smoothing) spectra (10 replicates), centered data..…….. page 889
Figure 284 Graph of the classification (automotive, architectural or container) error rate versus PC dimensions for HOO-CV with PCA reduced CVA for the first set of 30 glass first derivative (9-point smoothing) spectra (10 replicates), autoscaled data.……... page 892
Figure 285 Graph of the classification (window or container) error rate versus PC dimensions for HOO-CV with PCA reduced CVA for the first set of 30 glass first derivative (9-point smoothing) spectra (10 replicates), no data pretreatment.……..... page 894
Figure 286 Graph of the classification (window or container) error rate versus PC dimensions for HOO-CV with PCA reduced CVA for the first set of 30 glass first derivative (9-point smoothing) spectra (10 replicates), centered data.……..... page 896
Figure 287 Graph of the classification (window or container) error rate versus PC dimensions for HOO-CV with PCA reduced CVA for the first set of 30 glass first derivative (9-point smoothing) spectra (10 replicates), autoscaled data.……..... page 898
Figure 288 Graph of the discrimination error rate versus PC dimensions for HOO-CV with PCA reduced CVA for the first set of 20 window glass first derivative (9-point smoothing) spectra (10 replicates), no data pretreatment.……..... page 900
Figure 289 Graph of the discrimination error rate versus PC dimensions for HOO-CV with PCA reduced CVA for the first set of 20 window glass first derivative (9-point smoothing) spectra (10 replicates), centered data.……..... page 901
Figure 290 Graph of the discrimination error rate versus PC dimensions for HOO-CV with PCA reduced CVA for the first set of 20 window glass first derivative (9-point smoothing) spectra (10 replicates), autoscaled data.……..... page 903

Figure 291 Graph of the discrimination error rate versus PC dimensions for HOO-CV with PCA reduced CVA for the first set of 10 container glass first derivative (9-point smoothing) spectra (10 replicates), no data pretreatment.……..…….... page 905

Figure 292 Graph of the discrimination error rate versus PC dimensions for HOO-CV with PCA reduced CVA for the first set of 10 container glass first derivative (9-point smoothing) spectra (10 replicates), centered data.……..…….. page 906

Figure 293 Graph of the discrimination error rate versus PC dimensions for HOO-CV with PCA reduced CVA for the first set of 10 container glass first derivative (9-point smoothing) spectra (10 replicates), autoscaled data.……..……... page 908

Figure 294 Graph of the float classification error rate versus PC dimensions for HOO-CV with PCA reduced CVA for the first set of 20 window glass first derivative (9-point smoothing) spectra (10 replicates), no data pretreatment.……..…… page 910

Figure 295 Graph of the float classification error rate versus PC dimensions for HOO-CV with PCA reduced CVA for the first set of 20 window glass first derivative (9-point smoothing) spectra (10 replicates), centered data.……..…….. page 911

Figure 296 Graph of the float classification error rate versus PC dimensions for HOO-CV with PCA reduced CVA for the first set of 20 window glass first derivative (9-point smoothing) spectra (10 replicates), autoscaled data.……..……... page 913

Figure 297 Graph of the tempered classification error rate versus PC dimensions for HOO-CV with PCA reduced CVA for the first set of 20 window glass first derivative (9-point smoothing) spectra (10 replicates), no data pretreatment.……..…… page 915

Figure 298 Graph of the tempered classification error rate versus PC dimensions for HOO-CV with PCA reduced CVA for the first set of 20 window glass first derivative (9-point smoothing) spectra (10 replicates), centered data.……. page 916

Figure 299 Graph of the tempered classification error rate versus PC dimensions for HOO-CV with PCA reduced CVA for the first set of 20 window glass first derivative (9-point smoothing) spectra (10 replicates), autoscaled data.……. page 918

Figure 300 Graph of the discrimination error rate versus PC dimensions for HOO-CV with PCA reduced CVA for the first set of 30 glass second derivative (5-point smoothing) spectra (10 replicates), no data pretreatment.……..…… page 920

Figure 301 Graph of the discrimination error rate versus PC dimensions for HOO-CV with PCA reduced CVA for the first set of 30 glass second derivative (5-point smoothing) spectra (10 replicates), centered data.……..…….. page 922

Figure 302 Graph of the discrimination error rate versus PC dimensions for HOO-CV with PCA reduced CVA for the first set of 30 glass second derivative (5-point smoothing) spectra (10 replicates), autoscaled data..... page 925
Figure 303 Graph of the classification (automotive, architectural or container) error rate versus PC dimensions for HOO-CV with PCA reduced CVA for the first set of 30 glass second derivative (5-point smoothing) spectra (10 replicates), no data pretreatment..... page 927
Figure 304 Graph of the classification (automotive, architectural or container) error rate versus PC dimensions for HOO-CV with PCA reduced CVA for the first set of 30 glass second derivative (5-point smoothing) spectra (10 replicates), centered data..... page 929
Figure 305 Graph of the classification (automotive, architectural or container) error rate versus PC dimensions for HOO-CV with PCA reduced CVA for the first set of 30 glass second derivative (5-point smoothing) spectra (10 replicates), autoscaled data..... page 932
Figure 306 Graph of the classification (window or container) error rate versus PC dimensions for HOO-CV with PCA reduced CVA for the first set of 30 glass second derivative (5-point smoothing) spectra (10 replicates), no data pretreatment..... page 934
Figure 307 Graph of the classification (window or container) error rate versus PC dimensions for HOO-CV with PCA reduced CVA for the first set of 30 glass second derivative (5-point smoothing) spectra (10 replicates), centered data..... page 936
Figure 308 Graph of the classification (window or container) error rate versus PC dimensions for HOO-CV with PCA reduced CVA for the first set of 30 glass second derivative (5-point smoothing) spectra (10 replicates), autoscaled data..... page 939
Figure 309 Graph of the discrimination error rate versus PC dimensions for HOO-CV with PCA reduced CVA for the first set of 20 window glass second derivative (5-point smoothing) spectra (10 replicates), no data pretreatment..... page 941
Figure 310 Graph of the discrimination error rate versus PC dimensions for HOO-CV with PCA reduced CVA for the first set of 20 window glass second derivative (5-point smoothing) spectra (10 replicates), centered data..... page 943
Figure 311 Graph of the discrimination error rate versus PC dimensions for HOO-CV with PCA reduced CVA for the first set of 20 window glass second derivative (5-point smoothing) spectra (10 replicates), autoscaled data..... page 945
Figure 312 Graph of the discrimination error rate versus PC dimensions for HOO-CV with PCA reduced CVA for the first set of 10 container glass second derivative (5-point smoothing) spectra (10 replicates), no data pretreatment..... page 947

Figure 313 Graph of the discrimination error rate versus PC dimensions for HOO-CV with PCA reduced CVA for the first set of 10 container glass second derivative (5-point smoothing) spectra (10 replicates), centered data..... page 949
Figure 314 Graph of the discrimination error rate versus PC dimensions for HOO-CV with PCA reduced CVA for the first set of 10 container glass second derivative (5-point smoothing) spectra (10 replicates), autoscaled data..... page 951
Figure 315 Graph of the float classification error rate versus PC dimensions for HOO-CV with PCA reduced CVA for the first set of 20 window glass second derivative (5-point smoothing) spectra (10 replicates), no data pretreatment..... page 953
Figure 316 Graph of the float classification error rate versus PC dimensions for HOO-CV with PCA reduced CVA for the first set of 20 window glass second derivative (5-point smoothing) spectra (10 replicates), centered data..... page 955
Figure 317 Graph of the float classification error rate versus PC dimensions for HOO-CV with PCA reduced CVA for the first set of 20 window glass second derivative (5-point smoothing) spectra (10 replicates), autoscaled data..... page 957
Figure 318 Graph of the tempered classification error rate versus PC dimensions for HOO-CV with PCA reduced CVA for the first set of 20 window glass second derivative (5-point smoothing) spectra (10 replicates), no data pretreatment..... page 959
Figure 319 Graph of the tempered classification error rate versus PC dimensions for HOO-CV with PCA reduced CVA for the first set of 20 window glass second derivative (5-point smoothing) spectra (10 replicates), centered data..... page 961
Figure 320 Graph of the tempered classification error rate versus PC dimensions for HOO-CV with PCA reduced CVA for the first set of 20 window glass second derivative (5-point smoothing) spectra (10 replicates), autoscaled data..... page 963
Figure 321 Graph of the discrimination error rate versus PC dimensions for HOO-CV with PCA reduced CVA for the first set of 30 glass second derivative (9-point smoothing) spectra (10 replicates), no data pretreatment..... page 965
Figure 322 Graph of the discrimination error rate versus PC dimensions for HOO-CV with PCA reduced CVA for the first set of 30 glass second derivative (9-point smoothing) spectra (10 replicates), centered data..... page 966
Figure 323 Graph of the discrimination error rate versus PC dimensions for HOO-CV with PCA reduced CVA for the first set of 30 glass second derivative (9-point smoothing) spectra (10 replicates), autoscaled data..... page 969

Figure 324 Graph of the classification (automotive, architectural or container) error rate versus PC dimensions for HOO-CV with PCA reduced CVA for the first set of 30 glass second derivative (9-point smoothing) spectra (10 replicates), no data pretreatment…… page 971

Figure 325 Graph of the classification (automotive, architectural or container) error rate versus PC dimensions for HOO-CV with PCA reduced CVA for the first set of 30 glass second derivative (9-point smoothing) spectra (10 replicates), centered data..……... page 972

Figure 326 Graph of the classification (automotive, architectural or container) error rate versus PC dimensions for HOO-CV with PCA reduced CVA for the first set of 30 glass second derivative (9-point smoothing) spectra (10 replicates), autoscaled data..……..... page 975

Figure 327 Graph of the classification (window or container) error rate versus PC dimensions for HOO-CV with PCA reduced CVA for the first set of 30 glass second derivative (9-point smoothing) spectra (10 replicates), no data pretreatment..……. page 977

Figure 328 Graph of the classification (window or container) error rate versus PC dimensions for HOO-CV with PCA reduced CVA for the first set of 30 glass second derivative (9-point smoothing) spectra (10 replicates), centered data..……. page 978

Figure 329 Graph of the classification (window or container) error rate versus PC dimensions for HOO-CV with PCA reduced CVA for the first set of 30 glass second derivative (9-point smoothing) spectra (10 replicates), autoscaled data..…….. page 981

Figure 330 Graph of the discrimination error rate versus PC dimensions for HOO-CV with PCA reduced CVA for the first set of 20 window glass second derivative (9-point smoothing) spectra (10 replicates), no data pretreatment..……... page 982

Figure 331 Graph of the discrimination error rate versus PC dimensions for HOO-CV with PCA reduced CVA for the first set of 20 window glass second derivative (9-point smoothing) spectra (10 replicates), centered data..……... page 983

Figure 332 Graph of the discrimination error rate versus PC dimensions for HOO-CV with PCA reduced CVA for the first set of 20 window glass second derivative (9-point smoothing) spectra (10 replicates), autoscaled data..……... page 985

Figure 333 Graph of the discrimination error rate versus PC dimensions for HOO-CV with PCA reduced CVA for the first set of 10 container glass second derivative (9-point smoothing) spectra (10 replicates), no data pretreatment..…… page 986

Figure 334 Graph of the discrimination error rate versus PC dimensions for HOO-CV with PCA reduced CVA for the first set of 10 container glass second derivative (9-point smoothing) spectra (10 replicates), centered data..……... page 987

Figure 335 Graph of the discrimination error rate versus PC dimensions for HOO-CV with PCA reduced CVA for the first set of 10 container glass second derivative (9-point smoothing) spectra (10 replicates), autoscaled data..... page 989
Figure 336 Graph of the float classification error rate versus PC dimensions for HOO-CV with PCA reduced CVA for the first set of 20 window glass second derivative (9-point smoothing) spectra (10 replicates), no data pretreatment..... page 990
Figure 337 Graph of the float classification error rate versus PC dimensions for HOO-CV with PCA reduced CVA for the first set of 20 window glass second derivative (9-point smoothing) spectra (10 replicates), centered data..... page 991
Figure 338 Graph of the float classification error rate versus PC dimensions for HOO-CV with PCA reduced CVA for the first set of 20 window glass second derivative (9-point smoothing) spectra (10 replicates), autoscaled data..... page 993
Figure 339 Graph of the tempered classification error rate versus PC dimensions for HOO-CV with PCA reduced CVA for the first set of 20 window glass second derivative (9-point smoothing) spectra (10 replicates), no data pretreatment..... page 995
Figure 340 Graph of the tempered classification error rate versus PC dimensions for HOO-CV with PCA reduced CVA for the first set of 20 window glass second derivative (9-point smoothing) spectra (10 replicates), centered data..... page 996
Figure 341 Graph of the tempered classification error rate versus PC dimensions for HOO-CV with PCA reduced CVA for the first set of 20 window glass second derivative (9-point smoothing) spectra (10 replicates), autoscaled data..... page 998
Figure 342 PCA scree plot for the set of 153 glass first derivative (5-point smoothing) spectra (10 replicates), autoscaled..... page 1003
Figure 343 PCA scree plot for the set of 103 window glass first derivative (5-point smoothing) spectra (10 replicates), autoscaled..... page 1008
Figure 344 PCA scree plot for the set of 50 container glass first derivative (5-point smoothing) spectra (10 replicates), autoscaled..... page 1013
Figure 345 PCA scree plot for the set of 153 glass first derivative (9-point smoothing) spectra (10 replicates), autoscaled..... page 1018
Figure 346 PCA scree plot for the set of 153 glass second derivative (9-point smoothing) spectra (10 replicates), autoscaled..... page 1023
Figure 347 PCA scree plot for the set of 103 window glass second derivative (9-point smoothing) spectra (10 replicates), autoscaled..... page 1028
Figure 348 Graph of the discrimination error rate versus PC dimensions for HOO-CV with PCA reduced CVA for the set of 153 glass first derivative (5-point smoothing) spectra (10 replicates), autoscaled.... page 1031

Figure 349 Graph of the discrimination error rate versus PC dimensions for HOO-CV with PCA reduced CVA for the set of 103 window glass first derivative (5-point smoothing) spectra (10 replicates), autoscaled……..…….... page 1034
Figure 350 Graph of the discrimination error rate versus PC dimensions for HOO-CV with PCA reduced CVA for the set of 50 container glass first derivative (5-point smoothing) spectra (10 replicates), autoscaled…….……... page 1037
Figure 351 Graph of the discrimination error rate versus PC dimensions for HOO-CV with PCA reduced CVA for the set of 153 glass first derivative (9-point smoothing) spectra (10 replicates), autoscaled…….……... page 1039
Figure 352 Graph of the discrimination error rate versus PC dimensions for HOO-CV with PCA reduced CVA for the set of 153 glass second derivative (9-point smoothing) spectra (10 replicates), autoscaled...…….…..... page 1041
Figure 353 Graph of the tempered classification error rate versus PC dimensions for HOO-CV with PCA reduced CVA for the set of 103 window glass second derivative (9-point smoothing) spectra (10 replicates), autoscaled……. page 1043
Figure 354 PCA scree plot for the first set of 30 glass deconvolution data (10 replicates), no pretreatment…….…..... page 1044
Figure 355 PCA scree plot for the first set of 30 glass deconvolution data (10 replicates), centered…….……... page 1045
Figure 356 PCA scree plot for the first set of 30 glass deconvolution data (10 replicates), autoscaled…….……..... page 1046
Figure 357 PCA scree plot for the first set of 20 window glass deconvolution data (10 replicates), no pretreatment.……... page 1047
Figure 358 PCA scree plot for the first set of 20 window glass deconvolution data (10 replicates), centered…….…….….... page 1048
Figure 359 PCA scree plot for the first set of 20 window glass deconvolution data (10 replicates), autoscaled.……... page 1049
Figure 360 PCA scree plot for the first set of 10 container glass deconvolution data (10 replicates), no pretreatment.……... page 1050
Figure 361 PCA scree plot for the first set of 10 container glass deconvolution data (10 replicates), centered…….…….….... page 1051
Figure 362 PCA scree plot for the first set of 10 container glass deconvolution data (10 replicates), autoscaled…….…….. page 1052
Figure 363 PCA scree plot for the spectra of 21 glasses (10 replicates) with nominally similar RIs (same RI set 1), autoscaled.…….…..... page 1056
Figure 364 PCA scree plot for the first derivative spectra (5-point smoothing) of 21 glasses (10 replicates) with nominally similar RIs (same RI set 1), autoscaled…….……..... page 1059

Figure 365 PCA scree plot for the second derivative spectra (5-point smoothing) of 21 glasses (10 replicates) with nominally similar RIs (same RI set 1), autoscaled.……..……..... page 1062
Figure 366 PCA scree plot for the spectra of 30 glasses (10 replicates) with nominally similar RIs (same RI set 2), autoscaled.……..... page 1067
Figure 367 PCA scree plot for the first derivative spectra (5-point smoothing) of 30 glasses (10 replicates) with nominally similar RIs (same RI set 2), autoscaled.…….……..... page 1072
Figure 368 PCA scree plot for the second derivative spectra (5-point smoothing) of 30 glasses (10 replicates) with nominally similar RIs (same RI set 2), autoscaled.……. page 1076
Figure 369 Graph of the discrimination error rate versus PC dimensions for HOO-CV with PCA reduced CVA for the spectra of 21 glasses (10 replicates) with nominally similar RIs (same RI set 1), autoscaled……..……..... page 1078
Figure 370 Graph of the discrimination error rate versus PC dimensions for HOO-CV with PCA reduced CVA for the first derivative spectra (5-point smoothing) of 21 glasses (10 replicates) with nominally similar RIs (same RI set 1), autoscaled.……... page 1080
Figure 371 Graph of the discrimination error rate versus PC dimensions for HOO-CV with PCA reduced CVA for the second derivative spectra (5-point smoothing) of 21 glasses (10 replicates) with nominally similar RIs (same RI set 1), autoscaled.……...…… page 1082
Figure 372 Graph of the discrimination error rate versus PC dimensions for HOO-CV with PCA reduced CVA for the spectra of 30 glasses (10 replicates) with nominally similar RIs (same RI set 2), autoscaled…….……..... page 1085
Figure 373 Graph of the discrimination error rate versus PC dimensions for HOO-CV with PCA reduced CVA for the first derivative spectra (5-point smoothing) of 30 glasses (10 replicates) with nominally similar RIs (same RI set 2), autoscaled……... page 1088
Figure 374 Graph of the discrimination error rate versus PC dimensions for HOO-CV with PCA reduced CVA for the second derivative spectra (5-point smoothing) of 30 glasses (10 replicates) with nominally similar RIs (same RI set 2), autoscaled……... page 1091

LIST OF ABREVIATIONS

AAS	atomic absorption spectrometry
ANOVA	analysis of variance
ARO	all reflecting objective
ASTM	American Society for Testing Materials
ATR	attenuated total reflection
BPSG	borophosphosilicate glass
CL	cathodoluminescence
CLS	classical least-squares
cm	centimeter
cm^{-1}	reciprocal centimeter or wavenumber
CV	canonical variate
CVA	canonical variate analysis
DRC	dynamic reaction cell
DRC-ICP-MS	dynamic reaction cell inductively coupled plasma-mass spectrometry
EC	external calibraton
EC-ICP-MS	external calibraton inductively coupled plasma-mass spectrometry
EDS	energy dispersive X-ray spectrometry
EDXRF	energy dispersive X-ray fluorescence spectrometry
EPMA	wavelength-dispersive electron probe microanalysis
FBI	Federal Bureau of Investigation
FDLE	Florida Department of Law Enforcement
FT-IR	Fourier transform infrared spectroscopy
FTR	frustrated total reflection
g	gram
GRIM	glass refractive index measurement
HOO-CV	hold-one-out cross validation
HQI	hit quality index
HR-SF-ICP-MS	high resolution sector field inductively coupled plasma-mass spectrometry
ICP-AES	inductively coupled plasma-atomic emission spectrophotometry
ICP-MS	inductively coupled plasma-mass spectrometry
ICP-OES	inductively coupled plasma-optical emission spectrophotometry
ID	isotope dilution
ID-ICP-MS	isotope dilution inductively coupled plasma-mass spectrometry
IR	infrared
IRE	internal reflection element
LA	laser ablation
LA-ICP-MS	laser ablation-inductively coupled-mass spectrometry
LDA	linear discriminant analysis
LIBS	laser induced breakdown spectroscopy
LO	longitudinal-optic

MCT	mercury/cadmium telluride
mg	milligram
mm	millimeter
MSE	mean square for error
MSTr	mean square for treatments
NAA	neutron activation analysis
NBO/T	ratio of non-bridging oxygen per network forming tetrahedral
ng	nanogram
NIST	National Institute of Standards and Technology
nm	nanometer
NMR	nuclear magnetic resonance
PC	principle component
PCA	principle component analysis
PCA-CVA	principle component analysis canonical variate analysis
PCR	principle component regression
PLS	partial least squares
PLS-DA	partial least squares discriminant analysis
ppm	parts per million
RAS	reflection-absorption spectroscopy
RI	refractive index
RMS	root mean square
RSD	relative standard deviation
S/N	signal-to-noise ratio
SEM	scanning electron microscopy
SEM-EDS	scanning electron microscopy-energy dispersive X-ray spectrometry
SR-XRF	synchrotron radiation high-energy X-ray fluorescence spectrometry
SRM	standard reference material
SWGMAT	Scientific Working Group for Materials Analysis
TAKA	Thomas A. Kubic & Associates
TE	transverse electric
TM	transverse magnetic
TO	transverse-optic
UV	ultraviolet
WDS	wavelength dispersive X-ray spectrometry
WDXRF	wavelength dispersive X-ray fluorescence spectrometry
XAFS	X-ray absorption fine structure
XRF	X-ray fluorescence spectrometry
ΔRI	change of refractive index
µg	microgram
µm	micrometer
µXRF	micro-X-ray fluorescence spectrometry

CHAPTER 1: INTRODUCTION

1.A. Statement of the Problem

Glass is a ubiquitous material, and as a result it is commonly recovered as transfer evidence when glass objects are broken during the commission of a crime. Vehicle windows, architectural windows, containers, headlamps, light bulbs, and mirror glasses are some of the major sources of this evidence at a number of crime scenes, including but not limited to car accidents, robberies, vandalism, bombings, and homicides. Broken glass is readily transferred to the breaker and to any individual or object in the vicinity of the breaking event, thus it has the ability to associate a suspect with a crime scene location or item and in some cases the time of occurrence. The significance of glass evidence is enhanced when the fragments are determined to be indistinguishable in all measured properties from the broken glass object. Conversely, if the recovered fragments differ in their measured properties from the broken glass object, then that glass object can be eliminated as a possible source of the glass from the suspect.

The first step in any forensic glass comparison is to inspect the fragments visually and determine whether there is a fracture match between any of the recovered fragments. When the recovered fragments are large in size, there is a reasonably high chance of obtaining a fracture match. However such a match is rarely found when there are only a number of small glass fragments (De Forest, Gaensslen, and Lee, 1983). The second step is to measure physical and optical properties, such as color, thickness, curvature, and refractive index (RI). However, the glass fragments might be too small and not contain both original glass surfaces, thus making the original thickness and some of the other aforementioned properties impossible to determine. In addition, improvements in quality control during the manufacturing of glass have resulted in a narrowed range of RIs of the glasses produced, thus decreasing its power of discrimination.

Consequently, additional analytical methods for discrimination were required to be developed. The third step in the current analytical discrimination of glass fragment samples is the analysis of trace elements present. It is reported that several elemental analytical techniques, specifically laser ablation-inductively coupled-mass spectrometry (LA-ICP-MS), micro-X-ray fluorescence spectrometry (μXRF), and laser induced breakdown spectroscopy (LIBS), have the ability to discriminate 99% of glass samples, both alone and in combination with RI (Koons and Buscaglia, 2002; Trejos, Montero, and Almirall, 2003; Bridge et al., 2007; Naes et al., 2008). Three of the major disadvantages of elemental analyses are the cost, complexity of instrumentation, and steep learning curve for the analyst. These have prevented its widespread adoption by crime laboratories. Thus, there is need for an alternative method for the discrimination of glass samples that is simpler and less expensive then elemental analysis but more discriminating than RI.

The use of infrared (IR) microprobe analysis has great potential to aid in the discrimination of glass samples, which are frequently encountered as transfer evidence. Attenuated total reflection (ATR) mid-IR microspectroscopy will not only add to the battery of tests available for distinguishing between known and suspect samples of glass, but also it will provide information about the molecular chemistry which is not presently exploited by criminalists.

1.B. Glass Definitions, Structure and Properties

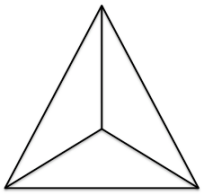
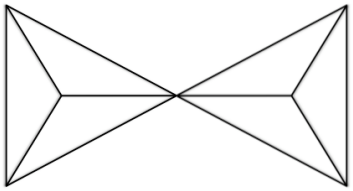
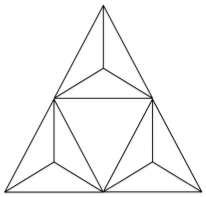
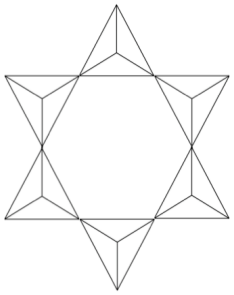
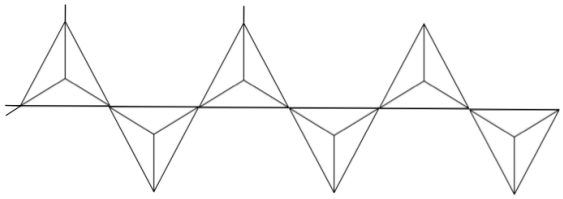
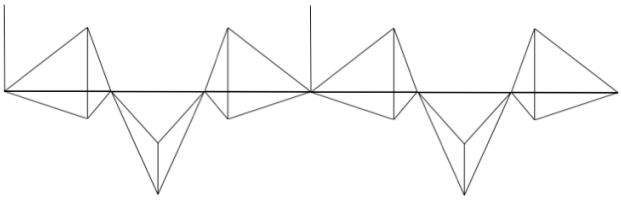
The American Society for Testing Materials (ASTM) defines glass as "the inorganic product of fusion which has cooled to a rigid condition without crystallizing" (ASTM C162-05, 2010). This standard definition of glass is very general hence this author prefers the definition

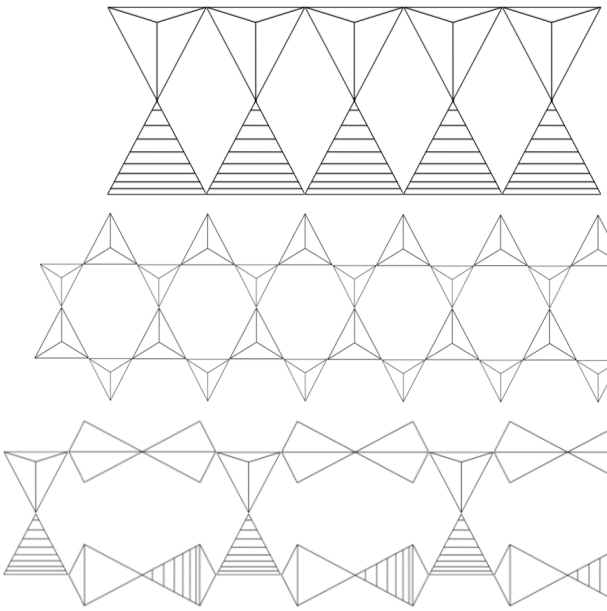
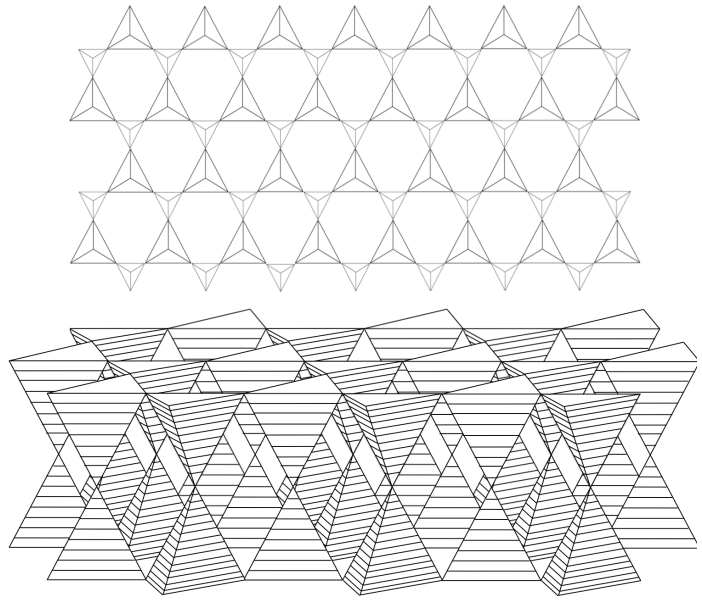
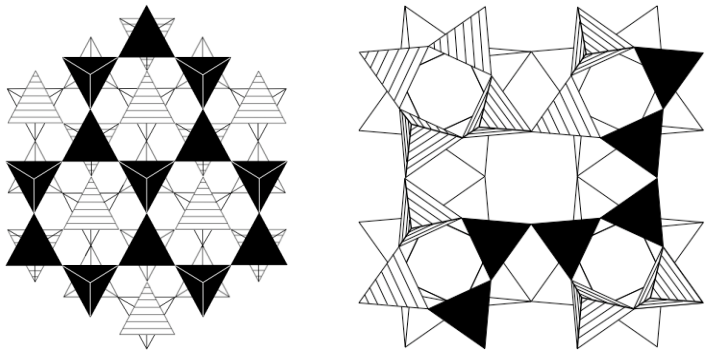
by Shelby (2009) of glass as "an amorphous solid completely lacking in long range, periodic atomic structure, and exhibiting a region of glass transformation behavior."

The term amorphous denotes "any condensed phase which lacks long-range order according to diffraction (x-ray, neutron, and electron) criteria" (Wong and Angell, 1976). Long-range order applies to crystalline materials, and is defined by Popescu (2005) to be "correlations between the positions of every two atoms situated as far as possible one from another". The Encyclopedia Britannica (2010) explains long-range order as "once the positions of an atom and its neighbours are known at one point, the place of each atom is known precisely throughout the crystal." Although a glass does not have long-range order, the structure of glass does possess short-to-medium range order. Short-range order is "defined by the interatomic correlations in the first coordination spheres of an arbitrary atom, e.g. up to the maximum distance where the atomic forces are acting." (Popescu, 2005)." Medium-range order extends the ordered arrangement of atoms beyond that of atomic forces, and is defined "as given by structural correlations in the range of 0.5 – 1 nm" (Popescu, 2005). The short-to-medium range order of silicate glass is composed of discrete silicate units, and the physiochemical properties of silicate glasses are controlled by the relative percentage of these co-existing silicate units (Bell et al. 1968; Dalby and King, 2006). As a result, it is necessary to identify and quantify these silicate units in order to understand the behavior of silicate glasses. Analytical techniques such as X-ray diffraction, nuclear magnetic resonance (NMR), X-ray absorption fine structure (XAFS), neutron diffraction, Raman spectroscopy and IR spectroscopy have been used to characterize the structural units in silicate glasses. (Mackenzie, 1960; Wong and Angell, 1976; Vogel, 1985; Vogel, 1994; Dalby and King, 2006; Shelby, 2009).

Most of the knowledge of the short-to-medium range order of glass is based on comparisons with studies of mineral silicates with known crystalline structures. The basic unit for all silicate structures is the SiO_4 tetrahedra. There are several different types of silicate structures, with the most important ones being island silicates (called nesosilicates, which is derived from the Greek word "nesos" for islands), group silicates (called sorosilicates, from the Greek word "soros" for groups), ring silicates (called cyclosilicates, from the Greek word "kyklos" for circle), chain silicates (called inosilicates, from the Greek word "inos" for fiber), layer (or sheet) silicates (called phylloosilicates, from the Greek where "phyllon" means block), and network silicates (called tectosilicates, from the Greek where "tektoneia" means lattice) (Vogel, 1985 and 1994; Deer, Howie, and Zussman, 1966). Table 1 shows the linkages of SiO_4 tetrahedra in each of the types of silicate structures and the corresponding silicon-oxygen building group. There are known minerals with each of these silicate structures, as described by Vogel (1985 and 1994). Examples of island silicates are phenacite ($Be_2[SiO_4]$), willemite ($Zn_2[SiO_4]$), and fosterite ($Mg_2[SiO_4]$). Thortveitite ($(Sc, Y)_2[Si_2O_7]$) is an example of group silicates. β-wollastonite ($Ca_3[Si_3O_9]$) and Beryl ($Al_2Be_3[Si_6O_{18}]$) are examples of 3-ring and 6-ring silicates, respectively. There are two types of single chain silicates, with enstanite ($Mg_2[Si_2O_6]$) and spodumene ($LiAl[Si_2O_6]$) being examples of the first type of single chain and α-wollastonite ($Ca_3[Si_3O_9]$) as the example of the second single chain. Sillimanite ($Al[AlSiO_5]$), tremolite ($Ca_2Mg_5[(OH_1F)]$ or $Ca_2Mg_5Si_8O_{22}(OH_2)$), and xonolith ($Ca_6[(OH)_2/Si_6O_{17}]$ are examples of the double chain, double binary chain, and double teriary chain silicates, respectively. The single layer silicates are exemplified by talcum ($Mg_3[(OH)_2/Si_4O_{10}]$ and montmorillonite ($Al_2[(OH)_2/Si_4O_{10}]$. Vogel (1985 and 1994) does not identify a mineral with the double layer silicate structure, but the formula is given as $CaAl_2Si_2O_8$(hex.). There are two types

Table 1: Silicate Structures (figures adapted from Vogel, 1985 and 1994).

Type of Silicate	Building Group	Linkage of SiO_4 tetrahedra
Island Silicates	$[SiO_4]^{4-}$	
Group Silicates	$[Si_2O_7]^{6-}$	
Ring Silicates		
3-ring	$[Si_3O_9]^{6-}$ - ring	
6-ring	$[Si_6O_{18}]^{12-}$ - ring	
Chain Silicates		
Single chain	$[SiO_3]_x^{2-}$ - chain	
	$[SiO_3]_x^{2-}$ - chain	

Double chain	$[Si_2O_5]_x^{2-}$- chain	
Double Binary Chain	$[Si_4O_{11}]_x^{6-}$- chain	
Double Teriary Chain	$[Si_6O_{17}]_x^{10-}$- chain	
Layer Silicates Single layer	$[Si_2O_5]_{xx}^{2-}$- layer	
Double layer		
Network Silicates	$[SiO_2]_{xxx}$ $(2SiO_2 = Si[SiO_4])$	

of network silicates, with high- and low-crystobalite (SiO_2), high- and low-tridymite(SiO_2), and high- and low-quartz (SiO_2) being examples of the first, and orthoclase ($KAlSi_3O_8$) and plagioclase ($(Na,Ca)Al(Si,Al)Si_2O_8$) being examples of the second. Analyzing these minerals and comparing the results with glass analytical data reveal the silicate structures that make up the short-to-medium range order of glasses. (Vogel, 1985 and 1994).

There are several theories concerning the structure of glasses. Gustav Tamman proposed the first theory of glass structure in 1903 in which glasses were considered to be strongly undercooled liquids (Vogel, 1985 and 1994). Although X-ray diffraction data has shown some agreement with this theory, it is considered to be very general and only a good start at understanding the structure of glasses. Victor Moritz Goldschmidt derived empirical rules for the formation of glasses based on ionic sizes (Vogel, 1985 and 1994). Goldschmidt proposed "a ratio of from 0.2 to 0.4 of radius-of cation (r_c) to radius-of-anion (r_a) as a condition of glass formation," with silicates (SiO_2), borates (B_2O_2), phosphates (P_2O_5), germanates (GeO_2), and others (such as arsenic trisulfide (As_2S_3) and beryllium fluoride (BeF_2)) fulfilling this condition (Vogel, 1985 and 1994). The microcrystal model of glass structure is based on the mineral crystal structure, where glasses are composed of very small, or micro, crystals (Shelby, 2009). A. A. Lebedev proposed the crystallite theory, which is based on the microcrystal theory with some modifications (Shelby, 2009; Vogel, 1985 and 1994). Lebedev said that instead of microcrystals, glasses are composed of crystallites connected by amorphous regions. Crystallites are deformed versions of silicate crystals that are not perfect lattices (Shelby, 2009; Vogel, 1985 and 1994). The most significant theory on the structure of glasses was proposed by W.J. Zachariasen and B.E. Warren and is known as the network theory. In 1932, W.J. Zachariasen published the paper "The Atomic Arrangement in Glass" which described the ability of various

oxides to form glass. This was the first work that used chemical composition for the understanding of glass structure. Warren's work in X-ray diffraction was critical in corroborating Zacharaisen's model, thus he is co-credited with the network theory. In the network theory, the relative glass-forming ability of oxides was evaluated and it was concluded that the ultimate condition for glass formation is that a substance can form extended three-dimensional networks lacking periodicity but with energy content comparable with that of the corresponding crystal network. From this condition, there are five rules for oxide structure that allow selection of those oxides that tend to form glasses (1) the oxide or compound must easily form polyhedral groups as the smallest building units, (2) the polyhedra share only one corner, not edges or faces, (3) the anions (oxide, sulfide, fluoride, etc…) should not bind to more than two central atoms of the polyhedra, (4) the polyhedra must have less than six corners, and (5) at least three of the corners of the polyhedra must be bound to neighbor polyhedra, thus linking them in a three-dimensional network (Zachariasen, 1932; Vogel, 1985 and 1994). Figure 1 shows an example of the structure of glass that agrees with the network theory, with silicate glass having the same tetrahedral linkages as crystalline silicates, but showing some irregular connections. Although the network theory continues to be the most commonly used model for glass structure, understanding the structure of glasses remains to be the subject of significant theoretical and analytical research.

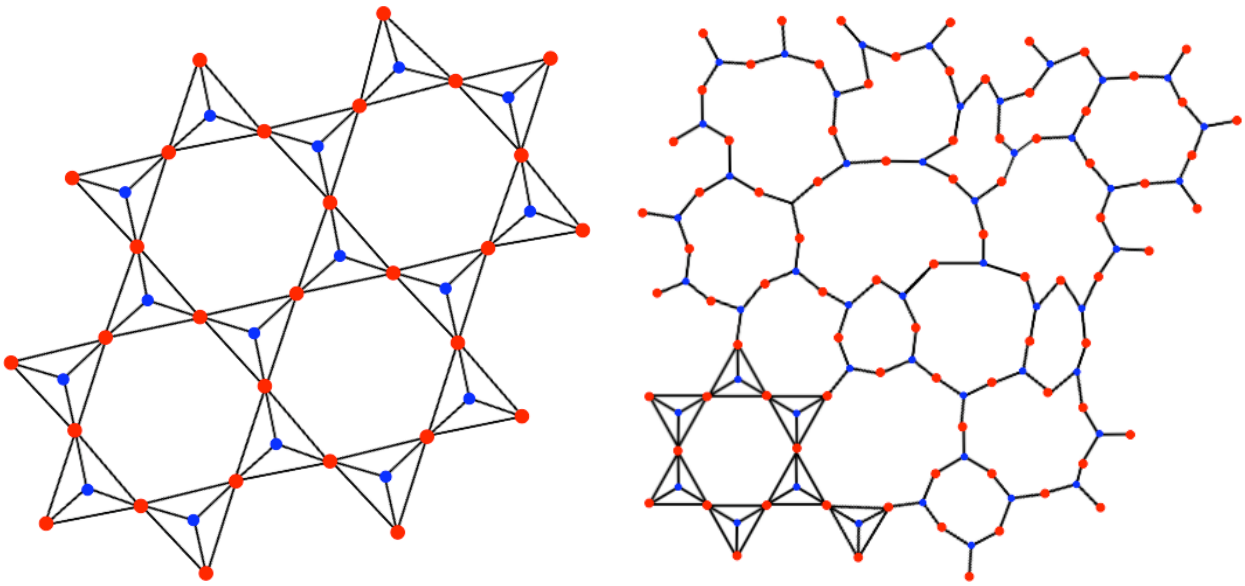


Figure 1: SiO_4 tetrahedral structures in crystalline and glassy silicates, adapted from Vogel, 1985 and 1994. The blue dots represent silicon and the red dots represent oxygen. A fourth oxygen would be located above or below each of the silicon atoms in the three-dimensional structures.

Glass transformation or transition refers to the change of a glass-forming liquid into a glass, which usually occurs upon rapid cooling. When the glass-forming liquid is slow cooled, the result is no longer a glass and instead is a crystal with long-range order. Glass transformation is a dynamic phenomenon occurring between two distinct states of matter (liquid and solid glass), each with different physical properties. Glass transformation behavior is represented on a diagram of enthalpy or volume versus temperature, as shown in Figure 2. The ordinate of the diagram can be either enthalpy or volume because these two properties behave similarly. To understand the glass transformation behavior, first consider a liquid at a temperature above its melting point. As the liquid is cooled, there are corresponding changes to the atomic and molecular structure and decreases in enthalpy (and volume). For many substances, when the melting point is reached, the liquid rapidly converts into a crystalline solid, which is accompanied by a rapid decrease in enthalpy. However, if the substance can be cooled below the

melting point without crystallization occurring, a supercooled liquid is formed. In the supercooled liquid region, the atomic structure continues to rearrange, the viscosity increases and there is no sudden decrease in enthalpy. Eventually the increase in viscosity prohibits further atomic and molecular rearrangement to the liquid's equilibrium structure. As a result, the enthalpy deviates from the liquid equilibrium line, as represented by a curve of decreasing slope, until it reaches the glass equilibrium line. The glass transformation range is defined as the temperature range between where the enthalpy corresponds to the liquid equilibrium and the glass equilibrium. The viscosity of the supercooled liquid controls the temperature where the enthalpy departs from the liquid equilibrium line, thus the use of a slower cooling rate enables the formation of a glass with a lower enthalpy. This results in glasses with different atomic and molecular structure. (Shelby, 2009).

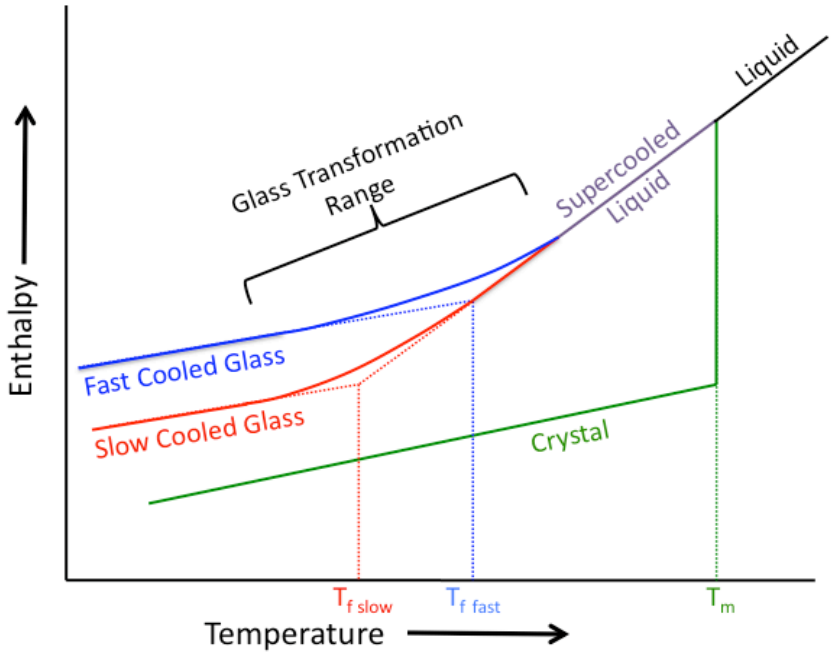


Figure 2: The glass transformation behavior diagram. The melting point of the crystal is T_m and the fictive temperature is T_f. (adapted from Shelby, 2009).

The glass transformation occurs over a range of temperatures, and as a result it is useful to describe the thermal history in terms of a single temperature. The glass transformation (or transition) temperature and fictive temperature are two such terms. The glass transformation temperature is the temperature at the beginning of the glass transformation range during heating, defined by changes in thermal analysis or expansion curves (Shelby, 2009). ASTM (C162-05, 2010) defines the glass transition temperature as "on heating, the temperature at which a glass transforms from an elastic to a viscoelastic material, characterized by the onset of a rapid change in thermal expansivity." The problem with using the glass transformation (or transition) temperature is that it is dependent on the heating rate, and thus is not constant for all experimental conditions (Shelby, 2009). The fictive temperature, as shown in Figure 2, is the extrapolated intersection of the glass and supercooled liquid equilibrium lines. Stolov and Simoff (2008) define the fictive temperature "as the equilibrium temperature at the moment of solidification."

There are many properties of silica glass that depend on the fictive temperature. Density, viscosity, thermal expansion coefficient, and RI are dependent on the fictive temperature. As an example of the relationship between fictive temperature and physical properties, Agarwal, Davis, and Tomozawa (1995) describe that "in the fictive temperature range of 1000-1400° C, with increasing fictive temperature, the room temperature density of silica glass was found to increase and the viscosity of silica glass at any given temperature was found to decrease." In addition, an increase in fictive temperature causes an increase in RI, however this relationship is not independent of the associated increase in density (Shelby, 2009). The fictive temperature is directly related to the average Si-O-Si bond angle, and therefore the vibrational frequency (Stolov and Simoff, 2008).

The optical properties of glass, specifically its transparency to visible light, have made glass an important material in all societies. Consequently, its ubiquity has made it a common form of forensic transfer evidence. There are several physical and optical properties, such as density, RI, and optical dispersion that are of considerable interest to various scientists, particularly forensic scientists.

Density is a physical property defined as the mass per unit volume (g/cm^3). The density of glass varies with its composition and thermal history, thus making it a useful property for forensic comparative analysis (SWGMAT, 2005b). The density of modern glass across a pane can vary, with typical variations being 0.001 g/cm^3 (Koons et al., 2002; Bottrell, 2009).

RI is defined by the Scientific Working Group for Materials Analysis (SWGMAT) (2005d) as "the ratio of the speed of light in one media compared to another, mathematically expressed as $n_i = v_1/v_2$, where RI = n_i at a specific wavelength i, and the speed of light in each media are v_1 and v_2. For glass analysis, v_1 is the speed of light in a vacuum." The RI is often measured by the application of Snell's Law:

$$n = \frac{\sin\Theta_1}{\sin\Theta_2}$$

where Θ_1 is the angle of incidence and Θ_2 is the angle of refraction for a ray of monochromatic light striking the boundary between two mediums. RI is a function of the composition and thermal history of the glass. RI is the most commonly measured optical property of glasses (Shelby, 2009).

Dispersion is a property of glass that is defined as "the change in refractive index with a change in wavelength of illumination" (SWGMAT, 2005d). Relative dispersion (V), or Abbe

value, is the measurement of dispersion that is most often used in forensic glass examinations and is calculated from the difference between RIs at different wavelengths, most commonly the sodium D line (nD, 589 nm), the hydrogen C line (nC, 486 nm), and the hydrogen F line (nF, 656 nm). The equation to calculate relative dispersion is: $V = (nD - 1)/(nF - nC)$. (ASTM C162-05, 2010; SWGMAT, 2005d).

1.C. Glass Manufacturing

The first production of glass by man was about 4000 years ago, by ancient Egyptians in furnaces used to make pottery. Glass was first used to make jewelry, but its favorable shaping properties extended its applications to include containers, windows, and lenses. Despite a plethora of applications, it wasn't until roughly 1800 that there was any significant advancement in glass manufacturing. This advancement was made by Guinand and Fraunhofer who developed special stirring methods for increasing the homogeneity of glass. Fraunhofer also recognized the need to measure the RI of glass at specific wavelengths, and as a result of further investigations, he is credited with inventing the spectrometer. (Vogel, 1985 and 1994).

The modern manufacturing process for all glasses generally follows a five-stage process, as described by Copley (2001): (1) raw materials, (2) melting, (3) forming, (4) annealing, and (5) warehouse or secondary processes.

The first stage is where the raw materials required for manufacture are obtained, weighed, and thoroughly mixed (Copley, 2001). The specific raw materials depend on the type of glass being manufactured. The raw materials for the production of soda-lime silicate glasses primarily include soda (Na_2O), lime (CaO), and silica (SiO_2), while borosilicate glass is

composed of silica and a boric oxide (B_2O_3) content above 4 weight percent (ASTM C162-05, 2010). Other glasses include lead, aluminosilicate, alkali barium silicate, borate, phosphate, and chalcogenide glasses (Copley, 2001). Cullet is an important raw material that aids in the melting process, and is defined by ASTM (C162-05, 2010) as "glass product or portions of product usually suitable for addition to raw batch." In glass manufacturing, the term batch has three meanings: (1) "the recipe of batch ingredients", (2) "the raw materials weighed but unmixed", and (3) "the raw materials, properly proportioned and mixed, for delivery to the furnace" (ASTM C162-05, 2010). The impurity of the raw materials of glass, specifically the silica sand, can impart a green tint to the final glass product. As a result, decolorisers such as selenium (for a pink coloring) and cobalt (for a blue coloring) are added to the batch to offset the green tint and ultimately produce colorless glass. Conversely, if color is desired in the end product, coloring compounds are added to the batch. (Copley, 2001).

The second stage is melting, which occurs in a melting furnace that can withstand temperatures of 1500°C (Copley, 2001). ASTM (C162-05, 2010) defines the melting furnace as "the complete unit of a glass melting assembly, including the melter, regenerators or recuperators, flues, refiners, forehearths, channels, throats, etc." The melter is the "melting unit constructed of refractory materials, with a glass level maintained essentially constant by feeding batch to replace glass continuously withdrawn" (ASTM C162-05, 2010). The regenerator is "a cyclic heat interchanger that alternately receives heat from gaseous combustion products and transfers heat to air or gas before combustion" (ASTM C162-05, 2010). Refiners are "a component of a melting furnace, for the purpose of conditioning the glass" (ASTM C162-05, 2010). In the melting furnace, the batch melts rapidly, the viscosity decreases, and the raw materials chemically react (Copley, 2001). The melting process and chemical reactions produce

undissolved gases (mainly carbon dioxide and water). These gases are detrimental to the appearance and optical properties of the final product, and therefore are removed in the fining (or refining) process (ASTM C162-05, 2010; Copley, 2001). Homogenization of the vitreous glass occurs by thermal and sometimes mechanical stirring (Copley, 2001). Lastly, the temperature is reduced as it travels through the furnace to the forming stages (Copley, 2001).

The third stage is the forming process, where the glass is shaped into the form of the final product. Forming occurs as the temperature decreases and viscosity increases. The specifics of the forming process depend on the particular product being manufactured, with different processes for the formation of flat glass, container glass, fiber glass, optical fiber glass, optical glass, glass-tubing, light-bulb glass, etc… (Copley, 2001; Shelby, 2009). The processes for the manufacture of container glass and flat glass are of particular significance to this research, and thus are considered in more detail.

The manufacturing of container glass was originally done by hand, where a gob of glass was collected at the end of a blowpipe and air was forced into the gob by blowing through the pipe. This formed a hollow bubble of glass that was rotated and shaped into its final form. The process of hand blowing glass is still used for specialty glass items, but modern manufacturing has automated the process. In the automated process, a gob of glass is mechanically collected at the end of a rod, transferred to a forming mold, cut free from the rod, and transported to a split mold where it is blown into rough shape. For some glass containers, such as wide-mouth containers, the gob is initially pressed to form the rough shape rather than blown. The glass is then moved to a blow mold where it is blown into its final shape. The majority of glass containers are made from soda-lime silicate glasses, made from 73% silica, 11% lime, 14% soda, and 2% alumina. Some container glasses can also contain small amounts of magnesium oxide

(MgO), potassium oxide (K_2O), and sulfur trioxide (SO_3). Borosilicate glass is commonly used for chemical and pharmaceutical containers because of its increased durability as well as the fact that it does not leach sodium into its contents when chemically attacked. (Shelby, 2009).

Shelby (2009) describes the various processes used in the manufacturing of flat glass. Flat glass was originally manufactured via the crown process, where a large gob of glass was blown into a bulb, opened, and then spun flat inside a furnace using centrifugal force. The flat glass was cut from the outer portion of the disk because the glass was thinner at the edges and thicker in the center. The variation in thickness of glass made by the crown process and the practice of installing these glass panes with the thicker end down has been used to debunk the myth that the glass windows in ancient cathedrals show evidence of flow. The manufacture of larger panes of flat glass was achieved by blowing or drawing a large gob of glass into a cylindrical shape, splitting the glass cylinders along their axis, and flattening by reheating the glass on a flat surface. Both of these processes produced flat glass of insufficient quality and were arduous and time consuming. Improvements in the manufacturing of flat glass came about with the Colburn sheet process, where a ribbon of glass is drawn directly from the melt over a bent roller to a horizontal position. ASTM (C162-05, 2010) defines sheet glass as "flat glass made by continuous drawing." There have been other variations on this continuous formation of sheet glass, with modern improvements enabling the manufacture of high quality sheet glass by this method. Another type of flat glass is plate glass, defined as "flat glass formed by a rolling process, ground, and polished on both sides, with surfaces essentially plane and parallel" (ASTM C162-05, 2010). There are two rolling processes: the rolling of molten glass into a sheet on a metal table or by continuous rolling between water-cooled rollers. Plate glass has better optical properties than sheet glass, however float glass is optically superior to plate glass. Most modern

glass is produced by the float process, and is thus called float glass, whereby molten glass is drawn into a flat sheet on top of a float bath. ASTM (C162-05, 2010) defines a float bath as "a pool of molten metal, commonly tin, contained within a refractory receptacle and protected from oxidation by an inert atmosphere." The molten glass on the float bath is held at a temperature of ~1000°C, which allows for the surface to become flat and parallel and enables irregularities to flow out (Copley, 2001). The glass is then slowly cooled to ~600°C, whereby it can be lifted from the float bath without damage. Current applications of the float process are limited to soda-lime silicate glasses. The equilibrium thickness of float glass on the tin bath is 7.1 mm, and in order to produce flat glass with other thicknesses the cooling melt must be stretched or compressed. Glass thicknesses ranging from 2.5 mm to 25 mm can be produced via the float process (Copley, 2001). The advantage of the float process is that neither the tin nor the atmosphere surfaces contain flaws, thus both have excellent finish and do not require further processing or polishing. In addition, superior control of optical properties is achieved with the float process. The expected variation of RIs within a single float source is in the range of +/- 4 X 10^{-5} for annealed glass and +/- 1.6 X 10^{-4} for tempered glass (SWGMAT, 2005d). The float process does impart a thin layer of tin, by thermal diffusion, into the surface of the glass that is in contact with the float bath. Yang, Townsend and Holgate (1994) measured the depth of tin diffusion in float glass using cathodoluminescence, and determined it to be 8-9 μm. Although there is also some tin contamination on the upper face of the glass from the tin vapor, this is in a much smaller concentration. Glass manufactured by the float method can be readily identified via the tin layer's ultraviolet (UV) fluorescence. Another high quality flat glass manufacturing method is the down draw method (or fusion process), which ASTM (C162-05, 2010) defines as the "process of continuously drawing glass downward from an orifice." In the down draw

method, the glass melt flows into a shallow trough where it is caused to overfill and flow over the sides. Just below the trough, the melt recombines into a single sheet. There are two significant advantages of the down draw method, despite it being slower than the float process. The first is its ability to be used to make any variety of glass, and the second is its ability to the control the glass thickness because the thickness is dependent on the pull rate. Pattern glass is manufactured by rolling the melt (at a temperature of ~1050°C) between two rollers. The bottom roller is engraved with the negative of the desired pattern while the top roller is smooth. The glass exits the rollers at a temperature of ~850°C, where it is brought to the annealing lehr by water-cooled steel rollers. Microsheet glass, which is very thin glass (less than 0.15 mm), is produced by drawing the melt through a platinum plate with a thin slit. The thickness of the glass is precisely controlled by the draw rate, and as a result this process is commonly used for the manufacturing of microscope cover slips. (Shelby, 2009; Copley, 2001).

Annealing is an important part of the manufacturing process because the cooling process can produce uncontrolled stress in the final glass. ASTM (C162-05, 2010) defines annealing as "a controlled cooling process for glass designed to reduce residual stress to a commercially acceptable level and modify structure." The stress is due to contraction of glass upon cooling, which does not occur uniformly because of the low thermal conductivity of glass. Implementing a slow cooling regimen minimizes this stress (Copley, 2001). Annealing occurs in a lehr, which is "a long tunnel-shaped oven for heat treating glass by continuous passage" (ASTM C162-05, 2010).

The last stage of glass manufacturing is either subjecting the glass to secondary processing or shipping the product to a warehouse from where it will be sold. There are a variety of secondary or finishing processes, including toughening or tempering, coating, and decorating

(Copley, 2001). ASTM (C162-05, 2010) defines tempered glass as "a general term for glass that has been subjected to a thermal treatment characterized by rapid cooling to produce a compressively stressed surface layer." Tempering is performed by uniformly reheating the glass to a temperature just above where deformation occurs, and then quickly cooling the surface. The inside of the glass remains hot, and it cools slowly. This cooling causes contraction which pulls the surface layers into compression that are balanced by the tension in the central layers. (Copley, 2001). Tempered glass is also known as heat-strengthened glass (ASTM C162-05, 2010). Coatings are applied to glass for numerous reasons, including decoration, protection, and strengthening (Copley, 2001). Coatings can be applied by vapor or spray, and there are two types of coating processes: hot end coating and cold end coating. Hot end coatings (such as tin or titanium) are applied to the glass before it enters the annealing lehr while cold end coatings (such as organic waxes, polyethylene emulsions, polyethylene glycols, and their fatty acid esters or fatty acids) are applied upon exiting the annealing lehr. The decorating of glass products involves adding to or removing glass from the surface. The latter process occurs via grinding or sand blasting the surface to produce a specified finish. Hydrofluoric acid can also be used to create a patterned or textured surface. (Copley, 2001)

1.D. Infrared Spectroscopy

1.D.a. Infrared Theory

The electromagnetic spectrum is the name for the range of wavelengths and photon energies of light. Radiation of the greatest energy (and shortest wavelength) corresponds to gamma radiation, and in order of decreasing energy (and increasing wavelength) are gamma rays, X-rays, UV radiation, visible light, IR radiation, microwave radiation, and radio waves.

The different range of energies coincides with different transitions in atoms and molecules, as shown in Figure 3.

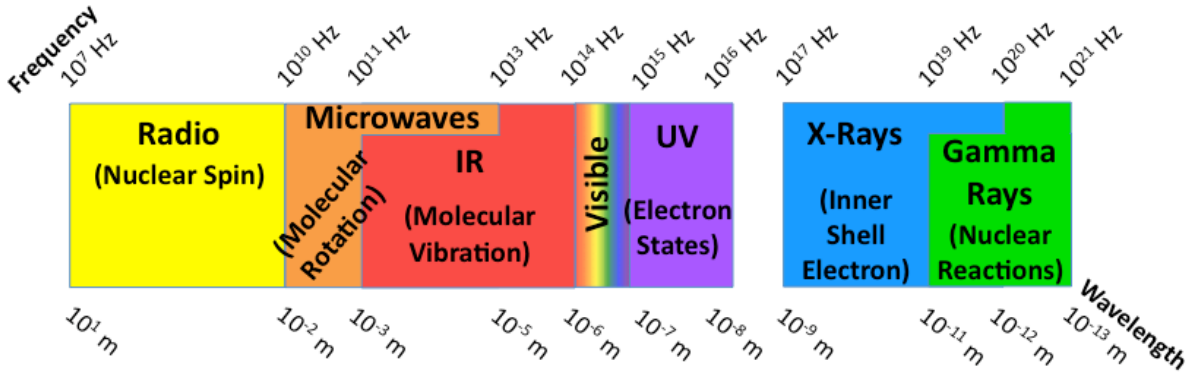


Figure 3: The Electromagnetic Spectrum with their different transitions in atoms and molecules (in parentheses), along with their respective wavelength and frequency ranges (*Skoog et al., 1998)*.

IR spectroscopy examines the interaction of IR radiation with molecules in a sample. IR radiation covers the spectral range of 12,800 to 10 cm^{-1} (wavenumbers), which is segmented into near- (12,800 to 4000 cm^{-1}), mid- (4000 to 200 cm^{-1}), and far- (200 to 10 cm^{-1}) IR regions. Mid-IR spectra occur from the absorption of energy due to the transition of molecules from one vibrational or rotational energy state to another. A net transfer of energy occurs when the frequency of the incident radiation is equivalent to the molecule's natural vibrational or rotational frequency in IR absorption spectroscopy. Other frequencies of IR radiation will not be absorbed and instead be transmitted. The absorption of the incident IR radiation causes a large proportion of molecules to be promoted to a higher energy state. IR absorption arises from a change in the dipole moment associated with rotational and vibrational energies of the bonds in a molecule. A change in dipole moment results when atoms within a molecule have different electron affinities so as to create an asymmetrical distribution of electron density. The distance between the centers of charge and the charge difference between the atoms will determine the

magnitude of the dipole moment. The larger the dipole moment in a molecule, the more intense the band will be in the IR spectrum. There are two main categories of molecular vibrations that cause IR absorption: stretching and bending. Stretching vibrations can be either symmetrical or asymmetrical. Bending vibrations are when there is a change in angle between bonds, and include the subclasses of scissoring, rocking, wagging, and twisting. Six types of molecular vibrations are shown in Figure 4. If a molecule has no change in dipole moment when any of the above actions take place, then it will be IR inactive. Molecules that are IR inactive will display weak or non-existent bands, and include homonuclear species such as O_2, N_2, and Cl_2. (Skoog et al., 1998).

The number of vibrational modes for simple diatomic and triatomic molecules can be calculated from its degrees of freedom and understanding the motion of the atoms in a molecule. More complex molecules can also be analyzed in a similar manner, however this analysis becomes more difficult. For polyatomic atoms, the degrees of freedom are equal to 3N, where the "3" comes from the three Cartesian coordinates for each point in space and the "N" is the number of atoms in the molecule. In addition, there are three additional considerations: (1) the molecule's translational motion of its center of gravity, (2) the molecule's rotational motion around its center of gravity, and (3) the relative motion of each atom (or vibration) to the other atoms. The atoms of a molecule move together through space, thus three coordinates are required to define this translational motion, and as a result the degrees of freedom are reduced by three. In addition, three degrees of freedom are needed to define the rotation of a molecule. Thus, the degrees of freedom for the interatomic motion of a molecule are equal to 3N - 6, which is equal to the number of possible vibrations for a molecule. Linear molecules represent a special case because of their straight-line molecular geometry. There are only two possible

rotational motions that cause a change in dipole moment, with rotation around the bond axis being impossible, thus there are only two degrees of freedom for its rotational motion. Thus, the degrees of freedom for the interatomic motion of a linear molecule are equal to 3N - 5. Each of the vibrations, calculated from 3N - 6 or 3N – 5, is called a normal mode. (Skoog et al., 1998).

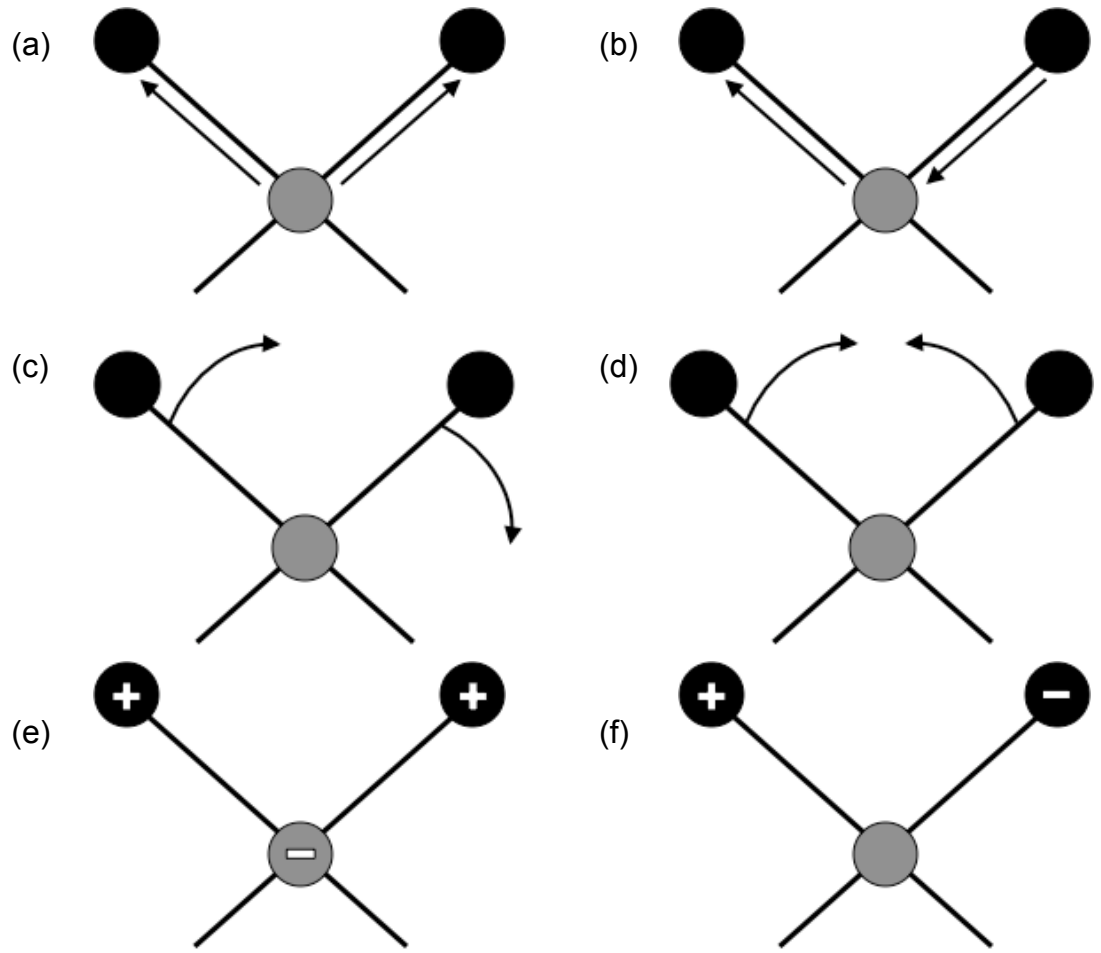


Figure 4: Six types of molecular vibrations: (a) symmetric stretching, (b) asymmetric stretching, (c) in-plane rocking, (d) in-plane scissoring, (e) out of plane wagging, and (f) out-of-plane twisting. The "+" symbol indicates motion from the page toward the reader and the "-" symbol indicates motion into the page away from the reader. These diagrams are adapted from figures by Skoog et al., 1998.

There are several conditions that cause there to be fewer or greater experimental peaks than theoretically predicted from the number of normal modes. There are four factors which cause there to be fewer peaks: (1) no change in dipole for a given vibration due to the molecule's symmetry, (2) two or more vibrations having identical or indistinguishable energies, (3) low absorption intensities prohibiting detection, and (4) the vibrational energy corresponds to a wavelength that is outside the range of the instrument. There are two main reasons why there might be more bands than expected: (1) overtone bands, and (2) combination bands. Overtone bands occur at a two or three times the original vibration's frequency (or wavenumber). Combination bands occur when two vibrational modes are excited simultaneously by one photon (quantum of energy), and its frequency is approximately equal to the sum of the two fundamental frequencies. (Skoog et al., 1998).

The energy and frequency (or wavenumber) of the vibrational bands can also be affected by other vibrators in the molecule, which is known as vibrational coupling. Skoog et al. (1998) details six factors that outline the requirements for vibrational coupling: (1) the strongest coupling of two stretching vibrations requires a common atom between the two vibrations, (2) the coupling of bending vibrations requires a common bond between the two vibrating groups, (3) the coupling of a bending and stretching vibration requires the stretching bond to be one side of the changing angle in the bending vibration, (4) the greatest coupling occurs when the two vibrations have approximately equal energies, (5) there is little or no coupling between vibrations that are separated by two or more bonds, (6) there is only coupling when the vibrations are of the same symmetry species. The phenomenon of vibrational coupling is very common and prevents an assignment of a specific frequency (or wavenumber) to an organic functional group. For example, the observed C-O stretching frequency is 1034 cm^{-1}, 1053 cm^{-1}, and 1105 cm^{-1} in

methanol, ethanol, and 2-butanol, respectively. Despite the uncertainties in the identification of functional groups that arise from vibrational coupling, it is the vibrational coupling that creates the unique spectra for each molecule which enables specific compounds to be positively identified. (Skoog et al., 1998).

Carbon dioxide (CO_2) is a linear molecule with a double bond connecting each of the carbon atoms to the central oxygen atom, and is a useful example for demonstrating the number of vibrational bands and vibrational coupling. The theoretical number of vibrations for a CO_2 molecule is 3 X 3 – 5 = 4. These four vibrational modes of CO_2 are shown in Figure 5, and include two stretching (symmetric and asymmetric) and two bending vibrations (both scissoring).

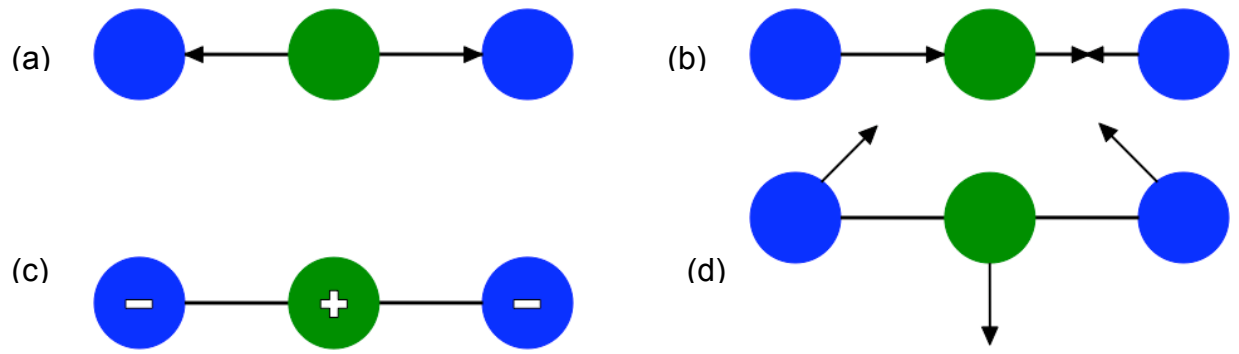


Figure 5: The four molecular vibrations of CO_2: (a) symmetric stretching, (b) asymmetric stretching, and both (c) and (d) scissoring. The "+" symbol indicates motion from the page toward the reader and the "-" symbol indicates motion into the page away from the reader. These diagrams are adapted from figures by Skoog et al., 1998.

The symmetric stretching vibration is IR inactive because it does not result in a change in dipole, as can be seen because the two oxygen atoms simultaneously move away from the central carbon atom. The asymmetric stretching, in which one oxygen atom moves away from the central carbon atom while the carbon atom moves towards the other oxygen atom, has a net change in dipole corresponding to a peak at 2330 cm^{-1}. The two bending vibrations are said to be degenerate because they have identical quantum states and energies, and thus produce one band

at 667 cm^{-1}. Coupling of the two C=O bonds in CO_2 are what cause there to be the two bands at 2330 cm^{-1} and 667 cm^{-1} rather than one band at ~1700 cm^{-1} due to a single C=O stretching vibration which is seen in aliphatic ketones. (Skoog et al., 1998).

The source of IR radiation in analytical instruments is commonly an electrically heated inert solid. When heated to between 1500 and 2200 K, the solid acts like a blackbody radiator emitting a continuous spectrum of radiation. This radiation is incident on a sample where some frequencies are absorbed and others transmitted through the instrument where they are detected and a spectrum obtained. The IR spectrum is plotted as absorbance (Abs) or percent transmittance (%T) versus wavenumber (cm^{-1}) or wavelength (μm). The transmittance is equal to the ratio of the power (or intensity) of the beam through the sample (P) to the power (or intensity) of the unobstructed beam (P_0), or $T = P/P_0$. The absorbance is equal to the negative log of the transmittance, Abs = -log (T). The vibrational spectrum of a sample is often considered to be a molecular 'fingerprint' capable of being used to identify the sample or the functional groups and backbone of the molecule. The spectral region that typically contains the most valuable information for identification by IR spectroscopy is from 1200 to 700 cm^{-1}, and is called the fingerprint region. There is also valuable information in the region from 700 to 200 cm^{-1}, however most IR instruments are not capable of detecting radiation below 450 cm^{-1} because these wavelengths are cut-off by the detector or the KBr beam splitter. (Skoog, et al., 1998)

Today, Fourier transform infrared (FT-IR) spectrometers are the most widely used IR instruments because of their "speed, high resolution, sensitivity, and unparalleled precision and accuracy" (Skoog, et al., 1998). There are four main advantages to Fourier transform instruments as compared to dispersive instruments. The Jaquinot, or throughput, advantage refers to the increased power that reaches the detector due to the fewer optical elements and the

absence of slits to attenuate the radiation. This enables a high signal resulting in a higher signal-to-noise ratio for Fourier transform instruments. The second is their high resolving power and wavelength reproducibility which allows for the analysis of complex spectra. The third is the high speed of analysis. All of the unabsorbed radiation from the source reaches the detector at once which enables the entire spectrum to be obtained within seconds. This data generated by the spectrometer are processed by a mathematical algorithm called a Fourier transform. The Fourier transform algorithm enables the instrument to analyze all of the wavelengths of IR light at once, and as a result a high quality spectrum is produced almost instantaneously. The fourth benefit of Fourier transform is the Fellgett, or multiplex, advantage which is made possible by the high speed of the instrument. This decrease in time for analysis allows for many spectra to be recorded and averaged, thus increasing the signal-to-noise ratio. If the noise is random, the signal-to-noise ratio improvement is theoretically proportional to the square root of the number of spectra co-added. This means if 4 spectra are taken then the increase in signal-to-noise is $\sqrt{4}$ = 2, and if 16 spectra are taken then there will be a 4-fold increase in signal-to-noise. These advantages are significant and are the reason why FT-IR instruments have eclipsed other IR spectrometers in modern laboratories (Skoog, et al., 1998). This occurred due to advances in computer power, the increased availability of lasers, and the attendant decrease in both their costs.

An interferometer is used in Fourier transform spectroscopy in order to attain a useable time-domain spectra, which pertains to changes in radiant power with time. "To obtain time-domain signals requires, therefore, a method of converting (*or modulating*) a high-frequency signal to one of measurable frequency without distorting the time relationships carried in the signal; that is, the frequencies in the modulated signal must be directly proportional to those in

the original" (Skoog, et al., 1998). Figure 6 diagrams a common design for an interferometer, called the Michelson interferometer, which is named for its inventor. The Michelson interferometer uses a

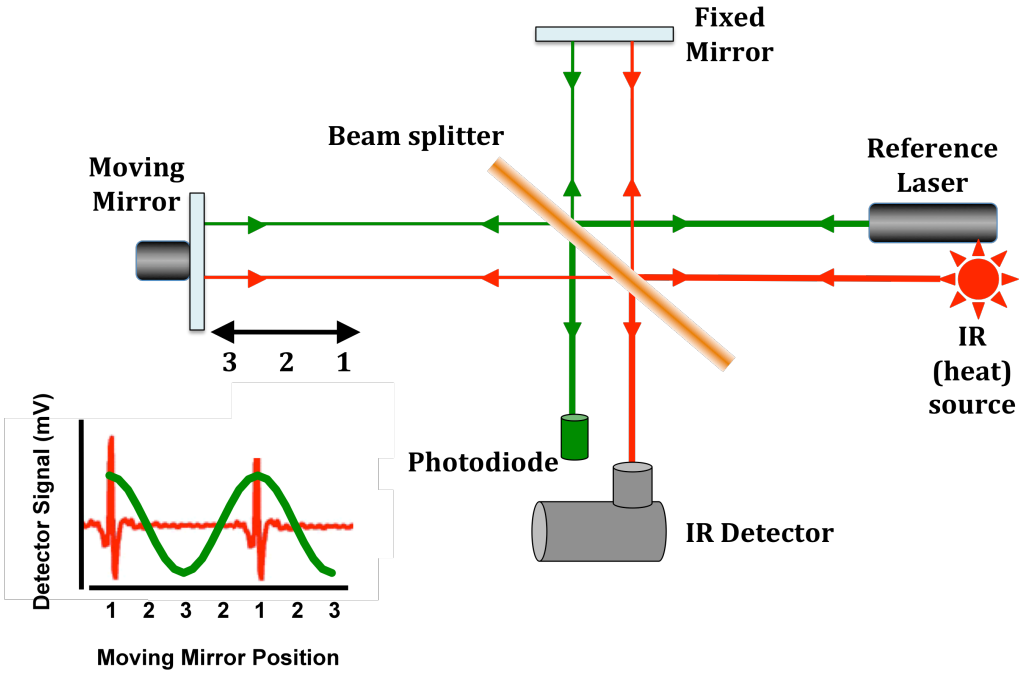


Figure 6: Schematics of IR spectrometer with Michelson interferometer.

beam splitter to separate the incident beam into two beams ideally of equal power. A commonly employed beam splitter is germanium on KBr, which is a thin layer of germanium with KBr on both sides. This is called a compensated beam splitter because it accounts for the path difference produced by the splitting of the beam through the beam splitter. The layering of the KBr ensures that both beams have the same optical path lengths through the beam splitter. Each beam is reflected from a mirror (one stationary and one moving at a constant velocity) and then recombined to produce an interference pattern. The united beam's intensity variations are a function of the difference in path lengths. A reference laser is used to measure the path lengths experienced by the two beams through changes in the mirror location. The difference between

the path length experienced by the radiation to the fixed mirror and the moving mirror is called the optical path difference. The total energy of the IR radiation changes as the optical path length difference changes. An interferogram, which is a plot of the IR energy (or detector signal) versus the optical path length difference, is generated. A Fourier transform of the interferogram is performed to produce a readable frequency-domain spectrum.

1.D.b. Attenuated Total Reflection

Attenuated total reflection (ATR) is an analytical method based on the total internal reflection of the incident radiation. In order to understand total internal reflection, the behavior of light when it encounters an interface must be understood.

When light strikes an interface between two media of different RIs, the beam will be partially transmitted and partially reflected. The transmitted beam is refracted (or bent), based on Snell's Law:

$$n_1 \sin i = n_2 \sin r$$

where n_1 and n_2 are the RIs of the two media, i is the angle of incidence and r is the angle of refraction. There is one scenario where the transmitted beam will not be refracted, and that is when the incident beam is normal to the interface between the two mediums ($i = 0°$). This results in the beam not being bent or refracted because the beam will be transmitted normal to the interface ($r = 0°$).

In Figure 7, the light is refracted into a medium of greater RI and as such it is bent towards the normal, as described by Snell's Law. When the light is refracted into a medium of a

lesser RI, as shown in Figure 8, it is bent away from the normal. As the angle of incidence increases, the refracted angle also increases. At a specific incident angle, known as the critical angle, the light will no longer be refracted to the new medium but instead will be refracted at a 90-degree angle from the normal to the surface and kept within the original medium. At any angle greater than the critical angle, the light is not transmitted and instead is reflected back into the medium. This phenomenon is known as total internal reflection.

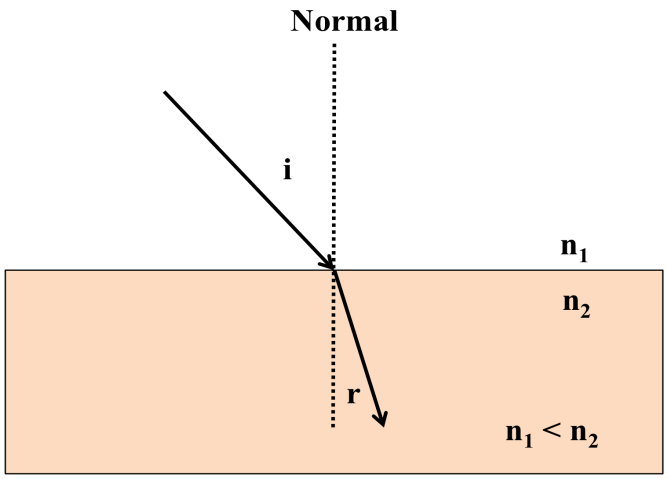


Figure 7: Refraction of light into a medium of higher RI.

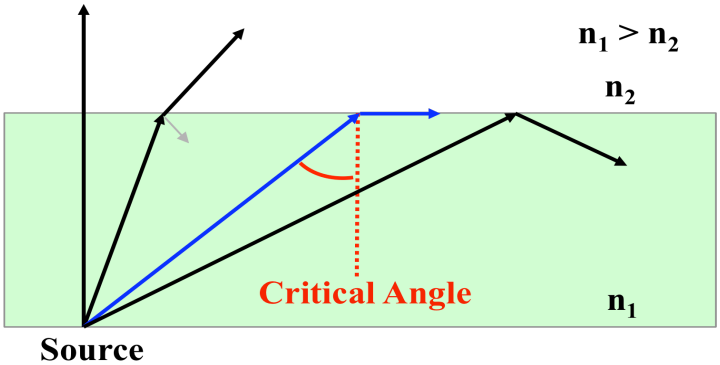


Figure 8: Refraction of light into a medium of lesser RI.

For the reflected beam, the angle of incidence equals the angle of reflection. The reflected beam has two components, one that has its electric field vector vibrating in the plane

perpendicular to the plane of incidence and one vibrating in the plane parallel to the plane of incidence, known as perpendicular polarization and parallel polarization, respectively. Perpendicular polarization is also known as transverse electric (TE) or senkrecht (s) waves, while parallel polarization is also known transverse magnetic (TM) or parallel (p) waves. The critical angle (Θ_C) required for total internal reflection is calculated from the following equation:

$$\Theta_C = \sin^{-1}(n_2 / n_1)$$

When total internal reflection occurs, the interface represents a mirror with an extremely high reflectivity, thus there is negligible attenuation of the beam due to reflection losses. (Harrick, 1987).

Even though the light does not enter the second medium, an electric field of the radiation penetrates some distance into the less refractive material. This electric field is called the evanescent wave. Harrick (1987) describes the evanescent wave as an "unusual disturbance" that has the same frequency as the incident wave and its electric field amplitude decreases exponentially as it penetrates into the second medium. The distance the evanescent wave extends into the less refractive material is called the depth of penetration (d_p). Harrick (1987) defines the depth of penetration for incident radiation to be "the distance required for the electric field amplitude to fall to e^{-1} of its value at the surface." The depth of penetration depends on the RIs of the two media (n_1 and n_2), the angle of incidence (Θ), and the wavelength of the incident radiation (λ), based on the following equation:

$$d_p = \lambda / \left[2\pi \left(n_1^2 \sin^2 \Theta - n_2^2 \right)^{1/2} \right]$$

An important factor of this equation is the wavelength dependence. As the wavelength increases (and the wavenumber decreases), so does the depth of penetration. This wavelength dependence on the depth of penetration is an important distinction between ATR and transmission spectra. The peak positions are similar, but there are differences in peak intensities. ATR spectra, as compared to transmission spectra, will have lesser peak intensities in the high wavenumber region and more intense peaks in the lower wavenumber region. Although an ATR correction can be applied to correct for the path length variation at different wavelengths, it is best to compare an ATR spectrum with other ATR spectra and likewise for transmission spectra.

When the evanescent wave penetrates into the sample, the radiation interacts (or couples) with the sample in two distinctly different methods. The first coupling mechanism, which gives rise to frustrated total reflection (FTR), redirects some or all of the energy and thus there is no energy loss. FTR is concerned with changes in RI, and has a wide range of applications including the making of continuously variable beam splitters, measuring RI, light modulators, and angle sensing, however this coupling interaction does not generate ATR spectra. The second coupling mechanism is what gives rise to ATR spectra, and involves the absorption of energy by the sample. The absorbed energy may be converted to heat. As a result of this absorption of the evanescent wave, the reflected radiation is lessened, or attenuated, at the wavelengths corresponding to the sample's absorption bands. The resulting spectrum is a measurement of this attenuation.

"The interaction of the evanescent wave for total internal reflection with the absorbing rarer medium is expressed exactly by Fresnel's equations using a complex refractive index" (Harrick, 1987). Fresnel's equations demonstrate the laws governing the intensity and polarization of reflected radiation. The reflected intensity can be calculated using the Fresnel

equations for absorbing materials, displayed below for a reflected beam polarized parallel, R_s, and polarized perpendicular, R_p, to the plane of incidence.

$$R_p = \left| \frac{n_1 \cos\Theta - \left[n_2 - ik_2^2 - n_1^2 \sin^2\Theta \right]^{1/2}}{n_1 \cos\Theta + \left[n_2 - ik_2^2 - n_1^2 \sin^2\Theta \right]^{1/2}} \right|^2$$

$$R_s = \left| \frac{n_2 - ik_2^2 \cos\Theta - n_1 \left[n_2 - ik_2^2 - n_1^2 \sin^2\Theta \right]^{1/2}}{n_2 - ik_2^2 \cos\Theta + n_1 \left[n_2 - ik_2^2 - n_1^2 \sin^2\Theta \right]^{1/2}} \right|^2$$

In these Fresnel equations, n_1 is the RI of the internal reflection element (IRE), Θ is the angle of incidence, $n_2 - ik_2$ is the term for the complex RI of the second medium, and i is the square root of -1. Fresnel's equation can be interpreted in terms of the critical angle, where by there is a specific Θ angle, where no energy is transmitted into the second medium and instead all of the energy is reflected at the interface. For any angle greater than or equal to the critical angle, total internal reflection occurs and $R_S = R_P = 100\%$. (Harrick, 1987).

Harrick (1987) also states that although Fresnel's equations are useful for determining reflection losses, they "do not yield any physical insight into the absorption mechanism or into the interaction of the penetrating field with the absorbing medium." Harrick (1987) details four factors that determine the strength of coupling of the evanescent wave by an absorbing medium: (1) the depth of penetration, (2) the electric field strength, (3) sample area, and (4) RI matching (Harrick, 1987). These factors can be seen from the equation for the effective thickness (d_e) of the sample when the sample's thickness is much greater than the depth of penetration (d_p):

$$d_e = \frac{(n_2/n_1)E_0^2 d_p}{2\cos\Theta}$$

where E_o is the incident or initial electric field strength. With increased depth of penetration, electric field strength, and sample area (which is proportional to $1/\cos\Theta$), there is greater coupling. There is also greater coupling when the RIs of the two mediums are closer together (e.g. n_2/n_1 approaches 1). (Harrick, 1987).

An ATR accessory is required for the collection of ATR mid-IR spectra. The accessory, which can usually be fit into the sampling area of most IR spectrometers, requires the sample to be in contact with the IRE, which is a transparent crystalline material with a high RI (usually germanium, silicon, diamond or zinc selenide). The incident angle is fixed, and the radiation can undergo a single internal reflection or multiple internal reflections in the IRE before passing to the detector. With each internal reflection, the radiation is attenuated by the interaction of the evanescent wave with the sample. ATR mid-IR spectroscopy is commonly employed for the IR analysis of samples that are difficult to analyze by IR transmission spectroscopy, such as "solids of limited solubilities, films, threads, pastes, adhesives, and powders" (Skoog, 1998).

1.E. Chemometrics

Chemometrics means performing calculations on measurements of chemical data. More recently, the common usage of the word refers to the use of linear algebra calculations or multivariate statistical analysis methods, to make either quantitative or qualitative measurements

of chemical data, primarily spectra. Chemometric analytical techniques are very powerful tools for extracting relevant information from complex spectra.

There are three potential uses of chemometric analysis: exploratory analysis, regression or classification. Exploratory analysis, such as principle component analysis (PCA), seeks to discover possible outliers and reveal whether there are patterns or trends in the data. Regression analysis is used to predict related properties with the goal of developing a model that correlates the information in the set of known measurements to the desired property. Partial least squares (PLS) and principle component regression (PCR) are examples of chemometric algorithms for performing regression. Chemometric classification is the assignment of samples to predefined categories and predicting an unknown sample as belonging to one of several distinct groups. Canonical variate analysis (CVA) and partial least squares discriminant analysis (PLS-DA) are examples of chemometric classification techniques. (Camo Software AS, *Chemometrics,* 2010). This research uses chemometric analysis for both exploratory analysis and classification, thus PCA, PCA-CVA, and PLS-DA are used to analyze the glass spectra.

PCA is a statistical data reduction technique that examines the variance patterns in complex multidimensional datasets, often providing clear ways for visual comparisons by allowing interpretation to be done graphically. PCA represents the data with new latent variables that are linear combinations of the original variables. These linear combinations, called principal components (PCs), are calculated along the direction of maximum variance and perpendicular to each other. Although PCA permits a summarized visualization of the data set, its primary function is to reveal structure in the data. (N.D.K. Petraco, 2011; Petraco, 2011; Camo Software AS, *Chemometrics,* 2010; Rencher, 2002; Joliffe, 2002)

CVA (also called Fisher discriminant analysis, linear Fisher discriminant analysis and linear discriminant analysis) is a method to find a linear combination of features that characterize or separate two or more classes of objects or events. CVA seeks to characterize the ratio of between group variance to within group variance. CVA is similar to PCA in that both techniques look for interesting directions in space, however unlike PCA, CVA is a supervised classification technique because it requires that the data be labeled with their identity and fed into the algorithm as groups. These a priori labeled samples operate as a training set in order to compute the canonical variates (CVs), Geometrically, the data is projected onto axes, defined by CVs, that best separate the samples into discrete groups or clusters. (N.D.K. Petraco, 2011; Petraco, 2011; Rencher, 2002)

For PCA-CVA, the purpose of PCA is not necessarily to reduce the size of the dataset, but instead to remove the correlation of the variables (Jackson, 2003). CVA does not work with co-linear variables, thus performing PCA of the spectral data reduces the data to a set of orthogonal variables that are appropriate for CVA while still retaining the chemical information needed for classification (N.D.K. Petraco, 2011; Petraco, 2011).

PLS-DA is a method for sharpening the separation between groups of data, by rotating PCA components such that a maximum separation among classes is obtained. Like CVA, PLS-DA is a supervised discrimination technique. The theory behind PLS-DA is to find an (approximate) linear relationship between experimental (explanatory) variables and group labels (response variables) in order to maximize group separation. PLS-DA is a popular chemometric technique for spectroscopic data because it works well with highly correlated variables. (N.D.K. Petraco, 2011; Camo Software AS, *PLS-DA*, 2010).

CHAPTER 2: REVIEW OF THE LITERATURE

2.A. Methods for Forensic Glass Analysis

Forensic glass examinations have been reported in the scientific literature for more than seventy years (Tryhorn, 1939). These examinations began with comparisons of physical and optical properties, and have evolved over the last forty years to include determinations of chemical composition.

There are three possible goals of forensic glass examination: classification, discrimination, and individualization. Classification of glass is defined as "the placement of a specimen into a particular product-use or manufacturer source category based upon the comparison of measured attributes with a database of known attributes for each category. Examples of classes include sheets, containers, light bulbs, tableware; or Libby-Owens-Ford, Pilkington, Corning; or float line A, float line B from a given manufacturing plant" (SWGMAT, 2005a). Discrimination is defined as "the ability to distinguish between two glass objects in the same class based on comparison of their measured attributes" (SWGMAT, 2005a). Individualization is the determination that a particular sample is unique, even amongst members of the same class. Individualization "may also refer to the demonstration that a questioned piece of physical evidence and a similar known sample have a common origin" (De Forest, Gaensslen, and Lee, 1983).

Prior to performing a forensic glass comparison or analysis, one must identify that the sample is indeed glass. There are several materials that can be mistaken for glass, however there are laboratory tests that forensic scientists use to identify a material as glass. These include the observance of conchoidal fractures (a break with surfaces that are irregularly curved and often striated) and amorphous structure, reaction to a hotpoint, measurement of relative

hardness, microscopy (glass is isotropic), and spectroscopy (Bottrell, 2009; Koons et al., 2002). Although there are some materials that can have some of these same properties, there are no known materials that mimic all of the same properties as glass. (Bottrell, 2009).

2.A.a. Physical Properties

No two objects can break exactly the same way every time (De Forest, Gaensslen, and Lee, 1983). The breaking of glass involves random processes which cause unique topological features on the fracture surfaces. Physical matching (also called a physical fit) is the association of the two sides of the fracture surfaces, and is considered the most incontrovertible evidence possible. The physical matching of two or more broken glass fragments (from commercially produced glass, e.g. container, automotive, and architectural) is the only forensic glass analytical method that is considered to establish an individualization of glass evidence as it enables an association of known and questioned glass fragments to the exclusion of all other sources (SWGMAT, 2005c; Bottrell, 2009). In the absence of a physical match, there are several physical properties that can be measured for the forensic analysis of glass, such as surface features, thickness, color, curvature, density, and optical properties (fluorescence, phosphorescence, cathodoluminescence, RI, and dispersion).

Surface features of glass can be useful for the comparison of known and questioned fragments, as they can be created either intentionally or accidentally during various stages of manufacturing, fabrication or during the product's end use (SWGMAT, 2005e; Bottrell, 2009; Koons et al., 2002). During a physical match examination, surface features can be useful marks for individualization and comparison. SWGMAT identifies three types of surface features: coatings, manufacturing features, and post-manufacturing surface features. Included in the

coatings category are thin films and mirrored backings. The thickness of coatings can vary from nanometer to micrometer thicknesses. Coatings and thin films are generally applied to the nonfloat side of flat glass, but can be on the float side or both sides. They are applied to automotive and architectural glasses for a variety of purposes such as increased strength, solar shading, and aesthetics (SWGMAT, 2005e). Coatings are not usually apparent to the naked eye nor through a light microscopy examination, and thus often require more sophisticated instrumentation for both recognition and comparison. Some instrumental techniques for the identification of coatings include transmission electron microscopy, scanning electron microscopy, differential interference contrast microscopy, atomic force microscopy, X-ray diffraction, X-ray fluorescence, and FT-IR spectroscopy (SWGMAT, 2005e; Bottrell, 2009; Koons et al., 2002). The tin layer that is produced during the float process is a surface feature that can be identified by its fluorescence, and will be discussed later in this chapter. Manufacturing features can be either intentional, such as etching, frosting, and texturing, or accidentally made via the manufacturing process, such as mold marks, ream (defined by ASTM C162-05 (2010) as "layers of glass that are not homogeneous within the main body of the glass"), rouge pits (defects due to polishing) or polish lines. Glass that is made from a mold, such as some container glass, has a texture like that of an "orange peel", which is quite distinct. These surface features can be useful for the identification of the manufacturing process which can aid in the classification of the glass evidence. Post-manufacturing surface features are unintentional and can include scratches, abrasions, and pitting, as well as unrelated materials stuck to the glass (such as dirt and debris). The latter surface features can be compared with a stereomicroscope, and any adhering material should be documented, analyzed, characterized and

preserved (if possible) in order to evaluate its evidentiary value. (SWGMAT, 2005e; Koons et al., 2002).

Flat and slightly curved glass products can be readily differentiated by thickness measurements, however both original parallel flat surfaces of the glass must be present. Glass samples encountered in forensic casework are often very small and do not possess the original surfaces. However, when they do then thickness measurements provide a simple means for comparison. Glass manufacturers tightly control the thickness of glass products, on the order of thousandths of an inch (Bottrell, 2009). ASTM lists the tolerances for flat glass on the order of +/- 0.25 mm (ASTM C10360-06, 2006) but Koons et al. (2002) have observed much lower tolerance ranges in casework samples. A micrometer or caliper with a precision of at least +/- 0.02 mm is used to measure the thickness of flat glass (SWGMAT, 2005e; Bottrell, 2009; Koons et al., 2002). Multiple locations for thickness measurements on a known pane of glass are important to determine if there is significant variations, such as with an automobile's curved windshield (SWGMAT, 2005e; Koons et al., 2002). When a questioned and known fragment of glass have statistically significant differences in thickness or the questioned fragment's thickness is outside the range for that of the known, it can be determined that they do not share a common source (SWGMAT, 2005e; Bottrell, 2009; Koons et al., 2002).

The color of glass is a useful and common property for preliminary differentiation, however it is often a more difficult comparison to make than one might expect. In the Collaborative Testing Services, Inc. (CTS) Forensic Testing Program's 2008 report, 74% of the 116 participating laboratories used color as a criteria for discriminating between questioned and known fragments in forensic glass comparisons. Glasses can be made in almost any color, and even the most colorless glass does in fact show a slight color (Koons et al., 2002). Figure 9

shows some of the most common colors of glass fragments found in casework, which includes clear colorless, clear light green, clear green, clear light blue, blue, clear blue green, brown, clear light grey, medium grey, and dark grey. The color is affected by the sample size and illumination, thus equal sized fragments should be used for side-by-side comparisons over a white surface. The glass fragment is viewed from its edge in order to assess the true color of the glass un-interfered with by a coating or thin film. Tints can also be distinguished with the aid of fluorescent and incandescent lights. Glass fragments are often too small or do not have enough color density for colorimetric analysis. Glass examiners must be careful when using color for exclusion because small differences in color can exist within a single glass object. Known and questioned glass fragments with significant differences in color can be excluded from coming from a common source. (SWGMAT, 2005e; Bottrell, 2009; Koons et al., 2002).



Figure 9: Photograph of ten different colored glass fragments (clear colorless, clear light green, clear green, clear light blue, blue, clear blue green, brown, clear light grey, medium grey, and dark grey). These represent the most common colors found in forensic glass casework. (*Printed with permission from Scott Ryland, FDLE)*

Measurement of the curvature or flatness of glass can be useful to differentiate a questioned and known fragment. This information can also potentially determine the broad product type of a questioned fragment, such as identifying a fragment as coming from flat or container glass. Large fragments can be analyzed with a stereomicroscope, whereas small fragments require interferometric measurements (SWGMAT, 2005e; Bottrell, 2009; Koons et al., 2002; Locke and Zoro, 1983; Locke and Elliott, 1984). Locke and Zoro (1983) studied the surfaces of bulk and casework sized glass fragments with a light microscope, monochromatic illumination, and an interference objective (an attachment consisting of a conventional objective combined with a micro interferometer). Interferometry is quite sensitive and as a result the occurrence of minute surface scratches or slight curvature of a surface has a significant effect on the appearance of an interference pattern. Locke and Zoro reported that the interference bands of curved glass show curved parallel lines whereas the interference fringes of flat glass (both float and non-float) are straight parallel lines. Using this information, container glass can be readily distinguished from flat window glass. In addition, irregular surface features such as patterned glass and 'orange peel' surfaces from molds produce intricate interference patterns that can be used for comparative analysis between questioned and known glass fragments. The authors concluded that this technique is ideal for forensic applications where subtle surface features could provide valuable additional evidence. Locke and Elliott (1984) expanded the study of interferometric measurements to window, container, tableware, and vehicle glasses. The authors found that objects with curved surfaces (tableware and containers) produced fragments that were almost always detectably curved while those from surfaces of both modern and old windows were clearly identified as flat. Additionally, the degree of curvature can be measured to further differentiate between different container glasses. Stereomicroscopic and interferometric analysis

of curvature is an inexpensive, quick, and relatively simple means of forensic glass analysis for both comparisons and identification of general product class.

The use of density comparisons was one of the first methods used in forensic glass examinations as demonstrated via its description in the earliest reports on forensic glass analysis (Tryhorn, 1939). It must be noted that early comparative glass analyses details the use of specific gravity rather than density (Tryhorn, 1939; Kirk and Russel, 1941; Gamble et al., 1943; Beeman, 1945; McCall, 1948; Kirk and Dollar, 1949), and although the two properties are often used interchangeably, they are not the same. Specific gravity, also known as relative density, is a physical property that is defined as the ratio of the mass of a solid or liquid to the mass of an equal volume of distilled water at 4°C. There are two primary types of glass density analysis, the density gradient column method and the sink/float method (SWGMAT, 2005b; Bottrell, 2009; Koons et al., 2002).

The density gradient column method is used for the comparison of a known and questioned fragment of glass by observing the fragment in a tube containing a liquid with a gradient of densities (Kirk, 1951; SWGMAT, 2005b; Bottrell, 2009; Koons et al., 2002). The glass fragments are suspended (neither sink nor float) when they reach the liquid with the same density. Therefore, if the questioned and known fragments are suspended at the same level, then it is determined that they have the same density. Koons et al. (2002) detail the problems associated with making absolute density determinations using a density gradient column, which include the difficulty in making uniform gradients, the inability to reuse a density gradient column because the gradient is changed when recovering glass fragments, and the time and space requirements for making and storing of density gradient columns. It is for these reasons that

more crime laboratories prefer the sink/float method of glass density determinations and comparisons.

The sink/float method can be used for both comparative and absolute density determinations (SWGMAT, 2005b; Bottrell, 2009; Koons et al., 2002). The sink/float method is similar to the density gradient method in that a glass fragment (or both the known and questioned fragments, although not usually together) is put into a tube with a liquid, and the fragment's rise, fall or float is monitored. Float refers to neutral buoyancy where the fragment remains suspended without rising or sinking. The difference between the two methods is that in the sink/float method the liquid is not a gradient and instead is a constant density solution made from two miscible liquids. The density of the solution is controlled by the addition of either of the two liquids until the glass fragments stay suspended in the tube. The tube is placed in a constant temperature bath because small changes in temperature will alter the density of the liquid (Tryhorn, 1939; Beeman, 1945; SWGMAT, 2005b; Bottrell, 2009; Koons et al., 2002). Traditional density determinations required the use of toxic solvents, typically bromobenzene and bromoform. However, recent developments have replaced these with the use of nontoxic, water-soluble tungsten salt (sodium polytungstate) and varying the concentration of the salt in order to control the density of the solution (Koons et al., 2002). Koons et al. (2002) report that the sink/float method is capable of detecting density differences as small as 5×10^{-5} g/cm^3, thus making it a very sensitive method of analysis. However, because the variation of density across a pane of glass can exceed this sensitivity, multiple fragments of the known glass sample must be analyzed to determine the range of density within the source (Koons et al., 2002). In comparative density determinations, if both the questioned and known fragments are suspended in the same mixture at the same temperature, then they have the same density. Tryhorn (1939)

describes this comparative method of glass analyses, however he suggested the use of different solvents--bromoform or methyl iodide and alcohol. For an absolute density determination, the density of the liquid in which the glass fragment is suspended is measured, traditionally by a pycnometer (Kirk and Russel, 1941), but current measurements are made with either by an analytical balance and plummet or by a density meter. Kubic, Galgan and Gillis (1975) compared the precision of absolute density determinations when employing either a pipet or a pychnometer, and found that the using the pychnometer had better results despite being more time consuming. They also stated that a specific gravity balance would provide the greatest discrimination power, but the density balance is the preferred method (when compared to using a pychnometer or pipet) for absolute density determinations of glass. Beveridge and Semen (1979) found that the precision of a digital density meter is 1×10^{-4} g/cm^3. The digital density meter measures the density of a suspending liquid mixture and consists of an analytical balance capable of accurately determining weights within 0.0001 g with a tall weighing chamber and a plummet that must sink in the liquid with a density above 2.6 g/cm^3. (SWGMAT, 2005b; Bottrell, 2009; Koons et al., 2002; Beveridge and Semen, 1979).

There are several disadvantages to the practice of density determinations that have contributed to its decline in use by trace evidence examiners. The first is the size requirement of the glass fragments (at least 5 mg or 2-3 mm in diameter), which prohibits its use on many casework samples that are smaller than this minimum size. In addition, the glass fragment must be meticulously clean and free of inclusions for accurate density determinations. Furthermore, the use of toxic solvents makes this procedure undesirable, despite the recent availability and application of safer chemicals. Last, the analysis of glass by other methods, specifically RI determination and elemental composition which have been shown to have better discriminating

power (Chapter 3.B), have replaced density determinations. (SWGMAT, 2005b; Bottrell, 2009; Koons et al., 2002). Despite these disadvantages, density determinations are still used by many forensic science laboratories, which is demonstrated by the Collaborative Testing Services, Inc. (CTS) Forensic Testing Program's 2008 report which showed that 32% of the 116 participating laboratories use this technique for forensic glass analysis.

2.A.a.i. Optical Properties

The fluorescence of glass is a property that has been described for use in forensic glass examinations in the earliest literature on the subject (Tryhorn, 1939). Tryhorn (1939) reported that fluorescence examinations with UV light were a routine test because of the simplicity and rapidity of this analysis. However he recognized that it was of limited discriminating power because glasses with similar compositions have indistinguishable fluorescent colors. The fluorescent color of most glasses is a brownish-violet, but the colors can vary to include black, brown, violet, purple, green, and blue. Tryhorn also recognized that increased discrimination could be achieved if the emitted fluorescence was measured spectroscopically.

The modern day use of fluorescence for forensic glass examinations is as an initial screening tool and is primarily used for the identification of float glass (Koons et al., 2002; Bottrell, 2009; SWGMAT, 2005e). Both short-wave (254 nm) and long-wave (350 nm) UV light are used in sequence to illuminate the questioned and known fragments simultaneously while they are side-by-side on a non-fluorescent background. The tin layer of float glass fluoresces yellow, thus allowing for its detection. It has been reported that some glass coatings also show fluorescence (Bottrell, 2009). Fluorescence throughout the bulk of the glass is also

still used for discrimination, and is caused by the presence of certain elements such as uranium in chrome-green glass (Koons et al., 2002; Bottrell, 2009).

Lloyd (1981) measured the excitation and fluorescence emission spectra of glasses and demonstrated its use for the discrimination of float glasses. Fluorescence spectra were obtained with conventional spectrometers from glass surfaces varying in area, with fragments as small as 0.05 mm^2 and 18 μg. Lloyd found that there are three fluorescence emissions of float glass, with the main emission being a very broad band at ~490 nm when excited at 280 nm. This fluorescence is from the tin layer of float glass. The second emission is possibly from arsenic, lead, and antimony, and is superimposed on the tin emission. This corresponds to an excitation in the 260 nm region. The third excitation occurs at 340 nm, with the corresponding emission peak at 375 nm, was also found in the fluorescence of nonfloat glass. As a result, this was called the "bulk" fluorescence. The nonfloat glass surface also showed an emission closely comparable to the major float surface emission (~490 nm with a 280 nm excitation), but at 15% of the float glass surfaces' intensity. The author showed that the emissions from the two surface emissions are qualitatively undifferentiated but can be clearly distinguished by the difference in intensity. Lloyd also found that there was negligible correlation between the tin fluorescence intensity and any RI feature. Lloyd concluded that float surface fragments could be unambiguously differentiated from other surface fragments by their fluorescence excitation and emission spectra.

Calloway and Jones (1978) showed that the phosphorescence component of the photoluminescence of glass could be used for the discrimination of glasses. The authors detail the advantages of phosphorescence, which include its low cost, high discriminating ability, small sample size (a minimum of 1 mg), and non-destructive nature. The authors found that the use of phosphorometric techniques enable the avoidance of some of the problems encountered in

fluorometric work on solids, however, the luminescence characteristic of float glass is a relatively prompt emission and must be treated as fluorescence for the purpose of its measurement. Calloway and Jones found that the phosphorescence spectrum of all glass samples consists of two principal bands (740 and 550 nm) with variable intensities. The authors used the ratios of the intensities of the two bands for discriminating among samples that could not be differentiated by RI, with further discrimination of 17 of 21 glass samples. Despite the successful discrimination of glasses by phosphorescence shown by Calloway and Jones, crime laboratories have not implemented this technique for the forensic analysis of glass.

Cathodoluminescence (CL) has recently been researched for the forensic analysis of glass (Stoecklein and Gobel, 1992; Palenik and Buscaglia, 2007; Bell et al., 2009). CL is the light (visible or near visible) emitted by a sample as a result of electron bombardment. The source of excitation required for CL is an electron beam or probe. This can be an electron gun in a vacuum chamber that is placed on the stage of a PLM or through a scanning electron microscope with a CL detector (D.K. Purcell, personal communication, March 5, 2012). The advantages of CL include the relatively low cost of instrumentation for the PLM with the electron gun accessory (approximately $50,000) in comparison to a SEM with CL detector (greater than $200,000) (D.K. Purcell, personal communication, March 5, 2012), its nondestructive nature, and ease of operation. Its current limitations for forensic glass discrimination are the lack of databases and standards, and the relatively low resolution of typical CL spectra (Bell et al., 2009). Stoecklin and Gobel (1992) published the first study on the CL of glass, and showed that the tin layer of the float surface could be distinguished from the nonfloat surface. Palenik and Buscaglia (2007) confirmed this work of Stoecklein and Gobel, and also showed that the nonfloat surface is more complex than the float surface because it showed a weak luminescence that appeared to be a

combination of a weak Sn^{2+} signal and the bulk glass. The nonfloat surface can be uncoated or coated with one or more nanolayers of a coating such as SnO_2, TiO_2, or Cr-spinel, none of which were shown to luminesce by CL. The analytical difficulty is that the coating is thinner than the electron penetration depth. As a result, the CL signal also originated from the bulk glass. Additionally, the nonfloat surface may also contain traces of Sn^{2+} from tin vapor over the bath in the float process. Bell et al. conducted a feasibility study on the use of CL for glass discrimination, and specifically applied the methods of forensic color analysis to the CL colors of glass. Bell et al. concluded that the results were encouraging and warrant continued research. The use of CL for forensic glass discrimination shows promise, but more research is required prior to its usage in casework by trace evidence examiners.

Measurement of RI is one of the oldest and most common techniques for forensic glass examinations and comparisons (Tryhorn, 1939; Koons et al., 2002; SWGMAT, 2005d). In the Collaborative Testing Services, Inc. (CTS) Forensic Testing Program's 2008 report, 92% of the 116 participating laboratories measured the RI of the questioned and known fragments, thus making RI measurement the most frequently employed technique for forensic glass examinations. The measurement of RI is often the first choice for glass comparisons because it only requires a minute sample amount and is a non-destructive method. However, most microscopic based measurement methods of RI require modification of the sample if it is too large because the glass fragment must be crushed.

There are a variety of microscopical techniques for measuring the RI of a glass fragment, all of which are immersion methods. The general procedure involves placing a glass particle into a liquid, observing the particle and liquid interface under a microscope, and then varying the composition of the liquid, the temperature and/or wavelength of light until the match point is

reached. The match point is defined by SWGMAT (2005d) to be "any combination of temperature and wavelength, at which two media have indistinguishable RIs. At the match point the glass will exhibit minimum contrast and visibility." Immersion methods include Becke line immersion, dispersion staining, single (or temperature) variation, Emmons double variation and automated glass RI measurement.

The Becke line method and dispersion staining are considered to be screening techniques for glass comparisons because neither technique is sensitive enough for establishing a positive association (Koons et al., 2002; SWGMAT, 2005d). The Becke line method involves determining the relative RI of the glass fragment to that of an immersion oil by observing the movement of a bright halo (called the Becke line) as the focus of the microscope is changed. The illumination can be white light however more precise measurements can be achieved when using monochromatic light (usually 589 nm). Different oils are used until the match point is reached or bracketed between two oils. Dispersion staining involves using a dispersion staining microscope objective and observing the colors on the edges of the glass particle in different immersion oils. In dispersion staining, two particles have the same RI at a specific wavelength of light if their match wavelengths are the same in a given immersion oil. The advantages of these techniques are that they are rapid and have minimal equipment requirements. The disadvantages include difficulty with recovering the fragments and cleaning them between liquids, extensive training for proper use of the dispersion staining technique, limited sensitivity (only to 1×10^{-3}), and the error associated with changing temperature (SWGMAT, 2005d).

In the early writings on forensic glass analysis, the Becke line method was not used for screening but for RI comparisons and determinations. Tryhorn, (1939) and Gamble, Burd, and Kirk (1943) describe using the Becke line method of comparative RI analysis, where the

questioned and known glass fragments are mounted and the movement of the Becke line is observed simultaneously. Gamble, Burd, and Kirk (1941) analyzed 100 randomly collected glass fragments using the Becke line method and were able to successfully differentiate all samples by their RI. They also determined that using the Becke line method, relative RIs can be determined to about +/- 5 X 10^{-4}, with sources of error being evaporation and variations in temperature. In 1956, Davis proposed a simplified method of glass comparison by the Becke line method in conjunction with the Christiansen effect (bright colored fringes or "halo" effect when nearing the matching RI of the immersion oil and the fragment). Davis (1956) found that this technique was simpler, more rapid and had an accuracy of 1 X 10^{-3} or better.

Ojena and De Forest (1972) proposed an improved method for the determination of RI for forensic glass comparisons that is known as the single (or temperature) variation method. Using this method, glass RI determination is based on the change of RI with temperature which varies for different materials. The glass fragment is immersed in an appropriate oil, and the temperature of the oil and glass is raised (using a hot stage on a phase contrast microscope) until the match point is reached at a specific wavelength of visible light (most often the sodium D line). The difference in RI (n) as a function of temperature (T) is dn/dT, with typical dn/dT of casework glass samples being on the order of 10^{-6} /°C and 10^{-4} /°C for most immersion oils (Koons et al., 2002). Ojena and De Forest (1972) determined that this technique is capable of measuring RI differences as small as 4 X 10^{-5}. McCrone (1974), using the single variation method, measured RIs of small glass fragments to within +/- 1 X 10^{-4}, which he wrote was smaller than the variation observed within most glass objects. More recent literature reveals that the precision of this method has been determined to be 1 X 10^{-5} (Cassista and Sandercock, 1994b) or 2 X 10^{-5} (Koons et al., 2002).

The Emmons double variation method is similar to the single variation method, however, both the temperature and wavelength of incident visible light are varied. The procedure for the Emmons double variation method involves mounting the glass fragment in a suitable immersion oil on a hot stage of a phase contrast microscope, heating the sample to within the stable range of the immersion oil, and then finding the match point by adjusting the wavelength of light. This procedure is repeated for at least three temperature values, and the data are then used to calculate or graphically determine (using a Hartmann net) the RI of the glass at nD, nC, and nF. The advantages of the Emmons double variation method are its rapidity of measuring RIs at multiple wavelengths and its precision of 4×10^{-5} to 6×10^{-5} (SWGMAT, 2005d; Cassista and Sandercock, 1994b). SWGMAT (2005d) identifies only one limitation to this method: it is not able to differentiate between glass samples from different sources with RI differences less than 1×10^{-4}. Heideman (1975) details three factors that play an important role in the accuracy and precision of the computed values of the RI obtained from the examinations using Emmons double variation method: the experience of the analyst performing the Becke line observations, the immersion oil used, and the manual construction of the curve through the points on the Hartmann net to obtain the calculated values of the RIs of the glass. Heideman (1975) showed that using a computer program to calculate the values for nD, nC, and nF instead of plotting the dispersion curve manually using a Hartmann net improved the reproducibility of the results obtained from using the Emmons double variation method.

The automated glass refractive index measurement (GRIM) instrument manufactured by Foster + Freeman is based on the single variation method with a phase contrast microscope. The advantages of the automated GRIM is its precision (2×10^{-5} or 3×10^{-5}, depending on the reference), the automatic generation and recording of RI, the removal of operator fatigue and

subjectivity, and its corresponding increase in reproducibility. ASTM E1967-98 (2003) states that the precision, as measured by the standard deviation, is 2×10^{-5} over 5 hrs and 3×10^{-5} over 5 days. In addition, there is no bias since the measurement of the sample is a direct comparison to the standard reference glasses used (ASTM E1967-98, 2003). The disadvantages include the need to keep the equipment scrupulously clean, the increased time associated with determining RIs at various wavelengths (such as that required for the calculation of dispersion), and the inability to differentiate between glasses with RI differences less than the precision of the instrument (SWGMAT, 2005d; Koons et al., 2002). Newton and Buckleton (2008) reported that the variability of the RI values is increased when fragment edge morphology becomes unsuitable for phase contrast microscopy, where an unsuitable edge can occur when the fragment is too thick, has a rough edge, or when there is strain in the glass. This is another potential pitfall of the automated GRIM.

There has been significant research into the variation of RI across (x- and y-axis) and through the thickness (z-axis) of glass, mostly focused on sheet glass (Davies, Dudley, and Smalldon, 1980; Underhill, 1980; Locke and Hayes, 1984; Zoro et al., 1988; Bennett et al., 2003; Newton et al., 2004). These studies showed that the variation across sheet glass was observable, but there were no systematic differences in RI across one pane of float glass (Locke and Hayes, 1984; Bennett et al., 2003). However, of particular interest is a phenomenon known as the surface RI effect, whereby the RI of the float surface/tin contact surface is higher than the bulk and the nonfloat surface is lower than the bulk. Most of the RI variation in the z-axis arises as a result of structural stress in the sheet. Thus, the float glass surface shows an anomalous RI result when immersion method RI determinations are made on the outermost layer of the glass. Underhill (1980) concluded that the surface RI effect could also be used to identify float glass

with certainty. Locke and Hayes (1984) showed that the surface RI effect is not exclusive to float glass, although it is most dramatically seen with float glass, because container glass also displayed variations across the thickness of the samples. Newton et al. (2004) investigated the effect of the surface RI effect on the probable distributions of RIs of the recovered glass given a range of casework type scenarios involving breakage and backscatter. As a consequence of the surface RI effect, a much larger variation in RI might be expected when float glass is encountered in casework, especially when surface fragments are over represented in the recovered glass sample. They discovered that the inclusion of surface fragments from the float surface of glass can have a profound effect on the comparison of questioned and known glass samples. The effect was most severe when the float side is facing the breaker because the properties of surface fragments from non-float glass samples are very similar to those of bulk fragments. In particular, Newton et al. found that the inclusion of a few surface fragments, even post grouping, was sufficient by itself to explain the observed differences in variance of RI between questioned and known groups. Newton et al. stated that surface fragments, if present, were likely to be treated as outliers and to be deemed as non-matching. The findings of Newton et al. challenge routine glass examination procedure and suggest that knowledge of which surface is facing the striker is valuable information in interpretation.

The distribution of RIs in the population of glass is of particular concern for forensic scientists when determining the significance of glass evidence, thus it has been the subject of research. Lambert and Evett (1984) analyzed the RI data collected on control glass samples submitted for examination in routine casework over a seven year time period. They determined that different types of glass have different RI distributions and that the distribution is changing with time. The most encountered class of forensic glass evidence, float glass, had RIs in the

range of 1.5165-1.5185 (Lambert and Evett, 1984). Koons and Buscaglia (2001) investigated the variation of the distribution of RI values using the FBI database. They compared the distribution of the RI values among flat glass from 1964-1979 with the distribution from 1980-1997. Koons and Buscaglia observed that the distribution of samples around the most frequently observed values are much narrower in the post-1980 samples than for those received prior to 1980. The observed narrowing of the spread among RI values has supported the necessity of using more discriminating methods, such as elemental analysis, that can be used to compare fragments of the glass having indistinguishable RI values.

The variation of RI across and through a pane of glass requires a forensic glass analyst to be concerned with the number of control glass fragments to analyze when performing a comparison. Sandercock (2000) compiled the RI data for four types of flat glass (toughened float glass, non-toughened float glass, non-float glass, and wired glass) in order to determine the number of control glass samples that should be analyzed. Sandercock suggested that, as a guideline, a minimum of seventeen RI measurements should be made when sampling a toughened float glass control, and a minimum of nine RI measurements must be made when sampling a non-toughened float glass control.

In 2011, Garvin and Koons published their research that evaluated eight different match (or test) criteria for the comparison of RI of glass fragments. This is a significant topic in the forensic glass examiner community because the authors discovered that there was no standard match criteria used in crime laboratories. Thus it is important to understand how different match criteria affect error rates. The test criteria compared were based on ranges, fixed intervals and multiples of standard deviations of the known source measurements. The authors did not attempt to determine which match criteria is best, because that depends on what other tests are being

conducted (i.e. if a more discriminating test is also being performed, a greater number of Type 2, or false inclusion, errors would be acceptable because RI determination would be treated more as a screening tool) and thus is "an ethical and administrative decision that has to date been up to each individual forensic laboratory or examiner".

Dispersion of glass can offer increased discrimination compared with RI at a single wavelength of light, although its value has been the subject of debate (Koons et al., 2002). Koons et al. (2002) report that dispersion can potentially offer increased discrimination for nonfloat glass samples. However, research by Slater and Fong (1982), Locke et al. (1986), and Cassista and Sandercock (1994b) indicates that dispersion offers little, if any, improvements over RI data obtained at nD with the single variation method. As a consequence of these studies, many forensic science laboratories do not calculate the dispersion for glass evidence.

The annealing procedure is used to increase the discrimination power of RI. SWGMAT (2005d) defines annealing as "the process of reducing residual strain in glass by controlled heating and cooling". The annealing process is based on a controlled slow cooling of glass fragments in specific temperature ranges, after prior heating to a selected temperature. The cooling during the annealing process should be slower than the cooling in the manufacturing process, except for optical glass because they are cooled very slowly during manufacturing. Annealing requires a slow cooling because slow cooling keeps the glass in a semi-liquid state, which allows changes in glass structure and thus releases structural strain. The resulting annealed glass (with the exception of optical glass) will have a greater RI and density than the original. Annealing is a non-destructive method, but it does change the glass that prevents repeat RI determinations. The disadvantages of annealing are that the process is labor intensive and time consuming. However, annealing is recommended by SWGMAT (2005d) when the known

and questioned glass fragments' RIs are indistinguishable because it can determine if the two fragments have similar thermal histories.

Locke, Sanger, and Roopnarine (1982) were the first to publish on the use of annealing for forensic glass examinations. The authors studied the identification of toughened glass by annealing, and showed that toughened glass could be completely discriminated from non-toughened glass using the annealing technique. However, their study showed a lack of reproducibility because of the slight differences in thermal environment within the muffle furnace experienced by the individual crucibles. Although Locke, Sanger, and Roopnarine showed that annealing was useful for identifying toughened glass, it could not provide additional discrimination between glasses of the same initial RI (except where one was toughened and the other was not). They suggested that additional discrimination could be possible with more careful and controlled annealing.

Locke, Hayes, and Sanger (1984) focused on improving and optimizing the annealing procedure, and tested the design of equipment and thermal routines, which included 5 parameters: the upper annealing temp, the time of holding the upper temp, the lower annealing temp, the time of the annealing process, and the cooling rate. The authors also recommended the use of a programmable furnace to control the temperature and a metal block to provide a uniform temperature.

Locke, Winstanley, Rocket, and Rydeard (1985) continued the refinement of the annealing method, using a mini-tube furnace with a programmable temperature controller and tested this equipment using the short 1-hour schedule against the muffle furnace with the overnight schedule used in previous reports by Locke. The authors showed excellent correlation between the 2 methods, but the absolute change in RI from the muffle furnace were always

greater than that for the mini-tube furnace. This was attributed to the different cooling rates for the 2 routines. The short 1-hour method was deemed the preferred approach because of the time savings and same precision. The authors suggested the use of annealing mainly for classification purposes

Winstanley and Rydeard (1984) were the first to use a shortened annealing schedule (less than 1 hour) by using a mini-tube furnace with a programmable temperature controller. The authors also introduced the relationship between the original thickness of a glass object and the change in RI value after annealing of small fragments. In 1985, Winstanley and Rydeard showed that the improved discrimination between glasses offered by annealing was limited to toughened, non-toughened and old windows, but not float glass.

Locke and Hayes (1984) devised a "short schedule" for annealing. The magnitude of the change of RI (ΔRI) subjected to the annealing "short schedule" has been shown to be useful for classification of glass fragments. When the "short schedule" is used, a ΔRI greater than +1 X 10^{-3} is indicative of tempered glass, less than +8 X 10^{-4} is indicative of annealed glass, between the ΔRI values for tempered and annealed glass falls heat-strengthened glass and some windshield glass, and a negative ΔRI is indicative of "an almost perfectly annealed glass, such as optical glass" (SWGMAT, 2005d).

Locke and Rocket (1985) studied the potential for greater discrimination between glasses using both the increased homogeneity displayed by annealed glasses and the change in RI. The authors suggested that annealing could be successfully used for further discrimination of glass fragments, beyond classification or identification of toughened glass.

Ryland (1986) reported on the value of source-type classification for small fragments of glass, and demonstrated the utility of annealing for discriminating between tempered and non-tempered glass. The author studied thirty window glasses, and classified most of them as tempered or non-tempered by the annealing process. However, Ryland discovered that only 3 out of 8 laminated glass samples, using an annealing procedure, fell into the tempered classification. In a later publication (Ryland, 1991), the author re-determined the samples and they fell into the non-tempered region. The cause of this 'misclassification' was the "crude method employed" (annealed in uncapped porcelain crucibles without the aid of a programmable muffle furnace or a stainless steal annealing block). The samples were re-determined using a more refined method (using an annealing block and controlled cool down of the furnace) and the data revealed them to be non-tempered. This demonstrated the importance of a careful and controlled method for annealing.

Marcouiller (1990) proposed an alternative schedule for the annealing procedure. The author recommended a long annealing schedule (28.5 hours) to ensure the correct and entire temperature, rate, and time program was run by the annealing equipment. Using this long schedule, toughened and non-toughened glass types were completely separated and all laminated samples fell into the non-tempered class. Marcouiller also recommended annealing mainly for classification purposes.

Cassista and Sandercock (1994a) studied the correlation between the change in RI and the change in density of glass after annealing. As expected, there was a high correlation. The authors recommended the use of the change in RI over the change in density because of the greater precision and the ease of measurement. Cassista and Sandercock also cautioned against using the change in RI values to discriminate between glass samples of the same type and having

similar RI values prior to annealing, thus indicating the use of annealing for classification purposes only.

Newton, Kitto, and Buckleton (2005) reviewed of the use of annealing in forensic glass casework and verified the usefulness of annealing as a supplementary technique in forensic glass examinations. The authors recommended that a continuous approach to the interpretation of data from annealing is better than the classification approach.

Pawluk-Kolc, Zieba-Palus, and Parczewski (2008) studied the RI distribution across toughened float glass, specifically architectural and automotive windows, both before and after annealing. The authors examined the variability of RI across a car windscreen and a windowpane, and then investigated the effect of re-annealing on this variability. The authors also sought to determine if the change in RI can be used for discrimination of two different types of toughened glass. The authors determined that the mean RI was significantly higher and the standard deviation was lower after annealing for both glasses. Furthermore, the distributions of RIs were not normal for either set (before or after annealing). The authors concluded that the difference in the values for the change in RI for both objects was not significant and thus it is not a good parameter to differentiate between two toughened glass objects. In addition, Pawluk-Kolc, Zieba-Palus, and Parczewski attempted to classify 181 glass samples on the basis of the RI and change of RI. The authors reported that there was increased discrimination when using both RI and change in RI. The authors found that the change in RI can be useful because the change of RI value can be significantly different for different glass samples and because after annealing the standard deviation of RIs is smaller. The authors concluded that annealing should mainly be used for classification purposes or identification of toughened glass, however annealing might be

successfully used for further discrimination of glass fragments, beyond classification or identification of toughened glass.

Rushton et al. (2011) studied the effect of annealing on the variation of glass RI over both a toughened (or tempered) and non-toughened pane of float glass. The authors used Bayesian statistical hierachical modeling and found that annealing increased the variability in RI for the non-toughened glass by a factor of 1.29 – 1.58 and for the toughened glass by a factor of 0.63-0.76. The authors also confirmed previous work that showed that there were observable, but not systematic differences in RI across both panes of glass.

2.A.b. Chemical Composition

Tryhorn (1939) wrote about the use of chemical composition in the first report on forensic glass analysis. However at that time, the procedure for obtaining a complete chemical analysis was too laborious, time consuming, and required too much material for it to be a realistic tool for the forensic glass examiner. In addition, physical and optical examinations were sufficient for discriminating between glasses. In the present day, advances in the quality of glass manufacturing technology, specifically improvements in quality control, have made discrimination, such as identification of the suspected source, more difficult. This is because the range of densities and RIs has narrowed within glass subtypes. As a result, the elemental analysis of glass has emerged as an important technique for glass analysis. Glasses from the same subtype may have the same gross elemental composition, but can have different trace and ultra-trace elemental signatures. SWGMAT (2005a) states that forensic glass examination using elemental analysis is potentially able "to differentiate among glasses made by different manufacturers, glasses from different production lines of a single manufacturer, specific

production runs of glass from a single manufacturer, and in some instances individual glass objects produced at the same production facility." Glass manufacturers control the concentrations of several elements to impart certain end-use properties to a specific product, and as a result these can be used to classify the product type of a questioned fragment. Despite this intentional control of element concentrations, there are variations with the manufacturer's acceptable ranges that can be used for discrimination. In addition, trace element concentrations are not generally controlled, with the exception of those used as colorants or those that can alter the physical or optical properties of the glass. The deviations in concentrations of trace elements can be used to differentiate glasses when the variation among objects exceeds the variation within each object. (SWGMAT, 2005a).

The elemental analysis of glass for forensic discrimination was documented as early as 1970 (Schmitt and Smith, 1970). Several instrumental techniques were originally investigated for the forensic discrimination of glass, such as neutron activation analysis (NAA) (Schmitt and Smith, 1970; Caldwell, 1972; Coleman and Goode, 1973), spark source mass spectrometry (German, B., Scaplehorn, 1972; Dabbs et al., 1973; Butterworth et al., 1974), atomic absorption spectrometry (AAS) (Fuller and Whitehead, 1974; Hughes, Catterick and Southeard, 1976), and Emission Spectrography (Blacklock et al., 1976), however these instrumental methods have largely been replaced by other methods of elemental analysis which provide increased discrimination, require smaller sample sizes, are less destructive, and/or are less laborious. The most commonly used techniques for elemental analysis are scanning electron microscopy-energy dispersive X-ray spectrometry (SEM-EDS), X-ray fluorescence spectrometry (XRF), inductively coupled plasma-optical emission spectrophotometry (ICP-OES) (also known as inductively coupled plasma-atomic emission spectrophotometry, ICP-AES), and inductively coupled plasma-

mass spectrometry (ICP-MS) (SWGMAT, 2005a). Although each technique has its strengths, each is limited by one or more of the following: sample size requirements, whether or not the technique is destructive, level of reliable detection and quantitation, sensitivity, linear concentration range, ability to control matrix effects and interferences, accuracy, precision, multi-element capability, cost of instrumentation, operator expertise required, or analysis time (Buscaglia, 1994; Almirall, 2001).

In scanning electron microscopy (SEM), an electron beam is scanned across a sample's surface. When the electrons strike the sample, a variety of signals are generated, and it is the detection of specific signals that produce an image or a sample's elemental composition. The three signals that provide the greatest amount of information in SEM are the secondary electrons, backscattered electrons, and X-rays. The first two provide visual information about the sample's morphology and the X-rays supply elemental information. X-rays are emitted via the interaction of the primary beam with atoms in the sample that cause inner shell transitions. The emitted X-ray has an energy and wavelength characteristic of the parent element, and it is the detection and measurement of this energy or wavelength that permits elemental analysis. The identity of the elements is identified by the wavelengths or energies of the emitted X-rays, and quantitative analysis of the elements uses the intensities of the peaks in the spectrum. There are two methods for X-ray detection that are defined by the manner in which the data are collected and displayed: wavelength dispersive X-ray spectrometry (WDS) and energy dispersive X-ray spectrometry (EDS). Although WDS offers better spectral resolution, lower levels of detection, and more reliable quantitative analysis than EDS, the increased cost and complexity of instrumentation have limited its use in forensic science laboratories (SWGMAT, 2005a; Kubic, 2002). As a

result, an SEM is most often paired with EDS for forensic elemental analyses. EDS provides rapid qualitative or, with adequate standards, quantitative analysis of elemental composition.

SEM-EDS has been used both for product-use classification and discrimination among sources (Keeley and Christofides 1979; Terry, Riessen, and Vowles, 1982; Ryland, 1986; Zadora, Brozek-Mucha, and Parczewski, 2001a; Zadora, Brozek-Mucha, and Parczewski, 2001b; Kubic, 2002; SWGMAT, 2005a). Zadora, Brozek-Mucha, and Parczewski (2001a) propose a classification scheme for glass by means of quantitative elemental analysis using SEM-EDS using the concentrations of aluminum, barium, calcium, iron, lead, magnesium, potassium, sodium, and zinc. The authors studied six categories of glass (car windows, car headlamps, external glass of car bulbs, internal glass of car bulbs, external glass of ordinary light bulbs, internal glass of ordinary light bulbs, and window sheets). Their presented approach led to the correct classification of most of the 153 glass samples studied with the exception of car windows and ordinary windows which revealed the same qualitative and very close quantitative elemental composition. Zadora, Brozek-Mucha, and Parczewski (2001b) then used chemometric cluster analysis to differentiate glass objects with similar qualitative and quantitative elemental contents, and were able to distinguish between car windows and ordinary windows.

SWGMAT (2005a) outlines the advantages and limitations of SEM-EDS for forensic glass analysis. The most important advantages of SEM-EDS is that it is nondestructive, applicable to very small samples, and many forensic laboratories already have the instrumentation because it is used for other forensic examinations. The most significant limitation of SEM-EDS is that precise and accurate quantitative determination of element concentrations is difficult because of the irregular shape and small size of forensic glass fragments. SEM-EDS has poor concentration detection limits, typically in the 0.1 percent range,

which limits the number of elements that can be quantified. Thus, several elements, such as barium and strontium, that are used for classification and source discrimination, are present in most glasses at concentrations that are not detectable using SEM-EDS. Additionally, the differences in elemental concentrations that are quantifiable by SEM-EDS will, in most instances, manifest themselves in readily distinguishable RI and/or density values. (SWGMAT, 2005a).

XRF is the emission of characteristic "secondary" (or fluorescent) X-rays from a material that has been excited by bombarding with high-energy X-rays. The elements present in the sample are identified by the energies or wavelengths of the detected X-rays and are quantified by their intensities. Similar to SEM with X-ray detection, there are two XRF spectrometry methods that are characterized by the way that the data is collected and displayed: wavelength dispersive (WDXRF) and energy dispersive (EDXRF). EDXRF has become the preferred method for forensic science laboratories over classic XRF instruments (WDXRF) because of its lower cost, ease of use, and applicability to smaller and irregularly shaped samples (SWGMAT, 2005a).

EDXRF has been used both for product-use classification and discrimination amongst sources (Reeve, Mathiesen, and Fong, 1976; Dudley et al., 1980; Howden, Dudley, and Smalldon, 1977; Howden, Dudley, and Smalldon, 1978; Ryland, 1986; SWGMAT, 2005a). Reeve, Mathiesen, and Fong (1976) used EDXRF for the semiquantitative analysis of 81 window glass samples of different origins. Using the element intensity ratios, they were able to successfully discriminate all but two of the 81 samples. Dudley et al. (1980) used EDXRF to discriminate between glass sources with indistinguishable RIs, and by using the element ratios to calcium, the glasses from 49 of the 50 pairs of samples of window and non-window origin were differentiated. Ryland (1986) was able to correctly classify 93% of glass fragments as

originating from either sheet or container glass by their element intensity ratios as determined by EDXRF.

SWGMAT (2005a) outlines the advantages and limitations of XRF for forensic glass analysis. The advantages of XRF are that it is rapid, nondestructive, fairly sensitive, and can be performed with minimal sample preparation. XRF also has lower limits of detection than SEM-EDS because it has a lower background signal and for heavier elements the cross section is greater for X-rays than electrons. Its most significant limitation is the need for using matrix-matched multi-element standards in order to obtain accurate quantitative results. In addition, using X-ray tubes at high powers may cause the discoloration of some glass samples. XRF is also less spatially discriminating than SEM-EDS because it has a larger beam size. However this higher special discrimination is seldom used because SEM-EDS uses a large raster size.

Hicks et al. (2003) used neural networks and linear discriminant analysis (LDA) using qualitative and semi-quantitative data to assess the potential of micro-XRF (μXRF) for the classification of glasses according to their respective origin and the differentiation among glasses with similar RI. Micro-XRF is non-destructive, rapid, and applicable to very small (0.3-0.5mm or 50-200 μg) fragments. The authors analyzed 119 windows collected from crime scenes, and the results showed that with RI it was possible to distinguish 6892 pairs, and out of the other 129 remaining pairs (not differentiated by RI), 112 were distinguished with μXRF. The product-use classification resulted in 5.4% error using LDA with leave-one-out, with the classes being containers, windows, light-bulbs, eye-glasses, headlamps, and vehicle window panes.

Nakanishi et al. (2008) assessed the applicability of synchrotron radiation high-energy XRF (SR-XRF) for the forensic discrimination of glass fragments. The authors state that traditional XRF's are not sensitive enough for the quantitative analysis of trace elements in glass,

but SR-XRF is more sensitive and thus could be useful. Nakanishi et al. determined that SR-XRF has a picogram lower limit of detection for barium, cerium, and samarium, and a 10 picogram lower limit of detection for strontium, zinc, tin, and hafnium. The most significant problem with using SR-XRF for the forensic discrimination of glass is that it is difficult to get beam time, however it is often free of charge. The authors conclude that SR-XRF could provide an effective approach to the nondestructive discrimination of small glass fragments in the field of forensic science.

Falcone, Sommariva, and Verita (2006) compared the use of three X-ray techniques for the forensic analysis of glass: WD-XRF, SEM/EDS, and wavelength-dispersive electron probe microanalysis (EPMA). The authors studied and compared the analytical sensitivity and accuracy of the various X-ray techniques for the analysis of small commercial glass fragments, with the final goal being the classification of glass by end-product and the discrimination between known and questioned samples. Falcone, Sommariva, and Verita conclude that WDXRF provides accurate analysis of major and minor components using glass beads prepared with at least 50 mg of powdered sample, with limits of detection for 50 mg samples ranging from 120 ppm for strontium, lead and copper oxides to 800 ppm for barium and zirconium oxides. For 200 mg samples, the limits of detection decreased and ranged from 30 ppm for strontium, lead and copper oxides to 200 ppm for barium and zirconium oxides. EPMA and SEM/EDS provide accurate analyses of the main components of embedded and polished glass particles down to 0.30 mm size, with limits of detection of 250-500 ppm by EPMA and 500-1000 ppm by SEM/EDS. The authors conclude that WDXRF is the preferred method of elemental glass analysis.

Both ICP-OES and ICP-MS techniques rely on an inductively coupled plasma to atomize, ionize, and excite the sample atoms. Almirall (2001) states that ICP methods provide the most information of all the elemental analysis methods. The inductively coupled plasma is initiated by an electrical discharge in a flowing stream of inert gas, usually argon, and then stabilized by a surrounding radio frequency field. The plasma appears as a small, constant glowing flame, with temperatures in the range of 7,000-10,000K. When the excited ions and atoms travel to lower temperature portions of the plasma, they drop to lower excited states and emit electromagnetic radiation at characteristic wavelengths that are used to identify the element(s) present. In an ICP-OES, a spectrophotometer disperses the emitted radiation and measures the intensity. Quantitative analysis is achieved by comparison of the emission intensities of a sample with those of standard solutions. ICP-MS uses the inductively coupled plasma torch as an ionization device, and the mass spectrometer isolates and detects the ion. There are several types of mass spectrometers, including quadrupole, time-of-flight, and magnetic-sector design with single or multiple electron multiplier detectors.

There are two primary methods for introducing glass samples into the ICP: (1) dissolution and nebulization or (2) direct solid sampling. In the dissolution procedure, glass samples weighing 0.2 to 8 mg are digested in high purity hydrofluoric acid (HF), nitric acid (HNO_3) or hydrochloric acid (HCl) (Catterick and Hickman 1981; Koons, Fiedler, and Rawalt, 1988; SWGMAT, 2005a). SWGMAT (2005a) details a standard procedure for dissolution that requires destruction of the sample and is labor and time intensive (sample preparation requires several days). Glass analysis via dissolution is performed with both ICP-OES and ICP-MS instruments. Conversely, direct solid sampling is more commonly used with ICP-MS than with ICP-OES. Laser ablation (LA) is used for direct sampling where a laser vaporizes a small

portion of the glass sample and it is swept into the ICP-MS. LA sampling results in the creation of small craters that are approximately 50 μm in diameter and 80 μm in depth (Trejos and Almirall, 2005b). LA sampling requires an instrument with a rapid scanning speed, thus it is paired with an ICP-MS that allows measurement of transient signals (SWGMAT, 2005a). LA sampling simplifies elemental analysis because it eliminates the need for extensive sample preparation, increases the speed of analysis, has minimal sample destruction and contamination, and extends elemental analysis to much smaller sized samples. The major disadvantage of LA is that it is very expensive, which precludes its use in many forensic laboratories.

SWGMAT (2005a) outlines the advantages and limitations of ICP-OES for forensic glass analysis. The most significant advantages of ICP-OES are its multielement analysis capabilities, long linear response ranges, the limited number of spectral and matrix interferences, low detection limits (0.01 to 0.1μg/g in glass) for many elements of interest, high precision (better than 2% relative standard deviation), and ease of automation of data handling. However, for small samples (less than 5mg), detection limits are slightly increased because of increased dilution factors. The limitations are that the dissolution of glass fragments is destructive, requires the use of corrosive acids and high purity reagents, and sample digestion is time-consuming compared to sample preparation for XRF, SEM-EDS, and LA-ICP-MS. In addition, the ICP-OES is expensive, requires more extensive operator training, and there are a limited number of forensic applications.

The first usage of elemental analysis with ICP-OES was the classification of glass into their product end-use categories (SWGMAT, 2005a). Catterick and Hickman (1981) developed a method for classification of glass with ICP-OES using the concentrations of five elements (manganese, iron, magnesium, aluminum, and barium). Hickman (1981) and Hickman,

Harbottle, and Sayre (1983) added additional elements for quantitative analysis, and classification into nine product categories was determined using a six to ten element classification scheme. According to SWGMAT (2005a), and based on the work of Koons, Fiedler, and Rawalt (1988), the most widely used protocol for forensic glass analysis uses the quantitation of ten elements (aluminum, barium, calcium, iron, magnesium, manganese, sodium, titanium, strontium, and zirconium), although sheet and container glass can be differentiated with a combination of five of these elements. Wolnik, Gaston, and Fricke (1989) used ICP-OES to associate food containers to the manufacturing plants in which they were made and to identify sources of contaminant glass in cases involving product tampering.

There has been considerable research on the use of ICP-OES for the discrimination of glasses within a product category. Koons, Fiedler, and Rawalt (1988) demonstrated how ICP-OES elemental analyses of nine elements can be statistically analyzed (using PCA and clustering) to correctly differentiate 180 of 184 samples and even to classify each sample into the correct manufacturing plant. Koons, Peters, and Rebbert (1991) measured the concentrations of 10 elements in automobile side-window glasses, and determined that the probability that two glasses from different vehicles would be indistinguishable was reported to be one in 1,080, compared with one in five for RI alone and one in ten for EDXRF spectrometry analysis alone. SWGMAT (2005a) reported that research showed that ICP-OES could differentiate between sheets of glass produced within minutes of each other in a single float-glass production line. Koons and Buscaglia (1999a and 2002) analyzed casework samples of glass with ICP-OES measurements of ten elements, and the authors reported that a very small likelihood exists for failing to discriminate between glass fragments from different sources, regardless of the matching procedure or significance level used. The authors analyzed 209 unrelated glass

specimens, and at a 95% confidence level, reported that there were only two type II errors made in 21,736 comparisons (0.009%) when using the equal variance t-test for comparison of sample means (Koons and Buscaglia, 2002). Thus, Koons and Buscaglia demonstrated the high discriminating power of ICP-OES measurements.

SWGMAT (2005a) outlines the advantages and limitations of ICP-MS for forensic glass analysis. The advantages of ICP-MS are similar to ICP-OES in that it is able to analyze a wide range of elements, has long linear response ranges, the limited number of spectral and matrix interferences, low detection limits (0.01 to 0.1μg/g in glass) for many elements of interest, high precision (better than 2% relative standard deviation), and ease of automation of data handling. ICP-MS has greater sensitivity and better detection limits than ICP-OES, thus ICP-MS enables the analysis of smaller fragments and additional elements that provide more points of comparison that potentially improves discrimination. ICP-MS is able to measure multiple isotopes of the same element that can potentially detect isotopic variations among sources or be used with the isotope dilution method for improved accuracy of element quantitation. The addition of LA as a sampling method for ICP-MS offers the rapid and direct determination of element concentrations in solid samples with minimal sample destruction and contamination. The limitations to the implementation of ICP-MS in forensic laboratories are "the high cost of instrumentation and laboratory support, the high level of operator training required, and the large time requirements for sample and standard preparation and analysis". ICP-MS also has poorer precision than ICP-OES, with the precision measurements for all elements when present in the middle of their respective concentration ranges generally equal to 10 percent or less relative standard deviation. Another significant limitation of ICP-MS is the increased risk of contamination because of its higher sensitivity and multielement capabilities, thus requiring strict

control of analyte elements during sample preparation and analysis. There are problematic interferences when using a quadrupole MS which are both well-known and difficult to correct, and these prohibit accurate quantitation of a few elements. High-resolution spectrometers or collision cell technology can remove some interference effects, particularly isobaric mass overlaps, however these are expensive and complicate instrument operation.

Zurhaar and Mullings (1990) were the first to use ICP-MS for forensic glass analysis. The authors evaluated the use of ICP-MS for its applicability to the characterization of window glass fragments, having identical RIs, and of the type that are frequently presented as physical evidence to a forensic laboratory. Zurhaar and Mullings analyzed samples with weights as small as 500 μg, and determined that sensitivity of ICP-MS using acid digestion had detection limits below 0.1 ng/mL. The authors analyzed 7 glass samples that were statistically indistinguishable by RI, and identified a group of 15 elements in window panes that could be used for discrimination among glasses. They were able to accurately quantitate the concentrations of 48 elements with a relative standard deviation of equal to or less than 4%. The authors stated that by quantitating 25 elements, the results of the discrimination test can then be considered unquestionable, with discrimination levels of 85-95%.

Parouchais et al. (1996) performed extensive investigation of ICP-MS analysis of glass with two purposes: (1) to find a suitable digestion procedure for glass that minimized interferences, loss of elements in the form of volatile salts and permitted use of a quartz sample introduction system, and (2) to investigate the applicability of ICP-MS to the forensic analysis of glass. The authors focused on the ability to discriminate glasses with matching RI, the ability to analyze small fragments (<1 mg), and determining the minimum volume that could be used for sample nebulization. The authors reported that a preparative scheme of HF:HNO_3:HCl in 2:1:1

ratio allowed the analysis of up to 62 elements via ICP-MS, minimizing interferences and analyte losses. Parouchais et al. used analysis of variance (ANOVA) to determine the variance components of 57 elements attributable to time (day to day), dissolution (sample to sample), calibration, and instrumental (internal) variance. The evaluation of the elements in terms of precision and accuracy resulted in a list of 45 elements with the greatest potential for discrimination. The authors successfully differentiated glasses of similar RI by comparing element concentrations and element ratios (e.g. strontium/barium). The advantage of using element ratios is that samples do not need to be weighed, thereby simplifying the analysis procedure. The authors determined that the smallest glass fragment that could be analyzed was estimated to be of the order of 100 μg for headlamp glass and 200 μg for container and sheet glass. The authors concluded that ICP-MS is a sensitive, accurate, and precise technique for the analysis of trace elements in glass, with detection limits on the order of ng/g level and analytical precision in the range of 1-5% RSD for most elements based on the analysis of 5 mL of a 1 mg/mL glass solution.

Duckworth et al. (2000) performed ANOVA on ICP-MS analyses of glass fragments to identify the source and magnitude of variation in elemental concentration determinations and to evaluate the accuracy in the multielement analysis. The authors studied 68 isotopes representing 57 elements in a NIST glass standard, and found that 40 isotopes representing 36 elements were shown to have good precision (RSD <10% and s<3 μg/g) and accuracy/small bias (relative bias <10%) and thus have the potential for being a highly discriminating tool. The authors made a list of potentially discriminating elements to be used for the development of an elemental concentration database for float glasses, with the final list consisting of 59 isotopes, representing

46 elements. Those not having both good precision and accuracy were critically examined before inclusion in the list of discriminating elements.

Duckworth et al. (2002) studied 76 automobile side windows with ICP-MS, that had previously been studied with ICP-OES, with two purposes: (1) to identify the elements with the greatest potential for discriminating float glass fragments sampled from a small population of vehicle side windows (using ANOVA), and (2) to compute the relative discriminating power of RI, ICP-OES, and ICP-MS. The authors used ANOVA analysis of ICP-MS to select 11 elements (barium, cerium, cobalt, cesium, hafnium, neodymium, rubidium, strontium, thallium, yttrium, and zirconium) for discriminating among the glass samples. The authors concluded that element quantitation using either ICP-OES or ICP-MS can significantly increase the discrimination of glass samples over RI measurements alone. The authors determined that ICP-OES has the advantage of measuring elemental concentrations with good precision but has a practical limitation on the number of elements that can be analyzed, and ICP-MS has the advantage of measuring a large number of elemental concentrations including different isotopes but has the limitation of reduced accuracy and precision due to required serial dilutions for measuring the major elements.

Recently, there have been a number of investigations into the use of LA sampling for ICP-MS (LA-ICP-MS) elemental glass analysis. Trejos and Almirall (2004) investigated the effect of fractionation on the forensic elemental analysis of glass with LA-ICP-MS. Fractionation is defined as "the phenomenon that produces a stoichiometry of laser products that is not representative of the sample composition", and poses one of the major challenges to using LA for in-situ trace elemental profiling of glass evidence. Trejos and Almiral concluded that although low levels of fractionation were found in the majority of the elements evaluated, the

small bias that can result from possible fractionation does not affect the precision and therefore does not significantly affect the quantitative analysis of glass. Trejos and Almirall (2005a and 2005b) investigated sampling strategies for the analysis of glass fragments by LA-ICP-MS, specifically looking at the micro-homogeneity of glass and the effect of sample size and sample shape. Trejos and Almirall (2005a) determined that float glass is homogeneous even at the micro-range level (200 ng) thus demonstrating the applicability of LA-ICP-MS as an alternative technique for the elemental analysis of glass. However, the variation of elemental composition of headlamps and containers (wine and beer bottles) is larger over the source than the instrumental variation due to inherent heterogeneity, thus sampling should be completed on the known from the top, middle, and bottom area of a container. The authors also concluded that the tempering process does not affect the elemental composition within glass fragments and is thus not a concern for forensic comparison. Trejos and Almirall (2005b) showed that there is no significant difference in the elemental composition of different sized fragments, and as a result the quantitative analysis of glass with internal standardization is possible for glass samples as small as 0.1 mm in length. The authors noted that their results could not be generalized for fragments measuring less than 0.2 mm by 0.1 mm.

The development and evaluation of a standard method for the quantitative determination of elements in glass samples by LA-ICP-MS has been investigated by Latkoczy et al. (2005) and Berends-Montero et al. (2006). Latkoczy et al. evaluated the results of four interlaboratory tests and concluded that for the analysis of forensic glass fragments it is essential to follow a dedicated LA optimization protocol. However, since the operating conditions of various LA-ICP-MS systems are so significantly different, matrix matched float glass calibration standards are required to produce comparable concentration values. The authors also determined that for

LA-ICP-MS to become a routine forensic technique, further studies must be carried out on the effects of a number of parameters, including instrumental variations. Berends-Montero et al. used ten elements (potassium, titanium, manganese, rubidium, strontium, zirconium, barium, lanthanum, cerium, and lead) in their LA-ICP-MS method. The authors determined that the method could be used for fragments 1 mm^2 with limits of detection in the order of μg/g and precision and accuracy <10 % for most of the measured elements. The authors determined the limit of detection and limit of quantitation values for all 10 elements that ranged from 0.2 μg/g (for strontium, lanthanum, and cerium) to 17 μg/g (for titanium) and 0.7-57 μg/g, respectively. Berends-Montero et al. also studied the heterogeneity of actual float glass panes, and defined the matching criteria for overlapping of intervals as concentration values of +/- 2 standard deviations.

Bajic et al. (2005) investigated the use of multivariate statistics for the analysis of LA-ICP-MS data. The authors studied LA-ICP-MS data with PCA of 26 glass samples, and determined that the significant advantage of using PCA to compare samples is the elimination of the need for elemental calibration and matrix-matched standards. PCA is essentially a pattern-matching analysis and does not rely on calibration of the spectra to known concentrations. This reduces the need for expensive, hazardous, and costly materials and procedures for analysis. A second advantage is the elimination of bias due to pre-selection of elements. The statistical comparison will determine which elements are significant for elimination or inclusion in the analysis. Bajic et al. demonstrated the usefulness of analyzing LA-ICP-MS data by PCA and concluded that by using PCA, the forensic scientist is able to perform a quantitative statistical comparison, which yields confidence intervals, for positive association of a questioned glass sample based on its trace elemental composition.

Trejos, Montero, and Almirall (2003) compared the discrimination potential of LA-ICP-MS previously reported solution ICP-MS methods using external calibration (EC) with internal standardization and solution isotope dilution (ID) method for the analysis of two different glass populations (headlamp and automotive glasses). A total of 91 different glass samples were used for the comparison study, and besides elemental composition, RI was also measured. The authors report that although the solution sample introduction methods using EC and ID presented excellent sensitivity and precision, these methods have the disadvantages of destroying the sample, and also involve complex sample preparation. For the 45 headlamp glasses (990 comparisons) analyzed, there were 44 (4.4%) and 21 (2.1%) undistinguishable pairs with EC-ICP-MS and LA-ICP-MS, respectively. When combined with RI analysis, there were 8 (0.8%) and 0 (0%) undistinguishable pairs with EC-ICP-MS and LA-ICP-MS, respectively. The RI alone had 102 undistinguishable pairs from the headlamp glasses. For the 46 automobile glasses (1035 comparisons) analyzed, there were 43 (4.2%) and 7 (0.7%) undistinguishable pairs with EC-ICP-MS and LA-ICP-MS, respectively. When combined with RI analysis, there were 27 (2.6%) and 3 (0.3%) undistinguishable pairs with EC-ICP-MS and LA-ICP-MS, respectively. The RI alone had 494 undistinguishable pairs from the automobile glasses. Trejos, Montero, and Almirall conclude that the LA method is preferred because it is simpler, faster, reduces contamination, is less destructive, does not require hazardous solvents, and produced comparable discrimination to the EC-ICP-MS and ID-ICP-MS.

Castro et al. (2008) investigated the analytical performance of high resolution sector field ICP-MS (HR-SF-ICP-MS) and quadrupole ICP-MS equipped with a dynamic reaction cell (DRC-ICP-MS) for the detection of iron in glass in terms of accuracy, precision, and method detection limits. This study was instigated because standard ICP-MS instruments suffer from

polyatomic interferences including $^{40}Ar^{16}O^{+}$, $^{40}Ar^{16}O^{1}H^{+}$, and refractory oxide $^{40}Ca^{16}O^{+}$ that compromise measurements of trace levels of $^{56}Fe^{+}$ and $^{57}Fe^{+}$, for example. This is a drawback in the analysis of glass fragments because iron had been previously identified as a good discriminating element. The authors also compared the results of conventional acid-digestion with LA sample introduction methods, with LA resulting in lower detection limits. Castro et al. determined that iron polyatomic interferences were reduced or resolved by using the DRC-ICP-MS and HR-SF-ICP-MS, with detection limits as low as 0.03 μg/g when LA sampling was employed. An advantage of DRC-ICP-MS is that it is less expensive and easier to use than HR-SF-ICP-MS. However, a significant limitation of DRC-ICP-MS is that it is limited to analysis of a few elements in the DRC mode because suppression of interferences is chemically dependent and other interferences that affect the analysis could be formed in the DRC. As a result, this limitation requires separate measurements for iron and for the other elements typically used in glass comparisons, because the transition from DRC to non-DRC mode is not fast enough for transient signals, thus using DRC would be time consuming and require more samples.

One of the most significant obstacles preventing LA-ICP-MS from being employed in forensic laboratories is the cost. The cost of equipping a laboratory with LA-ICP-MS is approximately $500,000, which includes the instrument, a special clean room and experienced users. Consequently, LA-ICP-MS is not the elemental analysis technique of choice for most forensic science laboratories. (Bush, 2011).

In the last five years there have been several studies about the applicability of using LIBS for the elemental analysis of glass (Bridge et al., 2007; Barnett, Cahoon and Almirall, 2008; Rodriguez-Celis et al.; 2008). LIBS is an atomic emission technique that involves focusing a high-power, short-pulse laser (usually in the nanosecond range) on a sample surface. A very

energetic plasma results that is rich in electrons, atoms, and ions. The plasma radiation, characteristic of the elements present in the sample, is observed and analyzed with a spectrophotometer. The advantages of LIBS for the elemental analysis of glass are that it is nearly non-destructive, requires little to no sample preparation, analysis time is only a few minutes, and provides multi-element analysis with low absolute detection limits (parts per million). A significant advantage of LIBS is that instrumentation is inexpensive, thus it provides an elemental analysis method that is affordable to most state and local crime laboratories. The disadvantages of LIBS are its poor precision (5-10%) relative to other elemental analytical techniques, matrix and spectral interferences, and its lower discriminating power and detection limits than LA-ICP-MS. In addition, LIBS is a very new analytical technique, and as of April 2011, only three forensic laboratories possess a LIBS instrument (Bush, 2011). Barnett, Cahoon and Almirall (2008) studied the effects of irradiation wavelength, ablation rate, and emission intensities on the analytical performance of LIBS for the elemental analysis of glass samples (5 NIST glasses and 6 automobile glasses). The authors concluded that the amount of material removed via LIBS is significantly influenced by the irradiation wavelength. Barnett, Cahoon, and Almirall determined that the 266 nm laser was more effective in mass removal and produced improved precision as compared to the 532 nm laser, however the emission from the 532 nm laser-produced plasma was found to be higher than that of 266 nm. The authors concluded that 266 nm is the preferred laser wavelength for the LIBS analysis of transparent glass samples due to the better precision, improved laser-to-sample coupling, and adequate intensity at the laser fluence (laser energy per area). Rodriguez-Celis et al. (2008) investigated the ability to identify glass fragments from their unique LIBS spectral "fingerprints" by using statistical correlation methods (linear and rank correlation techniques). The authors analyzed ten fragments from

seven automobile glasses (side and rear windows), and achieved 100% correct identification (95% confidence level for a type 1 error) by linear correlation when combined with a spectral mask (which eliminates regions of the spectra containing several intense lines common to all samples). Using the LIBS spectral "fingerprint" was advantageous because there was no need for quantification or calculation of intensity ratios.

Naes et al. (2008) compared LA-ICP-MS, μXRF spectroscopy, and LIBS in terms of discrimination power for a glass sample set consisting of 41 fragments from 14 different vehicles. The authors conclude that all methods are capable of excellent discrimination, with greater than 99% discrimination achieved for all techniques. Naes et al. also compare the three techniques based on several figures of merit. μXRF is easy to use, nondestructive, instrumentation is moderately expensive (~$120,000), provides semi-quantitative analysis, has fair to good precision (5-10% RSD), good sensitivity (100 ppm), very good to excellent discrimination, and analysis time is approximately 30 minutes per analysis. LA-ICP-MS is difficult to use, almost non-destructive, instrumentation is the most expensive, provides quantitative analysis, has excellent precision (<5% RSD), excellent sensitivity (<1 ppm), excellent discrimination, and instrument analysis time is approximately 3 minutes per analysis. LIBS is very easy to use, almost nondestructive, instrumentation is moderately expensive ($50,000-$150,000), provides semi-quantitative analysis, has fair to good precision (5-20% RSD), good sensitivity (10-50 ppm), very good to excellent discrimination, and analysis time is approximately 30 seconds per analysis. Naes et al. report that LIBS is a viable alternative to LA-ICP-MS and μXRF for use in the forensic laboratory because of its many advantages, most notably the reduced complexity, high sample throughput, good sensitivity, reduced cost of the instrumentation, and same discrimination ability of the other elemental methods.

2.B. Discrimination by Combined Analytical Methods

There has been significant research on the correlation between and increased discrimination provided by analyzing glass samples with multiple analytical methods. The advantages of using multiple techniques for glass analysis has been known since the beginning of forensic glass examinations, with Tryhorn (1939) detailing numerous methods including specific gravity, RI, hardness, color, UV fluorescence, and thermal analysis. Although Tryhorn did not determine the discrimination power or correlation between using multiple methods of analysis, there have been a plethora of subsequent studies with that goal.

The correlation between RI and density (or specific gravity) has been investigated for nearly seventy years. Gamble, Burd, and Kirk (1943) measured and compared the RI and specific gravity of 100 samples of glass, collected at random, and concluded that "each glass studied was distinguishable from all others, even though there is a definite parallelism between the two properties." The authors observed the correlation by plotting the specific gravity versus RI, however this did not preclude the increased discrimination provided by measuring both properties. Gamble, Burd, and Kirk also concluded that "specific gravity was not as valuable in distinguishing glass samples as was the refractive index" because all of the samples were able to be differentiated by RI alone but not all were able to be differentiated by density alone.

The correlation between RI and density has been the subject of numerous other investigations, including Cobb (1968), Dabbs and Pearson (1970), Dabbs and Pearson (1972), and Stoney and Thornton (1985). All of the research confirmed the existence of a correlation between RI and density. Stoney and Thornton (1985) examined the relationship between density and RI in order to identify considerations that may lead to conceptual errors in the interpretation of provenance. The authors argue for the necessity of an absolute determination of both RI and

density, as opposed to comparative determinations, for the proper forensic interpretation of glass evidence data. The authors recognize that when both properties are measured in a large number of samples, a high correlation between the two properties is apparent, as is evident from a study of 577 samples of window glass data from the FBI resulting in a correlation coefficient of 0.93. There are two potential conclusions derived at because of this correlation: (1) there is sufficient deviation from perfect correlation to justify the determinations of both density and RI, or (2) there is limited additional discrimination when both properties are measured and thus, only one should be used. Stoney and Thornton dismiss the second view because the high correlation does not in itself render the second property useless for individualization, nor does it imply that the second determination rarely provides additional discrimination. The authors conclude that although there is high correlation over the population, measuring one property does not determine the other, and thus Stoney and Thornton advocate the use both density and RI for forensic glass examinations.

Kirk (1951) proposed an analytical scheme for the forensic discrimination of glass. Kirk advocated comparing the density of a questioned and known fragment first using a density gradient tube, followed by comparative RI determination using the Becke line method rather than absolute RI determination.

Slater and Fong (1981) used statistical analysis of probabilities to evaluate the value of density, RI, and dispersion for identifying the source of glass samples. The authors concluded that density has the greatest differentiating power of the three parameters tested with a differentiating power approximately six times greater than that of RI when using equal thresholds of discrimination. In addition, Slater and Fong determined that dispersion offers little,

if any, improvement over RI. The authors conclude that density and RI together have a slightly greater discriminating power than density alone.

Koons, Peters, and Rebbert (1991) compared the discriminating power of elemental and optical analysis techniques. The authors compared ICP-OES, RI, and EDXRF on a sampling of 81 tempered sheet glasses and concluded that the highest degree of differentiation was achieved using ICP-OES. The authors determined that EDXRF was slightly more discriminating than RI but not as discriminating as ICP-OES.

There have been several proposed analytical schemes for the classification of glass that combines RI measurements and elemental analysis. Keeley and Christofides (1979) and Ryland (1986) advocate an analytical scheme that combines measurement of calcium/magnesium intensity ratios obtained using SEM-EDS with calcium/iron ratios obtained using XRF to classify glass fragments into sheet and container categories. Koons, Fiedler, and Rawalt (1988) used Ryland's scheme on 184 container and sheet glasses, and reported an 83% correct classification, with only a 51% correct classification rate for sheet glass. In a follow-up report, Ryland and Koons (1991) amended the conclusions of Koons, Fiedler, and Rawalt revealing a correct classification rate of 96% an inconclusive rate of 4%, with a 92% correct classification rate for sheet glass. Hickman (1981) proposed using RI and ICP-OES elemental data of five elements (manganese, iron, magnesium, aluminum, and barium) for the glass classification by the application of multivariate statistical procedures. Hickman analyzed 349 glass samples, and classified them into four categories (windows, vehicle, container, and tableware), and produced a rate of successful definite classifications of 91% with no wrong classifications. Almirall et al. (1998) used the RI and elemental concentrations of nine elements (aluminum, barium, calcium, iron, magnesium, manganese, strontium, titanium, and zirconium) as obtained from ICP-OES for

classifying glass into four product-use categories (headlamp glass, container glass, non-vehicle window float glass, and vehicle float glass). The authors used Fisher's linear discriminant modeling for the differentiation of the four glass types but concluded that further discrimination was not possible within a product-use category. Zadora (2009) analyzed 153 glass objects (23 building windows, 25 bulbs, 32 car windows, 57 containers, and 16 headlamps) by SEM-EDS and RI (before and after annealing), and concluded that the combination of these techniques was able to successfully classify all of the glass samples when using either likelihood ratios, support vector machines, and naïve Bayes classifiers. Zadora noted that because the elemental profile of building and car windows was very similar when analyzed with SEM-EDS, care must be taken when classifying them. Zadora concluded that the application of support vector machines and naïve Bayes classifiers gave slightly better results than application of the likelihood ratio model. However, the observed differences in misclassification rates were not great, and no single classification method was obviously more effective than any other. Despite the slight underperformance compared with support vector machines and naïve Bayes classifiers methods, Zadora recommends the likelihood model because it has the advantage that it is easily interpretable, does not act like a black box unlike the support vector machines, and does not require the investigator to make some assumption about prior belief as is required by the naïve Bayes classifiers method.

The discrimination power of combining physical, optical and elemental analytical techniques has been the topic of several investigations. Andrasko and Machly (1978) developed an analytical scheme including RI, density, emission spectrometry and SEM-EDS, and were able to distinguish 38 out of 40 window glasses. Koons and Buscaglia (1999a) evaluated the frequency distributions of RI (measured by the Emmons double variation method) and the

concentrations of ten elements (analyzed with ICP-OES) in 204 glass specimens received as evidence in casework. The authors concluded that all the 20,706 pairwise comparisons of the 204 specimens in this study were analytically distinguishable, and the corresponding low probability of two unrelated glass specimens being indistinguishable eliminates the need to collect extensive databases for the purpose of making exact probability calculations. This paper triggered a vivid discussion with Curran, Buckleton, and Triggs (1999) in the Journal of Forensic Sciences. Curran, Buckleton, and Triggs stated that despite the good power of discrimination of the combined elemental composition and RI measurements, it is particularly important that statistics, especially Bayesian statistics, be applied to the data to give an indication of the probability of two samples of glass matching "by chance". In response, Koons and Buscaglia (1999b) argued that statistics are important in the interpretation of any type of trace evidence analysis, but that it is more important to develop analytical methods capable of providing accurate, precise analytical data with the best possible powers of discrimination instead of using poorer analytical methods or data reduction in order that statistics can be calculated and having to rely on statistics for data interpretation. Bridge et al. (2006) compared the discriminating power of LIBS and LA-ICP-MS, each coupled with RI measurements, on 23 samples of automobile float glass from side and rear windows. The authors reported that 83% of the glass samples were discriminated with 99% confidence based on the LIBS spectra alone, 96-99% of the samples were discriminated based on LIBS spectra taken in conjunction with RI data at a 99% confidence level, and LA-ICP-MS data allowed for 100% discrimination of the samples without the need for RI data. Bridge et al. (2007) continued the prior work, and analyzed glass samples of 4 types (float glass taken from front and side automobile windows, automobile headlamp glass, automobile side mirror glass, and brown beverage container glass) by LIBS,

LA-ICP-MS and RI. Bridge et al. (2007) concluded that the largest discrimination was obtained by employing RI data in combination with LA-ICP-MS (98% discrimination of 666 pairwise comparisons at 95% confidence), while LIBS in combination with RI provided a somewhat lower discrimination (87.2% discrimination of 1122 pairwise comparisons at 95% confidence). The conclusions of both 2006 and 2007 papers is that the authors' results provide evidence to support the use of LIBS combined with RI for forensic analysis of float glass in laboratories that do not have access to a LA-ICP-MS.

2.C. Mid-IR Spectroscopy of Glass

Since the early 1900s, IR analysis has been an important tool for the determination of the molecular structure of glass (Mackenzie, 1960). Silicate glasses have been extensively investigated because of their scientific and technological importance. The molecular structure of glass has not only been studied to understand the glassy state of matter, but it has critical significance for the microelectronics industry and the manufacture of optical fibers.

In *Modern Aspects of the Vitreous State,* published in 1960, Mackenzie devotes an entire chapter to reviewing the knowledge about the vibrational spectra of glasses that had been collected from 1897 to 1959. The author noted that the major difficulty with performing IR transmission studies on glass involve sample preparation, and "one has to resort to very thin films (blown as bubbles from molten glass) or diluted fine powders in oil (Nujol) suspensions or compacted KBr pellets." Mackenzie identified six peaks in the mid-IR spectral region of vitreous silica: ~377, 465, 800, 950, 1100, and 1190 cm^{-1}. The author was able to assign only one band to a specific vibration: the greatest intensity peak at 1100 cm^{-1} is due to the Si-O-Si bond stretch. Mackenzie also noted a potential relationship between this band and the 1065 cm^{-1} band in

quartz and the 1085 cm^{-1} band in cristobalite. However, he only assumed, based on force constants, that the other high frequency peaks (around 1000 cm^{-1}) correspond to silicon-oxygen bond stretching while the medium and low frequency peaks (around 450 and 200 cm^{-1}, respectively) correspond to the weaker bond-bending forces. Wong and Angell's *Glass Structure by Spectroscopy* (1976), is a complementary text to Mackenzie's, as it extensively discusses the research on the molecular structure of glass using IR spectroscopy from 1960 to 1973.

In 1968, Bell, Bird, and Dean published their research on the vibrational frequency spectra of vitreous silica, germania, and beryllium fluoride. The authors computed the vibrational frequencies from atomic arrangements in physical models. Bell, Bird, and Dean confirmed the positions of bands in the computed spectra with experimentally observed bands in IR and Raman spectra. The authors assigned the three fundamental structural bands observed in the IR absorption spectra at 465, 800, and 1100 cm^{-1} as the rocking, bending, and stretching vibrations of Si-O-Si bridges, respectively. These vibrations are schematically represented in Figure 10. The stretching band at 1100 cm^{-1} is the most prominent in the IR spectra.

Wong (1973) studied the IR transmission spectra of a series of SiO_2 films vapor deposited on silicon from SiH_4 and O_2 at 450°C as a function of film thickness in the submicron range from 1000 to 9000 Å. Absorbances of band maxima observed in the frequency range 250-1400 cm^{-1} were shown to obey the Lambert-Bouguer's law in both as-deposited and heat-treated (800-1200°C) materials. The authors calculated the apparent absorption coefficients for the transmission minima at 1060, 800, and 450 cm^{-1} which were $2.5 \pm 0.1 \times 10^4$, $0.24 \pm 0.02 \times 10^4$, and $0.74 \pm 0.02 \times 10^4$ cm^{-1} for as-deposited films and $3.4 \pm 0.1 \times 10^4$, $0.34 \pm 0.02 \times 10^4$, and $1.06 \pm 0.02 \times 10^4$ cm^{-1} for heat-treated films, respectively. Wong concluded that the thickness of SiO_2

films as-deposited at 450°C as well as heat-treated to 800°C and above can be determined nondestructively using IR spectroscopy and the presented absorbance data.

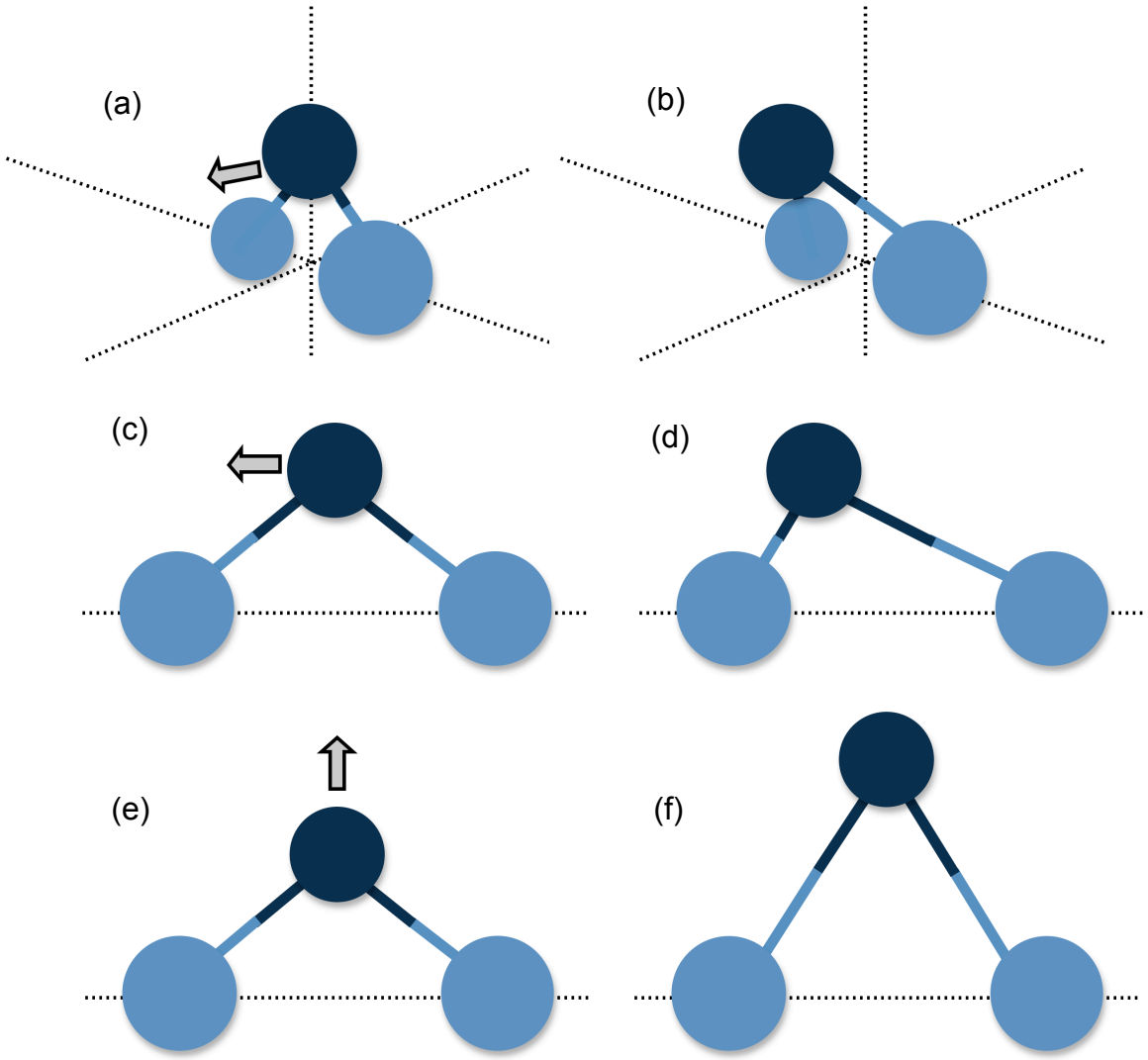


Figure 10: Schematic illustration of the vibrational motions of oxygen atoms (dark blue) with respect to the bridged silicon atoms (light blue): (a) and (b) represent the rocking vibration, which is a out of plane wagging motion perpendicular to the Si-O-Si plane; (c) and (d) represent the bending vibration, which is an antisymmetric stretching motion parallel to the Si-Si line between the two bridged cations; and (e) and (f) represent the stretching vibration, which is a symmetric stretching motion along the bisector of the Si-O-Si bridging angle. These diagrams are adapted from figures by Innocenzi, 2003.

In his 1974 book, *The infrared spectra of minerals*, Parke committed a chapter to describing some of the research on the IR and Raman spectroscopy on a variety of glasses, including silicate glasses (both binary and multi-component). A study of sodium silicate glasses showed that the peak at 1100 cm^{-1} decreased in intensity and moved to a lower frequency with increasing Na_2O content. Beyond 31 mol%, two maxima at 1050 and 960-920 cm^{-1} were observed. Parke described two theories on the identity of the 960-920 cm^{-1} band: 1) the formation of non-bridging oxygen ions, and 2) the crystallization or phase separation within the glass. Another study of silicate glasses showed that the peak at 780 cm^{-1}, which had been correlated with the Si-O-Si stretching vibration, also decreased in intensity and moved to a lower frequency with increasing alkali content. In a study of commercial soda-lime glasses and optical glasses containing high percentages of barium and lead, it was not possible to resolve a band at 950 cm^{-1}. At high concentrations, it is thought that the lead and barium ions take up network positions and thus reduce the number of non-bridging oxygens.

Boyd and Wilson (1982) studied the IR transmission spectra of a series of SiO_2 films grown on silicon wafers from a HCl and O_2 gas mixture at 850°C of film thicknesses down to 28 Å. The authors confirmed the use of the Lambert-Bouguer's Law for determining the thickness of thin films. Boyd and Wilson calculated the apparent absorption coefficient for the absorption at 1065 cm^{-1}, which was in good agreement with published data for thicker, vapor-deposited, and thermally grown films. The authors observed a continuous shift of the band near 1065 cm^{-1}, moving from an asymptotic limit maximum of 1072 cm^{-1} for thick films towards smaller wave numbers for thinner films; there was a ~20 cm^{-1} shift between the thinnest and thickest films. Boyd and Wilson discuss three possibilities for the origin of this shift: 1) oxygen deficiency in oxide films resulting in the band moving to ~1040 cm^{-1} for Si_2O_3 and to ~1000 cm^{-1} for SiO,

however the presence of Si_2O_3 would also be indicated by a band at 875 cm^{-1} which was not present; 2) bond strain due to constraint by the substrate, and/or 3) loss of interstitial oxygen from some substrates, which would cause a shift of ~7 cm^{-1}. The presence of interstitial oxygen is characterized by bands at 515 cm^{-1} and more visibly at 1106 cm^{-1}, which is due to vibrational modes of a nonlinear molecular unit of Si-O-Si. Boyd and Wilson describe the bands present in a spectrum of silicon dioxide film on a silicon wafer, which are due to four component: (1) the silicon dioxide peaks due to stretching (~1080 cm^{-1}), bending (800 cm^{-1}) and rocking (450 cm^{-1}) modes, (2) the absorption modes of the silicon lattice at 1302, 1107, 964, 890, 815, 740, 685, 607, and 568 cm^{-1}, (3) the carbon impurity band due to isolated substitutional carbon atoms at 602 cm^{-1} (which overlaps the silicon lattice band at 607 cm^{-1}), and (4) the oxygen impurity bands at 1107 and 515 cm^{-1}.

Boyd and Wilson (1987) used differential IR spectroscopy to study the silicon-oxygen stretching band of thin silicon dioxide films thermally grown on single-crystal silicon. The authors consistently observed an asymmetry in the spectra of films thicker than about 100 Å, of approximately 9 cm^{-1}. The peak position, width, and degree of asymmetry were also found to be sensitively dependent upon film thickness below 100-150 Å, while above this level these features were only very weakly dependent upon film thickness, indicating the presence of a thin layer of different structural or bonding properties. Boyd and Wilson conclude that the IR spectra of layers up to 100 Å thick are significantly affected by strain originating at the silicon-oxide interface.

Boyd (1987) furthers the analysis of the IR spectra of SiO_2 thin films using deconvolution. Boyd found that the characteristic IR band in the 1075 cm^{-1} region for thin films in the thickness range 28-450 Å mathematically deconvolute consistently into two distinctly

separate Gaussian profiles. The derived peaks are found around 1050 cm^{-1} with a full width at half-maximum transmission value (FWHM) of 65 cm^{-1}, and near 1085 cm^{-1} with a FWHM of 35 cm^{-1}. The relative band areas of these two features are consistently found to be approximately 0.76 and 0.24, respectively. Boyd concludes that these results support the theory that there are at least two structural models of amorphous SiO_2 repudiating the generally accepted continuous random network arrangement.

There has been considerable analysis of the IR spectrum of silicate glasses in terms of its transverse-optic (TO) and longitudinal-optic (LO) vibrational modes (Lange, 1989; Bensch and Bergholz, 1990; Almeida, 1992; Martinet and Devine, 1995; Ishikawa et al., 1997; Kirk, 1988; Koller, Schmidt, and Butler, 1988; Tan and Arndt, 2000; Innocenzi, 2003; Wang, Liu, and Tan, 2003). The TO and LO modes of silica glass are associated with the Si-O-Si vibrations, where the TO mode is associated with the vibrations parallel to the sample surface, while the LO mode is related to the vibrations perpendicular to the sample surface.

Innocenzi (2003) and Tan and Arndt (2000) describe the main absorption bands observed in the IR spectra of silica materials. There are three TO bands that are assigned to different vibrational modes of the Si–O–Si bonds: The TO_1 mode, the TO_2 mode, and the TO_3 mode. These three modes correspond with the three bands assigned by Bell, Bird, and Dean (1968). The TO_1 mode is the lowest frequency mode (460 cm^{-1}) and "is assigned to the TO rocking motions, perpendicular to the Si–O–Si plane, of the oxygens bridging two adjacent Si atoms" (Innocenzi, 2003), corresponding to Figure 10a and b. The TO_2 mode is observed near 800 cm^{-1}, and is a weak band "due to TO symmetric stretching of the O atom along a line bisecting the Si–O–Si angle, Θ, with some simultaneous motion of Si cations" (Innocenzi, 2003), corresponding to Figure 10c and d. The TO_3 mode is the main TO mode and corresponds to the band at ~1122

cm^{-1}. This highest frequency mode corresponds with the stretching vibration, which "involves motion back and forth of the oxygen atom along a line parallel to the Si–Si axis" (Innocenzi, 2003), as seen in Figure 10e and f. The motion results in opposite distortion of two neighboring Si–O bonds and is thus a TO antisymmetric stretching with a substantial amount of cationic motion. An intense shoulder at the high frequency side always accompanies the TO_3 band. The attribution of these bands to specific molecular motions is well established and these modes are taken as the silica fingerprint. Innocenzi also describes the LO–TO splitting of the vibrational modes, which are important features of IR spectra of silica glass. This splitting is attributed to long range coupling of Coulomb interactions. All three TO vibrational modes of glass show LO–TO splitting of different magnitudes: LO_1 (507 cm^{-1}) – TO_1 (457 cm^{-1}), LO_2 (820 cm^{-1}) – TO_2 (810 cm^{-1}), and LO_3 (1250 cm^{-1}) – TO_3 (1070 cm^{-1}). LO_1 and LO_2 are not observed in IR spectra, however LO_3 is associated with the high frequency shoulder of the TO_3 vibration band, even if the LO_3 mode is not detected in normal incidence transmission measurements where only TO modes are excited. The nature of the ~1250 cm^{-1} shoulder is explained as a broadened signature of the LO component of the TO_3 asymmetric stretching, or a mixed LO–TO mode with dominant LO character.

Kirk (1988) studied the IR absorption spectrum of SiO_2 in terms of its TO and LO vibrational modes. Kirk observed two coupled asymmetric stretching (AS) LO-TO frequency pairs called AS_1 (1256 and 1076 cm^{-1}) and AS_2 (1160 and 1200 cm^{-1}) in oblique-incidence p-polarized absorption spectra of thin SiO_2 films grown thermally on silicon wafers. Two additional LO-TO-mode pairs were observed in these spectra at approximately 820 and 810 cm^{-1} and 507 and 457 cm^{-1}. The least complicated explanation of the coupled-mode model that is consistent with experimental results is "one in which the AS_1-mode LO-TO frequency splitting is

due to the AS_1 transverse effective charge and the AS_2-mode LO-TO splitting is due to the mechanical coupling between these two modes and not to the AS_2 transverse effective charge, which is negligibly small".

Lange (1989) used IR spectroscopy to characterize thermal SiO_2 layers down to 15 nm thickness. From these measurements, performed in transmission mode under a 30° angle of incidence, the authors obtained a multiple resonance structure on the high-energy side of the main Si-O stretching vibration at 1075 cm^{-1}. Aside from a LO mode at 1254 cm^{-1}, Lange found experimental evidence for two additional vibrations: a TO mode at 1200 cm^{-1} and an LO mode at 1165 cm^{-1}. These features were explained by assuming disorder-induced vibrational coupling effects.

Ishikawa et al. (1997) investigated the structural properties of oxide films using IR spectroscopy, and discovered that the TO mode frequencies depended on the annealing temperature but the LO mode frequencies were constant in the bulk region. In a densified vitreous silica, both the TO and LO mode frequencies decrease. Thus, it was concluded that the TO mode frequencies correlate with the oxide density while the TO mode frequencies must be related to another property of the molecular structure.

Tan and Arndt (2000a) observed the splitting between LO and TO modes in the IR reflection spectra of silica glasses at different incident angles. The density of states and the frequency of the LO mode were found to increase with increasing incident angle. The authors used IR reflection spectroscopy to investigate the TO_3 mode, and found that the frequency of this band depended weakly on the incident angle. It increased from 1122 to 1124 cm^{-1} as the incident angle was increased from 0° to 20°. A sharp minimum in the reflectance was monitored at large incident angles. A transmission window was observed in the absorption spectra of silica glass

plates. The sharp minimum in the reflectance and appearance of the transmission window are thought to be the results produced by the Doppler effect due to the interaction of LO and TO modes in silica glass. The authors evaluated the phase velocity of the longitudinal mode in terms of the relativistic Doppler shift formula.

Wang, Liu, and Tan (2003) investigated the dependence of the frequency and reflectance of the TO and LO modes of silica glass on the angle of incidence and polarization direction of the incident light. In IR reflection spectra of silica glass, it was found that the positions and reflection bands are functions of the polarization state of the incident light and angle of incidence. The frequency of the TO band at 1129 cm^{-1} remained constant under different conditions, whereas the frequency of the LO band at ~1260 cm^{-1} and the ratio of the reflectance of the LO to TO (R_{LO}/R_{TO}) are functions of the polarization direction of the incident light and angle of incidence. The authors concluded that the dependence of the frequency of the LO band on the angle of incidence and polarization state of the incident light indicates the existence of a structural gradient from surface to bulk. This confirms prior observations that the structure of silica glass near the surface differs from that of the bulk. Specifically, the distribution of Si-O-Si angles varies from the surface to the inside of the glass because of the different fictive temperatures.

Agarwal, Davis, and Tomozawa (1995) investigated the ability to determine the fictive temperature of several types of silica glasses by IR spectroscopy. Fictive temperature of glasses are traditionally determined by differential scanning calorimetry analysis, but this method cannot be used for silica glasses because they show a negligible change in specific heat above and below the glass transition region. The authors state that it is known that silica glass structure varies with fictive temperature. In a separate study, it was demonstrated via X-ray analysis that as the

fictive temperature was increased from 1000 to 1500° C there was a decrease in the average Si-O-Si bond angle. In this research, the positions of both the fundamental structural band at ~1122 cm^{-1} monitored in IR reflection mode and an overtone of this band at ~2260 cm^{-1} monitored in IR transmission mode were found to be directly correlated with the glass fictive temperature. At any particular fictive temperature, the equilibrium structural band positions were found to be independent of the impurity content, such as hydroxyl, in different types of silica glass. The authors also relate the 1100 cm^{-1} band position, ν, to the Si-O-Si bond angle, Θ, by the following equation:

$$\nu = a\sqrt{\frac{2}{m}\left(\alpha \sin^2\frac{\Theta}{2} + \beta \cos^2\frac{\Theta}{2}\right)}$$

where m is the mass of the oxygen atom (in kg), the multiplying constant, a, is 5.305 X 10^{-12} s/cm, and α and β are the central and non-central force constants (in N/m). From the change in equilibrium position of the 1100 cm^{-1} band, the change in Si-O-Si bond angle was computed using values of α =600 N/m and β=100 N/m. The authors used the band shifts to compute the decrease in the average Si-O-Si bond angle, which was about 1.3° when the fictive temperature increased from 950 to 1400°C corresponding to a band shift of 2.50 cm^{-1}. The authors were able to determine the fictive temperatures of various as-received silica glasses using a calibration curve of fictive temperature versus wavenumber made from glasses with known fictive temperatures.

Haken et al. (2000) studied the influence of fictive temperature on IR peak positions, specifically the first overtone of the fundamental SiO_4-tetrahedron vibration mode at 2260 cm^{-1}. The authors concluded that the dependence of the RI on the fictive temperature is different for

the four types of silica glass studied because of the different types and concentrations of dopants. However, the authors were able to use the IR-absorption data to determine the fictive temperature of the four types of silica glass.

The FT-IR spectra of silica glasses have been studied using the ATR analysis technique. Nagai and Hashimoto (2001) used ATR to characterize the chemical bonding structures of ultra-thin SiO_2 films. The authors concluded that the shoulder band around 1150-1050 cm^{-1} reflects the interface roughness and the shoulder band around 1250-1150 cm^{-1} (LO mode) includes information about the change of Si-O-Si bonding angle and/or Si-O force constant. Rochat et al. (2003) investigated the capabilities and limitations of ATR FT-IR spectroscopy for the analysis of silicon oxide layers on silicon substrates, which are used in the microelectronics industry. The authors concluded that this technique was capable of comparing the structure of the silicon oxides. Rochat et al. used a homemade ATR with a Ge prism IRE, and collected IR data between 600-4500 cm^{-1}. The authors analyzed the Si-O-Si stretching vibrations (1000-1250 cm^{-1}), Si-H vibrations (2000-2300 cm^{-1}), and O-H vibrations (3000-3600 cm^{-1}) in order to elucidate the chemical structure. The Si-O-Si absorption band was determined to be composed of four contributions, as proposed by Kirk (1988), the LO and TO of two vibrational modes: 1) AS_1 mode for which adjacent O atoms move in phase; and 2) AS_2 mode in which the adjacent O atoms move 180° out of phase with each other.

Stolov and Simoff (2008) investigated the micro-ATR spectra of bulk silica glass for a variety of samples, including fused quartz slides, an optical fiber perform (which is glass that had not yet undergone final processing), and a series of optical fiber claddings. The authors noted that the band positions, shapes, and intensities of the TO_3 (~1070-1100 cm^{-1}) and the TO_2 (~800 cm^{-1}) bands varied depending on the measurement technique. The ATR spectra of the quartz

slide using a Ge (n = 4.003) IRE with the highest applied force (and best optical contact) had peaks at 1038 and 802 cm^{-1}, with the 1038 cm^{-1} peak having a broad high-frequency shoulder at about 1200 cm^{-1}. Using the Si (n = 3.418) IRE under the same conditions, the TO_3 and TO_2 peaks shift to 1026 cm^{-1} and 798 cm^{-1}, respectively. Using the ZnSe (n = 2.403) IRE under the same conditions, the TO_3 and TO_2 peaks shift to 980 cm^{-1} and 779 cm^{-1}, respectively. Using the diamond (n = 2.42) IRE under the same conditions, the TO_3 and TO_2 peaks shift to 969 cm^{-1} and 778 cm^{-1}, respectively. The authors contribute the shift of the TO_3 and TO_2 bands to the difference in RIs of the IRE, which "affects the IR beam penetration depth and the effective thickness of the sample" and "transforms the ATR band envelope, shifting its maximum to lower frequencies (with respect to the absorption spectrum)." Thus, the strongest shifts were observed for the IREs with the lower RIs (diamond and ZnSe). In addition, at certain conditions, a polariton peak was observed in the Si-O stretching region (1100-1160 cm^{-1}). "Surface polaritons are non-radiative waves localized at the boundary between media having one positive and the other negative dielectric constant", and cannot be assigned to the bulk TO or LO modes. Stolov and Simoff concluded that the polariton peak position was affected by the type of IRE (Ge, Si, ZnSe, or diamond), the IRE-sample distance, and the material used as an interlayer between the IRE and the sample (air or Nujol). The authors also determined that the polariton peak position is affected by the thermal history of the glass, and the authors attempted to correlate the observed changes with the glass fictive temperature. Prior work (Agarwal, Davis, and Tomozawa, 1995; Haken et al.; 2000) had shown that there is a linear correlation between the fictive temperature and the position of the TO_3 peak in reflection spectra. The authors expected that the position of the polariton peak position could be used for evaluating the glass fictive temperature because the fictive temperature affects the position of the entire band envelope. The authors concluded that

although the polariton peak position was sensitive to the fictive temperature, the accuracy of the micro-ATR technique was less than the accuracy when using IR reflection, thus using reflection spectra "seems more appropriate for the fictive temperature measurements".

Dalby and King (2006) proposed a new approach for determining glass structure with micro-reflectance FT-IR spectroscopy that is advantageous because it can be performed rapidly and inexpensively on small samples with minimal preparation. In prior IR studies (such as by Agarwal, Davis, and Tomozawa, 1995) structural information was inferred from the systematic shift of the single "peak" in the ~1100-900 cm^{-1} range which was thought to be caused by a decrease in the average Si-O bond angle in the bulk glass due to decreased polymerization of the glass network. Dalby and King hypothesized that the ~1100-900 cm^{-1} "peak" itself does not shift, and instead the peak position appears to shift because of the relative changes in intensities and FWHM of several "bands" with finite central positions, and that these bands relate to specific silicate units that have distinct molecular geometries. IR spectroscopy is able to detect silicate units because they each have a distinct molecular geometry that will scatter, emit, and/or absorb light at discrete band positions. The authors identify eight silicate unit vibrational modes in a collection of PbO-SiO_2 glasses using micro-reflectance FT-IR spectra that were transformed using the Kramers-Kronig relation. The transformed FT-IR spectra, in the 800 – 1200 cm^{-1} range, were deconvolved systematically into eight Voigt-shaped bands at centers that were predicted from the second derivative of the spectra. A Voigt shape, named after W. Voigt who completed the original work on the subject in 1912, is the term for a broadened spectral line due to the superposition of the Gaussian shape (from the Doppler effect) and an independent Lorentzian shape (which is the natural line width) (Posener, 1959). Dalby and King state that the deconvolution of the spectra can be performed in three ways: a model-independent fit, a model-

dependent fit, or a combined approach. In a model-independent fit, the bands are added arbitrarily to maximize goodness of fit and are subsequently assigned to silicate units based on previous work. In a model-dependent fit, bands are added at positions predicted for silicate units from empirical crystal chemical calculations. In the work by Dalby and King, the authors used a combined approach where the centers of the bands were predicted from the second derivative of the spectra, and the bands were added to obtain a goodness of fit. The structural units of silicate glasses, which typically contain more than one type of structural unit, were modeled using silicate units found in mineral crystals. The silicate units in crystals are a subgroup of the structural units, and they are grouped according to their ratio of non-bridging oxygen per network forming tetrahedral (NBO/T) to provide a measure of their polymerization. Therefore, the bulk NBO/T of a silicate glass is used to indicate its average polymerization state, such that a silicate glass with a low NBO/T has a highly polymerized structure presumably dominated by silicate units with low NBO/T. The authors used crystal chemical data, and previous Raman and IR band interpretations to assign bands to silicate units. The area of eight bands varied as a function of SiO_2 content, and these trends were combined with theoretical constraints to identify and assign the bands to seven silicate units: 1) isolated tetrahedral, SiO_4^{4-} (830 and 860 cm^{-1}), NBO/T = 4; 2) paired tetrahedral, $Si_2O_7^{6-}$ (900 cm^{-1}), NBO/T = 3; 3) ring, $Si_6O_{18}^{12-}$ (950 cm^{-1}), NBO/T = 2; 4) chain, $Si_2O_6^{4-}$ (980 cm^{-1}), NBO/T = 2; 5) double chain, $Si_4O_{11}^{6-}$ (1010 cm^{-1}), NBO/T = 1 or 2; 6) sheet, $Si_2O_5^{2-}$ (1050 cm^{-1}), NBO/T = 1; and 7) framework, SiO_2 (1100 cm^{-1}), NBO/T = 0. The data obtained by Dalby and King compared favorably with NMR data, thus validating their approach for determining glass structure with FT-IR spectroscopy.

There have been a plethora of experiments investigating the water-related species in silica glasses using IR spectroscopy (Mackenzie, 1960; Davis and Tomozawa, 1995a; Davis and

Tomozawa, 1995b; Davis et al., 1996; Humbach et al., 1996; Efimov and Pogareva, 2000; Tomozawa et al., 2001; Efimov, Pogareva, and Shashkin, 2003).

Efimov and Pogareva (2000) studied the water-related IR absorption spectra of some alkaline earth metaphosphate glasses, sodium silicate glasses, and window glass in the 1300-4000 cm^{-1} range. For the silicate glasses, there were four mode types associated with water-related vibrations: 1) four bands associated with four different stretching modes of the Si-O-H group participating in hydogen bonding (1580-1600, 1720-1760, 2080-2110, and ~2300-2400 cm^{-1}), 2) higher-frequency stretching modes of the Si-O-H group participating in hydrogen bonding (2600-2950 cm^{-1}), 3) stretching modes of the H_2O molecule (2800-3550 cm^{-1}), and 4) stretching mode of the free Si-O-H group (~3520-3600 cm^{-1}). Furthermore, for all glasses studied, four strong bands were found in the 1500-2600 cm^{-1} region. These bands, based on a similarity in their locations to those reported earlier for pyrophosphate glasses, were assigned to different stretching vibrations of the hydroxyl group participating in the strong hydrogen bonding of a single kind. Slight variations in band locations depending on glass composition were observed. For silicate glasses, the peak absorptivities for the low-frequency hydroxyl-related bands around 1590, 1740 and 2100 cm^{-1} were found to be greater by approximately 15, 15, and 4-5 times, respectively, than maximum absorptivities in the entire 2300-3700 cm^{-1} range. This rise in absorption with a decrease in wavenumber below 2300 cm^{-1} was considered to be the reason prior research missed these three bands.

Efimov, Pogareva, and Shashkin (2003) continued the study of water-related IR absorption spectra of silicate glasses, including a pane of float window glass. In the 1500-3700 cm^{-1} region, the spectra were seen to contain 14-15 bands. These bands were determined by deconvoluting the spectra. Ten bands located throughout the 1500-3700 cm^{-1} region (1539-

1606, 1670-1745, 1807-1840, 1903-1927, 2030-2107, 2302 +/-8, 2542, 2750, 3524, 3595 cm^{-1}) were shown to be due to the components of the stretching modes of the bound hydroxyl groups in three different structural sites. Four bands located within the 2850-3400 cm^{-1} region (2910, 2959, 3200, and 3393 cm^{-1}) were confirmed to be due to the components of the asymmetric and symmetric stretching modes of the H_2O molecule. The 1674 cm^{-1} band found in the spectrum of a water-enriched sample is assigned only to the bending mode of the interstitial H_2O molecule.

Effimov and Pogareva (2006) also studied the nature of the IR absorption bands in the 1300 to 5000 cm^{-1} region of vitreous silica and silicate glasses. The authors showed that the IR absorption bands in the spectra of silica glasses with frequencies around 1480, 1630, 1760, 1870, 1980, 2140, 2260, 2370, 2540, 2660, and 2810 cm^{-1} are due to the combination modes and overtones of the silica matrix, and the same is assumed for a weak 3140 cm^{-1} band. A weak band with frequency of ~3490 cm^{-1} was assigned tentatively to the symmetric stretching mode of interstitial H_2O molecules present in trace amounts.

IR spectroscopy has been used to determine the RI and optical dispersion of silica glass in the IR region (Tan, 1998; Tan and Arndt, 2000b; Tan and Arndt, 2001). This is of primary importance for understanding the properties and processes of optical fibers because of the small optical attenuation of IR radiation in silica glass. Tan (1998) measured the wavelength-dependent RIs for wavelengths ranging from 3 to 6.7 μm. In the strong absorption regions, RIs are commonly obtained by Kramers-Kronig analysis of reflectance data with moderate accuracy. Tan identifies the following absorption regions: an asymmetric band at 3672 cm^{-1} due to the location of the OH stretching band for SiOH in silica glass, bands at 2350 and 2393 cm^{-1} due to the absorption of CO_2 on the surfaces of sample, and bands at 2259 and 1632 cm^{-1} due to the vibrations of OH and molecular water in silica glass. In this research, Tan developed an

interferometric method for determining the RI of glass in the non-absorption IR range. Tan continued his research with Arndt which was printed in two articles (2000b and 2001). They determined the RI of silica glass at the positions of successive interference fringes in the wavelength region from 1.35 to 4.85 μm. The value of RI as a function of wavelength (λ) was evaluated which showed two maxima near 1.386 and 1.829 μm.

There are hundreds of articles devoted to the IR spectroscopic study of non-silicate glasses (borate, germinate, phosphate, nitrate, tellurite, vanadate, etc…) that have elucidated the molecular structure of these glassy systems. For example, Rada et al. (2008) investigated the structures of the boro-tellurite glasses using IR transmission spectroscopy in order to identify their molecular structure. The authors compared the FT-IR spectrum to the calculated spectrum, and were able to assign most of the observed IR bands. The centered band at about 470 cm^{-1} indicates the presence of BiO_6 units, a small peak appearing at 710 cm^{-1} is attributed to the B-O-B vibrations, a prominent band split into two components located at 875 and 981 cm^{-1} were assigned to the BiO_3 and BO_4 vibrations, respectively, and the band located at about 1267 cm^{-1} was assigned to the stretching of the B-O-B vibrations of the varied types BO_3 groups. It is beyond the scope of this literature review to discuss all of the IR studies on non-silicate glasses, however some are directly relevant to this research. Magdas et al. (2008) studied the structures of lead-phosphate glasses using IR transmission spectroscopy in order to elucidate the molecular structure. The authors use deconvolution of the IR spectrum to extract information about phosphate glass structure rather than the traditional analysis (peak positions) of IR spectra.

Of particular technological interest is the use of IR spectroscopy as a rapid method for the quantitative analysis of borophosphosilicate glass (BPSG) films on Si wafers for the microelectronics industry (Haaland, 1988; Adhihetty, McGuire, and Haaland, 1991; Zhang et al.,

1997; Niemczyk et al., 1999; Niemczyk, Zhang, and Haaland, 2001). Doped silicon oxide thin films are widely used as dielectrics, with the most commonly used doped silica being BPSG. The presence of boron (1 to 6 wt %) and phosphorus (2 to 8 wt %) dopants in these films modifies the film properties, thus their concentrations must be monitored carefully (Niemczyk et al., 1999). IR absorption and IR reflection are the most commonly used techniques for quality control of the BPSG deposition. Zhang et al. (1997) report that reflection spectroscopy is more advantageous than transmission spectroscopy because it does not require a transparent substrate below the thin-film sample, hence it can be applied to the determination of film properties when the films are deposited on product wafers. The examination of dielectric thin-film production with IR absorption and IR reflection techniques traditionally requires off-line analysis, however there have been studies for on-line monitoring using IR emission spectroscopy (Niemczyk et al., 1999, Niemczyk, Zhang, and Haaland, 2001).

Niemczyk et al. (1999) and Niemczyk, Zhang, and Haaland (2001) investigated the use of infrared emission spectroscopy (IRES) for the quantitative analysis of BPSG thin films on silicon monitor wafers. The authors determined that all of the film properties (boron content, phosphorus content, and film thickness) could be measured using IRES to the precision required for the manufacture and quality control in less than one second (with collection parameters of 1 scan and 32 cm^{-1} spectral resolution), thus permitting the potential for using the IRES technique for real-time monitoring of the BPSG film deposition process.

Chemometrics have been used to evaluate the data used in the quantitative analysis of glasses using IR spectroscopy. Haaland and Thomas (1988) used IR spectra of bulk seven-component, silicate based glasses to compare PLS methods for quantitative analyses with classical least-squares (CLS) and PCR methods. FT-IR spectra from 2300 – 4000 cm-1 were

obtained on eight samples of S-glass (5 mm thick) where the primary spectral variation in the glass was due to the B_2O_5 and OH components of the glass. The B_2O_5 and OH components are the most important to monitor for quality control of the glass since their concentrations are affected most by glass processing conditions. In addition, these components have the greatest influence on the final desired properties of the glass. The relative OH content was determined by measuring the peak height of the OH stretching band centered at 3650 cm^{-1}. Haaland and Thomas (1988) concluded that the PLS model approached the optimal prediction more rapidly and efficiently than the PCR model, and both PLS and PCR were superior to CLS methods for calibration when only one analyte is known. Haaland (1988) studied the use of CLS, PLS, and PCR methods for quantitative analysis of FT-IR spectra of BPSG films on silicon, which showed improved precision over standard peak-height measurements. PLS and PCR methods showed better analysis precision than CLS analysis. Haaland concluded that PLS is preferable to PCR because it achieves the same analysis precision but is computationally more efficient during calibration and generally requires a less complex model. Adhihetty, McGuire, and Haaland (1991) continued the previous work on BPSG glass on silicon wafers, and used quantitative IR spectral analysis to study the transfer of PLS calibration models between spectrometers. The authors showed that the PLS calibration model is robust to spectrometer variations and drift.

A feasibility study on the use of ATR mid-IR microspectroscopy for the discrimination of glass was performed by V.L. Martinez for her thesis work towards the completion of a Master's of Science in Forensic Science from John Jay College of Criminal Justice/CUNY in 2008. In the feasibility investigation, which analyzed different National Institute of Standards and Technology (NIST) glass standards, IR microprobe analysis was found to be very promising as a quick-and-easy screening method for the forensic discrimination of glass samples. ATR spectral

libraries produced by this study were useful and effective for rapidly differentiating glass samples, with the success rate for identifying the correct number one hit in the library searches being 96.49%, with the correct answer always being within the first two hits.

CHAPTER 3: EXPERIMENTAL DESIGN

3.A. Summary

This research investigated the use of the IlluminatIR™ IR microprobe analysis for elucidating the molecular structure of soda-lime silicate glasses and evaluates its use for forensic discrimination and classification. This research has four components, beginning with the ATR mid-IR spectra collection method development. The second stage was an attempt at correlating the mid-IR spectral bands with molecular structure. The third component of this research was to use chemometric analysis to investigate the use of IR microprobe analysis for the classification and discrimination of soda-lime silicate glasses. Last, the compatibility of IR microprobe analysis with GRIM analysis was investigated.

3.B. Hypotheses

Hypothesis One: The silicate units that are responsible for the short-to-medium range order of the structure of soda-lime silicate glasses can be identified by ATR mid-IR microspectroscopy.

Hypothesis Two: There exist measurable differences in the molecular structure of soda-lime silicate glasses from different sources that can be demonstrated by ATR mid-IR microspectroscopy, and thus the ATR mid-IR spectra of glasses can be used for forensic discrimination.

Hypothesis Three: There exist measurable similarities in the molecular structure of soda-lime silicate glasses within the same product class (window and container glasses or automotive, architectural and container glasses) and/or manufacturing process (float, tempered) that are

different between product classes and manufacturing processes that can be demonstrated, and thus classification by ATR mid-IR microspectroscopy is possible.

Hypothesis Four: Analysis of glass fragments by ATR mid-IR microspectroscopy can be efficiently integrated into a traditional forensic glass analytical scheme, specifically one that includes GRIM.

3.C. Sample Collection

This research focuses on the analysis of soda-lime silicate glasses with ATR mid-IR microspectroscopy. Other types of glass, such as borosilicate glass, may be the subject of a different future study. In addition, this research focuses on automotive, architectural, and container glass only. Other product-types, such as light bulb glass, glass fibers, and glass wool, may also be the subject of a different future study.

Glass samples were generously donated by Scott Ryland from the Materials Analysis Section of the Trace Evidence Unit of the Florida Department of Law Enforcement (FDLE) and Dr. Robert Koons and Dr. JoAnn Buscaglia from the Federal Bureau of Investigation (FBI) Laboratory. The FDLE has amassed a considerable collection of flat and container glass samples from known samples used in casework. Scott Ryland and his colleagues have analyzed these samples, thus most contain RI, thickness, and XRF elemental data as well as information on whether the samples are tempered and/or float glass. Scott Ryland kindly allowed me to sub-sample glass samples from these two collections. I collected more than 50 container and 100 flat glass samples (50 automotive and 50 architectural glasses) along with the accompanying data. Within these samples are two sets of glass with nominally similar RIs; the first set contains 30

glasses with nominal RIs of 1.5184 and 1.5185 at 20.0° C and the other contains 21 glasses with nominal RIs of 1.5180, 1.5181, and 1.5182 at 20.0° C. Drs. Robert Koons and JoAnn Buscaglia kindly sent me 50 automotive glass samples that had all been manufactured in the same year. These samples were collected from new cars that were crash-tested at the Insurance Institute for Highway Safety.

Mineral silicate standards were generously donated for this research by Dr. Thomas A. Kubic, Dr. John A. Reffner, Dr. JoAnn Buscaglia (FBI Laboratory), and Tony Nikischer (Excalibur Mineral Corp., 1000 North Division Street, Peekskill, NY 10566-1830). Dr. John A. Reffner provided the Cargille Reference Set No M-4 Comminuted Minerals (Cat No 34400) and the Wehrenberg Mineral Set (previously used by John P. Wehrenberg in his Manual for Forensic Mineralogy, a Short Course at the Spring Meeting of N.W.E.A.F.S., 1988).

3.D. Instrumentation

The IlluminatIR™ microprobe represents a significant advance in the field of IR microspectroscopy. The original IR microspectrometer and most that followed were benchtop IR spectrometers with a microscope attachment whereas the IlluminatIR™ is a FT-IR attachment for an infinity-corrected light microscope. This assemblage creates a unified instrument that combines polarized light microscopy with IR microspectroscopy which allows for the ability to take quality optical measurements, photomicrographs, and FT-IR spectrum simultaneously.



Figure 11: IlluminatIR™ II, from Smiths Detection.

The fundamental components of the IlluminatIR™ spectrometer are the IR source, the interferometer, and the detector. Optics (curved and flat mirrors) are present at several locations throughout the system and are used to redirect and refocus the light. Figure 12 shows the path of the mid-IR light as well as the reflected and transmitted visible light illuminations.

1. **Reflected light illumination**
2. **Transmitted light illumination**
3. **Mid-infrared radiation from FT-IR spectrometer.**
4. **Sample on microscope stage.**
5. **Common path of light and infrared radiation**
6. **Video camera for image recording.**
7. **Eyepieces for direct viewing.**

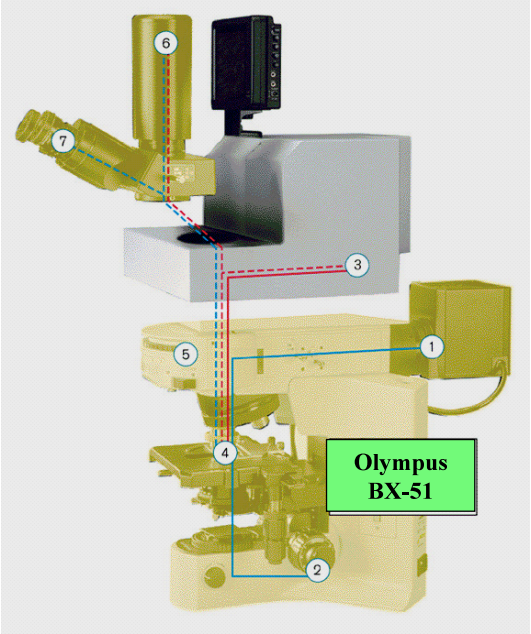


Figure 12: Schematics of IlluminatIR™ (*Reprinted with permission from Dr. John A Reffner).*

The IlluminatIR™ employs an electrically heated ceramic source. The spectrum of the mid-IR source, along with 3 spectral interferences (atmospheric water vapor, atmospheric carbon dioxide, and diamond sample interface), is displayed in the background spectrum shown in Figure 13.

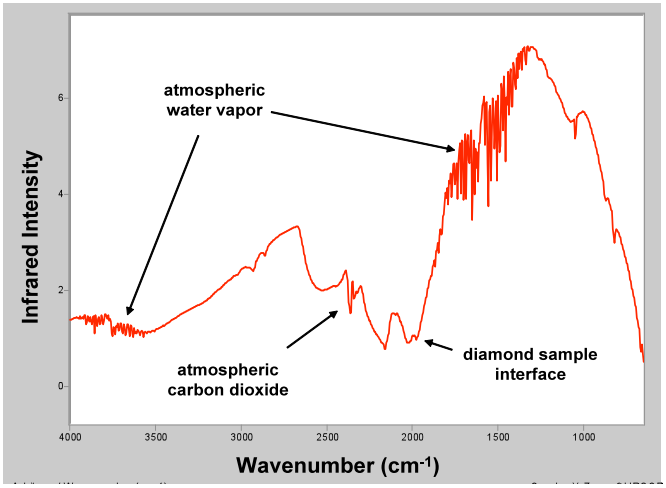


Figure 13: Background Spectrum of the IlluminatIR™, collected through the ATR objective (*Reprinted with permission from Dr. John A Reffner).*

The interferometer in the IlluminatIR™ has compensated germanium on KBr beam splitters, although the IlluminatIR™ can be fitted with other types of beam splitters. Figure 14 is a photograph of the layout of the interferometer in the IlluminatIR™.

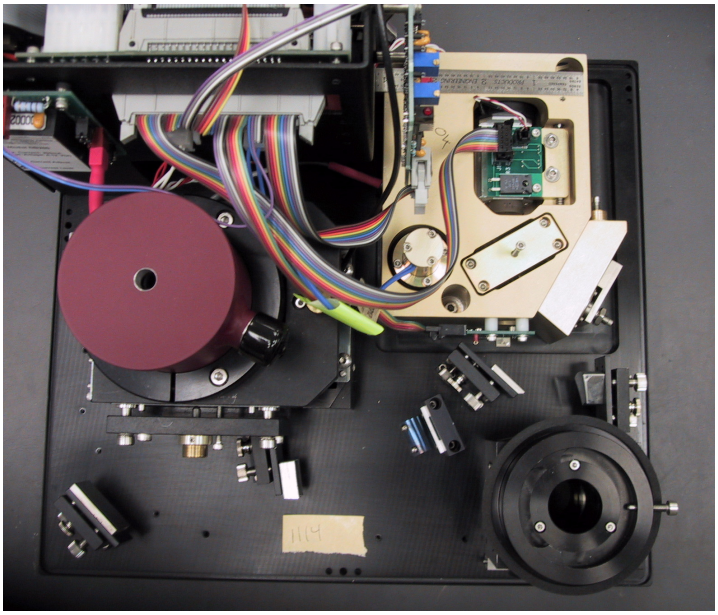
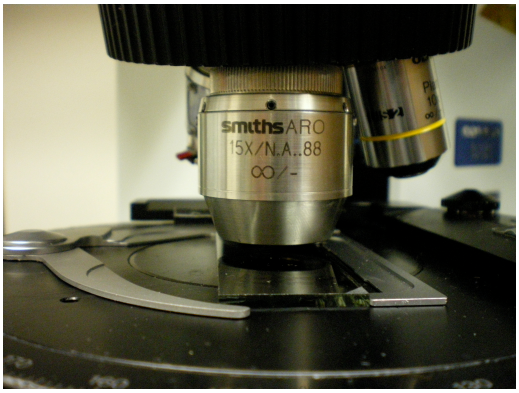


Figure 14: IlluminatIR™ interferometer layout (*Reprinted with permission from Dr. John A Reffner).*

A mercury/cadmium telluride (MCT) photoconductive detector is used in the IlluminatIR™. Photoconducting transistors are made by depositing a thin film of a semiconductor material onto a glass surface, and then protecting it from the atmosphere by sealing it in an evacuated envelope. In a MCT detector, both mercury telluride (HgTe) and cadmium telluride (CdTe) semiconductors are used. The electrical resistance of the semiconductor is decreased by the absorption of radiation which promotes nonconducting valence electrons to a higher energy conducting state. The photoconductor is in a series circuit with the voltage source and a load resistor. The decrease in resistance by the photoconductor

causes a decrease in voltage across a load resistor which functions to measure the radiation beam's power. (Skoog, et al., 1998).

The IlluminatIR™ is a mid-IR instrument with a spectral range from 4000 – 650 cm^{-1} (or 2.5 – 15.4 μm). The lower wavenumber is limited by the MCT detector.

(a) 

(b) 

Figures 15: The (a) ARO and (b) ATR Objectives.

The IlluminatIR™ employs two types of objectives capable of IR microprobe analysis: the all reflecting objective (ARO) which is used for reflection-absorption spectroscopy (RAS) and the attenuated total internal reflection (ATR) objective, pictured in Figures 15 a and b. The ARO and ATR have standard configuration magnifications of 15 times and 36 times, respectively. The ARO can also be configured for use with a hotstage accessory. This requires a longer-working-distance objective and, therefore, a 10-times ARO is an alternate option in these instances.

The ARO objective uses a parabolic reflector to image the IR radiation on the sample. The IR radiation from the interferometer travels through the sample where it is then reflected by a reflective surface (such as a gold or ReflectIR™ slide) back through the sample to another

parabolic reflector and lastly to the detector. This is known as "double-pass transmission" (Reffner and Martoglio, 1995) and is the hallmark of RAS. The IR radiation can also be reflected from the surface of the sample, which is known as specular or diffuse reflection. The visible light is transmitted through the center of the objective and is focused with a refractive imaging optic for visible light viewing of large fields. The refracting optic and the reflecting lens are parfocal, concentric, and have the same magnifying power.

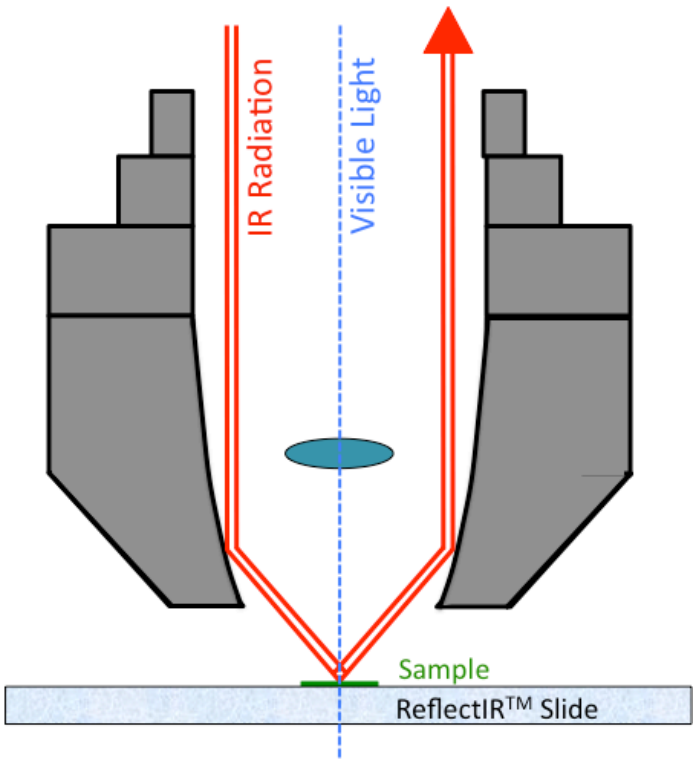


Figure 16: IR and Visible Light Path through ARO Objective.

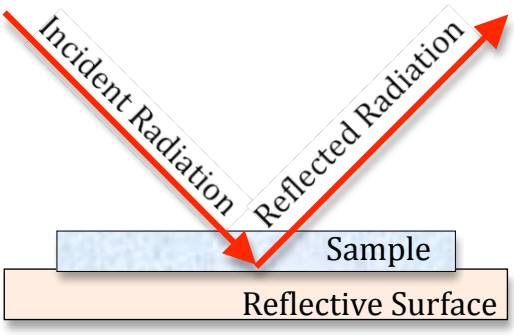


Figure 17: Reflection-Absorption IR Pathway.

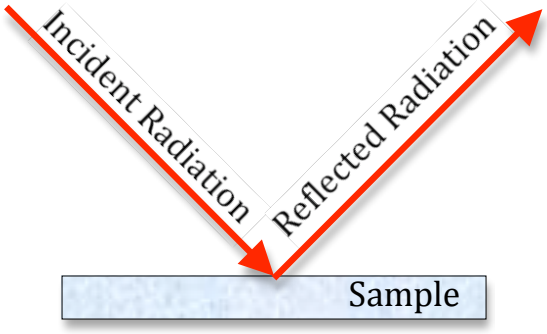


Figure 18: Specular Reflection IR Pathway.

The ReflectIR™ IR reflecting glass slide that is used for reflection-absorption IR microprobe analysis is a dichroic reflector that transmits visible light and reflects mid-IR radiation.

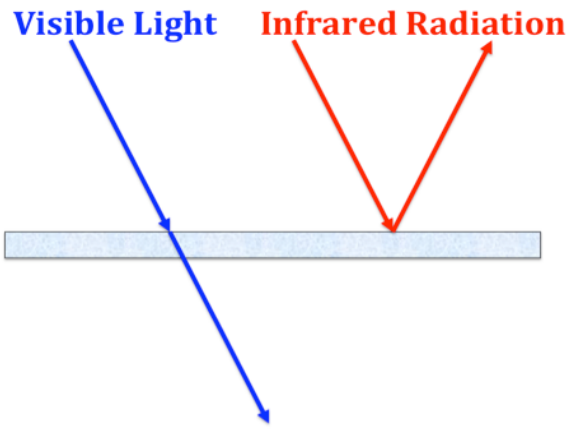


Figure 19: ReflectIR™ IR reflecting glass slide.

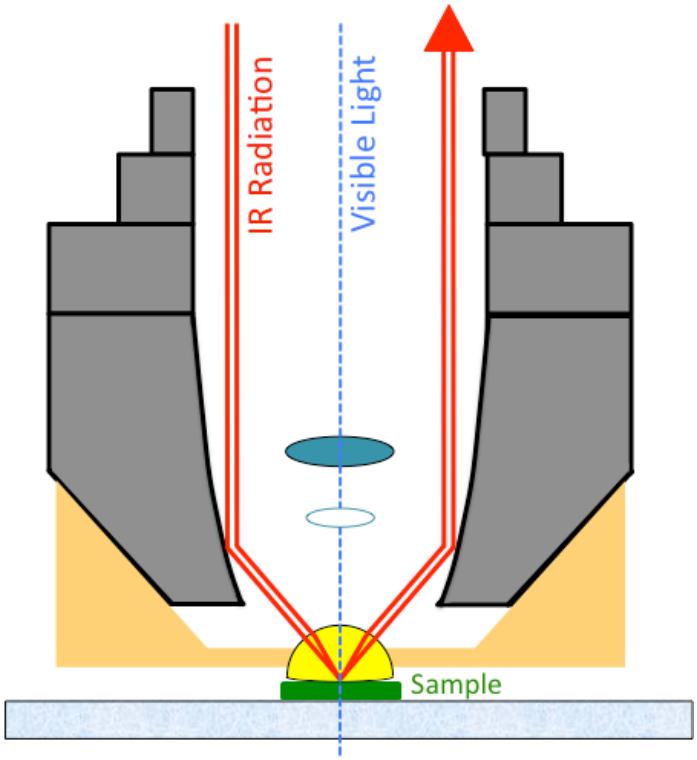


Figure 20: IR and Visible Light Path through ATR Objective.

The ATR objective uses a parabolic reflector to image the IR radiation onto the diamond-sample interface. The IR beam from the interferometer enters on one side of the diamond and reflects from the diamond-sample interface, returning to a second parabolic reflector and then the detector. Diamond is an ideal material for an IRE. It has a high index of refraction (n = 2.4) and is transparent through most of the mid-IR spectral region. It also has superior mechanical properties (such as its extreme hardness) and it is chemically inert, thus it can be used to analyze hard or corrosive samples.

When the diamond IRE is used, the depth of penetration of the evanescent wave is approximately equal to ¼ of the wavelength of incident light. This is calculated from the

equation described in Chapter 1.E.b: ($d_p = \lambda / \left[2\pi \left(n_1^2 \sin^2 \Theta - n_2^2 \right)^{1/2} \right]$), using the RI of diamond ($n_1 = 2.4$), a 45˚ angle of incidence ($\Theta = 45^{\circ}$), and a reasonable RI for the sample ($n_2 = 1.5$). The depth of penetration will vary based on wavelength, and increases from approximately 0.5 to 4 µm. The depth of penetration analysis using a diamond IRE are calculated and graphed in Appendix I, and show the depth of penetration variations with wavelength, wavenumber and angle of incidence.

In order for a sample to be analyzed by ATR, it must have a RI lower than that of the IRE. If the RI of the sample is greater than that of the IRE, total internal reflection will not occur and the incident radiation will be transmitted through the sample. The RI of diamond is relatively high, so this is not usually a concern, and with this study of glass, it is not a problem.

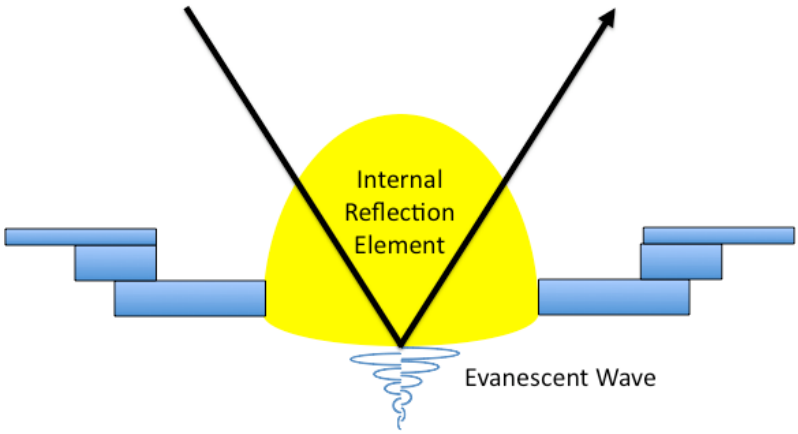


Figure 21: IR Light Path through IRE.

The ATR objective enables the sample to be observed and selected prior to contact and analysis. This is accomplished with two optical systems (visible and IR) and three operational modes (survey, contact, and scan) which are separated by Fourier plane masks (Reffner, et al., 1991). In the survey mode, the visible light travels through the center of the objective. The

visible light strikes the IRE at a near-normal angle which allows for the sample of interest to be visually found without physically disturbing it. In contact mode, the visible light is focused onto the diamond-sample interface at an angle less than the critical angle so that when diamond contact is made between the diamond and the sample, it can be visually confirmed. In the scan mode, the IR radiation strikes the diamond-sample interface at an angle greater than the critical angle which enables the internal reflection analysis of the sample.

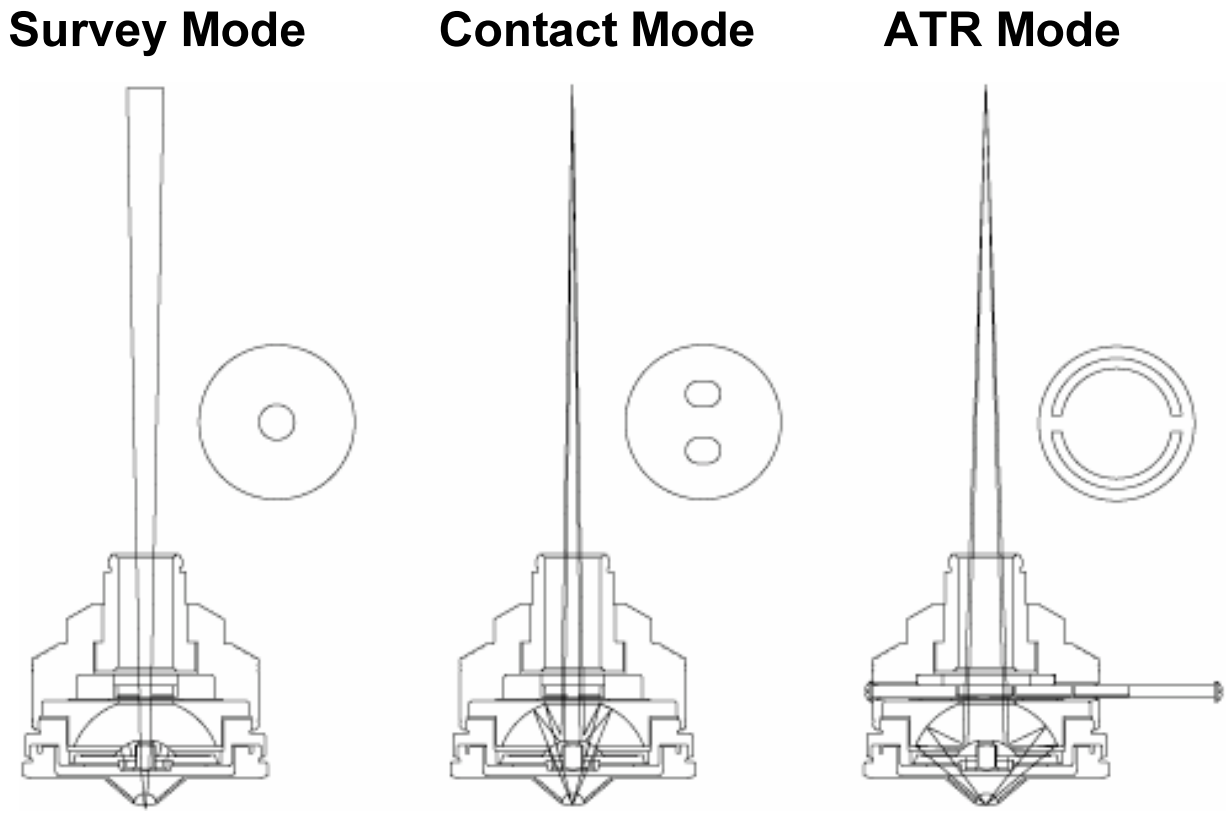


Figure 22: ATR Objective Modes (*Reprinted with permission from Dr. John A Reffner).*

3.E. Data Collection and Analysis

3.E.a. Instrument Validation

Performance validations were completed on the IlluminatIR™ FT-IR microspectrometer twelve times during the data collection period, from January 31, 2011 to January 03, 2012. The specifications for the tests in the performance validation ensure that the instrument is working properly according to the criteria set forth by the instrument manufacturer, Smiths Detection. The tests in the performance validation include: 1) ARO Objective: System Alignment and Electrical Settings, 2) ARO Objective: Signal-to-Noise Ratio with 100um aperture, 3) ATR Objective: Signal-to-Noise Ratio with 100um aperture, 4) ATR Objective: Baseline Stability, and 5) Laser Frequency Test. The performance validation reports and results are in Appendix II.

3.E.b. Method Development

The first stage of this research entailed developing a method for spectral data collection. The IlluminatIR™ IR microprobe has three parameters that can be controlled by the operator that will be investigated for optimal spectra collection. The three parameters are the number of co-added scans, the spectral resolution, and the IR beam aperture (or spot) size. Three NIST glass standards were analyzed with the varied parameters in order to determine the optimal method for glass analysis. The three NIST glass standards analyzed were SRM 620 (soda-lime flat glass), SRM 621 (soda-lime container glass), and SRM 1831 (SRM soda lime sheet glass). The NIST certificates are in Appendix III.

The first parameter is the number of co-added scans collected for a single spectrum. This parameter relates to the root mean square (RMS) noise and signal-to-noise ratio (S/N). It is well

known that a greater number of co-added scans cause a decrease in the RMS noise and an increase in the S/N. However, the S/N is proportional to (and the RMS noise inversely proportional to) the square root of the number of scans, thus increasing the number of scans beyond a certain number does not have a significant effect on the RMS noise and S/N. In this method development, the following number of scans was tested: 8, 16, 32, 64, 128, and 256. In addition, there is an increase in time required for analysis associated with a greater number of scans.

The second parameter is the spectral resolution, which can be set to 4, 8, or 16 cm^{-1}, all of which were tested in this method development. Resolution is a measure of the ability to distinguish between two peaks; analysis using a smaller wavenumber spectral resolution is able to distinguish between two peaks that are closer together than one with a greater wavenumber spectral resolution. In FT-IR spectroscopy, the spectral resolution is dependent on the difference in optical path lengths between the moving and stationary mirrors. The difference in optical path length (Δl) in cm is equal to the inverse of two times the spectral resolution (R) in cm^{-1}:

$$\Delta l = \frac{1}{2R}.$$

Thus, to attain a spectral resolution of 4 cm^{-1}, the difference in optical path length must be 1/8 cm. Spectral resolution is of particular interest to this study because of the deconvolution of the silicate band, which requires the broad silicate band to be separated and fit to multiple narrower peaks.

The third parameter is the IR beam aperture size, which determines the size of the IR radiation that is incident on the sample. It is obvious that a greater aperture size means a greater

amount of IR radiation, which results in a decrease in the RMS noise and an increase in the S/N. Thus, the largest aperture size is preferred for analysis. However, the entire IR beam must be incident on the sample, and consequently the aperture is limited by the size of the sample. In this method development, the following IR beam aperture sizes were tested: 10-, 25-, and 50-μm. The smallest possible IR beam aperture size that is capable of collecting quality ATR mid-IR spectra of glass was determined, and this determined the smallest sized glass fragment that can be analyzed with IR microprobe analysis.

For library searching, it is common practice to put an average spectrum of a known sample into an IR library rather than a single spectrum in order to have the library entry be the best representation of the sample. This is especially true when the sample is a mixture. Because glass is a mixture of various silicate units, a fourth factor that was evaluated is the optimal number of spectra collected from different fragments for each glass sample that will be averaged to produce one spectrum for library searching. This method development considered the following number of spectra to be averaged in order to produce one spectrum: 3, 5, 7, 10, 15, 20, and 30.

The determination of the optimal method collection parameters was evaluated based on the RMS noise, the S/N, and the time required for analysis. In addition, spectral libraries of all of the spectra collected at different parameters were searched with both a second set of spectra collected at each setting and the individual spectra used to make the library entries. The Hit Quality Index (HQI), or Quality, of the spectrum search was used to identify the optimal method collection parameters. HQI is a numerical rank obtained as a result of the spectrum search, with 0 being the best match and 1.414 or 1.000 being the worst match (this depends on the search

algorithm (Grams/AI Help Resource). The library that has the lowest average HQI was used to identify the optimal method collection parameters.

3.E.c. Glass Sample Preparation for ATR Mid-IR Microprobe Analysis

The preparation of glass for analysis with the diamond ATR objective is largely sample dependent because it depends on the size and shape of the sample. High-quality spectra are attained when good contact is made between the ATR objective and the sample. For a larger sample, such as the SRMs and the 'real world' window glass used in the method development (Chapter 3.E.b), there was essentially no sample preparation required because attaining good contact on a smooth flat surface is simple. However, most glass samples of forensic interest are microscopic in size and contain irregular surfaces. Consequently, a glass fragment requires a different sample preparation. Glass is brittle and does not compress with contact pressure, thus it will shatter when force is applied (Figures 23). This makes IR microprobe analysis quite difficult because of the scattering of the fragments.

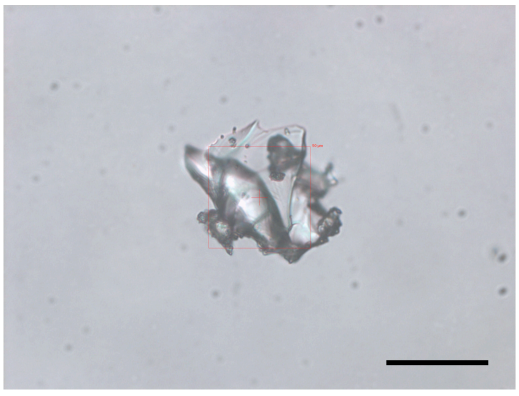
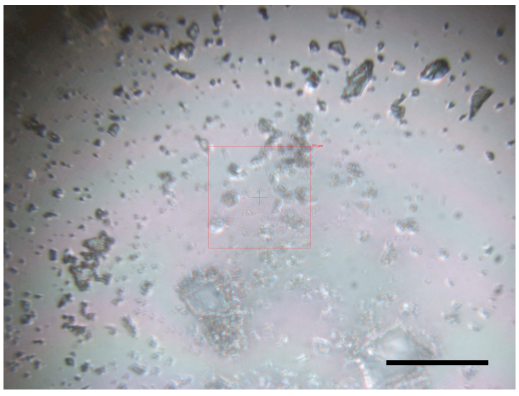
(a)  (b) 

Figure 23: (a) Photomicrograph of a dry mounted glass sample at 400 times magnification, prior to analysis, and (b) a photomicrograph of the same dry mounted glass sample at 360 times magnification after being shattered and scattered by the diamond ATR objective. The length of the black bar measures 50-µm.

A solution to this difficulty is to mount glass fragments in immersion oil, as microscopists have done for many years. The mounting of a sample in oil has three major advantages: the highest quality image is obtained because of the reduction in visible light scattering; optical properties, such as RI, are able to be measured, which has the potential to make this mid-IR analysis compatible with GRIM analysis; and the viscosity of the oil prevents the scattering of the shattered fragments. However, IR microscopists and spectroscopists are concerned with the effect of the oil on the resulting spectra, since oils are organic liquids with some IR absorption. As can be seen in Figure 25, when a glass fragment is mounted in oil, the viscosity of the oil prevents the scattering of the fragments and allows for IR analysis. As contact pressure is increased, the glass' peaks increase and the presence of the oil decreases, as seen in Figures 25 and 26. The contact between the diamond and the sample squeezes out the oil from between the two, thus the resulting IR spectrum is of the glass without significant interference from the oil.

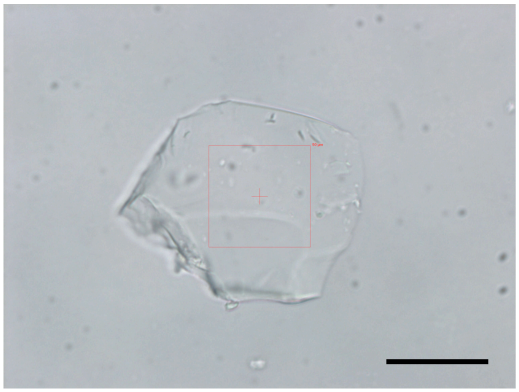


Figure 24: Photomicrograph of a glass sample in Nujol at 400 times magnification, prior to analysis. The length of the black bar measures 50-µm.

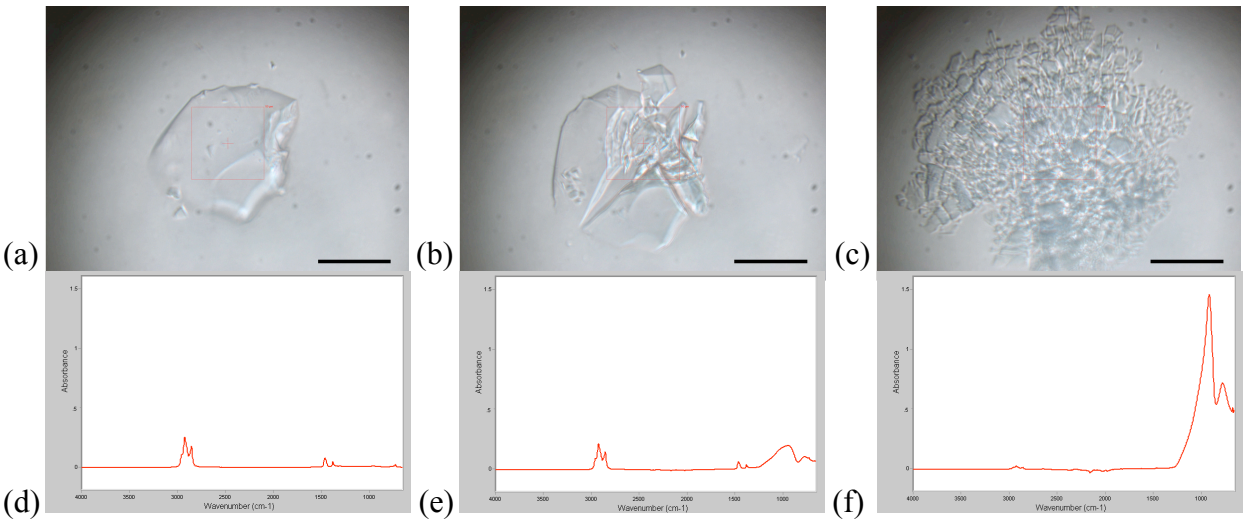


Figure 25: Photomicrographs of a glass sample in Nujol at 360 times magnification using the diamond ATR objective, varied by increasing the contact pressure: (a) after initial contact, (b) after some contact, and (c) after being crushed but not scattered. The length of the black bar measures 50-µm. Below each photomicrograph are their resulting mid-IR spectra (d-f), collected with a 50-µm aperture, 4 cm^{-1} spectral resolution, and 256 co-added scans. The spectra were produced using Grams® AI software.

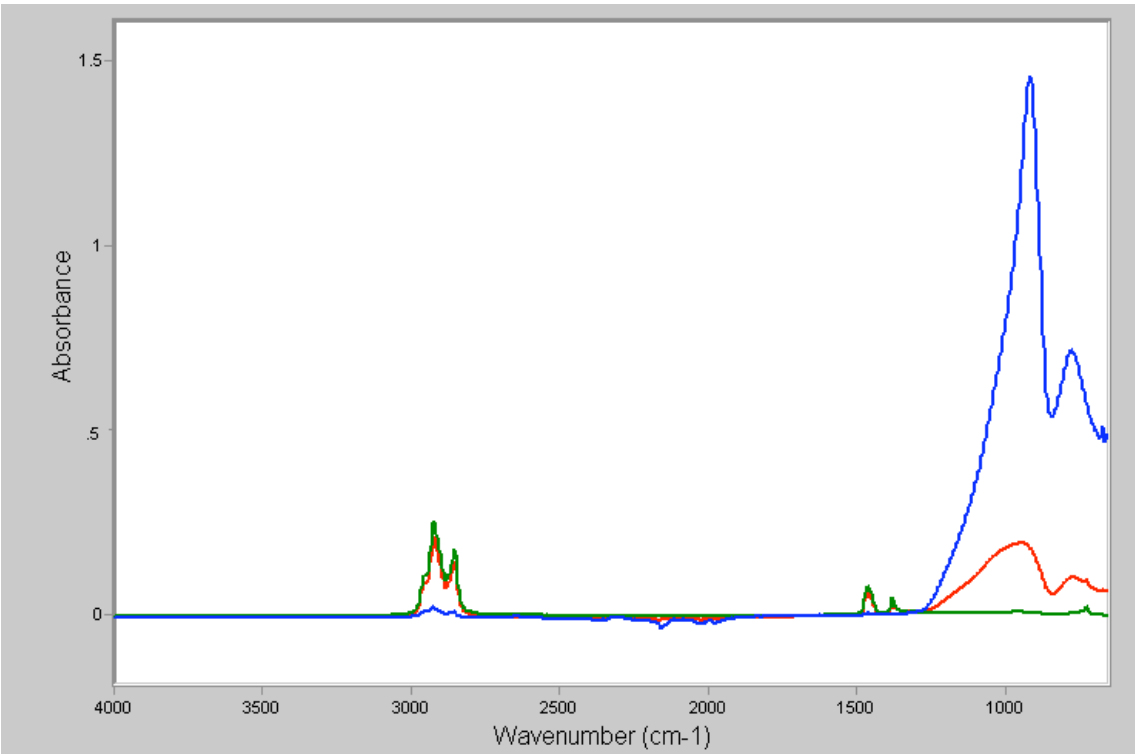


Figure 26: The mid-IR spectra of Figure 25 d-f overlaid, and produced using Grams® AI software. The red spectrum is after initial contact, the blue spectrum is after some contact, and the green spectrum is after being crushed but not scattered. As contact pressure is increased, the glass peaks are increase and the presence of the oil becomes insignificant.

This method is successful for glass samples as small as 10-µm which require IR analysis with a 10-µm aperture, and is shown in Figures 28 and 29.

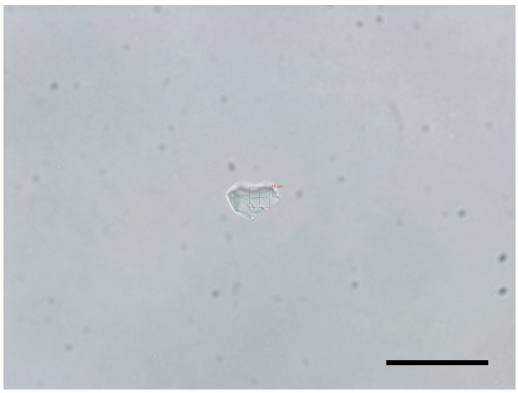


Figure 27: Photomicrograph of a glass sample in Nujol at 400 times magnification, prior to analysis. The length of the red square measures 10-µm and the black bar measures 50-µm.

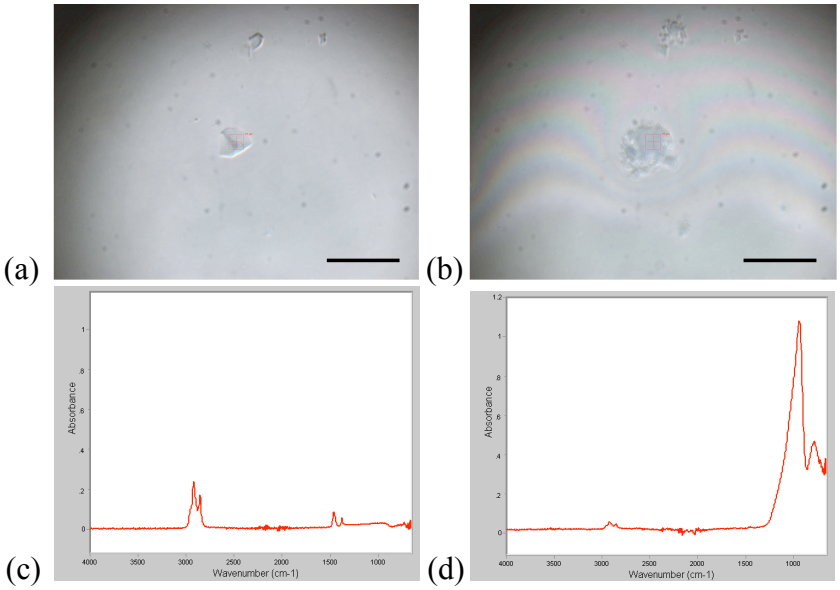


Figure 28: Photomicrographs of a glass sample in Nujol at 360 times magnification using the diamond ATR objective, varied by increasing the contact pressure: (a) after initial contact, and (b) after being crushed but not scattered. The length of the red square measures 10-µm and the black bar measures 50-µm. Below each photomicrograph are their resulting mid-IR spectra (c-d), collected with a 10-µm aperture, 4 cm^{-1} spectral resolution, and 256 co-added scans. The spectra were produced using Grams® AI software.

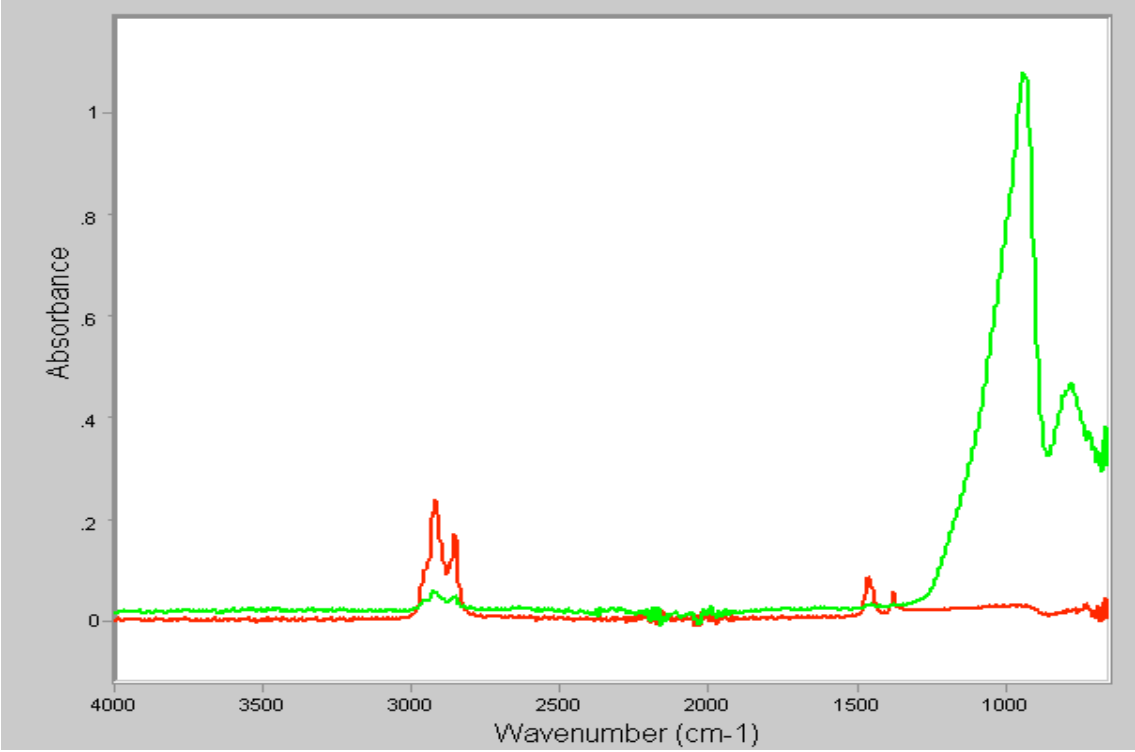


Figure 29: The mid-IR spectra of Figure 28 a-b overlaid, and produced using Grams® AI software. The red spectrum is after initial contact and the green spectrum is after being crushed but not scattered. When the glass sample is crushed, the contribution of the oil to the spectrum becomes insignificant in comparison to the spectrum of the glass.

The recommended sample preparation of glass fragments for IR microprobe analysis is a simple two-step process that is very similar to that for GRIM analysis. First, if the glass sample is too large for microscopic examination, it must be ground down to a size between 10 and 100-μm. The second and last step is to mount the fragments in viscous oil (Nujol was used in this research) on a ReflectIR™ microscope slide.

3.E.d. Correlation of Mid-IR Spectral Bands with Molecular Structure

The correlation of mid-IR spectral bands with molecular structure was completed as per similar methods to that discussed by Dalby and King (2006), which is detailed in Chapter 2.C. The silicate "peaks" in the region of 1300-650 cm^{-1} were deconvolved and correlated to the

different vibrational modes of soda-lime silicate bands. The deconvolution of the silicate band used three different methods for determining the individual silicate peak vibrations.

The first method for resolving the silicate peak vibration is a model-independent fit, and attempted to use the eight silicate unit vibrational modes identified and used by Dalby and King (2006). The identity and assignment of the eight bands to seven silicate units are: 1) isolated tetrahedral, SiO_4^{4-}, at 830 and 860 cm^{-1}; 2) paired tetrahedral, $Si_2O_7^{6-}$, at 900 cm^{-1}; 3) ring, $Si_6O_{18}^{12-}$, at 950 cm^{-1}; 4) chain, $Si_2O_6^{4-}$, at 980 cm^{-1}; 5) double chain, $Si_4O_{11}^{6-}$, at 1010 cm^{-1}; 6) sheet, $Si_2O_5^{2-}$, at 1050 cm^{-1}; and 7) framework, SiO_2, at 1100 cm^{-1}.

The second deconvolution method attempted to use the peak values obtained from the ATR mid-IR spectral analysis of silicate minerals with known structures. The silicate minerals and their structures are identified in the books by Vogel (1985 and 1994), and are diagrammed in Table 1. Three island silicate minerals were analyzed: phenakicite, willemite, and fosterite (all provided from Excalibur Minerals). The ring silicates were represented by beryl, and two sources of this mineral were analyzed (one provided by Dr. Kubic and the other from Dr. Reffner's Cargille mineral set). Three mineral varieties of the single chain silicate minerals were analyzed, two of which had two sources: enstatite (one provided by Dr. Buscaglia and the other from Dr. Reffner's Wehrenberg mineral set), spodumene (provided by Dr. Kubic), and α-wollastonite (one provided by Dr. Kubic and the other from Dr. Reffner's Cargille mineral set). The double chain silicates were represented by sillimanite, and two sources of this mineral were analyzed (both provided by Dr. Reffner). The double binary chain silicates were represented by tremolite, and two sources of this mineral were analyzed (both provided by Dr. Kubic with one being NIST SRM 1867). Xonolith, provided by Excalibur Minerals, was analyzed and has a double teriary chain silicate structure. Two mineral varieties of the single layer silicate minerals

were analyzed, both of which had two sources: talcum (from Dr. Reffner's Cargille and Wehrenberg mineral sets) and montmorillonite (both provided by Dr. Reffner). Four mineral varieties of the network silicate minerals were analyzed, three of which had two sources: crystobalite (provided by Dr. Kubic), quartz (one provided by Dr. Kubic and the other from Dr. Reffner's Wehrenberg mineral set), orthoclase (from Dr. Reffner's Cargille and Wehrenberg mineral sets), and plagioclase (from Dr. Reffner's Cargille and Wehrenberg mineral sets). Three-to-five replicate mid-IR spectra were collected for each mineral sample. The peaks for each mineral variety within a given silicate structure were compared to try to determine its mid-IR vibrational band(s).

The third deconvolution method is a combined approach, similar to that applied by Dalby and King (2006), and used the second derivative of the spectra combined with the peak picking function in the Grams® AI software program (©1991-2002 Thermo Galactic, Salem, NH) to identify the silicate peaks, and then used those peaks for the deconvolution of the soda-lime silicate glasses. The peaks were fit with Voigt line shapes. The peak fitting was then completed by using the iterate function, which adjusts the picked peaks (height, area, center X) to best match the original spectra, as determined by minimizing the residuals. The number of iterations was set to a value of 1000, which was repeated 3 – 5 times to ensure a best fit of the fitted trace to the original spectra.

Thirty soda-lime glass samples (10 container, 10 architectural, and 10 automotive glasses, listed in Table 2) obtained from Scott Ryland were deconvolved in an attempt to reveal their molecular structure. The results of the deconvolution, both peak positions (center X) and areas, were then analyzed with ANOVA to determine if the deconvolved data variations are significant. Microsoft®Excel:mac 2008 (©2007 Microsoft Corporation, Redmond, WA) and StatPlus®:mac

LE 2009 (©2001-2009 AnalystSoft Inc., Vancouver, BC) were used to perform ANOVA on the deconvolved data.

Table 2: A list of the 30 soda-lime silicate glasses, organized by end-use (architectural, automotive or container).

	Automotive	Architectural	Container
1	W10	W35	C50
2	W12	W50	C51
3	W13	W52	C52
4	W18	W153	C53
5	W442	W295	C54
6	W444	W360	C55
7	W445	W368	C56
8	W446	W394	C57
9	W448	W411	C58
10	W450	W412	C59

ANOVA is a statistical method used to determine if there is any difference in means. Unlike t-tests, ANOVA is used when determining the difference in means of more than two populations. However, this test can only reveal if two population means are significantly different but will not identify which of the populations can be differentiated. (Devore, 2008).

There are three steps for Single-Factor ANOVA. The first step is to state the null hypothesis (H_o), which in ANOVA is that the means of the groups or populations are equal. The alternative hypothesis (H_a) is also identified. The relevant hypotheses are:

$$H_o: \ \mu_1 = \mu_2 = \bullet\bullet\bullet = \mu_I$$

H_a: at least two of the μ_is are different

where I is the number of populations being compared, μ_1 is the mean of population 1, μ_2 is the mean of population 2, … μ_I is the mean of population I. If the null hypothesis is true, it means

that the different groups with their different sample means simply represent points on the same sampling distribution and thus cannot be differentiated. (Devore, 2008)

The second step is to choose a confidence level and consequently a critical value (alpha) for the test, where the confidence level is equal to 100(1-α)%. Thus a 95% confidence level corresponds to an alpha of 0.05. (Devore, 2008). The 95% confidence level was chosen for this research.

The third and final step is to calculate the test statistic for the data set. The test statistic used in single-factor ANOVA is F, where F is the ratio of the mean square for treatments (MSTr) to the mean square for error (MSE):

$$F = \frac{MSTr}{MSE}$$

MSTr is defined as:

$$MSTr = \frac{J}{I-1}\left[\left(\overline{X}_{1\bullet} - \overline{X}_{\bullet\bullet}\right)^2 + \left(\overline{X}_{2\bullet} - \overline{X}_{\bullet\bullet}\right)^2 + \bullet\bullet\bullet\left(\overline{X}_{I\bullet} - \overline{X}_{\bullet\bullet}\right)^2\right] = \frac{J}{I-1}\sum_i \left(\overline{X}_{i\bullet} - \overline{X}_{\bullet\bullet}\right)^2$$

where an individual mean of a population, $\overline{X}_{i,j}$ is:

$$\overline{X}_{i\bullet} = \frac{\sum_{j=1}^{J} X_{ij}}{J} \qquad i = 1, 2, \ldots, I$$

and the grand mean, $\overline{X}_{\bullet\bullet}$, which is the average of all observations, is calculated by:

$$\overline{X}_{\bullet\bullet} = \frac{\sum_{i=1}^{I}\sum_{j=1}^{J} X_{ij}}{IJ}$$

where $X_{i,j}$ is the random variable that denotes the jth measurement taken from the ith population and $x_{i,j}$ is the observed value of $X_{i,j}$ when the experiment is performed.

MSE is defined by:

$$MSE = \frac{S_1^2 + S_2^2 + \bullet\bullet\bullet + S_I^2}{I} \qquad i = 1, 2, \ldots, I$$

where S represents the sample variances and is calculated by:

$$S_i^2 = \frac{\sum_{j=1}^{J} \left(X_{ij} - \overline{X}_{i\bullet} \right)^2}{J - 1}$$

Once the F statistic is calculated, the null hypothesis is either rejected or not. If the calculated F statistic is larger than the F critical, the null hypothesis is rejected, which suggests that the means for at least two of the populations are significantly different. If the calculated F statistic is smaller than the F critical, the null hypothesis fails to be rejected, which indicates that there are no significant differences between the means. (Devore, 2008).

Since ANOVA only analyzes one variable at a time, it was used to determine if further analysis was warranted. If ANOVA revealed that there were no differences for a given peak (position or area) between the thirty glass samples, no further analysis would be completed. However, because the null hypothesis was rejected, the results of the deconvolution (both peak positions and areas) were used for evaluating the classification and discrimination potential of IR microprobe analysis of glass.

3.E.e. Classification and Discrimination Power

The ATR mid-IR spectra, first and second derivatives, and deconvolved peak areas and positions were analyzed to evaluate the classification and discrimination power of ATR mid-IR microspectroscopy of soda-lime silicate glasses. The derivatives and deconvolutions of the glass spectra were performed using the Grams® AI software program.

The first and second derivatives were performed using the Savitzky-Golay method, which is an algorithm that uses information from a limited portion of the spectrum to calculate the derivative at a particular wavelength. When performing a Savitzky-Golay derivative, it is important to control the amount of smoothing, which is determined by the size of the spectral segment to use for calculation of the derivative points, called the gap. The gap is often measured in wavelength span, but in the Grams® AI software program, it is in terms of data points. If the gap is too small, the resulting derivative will have too much noise. If it is too large, the peaks in the derivative will not represent the local behavior of the spectrum because either the peaks will be shifted or important information will be smoothed out. In this research, a 5-point smoothing scheme was applied to the second derivative spectra used in the ATR mid-IR spectral library searches, while both 5- and 9-point smoothing schemes were applied to the first and second derivative spectra used in the chemometric analyses. (Grams/AI Help Resource).

The analysis of the discrimination power was completed in three ways: 1) ATR IR library searching, 2) comparing the deconvolved peaks using a range test interval and 3) chemometric analysis. The ability of IR microprobe analysis for glass classification was evaluated using chemometric analysis.

The ATR mid-IR spectra of 153 soda-lime glass samples (50 container, 53 architectural, and 50 automotive glasses, listed in Table 3) obtained from Scott Ryland (FDLE) were collected.

Appendix IV contains additional information about the 153 soda-lime silicate glasses provided by Scott Ryland (FDLE). Ten replicate spectra were collected for each glass sample, with the term 'replicate' meaning a spectra from a different glass fragment from the same glass specimen. To assess the utility of these analytical methods, 30 of the soda-lime silicate glasses (10 container, 10 architectural, and 10 automotive glasses, listed in Table 2) were first analyzed with the ATR IR library searching and chemometrics. The methods that proved to be the most successful and having low error rates for classification and/or discrimination were then used to analyze the full set of 153 soda-lime silicate glasses (Table 3).

Table 3: A list of the 153 soda-lime silicate glasses, organized by end-use (architectural, automotive or container). The original 30 glasses used to assess the usefulness of the analytical methods are highlighted in yellow.

	Automotive (50)	Architectural (53)	Container (50)
1	W10	W35	C49
2	W12	W50	C50
3	W13	W52	C51
4	W18	W56	C52
5	W19	W58	C53
6	W20	W59	C54
7	W21	W60	C55
8	W22	W75	C56
9	W57	W80	C57
10	W264	W87	C58
11	W435	W129	C59
12	W436	W137	C60
13	W442	W153	C61
14	W444	W295	C62
15	W445	W360	C63
16	W446	W368	C64
17	W448	W371	C65
18	W449	W372	C66
19	W450	W383	C67

20	W451	W388	C68
21	W452	W392	C69
22	W455	W393	C70
23	W456	W394	C71
24	W457	W411	C72
25	W458	W412	C73
26	W474	W417	C74
27	W475	W418	C75
28	W476	W420	C76
29	W478	W423	C77
30	W481	W426	C78
31	W482	W443	C79
32	W484	W453	C80
33	W485	W454	C82
34	W486	W459	C83
35	W491	W461	C84
36	W492	W464	C85
37	W493	W469	C86
38	W494	W470	C87
39	W495	W471	C88
40	W501	W472	C89
41	W502	W477	C90
42	W503	W479	C91
43	W504	W480	C92
44	W505	W483	C93
45	W506	W487	C94
46	W509	W488	C97
47	W510	W489	C98
48	W514	W490	C99
49	W515	W498	C100
50	W516	W500	C101
51		W511	
52		W512	
53		W513	

To explore the ability of IR microprobe analysis to differentiate glasses that cannot be discriminated by RI, chemometric analysis was completed on two sets of glasses with nominally similar RIs. Table 4 contains a list of the glasses in each of the sets with nominally similar RIs.

Table 4: List of the glass samples contained in the 2 glass sets with nominally similar RIs. Glasses highlighted in yellow are also in the set of 153 glasses.

SAME RI SET 1 21- Nominally Similar Ris (1.5184-1.5185 nD)	**SAME RI SET 2** 30- Nominally Similar Ris (1.5180-1.5182 nD)
W23	W2
W33	W5
W49	W37
W62	W47
W79	W98
W83	W100
W95	W106
W103	W144
W107	W145
W129	W149
W132	W178
W142	W189
W143	W210
W152	W213
W153	W219
W165	W222
W174	W224
W193	W234
W204	W235
W206	W241
W232	W245
	W252
	W264
	W272
	W282
	W293
	W295
	W346
	W393
	W394

3.E.e.i. ATR Mid-IR Spectral Library Searching

The analysis of the discrimination power of IR microspectroscopy was completed in a similar method to that used by Martinez (2008) in her Master's thesis. It involved making two ATR mid-IR spectral libraries, one of the glass spectra and the other being the second derivative of the glass spectra. The second derivative is the rate of change of the slope of the spectrum, or a measure of curvature of the spectrum (O'Haver, 2008). Using the second derivative spectra mathematically enhances resolution, and this makes it easier to distinguish the individual components (both the number of bands and their corresponding wavenumbers) of the broad silicate bands (O'Haver, 2008). The library of the unprocessed spectra was then searched with different spectra of the same glass samples (collected from a different glass fragment). The library of the second derivative spectra was also searched with different second derivative spectra of the same glass samples (collected from a different glass fragment, but the same one used for the other library search). Two different library search statistical algorithms in Grams® AI software were used for this evaluation of discriminating power: a correlation algorithm and a first derivative correlation algorithm. The HQI of the spectral search is the feature that was used to compare the two library searches. The correlation algorithm of an unknown to a library entry is "effectively a normalized least squares dot product on the unknown", where "both the unknown and the library data are centered about their respective means before the vector dot products are calculated" (Grams/AI Help Resource). The following equation is used to calculate the HQI:

$$HQI = 1 - \frac{\left(Lib_m \bullet Unkn_m\right)^2}{\left(Lib_m \bullet Lib_m\right)\left(Unkn_m \bullet Unkn_m\right)}$$

In this equation, the library data (Lib_m) and the unknown data ($Unkn_m$) are defined as:

$$Lib_m = Lib - \frac{\sum_{i=1}^{n} Lib_i}{n} \qquad Unkn_m = Unkn - \frac{\sum_{i=1}^{n} Unkn_i}{n}$$

The advantage of centering the data is that it enables the HQI to be independent of the normalization of the spectra. This minimizes the effects on the HQI of a noisy baseline and sharp negative dips in the unknown spectrum due to the atmospheric interferences of water vapor and carbon dioxide peaks (Grams/AI Help Resource). The first derivative correlation algorithm is the same as the correlation algorithm, except prior to calculating the HQI, the first derivative of the library and known spectra are taken. The first derivative calculation is performed after mean centering. The first derivative calculation is done by subtracting previous points.

$$Lib_i = Lib_i - Lib_{i-1} \qquad Unkn_i = Unkn_i - Unkn_{i-1}$$

The most common advantage of this is to help correct for bad baselines. Another advantage is with the analysis of broad peaks, as the derivative reveals the slope of the tangent of the curve (Grams/AI Help Resource; O'Haver, 2008). The first derivative library search analysis of the second derivative spectra means that the third derivative of the spectra was compared. A comparison of the third derivative are sometimes useful for correcting for bad baselines and discriminating broad spectral features when the first and second derivatives are not sufficient (O'Haver, 2008).

An error rate for each of the library searches was calculated, based on the number of glass samples that were correctly identified as the first, second, and third hits. The first three hits

were used for calculation of the error rate because an analyst always looks at the top several hits from a spectral library search and not only at the first hit prior to making a chemical identification. Based on the comparison of the results of the two search algorithms, the preferred library search criterion was determined.

3.E.e.ii. Comparison of Deconvolved Peaks

The deconvolved peak areas and positions of the 30 glasses were compared using a range test interval to determine if this could be used for discriminating between different glasses. Comparison graphs for each peak, position (center X) and area, were made using Microsoft®Excel:mac 2008 to visually demonstrate overlapping and differentiated ranges.

3.E.e.iii. Chemometric Analysis

Three chemometric analytical methods, PCA, CVA, and PLS-DA were used to investigate the classification and discrimination power of IR microspectroscopy. The classification of glass into four different schemes was explored: 1) automotive, architectural or container, 2) window or container, 3) float or non-float, and 4) tempered or non-tempered. The discriminating power of the mid-IR spectra of glass was studied in three different glass groupings: 1) all glasses, 2) window glasses, and 3) container glasses. The underlying idea of examining the discriminating power within a specific class (window or container) is the combination of a classification and discrimination analysis, where an unknown glass sample's mid-IR spectra is first sourced as having being from a window or container and then discriminated among glasses of that class.

The deconvolution data, specifically the peak positions and areas, also were analyzed with hold-one-out cross validation (HOO-CV) PCA-CVA in order to investigate its ability to classify and discriminate glasses. The same 4 classification and 3 discrimination schemes that were used for the spectra were explored with this data.

The R program (R Foundation for Statistical Computing, 2010) was used for statistical processing and analysis. R is an open-source statistical environment that is an excellent analysis tool for forensic scientists. A significant advantage is that R is free and runs on UNIX, Windows and Macintosh. R has a comprehensive and user-friendly built-in help system, thus questions about the program can be quickly answered. R is a computer programming language modeled after S and S-Plus, thus is familiar to people with prior computer programming experience. Last, R has easy to learn syntax, a plethora of built-in statistical functions, and great graphing capabilities. (N.D.K. Petraco, 2011; Verzani, 2002).

Prior to importing the mid-IR spectra, first derivative spectra, second derivative spectra, and deconvolved data into R for statistical analysis, spectra or data from a given preprocess were arranged into an n×p data matrix (X):

$$\mathbf{X} = \begin{bmatrix} X_{11} & .. & X_{1j} & .. & X_{1p} \\ \vdots & & \vdots & & \vdots \\ X_{i1} & .. & X_{ij} & .. & X_{ip} \\ \vdots & & \vdots & & \vdots \\ X_{n1} & .. & X_{nj} & .. & X_{np} \end{bmatrix}$$

where n is the number of spectra (rows) and p is the number of data points (wavenumbers) in each spectra (columns). For the mid-IR spectra, the X_{ij} represents the absorbance value j in spectra i. For the derivative spectra, the X_{ij} represents the derivative value of absorbance j in spectra i. For the deconvolution data, the X_{ij} represents the peak position (in wavenumbers) j in peak i or the peak area j in peak i,

The mid-IR spectra collected in this research are from 4000 – 650 cm^{-1}, however the silicate bands are only in the region below 1300 cm^{-1}. Also, there is a considerable increase in noise in the region below 700 cm^{-1}. Consequently, all mid-IR spectra and derivative spectra were trimmed to eliminate unnecessary data and noise, thus they only include the region from 1300 – 700 cm^{-1}. This 600 cm^{-1} region, collected with 4 cm^{-1} spectral resolution, contains 323 data points. Accordingly, all of the spectral matrices contain a p = 323 which corresponds to 323 columns.

PCA is an exploratory algorithm that is designed to reduce large complex data sets into a series of optimized and interpretable size. In some applications, computing the principal components (PCs) is the end of the analysis. However, more often, the PCs that are obtained are used as input into another chemometric algorithm (Rencher, 2002; N.D.K. Petraco, 2011).

For the chemometric analysis used in this research, PCA was used to remove the correlation from the spectral data. In a spectrum, there is potentially a great deal of redundant information because proximal points in a profile are correlated. Thus, PCA was used to capture the essential information within the spectra while removing any correlations. (Joliffe, 2002; N.D.K. Petraco, 2011)

In PCA, information in a data set is measured through variance. The first PC is a linear combination of the original variables with maximum variance, or in other words, it is the

dimension along which the points in the data set (**X**) are maximally spread out. The second PC is the linear combination with second most variance, however it must be in a direction orthogonal to the first PC. The linear combinations of the original variables are used to form a new set of "derived variables" ($\mathbf{Z}_{PC}$):

$$Z_{ij} = \sum_{l=1}^{p} a_{il} X_{il}$$

In matrix form this is

$$Z_{PC} = XA_{PC}^{T}$$

where the superscript T indicates the transpose of $\mathbf{A}_{PC}$. The above equation is a transformation of the data (**X**) into the basis of PCs, where the transformation purely rotates the coordinate axes in feature space. The new data set (**Z**) is composed of derived variables that are equivalent to the original data (**X**), however the variables (columns) are ordered based on the amount of variance of the data set they contain, from largest to smallest. If the last variables (PCs) in **Z** contain a negligible amount of the variance, then they can be deleted without the data set loosing a significant amount of information. Thus, the dimensionality of the data set is effectively reduced to include only those variables that sufficiently represent the data. (N.D.K. Petraco, 2011; Petraco, 2011).

The matrix $\mathbf{A}_{PC}$ is computed by diagonalizing the $p \times p$ maximum likelihood covariance matrix (**S**) of **X**

$$\mathbf{S} = \frac{1}{n-1}\sum_{i=1}^{n}(\mathbf{X}_i - \bar{\mathbf{X}}) \otimes (\mathbf{X}_i - \bar{\mathbf{X}}).$$

where $\otimes$ is the Kronecker product of vectors. The ratio of eigenvalues (λ)

$$\lambda_i \Big/ \sum_{j=1}^{p} \lambda_j$$

gives the proportion of variance explained by the i^{th} principal component. The eigenvalue ratio can be useful in selecting the number of PCs required to effectively represent the data, however in this study, HOO-CV was used to select the number of PCs that would obtain good glass correct classification and discrimination rates while minimally risking over-fitting the PCA-CVA model. (N.D.K. Petraco, 2011; Petraco, 2011).

In addition to the spectral preprocessing of taking the first and second derivatives, data pretreatments (i.e. prior to PCA) of the matrix (**X**) can be performed using the R program. Two pretreatment schemes, mean centering and autoscaling, were individually applied to the glass data matrices to determine if they would increase the classification or discrimination power. Mean centering is performed by calculating the average data vector of all n rows in a data set and subtracting it point by point from each vector in the data set. Graphically, mean centering corresponds to a shift in the origin of the plot. Autoscaling is the combination of mean centering and variance scaling, where variance scaling is the process of normalizing each column so that the sum of squares equals 1. This is accomplished by dividing each column by its standard deviation. Variance scaling is performed in order to give equal weight or importance to all

variables (or wavenumbers) in the measured data set, and must be completed after mean centering. (N.D.K. Petraco, 2011; Gemperline, 2006).

CVA uses a between-group (**B**) to within-group (**W**) covariance matrix, $\mathbf{W}^{-1}\mathbf{B}$, to find the direction of best group separation. Canonical variates (CVs) are computed in p-dimensional space, min(p, k-1). CVA is similar to PCA in two ways. First, by retaining only the first few CVs, CVA can be used to reduce the dimensionality of the data. Second, CVA can be formulated as an eigenvector-eigenvalue problem where the number of retained CVs is determined by the magnitude of the eigenvalues. The CVs, $\mathbf{A}_{CV}$ and their eigenvalues $\mathbf{\Lambda}_{CV}$ are computed by diagonalizing the covariance matrix ($\mathbf{W}^{-1}\mathbf{B}$), where

$$B = \sum_{i=1}^{k} n_i \left(\overline{X}_i - \overline{X}\right) \otimes \left(\overline{X}_i - \overline{X}\right)^T$$

and

$$W = \sum_{i=1}^{k} \sum_{j=1}^{n_i} \left(\overline{X}_{i,j} - \overline{X}_i\right) \otimes \left(\overline{X}_{i,j} - \overline{X}_i\right)^T .$$

The non-singular **W** is inverted using a standard inversion method. $\mathbf{X}_{ij}$ represents the j^{th} glass spectra in the i^{th} sample and $\overline{\mathbf{X}}_i$ is the average of all the glass spectra in the i^{th} sample. Note that there are n_i glass spectra in sample i. It is important to also note that because the eigenproblem for CVA:

$$W^{-1}BA_{CV}^{T} = A_{CV}^{T}\Lambda_{CV}$$

is not symmetric, its eigenvectors are not necessarily orthogonal. Thus as opposed to PCA, the

CVs are often not perpendicular. As a consequence to this, covariance in the data causes the CVA model to fail, which is why spectral data must first undergo PCA. The last step in CVA is the transformation of the data on the basis of (retained) CVs as

$$Z = XA^T.$$

(Petraco, 2011; N.D.K. Petraco, 2011).

PLS-DA is a regression method that takes advantage of the covariance (as opposed to variance in PCA) in a data set by finding an approximately linear relationship between experimental (explanatory or predictor) variables and group labels (response) variables. "PLS is equivalent to successively finding linear functions of the predictor variables that have maximum covariance with the dependent variable, subject to each linear function being uncorrelated with previous ones" (Joliffe, 2002, pp. 185). In PLS, PCA is essentially applied iteratively to both the experimental matrix (X) and the group label matrix (Y) with the goal of finding regression coefficients that make Y = X. This is mathematically represented as

$$Y = X \bullet B_{pls} + F$$

where B_{pls} is a matrix of regression coefficients and F is a residual matrix. PLS-DA is used to improve the separation of groups identified by PCA on the experimental matrix. Similar to CVA (and unlike PCA), PLS-DA is a supervised learning method that requires the data to have assigned group labels. However, unlike CVA but similar to PCA, PLS-DA often works well with highly correlated variables. (Petraco, 2011; N.D.K. Petraco, 2011; Joliffe, 2002; Msimanga and Ollis, 2010).

An error rate, or misclassification rate, was calculated to determine the effectiveness of each of the classification algorithm at predicting group membership (called a classification error rate) or the discrimination algorithm at correct identification (called a discrimination error rate). An error or misclassification in this research occurs when the algorithm does not identify the unknown glass mid-IR spectrum as having come from a glass sample (or type of sample) when in reality it had, or the algorithm identifies the unknown glass mid-IR spectrum as having come from a specific glass sample or class when in fact it had not. The first of those errors is known as a Type 2 error or false negative, while the second is a Type 1 error or false positive.

HOO-CV is a robust method for estimating an algorithm's error rate (called the estimated error rate) for a population of glass mid-IR spectra using data from which it was not trained. A basic method for estimating the error rate is resubstitution, which is simply applying the classification or discrimination procedure to the set of data used to derive them. This calculates the apparent error rate, which is the percentage of misclassifications via the resubstitution method. The apparent error rate is a biased estimate that tends to be overly optimistic and requires correction. The first and simplest correction is HOO-CV, which computes the decision rules using all but one of the glass mid-IR spectra in the data set. The HOO-CV error rate is calculated by first determining whether the decision rule was correct on a held-out glass spectra, **x**, with true identity, **y**, where $g^{\text{hold-out-x}}(\mathbf{x})$ denote the identity of x assigned by the "hold-one-out" decision rules. Error or misclassifications are assigned a 1 and correct classifications a 0, which is symbolically written as:

$$1 - \delta_{y,g(x)}$$

where the Kronecker delta denotes

$$\delta_{y,g(x)} = \begin{cases} 1 & if \quad y = g(x) \\ 0 & if \quad y \neq g(x) \end{cases}$$

The HOO-CV procedure is then repeated for each glass mid-IR spectrum in the data set and the results are averaged to calculate an estimated error rate:

$$Err^{HOO-CV} = \frac{1}{n}\sum_{i=1}^{n} 1 - \delta_{y_i, g^{hold-out-x_i}(x_i)}$$

To assess the error rates of all of the mathematical models created for the classification and discrimination of glass, HOO-CV was used. (Efron, 1993; Rencher, 2002; Petraco, 2011; N.D.K. Petraco, 2011).

3.E.f. Mid-IR Microprobe Analysis Compatibility with GRIM

The compatibility of IR microprobe analysis with the modern RI analysis method using the GRIM was assessed in order to determine if IR microprobe analysis can be incorporated easily into an analytical scheme of glass analysis. The GRIM requires mounting glass samples in silicone immersion oils, and thus the collection of the ATR mid-IR spectra of glass samples was completed in the same immersion oils. Two NBS refractive index silicone liquids (SRM 1823) were tested that had been provided by Dr. Thomas A. Kubic: 1) Liquid I (nD at 20°C = 1.518) and 2) Liquid II (nD at 20°C = 1.559). The effect, if any, of the silicone oil on the glass's ATR mid-IR spectra was evaluated, specifically looking for the IR peaks of the oil and the glass.

CHAPTER 4: RESULTS

4.A. Method Development

The first method development experiment was designed to determine the optimal spectral resolution and number of co-added scans for glass analysis with an ATR mid-IR microprobe. It involved collecting ATR mid-IR spectra when no analyte or sample was in contact with the ATR, which in this experiment is called a blank and is analogous to the 100% line in IR transmission spectroscopy. By collecting the blank, which was done on 5 separate occasions for each sample area masking aperture size (50-, 25-, and 10-μm), the RMS noise in the region of interest (1300-850 cm^{-1}) was able to be calculated for all 18 combinations of spectral resolution (4, 8 or 16 cm^{-1}) and number of co-added scans (8, 16, 32, 64, 128, and 256). The RMS noise for the 10- and 25-μm aperture blanks was also collected with 512 co-added scans for all three spectral resolutions, thus making a total of 21 combinations for those apertures.

The nomenclature for all collected spectra is to name the sample and then identify the spectral resolution, the number of co-added scans, and the replicate number. Thus "Blank 4 256 1" is the first replicate of the blank spectra collected with 4 cm^{-1} spectral resolution and 256 co-added scans. For averages and other statistics, the replicate number is omitted, so "SRM 1831 8 64" refers to the designated statistic for all of the spectra of SRM 1831 collected with 8 cm^{-1} spectral resolution and 64 co-added scans.

Tables 5, 7 and 9 contain the RMS data and calculated averages, standard deviations, and percent relative standard deviations (% RSD) for the 50-μm, 25-μm, and 10-μm sample area masking aperture experiments, respectively. These data are represented graphically in Figures 30 - 32, 36 - 38, and 41 - 44 for the 50-μm, 25-μm and 10-μm aperture experiments, respectively.

Tables 6, 8, and 10 contain the analytical S/N for the 50-µm, 25-µm, and 10-µm aperture experiments, respectively. The 'signal' in the S/N was calculated by averaging the peak heights (in absorbance) for the three SRM glasses collected with the 50-µm aperture at all 18 combinations of spectral resolution and number of co-added scans, with 30 replicate spectra for each combination. The peak height data for the 3 SRM glasses are in Appendix V. The resulting average glass peak height was equal to 1.2422 absorbance units, with no systematic change in peak height for different resolutions or number of co-added scans. The S/N data are represented graphically in Figures 33 - 35, 39 - 41, and 45 - 47 for the 50-µm, 25-µm and 10-µm sample area masking aperture experiments, respectively.

Table 5: RMS noise for the spectra of blanks collected with the 50-µm aperture, calculated for the mid-IR region from 1300 – 850 cm^{-1}.

	1	2	3	4	5	Average Noise	Standard Deviation	% RSD
Blank 4 8	1.842E-04	1.891E-04	1.683E-04	1.757E-04	1.719E-04	1.778E-04	8.6369E-06	4.86
Blank 8 8	1.147E-04	1.209E-04	1.042E-04	1.187E-04	9.289E-05	1.103E-04	1.1650E-05	10.56
Blank 16 8	4.479E-05	6.656E-05	5.127E-05	7.206E-05	6.417E-05	5.977E-05	1.1328E-05	18.95
Blank 4 16	1.353E-04	1.451E-04	1.189E-04	1.166E-04	1.210E-04	1.274E-04	1.2304E-05	9.66
Blank 8 16	8.337E-05	9.457E-05	7.726E-05	6.518E-05	7.145E-05	7.836E-05	1.1300E-05	14.42
Blank 16 16	2.928E-05	5.000E-05	3.761E-05	3.210E-05	3.353E-05	3.651E-05	8.1210E-06	22.25
Blank 4 32	9.911E-05	9.535E-05	8.950E-05	7.592E-05	9.022E-05	9.002E-05	8.8035E-06	9.78
Blank 8 32	4.567E-05	5.020E-05	5.619E-05	4.209E-05	4.612E-05	4.805E-05	5.3815E-06	11.20
Blank 16 32	2.406E-05	2.563E-05	3.204E-05	2.736E-05	2.482E-05	2.678E-05	3.1834E-06	11.89
Blank 4 64	6.354E-05	8.238E-05	5.695E-05	6.640E-05	5.650E-05	6.515E-05	1.0524E-05	16.15
Blank 8 64	3.978E-05	5.179E-05	3.292E-05	4.084E-05	3.633E-05	4.033E-05	7.1198E-06	17.65
Blank 16 64	2.133E-05	3.650E-05	1.698E-05	6.366E-05	1.925E-05	3.154E-05	1.9518E-05	61.88
Blank 4 128	4.725E-05	5.158E-05	5.054E-05	5.376E-05	3.821E-05	4.827E-05	6.0913E-06	12.62
Blank 8 128	2.550E-05	3.756E-05	4.112E-05	3.441E-05	4.028E-05	3.577E-05	6.3129E-06	17.65
Blank 16 128	1.539E-05	2.084E-05	1.460E-05	6.305E-05	3.385E-05	2.954E-05	2.0251E-05	68.55
Blank 4 256	3.815E-05	5.061E-05	3.485E-05	4.265E-05	4.180E-05	4.161E-05	5.9106E-06	14.20
Blank 8 256	1.714E-05	2.307E-05	1.849E-05	2.439E-05	3.441E-05	2.350E-05	6.8092E-06	28.98
Blank 16 256	9.598E-06	1.104E-05	1.164E-05	5.507E-05	2.977E-05	2.342E-05	1.9528E-05	83.37

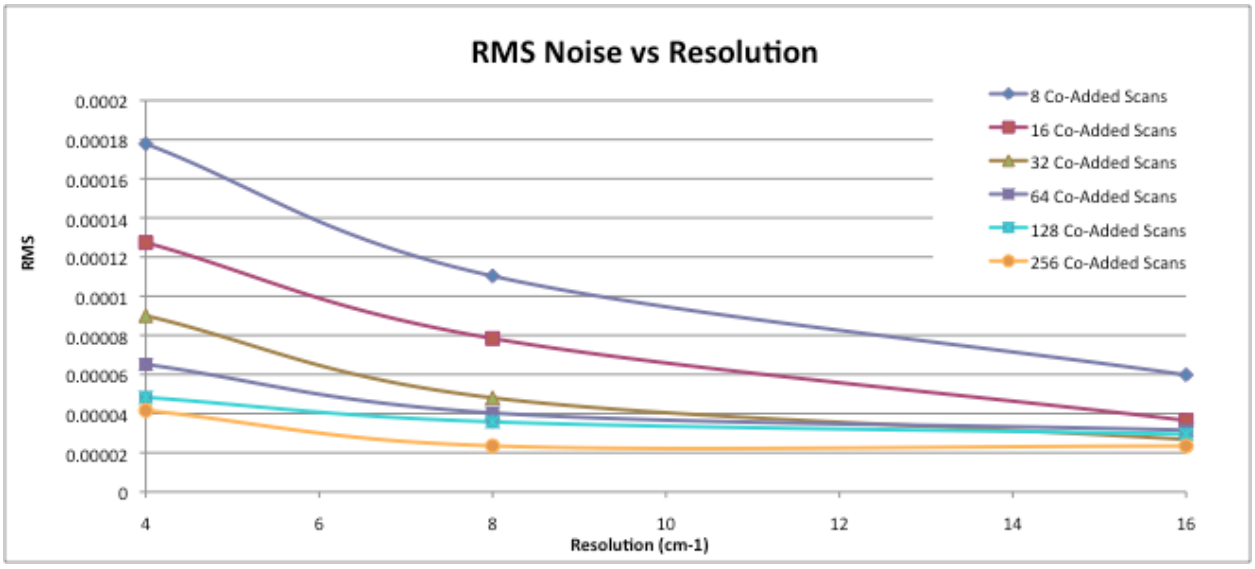


Figure 30: Graph of the RMS noise vs. spectral resolution for the 50-µm aperture.

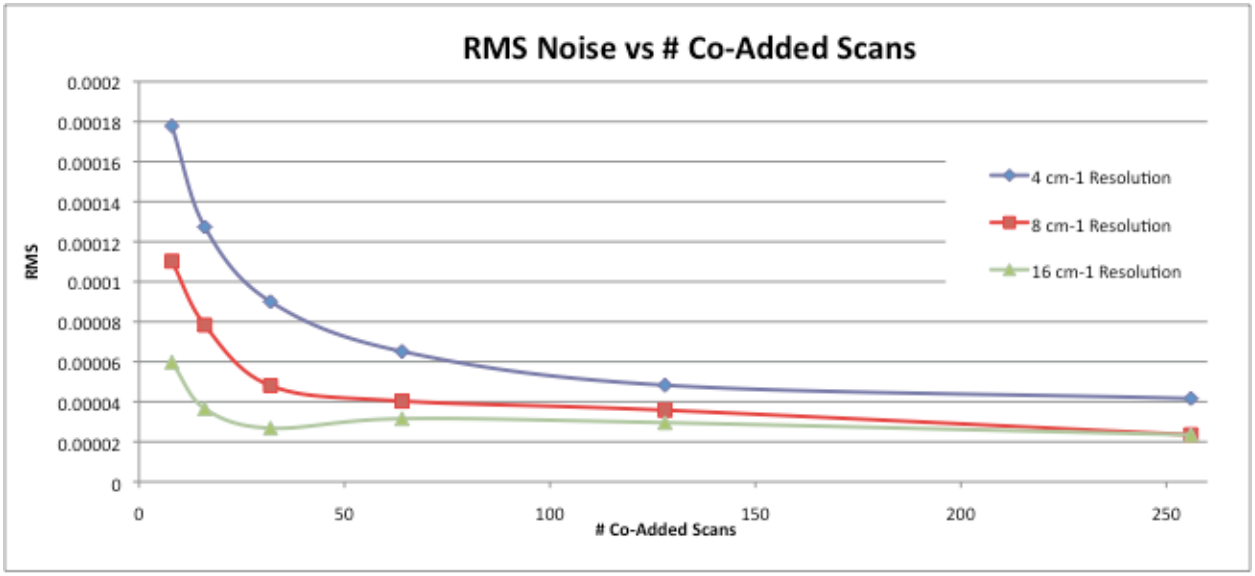


Figure 31: Graph of the RMS noise vs. the number of co-added scans for the 50-µm aperture.

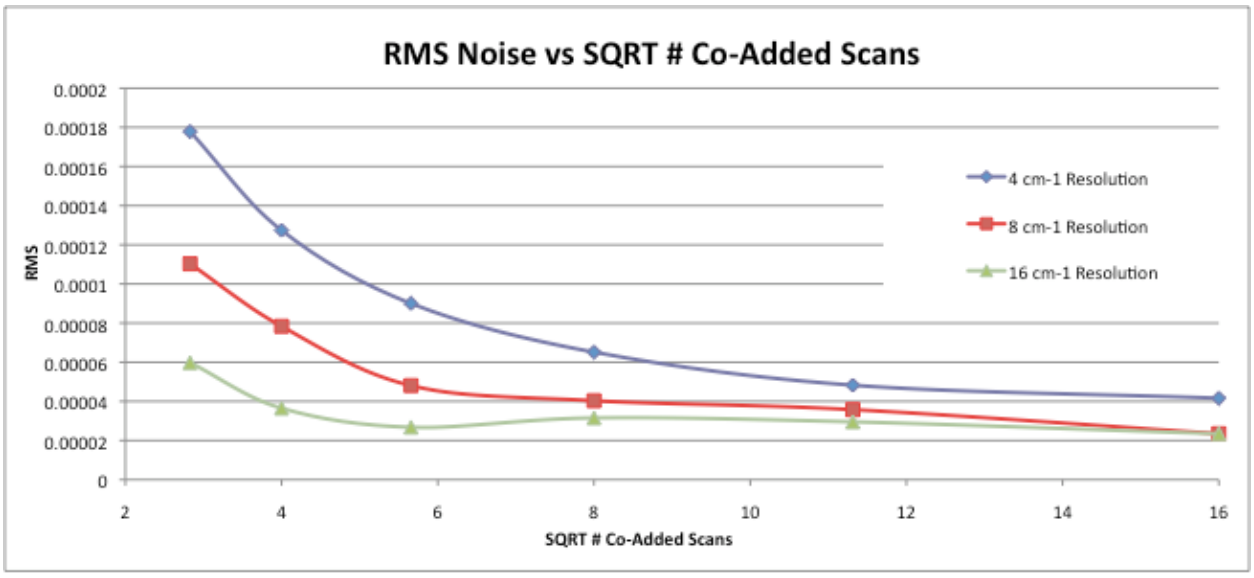


Figure 32: Graph of the RMS noise vs. the square root of the number of co-added scans for the 50-µm aperture.

Table 6: Analytical S/N for the spectra of blanks collected with the 50-µm aperture, calculated for the mid-IR region from 1300 – 850 cm^{-1}.

Spectral resolution & # of co-added scans	S/N
4 8	6985.56
8 8	11265.38
16 8	20783.55
4 16	9752.34
8 16	15852.25
16 16	34029.41
4 32	13799.27
8 32	25850.99
16 32	46379.23
4 64	19066.74
8 64	30800.76
16 64	39382.11
4 128	25737.36
8 128	34723.94
16 128	42046.53
4 256	29852.02
8 256	52862.04
16 256	53034.33

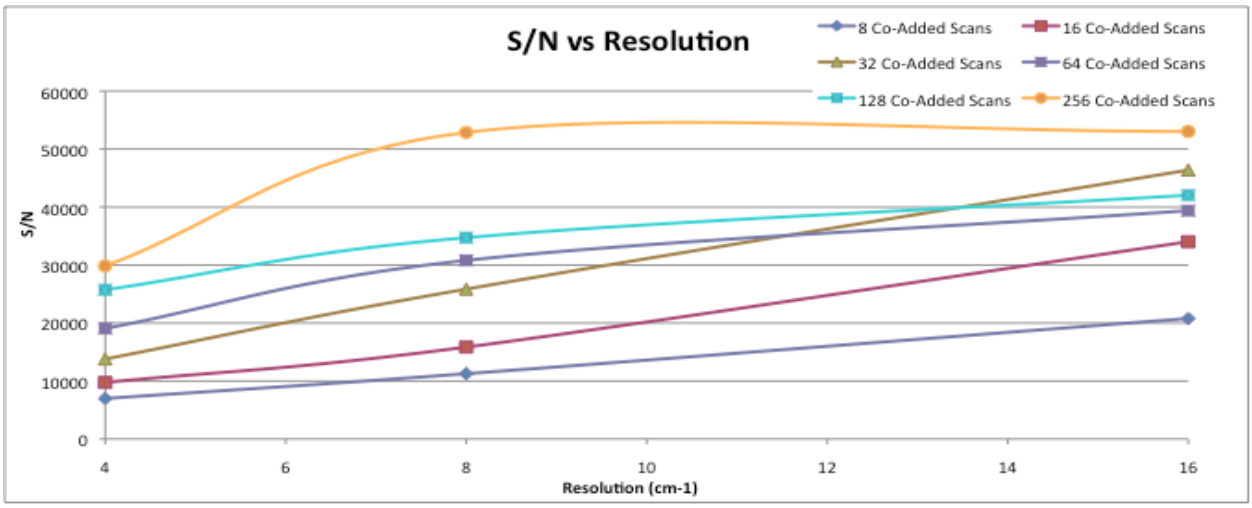


Figure 33: Graph of the S/N vs. spectral resolution for the 50-µm aperture.

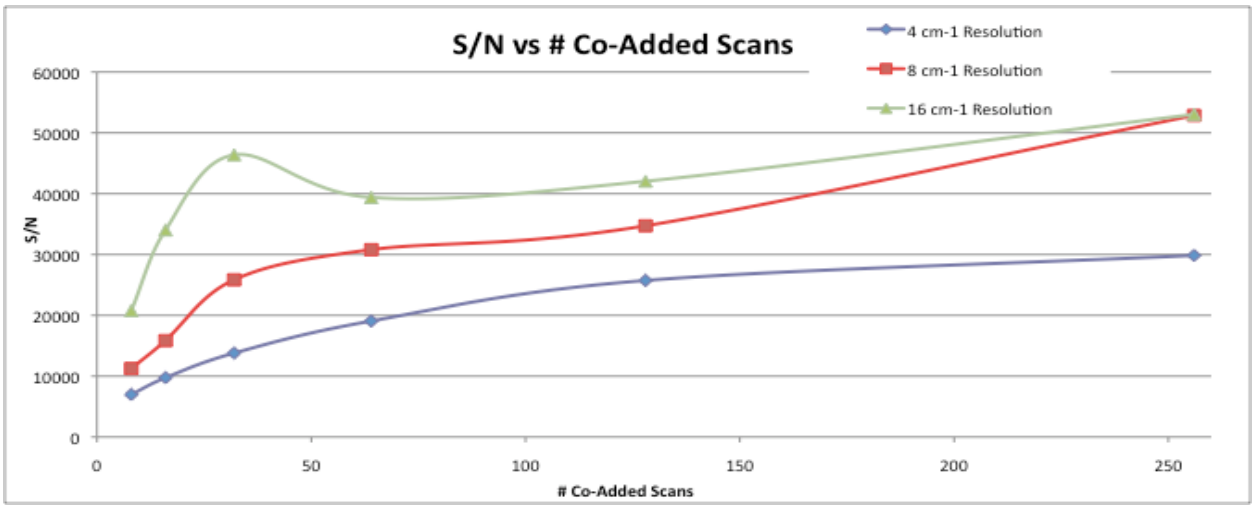


Figure 34: Graph of the S/N vs. the number of co-added scans for the 50-µm aperture.

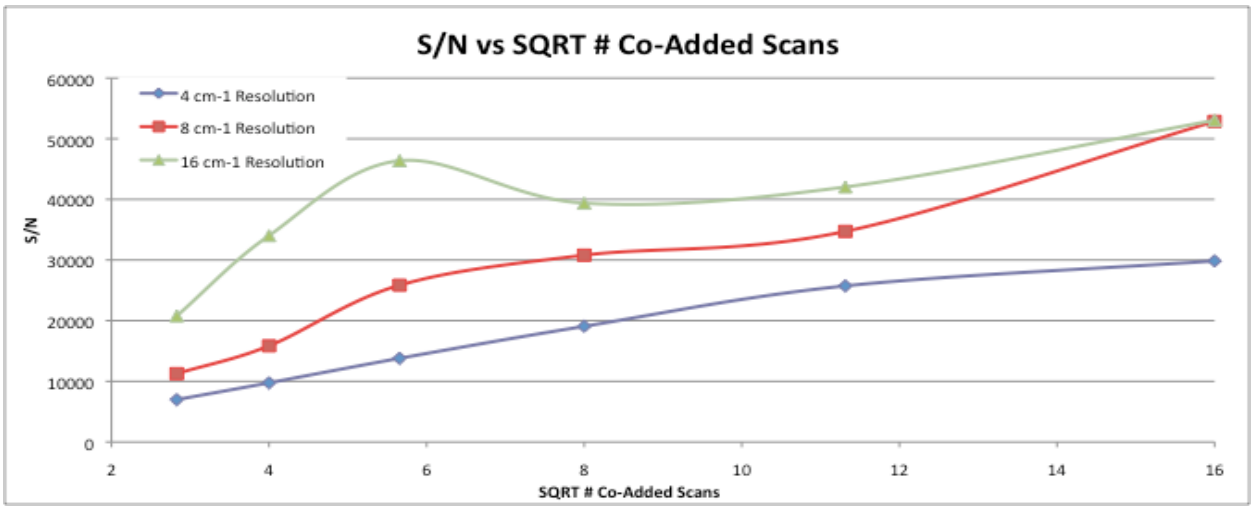


Figure 35: Graph of the S/N vs. the square root of the number of co-added scans for the 50-µm aperture.

Table 7: RMS noise for the spectra of blanks collected with the 25-μm aperture, calculated for the mid-IR region from 1300 – 850 cm^{-1}.

	1	2	3	4	5	Average Noise	Standard Deviation	% RSD
Blank 4 8	4.593E-04	4.450E-04	4.276E-04	4.866E-04	5.550E-04	4.747E-04	4.982E-05	10.49
Blank 8 8	2.710E-04	2.926E-04	2.712E-04	2.776E-04	3.082E-04	2.841E-04	1.607E-05	5.66
Blank 16 8	1.424E-04	1.557E-04	1.426E-04	1.466E-04	1.640E-04	1.503E-04	9.384E-06	6.25
Blank 4 16	3.322E-04	3.348E-04	3.877E-04	3.546E-04	3.197E-04	3.458E-04	2.654E-05	7.68
Blank 8 16	2.231E-04	2.211E-04	2.228E-04	1.926E-04	2.222E-04	2.163E-04	1.330E-05	6.15
Blank 16 16	9.827E-05	1.096E-04	1.332E-04	9.769E-05	1.521E-04	1.182E-04	2.378E-05	20.13
Blank 4 32	2.260E-04	2.146E-04	2.350E-04	2.564E-04	2.465E-04	2.357E-04	1.648E-05	6.99
Blank 8 32	1.328E-04	1.705E-04	1.342E-04	1.673E-04	1.436E-04	1.497E-04	1.804E-05	12.05
Blank 16 32	7.505E-05	9.623E-05	7.455E-05	7.670E-05	8.666E-05	8.184E-05	9.432E-06	11.53
Blank 4 64	1.558E-04	1.467E-04	1.469E-04	1.728E-04	1.697E-04	1.584E-04	1.234E-05	7.79
Blank 8 64	1.082E-04	1.019E-04	1.111E-04	8.274E-05	1.039E-04	1.016E-04	1.113E-05	10.95
Blank 16 64	5.834E-05	5.173E-05	4.434E-05	3.929E-05	6.663E-05	5.207E-05	1.089E-05	20.92
Blank 4 128	1.135E-04	1.298E-04	1.237E-04	1.048E-04	1.216E-04	1.187E-04	9.714E-06	8.19
Blank 8 128	6.743E-05	6.313E-05	8.722E-05	7.101E-05	8.184E-05	7.413E-05	1.008E-05	13.60
Blank 16 128	3.259E-05	3.670E-05	4.776E-05	4.538E-05	3.904E-05	4.029E-05	6.232E-06	15.47
Blank 4 256	8.165E-05	8.146E-05	8.298E-05	8.028E-05	8.620E-05	8.251E-05	2.273E-06	2.76
Blank 8 256	4.936E-05	5.889E-05	6.222E-05	4.908E-05	5.620E-05	5.515E-05	5.819E-06	10.55
Blank 16 256	2.238E-05	2.606E-05	2.226E-05	2.331E-05	2.887E-05	2.458E-05	2.847E-06	11.58
Blank 4 512	5.609E-05	6.384E-05	6.063E-05	6.533E-05	6.632E-05	6.244E-05	4.149E-06	6.64
Blank 8 512	3.566E-05	4.993E-05	3.947E-05	3.647E-05	3.814E-05	3.993E-05	5.781E-06	14.48
Blank 16 512	2.717E-05	2.034E-05	2.133E-05	2.033E-05	1.512E-05	2.086E-05	4.286E-06	20.55

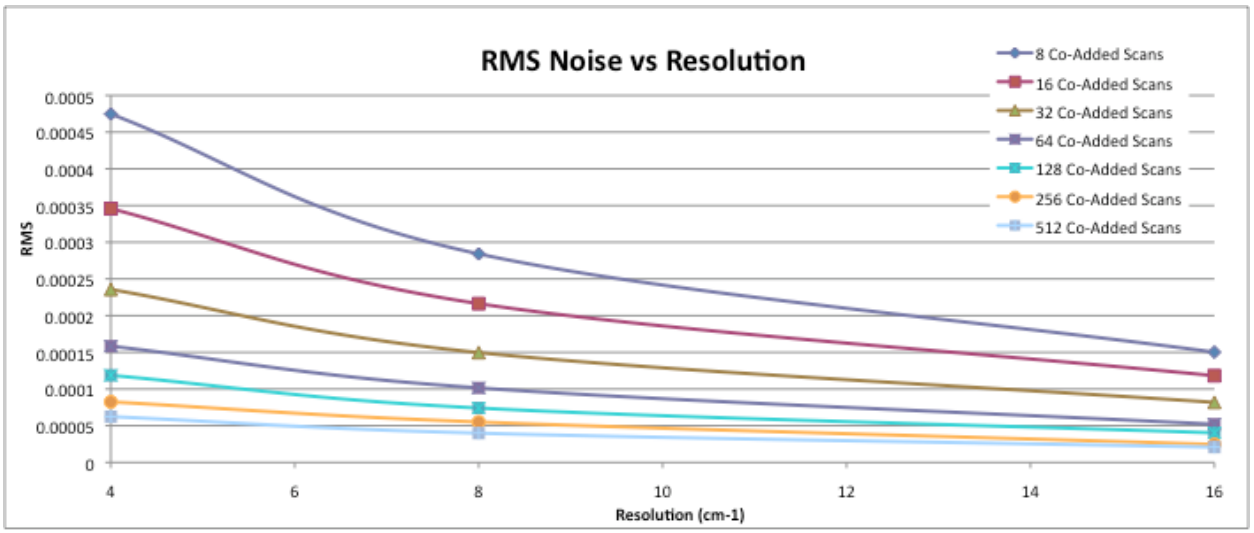


Figure 36: Graph of the RMS noise vs. spectral resolution for the 25-µm aperture.

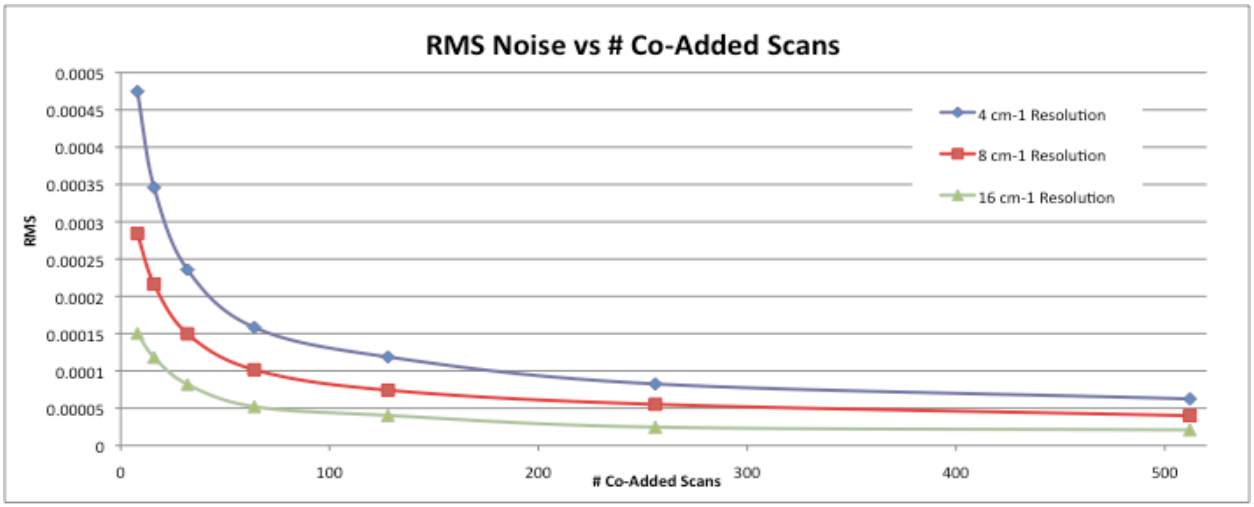


Figure 37: Graph of the RMS noise vs. the number of co-added scans for the 25-µm aperture.

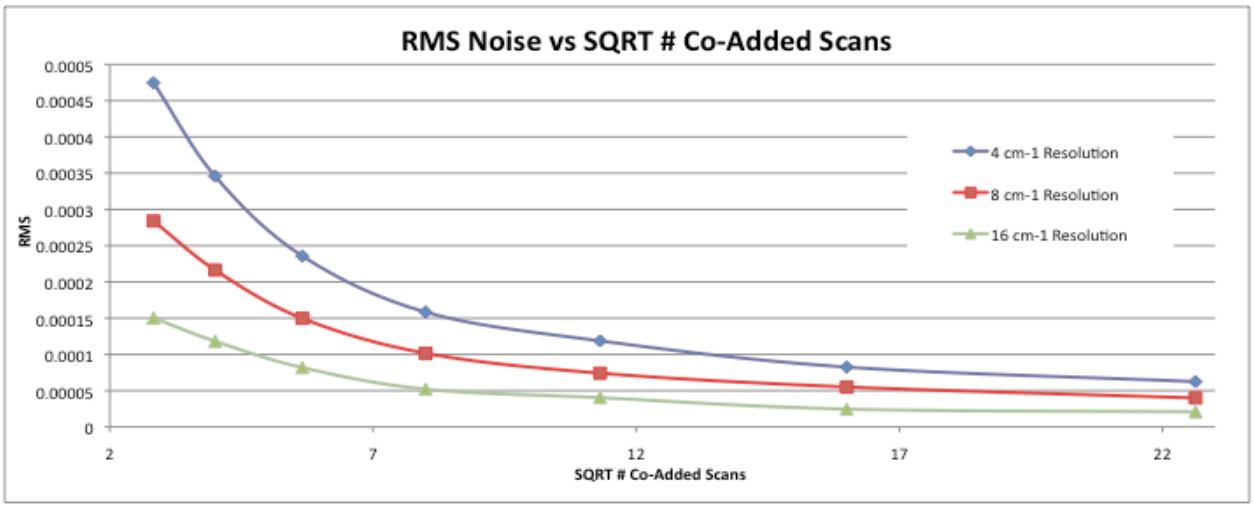


Figure 38: Graph of the RMS noise vs. the square root of the number of co-added scans for the 25-µm aperture.

Table 8: Analytical S/N for the spectra of blanks collected with the 25-µm aperture, calculated for the mid-IR region from 1300 – 850 cm^{-1}.

Spectral resolution & # of co-added scans	S/N
4 8	2616.75
8 8	4372.30
16 8	8267.18
4 16	3592.33
8 16	5741.88
16 16	10512.84
4 32	5270.83
8 32	8298.24
16 32	15178.87
4 64	7842.83
8 64	12232.34
16 64	23858.53
4 128	10467.64
8 128	16758.45
16 128	30829.30
4 256	15055.12
8 256	22524.79
16 256	50547.91
4 512	19894.07
8 512	31106.74
16 512	59557.62

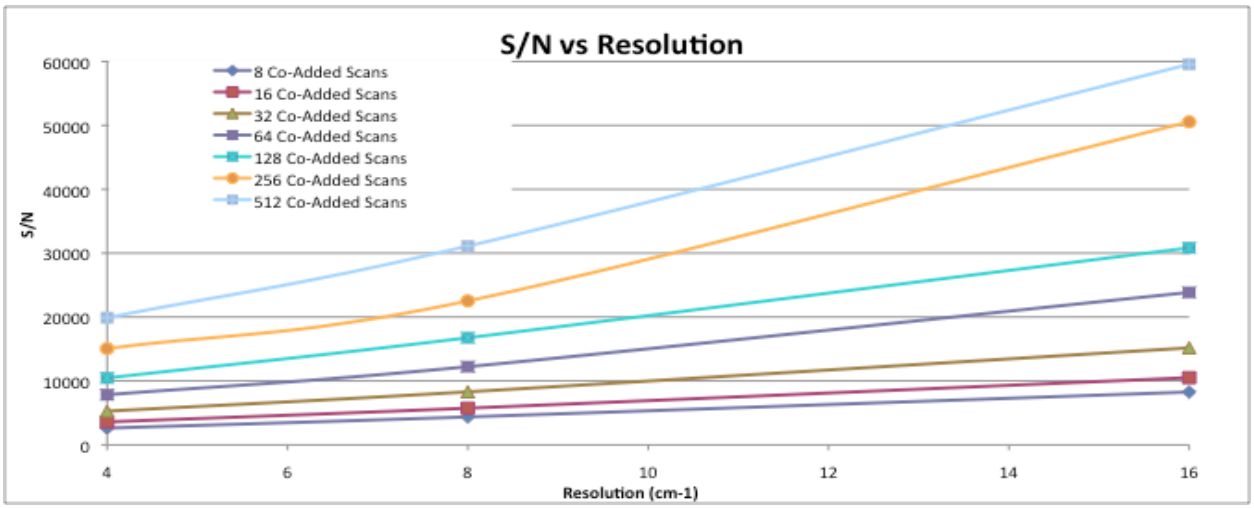


Figure 39: Graph of the S/N vs. spectral resolution for the 50-µm aperture.

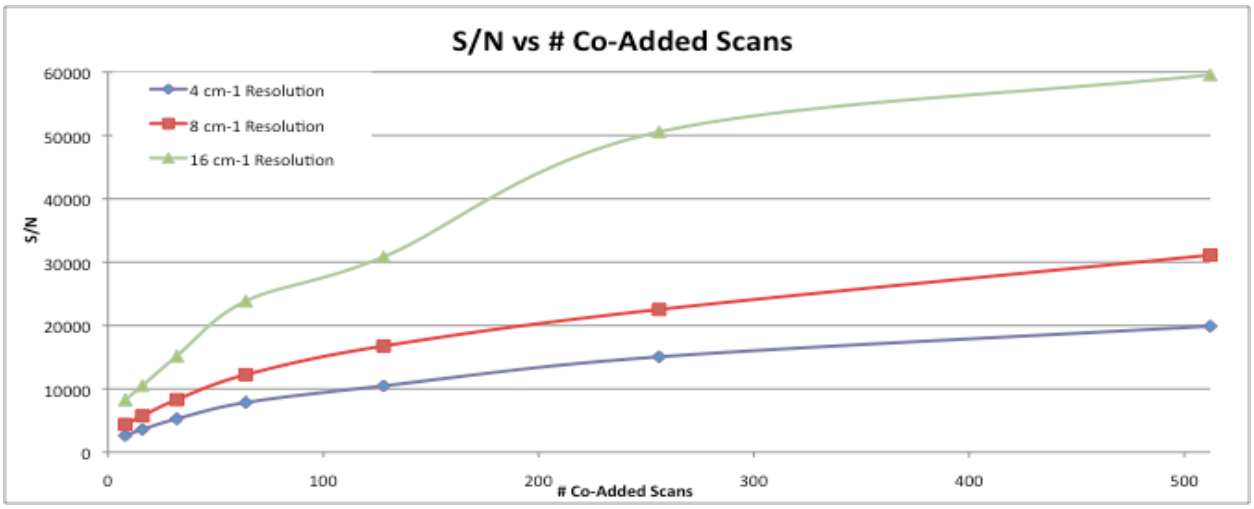


Figure 40: Graph of the S/N vs. the number of co-added scans for the 50-µm aperture.

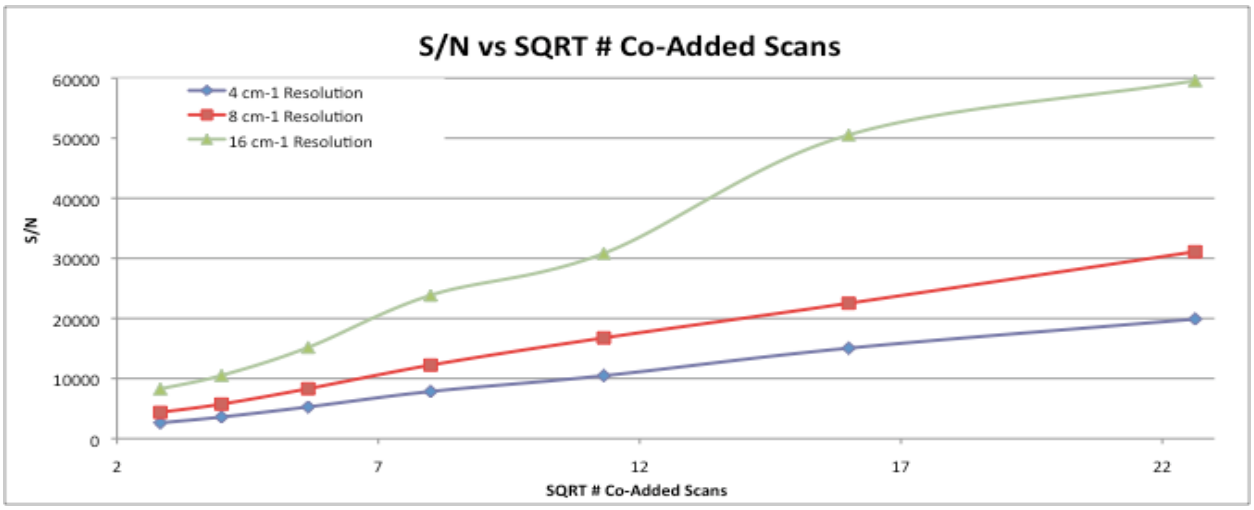


Figure 41: Graph of the S/N vs. the square root of the number of co-added scans for the 50-µm aperture.

Table 9: RMS noise for the spectra of blanks collected with the 10-µm aperture, calculated for the mid-IR region from 1300 – 850 cm^{-1}.

	1	2	3	4	5	Average Noise	Standard Deviation	% RSD
Blank 4 8	2.947E-03	2.800E-03	2.809E-03	3.403E-03	3.242E-03	3.040E-03	2.702E-04	8.89
Blank 8 8	2.198E-03	1.749E-03	2.101E-03	1.708E-03	2.000E-03	1.951E-03	2.156E-04	11.05
Blank 16 8	9.853E-04	8.474E-04	1.071E-03	7.845E-04	1.058E-03	9.494E-04	1.281E-04	13.49
Blank 4 16	2.018E-03	1.921E-03	2.089E-03	2.051E-03	2.233E-03	2.063E-03	1.141E-04	5.53
Blank 8 16	1.149E-03	1.069E-03	1.476E-03	1.492E-03	1.466E-03	1.330E-03	2.043E-04	15.35
Blank 16 16	8.082E-04	6.356E-04	7.419E-04	6.781E-04	7.089E-04	7.145E-04	6.543E-05	9.16
Blank 4 32	1.406E-03	1.655E-03	1.645E-03	1.570E-03	1.516E-03	1.559E-03	1.028E-04	6.59
Blank 8 32	8.585E-04	8.434E-04	9.630E-04	8.987E-04	9.645E-04	9.056E-04	5.677E-05	6.27
Blank 16 32	4.353E-04	4.984E-04	6.602E-04	4.890E-04	5.842E-04	5.334E-04	8.873E-05	16.64
Blank 4 64	1.036E-03	8.685E-04	1.066E-03	1.070E-03	1.110E-03	1.030E-03	9.413E-05	9.14
Blank 8 64	6.684E-04	6.716E-04	7.226E-04	6.265E-04	8.579E-04	7.094E-04	8.973E-05	12.65
Blank 16 64	3.048E-04	4.196E-04	4.058E-04	3.460E-04	4.844E-04	3.921E-04	6.929E-05	17.67
Blank 4 128	7.677E-04	6.625E-04	7.602E-04	7.214E-04	8.270E-04	7.478E-04	6.083E-05	8.13
Blank 8 128	5.312E-04	4.558E-04	5.337E-04	4.128E-04	6.012E-04	5.069E-04	7.360E-05	14.52
Blank 16 128	2.732E-04	2.379E-04	2.217E-04	1.983E-04	2.715E-04	2.405E-04	3.230E-05	13.43
Blank 4 256	4.999E-04	5.425E-04	5.313E-04	5.202E-04	5.584E-04	5.305E-04	2.219E-05	4.18
Blank 8 256	3.231E-04	3.119E-04	3.793E-04	3.009E-04	3.584E-04	3.347E-04	3.298E-05	9.85
Blank 16 256	1.861E-04	1.844E-04	1.758E-04	1.367E-04	1.865E-04	1.739E-04	2.126E-05	12.23
Blank 4 512	3.873E-04	3.274E-04	4.196E-04	3.681E-04	4.066E-04	3.818E-04	3.613E-05	9.46
Blank 8 512	1.906E-04	2.241E-04	2.398E-04	2.008E-04	2.754E-04	2.261E-04	3.363E-05	14.87
Blank 16 512	1.623E-04	1.163E-04	1.234E-04	1.090E-04	1.427E-04	1.307E-04	2.163E-05	16.54

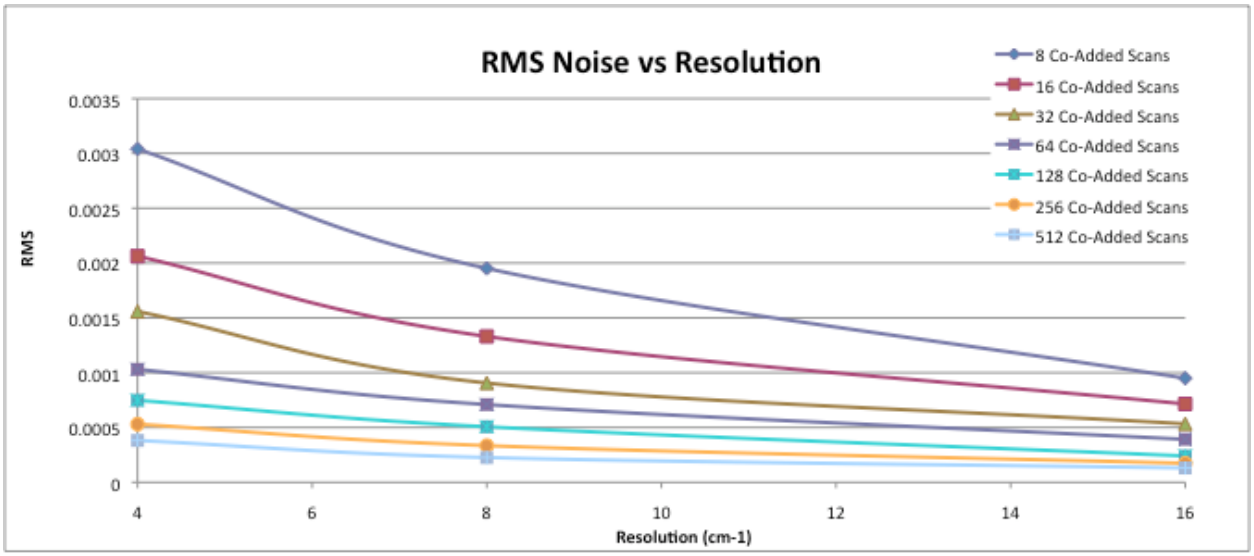


Figure 42: Graph of the RMS noise vs. spectral resolution for the 10-µm aperture.

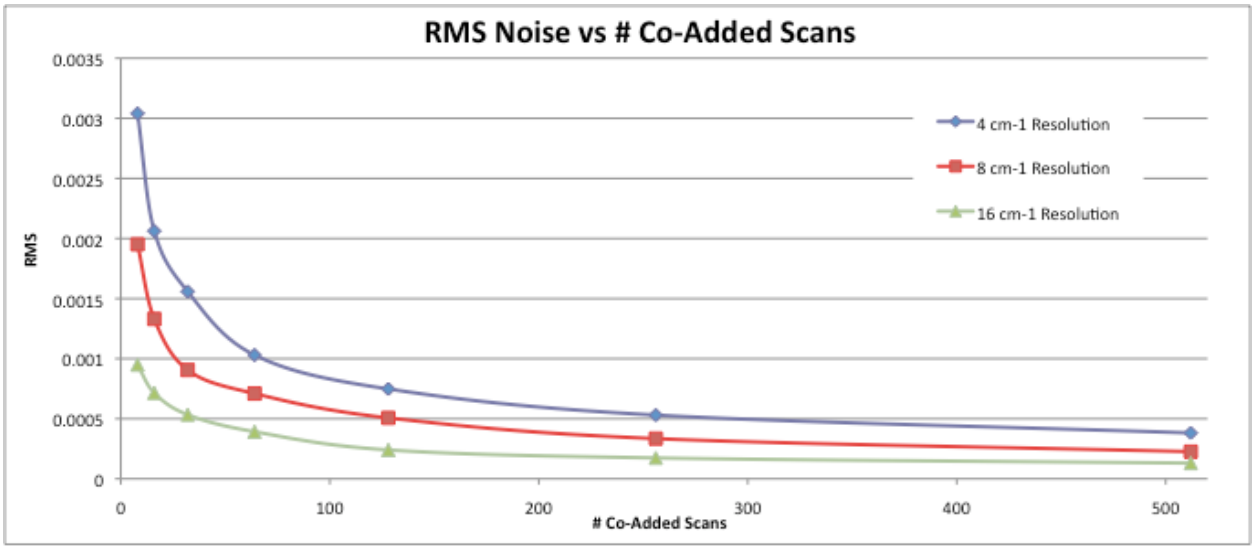


Figure 43: Graph of the RMS noise vs. the number of co-added scans for the 10-µm aperture.

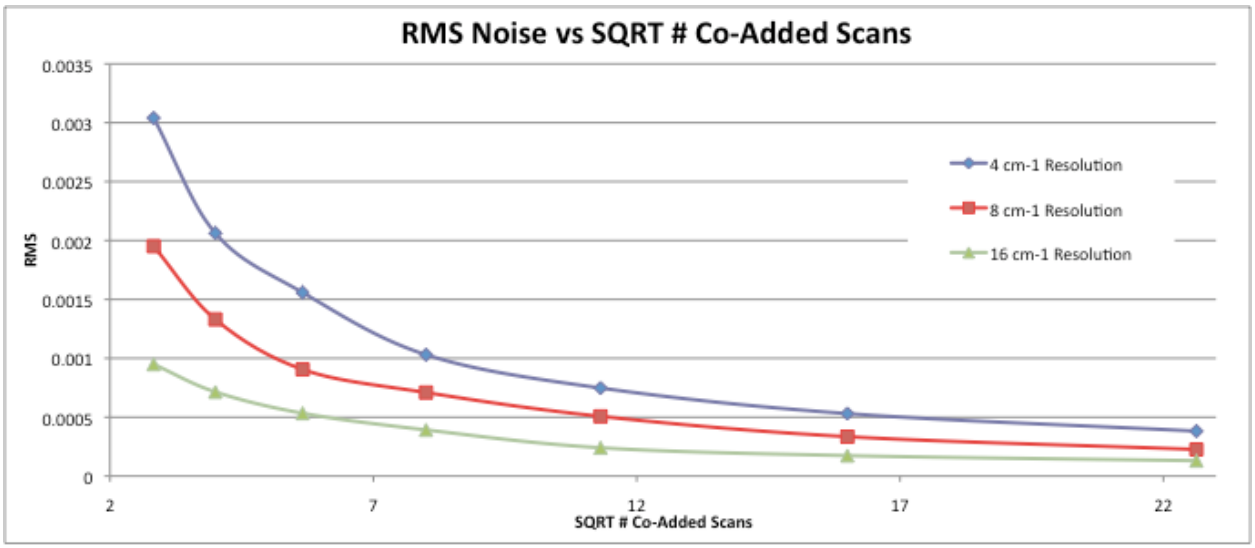


Figure 44: Graph of the RMS noise vs. the square root of the number of co-added scans for the 10-µm aperture.

Table 10: Analytical S/N for the spectra of blanks collected with the 10-µm aperture, calculated for the mid-IR region from 1300 – 850 cm^{-1}.

Spectral resolution & # of co-added scans	S/N
4 8	408.59
8 8	636.67
16 8	1308.51
4 16	602.28
8 16	933.68
16 16	1738.51
4 32	797.07
8 32	1371.73
16 32	2328.97
4 64	1205.88
8 64	1751.22
16 64	3168.29
4 128	1661.30
8 128	2450.46
16 128	5164.84
4 256	2341.82
8 256	3711.40
16 256	7143.94
4 512	3253.62
8 512	5493.28
16 512	9502.07

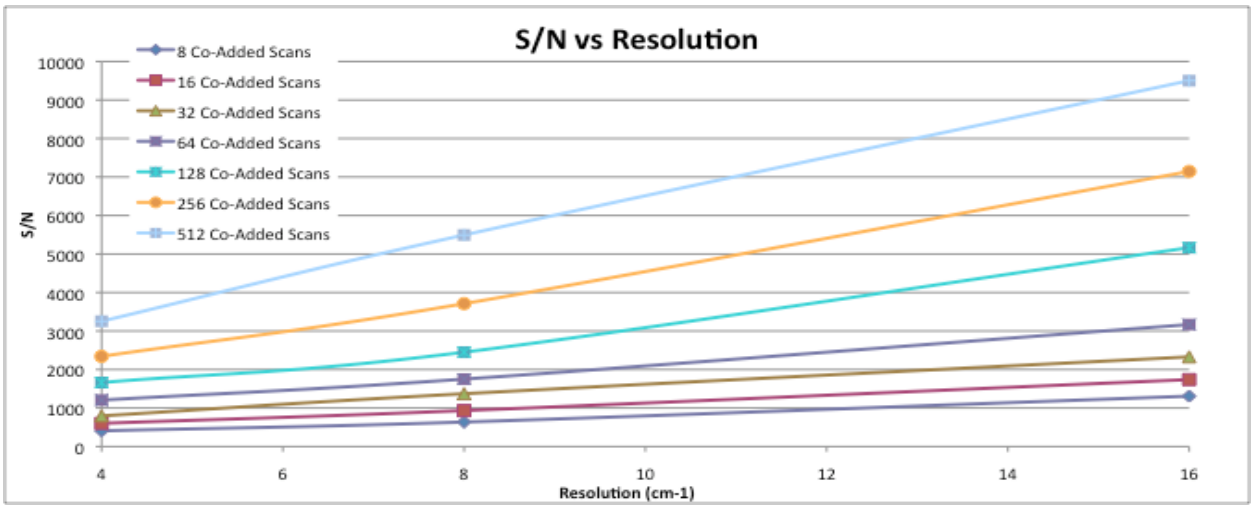


Figure 45: Graph of the S/N vs. spectral resolution for the 50-µm aperture.

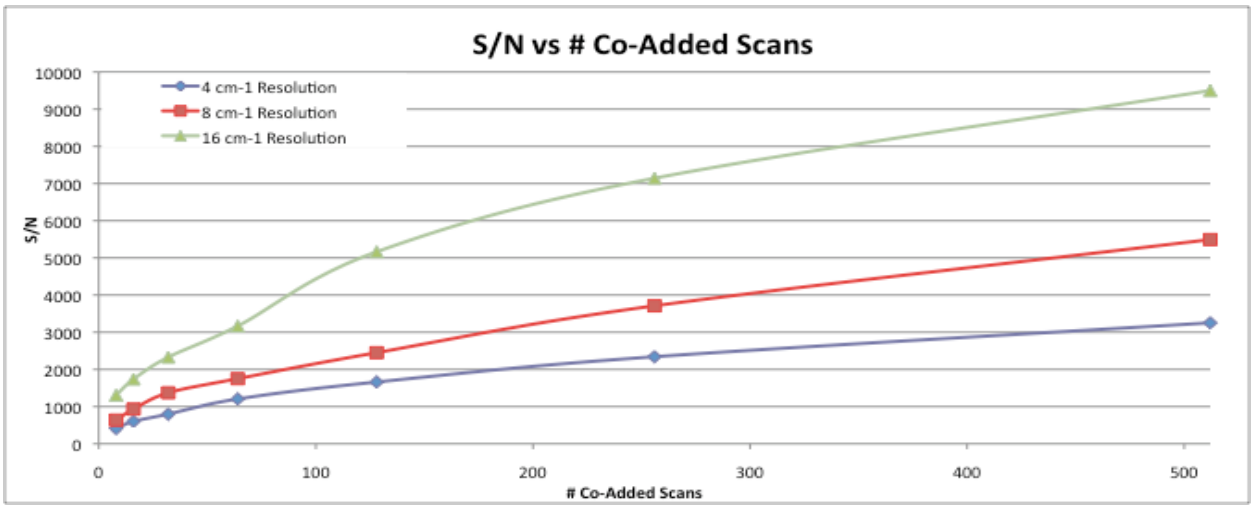


Figure 46: Graph of the S/N vs. the number of co-added scans for the 50-µm aperture.

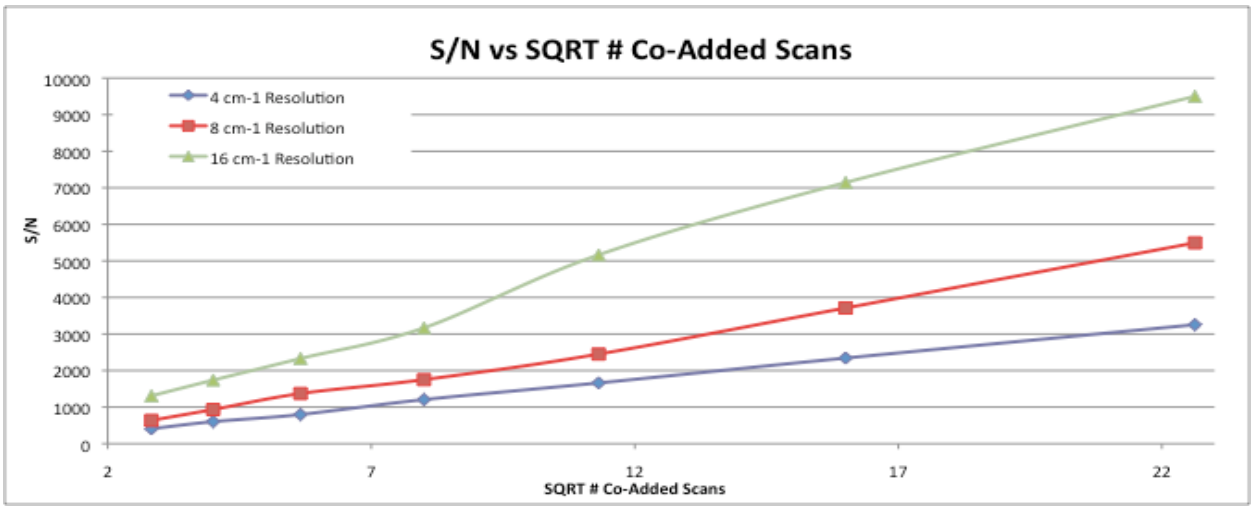


Figure 47: Graph of the S/N vs. the square root of the number of co-added scans for the 50-µm aperture.

As predicted by the Felgett advantage, the S/N increased with the square root of the number of co-added scans (or the RMS noise was inversely proportional to the square root of the number of co-added scans). The S/N also was proportional to the spectral resolution number: as the spectral resolution value increased (meaning a higher numerical value), so did the S/N. As a result, the combinations of 4 cm^{-1} spectral resolution and 256 co-added scans, 8 cm^{-1} spectral resolution and 64 co-added scans, and 16 cm^{-1} spectral resolution and 16 co-added scans all had roughly the same S/N (and RMS noise). There was also an unusually high S/N for the 50-μm aperture collected with a 16 cm^{-1} spectral resolution and 32 co-added scans, but this is for all of the spectra and not just one, which cannot be explained.

The time required for all of these analyses was minimal, with the longest time for one spectrum to be collected (not including sample preparation, which was less than 3 minutes) lasting approximately 90 seconds for the combination of 4 cm^{-1} spectral resolution and 256 co-added scans (or 2.5 minutes for the 4 cm^{-1} spectral resolution and 512 co-added scans). Reduced time for analysis was achieved with larger spectral resolutions or a lesser number of co-added scans. Still, 90 seconds of analysis time is not a long period of time, thus time for analysis was not a factor in determining the optimal parameters for the collection of glass mid-IR spectra.

As a result of these experiments, it was determined that all spectra of glass for this research were to be collected with the 50-μm aperture, 4 cm^{-1} spectral resolution, and 256 co-added scans. The spectra collected in this research were used for spectral deconvolutions and statistical analysis, thus the largest S/N (or smallest RMS noise) is desired. The larger aperture, 50-μm, and larger number of co-added scans, 256, provided the higher S/N, which is why those parameter values were chosen. Despite a larger S/N for lower spectral resolutions (higher numerical values), 4 cm^{-1} spectral resolution was chosen because the spectra are being

deconvolved and thus the most number of data points and highest spectral resolution is ideal. These combinations of parameters provided an analytical S/N of almost 30,000, which is excellent. To achieve a comparable S/N with smaller apertures, a significantly greater number of co-added scans must be used.

The second method development experiment was designed to determine the optimal number of spectra to be averaged and made into a searchable mid-IR glass library. It involved making searchable mid-IR libraries with glass spectra made from averaging different numbers of spectra (3, 5, 7, 10, 15, 20 and 30), and searching them with spectra of the same glass, both those used to make the averages and 5 spectra not used to make the library. Three SRM glasses were analyzed (SRM 620, 621, and 1831) as well as a 'real world' window glass. All glasses were analyzed with the 50-μm aperture and 4 cm^{-1} spectral resolution. In addition, the effect of using different numbers of co-added scans (8, 16, 32, 64, 128, and 256 co-added scans) was investigated in this experiment. Both the correlation and first derivative correlation search algorithms were used in this analysis and the HQI results are in Appendix VI.

Tables 11, 15, and 19 contain the calculated averages and standard deviations of the HQI data for library searches using the correlation algorithm of glass spectra not used in the making of the mid-IR libraries for SRM 620, 621 and 1831, respectively. This data is represented graphically in Figures 48, 52, and 56. Tables 12, 16, and 20 contain the calculated averages and standard deviations of the HQI data for library searches using the correlation algorithm of glass spectra used in the making of the mid-IR libraries for SRM 620, 621 and 1831, respectively. This data is represented graphically in Figures 49, 53, and 57. Tables 13, 17, and 21 contain the calculated averages and standard deviations of the HQI data for library searches using the first derivative correlation algorithm of glass spectra not used in the making of the mid-IR libraries

for SRM 620, 621 and 1831, respectively. This data is represented graphically in Figures 50, 54, and 58. Tables 14, 18, and 22 contain the calculated averages and standard deviations of the HQI data for library searches using the correlation algorithm of glass spectra used in the making of the mid-IR libraries for SRM 620, 621 and 1831, respectively. This data is represented graphically in Figures 51, 55, and 59.

In order to better compare the results from the 3 different SRM glasses with the combination of 4 cm^{-1} spectral resolution and 256 co-added scans, 4 graphs of the HQI data for all 3 SRMs were made (Figures 60 – 63): 1) correlation algorithm and HQI results from spectra not used in the making of the library, 2) correlation algorithm and HQI results from spectra used in the making of the library, 3) first derivative correlation algorithm and HQI results from spectra not used in the making of the library, and 4) first derivative correlation algorithm and HQI results from spectra used in the making of the library. In order to visually see the variance in the HQI results, these graphs included error bars equal to +/- 1 standard deviation. Also, an average of the 3 SRMs for each of the 4 data sets was calculated and is represented on each graph.

To confirm the results of the SRM glasses, the analysis was repeated for a 'real world' window glass sample. The analysis of the library search HQI data for the 'real world' window glass is in Tables 23 – 26 and is represented graphically in Figures 64 – 67.

Table 11: Average library search (correlation algorithm) HQI values (and standard deviations) for the SRM 620 glass spectra not used in the making of the mid-IR libraries. Each row has the data from a library made with spectra with different numbers of co-added scans (8, 16, 32, 64, 128, and 256). The columns are the different number of spectra averaged to make each entry in each mid-IR library.

	3 Ave	5 Ave	7 Ave	10 Ave	15 Ave	20 Ave
SRM 620 4 8	0.00252	0.00253	0.00245	0.00240	0.00250	0.00243
STD DEV	0.00037	0.00033	0.00029	0.00024	0.00031	0.00025
SRM 620 4 16	0.00446	0.00439	0.00433	0.00400	0.00374	0.00429
STD DEV	0.00039	0.00036	0.00037	0.00059	0.00031	0.00034
SRM 620 4 32	0.00278	0.00271	0.00273	0.00291	0.00288	0.00291
STD DEV	0.00119	0.00119	0.00117	0.00117	0.00124	0.00124
SRM 620 4 64	0.00271	0.00290	0.00286	0.00282	0.00282	0.00283
STD DEV	0.00020	0.00028	0.00029	0.00020	0.00022	0.00022
SRM 620 4 128	0.00242	0.00254	0.00275	0.00310	0.00313	0.00312
STD DEV	0.00019	0.00026	0.00044	0.00022	0.00021	0.00021
SRM 620 4 256	0.00310	0.00307	0.00289	0.00279	0.00306	0.00307
STD DEV	0.00030	0.00029	0.00040	0.00042	0.00031	0.00030

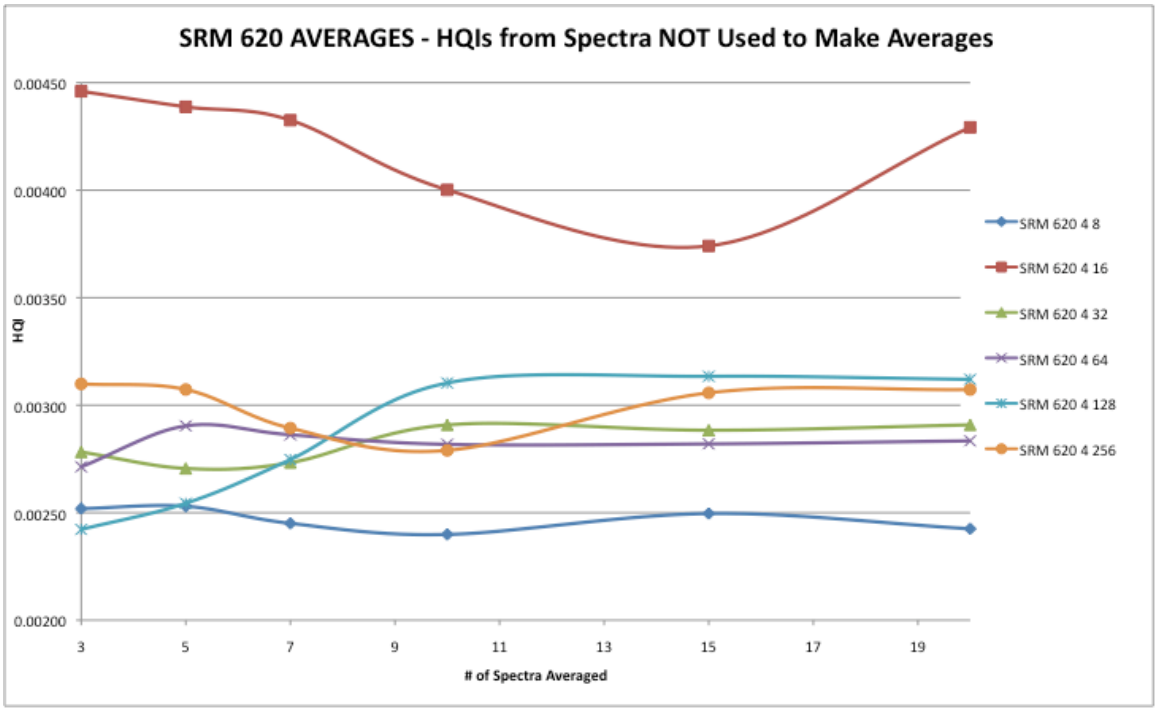


Figure 48: Graph of the HQI (correlation algorithm) from spectra not used to make the mid-IR library vs. the number that was averaged to make each spectrum in the library for SRM 620. Each line represents a data set with a different number of co-added scans.

Table 12: Average library search (correlation algorithm) HQI values (and standard deviations) for the SRM 620 glass spectra used in the making of the mid-IR libraries. Each row has the data from a library made with spectra with different numbers of co-added scans (8, 16, 32, 64, 128, and 256). The columns are the different number of spectra averaged to make each entry in each mid-IR library.

	3 Ave	5 Ave	7 Ave	10 Ave	15 Ave	20 Ave	30 Ave
SRM 620 4 8	0.00253	0.00258	0.00269	0.00264	0.00263	0.00272	0.00265
STD DEV	0.00045	0.00041	0.00045	0.00048	0.00047	0.00052	0.00051
SRM 620 4 16	0.00430	0.00429	0.00428	0.00390	0.00369	0.00432	0.00431
STD DEV	0.00038	0.00036	0.00027	0.00045	0.00029	0.00029	0.00030
SRM 620 4 32	0.00292	0.00257	0.00267	0.00286	0.00257	0.00285	0.00287
STD DEV	0.00034	0.00099	0.00090	0.00079	0.00078	0.00077	0.00079
SRM 620 4 64	0.00287	0.00307	0.00298	0.00299	0.00297	0.00298	0.00301
STD DEV	0.00023	0.00036	0.00031	0.00030	0.00029	0.00027	0.00034
SRM 620 4 128	0.00223	0.00233	0.00255	0.00293	0.00264	0.00268	0.00294
STD DEV	0.00015	0.00030	0.00048	0.00031	0.00040	0.00042	0.00028
SRM 620 4 256	0.00310	0.00309	0.00293	0.00290	0.00311	0.00313	0.00312
STD DEV	0.00030	0.00025	0.00033	0.00040	0.00025	0.00024	0.00025

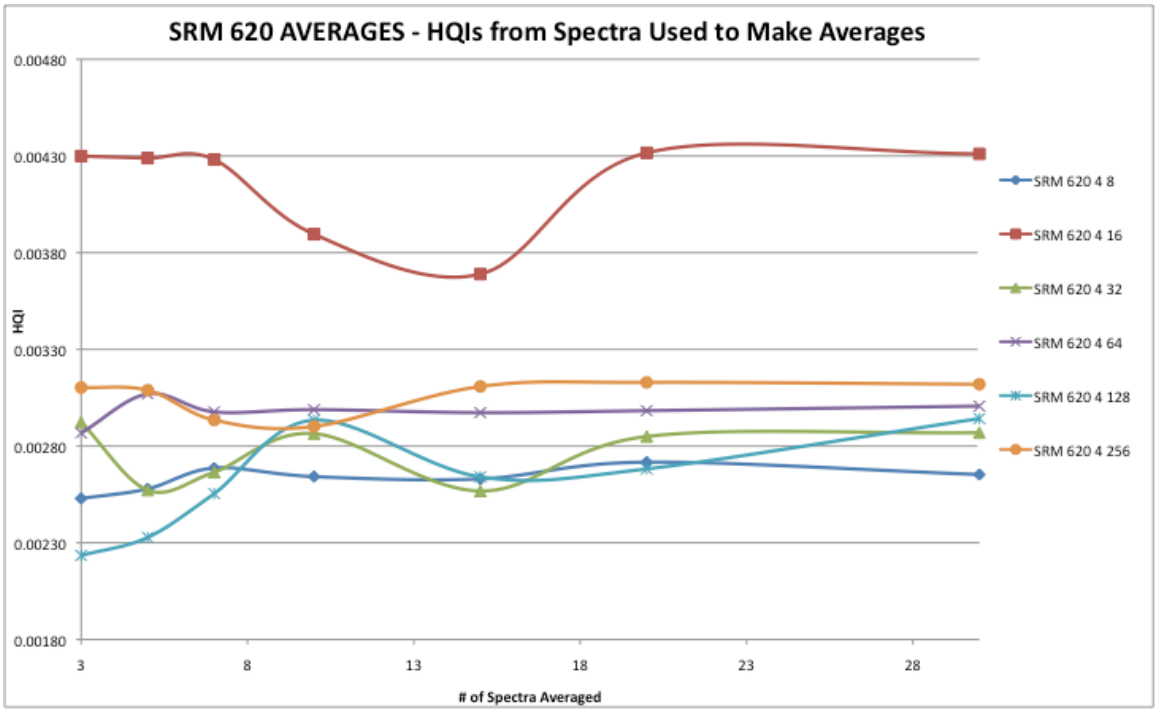


Figure 49: Graph of the HQI (correlation algorithm) from spectra used to make the mid-IR library vs. the number that was averaged to make each spectrum in the library for SRM 620. Each line represents a data set with a different number of co-added scans.

Table 13: Average library search (first derivative correlation algorithm) HQI values (and standard deviations) for the SRM 620 glass spectra not used in the making of the mid-IR libraries. Each row has the data from a library made with spectra with different numbers of co-added scans (8, 16, 32, 64, 128, and 256). The columns are the different number of spectra averaged to make each entry in each mid-IR library.

	3	5	7	10	15	20
SRM 620 4 8	0.04036	0.03760	0.03349	0.03535	0.03363	0.03318
STD DEV	0.00505	0.00479	0.00587	0.00508	0.00372	0.00485
SRM 620 4 16	0.17570	0.17715	0.17624	0.10678	0.02768	0.16921
STD DEV	0.00835	0.00807	0.00820	0.07684	0.00168	0.00718
SRM 620 4 32	0.13106	0.13316	0.13703	0.18144	0.18098	0.18110
STD DEV	0.07671	0.07840	0.08054	0.01295	0.01372	0.01407
SRM 620 4 64	0.17219	0.16718	0.16764	0.16469	0.16869	0.16956
STD DEV	0.01274	0.00603	0.00445	0.00606	0.00462	0.00482
SRM 620 4 128	0.02797	0.02748	0.07414	0.16210	0.16087	0.16072
STD DEV	0.00213	0.00278	0.06478	0.00684	0.00716	0.00713
SRM 620 4 256	0.16590	0.16509	0.11627	0.09604	0.15878	0.16788
STD DEV	0.00574	0.00609	0.06903	0.07535	0.00371	0.00436

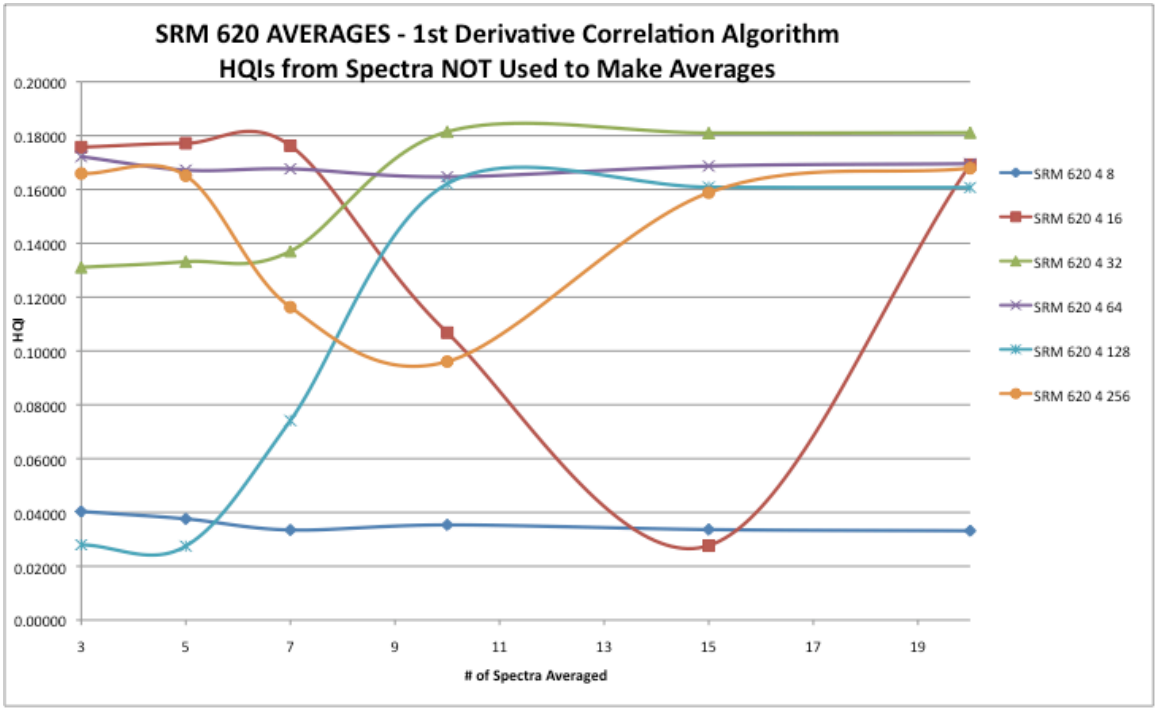


Figure 50: Graphs of the HQI (first derivative correlation algorithm) from spectra not used to make the mid-IR library vs. the number that was averaged to make each spectrum in the library for SRM 620. Each line represents a data set with a different number of co-added scans.

Table 14: Average library search (first derivative correlation algorithm) HQI values (and standard deviations) for the SRM 620 glass spectra used in the making of the mid-IR libraries. Each row has the data from a library made with spectra with different numbers of co-added scans (8, 16, 32, 64, 128, and 256). The columns are the different number of spectra averaged to make each entry in each mid-IR library.

	3	5	7	10	15	20	30
SRM 620 4 8	0.03597	0.03554	0.03356	0.03618	0.03535	0.03705	0.03583
STD DEV	0.01006	0.00808	0.00777	0.00714	0.00714	0.00695	0.00727
SRM 620 4 16	0.18086	0.18432	0.18241	0.08267	0.02648	0.17554	0.17425
STD DEV	0.01639	0.01438	0.01399	0.07638	0.00396	0.01146	0.01209
SRM 620 4 32	0.12256	0.12566	0.12879	0.17422	0.10132	0.17386	0.17363
STD DEV	0.07211	0.07302	0.07387	0.01338	0.07340	0.01354	0.01371
SRM 620 4 64	0.17073	0.16586	0.16586	0.16492	0.16870	0.16941	0.16885
STD DEV	0.01312	0.01166	0.01259	0.01010	0.00968	0.00994	0.00966
SRM 620 4 128	0.02575	0.02576	0.07513	0.16789	0.09571	0.09591	0.16464
STD DEV	0.00256	0.00306	0.06728	0.00850	0.06801	0.06897	0.00713
SRM 620 4 256	0.16615	0.16518	0.11622	0.11865	0.15867	0.16359	0.15887
STD DEV	0.00620	0.00667	0.06896	0.06930	0.00442	0.00599	0.00446

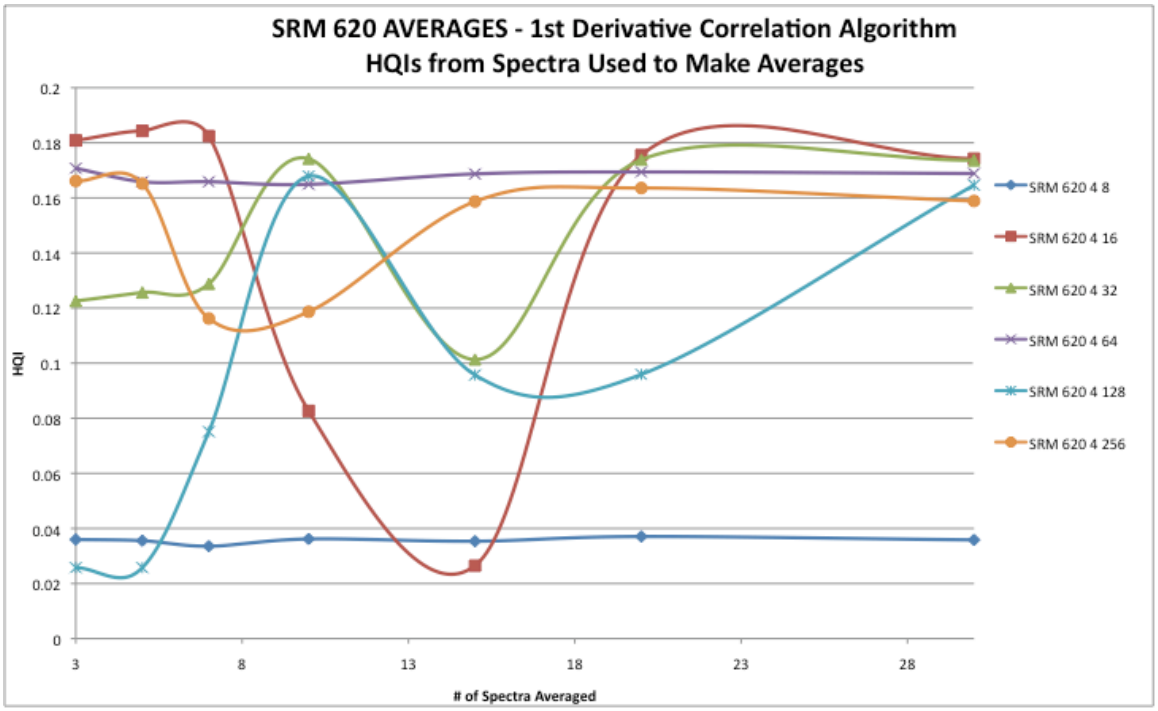


Figure 51: Graphs of the HQI (first derivative correlation algorithm) from spectra used to make the mid-IR library vs. the number that was averaged to make each spectrum in the library for SRM 620. Each line represents a data set with a different number of co-added scans.

Table 15: Average library search (correlation algorithm) HQI values (and standard deviations) for the SRM 621 glass spectra not used in the making of the mid-IR libraries. Each row has the data from a library made with spectra with different numbers of co-added scans (8, 16, 32, 64, 128, and 256). The columns are the different number of spectra averaged to make each entry in each mid-IR library.

	3	5	7	10	15	20
SRM 621 4 8	0.00229	0.00262	0.00313	0.00280	0.00252	0.00281
STD DEV	0.00101	0.00108	0.00140	0.00114	0.00097	0.00110
SRM 621 4 16	0.00173	0.00182	0.00171	0.00182	0.00194	0.00190
STD DEV	0.00051	0.00074	0.00060	0.00070	0.00060	0.00062
SRM 621 4 32	0.00219	0.00212	0.00191	0.00199	0.00223	0.00214
STD DEV	0.00060	0.00059	0.00051	0.00055	0.00061	0.00054
SRM 621 4 64	0.00151	0.00115	0.00142	0.00120	0.00116	0.00151
STD DEV	0.00055	0.00048	0.00053	0.00050	0.00051	0.00058
SRM 621 4 128	0.00198	0.00195	0.00213	0.00200	0.00186	0.00186
STD DEV	0.00037	0.00037	0.00037	0.00034	0.00031	0.00031
SRM 621 4 256	0.00468	0.00208	0.00205	0.00207	0.00206	0.00207
STD DEV	0.00395	0.00070	0.00055	0.00065	0.00059	0.00062

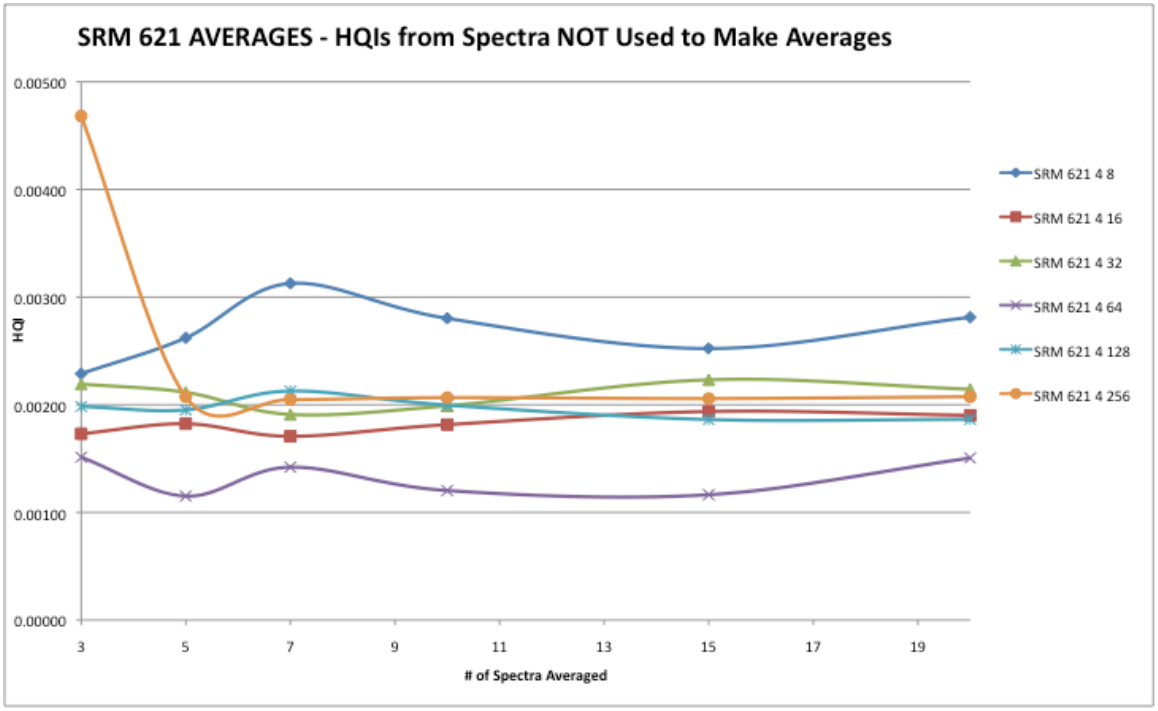


Figure 52: Graphs of the HQI (correlation algorithm) from spectra not used to make the mid-IR library vs. the number that was averaged to make each spectrum in the library for SRM 621. Each line represents a data set with a different number of co-added scans.

Table 16: Average library search (correlation algorithm) HQI values (and standard deviations) for the SRM 621 glass spectra used in the making of the mid-IR libraries. Each row has the data from a library made with spectra with different numbers of co-added scans (8, 16, 32, 64, 128, and 256). The columns are the different number of spectra averaged to make each entry in each mid-IR library.

	3	5	7	10	15	20	30
SRM 621 4 8	0.00188	0.00210	0.00231	0.00232	0.00236	0.00234	0.00209
STD DEV	0.00042	0.00060	0.00074	0.00090	0.00086	0.00082	0.00093
SRM 621 4 16	0.00152	0.00151	0.00146	0.00166	0.00182	0.00176	0.00150
STD DEV	0.00042	0.00033	0.00044	0.00044	0.00051	0.00048	0.00046
SRM 621 4 32	0.00191	0.00188	0.00178	0.00176	0.00181	0.00184	0.00199
STD DEV	0.00059	0.00066	0.00053	0.00051	0.00055	0.00051	0.00051
SRM 621 4 64	0.00165	0.00163	0.00182	0.00163	0.00156	0.00175	0.00187
STD DEV	0.00022	0.00044	0.00049	0.00044	0.00041	0.00052	0.00050
SRM 621 4 128	0.00168	0.00165	0.00188	0.00184	0.00165	0.00163	0.00194
STD DEV	0.00048	0.00035	0.00044	0.00046	0.00040	0.00041	0.00044
SRM 621 4 256	0.00442	0.00165	0.00169	0.00324	0.00170	0.00172	0.00172
STD DEV	0.00445	0.00053	0.00055	0.00226	0.00049	0.00050	0.00046

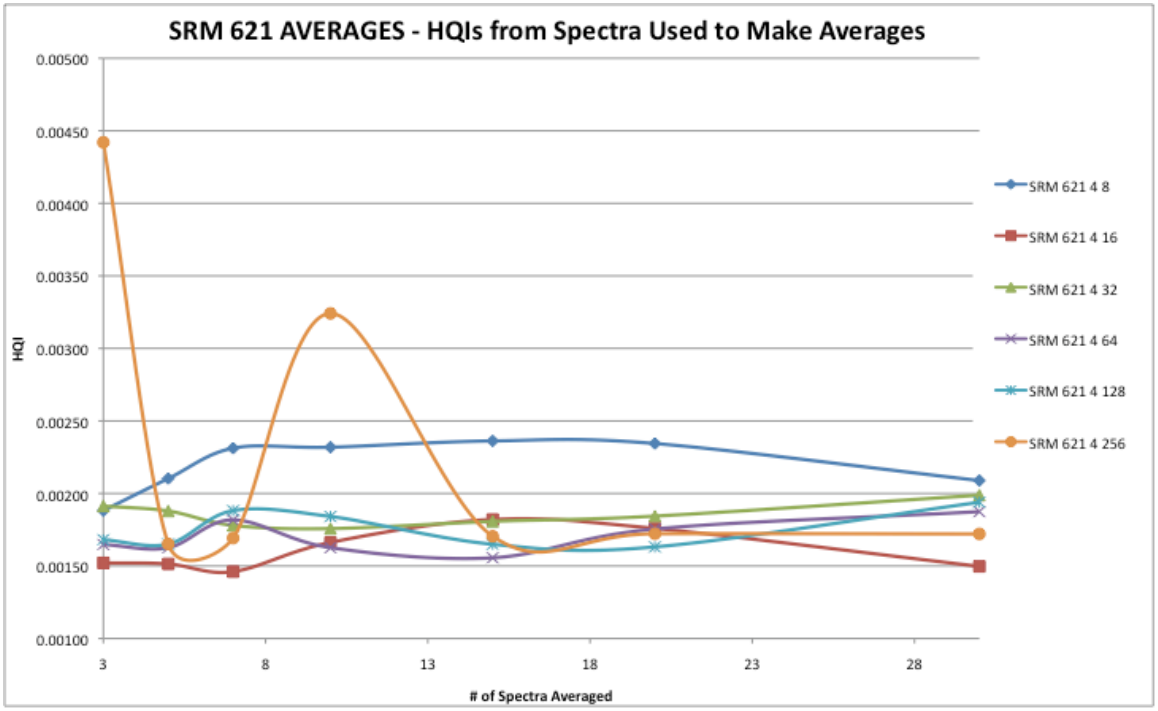


Figure 53: Graphs of the HQI (correlation algorithm) from spectra used to make the mid-IR library vs. the number that was averaged to make each spectrum in the library for SRM 621. Each line represents a data set with a different number of co-added scans.

Table 17: Average library search (first derivative correlation algorithm) HQI values (and standard deviations) for the SRM 621 glass spectra not used in the making of the mid-IR libraries. Each row has the data from a library made with spectra with different numbers of co-added scans (8, 16, 32, 64, 128, and 256). The columns are the different number of spectra averaged to make each entry in each mid-IR library.

	3	5	7	10	15	20
SRM 621 4 8	0.19966	0.21212	0.20782	0.20391	0.21072	0.21375
STD DEV	0.04835	0.04864	0.04584	0.04677	0.04814	0.04756
SRM 621 4 16	0.12404	0.11372	0.07986	0.13406	0.18360	0.18537
STD DEV	0.04797	0.05787	0.01215	0.06504	0.01765	0.01699
SRM 621 4 32	0.20033	0.15311	0.10754	0.12673	0.19157	0.18800
STD DEV	0.04198	0.07184	0.07188	0.07260	0.04111	0.04205
SRM 621 4 64	0.14374	0.06376	0.14071	0.05998	0.06459	0.18090
STD DEV	0.05692	0.00674	0.06151	0.00626	0.00751	0.01236
SRM 621 4 128	0.10793	0.10811	0.17779	0.12196	0.07432	0.07379
STD DEV	0.05321	0.05596	0.00764	0.05038	0.01004	0.00932
SRM 621 4 256	0.32356	0.06512	0.06606	0.06105	0.06045	0.05955
STD DEV	0.38153	0.00607	0.00486	0.00451	0.00452	0.00471

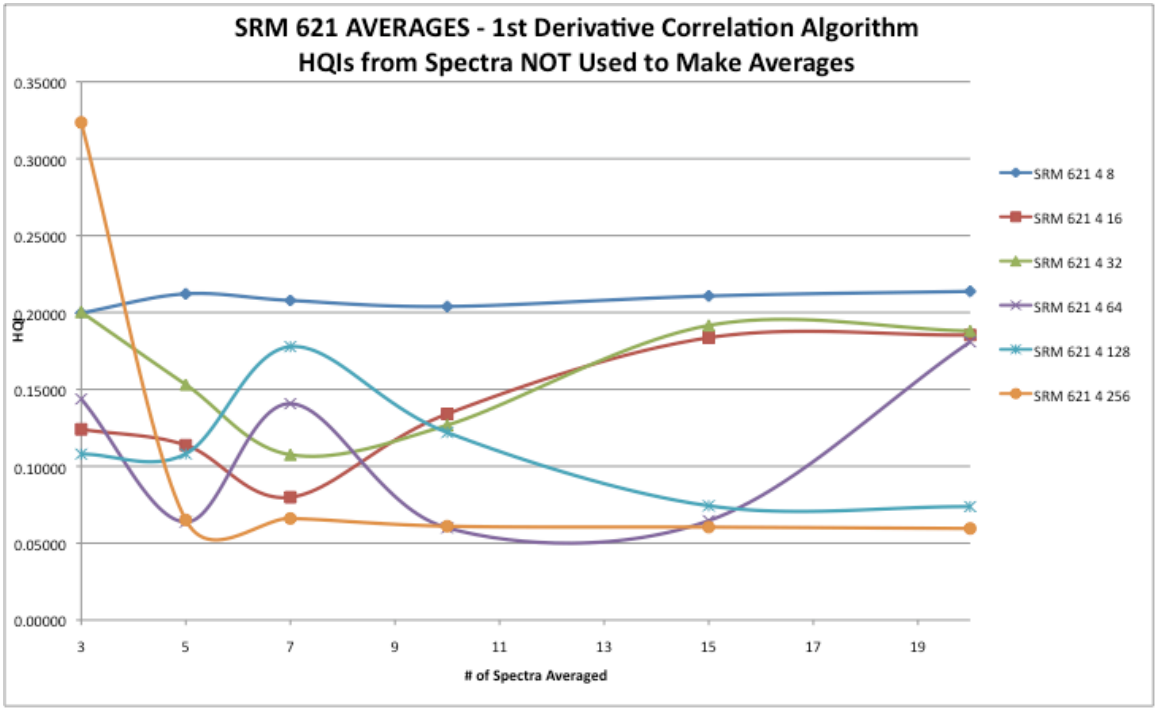


Figure 54: Graphs of the HQI (first derivative correlation algorithm) from spectra not used to make the mid-IR library vs. the number that was averaged to make each spectrum in the library for SRM 621. Each line represents a data set with a different number of co-added scans.

Table 18: Average library search (first derivative correlation algorithm) HQI values (and standard deviations) for the SRM 621 glass spectra used in the making of the mid-IR libraries. Each row has the data from a library made with spectra with different numbers of co-added scans (8, 16, 32, 64, 128, and 256). The columns are the different number of spectra averaged to make each entry in each mid-IR library.

	3	5	7	10	15	20	30
SRM 621 4 8	0.19746	0.19787	0.20120	0.20444	0.20961	0.20670	0.09128
STD DEV	0.02526	0.03757	0.04266	0.04650	0.04641	0.04868	0.02963
SRM 621 4 16	0.10393	0.10494	0.07133	0.14463	0.19431	0.19389	0.06800
STD DEV	0.06135	0.06380	0.01655	0.06526	0.02913	0.03071	0.01258
SRM 621 4 32	0.18350	0.14948	0.10061	0.09827	0.11948	0.12151	0.18319
STD DEV	0.01932	0.05970	0.05908	0.05673	0.06537	0.06143	0.02262
SRM 621 4 64	0.14445	0.06286	0.14237	0.10366	0.06256	0.11851	0.18013
STD DEV	0.05689	0.01013	0.05937	0.05954	0.00859	0.06063	0.01504
SRM 621 4 128	0.10084	0.10060	0.18084	0.13530	0.06539	0.06547	0.17257
STD DEV	0.06129	0.05784	0.01156	0.05061	0.00639	0.00618	0.01086
SRM 621 4 256	0.32235	0.06153	0.06310	0.29722	0.06113	0.06050	0.05863
STD DEV	0.39548	0.00562	0.00484	0.33286	0.00518	0.00551	0.00453

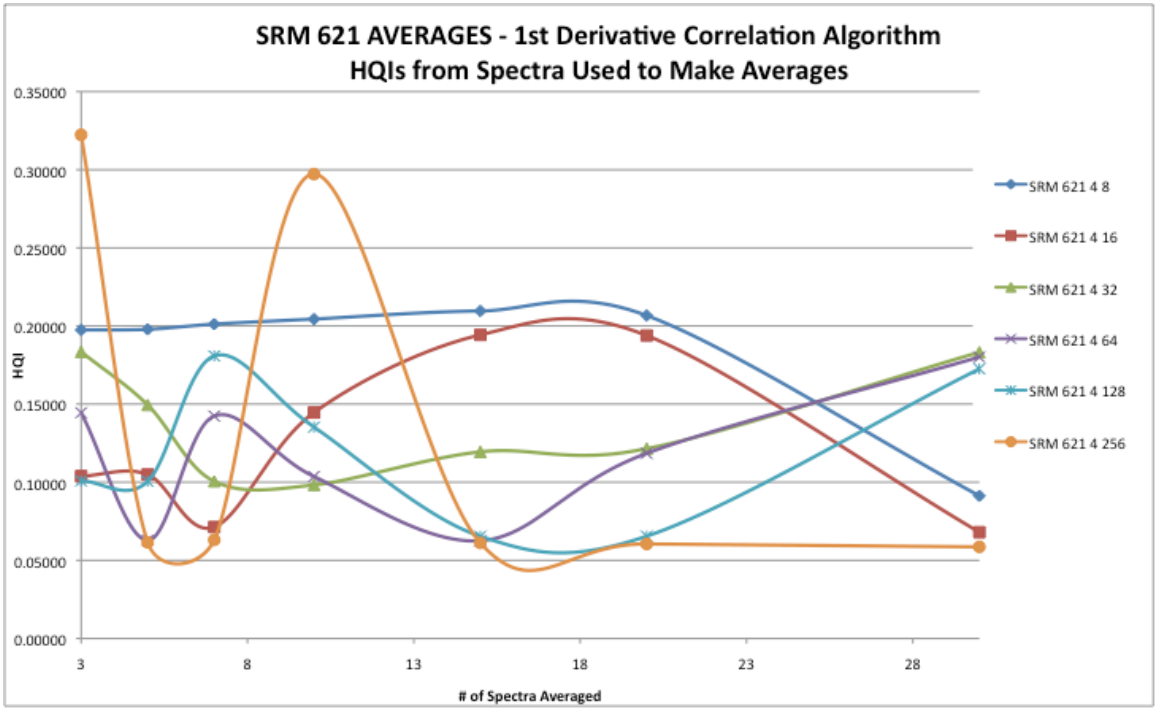


Figure 55: Graphs of the HQI (first derivative correlation algorithm) from spectra used to make the mid-IR library vs. the number that was averaged to make each spectrum in the library for SRM 621. Each line represents a data set with a different number of co-added scans.

Table 19: Average library search (correlation algorithm) HQI values (and standard deviations) for the SRM 1831 glass spectra not used in the making of the mid-IR libraries. Each row has the data from a library made with spectra with different numbers of co-added scans (8, 16, 32, 64, 128, and 256). The columns are the different number of spectra averaged to make each entry in each mid-IR library.

	3	5	7	10	15	20
SRM 1831 4 8	0.00271	0.00286	0.00262	0.00260	0.00261	0.00325
STD DEV	0.00023	0.00034	0.00018	0.00019	0.00019	0.00024
SRM 1831 4 16	0.00403	0.00403	0.00403	0.00403	0.00401	0.00403
STD DEV	0.00036	0.00036	0.00036	0.00037	0.00039	0.00039
SRM 1831 4 32	0.00496	0.00495	0.00468	0.00493	0.00493	0.00492
STD DEV	0.00010	0.00010	0.00038	0.00010	0.00011	0.00011
SRM 1831 4 64	0.00439	0.00435	0.00509	0.00471	0.00435	0.00507
STD DEV	0.00006	0.00006	0.00008	0.00038	0.00007	0.00007
SRM 1831 4 128	0.00486	0.00510	0.00744	0.00437	0.00509	0.00509
STD DEV	0.00038	0.00005	0.00341	0.00003	0.00004	0.00004
SRM 1831 4 256	0.00358	0.00364	0.00302	0.00361	0.00363	0.00357
STD DEV	0.00080	0.00061	0.00056	0.00058	0.00065	0.00060

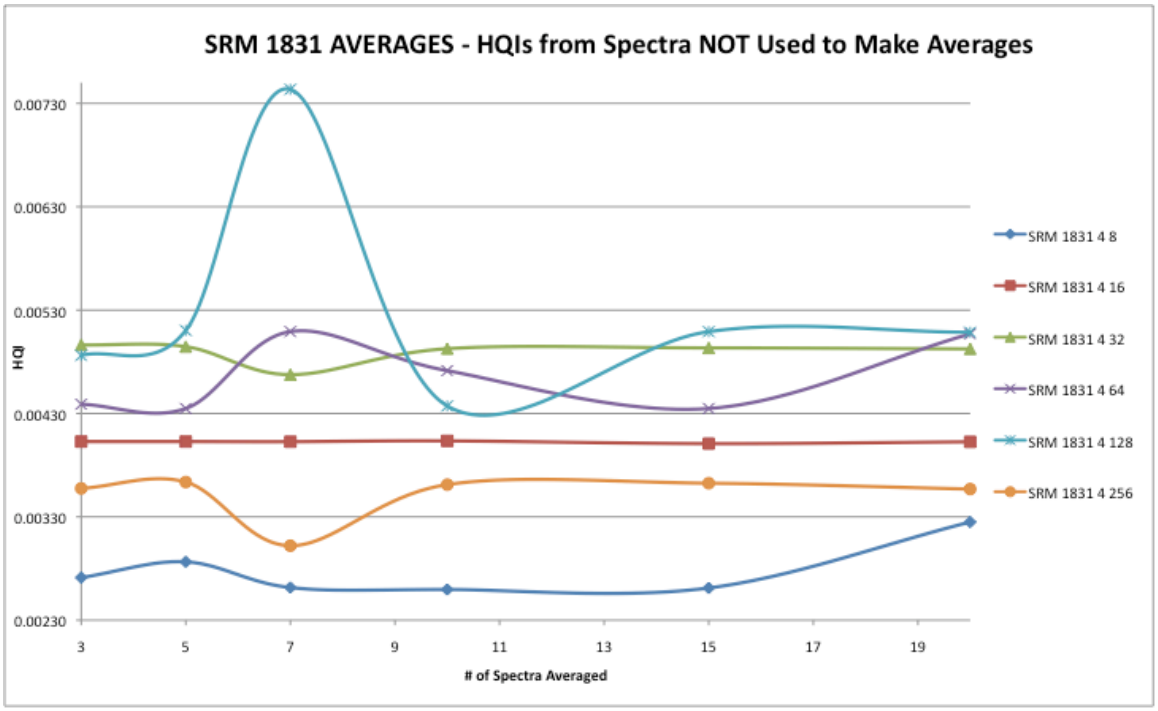


Figure 56: Graphs of the HQI (correlation algorithm) from spectra not used to make the mid-IR library vs. the number that was averaged to make each spectrum in the library for SRM 1831. Each line represents a data set with a different number of co-added scans.

Table 20: Average library search (correlation algorithm) HQI values (and standard deviations) for the SRM 1831 glass spectra used in the making of the mid-IR libraries. Each row has the data from a library made with spectra with different numbers of co-added scans (8, 16, 32, 64, 128, and 256). The columns are the different number of spectra averaged to make each entry in each mid-IR library.

	3	5	7	10	15	20	30
SRM 1831 4 8	0.00268	0.00292	0.00268	0.00270	0.00270	0.00330	0.00269
STD DEV	0.00032	0.00048	0.00028	0.00028	0.00028	0.00033	0.00028
SRM 1831 4 16	0.00402	0.00399	0.00398	0.00399	0.00399	0.00399	0.00467
STD DEV	0.00015	0.00017	0.00016	0.00020	0.00020	0.00019	0.00024
SRM 1831 4 32	0.00496	0.00493	0.00468	0.00494	0.00494	0.00493	0.00493
STD DEV	0.00025	0.00021	0.00037	0.00018	0.00017	0.00016	0.00017
SRM 1831 4 64	0.00435	0.00434	0.00509	0.00481	0.00434	0.00507	0.00505
STD DEV	0.00020	0.00017	0.00022	0.00039	0.00016	0.00019	0.00018
SRM 1831 4 128	0.00477	0.00502	0.00734	0.00456	0.00467	0.00467	0.00430
STD DEV	0.00042	0.00021	0.00337	0.00039	0.00039	0.00039	0.00017
SRM 1831 4 256	0.00345	0.00380	0.00318	0.00377	0.00347	0.00351	0.00376
STD DEV	0.00077	0.00063	0.00058	0.00066	0.00072	0.00068	0.00066

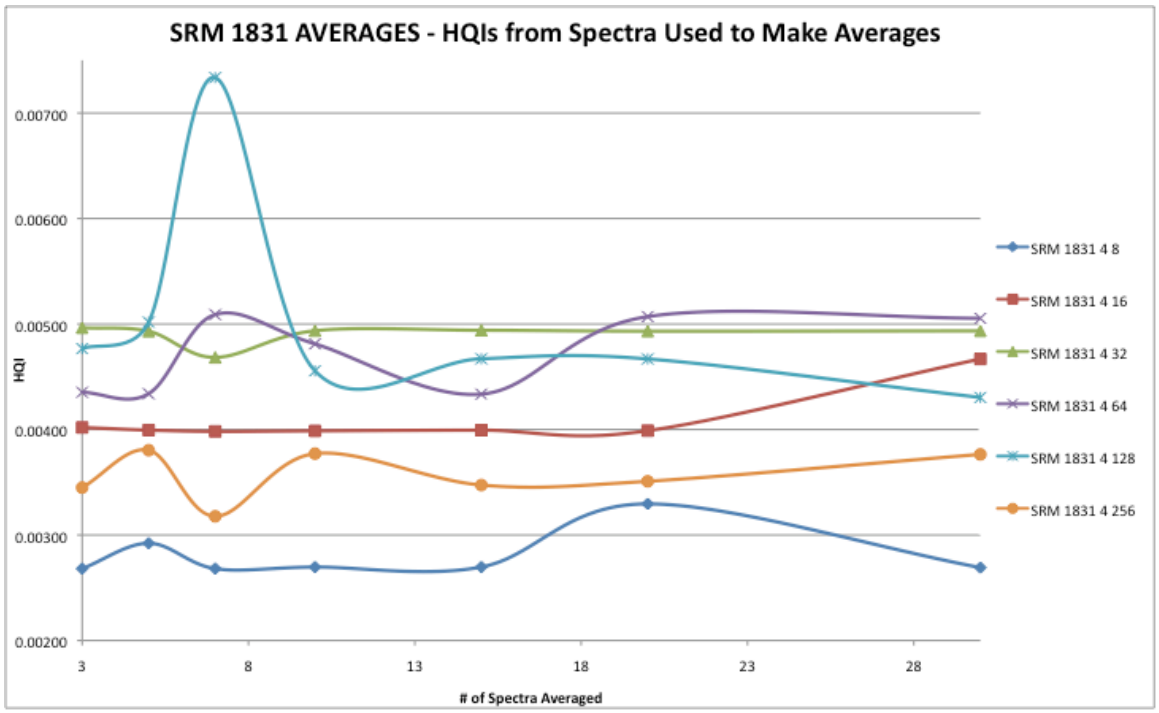


Figure 57: Graphs of the HQI (correlation algorithm) from spectra used to make the mid-IR library vs. the number that was averaged to make each spectrum in the library for SRM 1831. Each line represents a data set with a different number of co-added scans.

Table 21: Average library search (first derivative correlation algorithm) HQI values (and standard deviations) for the SRM 1831 glass spectra not used in the making of the mid-IR libraries. Each row has the data from a library made with spectra with different numbers of co-added scans (8, 16, 32, 64, 128, and 256). The columns are the different number of spectra averaged to make each entry in each mid-IR library.

	3	5	7	10	15	20
SRM 1831 4 8	0.03431	0.08021	0.03601	0.03254	0.03370	0.17597
SRM 1831 4 16	0.02555	0.02496	0.02479	0.02274	0.02165	0.02253
STD DEV	0.00552	0.00591	0.00440	0.00450	0.00475	0.00474
SRM 1831 4 32	0.19185	0.18846	0.13291	0.19481	0.19456	0.19441
STD DEV	0.01177	0.01163	0.08367	0.01141	0.01199	0.01215
SRM 1831 4 64	0.02192	0.01976	0.18177	0.09624	0.02047	0.17569
STD DEV	0.00248	0.00160	0.01109	0.08213	0.00158	0.00703
SRM 1831 4 128	0.12080	0.17267	0.36083	0.01979	0.17570	0.17512
STD DEV	0.07504	0.00583	0.27007	0.00098	0.00361	0.00369
SRM 1831 4 256	0.11688	0.16031	0.02622	0.16572	0.16117	0.16043
STD DEV	0.06566	0.00316	0.00240	0.00634	0.00327	0.00329

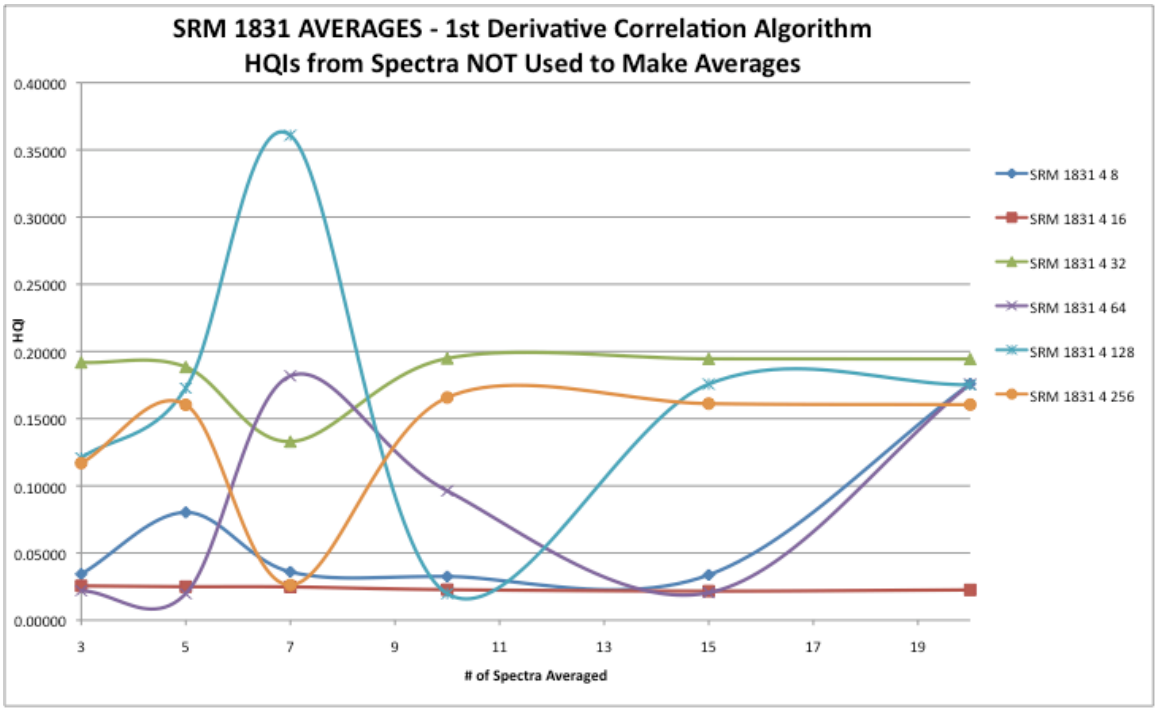


Figure 58: Graphs of the HQI (first derivative correlation algorithm) from spectra not used to make the mid-IR library vs. the number that was averaged to make each spectrum in the library for SRM 1831. Each line represents a data set with a different number of co-added scans.

Table 22: Average library search (first derivative correlation algorithm) HQI values (and standard deviations) for the SRM 1831 glass spectra used in the making of the mid-IR libraries. Each row has the data from a library made with spectra with different numbers of co-added scans (8, 16, 32, 64, 128, and 256). The columns are the different number of spectra averaged to make each entry in each mid-IR library.

	3	5	7	10	15	20	30
SRM 1831 4 8	0.03079	0.07617	0.03483	0.03375	0.03332	0.17145	0.03329
STD DEV	0.00696	0.07032	0.00724	0.00634	0.00698	0.02081	0.00706
SRM 1831 4 16	0.02315	0.02449	0.02479	0.02369	0.02319	0.02274	0.16676
STD DEV	0.00388	0.00451	0.00426	0.00525	0.00552	0.00474	0.01723
SRM 1831 4 32	0.17817	0.17432	0.12382	0.17848	0.17720	0.17616	0.17258
STD DEV	0.01118	0.00973	0.07386	0.01154	0.01267	0.01195	0.01214
SRM 1831 4 64	0.02178	0.01947	0.17920	0.12026	0.02010	0.17380	0.17340
STD DEV	0.00188	0.00133	0.01177	0.07419	0.00149	0.00581	0.00592
SRM 1831 4 128	0.12167	0.16409	0.36259	0.07332	0.09720	0.09826	0.01950
STD DEV	0.07749	0.04099	0.26681	0.07482	0.08194	0.07968	0.00121
SRM 1831 4 256	0.11677	0.16364	0.02563	0.16733	0.09527	0.09514	0.16423
STD DEV	0.06685	0.00440	0.00361	0.00588	0.07061	0.07036	0.00446

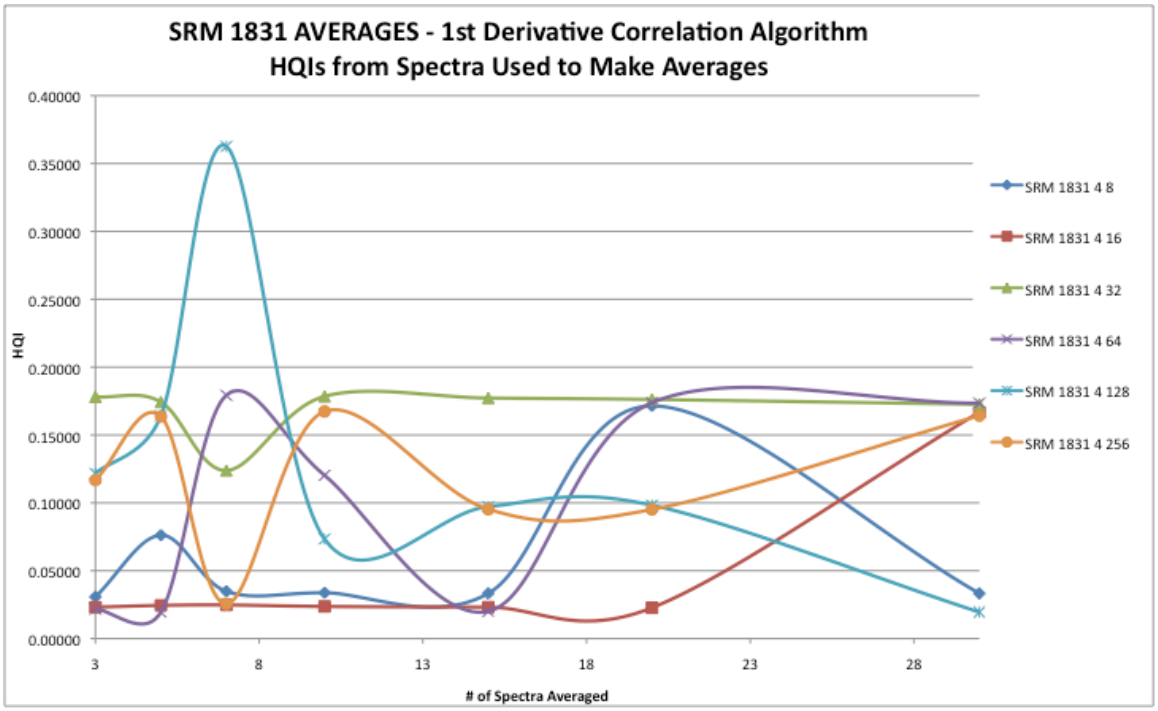


Figure 59: Graphs of the HQI (first derivative correlation algorithm) from spectra used to make the mid-IR library vs. the number that was averaged to make each spectrum in the library for SRM 1831. Each line represents a data set with a different number of co-added scans.

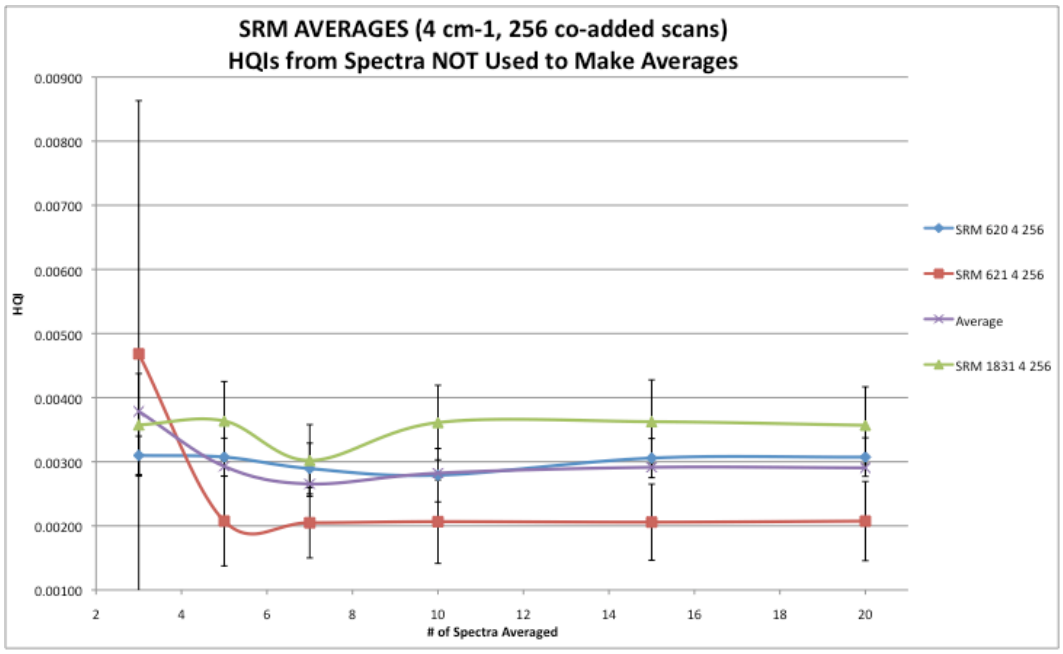


Figure 60: Graph of the HQI (correlation algorithm) from spectra not used to make the mid-IR library vs. the number that was averaged to make each spectrum in the library for SRM 620, 621 and 1831 (4 cm^{-1} spectral resolution and 256 co-added scans). Each data point for the three SRM data sets have +/-1 standard deviation error bars. An average of the three SRMs was made and is the purple data set.

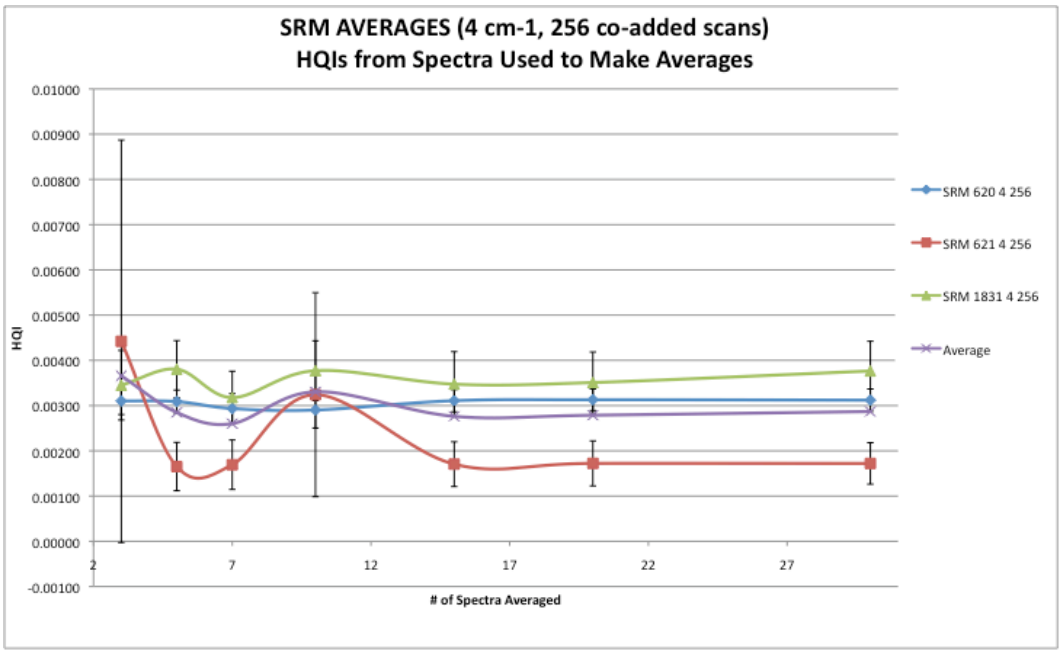


Figure 61: Graph of the HQI (correlation algorithm) from spectra used to make the mid-IR library vs. the number that was averaged to make each spectrum in the library for SRM 620, 621 and 1831 (4 cm^{-1} spectral resolution and 256 co-added scans). Each data point for the three SRM data sets have +/-1 standard deviation error bars. An average of the three SRMs was made and is the purple data set.

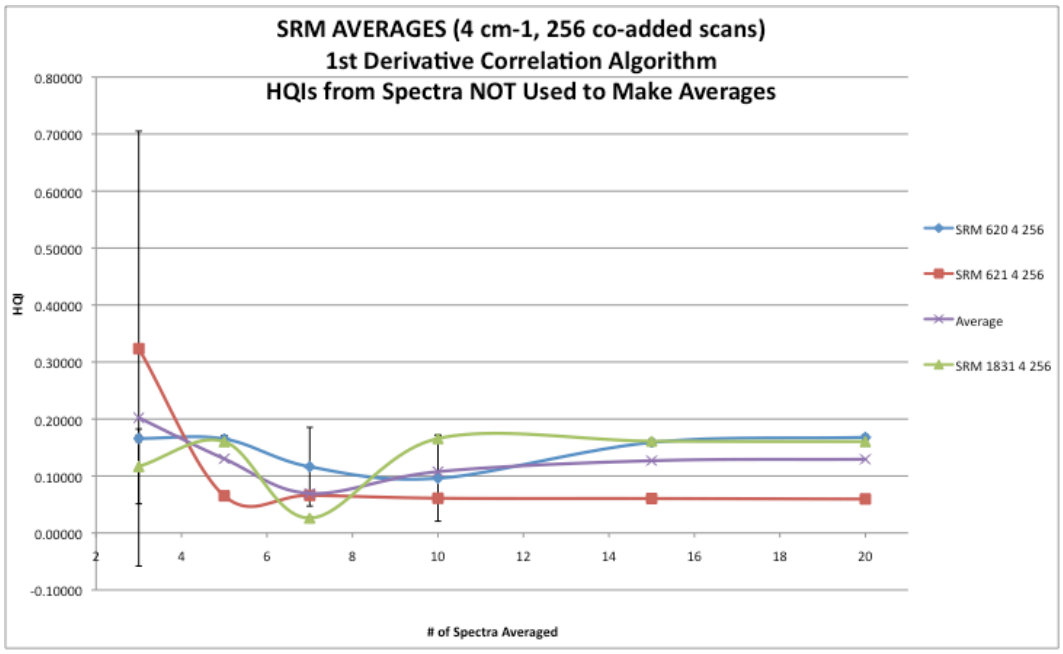


Figure 62: Graph of the HQI (first derivative correlation algorithm) from spectra not used to make the mid-IR library vs. the number that was averaged to make each spectrum in the library for SRM 620, 621 and 1831 (4 cm^{-1} spectral resolution and 256 co-added scans). Each data point for the three SRM data sets have +/-1 standard deviation error bars. An average of the three SRMs was made and is the purple data set.

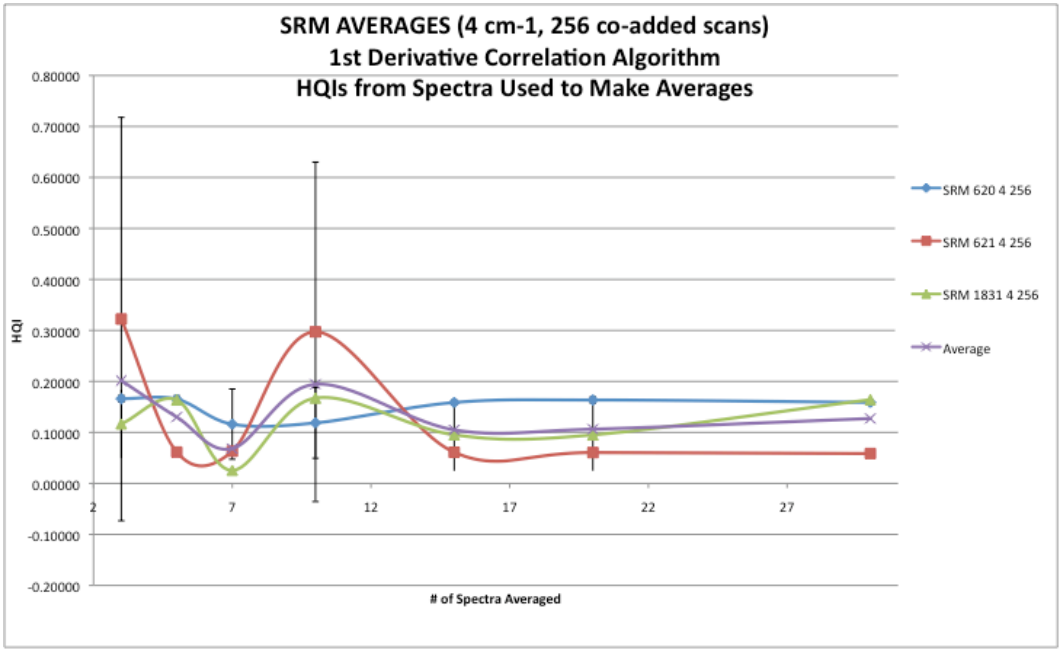


Figure 63: Graph of the HQI (first derivative correlation algorithm) from spectra used to make the mid-IR library vs. the number that was averaged to make each spectrum in the library for SRM 620, 621 and 1831 (4 cm^{-1} spectral resolution and 256 co-added scans). Each data point for the three SRM data sets have +/-1 standard deviation error bars. An average of the three SRMs was made and is the purple data set.

Table 23: Average library search (correlation algorithm) HQI values (and standard deviations) for a 'real world' window glass spectra not used in the making of the mid-IR libraries. Each row has the data from a library made with spectra with different numbers of co-added scans (8, 16, 32, 64, 128, and 256). The columns are the different number of spectra averaged to make each entry in each mid-IR library.

	3	5	7	10	15	20
Window NF 4 8	0.00021	0.00042	0.00020	0.00020	0.00082	0.00019
STD DEV	0.00003	0.00031	0.00002	0.00002	0.00008	0.00002
Window NF 4 16	0.00051	0.00068	0.00034	0.00068	0.00020	0.00068
STD DEV	0.00024	0.00004	0.00022	0.00005	0.00001	0.00005
Window NF 4 32	0.00035	0.00018	0.00018	0.00019	0.00018	0.00019
STD DEV	0.00024	0.00001	0.00001	0.00001	0.00001	0.00001
Window NF 4 64	0.00018	0.00019	0.00019	0.00049	0.00019	0.00019
STD DEV	0.00000	0.00001	0.00000	0.00032	0.00000	0.00000
Window NF 4 128	0.00019	0.00018	0.00018	0.00018	0.00019	0.00019
STD DEV	0.00001	0.00001	0.00001	0.00001	0.00001	0.00001
Window NF 4 256	0.00018	0.00018	0.00018	0.00080	0.00080	0.00080
STD DEV	0.00001	0.00000	0.00000	0.00001	0.00001	0.00001

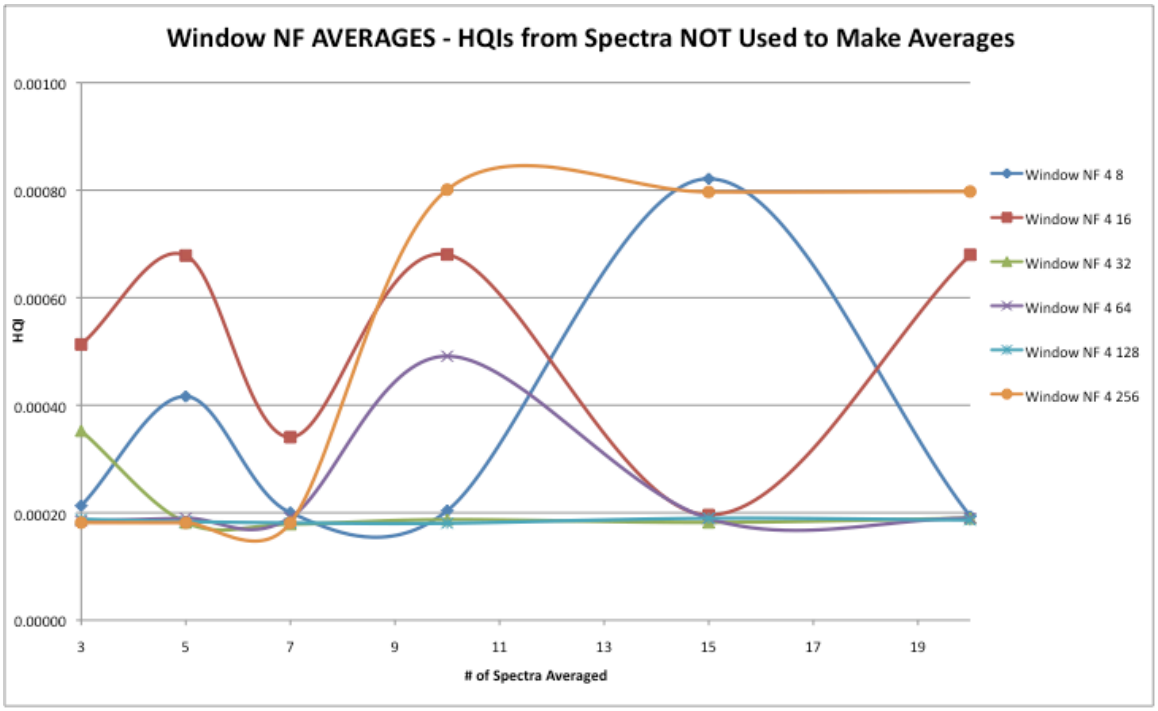


Figure 64: Graphs of the HQI (correlation algorithm) from spectra not used to make the mid-IR library vs. the number that was averaged to make each spectrum in the library for a 'real world' window. Each line represents a data set with a different number of co-added scans.

Table 24: Average library search (correlation algorithm) HQI values (and standard deviations) for a 'real world' window glass spectra used in the making of the mid-IR libraries. Each row has the data from a library made with spectra with different numbers of co-added scans (8, 16, 32, 64, 128, and 256). The columns are the different number of spectra averaged to make each entry in each mid-IR library.

	3	5	7	10	15	20	30
Window NF 4 8	0.00020	0.00040	0.00019	0.00043	0.00082	0.00019	0.00019
STD DEV	0.00002	0.00030	0.00001	0.00032	0.00008	0.00001	0.00002
Window NF 4 16	0.00051	0.00067	0.00035	0.00052	0.00045	0.00044	0.00068
STD DEV	0.00024	0.00003	0.00023	0.00023	0.00025	0.00025	0.00003
Window NF 4 32	0.00034	0.00019	0.00018	0.00019	0.00019	0.00019	0.00019
STD DEV	0.00023	0.00001	0.00001	0.00001	0.00001	0.00001	0.00001
Window NF 4 64	0.00018	0.00019	0.00019	0.00059	0.00019	0.00019	0.00067
STD DEV	0.00001	0.00001	0.00001	0.00029	0.00001	0.00001	0.00002
Window NF 4 128	0.00019	0.00018	0.00018	0.00018	0.00019	0.00018	0.00068
STD DEV	0.00000	0.00001	0.00001	0.00001	0.00001	0.00001	0.00001
Window NF 4 256	0.00018	0.00018	0.00018	0.00081	0.00080	0.00074	0.00068
STD DEV	0.00000	0.00000	0.00001	0.00002	0.00002	0.00006	0.00001

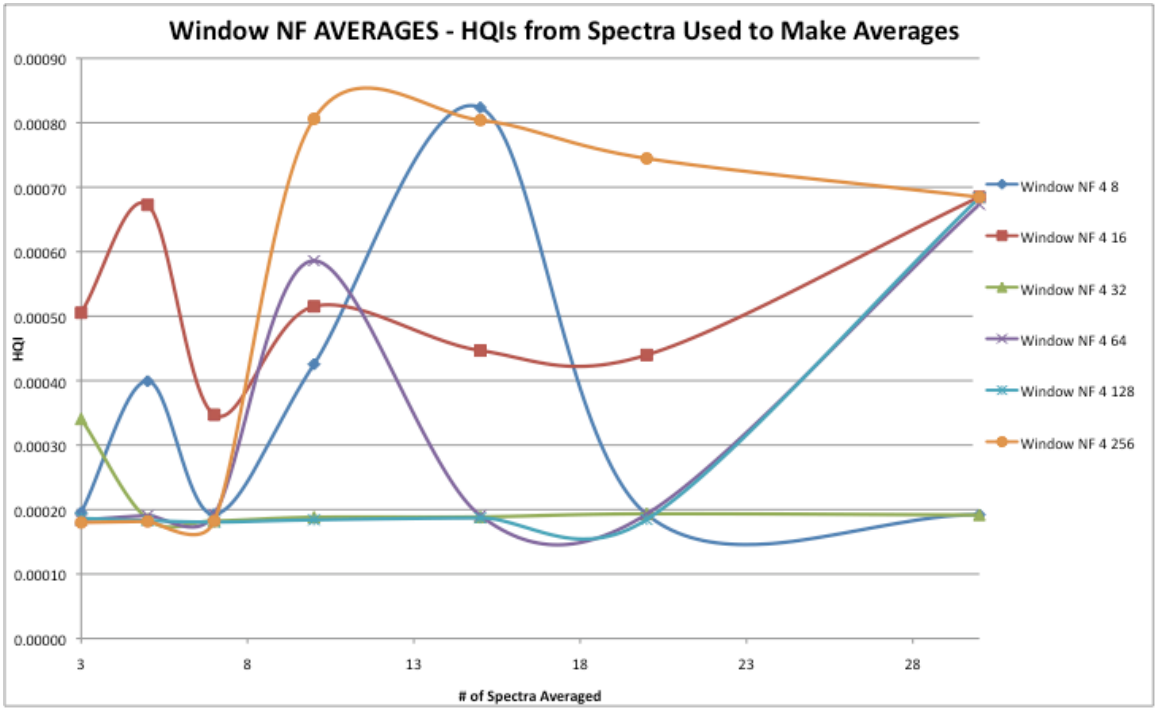


Figure 65: Graphs of the HQI (correlation algorithm) from spectra used to make the mid-IR library vs. the number that was averaged to make each spectrum in the library for a 'real world' window. Each line represents a data set with a different number of co-added scans.

Table 25: Average library search (first derivative correlation algorithm) HQI values (and standard deviations) for a 'real world' window glass spectra not used in the making of the mid-IR libraries. Each row has the data from a library made with spectra with different numbers of co-added scans (8, 16, 32, 64, 128, and 256). The columns are the different number of spectra averaged to make each entry in each mid-IR library.

	3	5	7	10	15	20
Window NF 4 8	0.03810	0.09174	0.03702	0.03952	0.20651	0.03662
STD DEV	0.00602	0.08113	0.00684	0.00876	0.01860	0.00586
Window NF 4 16	0.11412	0.15791	0.07024	0.15608	0.02817	0.15499
STD DEV	0.06348	0.01469	0.05698	0.01436	0.00281	0.01548
Window NF 4 32	0.07444	0.02270	0.02483	0.02446	0.02414	0.02232
STD DEV	0.07320	0.00500	0.00582	0.00496	0.00551	0.00558
Window NF 4 64	0.02293	0.02705	0.02557	0.10639	0.02450	0.02399
STD DEV	0.00198	0.00304	0.00209	0.08623	0.00205	0.00183
Window NF 4 128	0.02395	0.02568	0.02433	0.02599	0.02430	0.02682
STD DEV	0.00168	0.00300	0.00144	0.00251	0.00112	0.00110
Window NF 4 256	0.02109	0.02108	0.02158	0.18543	0.18528	0.18485
STD DEV	0.00200	0.00200	0.00216	0.00700	0.00748	0.00746

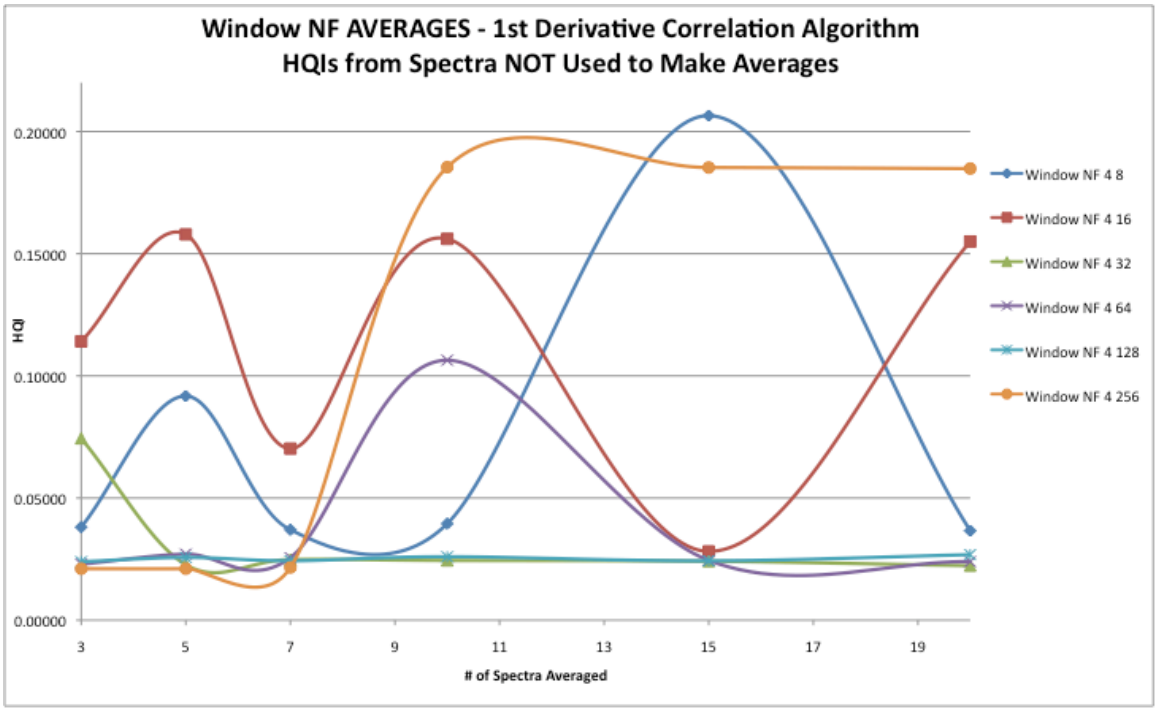


Figure 66: Graphs of the HQI (first derivative correlation algorithm) from spectra not used to make the mid-IR library vs. the number that was averaged to make each spectrum in the library for a 'real world' window. Each line represents a data set with a different number of co-added scans.

Table 26: Average library search (first derivative correlation algorithm) HQI values (and standard deviations) for a 'real world' window glass spectra used in the making of the mid-IR libraries. Each row has the data from a library made with spectra with different numbers of co-added scans (8, 16, 32, 64, 128, and 256). The columns are the different number of spectra averaged to make each entry in each mid-IR library.

	3	5	7	10	15	20	30
Window NF 4 8	0.03136	0.08812	0.03518	0.09545	0.20069	0.03744	0.03374
STD DEV	0.00287	0.07572	0.00572	0.08002	0.01681	0.00584	0.00562
Window NF 4 16	0.11264	0.16013	0.07096	0.11572	0.09466	0.09393	0.15959
STD DEV	0.06769	0.01103	0.06080	0.06392	0.06846	0.06859	0.01253
Window NF 4 32	0.06646	0.02437	0.02633	0.02497	0.02464	0.02435	0.02442
STD DEV	0.06539	0.00244	0.00364	0.00400	0.00394	0.00336	0.00326
Window NF 4 64	0.02198	0.02614	0.02482	0.12939	0.02370	0.02444	0.15702
STD DEV	0.00227	0.00371	0.00281	0.07785	0.00256	0.00250	0.00743
Window NF 4 128	0.02383	0.02561	0.02428	0.02675	0.02673	0.02817	0.16018
STD DEV	0.00177	0.00254	0.00172	0.00213	0.00263	0.00168	0.00430
Window NF 4 256	0.02078	0.02091	0.02205	0.18368	0.18385	0.16912	0.15500
STD DEV	0.00100	0.00122	0.00162	0.00577	0.00567	0.01502	0.00532

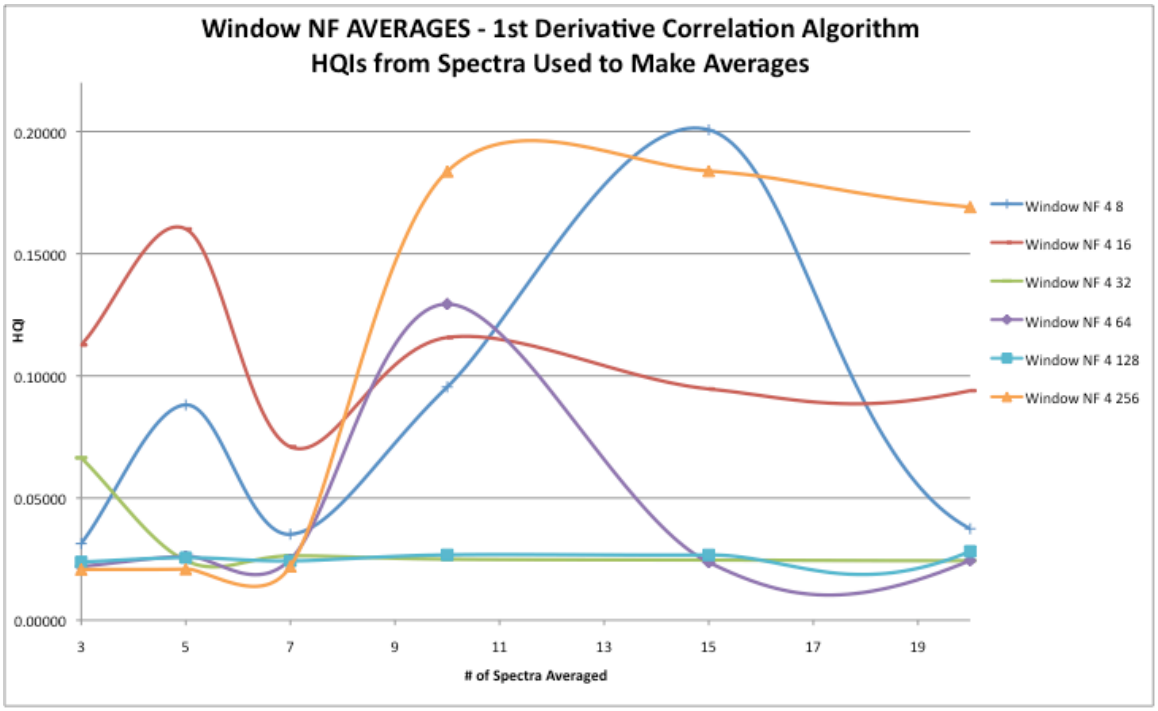


Figure 67: Graphs of the HQI (first derivative correlation algorithm) from spectra used to make the mid-IR library vs. the number that was averaged to make each spectrum in the library for a 'real world' window. Each line represents a data set with a different number of co-added scans.

The results of this second method development experiment demonstrated that an increase in the number of spectra averaged to compile a glass mid-IR searchable library does not provide a better hit quality, as measured by a lower HQI. For the 3 SRMs and the 'real world' window glass, there was no consistent or systematic change in HQI. This indicates that a glass mid-IR library compiled by averaging 3 spectra would be just as successful (as measured by a lower HQI) as one compiled from a greater number of spectra. Thus, the glass mid-IR spectral libraries that were made and analyzed in Chapter 4.C.a were compiled from glass averages of 3 spectra.

In addition, there was no systematic or consistent change in HQI for spectra collected with a different number of co-added scans. Thus, although there is a decrease in noise (or increase in S/N) when increasing the number of co-added scans, there is no added decrease in HQI value. This was surprising because it was thought that by reducing the noise, which is random and thus not reproducible, one would also get a better hit quality.

4.B. Correlation of Mid-IR Spectral Bands with Molecular Structure

Three methods were attempted to identify peaks for the deconvolution of the silicate vibrational band of soda-lime glass in order to correlate its mid-IR spectra with molecular structure: 1) using literature values, 2) using the vibrational bands from silicate minerals with known molecular structures, and 3) using the peak picking function of the Grams® AI software program. Only the latter method proved to be successful.

The first method attempted to deconvolve the glass spectral bands using the 8 silicate vibrations (7 silicate structures) from Dalby and King (2006): 1) 830 cm^{-1} (island silicate), 2) 860 cm^{-1} (island silicate), 3) 900 cm^{-1} (group silicate), 4) 950 cm^{-1} (ring silicate), 5) 980 cm^{-1} (chain

silicate), 6) 1010 cm^{-1} (double chain silicate), 7) 1050 cm^{-1} (layer silicate), and 8) 1100 cm^{-1} (network silicate). Figures 68 and 69 show the results of the deconvolution of the spectra of window and container glasses, respectively, using the literature peak values. Although the fitted trace (in navy blue) fits the original trace (in red) very well for both the window and the container glasses, three of the eight peaks (1050, 980, and 860 cm^{-1}) are inverted. In mid-IR spectroscopy, there are no negative peaks because negative absorbance values are nonsensical. Therefore, using the literature values of peaks for the deconvolution of glass spectral bands failed.

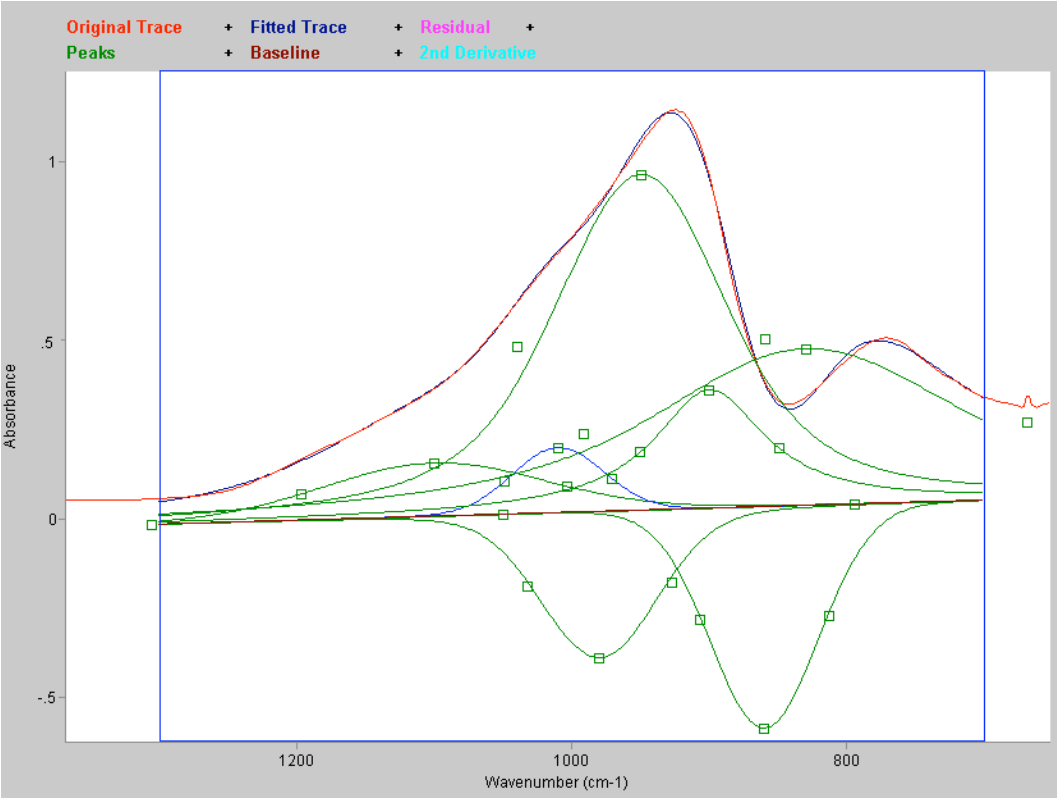


Figure 68: Results of deconvolution of automotive window glass W10 when using the reference literature values. The spectra were produced using Grams® AI software.

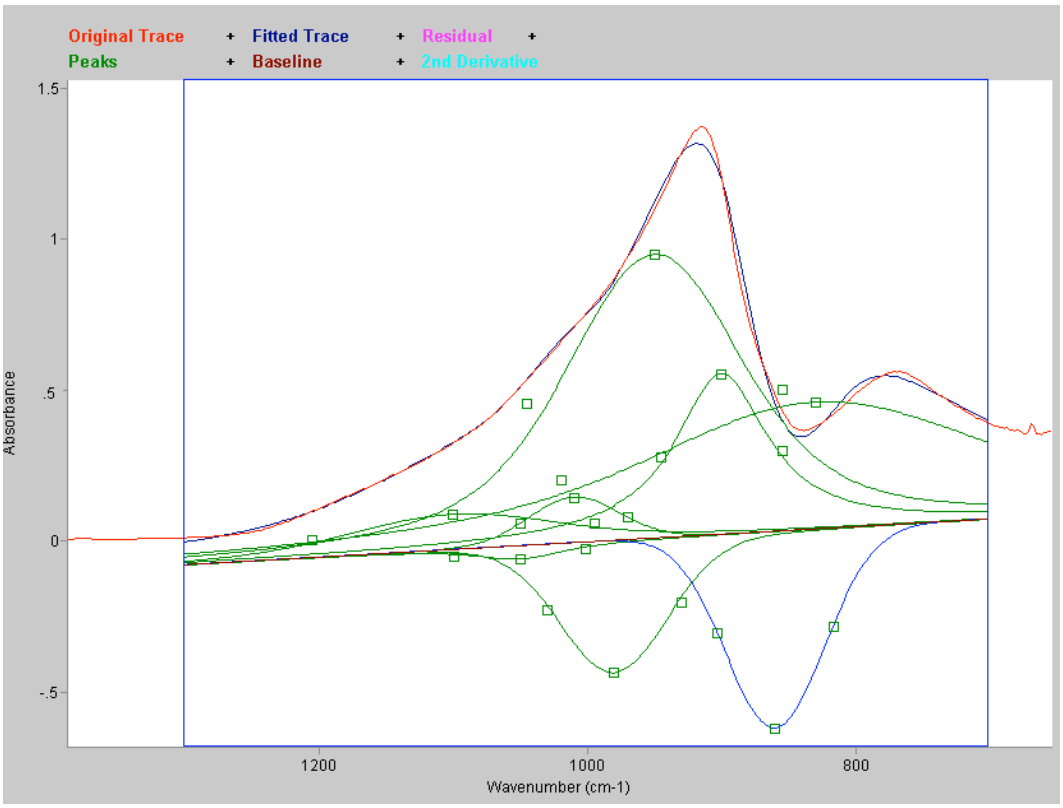


Figure 69: Results of deconvolution of container glass C50 when using the reference literature values. The spectra were produced using Grams® AI software.

The second method attempted to use the mid-IR spectra of minerals with known silicate structures to determine the peaks used for the glass deconvolution. The mid-IR spectra of the silicate minerals are in Appendix VII. In addition, Tables 27 through 34 have the data (center X peak positions) for each of the silicate minerals. For each mineral sample, an average was calculated of the 3 - 5 spectra. In addition, for those mineral varieties where two samples were analyzed, a grand average, which is an average of the two averages, was also calculated.

Table 27: Island silicate peak positions (center X, in wavenumbers) for peaks between 1300 – 700 cm^{-1}. Five replicate spectra were collected for each mineral standard, and the average position for each peak is in the last column.

Island Silicates	Silicate Peaks (cm^{-1})					
	1	2	3	4	5	Ave
Phenacite Excalibur	1093	1092	1092	1092	1093	1092
	955	943.9	947.9	948.9	934.9	946
	786.7	788.6	786.6	786.5	787	787
	759.6	759.6	759.4	759.4	759.3	759
	742.7	743.2	742.6	742.5	742.7	743
	721.5	723.3	720.6	721.1	720.7	721
Willemite Excalibur	972.4	977.8	974.1	976.9	975	975
	925.5	--	923.9	--	--	925
	879.3	--	878.6	--	--	879
	851.8	853.9	--	851.2	850.7	852
	844.8	--	846.9	841.2	--	844
Fosterite Excalibur	977.1	977.7	975.7	979	975.3	977
	855.3	855.5	858.3	855.5	859.5	857
	831.6	831.6	833.6	835.6	837.6	834

Table 28: Ring silicate peak position (center X, in wavenumbers) for peaks between 1300 – 700 cm^{-1}. Three replicate spectra were collected for each mineral standard, and two mineral standards were analyzed. An average position for each standard was calculated as well as a grand average of both standards.

Ring Silicates	Silicate Peaks (cm^{-1}) Sample 1				Silicate Peaks (cm^{-1}) Sample 2				GRAND AVE
	1	2	3	Ave	1	2	3	Ave	
Beryl 1- Cargille, 2- TAK	1188	1191	1179	1186	1193	1179	1190	1187	1187
	1012	1012	1012	1012	1013	1012	1013	1013	1012
	921.4	921.6	920.5	921	922.5	916.1	919.1	919	920
	804.1	801.9	798.7	802	802	800.8	800.7	801	801
	734.6	734.5	734.9	735	734.1	734.4	734.7	734	735

Table 29: Single chain silicate peak positions (center X, in wavenumbers) for peaks between 1300 – 700 cm^{-1}. Three-to-five replicate spectra were collected for each mineral standard, and two mineral standards were analyzed for each mineral type. An average position for each standard was calculated as well as a grand average of both standards.

Single Chain Silicates	Silicate Peaks (cm^{-1}) Sample 1				Silicate Peaks (cm^{-1}) Sample 2						GRAND AVE
	1	2	3	Ave	1	2	3	4	5	Ave	
Enstanite	1051	1050	1048	1050	1040	1045	1048	1046	1045	1045	1047
	1005	1006	1005	1005	1004	1004	1005	1007	1006	1005	1005
	917.3	915.4	916.9	917	914.1	915.3	916.6	915.1	916	915	916
1- Wehrenberg, 2- JAB	845.1	833.7	842.6	840	835.7	830.5	842.4	837.6	838.3	837	839
	734.4	744.4	744.1	741	744.6	745.3	744.4	746.1	744.8	745	743
	722.5	721.9	721.9	722	721.9	719.8	722.1	722.2	723.7	722	722
	689.7	690.1	692	691	691	688.5	691.6	695.7	689.4	691	691
Spodumene	1069	1065	1063	1066	--	--	--			--	--
	1007	1007	1006	1007	--	--	--			--	--
TAK	846.5	853.2	853.9	851	--	--	--			--	--
α-Wollastonite	1057	1058	1057	1057	1058	1057	1056			1057	1057
	1006	1004	998.9	1003	996.7	1003	999.4			1000	1001
	886.2	876.6	882	882	880.5	877.1	872.9			877	879
1- Cargille, 2- TAK	681.2	684.3	682.6	683	682.7	681.5	682.4			682	682

Table 30: Double chain silicate peak positions (center X, in wavenumbers) for peaks between 1300 – 700 cm^{-1}. Three replicate spectra were collected for each mineral standard, and two mineral standards were analyzed. An average position for each standard was calculated as well as a grand average of both standards.

Double Chain Silicates	Silicate Peaks (cm-1) - Sample 1				Silicate Peaks (cm-1) - Sample 2				GRAND AVE
	1	2	3	Ave	1	2	3	Ave	
Sillimanite	1169	1167	1167	1168	1168	1169	1168	1168	1168
	950.4	951.5	949	950	951.4	950.4	950.6	951	951
	881.8	881.8	881.9	882	882.7	884.9	882.8	883	883
1- JAR 2537, 2- JAR 2538	807.8	805.7	807.7	807	811.1	811.2	809.9	811	809
	685.1	689.6	686	687	682.6	686.4	720.8	697	692

Table 31: Double binary chain silicate peak positions (center X, in wavenumbers) for peaks between 1300 – 700 cm^{-1}. Five replicate spectra were collected for each mineral standard, and two mineral standards were analyzed. An average position for each standard was calculated as well as a grand average of both standards.

Double Binary Chain Silicates	Silicate peaks (cm^{-1}) Sample 1						Silicate Peaks (cm^{-1}) Sample 2						GRAND AVE
	1	2	3	4	5	Ave	1	2	3	4	5	Ave	
Tremolite	1082	1098	1087	1092	1087	1089	1091	1094	1089	1090	1089	1091	1090
	1034	1037	1035	1037	1036	1036	1032	1035	1033	--	1034	1034	1035
1- NIST SRM 1867,	911.6	915.7	906.2	905.6	913.3	910	904.9	912.1	914.9	917.4	911	912	911
2- TAK	758.8	754.7	753	755	760.9	756	755.9	755.2	758.7	759.7	760.8	758	757
	677.5	683	682.6	681.7	677.6	680	678.5	681.5	672.7	671.2	675.1	676	678

Table 32: Double tertiary chain silicate peak positions (center X, in wavenumbers) for peaks between 1300 – 700 cm^{-1}. Five replicate spectra were collected for the mineral standard, and the average position for each peak is in the last column.

Double Teriary Chain Silicates	Silicate Peaks (cm^{-1})					
	1	2	3	4	5	Ave
Xonolith	1199	1199	1199	1219	1195	1202
	1050	--	1051	--	1054	1052
Excalibur	940	--	942.2	--	942	941
	927.3	927.3	--	927.8	927.2	927

Table 33: Single layer silicate peak positions (center X, in wavenumbers) for peaks between 1300 – 700 cm^{-1}. Three-to-five replicate spectra were collected for each mineral standard, and two mineral standards were analyzed for each mineral type. An average position for each standard was calculated as well as a grand average of both standards.

Single Layer Silicates	Silicate Peaks (cm-1) - Sample 1						Silicate Peaks (cm-1) - Sample 2						GRAND AVE
	1	2	3	4	5	Ave	1	2	3	4	5	Ave	
Talcum	1076	1090	1087	1072	1069	1079	1071	1076	1078	1078	1072	1075	1077
	975.2	--	--	--	--	975	974.9	966.8	967.2	980.2	983.3	974	975
	949.4	938.2	941.6		937.7	942	958.1	946.3	945.9	956.7	958	953	947
1- Cargille, 2-	--	893.4	905	905.8	--	901	--	--	--	--	907.5	908	904
Wehrenberg	794	781.8	--	--	--	788	790.3	790.5	--	785.7	790.3	789	789
	--	757.5	761.5	761.1	--	760	--	--	--	--	--	--	--
Mont-morillonite	1115	1116	1115			1115	1117	1117	1117			1117	1116
	982.4	981.8	981.4			982	982	981	981.5			982	982
	914.8	914.5	915.1			915	917.2	918.9	916.7			918	916
1- JAR 2674	842.9	845.2	845			844	841.5	842	841.2			842	843
2- JAR 2675	792.8	793.9	786.5			791	794.4	793	794.5			794	793

Table 34: Network silicate peak positions (center X, in wavenumbers) for peaks between 1300 – 700 cm^{-1}. Three-to-five replicate spectra were collected for each mineral standard, and two mineral standards were analyzed for each mineral type, except for crystobalite. An average position for each standard was calculated as well as a grand average of both standards.

Network Silicates	Silicate Peaks (cm^{-1}) Sample 1						Silicate Peaks (cm^{-1}) Sample 2						GRAND AVE
	1	2	3	4	5	Ave	1	2	3	4	5	Ave	
Crystobalite NBS from TAK	1193	1192	1193	1192	--	1193							
	1051	1037	1043	1041	--	1043							
	--	1030	--	1038	--	1034							
	--	--	1013	--	1006	1010							
	789.2	788.8	786.9	787.1	783.1	787							
Quartz 1- NBS from TAK, 2- Wehrenberg	1161	1160	1161	1160	1158	1161	1160	1160	1160	1160	1158	1160	1160
	1037	1042	1050	1035	1014	1043	1026	1014	1009	1029	1009	1017	1030
	794.4	793.8	794.7	792.9	--	794	--	--	--	--	--	--	--
	776.1	776.2	777	775.7	773.4	776	772.7	772.5	771.9	773.2	770.1	772	774
	695.4	695.8	695.4	696	701.7	696	693.6	694.3	694.9	694	697.6	695	695
Orthoclase 1- Cargille, 2- Wehrenberg	1122	1124	--			1123	--	--	--			--	--
	--	--	1111			1111	--	--	--			--	--
	1089	--	1085			1087	1097	1090	1090			1092	1090
	969.8	969.9	964.9			968	958.4	953.3	953.6			955	962
	766.8	768.5	768.4			768	--	--	--			--	--
	723.5	724.8	724.7			724	720.6	723.1	724.1			723	723
Sodic Plagioclase/ Albite 1- Cargille, 2- Wehrenberg	1092	1092	1093			1092	1092	1093	--			1093	1092
	953.9	960.9	957.7			958	958.4	953.5	--			956	957
	787.7	787.1	786.2			787	786.1	788.1	--			787	787
	759.9	760.9	759.3			760	758.9	759.4	--			759	760
	744.3	742.3	742.4			743	741.8	744	--			743	743
	721.9	723.7	721.7			722	720.6	722.2	--			721	722

When comparing the silicate minerals, it was determined that there was too much variation in the spectra of minerals for a given silicate structure (island, group, etc…) to assign a peak value for each of the silicate structures. The probable reason for this is that the different minerals provide different environments for their silicate structures which cause considerable shifts in their molecular vibrations. It is these vibrational shifts that make these silicate minerals able to be differentiated by mid-IR spectroscopy, however it prohibits the use of minerals with known silicate structures from providing values for those silicate vibrations in glass.

The third method for determining the peaks for deconvolution relied on the second derivative of the spectra combined with the peak picking function of the Grams® AI software program. For all glasses, it was determined that there were 6 peaks that combine to make the broad silicate bands: 1) 1140 – 1100 cm^{-1}, 2) 1025 – 990 cm^{-1}, 3) 975 – 930 cm^{-1}, 4) 920 – 900 cm^{-1}, 5) 785 – 770 cm^{-1}, 6) and 760 – 710 cm^{-1}. Figures 70 through 72 show the results of the deconvolution of the spectra of an automotive window, an architectural window, and a container glass, respectively, using the combined approach.

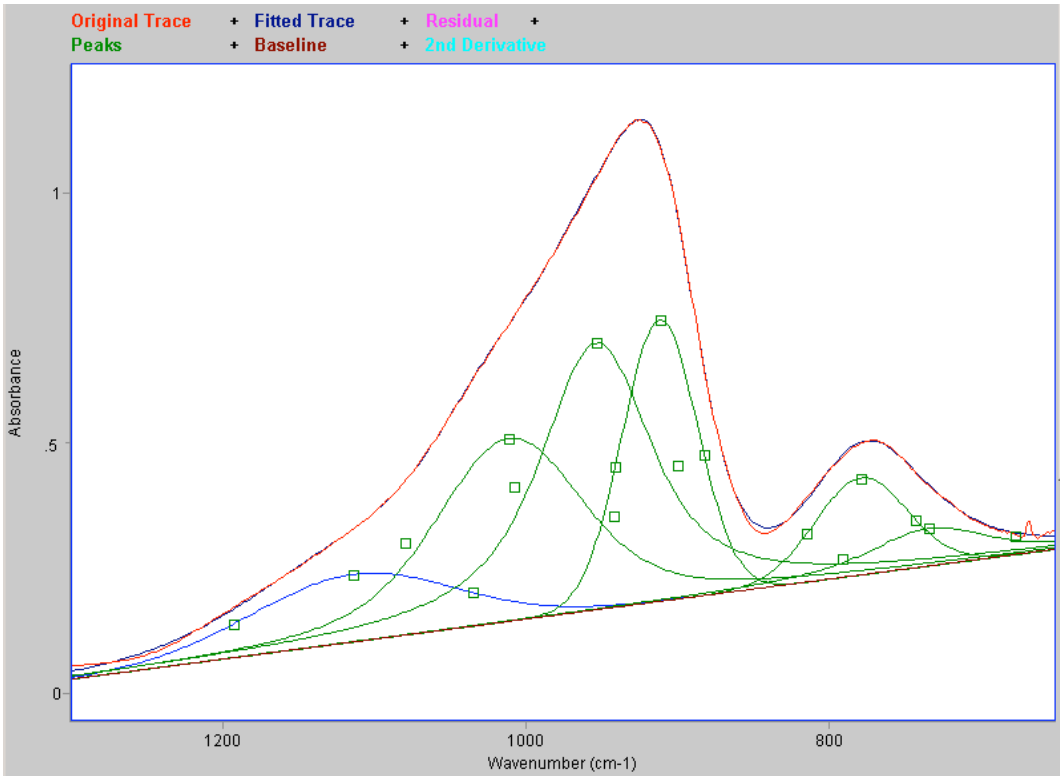


Figure 70: Results of deconvolution of automotive window glass W10 when using the combined approach to identify the silicate peaks. The spectra were produced using Grams® AI software.

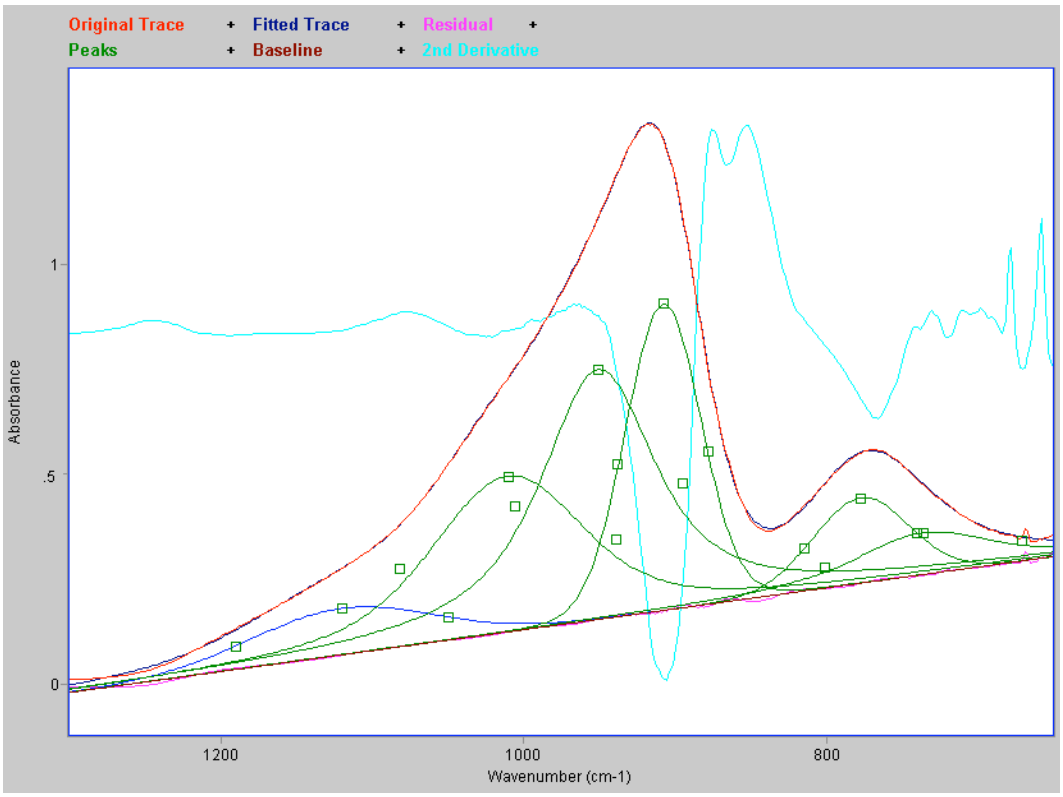


Figure 71: Results of deconvolution of architectural window glass W52 when using the combined approach to identify the silicate peaks. The spectra were produced using Grams® AI software.

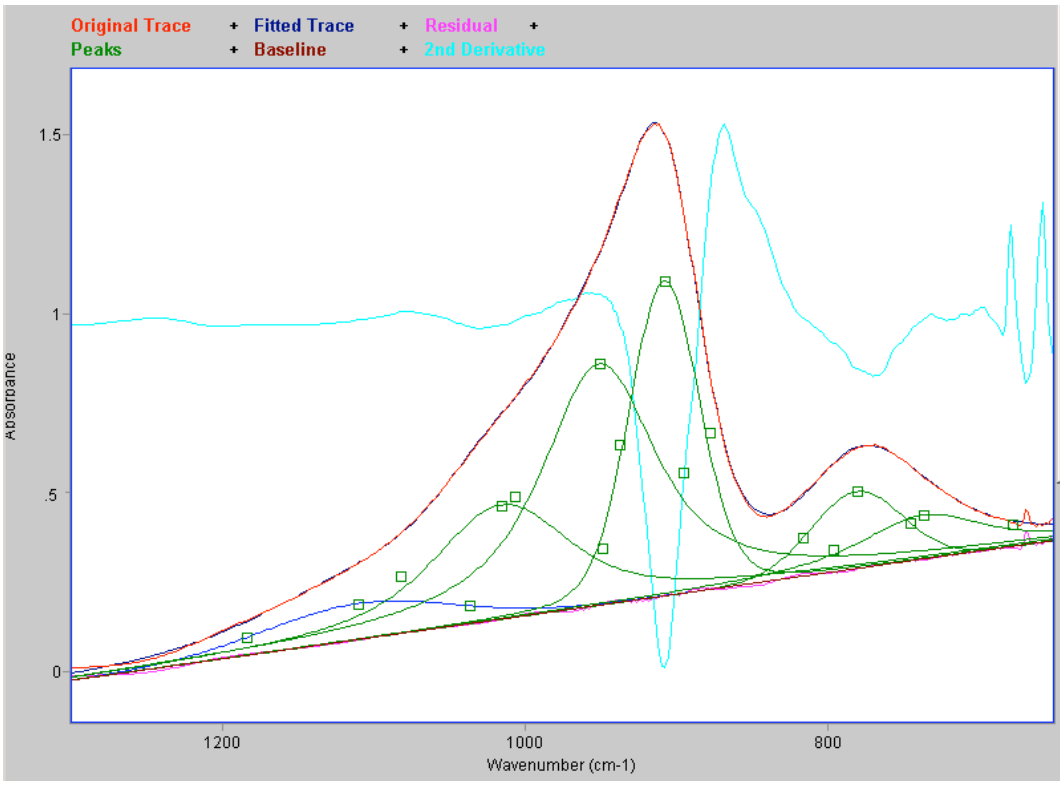


Figure 72: Results of deconvolution of container glass C50 when using the combined approach to identify the silicate peaks. The spectra were produced using Grams® AI software.

This combined approach for the deconvolution of the silicate bands of glass into 6 peaks appeared to be successful, where success was measured by a good match between the original spectra and the fitted trace. One of the major drawbacks of this peak picking method was that there was no process for correlating these peaks to specific silicate structures.

Once the spectra were deconvolved, ANOVA was used to determine if there was a significant difference in the peak positions (center X) or areas that could be used for discrimination and/or classification. The results of the ANOVA for each of the 6 peak positions and areas are in Tables 35 – 40 and Tables 41 – 46, respectively. The deconvolution results (peak position and area) for each of the 30 glasses are in Appendix VIII.

Table 35: Results of ANOVA for deconvolved peak 1 position.

Analysis of Variance (One-Way)

Summary

Groups	*Sample size*	*Sum*	*Mean*	*Variance*
W10	10	11177.423	1117.7423	25.8322
W12	10	11182.927	1118.2927	4.1184
W13	10	11208.848	1120.8848	18.0925
W18	10	11200.382	1120.0382	1.813
W35	10	11206.963	1120.6963	30.1902
W50	10	11176.742	1117.6742	4.7179
W52	10	11220.334	1122.0334	6.3207
W153	10	11248.324	1124.8324	11.3788
W295	10	11277.798	1127.7798	15.2885
W360	10	11289.137	1128.9137	6.1783
W368	10	11289.503	1128.9503	13.567
W394	10	11249.121	1124.9121	48.6571
W411	10	11277.327	1127.7327	6.6011
W412	10	11231.635	1123.1635	4.7439
W442	10	11237.144	1123.7144	1.8325
W444	10	11275.779	1127.5779	18.2226
W445	10	11260.494	1126.0494	6.8022
W446	10	11249.049	1124.9049	3.1331
W448	10	11276.204	1127.6204	7.1279
W450	10	11256.71	1125.671	9.0686
C50	10	11149.17	1114.917	5.3129
C51	10	11229.324	1122.9324	19.1617
C52	10	11174.931	1117.4931	19.111
C53	10	11197.837	1119.7837	24.6885
C54	10	11181.284	1118.1284	10.3702
C55	10	11208.557	1120.8557	15.8593
C56	10	11213.51	1121.351	19.3583
C57	10	11213.661	1121.3661	63.5
C58	10	11203.924	1120.3924	15.4807
C59	10	11105.458	1110.5458	5.1755

ANOVA

Source of Variation	*SS*	*df*	*MS*	*F*	*p-level*	*F crit*
Between Groups	5671.2059	29	195.5588	13.2821	0.%	1.5096
Within Groups	3975.3417	270	14.7235			
Total	9646.5476	299				

Table 36: Results of ANOVA for deconvolved peak 2 position.

Analysis of Variance (One-Way)

Summary

Groups	*Sample size*	*Sum*	*Mean*	*Variance*
W10	10	10109.456	1010.9456	29.3796
W12	10	10109.524	1010.9524	7.5899
W13	10	10110.306	1011.0306	8.574
W18	10	10119.679	1011.9679	0.9227
W35	10	10125.833	1012.5833	20.2903
W50	10	10120.598	1012.0598	6.132
W52	10	10126.364	1012.6364	1.1456
W153	10	10089.8581	1008.9858	28.3224
W295	10	10064.4614	1006.4461	16.8939
W360	10	10043.057	1004.3057	6.2724
W368	10	10046.681	1004.6681	5.2055
W394	10	10054.731	1005.4731	18.3872
W411	10	10048.3941	1004.8394	13.942
W412	10	10053.437	1005.3437	1.9535
W442	10	10046.357	1004.6357	3.8512
W444	10	10044.1871	1004.4187	10.7605
W445	10	10056.782	1005.6782	3.8398
W446	10	10062.824	1006.2824	2.3963
W448	10	10062.828	1006.2828	4.2501
W450	10	10069.609	1006.9609	1.9963
C50	10	10105.691	1010.5691	5.1446
C51	10	10110.337	1011.0337	10.0617
C52	10	10123.826	1012.3826	8.536
C53	10	10123.336	1012.3336	6.9352
C54	10	10127.969	1012.7969	3.9992
C55	10	10118.627	1011.8627	15.7826
C56	10	10113.544	1011.3544	8.6907
C57	10	10112.11	1011.211	17.5651
C58	10	10114.065	1011.4065	7.1469
C59	10	10076.513	1007.6513	7.6897

ANOVA

Source of Variation	*SS*	*df*	*MS*	*F*	*p-level*	*F crit*
Between Groups	2861.7247	29	98.6802	10.4366	0.%	1.5096
Within Groups	2552.9105	270	9.4552			
Total	5414.6352	299				

Table 37: Results of ANOVA for deconvolved peak 3 position.

Analysis of Variance (One-Way)

Summary

Groups	*Sample size*	*Sum*	*Mean*	*Variance*
W10	10	9537.2592	953.7259	68.4351
W12	10	9522.9594	952.2959	29.1775
W13	10	9496.2175	949.6218	33.9308
W18	10	9515.5906	951.5591	4.0705
W35	10	9510.2435	951.0244	34.7294
W50	10	9507.7382	950.7738	17.9338
W52	10	9552.3793	955.2379	5.337
W153	10	9487.7563	948.7756	37.1335
W295	10	9487.8101	948.781	34.8749
W360	10	9481.9032	948.1903	10.3673
W368	10	9476.2944	947.6294	22.4053
W394	10	9485.0786	948.5079	11.5182
W411	10	9479.6497	947.965	17.8726
W412	10	9495.6702	949.567	6.6714
W442	10	9499.7613	949.9761	5.2802
W444	10	9479.1202	947.912	26.4889
W445	10	9501.2762	950.1276	8.7677
W446	10	9507.6822	950.7682	7.2382
W448	10	9495.2696	949.527	13.657
W450	10	9506.215	950.6215	13.1863
C50	10	9511.2844	951.1284	1.938
C51	10	9535.4036	953.5404	10.9309
C52	10	9511.3349	951.1335	27.6
C53	10	9518.827	951.8827	21.2854
C54	10	9506.7465	950.6747	23.6598
C55	10	9541.0504	954.105	34.1456
C56	10	9501.6654	950.1665	8.4753
C57	10	9519.8514	951.9851	35.3949
C58	10	9492.666	949.2666	17.0219
C59	10	9503.2556	950.3256	5.9419

ANOVA

Source of Variation	*SS*	*df*	*MS*	*F*	*p-level*	*F crit*
Between Groups	1059.7535	29	36.5432	1.8411	0.69%	1.5096
Within Groups	5359.2258	270	19.849			
Total	6418.9793	299				

Table 38: Results of ANOVA for deconvolved peak 4 position.

Analysis of Variance (One-Way)

Summary

Groups	*Sample size*	*Sum*	*Mean*	*Variance*
W10	10	9110.0181	911.0018	18.3559
W12	10	9100.5706	910.0571	10.5467
W13	10	9087.7039	908.7704	6.6891
W18	10	9080.7214	908.0721	3.315
W35	10	9075.6362	907.5636	7.7966
W50	10	9093.0588	909.3059	3.5205
W52	10	9109.6671	910.9667	1.5484
W153	10	9081.5951	908.1595	4.6282
W295	10	9086.537	908.6537	8.6013
W360	10	9081.2161	908.1216	2.8923
W368	10	9083.6396	908.364	1.9226
W394	10	9082.3287	908.2329	2.1926
W411	10	9078.6519	907.8652	7.9164
W412	10	9063.8107	906.3811	4.1199
W442	10	9061.0392	906.1039	3.0628
W444	10	9088.9127	908.8913	10.0771
W445	10	9081.5486	908.1549	3.1834
W446	10	9078.1079	907.8108	2.4581
W448	10	9078.0362	907.8036	5.454
W450	10	9073.2492	907.3249	3.7099
C50	10	9091.0267	909.1027	0.9605
C51	10	9117.501	911.7501	4.7272
C52	10	9083.5719	908.3572	7.5662
C53	10	9093.9344	909.3934	5.7195
C54	10	9078.5866	907.8587	7.094
C55	10	9111.6454	911.1645	7.254
C56	10	9085.4995	908.55	1.9994
C57	10	9097.3798	909.738	8.6204
C58	10	9078.8014	907.8801	2.4506
C59	10	9061.5475	906.1548	1.6744

ANOVA

Source of Variation	*SS*	*df*	*MS*	*F*	*p-level*	*F crit*
Between Groups	566.2831	29	19.527	3.66	0.%	1.5096
Within Groups	1440.514	270	5.3352			
Total	2006.7971	299				

Table 39: Results of ANOVA for deconvolved peak 5 position.

Analysis of Variance (One-Way)

Summary

Groups	*Sample size*	*Sum*	*Mean*	*Variance*
W10	10	7787.3057	778.7306	1.4022
W12	10	7785.6777	778.5678	1.329
W13	10	7779.1914	777.9191	1.2733
W18	10	7775.846	777.5846	0.3683
W35	10	7775.3881	777.5388	3.8228
W50	10	7784.2668	778.4267	0.9213
W52	10	7783.181	778.3181	0.7707
W153	10	7790.3359	779.0336	3.2508
W295	10	7795.9469	779.5947	0.5916
W360	10	7775.4824	777.5482	1.8972
W368	10	7788.3436	778.8344	0.7593
W394	10	7796.9738	779.6974	0.5562
W411	10	7794.5506	779.4551	1.843
W412	10	7794.2605	779.4261	1.7663
W442	10	7803.9011	780.3901	2.3533
W444	10	7801.2174	780.1217	0.7749
W445	10	7789.1604	778.916	1.3552
W446	10	7801.9072	780.1907	0.9204
W448	10	7790.5378	779.0538	0.9529
W450	10	7801.2543	780.1254	1.779
C50	10	7790.5433	779.0543	2.0022
C51	10	7765.9607	776.5961	3.7181
C52	10	7765.7941	776.5794	3.0392
C53	10	7772.7152	777.2715	0.556
C54	10	7757.8028	775.7803	1.5381
C55	10	7770.6004	777.06	1.2841
C56	10	7757.9927	775.7993	2.9978
C57	10	7770.0445	777.0045	1.428
C58	10	7762.371	776.2371	0.7581
C59	10	7748.3985	774.8399	1.6987

ANOVA

Source of Variation	*SS*	*df*	*MS*	*F*	*p-level*	*F crit*
Between Groups	638.4493	29	22.0155	13.8439	0.%	1.5096
Within Groups	429.3706	270	1.5903			
Total	1067.8199	299				

Table 40: Results of ANOVA for deconvolved peak 6 position.

Analysis of Variance (One-Way)

Summary

Groups	*Sample size*	*Sum*	*Mean*	*Variance*
W10	10	7366.9409	736.6941	19.5541
W12	10	7407.653	740.7653	4.7247
W13	10	7415.901	741.5901	6.6347
W18	10	7402.9623	740.2962	3.3963
W35	10	7452.0148	745.2015	46.4803
W50	10	7392.7762	739.2776	1.7082
W52	10	7371.0313	737.1031	16.5885
W153	10	7398.4032	739.8403	11.3196
W295	10	7424.0331	742.4033	4.5092
W360	10	7429.3393	742.9339	12.8366
W368	10	7412.592	741.2592	3.1849
W394	10	7420.8584	742.0858	3.1694
W411	10	7403.144	740.3144	0.2222
W412	10	7399.7353	739.9735	2.7011
W442	10	7390.4837	739.0484	4.1575
W444	10	7423.1093	742.3109	8.0573
W445	10	7395.927	739.5927	2.2172
W446	10	7419.8389	741.9839	0.8906
W448	10	7413.7566	741.3757	4.007
W450	10	7417.2262	741.7226	2.4728
C50	10	7368.6066	736.8607	10.0087
C51	10	7333.1056	733.3106	56.6835
C52	10	7370.5671	737.0567	6.7908
C53	10	7382.8944	738.2894	12.0707
C54	10	7371.0439	737.1044	10.7718
C55	10	7354.7774	735.4777	4.9294
C56	10	7363.3845	736.3385	12.8582
C57	10	7354.1096	735.411	7.1353
C58	10	7370.7684	737.0768	3.8832
C59	10	7275.8861	727.5886	9.3976

ANOVA

Source of Variation	*SS*	*df*	*MS*	*F*	*p-level*	*F crit*
Between Groups	3484.0616	29	120.1401	12.2859	0.%	1.5096
Within Groups	2640.2517	270	9.7787			
Total	6124.3132	299				

Table 41: Results of ANOVA for deconvolved peak 1 area.

Analysis of Variance (One-Way)

Summary

Groups	*Sample size*	*Sum*	*Mean*	*Variance*
W10	10	182.5405	18.2541	4.3768
W12	10	180.6447	18.0645	4.3502
W13	10	158.6	15.86	2.8766
W18	10	162.5977	16.2598	0.8585
W35	10	144.6785	14.4678	7.2081
W50	10	163.4854	16.3485	3.3417
W52	10	179.7149	17.9715	2.1732
W153	10	139.5714	13.9571	3.5298
W295	10	138.0558	13.8056	6.1742
W360	10	141.3434	14.1343	1.5355
W368	10	146.6916	14.6692	3.1197
W394	10	150.4754	15.0475	8.4113
W411	10	130.4194	13.0419	5.5239
W412	10	148.8829	14.8883	3.304
W442	10	142.187	14.2187	1.7882
W444	10	138.5192	13.8519	12.4223
W445	10	148.3717	14.8372	3.8405
W446	10	155.586	15.5586	1.4874
W448	10	139.7601	13.976	4.9455
W450	10	150.901	15.0901	6.813
C50	10	170.9492	17.0949	3.0554
C51	10	183.0471	18.3047	8.0249
C52	10	160.9438	16.0944	6.1442
C53	10	163.049	16.3049	16.8988
C54	10	160.4275	16.0428	10.8781
C55	10	187.9809	18.7981	5.6317
C56	10	150.5369	15.0537	3.7108
C57	10	167.9539	16.7954	14.4622
C58	10	156.818	15.6818	5.4806
C59	10	145.8387	14.5839	4.3101

ANOVA

Source of Variation	*SS*	*df*	*MS*	*F*	*p-level*	*F crit*
Between Groups	692.6495	29	23.8845	4.2989	0.%	1.5096
Within Groups	1500.0947	270	5.5559			
Total	2192.7442	299				

Table 42: Results of ANOVA for deconvolved peak 2 area.

Analysis of Variance (One-Way)

Summary

Groups	*Sample size*	*Sum*	*Mean*	*Variance*
W10	10	521.865	52.1865	35.0016
W12	10	528.9527	52.8953	6.4272
W13	10	554.3278	55.4328	38.3233
W18	10	525.3279	52.5328	2.67
W35	10	521.9967	52.1997	39.3064
W50	10	525.2758	52.5276	7.1036
W52	10	529.0009	52.9001	4.9108
W153	10	586.6664	58.6666	49.1684
W295	10	616.6983	61.6698	43.942
W360	10	637.8099	63.781	24.0847
W368	10	628.7716	62.8772	21.596
W394	10	595.1219	59.5122	18.5628
W411	10	613.0689	61.3069	29.3714
W412	10	576.6326	57.6633	9.0027
W442	10	559.7467	55.9747	11.5595
W444	10	617.7171	61.7717	38.7879
W445	10	587.288	58.7288	10.3945
W446	10	579.589	57.9589	11.2467
W448	10	597.5127	59.7513	20.6715
W450	10	568.6243	56.8624	8.9971
C50	10	508.4974	50.8497	8.4282
C51	10	566.5512	56.6551	30.1166
C52	10	498.1718	49.8172	81.3589
C53	10	524.1044	52.4104	23.218
C54	10	519.1538	51.9154	18.6185
C55	10	524.2826	52.4283	16.6009
C56	10	542.8583	54.2858	27.6864
C57	10	544.3625	54.4362	70.8494
C58	10	545.4274	54.5427	25.0204
C59	10	484.3379	48.4338	6.5988

ANOVA

Source of Variation	*SS*	*df*	*MS*	*F*	*p-level*	*F crit*
Between Groups	4930.2737	29	170.0094	6.8958	0.%	1.5096
Within Groups	6656.6162	270	24.6541			
Total	11586.8899	299				

Table 43: Results of ANOVA for deconvolved peak 3 area.

Analysis of Variance (One-Way)

Summary

Groups	*Sample size*	*Sum*	*Mean*	*Variance*
W10	10	671.1151	67.1115	61.212
W12	10	685.1695	68.5169	77.9506
W13	10	742.647	74.2647	56.5828
W18	10	725.9794	72.5979	8.4286
W35	10	690.6821	69.0682	72.9264
W50	10	708.1098	70.811	39.0989
W52	10	641.7157	64.1716	46.0847
W153	10	629.8639	62.9864	31.3618
W295	10	618.0363	61.8036	28.1662
W360	10	636.6422	63.6642	18.9573
W368	10	629.9043	62.9904	29.8794
W394	10	623.9602	62.396	73.4418
W411	10	627.734	62.7734	19.2616
W412	10	572.0204	57.202	19.242
W442	10	573.3612	57.3361	12.4045
W444	10	625.3382	62.5338	52.5551
W445	10	598.3315	59.8331	29.6524
W446	10	578.8938	57.8894	13.6088
W448	10	610.6006	61.0601	51.144
W450	10	571.9556	57.1956	28.7227
C50	10	692.8489	69.2849	44.5226
C51	10	671.7503	67.175	61.4796
C52	10	706.0302	70.603	53.777
C53	10	698.5186	69.8519	86.1281
C54	10	676.2457	67.6246	49.6846
C55	10	650.0936	65.0094	131.2116
C56	10	675.8962	67.5896	32.7549
C57	10	696.1623	69.6162	44.0526
C58	10	722.2384	72.2238	40.6384
C59	10	593.5039	59.3504	83.0106

ANOVA

Source of Variation	*SS*	*df*	*MS*	*F*	*p-level*	*F crit*
Between Groups	7188.8851	29	247.8926	5.3198	0.%	1.5096
Within Groups	12581.4726	270	46.598			
Total	19770.3578	299				

Table 44: Results of ANOVA for deconvolved peak 4 area.

Analysis of Variance (One-Way)

Summary

Groups	*Sample size*	*Sum*	*Mean*	*Variance*
W10	10	428.4121	42.8412	74.6625
W12	10	440.5062	44.0506	170.9174
W13	10	449.4474	44.9447	113.8805
W18	10	457.3042	45.7304	13.2763
W35	10	500.6706	50.0671	105.4134
W50	10	437.5963	43.7596	20.4485
W52	10	411.6333	41.1633	15.3234
W153	10	401.6422	40.1642	42.3106
W295	10	450.5952	45.0595	48.231
W360	10	477.2276	47.7228	28.7107
W368	10	406.4645	40.6464	34.8812
W394	10	420.627	42.0627	51.2112
W411	10	467.5214	46.7521	71.1696
W412	10	448.3235	44.8324	43.4252
W442	10	443.3499	44.335	15.0082
W444	10	434.1659	43.4166	41.9062
W445	10	455.8079	45.5808	30.8747
W446	10	443.0353	44.3035	11.3591
W448	10	498.4766	49.8477	133.99
W450	10	445.4644	44.5464	46.3673
C50	10	435.6022	43.5602	50.276
C51	10	416.0319	41.6032	31.4542
C52	10	461.3278	46.1328	68.9301
C53	10	426.6979	42.6698	34.4097
C54	10	405.0719	40.5072	14.7056
C55	10	393.0488	39.3049	67.7503
C56	10	470.6499	47.065	77.6324
C57	10	423.9163	42.3916	31.5154
C58	10	410.1835	41.0183	27.3803
C59	10	446.8098	44.681	49.5041

ANOVA

Source of Variation	*SS*	*df*	*MS*	*F*	*p-level*	*F crit*
Between Groups	2084.6048	29	71.8829	1.3763	10.08%	1.5096
Within Groups	14102.3234	270	52.2308			
Total	16186.9283	299				

Table 45: Results of ANOVA for deconvolved peak 5 area.

Analysis of Variance (One-Way)

Summary

Groups	*Sample size*	*Sum*	*Mean*	*Variance*
W10	10	160.0162	16.0016	4.1488
W12	10	160.2283	16.0228	2.612
W13	10	167.0682	16.7068	4.6598
W18	10	167.195	16.7195	3.1097
W35	10	188.8776	18.8878	15.1008
W50	10	147.0402	14.704	3.8957
W52	10	133.3443	13.3344	4.2951
W153	10	158.1418	15.8142	10.8894
W295	10	151.886	15.1886	3.8185
W360	10	167.3188	16.7319	7.7659
W368	10	147.716	14.7716	4.9325
W394	10	136.9647	13.6965	2.3157
W411	10	147.0564	14.7056	2.6058
W412	10	123.3024	12.3302	6.5828
W442	10	119.7317	11.9732	3.5973
W444	10	134.8629	13.4863	10.302
W445	10	133.1497	13.315	2.9931
W446	10	128.8764	12.8876	2.1336
W448	10	152.4271	15.2427	4.5464
W450	10	123.5377	12.3538	4.5685
C50	10	123.4712	12.3471	4.8216
C51	10	155.1843	15.5184	6.912
C52	10	135.997	13.5997	2.9498
C53	10	148.0418	14.8042	13.4956
C54	10	135.7299	13.573	4.7566
C55	10	135.5822	13.5582	3.9142
C56	10	146.3944	14.6394	3.7823
C57	10	139.3811	13.9381	5.5669
C58	10	147.1268	14.7127	2.8377
C59	10	68.2304	6.823	1.9985

ANOVA

Source of Variation	*SS*	*df*	*MS*	*F*	*p-level*	*F crit*
Between Groups	1304.2947	29	44.9757	8.6542	0.%	1.5096
Within Groups	1403.1767	270	5.197			
Total	2707.4713	299				

Table 46: Results of ANOVA for deconvolved peak 6 area.

Analysis of Variance (One-Way)

Summary

Groups	*Sample size*	*Sum*	*Mean*	*Variance*
W10	10	95.2599	9.526	3.1052
W12	10	88.2426	8.8243	1.1513
W13	10	111.8066	11.1807	1.8658
W18	10	108.9275	10.8928	1.9576
W35	10	127.2727	12.7273	5.9389
W50	10	106.907	10.6907	3.404
W52	10	107.7252	10.7725	22.7079
W153	10	72.3604	7.236	3.3743
W295	10	91.1646	9.1165	1.0483
W360	10	114.0738	11.4074	2.1185
W368	10	90.7288	9.0729	0.5405
W394	10	84.0662	8.4066	4.3027
W411	10	100.142	10.0142	0.9036
W412	10	100.6096	10.061	2.1643
W442	10	93.7314	9.3731	0.9489
W444	10	94.0722	9.4072	0.7501
W445	10	102.7388	10.2739	0.9937
W446	10	85.49	8.549	0.454
W448	10	99.4401	9.944	2.4095
W450	10	87.6847	8.7685	3.8022
C50	10	121.2125	12.1212	2.5895
C51	10	110.1166	11.0117	5.7371
C52	10	138.5082	13.8508	4.2545
C53	10	125.3262	12.5326	6.8746
C54	10	125.0958	12.5096	8.1231
C55	10	112.9551	11.2955	3.9908
C56	10	145.6431	14.5643	9.6359
C57	10	135.5312	13.5531	2.8321
C58	10	135.4853	13.5485	4.7757
C59	10	190.3054	19.0305	15.4869

ANOVA

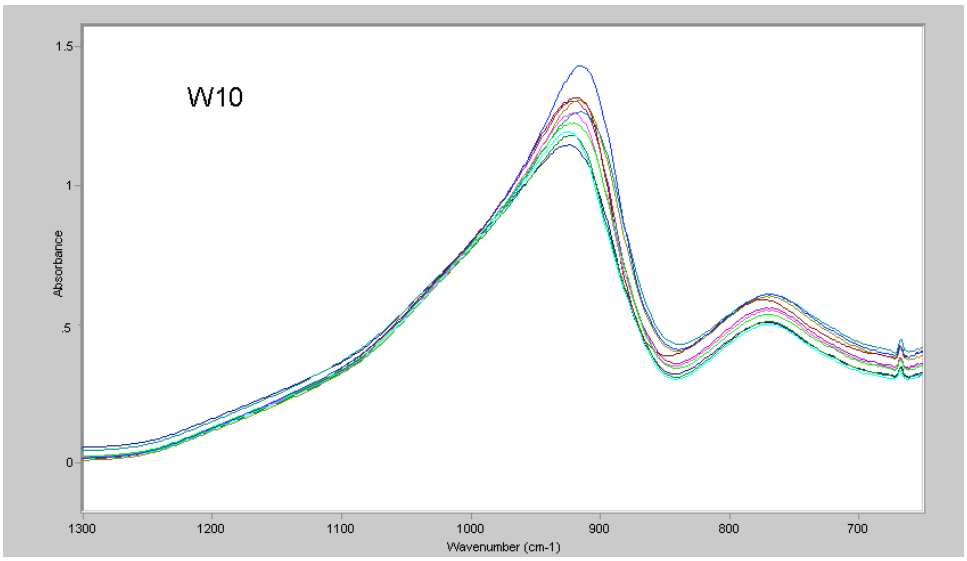
Source of Variation	*SS*	*df*	*MS*	*F*	*p-level*	*F crit*
Between Groups	1623.7342	29	55.9908	13.0981	0.%	1.5096
Within Groups	1154.1731	270	4.2747			
Total	2777.9073	299				

The results of ANOVA revealed that there were indeed statistically significant differences in the means of all 6 of the peak positions and 5 of the 6 peak areas. The F critical (1.5096) was larger than the F statistic (1.3763) for Peak 4's area, thus the null hypothesis was not rejected which indicated that there was no significant difference in that peak area's means for the different populations (glass samples). For the other 5 peak areas and the 6 peak positions, the F statistic was larger than the F critical. Thus, the null hypothesis was rejected which indicated that the means for at least 2 of the glass samples within the set of 30 are significantly different. However, ANOVA does not determine which glasses were differentiated; consequently further statistical analysis of the deconvolved peak data was warranted in order to determine its classification and discrimination power (Chapter 4.C.b).

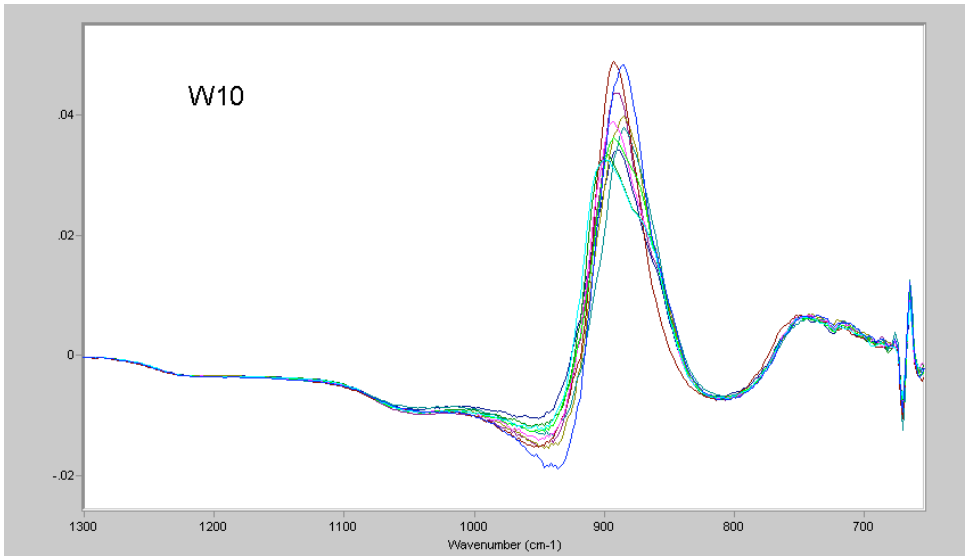
4.C. Classification and Discrimination Power

Prior to determining the discrimination and classification power of mid-IR microspectroscopy of glass, the first and second derivatives (5- and 9-point smoothing) of all of the spectra were calculated. Figures 73-75 show the unprocessed spectra and the first and the second derivative spectra (5- and 9-point smoothing) of an automotive, an architectural, and a window glass, respectively. Figure 76 shows the unprocessed spectra, the first derivative spectra and the second derivative spectra (5- and 9-point smoothing) of the automotive, architectural, and window glasses in Figures 73 – 75 overlaid.

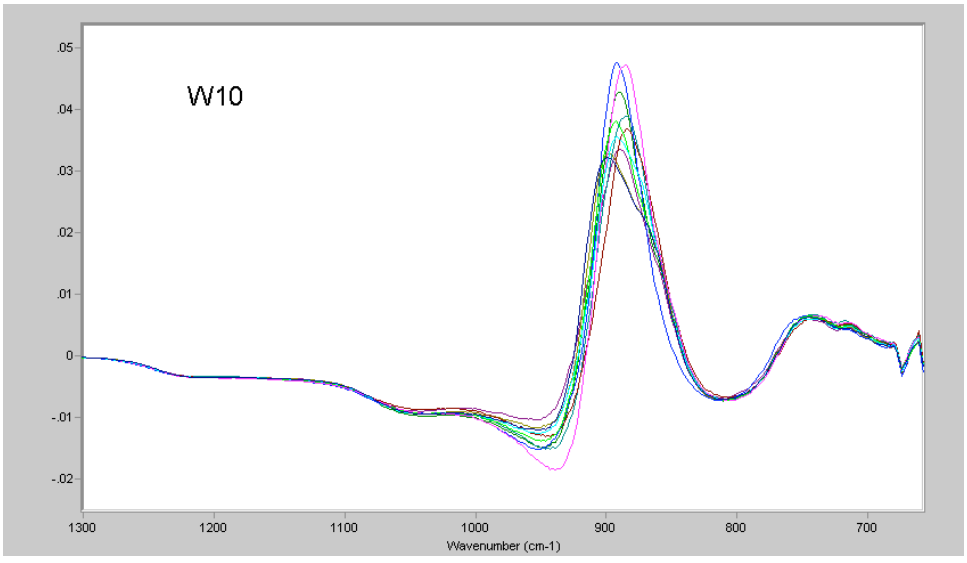
(a)


W10
Absorbance
1.5
1
.5
0
1300
1200
1100
1000
900
800
700
Wavenumber (cm-1)

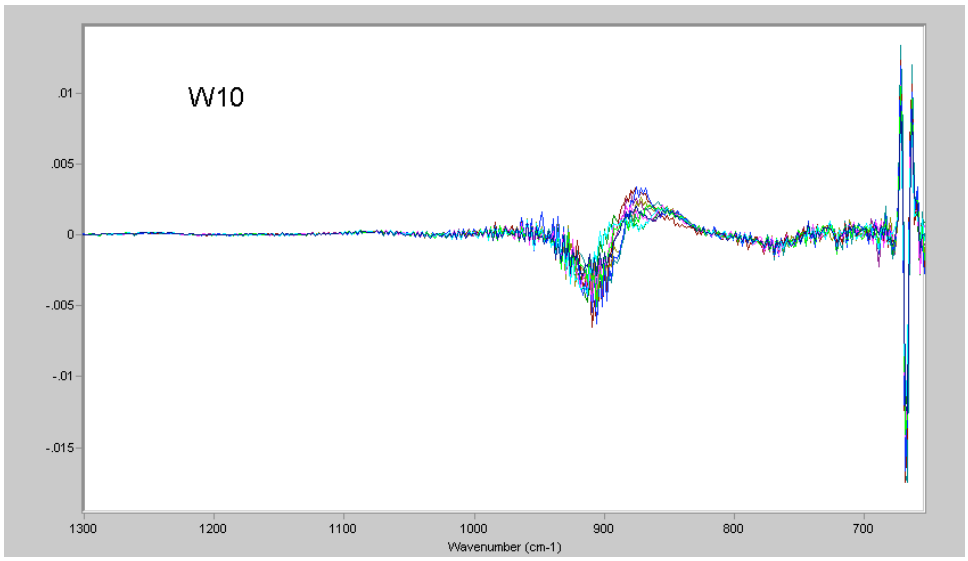
(b)


W10
.04
.02
0
-.02
1300
1200
1100
1000
900
800
700
Wavenumber (cm-1)

(c)


W10
.05
.04
.03
.02
.01
0
-.01
-.02
1300
1200
1100
1000
900
800
700
Wavenumber (cm-1)

(d)



(e)

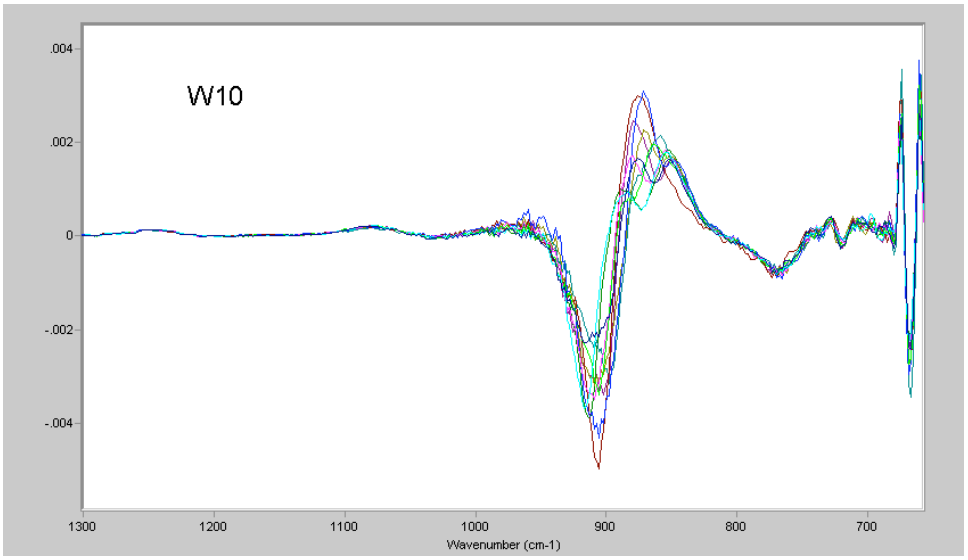
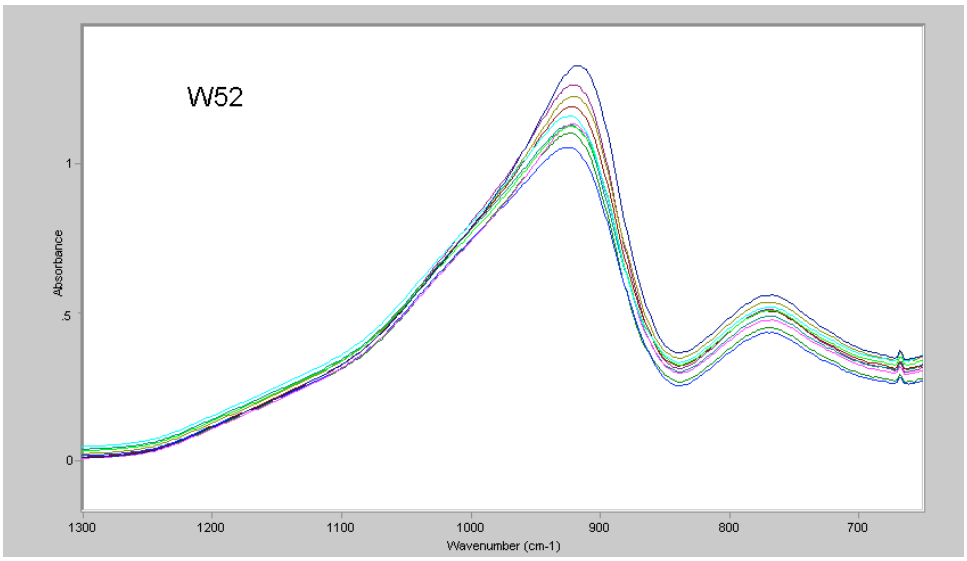
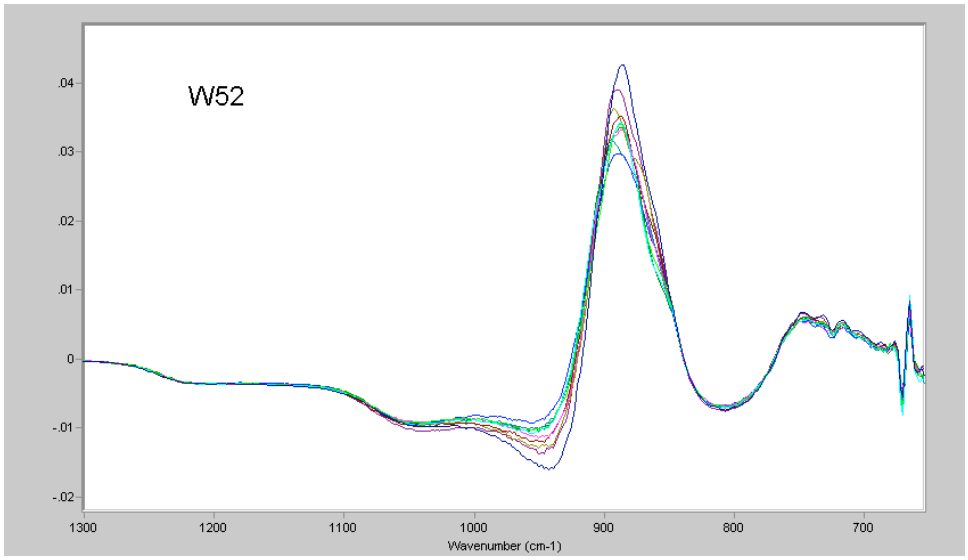


Figure 73: (a) The mid-IR spectra, collected with a 50-µm aperture, 4 cm^{-1} spectral resolution, and 256 co-added scans, of automotive glass W10 (10 replicates), (b) the first derivate spectra (5-point smoothing) of automotive glass W10 (10 replicates), (c) the first derivate spectra (9-point smoothing) of automotive glass W10 (10 replicates), (d) and the second derivative spectra (5-point smoothing) of automotive glass W10 (10 replicates), and (e) and the second derivative spectra (9-point smoothing) of automotive glass W10 (10 replicates). The spectra were produced using Grams® AI software.

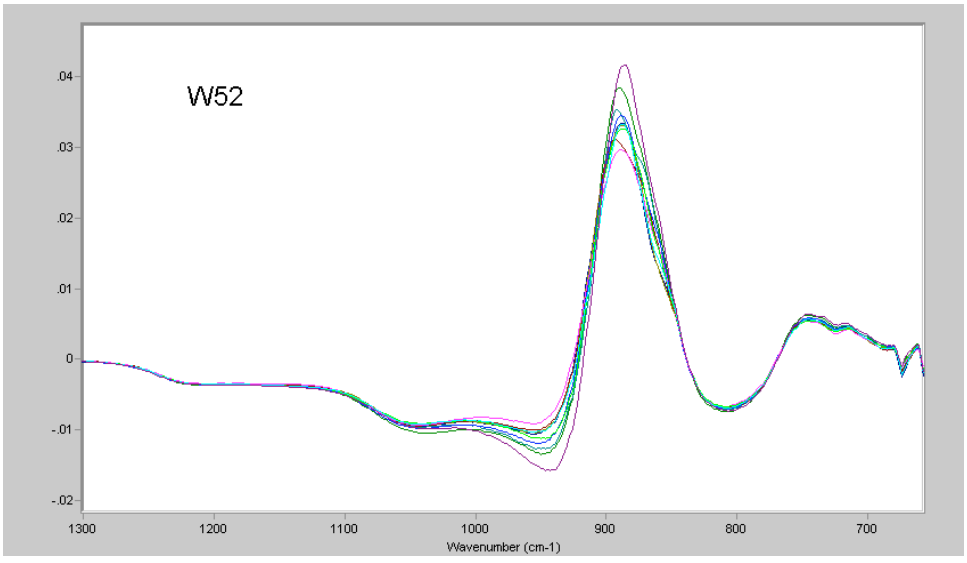
(a)


W52
Absorbance
1
.5
0
1300
1200
1100
1000
900
800
700
Wavenumber (cm-1)

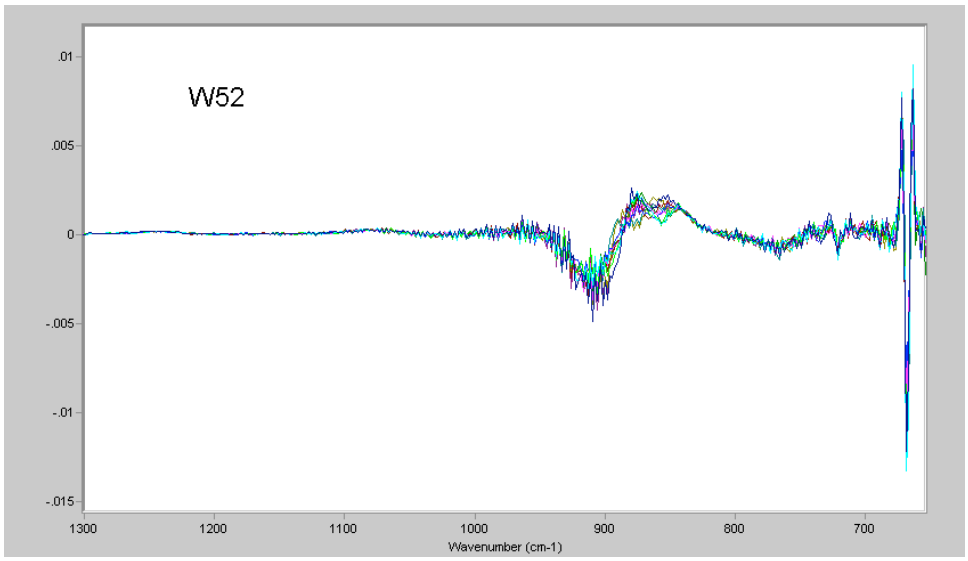
(b)


W52
.04
.03
.02
.01
0
-.01
-.02
1300
1200
1100
1000
900
800
700
Wavenumber (cm-1)

(c)


W52
.04
.03
.02
.01
0
-.01
-.02
1300
1200
1100
1000
900
800
700
Wavenumber (cm-1)

(d)



(e)

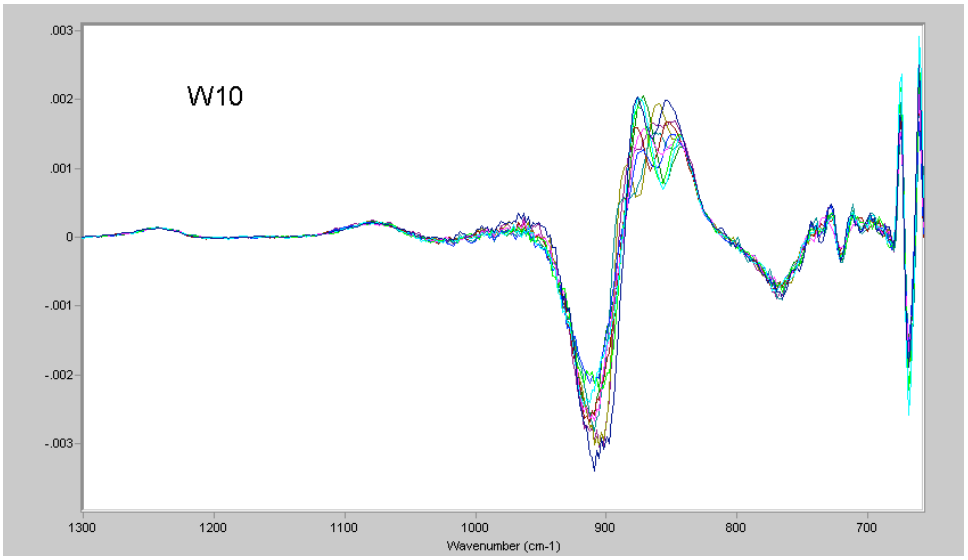
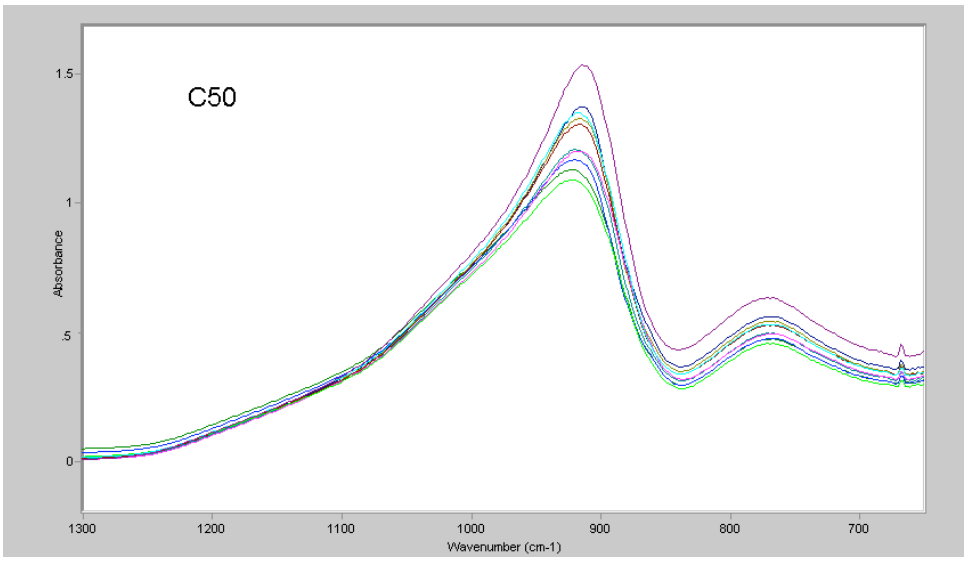
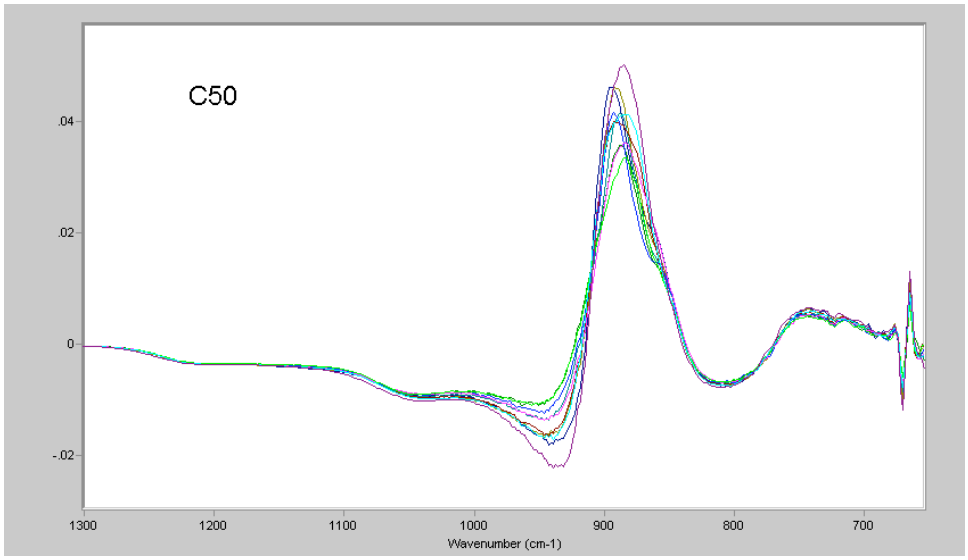


Figure 74: (a) The mid-IR spectra, collected with a 50-µm aperture, 4 cm^{-1} spectral resolution, and 256 co-added scans, of architectural glass W52 (10 replicates), (b) the first derivate spectra (5-point smoothing) of architectural glass W52 (10 replicates), (c) the first derivate spectra (9-point smoothing) of architectural glass W52 (10 replicates), (d) the second derivative spectra (5-point smoothing) of architectural glass W52 (10 replicates), and (e) the second derivative spectra (9-point smoothing) of architectural glass W52 (10 replicates). The spectra were produced using Grams® AI software.

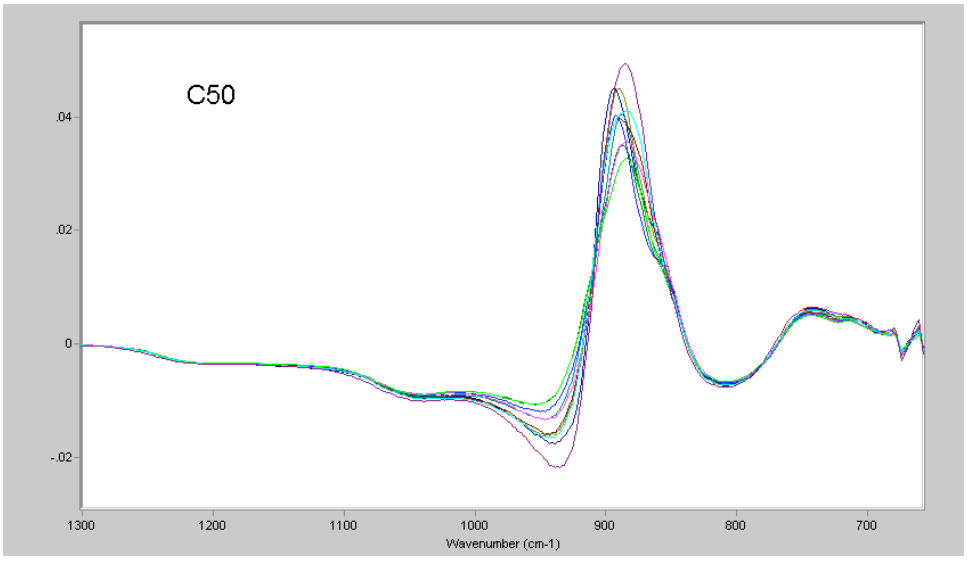
(a)


C50
Absorbance
1.5
1
.5
0
1300
1200
1100
1000
900
800
700
Wavenumber (cm-1)

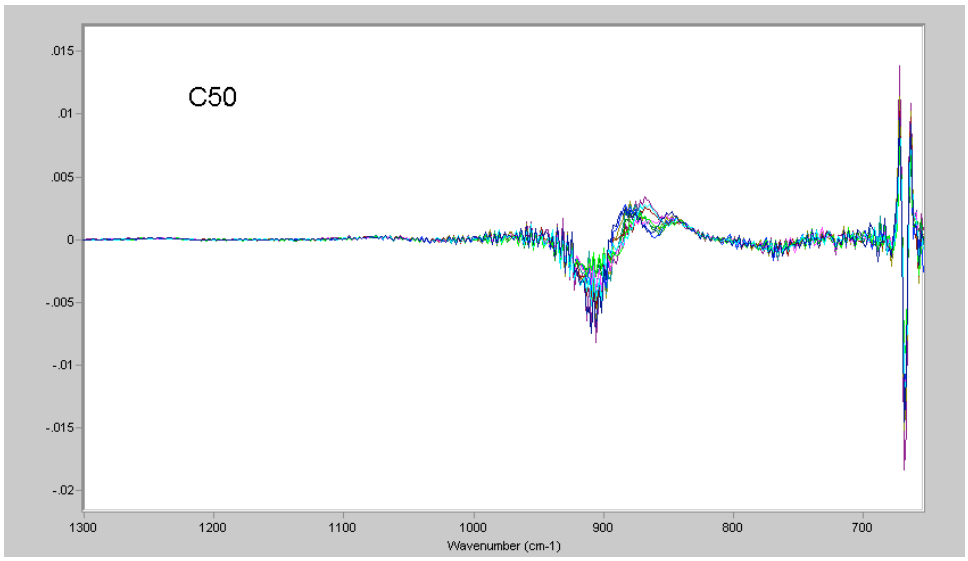
(b)


C50
.04
.02
0
-.02
1300
1200
1100
1000
900
800
700
Wavenumber (cm-1)

(c)


C50
.04
.02
0
-.02
1300
1200
1100
1000
900
800
700
Wavenumber (cm-1)

(d)



(e)

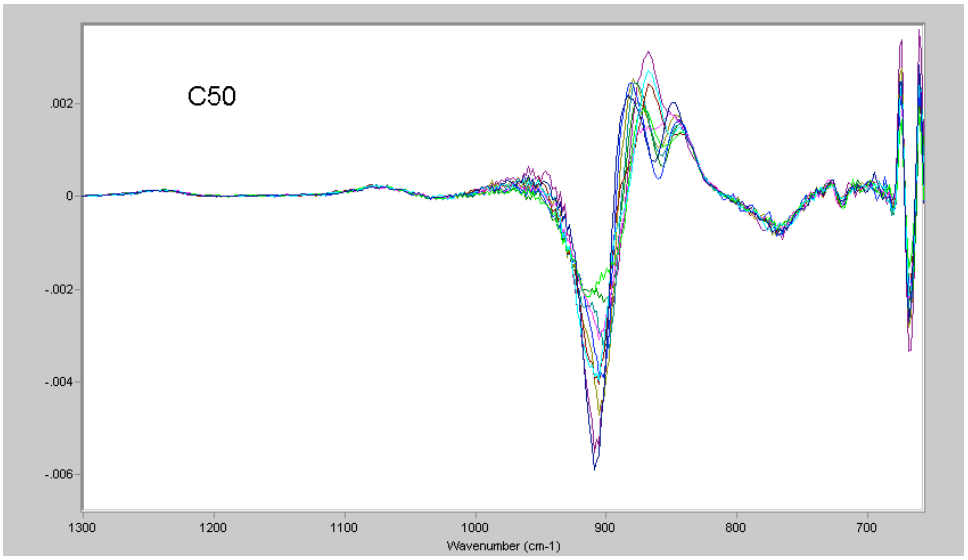
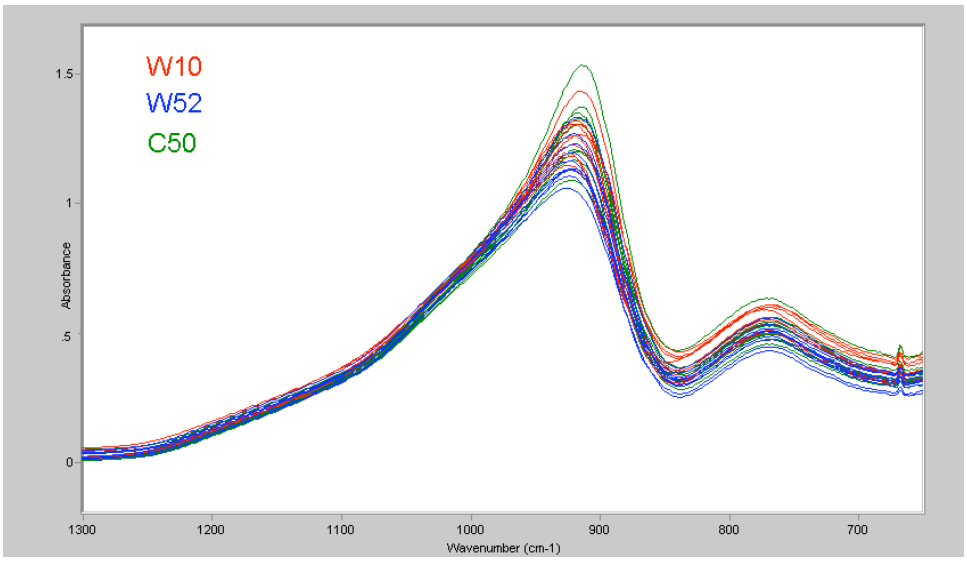
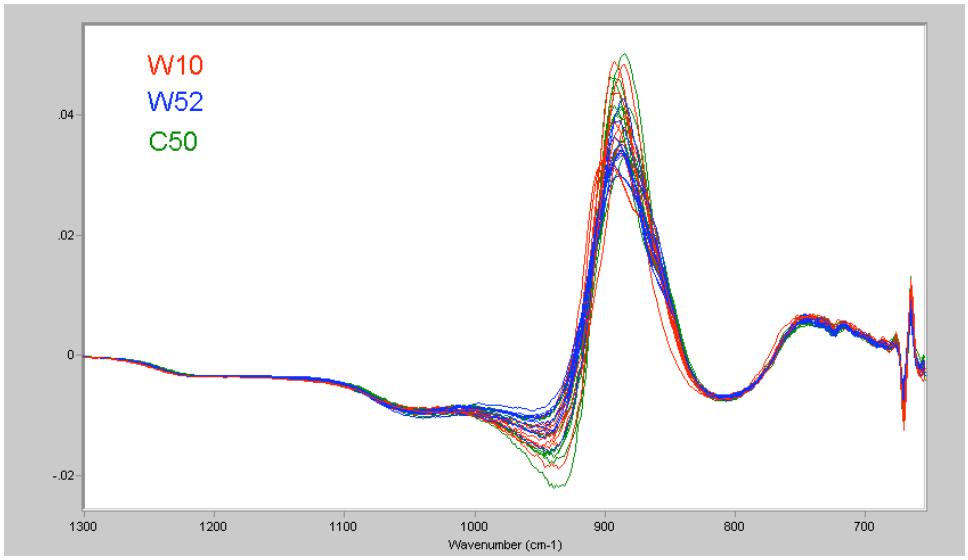


Figure 75: (a) The mid-IR spectra, collected with a 50-µm aperture, 4 cm^{-1} spectral resolution, and 256 co-added scans, of container glass C50 (10 replicates), (b) the first derivate spectra (5-point smoothing) of container glass C50 (10 replicates), (c) the first derivate spectra (9-point smoothing) of container glass C50 (10 replicates), (d) the second derivative spectra (5-point smoothing) of container glass C50 (10 replicates), (e) the second derivative spectra (9-point smoothing) of container glass C50 (10 replicates). The spectra were produced using Grams® AI software.

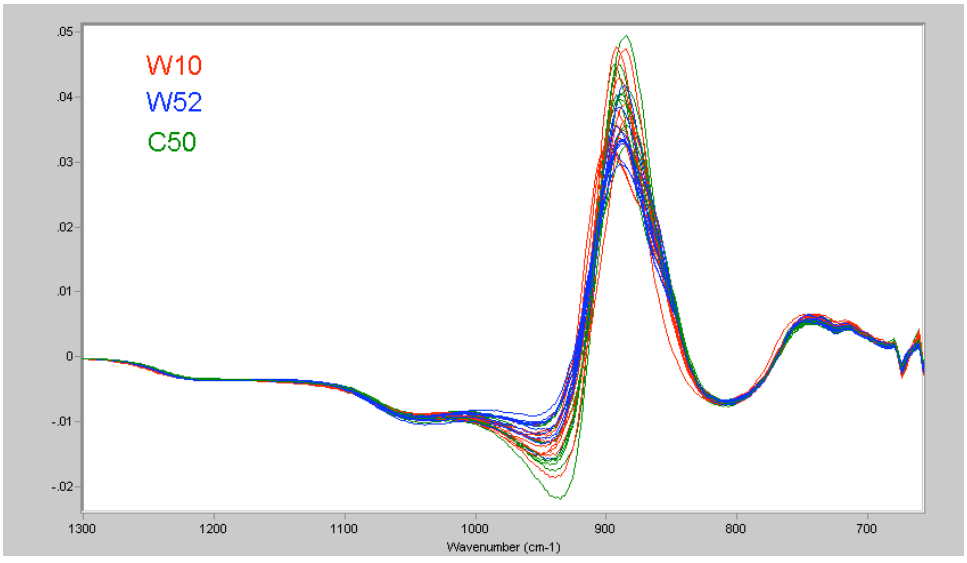
(a)


W10
W52
C50
Absorbance
1.5
1
.5
0
1300
1200
1100
1000
900
800
700
Wavenumber (cm-1)

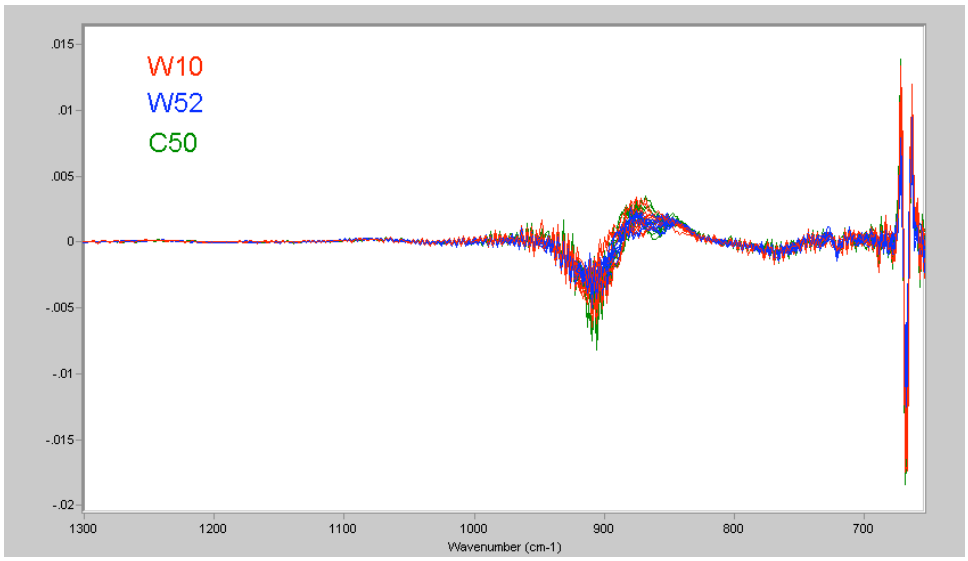
(b)


W10
W52
C50
.04
.02
0
-.02
1300
1200
1100
1000
900
800
700
Wavenumber (cm-1)

(c)


W10
W52
C50
.05
.04
.03
.02
.01
0
-.01
-.02
1300
1200
1100
1000
900
800
700
Wavenumber (cm-1)

(d)



(e)

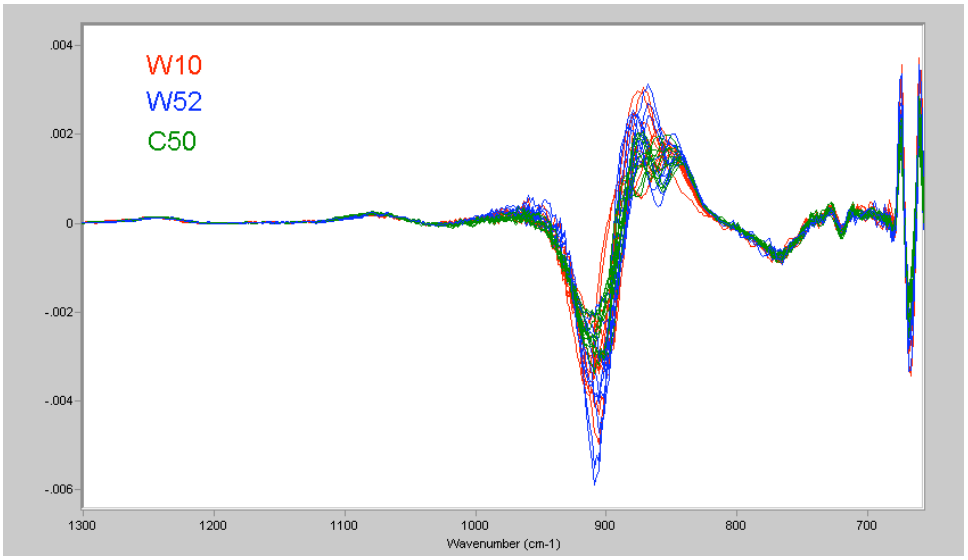


Figure 76: (a) The mid-IR spectra (collected with a 50-µm aperture, 4 cm^{-1} spectral resolution, and 256 co-added scans), (b) the first derivate spectra (5-point smoothing), (c) the first derivate spectra (9-point smoothing), (d) the second derivate spectra (5-point smoothing), and (e) the second derivate spectra (9-point smoothing) of automotive glass W10 (in red), architectural glass W52 (in blue) and container glass C50 (in green), all overlaid (10 replicates for each). The spectra were produced using Grams® AI software.

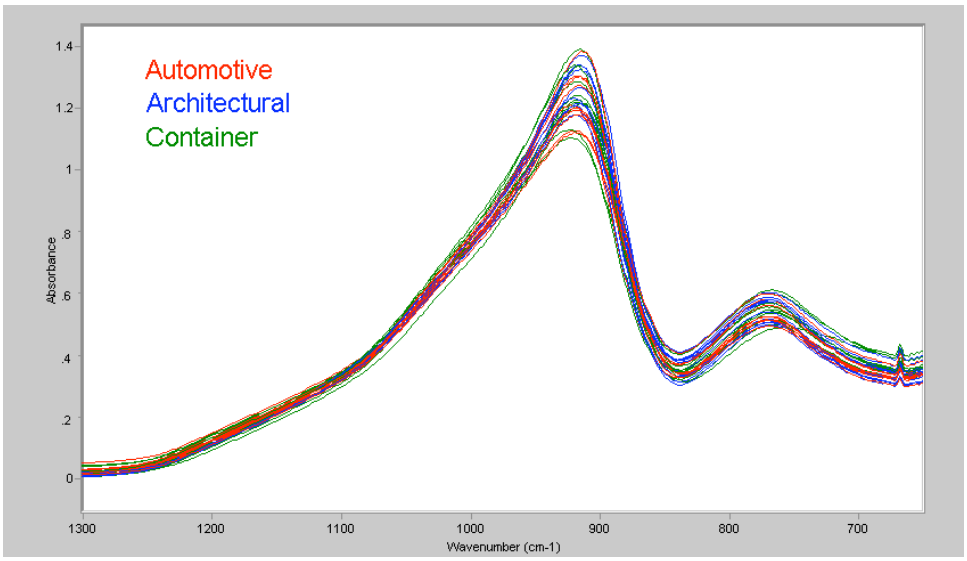
Figures 73a, 74a, and 75a show the mid-IR spectral variations that exist within a single glass source. There are considerable peak height variations within a given sample, which could have many explanations including, but not limited to varying amounts of contact with the IRE,

varying silicate structures in the analyzed fragments, and/or varying absorption due to orientation effects of the silicate structures. The variations in the mid-IR spectra within a given glass source can also be seen in the first and second derivate spectra (Figures 73b - e, 74b - e, and 75b - e). When comparing the spectra and derivative spectra of the 3 glasses (Figure 76), the different sources cannot be visually differentiated.

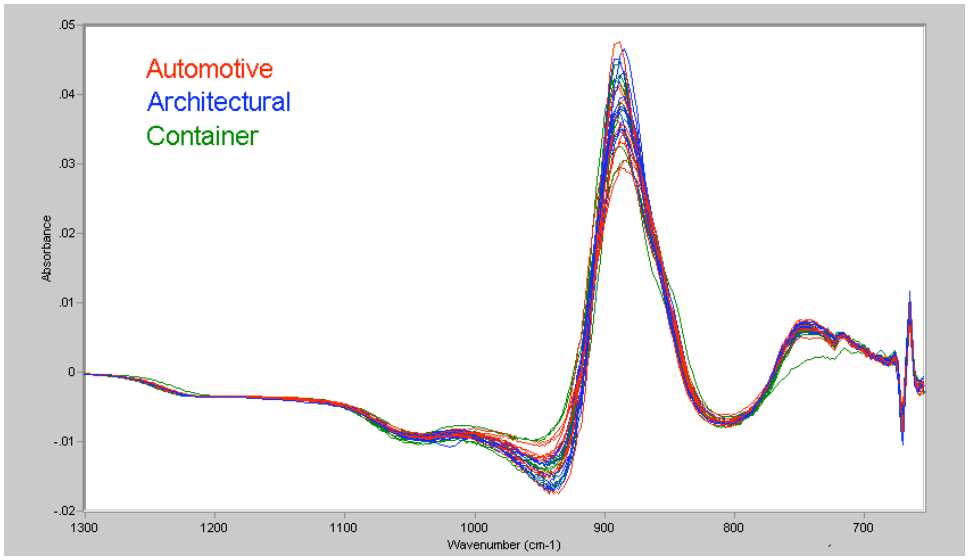
In addition, there are clear differences between the derivative spectra that underwent a 5-point smoothing (Figures 73b and d, 74b and d, 75b and d) and a 9-point smoothing (Figures 73c and e, 74c and e, and 75c and e). As expected, there is less noise with the derivate spectra that were 9-point smoothed than those that were 5-point smoothed. This is especially visible in the second derivative spectra. Furthermore, the ratios of peaks are different when the different smoothing schemes are used.

To determine if there were any visible differences in the mid-IR spectra or derivative spectra that could be used for source classification, the average of 3 spectra from 30 different glass sources (10 automotive, architectural, or container) were plotted and are shown in Figure 77a. The first and second derivative spectra (5- and 9-point smoothing) of the average spectra are also shown in Figures 77b – e. There are no visual differences that would enable a source classification of glasses by visual inspection of the mid-IR spectra and derivative spectra.

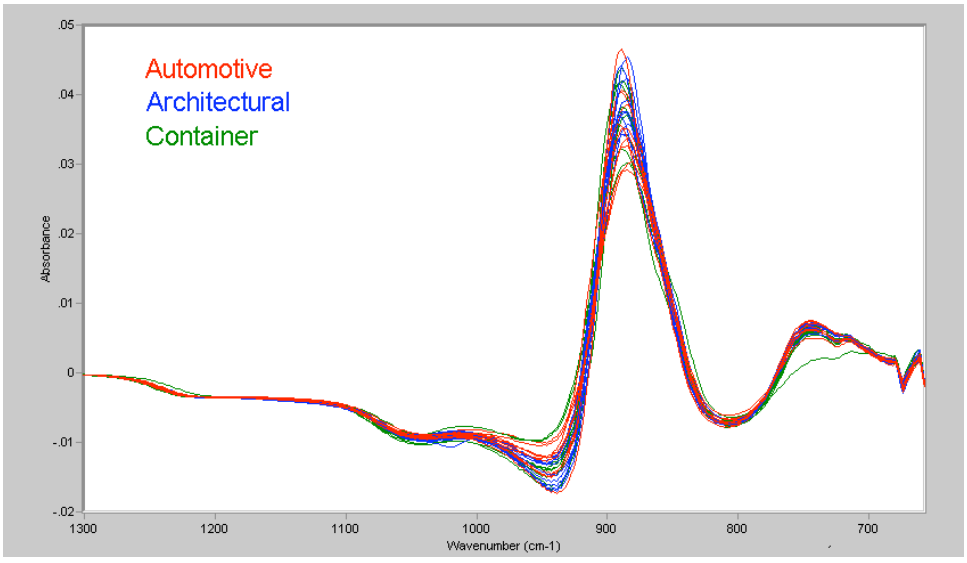
(a)


Automotive
Architectural
Container
Absorbance
1.4
1.2
1
.8
.6
.4
.2
0
1300
1200
1100
1000
900
800
700
Wavenumber (cm-1)

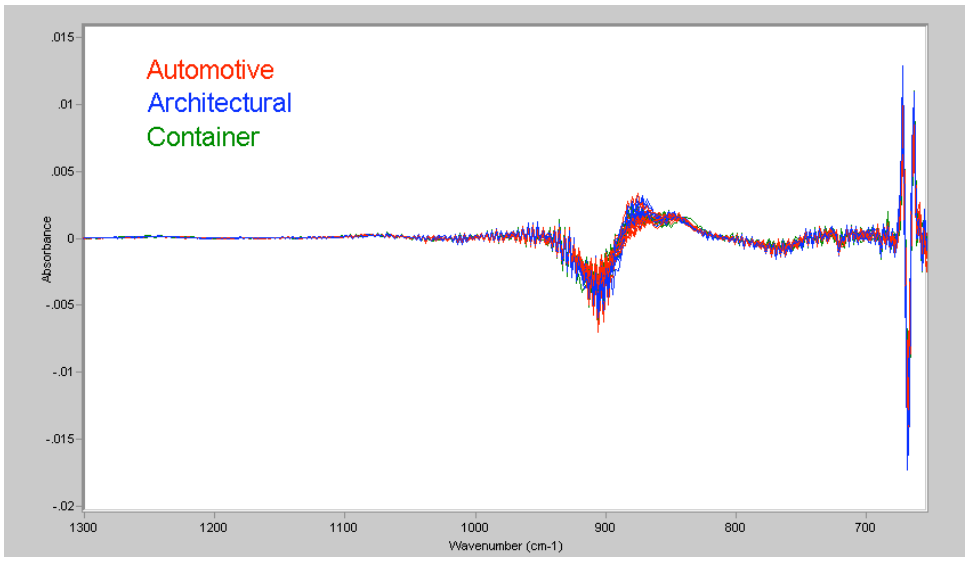
(b)


Automotive
Architectural
Container
Absorbance
.05
.04
.03
.02
.01
0
-.01
-.02
1300
1200
1100
1000
900
800
700
Wavenumber (cm-1)

(c)


Automotive
Architectural
Container
Absorbance
.05
.04
.03
.02
.01
0
-.01
-.02
1300
1200
1100
1000
900
800
700
Wavenumber (cm-1)

(d)



(e)

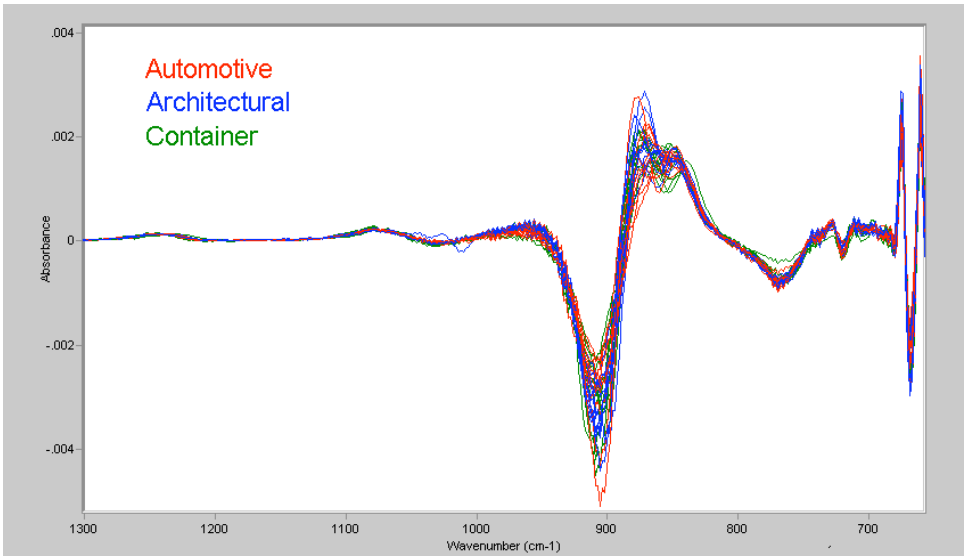


Figure 77: (a) The mid-IR spectra (collected with a 50-µm aperture, 4 cm^{-1} spectral resolution, and 256 co-added scans), (b) the first derivate spectra (5-point smoothing), (c) the first derivate spectra (9-point smoothing), (d) the second derivate spectra (5-point smoothing), and (e) the second derivate spectra (9-point smoothing) of 10 automotive glass averages (in red), 10 architectural glass averages (in blue) and 10 container glass averages C50 (in green), all overlaid (3 spectra used to make each of the averages). The spectra were produced using Grams® AI software.

4.C.a. ATR Mid-IR Spectral Library Searching

The ATR mid-IR spectral library searches were completed with 2 different search algorithms, the correlation and first derivative correlation, and 2 different mid-IR spectral libraries, one with the unprocessed spectra and the other with the second derivative (5-point smoothing) of the spectra. The results of the 4 ATR mid-IR spectral library searches are in Appendix IX. The results can be viewed in terms of the hit number and/or the HQI values. The hit list results are visually depicted in histograms for each of the 4 library searches in Figures 78 – 81.

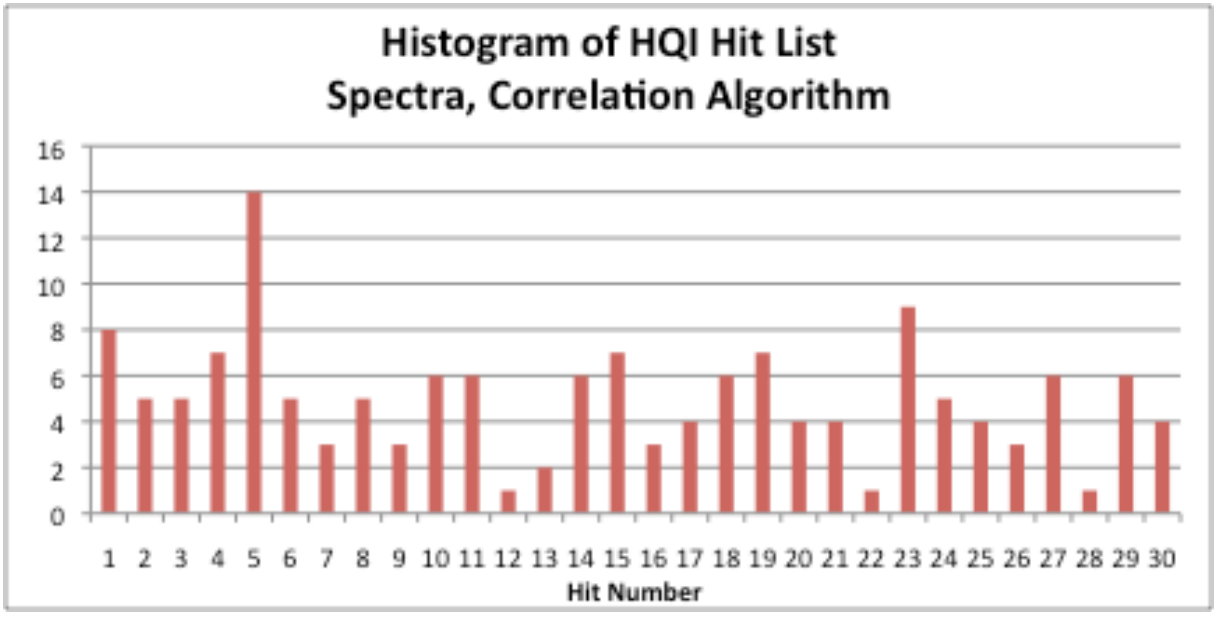


Figure 78: Histogram of the hit number for the ATR mid-IR spectral library search results for the 30 glass spectra (5 replicates) using the correlation search algorithm.

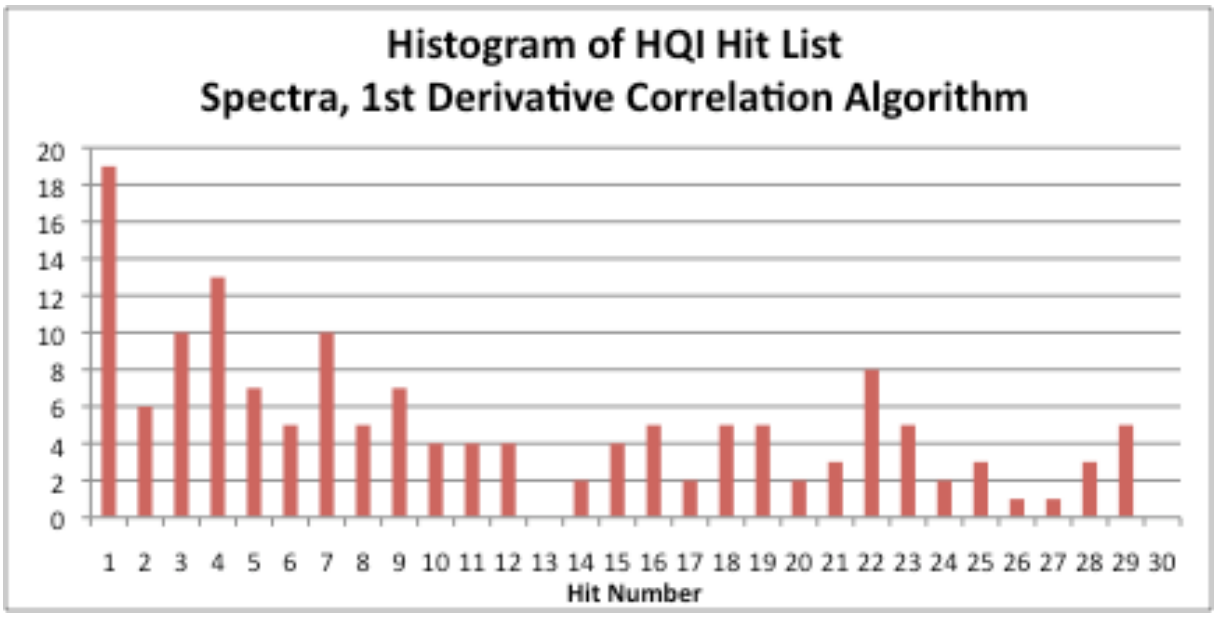


Figure 79: Histogram of the hit number for the ATR mid-IR spectral library search results for the 30 glass spectra (5 replicates) using the first derivative correlation search algorithm.

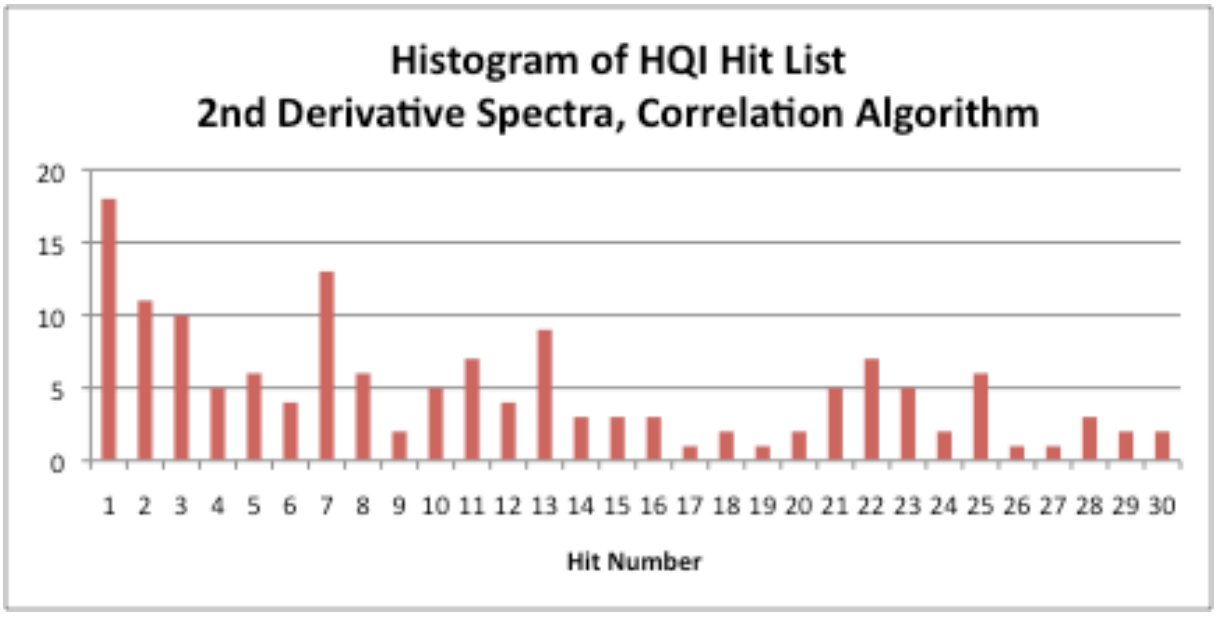


Figure 80: Histogram of the hit number for the ATR mid-IR spectral library search results for the 30 second derivative glass spectra (5 replicates) using the correlation search algorithm.

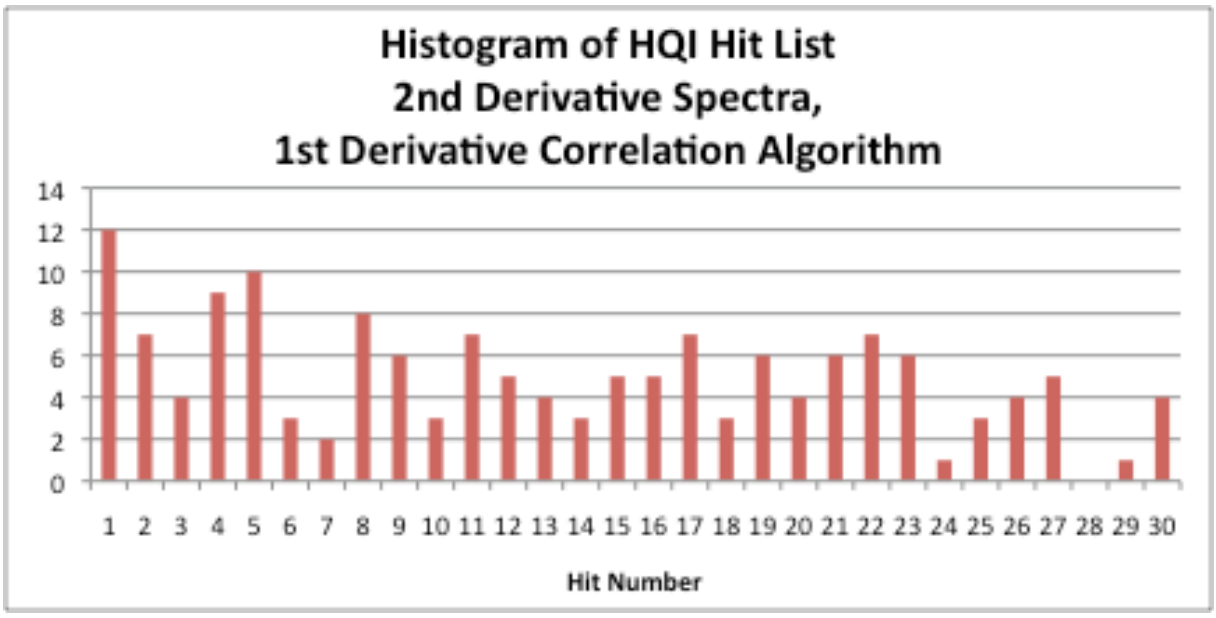


Figure 81: Histogram of the hit number for the ATR mid-IR spectral library search results for the 30 second derivative glass spectra (5 replicates) using the first derivative correlation search algorithm.

The histograms visually demonstrate the failure of all 4 of the ATR mid-IR spectral library search schemes to discriminate between the 30 glass samples because many of the glasses had high hit numbers. This failure is also seen in the average hit numbers and HQIs. The average "match" or correct hit for the library search of the 30 glass spectra using the correlation and first derivative correlation search algorithms was a hit number of 14 and 11, respectively, and an HQI of 0.0198 and 0.03179, respectively. The HQI values for both of these library search algorithms appear to be very good. However when considering their corresponding high hit number, it indicates that even a wrong hit has a low HQI value. The average "match" or correct hit for the library search of the 30 glass second derivative spectra using the correlation and first derivative correlation search algorithms was a hit number of 11 and 13, respectively, and a HQI of 0.121 and 0.584, respectively. The higher HQI for derivative spectral library searching is expected because of increase in noise and accentuation of spectral differences when taking

derivatives. The percentage of spectra that were correctly identified as the first, second or third hit was 12% and 23.3% for the correlation and first derivative correlation search algorithms, respectively. Accordingly, the error rates (where an error is defined as a failure for the correct identification to be the first, second or third hits) for the correlation and first derivative correlation search algorithms were 88% and 76.7%, respectively. For the second derivative spectra, the percentage of spectra that were correctly identified as the first, second or third hit was 26% and 15.3% for the correlation and first derivative correlation search algorithms, respectively. Thus, the error rates for the correlation and first derivative correlation search algorithms were 74% and 84.7%, respectively. Consequently, these results indicate that ATR mid-IR library searches of the spectra or second derivative spectra using the correlation or first derivative correlation algorithms are not useful for glass discrimination.

4.C.b. Comparison of Deconvolved Peaks

A comparison of the 30 glass deconvolved spectra was completed using a range test interval for each of the 6 peak positions and areas. The 6 peak position range comparisons for each of the 30 glasses are graphically represented in Figures 82 – 87. The 6 peak area range comparisons for each of the 30 glasses are graphically represented in Figures 88 – 93. For all comparison graphs, the identity of the 30 glasses is on the abscissa while the wavenumber (for peak position) or area is on the ordinate axes. Error bars show the range of wavenumber or area values while the average is represented with a diamond data point. Table 47 contains a summary of the results of the deconvolved peak position and area comparisons.

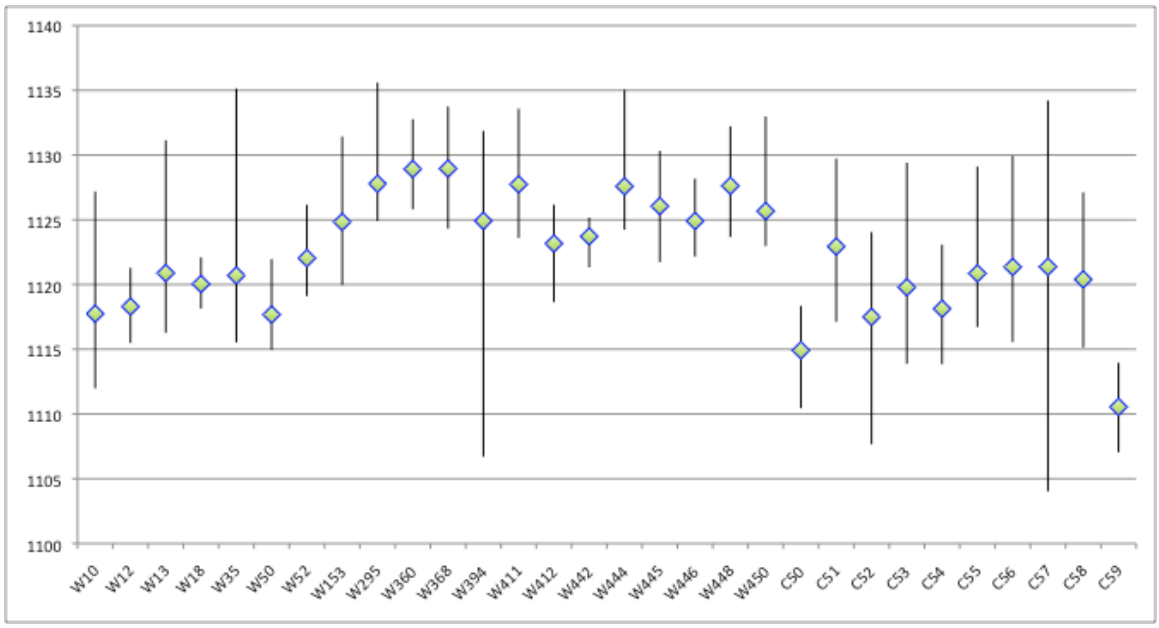


Figure 82: Graphic comparisons of the peak positions (center X, in wavenumbers) of Peak 1 from the deconvolution of the 30 glass spectra (10 replicates). The diamond data point shows the average peak position and the error bars show the range of peak position data for each glass sample.

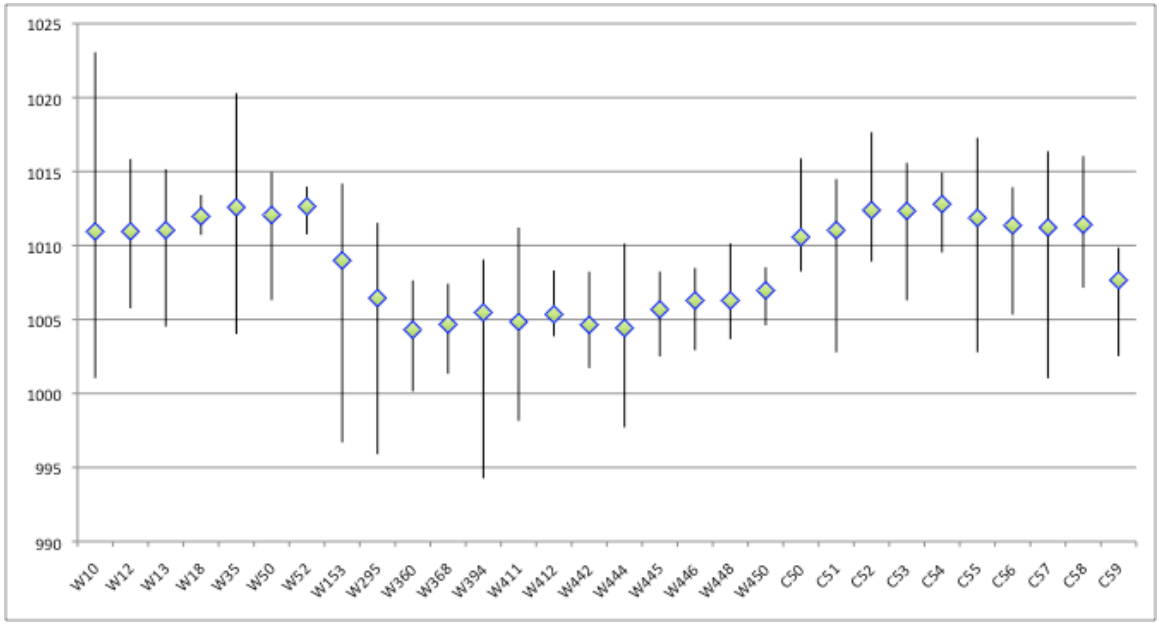


Figure 83: Graphic comparisons of the peak positions (center X, in wavenumbers) of Peak 2 from the deconvolution of the 30 glass spectra (10 replicates). The diamond data point shows the average peak position and the error bars show the range of peak position data for each glass sample.

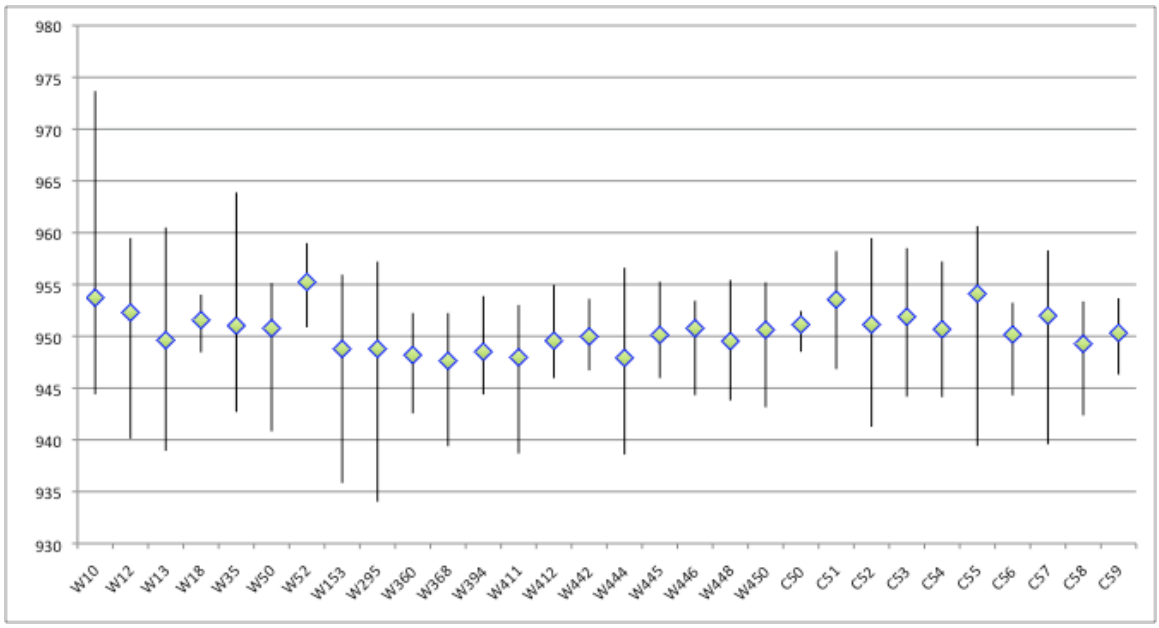


Figure 84: Graphic comparisons of the peak positions (center X, in wavenumbers) of Peak 3 from the deconvolution of the 30 glass spectra (10 replicates). The diamond data point shows the average peak position and the error bars show the range of peak position data for each glass sample.

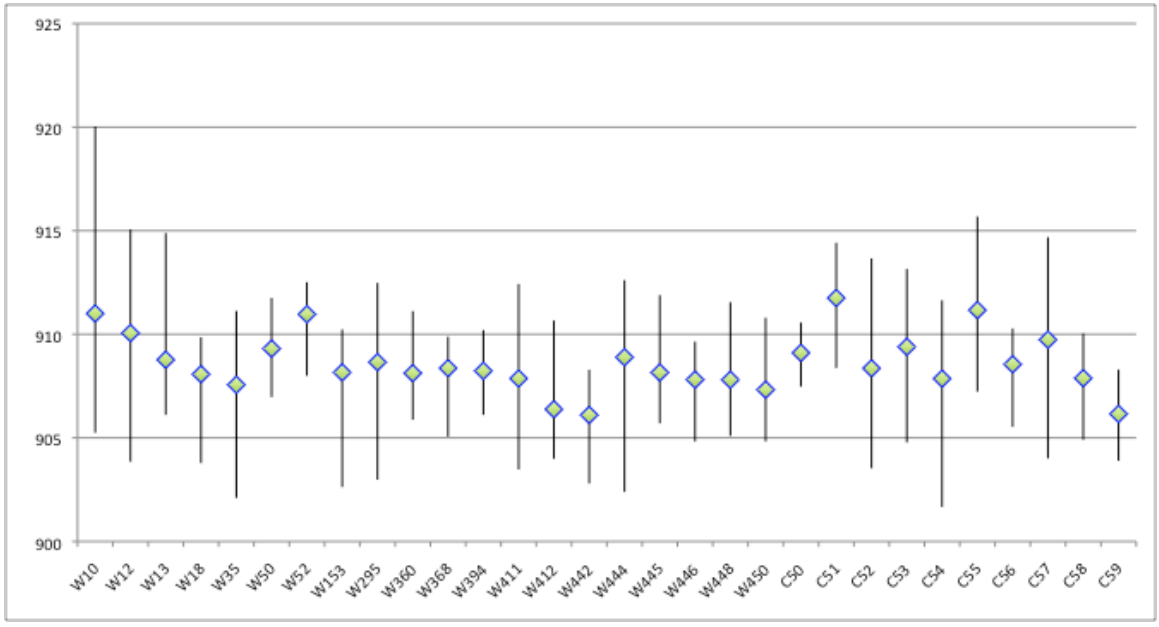


Figure 85: Graphic comparisons of the peak positions (center X, in wavenumbers) of Peak 4 from the deconvolution of the 30 glass spectra (10 replicates). The diamond data point shows the average peak position and the error bars show the range of peak position data for each glass sample.

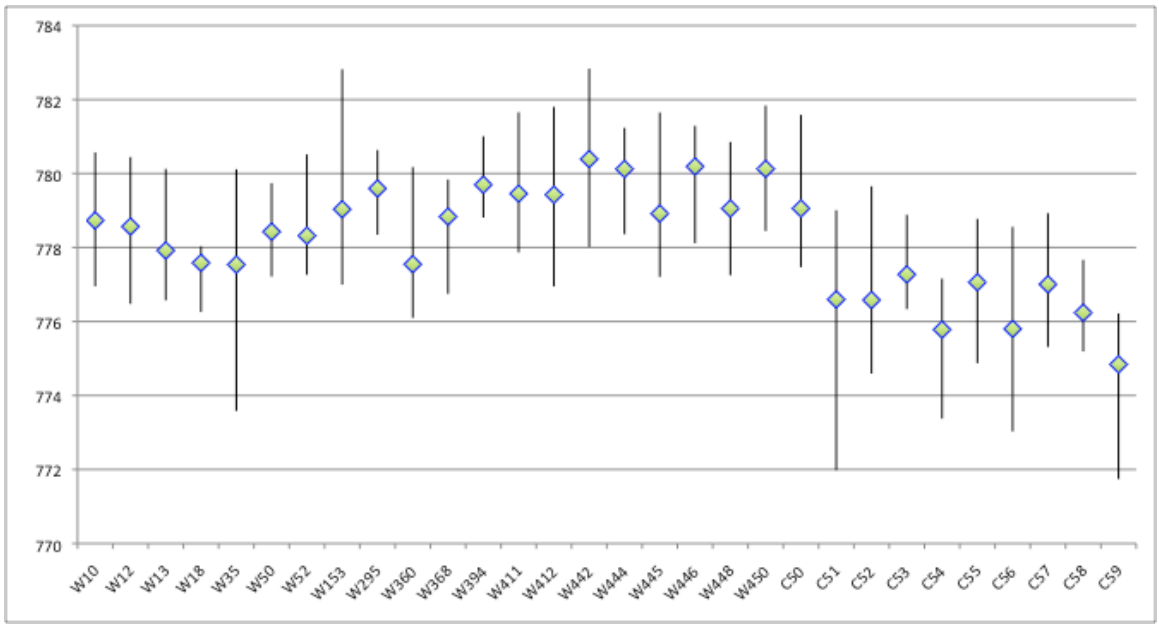


Figure 86: Graphic comparisons of the peak positions (center X, in wavenumbers) of Peak 5 from the deconvolution of the 30 glass spectra (10 replicates). The diamond data point shows the average peak position and the error bars show the range of peak position data for each glass sample.

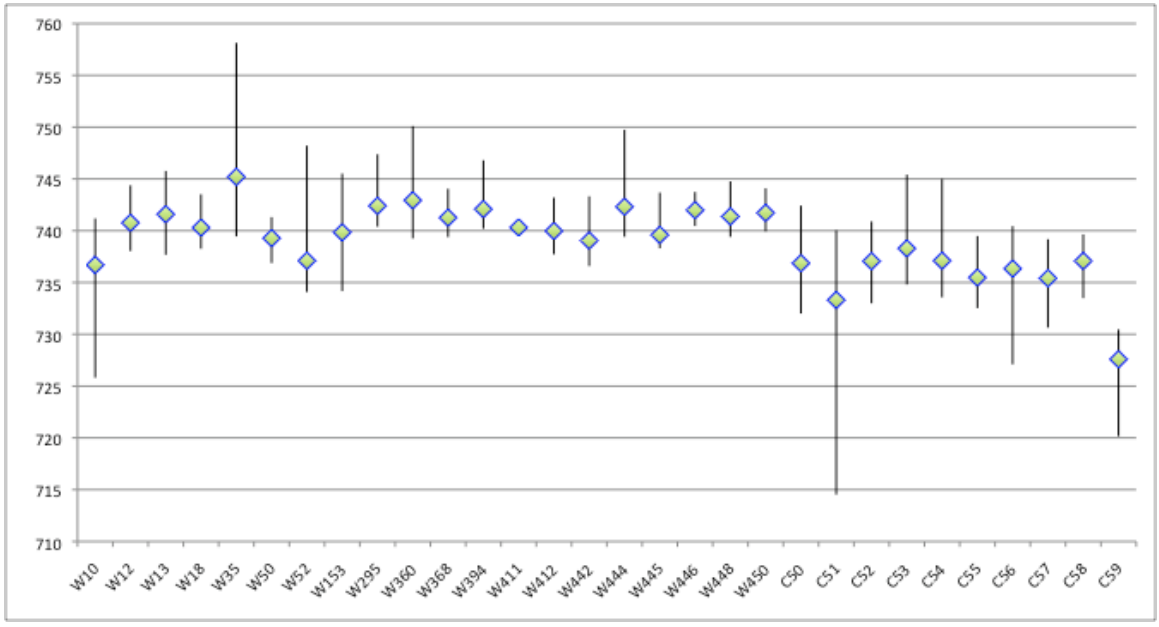


Figure 87: Graphic comparisons of the peak positions (center X, in wavenumbers) of Peak 6 from the deconvolution of the 30 glass spectra (10 replicates). The diamond data point shows the average peak position and the error bars show the range of peak position data for each glass sample.

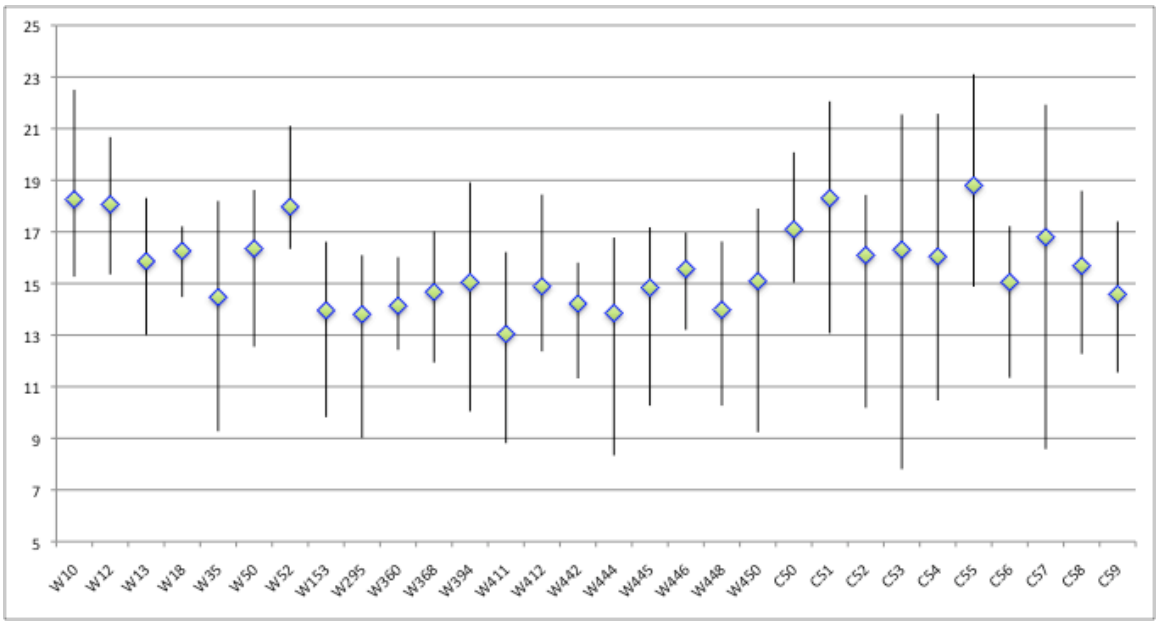


Figure 88: Graphic comparisons of the peak areas of Peak 1 from the deconvolution of the 30 glass spectra (10 replicates). The diamond data point shows the average peak area and the error bars show the range of peak area data for each glass sample.

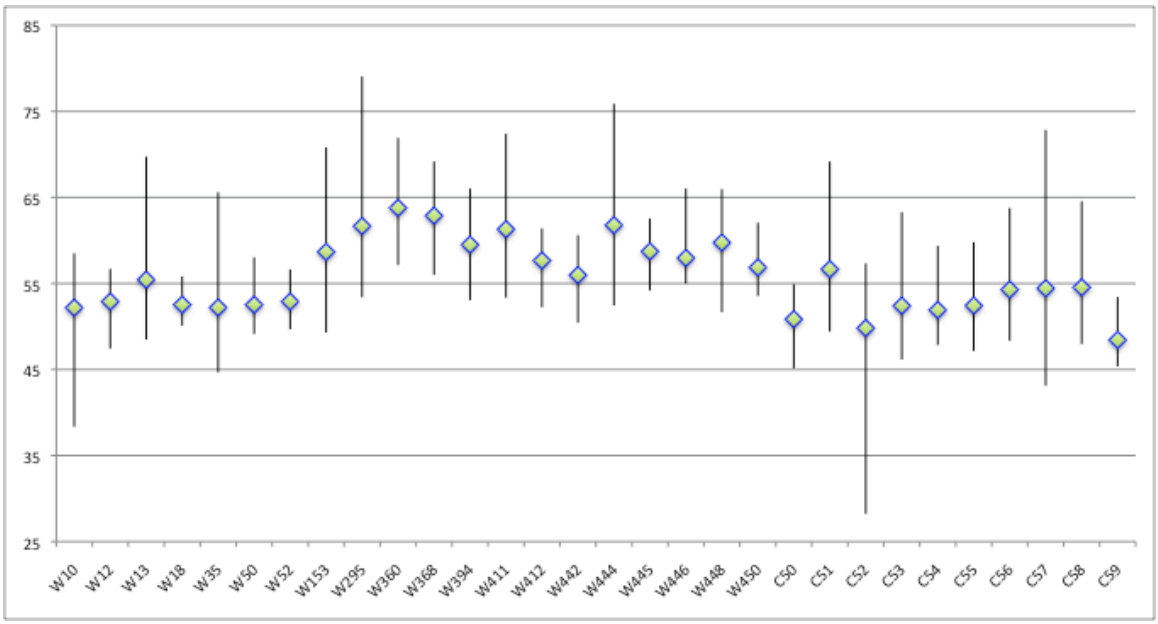


Figure 89: Graphic comparisons of the peak areas of Peak 2 from the deconvolution of the 30 glass spectra (10 replicates). The diamond data point shows the average peak area and the error bars show the range of peak area data for each glass sample.

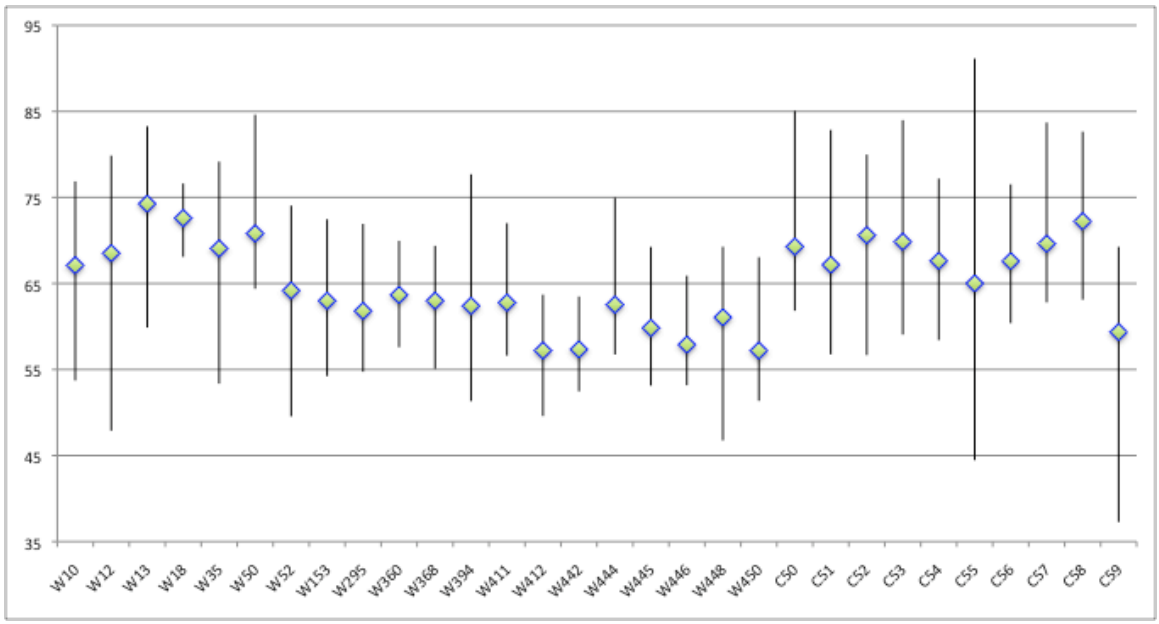


Figure 90: Graphic comparisons of the peak areas of Peak 3 from the deconvolution of the 30 glass spectra (10 replicates). The diamond data point shows the average peak area and the error bars show the range of peak area data for each glass sample.

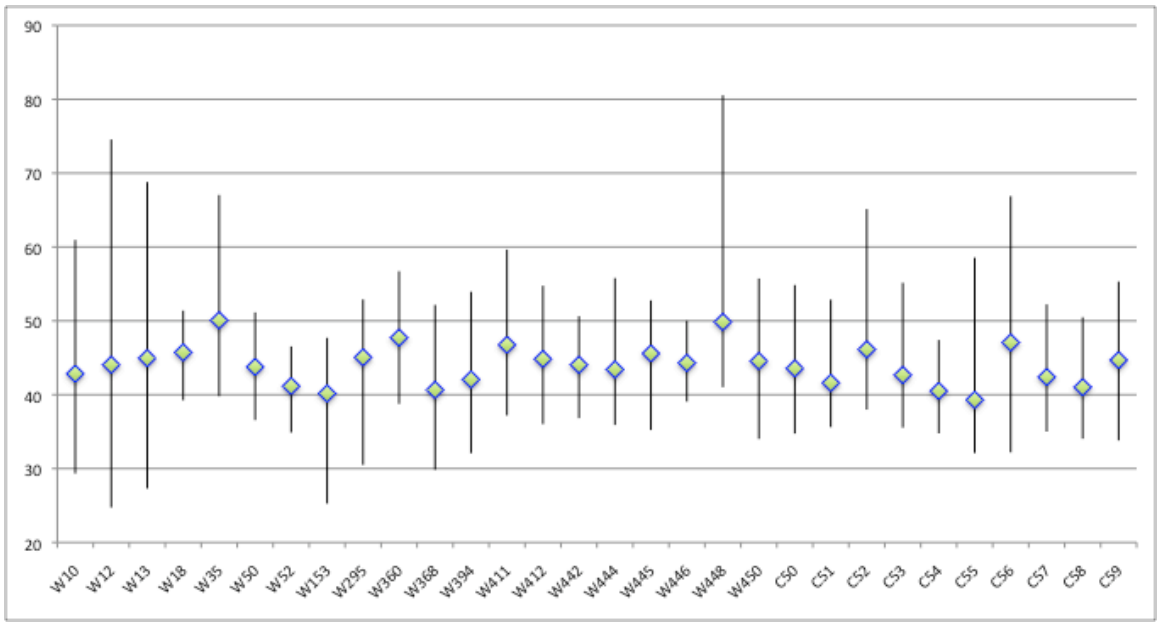


Figure 91: Graphic comparisons of the peak areas of Peak 4 from the deconvolution of the 30 glass spectra (10 replicates). The diamond data point shows the average peak area and the error bars show the range of peak area data for each glass sample.

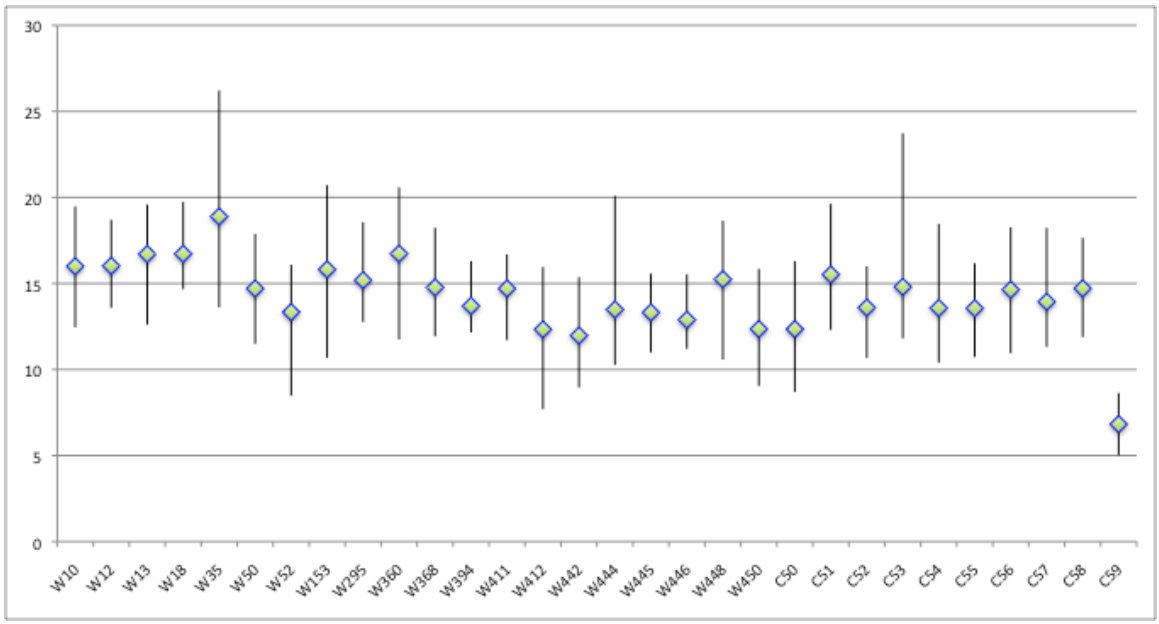


Figure 92: Graphic comparisons of the peak areas of Peak 5 from the deconvolution of the 30 glass spectra (10 replicates). The diamond data point shows the average peak area and the error bars show the range of peak area data for each glass sample.

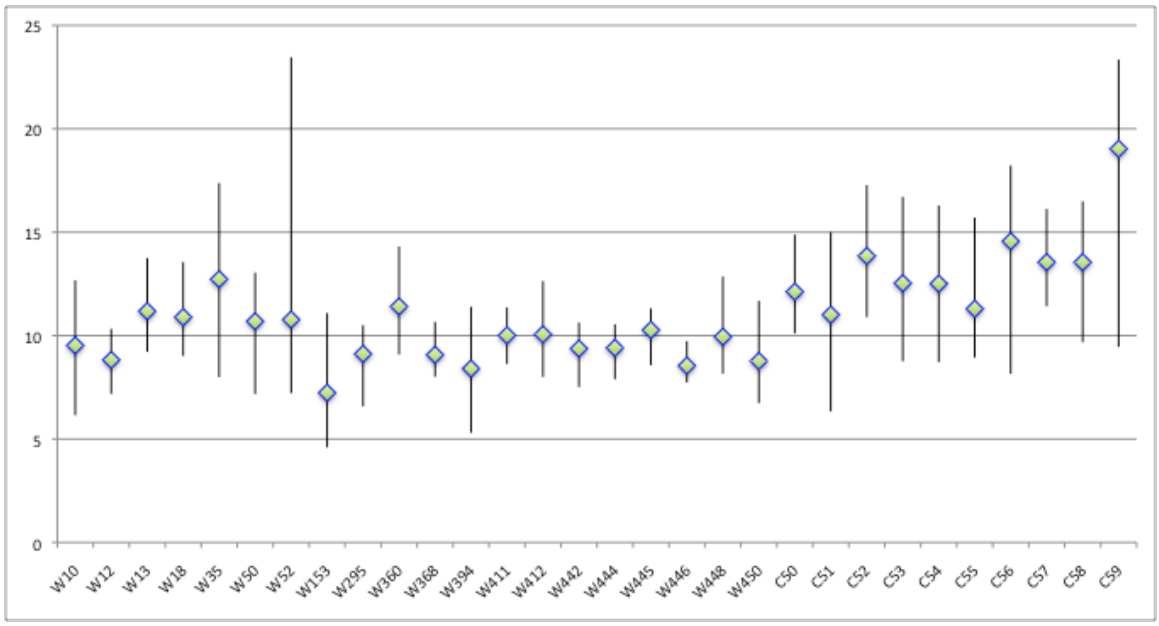


Figure 93: Graphic comparisons of the peak areas of Peak 6 from the deconvolution of the 30 glass spectra (10 replicates). The diamond data point shows the average peak area and the error bars show the range of peak area data for each glass sample.

Table 47: Results of the deconvolved peak position and area comparisons. For each glass sample (rows) where pairwise discrimination was successful, the specific peak position or area (column) has the identity(s) of the discriminated glass(es). The last three columns have the summary results for each glass sample which includes a list of all of the discriminated samples, the number of samples that could be discriminated (maximum of 29) and the percent of discriminated samples.

GLASS SAMPLE	W10	W12	W13	W18	W35
Peak 1 (location)	X	W295 W360 W368 W411 W444 W445 W446 W448 W450 C59	C59	W295 W360 W368 W411 W444 W446 W448 W450 C59	C59
Peak 2 (location)	X	X	X	W360 W368 W394 W412 W442 W444 W445 W446 W448 W450 C59.	X
Peak 3 (location)	X	X	X	X	X
Peak 4 (location)	X	X	X	X	X
Peak 5 (location)	C59	C59	C59	W295 W394 W446	X
Peak 6 location	X	C59	C59	C59	C57 C59
Peak 1 (area)	X	X	X	X	X
Peak 2 (area)	X	W360	X	W360 W368	X
Peak 3 (area)	X	X	X	W412 W442	X
Peak 4 (area)	X	X	X	X	X
Peak 5 (area)	C59	C59	C59	C59	C59
Peak 6 (area)	X	C52 C57	X	X	X
Discriminated Samples	C59	W295 W360 W368 W411 W444 W445 W446 W448 W450 C52 C59	C59	W295 W360 W368 W394 W411 W412 W442 W444 W445 W446 W448 W450 C59.	C57 C59
# of Samples Discriminated	1	11	1	13	2
% of Samples Discriminated	3.45	37.93	3.45	44.83	6.90

GLASS SAMPLE	W50	W52	W153	W295
Peak 1 (location)	W295 W360 W368 W411 W444 W446 W448 W450 C59	C50 C59	C50 C59	W12 W18 W50 C50 C52 C54 C59
Peak 2 (location)	X	W360 W368 W394 W412 W442 W444 W445 W446 W448 W450 C59.	X	X
Peak 3 (location)	X	X	X	X
Peak 4 (location)	X	X	X	X
Peak 5 (location)	C59	C54 C59	C59	W18 C54 C58 C59
Peak 6 location	C59	C59	C59	C51 C55 C57 C58 C59
Peak 1 (area)	X	W295 W360 W411	X	W52
Peak 2 (area)	X	W360	X	X
Peak 3 (area)	W412 W442	X	X	X
Peak 4 (area)	X	X	X	X
Peak 5 (area)	C59	X	C59	C59
Peak 6 (area)	X	X	C57	C52 C57
Discriminated Samples	W295 W360 W368 W411 W412 W442 W444 W446 W448 W450 C59	W295 W360 W368 W394 W411 W412 W442 W444 W445 W446 W448 W450 C50 C54 C59	C50 C57 C59	W12 W18 W50 W52 C50 C51 C52 C54 C55 C57 C58 C59
# of Samples Discriminated	11	15	3	12
% of Samples Discriminated	37.93	51.72	10.34	41.38

GLASS SAMPLE	W360	W368	W394	W411	W412
Peak 1 (location)	W12 W18 W50 W442 C50 C52 C54 C59	W12 W18 W50 C50 C52 C54 C59	X	W12 W18 W50 C50 C54 C59	C50 C59
Peak 2 (location)	W18 W52 C50 C52 C54	W18 W52 C50 C52 C54	W18 W52 C54	X	W18 W52 C52 C54
Peak 3 (location)	X	X	X	X	X
Peak 4 (location)	X	X	X	X	X
Peak 5 (location)	X	C59	W18 C54 C58 C59	C54 C58 C59	C59
Peak 6 location	C59	C57 C59	C51 C55 C57 C58 C59	C55 C57 C59	C59
Peak 1 (area)	W52	X	X	W52	X
Peak 2 (area)	W12 W18 W52 C50 C59	W18 C50 C59	X	X	X
Peak 3 (area)	X	X	X	X	W18 W50
Peak 4 (area)	X	X	X	X	X
Peak 5 (area)	C59	C59	C59	C59	X
Peak 6 (area)	X	C52 C57	X	X	X
Discriminated Samples	W12 W18 W50 W52 W442 C50 C52 C54 C59	W12 W18 W50 W52 C50 C52 C54 C57 C59	W18 W52 C51 C54 C55 C57 C58 C59	W12 W18 W50 W52 C50 C54 C55 C57 C58 C59	W18 W50 W52 C50 C52 C54 C59
# of Samples Discriminated	9	9	8	10	7
% of Samples Discriminated	31.03	31.03	27.59	34.48	24.14

GLASS SAMPLE	W442	W444	W445	W446	W448
Peak 1 (location)	W360 C50 C59	W12 W18 W50 C50 C52 C54 C59	W12 C50 C59	W12 W18 W50 C50 C59	W12 W18 W50 C50 C54 C59
Peak 2 (location)	W18 W52 C52 C54	W18 W52	W18 W52 C52 C54	W18 W52 C52 C54	W18 W52
Peak 3 (location)	X	X	X	X	X
Peak 4 (location)	C51	X	X	X	X
Peak 5 (location)	C54 C58 C59	C54 C58 C59	C59	W18 C54 C58 C59	C59
Peak 6 location	C59	C59	C59	C59	C59
Peak 1 (area)	X	X	X	X	X
Peak 2 (area)	X	X	C59	C50 C59	X
Peak 3 (area)	W18 W50	X	X	X	X
Peak 4 (area)	X	X	X	X	X
Peak 5 (area)	C59	C59	C59	C59	C59
Peak 6 (area)	C52 C57	C52 C57	C57	C50 C52 C57	X
Discriminated Samples	W18 W50 W52 W360 C50 C51 C52 C54 C57 C58 C59	W12 W18 W50 W52 C50 C52 C54 C57 C58 C59	W12 W18 C50 W52 C52 C54 C57 C59	W12 W18 W50 W52 C50 C52 C54 C57 C59	W12 W18 W50 W52 C50 C54 C59
# of Samples Discriminated	11	10	8	9	7
% of Samples Discriminated	37.93	34.48	27.59	31.03	24.14

GLASS SAMPLE	W450	C50	C51	C52	C53
Peak 1 (location)	W12 W18 W50 C50 C59	W52 W153 W295 W360 W368 W411 W412 W442 W444 W446 W448 W450	C59	W295 W360 W368 W444	X
Peak 2 (location)	W18 W52 C52 C54	W360 W368	X	W360 W368 W412 w442 W445 W446 W450	X
Peak 3 (location)	X	X	X	X	X
Peak 4 (location)	X	X	W442 C59	X	X
Peak 5 (location)	C54 C58 C59	C59	X	X	X
Peak 6 location	C59	C59	W295 W394	C59	C59
Peak 1 (area)	X	X	X	X	X
Peak 2 (area)	X	W360 W368 W445	X	X	X
Peak 3 (area)	X	X	X	X	X
Peak 4 (area)	X	X	X	X	X
Peak 5 (area)	C59	C59	C59	C59	C59
Peak 6 (area)	X	W446	X	W12 W295 W368 W442 W444 W446	X
Discriminated Samples	W12 W18 W50 W52 C50 C52 C54 C58 C59	W52 W153 W295 W360 W368 W411 W412 W442 W444 W445 W446 W448 W450 C59	W295 W394 W442 C59	W12 W295 W360 W368 W412 W442 W444 W445 W446 W450 C59	C59
# of Samples Discriminated	9	14	4	11	1
% of Samples Discriminated	31.03	48.28	13.79	37.93	3.45

GLASS SAMPLE	C54	C55	C56	C57
Peak 1 (location)	W295 W360 W368 W411 W444 W448	C59	C59	X
Peak 2 (location)	W360 W368 W394 W412 W442 W445 W446 W450	X	X	X
Peak 3 (location)	X	X	X	X
Peak 4 (location)	X	X	X	X
Peak 5 (location)	W52 W295 W394 W411 W442 W444 W446 W450 C50	X	X	X
Peak 6 location	C59	W295 W394 W411	X	W35 W295 W368 W394 W411
Peak 1 (area)	X	X	X	X
Peak 2 (area)	X	X	X	X
Peak 3 (area)	X	X	X	X
Peak 4 (area)	X	X	X	X
Peak 5 (area)	C59	C59	C59	C59
Peak 6 (area)	X	X	X	W12 W153 W295 W368 W442 W444 W445 W446
Discriminated Samples	W52 W295 W360 W368 W394 W411 W412 W442 W444 W445 W446 W448 W450 C50 C59	W295 W394 W411 C59	C59	W12 W35 W153 W295 W368 W394 W411 W442 W444 W445 W446 C59
# of Samples Discriminated	15	4	1	12
% of Samples Discriminated	51.72	13.79	3.45	41.38

GLASS SAMPLE	C58	C59
Peak 1 (location)	C59	W12 W13 W18 W35 W50 W52 W153 W295 W360 W368 W411 W412 W442 W444 W445 W446 W448 W450 C50 C51 C52 C54 C55 C56 C58
Peak 2 (location)	X	W18 W52
Peak 3 (location)	X	X
Peak 4 (location)	X	C51
Peak 5 (location)	W295 W394 W411 W442 W444 W446 W450	W10 W12 W13 W50 W52 W153 W295 W368 W394 W411 W412 W442 W444 W445 W446 W448 W450 C50 C53
Peak 6 location	W295 W394	W12 W13 W18 W35 W50 W52 W153 W295 W360 W368 W394 W411 W412 W442 W444 W445 W446 W448 W450 C50 C52 C53 C54 C55 C57 C58
Peak 1 (area)	X	X
Peak 2 (area)	X	W360 W368 W445 W446
Peak 3 (area)	X	X
Peak 4 (area)	X	X
Peak 5 (area)	C59	W10 W12 W13 W18 W35 W50 W153 W295 W360 W368 W394 W411 W442 W444 W445 W446 W448 W450 C50 C51 C52 C53 C54 C55 C56 C57 C58
Peak 6 (area)	X	X
Discriminated Samples	W295 W394 W411 W442 W444 W446 W450 C59	W10 W12 W13 W18 W35 W50 W52 W153 W295 W360 W368 W394 W411 W412 W442 W444 W445 W446 W448 W450 C50 C51 C52 C53 C54 C55 C56 C57 C58
# of Samples Discriminated	8	29
% of Samples Discriminated	27.59	100.00

Table 47 contains the results of the pair wise comparisons of the deconvolved peak position and area data of the first set of 30 glasses. Glass sample C59 was the only glass that was discriminated from all of the other glasses (100% discrimination), using the positions from peaks

1, 5 and 6 and areas from peaks 2 and 5. Glasses W10, W13, C53, and C56 could only be discriminated from C59 (3.45% discrimination), but no other glasses, using the position and/or area of peak 5. Glass W13 could also be discriminated from C59 using the position from peaks 1 and 6, and Glass C56 could also be discriminated from C59 using peak 1's position. W12 was discriminated from glasses W295, W360, W368, W411, W444, W445, W446, W448, W450, C52, and C59 (37.93% discrimination) using the peak 1 position and peak 6 area, although there was some repeated discrimination using the positions from peaks 5 and 6, and areas from peaks 2 and 5. Glass W18 was discriminated from glasses W295, W360, W368, W394, W411, W412, W442, W444, W445, W446, W448, W450, and C59 (44.83% discrimination) using the positions of peaks 1 and 2, although there was some repeated discrimination using the positions from peaks 5 and 6, and areas from peaks 2, 3 and 5. Glass W35 was discriminated from C57 and C59 (6.9% discrimination) using peak 6's position. Glass W50 was discriminated from glasses W295, W360, W368, W411, W412, W442, W444, W446, W448, W450, C59 (37.93% discrimination) using the position of peak 1 and area from peak 3, with was some repeated discrimination using the peak 5 area and positions from peak 5 and 6. Glass W52 was discriminated from 51.72% of the glasses (W295, W360, W368, W394, W411, W412, W442, W444, W445, W446, W448, W450, C50, C54, and C59) using the positions from peak 1, 2, and 5, and peak 1 area, although there was some repeated discrimination using peak 6's position and peak 2's area. Glass W153 was discriminated from C50, C57, and C59 (10.34% discrimination) using peak 1's position and peak 6's area, with repeated discrimination using positions from peaks 5 and 6, and areas from peak 5. Glass W295 was discriminated from glasses W12, W18, W50, W52, C50, C51, C52, C54, C55, C57, C58, and C59 (41.38% discrimination) using the positions of peaks 1, 5 and 6 with was some repeated discrimination using the areas from peaks

1, 5 and 6. Glass W360 was discriminated from glasses W12, W18, W50, W52, W442, C50, C52, C54, and C59 (31.03% discrimination) using the positions of peaks 1 and 2, with some repeated discrimination using peak 6's positions and the areas from peaks 1, 2, and 5. Glass W368 was discriminated from 31.03% of the glasses (W12, W18, W50, W52, C50, C52, C54, C57, and C59) using peak 6's area and the positions from peak 1, 2 and 6 with some repeated discrimination using the peak 5's location and the areas from peaks 2 and 5. Glass W394 was discriminated from 27.59% of the glasses (W18, W52, C51, C54, C55, C57, C58, and C59) using the positions from peaks 2, 5 and 6 with some repeated discrimination using peak 5's area. Glass W411 was discriminated from glasses W12, W18, W50, W52, C50, C54, C55, C57, C58, and C59 (34.48% discrimination) using peak 1's area and the positions of peaks 1, 5 and 6, with some repeated discrimination using peak 5's area. Glass W412 was discriminated from 24.14% of the glasses (W18, W50, W52, C50, C52, C54, C59) using the positions from peaks 1 and 2 with some repeated discrimination using peak 3's area and the position from peaks 5 and 6. Glass W442 was discriminated from glasses W18, W50, W52, W360, C50, C51, C52, C54, C57, C58, and C59 (37.93% discrimination) using the areas from peaks 3 and 6 and the positions of peaks 1, 2, 4 and 5, with some repeated discrimination using peak 6's position and peak 5's area. Glass W444 was discriminated from 34.48% of the glasses (W12, W18, W50, W52, C50, C52, C54, C57, C58, and C59) using peak 6's area and the positions from peaks 1, 2 and 5 with some repeated discrimination using peak 6's position and peak 5's area. Glass W445 was discriminated from glasses W12, W18, W52, C50, C52, C54, C57, and C59 (27.59% discrimination) using peak 6's area and the positions of peaks 1 and 2, with some repeated discrimination using the positions of peaks 5 and 6, and areas of peaks 2 and 5. Glass W446 was discriminated from glasses W12, W18, W50, W52, C50, C52, C54, C57, C58, and C59 (34.48%

discrimination) using peak 6's area and the positions of peaks 1, 2 and 5, with some repeated discrimination using peak 6's position and the areas of peaks 2 and 5. Glass W448 was discriminated from 24.14% of the glasses (W12, W18, W50, C50, C54, and C59) using the positions from peaks 1 and 2 with some repeated discrimination using the positions from peaks 5 and 6, and peak 5's area. Glass W450 was discriminated from 31.03% of the glasses (W12, W18, W50, W52, C50, C52, C54, C58, and C59) using the positions from peaks 1, 2 and 5 with some repeated discrimination using the peak 6's position and peak 5's area. Glass C50 was discriminated from glasses W52, W153, W295, W360, W368, W411, W412, W442, W444, W445, W446, W448, W450, and C59 (48.28% discrimination) using peak 2's area and the positions of peaks 1 and 2 with was some repeated discrimination using the locations and areas from peaks 5 and 6. Glass C51 was discriminated from 13.79% of the glasses (W 295, W394, W442, and C59) using the positions from peaks 4 and 6 with some repeated discrimination using peak 1's position and peak 5's area. Glass C52 was discriminated from glasses W12, W295, W360, W368, W412, W442, W444, W445, W446, W450, and C59 (37.93% discrimination) using peak 6's area and the positions of peaks 1 and 2, with some repeated discrimination using peak 6's position and peak 5's area. Glass C54 was discriminated from 51.72% of the glasses (W52, W295, W360, W368, W394, W411, W412, W442, W444, W445, W446, W448, W450, C50, and C59) using the positions from peak 1, 2, and 5, although there was some repeated discrimination using peak 6's position and peak 5's area. Glass C55 was discriminated from glasses W295, W394, W411, and C59 (13.79% discrimination) using peak 6's position and either peak 1's position or peak 5's area. Glass C57 was discriminated from 41.38% of the glasses (W12, W35, W153, W295, W368, W394, W411, W442, W444, W445, W446, and C59) using peak 6's position and area, although there was some repeated discrimination using peak 5's

area. Glass C58 was discriminated from glasses W295, W394, W411, W442, W444, W446, W450, and C59 (27.59% discrimination) using the positions from peaks 5 and 6 and either peak 1's position or peak 5's area.

Ten of the 12 peak areas and positions were capable of discriminating at least one pair of the glasses, with only peak 3's position and peak 4's area providing no discriminating ability. The lack of discrimination provided by peak 4's area is consistent with the ANOVA results in Chapter 4B.

The total number of discriminated pairs of glasses using the deconvolved peak position and area ranges was 133 out of a possible 435, thus having an overall 30.57% discrimination ability.

4.C.c. Chemometric Analysis

The results of the PCA analyses of the first set of 30 glasses are in Appendix X. Seven spectral preprocessing methods were explored: 1) the unprocessed spectra, 2) peak area normalization, 3) peak height normalization, 4) first derivative spectra with 5-point smoothing, 5) first derivative spectra with 9-point smoothing, 6) second derivative spectra with 5-point smoothing, and 7) second derivative spectra with 9-point smoothing. For each of the 7 preprocesses, the data was grouped into 3 different sets: 1) all glasses, 2) window glass, and 3) container glasses. Last, prior to making the PCA models, 3 additional data pretreatments were attempted: 1) none, 2) centering, and 3) autoscaling. Thus, a total of 63 PCA models were made. The PCA results include the percentage of variance in each of the calculated PCs, and this

information was then used to help determine the number of PCs to keep for the PCA-CVA discrimination and classification models.

The results of the HOO-CV of the PCA-CVA models are in Appendix XI. The results, in tables and graphs, show the HOO-CV error rates for each of the models when keeping different numbers of PC dimensions. In total, 147 different PCA-CVA chemometric models were made and error rates were calculated using HOO-CV, which were made from the different combinations of the 7 spectral preprocessing methods, the 7 different classification or discrimination groups, and the 3 data pretreatment schemes. These results are compared to the error rates for HOO-CV PLS-DA, in Tables 48 – 96. Tables 48 - 96 contain the HOO-CV error rates for the PCA-CVA and PLS-DA models made from the different combinations of the 7 spectral preprocessing methods and the 7 different classification or discrimination groups. Table 97 is a summary table that contains the lowest HOO-CV error rates for each of the chemometric models made with PCA-CVA and PLS-DA.

The R statistical program had two types of programming errors for the HOO-CV error rate calculations: one for PCA-CVA and the other for PLS-DA. The HOO-CV PCA-CVA programming error, which stated "Error in lda.default(x, grouping, ...) : variables … appear to be constant within groups", indicated that there was no measurable variance with additional PCs (i.e. variables). Thus the R program was not able to compute a PCA-CVA model with that number of PCs. The HOO-CV PLS-DA programming error, which stated that the R program "can't allocate region" and "cannot allocate vector of size", indicated that linear combination of variables (or vector) that made up the last PLS dimension was too small and thus the algorithm was not able to compute a PLS model with that number of dimensions. Consequently, no HOO-CV error rate was calculated when either of those programming errors occurred.

Table 48: Discrimination error rates for HOO-CV PCA-CVA (no pretreatment, centered and autoscaled) and HOO-CV PLS-DA models with varying number of PCs or PLS dimensions for the first set of 30 glass spectra (10 replicates). The smallest PC and PLS dimension with the minimum error rate is highlighted in yellow. The error rates associated with PC dimension containing at least 95, 99, and 99.9% of the variance are highlighted in blue, purple and red, respectively. Error* is an "Error in lda.default(x, grouping, ...) : variables 134 135 136… appear to be constant within groups".

Number of PCs for PCA & Dimensions for PLS-DA	Error Rate (%) for HOO-CV with PCA reduced CVA (no pretreatment)	Error Rate (%) for HOO-CV with PCA reduced CVA (centered)	Error Rate (%) for HOO-CV with PCA reduced CVA (autoscaled)	Error Rate (%) with HOO-CV with PLS-DA
3	90	90.67	92	92
4	89.67	89.33	84.67	89.67
5	72.33	70	70.67	88.67
6	62.67	61	57.67	85.67
7	61.67	61	51.67	83.65
8	55	56.67	48	80.67
10	46.33	46	44.33	74
30	15.67	16	13	44
50	15	14.67	11.67	42.67
75	14	14.67	11.67	41.67
80	12.67	13	10.33	36
90	12.67	12.33	10.33	33.33
100	11.33	11.33	9.67	37.67
133	11.67	12.33	8.67	32.33
136	Error*	Error*	7.33	33
150	Error*	Error*	8	32.67
200	Error*	Error*	13.33	39

Table 49: Classification (automotive, architectural, or container) error rates for HOO-CV PCA-CVA (no pretreatment, centered and autoscaled) and HOO-CV PLS-DA models with varying number of PCs or PLS dimensions for the first set of 30 glass spectra (10 replicates). The smallest PC and PLS dimension with the minimum error rate is highlighted in yellow. The error rates associated with PC dimension containing at least 95, 99, and 99.9% of the variance are highlighted in blue, purple and red, respectively. Error* is an "Error in lda.default(x, grouping, ...) : variables 136 137 138… appear to be constant within groups". Error** is an "Error in lda.default(x, grouping, ...) : variables 135 136 137… appear to be constant within groups".

Number of PCs for PCA & Dimensions for PLS-DA	Error Rate (%) for HOO-CV with PCA reduced CVA (no pretreatment)	Error Rate (%) for HOO-CV with PCA reduced CVA (centered)	Error Rate (%) for HOO-CV with PCA reduced CVA (autoscaled)	Error Rate (%) with HOO-CV with PLS-DA
3	66	65.33	67.33	35.67
4	65	66.33	61.33	36.33
5	31.67	30.67	29.67	31
6	33	33.33	26.67	29.33
7	28.67	29	26.33	31.67
8	29.33	28.67	21.67	30.67
10	23.67	23.33	21.33	27.33
30	16	17.67	15.67	23.33
42	17	16.67	14	22.33
50	18.33	19	16.33	23.67
75	19	17.67	18	24
80	18	18.67	18.33	23.67
90	20	20	19.67	23.33
100	20	20	21	25.33
134	19.67	20.33	20.33	36
150	Error*	Error**	19	37.67
200	Error*	Error**	21	46.67

Table 50: Classification (window or container) error rates for HOO-CV PCA-CVA (no pretreatment, centered and autoscaled) and HOO-CV PLS-DA models with varying number of PCs or PLS dimensions for the first set of 30 glass spectra (10 replicates). The smallest PC and PLS dimension with the minimum error rate is highlighted in yellow. The error rates associated with PC dimension containing at least 95, 99, and 99.9% of the variance are highlighted in blue, purple and red, respectively. Error* is an "Error in lda.default(x, grouping, ...) : variables 137 138 139… appear to be constant within groups". Error** is an "Error in lda.default(x, grouping, ...) : variables 135 136 137… appear to be constant within groups".

Number of PCs for PCA & Dimensions for PLS-DA	Error Rate (%) for HOO-CV with PCA reduced CVA (no pretreatment)	Error Rate (%) for HOO-CV with PCA reduced CVA (centered)	Error Rate (%) for HOO-CV with PCA reduced CVA (autoscaled)	Error Rate (%) with HOO-CV with PLS-DA
3	33.33	33.33	33.67	5.33
4	33.33	33.67	32.67	5.67
5	6.33	6	6.67	4.33
6	7.33	7	6.67	4
7	6.33	6.67	5.67	4
8	5.33	4.67	4	3.67
10	3.67	3.67	4	4
30	3.33	4	3.33	6.33
50	4	4.33	4	5.33
75	4.33	4.33	4.33	6
100	4.67	4.67	4.33	6.67
104	4.33	4.33	2.67	7.67
134	6.33	6.33	3.33	14.67
150	Error*	Error**	3	13.33
200	Error*	Error**	5.67	28

Table 51: Discrimination error rates for HOO-CV PCA-CVA (no pretreatment, centered and autoscaled) and HOO-CV PLS-DA models with varying number of PCs or PLS dimensions for the first set of 20 window glass spectra (10 replicates). The smallest PC and PLS dimension with the minimum error rate is highlighted in yellow. The error rates associated with PC dimension containing at least 95, 99, and 99.9% of the variance are highlighted in blue, purple and red, respectively. Error* is an "Error in lda.default(x, grouping, ...) : variables 124 125 126… appear to be constant within groups".

Number of PCs for PCA & Dimensions for PLS-DA	Error Rate (%) for HOO-CV with PCA reduced CVA (no pretreatment)	Error Rate (%) for HOO-CV with PCA reduced CVA (centered)	Error Rate (%) for HOO-CV with PCA reduced CVA (autoscaled)	Error Rate (%) with HOO-CV with PLS-DA
3	92.5	94	90.5	93.5
4	89	88.5	85.5	93
5	82	80.5	74.5	86.5
8	57.5	63	50	71.5
10	45.5	46.5	46.5	64
30	15	15.5	8	39
50	15.5	14.5	11.5	40.5
75	12	11.5	11.5	36.5
100	15.5	15	10.5	41.5
150	Error*	Error*	21.5	43.5

Table 52: Discrimination error rates for HOO-CV PCA-CVA (no pretreatment, centered and autoscaled) and HOO-CV PLS-DA models with varying number of PCs or PLS dimensions for the first set of 10 container glass spectra (10 replicates). The smallest PC and PLS dimension with the minimum error rate is highlighted in yellow. The error rates associated with PC dimension containing at least 95, 99, and 99.9% of the variance are highlighted in blue, purple and red, respectively.

Number of PCs for PCA & Dimensions for PLS-DA	Error Rate (%) for HOO-CV with PCA reduced CVA (no pretreatment)	Error Rate (%) for HOO-CV with PCA reduced CVA (centered)	Error Rate (%) for HOO-CV with PCA reduced CVA (autoscaled)	Error Rate (%) with HOO-CV with PLS-DA
3	72	69	74	76
5	62	63	62	69
9	43	48	45	55
10	46	44	37	58
30	13	13	8	20
32	13	13	6	19
50	13	9	10	24
75	20	16	16	25

Table 53: Float classification error rates for HOO-CV PCA-CVA (no pretreatment, centered and autoscaled) and HOO-CV PLS-DA models with varying number of PCs or PLS dimensions for the first set of 20 window glass spectra (10 replicates). The smallest PC and PLS dimension with the minimum error rate is highlighted in yellow. The error rates associated with PC dimension containing at least 95, 99, and 99.9% of the variance are highlighted in blue, purple and red, respectively. Error* is an "Error in lda.default(x, grouping, ...) : variables 125 126 127… appear to be constant within groups"

Number of PCs for PCA & Dimensions for PLS-DA	Error Rate (%) for HOO-CV with PCA reduced CVA (no pretreatment)	Error Rate (%) for HOO-CV with PCA reduced CVA (centered)	Error Rate (%) for HOO-CV with PCA reduced CVA (autoscaled)	Error Rate (%) with HOO-CV with PLS-DA
3	37	35.5	39	30
4	33	33	21.5	32
5	32.5	33	21	23.5
8	28.5	28	21.5	20
10	21	21	20	21.5
27	19.5	18	18	25
30	21.5	20.5	20.5	26.5
50	22.5	23	23.5	31.5
75	20.5	20.5	19	34
100	25.5	25.5	25	34
150	Error*	Error*	29	34.5

Table 54: Tempered classification error rates for HOO-CV PCA-CVA (no pretreatment, centered and autoscaled) and HOO-CV PLS-DA models with varying number of PCs or PLS dimensions for the first set of 20 window glass spectra (10 replicates). The smallest PC and PLS dimension with the minimum error rate is highlighted in yellow. The error rates associated with PC dimension containing at least 95, 99, and 99.9% of the variance are highlighted in blue, purple and red, respectively. Error* is an "Error in lda.default(x, grouping, ...) : variables 125 126 127… appear to be constant within groups".

Number of PCs for PCA & Dimensions for PLS-DA	Error Rate (%) for HOO-CV with PCA reduced CVA (no pretreatment)	Error Rate (%) for HOO-CV with PCA reduced CVA (centered)	Error Rate (%) for HOO-CV with PCA reduced CVA (autoscaled)	Error Rate (%) with HOO-CV with PLS-DA
3	31.5	33	32.5	30
4	30.5	30.5	32.5	26
5	32	32.5	31	27
8	29	31.5	29.5	28.5
10	27	27	28.5	25.5
30	18	19.5	15.5	22.5
50	18	16	16.5	21
75	18.5	18.5	21	20.5
100	21.5	21.5	16	19
138	Error*	Error*	11	19
150	Error*	Error*	13	19

Table 55: Discrimination error rates for HOO-CV PCA-CVA (no pretreatment, centered and autoscaled) and HOO-CV PLS-DA models with varying number of PCs or PLS dimensions for the first set of 30 normalized (peak area) glass spectra (10 replicates). The smallest PC and PLS dimension with the minimum error rate is highlighted in yellow. The error rates associated with PC dimension containing at least 90, 95, 99, and 99.9% of the variance are highlighted in green, blue, purple and red, respectively. Error* is an "Error in lda.default(x, grouping, ...) : variables 11 12 13… appear to be constant within groups". Error** is an "Error in lda.default(x, grouping, ...) : variables 10 11 12… appear to be constant within groups".

Number of PCs for PCA & Dimensions for PLS-DA	Error Rate (%) for HOO-CV with PCA reduced CVA (no pretreatment)	Error Rate (%) for HOO-CV with PCA reduced CVA (centered)	Error Rate (%) for HOO-CV with PCA reduced CVA (autoscaled)	Error Rate (%) with HOO-CV with PLS-DA
3	93.33	89	87.67	92
4	88.33	68.33	77.33	90
6	61.33	63.33	53	83
7	58.67	58.33	50	82
10	49.33	Error**	44.67	76.33
11	Error*	Error**	35.67	76
30	Error*	Error**	13.67	47.33
50	Error*	Error**	13.67	44
75	Error*	Error**	14	40.67
100	Error*	Error**	9.67	37.33
133	Error*	Error**	6.67	31
150	Error*	Error**	8.67	34
200	Error*	Error**	12	39.67

Table 56: Classification (automotive, architectural, or container) error rates for HOO-CV PCA-CVA (no pretreatment, centered and autoscaled) and HOO-CV PLS-DA models with varying number of PCs or PLS dimensions for the first set of 30 normalized (peak area) glass spectra (10 replicates). The smallest PC and PLS dimension with the minimum error rate is highlighted in yellow. The error rates associated with PC dimension containing at least 90, 95, 99, and 99.9% of the variance are highlighted in green, blue, purple and red, respectively. Error* is an "Error in lda.default(x, grouping, ...) : variables 11 12 13… appear to be constant within groups". Error** is an "Error in lda.default(x, grouping, ...) : variables 10 11 12 … appear to be constant within groups".

Number of PCs for PCA & Dimensions for PLS-DA	Error Rate (%) for HOO-CV with PCA reduced CVA (no pretreatment)	Error Rate (%) for HOO-CV with PCA reduced CVA (centered)	Error Rate (%) for HOO-CV with PCA reduced CVA (autoscaled)	Error Rate (%) with HOO-CV with PLS-DA
3	68	61.33	63	35.67
4	64.33	30.33	34.33	33
6	29.67	29.33	27.33	30.33
7	28	29.33	26.33	28
10	26.67	Error**	27	27.33
11	Error*	Error**	25.67	24
20	Error*	Error**	15	18
30	Error*	Error**	16	25
50	Error*	Error**	18	25
75	Error*	Error**	18.33	22.33
100	Error*	Error**	19.67	27.67
150	Error*	Error**	16.33	35.67
200	Error*	Error**	20.67	44.33

Table 57: Classification (window or container) error rates for HOO-CV PCA-CVA (no pretreatment, centered and autoscaled) and HOO-CV PLS-DA models with varying number of PCs or PLS dimensions for the first set of 30 normalized (peak area) glass spectra (10 replicates). The smallest PC and PLS dimension with the minimum error rate is highlighted in yellow. The error rates associated with PC dimension containing at least 90, 95, 99, and 99.9% of the variance are highlighted in green, blue, purple and red, respectively. Error* is an "Error in lda.default(x, grouping, ...): variables 11 12 13… appear to be constant within groups". Error** is an "Error in lda.default(x, grouping, ...): variables 10 11 12… appear to be constant within groups".

Number of PCs for PCA & Dimensions for PLS-DA	Error Rate (%) for HOO-CV with PCA reduced CVA (no pretreatment)	Error Rate (%) for HOO-CV with PCA reduced CVA (centered)	Error Rate (%) for HOO-CV with PCA reduced CVA (autoscaled)	Error Rate (%) with HOO-CV with PLS-DA
3	Error***	33.33	31	6.67
4	Error***	6	9.33	4.33
5	6.67	7	7.67	4
6	7	5.67	7.33	3.67
7	6.33	5.33	3.67	3.67
8	4.33	5.33	3.67	4
9	4	4	3.67	4
10	4	Error**	4.33	4
11	Error*	Error**	4	4
29	Error*	Error**	3	5.67
30	Error*	Error**	3.33	6
50	Error*	Error**	4	4
75	Error*	Error**	4.33	5
100	Error*	Error**	5	6.33
150	Error*	Error**	3.33	13
200	Error*	Error**	6.67	24.67

Table 58: Discrimination error rates for HOO-CV PCA-CVA (no pretreatment, centered and autoscaled) and HOO-CV PLS-DA models with varying number of PCs or PLS dimensions for the first set of 20 normalized (peak area) window glass spectra (10 replicates). The smallest PC and PLS dimension with the minimum error rate is highlighted in yellow. The error rates associated with PC dimension containing at least 95, 99, and 99.9% of the variance are highlighted in blue, purple and red, respectively. Error* is an "Error in lda.default(x, grouping, ...) : variables 10 11 12… appear to be constant within groups". Error** is an "Error in lda.default(x, grouping, ...) : variables 9 10 11… appear to be constant within groups".

Number of PCs for PCA & Dimensions for PLS-DA	Error Rate (%) for HOO-CV with PCA reduced CVA (no pretreatment)	Error Rate (%) for HOO-CV with PCA reduced CVA (centered)	Error Rate (%) for HOO-CV with PCA reduced CVA (autoscaled)	Error Rate (%) with HOO-CV with PLS-DA
3	92	90	90.5	93
6	78.5	79.5	54	77
10	Error*	Error**	49.5	69.5
11	Error*	Error**	48	68
30	Error*	Error**	15.5	40
50	Error*	Error**	16.5	38.5
75	Error*	Error**	13	36
77	Error*	Error**	12	36
100	Error*	Error**	13.5	40
150	Error*	Error**	20	45.5

Table 59: Discrimination error rates for HOO-CV PCA-CVA (no pretreatment, centered and autoscaled) and HOO-CV PLS-DA models with varying number of PCs or PLS dimensions for the first set of 10 normalized (peak area) container glass spectra (10 replicates). The smallest PC and PLS dimension with the minimum error rate is highlighted in yellow. The error rates associated with PC dimension containing at least 95, 99, and 99.9% of the variance are highlighted in blue, purple and red, respectively. Error* is an "Error in lda.default(x, grouping, ...) : variables 11 12 13… appear to be constant within groups". Error** is an "Error in lda.default(x, grouping, ...) : variables 10 11 12… appear to be constant within groups".

Number of PCs for PCA & Dimensions for PLS-DA	Error Rate (%) for HOO-CV with PCA reduced CVA (no pretreatment)	Error Rate (%) for HOO-CV with PCA reduced CVA (centered)	Error Rate (%) for HOO-CV with PCA reduced CVA (autoscaled)	Error Rate (%) with HOO-CV with PLS-DA
3	73	69	65	79
5	64	55	55	68
6	50	52	49	63
10	46	Error**	38	58
26	Error*	Error**	10	21
30	Error*	Error**	10	21
50	Error*	Error**	12	24
75	Error*	Error**	17	24

Table 60: Float classification error rates for HOO-CV PCA-CVA (no pretreatment, centered and autoscaled) and HOO-CV PLS-DA models with varying number of PCs or PLS dimensions for the first set of 20 normalized (peak area) window glass spectra (10 replicates). The smallest PC and PLS dimension with the minimum error rate is highlighted in yellow. The error rates associated with PC dimension containing at least 90, 95, 99, and 99.9% of the variance are highlighted in green, blue, purple and red, respectively. Error* is an "Error in lda.default(x, grouping, ...) : variables 11 12 13… appear to be constant within groups". Error** is an "Error in lda.default(x, grouping, ...) : variables 10 11 12… appear to be constant within groups".

Number of PCs for PCA & Dimensions for PLS-DA	Error Rate (%) for HOO-CV with PCA reduced CVA (no pretreatment)	Error Rate (%) for HOO-CV with PCA reduced CVA (centered)	Error Rate (%) for HOO-CV with PCA reduced CVA (autoscaled)	Error Rate (%) with HOO-CV with PLS-DA
3	38.5	33	34	33
6	33	31.5	32	22
10	22.5	Error**	22.5	19.5
11	Error*	Error**	22.5	20.5
30	Error*	Error**	18	27.5
33	Error*	Error**	16.5	26
50	Error*	Error**	22.5	31
75	Error*	Error**	19	34.5
100	Error*	Error**	24	34.5
150	Error*	Error**	29	33.5

Table 61: Tempered classification error rates for HOO-CV PCA-CVA (no pretreatment, centered and autoscaled) and HOO-CV PLS-DA models with varying number of PCs or PLS dimensions for the first set of 20 normalized (peak area) window glass spectra (10 replicates). The smallest PC and PLS dimension with the minimum error rate is highlighted in yellow. The error rates associated with PC dimension containing at least 90, 95, 99, and 99.9% of the variance are highlighted in green, blue, purple and red, respectively. Error* is an "Error in lda.default(x, grouping, ...) : variables 11 12 13… appear to be constant within groups". Error** is an "Error in lda.default(x, grouping, ...) : variables 10 11 12… appear to be constant within groups".

Number of PCs for PCA & Dimensions for PLS-DA	Error Rate (%) for HOO-CV with PCA reduced CVA (no pretreatment)	Error Rate (%) for HOO-CV with PCA reduced CVA (centered)	Error Rate (%) for HOO-CV with PCA reduced CVA (autoscaled)	Error Rate (%) with HOO-CV with PLS-DA
3	31.5	27	28	27
6	29	29	30.5	28
10	28.5	Error**	27	25
11	Error*	Error**	27.5	20.5
30	Error*	Error**	17	22
35	Error*	Error**	13.5	21
50	Error*	Error**	17	19.5
75	Error*	Error**	17.5	20.5
100	Error*	Error**	19	18.5
150	Error*	Error**	16	18.5

Table 62: Discrimination error rates for HOO-CV PCA-CVA (no pretreatment, centered and autoscaled) and HOO-CV PLS-DA models with varying number of PCs or PLS dimensions for the first set of 30 normalized (peak height) glass spectra (10 replicates). The smallest PC and PLS dimension with the minimum error rate is highlighted in yellow. The error rates associated with PC dimension containing at least 90, 95, 99, and 99.9% of the variance are highlighted in green, blue, purple and red, respectively. Error* is an "Error in lda.default(x, grouping, ...) : variables 121 122 123… appear to be constant within groups".

Number of PCs for PCA & Dimensions for PLS-DA	Error Rate (%) for HOO-CV with PCA reduced CVA (no pretreatment)	Error Rate (%) for HOO-CV with PCA reduced CVA (centered)	Error Rate (%) for HOO-CV with PCA reduced CVA (autoscaled)	Error Rate (%) with HOO-CV with PLS-DA
3	91	89	87.33	89
4	89	89.33	84.67	88
5	63	61	63.33	87
6	62	62.67	62.67	84
7	63.67	60.33	61	83.3
8	60	58	54.67	81.67
10	52.67	50.67	52.33	78
11	49.33	48	50.33	79
12	48.33	49.67	50	79.33
30	15.67	15.33	16.67	44.67
50	15	15.33	16.67	43
75	14.33	14.67	13.33	41
100	13	13	7.67	36.67
120	12.33	12.67	8.67	37.66
133	Error*	Error*	7.33	31.67
150	Error*	Error*	8	32.67
200	Error*	Error*	12.67	41.33

Table 63: Classification (automotive, architectural, or container) error rates for HOO-CV PCA-CVA (no pretreatment, centered and autoscaled) and HOO-CV PLS-DA models with varying number of PCs or PLS dimensions for the first set of 30 normalized (peak height) glass spectra (10 replicates). The smallest PC and PLS dimension with the minimum error rate is highlighted in yellow. The error rates associated with PC dimension containing at least 90, 95, 99, and 99.9% of the variance are highlighted in green, blue, purple and red, respectively. Error* is an "Error in lda.default(x, grouping, ...) : variables 124 125 126… appear to be constant within groups".

Number of PCs for PCA & Dimensions for PLS-DA	Error Rate (%) for HOO-CV with PCA reduced CVA (no pretreatment)	Error Rate (%) for HOO-CV with PCA reduced CVA (centered)	Error Rate (%) for HOO-CV with PCA reduced CVA (autoscaled)	Error Rate (%) with HOO-CV with PLS-DA
3	61	60	64.67	34.67
4	63	62.33	66.33	33.33
5	30.33	30	32	30.33
6	29.67	30	31	31.33
7	30.33	28.33	28	28.33
8	29.33	27.33	27.33	28
10	27	27	28.33	27
11	26.67	27	27.67	25.67
12	27.67	28	27.67	23
30	15.33	15.33	18.33	25.33
48	16.67	16.67	15	24.67
50	18	16.33	15.33	25.33
75	18	18	17	22.67
100	19.67	19.33	20	29.33
123	19.67	19.33	19.67	32.33
150	Error*	Error*	19	34.33
200	Error*	Error*	21	42

Table 64: Classification (window or container) error rates for HOO-CV PCA-CVA (no pretreatment, centered and autoscaled) and HOO-CV PLS-DA models with varying number of PCs or PLS dimensions for the first set of 30 normalized (peak height) glass spectra (10 replicates). The smallest PC and PLS dimension with the minimum error rate is highlighted in yellow. The error rates associated with PC dimension containing at least 90, 95, 99, and 99.9% of the variance are highlighted in green, blue, purple and red, respectively. Error* is an "Error in lda.default(x, grouping, ...) : variables 124 125 126… appear to be constant within groups".

Number of PCs for PCA & Dimensions for PLS-DA	Error Rate (%) for HOO-CV with PCA reduced CVA (no pretreatment)	Error Rate (%) for HOO-CV with PCA reduced CVA (centered)	Error Rate (%) for HOO-CV with PCA reduced CVA (autoscaled)	Error Rate (%) with HOO-CV with PLS-DA
3	34	33.33	30.67	6.67
4	34	33.67	30	4.33
5	6.67	7	7.67	4
6	7	5.33	7.33	3.67
7	5.67	5.67	5.67	4
8	7	6	4.67	3.67
10	4	4	4	3.67
11	4	4	4	3.67
12	4	4	3.67	3.67
30	4	4	3.67	6.33
50	4.67	4.67	3.67	4.33
75	5	5	4.67	4
100	5.33	5	4.33	6
123	5.33	5.33	5.67	9.67
150	Error*	Error*	6	12.67
171	Error*	Error*	2.67	13.67
200	Error*	Error*	3.67	24

Table 65: Discrimination error rates for HOO-CV PCA-CVA (no pretreatment, centered and autoscaled) and HOO-CV PLS-DA models with varying number of PCs or PLS dimensions for the first set of 20 normalized (peak height) window glass spectra (10 replicates). The smallest PC and PLS dimension with the minimum error rate is highlighted in yellow. The error rates associated with PC dimension containing at least 90, 95, 99, and 99.9% of the variance are highlighted in green, blue, purple and red, respectively. Error is an "Error in lda.default(x, grouping, ...) : variables 113 114 115… appear to be constant within groups".

Number of PCs for PCA & Dimensions for PLS-DA	Error Rate (%) for HOO-CV with PCA reduced CVA (no pretreatment)	Error Rate (%) for HOO-CV with PCA reduced CVA (centered)	Error Rate (%) for HOO-CV with PCA reduced CVA (autoscaled)	Error Rate (%) with HOO-CV with PLS-DA
3	91	92.5	90	91
4	84	89	81	88
6	83.5	83	69	76
7	81.5	63.5	62.5	76.5
10	53	53.3	54	71.5
11	50	50	55	69.5
12	53.5	51	52	66.5
30	15.5	15.5	17	38
50	16	16.5	16	38.5
75	15.5	14.5	12	35.5
96	14.5	13.5	10	38
100	14	13.5	12	40
150	Error*	Error*	17	45.5

Table 66: Discrimination error rates for HOO-CV PCA-CVA (no pretreatment, centered and autoscaled) and HOO-CV PLS-DA models with varying number of PCs or PLS dimensions for the first set of 10 normalized (peak height) container glass spectra (10 replicates). The smallest PC and PLS dimension with the minimum error rate is highlighted in yellow. The error rates associated with PC dimension containing at least 90, 95, 99, and 99.9% of the variance are highlighted in green, blue, purple and red, respectively.

Number of PCs for PCA & Dimensions for PLS-DA	Error Rate (%) for HOO-CV with PCA reduced CVA (no pretreatment)	Error Rate (%) for HOO-CV with PCA reduced CVA (centered)	Error Rate (%) for HOO-CV with PCA reduced CVA (autoscaled)	Error Rate (%) with HOO-CV with PLS-DA
3	76	70	69	75
4	69	63	66	72
6	58	59	55	62
10	42	40	43	61
11	46	46	49	55
26	17	17	9	24
30	11	14	10	25
50	15	15	12	22
75	21	24	25	24

Table 67: Float classification error rates for HOO-CV PCA-CVA (no pretreatment, centered and autoscaled) and HOO-CV PLS-DA models with varying number of PCs or PLS dimensions for the first set of 20 normalized (peak height) window glass spectra (10 replicates). The smallest PC and PLS dimension with the minimum error rate is highlighted in yellow. The error rates associated with PC dimension containing at least 90, 95, 99, and 99.9% of the variance are highlighted in green, blue, purple and red, respectively. Error* is an "Error in lda.default(x, grouping, ...) : variables 114 115 116… appear to be constant within groups".

Number of PCs for PCA & Dimensions for PLS-DA	Error Rate (%) for HOO-CV with PCA reduced CVA (no pretreatment)	Error Rate (%) for HOO-CV with PCA reduced CVA (centered)	Error Rate (%) for HOO-CV with PCA reduced CVA (autoscaled)	Error Rate (%) with HOO-CV with PLS-DA
3	37.5	33.5	37	33.5
4	33.5	33.5	32	29
6	31.5	33	32	23
7	31	34.5	32	24.5
10	23.5	23.5	23.5	21
11	23.5	22.5	25	19.5
12	24.5	23.5	26.5	22
15	20.5	19.5	17.5	20
30	22	22.5	21.5	27.5
50	23.5	23.5	20.5	32.5
75	20.5	19.5	21.5	34
100	25.5	26.5	26	36
150	Error*	Error*	23.5	36.5

Table 68: Tempered classification error rates for HOO-CV PCA-CVA (no pretreatment, centered and autoscaled) and HOO-CV PLS-DA models with varying number of PCs or PLS dimensions for the first set of 20 normalized (peak height) window glass spectra (10 replicates). The smallest PC and PLS dimension with the minimum error rate is highlighted in yellow. The error rates associated with PC dimension containing at least 90, 95, 99, and 99.9% of the variance are highlighted in green, blue, purple and red, respectively. Error* is an"Error in lda.default(x, grouping, ...) : variables 114 115 116… appear to be constant within groups".

Number of PCs for PCA & Dimensions for PLS-DA	Error Rate (%) for HOO-CV with PCA reduced CVA (no pretreatment)	Error Rate (%) for HOO-CV with PCA reduced CVA (centered)	Error Rate (%) for HOO-CV with PCA reduced CVA (autoscaled)	Error Rate (%) with HOO-CV with PLS-DA
3	29.5	27.5	31	28.5
4	27.5	28	28.5	26
6	29	29.5	31	29.5
7	29.5	29	30.5	26.5
10	25.5	25	26	27
11	28	28.5	27.5	25
12	28.5	28.5	27.5	23
30	21.5	20.5	21	21
36	17.5	18	17	22.5
50	19.5	20	17.5	20.5
75	19.5	19.5	19.5	19.5
100	22	24	22	18.5
150	Error*	Error*	19	19

Table 69: Discrimination error rates for HOO-CV PCA-CVA (no pretreatment, centered and autoscaled) and HOO-CV PLS-DA models with varying number of PCs or PLS dimensions for the first set of 30 glass first derivative (5-point smoothing) spectra (10 replicates). The smallest PC and PLS dimension with the minimum error rate is highlighted in yellow. The error rates associated with PC dimension containing at least 90, 95, 99, and 99.9% of the variance are highlighted in green, blue, purple and red, respectively. Error* is an "Error in lda.default(x, grouping, ...) : variables 72 73 74… appear to be constant within groups". Error** is an "Error in lda.default(x, grouping, ...) : variables 72 73 74… appear to be constant within groups".

Number of PCs for PCA & Dimensions for PLS-DA	Error Rate (%) for HOO-CV with PCA reduced CVA (no pretreatment)	Error Rate (%) for HOO-CV with PCA reduced CVA (centered)	Error Rate (%) for HOO-CV with PCA reduced CVA (autoscaled)	Error Rate (%) with HOO-CV with PLS-DA
3	94.33	95.33	84.33	91.67
4	92.67	94	78	90.33
5	91.67	84.33	60.33	93
6	80.67	82	52.67	90.67
7	83.67	84.67	49.33	88
9	58.33	57.33	47	82
10	59	57.33	40.33	79.67
30	31.67	30.67	19	52
36	25.33	27.67	14	52
37	26.33	26.33	13	52.33
50	20.67	20.67	9.67	48.33
70	20.67	19.67	7.67	48
71	21	Error**	7.33	46.67
75	Error*	Error**	7	42.33
96	Error*	Error**	4.67	38.33
100	Error*	Error**	5.67	34.67
102	Error*	Error**	6.67	33.67
150	Error*	Error**	11	34.67
200	Error*	Error**	14	43.67

Table 70: Classification (automotive, architectural, or container) error rates for HOO-CV PCA-CVA (no pretreatment, centered and autoscaled) and HOO-CV PLS-DA models with varying number of PCs or PLS dimensions for the first set of 30 glass first derivative (5-point smoothing) spectra (10 replicates). The smallest PC and PLS dimension with the minimum error rate is highlighted in yellow. The error rates associated with PC dimension containing at least 90, 95, 99, and 99.9% of the variance are highlighted in green, blue, purple and red, respectively. Error* is an "Error in lda.default(x, grouping, ...) : variables 75 76 77… appear to be constant within groups".

Number of PCs for PCA & Dimensions for PLS-DA	Error Rate (%) for HOO-CV with PCA reduced CVA (no pretreatment)	Error Rate (%) for HOO-CV with PCA reduced CVA (centered)	Error Rate (%) for HOO-CV with PCA reduced CVA (autoscaled)	Error Rate (%) with HOO-CV with PLS-DA
3	64.67	61	49	42.67
4	62.67	61.33	39.33	38.67
5	56.33	50.33	24	37.33
6	47	47.33	24.33	36.67
7	44.67	45	27	32.33
9	25.67	26.67	25.33	27.67
10	28	28.33	26.67	24.67
30	22.33	25.33	22.33	23.67
36	18	17	18	24.33
37	17.67	17.33	18	23.67
50	17	17.33	17.67	23.33
70	18.33	18.33	18	24.67
74	18.33	18.67	18.67	25.67
75	Error*	Error*	19	25.67
84	Error*	Error*	15.33	23.67
100	Error*	Error*	17.67	28
102	Error*	Error*	17.67	28.67
150	Error*	Error*	20.67	32.67
200	Error*	Error*	23.67	44

Table 71: Classification (window or container) error rates for HOO-CV PCA-CVA (no pretreatment, centered and autoscaled) and HOO-CV PLS-DA models with varying number of PCs or PLS dimensions for the first set of 30 glass first derivative (5-point smoothing) spectra (10 replicates). The smallest PC and PLS dimension with the minimum error rate is highlighted in yellow. The error rates associated with PC dimension containing at least 90, 95, 99, and 99.9% of the variance are highlighted in green, blue, purple and red, respectively. Error* is an "Error in lda.default(x, grouping, ...) : variables 75 76 77… appear to be constant within groups".

Number of PCs for PCA & Dimensions for PLS-DA	Error Rate (%) for HOO-CV with PCA reduced CVA (no pretreatment)	Error Rate (%) for HOO-CV with PCA reduced CVA (centered)	Error Rate (%) for HOO-CV with PCA reduced CVA (autoscaled)	Error Rate (%) with HOO-CV with PLS-DA
3	33.67	32.66	27.67	21.67
4	35.67	33.67	15.67	7.33
5	29	22.67	3.67	4
6	23	22.33	3.67	3.67
7	19.67	19.33	3.67	3.67
8	19.67	19.67	3.67	3.67
9	3.67	3.67	3.67	3.67
10	3.67	3.67	3.67	4.67
15	3.67	3.67	4	4
20	4.33	4	4	3.67
30	4	4.67	3.67	5.33
36	5	4.33	3.67	4.67
37	5	5	3.33	4.33
50	4	4.33	3.33	5.67
70	4	4	3.67	7.67
74	4	4	3.33	7.33
75	Error*	Error*	3.33	7
81	Error*	Error*	2.33	7
100	Error*	Error*	2.67	7.33
102	Error*	Error*	2.67	8
150	Error*	Error*	4	16
200	Error*	Error*	6	18.33

Table 72: Discrimination error rates for HOO-CV PCA-CVA (no pretreatment, centered and autoscaled) and HOO-CV PLS-DA models with varying number of PCs or PLS dimensions for the first set of 20 window glass first derivative (5-point smoothing) spectra (10 replicates). The smallest PC and PLS dimension with the minimum error rate is highlighted in yellow. The error rates associated with PC dimension containing at least 90, 95, 99, and 99.9% of the variance are highlighted in green, blue, purple and red, respectively. Error* is an "Error in lda.default(x, grouping, ...) : variables 67 68 69… appear to be constant within groups". Error** is an "Error in lda.default(x, grouping, ...) : variables 66 67 68… appear to be constant within groups".

Number of PCs for PCA & Dimensions for PLS-DA	Error Rate (%) for HOO-CV with PCA reduced CVA (no pretreatment)	Error Rate (%) for HOO-CV with PCA reduced CVA (centered)	Error Rate (%) for HOO-CV with PCA reduced CVA (autoscaled)	Error Rate (%) with HOO-CV with PLS-DA
3	90.5	94.5	85	93.5
4	90.5	90	78.5	94
5	88.5	90.5	67.5	87
6	87	87	55	83.5
7	86.5	86	55	78
9	68	70	43	77
10	68.5	64	39	73
12	54.5	55	31	63
30	29.5	29.5	16	48
35	32	27.5	12	43
41	26	26.5	11	45.5
50	21.5	21.5	9.5	40.5
61	21	21	6	38
75	Error*	Error**	8	37.5
97	Error*	Error**	10.5	39.5
100	Error*	Error**	9.5	37
150	Error*	Error**	29.5	43.5

Table 73: Discrimination error rates for HOO-CV PCA-CVA (no pretreatment, centered and autoscaled) and HOO-CV PLS-DA models with varying number of PCs or PLS dimensions for the first set of 10 container glass first derivative (5-point smoothing) spectra (10 replicates). The smallest PC and PLS dimension with the minimum error rate is highlighted in yellow. The error rates associated with PC dimension containing at least 90, 95, 99, and 99.9% of the variance are highlighted in green, blue, purple and red, respectively. Error* is an "Error in lda.default(x, grouping, ...) : variables 61 62 63… appear to be constant within groups". Error** is an "Error in lda.default(x, grouping, ...) : variables 60 61 62… appear to be constant within groups".

Number of PCs for PCA & Dimensions for PLS-DA	Error Rate (%) for HOO-CV with PCA reduced CVA (no pretreatment)	Error Rate (%) for HOO-CV with PCA reduced CVA (centered)	Error Rate (%) for HOO-CV with PCA reduced CVA (autoscaled)	Error Rate (%) with HOO-CV with PLS-DA
3	81	79	60	78
4	80	79	62	73
5	73	67	44	71
6	67	67	46	77
8	59	59	41	65
10	53	44	37	58
24	28	28	8	32
26	26	27	8	32
30	32	29	9	32
50	21	22	5	36
55	20	19	2	35
63	Error*	Error**	6	36
75	Error*	Error**	17	40

Table 74: Float classification error rates for HOO-CV PCA-CVA (no pretreatment, centered and autoscaled) and HOO-CV PLS-DA models with varying number of PCs or PLS dimensions for the first set of 20 window glass first derivative (5-point smoothing) spectra (10 replicates). The smallest PC and PLS dimension with the minimum error rate is highlighted in yellow. The error rates associated with PC dimension containing at least 90, 95, 99, and 99.9% of the variance are highlighted in green, blue, purple and red, respectively. Error* is an "Error in lda.default(x, grouping, ...) : variables 70 71 72… appear to be constant within groups".

Number of PCs for PCA & Dimensions for PLS-DA	Error Rate (%) for HOO-CV with PCA reduced CVA (no pretreatment)	Error Rate (%) for HOO-CV with PCA reduced CVA (centered)	Error Rate (%) for HOO-CV with PCA reduced CVA (autoscaled)	Error Rate (%) with HOO-CV with PLS-DA
3	33	33.5	27	32.5
4	35.5	34	27.5	25
5	36.5	34	28.5	26
6	31	31	25.5	23.5
7	28	28	24.5	19.5
9	26	28	18.5	19.5
10	23	27	20	22.5
12	23.5	22.5	20.5	22
27	22.5	19.5	13.5	22.5
30	20	20	15	23.5
35	22.5	22	17.5	27.5
41	23	22	17.5	25
50	23	23.5	16	26.5
75	Error*	Error*	18	27.5
97	Error*	Error*	22.5	28
100	Error*	Error*	24.5	28
150	Error*	Error*	24	27.5

Table 75: Tempered classification error rates for HOO-CV PCA-CVA (no pretreatment, centered and autoscaled) and HOO-CV PLS-DA models with varying number of PCs or PLS dimensions for the first set of 20 window glass first derivative (5-point smoothing) spectra (10 replicates). The smallest PC and PLS dimension with the minimum error rate is highlighted in yellow. The error rates associated with PC dimension containing at least 90, 95, 99, and 99.9% of the variance are highlighted in green, blue, purple and red, respectively. Error* is an "Error in lda.default(x, grouping, ...) : variables 70 71 72… appear to be constant within groups".

Number of PCs for PCA & Dimensions for PLS-DA	Error Rate (%) for HOO-CV with PCA reduced CVA (no pretreatment)	Error Rate (%) for HOO-CV with PCA reduced CVA (centered)	Error Rate (%) for HOO-CV with PCA reduced CVA (autoscaled)	Error Rate (%) with HOO-CV with PLS-DA
3	28.5	29	29.5	29
4	28.5	31	30	30
5	29.5	29.5	28	28
6	31	28	26.5	26
7	30.5	30	25	24
9	30	32.5	26	24.5
10	31.5	25	26.5	23.5
12	25.5	23.5	25	18
30	23.5	25	17.5	20.5
35	25	25.5	18	21
41	22	23.5	19	20.5
50	18	17.5	15	20.5
75	Error*	Error*	13	23.5
92	Error*	Error*	11.5	25.5
97	Error*	Error*	13.5	24.5
100	Error*	Error*	14	25
150	Error*	Error*	14.5	21.5

Table 76: Discrimination error rates for HOO-CV PCA-CVA (no pretreatment, centered and autoscaled) and HOO-CV PLS-DA models with varying number of PCs or PLS dimensions for the first set of 30 glass first derivative (9-point smoothing) spectra (10 replicates). The smallest PC and PLS dimension with the minimum error rate is highlighted in yellow. The error rates associated with PC dimension containing at least 90, 95, 99, and 99.9% of the variance are highlighted in green, blue, purple and red, respectively. Error* is an "Error in lda.default(x, grouping, ...) : variables 37 38 39… appear to be constant within groups".

Number of PCs for PCA & Dimensions for PLS-DA	Error Rate (%) for HOO-CV with PCA reduced CVA (no pretreatment)	Error Rate (%) for HOO-CV with PCA reduced CVA (centered)	Error Rate (%) for HOO-CV with PCA reduced CVA (autoscaled)	Error Rate (%) with HOO-CV with PLS-DA
3	94.33	94.33	87.67	94.67
4	93.67	93.67	78.33	90
5	90.67	90.33	67.33	89.67
6	80.67	80.67	57.33	90.33
7	78.67	80.67	53	88
8	78	77.67	51.67	86.67
10	59	59	41.33	80.33
14	42.67	43	36	73
27	23.67	23	20	47.67
30	23	24	20.33	46.67
37	Error*	Error*	14.67	44.33
50	Error*	Error*	11.33	37
75	Error*	Error*	6.67	33
100	Error*	Error*	8.67	29
123	Error*	Error*	5	28.33
150	Error*	Error*	7.67	32.33
200	Error*	Error*	9.33	35

Table 77: Classification (automotive, architectural, or container) error rates for HOO-CV PCA-CVA (no pretreatment, centered and autoscaled) and HOO-CV PLS-DA models with varying number of PCs or PLS dimensions for the first set of 30 glass first derivative (9-point smoothing) spectra (10 replicates). The smallest PC and PLS dimension with the minimum error rate is highlighted in yellow. The error rates associated with PC dimension containing at least 90, 95, 99, and 99.9% of the variance are highlighted in green, blue, purple and red, respectively. Error* is an "Error in lda.default(x, grouping, ...) : variables 39 40 41… appear to be constant within groups".

Number of PCs for PCA & Dimensions for PLS-DA	Error Rate (%) for HOO-CV with PCA reduced CVA (no pretreatment)	Error Rate (%) for HOO-CV with PCA reduced CVA (centered)	Error Rate (%) for HOO-CV with PCA reduced CVA (autoscaled)	Error Rate (%) with HOO-CV with PLS-DA
3	64.67	62.67	54	41
4	57.67	58.67	37	34
5	54	53.67	29.67	34
6	46.67	47.33	28	35.67
7	44.33	44.67	28.33	35.33
8	45.67	45	29	30.33
10	28.67	28.67	26	28.33
14	26.33	26.67	27.33	19
27	25.67	16	17.67	17.33
30	14.67	15.67	17.67	20.67
50	Error*	Error*	17	19.33
57	Error*	Error*	13.33	19
75	Error*	Error*	17	22.67
100	Error*	Error*	16.33	23.67
150	Error*	Error*	18	26.33
200	Error*	Error*	19.67	38

Table 78: Classification (window or container) error rates for HOO-CV PCA-CVA (no pretreatment, centered and autoscaled) and HOO-CV PLS-DA models with varying number of PCs or PLS dimensions for the first set of 30 glass first derivative (9-point smoothing) spectra (10 replicates). The smallest PC and PLS dimension with the minimum error rate is highlighted in yellow. The error rates associated with PC dimension containing at least 90, 95, 99, and 99.9% of the variance are highlighted in green, blue, purple and red, respectively. Error* is an "Error in lda.default(x, grouping, ...) : variables 39 40 41… appear to be constant within groups".

Number of PCs for PCA & Dimensions for PLS-DA	Error Rate (%) for HOO-CV with PCA reduced CVA (no pretreatment)	Error Rate (%) for HOO-CV with PCA reduced CVA (centered)	Error Rate (%) for HOO-CV with PCA reduced CVA (autoscaled)	Error Rate (%) with HOO-CV with PLS-DA
3	33.67	34	28.67	19.67
4	35	35	9.67	7.33
5	30	29.67	3.67	6
6	23.67	23	4.33	4.33
7	16	17	4.33	3.67
8	17	17	4	3.67
10	3.67	3.67	3.67	4
14	3.67	3.67	3.67	3.33
27	4	4	4.33	4
30	3.67	3.67	3.67	5.33
50	Error*	Error*	2.67	3.33
75	Error*	Error*	4	5.67
100	Error*	Error*	3.67	6.67
123	Error*	Error*	2	6.67
150	Error*	Error*	2.67	7.67
200	Error*	Error*	5	11

Table 79: Discrimination error rates for HOO-CV PCA-CVA (no pretreatment, centered and autoscaled) and HOO-CV PLS-DA models with varying number of PCs or PLS dimensions for the first set of 20 window glass first derivative (9-point smoothing) spectra (10 replicates). The smallest PC and PLS dimension with the minimum error rate is highlighted in yellow. The error rates associated with PC dimension containing at least 90, 95, 99, and 99.9% of the variance are highlighted in green, blue, purple and red, respectively. Error* is an "Error in lda.default(x, grouping, ...) : variables 35 36 37… appear to be constant within groups".

Number of PCs for PCA & Dimensions for PLS-DA	Error Rate (%) for HOO-CV with PCA reduced CVA (no pretreatment)	Error Rate (%) for HOO-CV with PCA reduced CVA (centered)	Error Rate (%) for HOO-CV with PCA reduced CVA (autoscaled)	Error Rate (%) with HOO-CV with PLS-DA
3	90	89.5	86	88
4	90.5	91	81	88.5
5	88.5	88.5	66.5	88
7	84	84.5	61.5	80
9	68	68.5	44.5	76.5
10	63.5	64.5	42	73.5
13	45.5	47	32.5	62
23	26	25	21.5	45
30	21	21	17.5	39.5
50	Error*	Error*	9	33
61	Error*	Error*	8	30
75	Error*	Error*	11.5	27
100	Error*	Error*	9	34
150	Error*	Error*	23.5	46

Table 80: Discrimination error rates for HOO-CV PCA-CVA (no pretreatment, centered and autoscaled) and HOO-CV PLS-DA models with varying number of PCs or PLS dimensions for the first set of 10 container glass first derivative (9-point smoothing) spectra (10 replicates). The smallest PC and PLS dimension with the minimum error rate is highlighted in yellow. The error rates associated with PC dimension containing at least 90, 95, 99, and 99.9% of the variance are highlighted in green, blue, purple and red, respectively. Error* is an "Error in lda.default(x, grouping, ...) : variables 36 37 38… appear to be constant within groups". Error** is an "Error in lda.default(x, grouping, ...) : variables 34 35 36… appear to be constant within groups".

Number of PCs for PCA & Dimensions for PLS-DA	Error Rate (%) for HOO-CV with PCA reduced CVA (no pretreatment)	Error Rate (%) for HOO-CV with PCA reduced CVA (centered)	Error Rate (%) for HOO-CV with PCA reduced CVA (autoscaled)	Error Rate (%) with HOO-CV with PLS-DA
3	80	79	60	76
4	80	78	62	74
5	72	68	44	73
6	65	68	46	77
7	56	68	43	66
10	51	47	35	59
12	37	42	38	58
13	35	38	32	62
30	18	20	8	33
33	17	18	6	28
35	16	Error**	7	31
50	Error*	Error**	9	28
75	Error*	Error**	22	27

Table 81: Float classification error rates for HOO-CV PCA-CVA (no pretreatment, centered and autoscaled) and HOO-CV PLS-DA models with varying number of PCs or PLS dimensions for the first set of 20 window glass first derivative (9-point smoothing) spectra (10 replicates). The smallest PC and PLS dimension with the minimum error rate is highlighted in yellow. The error rates associated with PC dimension containing at least 90, 95, 99, and 99.9% of the variance are highlighted in green, blue, purple and red, respectively. Error* is an "Error in lda.default(x, grouping, ...) : variables 36 37 38… appear to be constant within groups".

Number of PCs for PCA & Dimensions for PLS-DA	Error Rate (%) for HOO-CV with PCA reduced CVA (no pretreatment)	Error Rate (%) for HOO-CV with PCA reduced CVA (centered)	Error Rate (%) for HOO-CV with PCA reduced CVA (autoscaled)	Error Rate (%) with HOO-CV with PLS-DA
3	37.5	37.5	31.5	32
4	38	37	32	28
5	33	33	32	23.5
7	26.5	26.5	30	22
9	26	26	19	19
10	22	22.5	19.5	21
13	21	20.5	19.5	16.5
23	18	19	14	19.5
29	18.5	18.5	13	18.5
30	18.5	18	13.5	18.5
50	Error*	Error*	15.5	26.5
75	Error*	Error*	15.5	26
100	Error*	Error*	20	26
150	Error*	Error*	27.5	23.5

Table 82: Tempered classification error rates for HOO-CV PCA-CVA (no pretreatment, centered and autoscaled) and HOO-CV PLS-DA models with varying number of PCs or PLS dimensions for the first set of 20 window glass first derivative (9-point smoothing) spectra (10 replicates). The smallest PC and PLS dimension with the minimum error rate is highlighted in yellow. The error rates associated with PC dimension containing at least 90, 95, 99, and 99.9% of the variance are highlighted in green, blue, purple and red, respectively. Error* is an "Error in lda.default(x, grouping, ...) : variables 36 37 38… appear to be constant within groups".

Number of PCs for PCA & Dimensions for PLS-DA	Error Rate (%) for HOO-CV with PCA reduced CVA (no pretreatment)	Error Rate (%) for HOO-CV with PCA reduced CVA (centered)	Error Rate (%) for HOO-CV with PCA reduced CVA (autoscaled)	Error Rate (%) with HOO-CV with PLS-DA
3	29.5	29.5	31	28.5
4	30	30.5	27.5	27.5
5	30.5	30.5	26.5	28.5
7	30.5	30.5	27.5	26.5
9	30	30	26	25
10	29	29	25.5	24
13	29	28.5	26.5	23
23	22.5	22	26	16
30	22	20	20	16
50	Error*	Error*	16.5	16
71	Error*	Error*	14	17.5
75	Error*	Error*	18	16.5
100	Error*	Error*	18	19.5
150	Error*	Error*	15	20

Table 83: Discrimination error rates for HOO-CV PCA-CVA (no pretreatment, centered and autoscaled) and HOO-CV PLS-DA models with varying number of PCs or PLS dimensions for the first set of 30 glass second derivative (5-point smoothing) spectra (10 replicates). The smallest PC and PLS dimension with the minimum error rate is highlighted in yellow. The error rates associated with PC dimension containing at least 90, 95, 99, and 99.9% of the variance are highlighted in green, blue, purple and red, respectively. Error* is an "Error in lda.default(x, grouping, ...) : variables 82 83 84…. appear to be constant within groups". Error** is an "Error in lda.default(x, grouping, ...) : variables 85 86 87… appear to be constant within groups".

Number of PCs for PCA & Dimensions for PLS-DA	Error Rate (%) for HOO-CV with PCA reduced CVA (no pretreatment)	Error Rate (%) for HOO-CV with PCA reduced CVA (centered)	Error Rate (%) for HOO-CV with PCA reduced CVA (autoscaled)	Error Rate (%) with HOO-CV with PLS-DA
3	96.67	96.33	72.67	93.67
4	95.67	96.33	65	91.33
5	93.67	92	59	93.67
6	88	88.33	57.33	91
7	84.67	86.67	51.33	88.33
8	83.33	84.33	52	88.33
10	83	83	42.67	86.33
19	71.67	69.67	28.33	80
29	63.33	63.33	21	68.33
30	63.67	61.67	22	66.66
34	56.33	54.33	21	67.33
50	47.67	44.33	15.33	55.67
73	36	34.67	10.67	51.33
75	34	35.33	9.67	52
80	32.33	30	10.67	50.33
81	30	29	11	48.67
83	Error*	30.67	11.33	47.67
84	Error*	Error**	10.33	48
100	Error*	Error**	9	42.33
104	Error*	Error**	8.33	40.67
131	Error*	Error**	8	34.67
140	Error*	Error**	5	34.67
150	Error*	Error**	6.33	30
200	Error*	Error**	9	36
204	Error*	Error**	9.667	37.33

Table 84: Classification (automotive, architectural, or container) error rates for HOO-CV PCA-CVA (no pretreatment, centered and autoscaled) and HOO-CV PLS-DA models with varying number of PCs or PLS dimensions for the first set of 30 glass second derivative (5-point smoothing) spectra (10 replicates). The smallest PC and PLS dimension with the minimum error rate is highlighted in yellow. The error rates associated with PC dimension containing at least 90, 95, 99, and 99.9% of the variance are highlighted in green, blue, purple and red, respectively. Error* is an "Error in lda.default(x, grouping, ...) : variables 82 83 84…. appear to be constant within groups". Error** is an "Error in lda.default(x, grouping, ...) : variables 85 86 87… appear to be constant within groups".

Number of PCs for PCA & Dimensions for PLS-DA	Error Rate (%) for HOO-CV with PCA reduced CVA (no pretreatment)	Error Rate (%) for HOO-CV with PCA reduced CVA (centered)	Error Rate (%) for HOO-CV with PCA reduced CVA (autoscaled)	Error Rate (%) with HOO-CV with PLS-DA
3	62	63	59	54.33
4	62.33	59.33	57	55
5	57	58.33	58	47.67
6	57.33	57.67	53.67	41
7	58.33	58.33	54.67	38.67
8	58.67	59.33	54.67	33.33
10	60	60	51.67	33.33
19	50.67	51.67	34.33	27.67
29	44.67	46.33	30.67	26.33
30	45.67	44.67	29	26.67
34	43.67	44	30.67	25
50	38.67	36.67	32.67	22.33
73	33.33	33	28	23.33
75	31.67	31.33	26.33	24.67
80	29	29	25	25.33
81	29	28	25.67	24.67
84	26	27.67	27.33	25
85	26	26.67	27	25.33
100	Error*	Error*	25.67	27.67
104	Error*	Error*	26.67	29
131	Error*	Error*	22.67	37
150	Error*	Error*	21.67	36.67
159	Error*	Error*	16.67	36.67
200	Error*	Error*	21	37.67
204	Error*	Error*	21.67	38.67

Table 85: Classification (window or container) error rates for HOO-CV PCA-CVA (no pretreatment, centered and autoscaled) and HOO-CV PLS-DA models with varying number of PCs or PLS dimensions for the first set of 30 glass second derivative (5-point smoothing) spectra (10 replicates). The smallest PC and PLS dimension with the minimum error rate is highlighted in yellow. The error rates associated with PC dimension containing at least 90, 95, 99, and 99.9% of the variance are highlighted in green, blue, purple and red, respectively. Error* is an "Error in lda.default(x, grouping, ...) : variables 86 87 88 appear to be constant within groups".

Number of PCs for PCA & Dimensions for PLS-DA	Error Rate (%) for HOO-CV with PCA reduced CVA (no pretreatment)	Error Rate (%) for HOO-CV with PCA reduced CVA (centered)	Error Rate (%) for HOO-CV with PCA reduced CVA (autoscaled)	Error Rate (%) with HOO-CV with PLS-DA
3	32	33	33.33	33
4	33	33.67	29.33	25.33
5	34	31.67	29	19
6	31.67	32	30	16.33
7	32.33	32.67	30.67	11
8	33.67	33	30.33	8.33
10	34	32.67	28	7
19	32	30	13.67	6
29	26	25.67	12.33	4.33
30	26	21.67	12.33	4.33
34	21.67	20.33	12.67	3.33
50	16.33	12.67	10	4.33
73	6.67	6	6.67	5.33
75	5.33	5.67	6.67	5.67
80	6	5.67	8	6.67
81	5.67	6	8	7
83	6	5.33	7.67	7.33
84	5.67	6	8	7.33
85	5.67	6	7.67	7.65
100	Error*	Error*	5.67	10
104	Error*	Error*	6.33	11
131	Error*	Error*	3.67	12.33
142	Error*	Error*	2.33	13.33
150	Error*	Error*	2.67	14
200	Error*	Error*	5.33	22.33
204	Error*	Error*	5.67	23

Table 86: Discrimination error rates for HOO-CV PCA-CVA (no pretreatment, centered and autoscaled) and HOO-CV PLS-DA models with varying number of PCs or PLS dimensions for the first set of 20 window glass second derivative (5-point smoothing) spectra (10 replicates). The smallest PC and PLS dimension with the minimum error rate is highlighted in yellow. The error rates associated with PC dimension containing at least 90, 95, 99, and 99.9% of the variance are highlighted in green, blue, purple and red, respectively. Error* is an "Error in lda.default(x, grouping, ...) : variables 79 80 81… appear to be constant within groups". Error** is an "Error in lda.default(x, grouping, ...) : variables 78 79 80… appear to be constant within groups".

Number of PCs for PCA & Dimensions for PLS-DA	Error Rate (%) for HOO-CV with PCA reduced CVA (no pretreatment)	Error Rate (%) for HOO-CV with PCA reduced CVA (centered)	Error Rate (%) for HOO-CV with PCA reduced CVA (autoscaled)	Error Rate (%) with HOO-CV with PLS-DA
3	93.5	95.5	67.5	87.5
4	91.5	92.5	63	88
5	89	90.5	54.5	92
10	75	73	35	76.5
19	64	62	23.5	65.5
26	60.5	61	19	59
30	60	57.5	17	61
32	57	55	18.5	56
50	55	54	11.5	56.5
68	42.5	44	15	53.5
71	41.5	42.5	13	54.5
75	40.5	40	16	50
77	39	39	14.5	52
92	Error*	Error**	16.5	45.5
100	Error*	Error**	14.5	46
118	Error*	Error**	15	44
132	Error*	Error**	23.5	49
150	Error*	Error**	28.5	51
172	Error*	Error**	50	51

Table 87: Discrimination error rates for HOO-CV PCA-CVA (no pretreatment, centered and autoscaled) and HOO-CV PLS-DA models with varying number of PCs or PLS dimensions for the first set of 10 container glass second derivative (5-point smoothing) spectra (10 replicates). The smallest PC and PLS dimension with the minimum error rate is highlighted in yellow. The error rates associated with PC dimension containing at least 90, 95, 99, and 99.9% of the variance are highlighted in green, blue, purple and red, respectively. Error* is an "Error in lda.default(x, grouping, ...) : variables 68 69 70… appear to be constant within groups". Error** is an "Error in lda.default(x, grouping, ...) : variables 67 68 69… appear to be constant within groups".

Number of PCs for PCA & Dimensions for PLS-DA	Error Rate (%) for HOO-CV with PCA reduced CVA (no pretreatment)	Error Rate (%) for HOO-CV with PCA reduced CVA (centered)	Error Rate (%) for HOO-CV with PCA reduced CVA (autoscaled)	Error Rate (%) with HOO-CV with PLS-DA
3	84	83	33	77
4	77	75	28	73
5	69	73	26	69
10	62	59	16	56
14	50	45	11	55
22	39	44	7	51
24	39	42	6	46
29	36	35	5	43
30	38	35	5	40
47	28	30	9	39
50	30	27	8	41
59	30	31	9	35
61	32	29	10	35
75	Error*	Error**	14	35
81	Error*	Error**	22	35
83	Error*	Error**	15	34
97	Error*	Error**	99	33

Table 88: Float classification error rates for HOO-CV PCA-CVA (no pretreatment, centered and autoscaled) and HOO-CV PLS-DA models with varying number of PCs or PLS dimensions for the first set of 20 window glass second derivative (5-point smoothing) spectra (10 replicates). The smallest PC and PLS dimension with the minimum error rate is highlighted in yellow. The error rates associated with PC dimension containing at least 90, 95, 99, and 99.9% of the variance are highlighted in green, blue, purple and red, respectively. Error* is an "Error in lda.default(x, grouping, ...) : variables 81 82 83… appear to be constant within groups". Error** is an "Error in lda.default(x, grouping, ...) : variables 80 81 82… appear to be constant within groups".

Number of PCs for PCA & Dimensions for PLS-DA	Error Rate (%) for HOO-CV with PCA reduced CVA (no pretreatment)	Error Rate (%) for HOO-CV with PCA reduced CVA (centered)	Error Rate (%) for HOO-CV with PCA reduced CVA (autoscaled)	Error Rate (%) with HOO-CV with PLS-DA
3	34.5	37	33.5	32
4	38.5	40	28	26.5
5	36	40.5	27.5	29
10	33.5	31.5	23.5	26.5
19	32	31	25.5	26
26	33	29.5	23	26
30	26.5	25.5	21.5	24
31	24.5	25.5	20.5	23.5
32	25	25.5	21.5	25.5
50	28.5	30	23	30.5
68	30	31.5	24	34.5
71	32	31	24	34
75	33.5	35.5	24	34
77	33	35	25	35
92	Error*	Error**	27	36
100	Error*	Error**	29.5	37
118	Error*	Error**	26.5	36.5
132	Error*	Error**	25.5	37.5
150	Error*	Error**	27.5	37.5
172	Error*	Error**	38.5	37.5

Table 89: Tempered classification error rates for HOO-CV PCA-CVA (no pretreatment, centered and autoscaled) and HOO-CV PLS-DA models with varying number of PCs or PLS dimensions for the first set of 20 window glass second derivative (5-point smoothing) spectra (10 replicates). The smallest PC and PLS dimension with the minimum error rate is highlighted in yellow. The error rates associated with PC dimension containing at least 90, 95, 99, and 99.9% of the variance are highlighted in green, blue, purple and red, respectively. Error* is an "Error in lda.default(x, grouping, ...) : variables 81 82 83… appear to be constant within groups". Error** is an "Error in lda.default(x, grouping, ...) : variables 80 81 82… appear to be constant within groups".

Number of PCs for PCA & Dimensions for PLS-DA	Error Rate (%) for HOO-CV with PCA reduced CVA (no pretreatment)	Error Rate (%) for HOO-CV with PCA reduced CVA (centered)	Error Rate (%) for HOO-CV with PCA reduced CVA (autoscaled)	Error Rate (%) with HOO-CV with PLS-DA
3	35.5	40	27	28.5
4	31	36	26.5	27
5	32.5	34	29.5	25.5
10	27.5	28.5	27.5	24
19	25.5	28	25	21
26	29	29.5	25	17.5
30	31	29.5	19.5	16.5
32	30.5	31	20.5	16.5
50	25.5	27.5	15.5	14.5
68	27	25.5	17.5	12.5
71	25	28	18	12
75	25.5	26	17	12
77	28	28	16.5	11.5
92	Error*	Error**	15	11.5
100	Error*	Error**	15	12.5
113	Error*	Error**	11.5	12.5
118	Error*	Error**	13	12.5
132	Error*	Error**	14	11
150	Error*	Error**	14.5	11
172	Error*	Error**	18.5	11

Table 90: Discrimination error rates for HOO-CV PCA-CVA (no pretreatment, centered and autoscaled) and HOO-CV PLS-DA models with varying number of PCs or PLS dimensions for the first set of 30 glass second derivative (9-point smoothing) spectra (10 replicates). The smallest PC and PLS dimension with the minimum error rate is highlighted in yellow. The error rates associated with PC dimension containing at least 90, 95, 99, and 99.9% of the variance are highlighted in green, blue, purple and red, respectively. Error* is an "Error in lda.default(x, grouping, ...) : variables 27 28 29… appear to be constant within groups". Error** is an "Error in lda.default(x, grouping, ...) : variables 26 27 28… appear to be constant within groups."

Number of PCs for PCA & Dimensions for PLS-DA	Error Rate (%) for HOO-CV with PCA reduced CVA (no pretreatment)	Error Rate (%) for HOO-CV with PCA reduced CVA (centered)	Error Rate (%) for HOO-CV with PCA reduced CVA (autoscaled)	Error Rate (%) with HOO-CV with PLS-DA
3	96.67	96.67	79.67	96.67
4	94.67	95.33	66.33	96.33
5	92.33	93.67	63.33	95.67
6	93.67	95.33	62.33	94.33
7	95	90.67	57.67	93.67
8	88.33	87.67	54.33	91.67
10	78.33	76.33	43.67	86.67
21	53.33	51	25.67	70.33
25	47	46	19.67	65
30	Error*	Error**	20.33	59.33
41	Error*	Error**	15	49.67
50	Error*	Error**	10.33	54
60	Error*	Error**	9.33	52.67
64	Error*	Error**	9.33	49.67
75	Error*	Error**	6.33	42.67
100	Error*	Error**	10	32.67
106	Error*	Error**	8	31.33
150	Error*	Error**	10	32
164	Error*	Error**	7	34.67
166	Error*	Error**	6	34.67
200	Error*	Error**	11.67	41.67

Table 91: Classification (automotive, architectural, or container) error rates for HOO-CV PCA-CVA (no pretreatment, centered and autoscaled) and HOO-CV PLS-DA models with varying number of PCs or PLS dimensions for the first set of 30 glass second derivative (9-point smoothing) spectra (10 replicates). The smallest PC and PLS dimension with the minimum error rate is highlighted in yellow. The error rates associated with PC dimension containing at least 90, 95, 99, and 99.9% of the variance are highlighted in green, blue, purple and red, respectively. Error* is an "Error in lda.default(x, grouping, ...) : variables 30 31 32… appear to be constant within groups". Error** is an "Error in lda.default(x, grouping, ...) : variables 29 30 31… appear to be constant within groups".

Number of PCs for PCA & Dimensions for PLS-DA	Error Rate (%) for HOO-CV with PCA reduced CVA (no pretreatment)	Error Rate (%) for HOO-CV with PCA reduced CVA (centered)	Error Rate (%) for HOO-CV with PCA reduced CVA (autoscaled)	Error Rate (%) with HOO-CV with PLS-DA
3	63.67	64.33	67	57.33
4	61.67	59.33	39	51.33
5	58	59.33	36	43
6	58.33	59	33	36.67
7	59	58.33	34	33.67
8	58.33	53.67	32.67	33.33
10	47.67	44.33	26.33	27.33
21	29.67	29.67	24.67	21.33
25	27.33	27.33	27	21.33
30	Error*	Error**	23.33	22.67
41	Error*	Error**	20	25
50	Error*	Error**	19	21.67
60	Error*	Error**	17	24
61	Error*	Error**	16	23.33
64	Error*	Error**	18.33	23.33
75	Error*	Error**	17.67	24.67
100	Error*	Error**	19	27.67
106	Error*	Error**	18	27
150	Error*	Error**	20.67	30
164	Error*	Error**	22	31.33
200	Error*	Error**	25.33	35.55

Table 92: Classification (window or container) error rates for HOO-CV PCA-CVA (no pretreatment, centered and autoscaled) and HOO-CV PLS-DA models with varying number of PCs or PLS dimensions for the first set of 30 glass second derivative (9-point smoothing) spectra (10 replicates). The smallest PC and PLS dimension with the minimum error rate is highlighted in yellow. The error rates associated with PC dimension containing at least 90, 95, 99, and 99.9% of the variance are highlighted in green, blue, purple and red, respectively. Error* is an "Error in lda.default(x, grouping, ...) : variables 30 31 32… appear to be constant within groups". Error** is an "Error in lda.default(x, grouping, ...) : variables 29 30 31… appear to be constant within groups".

Number of PCs for PCA & Dimensions for PLS-DA	Error Rate (%) for HOO-CV with PCA reduced CVA (no pretreatment)	Error Rate (%) for HOO-CV with PCA reduced CVA (centered)	Error Rate (%) for HOO-CV with PCA reduced CVA (autoscaled)	Error Rate (%) with HOO-CV with PLS-DA
3	32.33	33.33	33.67	31.67
4	32.33	34.67	8.67	19.67
5	31	33	6.33	11.67
6	32	33	5	9.33
7	30.33	29.67	6.67	5.67
8	28.33	28	4.33	5
10	22.67	19.33	4	5
21	5.33	5.33	3.67	4
25	6	6	3.67	4.33
30	Error*	Error**	3.67	4.67
41	Error*	Error**	2.67	3.67
48	Error*	Error**	2	5.67
50	Error*	Error**	2.67	5.67
60	Error*	Error**	2.67	7
64	Error*	Error**	3	7.67
75	Error*	Error**	3	8
100	Error*	Error**	3.67	6.33
106	Error*	Error**	4	6
150	Error*	Error**	4	9
164	Error*	Error**	4.33	9.33
200	Error*	Error**	6.67	12.67

Table 93: Discrimination error rates for HOO-CV PCA-CVA (no pretreatment, centered and autoscaled) and HOO-CV PLS-DA models with varying number of PCs or PLS dimensions for the first set of 20 window glass second derivative (9-point smoothing) spectra (10 replicates). The smallest PC and PLS dimension with the minimum error rate is highlighted in yellow. The error rates associated with PC dimension containing at least 90, 95, 99, and 99.9% of the variance are highlighted in green, blue, purple and red, respectively. Error* is an "Error in lda.default(x, grouping, ...) : variables 26 27 28… appear to be constant within groups". Error** is an "Error in lda.default(x, grouping, ...) : variables 25 26 27… appear to be constant within groups.

Number of PCs for PCA & Dimensions for PLS-DA	Error Rate (%) for HOO-CV with PCA reduced CVA (no pretreatment)	Error Rate (%) for HOO-CV with PCA reduced CVA (centered)	Error Rate (%) for HOO-CV with PCA reduced CVA (autoscaled)	Error Rate (%) with HOO-CV with PLS-DA
3	94	96	77	92.5
4	91	93	73	95.5
5	87	92	66	92
6	88.5	88	66.5	91
10	78.5	81	46.5	77
21	59.5	57.5	28.5	62
22	60	58.5	24	59
30	Error*	Error**	22	56
41	Error*	Error**	19	43
50	Error*	Error**	17.5	42.5
58	Error*	Error**	11	37.5
61	Error*	Error**	11	39
69	Error*	Error**	7.5	40
75	Error*	Error**	12.5	35
99	Error*	Error**	10.5	32
100	Error*	Error**	11	32.5
146	Error*	Error**	23	44.5
150	Error*	Error**	21.5	45.5

Table 94: Discrimination error rates for HOO-CV PCA-CVA (no pretreatment, centered and autoscaled) and HOO-CV PLS-DA models with varying number of PCs or PLS dimensions for the first set of 10 container glass second derivative (9-point smoothing) spectra (10 replicates). The smallest PC and PLS dimension with the minimum error rate is highlighted in yellow. The error rates associated with PC dimension containing at least 90, 95, 99, and 99.9% of the variance are highlighted in green, blue, purple and red, respectively. Error* is an "Error in lda.default(x, grouping, ...) : variables 25 26 27… appear to be constant within groups". Error** is an "Error in lda.default(x, grouping, ...) : variables 24 25 26… appear to be constant within groups.

Number of PCs for PCA & Dimensions for PLS-DA	Error Rate (%) for HOO-CV with PCA reduced CVA (no pretreatment)	Error Rate (%) for HOO-CV with PCA reduced CVA (centered)	Error Rate (%) for HOO-CV with PCA reduced CVA (autoscaled)	Error Rate (%) with HOO-CV with PLS-DA
3	86	82	56	86
4	79	83	44	77
5	81	79	44	80
6	84	81	38	77
10	61	60	23	70
16	45	49	16	49
20	44	43	12	45
27	Error*	Error**	13	40
30	Error*	Error**	13	38
35	Error*	Error**	7	35
39	Error*	Error**	10	32
46	Error*	Error**	9	27
50	Error*	Error**	11	27
67	Error*	Error**	17	25
75	Error*	Error**	14	24
91	Error*	Error**	75	28

Table 95: Float classification error rates for HOO-CV PCA-CVA (no pretreatment, centered and autoscaled) and HOO-CV PLS-DA models with varying number of PCs or PLS dimensions for the first set of 20 window glass second derivative (9-point smoothing) spectra (10 replicates). The smallest PC and PLS dimension with the minimum error rate is highlighted in yellow. The error rates associated with PC dimension containing at least 90, 95, 99, and 99.9% of the variance are highlighted in green, blue, purple and red, respectively. Error* is an "Error in lda.default(x, grouping, ...) : variables 28 29 30… appear to be constant within groups". Error** is an "Error in lda.default(x, grouping, ...) : variables 27 28 29… appear to be constant within groups.

Number of PCs for PCA & Dimensions for PLS-DA	Error Rate (%) for HOO-CV with PCA reduced CVA (no pretreatment)	Error Rate (%) for HOO-CV with PCA reduced CVA (centered)	Error Rate (%) for HOO-CV with PCA reduced CVA (autoscaled)	Error Rate (%) with HOO-CV with PLS-DA
3	34	36.5	28	35
4	39.5	40.5	27	31
5	38	38	27.5	31
6	31	30	26.5	28
10	30	30	23.5	22
21	27	28	22.5	22.5
22	27	28	22.5	23.5
30	Error*	Error**	23	21
41	Error*	Error**	22.5	22.5
47	Error*	Error**	18.5	23.5
50	Error*	Error**	22	28
58	Error*	Error**	23	32.5
61	Error*	Error**	23.5	34
75	Error*	Error**	21	36
99	Error*	Error**	26	32
100	Error*	Error**	25	32
146	Error*	Error**	31	31
150	Error*	Error**	29.5	31

Table 96: Tempered classification error rates for HOO-CV PCA-CVA (no pretreatment, centered and autoscaled) and HOO-CV PLS-DA models with varying number of PCs or PLS dimensions for the first set of 20 window glass second derivative (9-point smoothing) spectra (10 replicates). The smallest PC and PLS dimension with the minimum error rate is highlighted in yellow. The error rates associated with PC dimension containing at least 90, 95, 99, and 99.9% of the variance are highlighted in green, blue, purple and red, respectively. Error* is an "Error in lda.default(x, grouping, ...) : variables 28 29 30… appear to be constant within groups". Error** is an "Error in lda.default(x, grouping, ...) : variables 27 28 29… appear to be constant within groups.

Number of PCs for PCA & Dimensions for PLS-DA	Error Rate (%) for HOO-CV with PCA reduced CVA (no pretreatment)	Error Rate (%) for HOO-CV with PCA reduced CVA (centered)	Error Rate (%) for HOO-CV with PCA reduced CVA (autoscaled)	Error Rate (%) with HOO-CV with PLS-DA
3	32	34	28.5	30
4	30.5	30.5	30.5	30
5	32.5	29	30	29
6	28	31	31	28.5
10	32.5	32.5	26	24
21	26	28	25.5	17.5
22	27.5	28	21.5	18
30	Error*	Error**	18.5	17.5
41	Error*	Error**	20.5	21
50	Error*	Error**	17.5	18
58	Error*	Error**	18	20
61	Error*	Error**	18.5	19
75	Error*	Error**	16	19
99	Error*	Error**	13	17.5
100	Error*	Error**	13.5	17.5
129	Error*	Error**	8	18.5
146	Error*	Error**	15	18.5
150	Error*	Error**	16	18.5

Table 97: A summary table of the lowest HOO-CV error rates for each of the chemometric models made with PCA-CVA and PLS-DA. The lowest HOO-CV error rate for each of the seven discrimination and container groupings is highlighted in yellow for the PCA-CVA models and blue for the PLS-DA models.

		Minimum HOO-CV PCA-CVA Error Rate (%) No Pre-treatment	Minimum HOO-CV PCA-CVA Error Rate (%) Centered	Minimum HOO-CV PCA-CVA Error Rate (%) Autoscaled	Minimum HOO-CV PLS-DA Error Rate (%)
Spectra	Discrimination	11.33	10.67	7.33	23.33
	Classification- Auto, Arch, Container	15.33	14.67	14	22.33
	Classification- Window or Container	3.33	3.33	2.67	3.67
	Discrimination Window	10	11.5	8	36.5
	Discrimination Container	11	9	6	19
	Float?	16.5	16.5	18	20
	Tempered?	16	16	11	19
1st Set Norm Peak Area	Discrimination	49.33	50.33	6.67	31
	Classification- Auto, Arch, Container	26.67	26.67	15	18
	Classification- Window or Container	4	4	3	3.67
	Discrimination Window	53	56.5	12	36
	Discrimination Container	42	42	10	21
	Float?	22.5	23.5	16.5	19.5
	Tempered?	28	25.5	13.5	18.5
1st Set Norm Peak Height	Discrimination	12	11.33	7.33	31.67
	Classification- Auto, Arch, Container	14	14	15	23
	Classification- Window or Container	3.67	3.67	2.67	3.67
	Discrimination Window	13.5	13.5	10	35.5
	Discrimination Container	11	10	9	22
	Float?	17.5	18	17.5	19.5
	Tempered?	16	16.5	17	18.5
First Derivative (5-point smoothing)	Discrimination	19	19.33	4.67	33.67
	Classification- Auto, Arch, Container	14.33	16	15.33	23.33
	Classification- Window or Container	3	3.67	2.33	3.67
	Discrimination Window	17.5	17.5	6	37
	Discrimination Container	18	15	2	32
	Float?	18	18	13.5	19.5
	Tempered?	16.5	17.5	11.5	18
First Derivative (9-point smoothing)	Discrimination	16	16	5	28.33
	Classification- Auto, Arch, Container	14.33	14.67	13.33	17.33
	Classification- Window or Container	3.33	3.33	2	3.33
	Discrimination Window	19.5	19	8	27
	Discrimination Container	16	18	6	27
	Float?	16.5	17.5	13	16.5
	Tempered?	19	18.5	14	16

Second Derivative (5-point smoothing)	Discrimination	30	29	5	30
	Classification- Auto, Arch, Container	26	26.33	16.67	23.33
	Classification- Window or Container	5.33	5.33	2.33	4.33
	Discrimination Window	38	38	11.5	44
	Discrimination Container	26	25	5	33
	Float?	24.5	25.5	20.5	23.5
	Tempered?	23.5	25	11.5	11.5
Second Derivative (9-point smoothing)	Discrimination	46.67	46	6	31.33
	Classification- Auto, Arch, Container	27	27	16	21.33
	Classification- Window or Container	5	5	2	3.67
	Discrimination Window	55	55.5	7.5	32
	Discrimination Container	39	41	7	24
	Float?	26.5	26.5	18.5	21
	Tempered?	26	26.5	8	17.5

Discrimination and classification results with autoscaled PCA-CVA had lower HOO-CV error rates than with PLS-DA, centered PCA-CVA, and PCA-CVA with no data pretreatment. There are no accepted criteria for choosing the number of PCs to retain for PCA-CVA, thus there is always some subjectivity in even deciding which criteria to use. For the preliminary set of 30 glasses, the number of retained PCs (and thus variance) was determined by which number of PCs resulted in a minimum error rate.

The lowest HOO-CV error rate for the discrimination of all 30 glasses was attained with PCA-CVA of the first derivative spectra (5-point smoothing, autoscaled), equaled 4.67%, and occurred first at PCA dimension 96 (99.879% variance retained). The corresponding PLS-DA HOO-CV error rate was 33.67%. The lowest HOO-CV error rate for the discrimination of the 20 window glasses was attained with PCA-CVA of the first derivative spectra (5-point smoothing, autoscaled), equaled 6%, and occurred first at PCA dimension 61 (99.561% variance retained). The corresponding PLS-DA HOO-CV error rate was 37%. The lowest HOO-CV error rate for the discrimination of 10 container glasses was attained with PCA-CVA of the first derivative spectra (5-point smoothing, autoscaled), equaled 2%, and occurred first at PCA dimension 55

(99.84% variance retained). The corresponding PLS-DA HOO-CV error rate was 32%. For all three discriminations, there was a large discrepancy between the HOO-CV error rates for the PCA-CVA and PLS-DA models, which could indicate that the PCA-CVA error rate is unreliable. Still, they warrant further study, and these chemometric analysis schemes were applied to the full set of 153 glasses.

The lowest HOO-CV error rate for the classification of all 30 glasses into the end-use categories of automotive, architectural or container glass was attained with PCA-CVA of the second derivative spectra (9-point smoothing, autoscaled), equaled 13.33%, and occurred first at PCA dimension 57 (94.469% variance retained). The corresponding PLS-DA HOO-CV error rate was 17.33%. These error rates were considered to be too high, thus further analysis on the classification into the end-use categories of automotive, architectural or container was not pursued. The high error rates for this discrimination was not surprising given the similarity in manufacturing processes of automotive and architectural glasses.

The lowest HOO-CV error rate for the classification of all 30 glasses into the end-use categories of window or container glass was attained with PCA-CVA of both the first and second derivative spectra (9-point smoothing, autoscaled), equaled 2%, and occurred first at PCA dimension 123 (99.999% variance retained) with the first derivative spectra and at PCA dimension 48 (92.349% variance retained) with the second derivative spectra. The corresponding PLS-DA HOO-CV error rates were 3.33% and 3.67%. These similar error rates support the success of classification into the end-use categories of window or container glasses, thus further analysis using these chemometric methods of the 153 glasses was completed.

The lowest HOO-CV error rate for the classification of the 20 window glasses into the manufacturing process categories of float or non-float was attained with PCA-CVA of the first

derivative spectra (9-point smoothing, autoscaled), equaled 13%, and occurred first at PCA dimension 29 (99.940% variance retained). The corresponding PLS-DA HOO-CV error rate was 16.5%. The similar error rates indicate that the models are working properly, however they are considered to be too high, thus there was no further analysis on the classification of glasses into the manufacturing process categories of float or non-float.

The lowest HOO-CV error rate for the classification of 20 window glasses into the manufacturing process categories of tempered or non-tempered was attained with PCA-CVA of the second derivative spectra (9-point smoothing, autoscaled), equaled 8%, and occurred first at PCA dimension 129 (99.754% variance retained). The corresponding PLS-DA HOO-CV error rate was 17.5%. The large discrepancy between the HOO-CV error rates could indicate that the PCA-CVA error rate is unreliable. Still, the low PCA-CVA HOO-CV error rate prompted the continued chemometric analysis of the full set of 153 glasses on the classification of glasses into the manufacturing process categories of tempered or non-tempered.

The results of the PCA analyses of the set of 153 glasses are in Appendix XII. Six PCA models, all autoscaled, were made for this data set: 1) the first derivative spectra (5-point smoothing) for all glasses, 2) the first derivative spectra (5-point smoothing) for window glasses, 3) the first derivative spectra (5-point smoothing) for container glasses, 4) the first derivative spectra (9-point smoothing) for all glasses, 5) the second derivative spectra (9-point smoothing) for all glasses, and 6) the second derivative spectra (9-point smoothing) for window glasses. Knowledge of the percentage of variance contained in the PCs was then used to help determine the number of PCs to keep for the PCA- CVA discrimination and classification models.

The results of the HOO-CV of the PCA-CVA models of the set of 153 glasses are in Appendix XIII. The results, in tables and graphs, show the error rates for each of the models

when keeping different numbers of PC dimensions. These results are compared to the error rates for HOO-CV PLS-DA, in Tables 98 – 103.

Table 98: Discrimination error rates for HOO-CV PCA-CVA (autoscaled) and HOO-CV PLS-DA models with varying number of PCs or PLS dimensions for all 153 glass first derivative (5-point smoothing) spectra (10 replicates). The smallest PC and PLS dimension with the minimum error rate is highlighted in yellow. The error rates associated with PC dimension containing at least 90, 95, 99, and 99.9% of the variance are highlighted in green, blue, purple and red, respectively. Error* denotes an error in the program where the R program "can't allocate region" and "cannot allocate vector of size", thus no HOO-CV error rate was computed.

Number of PCs for PCA & dimensions for PLS-DA	Error Rate (%) for HOO-CV with PCA reduced CVA (autoscaled)	Error Rate (%) with HOO-CV with PLS-DA
3	96.47	98.24
4	95.56	97.32
5	89.80	97.45
7	77.32	95.69
10	66.73	95.23
11	63.07	93.86
47	28.82	66.08
100	12.55	42.22
116	11.50	Error*
150	8.82	Error*
176	4.44	Error*
200	3.01	Error*
283	1.05	Error*

Table 99: Discrimination error rates for HOO-CV PCA-CVA (autoscaled) and HOO-CV PLS-DA models with varying number of PCs or PLS dimensions for 103 window glass first derivative (5-point smoothing) spectra (10 replicates). The smallest PC and PLS dimension with the minimum error rate is highlighted in yellow. The error rates associated with PC dimension containing at least 90, 95, 99, and 99.9% of the variance are highlighted in green, blue, purple and red, respectively.

Number of PCs for PCA & dimensions for PLS-DA	Error Rate (%) for HOO-CV with PCA reduced CVA (autoscaled)	Error Rate (%) with HOO-CV with PLS-DA
3	97.86	99.03
4	96.80	97.86
5	91.75	96.50
7	87.28	92.14
10	69.81	91.36
12	66.12	89.71
50	29.22	55.05
100	12.82	37.48
105	11.46	35.92
123	11.46	30.10
200	3.30	22.52
241	1.65	20.78

Table 100: Discrimination error rates for HOO-CV PCA-CVA (autoscaled) and HOO-CV PLS-DA models with varying number of PCs or PLS dimensions for 50 container glass first derivative (5-point smoothing) spectra (10 replicates). The smallest PC and PLS dimension with the minimum error rate is highlighted in yellow. The error rates associated with PC dimension containing at least 90, 95, 99, and 99.9% of the variance are highlighted in green, blue, purple and red, respectively.

Number of PCs for PCA & dimensions for PLS-DA	Error Rate (%) for HOO-CV with PCA reduced CVA (autoscaled)	Error Rate (%) with HOO-CV with PLS-DA
3	90.4	94.6
4	90	94.6
5	80.4	90.2
7	73.8	86.8
10	58.4	87.2
42	17.8	46
100	6.8	24.6
105	9.8	24.4
182	3.6	19.6
245	1.2	20.4

Table 101: Classification (window or container) error rates for HOO-CV PCA-CVA (autoscaled) and HOO-CV PLS-DA models with varying number of PCs or PLS dimensions for the all 153 glass first derivative (9-point smoothing) spectra (10 replicates). The smallest PC and PLS dimension with the minimum error rate is highlighted in yellow. The error rates associated with PC dimension containing at least 90, 95, 99, and 99.9% of the variance are highlighted in green, blue, purple and red, respectively.

Number of PCs for PCA & dimensions for PLS-DA	Error Rate (%) for HOO-CV with PCA reduced CVA (autoscaled)	Error Rate (%) with HOO-CV with PLS-DA
3	27.19	4.31
4	13.79	4.12
5	5.03	3.92
7	4.38	3.40
10	4.38	3.07
13	3.33	2.42
20	3.07	1.90
39	2.55	2.03
100	1.90	2.03
115	1.70	1.96
200	2.16	1.83

Table 102: Classification (window or container) error rates for HOO-CV PCA-CVA (autoscaled) and HOO-CV PLS-DA models with varying number of PCs or PLS dimensions for the all 153 glass second derivative (9-point smoothing) spectra (10 replicates). The smallest PC and PLS dimension with the minimum error rate is highlighted in yellow. The error rates associated with PC dimension containing at least 90, 95, 99, and 99.9% of the variance are highlighted in green, blue, purple and red, respectively.

Number of PCs for PCA & dimensions for PLS-DA	Error Rate (%) for HOO-CV with PCA reduced CVA (autoscaled)	Error Rate (%) with HOO-CV with PLS-DA
3	18.50	3.92
4	9.22	2.94
5	9.74	2.68
8	4.38	2.42
10	4.31	2.22
40	2.48	2.09
52	2.75	2.22
74	2.55	2.09
100	1.96	1.96
120	1.90	1.90
127	2.16	1.96
193	2.16	1.76

Table 103: Tempered classification error rates for HOO-CV PCA-CVA (autoscaled) and HOO-CV PLS-DA models with varying number of PCs or PLS dimensions for the 103 window glass second derivative (9-point smoothing) spectra (10 replicates). The smallest PC and PLS dimension with the minimum error rate is highlighted in yellow. The error rates associated with PC dimension containing at least 90, 95, 99, and 99.9% of the variance are highlighted in green, blue, purple and red, respectively.

Number of PCs for PCA & dimensions for PLS-DA	Error Rate (%) for HOO-CV with PCA reduced CVA (autoscaled)	Error Rate (%) with HOO-CV with PLS-DA
3	33.01	28.35
4	33.59	27.57
5	33.79	27.18
8	30.19	23.20
53	27.67	21.94
75	28.83	21.55
129	23.88	22.23
193	18.83	21.46
194	19.13	21.46

The discrimination and classification results with autoscaled PCA-CVA of the set of 153 glasses were fairly consistent with that from the preliminary set of 30 glasses, however there were some differences. When choosing the number of PCs for the full set of 153 glasses, 3 methods were used. The first was the same as for the original set of 30: the number of retained PCs (and thus variance) was determined by which number of PCs resulted in a minimum error rate. However, if too many PCs (and variance) are retained, then there is too much co-linearity retained in the data and this will cause the CVA model to fail. This prompted the use of more conservative approaches. The second method is used when there is an apparent plateau in the error rate, and from this the number of retained PCs (and variance) is chosen from the PC that begins the error rate plateau. This can be seen in Figures 94, 95, 97, and 98. The third method is when there is a sudden and sharp increase in error rate, and the number of retained PCs is chosen to be the PC immediately before the spike, as seen in Figure 96.

The lowest HOO-CV error rate for the discrimination of all 153 glasses was attained with PCA-CVA of the first derivative spectra (5-point smoothing, autoscaled), equaled 1.05%, and occurred first at PCA dimension 283 (100% variance). However, because this retains all of the variance, including all of the covariance, this error rate value is unreliable. Thus, a more conservative error rate of 4.44% occurring at 176 PCs (99.99% variance) was selected because it is at 176 PCs that the error rate plateau begins (Figure 94). The lowest HOO-CV error rate with PLS-DA of the first derivative spectra (5-point smoothing, autoscaled) equaled 42.22% with 100 PLS dimensions. The large discrepancy between the HOO-CV error rates could indicate that the PCA-CVA error rate is unreliable. The discrepancy could also show that PLS-DA is not an appropriate tool when attempting to make a many class model.

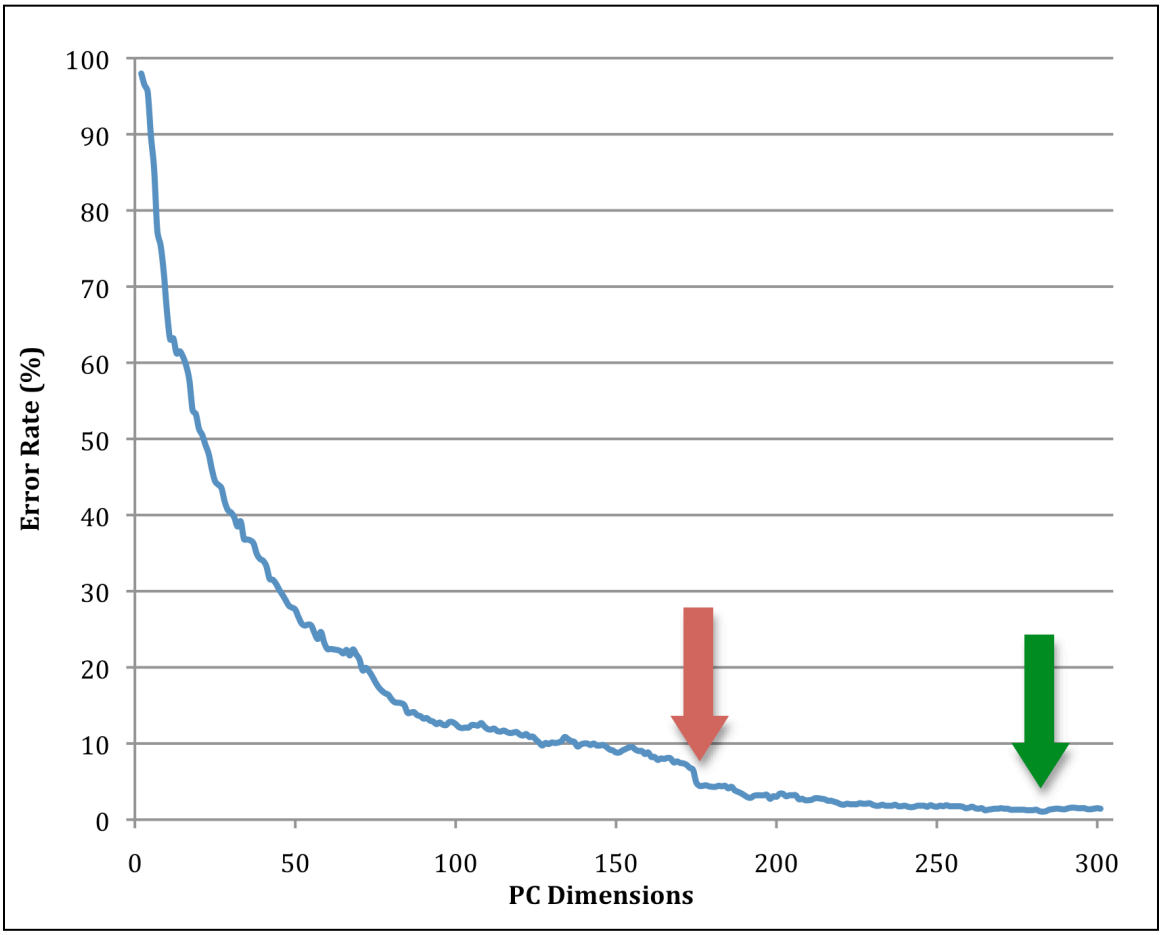


Figure 94: Graph of the discrimination error rate versus PC dimensions for HOO-CV with PCA reduced CVA for the set of 153 glass first derivative (5-point smoothing) spectra (10 replicates), autoscaled data. The green arrow points to the number of retained PC dimensions with the lowest error rate (283 PCs) while the red arrow points to the number of PC dimensions retained that begin a plateau (176 PCs).

The lowest HOO-CV error rate for the discrimination of 103 window glasses was attained with PCA-CVA of the first derivative spectra (5-point smoothing, autoscaled), equaled 1.65%, and occurred first at PCA dimension 241 (100% variance). However, because this retains all of the variance, similar to that for the discrimination of all glasses, this error rate value is not necessarily reliable. Thus, a more conservative error rate of 4.95% occurring at 182 PCs (99.99% variance) was selected because it is at 182 PCs that the error rate plateau begins (Figure 95). The lowest HOO-CV error rate with PLS-DA of the first derivative spectra (5-point

smoothing, autoscaled) equaled 20.78% with 241 PLS dimensions. The large discrepancy between the HOO-CV error rates could indicate either that the PCA-CVA error rate is unreliable or that PLS-DA is not useful for making a many class model.

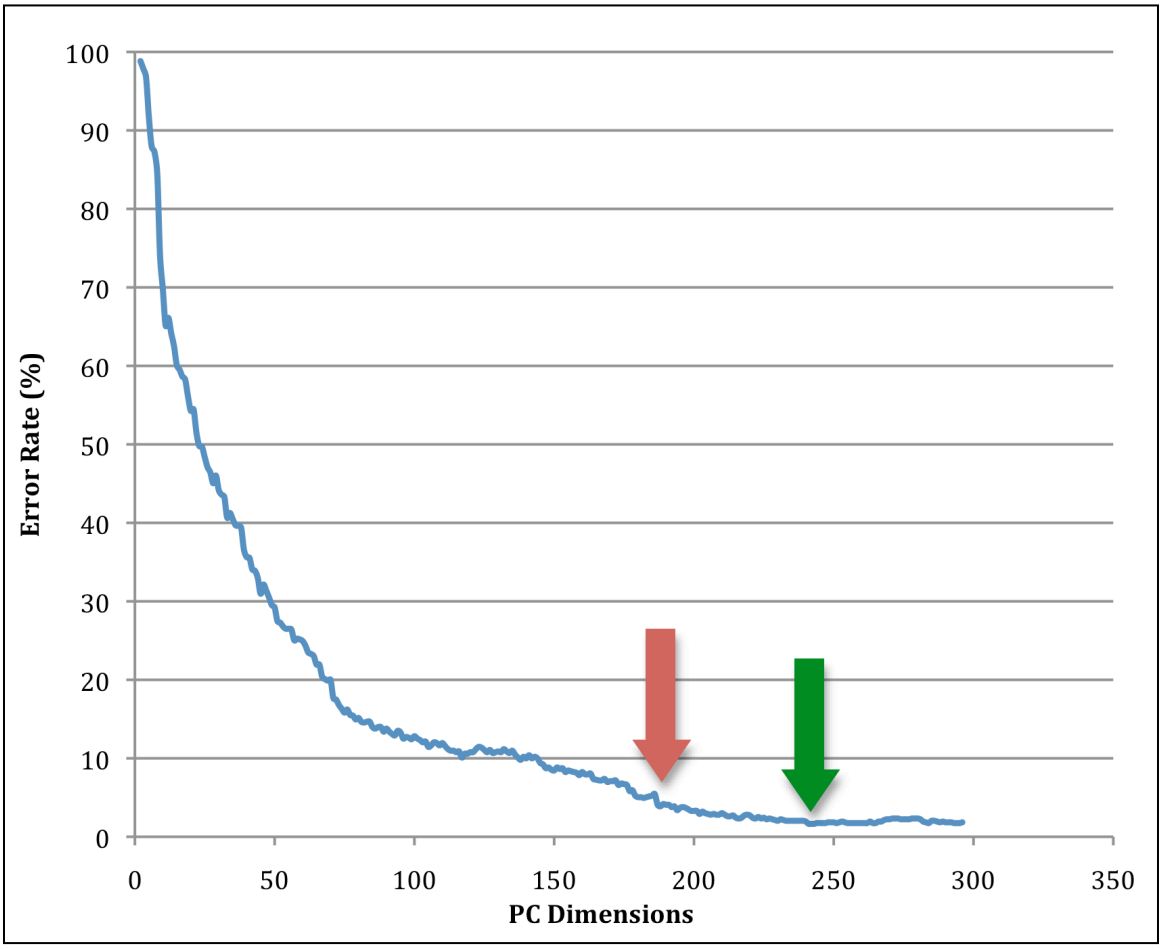


Figure 95: Graph of the discrimination error rate versus PC dimensions for HOO-CV with PCA reduced CVA for the set of 103 window glass first derivative (5-point smoothing) spectra (10 replicates), autoscaled data. The green arrow points to the number of retained PC dimensions with the lowest error rate (241 PCs) while the red arrow points to the number of PC dimensions retained that begin a plateau (182 PCs).

The lowest HOO-CV error rate for the discrimination of the 50 container glasses was attained with PCA-CVA of the first derivative spectra (5-point smoothing, autoscaled), equaled 1.2%, and occurred first at PCA dimension 245 (100% variance). However, because this retains

all of the variance, just like the previous discriminations, this error rate value is unreliable. Thus, a more conservative error rate of 6.8% occurring at 100 PCs (99.86% variance) was selected because it is immediately after 100 PCs that there is an error rate spike (Figure 96). The lowest HOO-CV error rate with PLS-DA of the first derivative spectra (5-point smoothing, autoscaled) equaled 19.6% with 182 PLS dimensions. The large discrepancy between the HOO-CV error rates could indicate that the PCA-CVA error rate is unreliable or that PLS-DA is not useful for making a many class model.

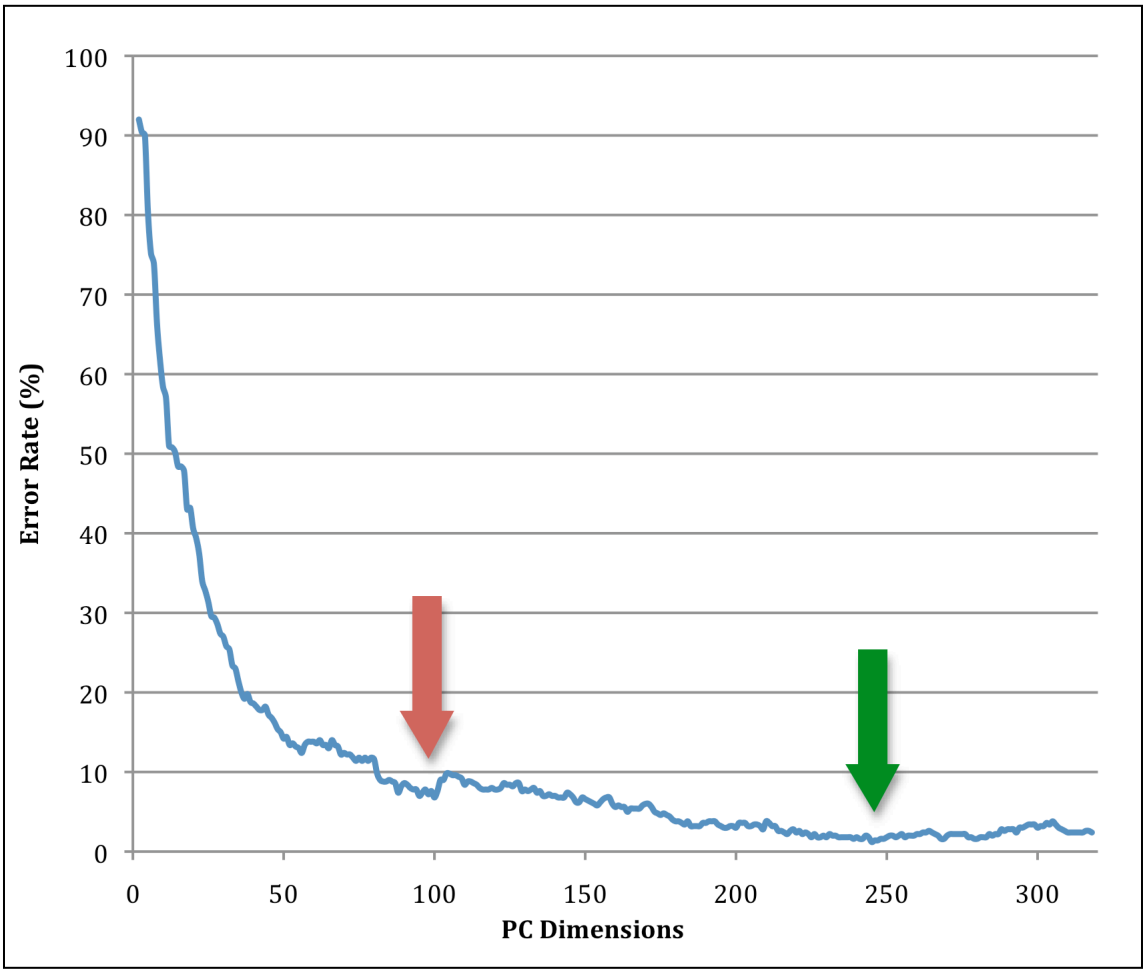


Figure 96: Graph of the discrimination error rate versus PC dimensions for HOO-CV with PCA reduced CVA for the set of 50 container glass first derivative (5-point smoothing) spectra (10 replicates), autoscaled data. The green arrow points to the number of retained PC dimensions with the lowest error rate (245 PCs) while the red arrow points to the number of PC dimensions retained that are immediately before an error rate spike (100 PCs).

The lowest HOO-CV error rate for the classification of 103 container glasses into the end-use categories of window or container glass was attained with PCA-CVA of the first derivative spectra (9-point smoothing, autoscaled), equaled 1.70%, and occurred first at PCA dimension 115 (100% variance). However, because this retains all of the variance, this error rate value is not necessarily reliable. Thus, a more conservative error rate of 1.83% occurring at 54 PCs (99.95% variance) was selected because it is at 54 PCs that the error rate plateau begins (Figure 97). The lowest HOO-CV error rate with PLS-DA of the first derivative spectra

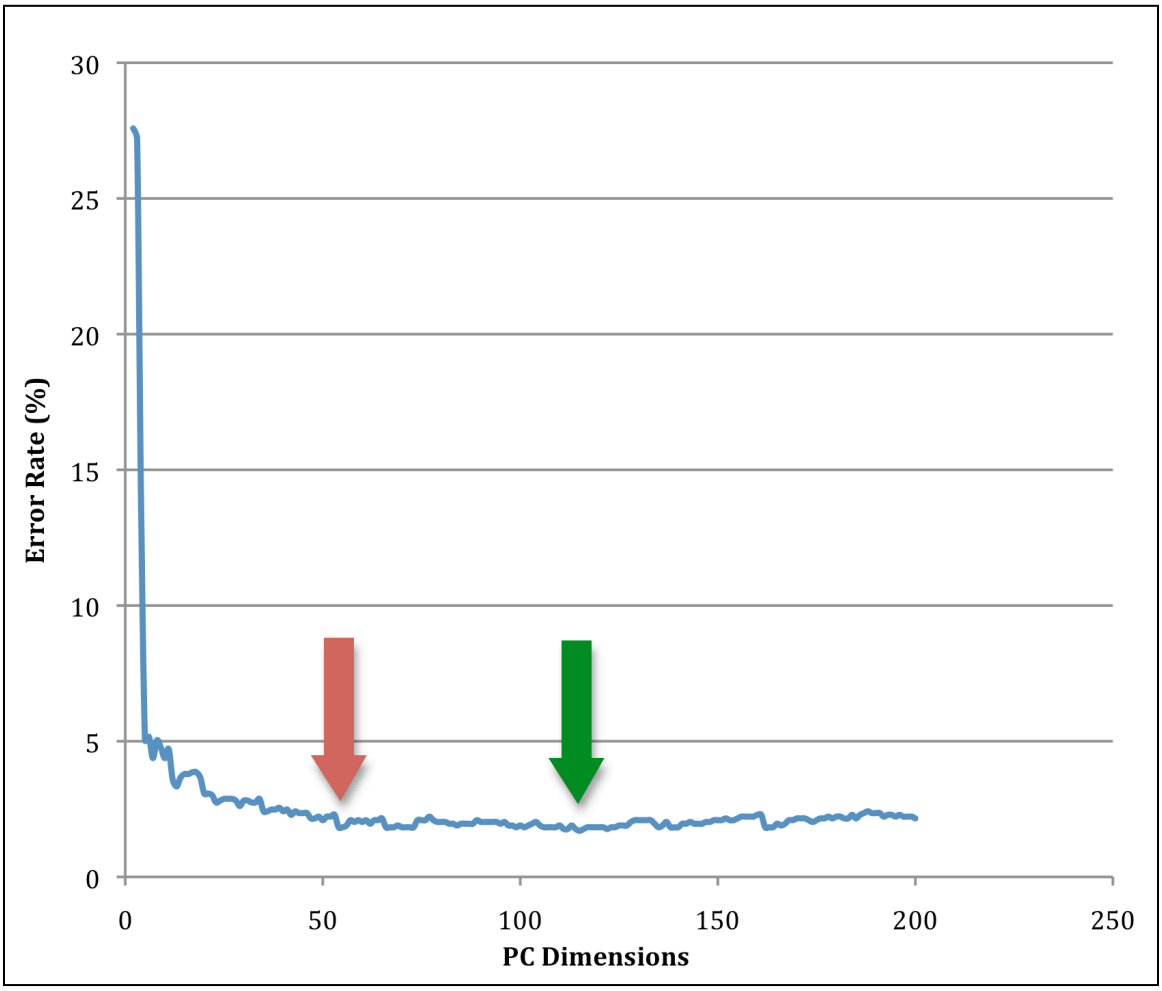


Figure 97: Graph of the classification (window or container) error rate versus PC dimensions for HOO-CV with PCA reduced CVA for the set of 103 container glass first derivative (9-point smoothing) spectra (10 replicates), autoscaled data. The green arrow points to the number of retained PC dimensions with the lowest error rate (115 PCs) while the red arrow points to the number of PC dimensions retained that that begin a plateau (54 PCs).

(9-point smoothing, autoscaled) was also equal to 1.83% with 200 PLS dimensions. The HOO-CV error rate for this classification was also investigated with the second derivative spectra (9-point smoothing, autoscaled), and resulted in a 1.90% error rate with 120 PCs (98.775% variance). A more conservative error rate, 2.48%, was also determined to be at 40 PCs (85.95% variance), which began the error rate plateau (Figure 98). The PLS-DA HOO-CV error rate for the second derivative spectra (9-point smoothing, autoscaled) was 1.76 with 193 PLS dimensions. The agreements between the HOO-CV error rates of PCA-CVA and PLS-DA for both derivatives strengthen the confidence in these models' error rate results.

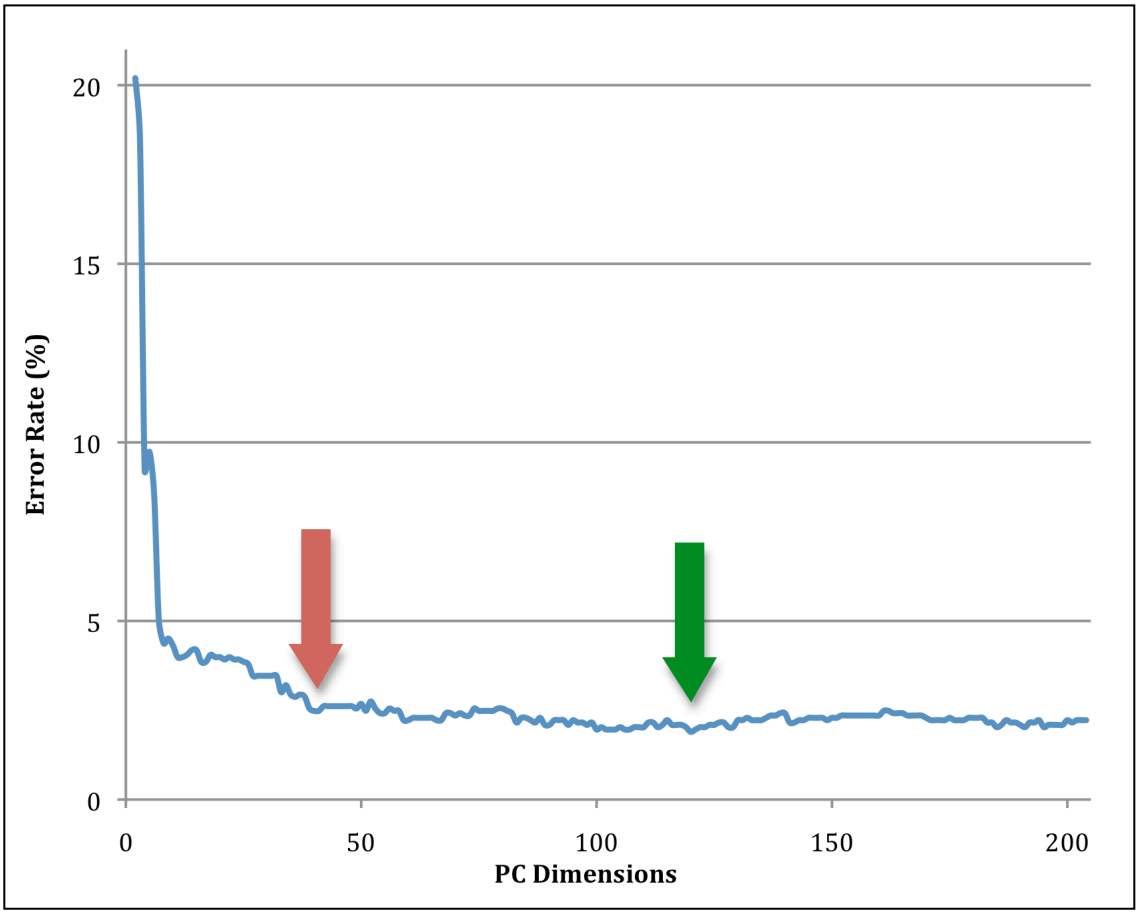


Figure 98: Graph of the classification (window or container) error rate versus PC dimensions for HOO-CV with PCA reduced CVA for the set of 103 container glass second derivative (9-point smoothing) spectra (10 replicates), autoscaled data. The green arrow points to the number of retained PC dimensions with the lowest error rate (120 PCs) while the red arrow points to the number of PC dimensions retained that that begin a plateau (40 PCs).

The lowest HOO-CV error rate for the classification of 103 window glasses into the manufacturing process categories of tempered or non-tempered was attained with PCA-CVA of the second derivative spectra (9-point smoothing, autoscaled), equaled 18.83%, and occurred first at PCA dimension 193 (99.898% variance). No conservative error rate was selected because of the already high error rate combined with the fact that there was neither a plateau nor an obvious spike (Figure 99). The lowest HOO-CV error rate with PLS-DA of the second derivative spectra (9-point smoothing, autoscaled) equaled 21.46% with 193 PLS dimensions. The agreement in error rates suggests that the models are reliable however the large error rates indicates that this is not a good method for tempered classification.

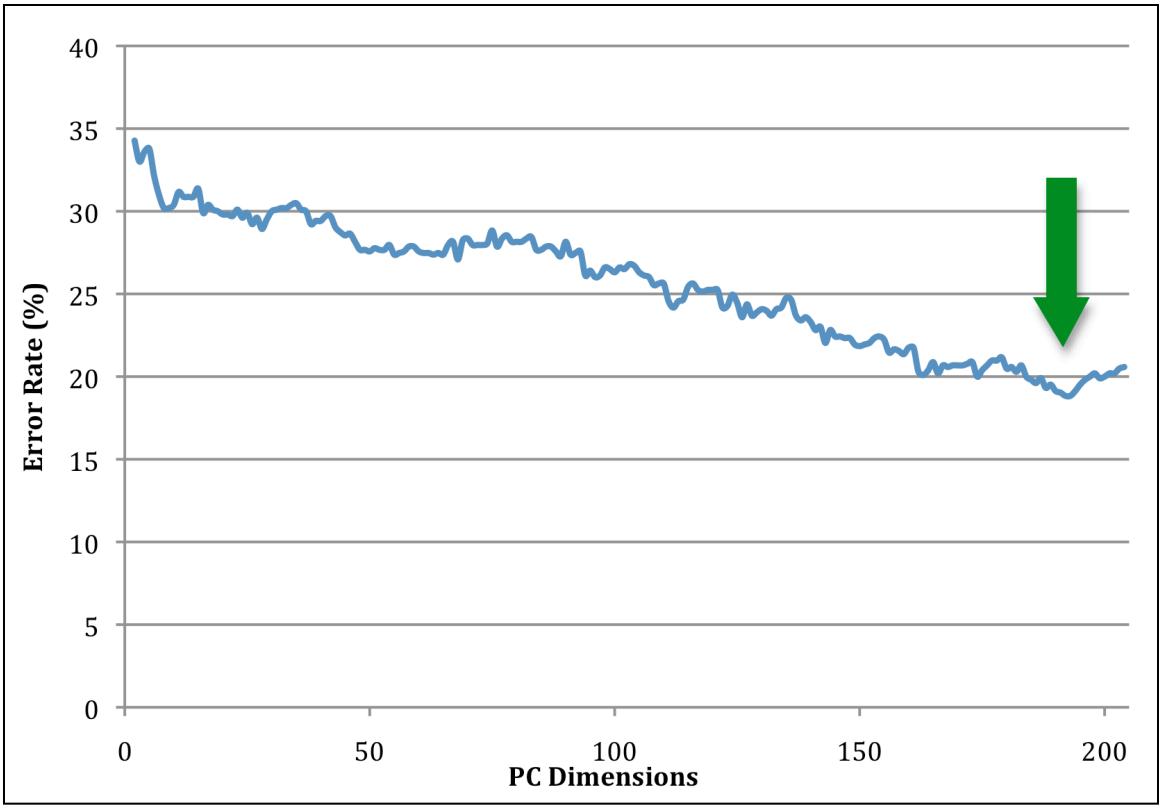


Figure 99: Graph of the classification (tempered or non-tempered) error rate versus PC dimensions for HOO-CV with PCA reduced CVA for the set of 103 container glass second derivative (9-point smoothing) spectra (10 replicates), autoscaled data. The green arrow points to the number of retained PC dimensions with the lowest error rate (193 PCs).

The results of the PCA analyses of the deconvolved data (peak positions and areas) of the first set of 30 glasses are in Appendix XIV. The deconvolved data was grouped into the same 3 sets of glasses that were used for the spectra and derivative spectra: 1) all glasses, 2) window glasses, and 3) container glasses. Also the same 3 additional data pretreatments were attempted: 1) none, 2) centering, and 3) autoscaling. Thus, a total of 9 PCA models were made which were used to help determine the number of PCs to keep for the PCA- CVA discrimination and classification models.

The results of the HOO-CV PCA-CVA for the deconvolved data (peak positions and areas) are compared to the error rates for HOO-CV PLS-DA, in Tables 104 – 110. Tables 104 - 110 contain the HOO-CV error rates for the PCA-CVA (no pretreatment, centered, autoscaled) and PLS-DA models made from the 7 different classification or discrimination groups.

Table 104: Discrimination error rates for HOO-CV PCA-CVA (no pretreatment, centered and autoscaled) and HOO-CV PLS-DA models with 2 - 12 PCs or PLS dimensions for the first set of 30 glass deconvolution data (10 replicates). The smallest PC and PLS dimension with the minimum error rate is highlighted in yellow. The error rates associated with PC dimension containing at least 90, 95, 99, and 99.9% of the variance are highlighted in green, blue, purple and red, respectively.

Number of PCs for PCA & Dimensions for PLS-DA	Error Rate (%) for HOO-CV with PCA reduced CVA (no pretreatment)	Error Rate (%) for HOO-CV with PCA reduced CVA (centered)	Error Rate (%) for HOO-CV with PCA reduced CVA (autoscaled)	Error Rate (%) with HOO-CV with PLS-DA
2	95	98	94	95.33
3	94	97	86.67	92.33
4	90.33	88.33	84.67	87.67
5	86.67	84.33	82	87
6	78.67	76.67	78.67	87
7	75.67	75.33	72.33	84
8	71.33	71.33	68.33	83.67
9	65.67	67.33	65.67	79
10	63.67	63.33	63	77
11	61.67	59.67	61	76
12	59	59	59	74.67

Table 105: Classification (automotive, architectural, or container) error rates for HOO-CV PCA-CVA (no pretreatment, centered and autoscaled) and HOO-CV PLS-DA models with 2 - 12 PCs or PLS dimensions for the first set of 30 glass deconvolution data (10 replicates). The smallest PC and PLS dimension with the minimum error rate is highlighted in yellow. The error rates associated with PC dimension containing at least 90, 95, 99, and 99.9% of the variance are highlighted in green, blue, purple and red, respectively.

Number of PCs for PCA & Dimensions for PLS-DA	Error Rate (%) for HOO-CV with PCA reduced CVA (no pretreatment)	Error Rate (%) for HOO-CV with PCA reduced CVA (centered)	Error Rate (%) for HOO-CV with PCA reduced CVA (autoscaled)	Error Rate (%) with HOO-CV with PLS-DA
2	59	54.33	43.33	41
3	47.67	47.33	42.67	37.33
4	50.67	45	42.67	36.33
5	43.67	44.33	43	31.67
6	40.67	38	35.67	32
7	35.33	35.33	33.67	32.67
8	34.33	34	33	31
9	35.33	33	34.67	30.67
10	30.67	30.67	33.67	30.67
11	31.33	31	30	30.33
12	31	31	31	30.33

Table 106: Classification (window or container) error rates for HOO-CV PCA-CVA (no pretreatment, centered and autoscaled) and HOO-CV PLS-DA models with 2 - 12 PCs or PLS dimensions for the first set of 30 glass deconvolution data (10 replicates). The smallest PC and PLS dimension with the minimum error rate is highlighted in yellow. The error rates associated with PC dimension containing at least 90, 95, 99, and 99.9% of the variance are highlighted in green, blue, purple and red, respectively.

Number of PCs for PCA & Dimensions for PLS-DA	Error Rate (%) for HOO-CV with PCA reduced CVA (no pretreatment)	Error Rate (%) for HOO-CV with PCA reduced CVA (centered)	Error Rate (%) for HOO-CV with PCA reduced CVA (autoscaled)	Error Rate (%) with HOO-CV with PLS-DA
2	30.67	26	17.67	8.33
3	22.67	27.33	11.67	8
4	24.33	16.67	11.67	7
5	14	15	12.67	8
6	10	10.67	7.67	7.33
7	10.33	10.33	7.67	8
8	10	9.3	7.33	8
9	7	6.67	7	8
10	7	7	8.33	8
11	8	7.33	7.33	8
12	7.67	7.67	7.67	8

Table 107: Discrimination error rates for HOO-CV PCA-CVA (no pretreatment, centered and autoscaled) and HOO-CV PLS-DA models with 2 - 12 PCs or PLS dimensions for the first set of 20 window glass deconvolution data (10 replicates). The smallest PC and PLS dimension with the minimum error rate is highlighted in yellow. The error rates associated with PC dimension containing at least 90, 95, 99, and 99.9% of the variance are highlighted in green, blue, purple and red, respectively.

Number of PCs for PCA & Dimensions for PLS-DA	Error Rate (%) for HOO-CV with PCA reduced CVA (no pretreatment)	Error Rate (%) for HOO-CV with PCA reduced CVA (centered)	Error Rate (%) for HOO-CV with PCA reduced CVA (autoscaled)	Error Rate (%) with HOO-CV with PLS-DA
2	95	100	90.5	92
3	95	94.5	89	88.5
4	88.5	88	88.5	87
5	84	85	84	86
6	78.5	81	81	84.5
7	78.5	77	79.5	84
8	71	72	70.5	79.5
9	67.5	68	68	76.5
10	68	63	65	71.5
11	59.5	58	59	68
12	56	56	56	67

Table 108: Discrimination error rates for HOO-CV PCA-CVA (no pretreatment, centered and autoscaled) and HOO-CV PLS-DA models with 2 - 12 PCs or PLS dimensions for the first set of 10 container glass deconvolution data (10 replicates). The smallest PC and PLS dimension with the minimum error rate is highlighted in yellow. The error rates associated with PC dimension containing at least 90, 95, 99, and 99.9% of the variance are highlighted in green, blue, purple and red, respectively.

Number of PCs for PCA & Dimensions for PLS-DA	Error Rate (%) for HOO-CV with PCA reduced CVA (no pretreatment)	Error Rate (%) for HOO-CV with PCA reduced CVA (centered)	Error Rate (%) for HOO-CV with PCA reduced CVA (autoscaled)	Error Rate (%) with HOO-CV with PLS-DA
2	80	90	84	89
3	79	79	84	78
4	75	72	72	75
5	76	76	69	65
6	69	72	66	61
7	65	64	60	63
8	66	62	64	66
9	61	62	61	62
10	61	62	55	64
11	59	59	61	64
12	59	59	59	62

Table 109: Float classification error rates for HOO-CV PCA-CVA (no pretreatment, centered and autoscaled) and HOO-CV PLS-DA models with 2 - 12 PCs or PLS dimensions for the first set of 30 glass deconvolution data (10 replicates). The smallest PC and PLS dimension with the minimum error rate is highlighted in yellow. The error rates associated with PC dimension containing at least 90, 95, 99, and 99.9% of the variance are highlighted in green, blue, purple and red, respectively.

Number of PCs for PCA & Dimensions for PLS-DA	Error Rate (%) for HOO-CV with PCA reduced CVA (no pretreatment)	Error Rate (%) for HOO-CV with PCA reduced CVA (centered)	Error Rate (%) for HOO-CV with PCA reduced CVA (autoscaled)	Error Rate (%) with HOO-CV with PLS-DA
2	41	37.5	11	10.5
3	39.5	12.5	11.5	10
4	12	12	11.5	10.5
5	11	10.5	10.5	10
6	12	11.5	10	10
7	11.5	11.5	10.5	9.5
8	10.5	10.5	10	9
9	11.5	10.5	10.5	9
10	10	8.5	11	9.5
11	9	9.5	10	9.5
12	9.5	9.5	9.5	9.5

Table 110: Tempered classification error rates for HOO-CV PCA-CVA (no pretreatment, centered and autoscaled) and HOO-CV PLS-DA models with 2 - 12 PCs or PLS dimensions for the first set of 30 glass deconvolution data (10 replicates). The smallest PC and PLS dimension with the minimum error rate is highlighted in yellow. The error rates associated with PC dimension containing at least 90, 95, 99, and 99.9% of the variance are highlighted in green, blue, purple and red, respectively.

Number of PCs for PCA & Dimensions for PLS-DA	Error Rate (%) for HOO-CV with PCA reduced CVA (no pretreatment)	Error Rate (%) for HOO-CV with PCA reduced CVA (centered)	Error Rate (%) for HOO-CV with PCA reduced CVA (autoscaled)	Error Rate (%) with HOO-CV with PLS-DA
2	40.5	40	37.5	29
3	39.5	38	37.5	29.5
4	33	37.5	35.5	28
5	30	35	31	27.5
6	32	29	31	29.5
7	30.5	29.5	32	29
8	31	30	27.5	29
9	29.5	31.5	28	29
10	30	32	28	29
11	29	28	29.5	29
12	29	29	29	29

The discrimination and classification error rates with HOO-CV PCA-CVA of the deconvolved data (peak positions and areas) were higher than those of the derivative spectra. This indicates that better chemometric classification and discrimination occurs when derivatives of the mid-IR spectra of glasses are computed rather than when the spectra are deconvolved. The only exception to this was for the classification into the manufacturing process categories of float or non-float, which had an 8.5% error rate with centered PCA-CVA that occurred with 10 PCs (99.97% variance). The lowest HOO-CV error rate with PLS-DA of the deconvolution data equaled 9% with 8 PLS dimensions. This agreement in error rates suggests that the float classification models are reliable.

The results of the PCA analyses of the two sets of glasses with nominally similar RIs are in Appendix XV. Three PCA models, all autoscaled, were made for each of these sets: 1) the unprocessed spectra 2) the first derivative spectra (5-point smoothing), 3) the second derivative spectra (5-point smoothing). Knowledge of the percentage of variance contained in the PCs was then used to help determine the number of PCs to keep for the PCA- CVA discrimination and classification models.

The results of the HOO-CV of the PCA-CVA models of the two sets of glasses with nominally similar RIs are in Appendix XVI. The results, in tables and graphs, show the error rates for each of the models when keeping different numbers of PC dimensions. These results are compared to the error rates for HOO-CV PLS-DA, in Tables 111 – 116.

Table 111: Discrimination error rates for HOO-CV PCA-CVA (autoscaled) and HOO-CV PLS-DA models with varying number of PCs or PLS dimensions for the spectra (10 replicates) of 21 glasses with nominally similar RIs (same RI set 1). The smallest PC and PLS dimension with the minimum error rate is highlighted in yellow. The error rates associated with PC dimension containing at least 95, 99, and 99.9% of the variance are highlighted in blue, purple and red, respectively.

# of PCs for PCA & dimensions for PLS-DA	Error Rate (%) for HOO-CV with PCA reduced CVA (autoscaled)	Error Rate (%) with HOO-CV with PLS-DA
3	88.10	89.52
4	85.24	91.43
5	82.86	85.24
8	79.05	78.57
30	30	47.62
32	28.57	47.62
97	21.90	38.10
163	31.90	44.29

Table 112: Discrimination error rates for HOO-CV PCA-CVA (autoscaled) and HOO-CV PLS-DA models with varying number of PCs or PLS dimensions for the spectra (10 replicates) of 30 glasses with nominally similar RIs (same RI set 2). The smallest PC and PLS dimension with the minimum error rate is highlighted in yellow. The error rates associated with PC dimension containing at least 95, 99, and 99.9% of the variance are highlighted in blue, purple and red, respectively.

# of PCs for PCA & dimensions for PLS-DA	Error Rate (%) for HOO-CV with PCA reduced CVA (autoscaled)	Error Rate (%) with HOO-CV with PLS-DA
3	93	94.67
4	93.67	93.67
5	93.33	94.67
9	89.33	90.33
31	37.67	60
97	23.67	37
170	19.33	42.33

Table 113: Discrimination error rates for HOO-CV PCA-CVA (autoscaled) and HOO-CV PLS-DA models with varying number of PCs or PLS dimensions for the first derivative spectra (5-point smoothing) (10 replicates) of 21 glasses with nominally similar RIs (same RI set 1). The smallest PC and PLS dimension with the minimum error rate is highlighted in yellow. The error rates associated with PC dimension containing at least 90, 95, 99, and 99.9% of the variance are highlighted in green, blue, purple and red, respectively.

# of PCs for PCA & dimensions for PLS-DA	Error Rate (%) for HOO-CV with PCA reduced CVA (autoscaled)	Error Rate (%) with HOO-CV with PLS-DA
3	91.42	90.48
4	89.53	83.81
5	81.90	80.48
6	80.48	76.19
10	61.90	73.81
39	28.10	30.95
94	17.14	30.95
97	18.57	33.33
150	32.38	41.90

Table 114: Discrimination error rates for HOO-CV PCA-CVA (autoscaled) and HOO-CV PLS-DA models with varying number of PCs or PLS dimensions for the first derivative spectra (5-point smoothing) (10 replicates) of 30 glasses with nominally similar RIs (same RI set 2). The smallest PC and PLS dimension with the minimum error rate is highlighted in yellow. The error rates associated with PC dimension containing at least 90, 95, 99, and 99.9% of the variance are highlighted in green, blue, purple and red, respectively.

# of PCs for PCA & dimensions for PLS-DA	Error Rate (%) for HOO-CV with PCA reduced CVA (autoscaled)	Error Rate (%) with HOO-CV with PLS-DA
3	92.33	95.33
4	92.33	94.67
5	93	92
6	89.33	85.67
11	74	85.33
43	39.33	41.33
107	16	29.33
150	21.33	29.67

Table 115: Discrimination error rates for HOO-CV PCA-CVA (autoscaled) and HOO-CV PLS-DA models with varying number of PCs or PLS dimensions for the second derivative spectra (5-point smoothing) (10 replicates) of 21 glasses with nominally similar RIs (same RI set 1). The smallest PC and PLS dimension with the minimum error rate is highlighted in yellow. The error rates associated with PC dimension containing at least 90, 95, 99, and 99.9% of the variance are highlighted in green, blue, purple and red, respectively.

# of PCs for PCA & dimensions for PLS-DA	Error Rate (%) for HOO-CV with PCA reduced CVA (autoscaled)	Error Rate (%) with HOO-CV with PLS-DA
3	74.76	88.57
4	72.86	80.95
5	70.95	80.48
42	25.24	22.86
69	18.57	28.57
85	12.38	30.48
90	15.24	30
132	25.71	30.96
175	44.76	40.86

Table 116: Discrimination error rates for HOO-CV PCA-CVA (autoscaled) and HOO-CV PLS-DA models with varying number of PCs or PLS dimensions for the second derivative spectra (5-point smoothing) (10 replicates) of 30 glasses with nominally similar RIs (same RI set 2). The smallest PC and PLS dimension with the minimum error rate is highlighted in yellow. The error rates associated with PC dimension containing at least 90, 95, 99, and 99.9% of the variance are highlighted in green, blue, purple and red, respectively.

# of PCs for PCA & dimensions for PLS-DA	Error Rate (%) for HOO-CV with PCA reduced CVA (autoscaled)	Error Rate (%) with HOO-CV with PLS-DA
3	85.67	95
4	84.00	91.33
5	79.67	92.67
26	33.33	49.67
79	23.67	33.67
98	19.33	34.33
102	20.00	35.67
149	21.00	35.67
203	22.33	41.67

The PCA-CVA and PLS-DA HOO-CV error rates for the discrimination of glasses with nominally similar RIs were fairly high for both sets of glasses and with all 3 pretreatment schemes. Consistent with the previous discrimination results, the derivative spectra had lower HOO-CV error rates than the unprocessed spectra.

The minimum PCA-CVA HOO-CV error rates for the autoscaled spectra were 21.90% (97 PCs, 100% variance) and 19.33% (170 PCs, 100% variance) for sets 1 and 2, respectively. Because these both retain all of the variance, and thus all of the covariance, these error rates could be unreliable. The corresponding minimum PLS-DA HOO-CV error rates were 38.10% (97 PLS dimensions) and 37% (97 PLS dimensions). The lowest PCA-CVA HOO-CV error rates for the autoscaled first derivative spectra (5-point smoothing) were 17.14% (94 PCs, 99.887% variance) and 16% (107 PCs, 99.901% variance) for sets 1 and 2, respectively. Again, these PCA-CVA models retain a large amount of the variance, thus making these error rates not necessarily reliable. The corresponding minimum PLS-DA HOO-CV error rates were 30.95% (39 PLS dimensions) and 29.33% (107 PLS dimensions). The minimum PCA-CVA HOO-CV error rates for the autoscaled second derivative spectra (5-point smoothing) were 12.38% (85 PCs, 94.143% variance) and 19.33% (98 PCs, 94.386% variance) for sets 1 and 2, respectively. The corresponding minimum PLS-DA HOO-CV error rates were 22.86% (42 PLS dimensions) and 33.67% (79 PLS dimensions).

The lowest error rate for discriminating between glasses with nominally similar RIs was achieved with the second derivative (5-point smoothing) preprocessing for set 1 (12.38%), but with the first derivative (5-point smoothing) preprocessing for set 2 (16%). Thus, there was no clear preprocessing scheme that provides better discrimination for glasses with the same RIs.

In addition, the HOO-CV error rate uses only 1 spectrum for comparison with the learning set, as might be observed when there is only 1 spectrum collected and/or 1 recovered glass fragment. It is likely that the error rate would decrease if multiple spectra were compared. Consequently, the error rates alone do not provide a complete picture of the discriminating power of this method. Tables 117, 119, 121, and 123 show the confusion matrices and Tables 118, 120, 122, and 124 provide the overall statistics of the HOO-CV PCA-CVA results for both sets of derivative spectra (using the number of PCs with the lowest error rate) from the glasses with nominally similar RIs.

The confusion matrices visually show the performance of the HOO-CV PCA-CVA models. Each row represents the predicted identity of the held-out sample while the columns show the actual identity. The number in each row shows the amount of times the test algorithm placed the held-out sample in a given class (column). Thus, if all 10 replicates for all samples were correctly identified, then every cell in the diagonal would have a "10".

The statistics calculated include the sensitivity, the specificity, the positive prediction value, the negative prediction value, the prevalence, the detection rate and the detection prevalence. The sensitivity, also called the true positive rate, is the probability that the test indicates an inclusion (t+) given that an association truly exists (S+), or Pr(t+|S+). The false negative or Type II error rate is equal to 1 – the sensitivity. The specificity, also called the true negative rate, is the probability that the test indicates an exclusion (t-) given that there is no association (S-), or Pr(t-|S-). The false positive or Type I error rate is equal to 1 – the specificity. The positive prediction value is the probability that an association truly exists given the test indicates an inclusion, or Pr(S+|t+). The negative prediction value is the probability that an association truly does not exists given the test indicates an exclusion (t-), or Pr(S-|t-). The

prevalence is the ratio of the number of samples in a specific glass to the total number of samples in the population. Thus, for set 1 (21 different glasses and 10 spectra collected for each glass), the prevalence is equal to 10 ÷ 210 = 0.04286, and for set 2 (30 different glasses and 10 spectra collected for each glass), the prevalence is equal to 10 ÷ 300 = 0.03333). The detection rate is the ratio of the number of times the test makes the correct inclusion to the total number of possible associations. The detection prevalence is the ratio of the number of times the test indicates inclusion to the total number of possible associations. (N.D.K. Petraco, 2011).

Table 117: Confusion matrix for the HOO-CV PCA-CVA results for the first derivative spectra (5-point smoothing, autoscaled) with 94 PCs of same RI set 1.

		Reference																				
		W23	W33	W49	W62	W79	W83	W95	W103	W107	W129	W132	W142	W143	W152	W153	W165	W174	W193	W204	W206	W232
Prediction	W23	10	0	0	0	0	0	0	0	0	0	0	0	0	0	0	0	0	0	0	0	0
	W33	0	10	0	0	0	0	0	0	0	0	0	0	0	0	0	0	0	0	0	0	0
	W49	0	0	8	0	0	0	0	0	0	0	1	0	0	0	0	0	0	0	0	0	1
	W62	0	0	0	10	0	0	0	0	0	0	0	0	0	0	0	0	0	0	0	0	0
	W79	0	0	0	0	9	0	0	0	0	0	0	0	0	0	0	0	0	0	0	0	0
	W83	0	0	0	0	0	8	1	0	0	1	0	0	0	0	0	0	0	0	0	0	0
	W95	0	0	2	0	0	2	7	1	1	4	0	0	0	0	0	0	1	0	0	0	0
	W103	0	0	0	0	0	0	0	8	0	0	1	0	0	0	0	0	0	0	0	0	1
	W107	0	0	0	0	0	0	0	0	7	0	0	0	1	0	0	0	0	0	0	0	0
	W129	0	0	0	0	0	0	1	0	1	5	0	0	0	0	0	0	0	0	0	0	0
	W132	0	0	0	0	0	0	1	0	0	0	4	0	2	0	0	0	0	0	0	0	0
	W142	0	0	0	0	1	0	0	0	1	0	0	10	0	0	0	0	0	0	0	1	0
	W143	0	0	0	0	0	0	0	0	0	0	2	0	6	1	0	0	0	0	0	0	0
	W152	0	0	0	0	0	0	0	0	0	0	0	0	0	8	0	0	0	0	0	2	0
	W153	0	0	0	0	0	0	0	0	0	0	0	0	0	0	10	0	0	0	0	0	0
	W165	0	0	0	0	0	0	0	0	0	0	0	0	0	0	0	10	0	0	0	0	0
	W174	0	0	0	0	0	0	0	0	0	0	1	0	0	0	0	0	9	0	0	0	0
	W193	0	0	0	0	0	0	0	0	0	0	0	0	0	0	0	0	0	10	0	0	0
	W204	0	0	0	0	0	0	0	0	0	0	0	0	0	0	0	0	0	0	10	0	0
	W206	0	0	0	0	0	0	0	0	0	0	1	0	1	1	0	0	0	0	0	7	0
	W232	0	0	0	0	0	0	0	1	0	0	0	0	0	0	0	0	0	0	0	0	8

Table 118: The HOO-CV PCA-CVA overall statistics for the first derivative spectra (5-point smoothing, autoscaled) with 94 PCs of same RI set 1.

Overall Statistics						
Accuracy:	0.8286					
95% CI:	(0.7707, 0.877)					
Statistic by Class						
Glass Identity	W23	W33	W49	W62	W79	
Sensitivity	1	1	0.8	1	0.9	
Specificity	1	1	0.99	1	1	
Pos Pred Value	1	1	0.8	1	1	
Neg Pred Value	1	1	0.99	1	0.99502	
Prevalence	0.04762	0.04762	0.04762	0.04762	0.04762	
Detection Rate	0.04762	0.04762	0.0381	0.04762	0.04286	
Detection Prevalence	0.04762	0.04762	0.04762	0.04762	0.04286	
Glass Identity	W83	W95	W103	W107	W129	
Sensitivity	0.8	0.7	0.8	0.7	0.5	
Specificity	0.99	0.945	0.99	0.995	0.99	
Pos Pred Value	0.8	0.38889	0.8	0.875	0.71429	
Neg Pred Value	0.99	0.98438	0.99	0.98515	0.97537	
Prevalence	0.04762	0.04762	0.04762	0.04762	0.04762	
Detection Rate	0.0381	0.03333	0.0381	0.03333	0.02381	
Detection Prevalence	0.04762	0.08571	0.04762	0.0381	0.03333	
Glass Identity	W132	W142	W143	W152	W153	
Sensitivity	0.4	1	0.6	0.8	1	
Specificity	0.985	0.985	0.985	0.99	1	
Pos Pred Value	0.57143	0.76923	0.66667	0.8	1	
Neg Pred Value	0.97044	1	0.9801	0.99	1	
Prevalence	0.04762	0.04762	0.04762	0.04762	0.04762	
Detection Rate	0.01905	0.04762	0.02857	0.0381	0.04762	
Detection Prevalence	0.03333	0.0619	0.04286	0.04762	0.04762	
Glass Identity	W165	W174	W193	W204	W206	W232
Sensitivity	1	0.9	1	1	0.7	0.8
Specificity	1	0.995	1	1	0.985	0.995
Pos Pred Value	1	0.9	1	1	0.7	0.88889
Neg Pred Value	1	0.995	1	1	0.985	0.99005
Prevalence	0.04762	0.04762	0.04762	0.04762	0.04762	0.04762
Detection Rate	0.04762	0.04286	0.04762	0.04762	0.03333	0.0381
Detection Prevalence	0.04762	0.04762	0.04762	0.04762	0.04762	0.04286

Table 119: Confusion matrix for the HOO-CV PCA-CVA results for the second derivative spectra (5-point smoothing, autoscaled) with 85 PCs of same RI set 1.

		Reference																				
		W23	W33	W49	W62	W79	W83	W95	W103	W107	W129	W132	W142	W143	W152	W153	W165	W174	W193	W204	W206	W232
Prediction	W23	9	0	0	0	0	0	0	0	0	0	0	0	0	0	0	0	0	0	0	0	0
	W33	0	10	0	0	0	0	0	0	0	0	0	0	0	0	0	0	0	0	0	0	0
	W49	1	0	9	0	0	0	0	0	0	0	0	0	0	0	0	0	0	0	0	0	0
	W62	0	0	0	9	0	0	0	0	0	0	0	0	0	0	0	0	0	0	0	0	0
	W79	0	0	1	0	10	0	0	0	0	0	0	1	0	0	0	0	0	0	0	0	0
	W83	0	0	0	0	0	8	0	0	0	0	0	0	0	0	0	0	0	0	0	0	0
	W95	0	0	0	0	0	1	6	0	2	1	0	0	0	0	0	0	0	0	0	0	0
	W103	0	0	0	0	0	0	0	7	0	0	0	0	1	0	0	0	0	0	0	0	0
	W107	0	0	0	0	0	1	1	0	7	0	1	1	0	0	0	0	0	0	0	0	0
	W129	0	0	0	0	0	0	1	1	1	7	1	0	0	0	0	0	0	0	0	0	0
	W132	0	0	0	0	0	0	0	0	0	0	7	0	0	0	0	0	0	0	0	0	0
	W142	0	0	0	1	0	0	1	0	0	1	0	8	0	0	0	0	0	0	0	0	0
	W143	0	0	0	0	0	0	1	1	0	1	0	0	9	0	0	0	0	0	0	0	0
	W152	0	0	0	0	0	0	0	0	0	0	0	0	0	10	0	0	0	1	0	0	0
	W153	0	0	0	0	0	0	0	0	0	0	0	0	0	0	10	0	0	0	0	0	0
	W165	0	0	0	0	0	0	0	0	0	0	0	0	0	0	0	10	0	0	0	0	0
	W174	0	0	0	0	0	0	0	0	0	0	0	0	0	0	0	0	10	0	0	0	0
	W193	0	0	0	0	0	0	0	0	0	0	1	0	0	0	0	0	0	9	0	0	0
	W204	0	0	0	0	0	0	0	0	0	0	0	0	0	0	0	0	0	0	10	0	0
	W206	0	0	0	0	0	0	0	0	0	0	0	0	0	0	0	0	0	0	0	9	0
	W232	0	0	0	0	0	0	0	1	0	0	0	0	0	0	0	0	0	0	0	1	10

Table 120: The HOO-CV PCA-CVA overall statistics for the second derivative spectra (5-point smoothing, autoscaled) with 85 PCs of same RI set 1.

Overall Statistics						
Accuracy:	0.8762					
95% CI:	(0.9239, 0.9175)					
Statistic by Class						
Glass Identity	W23	W33	W49	W62	W79	
Sensitivity	0.9	1	0.9	0.9	1	
Specificity	1	1	0.995	1	0.99	
Pos Pred Value	1	1	0.9	1	0.83333	
Neg Pred Value	0.99502	1	0.995	0.99502	1	
Prevalence	0.04762	0.04762	0.04762	0.04762	0.04762	
Detection Rate	0.04286	0.04762	0.04286	0.04286	0.04762	
Detection Prevalence	0.04286	0.04762	0.04762	0.04286	0.05714	
Glass Identity	W83	W95	W103	W107	W129	
Sensitivity	0.8	0.6	0.7	0.7	0.7	
Specificity	1	0.98	0.995	0.98	0.98	
Pos Pred Value	1	0.6	0.875	0.63636	0.63636	
Neg Pred Value	0.9901	0.98	0.98515	0.98492	0.98492	
Prevalence	0.04762	0.04762	0.04762	0.04762	0.04762	
Detection Rate	0.0381	0.02857	0.03333	0.03333	0.03333	
Detection Prevalence	0.0381	0.04762	0.0381	0.05238	0.05238	
Glass Identity	W132	W142	W143	W152	W153	
Sensitivity	0.7	0.8	0.9	1	1	
Specificity	1	0.985	0.985	0.995	1	
Pos Pred Value	1	0.72727	0.75	0.90909	1	
Neg Pred Value	0.98522	0.98995	0.99495	1	1	
Prevalence	0.04762	0.04762	0.04762	0.04762	0.04762	
Detection Rate	0.03333	0.0381	0.04286	0.04762	0.04762	
Detection Prevalence	0.03333	0.05238	0.05714	0.05238	0.04762	
Glass Identity	W165	W174	W193	W204	W206	W232
Sensitivity	1	1	0.9	1	0.9	1
Specificity	1	1	0.995	1	1	0.99
Pos Pred Value	1	1	0.9	1	1	0.83333
Neg Pred Value	1	1	0.995	1	0.99502	1
Prevalence	0.04762	0.04762	0.04762	0.04762	0.04762	0.04762
Detection Rate	0.04762	0.04762	0.04286	0.04762	0.04286	0.04762
Detection Prevalence	0.04762	0.04762	0.04762	0.04762	0.04286	0.05714

Table 121: Confusion matrix for the HOO-CV PCA-CVA results for the first derivative spectra (5-point smoothing, autoscaled) with 107 PCs of same RI set 2.

		Reference																													
		W2	W5	W37	W47	W98	W100	W106	W144	W1145	W149	W178	W189	W210	W213	W219	W222	W224	W234	W235	W241	W245	W252	W264	W272	W282	W293	W295	W346	W393	W394
Prediction	W2	9	2	0	0	0	0	0	0	0	0	0	0	0	0	0	0	0	0	0	0	0	0	0	0	0	0	0	0	0	0
	W5	1	8	0	0	0	0	0	0	0	0	0	0	0	0	0	0	0	0	0	0	0	0	0	0	0	0	0	0	0	0
	W37	0	0	9	0	0	0	0	0	0	0	0	0	0	0	0	0	0	0	0	0	0	0	0	0	0	0	0	0	0	0
	W47	0	0	0	10	0	0	0	0	0	0	0	0	0	0	0	0	0	0	0	0	0	0	0	0	0	0	0	0	0	0
	W98	0	0	1	0	8	0	0	1	1	1	0	0	0	0	0	0	0	0	0	0	0	0	0	0	0	0	0	0	0	0
	W100	0	0	0	0	0	10	0	0	0	0	0	0	0	0	0	0	0	0	0	0	0	0	0	0	0	0	0	0	0	0
	W106	0	0	0	0	0	0	9	1	0	0	0	0	0	0	0	0	0	0	0	0	0	0	0	0	0	0	0	0	0	0
	W144	0	0	0	0	2	0	0	8	0	0	0	0	0	0	0	0	0	0	0	0	0	0	0	0	0	0	0	0	0	0
	W1145	0	0	0	0	0	0	0	0	9	1	0	0	0	0	0	0	0	0	0	0	0	0	0	0	0	0	0	0	0	0
	W149	0	0	0	0	0	0	0	0	0	7	0	0	0	0	0	0	0	0	0	0	0	0	0	0	0	0	0	0	0	0
	W178	0	0	0	0	0	0	0	0	0	0	8	0	0	0	0	0	0	0	0	0	0	1	0	0	0	0	0	0	0	0
	W189	0	0	0	0	0	0	0	0	0	0	0	8	0	0	0	0	0	0	0	0	0	0	0	1	0	0	0	0	0	0
	W210	0	0	0	0	0	0	0	0	0	0	0	0	8	0	0	0	0	1	0	0	0	0	0	0	0	0	0	0	0	0
	W213	0	0	0	0	0	0	0	0	0	1	0	0	0	10	2	0	0	0	0	0	0	0	0	0	0	0	0	0	0	0
	W219	0	0	0	0	0	0	0	0	0	0	1	1	0	0	8	0	0	0	0	0	1	0	0	0	0	0	0	0	0	0
	W222	0	0	0	0	0	0	0	0	0	0	0	0	1	0	0	7	0	0	0	0	0	0	0	0	0	0	0	0	0	0
	W224	0	0	0	0	0	0	0	0	0	0	0	0	0	0	0	1	8	0	0	0	0	1	0	1	1	0	0	1	0	0
	W234	0	0	0	0	0	0	0	0	0	0	0	0	0	0	0	0	0	8	0	0	0	0	0	0	0	0	0	0	0	0
	W235	0	0	0	0	0	0	0	0	0	0	0	0	0	0	0	0	0	0	9	0	1	0	0	0	0	0	0	0	0	0
	W241	0	0	0	0	0	0	0	0	0	0	0	0	0	0	0	0	0	0	0	10	0	0	0	0	0	0	0	0	0	0
	W245	0	0	0	0	0	0	0	0	0	0	0	0	0	0	0	0	0	0	0	0	7	0	0	0	0	0	0	0	0	0
	W252	0	0	0	0	0	0	0	0	0	0	0	0	0	0	0	0	0	0	0	0	0	8	0	0	0	0	0	0	0	0
	W264	0	0	0	0	0	0	0	0	0	0	1	0	0	0	0	2	1	0	0	0	0	0	9	0	0	0	0	0	0	0
	W272	0	0	0	0	0	0	1	0	0	0	0	1	0	0	0	0	0	0	0	0	1	0	0	6	0	0	0	1	0	1
	W282	0	0	0	0	0	0	0	0	0	0	0	0	0	0	0	0	0	0	0	0	0	0	0	1	8	0	0	0	0	1
	W293	0	0	0	0	0	0	0	0	0	0	0	0	0	0	0	0	0	0	0	0	0	0	0	0	0	10	0	0	0	0
	W295	0	0	0	0	0	0	0	0	0	0	0	0	0	0	0	0	0	1	0	0	0	0	0	0	0	0	9	0	0	1
	W346	0	0	0	0	0	0	0	0	0	0	0	0	1	0	0	0	1	0	0	0	0	0	1	1	1	0	1	8	0	0
	W393	0	0	0	0	0	0	0	0	0	0	0	0	0	0	0	0	0	0	1	0	0	0	0	0	0	0	0	0	10	1
	W394	0	0	0	0	0	0	0	0	0	0	0	0	0	0	0	0	0	0	0	0	0	0	0	0	0	0	0	0	0	6

Table 122: The HOO-CV PCA-CVA overall statistics for the first derivative spectra (5-point smoothing, autoscaled) with 107 PCs of same RI set 2.

Overall Statistics								
Accuracy:	0.84							
95% CI:	(0.7935, 0.8796)							
Statistic by Class								
Glass Identity	W2	W5	W37	W47	W98	W100	W106	
Sensitivity	0.9	0.8	0.9	1	0.8	1	0.9	
Specificity	0.9931	0.99655	1	1	0.98621	1	0.99655	
Pos Pred Value	0.81818	0.88889	1	1	0.66667	1	0.9	
Neg Pred Value	0.99654	0.99313	0.99656	1	0.99306	1	0.99655	
Prevalence	0.03333	0.03333	0.03333	0.03333	0.03333	0.03333	0.03333	
Detection Rate	0.03	0.02667	0.03	0.03333	0.02667	0.03333	0.03	
Detection Prevalence	0.03667	0.03	0.03	0.03333	0.04	0.03333	0.03333	
Glass Identity	W144	W1145	W149	W178	W189	W210	W213	
Sensitivity	0.8	0.9	0.7	0.8	0.8	0.8	1	
Specificity	0.9931	0.99655	1	0.99655	0.99655	0.99655	0.98966	
Pos Pred Value	0.8	0.9	1	0.88889	0.88889	0.88889	0.76923	
Neg Pred Value	0.9931	0.99655	0.98976	0.99313	0.99313	0.99313	1	
Prevalence	0.03333	0.03333	0.03333	0.03333	0.03333	0.03333	0.03333	
Detection Rate	0.02667	0.03	0.02333	0.02667	0.02667	0.02667	0.03333	
Detection Prevalence	0.03333	0.03333	0.02333	0.03	0.03	0.03	0.04333	
Glass Identity	W219	W222	W224	W234	W235	W241	W245	W252
Sensitivity	0.8	0.7	0.8	0.8	0.9	1	0.7	0.8
Specificity	0.98966	0.99655	0.98276	1	0.99655	1	1	1
Pos Pred Value	0.72727	0.875	0.61538	1	0.9	1	1	1
Neg Pred Value	0.99308	0.98973	0.99303	0.99315	0.99655	1	0.98976	0.99315
Prevalence	0.03333	0.03333	0.03333	0.03333	0.03333	0.03333	0.03333	0.03333
Detection Rate	0.02667	0.02333	0.02667	0.02667	0.03	0.03333	0.02333	0.02667
Detection Prevalence	0.03667	0.02667	0.04333	0.02667	0.03333	0.03333	0.02333	0.02667
Glass Identity	W264	W272	W282	W293	W295	W346	W393	W394
Sensitivity	0.9	0.6	0.8	1	0.9	0.8	1	0.6
Specificity	0.98621	0.98276	0.9931	1	0.9931	0.97931	0.9931	1
Pos Pred Value	0.69231	0.54545	0.8	1	0.81818	0.57143	0.83333	1
Neg Pred Value	0.99652	0.98616	0.9931	1	0.99654	0.99301	1	0.98639
Prevalence	0.03333	0.03333	0.03333	0.03333	0.03333	0.03333	0.03333	0.03333
Detection Rate	0.03	0.02	0.02667	0.03333	0.03	0.02667	0.03333	0.02
Detection Prevalence	0.04333	0.03667	0.03333	0.03333	0.03667	0.04667	0.04	0.02

Table 123: Confusion matrix for the HOO-CV PCA-CVA results for the second derivative spectra (5-point smoothing, autoscaled) with 98 PCs of same RI set 2.

		Reference																													
		W2	W5	W37	W47	W98	W100	W106	W144	W1145	W149	W178	W189	W210	W213	W219	W222	W224	W234	W235	W241	W245	W252	W264	W272	W282	W293	W295	W346	W393	W394
Prediction	W2	10	1	0	0	0	0	0	0	0	0	0	0	0	0	0	0	0	0	0	0	0	0	0	0	0	0	0	0	0	0
	W5	0	9	0	0	0	0	0	0	0	0	0	0	0	0	0	0	0	0	0	0	0	0	0	0	0	0	0	0	0	0
	W37	0	0	10	0	0	0	0	0	0	0	0	0	0	0	0	0	0	0	0	0	0	0	0	0	0	0	0	0	0	0
	W47	0	0	0	10	0	0	0	0	0	0	0	0	0	0	0	0	0	0	0	0	0	0	0	0	0	0	0	0	0	0
	W98	0	0	0	0	7	0	0	0	1	0	0	1	0	0	0	1	0	0	0	0	0	0	0	0	0	0	0	0	0	0
	W100	0	0	0	0	1	8	0	0	0	0	0	0	0	0	0	0	0	0	0	0	0	0	0	0	0	0	0	0	0	0
	W106	0	0	0	0	0	0	10	0	0	0	0	0	0	0	0	0	0	0	0	0	0	0	0	0	0	0	0	0	0	0
	W144	0	0	0	0	0	1	0	8	0	0	0	0	0	0	0	0	0	0	0	0	0	0	0	0	0	0	0	0	0	0
	W1145	0	0	0	0	2	1	0	0	8	1	0	0	0	0	0	0	0	0	0	0	0	1	0	0	0	0	0	0	0	1
	W149	0	0	0	0	0	0	0	0	0	7	0	0	0	0	0	0	0	0	0	0	0	0	0	0	0	0	0	0	0	0
	W178	0	0	0	0	0	0	0	0	0	0	6	1	0	0	0	0	0	0	0	0	0	0	0	0	0	0	0	0	0	0
	W189	0	0	0	0	0	0	0	0	0	0	0	7	0	0	0	0	0	0	0	0	0	0	0	0	0	0	0	0	0	0
	W210	0	0	0	0	0	0	0	0	0	0	1	0	7	0	1	0	0	0	1	0	0	0	0	0	0	0	0	0	0	0
	W213	0	0	0	0	0	0	0	0	0	0	0	0	0	8	0	0	0	0	0	0	0	0	0	0	0	0	0	0	0	0
	W219	0	0	0	0	0	0	0	0	0	0	1	0	0	0	9	0	0	0	0	1	0	0	0	0	0	0	0	0	0	0
	W222	0	0	0	0	0	0	0	1	0	0	0	0	0	0	0	7	0	1	0	0	0	0	0	0	0	0	0	0	0	0
	W224	0	0	0	0	0	0	0	0	0	1	0	0	0	0	0	1	7	1	0	0	0	0	1	0	0	0	0	0	0	0
	W234	0	0	0	0	0	0	0	0	0	0	0	0	0	0	0	0	1	6	0	0	0	0	0	0	0	0	0	0	0	0
	W235	0	0	0	0	0	0	0	0	0	0	0	0	2	1	0	0	0	2	7	0	0	0	0	0	0	0	0	0	0	0
	W241	0	0	0	0	0	0	0	0	0	0	0	0	0	0	0	0	0	0	0	8	0	0	0	1	0	0	0	0	0	0
	W245	0	0	0	0	0	0	0	0	0	0	0	0	1	0	0	0	0	0	0	0	7	0	0	1	1	0	0	0	0	0
	W252	0	0	0	0	0	0	0	0	0	0	0	0	0	0	0	0	0	0	1	0	1	7	0	1	0	0	0	0	0	0
	W264	0	0	0	0	0	0	0	0	0	0	1	0	0	0	0	0	1	0	0	0	0	1	9	0	0	0	0	1	0	0
	W272	0	0	0	0	0	0	0	0	0	0	1	0	0	1	0	0	0	0	1	1	2	1	0	7	0	1	0	0	0	0
	W282	0	0	0	0	0	0	0	0	0	0	0	1	0	0	0	0	0	0	0	0	0	0	0	0	9	0	0	0	0	0
	W293	0	0	0	0	0	0	0	0	1	0	0	0	0	0	0	0	0	0	0	0	0	0	0	0	0	9	0	0	0	0
	W295	0	0	0	0	0	0	0	0	0	0	0	0	0	0	0	1	0	0	0	0	0	0	0	0	0	0	9	0	0	0
	W346	0	0	0	0	0	0	0	0	0	0	0	0	0	0	0	0	1	0	0	0	0	0	0	0	0	0	0	9	0	1
	W393	0	0	0	0	0	0	0	1	0	1	0	0	0	0	0	0	0	0	0	0	0	0	0	0	0	0	1	0	10	1
	W394	0	0	0	0	0	0	0	0	0	0	0	0	0	0	0	0	0	0	0	0	0	0	0	0	0	0	0	0	0	7

Table 124: The HOO-CV PCA-CVA overall statistics for the second derivative spectra (5-point smoothing, autoscaled) with 98 PCs of same RI set 2.

Overall Statistics								
Accuracy:	0.8067							
95% CI:	(0.7574, 0.8498)							
Statistic by Class								
Glass Identity	W2	W5	W37	W47	W98	W100	W106	
Sensitivity	1	0.9	1	1	0.7	0.8	1	
Specificity	0.99655	1	1	1	0.98966	0.99655	1	
Pos Pred Value	0.90909	1	1	1	0.7	0.88889	1	
Neg Pred Value	1	0.99656	1	1	0.98966	0.99313	1	
Prevalence	0.03333	0.03333	0.03333	0.03333	0.03333	0.03333	0.03333	
Detection Rate	0.03333	0.03	0.03333	0.03333	0.02333	0.02667	0.03333	
Detection Prevalence	0.03667	0.03	0.03333	0.03333	0.03333	0.03	0.03333	
Glass Identity	W144	W1145	W149	W178	W189	W210	W213	
Sensitivity	0.8	0.8	0.7	0.6	0.7	0.7	0.8	
Specificity	0.99655	0.97931	1	0.99655	1	0.98966	1	
Pos Pred Value	0.88889	0.57143	1	0.85714	1	0.7	1	
Neg Pred Value	0.99313	0.99301	0.98976	0.98635	0.98976	0.98966	0.99315	
Prevalence	0.03333	0.03333	0.03333	0.03333	0.03333	0.03333	0.03333	
Detection Rate	0.02667	0.02667	0.02333	0.02	0.02333	0.02333	0.02667	
Detection Prevalence	0.03	0.04667	0.02333	0.02333	0.02333	0.03333	0.02667	
Glass Identity	W219	W222	W224	W234	W235	W241	W245	W252
Sensitivity	0.9	0.7	0.7	0.6	0.7	0.8	0.7	0.7
Specificity	0.9931	0.9931	0.98621	0.99655	0.98276	0.99655	0.98966	0.98966
Pos Pred Value	0.81818	0.77778	0.63636	0.85714	0.58333	0.88889	0.7	0.7
Neg Pred Value	0.99654	0.98969	0.98962	0.98635	0.98958	0.99313	0.98966	0.98966
Prevalence	0.03333	0.03333	0.03333	0.03333	0.03333	0.03333	0.03333	0.03333
Detection Rate	0.03	0.02333	0.02333	0.02	0.02333	0.02667	0.02333	0.02333
Detection Prevalence	0.03667	0.03	0.03667	0.02333	0.04	0.03	0.03333	0.03333
Glass Identity	W264	W272	W282	W293	W295	W346	W393	W394
Sensitivity	0.9	0.7	0.9	0.9	0.9	0.9	1	0.7
Specificity	0.98621	0.97241	0.99655	0.99655	0.99655	0.9931	0.98621	1
Pos Pred Value	0.69231	0.46667	0.9	0.9	0.9	0.81818	0.71429	1
Neg Pred Value	0.99652	0.98947	0.99655	0.99655	0.99655	0.99654	1	0.98976
Prevalence	0.03333	0.03333	0.03333	0.03333	0.03333	0.03333	0.03333	0.03333
Detection Rate	0.03	0.02333	0.03	0.03	0.03	0.03	0.03333	0.02333
Detection Prevalence	0.04333	0.05	0.03333	0.03333	0.03333	0.03667	0.04667	0.02333

The confusion matrices and their corresponding statistics show that several of the glass samples within each population with the same RI could be differentiated from the other samples using each of the 10 of the spectra, with no false positives or false negatives. Within set 1, using

the first derivative spectra (5-point smoothing, autoscaled) for the PCA-CVA, 7 of the 21 glasses (W23, W33, W62, W153, W165, W193, and W204) were discriminated with 100% accuracy (both the sensitivity and specificity equal 1). Within set 1, using the second derivative spectra (5-point smoothing, autoscaled) for the PCA-CVA, 5 of the 21 glasses (W33, W153, W165, W174, and W204) were discriminated with 100% accuracy (both the sensitivity and specificity equal 1). Within set 2, using the first derivative spectra (5-point smoothing, autoscaled) for the PCA-CVA, 4 of the 30 glasses (W47, W100, W241, and W293) were discriminated with 100% accuracy (both the sensitivity and specificity equal 1). Within set 2, using the W37, W47, and W106) were discriminated with 100% accuracy (both the sensitivity and specificity equal 1).

Additionally, when considering all 10 replicates for each glass sample, a correct association was made for at least 7 of the 10 replicate first derivative spectra for 18 of the 21 glasses (86%) in set 1 and 28 of the 30 (93%) in set 2. For the second derivative spectra, a correct association was made for 20 of the 21 glasses (95%) in set 1 and 28 of the 30 (93%) in set 2. Consequently, if 8 - 10 derivative spectra of a questioned glass fragment were compared to a PCA-CVA model, it is likely that there would be a greater likelihood of making the correct source assignment than if only 1 spectra was compared. This shows that the mid-IR spectra can provide additional discrimination to glasses that cannot be differentiated by RI.

4.D. Mid-IR Microprobe Analysis Compatibility with GRIM

The sample preparation for the mid-IR microprobe analysis of glass is the same as that for GRIM in that both require mounting of a microscopic fragment of glass in oil. GRIM requires the use of designated refractive index silicone oils, and these oils have mid-IR peaks in the same region as glasses' silicate bands. It was thought that the silicone oil would not interfere

with a glass fragment's mid-IR spectra because it would be squeezed out from between the glass and the IRE during the ATR analysis, just like that with Nujol. However, as can be seen in Figures 100 – 103, the silicone oil's peaks distorted those from the glass. Specifically, the silicone oil's peaks at 727.4, 697.5, and 774.8 cm^{-1} distort one side of the ~790 cm^{-1} glass band.

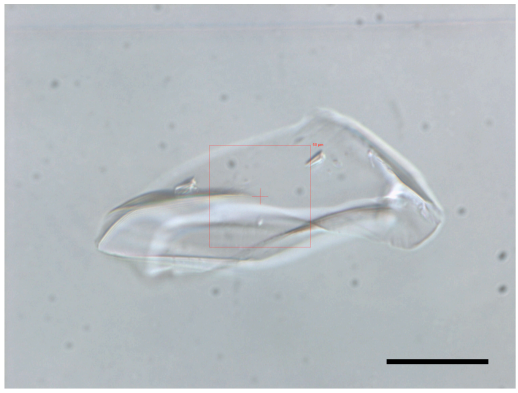


Figure 100: Photomicrograph of a glass sample in silicone oil II at 400 times magnification, prior to analysis. The length of the black bar measures 50-µm.

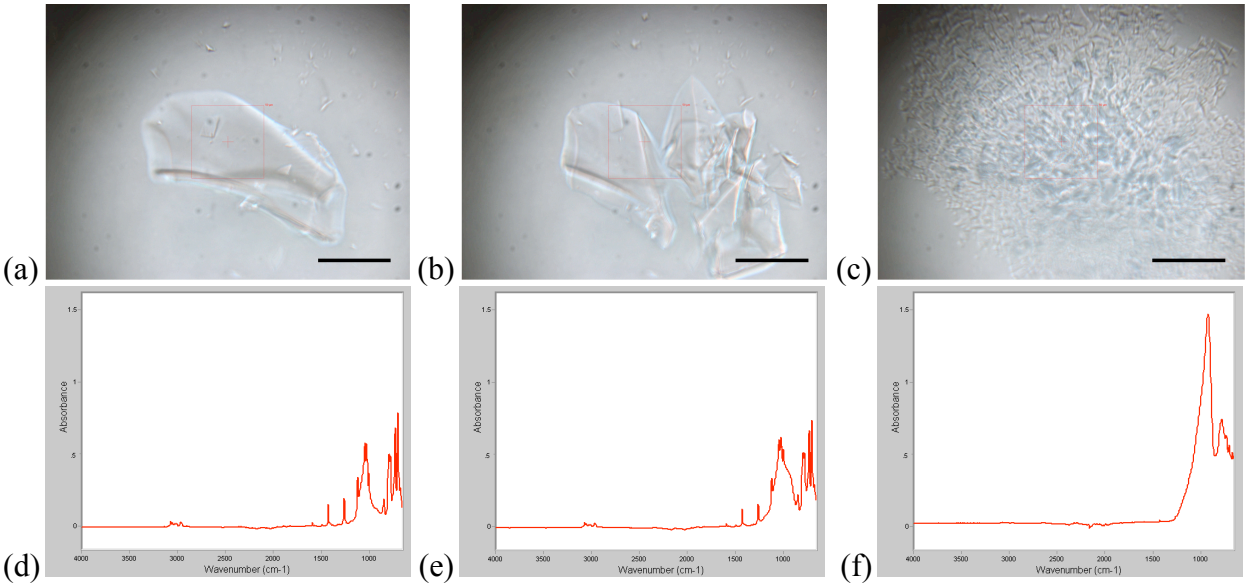


Figure 101: Photomicrographs of a glass sample in silicone oil II at 360 times magnification using the diamond ATR objective, varied by increasing the contact pressure: (a) after initial contact, (b) after some contact, and (c) after being crushed but not scattered. The length of the black bar measures 50-µm. Below each photomicrograph are their resulting mid-IR spectra, collected with a 50-µm aperture, 4 cm^{-1} spectral resolution, and 256 co-added scans. The spectra were produced using Grams® AI software.

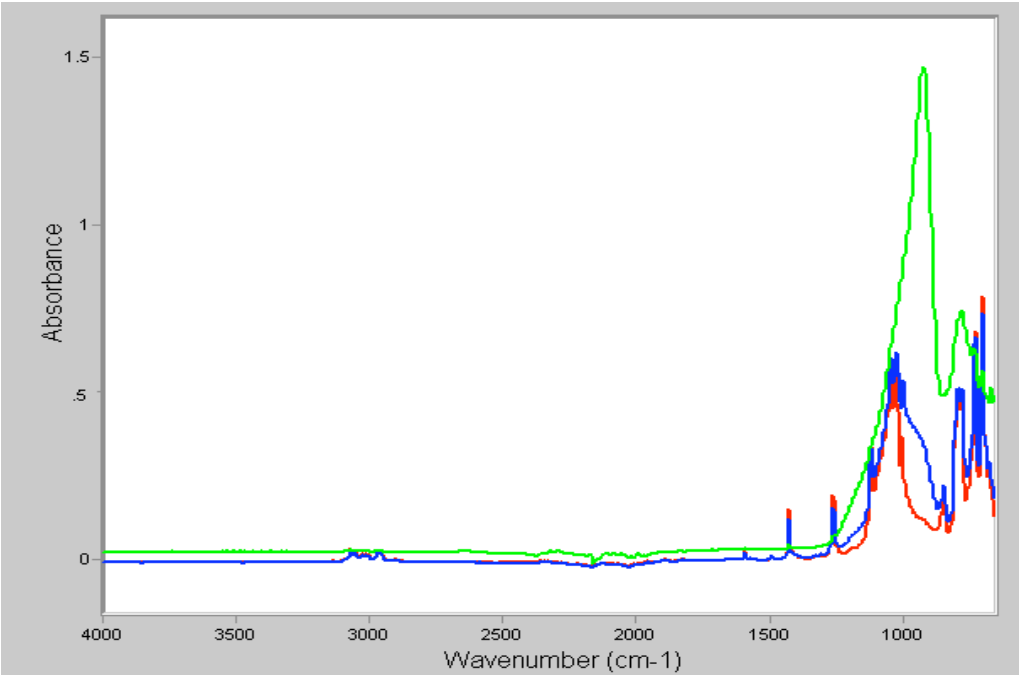


Figure 102: The mid-IR spectra of Figures 101 d-f overlaid, and produced using Grams® AI software. The red spectrum is after initial contact, the blue spectrum is after some contact, and the green spectrum is after being crushed but not scattered. As contact pressure is increased, the glass peaks are increase and the presence of the silicone oil decreases but does not disappear.

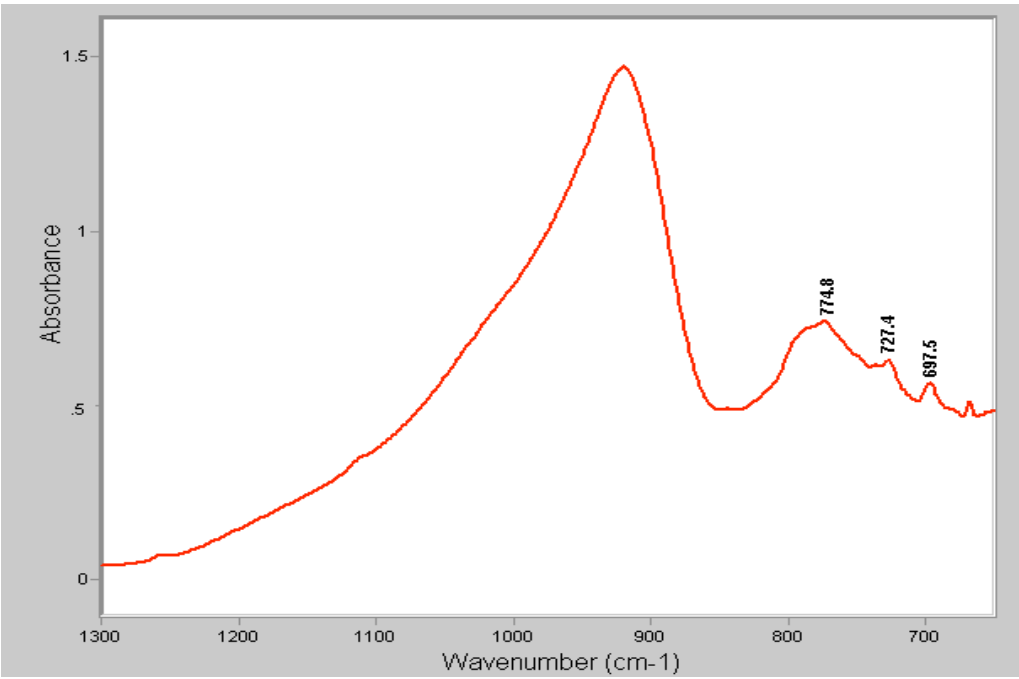


Figure 103: The mid-IR spectrum, from 1300-650 cm^{-1}, of the glass sample crushed in silicone oil produced using Grams® AI software. It is the same spectrum as in Figure 101 f, only zoomed in to the silicate peaks. The contribution of the silicone oil on the spectrum is considerable, as seen by the peaks at 727.4 cm^{-1} and 697.5 cm^{-1}, and the distortion of the peak at ~790 cm^{-1} with the 774.8 cm^{-1}.

Consequently, it was shown that ATR mid-IR analysis of glass could not be performed on fragments mounted in GRIM silicone oils. However, because the sample preparations are so similar with the exception of the mounting oil, an alternative procedure is proposed. After the glass sample is ground to an appropriate size for microscopy, two small portions of the fragments could be mounted separately: one in silicone oil for GRIM analysis and the other in Nujol for ATR mid-IR microprobe analysis. This would require minimal additional sample preparation for the criminalist.

CHAPTER 5: CONCLUSIONS

This research evaluated the suitability of ATR mid-IR microspectroscopy for the classification and discrimination of soda-lime silicate glasses. A method was developed and tested for the preparation and mid-IR analysis of glass fragments. The analytical protocol consisted of mounting microscopic glass fragments in immersion oil, specifically Nujol, and collecting the mid-IR spectra with a 50-µm aperture, a spectral resolution of 4 cm^{-1} and 256 co-added scans. These parameters produced spectra with a S/N of nearly 30,000, which is excellent. Even smaller samples, as small as 10-µm, were also shown to be able to be analyzed with the mid-IR microprobe to produce quality spectra. This mid-IR microprobe analysis of glass requires only minimal additional sample preparation to that which is already done for GRIM analysis and uses samples that are the same size and smaller than the ablated hole made in LA-ICP-MS.

Several methods were evaluated to determine the discriminating power of ATR mid-IR microspectroscopy, with PCA-CVA of first derivative spectra (5-point smoothing) proving to have the lowest error rates, as determined by HOO-CV. The methods that were not as successful as the chemometric analyses for the discrimination of soda-lime silicate glasses included using mid-IR spectral library searches (with both the correlation and first derivative correlation algorithm) and comparisons of the mid-IR deconvolution results (peak positions and areas) using the range test criteria. Conservative PCA-CVA HOO-CV error rate of 4.44% (176 PCs and 99.99% variance), 4.95% (182 PCs and 99.99% variance), and 6.8% (100 PCs and 99.86% variance) were calculated from sets of 153 glasses, 103 window glasses and 50 container glasses, respectively. For all 3 of these discriminations, there was a large discrepancy between the HOO-CV error rates of PCA-CVA and PLS-DA. This inconsistency could either indicate that the

PCA-CVA error rates are unreliable or that PLS-DA is not useful for making many class models. Furthermore, the HOO-CV error rate uses only 1 spectrum for comparison with the chemometric model, as might be observed when there is only 1 spectrum collected and/or 1 recovered glass fragment. When multiple spectra from multiple fragments are considered, the error rate would likely decrease.

The classification of glasses into their end use categories of window or container proved to very successful with both chemometric algorithms, PCA-CVA and PLS-DA. A conservative HOO-CV error rate of 1.83% was achieved with the first derivative spectra (9-point smoothing) using both PCA-CVA (54 PCs and 99.95% variance) and PLS-DA (200 PLS dimensions). With the second derivative spectra (9-point smoothing), conservative HOO-CV error rates of 2.48% (40 PCs and 85.95% variance) and 1.76% (193 PLS dimensions) were calculated with the PCA-CVA and PLS-DA models, respectively. The consistent error rate of approximately 2% for both sample preprocessing methods and for both chemometric models bolsters the credibility of this method for container and window glass classification.

Three of the classification schemes produced unacceptably high HOO-CV error rates, which show the inability of these chemometric algorithms to use the mid-IR spectra and derivatives for the classification of glasses into the end-use categories of automotive, architectural or container glasses or into the manufacturing processes of float or non-float and tempered or non-tempered. There was still some potential for the classification of glasses into float or non-float using the data from the deconvolution of 20 window glasses (10 replicates). The HOO-CV error rates were 8.5% and 9% with PCA-CVA (10 PCs and 99.97% variance) and PLS-DA (8 PLS dimensions). Further research should be completed to determine the reliability of using the deconvolution data to classify a glass as being float or non-float.

This research demonstrated the ability of mid-IR derivative spectra to provide increased discrimination of glasses that cannot be distinguished with RI. The lowest PCA-CVA HOO-CV error rates for discriminating between glasses with nominally similar RIs were 12.38% (second derivative spectra, 5-point smoothing) and 16% (first derivative, 5-point smoothing) for sets with 21 and 30 glasses with nominally similar RIs. However, these error rates alone do not show the whole picture because HOO-CV only uses 1 spectrum for comparison. Within both sets of glasses with nominally similar RIs, there were glasses that were able to be distinguished from the other glasses with all 10 replicate spectra. Seven of the 21 glasses in set 1 and 4 of the 30 glasses in set 2 (both using the first derivative spectra, 5-point smoothing) were able to be discriminated from the other glasses using all spectra in the PCA-CVA model (no false positives or false negatives). When multiple spectra were considered, the correct association rate increased. The majority of the glasses had correct associations for at least 7 of the 10 replicate derivative spectra. When using the first derivative (5-point smoothing) spectra, correct associations with atleast 7 of the 10 replicates was made for 86% and 93% of sets 1 and 2, respectively. With the second derivative (5-point smoothing) spectra, 95% and 93% of the glasses for sets 1 and 2, respectively, were correctly identified. This research demonstrated the power of mid-IR spectroscopy to provide additional discrimination to glasses that cannot be differentiated by RI.

CHAPTER 6: CONTRIBUTIONS TO FORENSIC SCIENCE AND CRIMINAL JUSTICE

There are important implications for forensic science and criminal justice policy and practice. This research provided additional evidence of the value of the molecular analysis of glass with ATR mid-IR microprobe analysis for the classification and discrimination of forensic glasses. This research takes advantage of a measurable property of glass, its molecular structure, which has not been used in the forensic analysis of glass. Most forensic laboratories have IR spectrometers and/or microprobes which are used in the analysis of a plethora of evidence types including but not limited to paint, fibers, plastics, adhesives, and illicit drugs. Thus this technique would not necessarily require a crime laboratory to purchase new instrumentation nor require extensive training for trace evidence examiners. As a result, the use of ATR mid-IR microspectroscopy for forensic glass comparisons and analysis could potentially be implemented by crime laboratories immediately and with minimal expense.

The usefulness of IR microprobe analysis of glass as an analytical method for legal purposes is that it is capable of satisfying both of the standards for admissibility of scientific evidence in US Courts. The first standard is based on the decision in *Frye v. United States*, where the District of Columbia Circuit Court determined that the method for assessing the reliability of scientific evidence was whether or not there was general acceptance in the relevant scientific community. The second is based on *Daubert v. Merrell Dow Pharmaceuticals, Inc.,* known as the Daubert standard, which bestows upon the judge the role of "gatekeeper" for the admissibility of scientific evidence. To aid judges in this role, the Supreme Court outlined four criteria for the determination of reliability: (1) testability and falsifiability, (2) peer review and publication, (3) a known or potential error rate, and (4) general acceptance. A fifth criterion is sometimes cited which is the use and maintenance of standards and controls. It is important to

note that these criteria were never intended to be used as a checklist, and they are neither mandatory nor exclusive. IR microspectroscopy is a method that is accepted by the relevant scientific community and courts widely recognize it as being reliable for the analysis of many different types of trace evidence. This research demonstrated the ability of mid-IR microspectroscopy to classify (into container and window glass) and discriminate soda-lime silicate glasses. Thus, this research expands this recognized analytical tool to include glass. In this research, the thorough method development, data collection, and chemometric analysis of the mid-IR data determined the optimum conditions, limits, and error rates for the technique, thus this research begins to satisfy the scientific testing requirements demanded of forensic methods presented in the courts of law.

CHAPTER 7: FURTHER CONSIDERATIONS

Upon completion of this work, there are at least four areas of research that warrant further consideration.

The first and most obvious is that more glasses should be analyzed to build a larger glass spectral database. It is well known that larger populations of samples provide more substantial statistics, thus additional glass samples should undergo this analytical protocol (which includes both the ATR mid-IR microprobe and chemometric analysis). In particular, more glasses with indistinguishable RIs should be analyzed to further establish the discrimination power of mid-IR microspectroscopy for glasses that cannot be discriminated by RI. In addition, glasses made in the same glass manufacturing plant at various time intervals should be analyzed to test the limits of this technique for glass discrimination.

A second area of further research is the homogeneity of fragments in a glass object. Although small-scale homogeneity was tested in this research through the use of analyzing 10 different fragments for each glass sample, larger-scale homogeneity was not tested. It is important to know whether fragments from different locations in a window or container would be associated with each other using these chemometric models.

The third is the use of additional chemometric algorithms and error rate estimates for the analysis of this glass spectral data. Specifically, using neural networks or support vector machines (SVM) on the PCA reduced data would provide alternative analyses to those of CVA and PLS-DA. Also, using different methods for estimating error rates, such as c-fold cross validation or bootstrapping, would provide additional support to the already calculated HOO-CV error rates. An important advantage of using SVM would be that it provides confidence intervals

around associations and error rates. The addition of confidence intervals would assist with the determination of match criteria when using chemometric models for discrimination.

The last area of further research is to determine exactly how this can and should be used by criminalists working on cases involving forensic glass evidence. The multivariate statistical methods for discrimination employed in this research do not lend themselves to a direct comparison between a known and questioned sample. These chemometric discriminations and classifications are accomplished by combinations of variables that cannot be reduced to a single spectral band or simple ratio of spectral bands. In addition, one must have a collection of sample data (i.e. a database), in order to use these chemometric methods for robust discrimination and classification determinations. Thus, prior to crime laboratories employing mid-IR microspectroscopy for glass classification and discrimination, it must be determined how to best use these chemometric methods in casework. One possible solution could be the creation of a PCA-CVA or other chemometric search algorithm for IR library searches. Although the mid-IR library searches were not successful at discriminating between glasses, the blame can be placed on the types of search algorithms. Correlation and first derivative correlation search algorithms are not successful with the discrimination of glasses or other samples with minimal differences. Thus, perhaps a search algorithm could be created which uses the library spectra as a learning set for making the chemometric model and the questioned spectra as the test sample. This could provide a powerful new tool for spectroscopic identification.

A STUDY OF THE MOLECULAR CHEMISTRY OF GLASSES BY INFRARED MICROSPECTROSCOPYAND ITS USE IN FORENSIC GLASS DISCRIMINATION AND CLASSIFICATION

by

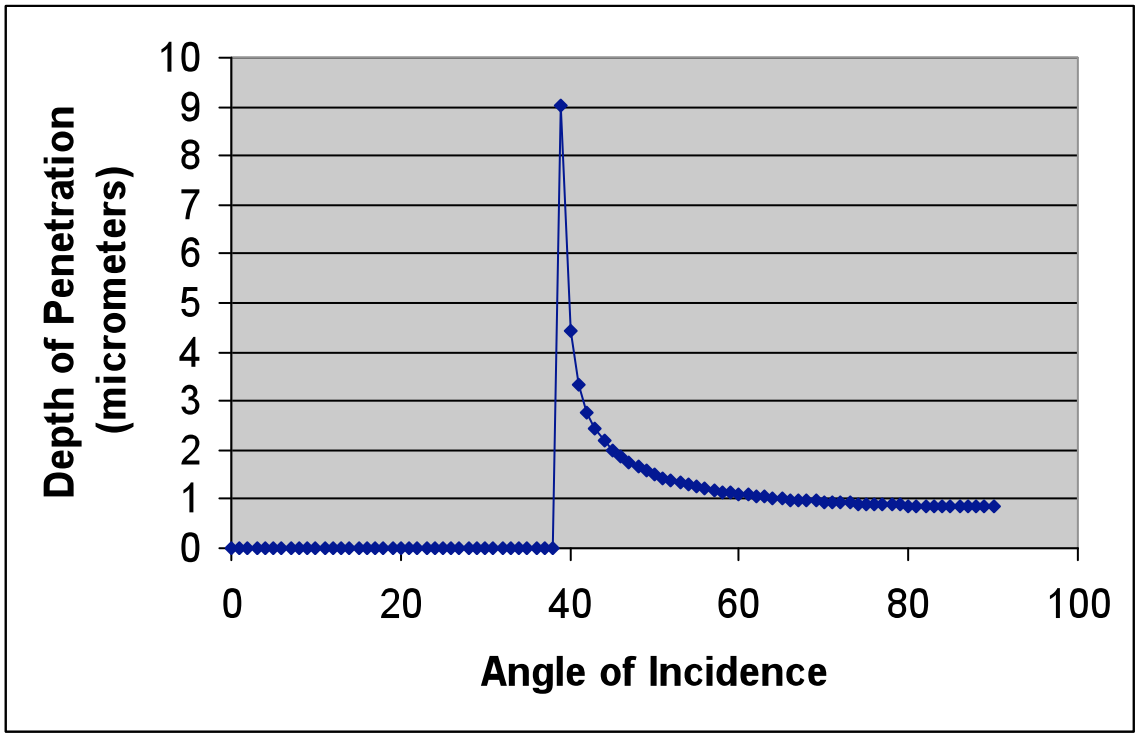
BROOKE WEINGER KAMMRATH

VOLUME II

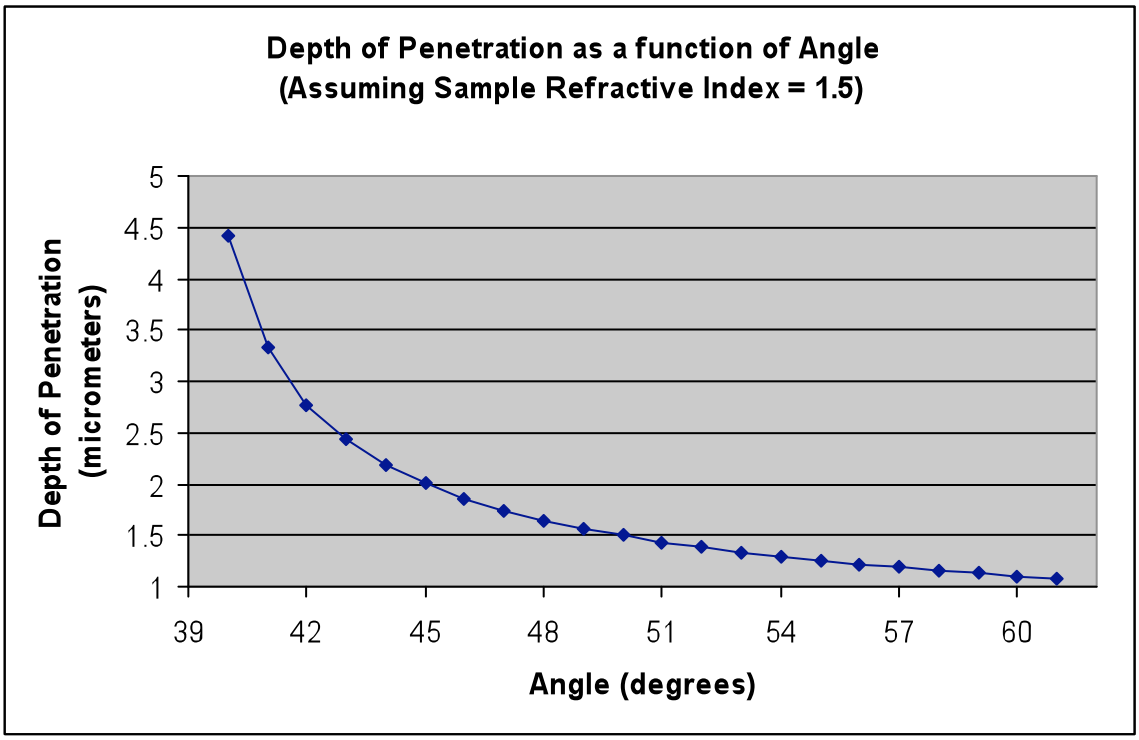
A dissertation submitted to the Graduate Faculty in Criminal Justice in partial fulfillment of the requirements for the degree of Doctor of Philosophy, The City University of New York

2012

APPENDIX I: DEPTH OF PENETRATION CALCULATIONS AND GRAPH



(a)



(b)

Figure 104: Depth of penetration variation as a function of the angle of incidence, from (a) 0 - 100° and (b) from 39 to 61°.

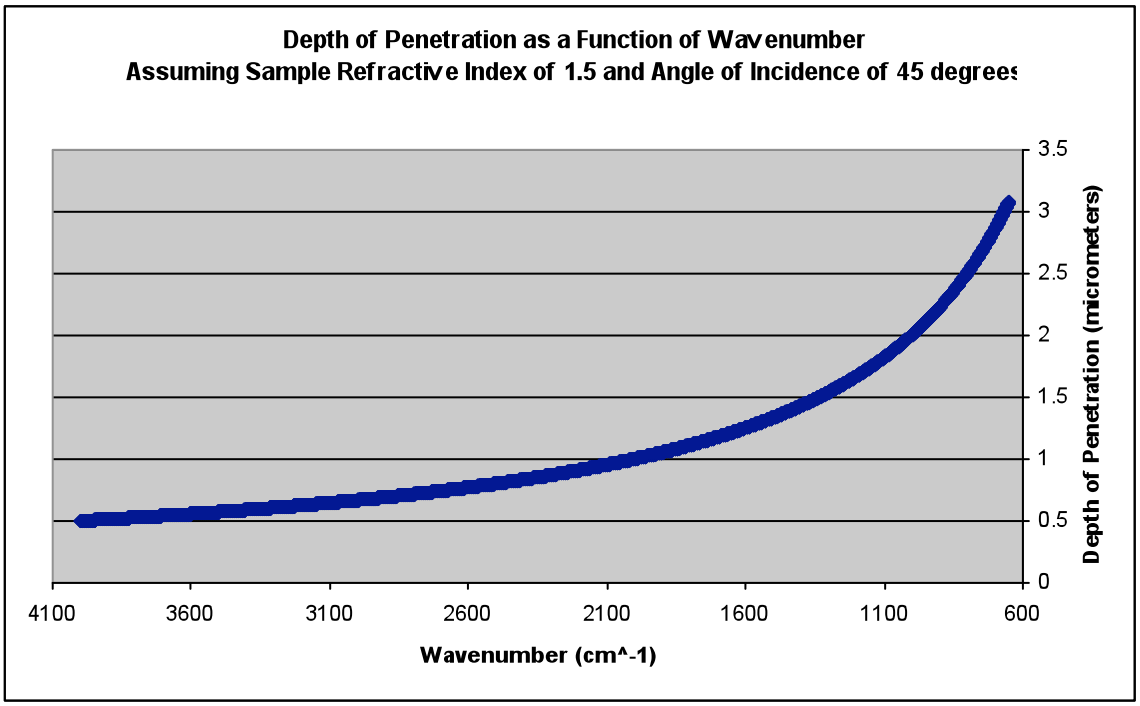
Table 125: Depth of penetration variation as a function of the angle of incident calculations.

	A	B	C	D	E	F	G	H	I	J	K
1	Depth of Penetration Variation with Angle of Incidence.										
2	θ (degrees)	θ (Radians)	Refractive Index of Sample	Refractive Index of Element	Sin^2 θ	¶	λ (μm)	2¶(Refractive Index of Element)	(Refractive Index of Sample/Refractive Index of Element)^2	θ (degrees)	Depth of Penetration (μm)
3	0	0	1.5	2.4	0	3.141592654	10	15.07964474	0.390625	0	#NUM!
4	1	0.0174533	1.5	2.4	0.000304586	3.141592654	10	15.07964474	0.390625	1	#NUM!
5	2	0.0349066	1.5	2.4	0.001217975	3.141592654	10	15.07964474	0.390625	2	#NUM!
6	3	0.0523599	1.5	2.4	0.002739052	3.141592654	10	15.07964474	0.390625	3	#NUM!
7	4	0.0698132	1.5	2.4	0.004865966	3.141592654	10	15.07964474	0.390625	4	#NUM!
8	5	0.0872665	1.5	2.4	0.007596123	3.141592654	10	15.07964474	0.390625	5	#NUM!
9	6	0.1047198	1.5	2.4	0.0109262	3.141592654	10	15.07964474	0.390625	6	#NUM!
10	7	0.122173	1.5	2.4	0.014852137	3.141592654	10	15.07964474	0.390625	7	#NUM!
11	8	0.1396263	1.5	2.4	0.019369152	3.141592654	10	15.07964474	0.390625	8	#NUM!
12	9	0.1570796	1.5	2.4	0.024471742	3.141592654	10	15.07964474	0.390625	9	#NUM!
13	10	0.1745329	1.5	2.4	0.03015369	3.141592654	10	15.07964474	0.390625	10	#NUM!
14	11	0.1919862	1.5	2.4	0.036408073	3.141592654	10	15.07964474	0.390625	11	#NUM!
15	12	0.2094395	1.5	2.4	0.043227271	3.141592654	10	15.07964474	0.390625	12	#NUM!
16	13	0.2268928	1.5	2.4	0.050602977	3.141592654	10	15.07964474	0.390625	13	#NUM!
17	14	0.2443461	1.5	2.4	0.058526204	3.141592654	10	15.07964474	0.390625	14	#NUM!
18	15	0.2617994	1.5	2.4	0.066987298	3.141592654	10	15.07964474	0.390625	15	#NUM!
19	16	0.2792527	1.5	2.4	0.075975952	3.141592654	10	15.07964474	0.390625	16	#NUM!
20	17	0.296706	1.5	2.4	0.085481214	3.141592654	10	15.07964474	0.390625	17	#NUM!
21	18	0.3141593	1.5	2.4	0.095491503	3.141592654	10	15.07964474	0.390625	18	#NUM!
22	19	0.3316126	1.5	2.4	0.105994623	3.141592654	10	15.07964474	0.390625	19	#NUM!
23	20	0.3490659	1.5	2.4	0.116977778	3.141592654	10	15.07964474	0.390625	20	#NUM!
24	21	0.3665191	1.5	2.4	0.128427587	3.141592654	10	15.07964474	0.390625	21	#NUM!
25	22	0.3839724	1.5	2.4	0.1403301	3.141592654	10	15.07964474	0.390625	22	#NUM!
26	23	0.4014257	1.5	2.4	0.152670815	3.141592654	10	15.07964474	0.390625	23	#NUM!
27	24	0.418879	1.5	2.4	0.165434697	3.141592654	10	15.07964474	0.390625	24	#NUM!
28	25	0.4363323	1.5	2.4	0.178606195	3.141592654	10	15.07964474	0.390625	25	#NUM!
29	26	0.4537856	1.5	2.4	0.192169262	3.141592654	10	15.07964474	0.390625	26	#NUM!
30	27	0.4712389	1.5	2.4	0.206107374	3.141592654	10	15.07964474	0.390625	27	#NUM!
31	28	0.4886922	1.5	2.4	0.220403548	3.141592654	10	15.07964474	0.390625	28	#NUM!
32	29	0.5061455	1.5	2.4	0.235040368	3.141592654	10	15.07964474	0.390625	29	#NUM!

	A	B	C	D	E	F	G	H	I	J	K
33	30	0.5235988	1.5	2.4	0.25	3.141592654	10	15.07964474	0.390625	30	#NUM!
34	31	0.5410521	1.5	2.4	0.265264219	3.141592654	10	15.07964474	0.390625	31	#NUM!
35	32	0.5585054	1.5	2.4	0.280814427	3.141592654	10	15.07964474	0.390625	32	#NUM!
36	33	0.5759587	1.5	2.4	0.296631678	3.141592654	10	15.07964474	0.390625	33	#NUM!
37	34	0.5934119	1.5	2.4	0.312696703	3.141592654	10	15.07964474	0.390625	34	#NUM!
38	35	0.6108652	1.5	2.4	0.328989928	3.141592654	10	15.07964474	0.390625	35	#NUM!
39	36	0.6283185	1.5	2.4	0.345491503	3.141592654	10	15.07964474	0.390625	36	#NUM!
40	37	0.6457718	1.5	2.4	0.362181322	3.141592654	10	15.07964474	0.390625	37	#NUM!
41	38	0.6632251	1.5	2.4	0.379039052	3.141592654	10	15.07964474	0.390625	38	#NUM!
42	39	0.6806784	1.5	2.4	0.396044155	3.141592654	10	15.07964474	0.390625	39	9.008305786
43	40	0.6981317	1.5	2.4	0.413175911	3.141592654	10	15.07964474	0.390625	40	4.415977408
44	41	0.715585	1.5	2.4	0.43041345	3.141592654	10	15.07964474	0.390625	41	3.324530962
45	42	0.7330383	1.5	2.4	0.447735768	3.141592654	10	15.07964474	0.390625	42	2.774916302
46	43	0.7504916	1.5	2.4	0.465121763	3.141592654	10	15.07964474	0.390625	43	2.429630263
47	44	0.7679449	1.5	2.4	0.482550252	3.141592654	10	15.07964474	0.390625	44	2.187215003
48	45	0.7853982	1.5	2.4	0.5	3.141592654	10	15.07964474	0.390625	45	2.005163806
49	46	0.8028515	1.5	2.4	0.517449748	3.141592654	10	15.07964474	0.390625	46	1.862116658
50	47	0.8203047	1.5	2.4	0.534878237	3.141592654	10	15.07964474	0.390625	47	1.746007506
51	48	0.837758	1.5	2.4	0.552264232	3.141592654	10	15.07964474	0.390625	48	1.649436122
52	49	0.8552113	1.5	2.4	0.56958655	3.141592654	10	15.07964474	0.390625	49	1.567577506
53	50	0.8726646	1.5	2.4	0.586824089	3.141592654	10	15.07964474	0.390625	50	1.497133047
54	51	0.8901179	1.5	2.4	0.603955845	3.141592654	10	15.07964474	0.390625	51	1.435760704
55	52	0.9075712	1.5	2.4	0.620960948	3.141592654	10	15.07964474	0.390625	52	1.381745404
56	53	0.9250245	1.5	2.4	0.637818678	3.141592654	10	15.07964474	0.390625	53	1.333798456
57	54	0.9424778	1.5	2.4	0.654508497	3.141592654	10	15.07964474	0.390625	54	1.29093024
58	55	0.9599311	1.5	2.4	0.671010072	3.141592654	10	15.07964474	0.390625	55	1.252366513
59	56	0.9773844	1.5	2.4	0.687303297	3.141592654	10	15.07964474	0.390625	56	1.217491678
60	57	0.9948377	1.5	2.4	0.703368322	3.141592654	10	15.07964474	0.390625	57	1.185809343
61	58	1.012291	1.5	2.4	0.719185573	3.141592654	10	15.07964474	0.390625	58	1.156914238
62	59	1.0297443	1.5	2.4	0.734735781	3.141592654	10	15.07964474	0.390625	59	1.130471844
63	60	1.0471976	1.5	2.4	0.75	3.141592654	10	15.07964474	0.390625	60	1.106203323
64	61	1.0646508	1.5	2.4	0.764959632	3.141592654	10	15.07964474	0.390625	61	1.083874218
65	62	1.0821041	1.5	2.4	0.779596452	3.141592654	10	15.07964474	0.390625	62	1.06328583
66	63	1.0995574	1.5	2.4	0.793892626	3.141592654	10	15.07964474	0.390625	63	1.044268579
67	64	1.1170107	1.5	2.4	0.807830738	3.141592654	10	15.07964474	0.390625	64	1.026676813
68	65	1.134464	1.5	2.4	0.821393805	3.141592654	10	15.07964474	0.390625	65	1.010384714

	A	B	C	D	E	F	G	H	I	J	K
69	66	1.1519173	1.5	2.4	0.834565303	3.141592654	10	15.07964474	0.390625	66	0.995283038
70	67	1.1693706	1.5	2.4	0.847329185	3.141592654	10	15.07964474	0.390625	67	0.981276491
71	68	1.1868239	1.5	2.4	0.8596699	3.141592654	10	15.07964474	0.390625	68	0.968281604
72	69	1.2042772	1.5	2.4	0.871572413	3.141592654	10	15.07964474	0.390625	69	0.956224999
73	70	1.2217305	1.5	2.4	0.883022222	3.141592654	10	15.07964474	0.390625	70	0.945041963
74	71	1.2391838	1.5	2.4	0.894005377	3.141592654	10	15.07964474	0.390625	71	0.934675264
75	72	1.2566371	1.5	2.4	0.904508497	3.141592654	10	15.07964474	0.390625	72	0.925074169
76	73	1.2740904	1.5	2.4	0.914518786	3.141592654	10	15.07964474	0.390625	73	0.916193626
77	74	1.2915436	1.5	2.4	0.924024048	3.141592654	10	15.07964474	0.390625	74	0.907993567
78	75	1.3089969	1.5	2.4	0.933012702	3.141592654	10	15.07964474	0.390625	75	0.900438328
79	76	1.3264502	1.5	2.4	0.941473796	3.141592654	10	15.07964474	0.390625	76	0.893496154
80	77	1.3439035	1.5	2.4	0.949397023	3.141592654	10	15.07964474	0.390625	77	0.887138778
81	78	1.3613568	1.5	2.4	0.956772729	3.141592654	10	15.07964474	0.390625	78	0.881341063
82	79	1.3788101	1.5	2.4	0.963591927	3.141592654	10	15.07964474	0.390625	79	0.8760807
83	80	1.3962634	1.5	2.4	0.96984631	3.141592654	10	15.07964474	0.390625	80	0.871337939
84	81	1.4137167	1.5	2.4	0.975528258	3.141592654	10	15.07964474	0.390625	81	0.867095375
85	82	1.43117	1.5	2.4	0.980630848	3.141592654	10	15.07964474	0.390625	82	0.863337751
86	83	1.4486233	1.5	2.4	0.985147863	3.141592654	10	15.07964474	0.390625	83	0.860051801
87	84	1.4660766	1.5	2.4	0.9890738	3.141592654	10	15.07964474	0.390625	84	0.857226108
88	85	1.4835299	1.5	2.4	0.992403877	3.141592654	10	15.07964474	0.390625	85	0.854850993
89	86	1.5009832	1.5	2.4	0.995134034	3.141592654	10	15.07964474	0.390625	86	0.852918417
90	87	1.5184364	1.5	2.4	0.997260948	3.141592654	10	15.07964474	0.390625	87	0.851421904
91	88	1.5358897	1.5	2.4	0.998782025	3.141592654	10	15.07964474	0.390625	88	0.850356481
92	89	1.553343	1.5	2.4	0.999695414	3.141592654	10	15.07964474	0.390625	89	0.849718626
93	90	1.5707963	1.5	2.4	1	3.141592654	10	15.07964474	0.390625	90	0.84950624

(a)



(b)

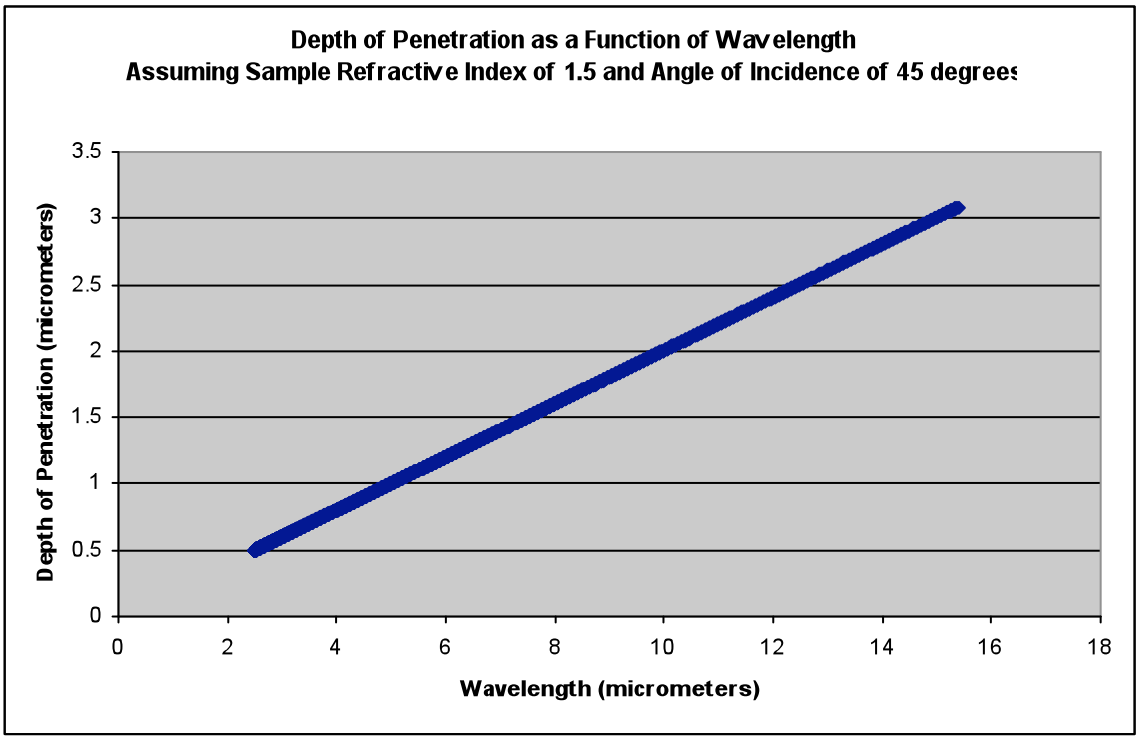


Figure 105: Depth of penetration variation as a function of the (a) wavenumber and (b) wavelength of the incident IR radiation.

Table 126: Depth of penetration variation as a function of the wavelength (or wavenumber) of the incident radiation calculations.

	A	B	C	D	E	F	G	H
1	Depth of Penetration Variation with Wavelength and Wavenumber							
2	Dp = λ /[(2 pi)*[n1^2* sin^2 theta - n2^2]^(1/2)							
3	Wavenumber (cm^-1)	Wavelength (cm)	Wavelength (micrometers)	2 * pi	n1^2 (n1 = 2.4)	sin^2 theta (theta = 45)	n2^2 (n2 = 1.5)	Depth of Penetration (micrometers)
4	650	0.001538462	15.38461538	6.283	5.76	0.5	2.25	3.084867394
5	651	0.001536098	15.3609831	6.283	5.76	0.5	2.25	3.080128735
6	652	0.001533742	15.33742331	6.283	5.76	0.5	2.25	3.075404611
7	653	0.001531394	15.31393568	6.283	5.76	0.5	2.25	3.070694956
8	654	0.001529052	15.29051988	6.283	5.76	0.5	2.25	3.065999704
9	655	0.001526718	15.26717557	6.283	5.76	0.5	2.25	3.061318788
10	656	0.00152439	15.24390244	6.283	5.76	0.5	2.25	3.056652144
11	657	0.00152207	15.22070015	6.283	5.76	0.5	2.25	3.051999705
12	658	0.001519757	15.19756839	6.283	5.76	0.5	2.25	3.047361408
13	659	0.001517451	15.17450683	6.283	5.76	0.5	2.25	3.042737187
14	660	0.001515152	15.15151515	6.283	5.76	0.5	2.25	3.038126979
15	661	0.001512859	15.12859304	6.283	5.76	0.5	2.25	3.033530721
16	662	0.001510574	15.10574018	6.283	5.76	0.5	2.25	3.028948348
17	663	0.001508296	15.08295626	6.283	5.76	0.5	2.25	3.024379799
18	664	0.001506024	15.06024096	6.283	5.76	0.5	2.25	3.01982501
19	665	0.001503759	15.03759398	6.283	5.76	0.5	2.25	3.015283919
20	666	0.001501502	15.01501502	6.283	5.76	0.5	2.25	3.010756466
21	667	0.00149925	14.99250375	6.283	5.76	0.5	2.25	3.006242588
22	668	0.001497006	14.97005988	6.283	5.76	0.5	2.25	3.001742225
23	669	0.001494768	14.94768311	6.283	5.76	0.5	2.25	2.997255316
24	670	0.001492537	14.92537313	6.283	5.76	0.5	2.25	2.992781801
25	671	0.001490313	14.90312966	6.283	5.76	0.5	2.25	2.988321619
26	672	0.001488095	14.88095238	6.283	5.76	0.5	2.25	2.983874712
27	673	0.001485884	14.85884101	6.283	5.76	0.5	2.25	2.97944102
28	674	0.00148368	14.83679525	6.283	5.76	0.5	2.25	2.975020484
29	675	0.001481481	14.81481481	6.283	5.76	0.5	2.25	2.970613047
30	676	0.00147929	14.79289941	6.283	5.76	0.5	2.25	2.966218649
31	677	0.001477105	14.77104874	6.283	5.76	0.5	2.25	2.961837233
32	678	0.001474926	14.74926254	6.283	5.76	0.5	2.25	2.957468741
33	679	0.001472754	14.7275405	6.283	5.76	0.5	2.25	2.953113117
34	680	0.001470588	14.70588235	6.283	5.76	0.5	2.25	2.948770304
35	681	0.001468429	14.68428781	6.283	5.76	0.5	2.25	2.944440244
36	682	0.001466276	14.66275666	6.283	5.76	0.5	2.25	2.940122883
37	683	0.001464129	14.64128843	6.283	5.76	0.5	2.25	2.935818165
38	684	0.001461988	14.61988304	6.283	5.76	0.5	2.25	2.931526033
39	685	0.001459854	14.59854015	6.283	5.76	0.5	2.25	2.927246433
40	686	0.001457726	14.57725948	6.283	5.76	0.5	2.25	2.92297931
41	687	0.001455604	14.55604076	6.283	5.76	0.5	2.25	2.918724609
42	688	0.001453488	14.53488372	6.283	5.76	0.5	2.25	2.914482277
43	689	0.001451379	14.5137881	6.283	5.76	0.5	2.25	2.910252259
44	690	0.001449275	14.49275362	6.283	5.76	0.5	2.25	2.906034502
45	691	0.001447178	14.47178003	6.283	5.76	0.5	2.25	2.901828953
46	692	0.001445087	14.45086705	6.283	5.76	0.5	2.25	2.897635558
47	693	0.001443001	14.43001443	6.283	5.76	0.5	2.25	2.893454266
48	694	0.001440922	14.4092219	6.283	5.76	0.5	2.25	2.889285024

	A	B	C	D	E	F	G	H
49	695	0.001438849	14.38848921	6.283	5.76	0.5	2.25	2.885127779
50	696	0.001436782	14.36781609	6.283	5.76	0.5	2.25	2.88098248
51	697	0.00143472	14.3472023	6.283	5.76	0.5	2.25	2.876849077
52	698	0.001432665	14.32664756	6.283	5.76	0.5	2.25	2.872727516
53	699	0.001430615	14.30615165	6.283	5.76	0.5	2.25	2.868617749
54	700	0.001428571	14.28571429	6.283	5.76	0.5	2.25	2.864519723
55	701	0.001426534	14.26533524	6.283	5.76	0.5	2.25	2.86043339
56	702	0.001424501	14.24501425	6.283	5.76	0.5	2.25	2.856358699
57	703	0.001422475	14.22475107	6.283	5.76	0.5	2.25	2.852295599
58	704	0.001420455	14.20454546	6.283	5.76	0.5	2.25	2.848244043
59	705	0.00141844	14.18439716	6.283	5.76	0.5	2.25	2.844203981
60	706	0.001416431	14.16430595	6.283	5.76	0.5	2.25	2.840175363
≈								≈
3321								
3322	3964	0.000252271	2.522704339	6.283	5.76	0.5	2.25	0.505843543
3323	3965	0.000252207	2.522068096	6.283	5.76	0.5	2.25	0.505715966
3324	3966	0.000252143	2.521432173	6.283	5.76	0.5	2.25	0.505588463
3325	3967	0.00025208	2.520796572	6.283	5.76	0.5	2.25	0.505461005
3326	3968	0.000252016	2.52016129	6.283	5.76	0.5	2.25	0.505333621
3327	3969	0.000251953	2.519526329	6.283	5.76	0.5	2.25	0.5052063
3328	3970	0.000251889	2.518891688	6.283	5.76	0.5	2.25	0.505079044
3329	3971	0.000251826	2.518257366	6.283	5.76	0.5	2.25	0.504951853
3330	3972	0.000251762	2.517623364	6.283	5.76	0.5	2.25	0.504824725
3331	3973	0.000251699	2.51698968	6.283	5.76	0.5	2.25	0.504697661
3332	3974	0.000251636	2.516356316	6.283	5.76	0.5	2.25	0.504570661
3333	3975	0.000251572	2.51572327	6.283	5.76	0.5	2.25	0.504443725
3334	3976	0.000251509	2.515090543	6.283	5.76	0.5	2.25	0.504316853
3335	3977	0.000251446	2.514458134	6.283	5.76	0.5	2.25	0.504190044
3336	3978	0.000251383	2.513826043	6.283	5.76	0.5	2.25	0.5040633
3337	3979	0.000251319	2.51319427	6.283	5.76	0.5	2.25	0.503936619
3338	3980	0.000251256	2.512562814	6.283	5.76	0.5	2.25	0.503810002
3339	3981	0.000251193	2.511931675	6.283	5.76	0.5	2.25	0.503683448
3340	3982	0.00025113	2.511300854	6.283	5.76	0.5	2.25	0.503556958
3341	3983	0.000251067	2.510670349	6.283	5.76	0.5	2.25	0.503430531
3342	3984	0.000251004	2.510040161	6.283	5.76	0.5	2.25	0.503304168
3343	3985	0.000250941	2.509410289	6.283	5.76	0.5	2.25	0.503177869
3344	3986	0.000250878	2.508780733	6.283	5.76	0.5	2.25	0.503051632
3345	3987	0.000250815	2.508151492	6.283	5.76	0.5	2.25	0.502925459
3346	3988	0.000250752	2.507522568	6.283	5.76	0.5	2.25	0.50279935
3347	3989	0.000250689	2.506893958	6.283	5.76	0.5	2.25	0.502673303
3348	3990	0.000250627	2.506265664	6.283	5.76	0.5	2.25	0.50254732
3349	3991	0.000250564	2.505637685	6.283	5.76	0.5	2.25	0.5024214
3350	3992	0.000250501	2.505010020	6.283	5.76	0.5	2.25	0.502295543
3351	3993	0.000250438	2.50438267	6.283	5.76	0.5	2.25	0.502169749
3352	3994	0.000250376	2.503755633	6.283	5.76	0.5	2.25	0.502044018
3353	3995	0.000250313	2.503128911	6.283	5.76	0.5	2.25	0.50191835
3354	3996	0.00025025	2.502502503	6.283	5.76	0.5	2.25	0.501792744
3355	3997	0.000250188	2.501876407	6.283	5.76	0.5	2.25	0.501667202
3356	3998	0.000250125	2.501250625	6.283	5.76	0.5	2.25	0.501541722
3357	3999	0.000250063	2.500625156	6.283	5.76	0.5	2.25	0.501416306
3358	4000	0.00025	2.5	6.283	5.76	0.5	2.25	0.501290952
3359								

APPENDIX II: PERFORMANCE VALIDATION REPORTS



Performance Validation Report

IlluminatIR FT-IR MicroSpectrometer System

This document contains the results of the spectroscopic performance tests for the IlluminatIR FT-IR Micro Spectrometer System. The specifications for these tests ensure that the IlluminatIR FT-IR system is in good working order and meets criteria set forth by Smiths Detection to determine suitability for the intended applications of the product. These specifications are not meant to indicate a minimum performance level for installed systems. The actual performance level may depend on the age of and application of the instrument. The procedures, tests, and results herein do not constitute a warranty, expressed or implied, including those of merchantability or fitness for any particular purpose not expressly set forth herein.

Date: 1-31-2011 @ 11h25m43s

System Serial No.: 2573

Part No.: 006-2202

ATR Objective Serial No.: 1111

Part No.: 006-5087

ARO Objective Serial No.: 1570

Part No.: 006-5046

1. ARO Objective: System Alignment and Electrical Settings

Interferogram Peak Intensity(>25000): -28232 PASS
Inteferogram Peak Location (1024 ± 50):995 PASS

2. ARO Objective: Signal-to-Noise Ratio with 100um aperture

Measurement Parameters

1 minute acquisition for background and sample using default acquisition settings: 4 cm-1 resolution, Happ-Genzel apodization, MCT detector (**FOR ALL TEST**).

Repeat data collections 5 times.

Root mean square (RMS) noise measured in the 1142-1042 cm-1 interval for a transmission spectrum.

Signal-to-noise ratio is calculated via:

$SNR_{(RMS)} = 100 / NOISE_{(RMS)}$

Mean SNR is calculated

Results

Run	RMS Noise (1142-1042 cm-1)	Signal-to-Noise Ratio
1	0.0070	14210
2	0.0072	13907
3	0.0061	16277
4	0.0072	13984
5	0.0082	12172

Mean RMS Noise - 0.0071

Mean SNR - 14110 PASS

Mean SNR should exceed 7000:1

3. ATR Objective: Signal-to-Noise Ratio with 100um aperture

Measurement Parameters

1 minute acquisition for background and sample.

Repeat data collections 5 times.

Root mean square (RMS) noise measured in the 1142-1042 cm-1 interval for a transmission spectrum.

Signal-to-noise ratio is calculated via:

$SNR_{(RMS)} = 100 / NOISE_{(RMS)}$
Mean SNR is calculated

Results

Run	RMS Noise (1142-1042 cm-1)	Signal-to-Noise Ratio
1	0.0072	13838
2	0.0067	14920
3	0.0084	11882
4	0.0067	14920
5	0.0079	12620

Mean RMS Noise - 0.0074
Mean SNR - 13636 PASS

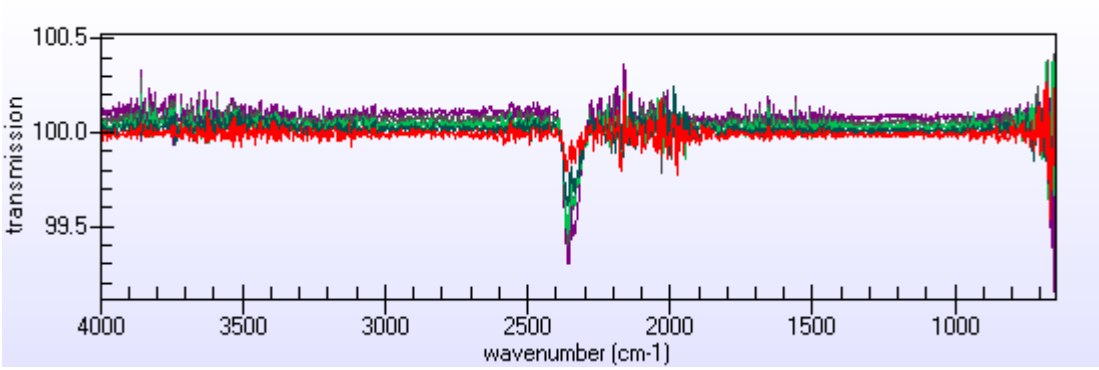
Mean SNR should exceed 7000:1

4. ATR Objective: Baseline Stability

Measurement Parameters

1 minute acquisition for background and sample.
5 acquisition (1 minute) samples ratioed to the same background.
Baseline drift is determined by measuring the difference between the maximum and minimum %transmittance between 3600-900 cm-1, ignoring the region 2400-1900 cm-1.

Results



(See Attached Page)

Baseline drift should be within 100 $\pm$ 2 %T for all five runs.

5. Laser Frequency Test(LFT)

Measurement Parameters

1 minute acquisition for background and sample.

1 minute acquisition polystyrene sample film. Determine the band positions (in cm-1) of the major absorption bands.

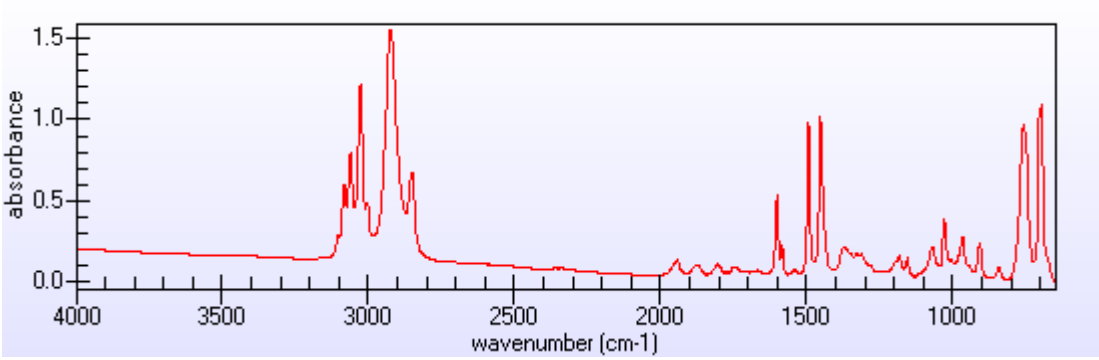
Compare the frequencies of the polystyrene measured to the NIST values for transmission (in vacuuo) for the 1921a polystyrene standard.

Results

Measured Frequencies (cm-1)	NIST Standard 1921a Frequencies (cm-1)	Difference (cm-1)
842.19	842.09	0.10
907.40	906.85	0.55
1028.51	1028.34	0.17
1069.50	1069.20	0.30
1155.21	1154.62	0.59
1583.76	1583.07	0.69
1602.39	1601.37	1.02
2850.77	2850.14	0.63
3025.91	3026.38	-0.47
3061.32	3060.03	1.29
3083.68	3082.14	1.54

Frequencies should be ± 3 cm-1 of the NIST standard.

(See Attached Polystyrene Spectrum) PASS



Tested by:

Brooke Weinger Kammrath_____

Performance Validation Report

IlluminatIR FT-IR MicroSpectrometer System

This document contains the results of the spectroscopic performance tests for the IlluminatIR FT-IR Micro Spectrometer System. The specifications for these tests ensure that the IlluminatIR FT-IR system is in good working order and meets criteria set forth by Smiths Detection to determine suitability for the intended applications of the product. These specifications are not meant to indicate a minimum performance level for installed systems. The actual performance level may depend on the age of and application of the instrument. The procedures, tests, and results herein do not constitute a warranty, expressed or implied, including those of merchantability or fitness for any particular purpose not expressly set forth herein.

Date: 4-21-2011 @ 15h1m52s

System Serial No.: 2573

Part No.: 006-2202

ATR Objective Serial No.: 1111

Part No.: 006-5087

ARO Objective Serial No.: 1570

Part No.: 006-5046

1. ARO Objective: System Alignment and Electrical Settings

Interferogram Peak Intensity(>25000):	-27518	PASS
Inteferogram Peak Location (1024 ± 50):	1001	PASS

2. ARO Objective: Signal-to-Noise Ratio with 100um aperture

Measurement Parameters

1 minute acquisition for background and sample using default acquisition settings: 4 cm-1 resolution, Happ-Genzel apodization, MCT detector (**FOR ALL TEST**).

Repeat data collections 5 times.

Root mean square (RMS) noise measured in the 1142-1042 cm-1 interval for a transmission spectrum.

Signal-to-noise ratio is calculated via:

$SNR_{(RMS)} = 100 / NOISE_{(RMS)}$

Mean SNR is calculated

Results

Run	RMS Noise (1142-1042 cm-1)	Signal-to-Noise Ratio
1	0.0053	18819
2	0.0064	15590
3	0.0070	14304
4	0.0049	20333
5	0.0067	14909

Mean RMS Noise - 0.0061

Mean SNR - 16791 PASS

Mean SNR should exceed 7000:1

3. ATR Objective: Signal-to-Noise Ratio with 100um aperture

Measurement Parameters

1 minute acquisition for background and sample.

Repeat data collections 5 times.

Root mean square (RMS) noise measured in the 1142-1042 cm-1 interval for a transmission spectrum.

Signal-to-noise ratio is calculated via:

$SNR_{(RMS)} = 100 / NOISE_{(RMS)}$
Mean SNR is calculated

Results

Run	RMS Noise (1142-1042 cm-1)	Signal-to-Noise Ratio
1	0.0074	13461
2	0.0049	20504
3	0.0082	12142
4	0.0067	15005
5	0.0065	15461

Mean RMS Noise - 0.0067
Mean SNR - 15315 PASS

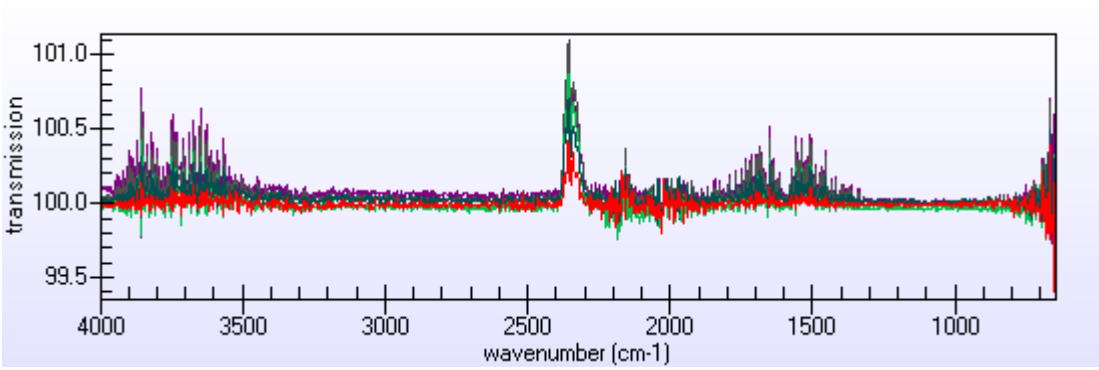
Mean SNR should exceed 7000:1

4. ATR Objective: Baseline Stability

Measurement Parameters

1 minute acquisition for background and sample.
5 acquisition (1 minute) samples ratioed to the same background.
Baseline drift is determined by measuring the difference between the maximum and minimum %transmittance between 3600-900 cm-1, ignoring the region 2400-1900 cm-1.

Results



(See Attached Page)

Baseline drift should be within 100 $\pm$ 2 %T for all five runs.

5. Laser Frequency Test(LFT)

Measurement Parameters

1 minute acquisition for background and sample.

1 minute acquisition polystyrene sample film. Determine the band positions (in cm-1) of the major absorption bands.

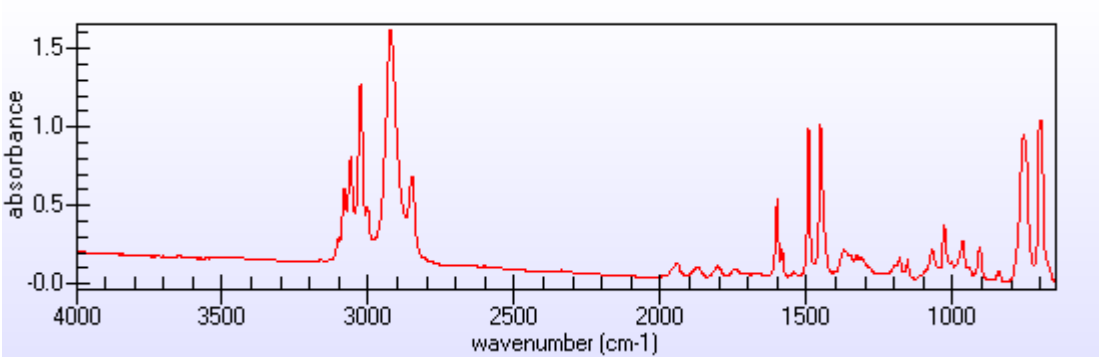
Compare the frequencies of the polystyrene measured to the NIST values for transmission (in vacuuo) for the 1921a polystyrene standard.

Results

Measured Frequencies (cm-1)	NIST Standard 1921a Frequencies (cm-1)	Difference (cm-1)
842.19	842.09	0.10
907.40	906.85	0.55
1028.51	1028.34	0.17
1069.50	1069.20	0.30
1155.21	1154.62	0.59
1583.76	1583.07	0.69
1602.39	1601.37	1.02
2850.77	2850.14	0.63
3025.91	3026.38	-0.47
3061.32	3060.03	1.29
3081.81	3082.14	-0.33

Frequencies should be ± 3 cm-1 of the NIST standard.

(See Attached Polystyrene Spectrum) PASS



Tested by:

Brooke Weinger Kammrath_____

Performance Validation Report

IlluminatIR FT-IR MicroSpectrometer System

This document contains the results of the spectroscopic performance tests for the IlluminatIR FT-IR Micro Spectrometer System. The specifications for these tests ensure that the IlluminatIR FT-IR system is in good working order and meets criteria set forth by Smiths Detection to determine suitability for the intended applications of the product. These specifications are not meant to indicate a minimum performance level for installed systems. The actual performance level may depend on the age of and application of the instrument. The procedures, tests, and results herein do not constitute a warranty, expressed or implied, including those of merchantability or fitness for any particular purpose not expressly set forth herein.

Date: 6-15-2011 @ 16h7m21s

System Serial No.: 2573

Part No.: 006-2202

ATR Objective Serial No.: 1111

Part No.: 006-5087

ARO Objective Serial No.: 1570

Part No.: 006-5046

1. ARO Objective: System Alignment and Electrical Settings

Interferogram Peak Intensity(>25000):	-28036	PASS
Inteferogram Peak Location (1024 ± 50):	1001	PASS

2. ARO Objective: Signal-to-Noise Ratio with 100um aperture

Measurement Parameters

1 minute acquisition for background and sample using default acquisition settings: 4 cm-1 resolution, Happ-Genzel apodization, MCT detector (**FOR ALL TEST**).

Repeat data collections 5 times.

Root mean square (RMS) noise measured in the 1142-1042 cm-1 interval for a transmission spectrum.

Signal-to-noise ratio is calculated via:

$SNR_{(RMS)} = 100 / NOISE_{(RMS)}$

Mean SNR is calculated

Results

Run	RMS Noise (1142-1042 cm-1)	Signal-to-Noise Ratio
1	0.0059	16986
2	0.0062	16163
3	0.0061	16262
4	0.0074	13547
5	0.0060	16803

Mean RMS Noise - 0.0063

Mean SNR - 15952 PASS

Mean SNR should exceed 7000:1

3. ATR Objective: Signal-to-Noise Ratio with 100um aperture

Measurement Parameters

1 minute acquisition for background and sample.

Repeat data collections 5 times.

Root mean square (RMS) noise measured in the 1142-1042 cm-1 interval for a transmission spectrum.

Signal-to-noise ratio is calculated via:

$SNR_{(RMS)} = 100 / NOISE_{(RMS)}$
Mean SNR is calculated

Results

Run	RMS Noise (1142-1042 cm-1)	Signal-to-Noise Ratio
1	0.0056	17761
2	0.0061	16398
3	0.0069	14520
4	0.0078	12877
5	0.0064	15663

Mean RMS Noise - 0.0066
Mean SNR - 15444 PASS

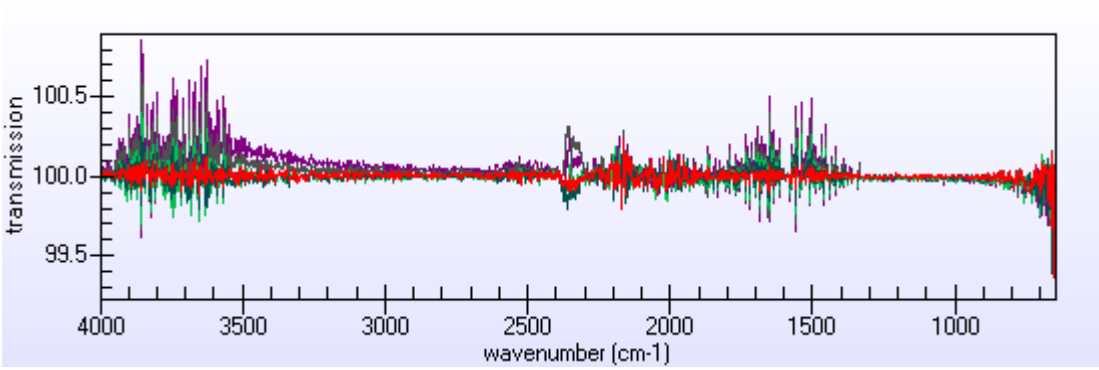
Mean SNR should exceed 7000:1

4. ATR Objective: Baseline Stability

Measurement Parameters

1 minute acquisition for background and sample.
5 acquisition (1 minute) samples ratioed to the same background.
Baseline drift is determined by measuring the difference between the maximum and minimum %transmittance between 3600-900 cm-1, ignoring the region 2400-1900 cm-1.

Results



(See Attached Page)

Baseline drift should be within 100 $\pm$ 2 %T for all five runs.

5. Laser Frequency Test(LFT)

Measurement Parameters

1 minute acquisition for background and sample.

1 minute acquisition polystyrene sample film. Determine the band positions (in cm-1) of the major absorption bands.

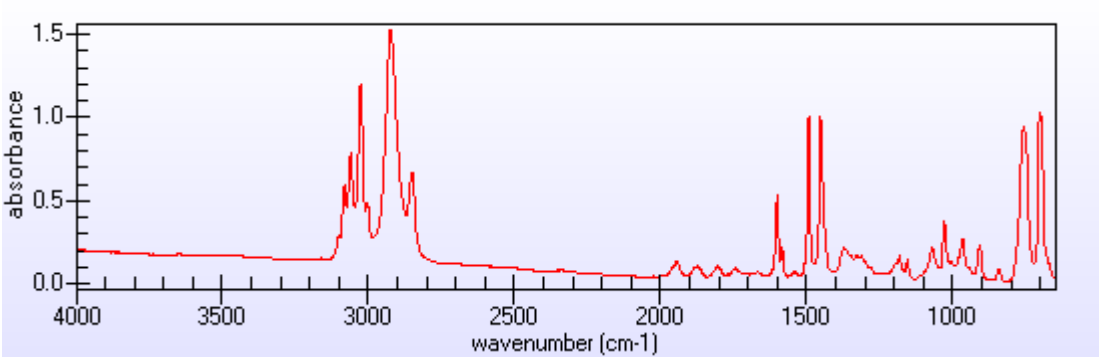
Compare the frequencies of the polystyrene measured to the NIST values for transmission (in vacuuo) for the 1921a polystyrene standard.

Results

Measured Frequencies (cm-1)	NIST Standard 1921a Frequencies (cm-1)	Difference (cm-1)
842.19	842.09	0.10
907.40	906.85	0.55
1028.51	1028.34	0.17
1069.50	1069.20	0.30
1155.21	1154.62	0.59
1583.76	1583.07	0.69
1602.39	1601.37	1.02
2848.91	2850.14	-1.23
3025.91	3026.38	-0.47
3061.32	3060.03	1.29
3081.81	3082.14	-0.33

Frequencies should be ± 3 cm-1 of the NIST standard.

(See Attached Polystyrene Spectrum) PASS



Tested by:

Brooke Weinger Kammrath_____

Performance Validation Report

IlluminatIR FT-IR MicroSpectrometer System

This document contains the results of the spectroscopic performance tests for the IlluminatIR FT-IR Micro Spectrometer System. The specifications for these tests ensure that the IlluminatIR FT-IR system is in good working order and meets criteria set forth by Smiths Detection to determine suitability for the intended applications of the product. These specifications are not meant to indicate a minimum performance level for installed systems. The actual performance level may depend on the age of and application of the instrument. The procedures, tests, and results herein do not constitute a warranty, expressed or implied, including those of merchantability or fitness for any particular purpose not expressly set forth herein.

Date: 7-13-2007 @ 13h19m25s

System Serial No.: 2573

Part No.: 006-2202

ATR Objective Serial No.: 1111

Part No.: 006-5087

ARO Objective Serial No.: 1570

Part No.: 006-5046

1. ARO Objective: System Alignment and Electrical Settings

Interferogram Peak Intensity(>25000): -26301 PASS
Inteferogram Peak Location (1024 ± 50):999 PASS

2. ARO Objective: Signal-to-Noise Ratio with 100um aperture

Measurement Parameters

1 minute acquisition for background and sample using default acquisition settings: 4 cm-1 resolution, Happ-Genzel apodization, MCT detector (**FOR ALL TEST**).

Repeat data collections 5 times.

Root mean square (RMS) noise measured in the 1142-1042 cm-1 interval for a transmission spectrum.

Signal-to-noise ratio is calculated via:

$SNR_{(RMS)} = 100 / NOISE_{(RMS)}$

Mean SNR is calculated

Results

Run	RMS Noise (1142-1042 cm-1)	Signal-to-Noise Ratio
1	0.0070	14352
2	0.0048	20863
3	0.0063	15786
4	0.0072	13929
5	0.0063	15838

Mean RMS Noise - 0.0063

Mean SNR - 16154 PASS

Mean SNR should exceed 7000:1

3. ATR Objective: Signal-to-Noise Ratio with 100um aperture

Measurement Parameters

1 minute acquisition for background and sample.

Repeat data collections 5 times.

Root mean square (RMS) noise measured in the 1142-1042 cm-1 interval for a transmission spectrum.

Signal-to-noise ratio is calculated via:
$SNR_{(RMS)} = 100 / NOISE_{(RMS)}$
Mean SNR is calculated

Results

Run	RMS Noise (1142-1042 cm-1)	Signal-to-Noise Ratio
1	0.0060	16531
2	0.0056	17929
3	0.0061	16516
4	0.0066	15216
5	0.0085	11819

Mean RMS Noise - 0.0065
Mean SNR - 15602 PASS

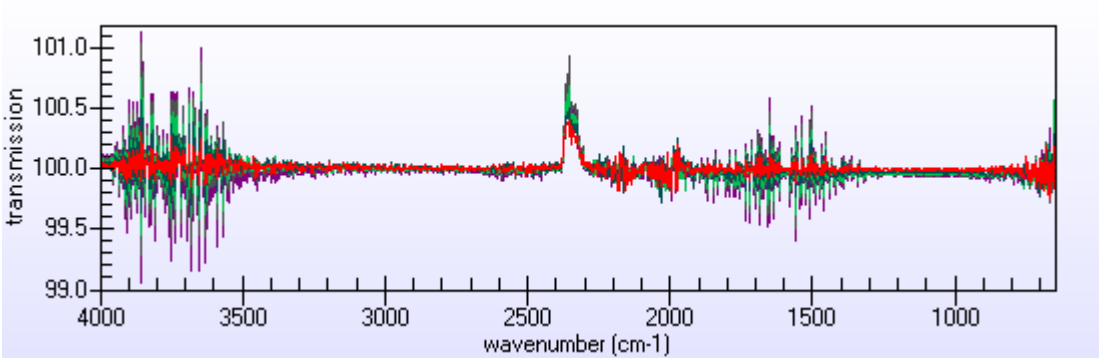
Mean SNR should exceed 7000:1

4. ATR Objective: Baseline Stability

Measurement Parameters

1 minute acquisition for background and sample.
5 acquisition (1 minute) samples ratioed to the same background.
Baseline drift is determined by measuring the difference between the maximum and minimum %transmittance between 3600-900 cm-1, ignoring the region 2400-1900 cm-1.

Results



(See Attached Page)

Baseline drift should be within 100 $\pm$ 2 %T for all five runs.

5. Laser Frequency Test(LFT)

Measurement Parameters

1 minute acquisition for background and sample.

1 minute acquisition polystyrene sample film. Determine the band positions (in cm-1) of the major absorption bands.

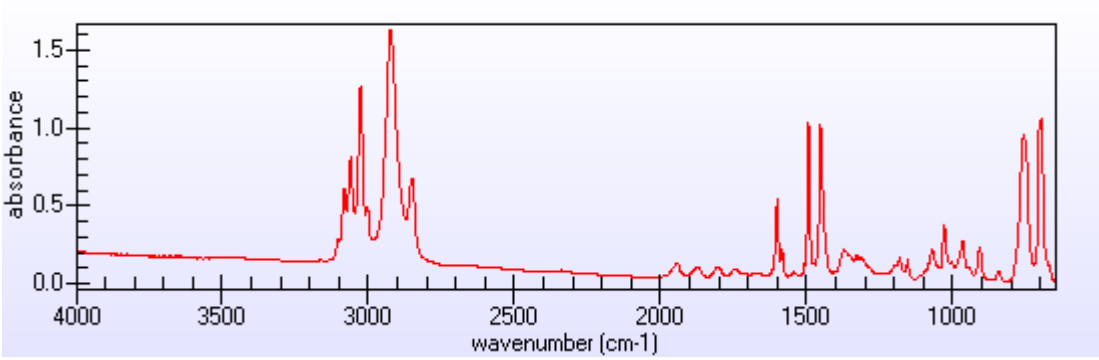
Compare the frequencies of the polystyrene measured to the NIST values for transmission (in vacuuo) for the 1921a polystyrene standard.

Results

Measured Frequencies (cm-1)	NIST Standard 1921a Frequencies (cm-1)	Difference (cm-1)
842.19	842.09	0.10
907.40	906.85	0.55
1028.51	1028.34	0.17
1069.50	1069.20	0.30
1155.21	1154.62	0.59
1583.76	1583.07	0.69
1602.39	1601.37	1.02
2850.77	2850.14	0.63
3025.91	3026.38	-0.47
3061.32	3060.03	1.29
3083.68	3082.14	1.54

Frequencies should be ± 3 cm-1 of the NIST standard.

(See Attached Polystyrene Spectrum) PASS



Tested by:

Brooke Weinger Kammrath_____

Performance Validation Report

IlluminatIR FT-IR MicroSpectrometer System

This document contains the results of the spectroscopic performance tests for the IlluminatIR FT-IR Micro Spectrometer System. The specifications for these tests ensure that the IlluminatIR FT-IR system is in good working order and meets criteria set forth by Smiths Detection to determine suitability for the intended applications of the product. These specifications are not meant to indicate a minimum performance level for installed systems. The actual performance level may depend on the age of and application of the instrument. The procedures, tests, and results herein do not constitute a warranty, expressed or implied, including those of merchantability or fitness for any particular purpose not expressly set forth herein.

Date: 8-2-2011 @ 12h24m27s

System Serial No.: 2573

Part No.: 006-2202

ATR Objective Serial No.: 1111

Part No.: 006-5087

ARO Objective Serial No.: 1570

Part No.: 006-5046

1. ARO Objective: System Alignment and Electrical Settings

Interferogram Peak Intensity(>25000):	-26989	PASS
Inteferogram Peak Location (1024 ± 50):	1001	PASS

2. ARO Objective: Signal-to-Noise Ratio with 100um aperture

Measurement Parameters

1 minute acquisition for background and sample using default acquisition settings: 4 cm-1 resolution, Happ-Genzel apodization, MCT detector (**FOR ALL TEST**).

Repeat data collections 5 times.

Root mean square (RMS) noise measured in the 1142-1042 cm-1 interval for a transmission spectrum.

Signal-to-noise ratio is calculated via:

$SNR_{(RMS)} = 100 / NOISE_{(RMS)}$

Mean SNR is calculated

Results

Run	RMS Noise (1142-1042 cm-1)	Signal-to-Noise Ratio
1	0.0054	18353
2	0.0049	20613
3	0.0070	14367
4	0.0065	15420
5	0.0059	16983

Mean RMS Noise - 0.0059

Mean SNR - 17147 PASS

Mean SNR should exceed 7000:1

3. ATR Objective: Signal-to-Noise Ratio with 100um aperture

Measurement Parameters

1 minute acquisition for background and sample.

Repeat data collections 5 times.

Root mean square (RMS) noise measured in the 1142-1042 cm-1 interval for a transmission spectrum.

Signal-to-noise ratio is calculated via:

$SNR_{(RMS)} = 100 / NOISE_{(RMS)}$
Mean SNR is calculated

Results

Run	RMS Noise (1142-1042 cm-1)	Signal-to-Noise Ratio
1	0.0073	13633
2	0.0053	18893
3	0.0082	12220
4	0.0058	17327
5	0.0088	11351

Mean RMS Noise - 0.0071
Mean SNR - 14685 PASS

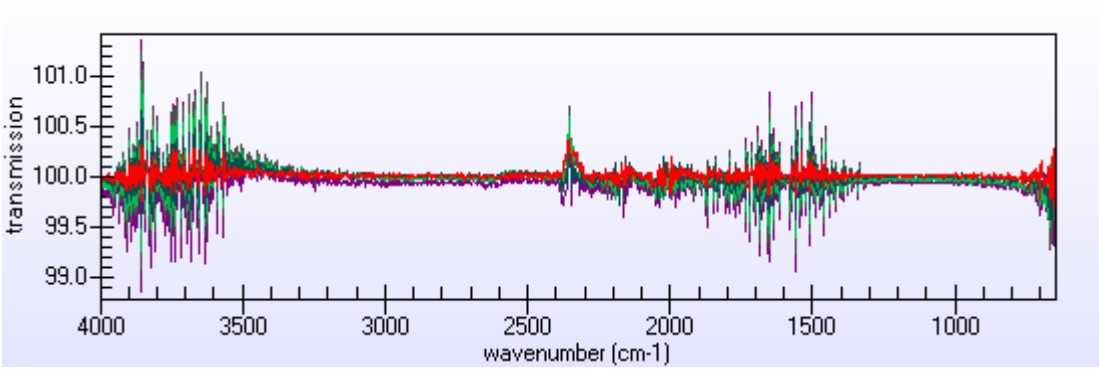
Mean SNR should exceed 7000:1

4. ATR Objective: Baseline Stability

Measurement Parameters

1 minute acquisition for background and sample.
5 acquisition (1 minute) samples ratioed to the same background.
Baseline drift is determined by measuring the difference between the maximum and minimum %transmittance between 3600-900 cm-1, ignoring the region 2400-1900 cm-1.

Results



(See Attached Page)

Baseline drift should be within 100 $\pm$ 2 %T for all five runs.

5. Laser Frequency Test(LFT)

Measurement Parameters

1 minute acquisition for background and sample.

1 minute acquisition polystyrene sample film. Determine the band positions (in cm-1) of the major absorption bands.

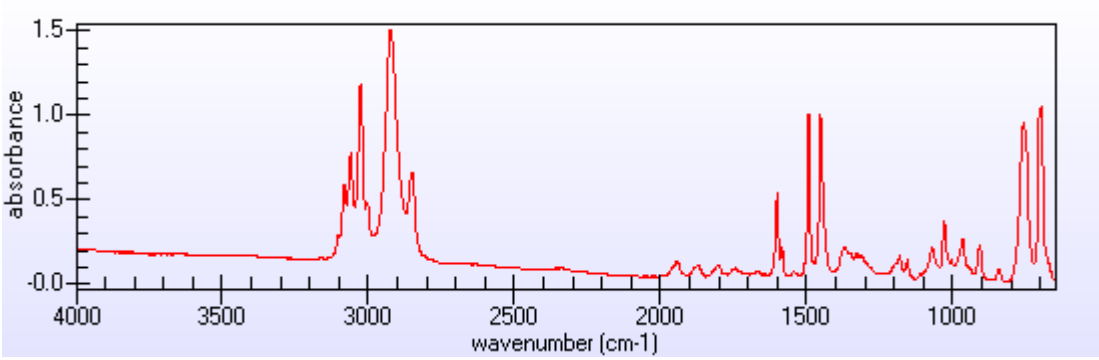
Compare the frequencies of the polystyrene measured to the NIST values for transmission (in vacuuo) for the 1921a polystyrene standard.

Results

Measured Frequencies (cm-1)	NIST Standard 1921a Frequencies (cm-1)	Difference (cm-1)
842.19	842.09	0.10
907.40	906.85	0.55
1028.51	1028.34	0.17
1069.50	1069.20	0.30
1155.21	1154.62	0.59
1583.76	1583.07	0.69
1602.39	1601.37	1.02
2850.77	2850.14	0.63
3025.91	3026.38	-0.47
3061.32	3060.03	1.29
3081.81	3082.14	-0.33

Frequencies should be ± 3 cm-1 of the NIST standard.

(See Attached Polystyrene Spectrum) PASS



Tested by:

Brooke Weinger Kammrath_____

Performance Validation Report

IlluminatIR FT-IR MicroSpectrometer System

This document contains the results of the spectroscopic performance tests for the IlluminatIR FT-IR Micro Spectrometer System. The specifications for these tests ensure that the IlluminatIR FT-IR system is in good working order and meets criteria set forth by Smiths Detection to determine suitability for the intended applications of the product. These specifications are not meant to indicate a minimum performance level for installed systems. The actual performance level may depend on the age of and application of the instrument. The procedures, tests, and results herein do not constitute a warranty, expressed or implied, including those of merchantability or fitness for any particular purpose not expressly set forth herein.

Date: 8-15-2011 @ 13h27m8s

System Serial No.: 2573

Part No.: 006-2202

ATR Objective Serial No.: 1111

Part No.: 006-5087

ARO Objective Serial No.: 1570

Part No.: 006-5046

1. ARO Objective: System Alignment and Electrical Settings

Interferogram Peak Intensity(>25000):	-26684	PASS
Inteferogram Peak Location (1024 ± 50):	1000	PASS

2. ARO Objective: Signal-to-Noise Ratio with 100um aperture

Measurement Parameters

1 minute acquisition for background and sample using default acquisition settings: 4 cm-1 resolution, Happ-Genzel apodization, MCT detector (**FOR ALL TEST**).

Repeat data collections 5 times.

Root mean square (RMS) noise measured in the 1142-1042 cm-1 interval for a transmission spectrum.

Signal-to-noise ratio is calculated via:

$SNR_{(RMS)} = 100 / NOISE_{(RMS)}$

Mean SNR is calculated

Results

Run	RMS Noise (1142-1042 cm-1)	Signal-to-Noise Ratio
1	0.0059	16871
2	0.0059	16855
3	0.0065	15289
4	0.0054	18391
5	0.0071	14116

Mean RMS Noise - 0.0062

Mean SNR - 16304 PASS

Mean SNR should exceed 7000:1

3. ATR Objective: Signal-to-Noise Ratio with 100um aperture

Measurement Parameters

1 minute acquisition for background and sample.

Repeat data collections 5 times.

Root mean square (RMS) noise measured in the 1142-1042 cm-1 interval for a transmission spectrum.

Signal-to-noise ratio is calculated via:

$SNR_{(RMS)} = 100 / NOISE_{(RMS)}$
Mean SNR is calculated

Results

Run	RMS Noise (1142-1042 cm-1)	Signal-to-Noise Ratio
1	0.0060	16601
2	0.0076	13220
3	0.0075	13263
4	0.0077	12995
5	0.0047	21164

Mean RMS Noise - 0.0067
Mean SNR - 15449 PASS

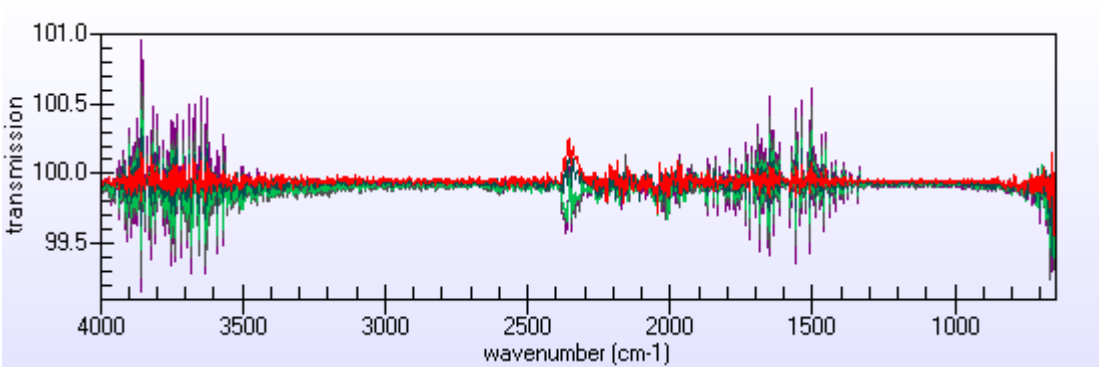
Mean SNR should exceed 7000:1

4. ATR Objective: Baseline Stability

Measurement Parameters

1 minute acquisition for background and sample.
5 acquisition (1 minute) samples ratioed to the same background.
Baseline drift is determined by measuring the difference between the maximum and minimum %transmittance between 3600-900 cm-1, ignoring the region 2400-1900 cm-1.

Results



(See Attached Page)

Baseline drift should be within 100 $\pm$ 2 %T for all five runs.

5. Laser Frequency Test(LFT)

Measurement Parameters

1 minute acquisition for background and sample.

1 minute acquisition polystyrene sample film. Determine the band positions (in cm-1) of the major absorption bands.

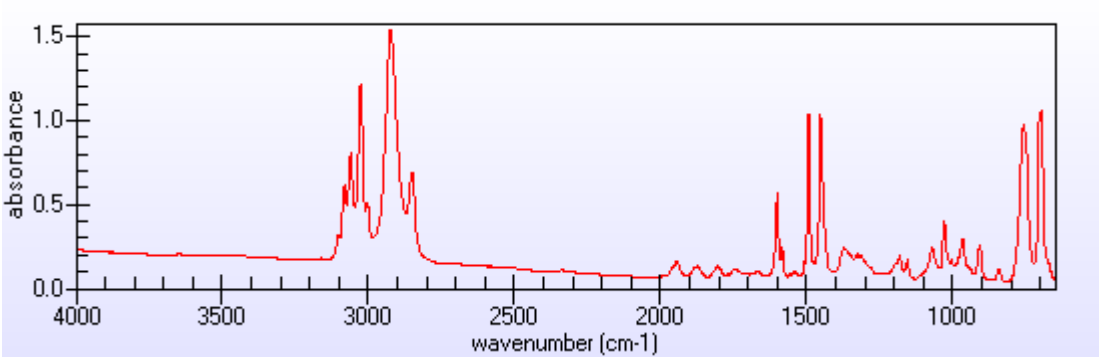
Compare the frequencies of the polystyrene measured to the NIST values for transmission (in vacuuo) for the 1921a polystyrene standard.

Results

Measured Frequencies (cm-1)	NIST Standard 1921a Frequencies (cm-1)	Difference (cm-1)
842.19	842.09	0.10
907.40	906.85	0.55
1028.51	1028.34	0.17
1069.50	1069.20	0.30
1155.21	1154.62	0.59
1583.76	1583.07	0.69
1602.39	1601.37	1.02
2848.91	2850.14	-1.23
3025.91	3026.38	-0.47
3061.32	3060.03	1.29
3081.81	3082.14	-0.33

Frequencies should be ± 3 cm-1 of the NIST standard.

(See Attached Polystyrene Spectrum) PASS



Tested by:

Brooke Weinger Kammrath_____

Performance Validation Report

IlluminatIR FT-IR MicroSpectrometer System

This document contains the results of the spectroscopic performance tests for the IlluminatIR FT-IR Micro Spectrometer System. The specifications for these tests ensure that the IlluminatIR FT-IR system is in good working order and meets criteria set forth by Smiths Detection to determine suitability for the intended applications of the product. These specifications are not meant to indicate a minimum performance level for installed systems. The actual performance level may depend on the age of and application of the instrument. The procedures, tests, and results herein do not constitute a warranty, expressed or implied, including those of merchantability or fitness for any particular purpose not expressly set forth herein.

Date: 8-30-2011 @ 11h33m42s

System Serial No.: 2573

Part No.: 006-2202

ATR Objective Serial No.: 1111

Part No.: 006-5087

ARO Objective Serial No.: 1570

Part No.: 006-5046

1. ARO Objective: System Alignment and Electrical Settings

Interferogram Peak Intensity(>25000): -26262 PASS
Inteferogram Peak Location (1024 ± 50):998 PASS

2. ARO Objective: Signal-to-Noise Ratio with 100um aperture

Measurement Parameters

1 minute acquisition for background and sample using default acquisition settings: 4 cm-1 resolution, Happ-Genzel apodization, MCT detector (**FOR ALL TEST**).

Repeat data collections 5 times.

Root mean square (RMS) noise measured in the 1142-1042 cm-1 interval for a transmission spectrum.

Signal-to-noise ratio is calculated via:

$SNR_{(RMS)} = 100 / NOISE_{(RMS)}$

Mean SNR is calculated

Results

Run	RMS Noise (1142-1042 cm-1)	Signal-to-Noise Ratio
1	0.0067	14821
2	0.0073	13645
3	0.0052	19399
4	0.0051	19609
5	0.0069	14541

Mean RMS Noise - 0.0062

Mean SNR - 16403 PASS

Mean SNR should exceed 7000:1

3. ATR Objective: Signal-to-Noise Ratio with 100um aperture

Measurement Parameters

1 minute acquisition for background and sample.

Repeat data collections 5 times.

Root mean square (RMS) noise measured in the 1142-1042 cm-1 interval for a transmission spectrum.

Signal-to-noise ratio is calculated via:

$SNR_{(RMS)} = 100 / NOISE_{(RMS)}$
Mean SNR is calculated

Results

Run	RMS Noise (1142-1042 cm-1)	Signal-to-Noise Ratio
1	0.0063	15992
2	0.0057	17430
3	0.0070	14374
4	0.0070	14207
5	0.0073	13785

Mean RMS Noise - 0.0066
Mean SNR - 15158 PASS

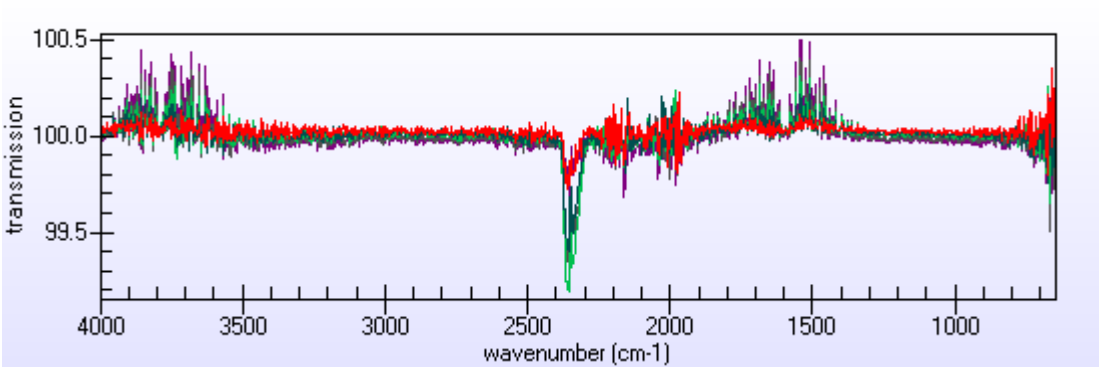
Mean SNR should exceed 7000:1

4. ATR Objective: Baseline Stability

Measurement Parameters

1 minute acquisition for background and sample.
5 acquisition (1 minute) samples ratioed to the same background.
Baseline drift is determined by measuring the difference between the maximum and minimum %transmittance between 3600-900 cm-1, ignoring the region 2400-1900 cm-1.

Results



(See Attached Page)

Baseline drift should be within 100 ± 2 %T for all five runs.

5. Laser Frequency Test(LFT)

Measurement Parameters

1 minute acquisition for background and sample.

1 minute acquisition polystyrene sample film. Determine the band positions (in cm-1) of the major absorption bands.

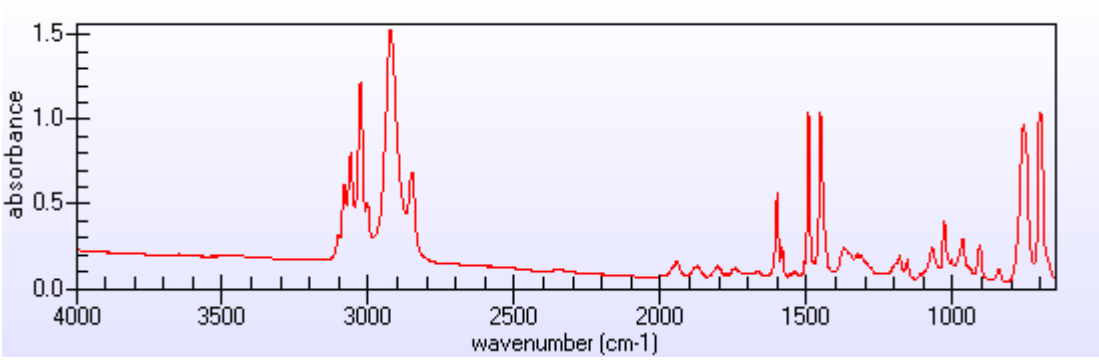
Compare the frequencies of the polystyrene measured to the NIST values for transmission (in vacuuo) for the 1921a polystyrene standard.

Results

Measured Frequencies (cm-1)	NIST Standard 1921a Frequencies (cm-1)	Difference (cm-1)
842.19	842.09	0.10
907.40	906.85	0.55
1028.51	1028.34	0.17
1069.50	1069.20	0.30
1155.21	1154.62	0.59
1583.76	1583.07	0.69
1602.39	1601.37	1.02
2850.77	2850.14	0.63
3025.91	3026.38	-0.47
3061.32	3060.03	1.29
3081.81	3082.14	-0.33

Frequencies should be ± 3 cm-1 of the NIST standard.

(See Attached Polystyrene Spectrum) PASS



Tested by:

Brooke Weinger Kammrath_____

Performance Validation Report

IlluminatIR FT-IR MicroSpectrometer System

This document contains the results of the spectroscopic performance tests for the IlluminatIR FT-IR Micro Spectrometer System. The specifications for these tests ensure that the IlluminatIR FT-IR system is in good working order and meets criteria set forth by Smiths Detection to determine suitability for the intended applications of the product. These specifications are not meant to indicate a minimum performance level for installed systems. The actual performance level may depend on the age of and application of the instrument. The procedures, tests, and results herein do not constitute a warranty, expressed or implied, including those of merchantability or fitness for any particular purpose not expressly set forth herein.

Date: 9-22-2011 @ 14h28m8s

System Serial No.: 2573

Part No.: 006-2202

ATR Objective Serial No.: 1111

Part No.: 006-5087

ARO Objective Serial No.: 1570

Part No.: 006-5046

1. ARO Objective: System Alignment and Electrical Settings

Interferogram Peak Intensity(>25000): -27319 PASS
Inteferogram Peak Location (1024 ± 50):997 PASS

2. ARO Objective: Signal-to-Noise Ratio with 100um aperture

Measurement Parameters

1 minute acquisition for background and sample using default acquisition settings: 4 cm-1 resolution, Happ-Genzel apodization, MCT detector (**FOR ALL TEST**).

Repeat data collections 5 times.

Root mean square (RMS) noise measured in the 1142-1042 cm-1 interval for a transmission spectrum.

Signal-to-noise ratio is calculated via:

$SNR_{(RMS)} = 100 / NOISE_{(RMS)}$

Mean SNR is calculated

Results

Run	RMS Noise (1142-1042 cm-1)	Signal-to-Noise Ratio
1	0.0050	19939
2	0.0076	13109
3	0.0060	16643
4	0.0047	21394
5	0.0068	14691

Mean RMS Noise - 0.0060

Mean SNR - 17155 PASS

Mean SNR should exceed 7000:1

3. ATR Objective: Signal-to-Noise Ratio with 100um aperture

Measurement Parameters

1 minute acquisition for background and sample.

Repeat data collections 5 times.

Root mean square (RMS) noise measured in the 1142-1042 cm-1 interval for a transmission spectrum.

Signal-to-noise ratio is calculated via:

$SNR_{(RMS)} = 100 / NOISE_{(RMS)}$
Mean SNR is calculated

Results

Run	RMS Noise (1142-1042 cm-1)	Signal-to-Noise Ratio
1	0.0153	6546
2	0.0152	6593
3	0.0121	8240
4	0.0147	6799
5	0.0101	9916

Mean RMS Noise - 0.0135
Mean SNR - 7619 PASS

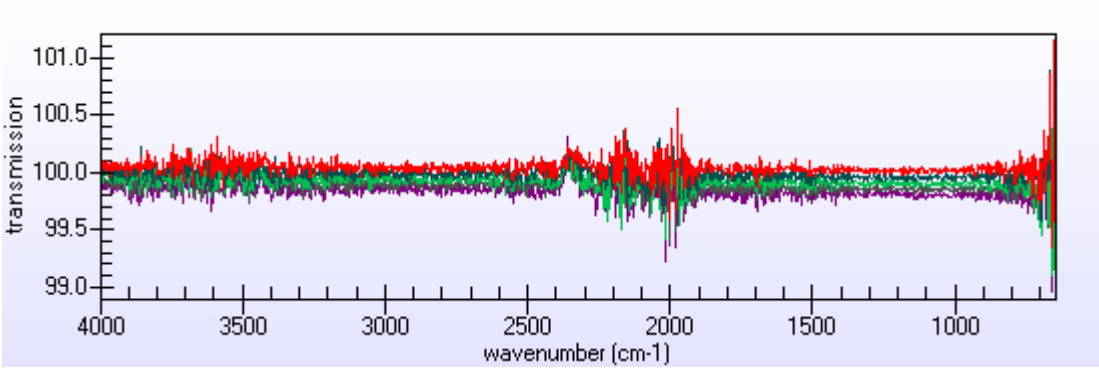
Mean SNR should exceed 7000:1

4. ATR Objective: Baseline Stability

Measurement Parameters

1 minute acquisition for background and sample.
5 acquisition (1 minute) samples ratioed to the same background.
Baseline drift is determined by measuring the difference between the maximum and minimum %transmittance between 3600-900 cm-1, ignoring the region 2400-1900 cm-1.

Results



(See Attached Page)

Baseline drift should be within 100 $\pm$ 2 %T for all five runs.

5. Laser Frequency Test(LFT)

Measurement Parameters

1 minute acquisition for background and sample.

1 minute acquisition polystyrene sample film. Determine the band positions (in cm-1) of the major absorption bands.

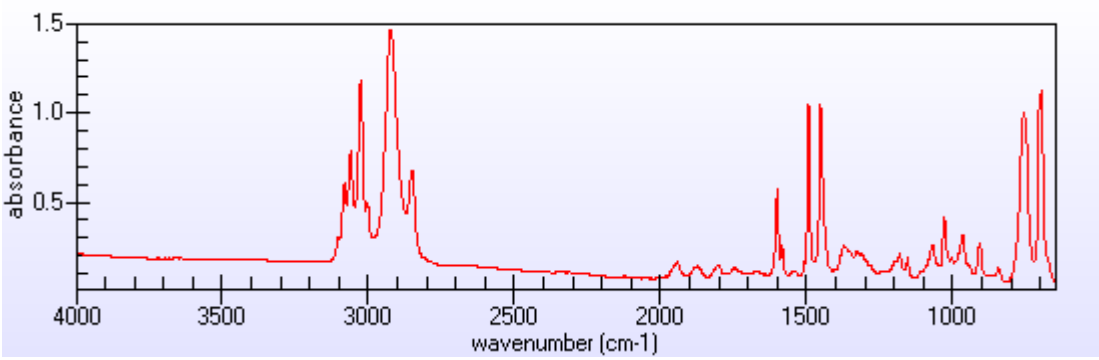
Compare the frequencies of the polystyrene measured to the NIST values for transmission (in vacuuo) for the 1921a polystyrene standard.

Results

Measured Frequencies (cm-1)	NIST Standard 1921a Frequencies (cm-1)	Difference (cm-1)
842.19	842.09	0.10
907.40	906.85	0.55
1028.51	1028.34	0.17
1069.50	1069.20	0.30
1155.21	1154.62	0.59
1583.76	1583.07	0.69
1602.39	1601.37	1.02
2848.91	2850.14	-1.23
3025.91	3026.38	-0.47
3061.32	3060.03	1.29
3081.81	3082.14	-0.33

Frequencies should be ± 3 cm-1 of the NIST standard.

(See Attached Polystyrene Spectrum) PASS



Tested by:

Brooke Weinger Kammrath_____

Performance Validation Report

IlluminatIR FT-IR MicroSpectrometer System

This document contains the results of the spectroscopic performance tests for the IlluminatIR FT-IR Micro Spectrometer System. The specifications for these tests ensure that the IlluminatIR FT-IR system is in good working order and meets criteria set forth by Smiths Detection to determine suitability for the intended applications of the product. These specifications are not meant to indicate a minimum performance level for installed systems. The actual performance level may depend on the age of and application of the instrument. The procedures, tests, and results herein do not constitute a warranty, expressed or implied, including those of merchantability or fitness for any particular purpose not expressly set forth herein.

Date: 10-19-2011 @ 12h59m22s

System Serial No.: 2573

Part No.: 006-2202

ATR Objective Serial No.: 1111

Part No.: 006-5087

ARO Objective Serial No.: 1570

Part No.: 006-5046

1. ARO Objective: System Alignment and Electrical Settings

Interferogram Peak Intensity(>25000): -25647 PASS
Inteferogram Peak Location (1024 ± 50):1006 PASS

2. ARO Objective: Signal-to-Noise Ratio with 100um aperture

Measurement Parameters

1 minute acquisition for background and sample using default acquisition settings: 4 cm-1 resolution, Happ-Genzel apodization, MCT detector (**FOR ALL TEST**).

Repeat data collections 5 times.

Root mean square (RMS) noise measured in the 1142-1042 cm-1 interval for a transmission spectrum.

Signal-to-noise ratio is calculated via:

$SNR_{(RMS)} = 100 / NOISE_{(RMS)}$

Mean SNR is calculated

Results

Run	RMS Noise (1142-1042 cm-1)	Signal-to-Noise Ratio
1	0.0066	15244
2	0.0055	18166
3	0.0052	19284
4	0.0056	17977
5	0.0083	11992

Mean RMS Noise - 0.0062

Mean SNR - 16533 PASS

Mean SNR should exceed 7000:1

3. ATR Objective: Signal-to-Noise Ratio with 100um aperture

Measurement Parameters

1 minute acquisition for background and sample.

Repeat data collections 5 times.

Root mean square (RMS) noise measured in the 1142-1042 cm-1 interval for a transmission spectrum.

Signal-to-noise ratio is calculated via:

$SNR_{(RMS)} = 100 / NOISE_{(RMS)}$
Mean SNR is calculated

Results

Run	RMS Noise (1142-1042 cm-1)	Signal-to-Noise Ratio
1	0.0155	6443
2	0.0153	6545
3	0.0161	6214
4	0.0131	7658
5	0.0120	8363

Mean RMS Noise - 0.0144
Mean SNR - 7045 PASS

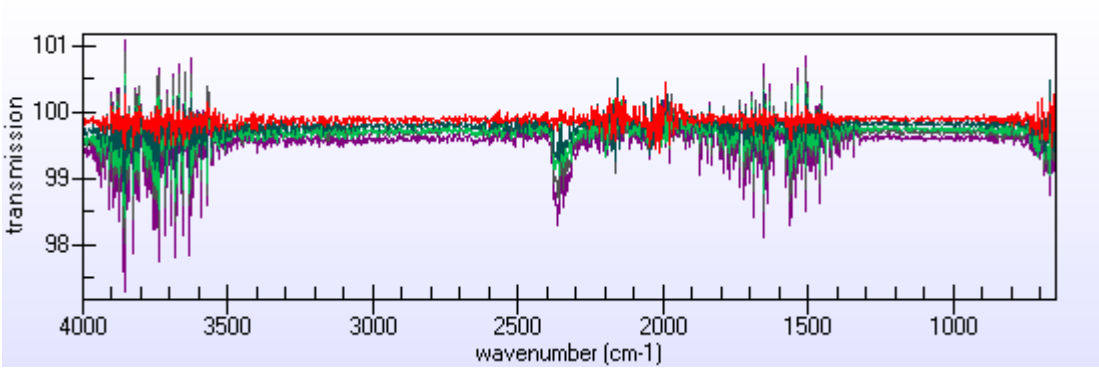
Mean SNR should exceed 7000:1

4. ATR Objective: Baseline Stability

Measurement Parameters

1 minute acquisition for background and sample.
5 acquisition (1 minute) samples ratioed to the same background.
Baseline drift is determined by measuring the difference between the maximum and minimum %transmittance between 3600-900 cm-1, ignoring the region 2400-1900 cm-1.

Results



(See Attached Page)

Baseline drift should be within 100 ± 2 %T for all five runs.

5. Laser Frequency Test(LFT)

Measurement Parameters

1 minute acquisition for background and sample.

1 minute acquisition polystyrene sample film. Determine the band positions (in cm-1) of the major absorption bands.

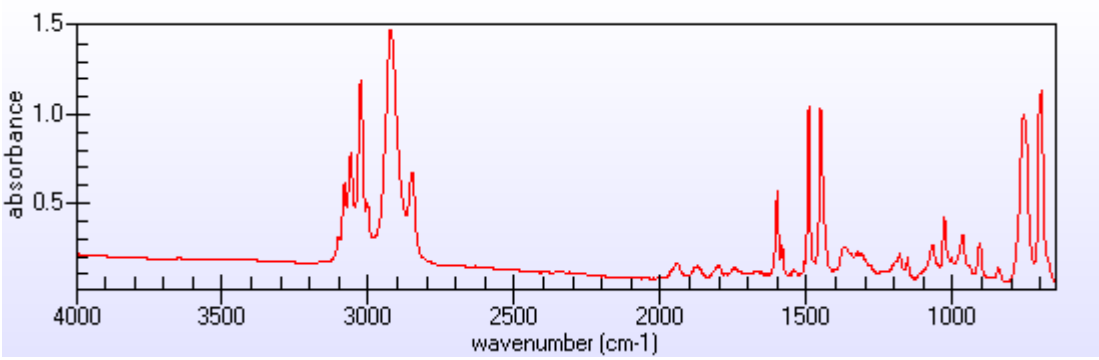
Compare the frequencies of the polystyrene measured to the NIST values for transmission (in vacuuo) for the 1921a polystyrene standard.

Results

Measured Frequencies (cm-1)	NIST Standard 1921a Frequencies (cm-1)	Difference (cm-1)
842.19	842.09	0.10
907.40	906.85	0.55
1028.51	1028.34	0.17
1069.50	1069.20	0.30
1155.21	1154.62	0.59
1583.76	1583.07	0.69
1600.53	1601.37	-0.84
2848.91	2850.14	-1.23
3025.91	3026.38	-0.47
3059.45	3060.03	-0.58
3081.81	3082.14	-0.33

Frequencies should be ± 3 cm-1 of the NIST standard.

(See Attached Polystyrene Spectrum) PASS



Tested by:

Brooke Weinger Kammrath_____

Performance Validation Report

IlluminatIR FT-IR MicroSpectrometer System

This document contains the results of the spectroscopic performance tests for the IlluminatIR FT-IR Micro Spectrometer System. The specifications for these tests ensure that the IlluminatIR FT-IR system is in good working order and meets criteria set forth by Smiths Detection to determine suitability for the intended applications of the product. These specifications are not meant to indicate a minimum performance level for installed systems. The actual performance level may depend on the age of and application of the instrument. The procedures, tests, and results herein do not constitute a warranty, expressed or implied, including those of merchantability or fitness for any particular purpose not expressly set forth herein.

Date: 10-31-2011 @ 11h49m33s

System Serial No.: 2573

Part No.: 006-2202

ATR Objective Serial No.: 1111

Part No.: 006-5087

ARO Objective Serial No.: 1570

Part No.: 006-5046

1. ARO Objective: System Alignment and Electrical Settings

Interferogram Peak Intensity(>25000):	-25743	PASS
Inteferogram Peak Location (1024 ± 50):	1004	PASS

2. ARO Objective: Signal-to-Noise Ratio with 100um aperture

Measurement Parameters

1 minute acquisition for background and sample using default acquisition settings: 4 cm-1 resolution, Happ-Genzel apodization, MCT detector (**FOR ALL TEST**).

Repeat data collections 5 times.

Root mean square (RMS) noise measured in the 1142-1042 cm-1 interval for a transmission spectrum.

Signal-to-noise ratio is calculated via:

$SNR_{(RMS)} = 100 / NOISE_{(RMS)}$

Mean SNR is calculated

Results

Run	RMS Noise (1142-1042 cm-1)	Signal-to-Noise Ratio
1	0.0081	12272
2	0.0051	19756
3	0.0067	14824
4	0.0062	16150
5	0.0069	14512

Mean RMS Noise - 0.0066

Mean SNR - 15503 PASS

Mean SNR should exceed 7000:1

3. ATR Objective: Signal-to-Noise Ratio with 100um aperture

Measurement Parameters

1 minute acquisition for background and sample.

Repeat data collections 5 times.

Root mean square (RMS) noise measured in the 1142-1042 cm-1 interval for a transmission spectrum.

Signal-to-noise ratio is calculated via:

$SNR_{(RMS)} = 100 / NOISE_{(RMS)}$
Mean SNR is calculated

Results

Run	RMS Noise (1142-1042 cm-1)	Signal-to-Noise Ratio
1	0.0106	9428
2	0.0109	9198
3	0.0098	10221
4	0.0091	10943
5	0.0096	10406

Mean RMS Noise - 0.0100
Mean SNR - 10039 PASS

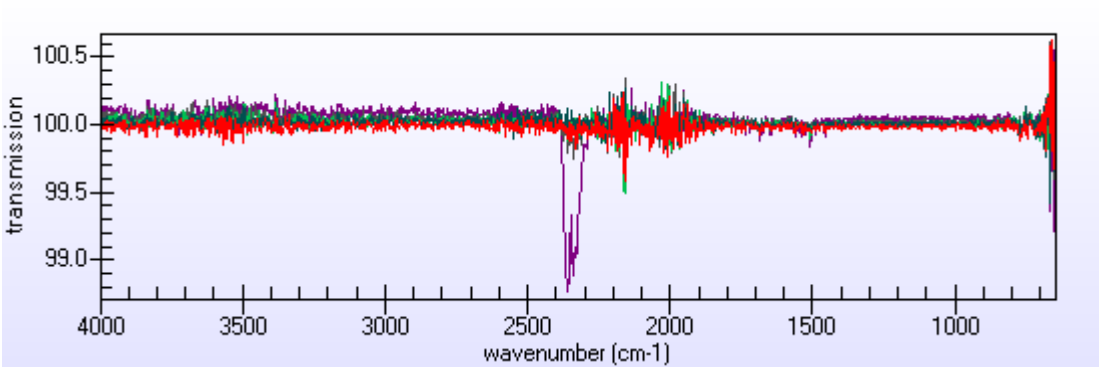
Mean SNR should exceed 7000:1

4. ATR Objective: Baseline Stability

Measurement Parameters

1 minute acquisition for background and sample.
5 acquisition (1 minute) samples ratioed to the same background.
Baseline drift is determined by measuring the difference between the maximum and minimum %transmittance between 3600-900 cm-1, ignoring the region 2400-1900 cm-1.

Results



(See Attached Page)

Baseline drift should be within 100 $\pm$ 2 %T for all five runs.

5. Laser Frequency Test(LFT)

Measurement Parameters

1 minute acquisition for background and sample.

1 minute acquisition polystyrene sample film. Determine the band positions (in cm-1) of the major absorption bands.

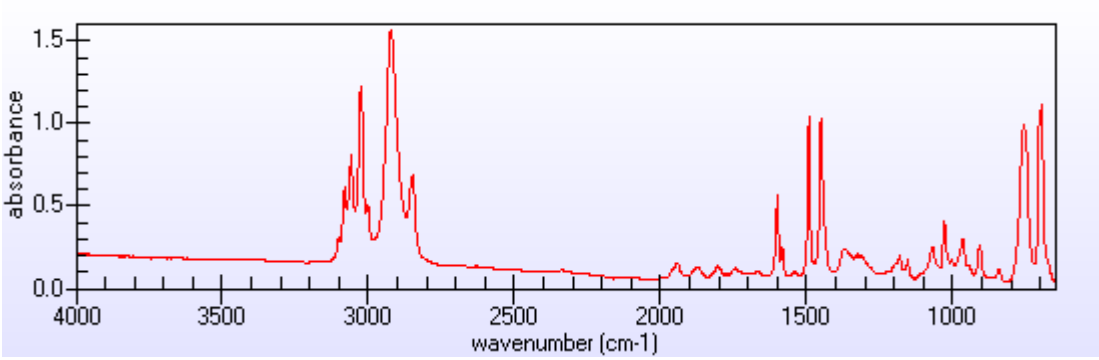
Compare the frequencies of the polystyrene measured to the NIST values for transmission (in vacuuo) for the 1921a polystyrene standard.

Results

Measured Frequencies (cm-1)	NIST Standard 1921a Frequencies (cm-1)	Difference (cm-1)
842.19	842.09	0.10
907.40	906.85	0.55
1028.51	1028.34	0.17
1069.50	1069.20	0.30
1155.21	1154.62	0.59
1583.76	1583.07	0.69
1600.53	1601.37	-0.84
2848.91	2850.14	-1.23
3024.05	3026.38	-2.33
3059.45	3060.03	-0.58
3081.81	3082.14	-0.33

Frequencies should be ± 3 cm-1 of the NIST standard.

(See Attached Polystyrene Spectrum) PASS



Tested by:

Brooke Weinger Kammrath_____

Performance Validation Report

IlluminatIR FT-IR MicroSpectrometer System

This document contains the results of the spectroscopic performance tests for the IlluminatIR FT-IR Micro Spectrometer System. The specifications for these tests ensure that the IlluminatIR FT-IR system is in good working order and meets criteria set forth by Smiths Detection to determine suitability for the intended applications of the product. These specifications are not meant to indicate a minimum performance level for installed systems. The actual performance level may depend on the age of and application of the instrument. The procedures, tests, and results herein do not constitute a warranty, expressed or implied, including those of merchantability or fitness for any particular purpose not expressly set forth herein.

Date: 12-13-2011 @ 13h15m23s

System Serial No.: 2573

Part No.: 006-2202

ATR Objective Serial No.: 1111

Part No.: 006-5087

ARO Objective Serial No.: 1570

Part No.: 006-5046

1. ARO Objective: System Alignment and Electrical Settings

Interferogram Peak Intensity(>25000): -25794 PASS
Inteferogram Peak Location (1024 ± 50):999 PASS

2. ARO Objective: Signal-to-Noise Ratio with 100um aperture

Measurement Parameters

1 minute acquisition for background and sample using default acquisition settings: 4 cm-1 resolution, Happ-Genzel apodization, MCT detector (**FOR ALL TEST**).

Repeat data collections 5 times.

Root mean square (RMS) noise measured in the 1142-1042 cm-1 interval for a transmission spectrum.

Signal-to-noise ratio is calculated via:

$SNR_{(RMS)} = 100 / NOISE_{(RMS)}$

Mean SNR is calculated

Results

Run	RMS Noise (1142-1042 cm-1)	Signal-to-Noise Ratio
1	0.0075	13311
2	0.0058	17147
3	0.0071	14084
4	0.0075	13394
5	0.0078	12885

Mean RMS Noise - 0.0071

Mean SNR - 14164 PASS

Mean SNR should exceed 7000:1

3. ATR Objective: Signal-to-Noise Ratio with 100um aperture

Measurement Parameters

1 minute acquisition for background and sample.

Repeat data collections 5 times.

Root mean square (RMS) noise measured in the 1142-1042 cm-1 interval for a transmission spectrum.

Signal-to-noise ratio is calculated via:

$SNR_{(RMS)} = 100 / NOISE_{(RMS)}$
Mean SNR is calculated

Results

Run	RMS Noise (1142-1042 cm-1)	Signal-to-Noise Ratio
1	0.0085	11700
2	0.0076	13125
3	0.0081	12354
4	0.0099	10068
5	0.0069	14549

Mean RMS Noise - 0.0082
Mean SNR - 12359 PASS

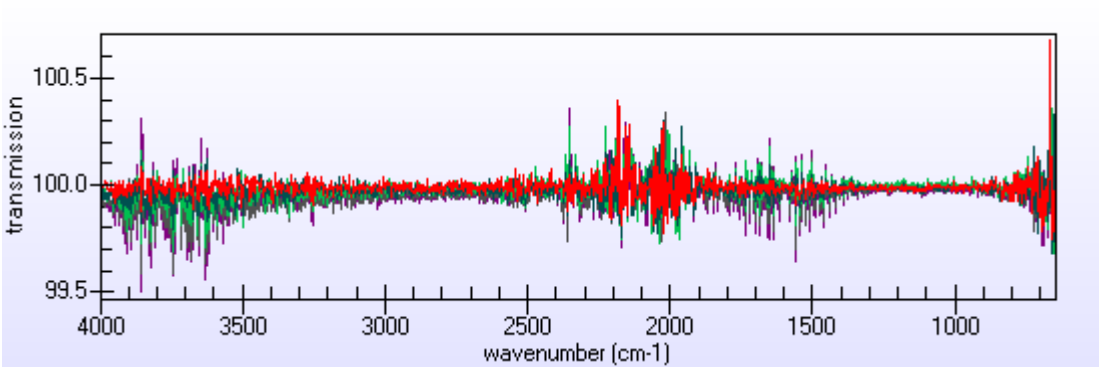
Mean SNR should exceed 7000:1

4. ATR Objective: Baseline Stability

Measurement Parameters

1 minute acquisition for background and sample.
5 acquisition (1 minute) samples ratioed to the same background.
Baseline drift is determined by measuring the difference between the maximum and minimum %transmittance between 3600-900 cm-1, ignoring the region 2400-1900 cm-1.

Results



(See Attached Page)

Baseline drift should be within 100 $\pm$ 2 %T for all five runs.

5. Laser Frequency Test(LFT)

Measurement Parameters

1 minute acquisition for background and sample.

1 minute acquisition polystyrene sample film. Determine the band positions (in cm-1) of the major absorption bands.

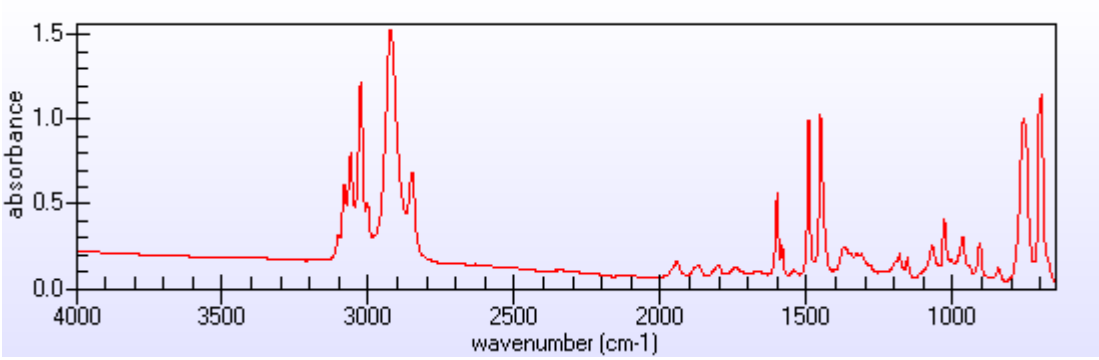
Compare the frequencies of the polystyrene measured to the NIST values for transmission (in vacuuo) for the 1921a polystyrene standard.

Results

Measured Frequencies (cm-1)	NIST Standard 1921a Frequencies (cm-1)	Difference (cm-1)
842.19	842.09	0.10
907.40	906.85	0.55
1028.51	1028.34	0.17
1069.50	1069.20	0.30
1155.21	1154.62	0.59
1583.76	1583.07	0.69
1602.39	1601.37	1.02
2850.77	2850.14	0.63
3025.91	3026.38	-0.47
3061.32	3060.03	1.29
3081.81	3082.14	-0.33

Frequencies should be ± 3 cm-1 of the NIST standard.

(See Attached Polystyrene Spectrum) PASS



Tested by:

Brooke Weinger Kammrath_____

Performance Validation Report

IlluminatIR FT-IR MicroSpectrometer System

This document contains the results of the spectroscopic performance tests for the IlluminatIR FT-IR Micro Spectrometer System. The specifications for these tests ensure that the IlluminatIR FT-IR system is in good working order and meets criteria set forth by Smiths Detection to determine suitability for the intended applications of the product. These specifications are not meant to indicate a minimum performance level for installed systems. The actual performance level may depend on the age of and application of the instrument. The procedures, tests, and results herein do not constitute a warranty, expressed or implied, including those of merchantability or fitness for any particular purpose not expressly set forth herein.

Date: 1-3-2012 @ 11h3m18s

System Serial No.: 2573

Part No.: 006-2202

ATR Objective Serial No.: 1111

Part No.: 006-5087

ARO Objective Serial No.: 1570

Part No.: 006-5046

1. ARO Objective: System Alignment and Electrical Settings

Interferogram Peak Intensity(>25000): -25732 PASS
Inteferogram Peak Location (1024 ± 50):996 PASS

2. ARO Objective: Signal-to-Noise Ratio with 100um aperture

Measurement Parameters

1 minute acquisition for background and sample using default acquisition settings: 4 cm-1 resolution, Happ-Genzel apodization, MCT detector (**FOR ALL TEST**).

Repeat data collections 5 times.

Root mean square (RMS) noise measured in the 1142-1042 cm-1 interval for a transmission spectrum.

Signal-to-noise ratio is calculated via:

$SNR_{(RMS)} = 100 / NOISE_{(RMS)}$

Mean SNR is calculated

Results

Run	RMS Noise (1142-1042 cm-1)	Signal-to-Noise Ratio
1	0.0065	15326
2	0.0069	14590
3	0.0064	15561
4	0.0065	15350
5	0.0056	17793

Mean RMS Noise - 0.0064

Mean SNR - 15724 PASS

Mean SNR should exceed 7000:1

3. ATR Objective: Signal-to-Noise Ratio with 100um aperture

Measurement Parameters

1 minute acquisition for background and sample.

Repeat data collections 5 times.

Root mean square (RMS) noise measured in the 1142-1042 cm-1 interval for a transmission spectrum.

Signal-to-noise ratio is calculated via:

$SNR_{(RMS)} = 100 / NOISE_{(RMS)}$
Mean SNR is calculated

Results

Run	RMS Noise (1142-1042 cm-1)	Signal-to-Noise Ratio
1	0.0098	10207
2	0.0076	13187
3	0.0084	11836
4	0.0097	10287
5	0.0093	10736

Mean RMS Noise - 0.0090
Mean SNR - 11251 PASS

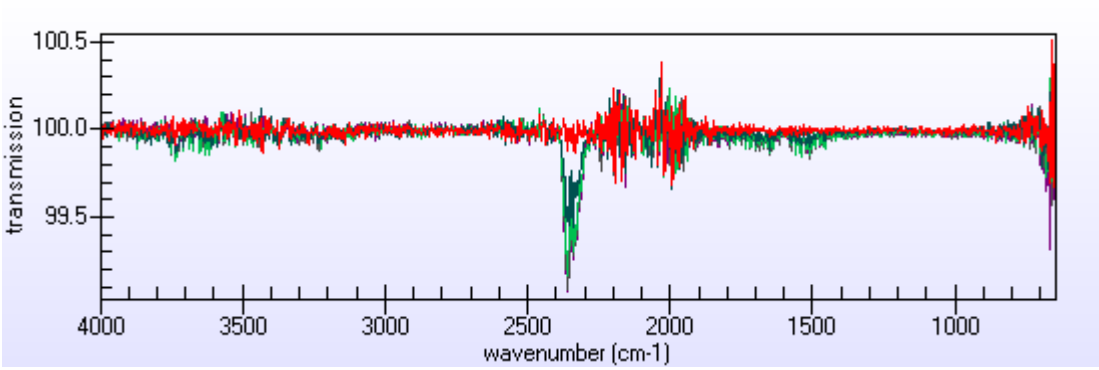
Mean SNR should exceed 7000:1

4. ATR Objective: Baseline Stability

Measurement Parameters

1 minute acquisition for background and sample.
5 acquisition (1 minute) samples ratioed to the same background.
Baseline drift is determined by measuring the difference between the maximum and minimum %transmittance between 3600-900 cm-1, ignoring the region 2400-1900 cm-1.

Results



(See Attached Page)

Baseline drift should be within 100 $\pm$ 2 %T for all five runs.

5. Laser Frequency Test(LFT)

Measurement Parameters

1 minute acquisition for background and sample.

1 minute acquisition polystyrene sample film. Determine the band positions (in cm-1) of the major absorption bands.

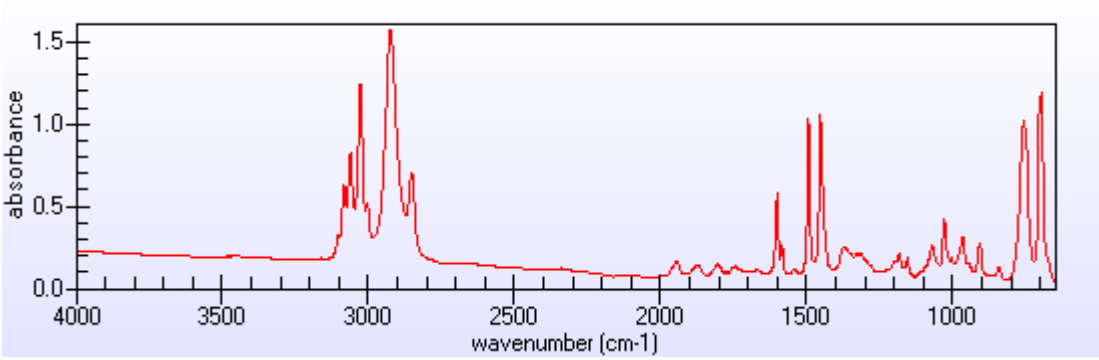
Compare the frequencies of the polystyrene measured to the NIST values for transmission (in vacuuo) for the 1921a polystyrene standard.

Results

Measured Frequencies (cm-1)	NIST Standard 1921a Frequencies (cm-1)	Difference (cm-1)
842.19	842.09	0.10
907.40	906.85	0.55
1028.51	1028.34	0.17
1069.50	1069.20	0.30
1155.21	1154.62	0.59
1583.76	1583.07	0.69
1602.39	1601.37	1.02
2850.77	2850.14	0.63
3025.91	3026.38	-0.47
3061.32	3060.03	1.29
3083.68	3082.14	1.54

Frequencies should be ± 3 cm-1 of the NIST standard.

(See Attached Polystyrene Spectrum) PASS



Tested by:

Brooke Weinger Kammrath_____

APPENDIX III: NIST CERTIFICATES

U. S. Department of Commerce
Malcolm Baldrige
Secretary

National Bureau of Standards
Ernest Ambler, Director

National Bureau of Standards

Certificate

Standard Reference Material 620

Soda–Lime Flat Glass

(In Cooperation with the American Society for Testing and Materials)

This Standard Reference Material is for use in checking chemical methods of analysis and for calibration in optical emission and x-ray spectrometric methods of analysis.

Constituent	Percent, by weight	Uncertainty
SiO_2	72.08	0.08
Na_2O	14.39	0.06
CaO	7.11	0.05
MgO	3.69	0.05
Al_2O_3	1.80	0.03
K_2O	0.41	0.03
SO_3	0.28	0.02
As_2O_3	0.056	0.003
Fe_2O_3	0.043	0.004
TiO_2	0.018	0.002

The certified values are the present best estimates of the "true" values based on the results of a cooperative analytical program. At NBS, fifteen statistically selected samples of the glass were extensively tested for homogeneity by S. D. Rasberry and C. K. Kim using x-ray fluorescence spectrometry. Based on their results the variations within and among samples are estimated to be less than the uncertainties given above.

The overall direction and coordination of the round-robin analysis leading to certification were performed by Paul Close, Chairman of ASTM Subcommittee C 14.02 on Chemical Analysis of Glass and Glass Products.

The technical and support aspects involved in the preparation, certification, and issuance of this Standard Reference Material were coordinated through the Office of Standard Reference Materials by G. W. Cleek and R. E. Michaelis.

Washington, D.C. 20234
January 13, 1982
(Revision of Certificate
dated 5/17/72)

George A. Uriano, Chief
Office of Standard Reference Materials

(over)

The material for this standard was prepared and furnished to NBS by American Saint Gobain Corporation (ASG), Jeannette Factory, Pennsylvania.

The following laboratories cooperated in the round-robin chemical analysis of this flat glass:

G. D. Bowling, Owens-Corning Fiberglass Corporation, Technical Center, Granville, Ohio

T. O. LaFramboise, Ford Motor Co., Glass Tech. Center, Lincoln Park, Michigan

Walter Gubar, Certain-Teed, Saint Gobain Insulation Corporation, Kansas City, Kansas

J. O. Hibbits, Owens-Illinois, Inc., Technical Center, Toledo, Ohio

Silve Kallman, Ledoux & Co., Teaneck, New Jersey

H. S. Moser, Owens-Illinois, Inc., Vineland, New Jersey

B. E. Pugh, Sharp-Schurtz Co., Lancaster, Ohio

R. E. Robertson, PPG Industries, Pittsburgh, Pennsylvania

Y. S. Su, Corning Glass Works, Corning, New York

L. E. Stadler, Emhart Corporation, Hartford Division, Hartford, Connecticut

K. M. Sappenfield, Analytical Chemistry Division, National Bureau of Standards, Gaithersburg, Maryland

U. S. Department of Commerce
Malcolm Baldrige
Secretary

National Bureau of Standards
Ernest Ambler, Director

National Bureau of Standards

Certificate

Standard Reference Material 621

Soda–Lime Container Glass

(In cooperation with the American Society for Testing and Materials)

This Standard Reference Material is for use in checking chemical methods of analysis and for calibrating optical emission and x-ray spectrometric methods of analysis.

Constituent	Percent by weight	Uncertainty
SiO_2	71.13	0.03
Na_2O	12.74	0.05
CaO	10.71	0.05
Al_2O_3	2.76	0.04
K_2O	2.01	0.03
MgO	0.27	0.03
SO_3	0.13	0.02
BaO	0.12	0.05
Fe_2O_3	0.040	0.003
As_2O_3	0.030	0.001
TiO_2	0.014	0.003
ZrO_2	0.007	0.001

The certified values are the present best estimates of the "true" values based on the results of a cooperative analytical program. At NBS twelve statistically selected samples of the glass were tested for homogeneity by S.D. Rasberry and L. Zinger using x-ray fluorescence spectrometry. Based on their results the variations among samples are estimated to be less than the uncertainties given above.

The overall direction and coordination of the round-robin analysis leading to certification were performed by Paul Close, Chairman of ASTM Subcommittee C-14.02 on Chemical Analysis of Glass and Glass Products.

The technical and support aspects involved in the preparation, certification, and issuance of this Standard Reference Material were coordinated through the Office of Standard Reference Materials by G.W. Cleek, C.L. Stanley, and R.E. Michaelis.

Washington, D.C. 20234
January 21, 1982
(Revision of certificate
dated 3/13/75.)

George A. Uriano, Chief
Office of Standard Reference Materials

(over)

The material for this SRM was prepared for NBS by Owens-Illinois, Inc., Technical Center, Toledo, Ohio. The following laboratories cooperated in the chemical analysis of this container glass:

T.B. Bodkin, Pennsylvania State University, University Park, Pennsylvania.

G.D. Bowling, Owens-Corning Fiberglass Corp., Technical Center, Granville; Ohio.

W.P. Close, Owens-Illinois, Inc., Technical Center, Toledo, Ohio.

H.S. Moser, Owens-Illinois, Inc., Vineland, New Jersey.

Y.S. Su, Corning Glass Works, Corning, New York.

L.E. Stadler, Emhart Corp., Hartford Division, Hartford, Connecticut.

E.J. Maienthal, Analytical Chemistry Division, National Bureau of Standards.

National Institute of Standards & Technology

Certificate of Analysis

Standard Reference Material® 1831

Soda-Lime Sheet Glass (1.2 % Al_2O_3)

(In Cooperation with ASTM)

This Standard Reference Material (SRM) is in the form of platelets approximately 38 mm square and is intended for use in checking chemical methods of analysis and in calibrating instrumental methods of analysis. The certified values are listed in Table 1 and represent the present best estimate of the "true value" based on the results of the cooperative program for certification. All values are reported as mass fractions [1].

The uncertainties listed are expressed as "combined uncertainties" calculated according to the ISO and NIST Guides [2]. Each uncertainty is based on the 95 % confidence limit of the "true value," and is intended to represent the combined effect of uncertainty components associated with various analytical factors such as method imprecision, possible systematic errors among methods, and material variability.

Table 1. Certified Mass Fractions

Constituent	Mass Fraction (in %)		
SiO_2	73.08[a,l]	±	0.08
Na_2O	13.32[a,m,f,c]	±	0.05
CaO	8.20[a,m,k,g]	±	0.05
MgO	3.51[a,m,i,k]	±	0.05
Al_2O_3	1.21[a,m,k,n,j,i,e]	±	0.04
K_2O	0.33[a,c,m,e]	±	0.02
SO_3	0.25[a,b]	±	0.01
Fe_2O_3 (total iron as)	0.087[a,m,h]	±	0.003
FeO	0.025[a]	±	0.007
TiO_2	0.019[a,d,h]	±	0.002

Methods Used: The primary procedures used in the analysis of this SRM are those recommended for referee analysis in ASTM C 169, Standard Methods for Chemical Analysis of Soda-Lime and Borosilicate Glass. All methods used in the certification of SRM 1831 are cited in Table 1.

[a]ASTM C 169 referee analysis	[f]Magnesium Uranyl Acetate	[k]Complexometric
[b]Combustion	[g]$KMnO_4$ Titration	[l]Gravimetric (Single-Dehydration)
[c]Flame Emission	[h]X-ray Fluorescence	[m]Atomic Absorption
[d]Spectrophotometry	[i]Gravimetric (8-Hydroxyquinoline)	[n]Gravimetric (Double Precipitate)
[e]Butyl Alcohol, $HClO_4$	[j]Gravimetric (Single-Precipitation)	

The technical and support aspects involved in the original preparation, certification, and issuance of this SRM were coordinated through the Standard Reference Materials Program by W.P. Reed and R.K. Kirby. Revision of this certificate was coordinated through the Standard Reference Materials Program by B.S. MacDonald.

Gaithersburg, MD 20899
Certificate Issue Date: May 21, 2007*
7/18/82 (original certificate date); 9/10/91 (iron oxide added)
*Removal of Table 2 and updated uncertainty values.

Thomas E. Gills, Chief
Standard Reference Materials Program

CAUTION: Before using the SRM in checking chemical analysis, it must be ground in agate to -200 mesh.

Homogeneity: This material was tested for homogeneity at NIST by P.A. Pella and R.L. Myklebust of the NIST Analytical Chemistry Division using X-ray fluorescence spectrometry. Three to five replicate measurements were made on at least 10 elements in each of 15 samples chosen at random from the lot of material. The results did not indicate any significant difference between the samples; the relative standard deviation for each element was less than 1 %.

The material for this SRM was prepared and furnished to NIST by The Pittsburgh Plate Glass Industries, Inc., Pittsburgh, PA.

Development of this SRM is part of the program of ASTM Subcommittee C14.91 on Standard Reference Materials, H.E. Hagy, Chairman. The overall direction and coordination of the cooperative analyses leading to certification originally and in revision to include iron oxide were performed by G.D. Bowling, Chairman of ASTM Subcommittee C14.02 on Chemical Properties and Analysis of Glass and Glass Products.

Cooperative analyses for certification were performed in the following laboratories:

Anchor Hocking Corp., Lancaster, OH
Broadway Glass Co., Inc., Brockway, PA
Corning Glass Works, Corning, NY
Emhart Industries, Inc., Windsor, CT
Ford Motor Co., Lincoln Park, MI
Libbey-Owens-Ford Co., Toledo, OH
Monarch Analytical Laboratories, Inc.,Toledo, OH
Owens-Corning Fiberglass Corp., Granville, OH
Owens-Illinois, Inc., Toledo, OH and Vineland, NJ
Pennsylvania State University, University Park, PA
Schott Glass Technologies, Inc., Duryea, PA
Sharp-Schurtz Co., Lancaster, PA
Thatcher Glass Co., Elmira, NY

REFERENCES

[1] Taylor, B.N., "Guide for the Use of the International System of Units (SI)," NIST Special Publication 811, 1995 Ed., (April 1995).

[2] *Guide to the Expression of Uncertainty in Measurement,* ISBN 92-67-10188-9, lst Ed. ISO, Geneva, Switzerland, (1993): see also Taylor, B.N. and Kuyatt, C.E., "Guidelines for Evaluating and Expressing the Uncertainty of NIST Measurement Results," NIST Technical Note 1297, U.S. Government Printing Office, Washington DC, (1994).

APPENDIX IV: GLASS SAMPLES

Table 127: Source information about the glasses analyzed in this research, as well as optical and physical properties (all provided by Scott Ryland, FDLE).

Sample ID	nD (20 deg.)	nC (20 deg.)	nF (20 deg.)	Density (25 deg.)	Thickness (mm)	Float	Tempered	Anneal (ΔnD)	Notes
W2	1.5181	1.5155	1.5243	2.4909	4.80	N	N		
W5	1.5181	1.5155	1.5242	2.4908	2.30	N	N		residence window
W10	1.5141	1.5114	1.5203	2.4732	5.70	N	Y		vehicle side window
W12	1.5178	1.5151	1.5241	2.4896	2.55	N	N		inside vehicle windshield
W13	1.5178	1.5152	1.5240	2.4894	2.45	N	N		outside vehicle windshield
W18	1.5193	1.5167	1.5256	2.4946		N	N		outside vehicle windshield
W19	1.5180	1.5153	1.5242	2.4899	2.60	N	N		inside vehicle windshield
W20	1.5165	1.5139	1.5225	2.4831	2.50	N	N		outside vehicle windshield
W21	1.5173	1.5146	1.5236	2.4866	2.50	N	N		inside vehicle windshield
W22	1.5195	1.5169	1.5257	2.4959	3.20	N	N		inside vehicle windshield
W23	1.5184	1.5158	1.5247	2.4907	5.95	Y	Y		vehicle side window
W33	1.5185	1.5158	1.5247	2.4880	4.75	Y	Y		vehicle side window
W35	1.5170	1.5144	1.5235	2.4866	4.70	N	Y		residence door window
W37	1.5181	1.5155	1.5243	2.4909	2.50	Y	N		
W47	1.5180	1.5154	1.5242	2.4914	3.10	Y	N		fire extinguisher case in motel
W49	1.5185	1.5160	1.5246	2.4923	2.40	Y	N		store window
W50	1.5135	1.5107	1.5199	2.4806	5.60	N	N		gas station window
W52	1.5159	1.5132	1.5222	2.4814	2.90	N	N		store window
W56	1.5230	1.5204	1.5293	2.5099	5.90	N	N		store window
W57	1.5201	1.5173	1.5267	2.4986	2.65	N	N		outside vehicle windshield
W58	1.5267	1.5241	1.5330	2.5261	5.90	N	N		store parallel-o-gray
W59	1.5229	1.5202	1.5295	2.5115	5.95	N	N		store window
W60	1.5187	1.5160	1.5249	2.4932	5.95	N	N		residential sliding door
W62	1.5184	1.5158	1.5246	2.4927	2.15	Y	N		hardware store window
W75	1.5143	1.5118	1.5204	2.4772	2.97	N	N		residence window
W79	1.5185	1.5159	1.5246	2.4931	5.79	Y	N		store plate glass (J.C.Penney Winter Park)
W80	1.5228	1.5202	1.5289		5.45	N	N		jalousie door window - surface orange peel textured
W83	1.5184	1.5156	1.5246	2.4901	3.95	Y	Y		vehicle side window
W87	1.5148	1.5121	1.5209	2.4748	5.75	N	Y		store door - Majik Market
W95	1.5185	1.5158	1.5247	2.4902	3.95	Y	Y		vehicle side window
W98	1.5180	1.5154	1.5242	2.4868	3.98	Y	Y		vehicle side window
W100	1.5182	1.5156	1.5244	2.4908	2.51	Y	N		outside vehicle windshield - colorless-Mercedes Benz
W103	1.5184	1.5158	1.5247	2.4899	4.81	Y	Y		vehicle side window
W106	1.5181	1.5155	1.5244	2.4895	4.69	Y	Y		store window - Circle K brown gray in color
W107	1.5185	1.5158	1.5248	2.4905	4.93	Y	Y		vehicle side window
W129	1.5185	1.5158	1.5248	2.4922	4.87	N	Y		sliding glass door brown in color
W132	1.5185	1.5159	1.5246	2.4933	5.61	Y	N		display case
W137	1.5148	1.5122	1.5210	2.4758	3.17	N	Y	20	store window (slight bulk fluor.)

W142	1.5185	1.5159	1.5246	2.4938	2.69	Y	N	9	laminated store window w/143
W143	1.5185	1.5159	1.5246	2.4942	2.69	Y	N	9	laminated store window w/142
W144	1.5181	1.5154	1.5243	2.4885	3.55	Y	Y		vehicle side window (rear)
W145	1.5181	1.5154	1.5244	2.4895	4.10	Y	Y		vehicle side window(front)
W149	1.5180	1.5153	1.5241	2.4891	4.76	Y	Y		parallel-o-bronze
W152	1.5185	1.5160	1.5249	2.4940	5.82	Y	N	8	bathroom window (outer pane)
W153	1.5185	1.5159	1.5248	2.4966	4.75	N	N	10	bathroom window patterned (inner pane)
W165	1.5184	1.5157	1.5246	2.4909	4.73	Y	Y		store window
W174	1.5184	1.5157	1.5247	2.4909	4.89	Y	Y	19	vehicle side window (passenger's side)
W178	1.5180	1.5154	1.5243	2.4917	2.25	Y	N		residence window
W189	1.5182	1.5156	1.5245		4.85	Y	Y	18	solar bronze
W193	1.5185	1.5159	1.5248	2.4902	4.08	Y	Y		vehicle rear window (frit)
W204	1.5185	1.5159	1.5248	2.4913	5.68	Y	N	7	store window
W206	1.5185	1.5158	1.5225	2.4916	5.69	Y	N	8	store window
W210	1.5180	1.5153	1.5244	2.4883	5.96	Y	Y	16	store window (brown)
W213	1.5181	1.5154	1.5246	2.4899	3.92	Y	Y	20	vehicle side window
W219	1.5181				4.74	Y	Y	17	store window
W222	1.5180				2.72	Y	N		store window
W224	1.5182			2.4865	5.78	Y	Y	18	business window - solar gray
W232	1.5185			2.4931	5.63	Y	N	7	business window
W234	1.5180			2.4925	2.69	Y	N	7	business window (door side A)
W235	1.5180			2.4926	2.7	Y	N	7	business window (door side B)
W241	1.5182				4.66	Y	Y	19	business door
W245	1.5181			2.4906	5.71	Y	Y	18	vehicle sunroof (reflect. surf)
W252	1.5182			2.4936	2.39	Y	N	9	residence window
W264	1.5182				2.98	N	N		vehicle outside rear view mirror
W272	1.5180				4.04	Y	Y		vehicle side window (rear pass side)
W282	1.5182				4.07	Y	Y		vehicle side window
W293	1.5181				5.68	Y	N	6	business window
W295	1.5181				5.73	Y	Y		business window
W346	1.5182				4.04	Y	Y		vehicle side window
W360	1.5184				2.29	Y	N	8	laminated business door (outside)
W368	1.5184				2.64	Y	N	9	residence window
W371	1.5206				2.23	Y	N		residence window (side 1 surf coat)
W372	1.5190				2.19	Y	N		residence window (side 2)
W383	1.5184				2.16	Y	N	9	residence window
W388	1.5207				2.20	Y	N		residence window
W392	1.5183				2.21	Y	N		residence window
W393	1.5181				2.67	Y	N	8	business door
W394	1.5181				2.67	Y	N	9	business door
W411	1.5178				3.10	Y	Y		residence door (front)
W412	1.5194				3.05	Y	Y		residence door (back)
W417	1.5136				6.06	Y	Y		business door
W418	1.5170				3.09	Y	Y		business door
W420	1.5203				2.96	Y	N	8	residential window
W423	1.5198				4.62	Y	N		business window
W426	1.5186				2.25	Y	N	10	business window
W442	1.5226				4.91	Y	Y		vehicle side window
W443	1.5194				3.33	Y	N	7	residential window (Solar gray)

W444	1.5215				2.22	Y	N	8	vehicle windshield (outside)
W445	1.5202				2.08	Y	N	8	vehicle windshield (inside)
W446	1.5199				3.84	Y	Y		vehicle side window
W448	1.5205				2.25	Y	N	10	vehicle windshield (side 1)
W449	1.5204			2.4994	2.26	Y	N	11	vehicle windshield (side 2)
W450	1.5211			2.4984	4.15	Y	Y	20	vehicle rear window
W451	1.5210				2.20	Y	N	9	vehicle windshield (outside)
W452	1.5214				2.08	Y	N	10	vehicle windshield (inside)
W453	1.5205				2.17	Y	N		business window
W454	1.5184				4.67	Y	Y	19	business window (Brown)
W455	1.5207				2.20	Y	N	10	vehicle windshield (inside)
W456	1.5207				2.32	Y	N	10	vehicle windshield (outside)
W457	1.5198				4.78	Y	Y	20	vehicle side window
W458	1.5185				4.4	Y	N		vehicle inside rear view mirror
W459	1.5184				2.25	Y	N		residential window
W461	1.5178				5.70	Y	N	16	business door
W464	1.5209				5.72	Y	Y	14	business door
W469	1.5204				5.65	Y	Y	15	business door
W470	1.5192				4.60	Y	Y	18	business door
W471	1.5189				2.78	Y	N	10	business door laminated (Side A)
W472	1.5189				2.78	Y	N	9	business door laminated (Side B)
W474	1.5182				3.52	Y	Y		vehicle side window
W475	1.5233				3.91	Y	Y		vehicle rear window
W476	1.5219				4.90	Y	Y		vehicle side window
W477	1.5192				5.89	Y	N	8	business window (Brown)
W478	1.5207				2.07	Y	N	9	vehicle windshield
W479	1.5208				5.69	Y	Y	18	business window
W480	1.5189				4.62	Y	Y	20	residence door
W481	1.5226				2.27	Y	N		vehicle windshield (outside)
W482	1.5226				2.27	Y	N		vehicle windshield (inside)
W483	1.5173				6.04	Y	Y	16	business window
W484	1.5201				2.02	Y	N	9	vehicle windshield (inside)
W485	1.5201				2.14	Y	N	9	vehicle windshield (outside)
W486	1.5209				4.10	Y	Y	21	vehicle side window
W487	1.5184				4.67	Y	Y	19	business door
W488	1.5199				4.71	Y	Y	18	business door
W489	1.5198				4.67	Y	Y		business door
W490	1.5175				4.59	Y	Y		business window
W491	1.5244				3.21	Y	Y		vehicle rear window (dark tint)
W492	1.5223				4.91	Y	Y		vehicle side window
W493	1.5204				3.89	Y	Y		vehicle side window
W494	1.5203				2.34	Y	N	10	vehicle windshield (inside)
W495	1.5203				2.34	Y	N	10	vehicle windshield (outside)
W498	1.5178				5.77	Y	Y		business door
W500	1.5188				3.01	Y	N		residence window
W501	1.5201				3.86	Y	Y		vehicle side window
W502	1.5219				2.32	Y	N		vehicle windshield (outside)
W503	1.5219				2.34	Y	N		vehicle windshield (inside)
W504	1.5243				4.08	Y	Y		vehicle window (dark tint)

W505	1.5201				3.84	Y	Y		vehicle side window
W506	1.5198				3.88	Y	Y		vehicle side window
W509	1.5183				3.38	Y	Y		vehicle side window
W510	1.5179				3.42	Y	Y		vehicle rear window
W511	1.5172				3.94	Y	Y	19	residence door
W512	1.5184				4.69	Y	Y		business door (brown)
W513	1.5184				4.66	Y	Y	17	business window
W514	1.5214				4.04	Y	Y	20	vehicle side window
W515	1.5225				4.09	Y	Y	19	vehicle side window (drk gray)
W516	1.5241				4.83	Y	Y		vehicle rear window (drk gray)
C49	1.52060								Thrifty Maid Apple Juice 1/2 gal.
C50	1.51700								Kraft Walnut Topping
C51	1.51774								Bluebird Apple Juice
C52	1.52153								White House Apple Juice
C53	1.51971								McCormick Minced Onion Seasoning
C54	1.51882								Frosted Bottle Jacquins Strawberry Dacquiri Mix
C55	1.51836								Pepsi Bottle no-returnable 16oz.
C56	1.51775								Pepsi Bottle Return
C57	1.51892								Strawberry Crush Dispo. Bottle
C58	1.52037								Clausseen Kosher Pickle Jar
C59	1.52079								Pepsi 1pt. Bottle
C60	1.51896								Dewar's White Label Scotch
C61	1.51745								Prego's Spaghetti Sauce
C62	1.51920								Johnnie Walker Scotch (miniature)
C63	1.52121								Canada Dry Tonic Water
C64	1.52004								Heinz Hickory Smoked BBQ Sauce
C65	1.52094								Reunete Duro Wine Bottle
C66	1.51787								Sunkist Orange Soda Disp. Bottle
C67	1.52182								Johnnie Walder Red 750ml Scotch Bottle Scotland
C68	1.52089								Pickel Jar (Clausen Dill)
C69	1.51814								Miracle Whip Jar (16oz)
C70	1.51859								Sugar Free Fraygo Diet Rock and Rye
C71	1.51721								Vlassic Sweet Midgets Pickles (16oz)
C72	1.51856								Johnny Walder Red Scotch Miniature
C73	1.51886								Dewars White Scotch Miniature
C74	1.51991								Nescafe (instant coffee) Decaf Rich & Natural 8oz
C75	1.51895								Pepsi 16oz Non-returnable Styrofoam Label
C76	1.52037								Los Hermanos 1985 White Cabernet 1.5L
C77	1.52039								Coke Bottle 16oz Returnable 1987
C78	1.51809								Smirnoff Vodka Bottle 35ml
C79	1.52109								Chevas Regal Scotch (1/5th)
C80	1.52114								Gordons Vodka Bottle 35ml
C81	1.51793								Kraft Tartar Sauce Jar 9oz
C82	1.52102								Beech Nut Baby Food Jar
C83	1.52132								Grey Poupon Mustard Jar 24oz
C84	1.51919								Quest Soda Bottle 10oz
C85	1.51650								Smirnoff Vodka Bottle 750ml
C86	1.52174								Bartles & James Wine Cooler Bottle 12oz

C87	1.52233								Chivas Regal Scotch 250ml from Scotland
C88	1.51658								Liquor Bottle from Jamaica
C89	1.52037								Weight Watchers Mayonnaise Jar 32oz
C90	1.52003								Old Time Soda Bottle 12oz
C91	1.52147								Clearly Canadian Soda Bottle 11oz
C92	1.51957								Very Fine Juice Bottle 10oz
C93	1.51839								Heinz Baby Food Jar 73/4oz
C94	1.52029								Eden Roc Champagne Bottle 750ml
C95	1.51435								Stoli Bottle
C96	1.51943								Sutter Home Wine Bottle 1.5L
C97	1.51997								Inglenook Wine Bottle 1.5L
C98	1.52129								Miller High Life Beer Bottle
C99	1.51900								Campbell's Tomato Juice Jar
C100	1.51998								Harry & David Wildn'Rare Preserves Jar(peach)
C101	1.52006								Harry & David Wildn'Rare Preserves Jar(strwberry)

APPENDIX V: METHOD DEVELOPMENT PEAK HEIGHTS FOR SRM GLASSES

Table 128: Peak Heights (in absorbance units) for SRMs 620, 621, 1831 taken with the 50-µm aperture and all 18 combinations of resolution and number of co-added scans (30 replicates). An average was calculated for each combination.

	1	2	3	4	5	6	7	8	9	10	11	12	13	14	15
SRM 620 4 8	1.431	1.435	1.467	1.470	1.432	1.469	1.417	1.405	1.330	1.385	1.502	1.306	1.272	1.263	1.489
SRM 620 8 8	1.386	1.392	1.377	1.425	1.370	1.313	1.395	1.328	1.450	1.382	1.305	1.405	1.462	1.527	1.433
SRM 620 16 8	1.464	1.421	1.474	1.438	1.414	1.350	1.464	1.403	1.378	1.381	1.337	1.412	1.439	1.475	1.430
SRM 620 4 16	1.444	1.444	1.447	1.378	1.365	1.440	1.419	1.401	1.419	1.349	1.438	1.418	1.380	1.386	1.471
SRM 620 8 16	1.457	1.463	1.408	1.447	1.351	1.362	1.428	1.406	1.439	1.402	1.457	1.352	1.390	1.410	1.407
SRM 620 16 16	1.396	1.453	1.439	1.404	1.451	1.452	1.453	1.432	1.447	1.392	1.373	1.422	1.458	1.463	1.458
SRM 620 4 32	1.471	1.482	1.483	1.377	1.457	1.401	1.362	1.400	1.433	1.448	1.444	1.420	1.405	1.411	1.411
SRM 620 8 32	1.394	1.466	1.476	1.462	1.437	1.451	1.400	1.444	1.383	1.474	1.488	1.474	1.478	1.438	1.414
SRM 620 16 32	1.487	1.466	1.495	1.467	1.467	1.477	1.432	1.423	1.431	1.464	1.503	1.507	1.485	1.514	1.438
SRM 620 4 64	1.421	1.511	1.450	1.460	1.368	1.565	1.560	1.507	1.492	1.537	1.484	1.466	1.464	1.416	1.399

SRM 621 4 16	SRM 621 16 8	SRM 621 8 8	SRM 621 4 8	SRM 620 16 256	SRM 620 8 256	SRM 620 4 256	SRM 620 16 128	SRM 620 8 128	SRM 620 4 128	SRM 620 16 64	SRM 620 8 64
0.684	0.570	0.625	0.529	1.590	1.600	1.565	1.536	1.522	1.540	1.492	1.512
0.707	0.736	0.605	0.837	1.469	1.574	1.584	1.512	1.433	1.558	1.511	1.519
0.832	0.806	0.623	0.851	1.481	1.588	1.559	1.441	1.540	1.547	1.493	1.484
0.824	0.660	0.694	0.721	1.468	1.597	1.570	1.531	1.513	1.526	1.500	1.535
0.610	0.602	0.629	0.741	1.479	1.584	1.561	1.536	1.524	1.567	1.484	1.433
0.823	0.541	0.838	0.517	1.517	1.584	1.536	1.559	1.553	1.543	1.525	1.408
0.804	0.728	0.615	0.749	1.456	1.593	1.504	1.310	1.523	1.494	1.500	1.501
0.844	0.720	0.625	0.822	1.466	1.579	1.507	1.565	1.427	1.509	1.555	1.460
0.761	0.727	0.785	0.685	1.542	1.589	1.476	1.562	1.492	1.512	1.570	1.445
0.591	0.677	0.679	0.669	1.525	1.599	1.557	1.559	1.529	1.522	1.573	1.449
0.597	0.922	0.684	0.814	1.448	1.599	1.562	1.579	1.575	1.484	1.547	1.516
0.760	0.597	0.856	0.784	1.431	1.594	1.543	1.570	1.481	1.410	1.542	1.519
0.594	0.661	0.740	0.608	1.414	1.591	1.578	1.588	1.559	1.481	1.520	1.520
0.691	0.564	0.721	0.768	1.544	1.596	1.499	1.509	1.577	1.457	1.443	1.524
0.710	0.673	0.829	0.547	1.484	1.605	1.503	1.442	1.361	1.411	1.529	1.535

SRM 621 4 256	SRM 621 16 128	SRM 621 8 128	SRM 621 4 128	SRM 621 16 64	SRM 621 8 64	SRM 621 4 64	SRM 621 16 32	SRM 621 8 32	SRM 621 4 32	SRM 621 16 16	SRM 621 8 16
0.685	0.633	0.610	0.553	0.556	0.631	0.631	0.611	0.669	0.677	0.640	0.691
0.759	0.660	0.616	0.683	0.610	0.553	0.749	0.612	0.598	0.608	0.791	0.517
0.743	0.844	0.604	0.544	0.580	0.563	0.502	0.663	0.675	0.727	0.815	0.741
0.648	0.719	0.678	0.583	0.483	0.827	0.620	0.632	0.655	0.652	0.640	0.696
0.748	0.668	0.554	0.672	0.575	0.595	0.600	0.608	0.646	0.549	0.759	0.569
0.762	0.501	0.575	0.820	0.694	0.611	0.741	0.618	0.589	0.689	0.600	0.802
0.746	0.703	0.684	0.577	0.561	0.669	0.636	0.581	0.622	0.748	0.670	0.705
0.595	0.603	0.685	0.986	0.630	0.663	0.605	0.575	0.650	0.667	0.615	0.766
0.826	0.569	0.627	0.571	0.726	0.675	0.880	0.635	0.669	0.784	0.735	0.673
0.784	0.608	0.621	0.575	0.528	0.705	0.675	0.668	0.556	0.660	0.616	0.792
0.785	0.741	0.611	0.594	0.518	0.690	0.758	0.677	0.670	0.819	0.733	0.664
0.699	0.631	0.617	0.746	0.790	0.749	0.815	0.638	0.612	0.601	0.788	0.659
0.672	0.658	0.765	0.615	0.538	0.814	0.835	0.538	0.685	0.693	0.582	0.738
0.496	0.649	0.752	0.634	0.627	0.805	0.632	0.581	0.734	0.594	0.748	0.848
0.647	0.696	0.603	0.809	0.571	0.766	0.625	0.614	0.769	0.690	0.626	0.707

SRM 1831 16 32	SRM 1831 8 32	SRM 1831 4 32	SRM 1831 16 16	SRM 1831 8 16	SRM 1831 4 16	SRM 1831 16 8	SRM 1831 8 8	SRM 1831 4 8	SRM 621 16 256	SRM 621 8 256
1.545	1.563	1.562	1.593	1.581	1.595	1.616	1.592	1.524	0.596	0.745
1.546	1.564	1.567	1.578	1.600	1.599	1.622	1.606	1.583	0.629	0.761
1.545	1.542	1.574	1.591	1.589	1.583	1.609	1.614	1.572	0.739	0.617
1.533	1.521	1.567	1.566	1.603	1.583	1.565	1.582	1.580	0.687	0.686
1.531	1.561	1.566	1.598	1.590	1.602	1.562	1.589	1.586	0.821	0.713
1.528	1.558	1.563	1.544	1.607	1.551	1.615	1.599	1.621	0.745	0.672
1.528	1.560	1.575	1.585	1.612	1.580	1.589	1.612	1.571	0.833	0.589
1.508	1.555	1.566	1.584	1.609	1.590	1.605	1.603	1.608	0.773	0.700
1.524	1.555	1.565	1.592	1.591	1.622	1.622	1.611	1.468	0.771	0.689
1.539	1.548	1.546	1.587	1.558	1.593	1.594	1.583	1.595	0.622	0.693
1.536	1.545	1.564	1.593	1.563	1.577	1.595	1.647	1.629	0.725	0.805
1.532	1.572	1.572	1.526	1.581	1.582	1.624	1.627	1.605	0.730	0.805
1.538	1.547	1.573	1.574	1.486	1.596	1.615	1.621	1.605	0.685	0.587
1.541	1.557	1.554	1.579	1.602	1.574	1.599	1.613	1.604	0.650	0.728
1.545	1.568	1.564	1.584	1.598	1.562	1.606	1.621	1.616	0.638	0.734

SRM 620 4 8	
1.437	16
1.445	17
1.446	18
1.388	19
1.432	20
1.412	21
1.417	22
1.455	23
1.494	24
1.487	25
1.507	26
1.486	27
1.446	28
1.492	29
1.419	30
1.428	Average Peak Height

SRM 1831 16 256	SRM 1831 8 256	SRM 1831 4 256	SRM 1831 16 128	SRM 1831 8 128	SRM 1831 4 128	SRM 1831 16 64	SRM 1831 8 64	SRM 1831 4 64
1.572	1.553	1.414	1.550	1.581	1.554	1.568	1.568	1.570
1.578	1.586	1.379	1.540	1.559	1.572	1.563	1.559	1.576
1.583	1.522	1.331	1.536	1.551	1.579	1.558	1.556	1.555
1.580	1.603	1.361	1.542	1.554	1.580	1.554	1.549	1.573
1.592	1.601	1.451	1.530	1.559	1.573	1.550	1.544	1.582
1.580	1.586	1.332	1.544	1.556	1.569	1.551	1.546	1.563
1.594	1.611	1.333	1.547	1.580	1.578	1.543	1.542	1.558
1.595	1.582	1.317	1.545	1.565	1.587	1.555	1.545	1.567
1.584	1.561	1.556	1.548	1.570	1.577	1.552	1.544	1.561
1.600	1.589	1.493	1.563	1.574	1.581	1.566	1.554	1.573
1.596	1.592	1.451	1.563	1.576	1.579	1.557	1.547	1.583
1.595	1.598	1.439	1.556	1.570	1.577	1.556	1.549	1.565
1.599	1.599	1.496	1.558	1.571	1.581	1.567	1.541	1.554
1.591	1.588	1.511	1.561	1.574	1.574	1.560	1.553	1.566
1.585	1.583	1.581	1.560	1.566	1.568	1.561	1.548	1.562

SRM 620 4 128	SRM 620 16 64	SRM 620 8 64	SRM 620 4 64	SRM 620 16 32	SRM 620 8 32	SRM 620 4 32	SRM 620 16 16	SRM 620 8 16	SRM 620 4 16	SRM 620 16 8	SRM 620 8 8
1.521	1.508	1.494	1.440	1.499	1.414	1.500	1.351	1.444	1.453	1.373	1.453
1.359	1.548	1.534	1.550	1.483	1.434	1.464	1.469	1.494	1.441	1.457	1.410
1.537	1.513	1.544	1.587	1.480	1.498	1.428	1.447	1.412	1.403	1.413	1.452
1.441	1.500	1.546	1.478	1.462	1.508	1.484	1.428	1.436	1.442	1.384	1.435
1.513	1.558	1.553	1.499	1.479	1.532	1.483	1.435	1.450	1.383	1.354	1.484
1.558	1.529	1.540	1.479	1.483	1.541	1.433	1.441	1.433	1.410	1.379	1.517
1.522	1.530	1.529	1.496	1.453	1.531	1.433	1.440	1.601	1.323	1.328	1.472
1.552	1.532	1.522	1.474	1.424	1.498	1.355	1.480	1.430	1.419	1.442	1.467
1.489	1.538	1.525	1.513	1.428	1.499	1.343	1.479	1.389	1.459	1.502	1.470
1.519	1.552	1.542	1.513	1.456	1.492	1.354	1.466	1.427	1.440	1.467	1.502
1.526	1.481	1.571	1.496	1.459	1.495	1.459	1.455	1.382	1.426	1.410	1.485
1.577	1.552	1.555	1.497	1.450	1.475	1.482	1.368	1.435	1.466	1.479	1.384
1.592	1.531	1.458	1.482	1.515	1.497	1.400	1.413	1.475	1.464	1.522	1.477
1.470	1.532	1.538	1.485	1.481	1.503	1.364	1.433	1.462	1.468	1.433	1.406
1.438	1.547	1.543	1.499	1.471	1.500	1.498	1.448	1.484	1.488	1.364	1.459
1.506	1.525	1.512	1.486	1.469	1.470	1.430	1.435	1.431	1.423	1.420	1.427

SRM 621 4 32	SRM 621 16 16	SRM 621 8 16	SRM 621 4 16	SRM 621 16 8	SRM 621 8 8	SRM 621 4 8	SRM 620 16 256	SRM 620 8 256	SRM 620 4 256	SRM 620 16 128	SRM 620 8 128
0.666	0.862	0.666	0.645	0.715	0.628	0.646	1.518	1.594	1.495	1.544	1.545
0.547	0.709	0.891	0.627	0.720	0.728	0.717	1.504	1.596	1.513	1.540	1.565
0.617	0.690	0.604	0.566	0.674	0.655	0.555	1.498	1.551	1.539	1.530	1.552
0.521	0.688	0.672	0.800	0.590	0.600	0.661	1.457	1.605	1.587	1.457	1.561
0.697	0.845	0.787	0.728	0.802	0.781	0.757	1.504	1.614	1.584	1.589	1.586
0.742	0.680	0.725	0.645	0.656	0.805	0.860	1.497	1.604	1.580	1.555	1.590
0.601	0.816	0.685	0.557	0.463	0.674	0.647	1.501	1.587	1.570	1.557	1.593
0.584	0.819	0.594	0.727	0.605	0.759	0.715	1.504	1.587	1.577	1.574	1.534
0.740	0.685	0.745	0.598	0.494	0.610	0.669	1.519	1.592	1.571	1.564	1.489
0.832	0.634	0.718	0.554	0.638	0.598	0.759	1.482	1.602	1.585	1.598	1.590
0.707	0.607	0.669	0.808	0.527	0.717	0.702	1.485	1.604	1.592	1.532	1.587
0.676	0.654	0.609	0.590	0.616	0.769	0.844	1.425	1.592	1.594	1.539	1.608
0.643	0.504	0.719	0.616	0.663	0.773	0.741	1.483	1.601	1.557	1.596	1.618
0.826	0.825	0.586	0.635	0.644	0.627	0.762	1.526	1.594	1.526	1.585	1.615
0.573	0.702	0.566	0.703	0.681	0.887	0.673	1.528	1.604	1.601	1.553	1.576
0.671	0.703	0.693	0.688	0.656	0.705	0.712	1.492	1.593	1.553	1.537	1.541

SRM 1831 4 8	SRM 621 16 256	SRM 621 8 256	SRM 621 4 256	SRM 621 16 128	SRM 621 8 128	SRM 621 4 128	SRM 621 16 64	SRM 621 8 64	SRM 621 4 64	SRM 621 16 32	SRM 621 8 32
1.584	0.691	0.688	0.703	0.616	0.682	0.615	0.648	0.677	0.744	0.632	0.614
1.594	0.621	0.812	0.552	0.604	0.704	0.600	0.623	0.588	0.814	0.646	0.576
1.598	0.800	0.620	0.689	0.663	0.751	0.804	0.581	0.584	0.628	0.632	0.771
1.589	0.617	0.626	0.573	0.613	0.604	0.665	0.778	0.566	0.592	0.622	0.711
1.599	0.735	0.531	0.678	0.750	0.690	0.620	0.666	0.715	0.626	0.773	0.627
1.615	0.645	0.741	0.565	0.547	0.703	0.734	0.853	0.725	0.676	0.624	0.539
1.587	0.688	0.647	0.679	0.778	0.557	0.587	0.724	0.768	0.656	0.572	0.549
1.569	0.674	0.629	0.592	0.602	0.639	0.703	0.912	0.674	0.564	0.656	0.459
1.574	0.677	0.639	0.578	0.836	0.744	0.656	0.708	0.666	0.646	0.682	0.520
1.579	0.668	0.799	0.588	0.834	0.607	0.745	0.542	0.738	0.687	0.634	0.542
1.589	0.729	0.642	0.710	---	0.599	0.700	0.782	0.720	0.617	0.584	0.636
1.621	0.645	0.628	0.735	0.656	0.668	0.702	0.832	0.645	0.696	0.646	0.610
1.566	0.641	0.708	0.722	0.590	0.729	0.662	0.766	0.701	0.592	0.657	0.681
1.575	0.682	0.583	0.783	0.715	0.737	0.704	0.751	0.633	0.532	0.700	0.647
1.615	0.557	0.582	0.754	0.687	0.630	0.623	0.713	0.650	0.650	0.653	0.583
1.587	0.690	0.680	0.683	0.668	0.655	0.669	0.662	0.679	0.667	0.632	0.629

SRM 1831 16 64	SRM 1831 8 64	SRM 1831 4 64	SRM 1831 16 32	SRM 1831 8 32	SRM 1831 4 32	SRM 1831 16 16	SRM 1831 8 16	SRM 1831 4 16	SRM 1831 16 8	SRM 1831 8 8
1.557	1.561	1.564	1.539	1.544	1.569	1.595	1.598	1.583	1.612	1.604
1.557	1.557	1.566	1.540	1.568	1.572	1.599	1.613	1.573	1.613	1.618
1.554	1.553	1.566	1.522	1.552	1.568	1.573	1.606	1.575	1.613	1.630
1.575	1.569	1.563	1.544	1.560	1.563	1.588	1.601	1.589	1.620	1.636
1.554	1.581	1.574	1.501	1.539	1.569	1.572	1.569	1.576	1.619	1.615
1.544	1.572	1.567	1.516	1.549	1.578	1.577	1.591	1.574	1.627	1.637
1.537	1.571	1.564	1.537	1.548	1.581	1.560	1.484	1.602	1.616	1.642
1.540	1.562	1.565	1.539	1.542	1.580	1.561	1.618	1.574	1.618	1.610
1.552	1.569	1.559	1.530	1.561	1.567	1.568	1.624	1.563	1.608	1.603
1.554	1.564	1.557	1.526	1.559	1.568	1.570	1.599	1.558	1.612	1.626
1.535	1.561	1.561	1.519	1.545	1.565	1.590	1.600	1.580	1.605	1.616
1.547	1.557	1.565	1.529	1.543	1.567	1.580	1.609	1.597	1.598	1.631
1.533	1.567	1.553	1.542	1.543	1.571	1.588	1.610	1.606	1.614	1.613
1.531	1.565	1.544	1.541	1.542	1.575	1.570	1.607	1.607	1.610	1.635
1.524	1.562	1.547	1.514	1.528	1.569	1.577	1.617	1.614	1.598	1.631
1.552	1.557	1.564	1.532	1.551	1.568	1.578	1.591	1.585	1.607	1.616

SRM 1831 16 256	SRM 1831 8 256	SRM 1831 4 256	SRM 1831 16 128	SRM 1831 8 128	SRM 1831 4 128
1.590	1.560	1.534	1.557	1.583	1.577
1.601	1.593	1.561	1.574	1.582	1.568
1.590	1.603	1.563	1.558	1.579	1.574
1.594	1.593	1.558	1.555	1.579	1.567
1.577	1.605	1.567	1.571	1.569	1.558
1.581	1.613	1.576	1.559	1.569	1.570
1.591	1.607	1.539	1.560	1.566	1.577
1.590	1.568	1.568	1.572	1.581	1.580
1.586	1.579	1.590	1.561	1.571	1.590
1.586	1.606	1.568	1.558	1.572	1.578
1.606	1.609	1.488	1.555	1.562	1.569
1.603	1.610	1.560	1.555	1.554	1.571
1.596	1.616	1.575	1.559	1.572	1.570
1.601	1.607	1.578	1.554	1.558	1.583
1.602	1.617	1.564	1.562	1.555	1.588
1.591	1.591	1.494	1.555	1.569	1.575

APPENDIX VI: METHOD DEVELOPMENT MID-IR SPECTRAL LIBRARY SEARCH HQI RESULTS

Table 129: Mid-IR spectral library results for SRM 620, correlation search algorithm.

	3A	3B	3C	5A	5B	5C	7A	7B	7C	10A	10B	10C	15A	15B	20A	20B	30A
SRM 620 481	0.00212	XXX	XXX	0.00232	XXX	XXX	0.00231	XXX	XXX	0.00216	XXX	XXX	0.00220	XXX	0.00213	XXX	0.00213
SRM 620 482	0.00256	0.00315	0.00239	0.00288	0.00244	0.00287	0.00285	0.00256	0.00238	0.00262	0.00243	0.00261	0.00269	0.00240	0.00255	0.00251	0.00256
SRM 620 483	XXX	XXX	0.00231	XXX	0.00236	XXX	XXX	0.00247	XXX	0.00253	XXX	XXX	0.00259	XXX	0.00247	XXX	0.00248
SRM 620 484	XXX	XXX	XXX	XXX	XXX	XXX	XXX	XXX	XXX	XXX	XXX	0.00284	XXX	0.00264	XXX	0.00274	0.00278
SRM 620 485	0.00247	0.00291	0.00237	0.00271	0.00240	0.00269	0.00269	0.00247	0.00236	0.00251	0.00239	0.00253	0.00256	0.00238	0.00248	0.00245	0.00247
SRM 620 486	XXX	XXX	XXX	XXX	XXX	XXX	XXX	XXX	XXX	XXX	XXX	0.00264	XXX	0.00244	XXX	0.00255	0.00259
SRM 620 487	0.00216	XXX	XXX	0.00235	XXX	XXX	0.00234	XXX	XXX	0.00220	XXX	XXX	0.00223	XXX	0.00218	XXX	0.00217
SRM 620 488	XXX	XXX	XXX	XXX	XXX	0.00225	XXX	0.00210	XXX	XXX	0.00205	XXX	0.00216	XXX	0.00211	0.00209	0.00210
SRM 620 489	0.00199	0.00204	0.00207	0.00199	0.00206	0.00199	0.00200	0.00200	0.00206	0.00200	0.00204	0.00201	0.00199	0.00205	0.00204	0.00202	0.00200
SRM 620 4810	XXX	XXX	0.00201	XXX	0.00202	XXX	0.00216	XXX	XXX	0.00206	XXX	XXX	0.00208	XXX	0.00207	XXX	0.00205

SRM 620 4 8 21	SRM 620 4 8 20	SRM 620 4 8 19	SRM 620 4 8 18	SRM 620 4 8 17	SRM 620 4 8 16	SRM 620 4 8 15	SRM 620 4 8 14	SRM 620 4 8 13	SRM 620 4 8 12	SRM 620 4 8 11
0.00267	0.00279	XXX	XXX	XXX	0.00237	XXX	XXX	XXX	XXX	XXX
0.00312	XXX	XXX	XXX	XXX	0.00284	XXX	0.00234	XXX	XXX	XXX
0.00258	XXX	XXX	XXX	XXX	0.00225	XXX	XXX	XXX	XXX	XXX
0.00292	0.00305	XXX	XXX	XXX	0.00263	XXX	0.00241	XXX	XXX	XXX
0.00261	XXX	XXX	0.00225	XXX	0.00228	XXX	XXX	XXX	XXX	XXX
0.00289	XXX	XXX	XXX	0.00298	0.00260	XXX	XXX	0.00224	XXX	XXX
0.00290	0.00303	XXX	XXX	XXX	0.00261	XXX	0.00243	XXX	XXX	XXX
0.00268	XXX	XXX	0.00236	0.00276	0.00237	XXX	XXX	0.00236	XXX	XXX
0.00256	XXX	XXX	XXX	XXX	0.00225	0.00305	XXX	XXX	0.00212	0.00278
0.00272	0.00284	XXX	0.00240	XXX	0.00242	XXX	0.00252	XXX	XXX	XXX
0.00259	XXX	XXX	XXX	0.00266	0.00227	0.00310	XXX	0.00246	XXX	0.00283
0.00273	XXX	0.00210	XXX	XXX	0.00243	XXX	XXX	XXX	0.00206	XXX
0.00277	0.00290	XXX	0.00245	0.00286	0.00247	XXX	0.00248	0.00231	XXX	XXX
0.00258	XXX	0.00203	XXX	XXX	0.00226	0.00309	XXX	XXX	0.00210	0.00282
0.00269	0.00280	XXX	0.00236	0.00276	0.00237	0.00325	0.00261	0.00242	XXX	0.00299
0.00265	XXX	0.00206	XXX	0.00274	0.00234	0.00321	XXX	0.00239	0.00207	0.00295
0.00268	0.00280	0.00207	0.00236	0.00276	0.00238	0.00326	0.00255	0.00236	0.00205	0.00301

SRM 620 4 16 2	SRM 620 4 16 1	SRM 620 4 8 30	SRM 620 4 8 29	SRM 620 4 8 28	SRM 620 4 8 27	SRM 620 4 8 26	SRM 620 4 8 25	SRM 620 4 8 24	SRM 620 4 8 23	SRM 620 4 8 22
0.00460	0.00457	XXX	XXX	XXX	XXX	XXX	XXX	XXX	XXX	XXX
0.00502	XXX	XXX	XXX	XXX	XXX	XXX	XXX	XXX	0.00304	0.00269
0.00459	XXX	XXX	XXX	XXX	XXX	XXX	XXX	0.00331	XXX	XXX
0.00472	0.00470	XXX	XXX	XXX	XXX	XXX	XXX	XXX	0.00281	XXX
0.00482	XXX	XXX	XXX	XXX	XXX	XXX	XXX	0.00337	XXX	0.00226
0.00439	XXX	0.00294	XXX	XXX	0.00309	XXX	XXX	XXX	XXX	XXX
0.00491	0.00487	XXX	XXX	XXX	XXX	XXX	XXX	XXX	0.00278	0.00251
0.00448	XXX	XXX	XXX	XXX	0.00281	XXX	XXX	0.00353	XXX	XXX
0.00430	XXX	0.00266	XXX	0.00278	XXX	0.00372	0.00336	XXX	XXX	XXX
0.00477	0.00474	XXX	XXX	XXX	XXX	XXX	XXX	0.00360	0.00257	0.00235
0.00368	XXX	0.00268	XXX	0.00281	0.00267	0.00378	0.00341	XXX	XXX	XXX
0.00389	XXX	XXX	0.00364	XXX	XXX	XXX	XXX	XXX	XXX	XXX
0.00397	0.00391	0.00284	XXX	XXX	0.00293	XXX	XXX	0.00369	0.00264	0.00239
0.00382	XXX	XXX	0.00338	0.00281	XXX	0.00377	0.00341	XXX	XXX	XXX
0.00453	0.00451	0.00277	XXX	0.00292	0.00281	0.00396	0.00357	0.00352	0.00253	0.00233
0.00446	XXX	0.00274	0.00350	0.00289	0.00278	0.00392	0.00353	XXX	XXX	XXX
0.00452	0.00450	0.00276	0.00354	0.00292	0.00282	0.00397	0.00358	0.00354	0.00253	0.00233

SRM 620 4 16 13	SRM 620 4 16 12	SRM 620 4 16 11	SRM 620 4 16 10	SRM 620 4 16 9	SRM 620 4 16 8	SRM 620 4 16 7	SRM 620 4 16 6	SRM 620 4 16 5	SRM 620 4 16 4	SRM 620 4 16 3
XXX	XXX	XXX	XXX	0.00411	XXX	0.00413	XXX	0.00410	XXX	XXX
XXX	XXX	XXX	XXX	0.00444	XXX	XXX	XXX	0.00432	XXX	XXX
XXX	XXX	XXX	0.00413	0.00415	XXX	XXX	XXX	0.00415	XXX	0.00454
XXX	XXX	XXX	XXX	0.00422	XXX	0.00425	XXX	0.00420	XXX	XXX
XXX	XXX	XXX	0.00418	0.00430	XXX	XXX	XXX	0.00422	XXX	0.00476
0.00369	XXX	XXX	XXX	0.00400	0.00416	XXX	XXX	0.00404	XXX	XXX
XXX	XXX	XXX	0.00421	0.00435	XXX	0.00439	XXX	0.00426	XXX	XXX
0.00374	XXX	XXX	XXX	0.00406	0.00422	XXX	XXX	0.00408	XXX	0.00442
XXX	0.00407	0.00428	XXX	0.00395	XXX	XXX	XXX	0.00403	XXX	XXX
XXX	XXX	XXX	0.00417	0.00426	XXX	0.00428	XXX	0.00421	XXX	0.00471
0.00308	XXX	0.00364	XXX	0.00337	0.00340	XXX	XXX	0.00339	XXX	XXX
XXX	0.00360	XXX	XXX	0.00350	XXX	XXX	0.00384	0.00347	0.00348	XXX
0.00323	XXX	XXX	0.00340	0.00356	0.00360	0.00358	XXX	0.00350	XXX	0.00397
XXX	0.00355	0.00378	XXX	0.00346	XXX	XXX	0.00377	0.00345	0.00346	XXX
0.00376	XXX	0.00449	0.00408	0.00408	0.00425	0.00410	XXX	0.00409	XXX	0.00447
0.00374	0.00419	0.00443	XXX	0.00404	0.00422	XXX	0.00435	0.00409	0.00405	XXX
0.00376	0.00422	0.00449	0.00408	0.00407	0.00424	0.00409	0.00441	0.00409	0.00406	0.00446

SRM 620 4 16 24	SRM 620 4 16 23	SRM 620 4 16 22	SRM 620 4 16 21	SRM 620 4 16 20	SRM 620 4 16 19	SRM 620 4 16 18	SRM 620 4 16 17	SRM 620 4 16 16	SRM 620 4 16 15	SRM 620 4 16 14
XXX	XXX	XXX	0.00404	0.00365	XXX	XXX	XXX	0.00485	XXX	XXX
XXX	0.00480	0.00396	0.00436	XXX	XXX	XXX	XXX	0.00526	XXX	0.00419
0.00473	XXX	XXX	0.00406	XXX	XXX	XXX	XXX	0.00483	XXX	XXX
XXX	0.00455	XXX	0.00414	0.00374	XXX	XXX	XXX	0.00497	XXX	0.00405
0.00498	XXX	0.00393	0.00421	XXX	XXX	0.00441	XXX	0.00506	XXX	XXX
XXX	XXX	XXX	0.00390	XXX	XXX	XXX	0.00435	0.00462	XXX	XXX
XXX	0.00470	0.00394	0.00427	0.00382	XXX	XXX	XXX	0.00515	XXX	0.00413
0.00460	XXX	XXX	0.00396	XXX	XXX	0.00417	0.00443	0.00471	XXX	XXX
XXX	XXX	XXX	0.00385	XXX	XXX	XXX	XXX	0.00452	0.00450	XXX
0.00493	0.00459	0.00393	0.00417	0.00376	XXX	0.00438	XXX	0.00502	XXX	0.00407
XXX	XXX	XXX	0.00330	XXX	XXX	XXX	0.00366	0.00385	0.00392	XXX
XXX	XXX	XXX	0.00345	XXX	0.00387	XXX	XXX	0.00408	XXX	XXX
0.00411	0.00385	0.00324	0.00350	0.00303	XXX	0.00364	0.00394	0.00416	XXX	0.00332
XXX	XXX	XXX	0.00340	XXX	0.00380	XXX	XXX	0.00400	0.00409	XXX
0.00466	0.00438	0.00389	0.00399	0.00364	XXX	0.00420	0.00448	0.00477	0.00477	0.00394
XXX	XXX	XXX	0.00395	XXX	0.00446	XXX	0.00442	0.00470	0.00469	XXX
0.00466	0.00437	0.00388	0.00398	0.00363	0.00452	0.00420	0.00448	0.00476	0.00477	0.00393

SRM 620 4 32 5	SRM 620 4 32 4	SRM 620 4 32 3	SRM 620 4 32 2	SRM 620 4 32 1	SRM 620 4 16 30	SRM 620 4 16 29	SRM 620 4 16 28	SRM 620 4 16 27	SRM 620 4 16 26	SRM 620 4 16 25
0.00322	XXX	XXX	0.00402	0.00341	XXX	XXX	XXX	XXX	XXX	XXX
0.00359	XXX	XXX	0.00446	XXX	XXX	XXX	XXX	XXX	XXX	XXX
0.00262	XXX	0.00281	0.00337	XXX	XXX	XXX	XXX	XXX	XXX	XXX
0.00346	XXX	XXX	0.00430	0.00366	XXX	XXX	XXX	XXX	XXX	XXX
0.00323	XXX	0.00338	0.00403	XXX	XXX	XXX	XXX	XXX	XXX	XXX
0.00250	XXX	XXX	0.00320	XXX	0.00436	XXX	XXX	0.00423	XXX	XXX
0.00336	XXX	XXX	0.00419	0.00356	XXX	XXX	XXX	XXX	XXX	XXX
0.00259	XXX	0.00277	0.00332	XXX	XXX	XXX	XXX	0.00432	XXX	XXX
0.00330	XXX	XXX	0.00412	XXX	0.00423	XXX	0.00446	XXX	0.00411	0.00431
0.00330	XXX	0.00348	0.00412	0.00349	XXX	XXX	XXX	XXX	XXX	XXX
0.00324	XXX	XXX	0.00404	XXX	0.00370	XXX	0.00386	0.00344	0.00345	0.00366
0.00319	0.00319	XXX	0.00398	XXX	XXX	0.00409	XXX	XXX	XXX	XXX
0.00325	XXX	0.00340	0.00405	0.00344	0.00407	XXX	XXX	0.00377	XXX	XXX
0.00258	0.00253	XXX	0.00332	XXX	XXX	0.00399	0.00403	XXX	0.00358	0.00381
0.00327	XXX	0.00343	0.00408	0.00347	0.00453	XXX	0.00474	0.00438	0.00431	0.00452
0.00320	0.00319	XXX	0.00399	XXX	0.00444	0.00461	0.00466	0.00430	0.00425	0.00446
0.00324	0.00321	0.00339	0.00404	0.00344	0.00452	0.00469	0.00474	0.00437	0.00430	0.00452

SRM 620 4 32 16	SRM 620 4 32 15	SRM 620 4 32 14	SRM 620 4 32 13	SRM 620 4 32 12	SRM 620 4 32 11	SRM 620 4 32 10	SRM 620 4 32 9	SRM 620 4 32 8	SRM 620 4 32 7	SRM 620 4 32 6
0.00078	XXX	XXX	XXX	XXX	XXX	XXX	0.00335	XXX	0.00294	XXX
0.00106	XXX	0.00311	XXX	XXX	XXX	XXX	0.00368	XXX	XXX	XXX
0.00037	XXX	XXX	XXX	XXX	XXX	0.00258	0.00269	XXX	XXX	XXX
0.00095	XXX	0.00302	XXX	XXX	XXX	XXX	0.00356	XXX	0.00306	XXX
0.00078	XXX	XXX	XXX	XXX	XXX	0.00311	0.00337	XXX	XXX	XXX
0.00027	XXX	XXX	0.00221	XXX	XXX	XXX	0.00260	0.00256	XXX	XXX
0.00089	XXX	0.00294	XXX	XXX	XXX	0.00325	0.00349	XXX	0.00303	XXX
0.00033	XXX	XXX	0.00227	XXX	XXX	XXX	0.00268	0.00261	XXX	XXX
0.00087	0.00319	XXX	XXX	0.00299	0.00318	XXX	0.00343	XXX	XXX	XXX
0.00084	XXX	0.00289	XXX	XXX	XXX	0.00319	0.00343	XXX	0.00297	XXX
0.00079	0.00314	XXX	0.00282	XXX	0.00312	XXX	0.00337	0.00326	XXX	XXX
0.00077	XXX	XXX	XXX	0.00291	XXX	XXX	0.00333	XXX	XXX	0.00323
0.00079	XXX	0.00285	0.00284	XXX	XXX	0.00313	0.00338	0.00326	0.00299	XXX
0.00034	0.00255	XXX	XXX	0.00240	0.00258	XXX	0.00266	XXX	XXX	0.00258
0.00081	0.00319	0.00286	0.00285	XXX	0.00317	0.00315	0.00340	0.00327	0.00300	XXX
0.00078	0.00312	XXX	0.00280	0.00291	0.00310	XXX	0.00334	0.00322	XXX	0.00324
0.00079	0.00316	0.00284	0.00283	0.00294	0.00314	0.00312	0.00337	0.00325	0.00298	0.00326

SRM 620 4 32 27	SRM 620 4 32 26	SRM 620 4 32 25	SRM 620 4 32 24	SRM 620 4 32 23	SRM 620 4 32 22	SRM 620 4 32 21	SRM 620 4 32 20	SRM 620 4 32 19	SRM 620 4 32 18	SRM 620 4 32 17
XXX	XXX	XXX	XXX	XXX	XXX	0.00291	0.00322	XXX	XXX	XXX
XXX	XXX	XXX	XXX	0.00292	0.00304	0.00324	XXX	XXX	XXX	XXX
XXX	XXX	XXX	0.00228	XXX	XXX	0.00238	XXX	XXX	XXX	XXX
XXX	XXX	XXX	XXX	0.00286	XXX	0.00312	0.00348	XXX	XXX	XXX
XXX	XXX	XXX	0.00289	XXX	0.00275	0.00293	XXX	XXX	0.00054	XXX
0.00252	XXX	XXX	XXX	XXX	XXX	0.00229	XXX	XXX	XXX	0.00014
XXX	XXX	XXX	XXX	0.00285	0.00286	0.00305	0.00338	XXX	XXX	XXX
0.00264	XXX	XXX	0.00228	XXX	XXX	0.00234	XXX	XXX	0.00013	0.00016
XXX	0.00326	0.00290	XXX	XXX	XXX	0.00302	XXX	XXX	XXX	XXX
XXX	XXX	XXX	0.00287	0.00279	0.00280	0.00298	0.00332	XXX	0.00055	XXX
0.00326	0.00320	0.00289	XXX	XXX	XXX	0.00296	XXX	XXX	XXX	0.00071
XXX	XXX	XXX	XXX	XXX	XXX	0.00290	XXX	0.00326	XXX	XXX
0.00327	XXX	XXX	0.00290	0.00282	0.00277	0.00295	0.00326	XXX	0.00055	0.00070
XXX	0.00252	0.00227	XXX	XXX	XXX	0.00234	XXX	0.00276	XXX	XXX
0.00330	0.00323	0.00288	0.00291	0.00283	0.00279	0.00298	0.00329	XXX	0.00055	0.00071
0.00322	0.00316	0.00286	XXX	XXX	XXX	0.00292	XXX	0.00327	XXX	0.00070
0.00326	0.00319	0.00287	0.00290	0.00282	0.00276	0.00294	0.00325	0.00331	0.00055	0.00071

SRM 620 4 64 8	SRM 620 4 64 7	SRM 620 4 64 6	SRM 620 4 64 5	SRM 620 4 64 4	SRM 620 4 64 3	SRM 620 4 64 2	SRM 620 4 64 1	SRM 620 4 32 30	SRM 620 4 32 29	SRM 620 4 32 28
XXX	0.00314	XXX	0.00260	XXX	XXX	0.00283	0.00254	XXX	XXX	XXX
XXX	XXX	XXX	0.00270	XXX	XXX	0.00316	XXX	XXX	XXX	XXX
XXX	XXX	XXX	0.00272	XXX	0.00272	0.00285	XXX	XXX	XXX	XXX
XXX	0.00334	XXX	0.00258	XXX	XXX	0.00296	0.00258	XXX	XXX	XXX
XXX	XXX	XXX	0.00320	XXX	0.00325	0.00337	XXX	XXX	XXX	XXX
0.00330	XXX	XXX	0.00295	XXX	XXX	0.00314	XXX	0.00241	XXX	XXX
XXX	0.00322	XXX	0.00263	XXX	XXX	0.00289	0.00259	XXX	XXX	XXX
0.00359	XXX	XXX	0.00316	XXX	0.00327	0.00343	XXX	XXX	XXX	XXX
XXX	XXX	XXX	0.00274	XXX	XXX	0.00305	XXX	0.00301	XXX	0.00267
XXX	0.00341	XXX	0.00280	XXX	0.00289	0.00308	0.00278	XXX	XXX	XXX
0.00323	XXX	XXX	0.00281	XXX	XXX	0.00307	XXX	0.00298	XXX	0.00264
XXX	XXX	0.00351	0.00272	0.00283	XXX	0.00311	XXX	XXX	0.00293	XXX
0.00324	0.00341	XXX	0.00282	XXX	0.00290	0.00308	0.00279	0.00296	XXX	XXX
XXX	XXX	0.00347	0.00271	0.00280	XXX	0.00307	XXX	XXX	0.00239	0.00209
0.00326	0.00343	XXX	0.00282	XXX	0.00291	0.00309	0.00279	0.00297	XXX	0.00264
0.00327	XXX	0.00348	0.00275	0.00283	XXX	0.00309	XXX	0.00294	0.00294	0.00260
0.00327	0.00345	0.00346	0.00276	0.00283	0.00287	0.00309	0.00275	0.00295	0.00295	0.00262

SRM 620 4 64 19	SRM 620 4 64 18	SRM 620 4 64 17	SRM 620 4 64 16	SRM 620 4 64 15	SRM 620 4 64 14	SRM 620 4 64 13	SRM 620 4 64 12	SRM 620 4 64 11	SRM 620 4 64 10	SRM 620 4 64 9
XXX	XXX	XXX	0.00243	XXX	XXX	XXX	XXX	XXX	XXX	0.00274
XXX	XXX	XXX	0.00257	XXX	0.00276	XXX	XXX	XXX	XXX	0.00303
XXX	XXX	XXX	0.00247	XXX	XXX	XXX	XXX	XXX	0.00326	0.00276
XXX	XXX	XXX	0.00246	XXX	0.00263	XXX	XXX	XXX	XXX	0.00286
XXX	0.00365	XXX	0.00277	XXX	XXX	XXX	XXX	XXX	0.00378	0.00327
XXX	XXX	0.00270	0.00257	XXX	XXX	0.00296	XXX	XXX	XXX	0.00302
XXX	XXX	XXX	0.00244	XXX	0.00264	XXX	XXX	XXX	0.00334	0.00278
XXX	0.00345	0.00254	0.00274	XXX	XXX	0.00325	XXX	XXX	XXX	0.00331
XXX	XXX	XXX	0.00252	0.00277	XXX	XXX	0.00281	0.00292	XXX	0.00293
XXX	0.00402	XXX	0.00252	XXX	0.00281	XXX	XXX	XXX	0.00354	0.00297
XXX	XXX	0.00288	0.00253	0.00283	XXX	0.00288	XXX	0.00294	XXX	0.00295
0.00308	XXX	XXX	0.00259	XXX	XXX	XXX	0.00287	XXX	XXX	0.00300
XXX	0.00399	0.00277	0.00251	XXX	0.00281	0.00289	XXX	XXX	0.00352	0.00296
0.00304	XXX	XXX	0.00255	0.00276	XXX	XXX	0.00283	0.00295	XXX	0.00296
XXX	0.00410	0.00284	0.00254	0.00285	0.00282	0.00291	XXX	0.00297	0.00355	0.00298
0.00307	XXX	0.00304	0.00254	0.00279	XXX	0.00288	0.00285	0.00297	XXX	0.00298
0.00308	0.00432	0.00299	0.00254	0.00281	0.00278	0.00289	0.00286	0.00297	0.00357	0.00298

SRM 620 4 64 30	SRM 620 4 64 29	SRM 620 4 64 28	SRM 620 4 64 27	SRM 620 4 64 26	SRM 620 4 64 25	SRM 620 4 64 24	SRM 620 4 64 23	SRM 620 4 64 22	SRM 620 4 64 21	SRM 620 4 64 20
XXX	XXX	XXX	XXX	XXX	XXX	XXX	XXX	XXX	0.00252	0.00270
XXX	XXX	XXX	XXX	XXX	XXX	XXX	0.00289	0.00299	0.00277	XXX
XXX	XXX	XXX	XXX	XXX	XXX	0.00280	XXX	XXX	0.00256	XXX
XXX	XXX	XXX	XXX	XXX	XXX	XXX	0.00275	XXX	0.00261	0.00282
XXX	XXX	XXX	XXX	XXX	XXX	0.00324	XXX	0.00318	0.00301	XXX
0.00295	XXX	XXX	0.00291	XXX	XXX	XXX	XXX	XXX	0.00279	XXX
XXX	XXX	XXX	XXX	XXX	XXX	XXX	0.00269	0.00276	0.00257	0.00275
XXX	XXX	XXX	0.00317	XXX	XXX	0.00329	XXX	XXX	0.00304	XXX
0.00291	XXX	0.00273	XXX	0.00284	0.00302	XXX	XXX	XXX	0.00270	XXX
XXX	XXX	XXX	XXX	XXX	XXX	0.00299	0.00284	0.00291	0.00272	0.00293
0.00291	XXX	0.00274	0.00287	0.00284	0.00301	XXX	XXX	XXX	0.00272	XXX
XXX	0.00284	XXX	XXX	XXX	XXX	XXX	XXX	XXX	0.00276	XXX
0.00292	XXX	XXX	0.00288	XXX	XXX	0.00299	0.00284	0.00291	0.00272	0.00293
XXX	0.00279	0.00278	XXX	0.00288	0.00308	XXX	XXX	XXX	0.00272	XXX
0.00294	XXX	0.00276	0.00290	0.00286	0.00303	0.00301	0.00286	0.00293	0.00274	0.00295
0.00295	0.00279	0.00277	0.00291	0.00288	0.00307	XXX	XXX	XXX	0.00273	XXX
0.00295	0.00280	0.00278	0.00291	0.00288	0.00306	0.00303	0.00287	0.00295	0.00273	0.00295

SRM 620 4 128 11	SRM 620 4 128 10	SRM 620 4 128 9	SRM 620 4 128 8	SRM 620 4 128 7	SRM 620 4 128 6	SRM 620 4 128 5	SRM 620 4 128 4	SRM 620 4 128 3	SRM 620 4 128 2	SRM 620 4 128 1
XXX	XXX	0.00218	XXX	0.00206	XXX	0.00259	XXX	XXX	0.00239	0.00223
XXX	XXX	0.00235	XXX	XXX	XXX	0.00283	XXX	XXX	0.00260	XXX
XXX	0.00224	0.00221	XXX	XXX	XXX	0.00263	XXX	0.00236	0.00242	XXX
XXX	XXX	0.00228	XXX	0.00216	XXX	0.00272	XXX	XXX	0.00251	0.00234
XXX	0.00225	0.00222	XXX	XXX	XXX	0.00263	XXX	0.00237	0.00243	XXX
XXX	XXX	0.00253	0.00254	XXX	XXX	0.00316	XXX	XXX	0.00286	XXX
XXX	0.00230	0.00226	XXX	0.00214	XXX	0.00269	XXX	XXX	0.00248	0.00232
XXX	XXX	0.00233	0.00233	XXX	XXX	0.00282	XXX	0.00251	0.00259	XXX
0.00288	XXX	0.00303	XXX	XXX	XXX	0.00365	XXX	XXX	0.00333	XXX
XXX	0.00289	0.00283	XXX	0.00272	XXX	0.00329	XXX	0.00297	0.00304	0.00288
0.00284	XXX	0.00297	0.00300	XXX	XXX	0.00355	XXX	XXX	0.00325	XXX
XXX	XXX	0.00284	XXX	XXX	0.00306	0.00332	0.00283	XXX	0.00305	XXX
XXX	0.00299	0.00293	0.00296	0.00281	XXX	0.00346	XXX	0.00310	0.00317	0.00300
0.00212	XXX	0.00226	XXX	XXX	0.00245	0.00271	0.00224	XXX	0.00250	XXX
0.00281	0.00298	0.00292	0.00294	0.00280	XXX	0.00344	XXX	0.00308	0.00316	0.00299
0.00217	XXX	0.00234	0.00235	XXX	0.00255	0.00283	0.00232	XXX	0.00260	XXX
0.00278	0.00295	0.00289	0.00292	0.00277	0.00313	0.00341	0.00288	0.00305	0.00313	0.00296

SRM 620 4 128 22	SRM 620 4 128 21	SRM 620 4 128 20	SRM 620 4 128 19	SRM 620 4 128 18	SRM 620 4 128 17	SRM 620 4 128 16	SRM 620 4 128 15	SRM 620 4 128 14	SRM 620 4 128 13	SRM 620 4 128 12
XXX	0.00236	0.00217	XXX	XXX	XXX	0.00220	XXX	XXX	XXX	XXX
0.00237	0.00256	XXX	XXX	XXX	XXX	0.00238	XXX	0.00210	XXX	XXX
XXX	0.00239	XXX	XXX	XXX	XXX	0.00224	XXX	XXX	XXX	XXX
XXX	0.00247	0.00228	XXX	XXX	XXX	0.00231	XXX	0.00206	XXX	XXX
0.00223	0.00239	XXX	XXX	0.00231	XXX	0.00224	XXX	XXX	XXX	XXX
XXX	0.00283	XXX	XXX	XXX	0.00216	0.00257	XXX	XXX	0.00226	XXX
0.00228	0.00245	0.00226	XXX	XXX	XXX	0.00229	XXX	0.00205	XXX	XXX
XXX	0.00255	XXX	XXX	0.00244	0.00225	0.00236	XXX	XXX	0.00212	XXX
XXX	0.00330	XXX	XXX	XXX	XXX	0.00307	0.00264	XXX	XXX	0.00261
0.00285	0.00301	0.00288	XXX	0.00291	XXX	0.00286	XXX	0.00262	XXX	XXX
XXX	0.00322	XXX	XXX	XXX	0.00278	0.00301	0.00264	XXX	0.00273	XXX
XXX	0.00303	XXX	0.00266	XXX	XXX	0.00287	XXX	XXX	XXX	0.00262
0.00295	0.00315	0.00298	XXX	0.00303	0.00285	0.00296	XXX	0.00265	0.00271	XXX
XXX	0.00246	XXX	0.00210	XXX	XXX	0.00229	0.00212	XXX	XXX	0.00206
0.00294	0.00313	0.00297	XXX	0.00301	0.00286	0.00295	0.00267	0.00265	0.00270	XXX
XXX	0.00256	XXX	0.00211	XXX	0.00226	0.00237	0.00212	XXX	0.00214	0.00206
0.00291	0.00310	0.00294	0.00267	0.00298	0.00285	0.00292	0.00266	0.00263	0.00268	0.00263

SRM 620 4 256 3	SRM 620 4 256 2	SRM 620 4 256 1	SRM 620 4 128 30	SRM 620 4 128 29	SRM 620 4 128 28	SRM 620 4 128 27	SRM 620 4 128 26	SRM 620 4 128 25	SRM 620 4 128 24	SRM 620 4 128 23
XXX	0.00304	0.00295	XXX	XXX	XXX	XXX	XXX	XXX	XXX	XXX
XXX	0.00310	XXX	XXX	XXX	XXX	XXX	XXX	XXX	XXX	0.00251
0.00276	0.00296	XXX	XXX	XXX	XXX	XXX	XXX	XXX	0.00206	XXX
XXX	0.00311	0.00301	XXX	XXX	XXX	XXX	XXX	XXX	XXX	0.00243
0.00276	0.00296	XXX	XXX	XXX	XXX	XXX	XXX	XXX	0.00207	XXX
XXX	0.00292	XXX	0.00216	XXX	XXX	0.00329	XXX	XXX	XXX	XXX
XXX	0.00307	0.00298	XXX	XXX	XXX	XXX	XXX	XXX	XXX	0.00240
0.00278	0.00297	XXX	XXX	XXX	XXX	0.00295	XXX	XXX	0.00215	XXX
XXX	0.00243	XXX	0.00268	XXX	0.00416	XXX	0.00307	0.00310	XXX	XXX
0.00222	0.00246	0.00238	XXX	XXX	XXX	XXX	XXX	XXX	0.00266	0.00296
XXX	0.00299	XXX	0.00267	XXX	0.00403	0.00371	0.00301	0.00303	XXX	XXX
XXX	0.00302	XXX	XXX	0.00272	XXX	XXX	XXX	XXX	XXX	XXX
0.00279	0.00298	0.00290	0.00267	XXX	XXX	0.00362	XXX	XXX	0.00273	0.00309
XXX	0.00300	XXX	XXX	0.00210	0.00316	XXX	0.00225	0.00229	XXX	XXX
0.00281	0.00299	0.00292	0.00268	XXX	0.00390	0.00360	0.00294	0.00297	0.00272	0.00307
XXX	0.00299	XXX	0.00212	0.00215	0.00330	0.00296	0.00233	0.00237	XXX	XXX
0.00281	0.00300	0.00292	0.00266	0.00276	0.00386	0.00356	0.00291	0.00294	0.00270	0.00304

SRM 620 4 256 14	SRM 620 4 256 13	SRM 620 4 256 12	SRM 620 4 256 11	SRM 620 4 256 10	SRM 620 4 256 9	SRM 620 4 256 8	SRM 620 4 256 7	SRM 620 4 256 6	SRM 620 4 256 5	SRM 620 4 256 4
XXX	XXX	XXX	XXX	XXX	0.00276	XXX	0.00276	XXX	0.00297	XXX
0.00332	XXX	XXX	XXX	XXX	0.00279	XXX	XXX	XXX	0.00302	XXX
XXX	XXX	XXX	XXX	0.00294	0.00271	XXX	XXX	XXX	0.00289	XXX
0.00334	XXX	XXX	XXX	XXX	0.00280	XXX	0.00281	XXX	0.00303	XXX
XXX	XXX	XXX	XXX	0.00293	0.00271	XXX	XXX	XXX	0.00289	XXX
XXX	0.00313	XXX	XXX	XXX	0.00274	0.00275	XXX	XXX	0.00287	XXX
0.00332	XXX	XXX	XXX	0.00304	0.00278	XXX	0.00279	XXX	0.00299	XXX
XXX	0.00325	XXX	XXX	XXX	0.00271	0.00274	XXX	XXX	0.00291	XXX
XXX	XXX	0.00253	0.00254	XXX	0.00225	XXX	XXX	XXX	0.00238	XXX
0.00264	XXX	XXX	XXX	0.00239	0.00217	XXX	0.00215	XXX	0.00237	XXX
XXX	0.00326	XXX	0.00314	XXX	0.00280	0.00280	XXX	XXX	0.00294	XXX
XXX	XXX	0.00311	XXX	XXX	0.00272	XXX	XXX	0.00286	0.00294	0.00297
0.00328	0.00326	XXX	XXX	0.00295	0.00274	0.00276	0.00275	XXX	0.00291	XXX
XXX	XXX	0.00310	0.00313	XXX	0.00274	XXX	XXX	0.00286	0.00293	0.00296
0.00330	0.00328	XXX	0.00313	0.00296	0.00276	0.00277	0.00277	XXX	0.00293	XXX
XXX	0.00327	0.00309	0.00312	XXX	0.00275	0.00276	XXX	0.00286	0.00292	0.00295
0.00329	0.00329	0.00310	0.00313	0.00297	0.00275	0.00277	0.00276	0.00287	0.00293	0.00296

SRM 620 4 256 25	SRM 620 4 256 24	SRM 620 4 256 23	SRM 620 4 256 22	SRM 620 4 256 21	SRM 620 4 256 20	SRM 620 4 256 19	SRM 620 4 256 18	SRM 620 4 256 17	SRM 620 4 256 16	SRM 620 4 256 15
XXX	XXX	XXX	XXX	0.00361	0.00318	XXX	XXX	XXX	0.00314	XXX
XXX	XXX	0.00361	0.00344	0.00368	XXX	XXX	XXX	XXX	0.00317	XXX
XXX	0.00297	XXX	XXX	0.00354	XXX	XXX	XXX	XXX	0.00309	XXX
XXX	XXX	0.00362	XXX	0.00369	0.00327	XXX	XXX	XXX	0.00319	XXX
XXX	0.00298	XXX	0.00331	0.00354	XXX	XXX	0.00296	XXX	0.00307	XXX
XXX	XXX	XXX	XXX	0.00348	XXX	XXX	XXX	0.00291	0.00308	XXX
XXX	XXX	0.00359	0.00342	0.00365	0.00323	XXX	XXX	XXX	0.00316	XXX
XXX	0.00299	XXX	XXX	0.00355	XXX	XXX	0.00297	0.00292	0.00308	XXX
0.00251	XXX	XXX	XXX	0.00290	XXX	XXX	XXX	XXX	0.00256	0.00288
XXX	0.00240	0.00289	0.00276	0.00296	0.00256	XXX	0.00238	XXX	0.00250	XXX
0.00314	XXX	XXX	XXX	0.00355	XXX	XXX	XXX	0.00298	0.00315	0.00350
XXX	XXX	XXX	XXX	0.00361	XXX	0.00358	XXX	XXX	0.00310	XXX
XXX	0.00299	0.00351	0.00333	0.00355	0.00314	XXX	0.00298	0.00294	0.00310	XXX
0.00319	XXX	XXX	XXX	0.00357	XXX	0.00352	XXX	XXX	0.00311	0.00346
0.00316	0.00300	0.00351	0.00334	0.00356	0.00314	XXX	0.00300	0.00296	0.00312	0.00347
0.00317	XXX	XXX	XXX	0.00356	XXX	0.00351	XXX	0.00294	0.00311	0.00346
0.00319	0.00301	0.00352	0.00335	0.00358	0.00316	0.00353	0.00300	0.00295	0.00312	0.00346

SRM 620 4 256 30	SRM 620 4 256 29	SRM 620 4 256 28	SRM 620 4 256 27	SRM 620 4 256 26
XXX	XXX	XXX	XXX	XXX
XXX	XXX	XXX	XXX	XXX
XXX	XXX	XXX	XXX	XXX
XXX	XXX	XXX	XXX	XXX
XXX	XXX	XXX	XXX	XXX
0.00330	XXX	XXX	0.00327	XXX
XXX	XXX	XXX	XXX	XXX
XXX	XXX	XXX	0.00336	XXX
0.00279	XXX	0.00240	XXX	0.00263
XXX	XXX	XXX	XXX	XXX
0.00340	XXX	0.00302	0.00333	0.00327
XXX	0.00300	XXX	XXX	XXX
0.00343	XXX	XXX	0.00336	XXX
XXX	0.00301	0.00301	XXX	0.00332
0.00343	XXX	0.00301	0.00336	0.00329
0.00343	0.00301	0.00302	0.00336	0.00330
0.00346	0.00302	0.00302	0.00338	0.00332

Table 130: Mid-IR spectral library results for SRM 621, correlation search algorithm.

	3A	3B	3C	5A	5B	5C	7A	7B	7C	10A	10B	10C	15A	15B	20A	20B	30A
SRM 621 4 8 1	0.00220	XXX	XXX	0.00224	XXX	XXX	0.00266	XXX	XXX	0.00298	XXX	XXX	0.00323	XXX	0.00363	XXX	0.00317
SRM 621 4 8 2	0.00152	0.00141	0.00213	0.00145	0.00209	0.00196	0.00151	0.00218	0.00276	0.00164	0.00219	0.00193	0.00174	0.00208	0.00192	0.00208	0.00157
SRM 621 4 8 3	XXX	XXX	0.00280	XXX	0.00274	XXX	XXX	0.00286	XXX	0.00205	XXX	XXX	0.00222	XXX	0.00249	XXX	0.00211
SRM 621 4 8 4	XXX	XXX	XXX	XXX	XXX	XXX	XXX	XXX	XXX	XXX	XXX	0.00203	XXX	0.00218	XXX	0.00218	0.00176

SRM 621 4 8 15	SRM 621 4 8 14	SRM 621 4 8 13	SRM 621 4 8 12	SRM 621 4 8 11	SRM 621 4 8 10	SRM 621 4 8 9	SRM 621 4 8 8	SRM 621 4 8 7	SRM 621 4 8 6	SRM 621 4 8 5
XXX	XXX	XXX	XXX	XXX	XXX	0.00196	XXX	0.00165	XXX	0.00158
XXX	0.00154	XXX	XXX	XXX	XXX	0.00185	XXX	XXX	XXX	0.00143
XXX	XXX	XXX	XXX	XXX	0.00153	0.00360	XXX	XXX	XXX	0.00231
XXX	0.00165	XXX	XXX	XXX	XXX	0.00197	XXX	0.00160	XXX	0.00151
XXX	XXX	XXX	XXX	XXX	0.00172	0.00349	XXX	XXX	XXX	0.00226
XXX	XXX	0.00235	XXX	XXX	XXX	0.00325	0.00251	XXX	XXX	0.00211
XXX	0.00176	XXX	XXX	XXX	0.00293	0.00231	XXX	0.00176	XXX	0.00160
XXX	XXX	0.00261	XXX	XXX	XXX	0.00364	0.00281	XXX	XXX	0.00235
0.00164	XXX	XXX	0.00362	0.00148	XXX	0.00462	XXX	XXX	XXX	0.00296
XXX	0.00192	XXX	XXX	XXX	0.00261	0.00260	XXX	0.00194	XXX	0.00175
0.00152	XXX	0.00264	XXX	0.00183	XXX	0.00370	0.00285	XXX	XXX	0.00236
XXX	XXX	XXX	0.00558	XXX	XXX	0.00314	XXX	XXX	0.00171	0.00207
XXX	0.00204	0.00208	XXX	XXX	0.00242	0.00280	0.00217	0.00207	XXX	0.00187
0.00157	XXX	XXX	0.00509	0.00196	XXX	0.00346	XXX	XXX	0.00179	0.00223
0.00157	0.00223	0.00230	XXX	0.00216	0.00205	0.00316	0.00244	0.00230	XXX	0.00206
0.00157	XXX	0.00251	0.00513	0.00198	XXX	0.00345	0.00268	XXX	0.00179	0.00223
0.00123	0.00178	0.00185	0.00576	0.00216	0.00195	0.00281	0.00218	0.00189	0.00143	0.00171

SRM 621 4 8 26	SRM 621 4 8 25	SRM 621 4 8 24	SRM 621 4 8 23	SRM 621 4 8 22	SRM 621 4 8 21	SRM 621 4 8 20	SRM 621 4 8 19	SRM 621 4 8 18	SRM 621 4 8 17	SRM 621 4 8 16
XXX	XXX	XXX	XXX	XXX	0.00168	0.00172	XXX	XXX	XXX	0.00279
XXX	XXX	XXX	0.00151	0.00196	0.00155	XXX	XXX	XXX	XXX	0.00274
XXX	XXX	0.00202	XXX	XXX	0.00267	XXX	XXX	XXX	XXX	0.00511
XXX	XXX	XXX	0.00158	XXX	0.00164	0.00168	XXX	XXX	XXX	0.00289
XXX	XXX	0.00197	XXX	0.00371	0.00259	XXX	XXX	0.00177	XXX	0.00497
XXX	XXX	XXX	XXX	XXX	0.00242	XXX	XXX	XXX	0.00208	0.00471
XXX	XXX	XXX	0.00181	0.00249	0.00180	0.00187	XXX	XXX	XXX	0.00339
XXX	XXX	0.00198	XXX	XXX	0.00269	XXX	XXX	0.00166	0.00197	0.00519
0.00193	0.00378	XXX	XXX	XXX	0.00343	XXX	XXX	XXX	XXX	0.00646
XXX	XXX	0.00160	0.00198	0.00279	0.00197	0.00201	XXX	0.00215	XXX	0.00379
0.00165	0.00298	XXX	XXX	XXX	0.00272	XXX	XXX	XXX	0.00184	0.00530
XXX	XXX	XXX	XXX	XXX	0.00236	XXX	0.00159	XXX	XXX	0.00450
XXX	XXX	0.00167	0.00213	0.00301	0.00211	0.00216	XXX	0.00204	0.00245	0.00408
0.00166	0.00285	XXX	XXX	XXX	0.00257	XXX	0.00164	XXX	XXX	0.00496
0.00160	0.00258	0.00179	0.00238	0.00338	0.00236	0.00239	XXX	0.00185	0.00219	0.00458
0.00166	0.00284	XXX	XXX	XXX	0.00256	XXX	0.00164	XXX	0.00201	0.00494
0.00121	0.00212	0.00150	0.00204	0.00296	0.00194	0.00192	0.00131	0.00172	0.00222	0.00408

SRM 621 4 16 7	SRM 621 4 16 6	SRM 621 4 16 5	SRM 621 4 16 4	SRM 621 4 16 3	SRM 621 4 16 2	SRM 621 4 16 1	SRM 621 4 8 30	SRM 621 4 8 29	SRM 621 4 8 28	SRM 621 4 8 27
0.00153	XXX	0.00232	XXX	XXX	0.00168	0.00242	XXX	XXX	XXX	XXX
XXX	XXX	0.00182	XXX	XXX	0.00137	XXX	XXX	XXX	XXX	XXX
XXX	XXX	0.00151	XXX	0.00129	0.00167	XXX	XXX	XXX	XXX	XXX
0.00119	XXX	0.00180	XXX	XXX	0.00138	0.00187	XXX	XXX	XXX	XXX
XXX	XXX	0.00140	XXX	0.00123	0.00162	XXX	XXX	XXX	XXX	XXX
XXX	XXX	0.00295	XXX	XXX	0.00161	XXX	0.00252	XXX	XXX	0.00143
0.00122	XXX	0.00186	XXX	XXX	0.00141	0.00193	XXX	XXX	XXX	XXX
XXX	XXX	0.00177	XXX	0.00126	0.00139	XXX	XXX	XXX	XXX	0.00144
XXX	XXX	0.00230	XXX	XXX	0.00120	XXX	0.00370	XXX	0.00179	XXX
0.00128	XXX	0.00158	XXX	0.00128	0.00146	0.00165	XXX	XXX	XXX	XXX
XXX	XXX	0.00256	XXX	XXX	0.00149	XXX	0.00287	XXX	0.00159	0.00142
XXX	0.00163	0.00235	0.00165	XXX	0.00153	XXX	XXX	0.00196	XXX	XXX
0.00153	XXX	0.00219	XXX	0.00171	0.00162	0.00229	0.00218	XXX	XXX	0.00155
XXX	0.00161	0.00233	0.00163	XXX	0.00150	XXX	XXX	0.00178	0.00164	XXX
0.00149	XXX	0.00216	XXX	0.00166	0.00156	0.00228	0.00245	XXX	0.00160	0.00148
XXX	0.00168	0.00245	0.00171	XXX	0.00150	XXX	0.00272	0.00178	0.00164	0.00148
0.00124	0.00136	0.00190	0.00136	0.00135	0.00129	0.00199	0.00212	0.00154	0.00129	0.00134

SRM 621 4 16 18	SRM 621 4 16 17	SRM 621 4 16 16	SRM 621 4 16 15	SRM 621 4 16 14	SRM 621 4 16 13	SRM 621 4 16 12	SRM 621 4 16 11	SRM 621 4 16 10	SRM 621 4 16 9	SRM 621 4 16 8
XXX	XXX	0.00302	XXX	XXX	XXX	XXX	XXX	XXX	0.00165	XXX
XXX	XXX	0.00238	XXX	0.00176	XXX	XXX	XXX	XXX	0.00127	XXX
XXX	XXX	0.00200	XXX	XXX	XXX	XXX	XXX	0.00129	0.00131	XXX
XXX	XXX	0.00238	XXX	0.00177	XXX	XXX	XXX	XXX	0.00128	XXX
0.00225	XXX	0.00185	XXX	XXX	XXX	XXX	XXX	0.00119	0.00121	XXX
XXX	0.00190	0.00387	XXX	XXX	0.00160	XXX	XXX	XXX	0.00199	0.00156
XXX	XXX	0.00244	XXX	0.00183	XXX	XXX	XXX	0.00143	0.00133	XXX
0.00290	0.00124	0.00240	XXX	XXX	0.00114	XXX	XXX	XXX	0.00132	0.00122
XXX	XXX	0.00312	0.00196	XXX	XXX	0.00117	0.00114	XXX	0.00154	XXX
0.00258	XXX	0.00210	XXX	0.00157	XXX	XXX	XXX	0.00126	0.00122	XXX
XXX	0.00172	0.00341	0.00228	XXX	0.00144	XXX	0.00146	XXX	0.00173	0.00141
XXX	XXX	0.00312	XXX	XXX	XXX	0.00171	XXX	XXX	0.00163	XXX
0.00346	0.00174	0.00288	XXX	0.00221	0.00144	XXX	XXX	0.00179	0.00156	0.00151
XXX	XXX	0.00312	0.00211	XXX	XXX	0.00163	0.00148	XXX	0.00161	XXX
0.00345	0.00169	0.00287	0.00196	0.00219	0.00139	XXX	0.00147	0.00177	0.00153	0.00144
XXX	0.00174	0.00325	0.00219	XXX	0.00143	0.00159	0.00148	XXX	0.00166	0.00143
0.00313	0.00132	0.00256	0.00165	0.00191	0.00114	0.00138	0.00117	0.00148	0.00133	0.00120

SRM 621 4 16 29	SRM 621 4 16 28	SRM 621 4 16 27	SRM 621 4 16 26	SRM 621 4 16 25	SRM 621 4 16 24	SRM 621 4 16 23	SRM 621 4 16 22	SRM 621 4 16 21	SRM 621 4 16 20	SRM 621 4 16 19
XXX	XXX	XXX	XXX	XXX	XXX	XXX	XXX	0.00150	0.00161	XXX
XXX	XXX	XXX	XXX	XXX	XXX	0.00109	0.00105	0.00109	XXX	XXX
XXX	XXX	XXX	XXX	XXX	0.00164	XXX	XXX	0.00138	XXX	XXX
XXX	XXX	XXX	XXX	XXX	XXX	0.00116	XXX	0.00113	0.00118	XXX
XXX	XXX	XXX	XXX	XXX	0.00153	XXX	0.00116	0.00128	XXX	XXX
XXX	XXX	0.00156	XXX	XXX	XXX	XXX	XXX	0.00159	XXX	XXX
XXX	XXX	XXX	XXX	XXX	XXX	0.00120	0.00114	0.00118	0.00123	XXX
XXX	XXX	0.00122	XXX	XXX	0.00196	XXX	XXX	0.00118	XXX	XXX
XXX	0.00160	XXX	0.00149	0.00119	XXX	XXX	XXX	0.00116	XXX	XXX
XXX	XXX	XXX	XXX	XXX	0.00175	0.00118	0.00110	0.00117	0.00113	XXX
XXX	0.00174	0.00139	0.00178	0.00157	XXX	XXX	XXX	0.00144	XXX	XXX
0.00206	XXX	XXX	XXX	XXX	XXX	XXX	XXX	0.00146	XXX	0.00154
XXX	XXX	0.00137	XXX	XXX	0.00259	0.00154	0.00156	0.00144	0.00151	XXX
0.00204	0.00160	XXX	0.00167	0.00167	XXX	XXX	XXX	0.00143	XXX	0.00147
XXX	0.00152	0.00133	0.00160	0.00173	0.00257	0.00151	0.00153	0.00140	0.00145	XXX
0.00212	0.00167	0.00137	0.00173	0.00165	XXX	XXX	XXX	0.00142	XXX	0.00144
0.00165	0.00138	0.00117	0.00132	0.00140	0.00212	0.00121	0.00115	0.00113	0.00112	0.00135

SRM 621 4 32 10	SRM 621 4 32 9	SRM 621 4 32 8	SRM 621 4 32 7	SRM 621 4 32 6	SRM 621 4 32 5	SRM 621 4 32 4	SRM 621 4 32 3	SRM 621 4 32 2	SRM 621 4 32 1	SRM 621 4 16 30
XXX	0.00158	XXX	0.00298	XXX	0.00154	XXX	XXX	0.00269	0.00157	XXX
XXX	0.00157	XXX	XXX	XXX	0.00186	XXX	XXX	0.00345	XXX	XXX
0.00252	0.00150	XXX	XXX	XXX	0.00161	XXX	0.00146	0.00295	XXX	XXX
XXX	0.00158	XXX	0.00324	XXX	0.00165	XXX	XXX	0.00291	0.00162	XXX
0.00224	0.00117	XXX	XXX	XXX	0.00130	XXX	0.00122	0.00271	XXX	XXX
XXX	0.00168	0.00274	XXX	XXX	0.00185	XXX	XXX	0.00320	XXX	0.00156
0.00248	0.00161	XXX	0.00318	XXX	0.00164	XXX	XXX	0.00288	0.00163	XXX
XXX	0.00124	0.00215	XXX	XXX	0.00133	XXX	0.00133	0.00260	XXX	XXX
XXX	0.00129	XXX	XXX	XXX	0.00132	XXX	XXX	0.00249	XXX	0.00118
0.00259	0.00155	XXX	0.00334	XXX	0.00166	XXX	0.00155	0.00303	0.00159	XXX
XXX	0.00134	0.00205	XXX	XXX	0.00135	XXX	XXX	0.00247	XXX	0.00142
XXX	0.00132	XXX	XXX	0.00128	0.00124	0.00133	XXX	0.00228	XXX	XXX
0.00267	0.00157	0.00264	0.00342	XXX	0.00171	XXX	0.00160	0.00307	0.00165	0.00146
XXX	0.00136	XXX	XXX	0.00131	0.00125	0.00132	XXX	0.00222	XXX	XXX
0.00252	0.00159	0.00251	0.00324	XXX	0.00166	XXX	0.00162	0.00291	0.00164	0.00141
XXX	0.00133	0.00196	XXX	0.00131	0.00129	0.00135	XXX	0.00237	XXX	0.00142
0.00246	0.00162	0.00244	0.00315	0.00155	0.00164	0.00168	0.00165	0.00283	0.00165	0.00118

SRM 621 4 32 21	SRM 621 4 32 20	SRM 621 4 32 19	SRM 621 4 32 18	SRM 621 4 32 17	SRM 621 4 32 16	SRM 621 4 32 15	SRM 621 4 32 14	SRM 621 4 32 13	SRM 621 4 32 12	SRM 621 4 32 11
0.00203	0.00137	XXX	XXX	XXX	0.00218	XXX	XXX	XXX	XXX	XXX
0.00256	XXX	XXX	XXX	XXX	0.00281	XXX	0.00254	XXX	XXX	XXX
0.00219	XXX	XXX	XXX	XXX	0.00237	XXX	XXX	XXX	XXX	XXX
0.00218	0.00145	XXX	XXX	XXX	0.00236	XXX	0.00216	XXX	XXX	XXX
0.00198	XXX	XXX	0.00126	XXX	0.00212	XXX	XXX	XXX	XXX	XXX
0.00241	XXX	XXX	XXX	0.00303	0.00264	XXX	XXX	0.00173	XXX	XXX
0.00216	0.00146	XXX	XXX	XXX	0.00234	XXX	0.00214	XXX	XXX	XXX
0.00190	XXX	XXX	0.00132	0.00254	0.00206	XXX	XXX	0.00129	XXX	XXX
0.00182	XXX	XXX	XXX	XXX	0.00198	0.00123	XXX	XXX	0.00145	0.00234
0.00226	0.00145	XXX	0.00158	XXX	0.00245	XXX	0.00224	XXX	XXX	XXX
0.00183	XXX	XXX	XXX	0.00237	0.00198	0.00128	XXX	0.00128	XXX	0.00233
0.00169	XXX	0.00118	XXX	XXX	0.00182	XXX	XXX	XXX	0.00136	XXX
0.00230	0.00149	XXX	0.00166	0.00298	0.00250	XXX	0.00227	0.00167	XXX	XXX
0.00165	XXX	0.00119	XXX	XXX	0.00177	0.00124	XXX	XXX	0.00134	0.00208
0.00218	0.00146	XXX	0.00159	0.00283	0.00237	0.00147	0.00216	0.00164	XXX	0.00283
0.00175	XXX	0.00121	XXX	0.00230	0.00189	0.00125	XXX	0.00126	0.00141	0.00222
0.00213	0.00146	0.00153	0.00157	0.00275	0.00231	0.00148	0.00211	0.00162	0.00173	0.00276

SRM 621 4 64 2	SRM 621 4 64 1	SRM 621 4 32 30	SRM 621 4 32 29	SRM 621 4 32 28	SRM 621 4 32 27	SRM 621 4 32 26	SRM 621 4 32 25	SRM 621 4 32 24	SRM 621 4 32 23	SRM 621 4 32 22
0.00053	0.00163	XXX	XXX	XXX	XXX	XXX	XXX	XXX	XXX	XXX
0.00054	XXX	XXX	XXX	XXX	XXX	XXX	XXX	XXX	0.00155	0.00159
0.00070	XXX	XXX	XXX	XXX	XXX	XXX	XXX	0.00163	XXX	XXX
0.00025	0.00128	XXX	XXX	XXX	XXX	XXX	XXX	XXX	0.00159	XXX
0.00040	XXX	XXX	XXX	XXX	XXX	XXX	XXX	0.00134	XXX	0.00120
0.00025	XXX	0.00178	XXX	XXX	0.00159	XXX	XXX	XXX	XXX	XXX
0.00047	0.00156	XXX	XXX	XXX	XXX	XXX	XXX	XXX	0.00162	0.00150
0.00060	XXX	XXX	XXX	XXX	0.00135	XXX	XXX	0.00145	XXX	XXX
0.00040	XXX	0.00167	XXX	0.00183	XXX	0.00213	0.00125	XXX	XXX	XXX
0.00029	0.00133	XXX	XXX	XXX	XXX	XXX	XXX	0.00175	0.00157	0.00147
0.00032	XXX	0.00172	XXX	0.00183	0.00142	0.00211	0.00130	XXX	XXX	XXX
0.00049	XXX	XXX	0.00235	XXX	XXX	XXX	XXX	XXX	XXX	XXX
0.00028	0.00131	0.00177	XXX	XXX	0.00156	XXX	XXX	0.00185	0.00157	0.00155
0.00031	XXX	XXX	0.00228	0.00166	XXX	0.00192	0.00128	XXX	XXX	XXX
0.00055	0.00165	0.00184	XXX	0.00222	0.00160	0.00253	0.00152	0.00178	0.00159	0.00152
0.00029	XXX	0.00176	0.00244	0.00176	0.00144	0.00204	0.00128	XXX	XXX	XXX
0.00052	0.00166	0.00188	0.00295	0.00216	0.00162	0.00246	0.00153	0.00177	0.00162	0.00153

SRM 621 4 64 13	SRM 621 4 64 12	SRM 621 4 64 11	SRM 621 4 64 10	SRM 621 4 64 9	SRM 621 4 64 8	SRM 621 4 64 7	SRM 621 4 64 6	SRM 621 4 64 5	SRM 621 4 64 4	SRM 621 4 64 3
XXX	XXX	XXX	XXX	0.00173	XXX	0.00178	XXX	0.00203	XXX	XXX
XXX	XXX	XXX	XXX	0.00156	XXX	XXX	XXX	0.00152	XXX	XXX
XXX	XXX	XXX	0.00138	0.00177	XXX	XXX	XXX	0.00249	XXX	0.00170
XXX	XXX	XXX	XXX	0.00130	XXX	0.00139	XXX	XXX	XXX	XXX
XXX	XXX	XXX	0.00122	0.00134	XXX	XXX	XXX	0.00183	XXX	0.00130
0.00177	XXX	XXX	XXX	0.00128	0.00204	XXX	XXX	0.00147	XXX	XXX
XXX	XXX	XXX	0.00158	0.00165	XXX	0.00168	XXX	0.00184	XXX	XXX
0.00174	XXX	XXX	XXX	0.00174	0.00296	XXX	XXX	0.00216	XXX	0.00166
XXX	0.00123	0.00145	XXX	0.00136	XXX	XXX	XXX	0.00192	XXX	XXX
XXX	XXX	XXX	0.00126	0.00131	XXX	0.00151	XXX	0.00166	XXX	0.00129
0.00163	XXX	0.00145	XXX	0.00135	0.00247	XXX	XXX	0.00175	XXX	XXX
XXX	0.00158	XXX	XXX	0.00166	XXX	XXX	0.00189	0.00205	0.00219	XXX
0.00171	XXX	XXX	0.00127	0.00129	0.00224	0.00149	XXX	0.00161	XXX	0.00128
XXX	0.00128	0.00149	XXX	0.00136	XXX	XXX	0.00167	0.00184	0.00200	XXX
0.00176	XXX	0.00174	0.00154	0.00169	0.00284	0.00187	XXX	0.00208	XXX	0.00163
0.00165	0.00130	0.00146	XXX	0.00134	0.00246	XXX	0.00161	0.00175	0.00189	XXX
0.00178	0.00158	0.00175	0.00155	0.00168	0.00283	0.00188	0.00190	0.00208	0.00223	0.00163

SRM 621 4 64 24	SRM 621 4 64 23	SRM 621 4 64 22	SRM 621 4 64 21	SRM 621 4 64 20	SRM 621 4 64 19	SRM 621 4 64 18	SRM 621 4 64 17	SRM 621 4 64 16	SRM 621 4 64 15	SRM 621 4 64 14
XXX	XXX	XXX	0.00177	0.00169	XXX	XXX	XXX	0.00148	XXX	XXX
XXX	0.00200	0.00183	0.00155	XXX	XXX	XXX	XXX	0.00177	XXX	0.00151
0.00129	XXX	XXX	0.00188	XXX	XXX	XXX	XXX	0.00137	XXX	XXX
XXX	0.00225	XXX	0.00136	0.00135	XXX	XXX	XXX	0.00133	XXX	0.00134
0.00141	XXX	0.00264	0.00142	XXX	XXX	0.00161	XXX	0.00122	XXX	XXX
XXX	XXX	XXX	0.00135	XXX	XXX	XXX	0.00132	0.00133	XXX	XXX
XXX	0.00271	0.00248	0.00168	0.00162	XXX	XXX	XXX	0.00154	XXX	0.00168
0.00167	XXX	XXX	0.00177	XXX	XXX	0.00193	0.00179	0.00147	XXX	XXX
XXX	XXX	XXX	0.00146	XXX	XXX	XXX	XXX	0.00124	0.00130	XXX
0.00163	0.00251	0.00236	0.00139	0.00136	XXX	0.00158	XXX	0.00127	XXX	0.00140
XXX	XXX	XXX	0.00143	XXX	XXX	XXX	0.00143	0.00126	0.00140	XXX
XXX	XXX	XXX	0.00172	XXX	0.00158	XXX	XXX	0.00149	XXX	XXX
0.00170	0.00242	0.00228	0.00136	0.00135	XXX	0.00156	0.00136	0.00129	XXX	0.00138
XXX	XXX	XXX	0.00147	XXX	0.00136	XXX	XXX	0.00126	0.00140	XXX
0.00172	0.00310	0.00286	0.00173	0.00164	XXX	0.00189	0.00174	0.00147	0.00160	0.00178
XXX	XXX	XXX	0.00143	XXX	0.00134	XXX	0.00146	0.00127	0.00144	XXX
0.00177	0.00309	0.00287	0.00173	0.00166	0.00157	0.00191	0.00177	0.00148	0.00164	0.00179

SRM 621 4 128 5	SRM 621 4 128 4	SRM 621 4 128 3	SRM 621 4 128 2	SRM 621 4 128 1	SRM 621 4 64 30	SRM 621 4 64 29	SRM 621 4 64 28	SRM 621 4 64 27	SRM 621 4 64 26	SRM 621 4 64 25
0.00236	XXX	XXX	0.00200	0.00245	XXX	XXX	XXX	XXX	XXX	XXX
0.00246	XXX	XXX	0.00233	XXX	XXX	XXX	XXX	XXX	XXX	XXX
0.00220	XXX	0.00128	0.00183	XXX	XXX	XXX	XXX	XXX	XXX	XXX
0.00212	XXX	XXX	0.00195	0.00227	XXX	XXX	XXX	XXX	XXX	XXX
0.00271	XXX	0.00158	0.00228	XXX	XXX	XXX	XXX	XXX	XXX	XXX
0.00206	XXX	XXX	0.00184	XXX	0.00212	XXX	XXX	0.00136	XXX	XXX
0.00265	XXX	XXX	0.00227	0.00279	XXX	XXX	XXX	XXX	XXX	XXX
0.00249	XXX	0.00156	0.00219	XXX	XXX	XXX	XXX	0.00199	XXX	XXX
0.00249	XXX	XXX	0.00212	XXX	0.00270	XXX	0.00131	XXX	0.00140	0.00174
0.00221	XXX	0.00126	0.00197	0.00235	XXX	XXX	XXX	XXX	XXX	XXX
0.00249	XXX	XXX	0.00215	XXX	0.00252	XXX	0.00133	0.00161	0.00146	0.00164
0.00284	0.00184	XXX	0.00238	XXX	XXX	0.00186	XXX	XXX	XXX	XXX
0.00217	XXX	0.00126	0.00193	0.00231	0.00230	XXX	XXX	0.00148	XXX	XXX
0.00234	0.00147	XXX	0.00200	XXX	XXX	0.00161	0.00134	XXX	0.00147	0.00171
0.00218	XXX	0.00126	0.00193	0.00231	0.00285	XXX	0.00157	0.00191	0.00171	0.00194
0.00228	0.00142	XXX	0.00198	XXX	0.00251	0.00156	0.00132	0.00161	0.00151	0.00164
0.00264	0.00172	0.00158	0.00225	0.00278	0.00284	0.00188	0.00157	0.00191	0.00175	0.00194

SRM 621 4 128 16	SRM 621 4 128 15	SRM 621 4 128 14	SRM 621 4 128 13	SRM 621 4 128 12	SRM 621 4 128 11	SRM 621 4 128 10	SRM 621 4 128 9	SRM 621 4 128 8	SRM 621 4 128 7	SRM 621 4 128 6
0.00221	XXX	XXX	XXX	XXX	XXX	XXX	0.00204	XXX	0.00158	XXX
0.00249	XXX	0.00241	XXX	XXX	XXX	XXX	0.00141	XXX	XXX	XXX
0.00204	XXX	XXX	XXX	XXX	XXX	0.00129	0.00185	XXX	XXX	XXX
0.00208	XXX	0.00207	XXX	XXX	XXX	XXX	0.00162	XXX	0.00128	XXX
0.00256	XXX	XXX	XXX	XXX	XXX	0.00166	0.00185	XXX	XXX	XXX
0.00199	XXX	XXX	0.00138	XXX	XXX	XXX	0.00175	0.00125	XXX	XXX
0.00251	XXX	0.00259	XXX	XXX	XXX	0.00166	0.00181	XXX	0.00160	XXX
0.00241	XXX	XXX	0.00172	XXX	XXX	XXX	0.00189	0.00149	XXX	XXX
0.00236	0.00154	XXX	XXX	0.00176	0.00165	XXX	0.00196	XXX	XXX	XXX
0.00214	XXX	0.00216	XXX	XXX	XXX	0.00139	0.00164	XXX	0.00130	XXX
0.00238	0.00155	XXX	0.00172	XXX	0.00164	XXX	0.00194	0.00150	XXX	XXX
0.00267	XXX	XXX	XXX	0.00196	XXX	XXX	0.00190	XXX	XXX	0.00194
0.00210	XXX	0.00213	0.00142	XXX	XXX	0.00138	0.00167	0.00123	0.00130	XXX
0.00222	0.00132	XXX	XXX	0.00154	0.00141	XXX	0.00173	XXX	XXX	0.00158
0.00211	0.00125	0.00213	0.00143	XXX	0.00131	0.00138	0.00167	0.00123	0.00130	XXX
0.00218	0.00128	XXX	0.00149	0.00150	0.00136	XXX	0.00168	0.00123	XXX	0.00155
0.00251	0.00156	0.00259	0.00178	0.00184	0.00163	0.00169	0.00187	0.00147	0.00160	0.00183

SRM 621 4 128 27	SRM 621 4 128 26	SRM 621 4 128 25	SRM 621 4 128 24	SRM 621 4 128 23	SRM 621 4 128 22	SRM 621 4 128 21	SRM 621 4 128 20	SRM 621 4 128 19	SRM 621 4 128 18	SRM 621 4 128 17
XXX	XXX	XXX	XXX	XXX	XXX	0.00171	0.00160	XXX	XXX	XXX
XXX	XXX	XXX	XXX	0.00131	0.00128	0.00132	XXX	XXX	XXX	XXX
XXX	XXX	XXX	0.00193	XXX	XXX	0.00151	XXX	XXX	XXX	XXX
XXX	XXX	XXX	XXX	0.00156	XXX	0.00144	0.00141	XXX	XXX	XXX
XXX	XXX	XXX	0.00236	XXX	0.00157	0.00152	XXX	XXX	0.00167	XXX
0.00191	XXX	XXX	XXX	XXX	XXX	0.00152	XXX	XXX	XXX	0.00135
XXX	XXX	XXX	XXX	0.00182	0.00153	0.00152	0.00167	XXX	XXX	XXX
0.00231	XXX	XXX	0.00217	XXX	XXX	0.00162	XXX	XXX	0.00163	0.00169
XXX	0.00304	0.00170	XXX	XXX	XXX	0.00163	XXX	XXX	XXX	XXX
XXX	XXX	XXX	0.00192	0.00156	0.00128	0.00142	0.00143	XXX	0.00131	XXX
0.00232	0.00304	0.00173	XXX	XXX	XXX	0.00164	XXX	XXX	XXX	0.00169
XXX	XXX	XXX	XXX	XXX	XXX	0.00155	XXX	0.00156	XXX	XXX
0.00201	XXX	XXX	0.00190	0.00159	0.00128	0.00144	0.00143	XXX	0.00131	0.00141
XXX	0.00291	0.00149	XXX	XXX	XXX	0.00144	XXX	0.00129	XXX	XXX
0.00202	0.00272	0.00153	0.00190	0.00159	0.00129	0.00144	0.00143	XXX	0.00132	0.00141
0.00212	0.00284	0.00149	XXX	XXX	XXX	0.00141	XXX	0.00126	XXX	0.00146
0.00246	0.00323	0.00167	0.00230	0.00185	0.00156	0.00155	0.00171	0.00152	0.00167	0.00176

SRM 621 4 256 8	SRM 621 4 256 7	SRM 621 4 256 6	SRM 621 4 256 5	SRM 621 4 256 4	SRM 621 4 256 3	SRM 621 4 256 2	SRM 621 4 256 1	SRM 621 4 128 30	SRM 621 4 128 29	SRM 621 4 128 28
XXX	0.00126	XXX	0.00222	XXX	XXX	0.00176	0.00167	XXX	XXX	XXX
XXX	XXX	XXX	0.00349	XXX	XXX	0.00288	XXX	XXX	XXX	XXX
XXX	XXX	XXX	0.01047	XXX	0.01105	0.01017	XXX	XXX	XXX	XXX
XXX	0.00148	XXX	0.00262	XXX	XXX	0.00211	0.00200	XXX	XXX	XXX
XXX	XXX	XXX	0.00242	XXX	0.00292	0.00194	XXX	XXX	XXX	XXX
0.00139	XXX	XXX	0.00383	XXX	XXX	0.00311	XXX	0.00142	XXX	XXX
XXX	0.00163	XXX	0.00289	XXX	XXX	0.00233	0.00221	XXX	XXX	XXX
0.00157	XXX	XXX	0.00285	XXX	0.00345	0.00231	XXX	XXX	XXX	XXX
XXX	XXX	XXX	0.00303	XXX	XXX	0.00241	XXX	0.00173	XXX	0.00186
XXX	0.00145	XXX	0.00255	XXX	0.00310	0.00204	0.00194	XXX	XXX	XXX
0.00140	XXX	XXX	0.00340	XXX	XXX	0.00273	XXX	0.00175	XXX	0.00187
XXX	XXX	0.00644	0.00692	0.00631	XXX	0.00652	XXX	XXX	0.00172	XXX
0.00151	0.00167	XXX	0.00294	XXX	0.00355	0.00237	0.00225	0.00149	XXX	XXX
XXX	XXX	0.00184	0.00236	0.00168	XXX	0.00191	XXX	XXX	0.00160	0.00171
0.00149	0.00168	XXX	0.00298	XXX	0.00360	0.00240	0.00228	0.00149	XXX	0.00161
0.00155	XXX	0.00211	0.00274	0.00193	XXX	0.00221	XXX	0.00154	0.00160	0.00167
0.00157	0.00152	0.00204	0.00264	0.00186	0.00321	0.00213	0.00203	0.00182	0.00176	0.00196

SRM 621 4 256 19	SRM 621 4 256 18	SRM 621 4 256 17	SRM 621 4 256 16	SRM 621 4 256 15	SRM 621 4 256 14	SRM 621 4 256 13	SRM 621 4 256 12	SRM 621 4 256 11	SRM 621 4 256 10	SRM 621 4 256 9
XXX	XXX	XXX	0.00176	XXX	XXX	XXX	XXX	XXX	XXX	0.00125
XXX	XXX	XXX	0.00155	XXX	0.00128	XXX	XXX	XXX	XXX	0.00168
XXX	XXX	XXX	0.01028	XXX	XXX	XXX	XXX	XXX	0.00974	0.00957
XXX	XXX	XXX	0.00161	XXX	0.00127	XXX	XXX	XXX	XXX	0.00131
XXX	0.00138	XXX	0.00184	XXX	XXX	XXX	XXX	XXX	0.00129	0.00141
XXX	XXX	0.00138	0.00139	XXX	XXX	0.00263	XXX	XXX	XXX	0.00185
XXX	XXX	XXX	0.00157	XXX	0.00133	XXX	XXX	XXX	0.00135	0.00146
XXX	0.00140	0.00139	0.00169	XXX	XXX	0.00198	XXX	XXX	XXX	0.00151
XXX	XXX	XXX	0.00152	0.00128	XXX	XXX	0.00202	0.00132	XXX	0.00156
XXX	0.00134	XXX	0.00170	XXX	0.00140	XXX	XXX	XXX	0.00129	0.00136
XXX	XXX	0.00129	0.00143	0.00133	XXX	0.00231	XXX	0.00131	XXX	0.00166
0.00580	XXX	XXX	0.00607	XXX	XXX	XXX	0.00621	XXX	XXX	0.00568
XXX	0.00136	0.00135	0.00161	XXX	0.00138	0.00203	XXX	XXX	0.00137	0.00151
0.00138	XXX	XXX	0.00184	0.00143	XXX	XXX	0.00168	0.00138	XXX	0.00134
XXX	0.00133	0.00132	0.00157	0.00135	0.00138	0.00204	XXX	0.00132	0.00135	0.00152
0.00154	XXX	0.00137	0.00167	0.00140	XXX	0.00190	0.00190	0.00135	XXX	0.00146
0.00150	0.00137	0.00137	0.00170	0.00141	0.00141	0.00184	0.00186	0.00135	0.00134	0.00141

SRM 621 4 256 30	SRM 621 4 256 29	SRM 621 4 256 28	SRM 621 4 256 27	SRM 621 4 256 26	SRM 621 4 256 25	SRM 621 4 256 24	SRM 621 4 256 23	SRM 621 4 256 22	SRM 621 4 256 21	SRM 621 4 256 20
XXX	XXX	XXX	XXX	XXX	XXX	XXX	XXX	XXX	0.00149	0.00116
XXX	XXX	XXX	XXX	XXX	XXX	XXX	0.00196	0.00148	0.00208	XXX
XXX	XXX	XXX	XXX	XXX	XXX	0.01018	XXX	XXX	0.00959	XXX
XXX	XXX	XXX	XXX	XXX	XXX	XXX	0.00151	XXX	0.00162	0.00126
XXX	XXX	XXX	XXX	XXX	XXX	0.00222	XXX	0.00127	0.00168	XXX
0.00135	XXX	XXX	0.00143	XXX	XXX	XXX	XXX	XXX	0.00238	XXX
XXX	XXX	XXX	XXX	XXX	XXX	XXX	0.00171	0.00127	0.00181	0.00133
XXX	XXX	XXX	0.00139	XXX	XXX	0.00261	XXX	XXX	0.00185	XXX
0.00123	XXX	0.00204	XXX	0.00139	0.00163	XXX	XXX	XXX	0.00196	XXX
XXX	XXX	XXX	XXX	XXX	XXX	0.00232	0.00157	0.00123	0.00166	0.00126
0.00127	XXX	0.00231	0.00136	0.00150	0.00184	XXX	XXX	XXX	0.00213	XXX
XXX	0.00668	XXX	XXX	XXX	XXX	XXX	XXX	XXX	0.00579	XXX
0.00135	XXX	XXX	0.00137	XXX	XXX	0.00268	0.00178	0.00130	0.00187	0.00136
XXX	0.00206	0.00163	XXX	0.00128	0.00144	XXX	XXX	XXX	0.00158	XXX
0.00131	XXX	0.00203	0.00135	0.00140	0.00168	0.00272	0.00181	0.00129	0.00190	0.00134
0.00135	0.00238	0.00188	0.00138	0.00135	0.00159	XXX	XXX	XXX	0.00177	XXX
0.00137	0.00230	0.00182	0.00137	0.00132	0.00155	0.00242	0.00163	0.00127	0.00171	0.00131

Table 131: Mid-IR spectral library results for SRM 1831, correlation search algorithm.

	3A	3B	3C	5A	5B	5C	7A	7B	7C	10A	10B	10C	15A	15B	20A	20B	30A
SRM 1831 481	0.00258	XXX	XXX	0.00258	XXX	XXX	0.00249	XXX	XXX	0.00244	XXX	XXX	0.00243	XXX	0.00300	XXX	0.00242
SRM 1831 482	0.00290	0.00278	0.00264	0.00286	0.00262	0.00337	0.00275	0.00261	0.00263	0.00270	0.00259	0.00273	0.00266	0.00267	0.00342	0.00342	0.00266
SRM 1831 483	XXX	XXX	0.00237	XXX	0.00234	XXX	XXX	0.00234	XXX	0.00241	XXX	XXX	0.00239	XXX	0.00301	XXX	0.00239
SRM 1831 484	XXX	XXX	XXX	XXX	XXX	XXX	XXX	XXX	XXX	XXX	XXX	0.00326	XXX	0.00320	XXX	0.00389	0.00319
SRM 1831 485	0.00279	0.00267	0.00254	0.00276	0.00252	0.00313	0.00265	0.00251	0.00253	0.00259	0.00249	0.00262	0.00256	0.00257	0.00317	0.00318	0.00256
SRM 1831 486	XXX	XXX	XXX	XXX	XXX	XXX	XXX	XXX	XXX	XXX	XXX	0.00304	XXX	0.00298	XXX	0.00355	0.00297
SRM 1831 487	0.00272	XXX	XXX	0.00270	XXX	XXX	0.00259	XXX	XXX	0.00254	XXX	XXX	0.00251	XXX	0.00313	XXX	0.00251
SRM 1831 488	XXX	XXX	XXX	XXX	XXX	0.00311	XXX	0.00268	XXX	XXX	0.00266	XXX	0.00274	XXX	0.00317	0.00318	0.00274
SRM 1831 489	0.00239	0.00238	0.00227	0.00241	0.00226	0.00298	0.00234	0.00230	0.00233	0.00229	0.00231	0.00236	0.00231	0.00230	0.00287	0.00290	0.00230
SRM 1831 4810	XXX	XXX	0.00267	XXX	0.00264	XXX	0.00279	XXX	XXX	0.00273	XXX	XXX	0.00269	XXX	0.00335	XXX	0.00269

SRM 1831 4 8 21	SRM 1831 4 8 20	SRM 1831 4 8 19	SRM 1831 4 8 18	SRM 1831 4 8 17	SRM 1831 4 8 16	SRM 1831 4 8 15	SRM 1831 4 8 14	SRM 1831 4 8 13	SRM 1831 4 8 12	SRM 1831 4 8 11
0.00310	0.00330	XXX	XXX	XXX	0.00294	XXX	XXX	XXX	XXX	XXX
0.00295	XXX	XXX	XXX	XXX	0.00282	XXX	0.00307	XXX	XXX	XXX
0.00281	XXX	XXX	XXX	XXX	0.00269	XXX	XXX	XXX	XXX	XXX
0.00305	0.00326	XXX	XXX	XXX	0.00292	XXX	0.00316	XXX	XXX	XXX
0.00278	XXX	XXX	0.00283	XXX	0.00266	XXX	XXX	XXX	XXX	XXX
0.00337	XXX	XXX	XXX	0.00392	0.00330	XXX	XXX	0.00351	XXX	XXX
0.00293	0.00314	XXX	XXX	XXX	0.00280	XXX	0.00305	XXX	XXX	XXX
0.00276	XXX	XXX	0.00282	0.00315	0.00265	XXX	XXX	0.00287	XXX	XXX
0.00278	XXX	XXX	XXX	XXX	0.00267	0.00287	XXX	XXX	0.00298	0.00274
0.00287	0.00308	XXX	0.00292	XXX	0.00274	XXX	0.00299	XXX	XXX	XXX
0.00274	XXX	XXX	XXX	0.00315	0.00264	0.00282	XXX	0.00286	XXX	0.00270
0.00289	XXX	0.00291	XXX	XXX	0.00278	XXX	XXX	XXX	0.00310	XXX
0.00282	0.00303	XXX	0.00288	0.00322	0.00270	XXX	0.00295	0.00294	XXX	XXX
0.00283	XXX	0.00285	XXX	XXX	0.00271	0.00292	XXX	XXX	0.00303	0.00280
0.00345	0.00362	XXX	0.00356	0.00398	0.00334	0.00355	0.00362	0.00358	XXX	0.00335
0.00345	XXX	0.00334	XXX	0.00399	0.00335	0.00356	XXX	0.00359	0.00370	0.00336
0.00282	0.00304	0.00284	0.00288	0.00322	0.00270	0.00291	0.00295	0.00294	0.00302	0.00279

SRM 1831 4 16 2	SRM 1831 4 16 1	SRM 1831 4 8 30	SRM 1831 4 8 29	SRM 1831 4 8 28	SRM 1831 4 8 27	SRM 1831 4 8 26	SRM 1831 4 8 25	SRM 1831 4 8 24	SRM 1831 4 8 23	SRM 1831 4 8 22
0.00456	0.00419	XXX	XXX	XXX	XXX	XXX	XXX	XXX	XXX	XXX
0.00455	XXX	XXX	XXX	XXX	XXX	XXX	XXX	XXX	0.00253	0.00260
0.00451	XXX	XXX	XXX	XXX	XXX	XXX	XXX	0.00231	XXX	XXX
0.00456	0.00419	XXX	XXX	XXX	XXX	XXX	XXX	XXX	0.00261	XXX
0.00453	XXX	XXX	XXX	XXX	XXX	XXX	XXX	0.00229	XXX	0.00244
0.00453	XXX	0.00349	XXX	XXX	0.00294	XXX	XXX	XXX	XXX	XXX
0.00454	0.00417	XXX	XXX	XXX	XXX	XXX	XXX	XXX	0.00251	0.00257
0.00456	XXX	XXX	XXX	XXX	0.00249	XXX	XXX	0.00229	XXX	XXX
0.00453	XXX	0.00290	XXX	0.00245	XXX	0.00233	0.00229	XXX	XXX	XXX
0.00455	0.00417	XXX	XXX	XXX	XXX	XXX	XXX	0.00236	0.00245	0.00252
0.00456	XXX	0.00286	XXX	0.00242	0.00248	0.00230	0.00225	XXX	XXX	XXX
0.00455	XXX	XXX	0.00243	XXX	XXX	XXX	XXX	XXX	XXX	XXX
0.00453	0.00415	0.00294	XXX	XXX	0.00255	XXX	XXX	0.00234	0.00243	0.00249
0.00457	XXX	XXX	0.00237	0.00247	XXX	0.00236	0.00231	XXX	XXX	XXX
0.00454	0.00417	0.00356	XXX	0.00294	0.00300	0.00291	0.00284	0.00289	0.00317	0.00296
0.00456	XXX	0.00357	0.00286	0.00296	0.00301	0.00293	0.00286	XXX	XXX	XXX
0.00535	0.00497	0.00294	0.00236	0.00246	0.00255	0.00235	0.00230	0.00234	0.00243	0.00249

SRM 1831 4 16 13	SRM 1831 4 16 12	SRM 1831 4 16 11	SRM 1831 4 16 10	SRM 1831 4 16 9	SRM 1831 4 16 8	SRM 1831 4 16 7	SRM 1831 4 16 6	SRM 1831 4 16 5	SRM 1831 4 16 4	SRM 1831 4 16 3
XXX	XXX	XXX	XXX	0.00421	XXX	0.00395	XXX	0.00405	XXX	XXX
XXX	XXX	XXX	XXX	0.00417	XXX	XXX	XXX	0.00403	XXX	XXX
XXX	XXX	XXX	0.00395	0.00415	XXX	XXX	XXX	0.00399	XXX	0.00428
XXX	XXX	XXX	XXX	0.00420	XXX	0.00395	XXX	0.00405	XXX	XXX
XXX	XXX	XXX	0.00396	0.00416	XXX	XXX	XXX	0.00401	XXX	0.00431
0.00411	XXX	XXX	XXX	0.00415	0.00394	XXX	XXX	0.00401	XXX	XXX
XXX	XXX	XXX	0.00398	0.00417	XXX	0.00394	XXX	0.00403	XXX	XXX
0.00414	XXX	XXX	XXX	0.00418	0.00396	XXX	XXX	0.00404	XXX	0.00433
XXX	0.00390	0.00386	XXX	0.00415	XXX	XXX	XXX	0.00401	XXX	XXX
XXX	XXX	XXX	0.00398	0.00418	XXX	0.00393	XXX	0.00403	XXX	0.00432
0.00413	XXX	0.00390	XXX	0.00418	0.00396	XXX	XXX	0.00404	XXX	XXX
XXX	0.00395	XXX	XXX	0.00417	XXX	XXX	0.00400	0.00403	0.00411	XXX
0.00411	XXX	XXX	0.00396	0.00415	0.00393	0.00391	XXX	0.00401	XXX	0.00430
XXX	0.00397	0.00393	XXX	0.00420	XXX	XXX	0.00401	0.00406	0.00413	XXX
0.00412	XXX	0.00389	0.00397	0.00417	0.00395	0.00393	XXX	0.00402	XXX	0.00432
0.00415	0.00395	0.00391	XXX	0.00419	0.00397	XXX	0.00400	0.00404	0.00412	XXX
0.00471	0.00460	0.00442	0.00471	0.00482	0.00461	0.00459	0.00460	0.00479	0.00489	0.00512

SRM 1831 4 16 24	SRM 1831 4 16 23	SRM 1831 4 16 22	SRM 1831 4 16 21	SRM 1831 4 16 20	SRM 1831 4 16 19	SRM 1831 4 16 18	SRM 1831 4 16 17	SRM 1831 4 16 16	SRM 1831 4 16 15	SRM 1831 4 16 14
XXX	XXX	XXX	0.00395	0.00396	XXX	XXX	XXX	0.00351	XXX	XXX
XXX	0.00389	0.00412	0.00392	XXX	XXX	XXX	XXX	0.00347	XXX	0.00400
0.00384	XXX	XXX	0.00390	XXX	XXX	XXX	XXX	0.00346	XXX	XXX
XXX	0.00392	XXX	0.00394	0.00395	XXX	XXX	XXX	0.00350	XXX	0.00402
0.00386	XXX	0.00413	0.00391	XXX	XXX	0.00387	XXX	0.00347	XXX	XXX
XXX	XXX	XXX	0.00392	XXX	XXX	XXX	0.00364	0.00347	XXX	XXX
XXX	0.00391	0.00414	0.00393	0.00395	XXX	XXX	XXX	0.00348	XXX	0.00401
0.00388	XXX	XXX	0.00394	XXX	XXX	0.00389	0.00365	0.00349	XXX	XXX
XXX	XXX	XXX	0.00390	XXX	XXX	XXX	XXX	0.00345	0.00392	XXX
0.00387	0.00391	0.00414	0.00393	0.00394	XXX	0.00388	XXX	0.00348	XXX	0.00401
XXX	XXX	XXX	0.00393	XXX	XXX	XXX	0.00364	0.00348	0.00396	XXX
XXX	XXX	XXX	0.00394	XXX	0.00392	XXX	XXX	0.00349	XXX	XXX
0.00385	0.00388	0.00411	0.00390	0.00392	XXX	0.00386	0.00362	0.00346	XXX	0.00398
XXX	XXX	XXX	0.00396	XXX	0.00394	XXX	XXX	0.00351	0.00398	XXX
0.00386	0.00390	0.00413	0.00392	0.00394	XXX	0.00387	0.00363	0.00347	0.00395	0.00400
XXX	XXX	XXX	0.00394	XXX	0.00392	XXX	0.00366	0.00349	0.00397	XXX
0.00444	0.00457	0.00475	0.00465	0.00468	0.00467	0.00462	0.00427	0.00410	0.00455	0.00467

SRM 1831 4 32 5	SRM 1831 4 32 4	SRM 1831 4 32 3	SRM 1831 4 32 2	SRM 1831 4 32 1	SRM 1831 4 16 30	SRM 1831 4 16 29	SRM 1831 4 16 28	SRM 1831 4 16 27	SRM 1831 4 16 26	SRM 1831 4 16 25
0.00504	XXX	XXX	0.00508	0.00487	XXX	XXX	XXX	XXX	XXX	XXX
0.00496	XXX	XXX	0.00502	XXX	XXX	XXX	XXX	XXX	XXX	XXX
0.00501	XXX	0.00529	0.00506	XXX	XXX	XXX	XXX	XXX	XXX	XXX
0.00500	XXX	XXX	0.00505	0.00484	XXX	XXX	XXX	XXX	XXX	XXX
0.00498	XXX	0.00527	0.00504	XXX	XXX	XXX	XXX	XXX	XXX	XXX
0.00497	XXX	XXX	0.00503	XXX	0.00418	XXX	XXX	0.00390	XXX	XXX
0.00500	XXX	XXX	0.00505	0.00485	XXX	XXX	XXX	XXX	XXX	XXX
0.00418	XXX	0.00447	0.00425	XXX	XXX	XXX	XXX	0.00393	XXX	XXX
0.00493	XXX	XXX	0.00498	XXX	0.00417	XXX	0.00413	XXX	0.00374	0.00402
0.00498	XXX	0.00526	0.00503	0.00483	XXX	XXX	XXX	XXX	XXX	XXX
0.00495	XXX	XXX	0.00500	XXX	0.00420	XXX	0.00416	0.00392	0.00378	0.00405
0.00501	0.00499	XXX	0.00505	XXX	XXX	0.00380	XXX	XXX	XXX	XXX
0.00497	XXX	0.00526	0.00503	0.00483	0.00417	XXX	XXX	0.00390	XXX	XXX
0.00499	0.00498	XXX	0.00503	XXX	XXX	0.00382	0.00419	XXX	0.00380	0.00408
0.00496	XXX	0.00525	0.00502	0.00482	0.00419	XXX	0.00415	0.00392	0.00377	0.00404
0.00497	0.00497	XXX	0.00502	XXX	0.00422	0.00380	0.00417	0.00394	0.00379	0.00406
0.00497	0.00497	0.00526	0.00502	0.00482	0.00481	0.00438	0.00483	0.00458	0.00453	0.00477

SRM 1831 4 32 16	SRM 1831 4 32 15	SRM 1831 4 32 14	SRM 1831 4 32 13	SRM 1831 4 32 12	SRM 1831 4 32 11	SRM 1831 4 32 10	SRM 1831 4 32 9	SRM 1831 4 32 8	SRM 1831 4 32 7	SRM 1831 4 32 6
0.00507	XXX	XXX	XXX	XXX	XXX	XXX	0.00496	XXX	0.00521	XXX
0.00501	XXX	0.00476	XXX	XXX	XXX	XXX	0.00489	XXX	XXX	XXX
0.00505	XXX	XXX	XXX	XXX	XXX	0.00452	0.00493	XXX	XXX	XXX
0.00504	XXX	0.00479	XXX	XXX	XXX	XXX	0.00493	XXX	0.00518	XXX
0.00503	XXX	XXX	XXX	XXX	XXX	0.00450	0.00491	XXX	XXX	XXX
0.00501	XXX	XXX	0.00503	XXX	XXX	XXX	0.00489	0.00470	XXX	XXX
0.00504	XXX	0.00479	XXX	XXX	XXX	0.00451	0.00492	XXX	0.00518	XXX
0.00428	XXX	XXX	0.00429	XXX	XXX	XXX	0.00416	0.00401	XXX	XXX
0.00497	0.00493	XXX	XXX	0.00477	0.00493	XXX	0.00486	XXX	XXX	XXX
0.00502	XXX	0.00477	XXX	XXX	XXX	0.00449	0.00491	XXX	0.00516	XXX
0.00499	0.00495	XXX	0.00501	XXX	0.00495	XXX	0.00488	0.00469	XXX	XXX
0.00505	XXX	XXX	XXX	0.00485	XXX	XXX	0.00493	XXX	XXX	0.00513
0.00502	XXX	0.00477	0.00503	XXX	XXX	0.00449	0.00490	0.00471	0.00515	XXX
0.00503	0.00498	XXX	XXX	0.00483	0.00498	XXX	0.00491	XXX	XXX	0.00511
0.00501	0.00496	0.00476	0.00502	XXX	0.00496	0.00448	0.00489	0.00470	0.00514	XXX
0.00501	0.00497	XXX	0.00503	0.00482	0.00497	XXX	0.00489	0.00471	XXX	0.00510
0.00501	0.00497	0.00477	0.00503	0.00482	0.00497	0.00449	0.00490	0.00471	0.00515	0.00510

SRM 1831 4 32 27	SRM 1831 4 32 26	SRM 1831 4 32 25	SRM 1831 4 32 24	SRM 1831 4 32 23	SRM 1831 4 32 22	SRM 1831 4 32 21	SRM 1831 4 32 20	SRM 1831 4 32 19	SRM 1831 4 32 18	SRM 1831 4 32 17
XXX	XXX	XXX	XXX	XXX	XXX	0.00482	0.00506	XXX	XXX	XXX
XXX	XXX	XXX	XXX	0.00475	0.00508	0.00475	XXX	XXX	XXX	XXX
XXX	XXX	XXX	0.00514	XXX	XXX	0.00480	XXX	XXX	XXX	XXX
XXX	XXX	XXX	XXX	0.00479	XXX	0.00479	0.00502	XXX	XXX	XXX
XXX	XXX	XXX	0.00511	XXX	0.00510	0.00477	XXX	XXX	0.00486	XXX
0.00469	XXX	XXX	XXX	XXX	XXX	0.00476	XXX	XXX	XXX	0.00501
XXX	XXX	XXX	XXX	0.00479	0.00512	0.00479	0.00502	XXX	XXX	XXX
0.00400	XXX	XXX	0.00436	XXX	XXX	0.00400	XXX	XXX	0.00413	0.00432
XXX	0.00505	0.00498	XXX	XXX	XXX	0.00472	XXX	XXX	XXX	XXX
XXX	XXX	XXX	0.00511	0.00477	0.00509	0.00477	0.00500	XXX	0.00486	XXX
0.00467	0.00507	0.00500	XXX	XXX	XXX	0.00474	XXX	XXX	XXX	0.00500
XXX	XXX	XXX	XXX	XXX	XXX	0.00479	XXX	0.00465	XXX	XXX
0.00469	XXX	XXX	0.00510	0.00476	0.00509	0.00476	0.00499	XXX	0.00485	0.00502
XXX	0.00511	0.00504	XXX	XXX	XXX	0.00477	XXX	0.00463	XXX	XXX
0.00468	0.00508	0.00502	0.00509	0.00475	0.00508	0.00475	0.00499	XXX	0.00484	0.00501
0.00469	0.00509	0.00502	XXX	XXX	XXX	0.00476	XXX	0.00462	XXX	0.00502
0.00469	0.00509	0.00503	0.00510	0.00476	0.00509	0.00476	0.00500	0.00462	0.00485	0.00502

SRM 1831 4 64 8	SRM 1831 4 64 7	SRM 1831 4 64 6	SRM 1831 4 64 5	SRM 1831 4 64 4	SRM 1831 4 64 3	SRM 1831 4 64 2	SRM 1831 4 64 1	SRM 1831 4 32 30	SRM 1831 4 32 29	SRM 1831 4 32 28
XXX	0.00435	XXX	0.00429	XXX	XXX	0.00443	0.00405	XXX	XXX	XXX
XXX	XXX	XXX	0.00427	XXX	XXX	0.00442	XXX	XXX	XXX	XXX
XXX	XXX	XXX	0.00427	XXX	0.00418	0.00442	XXX	XXX	XXX	XXX
XXX	0.00430	XXX	0.00422	XXX	XXX	0.00437	0.00400	XXX	XXX	XXX
XXX	XXX	XXX	0.00423	XXX	0.00415	0.00438	XXX	XXX	XXX	XXX
0.00420	XXX	XXX	0.00425	XXX	XXX	0.00440	XXX	0.00506	XXX	XXX
XXX	0.00499	XXX	0.00494	XXX	XXX	0.00510	0.00469	XXX	XXX	XXX
0.00491	XXX	XXX	0.00495	XXX	0.00483	0.00511	XXX	XXX	XXX	XXX
XXX	XXX	XXX	0.00504	XXX	XXX	0.00520	XXX	0.00502	XXX	0.00484
XXX	0.00433	XXX	0.00425	XXX	0.00416	0.00440	0.00402	XXX	XXX	XXX
0.00491	XXX	XXX	0.00495	XXX	XXX	0.00511	XXX	0.00504	XXX	0.00486
XXX	XXX	0.00503	0.00494	0.00510	XXX	0.00509	XXX	XXX	0.00514	XXX
0.00418	0.00431	XXX	0.00423	XXX	0.00414	0.00438	0.00401	0.00507	XXX	XXX
XXX	XXX	0.00432	0.00420	0.00436	XXX	0.00436	XXX	XXX	0.00512	0.00490
0.00491	0.00499	XXX	0.00496	XXX	0.00484	0.00512	0.00471	0.00506	XXX	0.00488
0.00489	XXX	0.00503	0.00494	0.00510	XXX	0.00510	XXX	0.00507	0.00511	0.00488
0.00490	0.00498	0.00504	0.00495	0.00511	0.00483	0.00510	0.00469	0.00507	0.00511	0.00489

SRM 1831 4 64 19	SRM 1831 4 64 18	SRM 1831 4 64 17	SRM 1831 4 64 16	SRM 1831 4 64 15	SRM 1831 4 64 14	SRM 1831 4 64 13	SRM 1831 4 64 12	SRM 1831 4 64 11	SRM 1831 4 64 10	SRM 1831 4 64 9
XXX	XXX	XXX	0.00439	XXX	XXX	XXX	XXX	XXX	XXX	0.00445
XXX	XXX	XXX	0.00439	XXX	0.00426	XXX	XXX	XXX	XXX	0.00443
XXX	XXX	XXX	0.00438	XXX	XXX	XXX	XXX	XXX	0.00448	0.00443
XXX	XXX	XXX	0.00433	XXX	0.00421	XXX	XXX	XXX	XXX	0.00439
XXX	0.00435	XXX	0.00435	XXX	XXX	XXX	XXX	XXX	0.00444	0.00439
XXX	XXX	0.00436	0.00436	XXX	XXX	0.00436	XXX	XXX	XXX	0.00441
XXX	XXX	XXX	0.00502	XXX	0.00490	XXX	XXX	XXX	0.00516	0.00512
XXX	0.00500	0.00503	0.00503	XXX	XXX	0.00504	XXX	XXX	XXX	0.00513
XXX	XXX	XXX	0.00512	0.00518	XXX	XXX	0.00504	0.00472	XXX	0.00522
XXX	0.00436	XXX	0.00436	XXX	0.00424	XXX	XXX	XXX	0.00446	0.00441
XXX	XXX	0.00504	0.00503	0.00509	XXX	0.00505	XXX	0.00464	XXX	0.00513
0.00500	XXX	XXX	0.00501	XXX	XXX	XXX	0.00494	XXX	XXX	0.00511
XXX	0.00434	0.00435	0.00435	XXX	0.00422	0.00435	XXX	XXX	0.00445	0.00440
0.00430	XXX	XXX	0.00432	0.00433	XXX	XXX	0.00422	0.00393	XXX	0.00437
XXX	0.00501	0.00504	0.00503	0.00509	0.00491	0.00505	XXX	0.00465	0.00518	0.00514
0.00501	XXX	0.00502	0.00501	0.00508	XXX	0.00503	0.00495	0.00463	XXX	0.00512
0.00501	0.00500	0.00503	0.00502	0.00508	0.00490	0.00504	0.00495	0.00464	0.00517	0.00512

SRM 1831 4 64 30	SRM 1831 4 64 29	SRM 1831 4 64 28	SRM 1831 4 64 27	SRM 1831 4 64 26	SRM 1831 4 64 25	SRM 1831 4 64 24	SRM 1831 4 64 23	SRM 1831 4 64 22	SRM 1831 4 64 21	SRM 1831 4 64 20
XXX	XXX	XXX	XXX	XXX	XXX	XXX	XXX	XXX	0.00443	0.00436
XXX	XXX	XXX	XXX	XXX	XXX	XXX	0.00462	0.00463	0.00442	XXX
XXX	XXX	XXX	XXX	XXX	XXX	0.00424	XXX	XXX	0.00441	XXX
XXX	XXX	XXX	XXX	XXX	XXX	XXX	0.00458	XXX	0.00437	0.00431
XXX	XXX	XXX	XXX	XXX	XXX	0.00421	XXX	0.00459	0.00438	XXX
0.00453	XXX	XXX	0.00452	XXX	XXX	XXX	XXX	XXX	0.00439	XXX
XXX	XXX	XXX	XXX	XXX	XXX	XXX	0.00534	0.00529	0.00510	0.00501
XXX	XXX	XXX	0.00525	XXX	XXX	0.00494	XXX	XXX	0.00511	XXX
0.00536	XXX	0.00548	XXX	0.00534	0.00537	XXX	XXX	XXX	0.00520	XXX
XXX	XXX	XXX	XXX	XXX	XXX	0.00423	0.00461	0.00462	0.00440	0.00434
0.00526	XXX	0.00539	0.00526	0.00525	0.00528	XXX	XXX	XXX	0.00511	XXX
XXX	0.00496	XXX	XXX	XXX	XXX	XXX	XXX	XXX	0.00509	XXX
0.00452	XXX	XXX	0.00451	XXX	XXX	0.00421	0.00459	0.00460	0.00438	0.00432
XXX	0.00423	0.00465	XXX	0.00451	0.00450	XXX	XXX	XXX	0.00435	XXX
0.00527	XXX	0.00539	0.00526	0.00525	0.00528	0.00494	0.00535	0.00531	0.00511	0.00502
0.00525	0.00497	0.00537	0.00524	0.00523	0.00526	XXX	XXX	XXX	0.00509	XXX
0.00526	0.00497	0.00538	0.00525	0.00524	0.00527	0.00493	0.00534	0.00530	0.00510	0.00501

SRM 1831 4 128 11	SRM 1831 4 128 10	SRM 1831 4 128 9	SRM 1831 4 128 8	SRM 1831 4 128 7	SRM 1831 4 128 6	SRM 1831 4 128 5	SRM 1831 4 128 4	SRM 1831 4 128 3	SRM 1831 4 128 2	SRM 1831 4 128 1
XXX	XXX	0.00519	XXX	0.00522	XXX	0.00517	XXX	XXX	0.00509	0.00501
XXX	XXX	0.00511	XXX	XXX	XXX	0.00510	XXX	XXX	0.00503	XXX
XXX	0.00437	0.00437	XXX	XXX	XXX	0.00435	XXX	0.00418	0.00429	XXX
XXX	XXX	0.00516	XXX	0.00519	XXX	0.00515	XXX	XXX	0.00507	0.00500
XXX	0.00510	0.00510	XXX	XXX	XXX	0.00508	XXX	0.00490	0.00502	XXX
XXX	XXX	0.00514	0.00519	XXX	XXX	0.00512	XXX	XXX	0.00506	XXX
XXX	0.00517	0.00516	XXX	0.00518	XXX	0.00514	XXX	XXX	0.00507	0.00501
XXX	XXX	0.00512	0.00517	XXX	XXX	0.00510	XXX	0.00492	0.00504	XXX
0.01216	XXX	0.01211	XXX	XXX	XXX	0.01211	XXX	XXX	0.01204	XXX
XXX	0.00442	0.00441	XXX	0.00440	XXX	0.00440	XXX	0.00423	0.00433	0.00426
0.00440	XXX	0.00439	0.00442	XXX	XXX	0.00437	XXX	XXX	0.00431	XXX
XXX	XXX	0.00512	XXX	XXX	0.00510	0.00511	0.00493	XXX	0.00504	XXX
XXX	0.00513	0.00512	0.00517	0.00515	XXX	0.00510	XXX	0.00492	0.00504	0.00498
0.00441	XXX	0.00440	XXX	XXX	0.00437	0.00438	0.00424	XXX	0.00432	XXX
0.00514	0.00512	0.00511	0.00517	0.00514	XXX	0.00510	XXX	0.00492	0.00503	0.00498
0.00441	XXX	0.00440	0.00443	XXX	0.00437	0.00438	0.00424	XXX	0.00432	XXX
0.00440	0.00440	0.00439	0.00442	0.00438	0.00436	0.00437	0.00424	0.00421	0.00431	0.00424

SRM 1831 4 128 22	SRM 1831 4 128 21	SRM 1831 4 128 20	SRM 1831 4 128 19	SRM 1831 4 128 18	SRM 1831 4 128 17	SRM 1831 4 128 16	SRM 1831 4 128 15	SRM 1831 4 128 14	SRM 1831 4 128 13	SRM 1831 4 128 12
XXX	0.00520	0.00458	XXX	XXX	XXX	0.00513	XXX	XXX	XXX	XXX
0.00512	0.00512	XXX	XXX	XXX	XXX	0.00506	XXX	0.00506	XXX	XXX
XXX	0.00437	XXX	XXX	XXX	XXX	0.00433	XXX	XXX	XXX	XXX
XXX	0.00517	0.00456	XXX	XXX	XXX	0.00511	XXX	0.00510	XXX	XXX
0.00510	0.00510	XXX	XXX	0.00506	XXX	0.00505	XXX	XXX	XXX	XXX
XXX	0.00515	XXX	XXX	XXX	0.00506	0.00509	XXX	XXX	0.00454	XXX
0.00517	0.00516	0.00456	XXX	XXX	XXX	0.00510	XXX	0.00510	XXX	XXX
XXX	0.00513	XXX	XXX	0.00508	0.00504	0.00507	XXX	XXX	0.00453	XXX
XXX	0.01215	XXX	XXX	XXX	XXX	0.01204	0.01212	XXX	XXX	0.01149
0.00443	0.00441	0.00385	XXX	0.00435	XXX	0.00437	XXX	0.00435	XXX	XXX
XXX	0.00439	XXX	XXX	XXX	0.00431	0.00435	0.00433	XXX	0.00384	XXX
XXX	0.00513	XXX	0.00521	XXX	XXX	0.00507	XXX	XXX	XXX	0.00457
0.00513	0.00513	0.00453	XXX	0.00508	0.00504	0.00507	XXX	0.00507	0.00453	XXX
XXX	0.00439	XXX	0.00447	XXX	XXX	0.00436	0.00434	XXX	XXX	0.00387
0.00512	0.00512	0.00453	XXX	0.00508	0.00504	0.00506	0.00507	0.00506	0.00452	XXX
XXX	0.00439	XXX	0.00447	XXX	0.00432	0.00436	0.00434	XXX	0.00384	0.00387
0.00440	0.00439	0.00383	0.00446	0.00433	0.00432	0.00435	0.00433	0.00433	0.00384	0.00387

SRM 1831 4 256 3	SRM 1831 4 256 2	SRM 1831 4 256 1	SRM 1831 4 128 30	SRM 1831 4 128 29	SRM 1831 4 128 28	SRM 1831 4 128 27	SRM 1831 4 128 26	SRM 1831 4 128 25	SRM 1831 4 128 24	SRM 1831 4 128 23
XXX	0.00311	0.00305	XXX	XXX	XXX	XXX	XXX	XXX	XXX	XXX
XXX	0.00328	XXX	XXX	XXX	XXX	XXX	XXX	XXX	XXX	0.00511
0.00251	0.00255	XXX	XXX	XXX	XXX	XXX	XXX	XXX	0.00424	XXX
XXX	0.00313	0.00294	XXX	XXX	XXX	XXX	XXX	XXX	XXX	0.00517
0.00317	0.00311	XXX	XXX	XXX	XXX	XXX	XXX	XXX	0.00496	XXX
XXX	0.00314	XXX	0.00517	XXX	XXX	0.00515	XXX	XXX	XXX	XXX
XXX	0.00255	0.00233	XXX	XXX	XXX	XXX	XXX	XXX	XXX	0.00516
0.00259	0.00257	XXX	XXX	XXX	XXX	0.00513	XXX	XXX	0.00498	XXX
XXX	0.00272	XXX	0.01212	XXX	0.01200	XXX	0.01209	0.01187	XXX	XXX
0.00314	0.00313	0.00291	XXX	XXX	XXX	XXX	XXX	XXX	0.00430	0.00444
XXX	0.00323	XXX	0.00443	XXX	0.00438	0.00439	0.00439	0.00423	XXX	XXX
XXX	0.00310	XXX	XXX	0.00512	XXX	XXX	XXX	XXX	XXX	XXX
0.00314	0.00311	0.00288	0.00515	XXX	XXX	0.00513	XXX	XXX	0.00499	0.00512
XXX	0.00256	XXX	XXX	0.00442	0.00439	XXX	0.00439	0.00424	XXX	XXX
0.00322	0.00315	0.00289	0.00515	XXX	0.00507	0.00513	0.00510	0.00493	0.00498	0.00512
XXX	0.00258	XXX	0.00444	0.00442	0.00439	0.00440	0.00439	0.00424	XXX	XXX
0.00314	0.00310	0.00287	0.00444	0.00441	0.00438	0.00439	0.00439	0.00423	0.00428	0.00442

SRM 1831 4 256 14	SRM 1831 4 256 13	SRM 1831 4 256 12	SRM 1831 4 256 11	SRM 1831 4 256 10	SRM 1831 4 256 9	SRM 1831 4 256 8	SRM 1831 4 256 7	SRM 1831 4 256 6	SRM 1831 4 256 5	SRM 1831 4 256 4
XXX	XXX	XXX	XXX	XXX	0.00448	XXX	0.00271	XXX	0.00315	XXX
0.00319	XXX	XXX	XXX	XXX	0.00333	XXX	XXX	XXX	0.00283	XXX
XXX	XXX	XXX	XXX	0.00304	0.00344	XXX	XXX	XXX	0.00242	XXX
0.00366	XXX	XXX	XXX	XXX	0.00396	XXX	0.00289	XXX	0.00297	XXX
XXX	XXX	XXX	XXX	0.00338	0.00365	XXX	XXX	XXX	0.00284	XXX
XXX	0.00328	XXX	XXX	XXX	0.00369	0.00329	XXX	XXX	0.00288	XXX
0.00294	XXX	XXX	XXX	0.00289	0.00322	XXX	0.00243	XXX	0.00234	XXX
XXX	0.00278	XXX	XXX	XXX	0.00327	0.00267	XXX	XXX	0.00237	XXX
XXX	XXX	0.00231	0.00268	XXX	0.00288	XXX	XXX	XXX	0.00232	XXX
0.00355	XXX	XXX	XXX	0.00351	0.00383	XXX	0.00294	XXX	0.00292	XXX
XXX	0.00324	XXX	0.00331	XXX	0.00358	0.00345	XXX	XXX	0.00289	XXX
XXX	XXX	0.00297	XXX	XXX	0.00400	XXX	XXX	0.00302	0.00296	0.00289
0.00349	0.00332	XXX	XXX	0.00345	0.00376	0.00322	0.00294	XXX	0.00289	XXX
XXX	XXX	0.00230	0.00272	XXX	0.00314	XXX	XXX	0.00261	0.00232	0.00241
0.00342	0.00326	XXX	0.00330	0.00340	0.00366	0.00331	0.00302	XXX	0.00287	XXX
XXX	0.00269	0.00231	0.00273	XXX	0.00314	0.00273	XXX	0.00263	0.00232	0.00243
0.00347	0.00330	0.00288	0.00331	0.00343	0.00374	0.00322	0.00294	0.00311	0.00287	0.00293

SRM 1831 4 256 25	SRM 1831 4 256 24	SRM 1831 4 256 23	SRM 1831 4 256 22	SRM 1831 4 256 21	SRM 1831 4 256 20	SRM 1831 4 256 19	SRM 1831 4 256 18	SRM 1831 4 256 17	SRM 1831 4 256 16	SRM 1831 4 256 15
XXX	XXX	XXX	XXX	0.00535	0.00477	XXX	XXX	XXX	0.00450	XXX
XXX	XXX	0.00395	0.00342	0.00404	XXX	XXX	XXX	XXX	0.00344	XXX
XXX	0.00441	XXX	XXX	0.00422	XXX	XXX	XXX	XXX	0.00347	XXX
XXX	XXX	0.00471	XXX	0.00477	0.00423	XXX	XXX	XXX	0.00402	XXX
XXX	0.00456	XXX	0.00369	0.00442	XXX	XXX	0.00403	XXX	0.00373	XXX
XXX	XXX	XXX	XXX	0.00446	XXX	XXX	XXX	0.00418	0.00377	XXX
XXX	XXX	0.00389	0.00322	0.00397	0.00343	XXX	XXX	XXX	0.00326	XXX
XXX	0.00419	XXX	XXX	0.00402	XXX	XXX	0.00364	0.00374	0.00331	XXX
0.00365	XXX	XXX	XXX	0.00357	XXX	XXX	XXX	XXX	0.00295	0.00349
XXX	0.00479	0.00456	0.00386	0.00462	0.00409	XXX	0.00422	XXX	0.00390	XXX
0.00446	XXX	XXX	XXX	0.00433	XXX	XXX	XXX	0.00407	0.00367	0.00427
XXX	XXX	XXX	XXX	0.00481	XXX	0.00432	XXX	XXX	0.00405	XXX
XXX	0.00470	0.00447	0.00379	0.00454	0.00402	XXX	0.00415	0.00426	0.00383	XXX
0.00399	XXX	XXX	XXX	0.00388	XXX	0.00346	XXX	XXX	0.00319	0.00383
0.00457	0.00457	0.00435	0.00370	0.00443	0.00391	XXX	0.00404	0.00415	0.00374	0.00438
0.00399	XXX	XXX	XXX	0.00388	XXX	0.00345	XXX	0.00361	0.00319	0.00382
0.00467	0.00468	0.00445	0.00377	0.00452	0.00399	0.00406	0.00412	0.00423	0.00381	0.00448

SRM 1831 4 256 30	SRM 1831 4 256 29	SRM 1831 4 256 28	SRM 1831 4 256 27	SRM 1831 4 256 26
XXX	XXX	XXX	XXX	XXX
XXX	XXX	XXX	XXX	XXX
XXX	XXX	XXX	XXX	XXX
XXX	XXX	XXX	XXX	XXX
XXX	XXX	XXX	XXX	XXX
0.00472	XXX	XXX	0.00432	XXX
XXX	XXX	XXX	XXX	XXX
XXX	XXX	XXX	0.00387	XXX
0.00378	XXX	0.00351	XXX	0.00271
XXX	XXX	XXX	XXX	XXX
0.00458	XXX	0.00432	0.00418	0.00339
XXX	0.00500	XXX	XXX	XXX
0.00480	XXX	XXX	0.00440	XXX
XXX	0.00403	0.00386	XXX	0.00287
0.00469	XXX	0.00443	0.00428	0.00343
0.00411	0.00402	0.00386	0.00372	0.00287
0.00478	0.00469	0.00453	0.00437	0.00347

Table 132: Mid-IR spectral library results for 'real world' window, correlation search algorithm.

	3A	3B	3C	5A	5B	5C	7A	7B	7C	10A	10B	10C	15A	15B	20A	20B	30A
Window 4 8 1	0.00018	XXX	XXX	0.00022	XXX	XXX	0.00021	XXX	XXX	0.00021	XXX	XXX	0.00094	XXX	0.00021	XXX	0.00021
Window 4 8 2	0.00021	0.00021	0.00024	0.00022	0.00080	0.00021	0.00021	0.00022	0.00022	0.00021	0.00024	0.00079	0.00079	0.00079	0.00021	0.00021	0.00021
Window 4 8 3	XXX	XXX	0.00021	XXX	0.00100	XXX	XXX	0.00021	XXX	0.00019	XXX	XXX	0.00098	XXX	0.00019	XXX	0.00019
Window 4 8 4	XXX	XXX	XXX	XXX	XXX	XXX	XXX	XXX	XXX	XXX	XXX	0.00089	XXX	0.00089	XXX	0.00019	0.00018
Window 4 8 5	0.00018	0.00019	0.00022	0.00019	0.00087	0.00018	0.00018	0.00019	0.00017	0.00017	0.00019	0.00087	0.00086	0.00086	0.00017	0.00018	0.00017

Window 4 8 17	Window 4 8 16	Window 4 8 15	Window 4 8 14	Window 4 8 13	Window 4 8 12	Window 4 8 11	Window 4 8 10	Window 4 8 9	Window 4 8 8	Window 4 8 7	Window 4 8 6
XXX	0.00025	XXX	XXX	XXX	XXX	XXX	XXX	0.00020	XXX	0.00018	XXX
XXX	0.00022	XXX	0.00020	XXX	XXX	XXX	XXX	0.00021	XXX	XXX	XXX
XXX	0.00026	XXX	XXX	XXX	XXX	XXX	0.00021	0.00024	XXX	XXX	XXX
XXX	0.00025	XXX	0.00022	XXX	XXX	XXX	XXX	0.00022	XXX	0.00020	XXX
XXX	0.00071	XXX	XXX	XXX	XXX	XXX	0.00082	0.00094	XXX	XXX	XXX
0.00019	0.00020	XXX	XXX	0.00021	XXX	XXX	XXX	0.00022	0.00018	XXX	XXX
XXX	0.00023	XXX	0.00020	XXX	XXX	XXX	0.00019	0.00021	XXX	0.00019	XXX
0.00019	0.00021	XXX	XXX	0.00022	XXX	XXX	XXX	0.00022	0.00019	XXX	XXX
XXX	0.00020	0.00017	XXX	XXX	0.00020	0.00019	XXX	0.00022	XXX	XXX	XXX
XXX	0.00022	XXX	0.00020	XXX	XXX	XXX	0.00019	0.00020	XXX	0.00019	XXX
0.00020	0.00021	0.00019	XXX	0.00022	XXX	0.00020	XXX	0.00023	0.00019	XXX	XXX
XXX	0.00072	XXX	XXX	XXX	0.00082	XXX	XXX	0.00093	XXX	XXX	0.00101
0.00078	0.00070	XXX	0.00083	0.00078	XXX	XXX	0.00081	0.00092	0.00087	0.00089	XXX
XXX	0.00071	0.00083	XXX	XXX	0.00081	0.00088	XXX	0.00092	XXX	XXX	0.00100
0.00019	0.00021	0.00018	0.00019	0.00021	XXX	0.00019	0.00019	0.00021	0.00018	0.00019	XXX
0.00019	0.00021	0.00019	XXX	0.00021	0.00020	0.00019	XXX	0.00021	0.00018	XXX	0.00022
0.00019	0.00021	0.00019	0.00020	0.00021	0.00019	0.00019	0.00019	0.00020	0.00018	0.00019	0.00022

Window 4 8 29	Window 4 8 28	Window 4 8 27	Window 4 8 26	Window 4 8 25	Window 4 8 24	Window 4 8 23	Window 4 8 22	Window 4 8 21	Window 4 8 20	Window 4 8 19	Window 4 8 18
XXX	XXX	XXX	XXX	XXX	XXX	XXX	XXX	0.00018	0.00018	XXX	XXX
XXX	XXX	XXX	XXX	XXX	XXX	0.00018	0.00019	0.00017	XXX	XXX	XXX
XXX	XXX	XXX	XXX	XXX	0.00022	XXX	XXX	0.00022	XXX	XXX	XXX
XXX	XXX	XXX	XXX	XXX	XXX	0.00019	XXX	0.00019	0.00020	XXX	XXX
XXX	XXX	XXX	XXX	XXX	0.00071	XXX	0.00077	0.00085	XXX	XXX	0.00071
XXX	XXX	0.00019	XXX	XXX	XXX	XXX	XXX	0.00018	XXX	XXX	XXX
XXX	XXX	XXX	XXX	XXX	XXX	0.00018	0.00020	0.00017	0.00018	XXX	XXX
XXX	XXX	0.00020	XXX	XXX	0.00019	XXX	XXX	0.00019	XXX	XXX	0.00021
XXX	0.00017	XXX	0.00017	0.00020	XXX	XXX	XXX	0.00017	XXX	XXX	XXX
XXX	XXX	XXX	XXX	XXX	0.00020	0.00017	0.00020	0.00017	0.00019	XXX	0.00021
XXX	0.00019	0.00020	0.00019	0.00023	XXX	XXX	XXX	0.00019	XXX	XXX	XXX
0.00084	XXX	XXX	XXX	XXX	XXX	XXX	XXX	0.00085	XXX	0.00086	XXX
XXX	XXX	0.00076	XXX	XXX	0.00070	0.00091	0.00077	0.00084	0.00083	XXX	0.00071
0.00083	0.00073	XXX	0.00086	0.00064	XXX	XXX	XXX	0.00083	XXX	0.00084	XXX
XXX	0.00018	0.00019	0.00018	0.00021	0.00019	0.00017	0.00020	0.00017	0.00018	XXX	0.00020
0.00017	0.00019	0.00021	0.00018	0.00022	XXX	XXX	XXX	0.00017	XXX	0.00016	XXX
0.00017	0.00019	0.00020	0.00018	0.00022	0.00020	0.00017	0.00020	0.00016	0.00018	0.00016	0.00020

Window 4 16 11	Window 4 16 10	Window 4 16 9	Window 4 16 8	Window 4 16 7	Window 4 16 6	Window 4 16 5	Window 4 16 4	Window 4 16 3	Window 4 16 2	Window 4 16 1	Window 4 8 30
XXX	XXX	0.00065	XXX	0.00068	XXX	0.00073	XXX	XXX	0.00068	0.00064	XXX
XXX	XXX	0.00019	XXX	XXX	XXX	0.00019	XXX	XXX	0.00018	XXX	XXX
XXX	0.00068	0.00068	XXX	XXX	XXX	0.00075	XXX	0.00071	0.00070	XXX	XXX
XXX	XXX	0.00066	XXX	0.00069	XXX	0.00074	XXX	XXX	0.00069	0.00066	XXX
XXX	0.00068	0.00067	XXX	XXX	XXX	0.00075	XXX	0.00071	0.00070	XXX	XXX
XXX	XXX	0.00067	0.00067	XXX	XXX	0.00076	XXX	XXX	0.00070	XXX	0.00019
XXX	0.00019	0.00019	XXX	0.00018	XXX	0.00018	XXX	XXX	0.00018	0.00021	XXX
XXX	XXX	0.00019	0.00020	XXX	XXX	0.00018	XXX	0.00018	0.00018	XXX	XXX
0.00069	XXX	0.00063	XXX	XXX	XXX	0.00071	XXX	XXX	0.00066	XXX	0.00018
XXX	0.00068	0.00066	XXX	0.00070	XXX	0.00075	XXX	0.00071	0.00070	0.00066	XXX
0.00074	XXX	0.00067	0.00067	XXX	XXX	0.00076	XXX	XXX	0.00070	XXX	0.00021
XXX	XXX	0.00020	XXX	XXX	0.00018	0.00019	0.00021	XXX	0.00018	XXX	XXX
XXX	0.00020	0.00020	0.00021	0.00019	XXX	0.00019	XXX	0.00019	0.00018	0.00022	0.00071
0.00073	XXX	0.00066	XXX	XXX	0.00072	0.00075	0.00068	XXX	0.00069	XXX	XXX
0.00074	0.00069	0.00067	0.00067	0.00071	XXX	0.00075	XXX	0.00071	0.00070	0.00067	0.00020
0.00018	XXX	0.00020	0.00020	XXX	0.00018	0.00019	0.00021	XXX	0.00018	XXX	0.00019
0.00073	0.00069	0.00066	0.00067	0.00070	0.00072	0.00075	0.00069	0.00071	0.00069	0.00067	0.00020

Window 4 16 23	Window 4 16 22	Window 4 16 21	Window 4 16 20	Window 4 16 19	Window 4 16 18	Window 4 16 17	Window 4 16 16	Window 4 16 15	Window 4 16 14	Window 4 16 13	Window 4 16 12
XXX	XXX	0.00063	0.00066	XXX	XXX	XXX	0.00062	XXX	XXX	XXX	XXX
0.00020	0.00017	0.00020	XXX	XXX	XXX	XXX	0.00020	XXX	0.00019	XXX	XXX
XXX	XXX	0.00065	XXX	XXX	XXX	XXX	0.00063	XXX	XXX	XXX	XXX
0.00066	XXX	0.00064	0.00067	XXX	XXX	XXX	0.00062	XXX	0.00067	XXX	XXX
XXX	0.00072	0.00065	XXX	XXX	0.00065	XXX	0.00063	XXX	XXX	XXX	XXX
XXX	XXX	0.00066	XXX	XXX	XXX	0.00069	0.00063	XXX	XXX	0.00064	XXX
0.00020	0.00017	0.00020	0.00019	XXX	XXX	XXX	0.00020	XXX	0.00019	XXX	XXX
XXX	XXX	0.00020	XXX	XXX	0.00019	0.00018	0.00019	XXX	XXX	0.00022	XXX
XXX	XXX	0.00061	XXX	XXX	XXX	XXX	0.00059	0.00067	XXX	XXX	0.00064
0.00066	0.00071	0.00064	0.00067	XXX	0.00065	XXX	0.00063	XXX	0.00067	XXX	XXX
XXX	XXX	0.00065	XXX	XXX	XXX	0.00069	0.00063	0.00071	XXX	0.00064	XXX
XXX	XXX	0.00021	XXX	0.00019	XXX	XXX	0.00020	XXX	XXX	XXX	0.00022
0.00021	0.00017	0.00020	0.00020	XXX	0.00020	0.00019	0.00020	XXX	0.00020	0.00023	XXX
XXX	XXX	0.00065	XXX	0.00077	XXX	XXX	0.00062	0.00070	XXX	XXX	0.00068
0.00067	0.00072	0.00065	0.00068	XXX	0.00065	0.00069	0.00063	0.00071	0.00068	0.00064	XXX
XXX	XXX	0.00020	XXX	0.00019	XXX	0.00019	0.00020	0.00019	XXX	0.00023	0.00021
0.00066	0.00072	0.00065	0.00067	0.00077	0.00065	0.00069	0.00063	0.00071	0.00067	0.00064	0.00068

Window 4 32 5	Window 4 32 4	Window 4 32 3	Window 4 32 2	Window 4 32 1	Window 4 16 30	Window 4 16 29	Window 4 16 28	Window 4 16 27	Window 4 16 26	Window 4 16 25	Window 4 16 24
0.00069	XXX	XXX	0.00070	0.00063	XXX	XXX	XXX	XXX	XXX	XXX	XXX
0.00020	XXX	XXX	0.00019	XXX	XXX	XXX	XXX	XXX	XXX	XXX	XXX
0.00018	XXX	0.00018	0.00017	XXX	XXX	XXX	XXX	XXX	XXX	XXX	0.00061
0.00018	XXX	XXX	0.00017	0.00019	XXX	XXX	XXX	XXX	XXX	XXX	XXX
0.00019	XXX	0.00019	0.00018	XXX	XXX	XXX	XXX	XXX	XXX	XXX	0.00061
0.00018	XXX	XXX	0.00017	XXX	0.00068	XXX	XXX	0.00069	XXX	XXX	XXX
0.00018	XXX	XXX	0.00018	0.00019	XXX	XXX	XXX	XXX	XXX	XXX	XXX
0.00018	XXX	0.00018	0.00017	XXX	XXX	XXX	XXX	0.00018	XXX	XXX	0.00019
0.00018	XXX	XXX	0.00017	XXX	0.00064	XXX	0.00065	XXX	0.00063	0.00068	XXX
0.00018	XXX	0.00019	0.00018	0.00019	XXX	XXX	XXX	XXX	XXX	XXX	0.00061
0.00019	XXX	XXX	0.00018	XXX	0.00068	XXX	0.00070	0.00069	0.00068	0.00072	XXX
0.00018	0.00017	XXX	0.00017	XXX	XXX	0.00020	XXX	XXX	XXX	XXX	XXX
0.00018	XXX	0.00019	0.00017	0.00019	0.00020	XXX	XXX	0.00019	XXX	XXX	0.00020
0.00018	0.00018	XXX	0.00018	XXX	XXX	0.00066	0.00069	XXX	0.00067	0.00072	XXX
0.00019	XXX	0.00019	0.00018	0.00020	0.00068	XXX	0.00069	0.00069	0.00067	0.00072	0.00062
0.00018	0.00018	XXX	0.00018	XXX	0.00019	0.00020	0.00020	0.00019	0.00018	0.00018	XXX
0.00019	0.00018	0.00019	0.00018	0.00020	0.00068	0.00066	0.00069	0.00069	0.00067	0.00072	0.00061

Window 4 32 17	Window 4 32 16	Window 4 32 15	Window 4 32 14	Window 4 32 13	Window 4 32 12	Window 4 32 11	Window 4 32 10	Window 4 32 9	Window 4 32 8	Window 4 32 7	Window 4 32 6
XXX	0.00062	XXX	XXX	XXX	XXX	XXX	XXX	0.00069	XXX	0.00066	XXX
XXX	0.00021	XXX	0.00020	XXX	XXX	XXX	XXX	0.00020	XXX	XXX	XXX
XXX	0.00019	XXX	XXX	XXX	XXX	XXX	0.00018	0.00018	XXX	XXX	XXX
XXX	0.00019	XXX	0.00018	XXX	XXX	XXX	XXX	0.00018	XXX	0.00019	XXX
XXX	0.00020	XXX	XXX	XXX	XXX	XXX	0.00019	0.00019	XXX	XXX	XXX
0.00019	0.00019	XXX	XXX	0.00018	XXX	XXX	XXX	0.00018	0.00019	XXX	XXX
XXX	0.00020	XXX	0.00018	XXX	XXX	XXX	0.00019	0.00018	XXX	0.00019	XXX
0.00019	0.00019	XXX	XXX	0.00018	XXX	XXX	XXX	0.00018	0.00019	XXX	XXX
XXX	0.00019	0.00018	XXX	XXX	0.00017	0.00018	XXX	0.00017	XXX	XXX	XXX
XXX	0.00020	XXX	0.00018	XXX	XXX	XXX	0.00019	0.00019	XXX	0.00020	XXX
0.00020	0.00020	0.00020	XXX	0.00019	XXX	0.00020	XXX	0.00019	0.00020	XXX	XXX
XXX	0.00019	XXX	XXX	XXX	0.00017	XXX	XXX	0.00018	XXX	XXX	0.00018
0.00019	0.00020	XXX	0.00018	0.00018	XXX	XXX	0.00019	0.00018	0.00019	0.00019	XXX
XXX	0.00020	0.00020	XXX	XXX	0.00018	0.00019	XXX	0.00018	XXX	XXX	0.00019
0.00020	0.00020	0.00020	0.00019	0.00019	XXX	0.00019	0.00020	0.00019	0.00020	0.00020	XXX
0.00020	0.00020	0.00020	XXX	0.00019	0.00018	0.00019	XXX	0.00018	0.00020	XXX	0.00019
0.00020	0.00020	0.00020	0.00019	0.00019	0.00018	0.00019	0.00019	0.00019	0.00020	0.00020	0.00019

Window 4 32 29	Window 4 32 28	Window 4 32 27	Window 4 32 26	Window 4 32 25	Window 4 32 24	Window 4 32 23	Window 4 32 22	Window 4 32 21	Window 4 32 20	Window 4 32 19	Window 4 32 18
XXX	XXX	XXX	XXX	XXX	XXX	XXX	XXX	0.00070	0.00066	XXX	XXX
XXX	XXX	XXX	XXX	XXX	XXX	0.00020	0.00019	0.00019	XXX	XXX	XXX
XXX	XXX	XXX	XXX	XXX	0.00018	XXX	XXX	0.00017	XXX	XXX	XXX
XXX	XXX	XXX	XXX	XXX	XXX	0.00018	XXX	0.00017	0.00018	XXX	XXX
XXX	XXX	XXX	XXX	XXX	0.00019	XXX	0.00018	0.00018	XXX	XXX	0.00018
XXX	XXX	0.00018	XXX	XXX	XXX	XXX	XXX	0.00017	XXX	XXX	XXX
XXX	XXX	XXX	XXX	XXX	XXX	0.00019	0.00018	0.00017	0.00018	XXX	XXX
XXX	XXX	0.00018	XXX	XXX	0.00018	XXX	XXX	0.00017	XXX	XXX	0.00018
XXX	0.00018	XXX	0.00017	0.00018	XXX	XXX	XXX	0.00017	XXX	XXX	XXX
XXX	XXX	XXX	XXX	XXX	0.00019	0.00019	0.00018	0.00018	0.00018	XXX	0.00018
XXX	0.00020	0.00019	0.00020	0.00020	XXX	XXX	XXX	0.00018	XXX	XXX	XXX
0.00021	XXX	XXX	XXX	XXX	XXX	XXX	XXX	0.00017	XXX	0.00018	XXX
XXX	XXX	0.00018	XXX	XXX	0.00019	0.00019	0.00018	0.00017	0.00018	XXX	0.00018
0.00022	0.00020	XXX	0.00019	0.00020	XXX	XXX	XXX	0.00018	XXX	0.00019	XXX
XXX	0.00020	0.00019	0.00020	0.00020	0.00020	0.00019	0.00019	0.00018	0.00019	XXX	0.00019
0.00022	0.00020	0.00019	0.00019	0.00020	XXX	XXX	XXX	0.00018	XXX	0.00019	XXX
0.00022	0.00020	0.00019	0.00019	0.00020	0.00019	0.00019	0.00019	0.00018	0.00019	0.00019	0.00018

Window 4 64 11	Window 4 64 10	Window 4 64 9	Window 4 64 8	Window 4 64 7	Window 4 64 6	Window 4 64 5	Window 4 64 4	Window 4 64 3	Window 4 64 2	Window 4 64 1	Window 4 32 30
XXX	XXX	0.00018	XXX	0.00019	XXX	0.00018	XXX	XXX	0.00018	0.00018	XXX
XXX	XXX	0.00018	XXX	XXX	XXX	0.00018	XXX	XXX	0.00018	XXX	XXX
XXX	0.00018	0.00018	XXX	XXX	XXX	0.00019	XXX	0.00018	0.00019	XXX	XXX
XXX	XXX	0.00018	XXX	0.00020	XXX	0.00019	XXX	XXX	0.00018	0.00018	XXX
XXX	0.00018	0.00018	XXX	XXX	XXX	0.00019	XXX	0.00018	0.00019	XXX	XXX
XXX	XXX	0.00019	0.00019	XXX	XXX	0.00020	XXX	XXX	0.00020	XXX	0.00019
XXX	0.00019	0.00018	XXX	0.00020	XXX	0.00019	XXX	XXX	0.00019	0.00019	XXX
XXX	XXX	0.00019	0.00018	XXX	XXX	0.00019	XXX	0.00018	0.00019	XXX	XXX
0.00018	XXX	0.00019	XXX	XXX	XXX	0.00019	XXX	XXX	0.00019	XXX	0.00018
XXX	0.00018	0.00018	XXX	0.00020	XXX	0.00019	XXX	0.00018	0.00018	0.00018	XXX
0.00086	XXX	0.00080	0.00081	XXX	XXX	0.00079	XXX	XXX	0.00081	XXX	0.00020
XXX	XXX	0.00080	XXX	XXX	0.00080	0.00078	0.00077	XXX	0.00080	XXX	XXX
XXX	0.00019	0.00018	0.00018	0.00020	XXX	0.00019	XXX	0.00018	0.00019	0.00019	0.00019
0.00018	XXX	0.00018	XXX	XXX	0.00018	0.00019	0.00019	XXX	0.00019	XXX	XXX
0.00018	0.00019	0.00019	0.00018	0.00020	XXX	0.00019	XXX	0.00018	0.00019	0.00019	0.00020
0.00018	XXX	0.00019	0.00018	XXX	0.00019	0.00019	0.00019	XXX	0.00019	XXX	0.00019
0.00072	0.00067	0.00068	0.00069	0.00065	0.00068	0.00067	0.00066	0.00068	0.00068	0.00069	0.00019

Window 4 64 23	Window 4 64 22	Window 4 64 21	Window 4 64 20	Window 4 64 19	Window 4 64 18	Window 4 64 17	Window 4 64 16	Window 4 64 15	Window 4 64 14	Window 4 64 13	Window 4 64 12
XXX	XXX	0.00019	0.00018	XXX	XXX	XXX	0.00019	XXX	XXX	XXX	XXX
0.00018	0.00019	0.00018	XXX	XXX	XXX	XXX	0.00018	XXX	0.00018	XXX	XXX
XXX	XXX	0.00019	XXX	XXX	XXX	XXX	0.00019	XXX	XXX	XXX	XXX
0.00018	XXX	0.00019	0.00018	XXX	XXX	XXX	0.00019	XXX	0.00019	XXX	XXX
XXX	0.00019	0.00019	XXX	XXX	0.00019	XXX	0.00019	XXX	XXX	XXX	XXX
XXX	XXX	0.00020	XXX	XXX	XXX	0.00020	0.00020	XXX	XXX	0.00020	XXX
0.00019	0.00020	0.00019	0.00019	XXX	XXX	XXX	0.00019	XXX	0.00019	XXX	XXX
XXX	XXX	0.00019	XXX	XXX	0.00019	0.00020	0.00019	XXX	XXX	0.00019	XXX
XXX	XXX	0.00020	XXX	XXX	XXX	XXX	0.00020	0.00019	XXX	XXX	0.00020
0.00018	0.00019	0.00019	0.00018	XXX	0.00019	XXX	0.00019	XXX	0.00019	XXX	XXX
XXX	XXX	0.00078	XXX	XXX	XXX	0.00079	0.00080	0.00083	XXX	0.00077	XXX
XXX	XXX	0.00077	XXX	0.00075	XXX	XXX	0.00079	XXX	XXX	XXX	0.00077
0.00019	0.00020	0.00019	0.00019	XXX	0.00019	0.00019	0.00019	XXX	0.00019	0.00019	XXX
XXX	XXX	0.00019	XXX	0.00020	XXX	XXX	0.00019	0.00018	XXX	XXX	0.00020
0.00019	0.00020	0.00019	0.00019	XXX	0.00019	0.00020	0.00019	0.00018	0.00020	0.00019	XXX
XXX	XXX	0.00019	XXX	0.00020	XXX	0.00020	0.00019	0.00019	XXX	0.00019	0.00020
0.00068	0.00062	0.00065	0.00069	0.00064	0.00070	0.00067	0.00067	0.00070	0.00067	0.00065	0.00066

Window 4 128 5	Window 4 128 4	Window 4 128 3	Window 4 128 2	Window 4 128 1	Window 4 64 30	Window 4 64 29	Window 4 64 28	Window 4 64 27	Window 4 64 26	Window 4 64 25	Window 4 64 24
0.00018	XXX	XXX	0.00018	0.00019	XXX	XXX	XXX	XXX	XXX	XXX	XXX
0.00018	XXX	XXX	0.00017	XXX	XXX	XXX	XXX	XXX	XXX	XXX	XXX
0.00019	XXX	0.00018	0.00018	XXX	XXX	XXX	XXX	XXX	XXX	XXX	0.00019
0.00018	XXX	XXX	0.00018	0.00019	XXX	XXX	XXX	XXX	XXX	XXX	XXX
0.00018	XXX	0.00018	0.00018	XXX	XXX	XXX	XXX	XXX	XXX	XXX	0.00019
0.00017	XXX	XXX	0.00017	XXX	0.00021	XXX	XXX	0.00020	XXX	XXX	XXX
0.00018	XXX	XXX	0.00018	0.00019	XXX	XXX	XXX	XXX	XXX	XXX	XXX
0.00019	XXX	0.00018	0.00018	XXX	XXX	XXX	XXX	0.00020	XXX	XXX	0.00020
0.00017	XXX	XXX	0.00016	XXX	0.00020	XXX	0.00020	XXX	0.00021	0.00019	XXX
0.00018	XXX	0.00018	0.00018	0.00019	XXX	XXX	XXX	XXX	XXX	XXX	0.00019
0.00017	XXX	XXX	0.00016	XXX	0.00081	XXX	0.00083	0.00081	0.00077	0.00078	XXX
0.00019	0.00019	XXX	0.00018	XXX	XXX	0.00084	XXX	XXX	XXX	XXX	XXX
0.00019	XXX	0.00018	0.00018	0.00019	0.00020	XXX	XXX	0.00019	XXX	XXX	0.00019
0.00018	0.00018	XXX	0.00017	XXX	XXX	0.00020	0.00020	XXX	0.00020	0.00019	XXX
0.00018	XXX	0.00018	0.00018	0.00019	0.00020	XXX	0.00020	0.00019	0.00020	0.00019	0.00019
0.00018	0.00018	XXX	0.00017	XXX	0.00021	0.00020	0.00020	0.00019	0.00021	0.00019	XXX
0.00070	0.00068	0.00070	0.00070	0.00067	0.00069	0.00072	0.00070	0.00069	0.00065	0.00066	0.00065

Window 4 128 17	Window 4 128 16	Window 4 128 15	Window 4 128 14	Window 4 128 13	Window 4 128 12	Window 4 128 11	Window 4 128 10	Window 4 128 9	Window 4 128 8	Window 4 128 7	Window 4 128 6
XXX	0.00020	XXX	XXX	XXX	XXX	XXX	XXX	0.00019	XXX	0.00018	XXX
XXX	0.00019	XXX	0.00019	XXX	XXX	XXX	XXX	0.00018	XXX	XXX	XXX
XXX	0.00020	XXX	XXX	XXX	XXX	XXX	0.00019	0.00020	XXX	XXX	XXX
XXX	0.00020	XXX	0.00019	XXX	XXX	XXX	XXX	0.00019	XXX	0.00019	XXX
XXX	0.00020	XXX	XXX	XXX	XXX	XXX	0.00019	0.00019	XXX	XXX	XXX
0.00018	0.00018	XXX	XXX	0.00017	XXX	XXX	XXX	0.00018	0.00018	XXX	XXX
XXX	0.00020	XXX	0.00019	XXX	XXX	XXX	0.00019	0.00019	XXX	0.00019	XXX
0.00019	0.00020	XXX	XXX	0.00018	XXX	XXX	XXX	0.00019	0.00019	XXX	XXX
XXX	0.00017	0.00017	XXX	XXX	0.00016	0.00016	XXX	0.00017	XXX	XXX	XXX
XXX	0.00020	XXX	0.00020	XXX	XXX	XXX	0.00019	0.00019	XXX	0.00019	XXX
0.00018	0.00018	0.00018	XXX	0.00017	XXX	0.00017	XXX	0.00018	0.00017	XXX	XXX
XXX	0.00020	XXX	XXX	XXX	0.00019	XXX	XXX	0.00019	XXX	XXX	0.00019
0.00020	0.00020	XXX	0.00020	0.00018	XXX	XXX	0.00019	0.00019	0.00019	0.00019	XXX
XXX	0.00019	0.00019	XXX	XXX	0.00018	0.00018	XXX	0.00019	XXX	XXX	0.00018
0.00019	0.00019	0.00020	0.00019	0.00018	XXX	0.00018	0.00019	0.00019	0.00019	0.00019	XXX
0.00019	0.00019	0.00019	XXX	0.00018	0.00018	0.00018	XXX	0.00018	0.00018	XXX	0.00018
0.00068	0.00067	0.00067	0.00066	0.00067	0.00067	0.00069	0.00071	0.00070	0.00071	0.00070	0.00069

Window 4 128 29	Window 4 128 28	Window 4 128 27	Window 4 128 26	Window 4 128 25	Window 4 128 24	Window 4 128 23	Window 4 128 22	Window 4 128 21	Window 4 128 20	Window 4 128 19	Window 4 128 18
XXX	XXX	XXX	XXX	XXX	XXX	XXX	XXX	0.00019	0.00019	XXX	XXX
XXX	XXX	XXX	XXX	XXX	XXX	0.00018	0.00018	0.00018	XXX	XXX	XXX
XXX	XXX	XXX	XXX	XXX	0.00019	XXX	XXX	0.00020	XXX	XXX	XXX
XXX	XXX	XXX	XXX	XXX	XXX	0.00018	XXX	0.00019	0.00019	XXX	XXX
XXX	XXX	XXX	XXX	XXX	0.00019	XXX	0.00019	0.00019	XXX	XXX	0.00019
XXX	XXX	0.00017	XXX	XXX	XXX	XXX	XXX	0.00018	XXX	XXX	XXX
XXX	XXX	XXX	XXX	XXX	XXX	0.00018	0.00019	0.00019	0.00019	XXX	XXX
XXX	XXX	0.00019	XXX	XXX	0.00019	XXX	XXX	0.00019	XXX	XXX	0.00019
XXX	0.00016	XXX	0.00017	0.00017	XXX	XXX	XXX	0.00017	XXX	XXX	XXX
XXX	XXX	XXX	XXX	XXX	0.00019	0.00019	0.00019	0.00019	0.00019	XXX	0.00019
XXX	0.00017	0.00017	0.00017	0.00018	XXX	XXX	XXX	0.00017	XXX	XXX	XXX
0.00019	XXX	XXX	XXX	XXX	XXX	XXX	XXX	0.00019	XXX	0.00020	XXX
XXX	XXX	0.00019	XXX	XXX	0.00019	0.00019	0.00019	0.00019	0.00019	XXX	0.00019
0.00018	0.00018	XXX	0.00018	0.00019	XXX	XXX	XXX	0.00019	XXX	0.00019	XXX
XXX	0.00018	0.00019	0.00019	0.00019	0.00019	0.00018	0.00019	0.00019	0.00019	XXX	0.00019
0.00018	0.00018	0.00018	0.00018	0.00018	XXX	XXX	XXX	0.00018	XXX	0.00019	XXX
0.00070	0.00069	0.00069	0.00068	0.00067	0.00068	0.00068	0.00068	0.00067	0.00068	0.00069	0.00066

Window 4 256 11	Window 4 256 10	Window 4 256 9	Window 4 256 8	Window 4 256 7	Window 4 256 6	Window 4 256 5	Window 4 256 4	Window 4 256 3	Window 4 256 2	Window 4 256 1	Window 4 128 30
XXX	XXX	0.00019	XXX	0.00018	XXX	0.00019	XXX	XXX	0.00019	0.00018	XXX
XXX	XXX	0.00018	XXX	XXX	XXX	0.00017	XXX	XXX	0.00017	XXX	XXX
XXX	0.00018	0.00018	XXX	XXX	XXX	0.00018	XXX	0.00018	0.00018	XXX	XXX
XXX	XXX	0.00018	XXX	0.00018	XXX	0.00018	XXX	XXX	0.00018	0.00017	XXX
XXX	0.00018	0.00018	XXX	XXX	XXX	0.00018	XXX	0.00018	0.00018	XXX	XXX
XXX	XXX	0.00018	0.00018	XXX	XXX	0.00018	XXX	XXX	0.00018	XXX	0.00018
XXX	0.00018	0.00018	XXX	0.00018	XXX	0.00018	XXX	XXX	0.00018	0.00018	XXX
XXX	XXX	0.00018	0.00017	XXX	XXX	0.00017	XXX	0.00017	0.00018	XXX	XXX
0.00018	XXX	0.00019	XXX	XXX	XXX	0.00018	XXX	XXX	0.00018	XXX	0.00017
XXX	0.00080	0.00079	XXX	0.00081	XXX	0.00081	XXX	0.00080	0.00080	0.00082	XXX
0.00082	XXX	0.00079	0.00079	XXX	XXX	0.00081	XXX	XXX	0.00080	XXX	0.00018
XXX	XXX	0.00080	XXX	XXX	0.00082	0.00082	0.00080	XXX	0.00080	XXX	XXX
XXX	0.00080	0.00079	0.00079	0.00081	XXX	0.00081	XXX	0.00079	0.00080	0.00081	0.00020
0.00082	XXX	0.00080	XXX	XXX	0.00082	0.00082	0.00080	XXX	0.00080	XXX	XXX
0.00082	0.00080	0.00079	0.00079	0.00081	XXX	0.00081	XXX	0.00079	0.00080	0.00081	0.00020
0.00070	XXX	0.00067	0.00067	XXX	0.00070	0.00069	0.00068	XXX	0.00068	XXX	0.00019
0.00070	0.00068	0.00067	0.00067	0.00069	0.00070	0.00069	0.00067	0.00068	0.00068	0.00069	0.00067

Window 4 256 23	Window 4 256 22	Window 4 256 21	Window 4 256 20	Window 4 256 19	Window 4 256 18	Window 4 256 17	Window 4 256 16	Window 4 256 15	Window 4 256 14	Window 4 256 13	Window 4 256 12
XXX	XXX	0.00019	0.00019	XXX	XXX	XXX	0.00019	XXX	XXX	XXX	XXX
0.00018	0.00017	0.00018	XXX	XXX	XXX	XXX	0.00018	XXX	0.00018	XXX	XXX
XXX	XXX	0.00018	XXX	XXX	XXX	XXX	0.00018	XXX	XXX	XXX	XXX
0.00018	XXX	0.00018	0.00018	XXX	XXX	XXX	0.00018	XXX	0.00019	XXX	XXX
XXX	0.00018	0.00018	XXX	XXX	0.00019	XXX	0.00019	XXX	XXX	XXX	XXX
XXX	XXX	0.00018	XXX	XXX	XXX	0.00018	0.00018	XXX	XXX	0.00018	XXX
0.00018	0.00018	0.00018	0.00018	XXX	XXX	XXX	0.00018	XXX	0.00019	XXX	XXX
XXX	XXX	0.00018	XXX	XXX	0.00018	0.00018	0.00018	XXX	XXX	0.00018	XXX
XXX	XXX	0.00018	XXX	XXX	XXX	XXX	0.00018	0.00019	XXX	XXX	0.00019
0.00078	0.00080	0.00079	0.00079	XXX	0.00078	XXX	0.00081	XXX	0.00085	XXX	XXX
XXX	XXX	0.00079	XXX	XXX	XXX	0.00080	0.00081	0.00083	XXX	0.00083	XXX
XXX	XXX	0.00079	XXX	0.00079	XXX	XXX	0.00081	XXX	XXX	XXX	0.00081
0.00078	0.00080	0.00078	0.00079	XXX	0.00078	0.00080	0.00081	XXX	0.00084	0.00083	XXX
XXX	XXX	0.00079	XXX	0.00079	XXX	XXX	0.00081	0.00083	XXX	XXX	0.00081
0.00078	0.00080	0.00078	0.00079	XXX	0.00078	0.00080	0.00081	0.00083	0.00084	0.00083	XXX
XXX	XXX	0.00067	XXX	0.00067	XXX	0.00068	0.00069	0.00071	XXX	0.00071	0.00069
0.00067	0.00068	0.00067	0.00067	0.00067	0.00066	0.00068	0.00069	0.00071	0.00072	0.00071	0.00069

Window 4 256 30	Window 4 256 29	Window 4 256 28	Window 4 256 27	Window 4 256 26	Window 4 256 25	Window 4 256 24
XXX	XXX	XXX	XXX	XXX	XXX	XXX
XXX	XXX	XXX	XXX	XXX	XXX	XXX
XXX	XXX	XXX	XXX	XXX	XXX	0.00018
XXX	XXX	XXX	XXX	XXX	XXX	XXX
XXX	XXX	XXX	XXX	XXX	XXX	0.00018
0.00018	XXX	XXX	0.00019	XXX	XXX	XXX
XXX	XXX	XXX	XXX	XXX	XXX	XXX
XXX	XXX	XXX	0.00018	XXX	XXX	0.00017
0.00018	XXX	0.00019	XXX	0.00019	0.00019	XXX
XXX	XXX	XXX	XXX	XXX	XXX	0.00080
0.00080	XXX	0.00080	0.00082	0.00080	0.00080	XXX
XXX	0.00081	XXX	XXX	XXX	XXX	XXX
0.00080	XXX	XXX	0.00082	XXX	XXX	0.00080
XXX	0.00081	0.00080	XXX	0.00081	0.00080	XXX
0.00080	XXX	0.00080	0.00082	0.00080	0.00080	0.00080
0.00068	0.00069	0.00068	0.00070	0.00068	0.00068	XXX
0.00068	0.00068	0.00068	0.00070	0.00068	0.00068	0.00068

Table 133: Mid-IR spectral library results for SRM 620, first derivative correlation search algorithm

	3A	3B	3C	5A	5B	5C	7A	7B	7C	10A	10B	10C	15A	15B	20A	20B	30
SRM 620 481	0.0265403	XXX	XXX	0.0276568	XXX	XXX	0.027891	XXX	XXX	0.0272444	XXX	XXX	0.0245921	XXX	0.0252572	XXX	0.0271339
SRM 620 482	0.0375977	0.037844	0.0382798	0.0379738	0.0356756	0.0337178	0.0361804	0.0267314	0.0286375	0.0365967	0.0314351	0.0305271	0.0322702	0.0297772	0.031501	0.0306354	0.0313379
SRM 620 483	XXX	XXX	0.0313845	XXX	0.0299794	XXX	XXX	0.0247878	XXX	0.031503	XXX	XXX	0.0279763	XXX	0.0270305	XXX	0.0266979
SRM 620 484	XXX	XXX	XXX	XXX	XXX	XXX	XXX	XXX	XXX	XXX	XXX	0.0358827	XXX	0.0345139	XXX	0.036301	0.0363049
SRM 620 485	0.0358628	0.0342255	0.03438	0.0347048	0.0358634	0.0340386	0.0353983	0.0291402	0.029555	0.0317333	0.0293627	0.0302611	0.0309678	0.0269466	0.028488	0.0276544	0.0277064
SRM 620 486	XXX	XXX	XXX	XXX	XXX	XXX	XXX	XXX	XXX	XXX	XXX	0.0380392	XXX	0.0366871	XXX	0.0400737	0.0393759
SRM 620 487	0.0584137	XXX	XXX	0.0584765	XXX	XXX	0.0578127	XXX	XXX	0.0627163	XXX	XXX	0.0550524	XXX	0.054968	XXX	0.0557427
SRM 620 488	XXX	XXX	XXX	XXX	XXX	0.0358908	XXX	0.0341	XXX	XXX	0.0380853	XXX	0.0391254	XXX	0.0382391	0.0398827	0.0402079
SRM 620 489	0.0405626	0.0482593	0.0392401	0.0393163	0.0441479	0.0342439	0.0400119	0.0322891	0.0360704	0.0399862	0.0356594	0.0332763	0.0324684	0.0390167	0.0357983	0.0387787	0.0351138
SRM 620 4810	XXX	XXX	0.0392043	XXX	0.0433028	XXX	0.043445	XXX	XXX	0.0440814	XXX	XXX	0.0359157	XXX	0.0402226	XXX	0.0384205

SRM 620 4 8 21	SRM 620 4 8 20	SRM 620 4 8 19	SRM 620 4 8 18	SRM 620 4 8 17	SRM 620 4 8 16	SRM 620 4 8 15	SRM 620 4 8 14	SRM 620 4 8 13	SRM 620 4 8 12	SRM 620 4 8 11
0.047279	0.0253873	XXX	XXX	XXX	0.0377723	XXX	XXX	XXX	XXX	XXX
0.0483121	XXX	XXX	XXX	XXX	0.0384901	XXX	0.0356998	XXX	XXX	XXX
0.048063	XXX	XXX	XXX	XXX	0.0391988	XXX	XXX	XXX	XXX	XXX
0.0472812	0.0247878	XXX	XXX	XXX	0.038847	XXX	0.0399209	XXX	XXX	XXX
0.0451505	XXX	XXX	0.0313875	XXX	0.0347511	XXX	XXX	XXX	XXX	XXX
0.0385164	XXX	XXX	XXX	0.0370521	0.0298347	XXX	XXX	0.0379231	XXX	XXX
0.0470116	0.0266423	XXX	XXX	XXX	0.0378781	XXX	0.0388166	XXX	XXX	XXX
0.0370384	XXX	XXX	0.0273527	0.0348031	0.0257418	XXX	XXX	0.0368619	XXX	XXX
0.0336577	XXX	XXX	XXX	XXX	0.0270218	0.0355588	XXX	XXX	0.0352659	0.0320307
0.0456001	0.027805	XXX	0.0350381	XXX	0.0377189	XXX	0.0387493	XXX	XXX	XXX
0.0358768	XXX	XXX	XXX	0.0367716	0.0295527	0.0426216	XXX	0.0424102	XXX	0.0356221
0.0407013	XXX	0.0423373	XXX	XXX	0.0326209	XXX	XXX	XXX	0.0435204	XXX
0.0402065	0.022955	XXX	0.0291381	0.042374	0.0322479	XXX	0.0342257	0.0436926	XXX	XXX
0.0376214	XXX	0.0416439	XXX	XXX	0.0292169	0.0468425	XXX	XXX	0.0432142	0.0367669
0.0403134	0.0211178	XXX	0.0298692	0.0409994	0.0297816	0.0474167	0.0383999	0.0442992	XXX	0.0380785
0.0408219	XXX	0.0432468	XXX	0.0413585	0.0308769	0.0471031	XXX	0.0449144	0.0446605	0.0381649
0.0392369	0.0219739	0.042803	0.0306986	0.0419006	0.0316209	0.0475142	0.0364855	0.0440036	0.0425609	0.0360702

SRM 620 4 16 2	SRM 620 4 16 1	SRM 620 4 8 30	SRM 620 4 8 29	SRM 620 4 8 28	SRM 620 4 8 27	SRM 620 4 8 26	SRM 620 4 8 25	SRM 620 4 8 24	SRM 620 4 8 23	SRM 620 4 8 22
0.177265	0.189671	XXX	XXX	XXX	XXX	XXX	XXX	XXX	XXX	XXX
0.18985	XXX	XXX	XXX	XXX	XXX	XXX	XXX	XXX	0.0318277	0.0426645
0.177238	XXX	XXX	XXX	XXX	XXX	XXX	XXX	0.0325955	XXX	XXX
0.187172	0.199891	XXX	XXX	XXX	XXX	XXX	XXX	XXX	0.0342412	XXX
0.185846	XXX	XXX	XXX	XXX	XXX	XXX	XXX	0.0293993	XXX	0.0389738
0.177749	XXX	0.0321463	XXX	XXX	0.032016	XXX	XXX	XXX	XXX	XXX
0.188028	0.203487	XXX	XXX	XXX	XXX	XXX	XXX	XXX	0.0348019	0.0414625
0.17529	XXX	XXX	XXX	XXX	0.0309004	XXX	XXX	0.0216614	XXX	XXX
0.18325	XXX	0.0301489	XXX	0.0325002	XXX	0.0311187	0.026774	XXX	XXX	XXX
0.185566	0.201396	XXX	XXX	XXX	XXX	XXX	XXX	0.0298523	0.0324053	0.0399747
0.0310442	XXX	0.0332097	XXX	0.0350153	0.0300437	0.03572	0.0291293	XXX	XXX	XXX
0.0246893	XXX	XXX	0.0273318	XXX	XXX	XXX	XXX	XXX	XXX	XXX
0.026185	0.0263331	0.0354271	XXX	XXX	0.0364455	XXX	XXX	0.028457	0.033575	0.0346695
0.0265012	XXX	XXX	0.0252166	0.0392844	XXX	0.0387621	0.031426	XXX	XXX	XXX
0.175204	0.190667	0.0369538	XXX	0.0387809	0.0358633	0.0398153	0.0331391	0.0250775	0.0316388	0.0358153
0.175606	XXX	0.0382199	0.0270159	0.0392959	0.0374293	0.0404172	0.0321802	XXX	XXX	XXX
0.174044	0.190714	0.0367907	0.024488	0.0383612	0.0357885	0.0393052	0.0330234	0.0265349	0.030648	0.0370771

SRM 620 4 16 13	SRM 620 4 16 12	SRM 620 4 16 11	SRM 620 4 16 10	SRM 620 4 16 9	SRM 620 4 16 8	SRM 620 4 16 7	SRM 620 4 16 6	SRM 620 4 16 5	SRM 620 4 16 4	SRM 620 4 16 3
XXX	XXX	XXX	XXX	0.176729	XXX	0.149684	XXX	0.169922	XXX	XXX
XXX	XXX	XXX	XXX	0.188652	XXX	XXX	XXX	0.179786	XXX	XXX
XXX	XXX	XXX	0.190632	0.177102	XXX	XXX	XXX	0.170455	XXX	0.165344
XXX	XXX	XXX	XXX	0.184994	XXX	0.158409	XXX	0.178362	XXX	XXX
XXX	XXX	XXX	0.199647	0.185036	XXX	XXX	XXX	0.175624	XXX	0.174961
0.181005	XXX	XXX	XXX	0.178565	0.191133	XXX	XXX	0.169237	XXX	XXX
XXX	XXX	XXX	0.198652	0.186218	XXX	0.160323	XXX	0.177866	XXX	XXX
0.180325	XXX	XXX	XXX	0.175544	0.191999	XXX	XXX	0.168993	XXX	0.164424
XXX	0.170167	0.173015	XXX	0.185695	XXX	XXX	XXX	0.17501	XXX	XXX
XXX	XXX	XXX	0.200142	0.183992	XXX	0.158752	XXX	0.176904	XXX	0.173971
0.0281002	XXX	0.033873	XXX	0.0339974	0.0228934	XXX	XXX	0.0354567	XXX	XXX
XXX	0.0309617	XXX	XXX	0.0254412	XXX	XXX	0.0277596	0.0280532	0.0277251	XXX
0.0236244	XXX	XXX	0.0212486	0.0273653	0.0196136	0.0356547	XXX	0.028226	XXX	0.0289235
XXX	0.0310847	0.0293802	XXX	0.0278097	XXX	XXX	0.0280314	0.0312714	0.0305489	XXX
0.179827	XXX	0.163546	0.189596	0.175611	0.190799	0.150105	XXX	0.165693	XXX	0.164309
0.179522	0.162127	0.164409	XXX	0.176022	0.191714	XXX	0.165424	0.167933	0.177093	XXX
0.179823	0.162023	0.163677	0.189716	0.174854	0.190254	0.149558	0.164945	0.165064	0.173743	0.163784

SRM 620 4 16 24	SRM 620 4 16 23	SRM 620 4 16 22	SRM 620 4 16 21	SRM 620 4 16 20	SRM 620 4 16 19	SRM 620 4 16 18	SRM 620 4 16 17	SRM 620 4 16 16	SRM 620 4 16 15	SRM 620 4 16 14
XXX	XXX	XXX	0.161134	0.20107	XXX	XXX	XXX	0.174075	XXX	XXX
XXX	0.18191	0.195896	0.170603	XXX	XXX	XXX	XXX	0.185188	XXX	0.169952
0.183613	XXX	XXX	0.161832	XXX	XXX	XXX	XXX	0.175649	XXX	XXX
XXX	0.181735	XXX	0.169095	0.21005	XXX	XXX	XXX	0.182589	XXX	0.1723
0.193492	XXX	0.196823	0.168221	XXX	XXX	0.174922	XXX	0.182328	XXX	XXX
XXX	XXX	XXX	0.15903	XXX	XXX	XXX	0.164428	0.173354	XXX	XXX
XXX	0.181809	0.195536	0.169259	0.210572	XXX	XXX	XXX	0.181175	XXX	0.171377
0.182651	XXX	XXX	0.158213	XXX	XXX	0.165945	0.164636	0.172532	XXX	XXX
XXX	XXX	XXX	0.167067	XXX	XXX	XXX	XXX	0.17945	0.188759	XXX
0.19327	0.180412	0.197205	0.168316	0.209456	XXX	0.175443	XXX	0.182833	XXX	0.172589
XXX	XXX	XXX	0.0380744	XXX	XXX	XXX	0.0332735	0.0316568	0.028734	XXX
XXX	XXX	XXX	0.0314044	XXX	0.0207404	XXX	XXX	0.0269823	XXX	XXX
0.0228981	0.0247468	0.0227282	0.0302955	0.0188893	XXX	0.0282709	0.0265083	0.0263114	XXX	0.0319386
XXX	XXX	XXX	0.030028	XXX	0.0223816	XXX	XXX	0.0270139	0.0238642	XXX
0.18078	0.17114	0.186512	0.158543	0.199462	XXX	0.163027	0.163248	0.170994	0.180532	0.162612
XXX	XXX	XXX	0.157173	XXX	0.189495	XXX	0.163717	0.171623	0.180234	XXX
0.180868	0.170727	0.186381	0.15784	0.198505	0.189148	0.163309	0.162882	0.171695	0.180377	0.162686

SRM 620 4 32 5	SRM 620 4 32 4	SRM 620 4 32 3	SRM 620 4 32 2	SRM 620 4 32 1	SRM 620 4 16 30	SRM 620 4 16 29	SRM 620 4 16 28	SRM 620 4 16 27	SRM 620 4 16 26	SRM 620 4 16 25
0.178497	XXX	XXX	0.183683	0.175161	XXX	XXX	XXX	XXX	XXX	XXX
0.200857	XXX	XXX	0.207425	XXX	XXX	XXX	XXX	XXX	XXX	XXX
0.0242597	XXX	0.0279864	0.0276581	XXX	XXX	XXX	XXX	XXX	XXX	XXX
0.19838	XXX	XXX	0.20515	0.195636	XXX	XXX	XXX	XXX	XXX	XXX
0.188805	XXX	0.170983	0.193726	XXX	XXX	XXX	XXX	XXX	XXX	XXX
0.0233435	XXX	XXX	0.0248259	XXX	0.177447	XXX	XXX	0.188531	XXX	XXX
0.198178	XXX	XXX	0.204929	0.194906	XXX	XXX	XXX	XXX	XXX	XXX
0.0244392	XXX	0.0286995	0.0256688	XXX	XXX	XXX	XXX	0.187162	XXX	XXX
0.199776	XXX	XXX	0.205237	XXX	0.184845	XXX	0.171026	XXX	0.190631	0.193332
0.188552	XXX	0.171954	0.194943	0.184839	XXX	XXX	XXX	XXX	XXX	XXX
0.188922	XXX	XXX	0.194208	XXX	0.0292711	XXX	0.0351718	0.0285783	0.0288994	0.024494
0.187077	0.1898	XXX	0.192484	XXX	XXX	0.0269949	XXX	XXX	XXX	XXX
0.188711	XXX	0.171239	0.193244	0.185391	0.026331	XXX	XXX	0.0238541	XXX	XXX
0.0246984	0.0255852	XXX	0.0271529	XXX	XXX	0.0279295	0.0307744	XXX	0.0240335	0.0222215
0.188125	XXX	0.170469	0.195053	0.184102	0.176821	XXX	0.163025	0.187043	0.181723	0.184411
0.18753	0.189807	XXX	0.192406	XXX	0.176322	0.173955	0.164271	0.187646	0.182883	0.18526
0.187904	0.189931	0.170483	0.193443	0.185122		0.172847	0.162311	0.186085	0.181513	0.18398

SRM 620 4 32 16	SRM 620 4 32 15	SRM 620 4 32 14	SRM 620 4 32 13	SRM 620 4 32 12	SRM 620 4 32 11	SRM 620 4 32 10	SRM 620 4 32 9	SRM 620 4 32 8	SRM 620 4 32 7	SRM 620 4 32 6
0.164147	XXX	XXX	XXX	XXX	XXX	XXX	0.179003	XXX	0.153086	XXX
0.186702	XXX	0.166784	XXX	XXX	XXX	XXX	0.200781	XXX	XXX	XXX
0.0311627	XXX	XXX	XXX	XXX	XXX	0.0261487	0.0252161	XXX	XXX	XXX
0.183526	XXX	0.166979	XXX	XXX	XXX	XXX	0.197508	XXX	0.171185	XXX
0.172835	XXX	XXX	XXX	XXX	XXX	0.174894	0.189714	XXX	XXX	XXX
0.0311654	XXX	XXX	0.0301451	XXX	XXX	XXX	0.0246177	0.0254384	XXX	XXX
0.182275	XXX	0.165772	XXX	XXX	XXX	0.184792	0.198945	XXX	0.170605	XXX
0.0310377	XXX	XXX	0.0292656	XXX	XXX	XXX	0.0266038	0.0264483	XXX	XXX
0.184182	0.18949	XXX	XXX	0.172958	0.163876	XXX	0.199628	XXX	XXX	XXX
0.173048	XXX	0.157064	XXX	XXX	XXX	0.174641	0.189201	XXX	0.16117	XXX
0.173128	0.177712	XXX	0.167582	XXX	0.154143	XXX	0.189374	0.186002	XXX	XXX
0.173084	XXX	XXX	XXX	0.162596	XXX	XXX	0.187835	XXX	XXX	0.187
0.172487	XXX	0.156805	0.166648	XXX	XXX	0.175019	0.189456	0.18634	0.1623	XXX
0.0312945	0.0261075	XXX	XXX	0.0325396	0.0355454	XXX	0.0248844	XXX	XXX	0.0255147
0.172884	0.178298	0.156122	0.167118	XXX	0.153612	0.17558	0.188841	0.187453	0.162424	XXX
0.173102	0.17783	XXX	0.167053	0.163277	0.153952	XXX	0.187482	0.185518	XXX	0.187799
0.172465	0.177035	0.155687	0.166388	0.161437	0.153208	0.175089	0.188752	0.186325	0.162147	0.187813

SRM 620 4 32 27	SRM 620 4 32 26	SRM 620 4 32 25	SRM 620 4 32 24	SRM 620 4 32 23	SRM 620 4 32 22	SRM 620 4 32 21	SRM 620 4 32 20	SRM 620 4 32 19	SRM 620 4 32 18	SRM 620 4 32 17
XXX	XXX	XXX	XXX	XXX	XXX	0.15155	0.177672	XXX	XXX	XXX
XXX	XXX	XXX	XXX	0.169743	0.17968	0.173097	XXX	XXX	XXX	XXX
XXX	XXX	XXX	0.0267357	XXX	XXX	0.0318462	XXX	XXX	XXX	XXX
XXX	XXX	XXX	XXX	0.166622	XXX	0.169844	0.199476	XXX	XXX	XXX
XXX	XXX	XXX	0.183004	XXX	0.167743	0.161952	XXX	XXX	0.152504	XXX
0.0262087	XXX	XXX	XXX	XXX	XXX	0.0319754	XXX	XXX	XXX	0.0212047
XXX	XXX	XXX	XXX	0.169035	0.17809	0.170814	0.198913	XXX	XXX	XXX
0.0250325	XXX	XXX	0.0266485	XXX	XXX	0.0320882	XXX	XXX	0.0346735	0.0242235
XXX	0.201338	0.18073	XXX	XXX	XXX	0.171646	XXX	XXX	XXX	XXX
XXX	XXX	XXX	0.182187	0.159708	0.168001	0.161466	0.188608	XXX	0.152134	XXX
0.180097	0.191072	0.171168	XXX	XXX	XXX	0.161528	XXX	XXX	XXX	0.198946
XXX	XXX	XXX	XXX	XXX	XXX	0.159601	XXX	0.162584	XXX	XXX
0.178983	XXX	XXX	0.18291	0.159489	0.167233	0.161018	0.187874	XXX	0.15266	0.199004
XXX	0.0228565	0.0316613	XXX	XXX	XXX	0.0335093	XXX	0.033395	XXX	XXX
0.1793	0.190481	0.171028	0.183601	0.159488	0.167814	0.160606	0.189247	XXX	0.152331	0.197875
0.179405	0.190009	0.171211	XXX	XXX	XXX	0.160137	XXX	0.162602	XXX	0.197774
0.179087	0.19029	0.170767	0.183949	0.15919	0.166899	0.160464	0.188601	0.161591	0.152283	0.198557

SRM 620 4 64 8	SRM 620 4 64 7	SRM 620 4 64 6	SRM 620 4 64 5	SRM 620 4 64 4	SRM 620 4 64 3	SRM 620 4 64 2	SRM 620 4 64 1	SRM 620 4 32 30	SRM 620 4 32 29	SRM 620 4 32 28
XXX	0.158186	XXX	0.160698	XXX	XXX	0.159735	0.178867	XXX	XXX	XXX
XXX	XXX	XXX	0.186642	XXX	XXX	0.187961	XXX	XXX	XXX	XXX
XXX	XXX	XXX	0.168984	XXX	0.179139	0.167741	XXX	XXX	XXX	XXX
XXX	0.169012	XXX	0.168557	XXX	XXX	0.169153	0.188574	XXX	XXX	XXX
XXX	XXX	XXX	0.172353	XXX	0.182403	0.170581	XXX	XXX	XXX	XXX
0.171301	XXX	XXX	0.161496	XXX	XXX	0.16137	XXX	0.0328726	XXX	XXX
XXX	0.168479	XXX	0.16799	XXX	XXX	0.168574	0.188772	XXX	XXX	XXX
0.176806	XXX	XXX	0.166104	XXX	0.176505	0.164536	XXX	XXX	XXX	XXX
XXX	XXX	XXX	0.169853	XXX	XXX	0.1694	XXX	0.170599	XXX	0.168497
XXX	0.168915	XXX	0.168594	XXX	0.180141	0.16839	0.188488	XXX	XXX	XXX
0.171001	XXX	XXX	0.161346	XXX	XXX	0.160121	XXX	0.161324	XXX	0.15944
XXX	XXX	0.170418	0.169191	0.175314	XXX	0.169663	XXX	XXX	0.163717	XXX
0.180313	0.168788	XXX	0.168864	XXX	0.179989	0.16844	0.188558	0.16043	XXX	XXX
XXX	XXX	0.172145	0.170187	0.176628	XXX	0.170864	XXX	XXX	0.0373524	0.0353114
0.18116	0.168923	XXX	0.169868	XXX	0.180009	0.169008	0.189381	0.159886	XXX	0.158818
0.182808	XXX	0.172137	0.171088	0.1772	XXX	0.169818	XXX	0.160054	0.163954	0.158629
0.181274	0.170605	0.170023	0.169905	0.175883	0.18082	0.169971	0.19005	0.160468	0.164801	0.158638

SRM 620 4 64 19	SRM 620 4 64 18	SRM 620 4 64 17	SRM 620 4 64 16	SRM 620 4 64 15	SRM 620 4 64 14	SRM 620 4 64 13	SRM 620 4 64 12	SRM 620 4 64 11	SRM 620 4 64 10	SRM 620 4 64 9
XXX	XXX	XXX	0.166433	XXX	XXX	XXX	XXX	XXX	XXX	0.161359
XXX	XXX	XXX	0.195017	XXX	0.192654	XXX	XXX	XXX	XXX	0.18814
XXX	XXX	XXX	0.174712	XXX	XXX	XXX	XXX	XXX	0.167975	0.168334
XXX	XXX	XXX	0.175957	XXX	0.173698	XXX	XXX	XXX	XXX	0.169289
XXX	0.147903	XXX	0.17676	XXX	XXX	XXX	XXX	XXX	0.171922	0.17182
XXX	XXX	0.147267	0.166397	XXX	XXX	0.167795	XXX	XXX	XXX	0.161197
XXX	XXX	XXX	0.17491	XXX	0.173242	XXX	XXX	XXX	0.169875	0.16852
XXX	0.137872	0.146503	0.169723	XXX	XXX	0.173794	XXX	XXX	XXX	0.166112
XXX	XXX	XXX	0.175053	0.182652	XXX	XXX	0.16571	0.165321	XXX	0.169925
XXX	0.152099	XXX	0.175758	XXX	0.174664	XXX	XXX	XXX	0.169885	0.168477
XXX	XXX	0.147804	0.166372	0.17392	XXX	0.168151	XXX	0.156878	XXX	0.161624
0.159626	XXX	XXX	0.176328	XXX	XXX	XXX	0.166778	XXX	XXX	0.169183
XXX	0.151477	0.156202	0.175354	XXX	0.174459	0.177048	XXX	XXX	0.169674	0.168487
0.160775	XXX	XXX	0.176758	0.185034	XXX	XXX	0.167375	0.168141	XXX	0.170368
XXX	0.152169	0.158453	0.176246	0.184773	0.174395	0.177441	XXX	0.165607	0.170304	0.170038
0.16089	XXX	0.158483	0.176399	0.186083	XXX	0.178379	0.167512	0.168121	XXX	0.171012
0.159361	0.154051	0.157843	0.176087	0.184642	0.175102	0.177716	0.167093	0.166579	0.17102	0.169483

SRM 620 4 64 30	SRM 620 4 64 29	SRM 620 4 64 28	SRM 620 4 64 27	SRM 620 4 64 26	SRM 620 4 64 25	SRM 620 4 64 24	SRM 620 4 64 23	SRM 620 4 64 22	SRM 620 4 64 21	SRM 620 4 64 20
XXX	XXX	XXX	XXX	XXX	XXX	XXX	XXX	XXX	0.153626	0.156825
XXX	XXX	XXX	XXX	XXX	XXX	XXX	0.172523	0.178143	0.18184	XXX
XXX	XXX	XXX	XXX	XXX	XXX	0.152218	XXX	XXX	0.161579	XXX
XXX	XXX	XXX	XXX	XXX	XXX	XXX	0.154456	XXX	0.163277	0.165549
XXX	XXX	XXX	XXX	XXX	XXX	0.153642	XXX	0.161093	0.164263	XXX
0.166322	XXX	XXX	0.166979	XXX	XXX	XXX	XXX	XXX	0.155214	XXX
XXX	XXX	XXX	XXX	XXX	XXX	XXX	0.154265	0.159337	0.162606	0.165814
XXX	XXX	XXX	0.169821	XXX	XXX	0.148692	XXX	XXX	0.158258	XXX
0.175652	XXX	0.153005	XXX	0.171858	0.159069	XXX	XXX	XXX	0.162971	XXX
XXX	XXX	XXX	XXX	XXX	XXX	0.152794	0.15372	0.158975	0.162302	0.164581
0.165871	XXX	0.144081	0.164999	0.163791	0.149992	XXX	XXX	XXX	0.153954	XXX
XXX	0.15738	XXX	XXX	XXX	XXX	XXX	XXX	XXX	0.163856	XXX
0.174926	XXX	XXX	0.174568	XXX	XXX	0.152828	0.154045	0.158738	0.162303	0.165135
XXX	0.157971	0.156915	XXX	0.175173	0.160679	XXX	XXX	XXX	0.165341	XXX
0.17618	XXX	0.153607	0.17454	0.172704	0.159575	0.153265	0.155665	0.159245	0.162655	0.166684
0.176815	0.156838	0.155027	0.176183	0.17363	0.160071	XXX	XXX	XXX	0.163806	XXX
0.17592	0.157679	0.154487	0.176245	0.173298	0.159753	0.153947	0.155568	0.160227	0.163876	0.167102

SRM 620 4 128 11	SRM 620 4 128 10	SRM 620 4 128 9	SRM 620 4 128 8	SRM 620 4 128 7	SRM 620 4 128 6	SRM 620 4 128 5	SRM 620 4 128 4	SRM 620 4 128 3	SRM 620 4 128 2	SRM 620 4 128 1
XXX	XXX	0.0252152	XXX	0.0257209	XXX	0.0253747	XXX	XXX	0.0286366	0.0305033
XXX	XXX	0.0269988	XXX	XXX	XXX	0.028762	XXX	XXX	0.032883	XXX
XXX	0.0252009	0.0259148	XXX	XXX	XXX	0.0258357	XXX	0.0284831	0.029798	XXX
XXX	XXX	0.0285938	XXX	0.0287722	XXX	0.0283817	XXX	XXX	0.0327438	0.0342866
XXX	0.0234162	0.0242432	XXX	XXX	XXX	0.0248047	XXX	0.0268603	0.0289764	XXX
XXX	XXX	0.0232312	0.0226463	XXX	XXX	0.0260013	XXX	XXX	0.0292476	XXX
XXX	0.0276305	0.0287273	XXX	0.0289597	XXX	0.0290368	XXX	XXX	0.0330291	0.0354446
XXX	XXX	0.0271981	0.0271494	XXX	XXX	0.027591	XXX	0.0309241	0.0319773	XXX
0.170532	XXX	0.162619	XXX	XXX	XXX	0.174785	XXX	XXX	0.155205	XXX
XXX	0.162673	0.161645	XXX	0.161054	XXX	0.172571	XXX	0.153572	0.153642	0.148053
0.171505	XXX	0.163215	0.164318	XXX	XXX	0.175282	XXX	XXX	0.156347	XXX
XXX	XXX	0.171858	XXX	XXX	0.179797	0.18259	0.164624	XXX	0.162979	XXX
XXX	0.162542	0.161222	0.162343	0.16087	XXX	0.17266	XXX	0.15353	0.153605	0.147843
0.0261866	XXX	0.0288592	XXX	XXX	0.0277186	0.0283562	0.0320482	XXX	0.0326247	XXX
0.169898	0.162325	0.161093	0.161942	0.160555	XXX	0.172465	XXX	0.153454	0.1535	0.147593
0.0241941	XXX	0.0267459	0.027111	XXX	0.0256116	0.0268754	0.0308672	XXX	0.0315667	XXX
0.170634	0.163421	0.162129	0.163071	0.161864	0.170223	0.173213	0.155573	0.154569	0.154209	0.148428

SRM 620 4 128 22	SRM 620 4 128 21	SRM 620 4 128 20	SRM 620 4 128 19	SRM 620 4 128 18	SRM 620 4 128 17	SRM 620 4 128 16	SRM 620 4 128 15	SRM 620 4 128 14	SRM 620 4 128 13	SRM 620 4 128 12
XXX	0.0283698	0.0219153	XXX	XXX	XXX	0.025986	XXX	XXX	XXX	XXX
0.0242995	0.029992	XXX	XXX	XXX	XXX	0.029165	XXX	0.0234696	XXX	XXX
XXX	0.0291051	XXX	XXX	XXX	XXX	0.0275619	XXX	XXX	XXX	XXX
XXX	0.032169	0.0236217	XXX	XXX	XXX	0.0291654	XXX	0.0256397	XXX	XXX
0.0222536	0.0264707	XXX	XXX	0.0263446	XXX	0.0259489	XXX	XXX	XXX	XXX
XXX	0.0273945	XXX	XXX	XXX	0.0274578	0.024868	XXX	XXX	0.0241535	XXX
0.026632	0.0320323	0.0242604	XXX	XXX	XXX	0.0294356	XXX	0.0256711	XXX	XXX
XXX	0.0313849	XXX	XXX	0.0304244	0.0341273	0.0293938	XXX	XXX	0.0286387	XXX
XXX	0.159431	XXX	XXX	XXX	XXX	0.160221	0.165626	XXX	XXX	0.16251
0.169053	0.157728	0.171939	XXX	0.152422	XXX	0.159079	XXX	0.173324	XXX	XXX
XXX	0.160444	XXX	XXX	XXX	0.166296	0.161011	0.167644	XXX	0.159661	XXX
XXX	0.168096	XXX	0.178589	XXX	XXX	0.16913	XXX	XXX	XXX	0.172756
0.168469	0.157569	0.172267	XXX	0.152496	0.16523	0.159296	XXX	0.17286	0.157734	XXX
XXX	0.0329424	XXX	0.0283446	XXX	XXX	0.029274	0.0308876	XXX	XXX	0.031399
0.168452	0.157516	0.172096	XXX	0.152407	0.164838	0.159012	0.166289	0.172929	0.157705	XXX
XXX	0.0306764	XXX	0.0269492	XXX	0.0339416	0.0289901	0.0289277	XXX	0.0288343	0.0300434
0.169868	0.158591	0.173271	0.168698	0.153459	0.165891	0.159845	0.167241	0.17382	0.159165	0.163073

SRM 620 4 256 3	SRM 620 4 256 2	SRM 620 4 256 1	SRM 620 4 128 30	SRM 620 4 128 29	SRM 620 4 128 28	SRM 620 4 128 27	SRM 620 4 128 26	SRM 620 4 128 25	SRM 620 4 128 24	SRM 620 4 128 23
XXX	0.17343	0.169351	XXX	XXX	XXX	XXX	XXX	XXX	XXX	XXX
XXX	0.174664	XXX	XXX	XXX	XXX	XXX	XXX	XXX	XXX	0.025918
0.173169	0.163562	XXX	XXX	XXX	XXX	XXX	XXX	XXX	0.0262199	XXX
XXX	0.173357	0.168705	XXX	XXX	XXX	XXX	XXX	XXX	XXX	0.0276163
0.17266	0.163085	XXX	XXX	XXX	XXX	XXX	XXX	XXX	0.0243338	XXX
XXX	0.17374	XXX	0.0236652	XXX	XXX	0.0253687	XXX	XXX	XXX	XXX
XXX	0.172516	0.16767	XXX	XXX	XXX	XXX	XXX	XXX	XXX	0.0269188
0.172812	0.163917	XXX	XXX	XXX	XXX	0.0278792	XXX	XXX	0.0278966	XXX
XXX	0.0207565	XXX	0.165059	XXX	0.171163	XXX	0.16808	0.172169	XXX	XXX
0.0213151	0.0232024	0.0229192	XXX	XXX	XXX	XXX	XXX	XXX	0.161357	0.16372
XXX	0.172606	XXX	0.166203	XXX	0.172231	0.170241	0.168972	0.173103	XXX	XXX
XXX	0.173996	XXX	XXX	0.187269	XXX	XXX	XXX	XXX	XXX	XXX
0.172658	0.163385	0.159192	0.164799	XXX	XXX	0.168727	XXX	XXX	0.161205	0.164767
XXX	0.163301	XXX	XXX	0.0260338	0.0286383	XXX	0.0269522	0.0254941	XXX	XXX
0.183035	0.173364	0.168632	0.164626	XXX	0.169401	0.168456	0.167057	0.170742	0.161042	0.164666
XXX	0.164049	XXX	0.0288172	0.0236908	0.028285	0.0278804	0.025815	0.0240675	XXX	XXX
0.172918	0.163578	0.159122		0.177238	0.170343	0.169505	0.167753	0.171343	0.161871	0.166253

SRM 620 4 256 14	SRM 620 4 256 13	SRM 620 4 256 12	SRM 620 4 256 11	SRM 620 4 256 10	SRM 620 4 256 9	SRM 620 4 256 8	SRM 620 4 256 7	SRM 620 4 256 6	SRM 620 4 256 5	SRM 620 4 256 4
XXX	XXX	XXX	XXX	XXX	0.167919	XXX	0.173222	XXX	0.172096	XXX
0.170424	XXX	XXX	XXX	XXX	0.166704	XXX	XXX	XXX	0.172526	XXX
XXX	XXX	XXX	XXX	0.160975	0.158736	XXX	XXX	XXX	0.162633	XXX
0.170502	XXX	XXX	XXX	XXX	0.166298	XXX	0.172888	XXX	0.171415	XXX
XXX	XXX	XXX	XXX	0.160311	0.156957	XXX	XXX	XXX	0.162073	XXX
XXX	0.167367	XXX	XXX	XXX	0.166992	0.172919	XXX	XXX	0.172564	XXX
0.169815	XXX	XXX	XXX	0.169364	0.16576	XXX	0.172464	XXX	0.170773	XXX
XXX	0.158872	XXX	XXX	XXX	0.157613	0.162971	XXX	XXX	0.16245	XXX
XXX	XXX	0.0211296	0.0201108	XXX	0.0245968	XXX	XXX	XXX	0.0198421	XXX
0.0245276	XXX	XXX	XXX	0.0226962	0.0264478	XXX	0.0246395	XXX	0.021899	XXX
XXX	0.166548	XXX	0.16733	XXX	0.165997	0.172261	XXX	XXX	0.171245	XXX
XXX	XXX	0.168267	XXX	XXX	0.167704	XXX	XXX	0.170112	0.172317	0.167868
0.161036	0.158291	XXX	XXX	0.160233	0.157524	0.162843	0.162918	XXX	0.161842	XXX
XXX	XXX	0.156926	0.158376	XXX	0.156569	XXX	XXX	0.159157	0.161428	0.156352
0.169961	0.167034	XXX	0.167893	0.169488	0.166327	0.172443	0.172534	XXX	0.171572	XXX
XXX	0.159007	0.158122	0.159794	XXX	0.158288	0.163551	XXX	0.160273	0.162517	0.157772
0.160941	0.15823	0.157225	0.15886	0.160315	0.157272	0.162986	0.163075	0.159647	0.161752	0.156731

SRM 620 4 256 25	SRM 620 4 256 24	SRM 620 4 256 23	SRM 620 4 256 22	SRM 620 4 256 21	SRM 620 4 256 20	SRM 620 4 256 19	SRM 620 4 256 18	SRM 620 4 256 17	SRM 620 4 256 16	SRM 620 4 256 15
XXX	XXX	XXX	XXX	0.167383	0.167225	XXX	XXX	XXX	0.164756	XXX
XXX	XXX	0.165982	0.158308	0.165997	XXX	XXX	XXX	XXX	0.164414	XXX
XXX	0.156657	XXX	XXX	0.157945	XXX	XXX	XXX	XXX	0.155661	XXX
XXX	XXX	0.164954	XXX	0.165792	0.16616	XXX	XXX	XXX	0.163768	XXX
XXX	0.154992	XXX	0.148893	0.156285	XXX	XXX	0.162635	XXX	0.154422	XXX
XXX	XXX	XXX	XXX	0.165719	XXX	XXX	XXX	0.16579	0.163926	XXX
XXX	XXX	0.164274	0.157071	0.164672	0.165106	XXX	XXX	XXX	0.163275	XXX
XXX	0.155737	XXX	XXX	0.157327	XXX	XXX	0.163087	0.155915	0.154896	XXX
0.0200708	XXX	XXX	XXX	0.0213475	XXX	XXX	XXX	XXX	0.0243163	0.0227902
XXX	0.0249685	0.0242719	0.0264557	0.0248554	0.0247154	XXX	0.0223325	XXX	0.0266698	XXX
0.170053	XXX	XXX	XXX	0.1644	XXX	XXX	XXX	0.164855	0.163081	0.166533
XXX	XXX	XXX	XXX	0.168025	XXX	0.178873	XXX	XXX	0.164749	XXX
XXX	0.155035	0.155488	0.149317	0.156622	0.157028	XXX	0.162688	0.155401	0.154515	XXX
0.161377	XXX	XXX	XXX	0.155589	XXX	0.166685	XXX	XXX	0.154042	0.156719
0.170529	0.163613	0.164386	0.157723	0.164763	0.165791	XXX	0.171727	0.164641	0.163382	0.166606
0.162534	XXX	XXX	XXX	0.157359	XXX	0.168022	XXX	0.156183	0.155232	0.158182
0.161724	0.154636	0.155462	0.148935	0.156047	0.156665	0.166858	0.162642	0.155483	0.154563	0.15736

SRM 620 4 256 30	SRM 620 4 256 29	SRM 620 4 256 28	SRM 620 4 256 27	SRM 620 4 256 26
XXX	XXX	XXX	XXX	XXX
XXX	XXX	XXX	XXX	XXX
XXX	XXX	XXX	XXX	XXX
XXX	XXX	XXX	XXX	XXX
XXX	XXX	XXX	XXX	XXX
0.164263	XXX	XXX	0.16461	XXX
XXX	XXX	XXX	XXX	XXX
XXX	XXX	XXX	0.156463	XXX
0.0220928	XXX	0.0220406	XXX	0.0208322
XXX	XXX	XXX	XXX	XXX
0.163058	XXX	0.163265	0.163177	0.166779
XXX	0.169346	XXX	XXX	XXX
0.155197	XXX	XXX	0.155771	XXX
XXX	0.15786	0.154606	XXX	0.158026
0.163922	XXX	0.163835	0.164071	0.16754
0.155928	0.159392	0.156238	0.156475	0.159261
0.155275	0.158515	0.155297	0.155632	0.15841

Table 134: Mid-IR spectral library results for SRM 621, first derivative correlation search algorithm.

	3A	3B	3C	5A	5B	5C	7A	7B	7C	10A	10B	10C	15A	15B	20A	20B	30A
SRM 621 4 8 1	0.179532	XXX	XXX	0.201078	XXX	XXX	0.185896	XXX	XXX	0.189483	XXX	XXX	0.211835	XXX	0.215937	XXX	0.0844081
SRM 621 4 8 2	0.174776	0.210424	0.179221	0.192342	0.18355	0.220022	0.17693	0.204186	0.203576	0.176868	0.204733	0.186006	0.194964	0.188646	0.197947	0.187984	0.0835365
SRM 621 4 8 3	XXX	XXX	0.180908	XXX	0.190289	XXX	XXX	0.217472	XXX	0.186376	XXX	XXX	0.209467	XXX	0.214824	XXX	0.0710848
SRM 621 4 8 4	XXX	XXX	XXX	XXX	XXX	XXX	XXX	XXX	XXX	XXX	XXX	0.165672	XXX	0.168092	XXX	0.169905	0.107074

SRM 621 4 8 15	SRM 621 4 8 14	SRM 621 4 8 13	SRM 621 4 8 12	SRM 621 4 8 11	SRM 621 4 8 10	SRM 621 4 8 9	SRM 621 4 8 8	SRM 621 4 8 7	SRM 621 4 8 6	SRM 621 4 8 5
XXX	XXX	XXX	XXX	XXX	XXX	0.134586	XXX	0.189626	XXX	0.159223
XXX	0.21299	XXX	XXX	XXX	XXX	0.165509	XXX	XXX	XXX	0.195728
XXX	XXX	XXX	XXX	XXX	0.250625	0.144216	XXX	XXX	XXX	0.162815
XXX	0.194292	XXX	XXX	XXX	XXX	0.14688	XXX	0.20693	XXX	0.173492
XXX	XXX	XXX	XXX	XXX	0.280289	0.151056	XXX	XXX	XXX	0.175595
XXX	XXX	0.250746	XXX	XXX	XXX	0.185147	0.153162	XXX	XXX	0.208752
XXX	0.184229	XXX	XXX	XXX	0.27678	0.137375	XXX	0.199894	XXX	0.160367
XXX	XXX	0.238294	XXX	XXX	XXX	0.174402	0.14001	XXX	XXX	0.19804
0.260075	XXX	XXX	0.224086	0.133347	XXX	0.166203	XXX	XXX	XXX	0.186468
XXX	0.190361	XXX	XXX	XXX	0.282486	0.142244	XXX	0.205612	XXX	0.164972
0.259866	XXX	0.236078	XXX	0.142844	XXX	0.16904	0.138545	XXX	XXX	0.189752
XXX	XXX	XXX	0.226775	XXX	XXX	0.150102	XXX	XXX	0.177529	0.176288
XXX	0.211904	0.229329	XXX	XXX	0.306308	0.161025	0.128644	0.225888	XXX	0.185662
0.252799	XXX	XXX	0.233764	0.132621	XXX	0.158169	XXX	XXX	0.182691	0.178711
0.261732	0.215833	0.232784	XXX	0.13684	0.3137	0.16551	0.131498	0.230858	XXX	0.189504
0.252471	XXX	0.220893	0.231727	0.134172	XXX	0.157372	0.129554	XXX	0.182056	0.179666
0.0589112	0.0836709	0.0730013	0.120968	0.186379	0.0920903	0.110393	0.12773	0.0656726	0.0897647	0.0986629

SRM 621 4 8 26	SRM 621 4 8 25	SRM 621 4 8 24	SRM 621 4 8 23	SRM 621 4 8 22	SRM 621 4 8 21	SRM 621 4 8 20	SRM 621 4 8 19	SRM 621 4 8 18	SRM 621 4 8 17	SRM 621 4 8 16
XXX	XXX	XXX	XXX	XXX	0.267983	0.215103	XXX	XXX	XXX	0.197236
XXX	XXX	XXX	0.198748	0.179321	0.302932	XXX	XXX	XXX	XXX	0.234078
XXX	XXX	0.170282	XXX	XXX	0.258871	XXX	XXX	XXX	XXX	0.207357
XXX	XXX	XXX	0.180328	XXX	0.282289	0.231387	XXX	XXX	XXX	0.218586
XXX	XXX	0.172543	XXX	0.163579	0.268034	XXX	XXX	0.200532	XXX	0.208501
XXX	XXX	XXX	XXX	XXX	0.314769	XXX	XXX	XXX	0.133023	0.252821
XXX	XXX	XXX	0.168529	0.159264	0.265402	0.225338	XXX	XXX	XXX	0.203238
XXX	XXX	0.190179	XXX	XXX	0.290377	XXX	XXX	0.215133	0.118392	0.228431
0.237004	0.227627	XXX	XXX	XXX	0.288976	XXX	XXX	XXX	XXX	0.233378
XXX	XXX	0.171098	0.169063	0.159037	0.264424	0.222659	XXX	0.205861	XXX	0.201556
0.243104	0.235184	XXX	XXX	XXX	0.291273	XXX	XXX	XXX	0.120809	0.234208
XXX	XXX	XXX	XXX	XXX	0.275513	XXX	0.212495	XXX	XXX	0.21865
XXX	XXX	0.189138	0.189781	0.184096	0.286199	0.243384	XXX	0.23066	0.124594	0.225767
0.233511	0.2241	XXX	XXX	XXX	0.277428	XXX	0.215147	XXX	XXX	0.216434
0.23982	0.233651	0.189598	0.19335	0.18408	0.289405	0.243021	XXX	0.228591	0.121783	0.226372
0.231711	0.223137	XXX	XXX	XXX	0.276264	XXX	0.214372	XXX	0.115635	0.216348
0.0828832	0.0628672	0.0855084	0.0776842	0.0973285	0.0504716	0.0577875	0.106121	0.102418	0.163025	0.0679232

SRM 621 4 16 7	SRM 621 4 16 6	SRM 621 4 16 5	SRM 621 4 16 4	SRM 621 4 16 3	SRM 621 4 16 2	SRM 621 4 16 1	SRM 621 4 8 30	SRM 621 4 8 29	SRM 621 4 8 28	SRM 621 4 8 27
0.185768	XXX	0.192534	XXX	XXX	0.176562	0.160213	XXX	XXX	XXX	XXX
XXX	XXX	0.099182	XXX	XXX	0.118746	XXX	XXX	XXX	XXX	XXX
XXX	XXX	0.0730534	XXX	0.067028	0.0877819	XXX	XXX	XXX	XXX	XXX
0.0672877	XXX	0.0666334	XXX	XXX	0.0815421	0.0808517	XXX	XXX	XXX	XXX
XXX	XXX	0.074117	XXX	0.0637995	0.0844531	XXX	XXX	XXX	XXX	XXX
XXX	XXX	0.199085	XXX	XXX	0.183293	XXX	0.189956	XXX	XXX	0.219861
0.0682207	XXX	0.0675657	XXX	XXX	0.0815776	0.0827977	XXX	XXX	XXX	XXX
XXX	XXX	0.0714635	XXX	0.0608562	0.0829986	XXX	XXX	XXX	XXX	0.196646
XXX	XXX	0.0912027	XXX	XXX	0.0973288	XXX	0.172954	XXX	0.254068	XXX
0.0705324	XXX	0.0684277	XXX	0.0625949	0.0813858	0.0822097	XXX	XXX	XXX	XXX
XXX	XXX	0.200748	XXX	XXX	0.189498	XXX	0.174577	XXX	0.262204	0.200078
XXX	0.18779	0.186459	0.181166	XXX	0.177767	XXX	XXX	0.319005	XXX	XXX
0.190219	XXX	0.18843	XXX	0.190759	0.178526	0.164742	0.17135	XXX	XXX	0.196707
XXX	0.194283	0.190486	0.188275	XXX	0.184913	XXX	XXX	0.316572	0.256644	XXX
0.191711	XXX	0.191289	XXX	0.193983	0.180087	0.167965	0.171857	XXX	0.263086	0.199632
XXX	0.194321	0.193825	0.18869	XXX	0.179074	XXX	0.164895	0.314356	0.253876	0.189168
0.0667819	0.0653813	0.0679307	0.0674186	0.0637518	0.0741455	0.076999	0.0924582	0.0670875	0.0729593	0.0984399

SRM 621 4 16 18	SRM 621 4 16 17	SRM 621 4 16 16	SRM 621 4 16 15	SRM 621 4 16 14	SRM 621 4 16 13	SRM 621 4 16 12	SRM 621 4 16 11	SRM 621 4 16 10	SRM 621 4 16 9	SRM 621 4 16 8
XXX	XXX	0.166358	XXX	XXX	XXX	XXX	XXX	XXX	0.18315	XXX
XXX	XXX	0.113566	XXX	0.0809865	XXX	XXX	XXX	XXX	0.10473	XXX
XXX	XXX	0.0913827	XXX	XXX	XXX	XXX	XXX	0.0700953	0.0811926	XXX
XXX	XXX	0.0810129	XXX	0.0630678	XXX	XXX	XXX	XXX	0.0706338	XXX
0.0689133	XXX	0.0809567	XXX	XXX	XXX	XXX	XXX	0.0703817	0.0816801	XXX
XXX	0.180781	0.173655	XXX	XXX	0.179469	XXX	XXX	XXX	0.187217	0.188996
XXX	XXX	0.0806144	XXX	0.0614652	XXX	XXX	XXX	0.0653179	0.0729878	XXX
0.0699695	0.0792321	0.0812827	XXX	XXX	0.0714663	XXX	XXX	XXX	0.0742873	0.076057
XXX	XXX	0.101836	0.0988433	XXX	XXX	0.073646	0.0792851	XXX	0.0948336	XXX
0.0684709	XXX	0.0788316	XXX	0.0631761	XXX	XXX	XXX	0.0663803	0.0738373	XXX
XXX	0.182305	0.173213	0.161596	XXX	0.185401	XXX	0.207731	XXX	0.192225	0.195367
XXX	XXX	0.163758	XXX	XXX	XXX	0.21688	XXX	XXX	0.177913	XXX
0.183636	0.1812	0.161376	XXX	0.195967	0.18071	XXX	XXX	0.184495	0.179811	0.183664
XXX	XXX	0.168451	0.161124	XXX	XXX	0.21973	0.208579	XXX	0.180853	XXX
0.183684	0.185622	0.162675	0.156959	0.197804	0.182185	XXX	0.203738	0.188902	0.18348	0.185518
XXX	0.183997	0.165556	0.157643	XXX	0.182373	0.215994	0.205552	XXX	0.1843	0.185297
0.06876	0.0741339	0.0758574	0.0749269	0.0636574	0.0715269	0.0561361	0.0631454	0.0668605	0.0694552	0.0714208

SRM 621 4 16 29	SRM 621 4 16 28	SRM 621 4 16 27	SRM 621 4 16 26	SRM 621 4 16 25	SRM 621 4 16 24	SRM 621 4 16 23	SRM 621 4 16 22	SRM 621 4 16 21	SRM 621 4 16 20	SRM 621 4 16 19
XXX	XXX	XXX	XXX	XXX	XXX	XXX	XXX	0.211679	0.202827	XXX
XXX	XXX	XXX	XXX	XXX	XXX	0.0741933	0.0538061	0.0844685	XXX	XXX
XXX	XXX	XXX	XXX	XXX	0.0404413	XXX	XXX	0.0761703	XXX	XXX
XXX	XXX	XXX	XXX	XXX	XXX	0.0658925	XXX	0.0614908	0.0634385	XXX
XXX	XXX	XXX	XXX	XXX	0.0371974	XXX	0.042002	0.0660784	XXX	XXX
XXX	XXX	0.186271	XXX	XXX	XXX	XXX	XXX	0.214015	XXX	XXX
XXX	XXX	XXX	XXX	XXX	XXX	0.0650941	0.0425889	0.0625137	0.0662357	XXX
XXX	XXX	0.074881	XXX	XXX	0.0388651	XXX	XXX	0.0632303	XXX	XXX
XXX	0.113265	XXX	0.0855232	0.0551433	XXX	XXX	XXX	0.0742301	XXX	XXX
XXX	XXX	XXX	XXX	XXX	0.0366864	0.0671036	0.0466483	0.064505	0.0689822	XXX
XXX	0.145459	0.190579	0.188455	0.281051	XXX	XXX	XXX	0.217929	XXX	XXX
0.154318	XXX	XXX	XXX	XXX	XXX	XXX	XXX	0.209285	XXX	0.168064
XXX	XXX	0.187407	XXX	XXX	0.257712	0.214691	0.250229	0.209846	0.205443	XXX
0.154617	0.140199	XXX	0.187434	0.27461	XXX	XXX	XXX	0.21212	XXX	0.173763
XXX	0.140258	0.189399	0.183434	0.275625	0.257609	0.214925	0.25083	0.209318	0.206529	XXX
0.153938	0.140858	0.187992	0.187895	0.277324	XXX	XXX	XXX	0.208521	XXX	0.171289
0.0826199	0.0932252	0.068698	0.0720909	0.0523253	0.0373956	0.0684526	0.0497757	0.0583827	0.0581378	0.104951

SRM 621 4 32 10	SRM 621 4 32 9	SRM 621 4 32 8	SRM 621 4 32 7	SRM 621 4 32 6	SRM 621 4 32 5	SRM 621 4 32 4	SRM 621 4 32 3	SRM 621 4 32 2	SRM 621 4 32 1	SRM 621 4 16 30
XXX	0.249659	XXX	0.195961	XXX	0.246267	XXX	XXX	0.171295	0.164234	XXX
XXX	0.265134	XXX	XXX	XXX	0.265232	XXX	XXX	0.190996	XXX	XXX
0.180424	0.223086	XXX	XXX	XXX	0.225031	XXX	0.186247	0.154396	XXX	XXX
XXX	0.249438	XXX	0.195736	XXX	0.24587	XXX	XXX	0.171134	0.165471	XXX
0.0566007	0.0455717	XXX	XXX	XXX	0.0461299	XXX	0.0592853	0.078267	XXX	XXX
XXX	0.237308	0.205594	XXX	XXX	0.237665	XXX	XXX	0.166998	XXX	0.215678
0.199552	0.2469	XXX	0.193684	XXX	0.24373	XXX	XXX	0.171	0.165141	XXX
XXX	0.046978	0.0489275	XXX	XXX	0.0434754	XXX	0.0555808	0.0728567	XXX	XXX
XXX	0.051328	XXX	XXX	XXX	0.0398891	XXX	XXX	0.0706654	XXX	0.0691749
0.189531	0.233402	XXX	0.185925	XXX	0.234124	XXX	0.197194	0.163087	0.155426	XXX
XXX	0.0491771	0.0533427	XXX	XXX	0.0426828	XXX	XXX	0.0757322	XXX	0.221536
XXX	0.040879	XXX	XXX	0.0537193	0.0403283	0.0501455	XXX	0.0682842	XXX	XXX
0.192802	0.236195	0.205664	0.18746	XXX	0.236214	XXX	0.200493	0.164439	0.157738	0.218942
XXX	0.0458328	XXX	XXX	0.0557185	0.0373914	0.0502485	XXX	0.0679793	XXX	XXX
0.188545	0.234102	0.202979	0.183821	XXX	0.233168	XXX	0.197108	0.160571	0.153915	0.217529
XXX	0.0480293	0.0520748	XXX	0.0574323	0.0410231	0.0562586	XXX	0.0743476	XXX	0.216799
0.188306	0.233385	0.203044	0.182944	0.197839	0.232134	0.19336	0.196152	0.160304	0.154611	0.0557104

SRM 621 4 32 21	SRM 621 4 32 20	SRM 621 4 32 19	SRM 621 4 32 18	SRM 621 4 32 17	SRM 621 4 32 16	SRM 621 4 32 15	SRM 621 4 32 14	SRM 621 4 32 13	SRM 621 4 32 12	SRM 621 4 32 11
0.162057	0.17482	XXX	XXX	XXX	0.17554	XXX	XXX	XXX	XXX	XXX
0.177604	XXX	XXX	XXX	XXX	0.196143	XXX	0.210154	XXX	XXX	XXX
0.143393	XXX	XXX	XXX	XXX	0.159118	XXX	XXX	XXX	XXX	XXX
0.160601	0.179343	XXX	XXX	XXX	0.175052	XXX	0.190284	XXX	XXX	XXX
0.0859842	XXX	XXX	0.08024	XXX	0.0770282	XXX	XXX	XXX	XXX	XXX
0.153425	XXX	XXX	XXX	0.200106	0.166205	XXX	XXX	0.188761	XXX	XXX
0.160562	0.176642	XXX	XXX	XXX	0.174752	XXX	0.189383	XXX	XXX	XXX
0.0789292	XXX	XXX	0.0745723	0.0572201	0.0689243	XXX	XXX	0.0568482	XXX	XXX
0.0758712	XXX	XXX	XXX	XXX	0.0671702	0.0738773	XXX	XXX	0.0697165	0.0462504
0.151303	0.168439	XXX	0.153993	XXX	0.166907	XXX	0.181315	XXX	XXX	XXX
0.0802997	XXX	XXX	XXX	0.0577684	0.0706004	0.076509	XXX	0.0583199	XXX	0.0488851
0.0744908	XXX	0.0567721	XXX	XXX	0.0642237	XXX	XXX	XXX	0.0682747	XXX
0.153158	0.171546	XXX	0.15587	0.200081	0.167853	XXX	0.183902	0.187775	XXX	XXX
0.0738588	XXX	0.0584769	XXX	XXX	0.0636195	0.0720675	XXX	XXX	0.0687048	0.0439651
0.148466	0.168214	XXX	0.153296	0.196313	0.163703	0.169318	0.17941	0.184975	XXX	0.204576
0.0824491	XXX	0.0639405	XXX	0.0583253	0.0716609	0.0791774	XXX	0.058051	0.0756076	0.048064
0.148765	0.167724	0.199635	0.151937	0.195355	0.16316	0.169005	0.178826	0.184313	0.157148	0.203591

SRM 621 4 64 2	SRM 621 4 64 1	SRM 621 4 32 30	SRM 621 4 32 29	SRM 621 4 32 28	SRM 621 4 32 27	SRM 621 4 32 26	SRM 621 4 32 25	SRM 621 4 32 24	SRM 621 4 32 23	SRM 621 4 32 22
0.183449	0.189591	XXX	XXX	XXX	XXX	XXX	XXX	XXX	XXX	XXX
0.155813	XXX	XXX	XXX	XXX	XXX	XXX	XXX	XXX	0.210541	0.154331
0.0734099	XXX	XXX	XXX	XXX	XXX	XXX	XXX	0.174767	XXX	XXX
0.0651081	0.0606415	XXX	XXX	XXX	XXX	XXX	XXX	XXX	0.19614	XXX
0.0714199	XXX	XXX	XXX	XXX	XXX	XXX	XXX	0.0592143	XXX	0.0935011
0.0700049	XXX	0.189061	XXX	XXX	0.182882	XXX	XXX	XXX	XXX	XXX
0.168695	0.178724	XXX	XXX	XXX	XXX	XXX	XXX	XXX	0.19479	0.141258
0.174091	XXX	XXX	XXX	XXX	0.0647817	XXX	XXX	0.0598215	XXX	XXX
0.0664794	XXX	0.066301	XXX	0.0580858	XXX	0.0594307	0.0608929	XXX	XXX	XXX
0.0637144	0.0626348	XXX	XXX	XXX	XXX	XXX	XXX	0.188812	0.184807	0.131184
0.0674902	XXX	0.0688078	XXX	0.0597537	0.0666261	0.0619983	0.0629963	XXX	XXX	XXX
0.167609	XXX	XXX	0.0499575	XXX	XXX	XXX	XXX	XXX	XXX	XXX
0.0710627	0.0690977	0.190876	XXX	XXX	0.18302	XXX	XXX	0.190598	0.187012	0.133999
0.0620802	XXX	XXX	0.0465853	0.0544218	XXX	0.0573284	0.0592482	XXX	XXX	XXX
0.17204	0.181254	0.187711	XXX	0.187768	0.180883	0.183875	0.185542	0.186904	0.182895	0.129392
0.0637732	XXX	0.0705903	0.0543887	0.0637217	0.0695324	0.0630559	0.0653253	XXX	XXX	XXX
0.169148	0.178314	0.188582	0.201918	0.18726	0.181148	0.184471	0.187337	0.18883	0.183137	0.131387

SRM 621 4 64 13	SRM 621 4 64 12	SRM 621 4 64 11	SRM 621 4 64 10	SRM 621 4 64 9	SRM 621 4 64 8	SRM 621 4 64 7	SRM 621 4 64 6	SRM 621 4 64 5	SRM 621 4 64 4	SRM 621 4 64 3
XXX	XXX	XXX	XXX	0.213235	XXX	0.176502	XXX	0.18288	XXX	XXX
XXX	XXX	XXX	XXX	0.192976	XXX	XXX	XXX	0.158945	XXX	XXX
XXX	XXX	XXX	0.0558972	0.0580781	XXX	XXX	XXX	0.0710506	XXX	0.0667951
XXX	XXX	XXX	XXX	0.0532044	XXX	0.0648468	XXX	0.0597825	XXX	XXX
XXX	XXX	XXX	0.0536129	0.0566505	XXX	XXX	XXX	0.06803	XXX	0.0675156
0.0696341	XXX	XXX	XXX	0.0520058	0.0589329	XXX	XXX	0.063553	XXX	XXX
XXX	XXX	XXX	0.203624	0.201027	XXX	0.165294	XXX	0.169598	XXX	XXX
0.178616	XXX	XXX	XXX	0.204553	0.183978	XXX	XXX	0.17439	XXX	0.18312
XXX	0.0585184	0.0721604	XXX	0.0459726	XXX	XXX	XXX	0.0600351	XXX	XXX
XXX	XXX	XXX	0.0483206	0.0511867	XXX	0.0656561	XXX	0.058988	XXX	0.0604065
0.0639266	XXX	0.0739144	XXX	0.0484752	0.0578111	XXX	XXX	0.0613601	XXX	XXX
XXX	0.188059	XXX	XXX	0.200296	XXX	XXX	0.169081	0.170191	0.193167	XXX
0.0708384	XXX	XXX	0.0516887	0.0533009	0.0606634	0.0706666	XXX	0.0651073	XXX	0.0663697
XXX	0.056411	0.0710794	XXX	0.0473335	XXX	XXX	0.0601574	0.0591483	0.0506419	XXX
0.176984	XXX	0.16325	0.201674	0.200283	0.181367	0.16711	XXX	0.1721	XXX	0.178911
0.0631136	0.0573057	0.0711152	XXX	0.0482435	0.0563937	XXX	0.0608716	0.0591332	0.0489308	XXX
0.17662	0.189167	0.164573	0.203949	0.201154	0.181529	0.167183	0.16839	0.171243	0.195021	0.177382

SRM 621 4 64 24	SRM 621 4 64 23	SRM 621 4 64 22	SRM 621 4 64 21	SRM 621 4 64 20	SRM 621 4 64 19	SRM 621 4 64 18	SRM 621 4 64 17	SRM 621 4 64 16	SRM 621 4 64 15	SRM 621 4 64 14
XXX	XXX	XXX	0.198282	0.185308	XXX	XXX	XXX	0.188868	XXX	XXX
XXX	0.190806	0.181374	0.172154	XXX	XXX	XXX	XXX	0.165715	XXX	0.166608
0.0871977	XXX	XXX	0.0646045	XXX	XXX	XXX	XXX	0.0767101	XXX	XXX
XXX	0.0447514	XXX	0.0566907	0.067092	XXX	XXX	XXX	0.0676363	XXX	0.0570485
0.0870244	XXX	0.0574414	0.0658037	XXX	XXX	0.0748828	XXX	0.0741994	XXX	XXX
XXX	XXX	XXX	0.0636503	XXX	XXX	XXX	0.0531445	0.0685928	XXX	XXX
XXX	0.207927	0.19949	0.185539	0.172201	XXX	XXX	XXX	0.174915	XXX	0.179049
0.151009	XXX	XXX	0.18926	XXX	XXX	0.164085	0.204113	0.178551	XXX	XXX
XXX	XXX	XXX	0.0571344	XXX	XXX	XXX	XXX	0.0604435	0.0667297	XXX
0.0770472	0.046118	0.0521181	0.0569578	0.0651571	XXX	0.0665089	XXX	0.0666347	XXX	0.056575
XXX	XXX	XXX	0.0612577	XXX	XXX	XXX	0.0483925	0.0637793	0.0705225	XXX
XXX	XXX	XXX	0.183031	XXX	0.191325	XXX	XXX	0.174481	XXX	XXX
0.0844315	0.0497198	0.0569028	0.0619126	0.0691519	XXX	0.073024	0.0555201	0.0715782	XXX	0.0640488
XXX	XXX	XXX	0.056834	XXX	0.0538915	XXX	XXX	0.0627362	0.0724915	XXX
0.148477	0.209921	0.20172	0.186284	0.171037	XXX	0.160656	0.19885	0.173788	0.161975	0.180347
XXX	XXX	XXX	0.057299	XXX	0.054333	XXX	0.04855	0.0623689	0.0714269	XXX
0.149329	0.208605	0.203882	0.185088	0.174552	0.190142	0.160382	0.200595	0.173611	0.163916	0.181517

SRM 621 4 128 5	SRM 621 4 128 4	SRM 621 4 128 3	SRM 621 4 128 2	SRM 621 4 128 1	SRM 621 4 64 30	SRM 621 4 64 29	SRM 621 4 64 28	SRM 621 4 64 27	SRM 621 4 64 26	SRM 621 4 64 25
0.186517	XXX	XXX	0.166909	0.185265	XXX	XXX	XXX	XXX	XXX	XXX
0.0656535	XXX	XXX	0.0781574	XXX	XXX	XXX	XXX	XXX	XXX	XXX
0.0573152	XXX	0.059657	0.0649237	XXX	XXX	XXX	XXX	XXX	XXX	XXX
0.0633952	XXX	XXX	0.0759803	0.0671575	XXX	XXX	XXX	XXX	XXX	XXX
0.191126	XXX	0.183394	0.170181	XXX	XXX	XXX	XXX	XXX	XXX	XXX
0.055745	XXX	XXX	0.0701954	XXX	0.0667718	XXX	XXX	0.059488	XXX	XXX
0.179104	XXX	XXX	0.159511	0.178113	XXX	XXX	XXX	XXX	XXX	XXX
0.188949	XXX	0.182053	0.171768	XXX	XXX	XXX	XXX	0.179715	XXX	XXX
0.188432	XXX	XXX	0.17085	XXX	0.0631385	XXX	0.0639878	XXX	0.0579159	0.056342
0.0634575	XXX	0.0664494	0.0742916	0.0652823	XXX	XXX	XXX	XXX	XXX	XXX
0.176275	XXX	XXX	0.159807	XXX	0.065527	XXX	0.0689047	0.0575732	0.0648852	0.059602
0.178034	0.162732	XXX	0.160729	XXX	XXX	0.202806	XXX	XXX	XXX	XXX
0.0635657	XXX	0.0666468	0.0750916	0.0672101	0.070917	XXX	XXX	0.0622952	XXX	XXX
0.0548952	0.0613693	XXX	0.0664749	XXX	XXX	0.0543309	0.070911	XXX	0.0655195	0.0579876
0.0633821	XXX	0.066848	0.0748973	0.0673918	0.167702	XXX	0.163676	0.177625	0.175708	0.175132
0.0560129	0.0628387	XXX	0.0680461	XXX	0.0667267	0.0535492	0.0704531	0.0578885	0.0661021	0.0593381
0.177286	0.162961	0.170043	0.159688	0.178796	0.17036	0.2029	0.164914	0.177923	0.176763	0.175802

SRM 621 4 128 16	SRM 621 4 128 15	SRM 621 4 128 14	SRM 621 4 128 13	SRM 621 4 128 12	SRM 621 4 128 11	SRM 621 4 128 10	SRM 621 4 128 9	SRM 621 4 128 8	SRM 621 4 128 7	SRM 621 4 128 6
0.180453	XXX	XXX	XXX	XXX	XXX	XXX	0.183898	XXX	0.186131	XXX
0.0742524	XXX	0.0593601	XXX	XXX	XXX	XXX	0.0895025	XXX	XXX	XXX
0.0637508	XXX	XXX	XXX	XXX	XXX	0.0498116	0.0930238	XXX	XXX	XXX
0.0716632	XXX	0.0584782	XXX	XXX	XXX	XXX	0.0897017	XXX	0.0709777	XXX
0.184559	XXX	XXX	XXX	XXX	XXX	0.195234	0.189755	XXX	XXX	XXX
0.0619201	XXX	XXX	0.0640537	XXX	XXX	XXX	0.0755011	0.0563862	XXX	XXX
0.17369	XXX	0.187519	XXX	XXX	XXX	0.18456	0.176828	XXX	0.178076	XXX
0.181196	XXX	XXX	0.174018	XXX	XXX	XXX	0.180533	0.197105	XXX	XXX
0.18235	0.183152	XXX	XXX	0.180926	0.174106	XXX	0.17996	XXX	XXX	XXX
0.0713808	XXX	0.057882	XXX	XXX	XXX	0.0596022	0.0947312	XXX	0.072918	XXX
0.170434	0.172216	XXX	0.163324	XXX	0.164015	XXX	0.16768	0.184924	XXX	XXX
0.172715	XXX	XXX	XXX	0.171549	XXX	XXX	0.170548	XXX	XXX	0.161496
0.0709001	XXX	0.0579731	0.0714061	XXX	XXX	0.0614413	0.0906511	0.0683871	0.0706396	XXX
0.0615677	0.0565903	XXX	XXX	0.0605486	0.0651124	XXX	0.079837	XXX	XXX	0.0642466
0.0705192	0.0648469	0.0580772	0.0711512	XXX	0.0739472	0.0618726	0.0886742	0.0671893	0.06957	XXX
0.0627599	0.0575273	XXX	0.0637484	0.0614816	0.0674587	XXX	0.0795277	0.0593156	XXX	0.0648714
0.171588	0.173333	0.187996	0.163632	0.170321	0.164515	0.18788	0.168682	0.186939	0.17312	0.161497

SRM 621 4 128 27	SRM 621 4 128 26	SRM 621 4 128 25	SRM 621 4 128 24	SRM 621 4 128 23	SRM 621 4 128 22	SRM 621 4 128 21	SRM 621 4 128 20	SRM 621 4 128 19	SRM 621 4 128 18	SRM 621 4 128 17
XXX	XXX	XXX	XXX	XXX	XXX	0.178669	0.174544	XXX	XXX	XXX
XXX	XXX	XXX	XXX	0.0543853	0.073503	0.0714116	XXX	XXX	XXX	XXX
XXX	XXX	XXX	0.0649256	XXX	XXX	0.0644731	XXX	XXX	XXX	XXX
XXX	XXX	XXX	XXX	0.0566407	XXX	0.0721145	0.069839	XXX	XXX	XXX
XXX	XXX	XXX	0.169121	XXX	0.170423	0.18253	XXX	XXX	0.176628	XXX
0.0567678	XXX	XXX	XXX	XXX	XXX	0.067209	XXX	XXX	XXX	0.0587506
XXX	XXX	XXX	XXX	0.20184	0.158307	0.169826	0.166626	XXX	XXX	XXX
0.188245	XXX	XXX	0.168498	XXX	XXX	0.182108	XXX	XXX	0.171449	0.177269
XXX	0.201103	0.187674	XXX	XXX	XXX	0.181685	XXX	XXX	XXX	XXX
XXX	XXX	XXX	0.0739754	0.0566807	0.073227	0.0706557	0.0687676	XXX	0.078626	XXX
0.175765	0.188917	0.17574	XXX	XXX	XXX	0.17093	XXX	XXX	XXX	0.167086
XXX	XXX	XXX	XXX	XXX	XXX	0.170863	XXX	0.170486	XXX	XXX
0.0637431	XXX	XXX	0.074312	0.0579912	0.074367	0.0714023	0.0700692	XXX	0.0768289	0.0699195
XXX	0.0529337	0.0605094	XXX	XXX	XXX	0.0642793	XXX	0.0642771	XXX	XXX
0.062984	0.0598166	0.0699275	0.0743438	0.0576333	0.0744003	0.0714527	0.0707848	XXX	0.0756878	0.0688479
0.0578404	0.0541965	0.0612495	XXX	XXX	XXX	0.0657094	XXX	0.0659294	XXX	0.061388
0.177694	0.18973	0.177163	0.15849	0.20019	0.157824	0.169447	0.166765	0.168923	0.163625	0.169508

SRM 621 4 256 8	SRM 621 4 256 7	SRM 621 4 256 6	SRM 621 4 256 5	SRM 621 4 256 4	SRM 621 4 256 3	SRM 621 4 256 2	SRM 621 4 256 1	SRM 621 4 128 30	SRM 621 4 128 29	SRM 621 4 128 28
XXX	0.055953	XXX	0.0570297	XXX	XXX	0.0585608	0.0571125	XXX	XXX	XXX
XXX	XXX	XXX	0.0647188	XXX	XXX	0.0653003	XXX	XXX	XXX	XXX
XXX	XXX	XXX	0.851497	XXX	0.845991	0.840203	XXX	XXX	XXX	XXX
XXX	0.0556148	XXX	0.058565	XXX	XXX	0.0596377	0.0572774	XXX	XXX	XXX
XXX	XXX	XXX	0.0623025	XXX	0.0635841	0.0647892	XXX	XXX	XXX	XXX
0.0707615	XXX	XXX	0.0687969	XXX	XXX	0.0741347	XXX	0.0551244	XXX	XXX
XXX	0.0636945	XXX	0.0657187	XXX	XXX	0.0672913	0.0639943	XXX	XXX	XXX
0.0675859	XXX	XXX	0.062974	XXX	0.0666409	0.0667317	XXX	XXX	XXX	XXX
XXX	XXX	XXX	0.0633293	XXX	XXX	0.0690856	XXX	0.190938	XXX	0.166113
XXX	0.0576942	XXX	0.0599848	XXX	0.060701	0.0614827	0.0590215	XXX	XXX	XXX
0.0628993	XXX	XXX	0.0599387	XXX	XXX	0.0640175	XXX	0.178927	XXX	0.154891
XXX	XXX	0.764075	0.753938	0.761444	XXX	0.740457	XXX	XXX	0.18432	XXX
0.0638028	0.0580456	XXX	0.0589028	XXX	0.0608197	0.0615992	0.0599082	0.0658403	XXX	XXX
XXX	XXX	0.0566572	0.0627726	0.0569543	XXX	0.0674016	XXX	XXX	0.0642498	0.0680789
0.063123	0.0586622	XXX	0.0585394	XXX	0.0613679	0.0618165	0.060338	0.0650672	XXX	0.0774622
0.0697244	XXX	0.0557219	0.0624187	0.0563415	XXX	0.0676563	XXX	0.0580686	0.0635522	0.0694275
0.0643528	0.0575229	0.0526404	0.0577423	0.0512103	0.0592621	0.0598268	0.0585266	0.180832	0.182899	0.155646

SRM 621 4 256 19	SRM 621 4 256 18	SRM 621 4 256 17	SRM 621 4 256 16	SRM 621 4 256 15	SRM 621 4 256 14	SRM 621 4 256 13	SRM 621 4 256 12	SRM 621 4 256 11	SRM 621 4 256 10	SRM 621 4 256 9
XXX	XXX	XXX	0.0627449	XXX	XXX	XXX	XXX	XXX	XXX	0.0546967
XXX	XXX	XXX	0.0664826	XXX	0.0685205	XXX	XXX	XXX	XXX	0.0594054
XXX	XXX	XXX	0.843049	XXX	XXX	XXX	XXX	XXX	0.853963	0.853914
XXX	XXX	XXX	0.0622239	XXX	0.062702	XXX	XXX	XXX	XXX	0.0546335
XXX	0.0654079	XXX	0.0683841	XXX	XXX	XXX	XXX	XXX	0.0664761	0.059895
XXX	XXX	0.0699257	0.0669629	XXX	XXX	0.0677609	XXX	XXX	XXX	0.0606883
XXX	XXX	XXX	0.0676655	XXX	0.0700926	XXX	XXX	XXX	0.065143	0.0610811
XXX	0.0640195	0.0699593	0.0670288	XXX	XXX	0.0688677	XXX	XXX	XXX	0.059502
XXX	XXX	XXX	0.0645978	0.0643665	XXX	XXX	0.0629164	0.0657022	XXX	0.0571966
XXX	0.0604193	XXX	0.0620257	XXX	0.0650249	XXX	XXX	XXX	0.0605609	0.0559049
XXX	XXX	0.0618906	0.0594019	0.0575204	XXX	0.0605999	XXX	0.060387	XXX	0.0531587
0.750226	XXX	XXX	0.744089	XXX	XXX	XXX	0.749548	XXX	XXX	0.757064
XXX	0.0583529	0.0642483	0.0604921	XXX	0.0645231	0.0654086	XXX	XXX	0.0582136	0.0543953
0.0614655	XXX	XXX	0.0687333	0.068089	XXX	XXX	0.0653692	0.0712734	XXX	0.0594051
XXX	0.0568591	0.0624838	0.0588947	0.0570281	0.0646946	0.0619548	XXX	0.0624478	0.056049	0.0528563
0.0604389	XXX	0.0714282	0.0676153	0.0671971	XXX	0.067076	0.0649724	0.0694412	XXX	0.0590124
0.0556159	0.0591328	0.0658264	0.0624329	0.0604485	0.0646292	0.0651979	0.0621724	0.0666018	0.0597455	0.0543199

SRM 621 4 256 30	SRM 621 4 256 29	SRM 621 4 256 28	SRM 621 4 256 27	SRM 621 4 256 26	SRM 621 4 256 25	SRM 621 4 256 24	SRM 621 4 256 23	SRM 621 4 256 22	SRM 621 4 256 21	SRM 621 4 256 20
XXX	XXX	XXX	XXX	XXX	XXX	XXX	XXX	XXX	0.066243	0.0589186
XXX	XXX	XXX	XXX	XXX	XXX	XXX	0.0607451	0.0510505	0.0744979	XXX
XXX	XXX	XXX	XXX	XXX	XXX	0.848859	XXX	XXX	0.835127	XXX
XXX	XXX	XXX	XXX	XXX	XXX	XXX	0.0553843	XXX	0.0682801	0.0606642
XXX	XXX	XXX	XXX	XXX	XXX	0.0594599	XXX	0.0529417	0.0726776	XXX
0.0580057	XXX	XXX	0.0570272	XXX	XXX	XXX	XXX	XXX	0.0748037	XXX
XXX	XXX	XXX	XXX	XXX	XXX	XXX	0.0630086	0.0540499	0.0752537	0.0658787
XXX	XXX	XXX	0.0571804	XXX	XXX	0.0625565	XXX	XXX	0.0725429	XXX
0.0563171	XXX	0.0540086	XXX	0.0569014	0.0622594	XXX	XXX	XXX	0.0708949	XXX
XXX	XXX	XXX	XXX	XXX	XXX	0.055904	0.0569715	0.0502422	0.0681254	0.0596737
0.052243	XXX	0.0505368	0.0501744	0.0532305	0.0580145	XXX	XXX	XXX	0.0664498	XXX
XXX	0.762605	XXX	XXX	XXX	XXX	XXX	XXX	XXX	0.734381	XXX
0.0587426	XXX	XXX	0.0523363	XXX	XXX	0.056653	0.0573367	0.0503146	0.0668767	0.0575116
XXX	0.0587832	0.0558436	XXX	0.0601973	0.0633296	XXX	XXX	XXX	0.0715137	XXX
0.055428	XXX	0.0502641	0.0507855	0.0537838	0.0571493	0.0571662	0.0573561	0.0509788	0.0656522	0.0557986
0.0615624	0.05845	0.0557546	0.0583666	0.0590863	0.0632212	XXX	XXX	XXX	0.0707437	XXX
0.060474	0.0545192	0.0518028	0.0543319	0.0545288	0.057096	0.0566284	0.0568386	0.0513441	0.0655695	0.0584733

Table 135: Mid-IR spectral library results for SRM 1831, first derivative correlation search algorithm.

	3A	3B	3C	5A	5B	5C	7A	7B	7C	10A	10B	10C	15A	15B	20A	20B	30A
SRM 1831 4 8 1	0.0426293	XXX	XXX	0.0450747	XXX	XXX	0.0483089	XXX	XXX	0.0440506	XXX	XXX	0.0459842	XXX	0.14484	XXX	0.0435076
SRM 1831 4 8 2	0.02584	0.0221724	0.0213889	0.0237376	0.0189197	0.215648	0.0269306	0.026349	0.0259765	0.0227197	0.0234444	0.0262635	0.0237123	0.0214394	0.214464	0.215294	0.0224984
SRM 1831 4 8 3	XXX	XXX	0.0295968	XXX	0.0259561	XXX	XXX	0.0314175	XXX	0.0301137	XXX	XXX	0.032367	XXX	0.161939	XXX	0.0316312
SRM 1831 4 8 4	XXX	XXX	XXX	XXX	XXX	XXX	XXX	XXX	XXX	XXX	XXX	0.0356954	XXX	0.0351132	XXX	0.172115	0.0349899
SRM 1831 4 8 5	0.044831	0.0394635	0.0361708	0.0387245	0.0346804	0.164204	0.0446386	0.0400323	0.0375245	0.0390178	0.0367778	0.0412435	0.0404793	0.0381497	0.163836	0.165519	0.0398872
SRM 1831 4 8 6	XXX	XXX	XXX	XXX	XXX	XXX	XXX	XXX	XXX	XXX	XXX	0.0349191	XXX	0.030885	XXX	0.173197	0.0309318
SRM 1831 4 8 7	0.0318729	XXX	XXX	0.0335679	XXX	XXX	0.0384802	XXX	XXX	0.0350691	XXX	XXX	0.0368463	XXX	0.181176	XXX	0.0333236
SRM 1831 4 8 8	XXX	XXX	XXX	XXX	XXX	0.132663	XXX	0.0518291	XXX	XXX	0.049481	XXX	0.0525119	XXX	0.135701	0.137608	0.0541593
SRM 1831 4 8 9	0.0410992	0.0374975	0.0374744	0.0367521	0.0341702	0.165924	0.0433046	0.0406932	0.0409003	0.0381939	0.0394012	0.039707	0.0396221	0.0351043	0.164704	0.165659	0.0375164
SRM 1831 4 8 10	XXX	XXX	0.0258188	XXX	0.0222093	XXX	0.0312211	XXX	XXX	0.0282513	XXX	XXX	0.0283745	XXX	0.170791	XXX	0.0268105

SRM 1831 4 8 21	SRM 1831 4 8 20	SRM 1831 4 8 19	SRM 1831 4 8 18	SRM 1831 4 8 17	SRM 1831 4 8 16	SRM 1831 4 8 15	SRM 1831 4 8 14	SRM 1831 4 8 13	SRM 1831 4 8 12	SRM 1831 4 8 11
0.0339773	0.0337824	XXX	XXX	XXX	0.0398314	XXX	XXX	XXX	XXX	XXX
0.0295004	XXX	XXX	XXX	XXX	0.0363496	XXX	0.0252439	XXX	XXX	XXX
0.0306711	XXX	XXX	XXX	XXX	0.0383914	XXX	XXX	XXX	XXX	XXX
0.0285218	0.0328776	XXX	XXX	XXX	0.0400511	XXX	0.0269137	XXX	XXX	XXX
0.0293113	XXX	XXX	0.0208239	XXX	0.0329611	XXX	XXX	XXX	XXX	XXX
0.169386	XXX	XXX	XXX	0.192981	0.170148	XXX	XXX	0.195381	XXX	XXX
0.0334155	0.0381996	XXX	XXX	XXX	0.0416113	XXX	0.0322804	XXX	XXX	XXX
0.0345425	XXX	XXX	0.0277071	0.026208	0.0382025	XXX	XXX	0.0245679	XXX	XXX
0.0303338	XXX	XXX	XXX	XXX	0.0357019	0.0309619	XXX	XXX	0.0264752	0.0385942
0.028811	0.0338814	XXX	0.0263299	XXX	0.0356841	XXX	0.0292476	XXX	XXX	XXX
0.030607	XXX	XXX	XXX	0.0273491	0.0307502	0.0238094	XXX	0.0246069	XXX	0.0321579
0.0317886	XXX	0.0406182	XXX	XXX	0.0369756	XXX	XXX	XXX	0.0290621	XXX
0.0304343	0.033949	XXX	0.0268184	0.0277385	0.0342306	XXX	0.0295073	0.0280139	XXX	XXX
0.025562	XXX	0.0373463	XXX	XXX	0.032256	0.0245014	XXX	XXX	0.0257962	0.0360691
0.167855	0.162568	XXX	0.187052	0.192736	0.169003	0.210847	0.184179	0.195928	XXX	0.168605
0.16767	XXX	0.150712	XXX	0.194004	0.17158	0.21322	XXX	0.196866	0.193901	0.170946
0.0269736	0.0353979	0.0372372	0.0254501	0.0276835	0.0329845	0.0274376	0.0288369	0.025698	0.025966	0.0386148

SRM 1831 4 16 2	SRM 1831 4 16 1	SRM 1831 4 8 30	SRM 1831 4 8 29	SRM 1831 4 8 28	SRM 1831 4 8 27	SRM 1831 4 8 26	SRM 1831 4 8 25	SRM 1831 4 8 24	SRM 1831 4 8 23	SRM 1831 4 8 22
0.0265301	0.0192923	XXX	XXX	XXX	XXX	XXX	XXX	XXX	XXX	XXX
0.0248536	XXX	XXX	XXX	XXX	XXX	XXX	XXX	XXX	0.0186108	0.0352689
0.0200116	XXX	XXX	XXX	XXX	XXX	XXX	XXX	0.0343051	XXX	XXX
0.0233412	0.0177766	XXX	XXX	XXX	XXX	XXX	XXX	XXX	0.020845	XXX
0.0258228	XXX	XXX	XXX	XXX	XXX	XXX	XXX	0.0323261	XXX	0.0323294
0.0203975	XXX	0.173408	XXX	XXX	0.155141	XXX	XXX	XXX	XXX	XXX
0.0231903	0.0193994	XXX	XXX	XXX	XXX	XXX	XXX	XXX	0.0263788	0.0402705
0.0228985	XXX	XXX	XXX	XXX	0.0396778	XXX	XXX	0.0411498	XXX	XXX
0.026148	XXX	0.0317867	XXX	0.0379407	XXX	0.0320756	0.035851	XXX	XXX	XXX
0.0225529	0.018543	XXX	XXX	XXX	XXX	XXX	XXX	0.0400517	0.023171	0.0356229
0.0205042	XXX	0.033654	XXX	0.0392429	0.0367162	0.0301108	0.0349083	XXX	XXX	XXX
0.0219625	XXX	XXX	0.0383855	XXX	XXX	XXX	XXX	XXX	XXX	XXX
0.0210109	0.0164851	0.0329941	XXX	XXX	0.0430876	XXX	XXX	0.0425789	0.022961	0.0387585
0.020907	XXX	XXX	0.0329063	0.0368557	XXX	0.0316364	0.0334812	XXX	XXX	XXX
0.0217762	0.0176558	0.17119	XXX	0.150093	0.157342	0.167727	0.156931	0.147552	0.207856	0.138653
0.0186323	XXX	0.17327	0.163307	0.152045	0.157566	0.169721	0.159912	XXX	XXX	XXX
0.178078	0.19249	0.0295636	0.0346035	0.0376929	0.0434872	0.032051	0.0343392	0.0402646	0.0221966	0.0368612

SRM 1831 4 16 13	SRM 1831 4 16 12	SRM 1831 4 16 11	SRM 1831 4 16 10	SRM 1831 4 16 9	SRM 1831 4 16 8	SRM 1831 4 16 7	SRM 1831 4 16 6	SRM 1831 4 16 5	SRM 1831 4 16 4	SRM 1831 4 16 3
XXX	XXX	XXX	XXX	0.031617	XXX	0.0288218	XXX	0.0230972	XXX	XXX
XXX	XXX	XXX	XXX	0.0294437	XXX	XXX	XXX	0.0199767	XXX	XXX
XXX	XXX	XXX	0.0184808	0.0246496	XXX	XXX	XXX	0.0200697	XXX	0.0220504
XXX	XXX	XXX	XXX	0.0300445	XXX	0.029388	XXX	0.0214303	XXX	XXX
XXX	XXX	XXX	0.020443	0.0314061	XXX	XXX	XXX	0.0222895	XXX	0.0274631
0.0251352	XXX	XXX	XXX	0.021522	0.0271382	XXX	XXX	0.0216062	XXX	XXX
XXX	XXX	XXX	0.021153	0.0257271	XXX	0.0278775	XXX	0.0208351	XXX	XXX
0.0279687	XXX	XXX	XXX	0.0244648	0.0284118	XXX	XXX	0.0211304	XXX	0.0234969
XXX	0.0219496	0.0340244	XXX	0.0280425	XXX	XXX	XXX	0.0229026	XXX	XXX
XXX	XXX	XXX	0.0223477	0.0250114	XXX	0.0268709	XXX	0.0212225	XXX	0.0238187
0.0255289	XXX	0.0288574	XXX	0.0241232	0.0266354	XXX	XXX	0.0191096	XXX	XXX
XXX	0.0206477	XXX	XXX	0.0237132	XXX	XXX	0.040778	0.0214493	0.0210292	XXX
0.0256789	XXX	XXX	0.0182298	0.0226797	0.0268866	0.0241667	XXX	0.0190471	XXX	0.0218553
XXX	0.022233	0.033985	XXX	0.0241263	XXX	XXX	0.0404882	0.020672	0.0209826	XXX
0.0267267	XXX	0.0293572	0.0195428	0.0235085	0.0275264	0.0248909	XXX	0.0196737	XXX	0.0226667
0.0266285	0.0202726	0.030435	XXX	0.0216809	0.0270593	XXX	0.0368241	0.0189019	0.0192633	XXX
0.149776	0.174045	0.139872	0.179744	0.165468	0.146513	0.156758	0.127459	0.183384	0.186271	0.168231

SRM 1831 4 16 24	SRM 1831 4 16 23	SRM 1831 4 16 22	SRM 1831 4 16 21	SRM 1831 4 16 20	SRM 1831 4 16 19	SRM 1831 4 16 18	SRM 1831 4 16 17	SRM 1831 4 16 16	SRM 1831 4 16 15	SRM 1831 4 16 14
XXX	XXX	XXX	0.0209637	0.0206519	XXX	XXX	XXX	0.0380784	XXX	XXX
XXX	0.0207902	0.0262142	0.0216284	XXX	XXX	XXX	XXX	0.0307716	XXX	0.0234906
0.0285139	XXX	XXX	0.0206403	XXX	XXX	XXX	XXX	0.030954	XXX	XXX
XXX	0.0247326	XXX	0.0194718	0.0207914	XXX	XXX	XXX	0.0340105	XXX	0.0219975
0.0336823	XXX	0.0314009	0.0215846	XXX	XXX	0.0209158	XXX	0.0370873	XXX	XXX
XXX	XXX	XXX	0.0163225	XXX	XXX	XXX	0.0212665	0.0280278	XXX	XXX
XXX	0.0242297	0.030004	0.0201625	0.0228999	XXX	XXX	XXX	0.0319468	XXX	0.0231943
0.0304636	XXX	XXX	0.0188853	XXX	XXX	0.0179211	0.0224849	0.0309676	XXX	XXX
XXX	XXX	XXX	0.0217154	XXX	XXX	XXX	XXX	0.0327985	0.0288796	XXX
0.0324473	0.0234216	0.029301	0.0186856	0.0209923	XXX	0.0187985	XXX	0.0309071	XXX	0.0235703
XXX	XXX	XXX	0.0166645	XXX	XXX	XXX	0.0212792	0.0286059	0.0254896	XXX
XXX	XXX	XXX	0.0193723	XXX	0.0187862	XXX	XXX	0.0287854	XXX	XXX
0.0293628	0.020086	0.0249882	0.0164448	0.0194335	XXX	0.0157372	0.0203503	0.0290617	XXX	0.0204772
XXX	XXX	XXX	0.019001	XXX	0.0170826	XXX	XXX	0.0302127	0.027782	XXX
0.0299471	0.0210224	0.02592	0.0176739	0.0204613	XXX	0.0170269	0.021644	0.0300417	0.0257033	0.0220079
XXX	XXX	XXX	0.0172129	XXX	0.0150516	XXX	0.0225883	0.0275844	0.0250827	XXX
0.140834	0.169021	0.144486	0.181121	0.177336	0.188723	0.18813	0.161865	0.163213	0.153865	0.172086

SRM 1831 4 32 5	SRM 1831 4 32 4	SRM 1831 4 32 3	SRM 1831 4 32 2	SRM 1831 4 32 1	SRM 1831 4 16 30	SRM 1831 4 16 29	SRM 1831 4 16 28	SRM 1831 4 16 27	SRM 1831 4 16 26	SRM 1831 4 16 25
0.194532	XXX	XXX	0.174988	0.186936	XXX	XXX	XXX	XXX	XXX	XXX
0.203928	XXX	XXX	0.182508	XXX	XXX	XXX	XXX	XXX	XXX	XXX
0.204304	XXX	0.182754	0.184211	XXX	XXX	XXX	XXX	XXX	XXX	XXX
0.193692	XXX	XXX	0.173956	0.18611	XXX	XXX	XXX	XXX	XXX	XXX
0.204735	XXX	0.182825	0.183077	XXX	XXX	XXX	XXX	XXX	XXX	XXX
0.194532	XXX	XXX	0.175051	XXX	0.0228405	XXX	XXX	0.0223124	XXX	XXX
0.194168	XXX	XXX	0.174146	0.187211	XXX	XXX	XXX	XXX	XXX	XXX
0.0176478	XXX	0.021262	0.0216158	XXX	XXX	XXX	XXX	0.0246119	XXX	XXX
0.203405	XXX	XXX	0.182052	XXX	0.0272105	XXX	0.0220549	XXX	0.0181993	0.0242505
0.20483	XXX	0.183068	0.184017	0.196875	XXX	XXX	XXX	XXX	XXX	XXX
0.204577	XXX	XXX	0.182631	XXX	0.0221701	XXX	0.0174973	0.0211927	0.0140423	0.0202215
0.192508	0.174795	XXX	0.17144	XXX	XXX	0.0296444	XXX	XXX	XXX	XXX
0.204606	XXX	0.182716	0.182959	0.196939	0.0226552	XXX	XXX	0.0227044	XXX	XXX
0.194117	0.176135	XXX	0.172587	XXX	XXX	0.0297262	0.0200702	XXX	0.0166143	0.0228524
0.204381	XXX	0.183155	0.182754	0.197144	0.0234609	XXX	0.0198506	0.0234586	0.0149876	0.0209079
0.193868	0.176413	XXX	0.172594	XXX	0.0238973	0.0267256	0.0176302	0.0235435	0.0152796	0.0203863
0.193883	0.17642	0.174605	0.172641	0.186916	0.161073	0.149707	0.170892	0.161152	0.193766	0.177296

SRM 1831 4 32 16	SRM 1831 4 32 15	SRM 1831 4 32 14	SRM 1831 4 32 13	SRM 1831 4 32 12	SRM 1831 4 32 11	SRM 1831 4 32 10	SRM 1831 4 32 9	SRM 1831 4 32 8	SRM 1831 4 32 7	SRM 1831 4 32 6
0.174113	XXX	XXX	XXX	XXX	XXX	XXX	0.185507	XXX	0.18753	XXX
0.18276	XXX	0.16315	XXX	XXX	XXX	XXX	0.193905	XXX	XXX	XXX
0.183032	XXX	XXX	XXX	XXX	XXX	0.183934	0.19508	XXX	XXX	XXX
0.174152	XXX	0.155034	XXX	XXX	XXX	XXX	0.184995	XXX	0.187659	XXX
0.182609	XXX	XXX	XXX	XXX	XXX	0.184145	0.194437	XXX	XXX	XXX
0.173268	XXX	XXX	0.170943	XXX	XXX	XXX	0.185981	0.174428	XXX	XXX
0.17455	XXX	0.155249	XXX	XXX	XXX	0.174014	0.184655	XXX	0.188727	XXX
0.0200382	XXX	XXX	0.0225335	XXX	XXX	XXX	0.0203141	0.0227489	XXX	XXX
0.181667	0.166476	XXX	XXX	0.177777	0.16579	XXX	0.194121	XXX	XXX	XXX
0.182751	XXX	0.163279	XXX	XXX	XXX	0.184057	0.195137	XXX	0.198435	XXX
0.182285	0.166755	XXX	0.180159	XXX	0.167615	XXX	0.193753	0.184107	XXX	XXX
0.17223	XXX	XXX	XXX	0.168445	XXX	XXX	0.182969	XXX	XXX	0.191268
0.182499	XXX	0.163181	0.180619	XXX	XXX	0.184018	0.194212	0.184194	0.198293	XXX
0.172267	0.157113	XXX	XXX	0.169671	0.158048	XXX	0.18297	XXX	XXX	0.192925
0.182214	0.166973	0.16319	0.18061	XXX	0.167326	0.183721	0.193917	0.184357	0.198365	XXX
0.172569	0.157268	XXX	0.17088	0.169944	0.15829	XXX	0.183144	0.175264	XXX	0.193305
0.172589	0.157309	0.154045	0.170882	0.16992	0.158304	0.173713	0.183158	0.17525	0.187831	0.193344

SRM 1831 4 32 27	SRM 1831 4 32 26	SRM 1831 4 32 25	SRM 1831 4 32 24	SRM 1831 4 32 23	SRM 1831 4 32 22	SRM 1831 4 32 21	SRM 1831 4 32 20	SRM 1831 4 32 19	SRM 1831 4 32 18	SRM 1831 4 32 17
XXX	XXX	XXX	XXX	XXX	XXX	0.200988	0.157358	XXX	XXX	XXX
XXX	XXX	XXX	XXX	0.188953	0.176121	0.207151	XXX	XXX	XXX	XXX
XXX	XXX	XXX	0.176777	XXX	XXX	0.210675	XXX	XXX	XXX	XXX
XXX	XXX	XXX	XXX	0.179647	XXX	0.199142	0.157435	XXX	XXX	XXX
XXX	XXX	XXX	0.176673	XXX	0.176553	0.208549	XXX	XXX	0.176901	XXX
0.166601	XXX	XXX	XXX	XXX	XXX	0.198661	XXX	XXX	XXX	0.166142
XXX	XXX	XXX	XXX	0.180004	0.168779	0.199708	0.157724	XXX	XXX	XXX
0.0234515	XXX	XXX	0.0211044	XXX	XXX	0.0172124	XXX	XXX	0.0239243	0.0241559
XXX	0.195577	0.167351	XXX	XXX	XXX	0.208396	XXX	XXX	XXX	XXX
XXX	XXX	XXX	0.176672	0.190554	0.177334	0.209392	0.165978	XXX	0.177223	XXX
0.175951	0.195739	0.169023	XXX	XXX	XXX	0.208775	XXX	XXX	XXX	0.175635
XXX	XXX	XXX	XXX	XXX	XXX	0.198058	XXX	0.150649	XXX	XXX
0.175713	XXX	XXX	0.17662	0.190614	0.176649	0.208502	0.165523	XXX	0.176747	0.175707
XXX	0.185251	0.159542	XXX	XXX	XXX	0.197934	XXX	0.151171	XXX	XXX
0.17564	0.19601	0.169162	0.176868	0.190171	0.176833	0.208775	0.165718	XXX	0.176917	0.175636
0.166201	0.185506	0.159682	XXX	XXX	XXX	0.198597	XXX	0.150669	XXX	0.16586
0.166234	0.185517	0.15967	0.168161	0.180083	0.167337	0.198594	0.156988	0.150643	0.167212	0.165866

SRM 1831 4 64 8	SRM 1831 4 64 7	SRM 1831 4 64 6	SRM 1831 4 64 5	SRM 1831 4 64 4	SRM 1831 4 64 3	SRM 1831 4 64 2	SRM 1831 4 64 1	SRM 1831 4 32 30	SRM 1831 4 32 29	SRM 1831 4 32 28
XXX	0.0194703	XXX	0.0211305	XXX	XXX	0.0184547	0.0211499	XXX	XXX	XXX
XXX	XXX	XXX	0.0237537	XXX	XXX	0.0220867	XXX	XXX	XXX	XXX
XXX	XXX	XXX	0.0236555	XXX	0.0247633	0.0217534	XXX	XXX	XXX	XXX
XXX	0.0199737	XXX	0.0209596	XXX	XXX	0.0189809	0.0213004	XXX	XXX	XXX
XXX	XXX	XXX	0.0205626	XXX	0.0207174	0.0189175	XXX	XXX	XXX	XXX
0.0184822	XXX	XXX	0.0195741	XXX	XXX	0.0186407	XXX	0.173738	XXX	XXX
XXX	0.170012	XXX	0.178488	XXX	XXX	0.178712	0.172662	XXX	XXX	XXX
0.178141	XXX	XXX	0.178449	XXX	0.165	0.179109	XXX	XXX	XXX	XXX
XXX	XXX	XXX	0.1967	XXX	XXX	0.197424	XXX	0.183803	XXX	0.172461
XXX	0.0193221	XXX	0.0190494	XXX	0.0203437	0.0175339	0.0196904	XXX	XXX	XXX
0.175862	XXX	XXX	0.176478	XXX	XXX	0.177452	XXX	0.183601	XXX	0.174259
XXX	XXX	0.170267	0.176991	0.17977	XXX	0.177435	XXX	XXX	0.170697	XXX
0.0196495	0.0206714	XXX	0.0213628	XXX	0.0221507	0.019892	0.0224321	0.183185	XXX	XXX
XXX	XXX	0.0199077	0.0184933	0.0183672	XXX	0.0178921	XXX	XXX	0.171397	0.164067
0.177743	0.170805	XXX	0.179172	XXX	0.164302	0.179489	0.173717	0.18376	XXX	0.174397
0.17678	XXX	0.170748	0.177632	0.180046	XXX	0.178465	XXX	0.174337	0.171277	0.164662
0.177248	0.170171	0.170333	0.178037	0.180328	0.163596	0.178669	0.172665	0.17436	0.171282	0.164645

SRM 1831 4 64 19	SRM 1831 4 64 18	SRM 1831 4 64 17	SRM 1831 4 64 16	SRM 1831 4 64 15	SRM 1831 4 64 14	SRM 1831 4 64 13	SRM 1831 4 64 12	SRM 1831 4 64 11	SRM 1831 4 64 10	SRM 1831 4 64 9
XXX	XXX	XXX	0.0217952	XXX	XXX	XXX	XXX	XXX	XXX	0.0183598
XXX	XXX	XXX	0.0264693	XXX	0.0224699	XXX	XXX	XXX	XXX	0.021059
XXX	XXX	XXX	0.026651	XXX	XXX	XXX	XXX	XXX	0.0215442	0.0203449
XXX	XXX	XXX	0.0220709	XXX	0.0191028	XXX	XXX	XXX	XXX	0.0185665
XXX	0.0210335	XXX	0.0228514	XXX	XXX	XXX	XXX	XXX	0.0184073	0.017331
XXX	XXX	0.0206021	0.0220307	XXX	XXX	0.018953	XXX	XXX	XXX	0.0183796
XXX	XXX	XXX	0.16455	XXX	0.173502	XXX	XXX	XXX	0.176998	0.182337
XXX	0.165473	0.166365	0.165004	XXX	XXX	0.170343	XXX	XXX	XXX	0.183094
XXX	XXX	XXX	0.182652	0.197286	XXX	XXX	0.19326	0.186158	XXX	0.201531
XXX	0.0208137	XXX	0.0215355	XXX	0.0185624	XXX	XXX	XXX	0.0177007	0.0166213
XXX	XXX	0.164792	0.163008	0.177178	XXX	0.168758	XXX	0.166982	XXX	0.181087
0.167889	XXX	XXX	0.163947	XXX	XXX	XXX	0.173794	XXX	XXX	0.181292
XXX	0.0219334	0.0219981	0.0227051	XXX	0.0201032	0.0200693	XXX	XXX	0.0194925	0.0186464
0.0216419	XXX	XXX	0.0223755	0.019267	XXX	XXX	0.0188311	0.0207107	XXX	0.0177203
XXX	0.165875	0.166574	0.164482	0.178539	0.173335	0.170493	XXX	0.168721	0.177972	0.182005
0.167769	XXX	0.166381	0.164207	0.177613	XXX	0.169907	0.174285	0.167493	XXX	0.181323
0.168133	0.165547	0.165919	0.163932	0.178185	0.17285	0.170157	0.174065	0.16842	0.17735	0.180956

SRM 1831 4 64 30	SRM 1831 4 64 29	SRM 1831 4 64 28	SRM 1831 4 64 27	SRM 1831 4 64 26	SRM 1831 4 64 25	SRM 1831 4 64 24	SRM 1831 4 64 23	SRM 1831 4 64 22	SRM 1831 4 64 21	SRM 1831 4 64 20
XXX	XXX	XXX	XXX	XXX	XXX	XXX	XXX	XXX	0.0191752	0.0197456
XXX	XXX	XXX	XXX	XXX	XXX	XXX	0.0218613	0.0245022	0.0223749	XXX
XXX	XXX	XXX	XXX	XXX	XXX	0.0205065	XXX	XXX	0.0217944	XXX
XXX	XXX	XXX	XXX	XXX	XXX	XXX	0.01982	XXX	0.0196743	0.0205632
XXX	XXX	XXX	XXX	XXX	XXX	0.017072	XXX	0.0203424	0.0183265	XXX
0.0179772	XXX	XXX	0.0176645	XXX	XXX	XXX	XXX	XXX	0.0195935	XXX
XXX	XXX	XXX	XXX	XXX	XXX	XXX	0.178512	0.165821	0.17292	0.167931
XXX	XXX	XXX	0.181837	XXX	XXX	0.176228	XXX	XXX	0.173701	XXX
0.201791	XXX	0.189331	XXX	0.187332	0.199135	XXX	XXX	XXX	0.191865	XXX
XXX	XXX	XXX	XXX	XXX	XXX	0.0178665	0.0191327	0.0201536	0.0175781	0.0199962
0.181453	XXX	0.169014	0.180143	0.167708	0.179027	XXX	XXX	XXX	0.172098	XXX
XXX	0.181031	XXX	XXX	XXX	XXX	XXX	XXX	XXX	0.172099	XXX
0.0185131	XXX	XXX	0.0189685	0.0217631	XXX	0.0196543	0.0197703	0.0219963	0.0197481	0.0216058
XXX	0.0178922	0.0210495	XXX	0.0207476	0.0183595	XXX	XXX	XXX	0.0191246	XXX
0.182981	XXX	0.171246	0.182286	0.169511	0.180661	0.175654	0.179077	0.165875	0.173284	0.168712
0.182026	0.181092	0.169821	0.181152	0.16847	0.17999	XXX	XXX	XXX	0.172788	XXX
0.1826	0.181206	0.170718	0.182173	0.168858	0.17993	0.174925	0.179081	0.165076	0.172317	0.168704

SRM 1831 4 128 11	SRM 1831 4 128 10	SRM 1831 4 128 9	SRM 1831 4 128 8	SRM 1831 4 128 7	SRM 1831 4 128 6	SRM 1831 4 128 5	SRM 1831 4 128 4	SRM 1831 4 128 3	SRM 1831 4 128 2	SRM 1831 4 128 1
XXX	XXX	0.166759	XXX	0.175768	XXX	0.17064	XXX	XXX	0.167574	0.172114
XXX	XXX	0.174997	XXX	XXX	XXX	0.178857	XXX	XXX	0.176386	XXX
XXX	0.0184283	0.0182306	XXX	XXX	XXX	0.0179188	XXX	0.0180107	0.0182438	XXX
XXX	XXX	0.175202	XXX	0.185274	XXX	0.179982	XXX	XXX	0.17697	0.181548
XXX	0.17573	0.173596	XXX	XXX	XXX	0.17792	XXX	0.177368	0.175487	XXX
XXX	XXX	0.164787	0.171039	XXX	XXX	0.168756	XXX	XXX	0.166357	XXX
XXX	0.17764	0.175322	XXX	0.185179	XXX	0.179693	XXX	XXX	0.177185	0.181921
XXX	XXX	0.174457	0.181007	XXX	XXX	0.17877	XXX	0.178163	0.176031	XXX
0.737043	XXX	0.728288	XXX	XXX	XXX	0.732955	XXX	XXX	0.729978	XXX
XXX	0.0208406	0.0205526	XXX	0.0189261	XXX	0.0201595	XXX	0.0195968	0.0205625	0.0195129
0.0172214	XXX	0.0189862	0.0179887	XXX	XXX	0.0186139	XXX	XXX	0.0189835	XXX
XXX	XXX	0.173815	XXX	XXX	0.18138	0.178084	0.170413	XXX	0.175867	XXX
XXX	0.176599	0.174113	0.180744	0.183938	XXX	0.178585	XXX	0.178022	0.175822	0.180971
0.0151124	XXX	0.0165469	XXX	XXX	0.0160046	0.0157576	0.0176464	XXX	0.0164207	XXX
0.181004	0.176166	0.173565	0.180119	0.183413	XXX	0.17795	XXX	0.177486	0.175266	0.180299
0.0178608	XXX	0.0196179	0.0182874	XXX	0.018826	0.0186642	0.0208573	XXX	0.0194517	XXX
0.0176653	0.019969	0.0194986	0.0183472	0.0174471	0.0187665	0.0186126	0.0210313	0.0186313	0.0195459	0.0185811

SRM 1831 4 128 22	SRM 1831 4 128 21	SRM 1831 4 128 20	SRM 1831 4 128 19	SRM 1831 4 128 18	SRM 1831 4 128 17	SRM 1831 4 128 16	SRM 1831 4 128 15	SRM 1831 4 128 14	SRM 1831 4 128 13	SRM 1831 4 128 12
XXX	0.171763	0.169328	XXX	XXX	XXX	0.163224	XXX	XXX	XXX	XXX
0.176071	0.178941	XXX	XXX	XXX	XXX	0.170661	XXX	0.179745	XXX	XXX
XXX	0.0180914	XXX	XXX	XXX	XXX	0.01973	XXX	XXX	XXX	XXX
XXX	0.180329	0.178252	XXX	XXX	XXX	0.171538	XXX	0.181184	XXX	XXX
0.175	0.178527	XXX	XXX	0.177458	XXX	0.169785	XXX	XXX	XXX	XXX
XXX	0.169706	XXX	XXX	XXX	0.166636	0.161146	XXX	XXX	0.171772	XXX
0.177167	0.180294	0.178762	XXX	XXX	XXX	0.171469	XXX	0.181063	XXX	XXX
XXX	0.179577	XXX	XXX	0.178557	0.176466	0.170741	XXX	XXX	0.181682	XXX
XXX	0.734047	XXX	XXX	XXX	XXX	0.723627	0.734507	XXX	XXX	0.732889
0.0205608	0.019807	0.0201283	XXX	0.0195961	XXX	0.0215865	XXX	0.0191096	XXX	XXX
XXX	0.0186309	XXX	XXX	XXX	0.0202838	0.0199848	0.0185369	XXX	0.017491	XXX
XXX	0.179621	XXX	0.177433	XXX	XXX	0.170269	XXX	XXX	XXX	0.178159
0.176357	0.179462	0.177568	XXX	0.178409	0.176363	0.170494	XXX	0.179924	0.18154	XXX
XXX	0.0164203	XXX	0.0171632	XXX	XXX	0.0171874	0.0158931	XXX	XXX	0.0158816
0.175795	0.179065	0.177176	XXX	0.177894	0.176077	0.169778	0.179388	0.179422	0.180961	XXX
XXX	0.0192648	XXX	0.0201384	XXX	0.0210772	0.0204197	0.0187281	XXX	0.0178968	0.0187929
0.01965	0.0192149	0.019523	0.0200727	0.018737	0.0210793	0.0201615	0.0186926	0.0182514	0.0177055	0.0187694

SRM 1831 4 256 3	SRM 1831 4 256 2	SRM 1831 4 256 1	SRM 1831 4 128 30	SRM 1831 4 128 29	SRM 1831 4 128 28	SRM 1831 4 128 27	SRM 1831 4 128 26	SRM 1831 4 128 25	SRM 1831 4 128 24	SRM 1831 4 128 23
XXX	0.159982	0.161506	XXX	XXX	XXX	XXX	XXX	XXX	XXX	XXX
XXX	0.162312	XXX	XXX	XXX	XXX	XXX	XXX	XXX	XXX	0.166588
0.0316285	0.0289744	XXX	XXX	XXX	XXX	XXX	XXX	XXX	0.0189737	XXX
XXX	0.159643	0.160949	XXX	XXX	XXX	XXX	XXX	XXX	XXX	0.167691
0.16462	0.161083	XXX	XXX	XXX	XXX	XXX	XXX	XXX	0.017429	XXX
XXX	0.160655	XXX	0.166293	XXX	XXX	0.16866	XXX	XXX	XXX	XXX
XXX	0.028766	0.0257777	XXX	XXX	XXX	XXX	XXX	XXX	XXX	0.168134
0.0325644	0.0292292	XXX	XXX	XXX	XXX	0.178556	XXX	XXX	0.17467	XXX
XXX	0.0317753	XXX	0.729773	XXX	0.726656	XXX	0.727172	0.727456	XXX	XXX
0.174205	0.170855	0.171467	XXX	XXX	XXX	XXX	XXX	XXX	0.0206879	0.0228416
XXX	0.16221	XXX	0.0197561	XXX	0.0203547	0.0188442	0.0193882	0.0193257	XXX	XXX
XXX	0.160221	XXX	XXX	0.170031	XXX	XXX	XXX	XXX	XXX	XXX
0.164633	0.161728	0.162515	0.176054	XXX	XXX	0.178375	XXX	XXX	0.174491	0.166388
XXX	0.0300699	XXX	XXX	0.018159	0.018824	XXX	0.0168613	0.0164038	XXX	XXX
0.164671	0.160716	0.161677	0.175592	XXX	0.17283	0.178114	0.172797	0.173099	0.173956	0.166228
XXX	0.0296185	XXX	0.0205441	0.0214074	0.0219096	0.0194148	0.0199451	0.019475	XXX	XXX
0.164418	0.161613	0.162348	0.0204917	0.0212768	0.021513	0.0194413	0.0200616	0.0194689	0.0203493	0.0224852

SRM 1831 4 256 14	SRM 1831 4 256 13	SRM 1831 4 256 12	SRM 1831 4 256 11	SRM 1831 4 256 10	SRM 1831 4 256 9	SRM 1831 4 256 8	SRM 1831 4 256 7	SRM 1831 4 256 6	SRM 1831 4 256 5	SRM 1831 4 256 4
XXX	XXX	XXX	XXX	XXX	0.162524	XXX	0.156864	XXX	0.157466	XXX
0.159693	XXX	XXX	XXX	XXX	0.157314	XXX	XXX	XXX	0.157512	XXX
XXX	XXX	XXX	XXX	0.0240323	0.0281082	XXX	XXX	XXX	0.0266871	XXX
0.160007	XXX	XXX	XXX	XXX	0.158804	XXX	0.158308	XXX	0.155986	XXX
XXX	XXX	XXX	XXX	0.16285	0.158245	XXX	XXX	XXX	0.156966	XXX
XXX	0.168832	XXX	XXX	XXX	0.157815	0.167923	XXX	XXX	0.156696	XXX
0.0238541	XXX	XXX	XXX	0.0228014	0.0257746	XXX	0.0348858	XXX	0.0258599	XXX
XXX	0.0220698	XXX	XXX	XXX	0.0262915	0.0328789	XXX	XXX	0.0266433	XXX
XXX	XXX	0.0250225	0.0260762	XXX	0.024981	XXX	XXX	XXX	0.0273734	XXX
0.17072	XXX	XXX	XXX	0.173049	0.168407	XXX	0.170073	XXX	0.166563	XXX
XXX	0.169169	XXX	0.159701	XXX	0.158033	0.170078	XXX	XXX	0.157274	XXX
XXX	XXX	0.167513	XXX	XXX	0.160336	XXX	XXX	0.159489	0.157039	0.163412
0.160961	0.169506	XXX	XXX	0.163638	0.159	0.169026	0.161241	XXX	0.157373	XXX
XXX	XXX	0.0241462	0.0251185	XXX	0.0256044	XXX	XXX	0.035002	0.0266412	0.0302299
0.160364	0.169277	XXX	0.159061	0.163035	0.158154	0.168368	0.159965	XXX	0.15694	XXX
XXX	0.0217012	0.0238482	0.0253626	XXX	0.0252787	0.0336339	XXX	0.0345341	0.0267053	0.0300316
0.16086	0.169435	0.167885	0.159283	0.163563	0.158942	0.168833	0.160991	0.161452	0.157167	0.1647

SRM 1831 4 256 25	SRM 1831 4 256 24	SRM 1831 4 256 23	SRM 1831 4 256 22	SRM 1831 4 256 21	SRM 1831 4 256 20	SRM 1831 4 256 19	SRM 1831 4 256 18	SRM 1831 4 256 17	SRM 1831 4 256 16	SRM 1831 4 256 15
XXX	XXX	XXX	XXX	0.165583	0.173439	XXX	XXX	XXX	0.169294	XXX
XXX	XXX	0.16354	0.151859	0.159649	XXX	XXX	XXX	XXX	0.165073	XXX
XXX	0.0283447	XXX	XXX	0.0276262	XXX	XXX	XXX	XXX	0.0250426	XXX
XXX	XXX	0.166113	XXX	0.161364	0.169843	XXX	XXX	XXX	0.165916	XXX
XXX	0.165199	XXX	0.152838	0.160311	XXX	XXX	0.162158	XXX	0.165451	XXX
XXX	XXX	XXX	XXX	0.16046	XXX	XXX	XXX	0.163394	0.165184	XXX
XXX	XXX	0.025206	0.0269502	0.0259108	0.0232601	XXX	XXX	XXX	0.0237256	XXX
XXX	0.027116	XXX	XXX	0.0264577	XXX	XXX	0.0253571	0.0248608	0.0234134	XXX
0.0218335	XXX	XXX	XXX	0.0244558	XXX	XXX	XXX	XXX	0.0225779	0.0225681
XXX	0.176119	0.176279	0.16326	0.171442	0.180369	XXX	0.173072	XXX	0.176796	XXX
0.170569	XXX	XXX	XXX	0.16028	XXX	XXX	XXX	0.163741	0.165336	0.167852
XXX	XXX	XXX	XXX	0.162828	XXX	0.159461	XXX	XXX	0.167449	XXX
XXX	0.166505	0.166048	0.153427	0.161789	0.170468	XXX	0.162787	0.164948	0.165969	XXX
0.0226884	XXX	XXX	XXX	0.0251489	XXX	0.0257574	XXX	XXX	0.0225334	0.0233902
0.171431	0.165326	0.164827	0.152882	0.160835	0.169295	XXX	0.162494	0.163778	0.165507	0.168528
0.0224139	XXX	XXX	XXX	0.0252366	XXX	0.0254501	XXX	0.0236466	0.0228045	0.0234517
0.172322	0.166426	0.16595	0.15338	0.161746	0.170353	0.158495	0.162724	0.164913	0.165919	0.169134

SRM 1831 4 256 30	SRM 1831 4 256 29	SRM 1831 4 256 28	SRM 1831 4 256 27	SRM 1831 4 256 26
XXX	XXX	XXX	XXX	XXX
XXX	XXX	XXX	XXX	XXX
XXX	XXX	XXX	XXX	XXX
XXX	XXX	XXX	XXX	XXX
XXX	XXX	XXX	XXX	XXX
0.166084	XXX	XXX	0.165479	XXX
XXX	XXX	XXX	XXX	XXX
XXX	XXX	XXX	0.0249417	XXX
0.0236098	XXX	0.0226895	XXX	0.0239768
XXX	XXX	XXX	XXX	XXX
0.165907	XXX	0.17014	0.164848	0.161503
XXX	0.168584	XXX	XXX	XXX
0.166899	XXX	XXX	0.166383	XXX
XXX	0.02533	0.0235817	XXX	0.0239392
0.166595	XXX	0.170964	0.165536	0.162047
0.0249924	0.0252881	0.0236745	0.0240123	0.0238145
0.166797	0.166789	0.171589	0.166293	0.162716

Table 136: Mid-IR spectral library results for 'real world' window, first derivative correlation search algorithm.

	3A	3B	3C	5A	5B	5C	7A	7B	7C	10A	10B	10C	15A	15B	20A	20B	30A
Window 4 8 1	0.0297069	XXX	XXX	0.0373681	XXX	XXX	0.034944	XXX	XXX	0.0343273	XXX	XXX	0.209937	XXX	0.0378961	XXX	0.0356387
Window 4 8 2	0.0430946	0.0385866	0.0503685	0.0398853	0.177322	0.0472887	0.0367383	0.0508415	0.0463329	0.0411768	0.057783	0.178447	0.181451	0.178296	0.0451483	0.0434474	0.0409602
Window 4 8 3	XXX	XXX	0.0266305	XXX	0.214333	XXX	XXX	0.033248	XXX	0.0257894	XXX	XXX	0.218641	XXX	0.0289179	XXX	0.0303587
Window 4 8 4	XXX	XXX	XXX	XXX	XXX	XXX	XXX	XXX	XXX	XXX	XXX	0.190096	XXX	0.190798	XXX	0.0421207	0.0344932
Window 4 8 5	0.0292874	0.0291037	0.0364498	0.0279464	0.220843	0.03309	0.0265411	0.0338307	0.025824	0.0257939	0.0359922	0.226419	0.226165	0.223981	0.0287082	0.0286891	0.0241897

Window 4 8 17	Window 4 8 16	Window 4 8 15	Window 4 8 14	Window 4 8 13	Window 4 8 12	Window 4 8 11	Window 4 8 10	Window 4 8 9	Window 4 8 8	Window 4 8 7	Window 4 8 6
XXX	0.0368476	XXX	XXX	XXX	XXX	XXX	XXX	0.0358737	XXX	0.0319319	XXX
XXX	0.039277	XXX	0.0323448	XXX	XXX	XXX	XXX	0.0326045	XXX	XXX	XXX
XXX	0.0374539	XXX	XXX	XXX	XXX	XXX	0.0341393	0.0419036	XXX	XXX	XXX
XXX	0.0347911	XXX	0.033543	XXX	XXX	XXX	XXX	0.034264	XXX	0.0349124	XXX
XXX	0.216073	XXX	XXX	XXX	XXX	XXX	0.171612	0.189229	XXX	XXX	XXX
0.040464	0.0372758	XXX	XXX	0.0418818	XXX	XXX	XXX	0.0376315	0.0353743	XXX	XXX
XXX	0.0344871	XXX	0.0314242	XXX	XXX	XXX	0.0313491	0.0320567	XXX	0.0329617	XXX
0.0403092	0.0402636	XXX	XXX	0.0458357	XXX	XXX	XXX	0.0396703	0.0393822	XXX	XXX
XXX	0.0344457	0.029682	XXX	XXX	0.037618	0.0281075	XXX	0.039869	XXX	XXX	XXX
XXX	0.0334789	XXX	0.0327778	XXX	XXX	XXX	0.0335874	0.0331046	XXX	0.0377051	XXX
0.0403027	0.0428187	0.0395294	XXX	0.0477432	XXX	0.0326621	XXX	0.0452982	0.0454468	XXX	XXX
XXX	0.220897	XXX	XXX	XXX	0.18181	XXX	XXX	0.193828	XXX	XXX	0.224639
0.237783	0.222114	XXX	0.191796	0.18941	XXX	XXX	0.177913	0.195341	0.199029	0.190786	XXX
XXX	0.219538	0.197323	XXX	XXX	0.181215	0.218354	XXX	0.193365	XXX	XXX	0.223782
0.0364211	0.0354924	0.0365668	0.0368893	0.0454235	XXX	0.02925	0.0376404	0.0362965	0.0354925	0.042652	XXX
0.032061	0.0305141	0.0346437	XXX	0.041931	0.0403736	0.0280992	XXX	0.0373247	0.0376208	XXX	0.031689
0.0274939	0.0316106	0.0309908	0.0326102	0.0402036	0.0350048	0.0235368	0.0376477	0.0318219	0.0312692	0.0347419	0.0290263

Window 4 8 29	Window 4 8 28	Window 4 8 27	Window 4 8 26	Window 4 8 25	Window 4 8 24	Window 4 8 23	Window 4 8 22	Window 4 8 21	Window 4 8 20	Window 4 8 19	Window 4 8 18
XXX	XXX	XXX	XXX	XXX	XXX	XXX	XXX	0.0347348	0.0307351	XXX	XXX
XXX	XXX	XXX	XXX	XXX	XXX	0.0298298	0.035106	0.037485	XXX	XXX	XXX
XXX	XXX	XXX	XXX	XXX	0.0310888	XXX	XXX	0.048397	XXX	XXX	XXX
XXX	XXX	XXX	XXX	XXX	XXX	0.0308229	XXX	0.0342877	0.0337657	XXX	XXX
XXX	XXX	XXX	XXX	XXX	0.199218	XXX	0.177855	0.204651	XXX	XXX	0.190607
XXX	XXX	0.0435258	XXX	XXX	XXX	XXX	XXX	0.0414985	XXX	XXX	XXX
XXX	XXX	XXX	XXX	XXX	XXX	0.0295788	0.0348075	0.0336209	0.0323795	XXX	XXX
XXX	XXX	0.0450647	XXX	XXX	0.0348844	XXX	XXX	0.0444651	XXX	XXX	0.0421615
XXX	0.0295197	XXX	0.0283253	0.0451064	XXX	XXX	XXX	0.0362733	XXX	XXX	XXX
XXX	XXX	XXX	XXX	XXX	0.0332691	0.0290015	0.0411184	0.0359468	0.0368837	XXX	0.037648
XXX	0.038253	0.0527531	0.0381333	0.0553753	XXX	XXX	XXX	0.0437777	XXX	XXX	XXX
0.190635	XXX	XXX	XXX	XXX	XXX	XXX	XXX	0.202692	XXX	0.226231	XXX
XXX	XXX	0.201433	XXX	XXX	0.208589	0.210414	0.186021	0.207482	0.189179	XXX	0.199942
0.190599	0.201536	XXX	0.204167	0.159733	XXX	XXX	XXX	0.201018	XXX	0.22303	XXX
XXX	0.0355846	0.0412194	0.0382881	0.0483779	0.034755	0.0304458	0.0446711	0.0374638	0.0406362	XXX	0.0391838
0.0388455	0.0367208	0.0518898	0.0375386	0.0493519	XXX	XXX	XXX	0.0332715	XXX	0.0282674	XXX
0.0355898	0.0316719	0.0457604	0.0353921	0.0483886	0.0363418	0.030484	0.0386921	0.0283782	0.0358317	0.0257049	0.0344896

Window 4 16 11	Window 4 16 10	Window 4 16 9	Window 4 16 8	Window 4 16 7	Window 4 16 6	Window 4 16 5	Window 4 16 4	Window 4 16 3	Window 4 16 2	Window 4 16 1	Window 4 8 30
XXX	XXX	0.149417	XXX	0.173191	XXX	0.177791	XXX	XXX	0.164835	0.146667	XXX
XXX	XXX	0.0294323	XXX	XXX	XXX	0.0244532	XXX	XXX	0.0258843	XXX	XXX
XXX	0.158912	0.155564	XXX	XXX	XXX	0.175312	XXX	0.164635	0.165606	XXX	XXX
XXX	XXX	0.146106	XXX	0.171464	XXX	0.178207	XXX	XXX	0.161568	0.146894	XXX
XXX	0.164788	0.156302	XXX	XXX	XXX	0.18621	XXX	0.173533	0.169482	XXX	XXX
XXX	XXX	0.152125	0.15692	XXX	XXX	0.180679	XXX	XXX	0.163521	XXX	0.0364527
XXX	0.0253191	0.0295027	XXX	0.0241731	XXX	0.0265291	XXX	XXX	0.0276991	0.0259112	XXX
XXX	XXX	0.0362593	0.0375815	XXX	XXX	0.03049	XXX	0.0282675	0.0309954	XXX	XXX
0.152099	XXX	0.141908	XXX	XXX	XXX	0.169534	XXX	XXX	0.153201	XXX	0.0320012
XXX	0.158682	0.148164	XXX	0.173406	XXX	0.178243	XXX	0.166766	0.164292	0.146274	XXX
0.163417	XXX	0.151457	0.160242	XXX	XXX	0.179367	XXX	XXX	0.163766	XXX	0.0406356
XXX	XXX	0.0306515	XXX	XXX	0.019252	0.0269634	0.0375081	XXX	0.0252572	XXX	XXX
XXX	0.029212	0.0288315	0.0311251	0.0236582	XXX	0.0253364	XXX	0.0244709	0.0252936	0.0273531	0.203189
0.16126	XXX	0.147424	XXX	XXX	0.177732	0.178267	0.145929	XXX	0.162017	XXX	XXX
0.161743	0.159632	0.148637	0.15786	0.174277	XXX	0.178616	XXX	0.167644	0.162366	0.14874	0.0381731
0.0224584	XXX	0.0299947	0.0300792	XXX	0.0178251	0.0243979	0.0376873	XXX	0.0246915	XXX	0.0346703
0.161201	0.160993	0.147104	0.158194	0.173547	0.177404	0.178365	0.145724	0.168196	0.161835	0.148198	0.0338646

Window 4 16 23	Window 4 16 22	Window 4 16 21	Window 4 16 20	Window 4 16 19	Window 4 16 18	Window 4 16 17	Window 4 16 16	Window 4 16 15	Window 4 16 14	Window 4 16 13	Window 4 16 12
XXX	XXX	0.143739	0.150327	XXX	XXX	XXX	0.14439	XXX	XXX	XXX	XXX
0.0259668	0.0216294	0.0316691	XXX	XXX	XXX	XXX	0.0316517	XXX	0.0214968	XXX	XXX
XXX	XXX	0.145818	XXX	XXX	XXX	XXX	0.146221	XXX	XXX	XXX	XXX
0.162297	XXX	0.142728	0.151023	XXX	XXX	XXX	0.141772	XXX	0.16435	XXX	XXX
XXX	0.167395	0.14924	XXX	XXX	0.145599	XXX	0.148703	XXX	XXX	XXX	XXX
XXX	XXX	0.146938	XXX	XXX	XXX	0.165632	0.145015	XXX	XXX	0.13649	XXX
0.0254857	0.0230651	0.0329739	0.0285716	XXX	XXX	XXX	0.0314599	XXX	0.0235324	XXX	XXX
XXX	XXX	0.0364952	XXX	XXX	0.0363939	0.0272051	0.034716	XXX	XXX	0.0449934	XXX
XXX	XXX	0.136023	XXX	XXX	XXX	XXX	0.135862	0.154073	XXX	XXX	0.13126
0.162165	0.160894	0.14128	0.150741	XXX	0.139929	XXX	0.142579	XXX	0.165587	XXX	XXX
XXX	XXX	0.146175	XXX	XXX	XXX	0.164826	0.145473	0.163792	XXX	0.135535	XXX
XXX	XXX	0.034006	XXX	0.0241945	XXX	XXX	0.0300565	XXX	XXX	XXX	0.0357278
0.0272781	0.0221734	0.0317468	0.0274533	XXX	0.0311272	0.0258365	0.0296315	XXX	0.0240566	0.0436671	XXX
XXX	XXX	0.144274	XXX	0.173769	XXX	XXX	0.14214	0.165172	XXX	XXX	0.140743
0.163538	0.162448	0.143283	0.150754	XXX	0.139714	0.164373	0.142026	0.163743	0.166042	0.136449	XXX
XXX	XXX	0.0320977	XXX	0.0223137	XXX	0.0248414	0.0296815	0.0238787	XXX	0.0418588	0.0331327
0.16353	0.161869	0.14305	0.15043	0.172918	0.139678	0.164117	0.141434	0.164257	0.165932	0.136785	0.140252

Window 4 32 5	Window 4 32 4	Window 4 32 3	Window 4 32 2	Window 4 32 1	Window 4 16 30	Window 4 16 29	Window 4 16 28	Window 4 16 27	Window 4 16 26	Window 4 16 25	Window 4 16 24
0.17838	XXX	XXX	0.187225	0.145826	XXX	XXX	XXX	XXX	XXX	XXX	XXX
0.025685	XXX	XXX	0.0266658	XXX	XXX	XXX	XXX	XXX	XXX	XXX	XXX
0.0222869	XXX	0.0224041	0.0166124	XXX	XXX	XXX	XXX	XXX	XXX	XXX	0.150893
0.0192551	XXX	XXX	0.018763	0.0282402	XXX	XXX	XXX	XXX	XXX	XXX	XXX
0.0222873	XXX	0.0265972	0.0202791	XXX	XXX	XXX	XXX	XXX	XXX	XXX	0.158832
0.0215633	XXX	XXX	0.0183657	XXX	0.16163	XXX	XXX	0.175151	XXX	XXX	XXX
0.0204043	XXX	XXX	0.019733	0.0294938	XXX	XXX	XXX	XXX	XXX	XXX	XXX
0.0206395	XXX	0.0275543	0.0195319	XXX	XXX	XXX	XXX	0.0286244	XXX	XXX	0.0324122
0.0272954	XXX	XXX	0.024887	XXX	0.149423	XXX	0.167713	XXX	0.161853	0.162128	XXX
0.0227234	XXX	0.0272556	0.0213951	0.0311951	XXX	XXX	XXX	XXX	XXX	XXX	0.15401
0.0233036	XXX	XXX	0.0200319	XXX	0.159842	XXX	0.179013	0.17312	0.171804	0.172283	XXX
0.0196647	0.022873	XXX	0.0158455	XXX	XXX	0.0297783	XXX	XXX	XXX	XXX	XXX
0.0221347	XXX	0.0291627	0.0206801	0.031346	0.0294261	XXX	XXX	0.0259491	XXX	XXX	0.0292055
0.0198034	0.0227278	XXX	0.0168406	XXX	XXX	0.156466	0.178887	XXX	0.171136	0.172532	XXX
0.0198635	XXX	0.0274767	0.0191593	0.0287992	0.158741	XXX	0.177411	0.172861	0.170198	0.17264	0.15318
0.0205853	0.0236048	XXX	0.0174255	XXX	0.0268602	0.0293148	0.019611	0.0249421	0.0206026	0.0190397	XXX
0.0207891	0.0241526	0.0290885	0.0179986	0.0301549	0.160053	0.155672	0.178078	0.173346	0.170487	0.172207	0.152985

Window 4 32 17	Window 4 32 16	Window 4 32 15	Window 4 32 14	Window 4 32 13	Window 4 32 12	Window 4 32 11	Window 4 32 10	Window 4 32 9	Window 4 32 8	Window 4 32 7	Window 4 32 6
XXX	0.1479	XXX	XXX	XXX	XXX	XXX	XXX	0.170944	XXX	0.156216	XXX
XXX	0.0368761	XXX	0.0246272	XXX	XXX	XXX	XXX	0.0308161	XXX	XXX	XXX
XXX	0.0271502	XXX	XXX	XXX	XXX	XXX	0.0209268	0.0211105	XXX	XXX	XXX
XXX	0.030833	XXX	0.0208014	XXX	XXX	XXX	XXX	0.0223101	XXX	0.0257879	XXX
XXX	0.0323746	XXX	XXX	XXX	XXX	XXX	0.0254107	0.0248101	XXX	XXX	XXX
0.0248662	0.0313514	XXX	XXX	0.0235732	XXX	XXX	XXX	0.0231219	0.0282605	XXX	XXX
XXX	0.0318547	XXX	0.0221636	XXX	XXX	XXX	0.026085	0.0234225	XXX	0.0267194	XXX
0.0227625	0.0322223	XXX	XXX	0.0237393	XXX	XXX	XXX	0.0240482	0.0265846	XXX	XXX
XXX	0.0381582	0.0346772	XXX	XXX	0.0248065	0.0304842	XXX	0.0282308	XXX	XXX	XXX
XXX	0.0324349	XXX	0.0222282	XXX	XXX	XXX	0.0267326	0.0259035	XXX	0.0294264	XXX
0.0275569	0.0338309	0.0320522	XXX	0.0258145	XXX	0.0267892	XXX	0.0243239	0.028751	XXX	XXX
XXX	0.0299675	XXX	XXX	XXX	0.0188514	XXX	XXX	0.0202194	XXX	XXX	0.0264148
0.023649	0.0331026	XXX	0.0230508	0.0249801	XXX	XXX	0.0260419	0.0254778	0.0279136	0.0287201	XXX
XXX	0.0311928	0.0303982	XXX	XXX	0.0191758	0.0230474	XXX	0.0202459	XXX	XXX	0.0268333
0.0228195	0.0316942	0.0275729	0.0227985	0.0240791	XXX	0.0223399	0.0258856	0.023035	0.0256382	0.0276365	XXX
0.0270826	0.0317195	0.0307502	XXX	0.0247346	0.019721	0.0235054	XXX	0.0210283	0.0261126	XXX	0.0274621
0.0247577	0.0305503	0.0289363	0.0236343	0.0238353	0.0191072	0.0236605	0.0237568	0.0216944	0.025916	0.0265656	0.0271119

Window 4 32 29	Window 4 32 28	Window 4 32 27	Window 4 32 26	Window 4 32 25	Window 4 32 24	Window 4 32 23	Window 4 32 22	Window 4 32 21	Window 4 32 20	Window 4 32 19	Window 4 32 18
XXX	XXX	XXX	XXX	XXX	XXX	XXX	XXX	0.183445	0.158443	XXX	XXX
XXX	XXX	XXX	XXX	XXX	XXX	0.0260783	0.0232403	0.0235271	XXX	XXX	XXX
XXX	XXX	XXX	XXX	XXX	0.0203519	XXX	XXX	0.0179482	XXX	XXX	XXX
XXX	XXX	XXX	XXX	XXX	XXX	0.0224891	XXX	0.0177937	0.0245439	XXX	XXX
XXX	XXX	XXX	XXX	XXX	0.0234959	XXX	0.0203782	0.0187064	XXX	XXX	0.0246929
XXX	XXX	0.021107	XXX	XXX	XXX	XXX	XXX	0.0186428	XXX	XXX	XXX
XXX	XXX	XXX	XXX	XXX	XXX	0.0237042	0.0211627	0.0185762	0.0258129	XXX	XXX
XXX	XXX	0.0210706	XXX	XXX	0.0226243	XXX	XXX	0.0183319	XXX	XXX	0.0258608
XXX	0.0292893	XXX	0.0265284	0.031424	XXX	XXX	XXX	0.0250494	XXX	XXX	XXX
XXX	XXX	XXX	XXX	XXX	0.0238961	0.0246608	0.0214521	0.019929	0.0264742	XXX	0.0255351
XXX	0.0255107	0.0231379	0.0223205	0.0272491	XXX	XXX	XXX	0.0206879	XXX	XXX	XXX
0.0267662	XXX	XXX	XXX	XXX	XXX	XXX	XXX	0.0171099	XXX	0.0283191	XXX
XXX	XXX	0.0223143	XXX	XXX	0.0237115	0.0244677	0.0219501	0.019326	0.0265191	XXX	0.0264946
0.0275802	0.0232196	XXX	0.0188899	0.0248846	XXX	XXX	XXX	0.01806	XXX	0.0282253	XXX
XXX	0.0219951	0.0208614	0.0197542	0.0254341	0.0225358	0.0227507	0.0208589	0.0178256	0.0256565	XXX	0.0259952
0.0281411	0.023966	0.0222256	0.0196378	0.0259816	XXX	XXX	XXX	0.0185993	XXX	0.0290296	XXX
0.0280593	0.0235282	0.021046	0.0196308	0.0251171	0.0245819	0.0249598	0.0239103	0.0187008	0.0248961	0.027038	0.0248401

Window 4 64 11	Window 4 64 10	Window 4 64 9	Window 4 64 8	Window 4 64 7	Window 4 64 6	Window 4 64 5	Window 4 64 4	Window 4 64 3	Window 4 64 2	Window 4 64 1	Window 4 32 30
XXX	XXX	0.0207166	XXX	0.0268188	XXX	0.0249886	XXX	XXX	0.0212715	0.0195596	XXX
XXX	XXX	0.0202399	XXX	XXX	XXX	0.0234097	XXX	XXX	0.0197914	XXX	XXX
XXX	0.0212624	0.0222103	XXX	XXX	XXX	0.0262417	XXX	0.0202068	0.0214469	XXX	XXX
XXX	XXX	0.0224902	XXX	0.028965	XXX	0.0269108	XXX	XXX	0.0223345	0.0217908	XXX
XXX	0.0233268	0.0243353	XXX	XXX	XXX	0.0291418	XXX	0.0220307	0.0238205	XXX	XXX
XXX	XXX	0.0276862	0.0291575	XXX	XXX	0.0321362	XXX	XXX	0.0291616	XXX	0.0253031
XXX	0.0229933	0.0239144	XXX	0.0290962	XXX	0.0279558	XXX	XXX	0.0231669	0.0219233	XXX
XXX	XXX	0.0219148	0.0218395	XXX	XXX	0.0267356	XXX	0.0210333	0.022429	XXX	XXX
0.0247881	XXX	0.0243742	XXX	XXX	XXX	0.0288863	XXX	XXX	0.0257728	XXX	0.0304579
XXX	0.0230125	0.0224134	XXX	0.0289883	XXX	0.0269657	XXX	0.0215648	0.0224162	0.0217012	XXX
0.192008	XXX	0.19469	0.190887	XXX	XXX	0.180973	XXX	XXX	0.193944	XXX	0.0267401
XXX	XXX	0.192223	XXX	XXX	0.191839	0.177618	0.179781	XXX	0.19034	XXX	XXX
XXX	0.0225829	0.0223948	0.0221363	0.0291885	XXX	0.0268768	XXX	0.0210064	0.0223271	0.0217269	0.0277735
0.0207412	XXX	0.0204447	XXX	XXX	0.0220847	0.0241517	0.0244502	XXX	0.0207322	XXX	XXX
0.02229	0.0225745	0.0217231	0.0223492	0.0283789	XXX	0.0260196	XXX	0.0212001	0.0224313	0.0224155	0.0262396
0.0222748	XXX	0.0222063	0.02352	XXX	0.023609	0.0254501	0.0257324	XXX	0.0225616	XXX	0.0254506
0.161351	0.158079	0.164382	0.160824	0.146509	0.162122	0.151069	0.152502	0.160726	0.16284	0.162611	0.0246973

Window 4 64 23	Window 4 64 22	Window 4 64 21	Window 4 64 20	Window 4 64 19	Window 4 64 18	Window 4 64 17	Window 4 64 16	Window 4 64 15	Window 4 64 14	Window 4 64 13	Window 4 64 12
XXX	XXX	0.0244932	0.0211869	XXX	XXX	XXX	0.0242145	XXX	XXX	XXX	XXX
0.0204516	0.0238002	0.0225714	XXX	XXX	XXX	XXX	0.0226162	XXX	0.0213054	XXX	XXX
XXX	XXX	0.0251547	XXX	XXX	XXX	XXX	0.0246199	XXX	XXX	XXX	XXX
0.0230417	XXX	0.0258705	0.0223732	XXX	XXX	XXX	0.0260067	XXX	0.0249926	XXX	XXX
XXX	0.0275239	0.0266311	XXX	XXX	0.0230714	XXX	0.0273644	XXX	XXX	XXX	XXX
XXX	XXX	0.0310825	XXX	XXX	XXX	0.0338618	0.0308284	XXX	XXX	0.0316683	XXX
0.0237527	0.0272769	0.0261805	0.0228678	XXX	XXX	XXX	0.0267274	XXX	0.0258671	XXX	XXX
XXX	XXX	0.0257052	XXX	XXX	0.0208284	0.0268358	0.0247191	XXX	XXX	0.0244037	XXX
XXX	XXX	0.027257	XXX	XXX	XXX	XXX	0.0277676	0.0236742	XXX	XXX	0.0296999
0.0227894	0.0275153	0.0258445	0.0223504	XXX	0.0207	XXX	0.0257864	XXX	0.0251971	XXX	XXX
XXX	XXX	0.18657	XXX	XXX	XXX	0.176149	0.18434	0.2006	XXX	0.184251	XXX
XXX	XXX	0.18237	XXX	0.167877	XXX	XXX	0.182012	XXX	XXX	XXX	0.182609
0.022789	0.0272323	0.0257339	0.0222216	XXX	0.0209493	0.0272156	0.0251767	XXX	0.0250914	0.0243641	XXX
XXX	XXX	0.0228373	XXX	0.0293164	XXX	XXX	0.0242493	0.0203978	XXX	XXX	0.025748
0.0224983	0.0273716	0.024995	0.0219763	XXX	0.0204057	0.0270038	0.0247946	0.019622	0.0255948	0.0244834	XXX
XXX	XXX	0.0254096	XXX	0.029976	XXX	0.0279401	0.0249277	0.0217418	XXX	0.0258084	0.0266538
0.157161	0.145938	0.156346	0.161887	0.140623	0.169572	0.147046	0.154833	0.169728	0.154602	0.154682	0.154686

Window 4 128 5	Window 4 128 4	Window 4 128 3	Window 4 128 2	Window 4 128 1	Window 4 64 30	Window 4 64 29	Window 4 64 28	Window 4 64 27	Window 4 64 26	Window 4 64 25	Window 4 64 24
0.023961	XXX	XXX	0.0225041	0.0252962	XXX	XXX	XXX	XXX	XXX	XXX	XXX
0.0231508	XXX	XXX	0.0213746	XXX	XXX	XXX	XXX	XXX	XXX	XXX	XXX
0.0259748	XXX	0.0240855	0.0241147	XXX	XXX	XXX	XXX	XXX	XXX	XXX	0.0231914
0.0232286	XXX	XXX	0.0212587	0.024073	XXX	XXX	XXX	XXX	XXX	XXX	XXX
0.0252795	XXX	0.0233982	0.0238005	XXX	XXX	XXX	XXX	XXX	XXX	XXX	0.0250813
0.0297394	XXX	XXX	0.0279503	XXX	0.027595	XXX	XXX	0.0276821	XXX	XXX	XXX
0.0241767	XXX	XXX	0.0222676	0.0251849	XXX	XXX	XXX	XXX	XXX	XXX	XXX
0.0245076	XXX	0.022229	0.0230183	XXX	XXX	XXX	XXX	0.0230315	XXX	XXX	0.0234316
0.0255635	XXX	XXX	0.0240924	XXX	0.0246013	XXX	0.0264111	XXX	0.0310228	0.0257923	XXX
0.0241556	XXX	0.0223992	0.0224252	0.0253589	XXX	XXX	XXX	XXX	XXX	XXX	0.0232336
0.0280768	XXX	XXX	0.0265893	XXX	0.192751	XXX	0.182945	0.190873	0.169834	0.184643	XXX
0.0286582	0.0279018	XXX	0.0270222	XXX	XXX	0.196386	XXX	XXX	XXX	XXX	XXX
0.0249403	XXX	0.02318	0.022819	0.0267071	0.0231488	XXX	XXX	0.023079	XXX	XXX	0.0237106
0.0290928	0.0285017	XXX	0.0276869	XXX	XXX	0.0224157	0.0256173	XXX	0.0283556	0.0230401	XXX
0.0273814	XXX	0.0257794	0.0256796	0.0291711	0.0231547	XXX	0.0252128	0.0224324	0.0277603	0.0251074	0.0241958
0.0294496	0.0287865	XXX	0.0280541	XXX	0.0245323	0.0230462	0.0269159	0.0236279	0.0300914	0.0254189	XXX
0.159314	0.160178	0.16594	0.164317	0.154068	0.163865	0.166717	0.154951	0.161759	0.142378	0.15583	0.155106

Window 4 128 17	Window 4 128 16	Window 4 128 15	Window 4 128 14	Window 4 128 13	Window 4 128 12	Window 4 128 11	Window 4 128 10	Window 4 128 9	Window 4 128 8	Window 4 128 7	Window 4 128 6
XXX	0.0237459	XXX	XXX	XXX	XXX	XXX	XXX	0.023076	XXX	0.0223653	XXX
XXX	0.0222976	XXX	0.0224737	XXX	XXX	XXX	XXX	0.0228774	XXX	XXX	XXX
XXX	0.0253808	XXX	XXX	XXX	XXX	XXX	0.0238426	0.0244244	XXX	XXX	XXX
XXX	0.0227151	XXX	0.0232547	XXX	XXX	XXX	XXX	0.0222184	XXX	0.0218732	XXX
XXX	0.0247727	XXX	XXX	XXX	XXX	XXX	0.0240476	0.0240382	XXX	XXX	XXX
0.027629	0.0287545	XXX	XXX	0.027299	XXX	XXX	XXX	0.0290125	0.0279274	XXX	XXX
XXX	0.0230114	XXX	0.0236489	XXX	XXX	XXX	0.0227189	0.0226907	XXX	0.0222672	XXX
0.0227027	0.0235729	XXX	XXX	0.0225681	XXX	XXX	XXX	0.0240865	0.0227346	XXX	XXX
XXX	0.0253962	0.0257945	XXX	XXX	0.0234328	0.0237922	XXX	0.0244391	XXX	XXX	XXX
XXX	0.0238235	XXX	0.0246139	XXX	XXX	XXX	0.0229422	0.02324	XXX	0.0235069	XXX
0.0267578	0.0280293	0.0278598	XXX	0.0262025	XXX	0.0268157	XXX	0.0271227	0.0267361	XXX	XXX
XXX	0.0289256	XXX	XXX	XXX	0.0266469	XXX	XXX	0.0278723	XXX	XXX	0.0277085
0.0232252	0.0239508	XXX	0.0246721	0.0226141	XXX	XXX	0.0236666	0.0240122	0.0229961	0.0232868	XXX
XXX	0.0291221	0.0294936	XXX	XXX	0.0271199	0.0278495	XXX	0.0281021	XXX	XXX	0.0280501
0.0256398	0.0263321	0.0275712	0.0271668	0.0250616	XXX	0.0257069	0.0258237	0.0262721	0.0260084	0.0259526	XXX
0.0286283	0.0295585	0.0299599	XXX	0.0276387	0.0274996	0.0282914	XXX	0.028574	0.0281876	XXX	0.0284941
0.164604	0.161076	0.157666	0.157943	0.162337	0.167389	0.16438	0.16545	0.162304	0.164739	0.161458	0.163336

Window 4 128 29	Window 4 128 28	Window 4 128 27	Window 4 128 26	Window 4 128 25	Window 4 128 24	Window 4 128 23	Window 4 128 22	Window 4 128 21	Window 4 128 20	Window 4 128 19	Window 4 128 18
XXX	XXX	XXX	XXX	XXX	XXX	XXX	XXX	0.0256628	0.0239585	XXX	XXX
XXX	XXX	XXX	XXX	XXX	XXX	0.0233317	0.0215795	0.0229083	XXX	XXX	XXX
XXX	XXX	XXX	XXX	XXX	0.0275155	XXX	XXX	0.0278521	XXX	XXX	XXX
XXX	XXX	XXX	XXX	XXX	XXX	0.0236126	XXX	0.0248558	0.0229678	XXX	XXX
XXX	XXX	XXX	XXX	XXX	0.0270339	XXX	0.0254834	0.026592	XXX	XXX	0.0267691
XXX	XXX	0.0277357	XXX	XXX	XXX	XXX	XXX	0.0310438	XXX	XXX	XXX
XXX	XXX	XXX	XXX	XXX	XXX	0.0243186	0.0235592	0.0246133	0.0232222	XXX	XXX
XXX	XXX	0.0230198	XXX	XXX	0.0265119	XXX	XXX	0.0254056	XXX	XXX	0.0256872
XXX	0.0255031	XXX	0.0255607	0.0277973	XXX	XXX	XXX	0.0280644	XXX	XXX	XXX
XXX	XXX	XXX	XXX	XXX	0.026288	0.0249859	0.0250364	0.0261825	0.0244323	XXX	0.0253185
XXX	0.028002	0.0271102	0.027794	0.029868	XXX	XXX	XXX	0.0302297	XXX	XXX	XXX
0.0286348	XXX	XXX	XXX	XXX	XXX	XXX	XXX	0.0314661	XXX	0.028981	XXX
XXX	XXX	0.0231938	XXX	XXX	0.0266938	0.0253538	0.0247037	0.0257824	0.0244395	XXX	0.0263823
0.0289521	0.0295306	XXX	0.0288451	0.0312943	XXX	XXX	XXX	0.0313863	XXX	0.0293457	XXX
XXX	0.0268957	0.0260557	0.0269888	0.0288927	0.0292655	0.0280273	0.0275126	0.0284504	0.0273005	XXX	0.0286163
0.0293956	0.0298908	0.0284321	0.0292448	0.0316346	XXX	XXX	XXX	0.0317547	XXX	0.0296785	XXX
0.163602	0.159959	0.162418	0.158455	0.154248	0.153032	0.155665	0.158372	0.15487	0.159152	0.163353	0.151866

Window 4 256 11	Window 4 256 10	Window 4 256 9	Window 4 256 8	Window 4 256 7	Window 4 256 6	Window 4 256 5	Window 4 256 4	Window 4 256 3	Window 4 256 2	Window 4 256 1	Window 4 128 30
XXX	XXX	0.0239505	XXX	0.0199879	XXX	0.0201962	XXX	XXX	0.0194845	0.0196793	XXX
XXX	XXX	0.0231451	XXX	XXX	XXX	0.0189308	XXX	XXX	0.0186023	XXX	XXX
XXX	0.0212664	0.0222874	XXX	XXX	XXX	0.0193188	XXX	0.020025	0.0183659	XXX	XXX
XXX	XXX	0.0227316	XXX	0.019302	XXX	0.0192082	XXX	XXX	0.0184878	0.0184936	XXX
XXX	0.0224577	0.0236234	XXX	XXX	XXX	0.0199957	XXX	0.0203848	0.0191306	XXX	XXX
XXX	XXX	0.0232544	0.020561	XXX	XXX	0.0192014	XXX	XXX	0.0182722	XXX	0.0311013
XXX	0.0222191	0.0233582	XXX	0.0201343	XXX	0.0195373	XXX	XXX	0.0188311	0.0195184	XXX
XXX	XXX	0.0229544	0.0206409	XXX	XXX	0.0189375	XXX	0.0199888	0.0183787	XXX	XXX
0.0238744	XXX	0.0247124	XXX	XXX	XXX	0.0210157	XXX	XXX	0.0201774	XXX	0.0275629
XXX	0.181823	0.178014	XXX	0.192596	XXX	0.191494	XXX	0.186972	0.194113	0.194611	XXX
0.178584	XXX	0.17771	0.183067	XXX	XXX	0.190925	XXX	XXX	0.193461	XXX	0.0301596
XXX	XXX	0.178367	XXX	XXX	0.193473	0.191813	0.192996	XXX	0.19428	XXX	XXX
XXX	0.181436	0.177314	0.182996	0.192025	XXX	0.190954	XXX	0.186408	0.193786	0.193869	0.0263711
0.17962	XXX	0.178382	XXX	XXX	0.193975	0.192042	0.193306	XXX	0.19456	XXX	XXX
0.178499	0.180989	0.176896	0.182962	0.191587	XXX	0.190675	XXX	0.186395	0.193334	0.193627	0.0285429
0.15041	XXX	0.149025	0.154545	XXX	0.163746	0.161756	0.163346	XXX	0.164278	XXX	0.0318057
0.150767	0.15306	0.14934	0.154742	0.162963	0.163987	0.162113	0.163542	0.157962	0.164691	0.165069	0.153981

Window 4 256 23	Window 4 256 22	Window 4 256 21	Window 4 256 20	Window 4 256 19	Window 4 256 18	Window 4 256 17	Window 4 256 16	Window 4 256 15	Window 4 256 14	Window 4 256 13	Window 4 256 12
XXX	XXX	0.0237154	0.0225689	XXX	XXX	XXX	0.0209905	XXX	XXX	XXX	XXX
0.0216472	0.0214738	0.0233377	XXX	XXX	XXX	XXX	0.0214928	XXX	0.0205088	XXX	XXX
XXX	XXX	0.0228403	XXX	XXX	XXX	XXX	0.019655	XXX	XXX	XXX	XXX
0.0213088	XXX	0.0228769	0.0213514	XXX	XXX	XXX	0.0200261	XXX	0.0210019	XXX	XXX
XXX	0.0215702	0.0237796	XXX	XXX	0.0236304	XXX	0.0217875	XXX	XXX	XXX	XXX
XXX	XXX	0.0229034	XXX	XXX	XXX	0.0215196	0.0209546	XXX	XXX	0.0200373	XXX
0.0219106	0.0226714	0.0233229	0.0216121	XXX	XXX	XXX	0.0205546	XXX	0.0213125	XXX	XXX
XXX	XXX	0.0233576	XXX	XXX	0.0233817	0.0215402	0.0211649	XXX	XXX	0.0202676	XXX
XXX	XXX	0.0249185	XXX	XXX	XXX	XXX	0.0224251	0.0231256	XXX	XXX	0.0257915
0.179226	0.181507	0.178076	0.180623	XXX	0.174434	XXX	0.186541	XXX	0.183113	XXX	XXX
XXX	XXX	0.177472	XXX	XXX	XXX	0.184414	0.186467	0.181878	XXX	0.181873	XXX
XXX	XXX	0.178337	XXX	0.182539	XXX	XXX	0.186701	XXX	XXX	XXX	0.173049
0.17874	0.180867	0.177914	0.180426	XXX	0.173882	0.184123	0.186421	XXX	0.182822	0.182247	XXX
XXX	XXX	0.178624	XXX	0.182948	XXX	XXX	0.186761	0.183274	XXX	XXX	0.173447
0.178934	0.180716	0.177595	0.180301	XXX	0.173534	0.183938	0.185764	0.18177	0.182861	0.182012	XXX
XXX	XXX	0.149622	XXX	0.153203	XXX	0.155489	0.15716	0.153525	XXX	0.15372	0.144455
0.15074	0.15265	0.149893	0.152377	0.153353	0.146053	0.155745	0.157599	0.153757	0.154475	0.153879	0.144637

Window 4 256 30	Window 4 256 29	Window 4 256 28	Window 4 256 27	Window 4 256 26	Window 4 256 25	Window 4 256 24
XXX	XXX	XXX	XXX	XXX	XXX	XXX
XXX	XXX	XXX	XXX	XXX	XXX	XXX
XXX	XXX	XXX	XXX	XXX	XXX	0.0198693
XXX	XXX	XXX	XXX	XXX	XXX	XXX
XXX	XXX	XXX	XXX	XXX	XXX	0.0205795
0.0204188	XXX	XXX	0.0209603	XXX	XXX	XXX
XXX	XXX	XXX	XXX	XXX	XXX	XXX
XXX	XXX	XXX	0.0213681	XXX	XXX	0.0207302
0.0220195	XXX	0.0246569	XXX	0.0232399	0.0230851	XXX
XXX	XXX	XXX	XXX	XXX	XXX	0.183499
0.183269	XXX	0.177478	0.183547	0.179413	0.182351	XXX
XXX	0.184082	XXX	XXX	XXX	XXX	XXX
0.18439	XXX	XXX	0.183706	XXX	XXX	0.183129
XXX	0.184672	0.178712	XXX	0.181119	0.183074	XXX
0.184012	XXX	0.177814	0.183379	0.179892	0.181823	0.183271
0.155678	0.154894	0.149835	0.15507	0.151829	0.153506	XXX
0.156025	0.154844	0.149804	0.155202	0.151834	0.153927	0.154843

APPENDIX VII: MINERAL SILICATE MID-IR SPECTRA

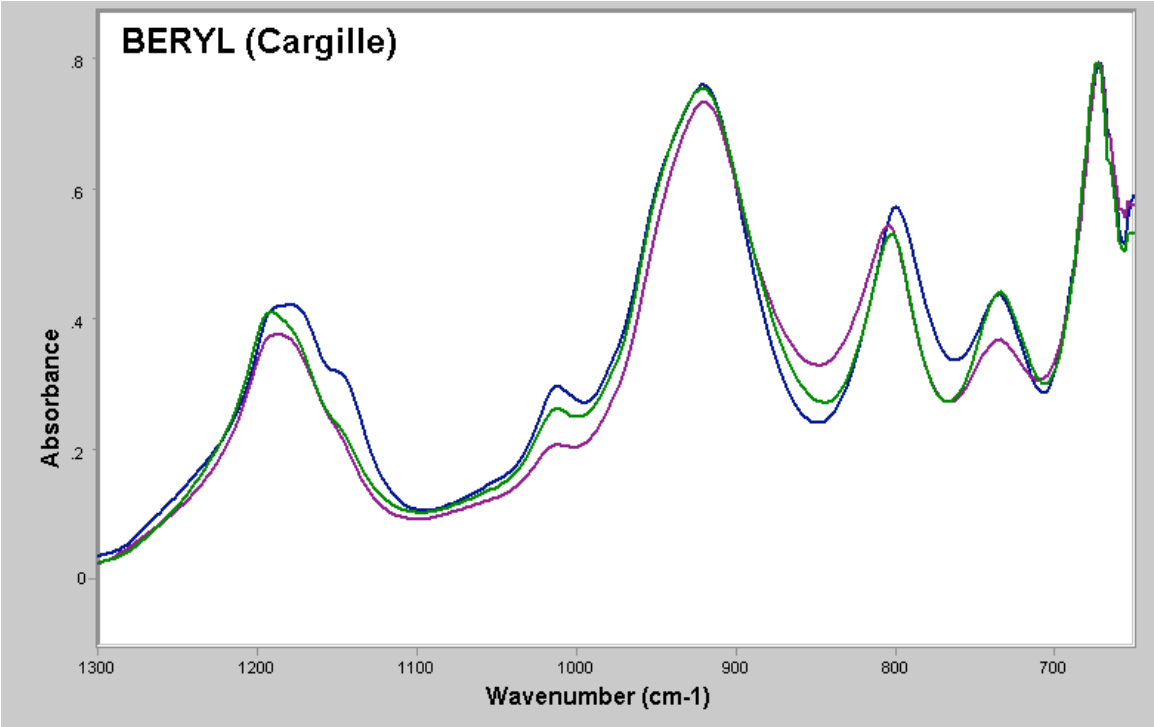


Figure 106: Mid-IR Spectra of Beryl. The mineral silicate sample was from the Cargille Reference Set.

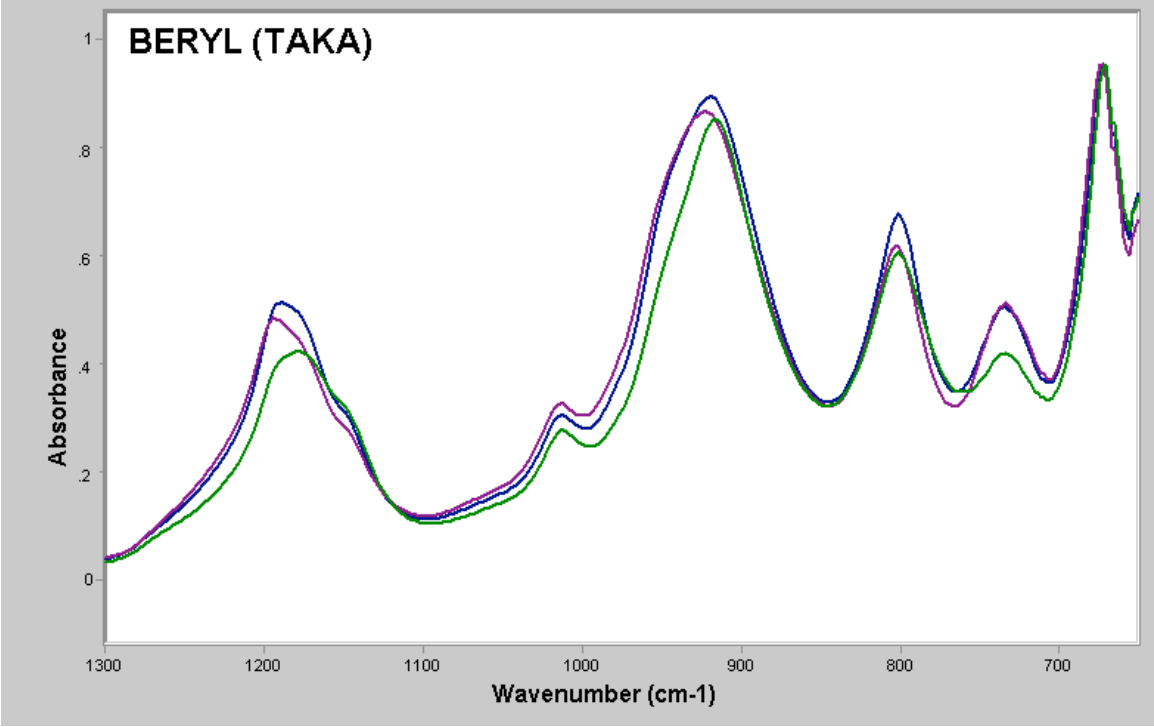


Figure 107: Mid-IR Spectra of Beryl. The mineral silicate sample was provided by Dr. Thomas A. Kubic (TAKA).

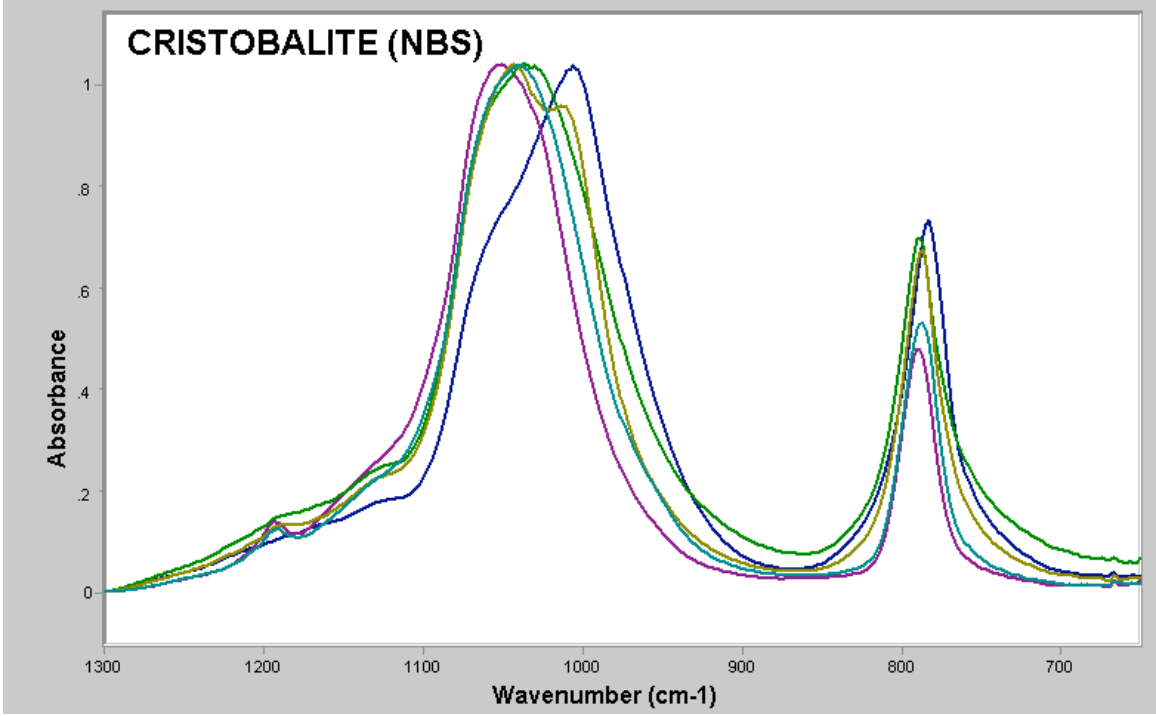


Figure 108: Mid-IR Spectra of Cristobalite. The mineral silicate sample was a NBS standard provided by Dr. Thomas A. Kubic (TAKA).

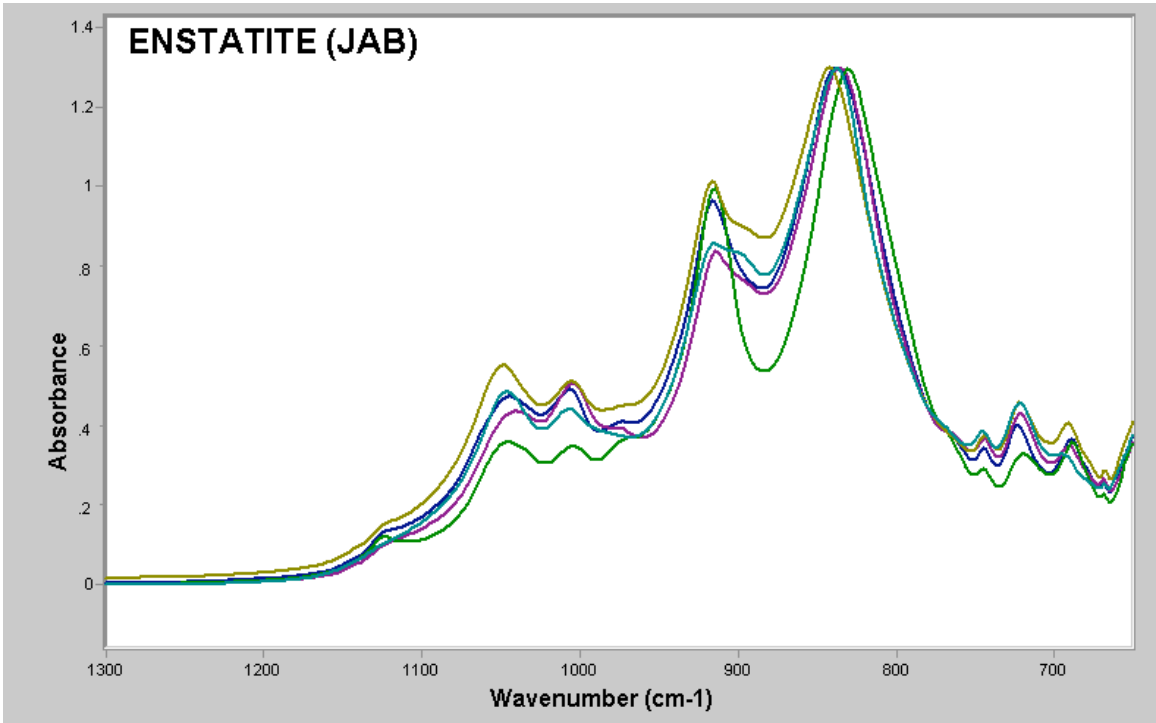


Figure 109: Mid-IR Spectra of Enstatite. The mineral silicate sample was provided by Dr. JoAnn Buscaglia.

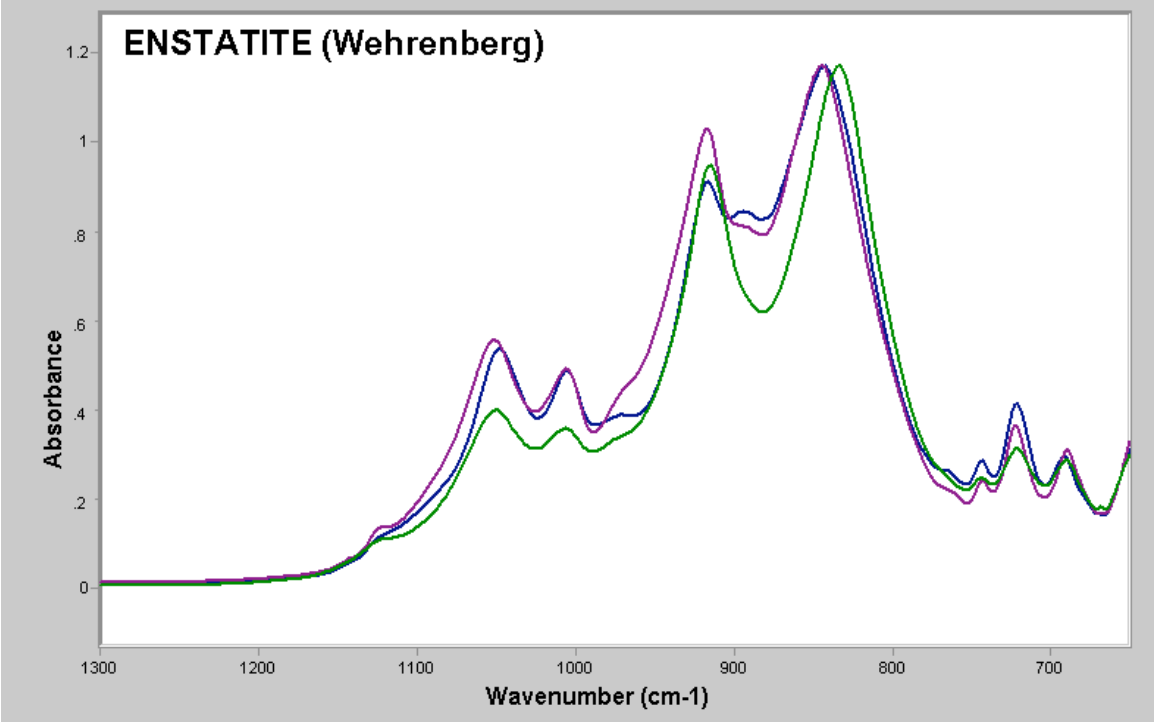


Figure 110: Mid-IR Spectra of Enstatite. The mineral silicate sample was from the Wehrenberg Mineral Set.

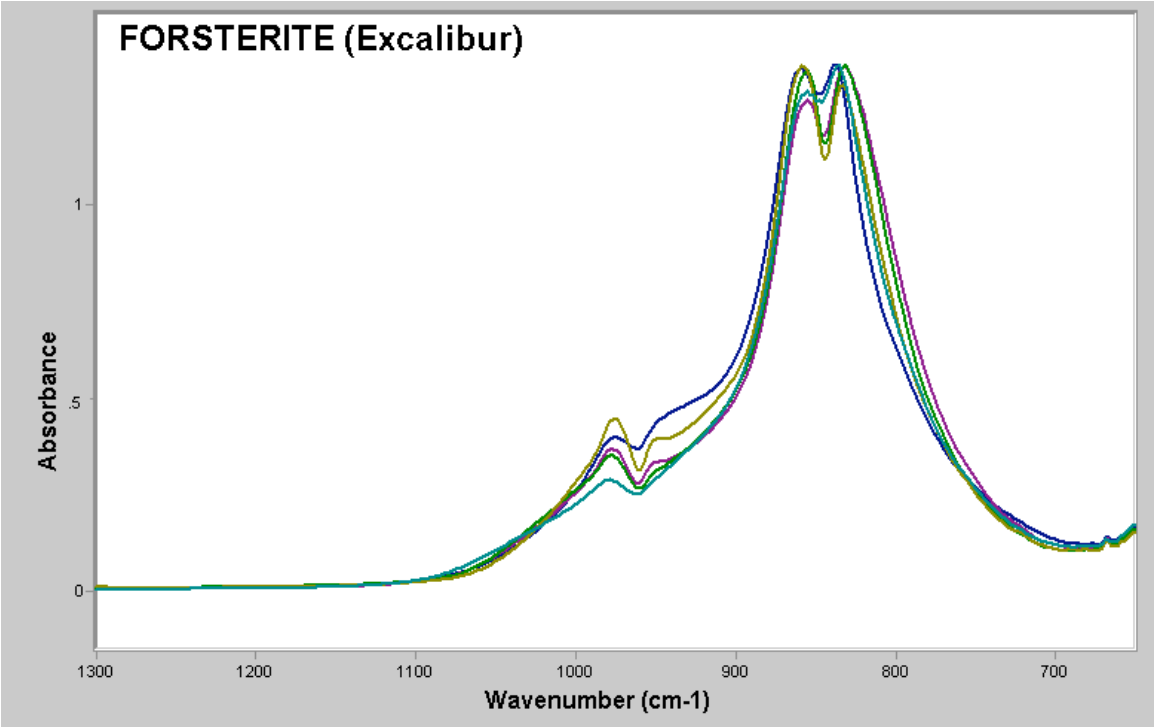


Figure 111: Mid-IR Spectra of Forsterite. The mineral silicate sample was provided by Tony Nikischer (Excalibur Mineral Corp).

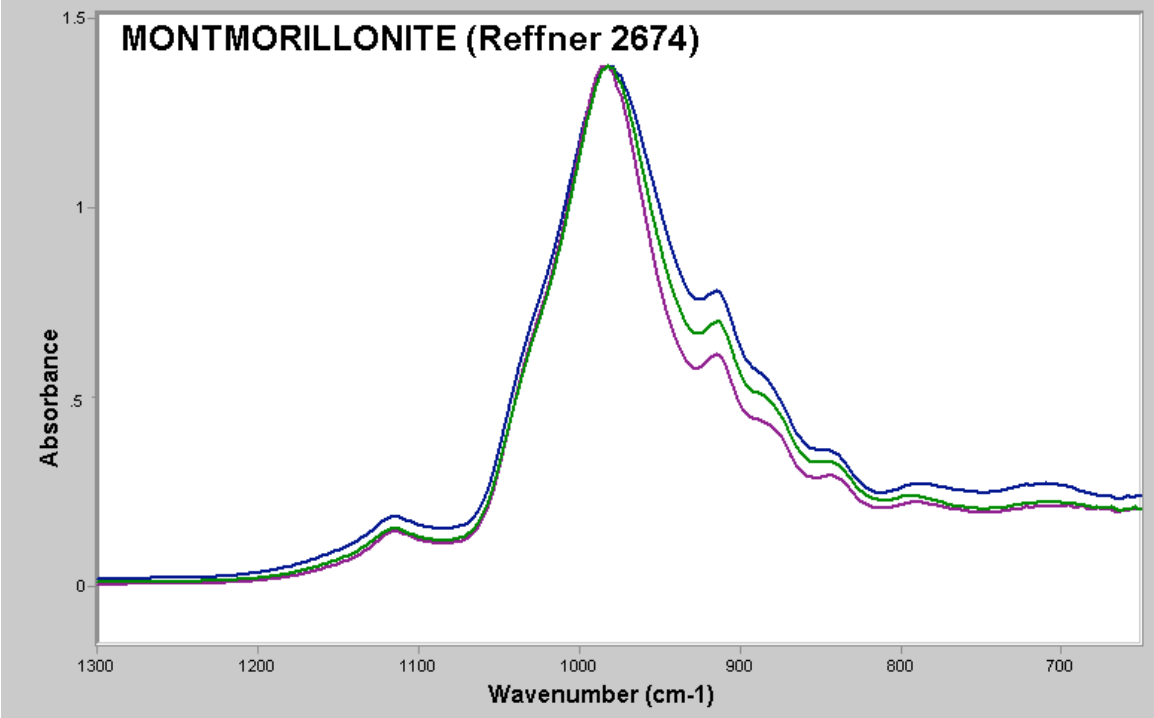


Figure 112: Mid-IR Spectra of Montmorillonite. The mineral silicate sample was provided by Dr. John A. Reffner.

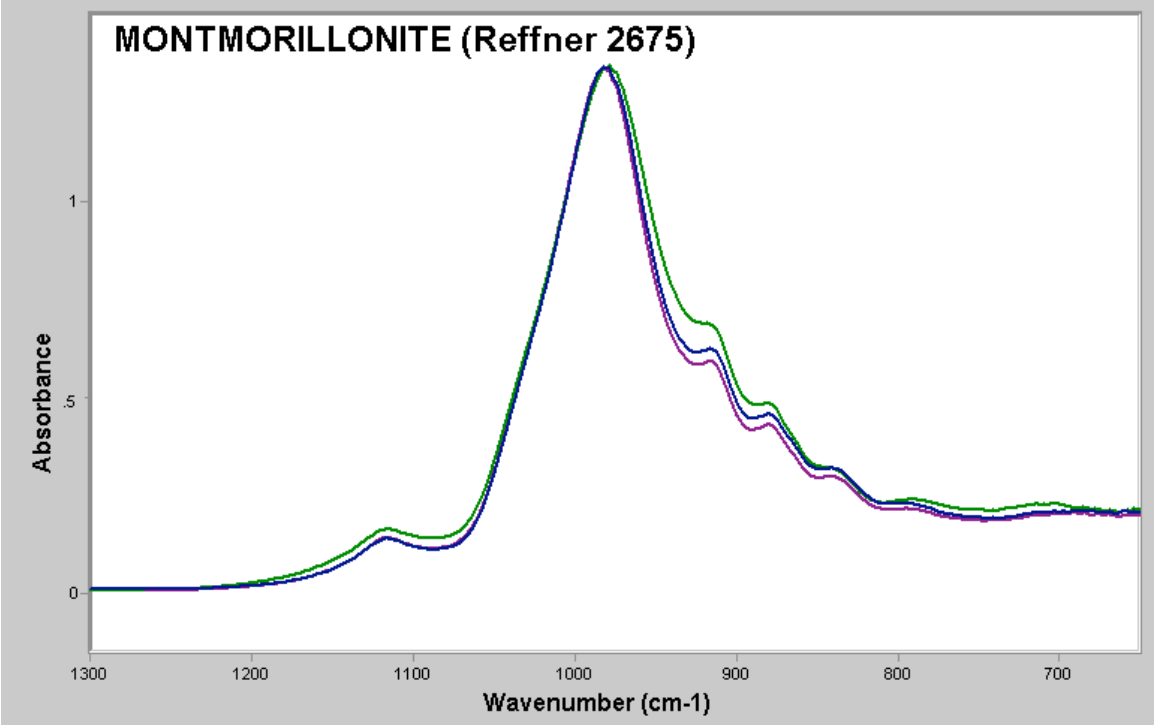


Figure 113: Mid-IR Spectra of Montmorillonite. The mineral silicate sample was provided by Dr. John A. Reffner.

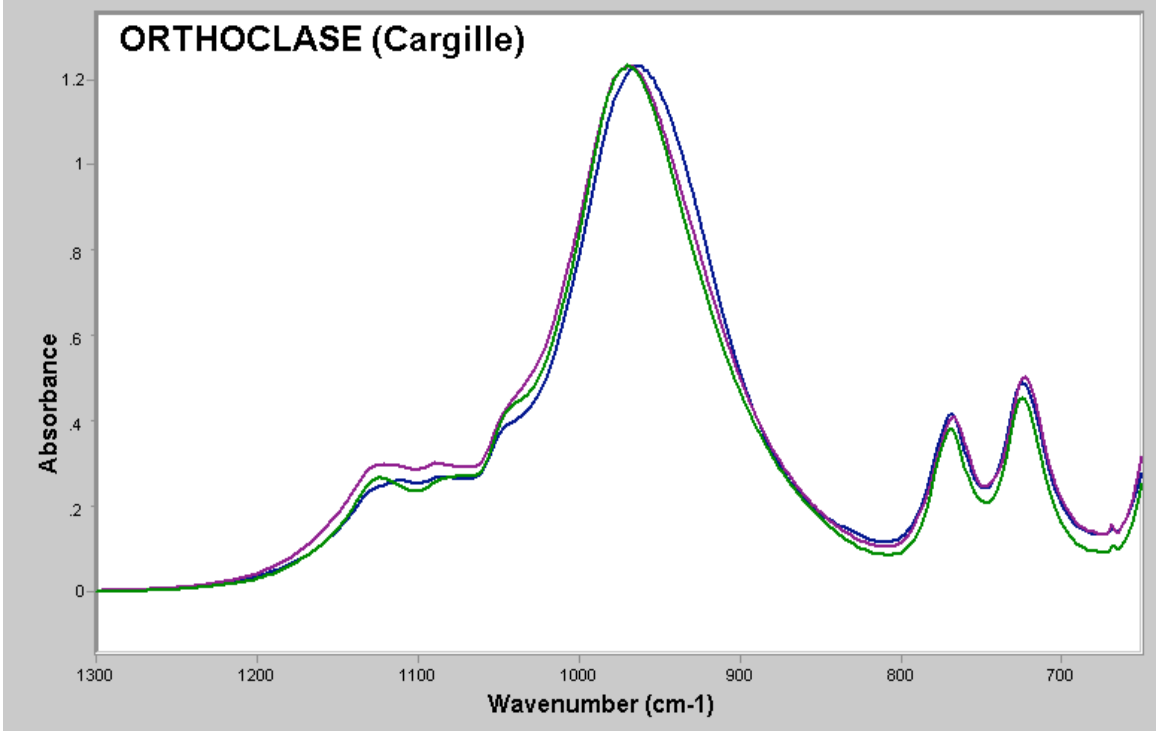


Figure 114: Mid-IR Spectra of Orthoclase. The mineral silicate sample was from the Cargille Reference Set.

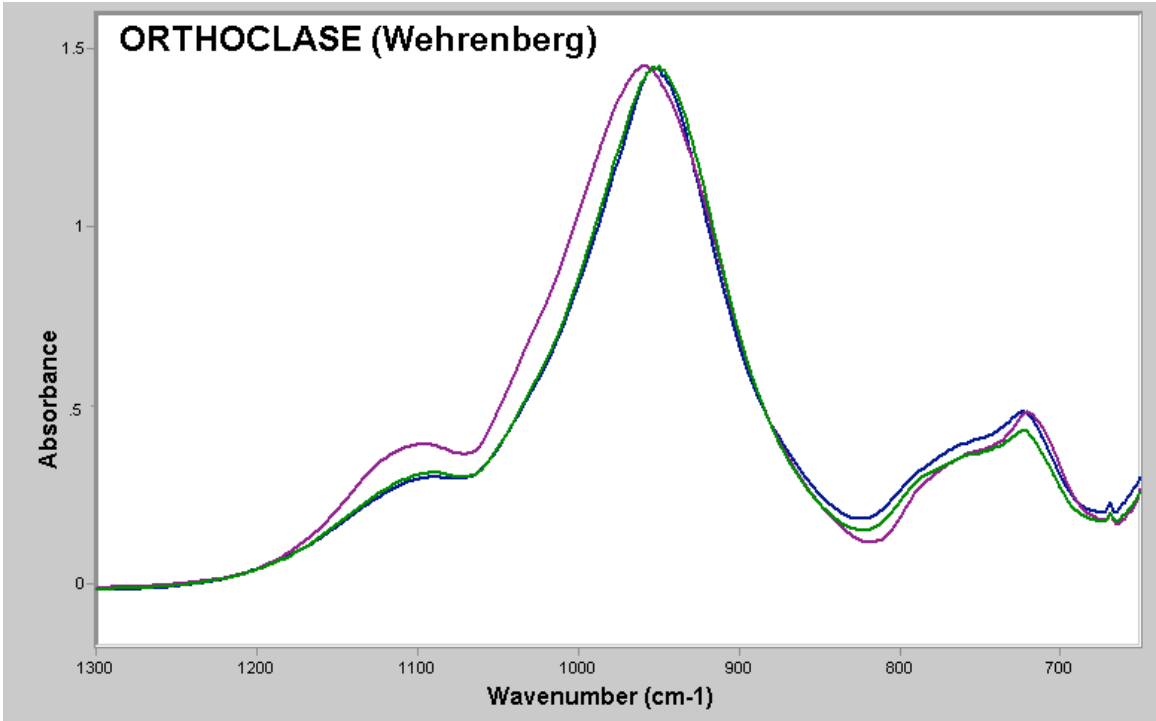


Figure 115: Mid-IR Spectra of Orthoclase. The mineral silicate sample was from the Wehrenberg Mineral Set.

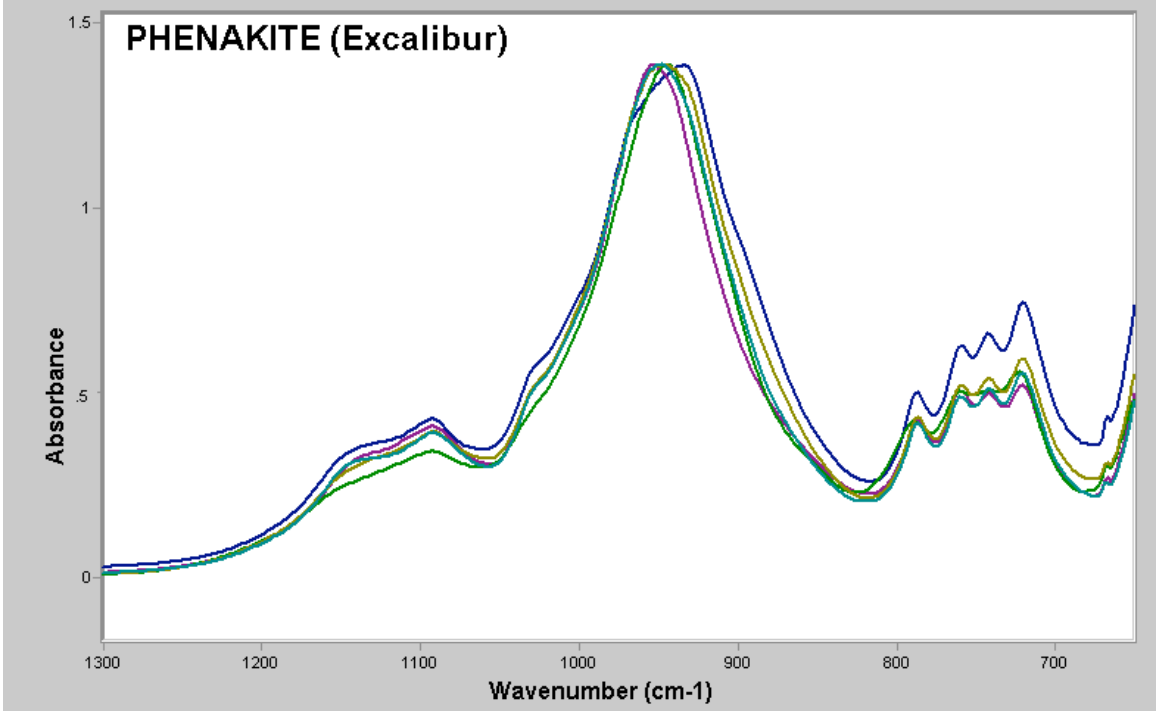


Figure 116: Mid-IR Spectra of Phenakite. The mineral silicate sample was provided by Tony Nikischer (Excalibur Mineral Corp).

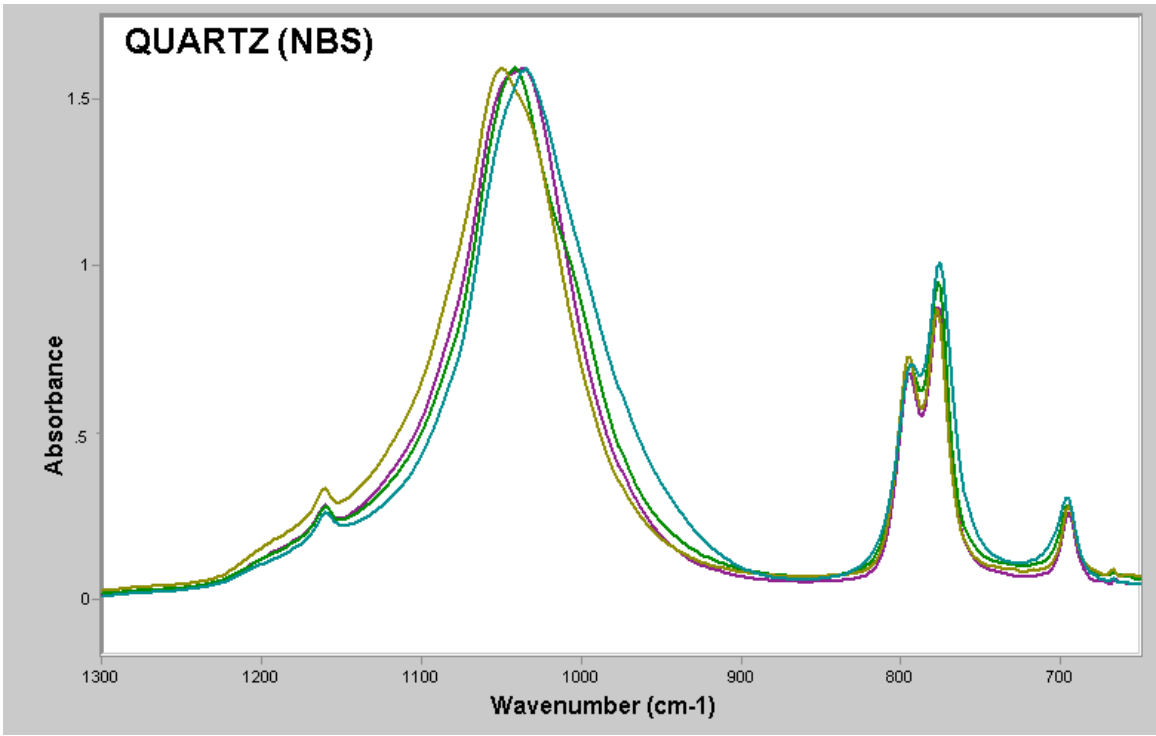


Figure 117: Mid-IR Spectra of Quartz. The mineral silicate sample was a NBS standard provided by Dr. Thomas A. Kubic (TAKA).

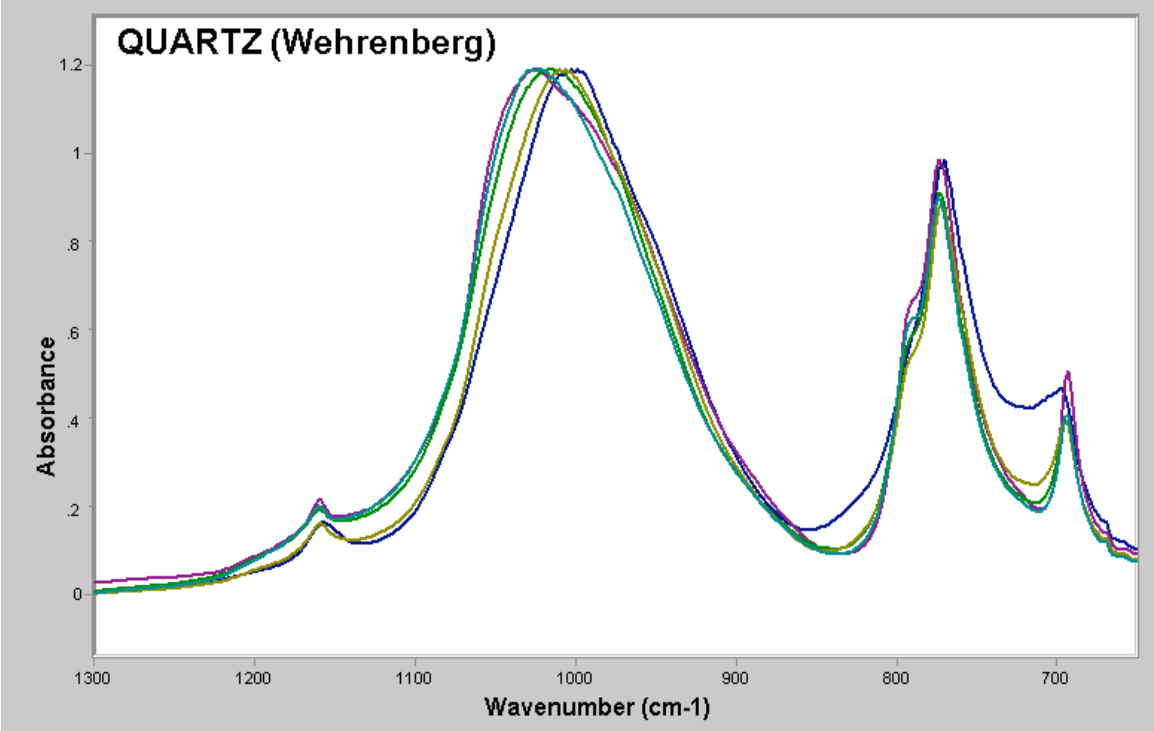


Figure 118: Mid-IR Spectra of Quartz. The mineral silicate sample was from the Wehrenberg Mineral Set.

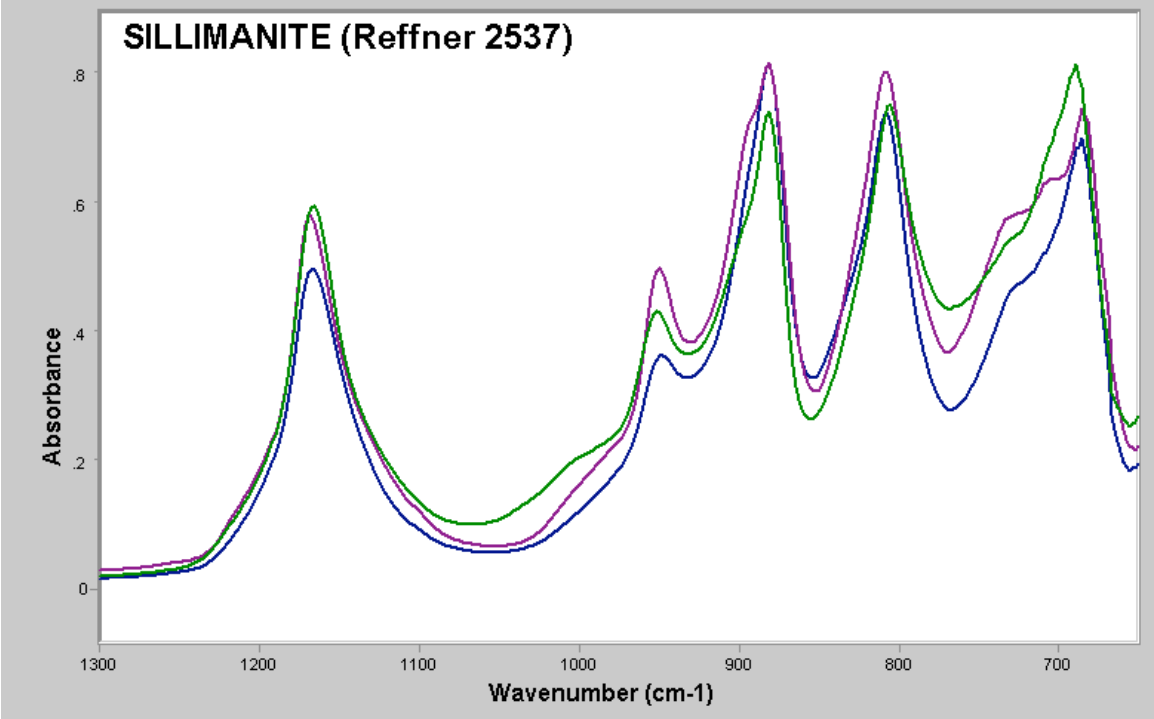


Figure 119: Mid-IR Spectra of Sillimanite. The mineral silicate sample was provided by Dr. John A. Reffner.

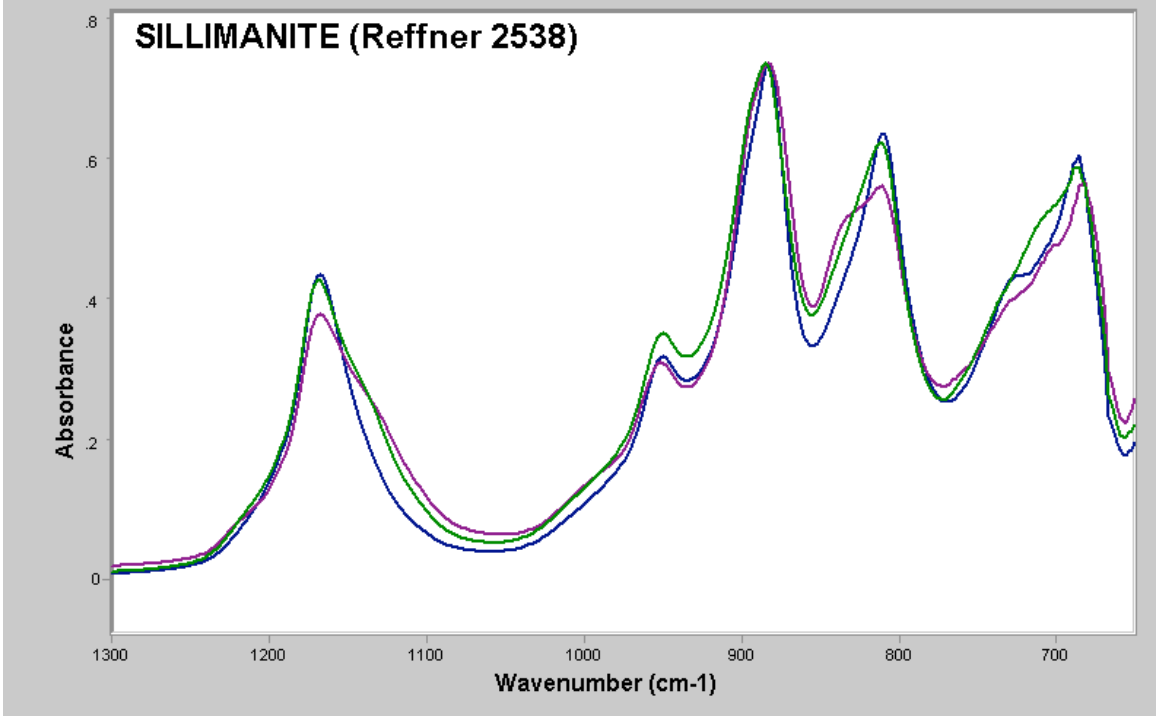


Figure 120: Mid-IR Spectra of Sillimanite. The mineral silicate sample was provided by Dr. John A. Reffner.

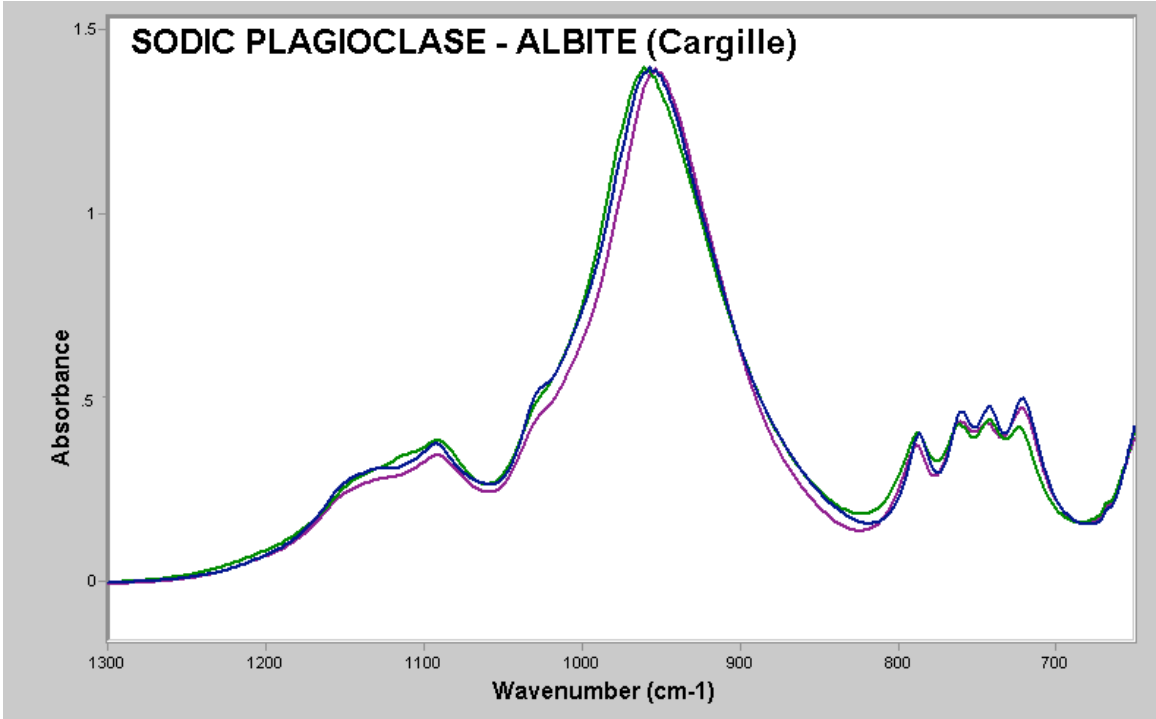


Figure 121: Mid-IR Spectra of Sodic Plagioclase - Albite. The mineral silicate sample was from the Cargille Reference Set.

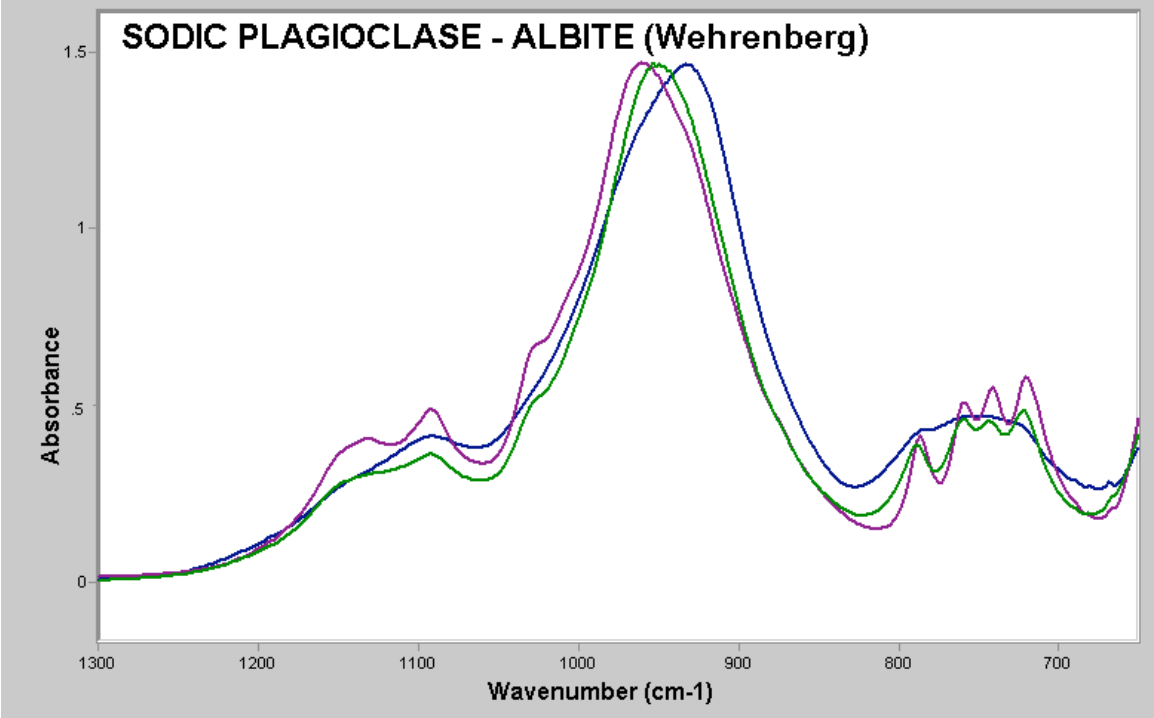


Figure 122: Mid-IR Spectra of Sodic Plagioclase - Albite. The mineral silicate sample was from the Wehrenberg Mineral Set.

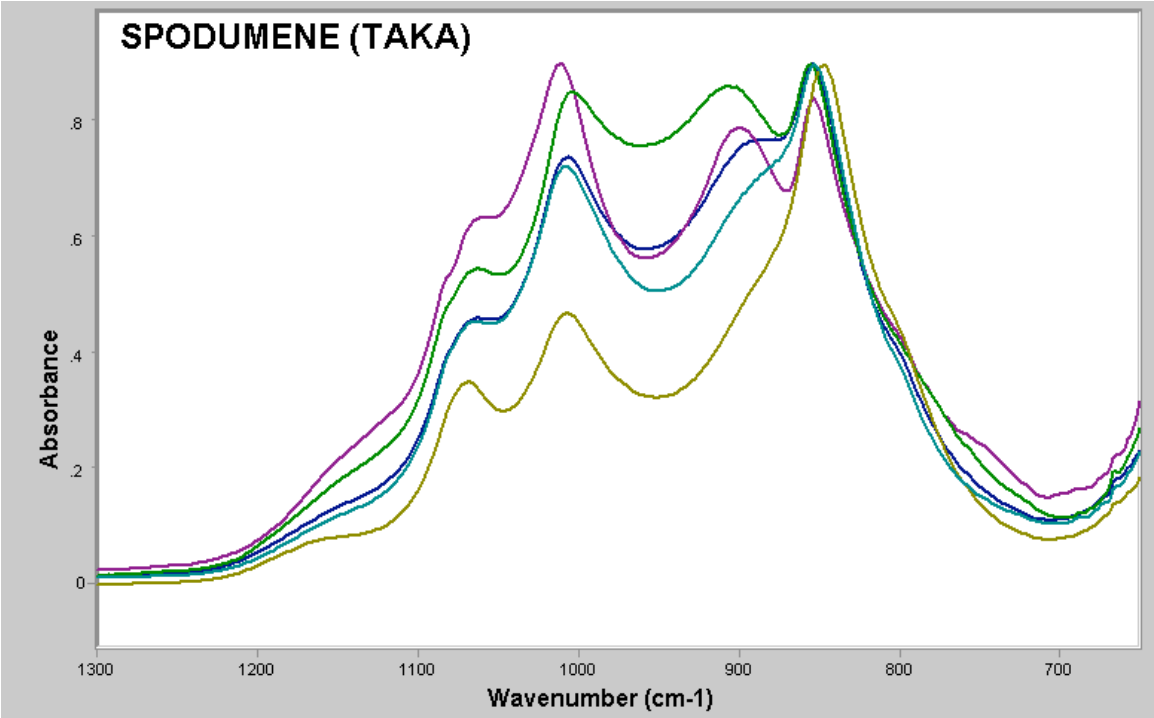


Figure 123: Mid-IR Spectra of Spodumene. The mineral silicate sample was provided by Dr. Thomas A. Kubic (TAKA).

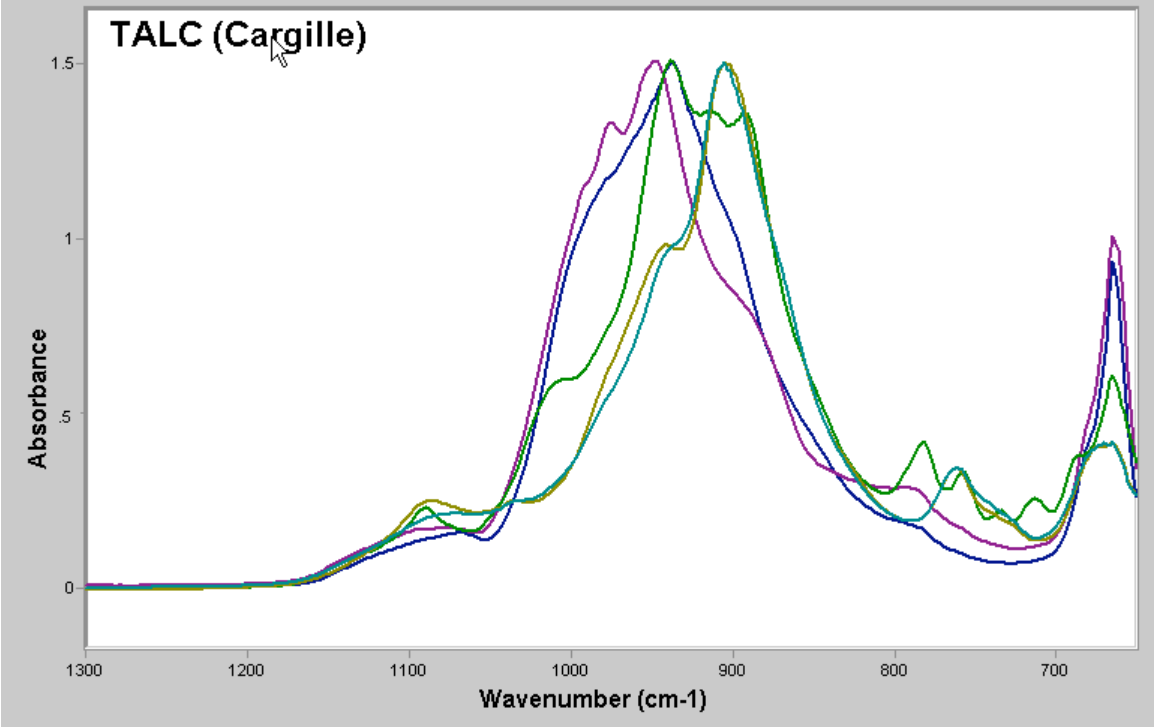


Figure 124: Mid-IR Spectra of Talc. The mineral silicate sample was from the Cargille Reference Set.

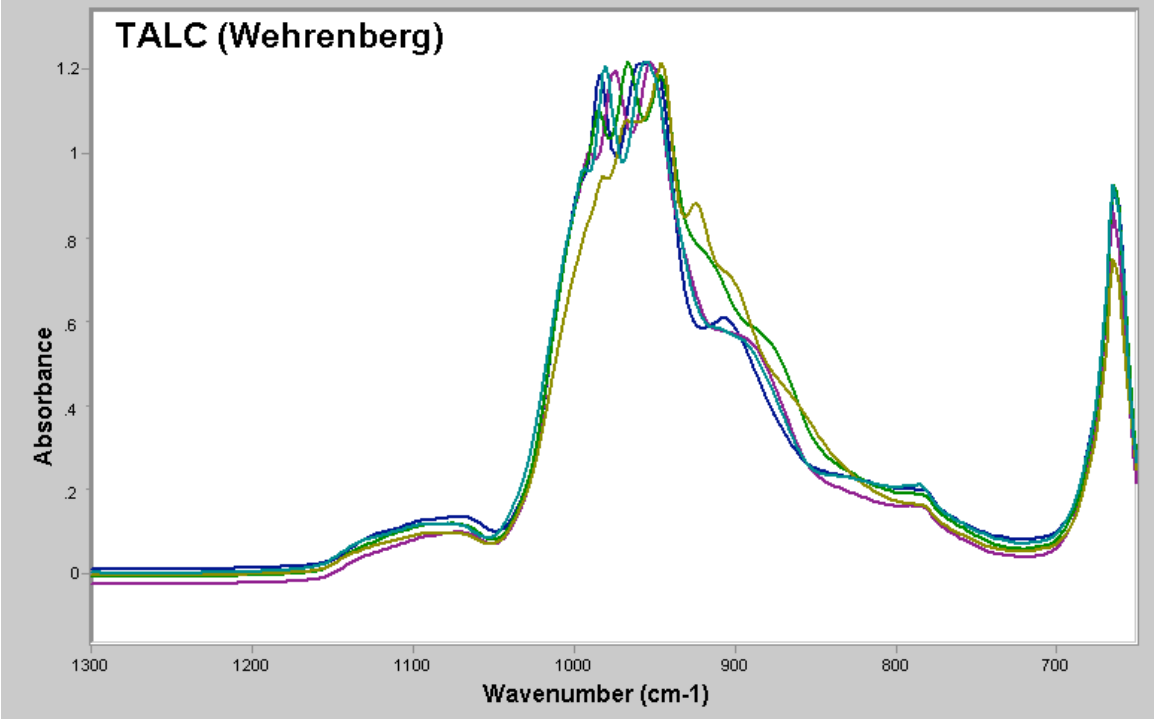


Figure 125: Mid-IR Spectra of Talc. The mineral silicate sample was from the Wehrenberg Mineral Set.

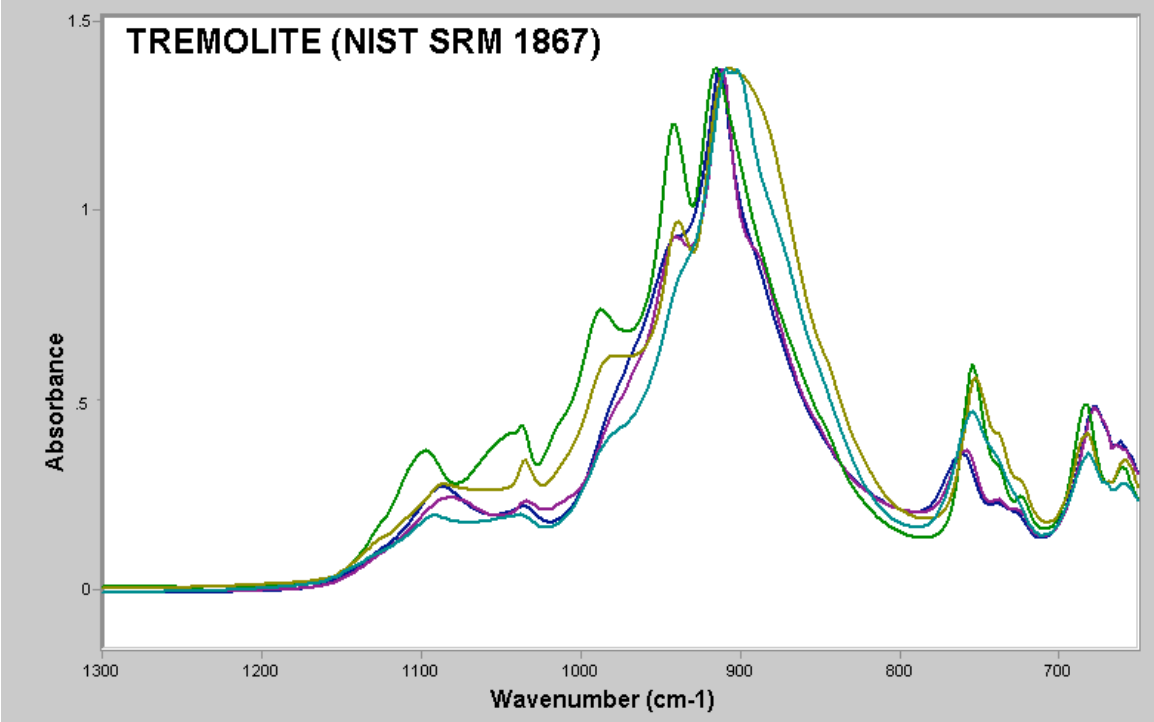


Figure 126: Mid-IR Spectra of Tremolite. The mineral silicate sample was a NIST standard (SRM 1867) provided by Dr. Thomas A. Kubic (TAKA).

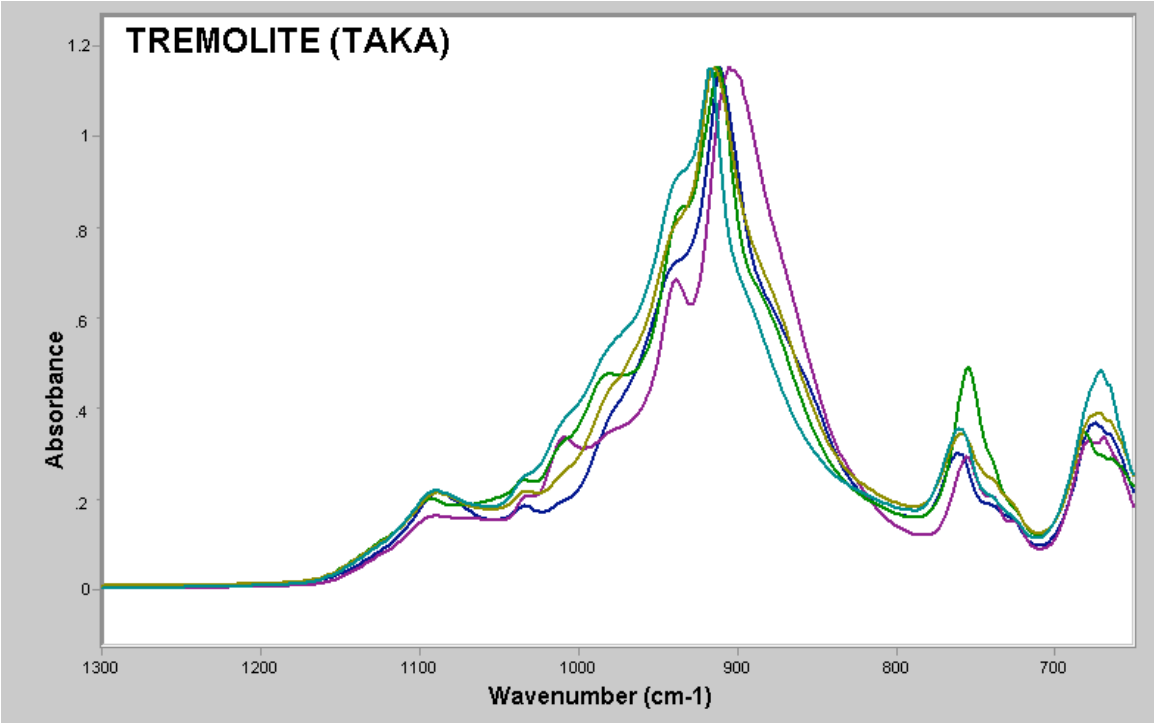


Figure 127: Mid-IR Spectra of Tremolite. The mineral silicate sample was provided by Dr. Thomas A. Kubic (TAKA).

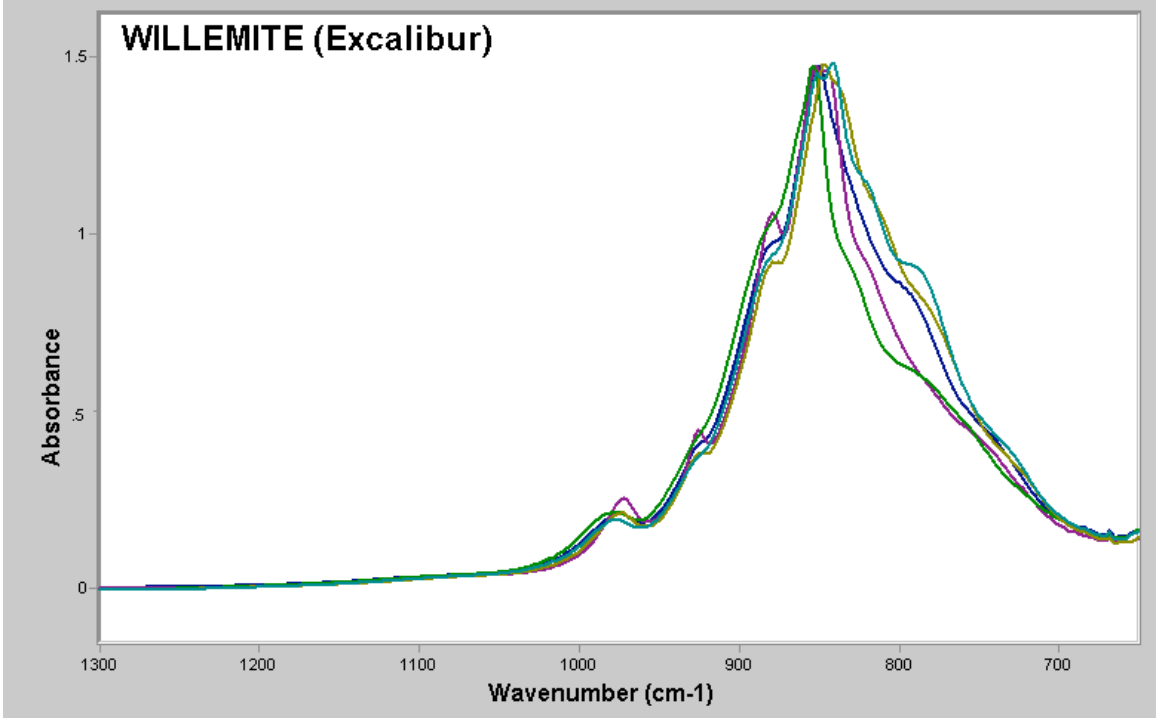


Figure 128: Mid-IR Spectra of Willemite. The mineral silicate sample was provided by Tony Nikischer (Excalibur Mineral Corp).

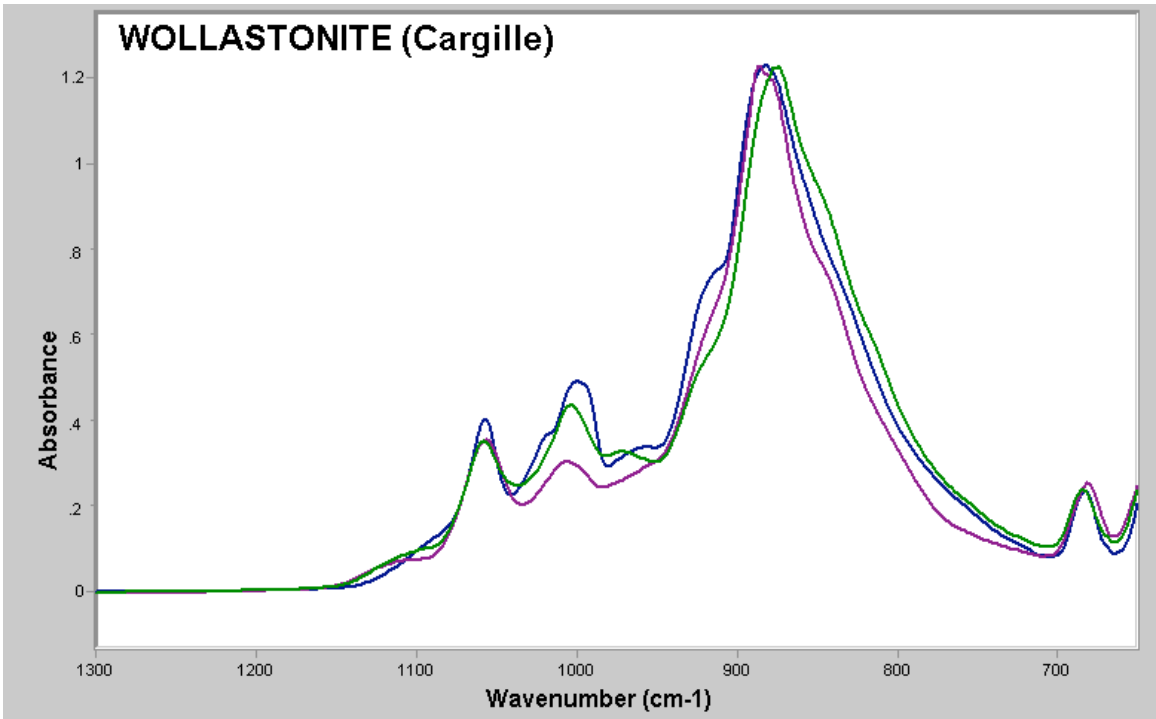


Figure 129: Mid-IR Spectra of Wollastonite. The mineral silicate sample was from the Cargille Reference Set.

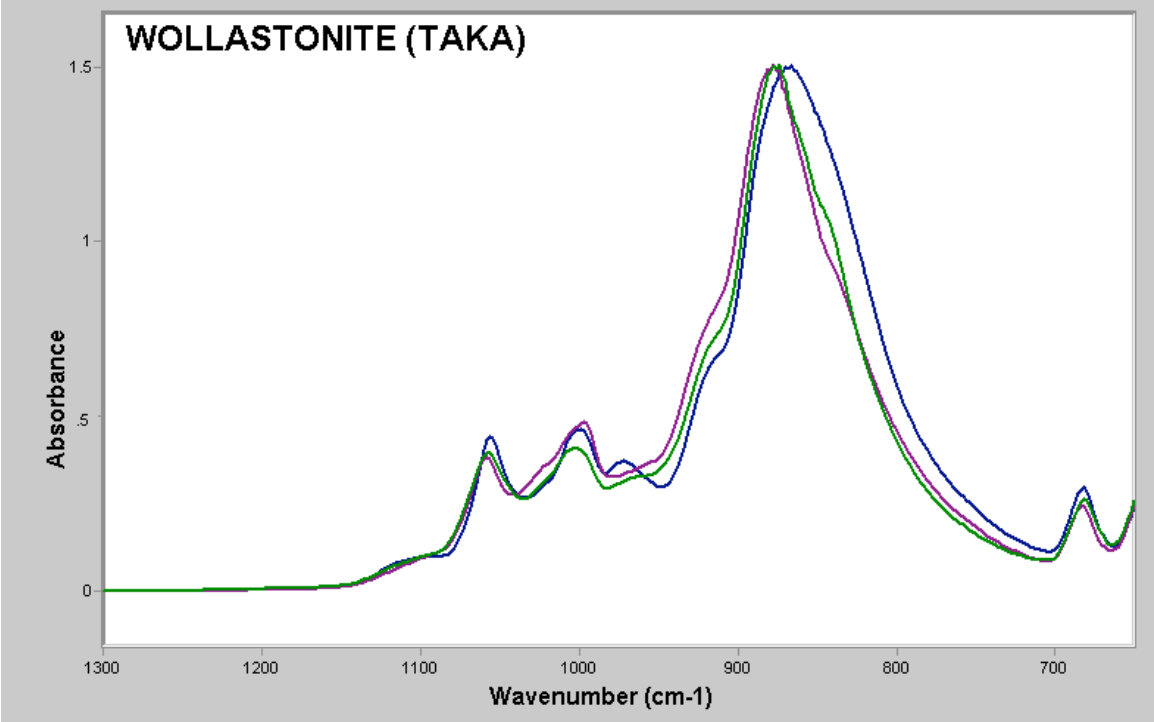


Figure 130: Mid-IR Spectra of Wollastonite. The mineral silicate sample was provided by Dr. Thomas A. Kubic (TAKA).

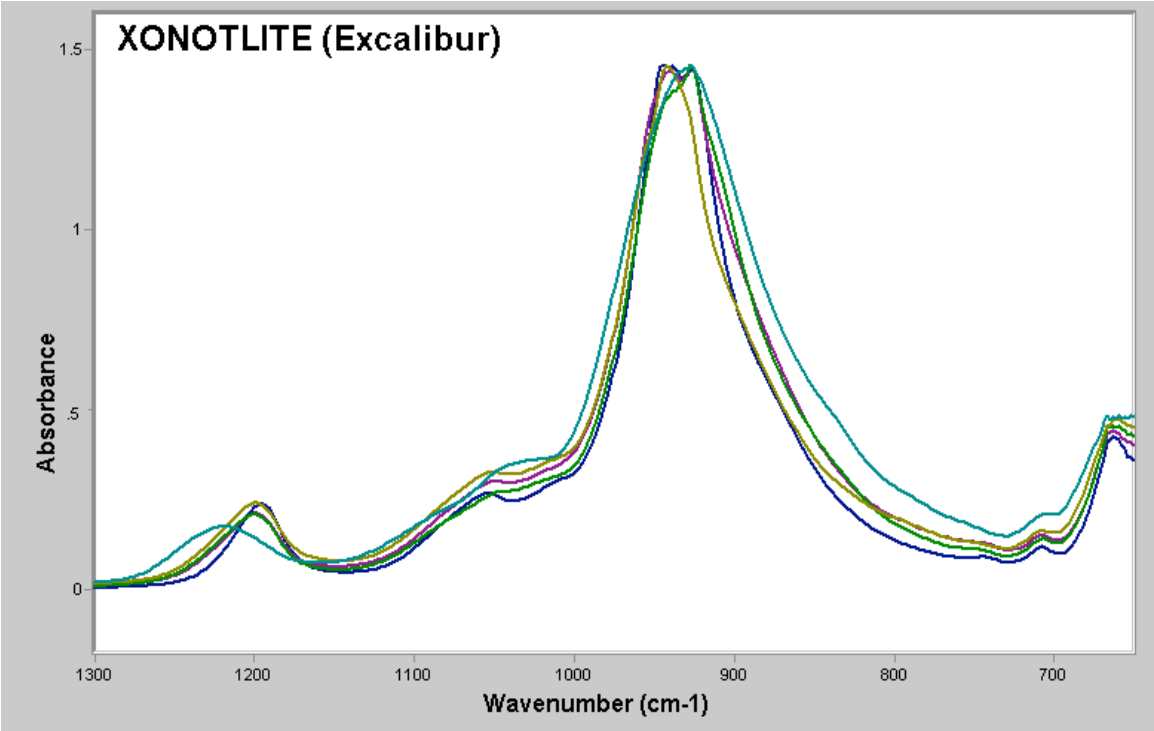


Figure 131: Mid-IR Spectra of Xonotlite. The mineral silicate sample was provided by Tony Nikischer (Excalibur Mineral Corp).

APPENDIX VIII: DECONVOLUTION DATA

Table 137: Peak positions (center X, in wavenumbers) from the deconvolution of 30 glass samples (10 replicates) into 6 peaks.

GLASS SAMPLE	Peak 1	Peak 2	Peak 3	Peak 4	Peak 5	Peak 6
W10 1	1114.503	1011.098	953.7268	911.556	778.6569	733.9703
W10 2	1121.96	1009.286	949.8505	910.2796	778.7568	736.9141
W10 3	1127.183	1011.829	960.0194	915.533	780.5713	739.6229
W10 4	1112.122	1011.744	951.2139	908.1649	778.492	738.257
W10 5	1111.992	1008.946	948.882	905.2473	777.2865	738.909
W10 6	1111.975	1001.04	944.3956	908.9694	779.2497	725.8046
W10 7	1120.209	1008.301	947.0294	907.2155	776.9516	739.5914
W10 8	1118.723	1013.023	954.9818	912.5369	778.7981	737.9479
W10 9	1117.834	1011.129	953.4844	910.4812	778.0346	734.7345
W10 10	1120.922	1023.06	973.6754	920.0343	780.5082	741.1892
W12 1	1120.834	1005.759	940.1134	903.8424	777.8744	738.9419
W12 2	1121.29	1013.008	952.4211	910.5235	778.6439	742.4755
W12 3	1117.45	1011.171	953.2573	910.0672	778.2482	739.1704
W12 4	1115.476	1011.843	953.508	909.9742	778.3399	738.0299
W12 5	1116.356	1011.253	952.1044	908.2271	777.6309	738.8089
W12 6	1120.294	1008.75	959.4862	915.0695	780.4456	743.3506
W12 7	1119.525	1009.355	948.4445	907.0103	776.477	744.3858
W12 8	1117.17	1009.752	950.2993	909.7971	778.7505	739.5102
W12 9	1116.856	1012.783	955.4212	913.567	779.9794	741.5214
W12 10	1117.676	1015.85	957.904	912.4923	779.2879	741.4584
W13 1	1118.281	1010.684	949.402	906.1094	776.5706	742.5578
W13 2	1121.819	1011.879	951.3624	907.8303	777.1551	741.423
W13 3	1131.145	1004.514	938.939	907.7908	778.8955	739.9917
W13 4	1118.871	1011.616	949.746	908.412	777.1715	741.7485
W13 5	1116.258	1011.649	947.009	908.895	778.9966	745.7671
W13 6	1121.566	1011.551	948.4567	906.568	776.716	743.7444
W13 7	1118.496	1012.583	953.012	910.2981	777.6665	738.0386
W13 8	1117.507	1012.827	953.8446	910.2407	777.953	737.6722
W13 9	1123.44	1007.842	943.9428	906.6742	777.9404	743.9849
W13 10	1121.465	1015.161	960.503	914.8854	780.1262	740.9728
W18 1	1118.135	1011.426	950.2435	909.022	777.9654	739.4047
W18 2	1118.595	1010.716	948.4464	903.7828	776.2585	743.5208
W18 3	1120.414	1010.895	950.7012	908.6654	777.6849	740.0144
W18 4	1119.119	1013.319	952.8981	908.6472	778.0261	738.7141
W18 5	1120.963	1011.984	953.7178	909.3247	777.8723	739.1569
W18 6	1118.901	1012.235	948.9961	905.9949	777.6249	743.2513
W18 7	1121.163	1010.987	950.6189	908.1371	777.846	741.0765
W18 8	1122.098	1012.501	954.0191	908.4031	776.697	738.9197
W18 9	1121.377	1013.415	953.4812	909.8589	777.838	740.6419

W18 10	1119.617	1012.201	952.4683	908.8853	778.0329	738.262
W35 1	1115.524	1012.763	952.4704	908.2974	776.8169	741.3242
W35 2	1120.789	1010.396	945.6775	905.7841	776.5247	748.7633
W35 3	1117.792	1014.752	954.4975	910.1186	779.1973	740.4446
W35 4	1120.009	1016.283	953.812	910.4101	780.1137	742.4289
W35 5	1116.792	1011.97	952.2306	908.778	777.919	739.4545
W35 6	1121.252	1011.696	949.4398	907.2952	776.427	739.8827
W35 7	1135.135	1004.022	946.8425	906.8409	779.507	741.405
W35 8	1119.712	1008.347	942.693	902.0977	773.5822	755.9792
W35 9	1122.217	1020.305	963.897	911.1292	776.5229	758.1391
W35 10	1117.741	1015.299	948.6832	904.885	778.7774	744.1933
W50 1	1117.791	1012.784	952.5513	911.7556	779.7366	740.8755
W50 2	1116.391	1013.247	953.201	908.445	777.4453	736.8788
W50 3	1115.454	1011.513	952.0416	910.0413	778.6459	739.5866
W50 4	1118.622	1012.972	953.5474	909.8484	777.6056	738.7259
W50 5	1117.845	1014.136	955.1428	911.4744	778.4789	737.8498
W50 6	1115.702	1014.97	953.5151	911.5702	779.0825	741.3144
W50 7	1118.097	1012.19	950.4869	907.7807	777.4132	739.2088
W50 8	1121.962	1006.302	940.8238	907.0475	778.9043	739.1212
W50 9	1114.951	1009.687	949.6739	906.9693	777.2129	739.2669
W50 10	1119.927	1012.797	946.7544	908.1264	779.7416	739.9483
W52 1	1120.388	1010.752	950.87	907.9948	777.5475	736.3903
W52 2	1123.695	1011.776	954.0792	910.2878	778.1122	735.7885
W52 3	1119.324	1011.569	953.7293	911.359	777.2613	734.0716
W52 4	1119.101	1012.813	954.4771	910.2709	778.3693	735.7079
W52 5	1120.169	1013.576	957.1159	911.9441	778.1588	736.2745
W52 6	1126.167	1013.408	956.3042	911.3332	778.5318	735.6205
W52 7	1124.567	1012.476	959.0082	912.5179	780.5198	748.2231
W52 8	1124.654	1013.801	956.3518	911.112	777.9274	734.3352
W52 9	1121.214	1013.981	956.7444	911.2367	778.603	738.2149
W52 10	1121.055	1012.212	953.6992	911.6107	778.1499	736.4048
W153 1	1131.435	1005.359	944.161	907.9449	780.7004	742.5127
W153 2	1124.682	1013.771	953.1596	909.5471	777.0538	739.517
W153 3	1119.969	1005.788	943.222	907.8206	782.8214	745.5201
W153 4	1128.7	1007.565	947.7121	908.2492	779.4141	741.4162
W153 5	1121.709	1014.187	955.9508	910.2321	778.9733	739.807
W153 6	1122.759	1011.267	952.329	909.5278	778.1411	739.0308
W153 7	1125.132	1011.313	950.7353	907.4201	778.1936	742.3348
W153 8	1126.1	996.6901	935.8411	902.6288	780.1191	735.4244
W153 9	1122.744	1011.773	951.5169	909.5816	776.9971	734.1716
W153 10	1125.094	1012.145	953.1285	908.6429	777.922	738.6686
W295 1	1125.69	1006.492	949.9012	909.1007	778.3465	747.3831
W295 2	1125.333	1011.538	957.2192	912.4831	780.6352	742.4848
W295 3	1124.907	1006.223	949.4636	908.1421	779.6217	740.8266
W295 4	1124.99	1005.858	950.9684	908.6492	779.3907	740.3836

W295 5	1125.17	1006.09	951.224	908.9926	779.7494	741.046
W295 6	1125.109	1006.636	948.462	904.8918	779.3534	741.9232
W295 7	1128.394	1008.31	950.1754	911.573	780.2285	741.3791
W295 8	1135.598	995.8914	934.025	902.9809	778.3443	744.2415
W295 9	1128.966	1008.255	950.3882	911.3446	780.1758	741.0392
W295 10	1133.641	1009.168	945.9831	908.379	780.1014	743.326
W360 1	1125.875	1007.644	951.7726	911.1198	780.176	741.3247
W360 2	1129.051	1003.571	946.3485	905.8705	776.705	740.376
W360 3	1125.813	1003.881	950.7849	907.2498	776.0965	745.6877
W360 4	1131.099	1001.037	944.6718	907.3328	776.5948	746.5125
W360 5	1126.782	1005.125	950.1023	907.7705	776.8769	740.0355
W360 6	1130.068	1007.202	949.1007	910.963	779.7282	739.5311
W360 7	1132.77	1000.14	942.5528	907.3584	776.6429	743.8895
W360 8	1131.2	1003.153	945.9161	906.9007	777.0256	750.1054
W360 9	1126.646	1006.778	952.2505	908.6711	777.7984	739.2473
W360 10	1129.833	1004.526	948.403	907.9795	777.8381	742.6296
W368 1	1124.891	1007.424	952.1075	908.4087	779.1468	739.8094
W368 2	1132.892	1001.957	939.3878	905.0595	776.7453	744.0536
W368 3	1125.689	1006.404	951.5723	909.6713	779.1798	739.3816
W368 4	1124.31	1006.641	952.2445	908.9398	779.1505	739.8594
W368 5	1125.612	1006.497	952.0827	909.888	779.3271	740.1112
W368 6	1130.319	1006.224	950.2585	909.5669	778.6249	743.8797
W368 7	1128.097	1004.811	947.4306	908.3202	778.5899	740.3335
W368 8	1130.772	1003.087	945.245	907.9339	778.2399	742.7009
W368 9	1133.168	1002.301	942.2169	907.9295	779.5011	740.1953
W368 10	1133.753	1001.335	943.7486	907.9218	779.8383	742.2674
W394 1	1131.688	1007.947	946.4588	906.3469	779.8874	741.4185
W394 2	1127.409	1005.332	948.6592	910.2076	779.0697	740.186
W394 3	1106.688	994.26	944.7345	907.4151	778.8081	746.803
W394 4	1125.962	1008.873	944.3808	906.11	779.0058	741.0607
W394 5	1131.868	1005.829	945.3439	906.9678	778.9997	742.0894
W394 6	1125.67	1006.774	951.5398	908.7823	780.6811	742.6742
W394 7	1126.387	1003.945	947.0767	908.5593	779.9998	741.8462
W394 8	1123.89	1009.063	953.8892	909.4923	781.0083	741.6601
W394 9	1124.372	1007.669	951.2966	908.3452	779.6248	741.4387
W394 10	1125.187	1005.039	951.6991	910.1022	779.8891	741.6816
W411 1	1127.419	1003.827	946.9384	907.6564	779.5867	740.7852
W411 2	1126.892	1003.799	948.6418	907.255	778.3076	740.2596
W411 3	1133.582	998.1531	938.6801	903.4763	778.0484	740.4029
W411 4	1123.593	1005.999	951.59	908.4974	780.4736	740.5291
W411 5	1127.21	1003.27	947.6796	907.2678	777.8666	741.1233
W411 6	1125.817	1011.212	946.8625	905.0047	781.6568	739.9242
W411 7	1127.291	1005.083	948.2876	908.432	779.6582	739.5516
W411 8	1129.344	1008.533	952.9041	912.4281	780.7669	740.2517
W411 9	1127.726	1007.411	953.0275	912.2559	780.2849	739.7843

W411 10	1128.453	1001.107	945.0381	906.3783	777.9009	740.5321
W412 1	1122.405	1004.21	949.4476	907.4551	778.1554	737.7129
W412 2	1123.087	1005.089	951.4131	908.3987	779.512	739.796
W412 3	1123.187	1005.771	948.3614	904.5969	779.658	740.1417
W412 4	1122.974	1006.858	950.2535	905.4726	780.3553	740.617
W412 5	1118.632	1008.318	954.9716	910.6687	781.8057	743.2074
W412 6	1124.959	1004.044	945.9485	905.7437	778.9653	739.1898
W412 7	1126.167	1003.854	948.7278	906.0603	776.949	738.9066
W412 8	1121.793	1005.45	951.3699	906.7936	780.4298	741.3115
W412 9	1122.602	1005.484	948.1397	903.9871	778.8614	737.9899
W412 10	1125.829	1004.359	947.0371	904.634	779.5686	740.8625
W442 1	1123.364	1004.76	951.4114	908.014	780.1091	737.8955
W442 2	1123.947	1008.234	953.6185	907.827	782.8365	743.321
W442 3	1124.532	1004.691	949.9143	906.9768	779.3344	736.5861
W442 4	1123.567	1006.188	952.5444	908.2875	781.9502	740.8751
W442 5	1121.467	1005.703	951.8258	905.9735	781.6715	740.4527
W442 6	1121.327	1005.446	948.3575	902.7997	781.644	739.6437
W442 7	1125.123	1001.938	947.3793	905.7274	779.3337	738.2016
W442 8	1125.166	1001.716	946.7097	904.1183	778.0149	738.1216
W442 9	1124.461	1003.381	949.3437	905.6639	779.3965	737.0383
W442 10	1124.19	1004.3	948.6567	905.6511	779.6103	738.3481
W444 1	1125.1	1004.185	949.0376	910.8093	781.1219	742.3532
W444 2	1134.503	1007.287	944.2829	908.0178	779.984	741.5591
W444 3	1135.046	997.7091	938.5826	904.4054	779.3261	742.7385
W444 4	1124.227	1004.618	950.422	909.1581	779.5867	739.4134
W444 5	1124.485	1004.212	950.0225	910.4678	780.721	741.8399
W444 6	1124.964	1010.138	956.6257	912.6165	780.0461	740.3453
W444 7	1131.124	1001.591	941.543	902.387	778.3582	749.7419
W444 8	1125.257	1005.969	950.6077	911.0768	781.2367	742.6651
W444 9	1125.861	1004.618	949.1599	910.3125	780.6845	742.1173
W444 10	1125.212	1003.86	948.8363	909.6615	780.1522	740.3356
W445 1	1123.585	1007.458	953.2488	907.8606	781.6525	743.687
W445 2	1123.292	1008.244	955.2762	911.8926	779.5701	739.3495
W445 3	1127.571	1004.047	947.4088	905.7255	778.2758	739.8089
W445 4	1121.734	1002.504	947.8329	907.6532	778.9792	739.1468
W445 5	1127.883	1003.92	948.7061	907.8248	777.2033	739.4374
W445 6	1124.967	1007.546	952.7088	908.4455	778.676	738.3027
W445 7	1127.335	1005.562	950.8763	909.597	779.3119	739.1199
W445 8	1130.323	1007.719	945.9621	905.7025	778.1604	739.0003
W445 9	1127.494	1005.082	948.4223	908.3594	778.559	738.977
W445 10	1126.31	1004.7	950.8339	908.4875	778.7722	739.0975
W446 1	1125.18	1008.489	953.4423	909.6469	781.2901	742.3137
W446 2	1122.157	1007.307	952.5059	908.4815	780.8828	741.8117
W446 3	1125.282	1004.602	948.9571	905.9804	779.3459	742.1087
W446 4	1127.046	1006.488	949.4496	909.2453	780.421	741.7065

W446 5	1128.182	1002.92	944.3024	904.8244	778.1161	743.7394
W446 6	1124.841	1006.101	952.1838	908.8307	780.8943	743.1938
W446 7	1123.053	1006.299	951.1692	906.9764	781.0456	741.8581
W446 8	1124.143	1006.372	951.1644	907.0303	779.8038	741.4433
W446 9	1125.247	1007.02	951.4132	908.0224	779.8169	740.4601
W446 10	1123.918	1007.226	953.0943	909.0696	780.2907	741.2036
W448 1	1126.659	1006.253	949.8062	907.2062	778.4266	740.7623
W448 2	1124.632	1005.812	950.8266	908.3404	779.2828	739.8382
W448 3	1126.815	1004.128	950.1621	909.0096	779.0042	740.8777
W448 4	1130.285	1007.842	946.5723	905.0954	779.8134	739.518
W448 5	1126.752	1006.459	951.7209	909.4969	779.3437	739.7259
W448 6	1126.826	1010.151	953.9955	911.5532	780.8539	742.874
W448 7	1132.217	1005.417	943.804	905.7019	778.1881	741.5688
W448 8	1123.667	1008.578	955.4367	910.5999	779.4896	739.408
W448 9	1130.511	1003.669	945.8032	905.4023	778.887	744.7658
W448 10	1127.84	1004.519	947.1421	905.6304	777.2485	744.4179
W450 1	1123.566	1007.795	952.2089	906.7061	781.5027	742.9076
W450 2	1124.465	1008.488	954.6023	910.0502	781.7724	743.9556
W450 3	1125.123	1007.245	951.9937	907.8874	780.597	742.1507
W450 4	1123.683	1007.661	952.8623	908.2327	780.9019	742.0723
W450 5	1128.311	1007.628	948.6015	905.9876	779.0524	740.0335
W450 6	1132.984	1006.904	943.1466	904.827	779.3891	741.0513
W450 7	1122.969	1008.533	955.2176	910.7986	781.8404	744.1024
W450 8	1126.009	1004.712	947.3391	906.6216	778.861	740.0412
W450 9	1125.824	1004.609	949.3957	905.4795	778.4467	740.9826
W450 10	1123.776	1006.034	950.8473	906.6585	778.8907	739.929
C50 1	1115.353	1012.456	951.8797	910.5727	781.5864	742.4306
C50 2	1110.448	1015.902	951.0786	907.9472	780.7321	736.7267
C50 3	1113.47	1009.535	951.7757	909.6053	778.6783	736.654
C50 4	1118.353	1008.821	948.5026	908.8393	779.6036	738.6768
C50 5	1116.437	1008.238	949.0374	908.4535	778.3301	736.489
C50 6	1117.569	1010.666	951.7959	909.3409	777.9595	734.5817
C50 7	1114.365	1008.419	950.3501	910.3981	780.2797	741.1968
C50 8	1113.561	1010.82	952.3881	907.4743	778.2552	735.4106
C50 9	1113.748	1010.433	952.4479	909.2167	777.4694	732.0052
C50 10	1115.866	1010.401	952.0284	909.1787	777.649	734.4352
C51 1	1119.253	1014.499	958.2366	913.7381	778.2524	738.7536
C51 2	1119.063	1012.384	954.2709	911.5114	777.2343	733.9083
C51 3	1129.735	1011.513	950.706	909.6757	776.5428	740.0468
C51 4	1129.513	1002.78	946.8252	909.8757	771.9792	714.5231
C51 5	1117.12	1013.304	956.7815	913.2929	776.9878	731.9494
C51 6	1123.097	1011.418	951.5845	908.3744	776.3567	738.0629
C51 7	1124.801	1009.657	955.3608	914.4203	779.0073	738.3895
C51 8	1124.452	1011.202	955.3814	914.2483	775.2625	728.4662
C51 9	1123.19	1011.776	952.3254	909.9723	777.6856	736.1273

C51 10	1119.1	1011.804	953.9313	912.3919	776.6521	732.8785
C52 1	1114.521	1012.312	951.6372	907.3438	776.6976	736.7021
C52 2	1116.576	1016.834	959.4862	913.6657	779.6559	740.9037
C52 3	1118.358	1012.64	951.4286	907.5814	776.1661	736.5372
C52 4	1119.168	1013.132	953.5578	909.7983	775.7805	734.3041
C52 5	1120.635	1009.453	946.4749	907.9588	777.5302	740.0265
C52 6	1115.693	1011.628	952.2704	907.9511	774.5903	732.9896
C52 7	1119.576	1011.396	950.5696	908.0757	775.074	734.9268
C52 8	1118.691	1008.911	947.3909	906.3771	774.7988	736.2234
C52 9	1107.655	1017.659	957.2619	911.2889	779.1691	739.4125
C52 10	1124.058	1009.861	941.2574	903.5311	776.3316	738.5412
C53 1	1126.892	1013.136	944.1712	904.7805	777.2176	745.4117
C53 2	1116.642	1012.467	955.1876	911.1632	777.4441	735.6232
C53 3	1118.408	1012.505	954.5527	910.453	776.8935	735.4407
C53 4	1129.407	1006.293	950.6887	907.9556	776.495	735.9824
C53 5	1115.573	1013.353	955.3197	910.7699	777.5127	734.8085
C53 6	1118.248	1015.581	950.7153	910.5911	778.8847	741.6152
C53 7	1121.505	1012.758	955.2548	909.487	776.3339	736.4472
C53 8	1120.476	1010.384	946.8092	906.9986	777.5827	738.8327
C53 9	1113.872	1011.523	947.6074	908.5815	776.6415	741.3884
C53 10	1116.814	1015.336	958.5204	913.154	777.7095	737.3444
C54 1	1117.427	1014.246	954.2454	910.5253	775.1484	733.5602
C54 2	1113.846	1014.932	957.2296	911.641	776.8373	735.3929
C54 3	1114.947	1014.108	953.4264	907.4843	776.4867	736.186
C54 4	1116.615	1014.521	954.5715	908.5854	776.4085	735.6464
C54 5	1120.033	1012.65	951.2275	907.2	775.2063	735.8688
C54 6	1120.391	1012.728	949.4478	907.3147	774.4298	737.4389
C54 7	1116.505	1011.36	944.3908	901.6631	773.3735	745.0208
C54 8	1122.669	1009.527	944.1216	907.3442	777.1621	739.1096
C54 9	1115.77	1014.231	953.781	909.3535	775.7155	734.2661
C54 10	1123.081	1009.666	944.3049	907.4751	777.0347	738.5542
C55 1	1117.928	1013.726	955.8363	912.0993	776.3655	732.5287
C55 2	1119.08	1011.841	953.6222	912.1802	778.6377	738.9115
C55 3	1122.658	1011.463	951.2129	908.4151	774.8732	733.1824
C55 4	1118.795	1013.127	955.4342	910.8383	777.2064	735.1163
C55 5	1116.717	1013.757	957.4221	912.5256	777.5695	735.3516
C55 6	1126.232	1007.799	960.644	915.6869	777.0163	735.4722
C55 7	1129.109	1002.784	939.4072	907.2291	776.5772	734.9315
C55 8	1120.61	1017.284	958.491	913.9549	778.7771	739.4913
C55 9	1118.969	1013.543	952.9691	908.0145	777.0982	735.7259
C55 10	1118.459	1013.303	956.0114	910.7015	776.4793	734.066
C56 1	1115.554	1013.242	951.3757	905.5301	774.9369	736.3473
C56 2	1119.263	1013.387	953.2554	910.2806	775.985	735.5883
C56 3	1122.96	1013.433	952.5943	908.8287	775.4175	737.528
C56 4	1115.677	1009.897	950.0153	908.6811	778.5598	736.1802

C56 5	1126.02	1005.329	946.1208	910.1533	773.026	727.0958
C56 6	1129.938	1007.659	944.2833	908.9684	777.1822	737.1964
C56 7	1119.997	1012.864	951.1029	906.8848	774.8327	738.2089
C56 8	1119.965	1010.387	949.4771	908.8896	778.257	740.4473
C56 9	1121.307	1013.4	952.7684	908.9006	774.5573	735.8246
C56 10	1122.829	1013.946	950.6722	908.3823	775.2383	738.9677
C57 1	1129.415	1007.98	939.5665	904.005	777.277	739.1814
C57 2	1120.753	1016.379	958.3014	914.6906	778.9287	738.1987
C57 3	1124.698	1011.744	952.6053	908.7211	775.308	734.5001
C57 4	1119.696	1011.509	953.2012	912.7034	778.9308	738.7264
C57 5	1117.417	1012.923	954.7489	911.3162	776.451	733.2085
C57 6	1104.018	1013.605	955.0953	907.5374	775.9585	730.6403
C57 7	1134.22	1001.024	943.1934	908.245	776.9992	735.0923
C57 8	1120.493	1013.788	956.6801	910.013	776.3687	734.5549
C57 9	1119.252	1012.359	954.4185	910.5722	777.4875	735.9068
C57 10	1123.699	1010.799	952.0408	909.5759	776.3351	734.1002
C58 1	1118.165	1016.041	953.1214	909.5665	776.9642	738.6583
C58 2	1118.789	1011.057	948.8247	907.4924	775.6107	736.0703
C58 3	1123.842	1012.994	952.8632	908.1962	776.5023	736.9718
C58 4	1118.032	1011.403	951.1111	910.0444	776.7529	736.9899
C58 5	1119.739	1010.469	945.4042	904.9081	775.1911	739.647
C58 6	1125.547	1007.145	942.3595	907.3669	777.6655	738.6747
C58 7	1115.122	1012.862	952.8554	907.3019	775.9003	734.3322
C58 8	1127.115	1007.343	943.8445	908.0559	777.0822	737.5935
C58 9	1120.931	1011.804	948.9192	906.3838	775.2222	738.3401
C58 10	1116.642	1012.947	953.3628	909.4853	775.4796	733.4906
C59 1	1110.413	1002.524	946.3029	906.5533	771.7389	720.1516
C59 2	1108.435	1002.691	953.6781	908.2982	774.4903	730.475
C59 3	1112.007	1008.24	948.33	903.894	774.1197	724.6538
C59 4	1109.621	1009.858	953.007	905.6678	775.0349	729.2964
C59 5	1111.423	1009.734	951.9947	906.5177	776.1816	729.8699
C59 6	1113.846	1009.024	948.2222	904.653	776.2181	728.5861
C59 7	1113.969	1009.367	950.4182	905.4081	775.6146	728.5048
C59 8	1108.806	1007.87	949.5689	906.571	775.3213	729.074
C59 9	1107.04	1009.621	952.6705	907.4655	775.3199	727.3557
C59 10	1109.898	1007.584	949.0631	906.5189	774.3592	727.9188

Table 138: Peak areas (in absorbance units) from the deconvolution of 30 glass samples (10 replicates into 6 peaks.

GLASS SAMPLE	Peak 1	Peak 2	Peak 3	Peak 4	Peak 5	Peak 6
W10 1	22.50378	51.73519	63.78723	35.32942	14.82216	8.372366
W10 2	16.39921	57.79991	73.09708	38.94126	15.92779	9.682471
W10 3	16.55988	52.66086	54.30797	51.09776	12.4572	9.763576
W10 4	17.54026	48.429	73.11313	45.35826	17.7393	12.67799
W10 5	18.42793	52.69124	67.5819	39.96299	17.49534	9.764414
W10 6	20.22182	58.50165	72.26401	29.33054	19.47861	6.147725
W10 7	15.2626	58.08453	76.86737	43.28776	17.16286	11.20953
W10 8	17.57223	50.77084	68.66611	43.73687	15.17667	9.755783
W10 9	19.053	52.84702	67.71116	40.41253	15.74002	9.827101
W10 10	18.99983	38.34478	53.71909	60.95466	14.0162	8.058906
W12 1	15.34935	54.02953	79.86235	24.72498	16.92704	7.183779
W12 2	15.67317	54.10141	77.40058	49.81264	18.70049	10.32964
W12 3	19.82489	53.79552	69.82068	42.36161	16.73046	8.973098
W12 4	20.67221	52.34959	65.87575	38.87929	15.0856	8.334989
W12 5	20.28972	51.34102	65.36458	36.8883	15.64102	8.234101
W12 6	16.62359	52.76003	47.87835	74.56317	16.26927	9.767168
W12 7	15.89827	56.70408	75.3365	43.22158	17.73136	9.69045
W12 8	18.54431	55.08515	67.92182	36.59309	13.7908	8.031359
W12 9	20.08185	51.35905	66.95574	41.78114	13.57916	7.725239
W12 10	17.6873	47.42732	68.75313	51.68035	15.77311	9.97276
W13 1	16.4441	55.50019	74.22871	46.73663	17.51854	11.17961
W13 2	15.88399	52.67417	72.45078	44.28162	18.03333	10.92215
W13 3	13.00089	69.74402	81.21667	27.28883	14.21935	11.49114
W13 4	16.65163	54.42596	75.58418	41.94072	18.63302	10.54277
W13 5	15.65864	53.34777	83.29028	48.54742	17.24847	13.75187
W13 6	14.18422	55.45937	79.53371	51.03475	19.5894	12.62987
W13 7	18.19101	50.79517	66.2757	37.71819	12.60295	9.216186
W13 8	18.31785	51.837	69.00296	43.32121	15.16101	9.328706
W13 9	14.30667	62.07771	81.1923	39.78108	17.91927	11.64438
W13 10	15.96095	48.46646	59.87172	68.79696	16.14287	11.09994
W18 1	17.21689	52.59016	70.63514	39.23654	14.65963	9.988101
W18 2	14.98618	52.75722	72.78525	47.78327	18.20008	13.55287
W18 3	16.70387	55.8248	74.92398	43.63106	17.89659	10.09849
W18 4	16.82071	50.384	70.01017	45.29164	15.40474	10.79679
W18 5	17.19813	52.32098	69.70445	44.37519	15.69571	10.29992
W18 6	14.47248	52.69921	76.6296	51.38902	19.73547	13.11238
W18 7	15.87673	54.04777	75.07155	46.87897	17.22922	10.77276
W18 8	16.44087	50.08671	68.08797	41.71951	14.84597	9.009096
W18 9	16.01875	52.12174	75.56047	49.47515	18.2672	10.89689
W18 10	16.86309	52.49526	72.57085	47.52381	15.26043	10.40021
W35 1	17.51622	49.44641	68.34725	41.82792	19.26038	11.74307

W35 2	13.91782	56.8559	78.84309	42.92656	21.61143	13.53504
W35 3	16.86838	47.98445	67.92148	48.62651	14.74507	12.31883
W35 4	14.64438	47.16576	72.34	56.67241	13.6103	14.09091
W35 5	18.19787	51.73102	68.54246	40.61446	17.31129	7.99403
W35 6	15.05748	52.10292	71.25137	39.78106	16.21557	11.14598
W35 7	9.272777	65.60194	53.35729	67.04603	17.74758	11.67129
W35 8	12.19045	57.83964	79.16859	44.27592	23.21591	14.04597
W35 9	14.28111	44.66158	56.2833	66.19873	26.21403	17.38142
W35 10	12.732	48.60709	74.62725	52.70098	18.946	13.34612
W50 1	17.13262	51.12834	68.06216	44.07389	12.44185	11.3119
W50 2	17.21127	49.13	64.756	42.24432	13.67632	10.90613
W50 3	18.62154	51.64717	64.37646	38.1009	11.48781	9.382899
W50 4	17.2174	52.23604	68.41505	44.07214	14.08618	10.3025
W50 5	18.3143	50.85451	66.25548	41.59699	14.08865	8.775143
W50 6	16.51415	49.87065	69.28597	43.54189	17.88013	7.176763
W50 7	15.14437	53.06603	73.45844	51.14536	16.06757	12.81426
W50 8	14.62776	58.03929	84.62417	36.55807	14.59212	13.04362
W50 9	16.15533	54.55655	71.85689	47.84641	15.94705	11.03228
W50 10	12.54663	54.74722	77.01922	48.41633	16.77253	12.16147
W52 1	16.54323	54.75471	74.05669	46.54011	16.0856	12.56861
W52 2	17.69292	56.6365	71.51148	44.44099	14.56643	11.54214
W52 3	19.00279	52.35362	65.7493	35.03569	12.62194	9.716581
W52 4	17.79183	51.03177	68.06923	43.84076	14.51388	10.19015
W52 5	19.18532	50.27287	62.16321	39.63717	12.46228	8.186174
W52 6	16.55622	54.72948	64.12668	43.53499	14.93495	8.469962
W52 7	21.10804	54.30586	49.53879	42.91502	8.478881	23.46368
W52 8	16.33508	52.26317	60.64814	41.37193	13.8659	8.102055
W52 9	17.39264	49.67961	60.49499	39.43806	13.15646	8.269149
W52 10	18.10684	52.9733	65.35723	34.87853	12.65797	7.216689
W153 1	9.820094	68.48188	70.78529	42.2287	15.30002	8.259492
W153 2	13.93716	55.30392	61.85763	47.70569	18.79088	7.374022
W153 3	16.61892	52.84986	72.47089	36.23654	10.6741	11.09171
W153 4	12.52179	64.90263	66.99689	41.44119	13.25676	8.838111
W153 5	15.38938	49.29369	54.22266	38.47758	13.85236	5.573405
W153 6	15.30432	55.37136	58.63365	36.29385	12.6727	6.261577
W153 7	13.29814	57.72782	63.21004	43.78955	18.14601	6.356485
W153 8	13.49796	70.82577	60.69093	25.25082	20.7146	4.588522
W153 9	14.90036	55.94025	59.92063	44.70832	19.35788	6.64211
W153 10	14.28331	55.96918	61.07529	45.50993	15.37647	7.374965
W295 1	14.65521	60.72954	61.53588	42.25425	18.55687	9.411942
W295 2	16.02797	53.3901	54.73829	50.27353	14.11881	8.642967
W295 3	15.75307	59.45535	57.00639	36.09052	12.76234	6.575468
W295 4	15.76453	60.5599	59.58834	46.27755	14.44864	9.299704
W295 5	16.09833	59.7567	59.8106	46.12806	14.04262	8.924574
W295 6	13.47407	59.50484	59.31622	47.55796	15.6069	9.255131

W295 7	13.60094	59.75027	61.30407	49.16867	13.20438	9.184517
W295 8	10.08743	79.06728	69.59894	30.49719	18.12446	9.650656
W295 9	13.58393	60.73463	63.21366	52.90561	14.7389	9.713804
W295 10	9.010311	63.74972	71.92393	49.44189	16.2821	10.50588
W360 1	15.80834	58.43814	58.51784	44.91477	11.75169	9.084729
W360 2	13.59016	64.6327	65.40958	52.48822	18.39797	11.75604
W360 3	14.03655	61.23722	59.11331	56.71951	19.10335	12.41219
W360 4	13.61598	69.25462	66.88948	42.21198	17.93178	11.50896
W360 5	15.53767	60.45591	61.04821	44.69789	15.07297	10.12047
W360 6	13.51826	62.24214	63.5839	50.56779	14.55705	10.96377
W360 7	12.88475	71.93642	69.95384	38.75367	18.76982	12.41294
W360 8	12.4256	68.96641	67.71562	49.86062	20.59154	14.31227
W360 9	16.02117	57.13549	57.57433	45.95669	13.83553	10.3232
W360 10	13.90492	63.51088	66.83613	51.05647	17.30707	11.17921
W368 1	16.31138	56.00251	55.06756	40.85688	12.54927	9.263567
W368 2	13.77679	69.18944	66.39761	35.12292	17.80354	8.435302
W368 3	16.24195	59.11193	58.99938	42.25814	14.57109	9.061791
W368 4	16.7483	57.28713	55.88695	40.87652	12.76669	8.938793
W368 5	17.01602	59.77774	58.30636	42.84664	13.01317	9.136277
W368 6	13.33355	63.84488	67.42356	52.15976	18.23491	10.66086
W368 7	14.30164	63.90567	63.64472	37.22841	14.86874	8.014067
W368 8	13.19031	68.79818	69.37444	40.79469	16.12926	9.478225
W368 9	11.93369	66.46872	69.19739	44.48546	15.85262	9.375044
W368 10	13.83796	64.38536	65.60629	29.83504	11.92671	8.364848
W394 1	10.03954	61.95247	70.35334	53.95323	16.29862	10.64707
W394 2	15.42239	62.76805	61.77759	38.32435	12.63157	8.583353
W394 3	18.92058	59.4099	66.08323	46.74982	14.78072	9.924492
W394 4	12.76499	53.0572	77.69429	48.24567	14.45703	11.39818
W394 5	10.71746	66.04483	70.52363	48.07773	15.6953	9.98983
W394 6	16.10628	58.24562	55.14969	39.04126	12.78278	7.127709
W394 7	16.16841	64.01436	59.93864	32.07188	12.15044	6.220221
W394 8	17.09359	53.63427	51.31748	37.81208	12.27662	6.443109
W394 9	16.67303	56.39362	53.45511	33.08002	12.30607	5.301526
W394 10	16.56912	59.60155	57.66719	43.27098	13.58555	8.430759
W411 1	13.85641	63.9864	63.38807	37.18893	15.92829	8.620701
W411 2	14.09	62.34947	62.90841	45.61168	15.34901	9.954336
W411 3	9.056815	72.40665	72.01964	41.9435	15.94935	11.29179
W411 4	16.21598	57.84983	56.60654	42.36482	14.16909	8.963959
W411 5	13.88273	62.80413	63.65224	42.66408	15.55963	9.875328
W411 6	8.809511	53.33254	63.30732	59.26066	16.6893	9.66794
W411 7	13.51866	58.17236	57.64806	41.62319	11.70293	9.961838
W411 8	13.24914	57.46743	60.96089	59.64364	13.46749	11.05557
W411 9	14.80165	58.58542	60.67308	56.75968	12.74021	11.36637
W411 10	12.93848	66.11467	66.56978	40.46121	15.50109	9.384217
W412 1	16.42562	58.68292	56.8787	37.61984	11.32059	8.806654

W412 2	15.7717	57.03731	56.49799	48.4757	10.84237	11.17368
W412 3	13.57633	58.25693	59.77558	51.23351	13.97838	10.65065
W412 4	14.35491	54.77354	54.39341	45.60951	11.55666	9.996356
W412 5	18.44646	52.21874	49.5865	39.56556	7.693705	8.003755
W412 6	14.04859	61.1743	58.19966	36.01954	11.02061	8.111504
W412 7	13.30286	60.66864	63.5675	52.29488	15.96441	12.63989
W412 8	16.30045	55.32146	53.3249	40.90848	11.02172	9.531431
W412 9	14.28812	57.08467	56.09111	41.83925	14.31244	11.08545
W412 10	12.36786	61.4141	63.70506	54.75727	15.59155	10.61023
W442 1	15.8075	56.96564	57.15767	40.97208	11.8058	8.440995
W442 2	14.36053	50.43279	52.44964	46.83956	8.95148	9.72897
W442 3	14.87624	56.58094	56.42472	36.82902	11.79718	7.510048
W442 4	15.26901	54.28928	55.51322	46.06788	9.758494	9.32489
W442 5	15.47342	53.46918	53.30805	43.10373	11.05753	8.743394
W442 6	11.32521	51.95941	55.72333	50.63927	12.71352	9.722453
W442 7	13.95027	60.61421	62.11878	41.86511	13.39773	9.062532
W442 8	12.94384	60.50452	63.48284	47.56585	15.37027	10.61051
W442 9	14.50125	57.81442	59.27819	44.60536	13.64178	10.63295
W442 10	13.67977	57.11626	57.90475	44.86207	11.23787	9.954703
W444 1	16.22942	61.10654	58.37559	40.80994	10.26227	9.609944
W444 2	8.335113	63.57687	73.62288	51.53564	15.41919	10.15754
W444 3	9.039167	75.88857	74.98457	39.3928	17.21052	10.55085
W444 4	16.22187	59.29887	58.27236	38.12243	12.65119	8.47335
W444 5	16.77805	60.16624	57.17376	38.18862	10.45285	9.162525
W444 6	15.48968	52.43974	56.73775	55.79335	13.33434	9.591956
W444 7	8.987246	66.94458	69.6443	47.94681	20.09566	10.54466
W444 8	15.58995	57.94933	57.25518	44.38666	10.97569	9.096048
W444 9	15.46977	58.78643	58.63273	42.08828	11.32089	9.00023
W444 10	16.37898	61.55991	60.63905	35.90135	13.14031	7.885074
W445 1	17.17708	55.37653	53.11831	43.1021	10.98528	8.771594
W445 2	16.9803	54.27516	53.45219	42.28087	11.91596	9.433318
W445 3	13.5159	62.39782	63.89426	49.49303	15.58285	11.24023
W445 4	15.0125	57.43616	56.85345	43.25715	12.11851	10.45043
W445 5	14.28325	62.56226	64.20629	45.50548	15.45255	10.83855
W445 6	15.99129	54.16589	54.23735	41.59185	12.11452	10.55861
W445 7	14.91521	60.54841	62.51918	51.2154	14.17999	11.01143
W445 8	10.26357	61.21056	69.25561	51.3607	15.03538	10.5433
W445 9	15.08761	59.0946	58.32103	35.22381	11.68122	8.570413
W445 10	15.145	60.22056	62.47382	52.77754	14.08347	11.32093
W446 1	16.27761	55.16457	54.84163	43.81418	11.54167	8.008287
W446 2	16.83329	55.42263	53.17173	40.80491	11.19652	7.939497
W446 3	14.5686	59.92794	61.30904	50.02372	14.97789	9.737528
W446 4	14.36456	58.82698	59.39577	45.51198	11.38022	9.101162
W446 5	13.20035	66.04029	65.89915	39.06777	15.53456	8.013832
W446 6	16.97082	59.41973	59.10336	47.68413	12.51875	8.064784

W446 7	16.67879	57.18879	55.82372	41.09782	13.67441	7.733056
W446 8	15.56447	56.4372	56.19848	44.56016	12.66169	8.931685
W446 9	15.44426	56.16453	57.1927	43.71047	12.73651	8.991563
W446 10	15.68321	54.99629	55.95823	46.76014	12.65418	8.968573
W448 1	14.61853	59.34963	59.5847	42.62388	15.10559	8.964507
W448 2	16.62687	59.31915	58.51947	41.02336	14.30731	8.157766
W448 3	16.09006	61.55397	62.5285	46.14426	14.92816	9.513883
W448 4	10.98933	61.32412	69.27242	54.56584	16.10424	11.22376
W448 5	15.53592	58.56416	59.10481	45.02688	13.86418	8.803114
W448 6	15.58491	52.95038	53.61687	44.40892	10.58051	8.249662
W448 7	10.26483	64.27297	67.88311	45.54182	15.68052	10.09454
W448 8	14.6747	51.6644	46.74998	80.54826	16.42033	12.86631
W448 9	11.95383	65.96936	68.73892	52.85959	18.64331	11.66886
W448 10	13.42111	62.54457	64.6018	45.73378	16.79299	9.897654
W450 1	15.85813	53.55462	52.08136	40.44316	11.87041	7.218368
W450 2	17.51977	55.22188	53.99394	42.66068	10.1406	7.712683
W450 3	15.91046	56.0675	55.39101	43.72173	12.30701	7.464584
W450 4	16.70801	54.14818	52.37436	40.22822	10.95305	7.544055
W450 5	12.13032	56.08668	60.34672	48.83462	13.73887	10.31564
W450 6	9.2366	62.06982	68.05321	55.73951	15.84728	11.6795
W450 7	17.90298	54.2072	51.35774	39.09867	9.043182	7.187175
W450 8	15.4287	60.81559	58.8992	34.00987	12.36789	6.733109
W450 9	14.6119	59.84262	62.72573	53.9366	15.31636	11.53881
W450 10	15.59414	56.61017	56.73228	46.79129	11.95307	10.29076
C50 1	15.02952	48.43063	70.32021	54.37006	10.47682	14.23627
C50 2	15.73907	45.14037	85.06512	54.85727	16.30064	14.88108
C50 3	20.08285	51.50379	63.42953	34.74558	10.67647	10.10825
C50 4	15.32735	54.92194	72.67752	44.67857	12.40652	13.48248
C50 5	16.528	53.70066	68.12379	37.83116	11.79352	11.04099
C50 6	15.87489	51.3673	70.2005	44.87074	13.84942	12.19595
C50 7	18.82245	52.69941	64.51334	37.82076	8.690818	11.81727
C50 8	17.28183	49.45323	64.98721	43.58661	12.33612	11.52327
C50 9	19.21873	48.83185	61.83102	36.30104	12.24257	10.2538
C50 10	17.04452	52.44817	71.70064	46.54045	14.6983	11.67313
C51 1	18.85753	49.40029	65.73497	46.04708	12.73089	11.79745
C51 2	20.66863	53.86511	68.17922	38.91972	14.94596	11.1246
C51 3	13.07117	58.42931	82.85164	52.88445	19.62789	15.00185
C51 4	15.53859	69.19296	63.66556	35.60424	19.30057	6.338134
C51 5	22.05547	51.16483	62.24076	36.16188	13.55315	9.517363
C51 6	15.12302	54.99941	75.16927	47.99043	17.89658	14.13692
C51 7	19.23575	59.81696	56.7542	40.65589	12.29336	10.73036
C51 8	19.84055	57.97514	58.12052	39.87183	13.90647	10.13513
C51 9	18.38556	57.3331	70.60314	40.44602	15.90877	10.38874
C51 10	20.27083	54.3741	68.43099	37.45038	15.02064	10.94609
C52 1	17.21784	49.20238	63.43863	37.98391	12.42364	10.89334

C52 2	18.0919	41.06613	56.67118	55.29356	10.67116	12.70557
C52 3	15.32833	52.3391	71.83284	47.46461	15.99201	14.1204
C52 4	16.97851	52.31424	69.53049	42.91287	14.62004	13.06574
C52 5	14.33143	57.33205	75.2172	44.0795	11.4045	15.52972
C52 6	18.36475	50.2418	64.5442	39.3105	12.66877	12.23292
C52 7	16.03773	53.04356	71.44998	41.55924	14.66075	12.96883
C52 8	15.97784	57.2735	73.91443	41.13384	15.08393	12.91235
C52 9	18.43163	28.22054	79.98372	65.13636	14.25049	17.27574
C52 10	10.1838	57.13845	79.44751	46.45337	14.22175	16.80355
C53 1	7.804938	55.43123	80.42892	47.16503	23.73165	14.43053
C53 2	20.16426	51.37613	64.55766	39.42314	12.56752	10.40901
C53 3	19.42214	51.53795	66.59611	39.07929	13.23287	11.05907
C53 4	16.0722	63.28302	59.05841	39.35662	13.01151	10.86995
C53 5	21.55124	49.8089	60.85692	35.5383	12.26017	8.759456
C53 6	12.9412	47.74175	81.0329	55.15362	15.50852	16.71062
C53 7	16.64331	51.02958	68.87216	45.96796	12.21842	14.07956
C53 8	13.9594	55.59626	72.88919	38.84053	16.8061	12.43329
C53 9	15.12958	52.14215	83.9836	46.43913	16.90253	15.89403
C53 10	19.3607	46.15742	60.24272	39.7343	11.80252	10.68073
C54 1	18.92033	49.64441	63.38811	36.35436	12.40373	9.930293
C54 2	21.57352	48.57204	58.41178	36.69702	10.39682	8.712147
C54 3	17.66093	48.13684	62.23679	39.73994	13.23518	10.96897
C54 4	17.28008	47.84448	62.10483	40.8604	12.53684	11.24157
C54 5	16.15722	50.72963	62.66772	34.77673	12.31151	9.387452
C54 6	14.51587	53.62044	74.00295	44.28927	15.58484	13.98476
C54 7	10.46876	52.56807	73.72405	47.41061	18.46708	16.2921
C54 8	13.31231	59.38372	77.20265	42.49246	13.16295	15.91986
C54 9	17.8008	49.41617	65.58297	41.00126	14.19636	12.99346
C54 10	12.7377	59.23797	76.92387	41.44984	13.4346	15.66519
C55 1	20.69771	49.80019	62.6683	35.18639	13.21477	8.934548
C55 2	20.07156	52.76204	64.27904	35.06771	10.95166	10.03035
C55 3	17.59361	53.84839	69.78029	35.6538	16.17636	12.55565
C55 4	19.72066	51.80062	65.90002	39.67668	13.13354	10.77097
C55 5	23.10889	50.70573	59.58369	34.80061	10.72397	9.178891
C55 6	17.87947	58.82077	44.454	58.56791	15.08733	12.28657
C55 7	14.87351	59.80458	91.15346	32.0915	15.88379	15.70724
C55 8	16.22756	47.15611	67.07301	49.21425	14.01506	11.18144
C55 9	17.98379	49.64372	62.59057	35.20088	14.78412	10.17966
C55 10	19.82416	49.94048	62.61117	37.58902	11.61158	12.12974
C56 1	16.26261	48.33512	63.19347	41.18726	13.97536	13.8365
C56 2	17.12393	52.11929	68.81109	44.16857	13.44667	14.12013
C56 3	15.15718	53.22639	72.72842	47.90251	15.25772	14.69517
C56 4	17.22459	49.67141	61.43535	32.19259	10.94451	8.153828
C56 5	15.65271	63.55009	60.38357	44.70461	16.06975	10.8523
C56 6	11.34481	63.77919	69.67833	50.96942	15.86347	17.14934

C56 7	14.57492	52.20177	72.42365	50.12158	14.54754	17.14806
C56 8	12.65991	51.97954	60.87319	66.89063	13.45852	18.22593
C56 9	16.44283	53.3349	69.84397	44.09502	14.55979	14.83162
C56 10	14.09341	54.66064	76.52516	48.4177	18.27102	16.63027
C57 1	8.582361	62.33698	83.70645	43.81305	18.2365	15.96292
C57 2	17.17722	48.93254	69.75897	52.23345	12.98176	14.51011
C57 3	15.65458	55.7129	76.53424	49.39887	16.47745	16.1291
C57 4	19.20434	54.67256	67.20312	37.89387	11.31401	11.88504
C57 5	19.5552	50.53678	63.69126	36.11294	11.74623	11.85977
C57 6	21.9273	43.10807	63.57287	45.37485	12.91132	13.254
C57 7	12.74564	72.84034	70.45584	35.00098	15.19251	12.47312
C57 8	17.39228	47.08528	62.79485	40.8354	11.57966	13.67424
C57 9	18.9733	52.7069	65.68239	39.51822	13.08968	11.41928
C57 10	16.74165	56.4301	72.76228	43.73467	15.85198	14.3636
C58 1	15.58449	47.94882	70.08519	46.36771	13.80446	13.21406
C58 2	16.71569	53.36839	68.52641	35.24812	13.28698	11.46423
C58 3	15.85568	55.76356	71.81373	46.56107	14.83381	13.89439
C58 4	18.33013	53.69341	67.0134	34.04521	11.87893	9.680391
C58 5	13.97148	54.66052	73.27229	40.57439	15.3792	16.49483
C58 6	12.2679	64.55439	81.44506	40.05705	16.69142	15.93065
C58 7	18.58959	48.84811	63.10832	38.64563	13.54344	12.32695
C58 8	13.03404	60.54972	82.64956	38.28426	15.20488	14.29273
C58 9	13.93817	54.55605	76.75883	50.48993	17.65361	15.88905
C58 10	18.5308	51.4844	67.5656	39.91008	14.85004	12.29802
C59 1	15.01529	53.42615	59.15121	39.24273	8.435354	18.06268
C59 2	17.40789	46.51039	37.26272	45.64049	6.564992	9.452001
C59 3	11.94921	48.92213	63.23058	47.18417	8.572827	20.0982
C59 4	15.23789	45.45484	57.50785	46.09611	5.012925	20.52824
C59 5	14.11224	48.35288	64.80691	51.35644	6.336553	21.47643
C59 6	11.54896	51.06467	68.87839	51.27391	8.633903	22.79968
C59 7	12.15146	49.20198	69.26459	55.32772	7.765513	23.34978
C59 8	15.95473	46.54601	56.35038	33.80579	5.327511	16.94888
C59 9	16.78219	45.36134	56.12446	40.5922	6.113094	18.68411
C59 10	15.6788	49.49749	60.92677	36.29028	5.467733	18.90543

APPENDIX IX: ATR MID-IR SPECTRAL LIBRARY SEARCH RESULTS

Table 139: ATR mid-IR spectral library search results for 30 glass spectra (5 replicates) using the correlation search algorithm.

Glass Spectra	1st Hit		2nd Hit		3rd Hit		If not 1-3….	
		Hit Quality		Hit Quality		Hit Quality	Hit #	Hit Quality
W10 6	C51	0.0056	W50	0.0089	W52	0.0094	25	0.0247
W10 7	C50	0.0042	W394	0.0056	W444	0.0064	28	0.0414
W10 8	C51	0.0041	W52	0.0050	W50	0.0054	24	0.0234
W10 9	W52	0.0043	C51	0.0049	W50	0.0051	23	0.0238
W10 10	C55	0.0075	C54	0.0105	W52	0.0127	15	0.0276
W12 6	C51	0.0056	C50	0.0058	W153	0.0079	29	0.0591
W12 7	C50	0.0042	W394	0.0062	C56	0.0064	30	0.0609
W12 8	W52	0.0060	W50	0.0065	C54	0.0071	29	0.0675
W12 9	C55	0.0106	C54	0.0132	W52	0.0140	29	0.0811
W12 10	C51	0.0044	W52	0.0054	W50	0.0057	29	0.0621
W13 6	W411	0.0054	W444	0.0055	W360	0.0065	29	0.0597
W13 7	C55	0.0068	W52	0.0080	W50	0.0091	30	0.0779
W13 8	W52	0.0044	W50	0.0050	C51	0.0056	30	0.0665
W13 9	C50	0.0033	W394	0.0041	C57	0.0048	29	0.0564
W13 10	C51	0.0042	C50	0.0057	W295	0.0065	30	0.0597
W18 6	W411	0.0058	W444	0.0066	W360	0.0079	25	0.0352
W18 7	C50	0.0042	C56	0.0059	W448	0.0065	27	0.0352
W18 8	W52	0.0057	W448	0.0070	W50	0.0072	27	0.0442
W18 9	C50	0.0043	C51	0.0057	C56	0.0060	27	0.0357
W18 10	W448	0.0055	C50	0.0058	W52	0.0062	27	0.0372
W35 6	C50	0.0037	C56	0.0039	W448	0.0047	19	0.0080
W35 7	W411	0.0106	W444	0.0115	C57	0.0138	4	0.0146
W35 8	W411	0.0150	W444	0.0179	W360	0.0204	5	0.0211
W35 9	W411	0.0081	W444	0.0088	C57	0.0093	4	0.0093
W35 10	W411	0.0119	W444	0.0140	W35	0.0152		
W50 6	C51	0.0042	W295	0.0049	C50	0.0053	6	0.0060
W50 7	C50	0.0053	W394	0.0067	W444	0.0074	19	0.0164
W50 8	C50	0.0032	W153	0.0054	W394	0.0054	19	0.0107
W50 9	C50	0.0047	W394	0.0059	W360	0.0066	20	0.0140
W50 10	W444	0.0041	W411	0.0047	C57	0.0051	20	0.0215
W52 6	W52	0.0053	C54	0.0057	W50	0.0064		
W52 7	C55	0.0117	C54	0.0126	W52	0.0189		
W52 8	W52	0.0056	C54	0.0056	W50	0.0066		
W52 9	C54	0.0046	C55	0.0047	W52	0.0064		
W52 10	C55	0.0054	C54	0.0068	W52	0.0100		
W153 6	W52	0.0062	C54	0.0066	W50	0.0068	18	0.0219

W153 7	C50	0.0038	C56	0.0046	W412	0.0050	11	0.0063
W153 8	W35	0.0042	W153	0.0052	C57	0.0052		
W153 9	C50	0.0041	C56	0.0049	C51	0.0050	10	0.0064
W153 10	W448	0.0046	C50	0.0049	C56	0.0050	17	0.0090
W295 6	W360	0.0063	W411	0.0069	W394	0.0072	18	0.0151
W295 7	C51	0.0038	W50	0.0049	W52	0.0052	5	0.0060
W295 8	W411	0.0046	W444	0.0050	C57	0.0060	17	0.0181
W295 9	C51	0.0045	C50	0.0051	W448	0.0062	8	0.0070
W295 10	W444	0.0041	C57	0.0049	W411	0.0052	15	0.0159
W360 6	C51	0.0040	C50	0.0053	W448	0.0058	18	0.0106
W360 7	C50	0.0033	W394	0.0047	W153	0.0051	6	0.0059
W360 8	W444	0.0049	W411	0.0052	C57	0.0060	5	0.0067
W360 9	W52	0.0056	W448	0.0066	W50	0.0068	19	0.0168
W360 10	C50	0.0040	W394	0.0058	C56	0.0063	4	0.0070
W368 6	C50	0.0011	W394	0.0019	C57	0.0022	15	0.0067
W368 7	W52	0.0042	C51	0.0046	W50	0.0047	5	0.0058
W368 8	C50	0.0041	C51	0.0055	C56	0.0059	5	0.0071
W368 9	C50	0.0032	W394	0.0046	W153	0.0046	15	0.0086
W368 10	W52	0.0050	W50	0.0057	C54	0.0060	8	0.0086
W394 6	W52	0.0050	C54	0.0051	W50	0.0055	18	0.0182
W394 7	C54	0.0066	C55	0.0068	W52	0.0078	20	0.0274
W394 8	C54	0.0044	C55	0.0058	W450	0.0076	19	0.0263
W394 9	C54	0.0049	C55	0.0063	W450	0.0089	19	0.0292
W394 10	W52	0.0055	W50	0.0064	C51	0.0065	17	0.0185
W411 6	W411	0.0205	W444	0.0233	W35	0.0259		
W411 7	W448	0.0042	C56	0.0043	W368	0.0045	24	0.0133
W411 8	C50	0.0044	C51	0.0050	C56	0.0065	21	0.0129
W411 9	C51	0.0048	W52	0.0060	W50	0.0066	24	0.0199
W411 10	C50	0.0040	W394	0.0057	C56	0.0063	9	0.0084
W412 6	W448	0.0052	W445	0.0053	W446	0.0054	5	0.0059
W412 7	C50	0.0072	W394	0.0076	W360	0.0079	4	0.0083
W412 8	W450	0.0053	W52	0.0062	W445	0.0063	10	0.0083
W412 9	W412	0.0054	C56	0.0069	W446	0.0069		
W412 10	W411	0.0090	W444	0.0105	W360	0.0108	8	0.0142
W442 6	W411	0.0150	W35	0.0176	W360	0.0183	14	0.0322
W442 7	W412	0.0045	C50	0.0054	C56	0.0055	11	0.0073
W442 8	W411	0.0081	W360	0.0084	W394	0.0090	17	0.0176
W442 9	W412	0.0047	C56	0.0060	C50	0.0062	11	0.0076
W442 10	W412	0.0046	C50	0.0067	C56	0.0068	10	0.0084
W444 6	C51	0.0054	W52	0.0058	W50	0.0064	23	0.0181
W444 7	W411	0.0180	W444	0.0212	C57	0.0247		
W444 8	W52	0.0051	W50	0.0055	C51	0.0060	23	0.0251
W444 9	W52	0.0056	W50	0.0064	C51	0.0067	23	0.0267

W444 10	W52	0.0066	C54	0.0077	W50	0.0078	24	0.0319
W445 6	C54	0.0058	W450	0.0059	W52	0.0059	6	0.0079
W445 7	C50	0.0054	W448	0.0062	C51	0.0063	7	0.0074
W445 8	W411	0.0054	W444	0.0062	W360	0.0067	14	0.0163
W445 9	C54	0.0060	W52	0.0065	C55	0.0073	9	0.0113
W445 10	C50	0.0058	W412	0.0068	W448	0.0069	5	0.0077
W446 6	W52	0.0058	W448	0.0066	W50	0.0069	7	0.0080
W446 7	W450	0.0046	W448	0.0050	W445	0.0050	4	0.0051
W446 8	W445	0.0046	W446	0.0046	W448	0.0047		
W446 9	W448	0.0049	W445	0.0052	W450	0.0052	5	0.0054
W446 10	W448	0.0043	W445	0.0047	W52	0.0048	5	0.0051
W448 6	C54	0.0049	C55	0.0056	W52	0.0072	7	0.0103
W448 7	W411	0.0047	W444	0.0052	W360	0.0053	16	0.0147
W448 8	W444	0.0053	W411	0.0058	C57	0.0061	16	0.0179
W448 9	W411	0.0067	W444	0.0072	W360	0.0084	15	0.0197
W448 10	C50	0.0051	W360	0.0053	W394	0.0054	14	0.0086
W450 6	W411	0.0101	W444	0.0113	W360	0.0132	20	0.0387
W450 7	C54	0.0104	C55	0.0115	W52	0.0157	4	0.0166
W450 8	W52	0.0065	C54	0.0067	W450	0.0069		
W450 9	W412	0.0073	C50	0.0083	W360	0.0087	19	0.0169
W450 10	W412	0.0064	W446	0.0068	W448	0.0070	6	0.0084
C50 6	C50	0.0052	C51	0.0063	C56	0.0068		
C50 7	W52	0.0085	W50	0.0096	C54	0.0097	14	0.0200
C50 8	W412	0.0053	W448	0.0058	W445	0.0059	6	0.0064
C50 9	C54	0.0061	W52	0.0066	C55	0.0075	16	0.0184
C50 10	C50	0.0065	C51	0.0078	W52	0.0081		
C51 6	C50	0.0033	W394	0.0043	C56	0.0044	13	0.0074
C51 7	C55	0.0110	C54	0.0156	W52	0.0215	5	0.0236
C51 8	C55	0.0131	C54	0.0175	W52	0.0247	5	0.0278
C51 9	W52	0.0043	C51	0.0047	W50	0.0051		
C51 10	C55	0.0063	C54	0.0091	W52	0.0113	5	0.0126
C52 6	W52	0.0054	W50	0.0064	W448	0.0073	14	0.0111
C52 7	C50	0.0053	C56	0.0053	C51	0.0053	11	0.0072
C52 8	C55	0.0131	C54	0.0175	W52	0.0247	14	0.0435
C52 9	C57	0.0043	W444	0.0044	W411	0.0051	11	0.0108
C52 10	W411	0.0107	W444	0.0128	C57	0.0150	12	0.0263
C53 6	C57	0.0053	W444	0.0055	W411	0.0069	9	0.0105
C53 7	W52	0.0049	W50	0.0065	W448	0.0068	18	0.0156
C53 8	C57	0.0033	C53	0.0037	W35	0.0041		
C53 9	W444	0.0052	C57	0.0054	C50	0.0061	10	0.0104
C53 10	C55	0.0054	C54	0.0069	W52	0.0116	18	0.0312
C54 6	C50	0.0035	C56	0.0047	W394	0.0052	23	0.0209
C54 7	W411	0.0226	W444	0.0269	W35	0.0295	27	0.0893

C54 8	C50	0.0035	W394	0.0051	W153	0.0053	23	0.0245
C54 9	W52	0.0041	W50	0.0042	C51	0.0048	11	0.0061
C54 10	C50	0.0035	C57	0.0046	W153	0.0048	23	0.0249
C55 6	C55	0.0058	C51	0.0076	C54	0.0081		
C55 7	C50	0.0041	C51	0.0058	W153	0.0060	24	0.0223
C55 8	C51	0.0039	W50	0.0054	W295	0.0057	8	0.0080
C55 9	C54	0.0044	W450	0.0054	W50	0.0061	4	0.0061
C55 10	C55	0.0076	C54	0.0077	W52	0.0129		
C56 6	C57	0.0049	W444	0.0051	W153	0.0061	10	0.0102
C56 7	C50	0.0052	W394	0.0057	W360	0.0059	5	0.0066
C56 8	W411	0.0077	W444	0.0079	C57	0.0091	10	0.0183
C56 9	C51	0.0050	W52	0.0050	W50	0.0056	5	0.0060
C56 10	C50	0.0037	C57	0.0039	W394	0.0042	8	0.0057
C57 6	W445	0.0046	W446	0.0047	W442	0.0049	21	0.0131
C57 7	C51	0.0031	C50	0.0057	W50	0.0058	15	0.0100
C57 8	C54	0.0047	C55	0.0061	W52	0.0064	21	0.0259
C57 9	C54	0.0054	C55	0.0056	W52	0.0060	22	0.0272
C57 10	C51	0.0040	W52	0.0050	W50	0.0059	21	0.0150
C58 6	C57	0.0049	W444	0.0049	C50	0.0054	23	0.0287
C58 7	W450	0.0049	W52	0.0054	C54	0.0055	25	0.0269
C58 8	C50	0.0036	W153	0.0054	W394	0.0059	25	0.0264
C58 9	W411	0.0055	W444	0.0059	W394	0.0068	23	0.0311
C58 10	W52	0.0044	W50	0.0051	C54	0.0055	26	0.0291
C59 6	W411	0.0105	W444	0.0134	W360	0.0153	13	0.0262
C59 7	W411	0.0164	W444	0.0187	W360	0.0190	15	0.0302
C59 8	W52	0.0084	W50	0.0096	W445	0.0098	27	0.0325
C59 9	W412	0.0079	W445	0.0085	C56	0.0088	26	0.0278
C59 10	W52	0.0098	W412	0.0106	W445	0.0112	26	0.0331

Table 140: ATR mid-IR spectral library search results for 30 glass spectra (5 replicates) using the first derivative correlation search algorithm.

Glass Spectra	1st Hit		2nd Hit		3rd Hit		If not 1-3….	
		Hit Quality		Hit Quality		Hit Quality	Hit #	Hit Quality
W10 6	C51	0.0347	W12	0.0389	W153	0.0415	4	0.0439
W10 7	W394	0.0097	W411	0.0122	W35	0.0151	29	0.0692
W10 8	C51	0.0109	W10	0.0110	W50	0.0168		
W10 9	W295	0.0130	W52	0.0130	W50	0.0147	5	0.0155
W10 10	W10	0.0297	C55	0.0401	C51	0.0521		
W12 6	C51	0.0288	W10	0.0425	W50	0.0457	7	0.0494
W12 7	W394	0.0098	W35	0.0107	W411	0.0127	8	0.0180
W12 8	W50	0.0115	C51	0.0160	W52	0.0167	4	0.0179
W12 9	W10	0.0165	C51	0.0230	C55	0.0278	7	0.0439
W12 10	C51	0.0123	W295	0.0158	W50	0.0174	6	0.0206
W13 6	W411	0.0164	W35	0.0168	W360	0.0169	6	0.0220
W13 7	C55	0.0122	W52	0.0140	W50	0.0145	19	0.0314
W13 8	W50	0.0111	W295	0.0116	W52	0.0121	11	0.0190
W13 9	W394	0.0134	W153	0.0152	W444	0.0155	5	0.0172
W13 10	C51	0.0225	W10	0.0300	W50	0.0345	11	0.0502
W18 6	W360	0.0205	W411	0.0207	W35	0.0215	4	0.0234
W18 7	W13	0.0103	W35	0.0119	W360	0.0122	8	0.0136
W18 8	W368	0.0116	W442	0.0118	W445	0.0128	15	0.0210
W18 9	W12	0.0131	W295	0.0141	W35	0.0147	16	0.0221
W18 10	C56	0.0095	W368	0.0108	C53	0.0112	7	0.0132
W35 6	W394	0.0093	W18	0.0104	W360	0.0111	4	0.0112
W35 7	W444	0.0263	W411	0.0340	W360	0.0368	6	0.0382
W35 8	W411	0.0483	C59	0.0606	W412	0.0615	7	0.0729
W35 9	W35	0.0292	W360	0.0314	W295	0.0361		
W35 10	W411	0.0281	W360	0.0295	W412	0.0297	5	0.0344
W50 6	C51	0.0122	W295	0.0145	W12	0.0169	4	0.0178
W50 7	W35	0.0147	W394	0.0149	W360	0.0153	5	0.0164
W50 8	W153	0.0106	W444	0.0123	C50	0.0175	8	0.0285
W50 9	W360	0.0140	W35	0.0144	W394	0.0146	25	0.0427
W50 10	W153	0.0107	W444	0.0109	C50	0.0144	16	0.0345
W52 6	W52	0.0116	C55	0.0140	W10	0.0140		
W52 7	C55	0.0127	C54	0.0153	W10	0.0214	4	0.0258
W52 8	W52	0.0098	W295	0.0118	C54	0.0124		
W52 9	C55	0.0112	C54	0.0141	W52	0.0145		
W52 10	C55	0.0093	W10	0.0136	C54	0.0207	4	0.0222
W153 6	W50	0.0124	W52	0.0126	C58	0.0136	22	0.0236
W153 7	W360	0.0086	W35	0.0086	W18	0.0095	22	0.0257
W153 8	W35	0.0211	W411	0.0213	W394	0.0217	17	0.0371

W153 9	W295	0.0130	W12	0.0154	W35	0.0166	22	0.0294
W153 10	C56	0.0087	W360	0.0088	W18	0.0099	23	0.0219
W295 6	W412	0.0177	W360	0.0249	W18	0.0250	22	0.0542
W295 7	C51	0.0153	W50	0.0182	W10	0.0255	8	0.0281
W295 8	W411	0.0103	W394	0.0149	W360	0.0171	22	0.0428
W295 9	C51	0.0138	W50	0.0174	C50	0.0201	7	0.0244
W295 10	W444	0.0135	W153	0.0156	C50	0.0207	19	0.0530
W360 6	C51	0.0160	W50	0.0180	W153	0.0216	20	0.0401
W360 7	W12	0.0119	W394	0.0121	C57	0.0159	11	0.0199
W360 8	W411	0.0121	W394	0.0130	W35	0.0160	4	0.0189
W360 9	W368	0.0092	W445	0.0096	W446	0.0107	16	0.0182
W360 10	W360	0.0084	W394	0.0086	W35	0.0093		
W368 6	W35	0.0137	C50	0.0139	W394	0.0140	18	0.0265
W368 7	W52	0.0124	W12	0.0132	W295	0.0135	7	0.0159
W368 8	W394	0.0104	W12	0.0116	C50	0.0145	21	0.0255
W368 9	W153	0.0125	W444	0.0137	C50	0.0184	21	0.0458
W368 10	W50	0.0142	W52	0.0160	C55	0.0189	10	0.0227
W394 6	W368	0.0109	W448	0.0132	W52	0.0145	25	0.0286
W394 7	C55	0.0169	W50	0.0176	W52	0.0178	18	0.0353
W394 8	C54	0.0136	W450	0.0145	W368	0.0166	24	0.0483
W394 9	C54	0.0106	W442	0.0189	W450	0.0197	22	0.0423
W394 10	W50	0.0101	W12	0.0121	C51	0.0124	18	0.0244
W411 6	W411	0.0409	W360	0.0455	W412	0.0479		
W411 7	W50	0.0120	W13	0.0123	C57	0.0129	24	0.0299
W411 8	C51	0.0219	C50	0.0303	W50	0.0309	29	0.0767
W411 9	C51	0.0157	W50	0.0209	C50	0.0259	29	0.0702
W411 10	W411	0.0099	W394	0.0103	W35	0.0158		
W412 6	W412	0.0141	W18	0.0146	W360	0.0162		
W412 7	W412	0.0168	W360	0.0188	W18	0.0207		
W412 8	W442	0.0107	W450	0.0112	W446	0.0122	5	0.0159
W412 9	W412	0.0172	W446	0.0259	W442	0.0262		
W412 10	W412	0.0281	W411	0.0291	C59	0.0317		
W442 6	W412	0.0445	C59	0.0542	W446	0.0591	4	0.0603
W442 7	W412	0.0111	W18	0.0154	W442	0.0160		
W442 8	W412	0.0235	W411	0.0291	C59	0.0309	9	0.0439
W442 9	W412	0.0099	W442	0.0152	W446	0.0159		
W442 10	W412	0.0094	W360	0.0171	W18	0.0175	6	0.0203
W444 6	C51	0.0149	W295	0.0180	W50	0.0216	28	0.0483
W444 7	W411	0.0479	C59	0.0636	W412	0.0691	8	0.0892
W444 8	W50	0.0145	C51	0.0172	W10	0.0219	21	0.0431
W444 9	W50	0.0118	C51	0.0168	W52	0.0213	22	0.0379
W444 10	W52	0.0140	C55	0.0147	W50	0.0159	28	0.0498
W445 6	W450	0.0105	W442	0.0117	C54	0.0123	4	0.0128

W445 7	C52	0.0111	C56	0.0113	W12	0.0122	19	0.0168
W445 8	W411	0.0142	W360	0.0197	W394	0.0198	20	0.0412
W445 9	C54	0.0161	W52	0.0162	C58	0.0179	10	0.0216
W445 10	W360	0.0098	C56	0.0099	C52	0.0110	9	0.0128
W446 6	W368	0.0078	W446	0.0091	W445	0.0098		
W446 7	W450	0.0107	W446	0.0107	W442	0.0112		
W446 8	W446	0.0091	W442	0.0103	W412	0.0105		
W446 9	W445	0.0095	W442	0.0101	W446	0.0106		
W446 10	W368	0.0084	W446	0.0095	W445	0.0100		
W448 6	W50	0.0203	W10	0.0239	C55	0.0239	11	0.0343
W448 7	W411	0.0120	W394	0.0129	W360	0.0137	18	0.0294
W448 8	C50	0.0245	C57	0.0255	W444	0.0259	17	0.0454
W448 9	W411	0.0187	W360	0.0220	W18	0.0235	16	0.0404
W448 10	W412	0.0119	W18	0.0131	W360	0.0135	9	0.0220
W450 6	W411	0.0331	W360	0.0358	W444	0.0358	23	0.0774
W450 7	C54	0.0122	C55	0.0186	W450	0.0203		
W450 8	C58	0.0152	W368	0.0160	W448	0.0161	12	0.0200
W450 9	W412	0.0126	W360	0.0214	W18	0.0220	14	0.0339
W450 10	W412	0.0086	W446	0.0115	W445	0.0138	7	0.0176
C50 6	C50	0.0111	W12	0.0112	C57	0.0118		
C50 7	W50	0.0158	C51	0.0217	W10	0.0266	7	0.0310
C50 8	W412	0.0086	W446	0.0112	C56	0.0113	22	0.0262
C50 9	C54	0.0109	W52	0.0140	W368	0.0168	26	0.0417
C50 10	W394	0.0112	W35	0.0130	W12	0.0133	4	0.0139
C51 6	W35	0.0089	W394	0.0100	W360	0.0100	23	0.0240
C51 7	W10	0.0288	C55	0.0347	C51	0.0454		
C51 8	W10	0.0281	C55	0.0321	C51	0.0469		
C51 9	W52	0.0121	W50	0.0122	C51	0.0126		
C51 10	W10	0.0118	C55	0.0122	C51	0.0249		
C52 6	W448	0.0137	W368	0.0139	C52	0.0140		
C52 7	W394	0.0102	C56	0.0123	C58	0.0124	5	0.0125
C52 8	W10	0.0281	C55	0.0321	C51	0.0469	9	0.0787
C52 9	C50	0.0227	C57	0.0258	W153	0.0273	9	0.0369
C52 10	W411	0.0337	C59	0.0387	W444	0.0499	18	0.0815
C53 6	W153	0.0263	C50	0.0278	W444	0.0281	15	0.0590
C53 7	W368	0.0112	W445	0.0122	C54	0.0130	12	0.0176
C53 8	W13	0.0117	W153	0.0119	C57	0.0122	7	0.0146
C53 9	W444	0.0175	W153	0.0204	C50	0.0283	12	0.0511
C53 10	C55	0.0125	W10	0.0136	C54	0.0235	15	0.0444
C54 6	W394	0.0102	W35	0.0119	W411	0.0127	28	0.0460
C54 7	W411	0.0651	C59	0.0653	W412	0.0745	27	0.1675
C54 8	W444	0.0124	W153	0.0153	C57	0.0202	29	0.0817
C54 9	C52	0.0103	W368	0.0103	W448	0.0119	9	0.0148

C54 10	W444	0.0117	W153	0.0137	C57	0.0182	29	0.0773
C55 6	W10	0.0162	C51	0.0223	C55	0.0265		
C55 7	W153	0.0158	W444	0.0212	C57	0.0234	23	0.0624
C55 8	W10	0.0161	C51	0.0179	W50	0.0260	4	0.0286
C55 9	C54	0.0121	W368	0.0146	W445	0.0150	14	0.0236
C55 10	C54	0.0112	C55	0.0127	W52	0.0216		
C56 6	W444	0.0237	W153	0.0240	C50	0.0295	12	0.0578
C56 7	W360	0.0118	W412	0.0137	W18	0.0143	6	0.0162
C56 8	W444	0.0228	W153	0.0309	C50	0.0326	10	0.0526
C56 9	C56	0.0100	C52	0.0101	W368	0.0113		
C56 10	W394	0.0099	W35	0.0107	C57	0.0123	9	0.0167
C57 6	W442	0.0121	W446	0.0129	W450	0.0139	23	0.0449
C57 7	W153	0.0195	W50	0.0210	W12	0.0221	5	0.0246
C57 8	C54	0.0105	W450	0.0159	W442	0.0183	25	0.0501
C57 9	W50	0.0123	W52	0.0132	C55	0.0151	19	0.0303
C57 10	W12	0.0114	W50	0.0115	C51	0.0128	4	0.0145
C58 6	W444	0.0153	W153	0.0163	C57	0.0251	16	0.0471
C58 7	W446	0.0102	W445	0.0109	W442	0.0112	10	0.0162
C58 8	W153	0.0152	W444	0.0159	C57	0.0239	15	0.0449
C58 9	W411	0.0193	W360	0.0199	W394	0.0220	19	0.0370
C58 10	W52	0.0116	W295	0.0119	W368	0.0124	7	0.0153
C59 6	C59	0.0259	W411	0.0421	W412	0.0482		
C59 7	C59	0.0217	W412	0.0397	W411	0.0439		
C59 8	C59	0.0180	W412	0.0268	W442	0.0289		
C59 9	C59	0.0181	W412	0.0189	W442	0.0209		
C59 10	C59	0.0168	W412	0.0277	W442	0.0316		

Table 141: ATR mid-IR spectral library search results for 30 second derivative glass spectra (5 replicates) using the correlation search algorithm.

Glass Spectra	1st Hit		2nd Hit		3rd Hit		If not 1-3….	
		Hit Quality		Hit Quality		Hit Quality	Hit #	Hit Quality
W10 6	W444	0.0813	C57	0.0954	W153	0.0962	16	0.1711
W10 7	W394	0.0430	W12	0.0472	W35	0.0607	30	0.1829
W10 8	W10	0.0368	C51	0.0472	W50	0.0855		
W10 9	W12	0.0687	W446	0.0766	W368	0.0874	16	0.1174
W10 10	W10	0.1681	C51	0.2292	W295	0.2401		
W12 6	C51	0.1293	W10	0.1518	C50	0.1930	8	0.2440
W12 7	W35	0.0516	W394	0.0540	W360	0.0590	5	0.0665
W12 8	W153	0.0487	W50	0.0614	C56	0.0826	11	0.1091
W12 9	C51	0.0673	W10	0.0725	W50	0.0901	8	0.1420
W12 10	C51	0.0467	W10	0.0672	C52	0.0822	7	0.1138
W13 6	C56	0.0685	W360	0.0852	W448	0.0881	7	0.0914
W13 7	W52	0.0476	C58	0.0504	C55	0.0573	25	0.1162
W13 8	W368	0.0576	W50	0.0590	W13	0.0607		
W13 9	W411	0.0522	W444	0.0770	W153	0.0872	14	0.1192
W13 10	C51	0.1060	W10	0.1459	C50	0.1671	11	0.2317
W18 6	W13	0.0609	W360	0.0709	W35	0.0744	5	0.0854
W18 7	C56	0.0557	W13	0.0613	W368	0.0623	13	0.1035
W18 8	C54	0.0547	W448	0.0620	W442	0.0635	5	0.0699
W18 9	W35	0.0913	W12	0.1042	W13	0.1083	15	0.1502
W18 10	C56	0.0319	W52	0.0568	W448	0.0676	13	0.0816
W35 6	W394	0.0365	W18	0.0513	C58	0.0544	13	0.0882
W35 7	W444	0.0700	C57	0.0706	W13	0.0732	8	0.1256
W35 8	W411	0.1454	W412	0.1621	W18	0.1706	7	0.2050
W35 9	W295	0.1464	W35	0.1762	W442	0.1842		
W35 10	W360	0.0450	W35	0.0573	W18	0.0620		
W50 6	W10	0.0521	C51	0.0597	W295	0.0629	7	0.0925
W50 7	W13	0.0524	W360	0.0572	C57	0.0582	11	0.0984
W50 8	W153	0.0459	W444	0.0522	C57	0.0742	4	0.0767
W50 9	W35	0.0528	W360	0.0564	W13	0.0573	23	0.1358
W50 10	W153	0.0389	W444	0.0426	C57	0.0449	4	0.0492
W52 6	W52	0.0509	W295	0.0544	W10	0.0547		
W52 7	C55	0.0573	C54	0.0687	W10	0.0702	6	0.0763
W52 8	W52	0.0449	W295	0.0542	C52	0.0546		
W52 9	W52	0.0622	C55	0.0654	C58	0.0721		
W52 10	C55	0.0492	C58	0.0660	W52	0.0688		
W153 6	C58	0.0655	C55	0.0741	W394	0.0795	10	0.0968
W153 7	W448	0.0607	W394	0.0632	W360	0.0668	26	0.1390
W153 8	W411	0.0809	W18	0.1050	W448	0.1127	25	0.2113

W153 9	W295	0.0645	W448	0.0832	C54	0.0880	25	0.1807
W153 10	W360	0.0372	W35	0.0389	W52	0.0470	23	0.0946
W295 6	W360	0.0882	W446	0.0892	W18	0.0892	22	0.1579
W295 7	C51	0.0591	C50	0.0730	W50	0.0841	13	0.1460
W295 8	W411	0.0242	W394	0.0473	W18	0.0523	22	0.1189
W295 9	C51	0.0529	W50	0.0764	C57	0.0823	15	0.1448
W295 10	W444	0.0609	C57	0.0697	W153	0.0783	23	0.2192
W360 6	C50	0.0703	C51	0.0750	W50	0.0899	11	0.1411
W360 7	W411	0.0386	W394	0.0484	C53	0.0504	7	0.0742
W360 8	W411	0.0351	W394	0.0401	W35	0.0504	4	0.0509
W360 9	W360	0.0394	C52	0.0396	W35	0.0495		
W360 10	C53	0.0413	W394	0.0451	W360	0.0453		
W368 6	W35	0.0680	W295	0.0716	C52	0.0744	21	0.1434
W368 7	C58	0.0667	W411	0.0768	W394	0.0835	20	0.1437
W368 8	W411	0.0503	C58	0.0542	W394	0.0592	24	0.1353
W368 9	W444	0.0383	W153	0.0702	C57	0.0883	18	0.1959
W368 10	W153	0.0846	C58	0.1008	C55	0.1011	15	0.1354
W394 6	W448	0.0696	W368	0.0704	W450	0.0806	25	0.1518
W394 7	C55	0.1168	C58	0.1199	W411	0.1206	7	0.1385
W394 8	W450	0.0532	W368	0.0537	W448	0.0712	27	0.1735
W394 9	C54	0.0968	W412	0.0993	W445	0.1130	8	0.1403
W394 10	W50	0.0525	C51	0.0605	W368	0.0616	22	0.1214
W411 6	W360	0.0937	W35	0.0988	W13	0.1003	17	0.1548
W411 7	W153	0.0332	W50	0.0376	C57	0.0477	22	0.1133
W411 8	C51	0.1027	W10	0.1530	W50	0.1630	28	0.3621
W411 9	C51	0.0784	C50	0.1159	W50	0.1185	28	0.3022
W411 10	W411	0.0363	W394	0.0436	W18	0.0631		
W412 6	W411	0.0831	C58	0.0894	C59	0.0896	6	0.1243
W412 7	W18	0.0865	W360	0.0887	W448	0.0946	8	0.1191
W412 8	W450	0.0625	W412	0.0711	W446	0.0760		
W412 9	W442	0.1053	W412	0.1262	W18	0.1264		
W412 10	W412	0.0603	W18	0.0703	W360	0.0781		
W442 6	W442	0.1371	W18	0.1461	W446	0.1481		
W442 7	W411	0.0782	W18	0.0872	W442	0.0928		
W442 8	W18	0.1005	W412	0.1110	W442	0.1112		
W442 9	W442	0.0576	W18	0.0750	W360	0.0835		
W442 10	W18	0.0324	W360	0.0556	W412	0.0574	10	0.0663
W444 6	W10	0.0716	C51	0.0778	W295	0.0936	28	0.2665
W444 7	W411	0.1117	W18	0.1194	C59	0.1422	25	0.2556
W444 8	W50	0.0798	C51	0.0923	C50	0.0946	9	0.1388
W444 9	W50	0.0494	W153	0.0567	C50	0.0698	5	0.0825
W444 10	C55	0.0550	C58	0.0553	W52	0.0595	30	0.1747
W445 6	W445	0.0506	W448	0.0555	W450	0.0593		

W445 7	W52	0.0463	W445	0.0508	C52	0.0536		
W445 8	C59	0.0500	W411	0.0783	W18	0.0898	20	0.1541
W445 9	C58	0.0709	W411	0.0995	W52	0.1011	6	0.1112
W445 10	W360	0.0420	W448	0.0440	W445	0.0471		
W446 6	W446	0.0361	W360	0.0434	C52	0.0443		
W446 7	W446	0.0496	W450	0.0698	C56	0.0746		
W446 8	W412	0.0340	W445	0.0371	W448	0.0441	10	0.0693
W446 9	W445	0.0475	W52	0.0653	C58	0.0681	5	0.0715
W446 10	W446	0.0406	W368	0.0416	W450	0.0489		
W448 6	W50	0.0875	C51	0.0979	W10	0.1037	19	0.1704
W448 7	W18	0.0494	W411	0.0510	W394	0.0535	13	0.0904
W448 8	C51	0.1155	C50	0.1175	C57	0.1255	21	0.2132
W448 9	C56	0.0571	W18	0.0831	W446	0.0840	7	0.0921
W448 10	W18	0.0585	W442	0.0650	W412	0.0744	7	0.0864
W450 6	W13	0.0899	W444	0.0979	C57	0.1067	23	0.1850
W450 7	C54	0.0647	W450	0.0648	W295	0.0673		
W450 8	W411	0.0635	W18	0.0661	C58	0.0725	21	0.1413
W450 9	W412	0.0466	W18	0.0560	W448	0.0679	6	0.0731
W450 10	W368	0.0515	W360	0.0530	W18	0.0530	7	0.0640
C50 6	C52	0.0493	C50	0.0521	W360	0.0550		
C50 7	W444	0.0689	W50	0.0916	W153	0.0960		
C50 8	W360	0.0362	C53	0.0433	W18	0.0443	22	0.0811
C50 9	C58	0.0649	C54	0.0680	C55	0.0719	25	0.1515
C50 10	W35	0.0518	W12	0.0535	W295	0.0550	12	0.0805
C51 6	W35	0.0258	W360	0.0284	C53	0.0337	13	0.0631
C51 7	C51	0.1060	W50	0.1206	W10	0.1282		
C51 8	C51	0.1265	W50	0.1291	W10	0.1372		
C51 9	C56	0.0740	W52	0.0747	W50	0.0838	7	0.0973
C51 10	W10	0.0420	C51	0.0646	W52	0.0665		
C52 6	C54	0.0731	W394	0.0754	W35	0.0756	10	0.0886
C52 7	W394	0.0478	W12	0.0679	W360	0.0681	9	0.0792
C52 8	W411	0.0515	W394	0.0529	W18	0.0613	12	0.1050
C52 9	C50	0.1103	C51	0.1148	C57	0.1461	4	0.1477
C52 10	C59	0.0864	W411	0.0975	W13	0.1354	22	0.2130
C53 6	C50	0.1077	C51	0.1125	C57	0.1179	13	0.2069
C53 7	C52	0.0431	C53	0.0444	W52	0.0515		
C53 8	W444	0.0469	C57	0.0477	W153	0.0683	5	0.0833
C53 9	W444	0.0378	W153	0.0656	C57	0.0794	8	0.1378
C53 10	W10	0.0543	C51	0.0648	C52	0.0903	14	0.1330
C54 6	W394	0.0692	W411	0.0768	W18	0.0803	12	0.1123
C54 7	C59	0.1412	W412	0.1548	W18	0.1575	22	0.2969
C54 8	W153	0.0846	W444	0.1279	C50	0.1314	29	0.2840
C54 9	W448	0.0543	W368	0.0584	W295	0.0688	7	0.0738

C54 10	W444	0.0406	W153	0.0567	C57	0.0723	29	0.2629
C55 6	C51	0.0714	W10	0.0763	W50	0.1078	7	0.1505
C55 7	W444	0.0600	W153	0.0636	C57	0.0986	21	0.2066
C55 8	C51	0.0895	W10	0.1049	C52	0.1323	11	0.1794
C55 9	W445	0.0665	W412	0.0771	C54	0.0985	11	0.1263
C55 10	C55	0.0588	W445	0.0625	W368	0.0694		
C56 6	C50	0.1112	W153	0.1145	W444	0.1173	13	0.2094
C56 7	W18	0.0342	W360	0.0434	W412	0.0465	10	0.0683
C56 8	W444	0.0970	C50	0.1110	W13	0.1117	12	0.1844
C56 9	W13	0.0654	C56	0.0697	W448	0.0714		
C56 10	W394	0.0594	W360	0.0605	C52	0.0634	18	0.1047
C57 6	W450	0.0543	W446	0.0597	W448	0.0704	21	0.1589
C57 7	W153	0.0660	W444	0.0853	C57	0.1051		
C57 8	W446	0.0614	W52	0.0719	W445	0.0775	23	0.1278
C57 9	C56	0.0500	W52	0.0702	W50	0.0739	4	0.0829
C57 10	W153	0.0522	C56	0.0546	C57	0.0637		
C58 6	W153	0.0605	W444	0.0767	C57	0.0944	14	0.1583
C58 7	W412	0.0403	W445	0.0481	W18	0.0617	7	0.0704
C58 8	W153	0.0631	W444	0.0709	C57	0.1044	16	0.1889
C58 9	W13	0.0786	C56	0.0947	W360	0.1031	24	0.1663
C58 10	C54	0.0562	W295	0.0598	C52	0.0726	13	0.0982
C59 6	W411	0.0898	W18	0.0958	C59	0.0977		
C59 7	W412	0.0599	W18	0.0729	C59	0.0795		
C59 8	C59	0.0876	W411	0.1096	W394	0.1224		
C59 9	W442	0.0677	W18	0.0749	W448	0.0828	11	0.1002
C59 10	W411	0.1057	C59	0.1083	W394	0.1267		

Table 142: ATR mid-IR spectral library search results for 30 second derivative glass spectra (5 replicates) using the first derivative correlation search algorithm.

Glass Spectra	1st Hit		2nd Hit		3rd Hit		If not 1-3….	
		Hit Quality		Hit Quality		Hit Quality	Hit #	Hit Quality
W10 6	W13	0.4711	W444	0.4891	W153	0.4927	17	0.5899
W10 7	W394	0.3036	W12	0.3533	W18	0.4066	21	0.5874
W10 8	W10	0.4155	C51	0.4270	C56	0.4937		
W10 9	W35	0.4250	W12	0.4257	W446	0.4574	11	0.5192
W10 10	W10	0.5691	W295	0.6791	C54	0.7305		
W12 6	C50	0.6285	W10	0.6436	C52	0.6552	21	0.8250
W12 7	C50	0.4540	W360	0.4880	C57	0.4922	10	0.5649
W12 8	W153	0.4944	C56	0.4998	W444	0.5096	21	0.7269
W12 9	C50	0.3657	W35	0.4286	C57	0.4316	16	0.5966
W12 10	C51	0.4073	C52	0.4505	W10	0.4562	15	0.5932
W13 6	C56	0.5295	W50	0.5777	C53	0.5842	19	0.7073
W13 7	W445	0.4230	W412	0.4456	C58	0.4674	27	0.6708
W13 8	W450	0.3736	W13	0.3773	W50	0.4136		
W13 9	W411	0.3681	W444	0.3930	W153	0.4144	19	0.6138
W13 10	C51	0.1060	W10	0.1459	C50	0.1671	11	0.2317
W18 6	W13	0.4041	W448	0.4076	C50	0.4699	16	0.6156
W18 7	C56	0.4493	W13	0.4975	W153	0.5287	21	0.7392
W18 8	W442	0.4090	W295	0.4608	C54	0.4707	4	0.5060
W18 9	W35	0.4740	W368	0.4879	W13	0.4884	13	0.6283
W18 10	C56	0.4903	W448	0.5112	W10	0.5383	19	0.6982
W35 6	W394	0.2786	W445	0.3952	W18	0.4299	17	0.6082
W35 7	C57	0.3596	C50	0.4116	W13	0.4216	16	0.5820
W35 8	W412	0.5126	C58	0.5619	W442	0.5735	4	0.6072
W35 9	W295	0.5870	W394	0.5877	C54	0.6213	7	0.7013
W35 10	W360	0.3326	C53	0.3625	C50	0.3629	5	0.4189
W50 6	C52	0.4173	W360	0.4637	C50	0.4674	23	0.6211
W50 7	W360	0.4064	C57	0.4300	C50	0.4359	14	0.5409
W50 8	C50	0.3849	W444	0.3891	W153	0.4011	8	0.4892
W50 9	W360	0.3711	W35	0.3903	W12	0.3952	21	0.5756
W50 10	W50	0.3524	W35	0.3823	W153	0.3927		
W52 6	W445	0.4253	W394	0.4381	W12	0.4580	13	0.5608
W52 7	C51	0.4704	W295	0.5228	W10	0.5296	15	0.6083
W52 8	W35	0.5385	W18	0.5507	W442	0.5661	8	0.6106
W52 9	W18	0.4600	W52	0.4798	C57	0.4968		
W52 10	C58	0.3654	W445	0.3905	C55	0.4261	4	0.4772
W153 6	W52	0.4211	W394	0.4374	C58	0.4392	8	0.5205
W153 7	W394	0.4555	W35	0.4566	W12	0.5092	11	0.5715
W153 8	W411	0.4638	W35	0.5991	W448	0.6215	15	0.7327

W153 9	W52	0.4529	W368	0.5073	C54	0.5094	17	0.6456
W153 10	W35	0.3983	W360	0.4147	C50	0.4227	11	0.5436
W295 6	W360	0.4452	C50	0.4560	W448	0.5376	22	0.7312
W295 7	C50	0.2970	W360	0.3238	C57	0.3829	15	0.4961
W295 8	C53	0.3658	W411	0.3789	W394	0.4018	23	0.5538
W295 9	C51	0.3422	C57	0.3589	C50	0.3606	16	0.4937
W295 10	W50	0.3589	C57	0.3695	C50	0.3818	23	0.6630
W360 6	C50	0.2802	W360	0.3649	W153	0.3976		
W360 7	W411	0.3113	C53	0.3457	W360	0.3822		
W360 8	W360	0.3442	C53	0.3687	W411	0.3739		
W360 9	W35	0.3369	C52	0.3721	W360	0.3809		
W360 10	W13	0.4774	W394	0.4806	W52	0.4934	17	0.5899
W368 6	C52	0.5141	W360	0.5511	W442	0.5585	30	0.8466
W368 7	W411	0.5081	C58	0.5190	W412	0.5461	25	0.7872
W368 8	W411	0.4267	C58	0.4989	W52	0.5043	19	0.6230
W368 9	W444	0.2778	W153	0.4251	W13	0.4497	18	0.6789
W368 10	W153	0.4544	W411	0.4577	W12	0.4814	14	0.5808
W394 6	C57	0.3983	W153	0.4275	W446	0.4347	26	0.6748
W394 7	W411	0.4826	W52	0.4938	W18	0.5046	23	0.6560
W394 8	W368	0.4840	W448	0.4847	W450	0.5220	27	0.7770
W394 9	W394	0.4777	W412	0.4827	W18	0.5116		
W394 10	W450	0.3255	C51	0.3308	W12	0.3599	20	0.6082
W411 6	W446	0.4704	W368	0.5082	C51	0.5354	22	0.6936
W411 7	W50	0.3950	C56	0.4070	W153	0.4113	17	0.5237
W411 8	C51	0.4474	W10	0.4998	W295	0.5141	27	0.8324
W411 9	C50	0.4149	C52	0.4422	W360	0.4654	19	0.7229
W411 10	C52	0.4981	W394	0.5107	W360	0.5114	4	0.5137
W412 6	W394	0.4574	C58	0.5878	W445	0.5884	9	0.6448
W412 7	W360	0.5485	W13	0.5551	W450	0.5651	30	0.8464
W412 8	W412	0.5167	W360	0.5308	W12	0.5530		
W412 9	W360	0.5908	W442	0.6189	C52	0.6453	10	0.7098
W412 10	W360	0.4365	C50	0.4550	W35	0.4633	11	0.5720
W442 6	W411	0.5899	W18	0.5974	W360	0.6071	17	0.7401
W442 7	W411	0.3924	W448	0.4927	W52	0.5289	22	0.7266
W442 8	W442	0.4156	W35	0.4223	C58	0.5092		
W442 9	W448	0.4866	W360	0.5198	W295	0.5293	5	0.5464
W442 10	W18	0.3867	W446	0.4458	W394	0.4539	6	0.4731
W444 6	W10	0.3946	C52	0.4809	C50	0.4894	22	0.6793
W444 7	W448	0.4667	W12	0.4684	W411	0.4705	15	0.6255
W444 8	W153	0.3890	W13	0.3946	W10	0.4019	8	0.4563
W444 9	W153	0.3340	W444	0.3702	W13	0.3905		
W444 10	C55	0.4367	C58	0.4473	W52	0.4723	30	0.7527
W445 6	W52	0.3725	W295	0.4455	W445	0.4474		

W445 7	W412	0.4114	W52	0.4260	W18	0.4294	4	0.4523
W445 8	C59	0.5129	W412	0.6171	W368	0.6228	26	0.8204
W445 9	C58	0.4309	W412	0.4684	C56	0.4870	5	0.5293
W445 10	W52	0.3912	C50	0.4222	W360	0.4396	9	0.5156
W446 6	W450	0.4037	W18	0.4230	W448	0.4412	6	0.4713
W446 7	C53	0.4347	W448	0.4862	W10	0.4883	4	0.5067
W446 8	W295	0.3854	W52	0.4123	W12	0.4191	6	0.4314
W446 9	W445	0.3853	W411	0.3892	W35	0.4304	19	0.5827
W446 10	W446	0.3817	W368	0.3875	C54	0.4105		
W448 6	W444	0.4039	C51	0.4043	C50	0.4109	13	0.5440
W448 7	C58	0.4032	C55	0.4113	W13	0.4177	20	0.5445
W448 8	C51	0.3969	C50	0.4398	C52	0.4413	26	0.6735
W448 9	C56	0.4033	W448	0.4789	W446	0.5180		
W448 10	W442	0.2850	W412	0.3981	C58	0.4066	21	0.6368
W450 6	C56	0.4445	W50	0.4536	W153	0.4673	12	0.5948
W450 7	W52	0.4607	C55	0.4873	W448	0.4879	22	0.6593
W450 8	W12	0.5140	W18	0.5520	W394	0.5581	25	0.7081
W450 9	W442	0.4288	W412	0.4505	C53	0.4534	23	0.6600
W450 10	W360	0.4397	W445	0.4445	W153	0.4488	25	0.6268
C50 6	W360	0.3850	C52	0.4074	C50	0.4494		
C50 7	W153	0.3637	W444	0.3974	C57	0.4279	5	0.4591
C50 8	W35	0.4049	W411	0.4254	W153	0.4456	5	0.4880
C50 9	W411	0.4986	W448	0.4992	C55	0.5041	18	0.6334
C50 10	C51	0.4464	W13	0.4557	W295	0.5112	12	0.5853
C51 6	W448	0.3211	W35	0.3427	C50	0.3808	8	0.4884
C51 7	C51	0.3085	W50	0.3305	W153	0.4330		
C51 8	W444	0.4578	W50	0.4802	W13	0.4896	4	0.4951
C51 9	W412	0.6680	W52	0.6696	C56	0.6697	9	0.7474
C51 10	W18	0.3434	W10	0.3592	C58	0.4095	7	0.4733
C52 6	W35	0.4218	C55	0.4265	W442	0.4290	8	0.4908
C52 7	W394	0.3016	W12	0.4283	W295	0.4336	8	0.5448
C52 8	W360	0.3780	C50	0.3819	W394	0.3894	5	0.4292
C52 9	C50	0.4246	W444	0.5061	W35	0.5260	9	0.6250
C52 10	C56	0.4932	W13	0.5150	W411	0.5507	9	0.6629
C53 6	C57	0.4094	C50	0.4476	W360	0.4927	12	0.5647
C53 7	C53	0.3801	W35	0.4152	W411	0.4665		
C53 8	C57	0.3339	W444	0.3851	W153	0.4323	8	0.5078
C53 9	W444	0.2464	W153	0.3089	C57	0.3533	5	0.4009
C53 10	C50	0.3791	C57	0.4206	W10	0.4589	5	0.4634
C54 6	W411	0.4862	W360	0.5371	C50	0.5467	13	0.6994
C54 7	C56	0.6060	W411	0.6215	C59	0.6520	26	0.8514
C54 8	C56	0.3608	C59	0.4782	W153	0.4960	30	0.8358
C54 9	W368	0.4636	W13	0.5165	W35	0.5245	18	0.6194

C54 10	W444	0.3252	W153	0.3491	C57	0.3738	29	0.8024
C55 6	C51	0.3956	W10	0.4525	W12	0.4647	16	0.6160
C55 7	W153	0.3837	C56	0.5087	W13	0.5088	23	0.7495
C55 8	C52	0.4366	W35	0.4425	W360	0.4515	9	0.5167
C55 9	W445	0.5195	W52	0.5260	C54	0.5269	14	0.6121
C55 10	C58	0.4385	W445	0.4915	W10	0.4924	5	0.5194
C56 6	W13	0.3911	C52	0.4263	C50	0.4521	11	0.5514
C56 7	W394	0.3641	W18	0.3783	C57	0.4050	22	0.6222
C56 8	C50	0.3825	W153	0.3901	W444	0.4096	10	0.5642
C56 9	C59	0.6299	W446	0.6607	W153	0.6625	4	0.6732
C56 10	W442	0.4955	W412	0.5181	W394	0.5479	11	0.6748
C57 6	W360	0.4785	W446	0.4891	W448	0.4984	5	0.5279
C57 7	W444	0.3948	C57	0.5033	W153	0.5060		
C57 8	W445	0.4647	C58	0.4736	C55	0.4879	12	0.5478
C57 9	C56	0.3698	W10	0.4775	W153	0.5038	12	0.5953
C57 10	W444	0.4618	C57	0.4715	W153	0.5053		
C58 6	W153	0.4265	C56	0.4344	C59	0.5247	17	0.6398
C58 7	W446	0.3677	W412	0.4766	W368	0.4792	4	0.4913
C58 8	W153	0.4199	C56	0.4838	W444	0.4925	24	0.7417
C58 9	C56	0.5254	W153	0.5261	C53	0.5407	27	0.7759
C58 10	W295	0.4026	C55	0.4272	C54	0.4309	22	0.6379
C59 6	C57	0.5791	W444	0.5835	W448	0.5907	20	0.7388
C59 7	W35	0.4236	W445	0.4626	C53	0.4989	27	0.6855
C59 8	C59	0.4962	W394	0.5227	W412	0.6869		
C59 9	W35	0.4596	W448	0.4873	W368	0.5233	20	0.6376
C59 10	C59	0.6176	W394	0.6268	W442	0.6986		

APPENDIX X: PCA RESULTS FOR CHEMOMETRIC ANALYSIS OF THE FIRST SET OF 30 GLASSES

A. PCA Results for the Unprocessed Spectra

Table 143: PCA results for the first set of 30 glass spectra (10 replicates), no data pretreatment.

Importance of components:

	PC1	PC2	PC3	PC4	PC5	PC6	PC7	PC8	PC9	PC10
Standard deviation	10.530	0.49581	0.21785	0.15386	0.07987	0.07339	0.04303	0.03789	0.02937	0.02771
Proportion of Variance	0.997	0.00221	0.00043	0.00021	0.00006	0.00005	0.00002	0.00001	0.00001	0.00001
Cumulative Proportion	0.997	0.99920	0.99963	0.99984	0.99990	0.99995	0.99997	0.99998	0.99999	0.99999

	PC11	PC12	PC13	PC14	PC15	PC16	PC17	PC18	PC19
Standard deviation	0.01429	0.01316	0.008203	0.006933	0.00632	0.005054	0.003402	0.002934	0.002228
Proportion of Variance	0.00000	0.00000	0.000000	0.000000	0.00000	0.000000	0.000000	0.000000	0.000000
Cumulative Proportion	1.00000	1.00000	1.000000	1.000000	1.00000	1.000000	1.000000	1.000000	1.000000

	PC20	PC21	PC22	PC23	PC24	PC25	PC26	PC27
Standard deviation	0.002084	0.001859	0.001490	0.001179	0.001104	0.001043	0.001012	0.0009533
Proportion of Variance	0.000000	0.000000	0.000000	0.000000	0.000000	0.000000	0.000000	0.0000000
Cumulative Proportion	1.000000	1.000000	1.000000	1.000000	1.000000	1.000000	1.000000	1.0000000

	PC28	PC29	PC30	PC31	PC32	PC33	PC34	PC35
Standard deviation	0.0009254	0.0008772	0.0008722	0.000815	0.000797	0.0007777	0.0007618	0.0007343
Proportion of Variance	0.0000000	0.0000000	0.0000000	0.000000	0.000000	0.0000000	0.0000000	0.0000000
Cumulative Proportion	1.0000000	1.0000000	1.0000000	1.000000	1.000000	1.0000000	1.0000000	1.0000000

	PC36	PC37	PC38	PC39	PC40	PC41	PC42	PC43
Standard deviation	0.000726	0.0007025	0.000675	0.0006638	0.0006444	0.0006317	0.0006165	0.0006065
Proportion of Variance	0.000000	0.0000000	0.000000	0.0000000	0.0000000	0.0000000	0.0000000	0.0000000
Cumulative Proportion	1.000000	1.0000000	1.000000	1.0000000	1.0000000	1.0000000	1.0000000	1.0000000

	PC44	PC45	PC46	PC47	PC48	PC49	PC50	PC51
Standard deviation	0.0006006	0.0005809	0.0005695	0.000557	0.0005426	0.000529	0.0005148	0.000508
Proportion of Variance	0.0000000	0.0000000	0.0000000	0.000000	0.0000000	0.000000	0.0000000	0.000000
Cumulative Proportion	1.0000000	1.0000000	1.0000000	1.000000	1.0000000	1.000000	1.0000000	1.000000

	PC52	PC53	PC54	PC55	PC56	PC57	PC58
Standard deviation	0.0004872	0.0004833	0.0004814	0.0004673	0.0004615	0.0004524	0.0004487
Proportion of Variance	0.0000000	0.0000000	0.0000000	0.0000000	0.0000000	0.0000000	0.0000000
Cumulative Proportion	1.0000000	1.0000000	1.0000000	1.0000000	1.0000000	1.0000000	1.0000000

	PC59	PC60	PC61	PC62	PC63	PC64	PC65	PC66
Standard deviation	0.0004398	0.0004281	0.0004226	0.0004061	0.0004036	0.0003909	0.0003858	0.000379
Proportion of Variance	0.0000000	0.0000000	0.0000000	0.0000000	0.0000000	0.0000000	0.0000000	0.000000
Cumulative Proportion	1.0000000	1.0000000	1.0000000	1.0000000	1.0000000	1.0000000	1.0000000	1.000000

	PC67	PC68	PC69	PC70	PC71	PC72	PC73
Standard deviation	0.0003732	0.0003651	0.0003525	0.0003423	0.0003421	0.0003294	0.0003217
Proportion of Variance	0.0000000	0.0000000	0.0000000	0.0000000	0.0000000	0.0000000	0.0000000
Cumulative Proportion	1.0000000	1.0000000	1.0000000	1.0000000	1.0000000	1.0000000	1.0000000

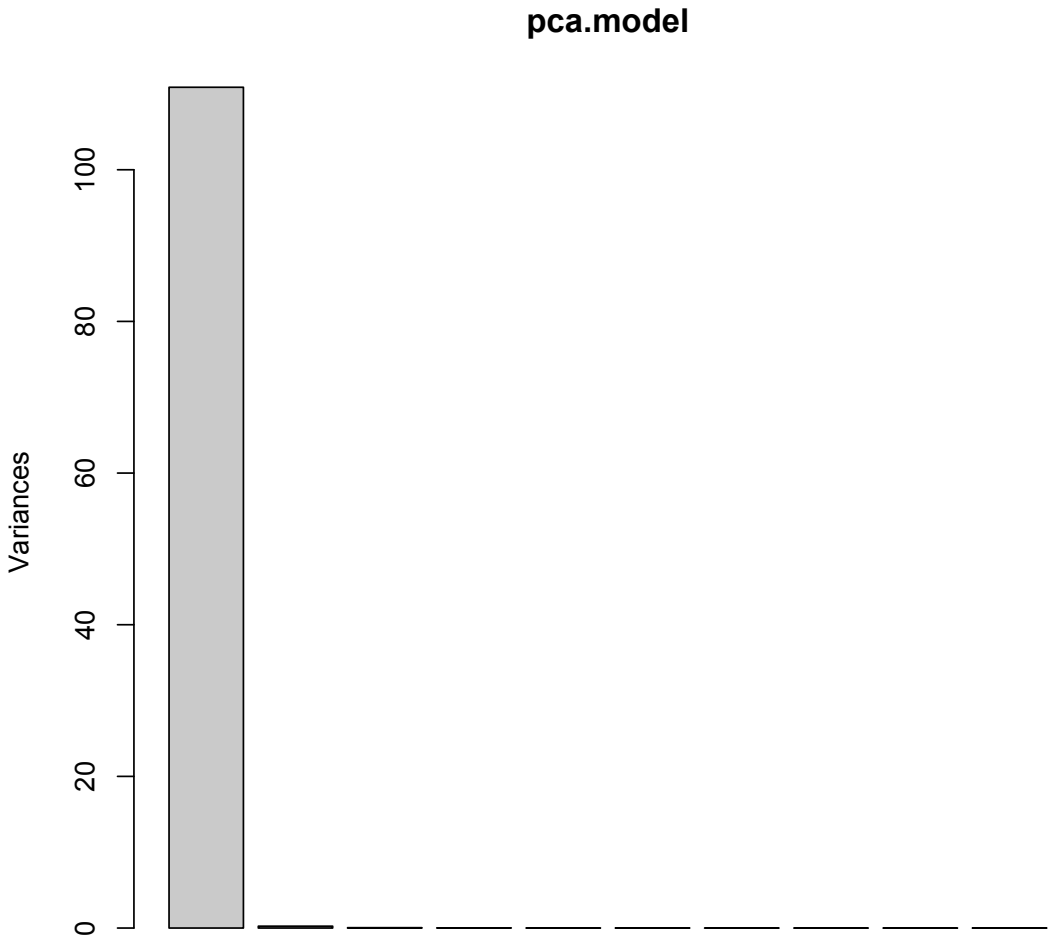


Figure 132: PCA scree plot for the first set of 30 glass spectra (10 replicates), no data pretreatment.

Table 144: PCA results for the first set of 30 glass spectra (10 replicates), centered.

Importance of components:

	PC1	PC2	PC3	PC4	PC5	PC6	PC7	PC8	PC9
Standard deviation	0.8564	0.26780	0.21736	0.11207	0.07950	0.05888	0.04268	0.03239	0.02872
Proportion of Variance	0.8339	0.08155	0.05372	0.01428	0.00719	0.00394	0.00207	0.00119	0.00094
Cumulative Proportion	0.8339	0.91544	0.96916	0.98344	0.99063	0.99457	0.99664	0.99783	0.99877

	PC10	PC11	PC12	PC13	PC14	PC15	PC16	PC17
Standard deviation	0.02217	0.01429	0.01307	0.008082	0.00644	0.005215	0.005023	0.003105
Proportion of Variance	0.00056	0.00023	0.00019	0.000070	0.00005	0.000030	0.000030	0.000010
Cumulative Proportion	0.99933	0.99956	0.99976	0.999830	0.99988	0.999910	0.999940	0.999950

	PC18	PC19	PC20	PC21	PC22	PC23	PC24	PC25
Standard deviation	0.002934	0.002224	0.001994	0.00178	0.001490	0.001163	0.001051	0.001034
Proportion of Variance	0.000010	0.000010	0.000000	0.00000	0.000000	0.000000	0.000000	0.000000
Cumulative Proportion	0.999960	0.999960	0.999970	0.99997	0.999970	0.999980	0.999980	0.999980

	PC26	PC27	PC28	PC29	PC30	PC31	PC32
Standard deviation	0.001001	0.0009526	0.0009124	0.0008738	0.0008549	0.0008049	0.0007898
Proportion of Variance	0.000000	0.0000000	0.0000000	0.0000000	0.0000000	0.0000000	0.0000000
Cumulative Proportion	0.999980	0.9999800	0.9999800	0.9999800	0.9999800	0.9999800	0.9999800

	PC33	PC34	PC35	PC36	PC37	PC38	PC39
Standard deviation	0.0007738	0.0007617	0.0007274	0.000718	0.0006907	0.000671	0.0006628
Proportion of Variance	0.0000000	0.0000000	0.0000000	0.000000	0.0000000	0.000000	0.0000000
Cumulative Proportion	0.9999800	0.9999900	0.9999900	0.999990	0.9999900	0.999990	0.9999900

	PC40	PC41	PC42	PC43	PC44	PC45	PC46
Standard deviation	0.0006422	0.0006286	0.0006163	0.0006029	0.0005941	0.00058	0.0005645
Proportion of Variance	0.0000000	0.0000000	0.0000000	0.0000000	0.0000000	0.00000	0.0000000
Cumulative Proportion	0.9999900	0.9999900	0.9999900	0.9999900	0.9999900	0.99999	0.9999900

	PC47	PC48	PC49	PC50	PC51	PC52	PC53
Standard deviation	0.0005544	0.0005426	0.0005277	0.0005111	0.0005066	0.0004859	0.0004833
Proportion of Variance	0.0000000	0.0000000	0.0000000	0.0000000	0.0000000	0.0000000	0.0000000
Cumulative Proportion	0.9999900	0.9999900	0.9999900	0.9999900	0.9999900	0.9999900	0.9999900

	PC54	PC55	PC56	PC57	PC58	PC59	PC60
Standard deviation	0.000474	0.0004664	0.000459	0.0004524	0.0004469	0.000439	0.0004281
Proportion of Variance	0.000000	0.0000000	0.000000	0.0000000	0.0000000	0.000000	0.0000000
Cumulative Proportion	0.999990	0.9999900	0.999990	0.9999900	0.9999900	0.999990	0.9999900

	PC61	PC62	PC63	PC64	PC65	PC66	PC67
Standard deviation	0.0004226	0.0004058	0.0004036	0.0003902	0.0003836	0.0003743	0.0003684
Proportion of Variance	0.0000000	0.0000000	0.0000000	0.0000000	0.0000000	0.0000000	0.0000000
Cumulative Proportion	1.0000000	1.0000000	1.0000000	1.0000000	1.0000000	1.0000000	1.0000000

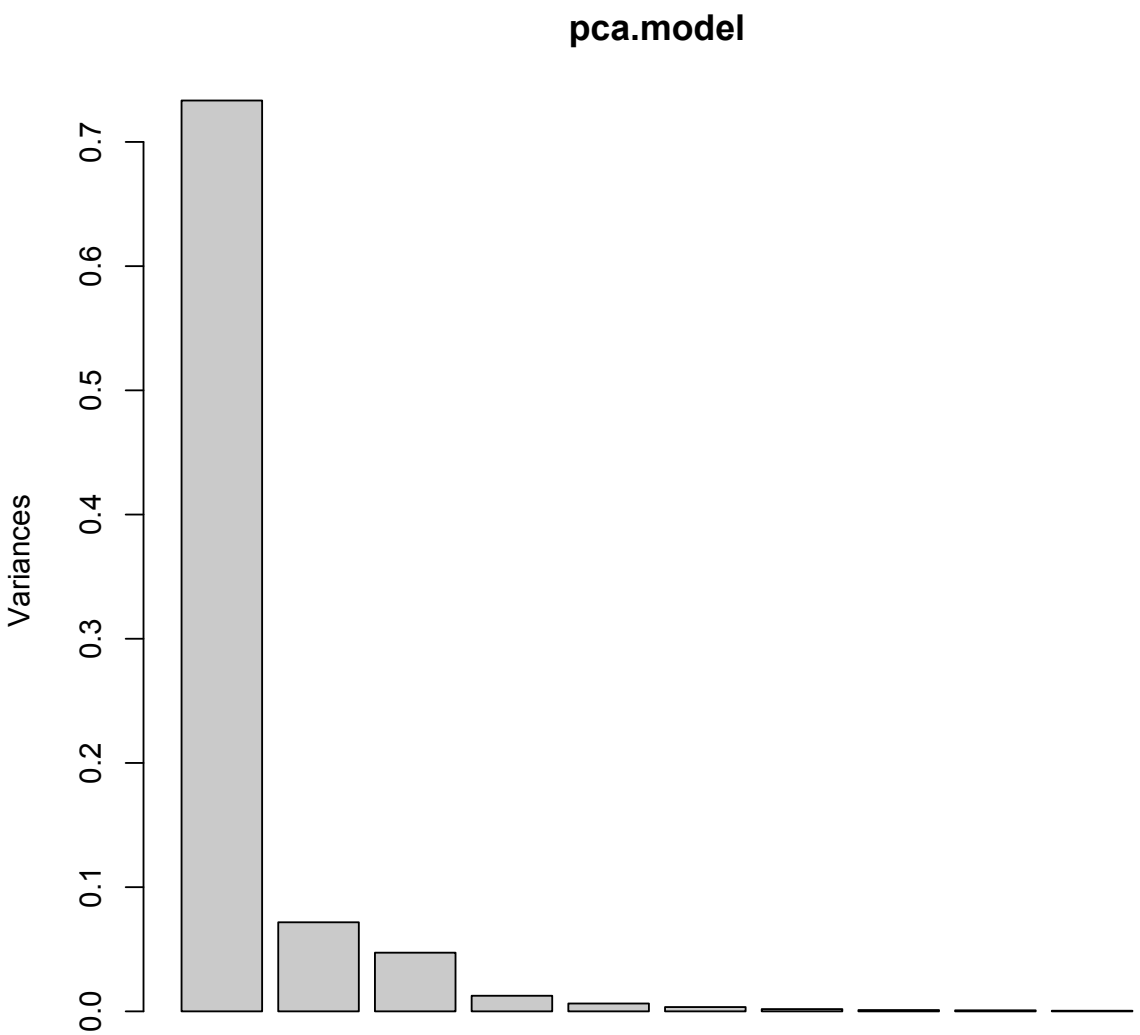


Figure 133: PCA scree plot for the first set of 30 glass spectra (10 replicates), centered.

Table 145: PCA results for the first set of 30 glass spectra (10 replicates), autoscaled.

Importance of components:

	PC1	PC2	PC3	PC4	PC5	PC6	PC7	PC8	PC9
Standard deviation	12.2744	11.7822	4.80850	2.04453	1.56510	1.19569	1.1369	0.61341	0.46886
Proportion of Variance	0.4664	0.4298	0.07158	0.01294	0.00758	0.00443	0.0040	0.00116	0.00068
Cumulative Proportion	0.4664	0.8962	0.96781	0.98075	0.98833	0.99276	0.9968	0.99793	0.99861

	PC10	PC11	PC12	PC13	PC14	PC15	PC16	PC17	PC18
Standard deviation	0.39542	0.3125	0.2519	0.21947	0.16863	0.14098	0.10460	0.06698	0.05410
Proportion of Variance	0.00048	0.0003	0.0002	0.00015	0.00009	0.00006	0.00003	0.00001	0.00001
Cumulative Proportion	0.99909	0.9994	0.9996	0.99974	0.99983	0.99989	0.99992	0.99994	0.99995

	PC19	PC20	PC21	PC22	PC23	PC24	PC25	PC26	PC27
Standard deviation	0.05132	0.04746	0.03754	0.03448	0.03125	0.02891	0.02387	0.02207	0.01967
Proportion of Variance	0.00001	0.00001	0.00000	0.00000	0.00000	0.00000	0.00000	0.00000	0.00000
Cumulative Proportion	0.99995	0.99996	0.99996	0.99997	0.99997	0.99997	0.99998	0.99998	0.99998

	PC28	PC29	PC30	PC31	PC32	PC33	PC34	PC35	PC36
Standard deviation	0.01796	0.01600	0.01512	0.01490	0.01442	0.01389	0.01364	0.01338	0.01298
Proportion of Variance	0.00000	0.00000	0.00000	0.00000	0.00000	0.00000	0.00000	0.00000	0.00000
Cumulative Proportion	0.99998	0.99998	0.99998	0.99998	0.99998	0.99998	0.99998	0.99998	0.99998

	PC37	PC38	PC39	PC40	PC41	PC42	PC43	PC44	PC45
Standard deviation	0.01279	0.01239	0.01211	0.01200	0.01167	0.01096	0.01085	0.01081	0.01055
Proportion of Variance	0.00000	0.00000	0.00000	0.00000	0.00000	0.00000	0.00000	0.00000	0.00000
Cumulative Proportion	0.99999	0.99999	0.99999	0.99999	0.99999	0.99999	0.99999	0.99999	0.99999

	PC46	PC47	PC48	PC49	PC50	PC51	PC52	PC53
Standard deviation	0.01047	0.01018	0.01010	0.009874	0.009853	0.00951	0.009367	0.009314
Proportion of Variance	0.00000	0.00000	0.00000	0.000000	0.000000	0.00000	0.000000	0.000000
Cumulative Proportion	0.99999	0.99999	0.99999	0.999990	0.999990	0.99999	0.999990	0.999990

	PC54	PC55	PC56	PC57	PC58	PC59	PC60	PC61
Standard deviation	0.009064	0.00899	0.008887	0.008447	0.008434	0.00829	0.008238	0.007902
Proportion of Variance	0.000000	0.00000	0.000000	0.000000	0.000000	0.00000	0.000000	0.000000
Cumulative Proportion	0.999990	0.99999	0.999990	0.999990	0.999990	0.99999	0.999990	0.999990

	PC62	PC63	PC64	PC65	PC66	PC67	PC68	PC69
Standard deviation	0.007886	0.007817	0.007782	0.007607	0.007485	0.007456	0.00731	0.007248
Proportion of Variance	0.000000	0.000000	0.000000	0.000000	0.000000	0.000000	0.00000	0.000000
Cumulative Proportion	0.999990	0.999990	0.999990	0.999990	0.999990	0.999990	0.99999	0.999990

	PC70	PC71	PC72	PC73	PC74	PC75	PC76	PC77
Standard deviation	0.007101	0.006964	0.006872	0.00668	0.006676	0.006604	0.006491	0.006343
Proportion of Variance	0.000000	0.000000	0.000000	0.00000	0.000000	0.000000	0.000000	0.000000
Cumulative Proportion	0.999990	0.999990	0.999990	0.99999	0.999990	1.000000	1.000000	1.000000

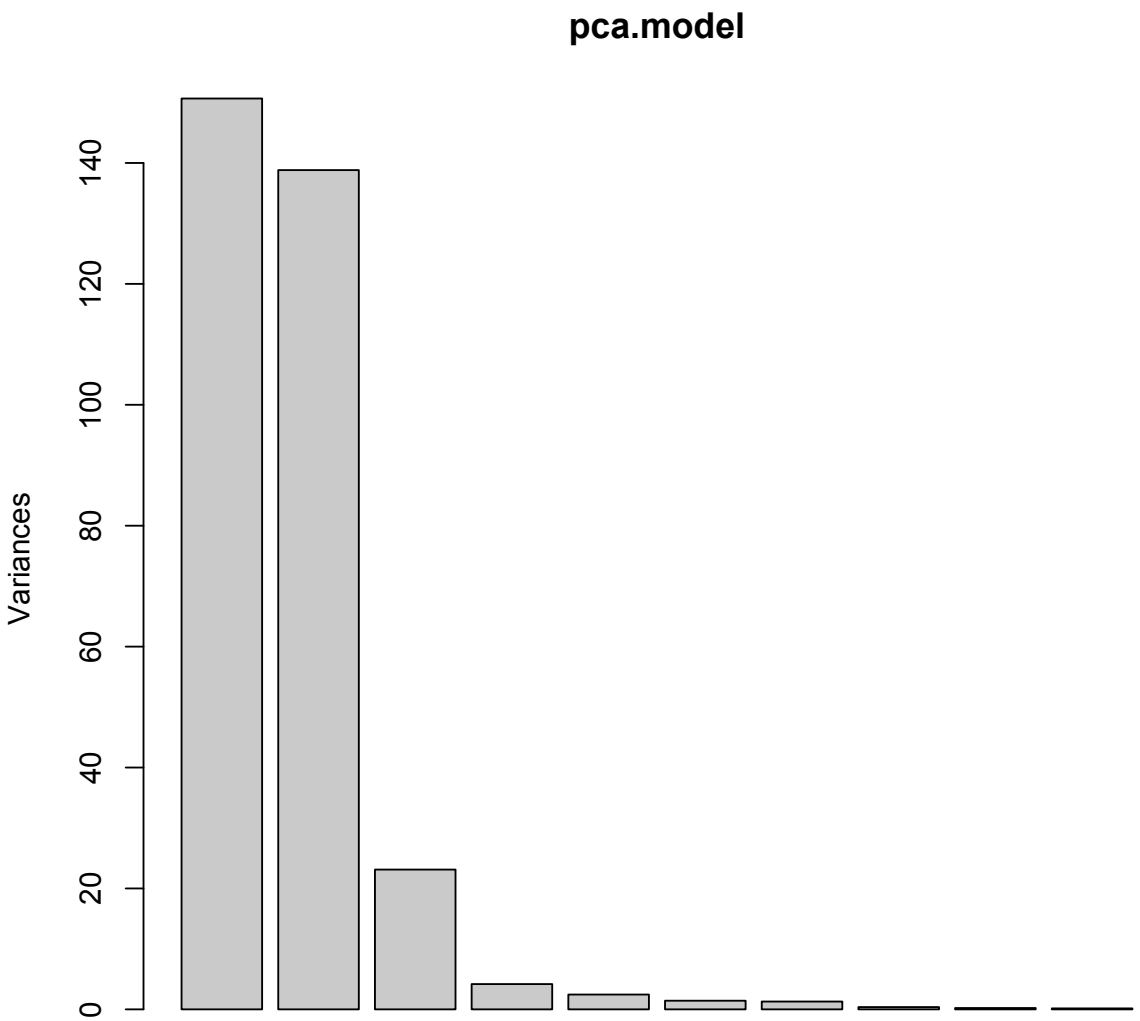


Figure 134: PCA scree plot for the first set of 30 glass spectra (10 replicates), autoscaled.

Table 146: PCA results for the first set of 20 window glass spectra (10 replicates), no data pretreatment.

Importance of components:

	PC1	PC2	PC3	PC4	PC5	PC6	PC7	PC8	PC9	PC10	PC11	PC12
Standard deviation	10.5509	0.45933	0.2107	0.13570	0.07156	0.04238	0.03733	0.03212	0.02860	0.0189	0.01376	0.01252
Proportion of Variance	0.9974	0.00189	0.0004	0.00017	0.00005	0.00002	0.00001	0.00001	0.00001	0.0000	0.00000	0.00000
Cumulative Proportion	0.9974	0.99934	0.9997	0.99990	0.99995	0.99996	0.99998	0.99998	0.99999	1.0000	1.00000	1.00000

	PC13	PC14	PC15	PC16	PC17	PC18	PC19	PC20	PC21	PC22
Standard deviation	0.007539	0.006848	0.005076	0.00475	0.00336	0.002493	0.001935	0.001846	0.001614	0.001282
Proportion of Variance	0.000000	0.000000	0.000000	0.00000	0.00000	0.000000	0.000000	0.000000	0.000000	0.000000
Cumulative Proportion	1.000000	1.000000	1.000000	1.00000	1.00000	1.000000	1.000000	1.000000	1.000000	1.000000

	PC23	PC24	PC25	PC26	PC27	PC28	PC29	PC30	PC31
Standard deviation	0.001160	0.001108	0.001008	0.00097	0.0009197	0.0008903	0.0008292	0.0008253	0.0007883
Proportion of Variance	0.000000	0.000000	0.000000	0.00000	0.0000000	0.0000000	0.0000000	0.0000000	0.0000000
Cumulative Proportion	1.000000	1.000000	1.000000	1.00000	1.0000000	1.0000000	1.0000000	1.0000000	1.0000000

	PC32	PC33	PC34	PC35	PC36	PC37	PC38	PC39	PC40
Standard deviation	0.0007826	0.0007612	0.0007218	0.000713	0.0006938	0.0006865	0.0006684	0.0006389	0.0006358
Proportion of Variance	0.0000000	0.0000000	0.0000000	0.000000	0.0000000	0.0000000	0.0000000	0.0000000	0.0000000
Cumulative Proportion	1.0000000	1.0000000	1.0000000	1.000000	1.0000000	1.0000000	1.0000000	1.0000000	1.0000000

	PC41	PC42	PC43	PC44	PC45	PC46	PC47	PC48	PC49
Standard deviation	0.0006238	0.000592	0.0005633	0.0005562	0.0005523	0.0005409	0.0005312	0.0005231	0.0005162
Proportion of Variance	0.0000000	0.000000	0.0000000	0.0000000	0.0000000	0.0000000	0.0000000	0.0000000	0.0000000
Cumulative Proportion	1.0000000	1.000000	1.0000000	1.0000000	1.0000000	1.0000000	1.0000000	1.0000000	1.0000000

	PC50	PC51	PC52	PC53	PC54	PC55	PC56	PC57	PC58
Standard deviation	0.0005043	0.00049	0.0004773	0.000468	0.0004557	0.0004498	0.0004301	0.0004245	0.0004098
Proportion of Variance	0.0000000	0.00000	0.0000000	0.000000	0.0000000	0.0000000	0.0000000	0.0000000	0.0000000
Cumulative Proportion	1.0000000	1.00000	1.0000000	1.000000	1.0000000	1.0000000	1.0000000	1.0000000	1.0000000

	PC59	PC60	PC61	PC62	PC63	PC64	PC65	PC66	PC67
Standard deviation	0.0004017	0.0003911	0.0003843	0.0003775	0.0003741	0.0003627	0.0003533	0.000351	0.0003409
Proportion of Variance	0.0000000	0.0000000	0.0000000	0.0000000	0.0000000	0.0000000	0.0000000	0.000000	0.0000000
Cumulative Proportion	1.0000000	1.0000000	1.0000000	1.0000000	1.0000000	1.0000000	1.0000000	1.000000	1.0000000

	PC68	PC69	PC70	PC71	PC72	PC73	PC74	PC75	PC76
Standard deviation	0.0003377	0.0003227	0.000315	0.0003085	0.0003008	0.0002978	0.0002929	0.0002808	0.0002735
Proportion of Variance	0.0000000	0.0000000	0.000000	0.0000000	0.0000000	0.0000000	0.0000000	0.0000000	0.0000000
Cumulative Proportion	1.0000000	1.0000000	1.000000	1.0000000	1.0000000	1.0000000	1.0000000	1.0000000	1.0000000

	PC77	PC78	PC79	PC80	PC81	PC82	PC83	PC84	PC85
Standard deviation	0.0002685	0.0002629	0.0002576	0.0002522	0.0002434	0.0002398	0.0002365	0.0002332	0.0002248
Proportion of Variance	0.0000000	0.0000000	0.0000000	0.0000000	0.0000000	0.0000000	0.0000000	0.0000000	0.0000000
Cumulative Proportion	1.0000000	1.0000000	1.0000000	1.0000000	1.0000000	1.0000000	1.0000000	1.0000000	1.0000000

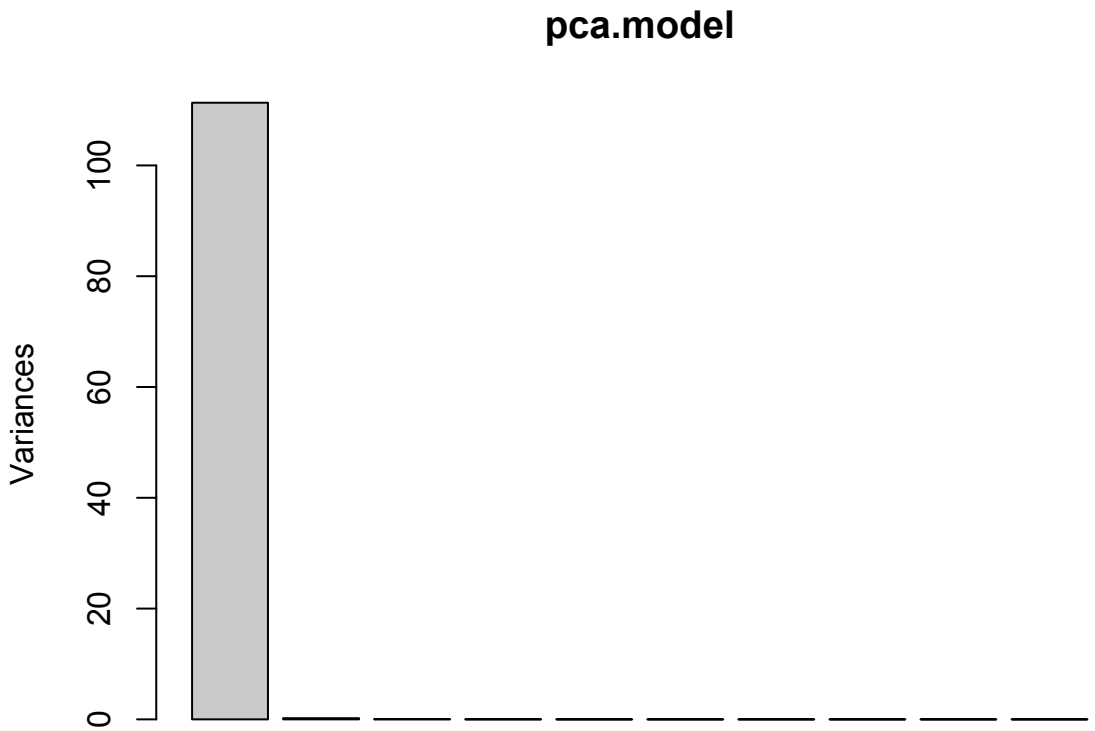


Figure 135: PCA scree plot for the first set of 20 window glass spectra (10 replicates), no data pretreatment.

Table 147: PCA results for the first set of 20 window glass spectra (10 replicates), centered.

Importance of components:

	PC1	PC2	PC3	PC4	PC5	PC6	PC7	PC8	PC9	PC10	PC11
Standard deviation	0.8126	0.23954	0.19899	0.10782	0.05450	0.04113	0.03214	0.02987	0.02371	0.01889	0.01373
Proportion of Variance	0.8499	0.07385	0.05096	0.01496	0.00382	0.00218	0.00133	0.00115	0.00072	0.00046	0.00024
Cumulative Proportion	0.8499	0.92374	0.97471	0.98967	0.99349	0.99567	0.99700	0.99815	0.99887	0.99933	0.99957

	PC12	PC13	PC14	PC15	PC16	PC17	PC18	PC19	PC20	PC21
Standard deviation	0.01210	0.007515	0.006203	0.005033	0.004478	0.003006	0.002475	0.001898	0.001740	0.001583
Proportion of Variance	0.00019	0.000070	0.000050	0.000030	0.000030	0.000010	0.000010	0.000000	0.000000	0.000000
Cumulative Proportion	0.99976	0.999830	0.999880	0.999910	0.999940	0.999950	0.999960	0.999960	0.999970	0.999970

	PC22	PC23	PC24	PC25	PC26	PC27	PC28	PC29	PC30
Standard deviation	0.001278	0.001151	0.001090	0.0009991	0.0009565	0.0009164	0.000888	0.0008258	0.0008102
Proportion of Variance	0.000000	0.000000	0.000000	0.0000000	0.0000000	0.0000000	0.000000	0.0000000	0.0000000
Cumulative Proportion	0.999970	0.999970	0.999980	0.9999800	0.9999800	0.9999800	0.999980	0.9999800	0.9999800

	PC31	PC32	PC33	PC34	PC35	PC36	PC37	PC38	PC39
Standard deviation	0.0007872	0.0007645	0.0007518	0.0007211	0.000712	0.000693	0.000683	0.000649	0.0006386
Proportion of Variance	0.0000000	0.0000000	0.0000000	0.0000000	0.000000	0.000000	0.000000	0.000000	0.0000000
Cumulative Proportion	0.9999800	0.9999800	0.9999900	0.9999900	0.999990	0.999990	0.999990	0.999990	0.9999900

	PC40	PC41	PC42	PC43	PC44	PC45	PC46	PC47	PC48
Standard deviation	0.000624	0.0006153	0.000582	0.0005597	0.0005554	0.0005462	0.0005385	0.0005306	0.0005231
Proportion of Variance	0.000000	0.0000000	0.000000	0.0000000	0.0000000	0.0000000	0.0000000	0.0000000	0.0000000
Cumulative Proportion	0.999990	0.9999900	0.999990	0.9999900	0.9999900	0.9999900	0.9999900	0.9999900	0.9999900

	PC49	PC50	PC51	PC52	PC53	PC54	PC55	PC56	PC57
Standard deviation	0.0005061	0.0004938	0.0004871	0.0004725	0.0004663	0.0004529	0.0004495	0.0004292	0.0004227
Proportion of Variance	0.0000000	0.0000000	0.0000000	0.0000000	0.0000000	0.0000000	0.0000000	0.0000000	0.0000000
Cumulative Proportion	0.9999900	0.9999900	0.9999900	0.9999900	0.9999900	0.9999900	0.9999900	0.9999900	0.9999900

	PC58	PC59	PC60	PC61	PC62	PC63	PC64	PC65	PC66
Standard deviation	0.0004093	0.0004016	0.0003911	0.0003831	0.0003767	0.0003691	0.0003556	0.0003517	0.0003488
Proportion of Variance	0.0000000	0.0000000	0.0000000	0.0000000	0.0000000	0.0000000	0.0000000	0.0000000	0.0000000
Cumulative Proportion	1.0000000	1.0000000	1.0000000	1.0000000	1.0000000	1.0000000	1.0000000	1.0000000	1.0000000

	PC67	PC68	PC69	PC70	PC71	PC72	PC73	PC74	PC75
Standard deviation	0.0003399	0.0003373	0.0003224	0.0003091	0.0003085	0.0003007	0.0002966	0.0002884	0.0002807
Proportion of Variance	0.0000000	0.0000000	0.0000000	0.0000000	0.0000000	0.0000000	0.0000000	0.0000000	0.0000000
Cumulative Proportion	1.0000000	1.0000000	1.0000000	1.0000000	1.0000000	1.0000000	1.0000000	1.0000000	1.0000000

	PC76	PC77	PC78	PC79	PC80	PC81	PC82	PC83	PC84
Standard deviation	0.0002706	0.0002685	0.0002585	0.0002575	0.0002506	0.0002429	0.0002397	0.0002365	0.0002288
Proportion of Variance	0.0000000	0.0000000	0.0000000	0.0000000	0.0000000	0.0000000	0.0000000	0.0000000	0.0000000
Cumulative Proportion	1.0000000	1.0000000	1.0000000	1.0000000	1.0000000	1.0000000	1.0000000	1.0000000	1.0000000

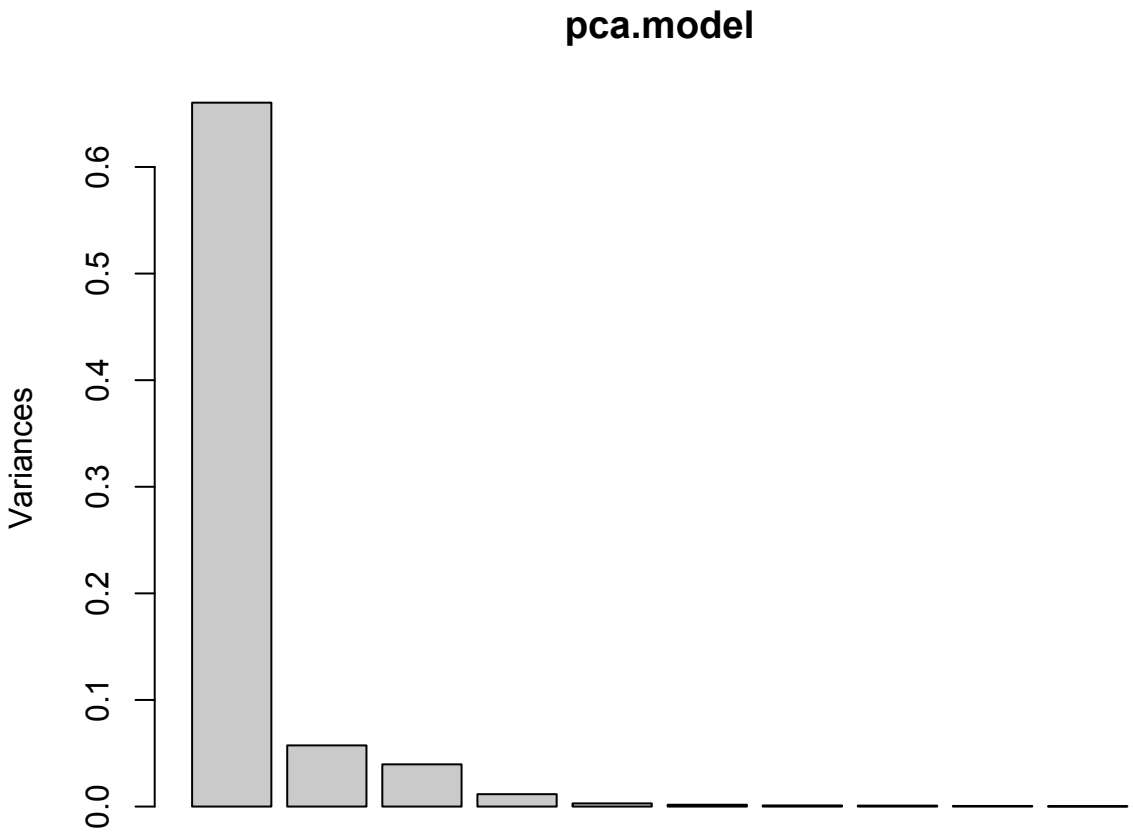


Figure 136: PCA scree plot for the first set of 20 window glass spectra (10 replicates), centered.

Table 148: PCA results for the first set of 20 window glass spectra (10 replicates), autoscaled.

Importance of components:

	PC1	PC2	PC3	PC4	PC5	PC6	PC7	PC8	PC9	PC10	PC11	PC12
Standard deviation	12.5486	11.5560	4.92907	1.93469	1.2063	1.0171	0.69916	0.55830	0.4417	0.4024	0.28843	0.28207
Proportion of Variance	0.4875	0.4134	0.07522	0.01159	0.0045	0.0032	0.00151	0.00097	0.0006	0.0005	0.00026	0.00025
Cumulative Proportion	0.4875	0.9010	0.97618	0.98777	0.9923	0.9955	0.99699	0.99795	0.9986	0.9991	0.99932	0.99956

	PC13	PC14	PC15	PC16	PC17	PC18	PC19	PC20	PC21	PC22	PC23
Standard deviation	0.24169	0.16356	0.14381	0.10879	0.06529	0.05185	0.04983	0.03897	0.03502	0.03344	0.0315
Proportion of Variance	0.00018	0.00008	0.00006	0.00004	0.00001	0.00001	0.00001	0.00000	0.00000	0.00000	0.0000
Cumulative Proportion	0.99974	0.99983	0.99989	0.99993	0.99994	0.99995	0.99996	0.99996	0.99997	0.99997	1.0000

	PC24	PC25	PC26	PC27	PC28	PC29	PC30	PC31	PC32	PC33	PC34
Standard deviation	0.02652	0.0233	0.01992	0.01781	0.01742	0.01688	0.01633	0.01601	0.01535	0.01465	0.01465
Proportion of Variance	0.00000	0.0000	0.00000	0.00000	0.00000	0.00000	0.00000	0.00000	0.00000	0.00000	0.00000
Cumulative Proportion	0.99997	1.0000	0.99998	0.99998	0.99998	0.99998	0.99998	0.99998	0.99998	0.99998	0.99998

	PC35	PC36	PC37	PC38	PC39	PC40	PC41	PC42	PC43	PC44	PC45
Standard deviation	0.01381	0.01363	0.01329	0.01311	0.01270	0.01216	0.01162	0.01150	0.01142	0.01133	0.01098
Proportion of Variance	0.00000	0.00000	0.00000	0.00000	0.00000	0.00000	0.00000	0.00000	0.00000	0.00000	0.00000
Cumulative Proportion	0.99998	0.99998	0.99999	0.99999	0.99999	0.99999	0.99999	0.99999	0.99999	0.99999	0.99999

	PC46	PC47	PC48	PC49	PC50	PC51	PC52	PC53	PC54	PC55	PC56
Standard deviation	0.01089	0.0105	0.01046	0.01027	0.01012	0.009983	0.00978	0.009504	0.009433	0.009295	0.009131
Proportion of Variance	0.00000	0.0000	0.00000	0.00000	0.00000	0.000000	0.00000	0.000000	0.000000	0.000000	0.000000
Cumulative Proportion	0.99999	1.0000	0.99999	0.99999	0.99999	0.999990	0.99999	0.999990	0.999990	0.999990	0.999990

	PC57	PC58	PC59	PC60	PC61	PC62	PC63	PC64	PC65	PC66
Standard deviation	0.008904	0.008873	0.008728	0.008593	0.008531	0.008356	0.008203	0.008042	0.007935	0.007719
Proportion of Variance	0.000000	0.000000	0.000000	0.000000	0.000000	0.000000	0.000000	0.000000	0.000000	0.000000
Cumulative Proportion	0.999990	0.999990	0.999990	0.999990	0.999990	0.999990	0.999990	0.999990	0.999990	0.999990

	PC67	PC68	PC69	PC70	PC71	PC72	PC73	PC74	PC75	PC76
Standard deviation	0.007687	0.00752	0.007385	0.007358	0.007267	0.00709	0.007014	0.006914	0.006795	0.006644
Proportion of Variance	0.000000	0.00000	0.000000	0.000000	0.000000	0.00000	0.000000	0.000000	0.000000	0.000000
Cumulative Proportion	0.999990	0.99999	0.999990	0.999990	0.999990	1.00000	1.000000	1.000000	1.000000	1.000000

	PC77	PC78	PC79	PC80	PC81	PC82	PC83	PC84	PC85	PC86
Standard deviation	0.006504	0.006439	0.006338	0.006216	0.006114	0.006037	0.006022	0.005822	0.005766	0.005684
Proportion of Variance	0.000000	0.000000	0.000000	0.000000	0.000000	0.000000	0.000000	0.000000	0.000000	0.000000
Cumulative Proportion	1.000000	1.000000	1.000000	1.000000	1.000000	1.000000	1.000000	1.000000	1.000000	1.000000

	PC87	PC88	PC89	PC90	PC91	PC92	PC93	PC94	PC95	PC96
Standard deviation	0.005648	0.005631	0.005505	0.005386	0.005324	0.005269	0.005217	0.005068	0.004969	0.004916
Proportion of Variance	0.000000	0.000000	0.000000	0.000000	0.000000	0.000000	0.000000	0.000000	0.000000	0.000000
Cumulative Proportion	1.000000	1.000000	1.000000	1.000000	1.000000	1.000000	1.000000	1.000000	1.000000	1.000000

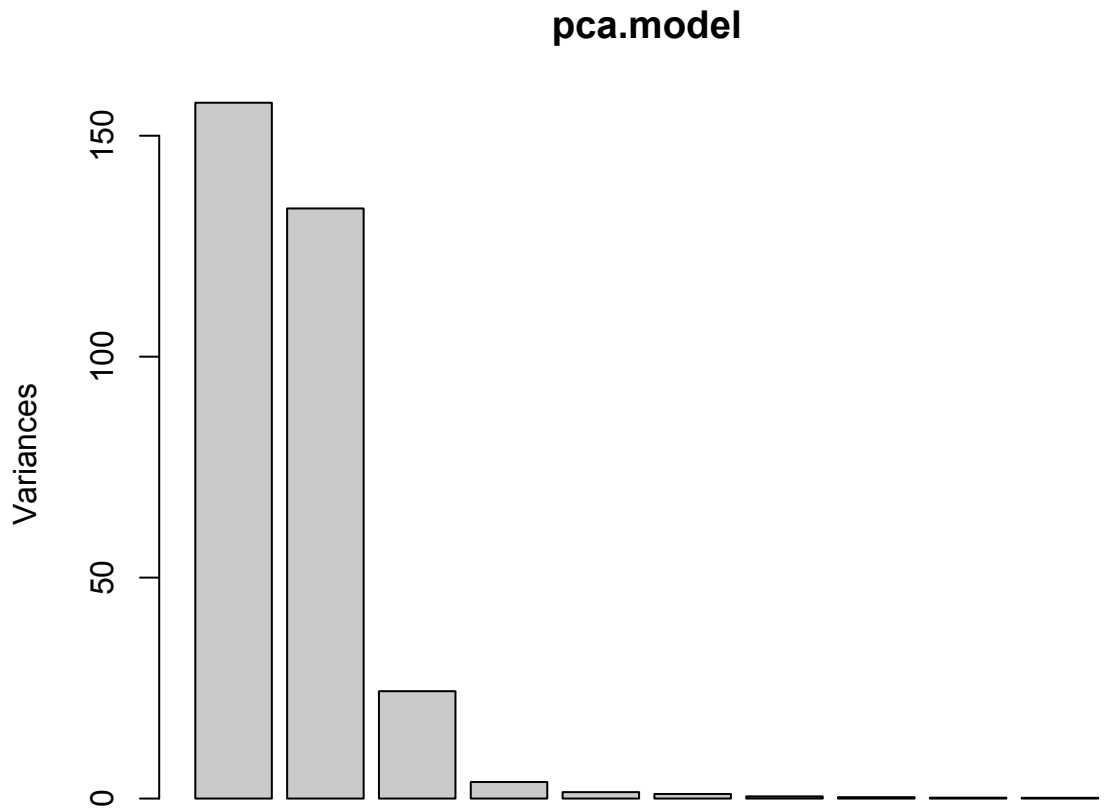


Figure 137: PCA scree plot for the first set of 20 window glass spectra (10 replicates), autoscaled.

Table 149: PCA results for the first set of 10 container glass spectra (10 replicates), no data pretreatment.

Importance of components:

	PC1	PC2	PC3	PC4	PC5	PC6	PC7	PC8	PC9	PC10	PC11
Standard deviation	10.5416	0.56378	0.2356	0.17791	0.07655	0.06497	0.04125	0.03709	0.02466	0.02345	0.01504
Proportion of Variance	0.9962	0.00285	0.0005	0.00028	0.00005	0.00004	0.00002	0.00001	0.00001	0.00000	0.00000
Cumulative Proportion	0.9962	0.99909	0.9996	0.99987	0.99992	0.99996	0.99997	0.99998	0.99999	0.99999	1.00000

	PC12	PC13	PC14	PC15	PC16	PC17	PC18	PC19	PC20	PC21
Standard deviation	0.01270	0.007188	0.006246	0.004788	0.003678	0.002933	0.00228	0.002199	0.001856	0.001589
Proportion of Variance	0.00000	0.000000	0.000000	0.000000	0.000000	0.000000	0.00000	0.000000	0.000000	0.000000
Cumulative Proportion	1.00000	1.000000	1.000000	1.000000	1.000000	1.000000	1.00000	1.000000	1.000000	1.000000

	PC22	PC23	PC24	PC25	PC26	PC27	PC28	PC29	PC30
Standard deviation	0.001315	0.001179	0.001121	0.001039	0.0009734	0.0009234	0.0009198	0.0008582	0.000852
Proportion of Variance	0.000000	0.000000	0.000000	0.000000	0.0000000	0.0000000	0.0000000	0.0000000	0.000000
Cumulative Proportion	1.000000	1.000000	1.000000	1.000000	1.0000000	1.0000000	1.0000000	1.0000000	1.000000

	PC31	PC32	PC33	PC34	PC35	PC36	PC37	PC38	PC39
Standard deviation	0.000833	0.0007774	0.000762	0.0007469	0.0007242	0.0006742	0.0006617	0.0006593	0.000611
Proportion of Variance	0.000000	0.0000000	0.000000	0.0000000	0.0000000	0.0000000	0.0000000	0.0000000	0.000000
Cumulative Proportion	1.000000	1.0000000	1.000000	1.0000000	1.0000000	1.0000000	1.0000000	1.0000000	1.000000

	PC40	PC41	PC42	PC43	PC44	PC45	PC46	PC47	PC48
Standard deviation	0.0006015	0.0005896	0.000562	0.0005341	0.0005173	0.0005007	0.0004902	0.0004788	0.000463
Proportion of Variance	0.0000000	0.0000000	0.000000	0.0000000	0.0000000	0.0000000	0.0000000	0.0000000	0.000000
Cumulative Proportion	1.0000000	1.0000000	1.000000	1.0000000	1.0000000	1.0000000	1.0000000	1.0000000	1.000000

	PC49	PC50	PC51	PC52	PC53	PC54	PC55	PC56	PC57
Standard deviation	0.0004483	0.0004448	0.0004303	0.0004143	0.0004105	0.0003856	0.0003787	0.000375	0.0003615
Proportion of Variance	0.0000000	0.0000000	0.0000000	0.0000000	0.0000000	0.0000000	0.0000000	0.000000	0.0000000
Cumulative Proportion	1.0000000	1.0000000	1.0000000	1.0000000	1.0000000	1.0000000	1.0000000	1.000000	1.0000000

	PC58	PC59	PC60	PC61	PC62	PC63	PC64	PC65	PC66
Standard deviation	0.0003573	0.0003441	0.0003191	0.0003144	0.0003084	0.0003030	0.0002967	0.0002942	0.0002812
Proportion of Variance	0.0000000	0.0000000	0.0000000	0.0000000	0.0000000	0.0000000	0.0000000	0.0000000	0.0000000
Cumulative Proportion	1.0000000	1.0000000	1.0000000	1.0000000	1.0000000	1.0000000	1.0000000	1.0000000	1.0000000

	PC67	PC68	PC69	PC70	PC71	PC72	PC73	PC74	PC75
Standard deviation	0.0002766	0.0002707	0.0002648	0.0002622	0.000245	0.0002322	0.0002299	0.0002258	0.0002208
Proportion of Variance	0.0000000	0.0000000	0.0000000	0.0000000	0.000000	0.0000000	0.0000000	0.0000000	0.0000000
Cumulative Proportion	1.0000000	1.0000000	1.0000000	1.0000000	1.000000	1.0000000	1.0000000	1.0000000	1.0000000

	PC76	PC77	PC78	PC79	PC80	PC81	PC82	PC83	PC84
Standard deviation	0.0002135	0.0001976	0.0001942	0.0001898	0.0001851	0.0001788	0.0001703	0.0001678	0.0001635
Proportion of Variance	0.0000000	0.0000000	0.0000000	0.0000000	0.0000000	0.0000000	0.0000000	0.0000000	0.0000000
Cumulative Proportion	1.0000000	1.0000000	1.0000000	1.0000000	1.0000000	1.0000000	1.0000000	1.0000000	1.0000000

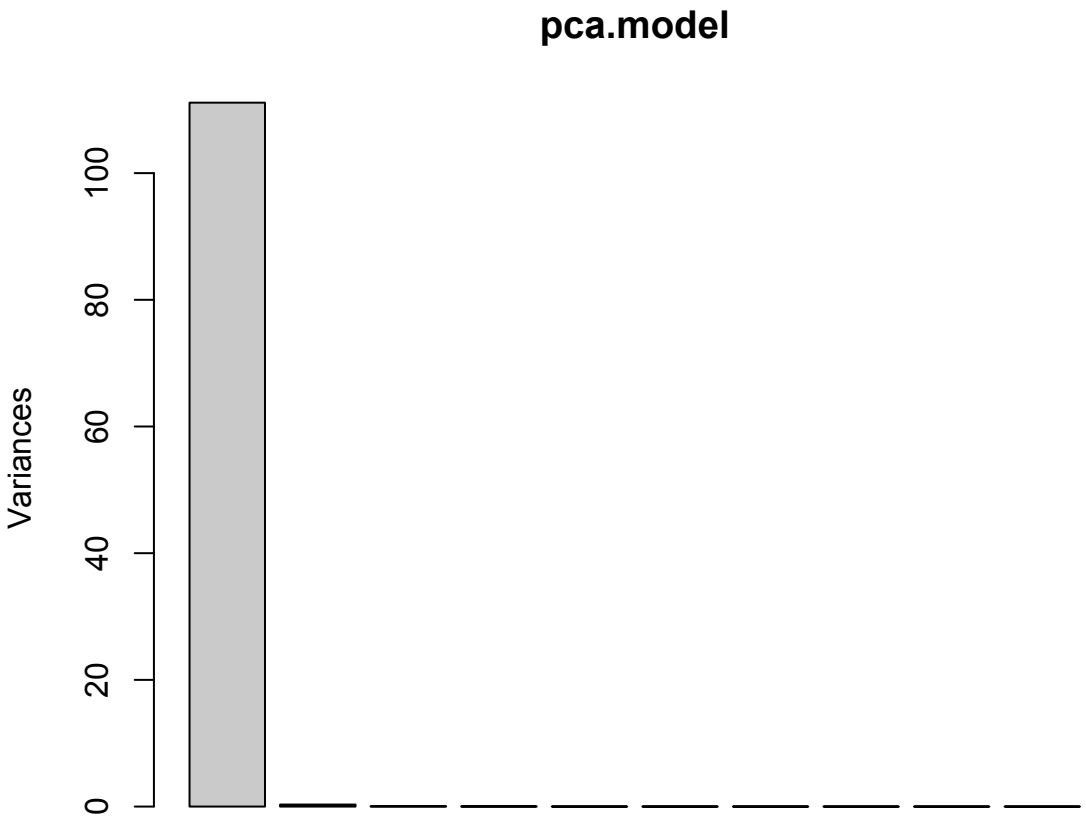


Figure 138: PCA scree plot for the first set of 10 container glass spectra (10 replicates), no data pretreatment.

Table 150: PCA results for the first set of 10 container glass spectra (10 replicates), centered.

Importance of components:

	PC1	PC2	PC3	PC4	PC5	PC6	PC7	PC8	PC9	PC10	PC11
Standard deviation	0.9405	0.3362	0.2284	0.11532	0.07065	0.05951	0.03747	0.02988	0.02426	0.01951	0.01451
Proportion of Variance	0.8226	0.1051	0.0485	0.01237	0.00464	0.00329	0.00131	0.00083	0.00055	0.00035	0.00020
Cumulative Proportion	0.8226	0.9277	0.9762	0.98854	0.99318	0.99648	0.99778	0.99861	0.99916	0.99951	0.99971

	PC12	PC13	PC14	PC15	PC16	PC17	PC18	PC19	PC20	PC21
Standard deviation	0.01266	0.006966	0.005367	0.004619	0.003364	0.002901	0.002200	0.002034	0.001778	0.001585
Proportion of Variance	0.00015	0.000050	0.000030	0.000020	0.000010	0.000010	0.000000	0.000000	0.000000	0.000000
Cumulative Proportion	0.99986	0.999900	0.999930	0.999950	0.999960	0.999970	0.999970	0.999980	0.999980	0.999980

	PC22	PC23	PC24	PC25	PC26	PC27	PC28	PC29	PC30
Standard deviation	0.001281	0.001177	0.001072	0.001024	0.0009491	0.0009233	0.0009015	0.0008574	0.0008439
Proportion of Variance	0.000000	0.000000	0.000000	0.000000	0.0000000	0.0000000	0.0000000	0.0000000	0.0000000
Cumulative Proportion	0.999980	0.999980	0.999990	0.999990	0.9999900	0.9999900	0.9999900	0.9999900	0.9999900

	PC31	PC32	PC33	PC34	PC35	PC36	PC37	PC38	PC39
Standard deviation	0.0008184	0.0007754	0.0007605	0.0007262	0.0006782	0.0006653	0.0006602	0.0006489	0.0006058
Proportion of Variance	0.0000000	0.0000000	0.0000000	0.0000000	0.0000000	0.0000000	0.0000000	0.0000000	0.0000000
Cumulative Proportion	0.9999900	0.9999900	0.9999900	0.9999900	0.9999900	0.9999900	0.9999900	0.9999900	0.9999900

	PC40	PC41	PC42	PC43	PC44	PC45	PC46	PC47	PC48
Standard deviation	0.0005897	0.0005842	0.0005614	0.0005338	0.0005146	0.0005007	0.0004901	0.0004632	0.0004537
Proportion of Variance	0.0000000	0.0000000	0.0000000	0.0000000	0.0000000	0.0000000	0.0000000	0.0000000	0.0000000
Cumulative Proportion	0.9999900	1.0000000	1.0000000	1.0000000	1.0000000	1.0000000	1.0000000	1.0000000	1.0000000

	PC49	PC50	PC51	PC52	PC53	PC54	PC55	PC56	PC57
Standard deviation	0.0004477	0.0004319	0.0004237	0.0004105	0.0004044	0.0003821	0.0003785	0.0003636	0.0003573
Proportion of Variance	0.0000000	0.0000000	0.0000000	0.0000000	0.0000000	0.0000000	0.0000000	0.0000000	0.0000000
Cumulative Proportion	1.0000000	1.0000000	1.0000000	1.0000000	1.0000000	1.0000000	1.0000000	1.0000000	1.0000000

	PC58	PC59	PC60	PC61	PC62	PC63	PC64	PC65	PC66
Standard deviation	0.0003451	0.0003332	0.0003158	0.0003120	0.0003066	0.0003006	0.0002943	0.0002853	0.0002810
Proportion of Variance	0.0000000	0.0000000	0.0000000	0.0000000	0.0000000	0.0000000	0.0000000	0.0000000	0.0000000
Cumulative Proportion	1.0000000	1.0000000	1.0000000	1.0000000	1.0000000	1.0000000	1.0000000	1.0000000	1.0000000

	PC67	PC68	PC69	PC70	PC71	PC72	PC73	PC74	PC75
Standard deviation	0.0002745	0.0002662	0.0002638	0.0002547	0.0002322	0.0002299	0.0002269	0.0002213	0.0002137
Proportion of Variance	0.0000000	0.0000000	0.0000000	0.0000000	0.0000000	0.0000000	0.0000000	0.0000000	0.0000000
Cumulative Proportion	1.0000000	1.0000000	1.0000000	1.0000000	1.0000000	1.0000000	1.0000000	1.0000000	1.0000000

	PC76	PC77	PC78	PC79	PC80	PC81	PC82	PC83	PC84
Standard deviation	0.0002112	0.000197	0.0001904	0.0001898	0.0001808	0.0001781	0.0001703	0.0001636	0.0001619
Proportion of Variance	0.0000000	0.000000	0.0000000	0.0000000	0.0000000	0.0000000	0.0000000	0.0000000	0.0000000
Cumulative Proportion	1.0000000	1.000000	1.0000000	1.0000000	1.0000000	1.0000000	1.0000000	1.0000000	1.0000000

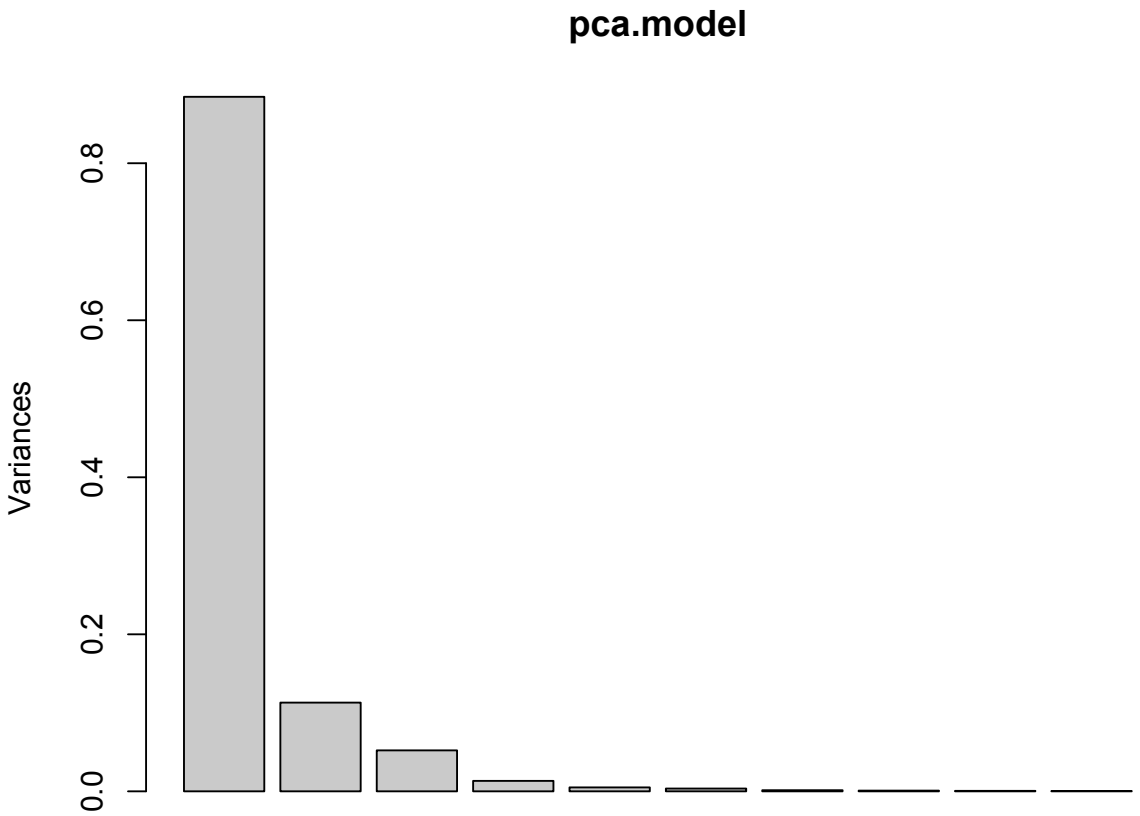


Figure 139: PCA scree plot for the first set of 10 container glass spectra (10 replicates), centered.

Table 151: PCA results for the first set of 10 container glass spectra (10 replicates), autoscaled.

Importance of components:

	PC1	PC2	PC3	PC4	PC5	PC6	PC7	PC8	PC9	PC10	PC11
Standard deviation	12.203	12.0657	4.44795	2.20665	1.11259	1.08769	0.8797	0.4419	0.39253	0.35276	0.24997
Proportion of Variance	0.461	0.4507	0.06125	0.01508	0.00383	0.00366	0.0024	0.0006	0.00048	0.00039	0.00019
Cumulative Proportion	0.461	0.9117	0.97299	0.98806	0.99190	0.99556	0.9980	0.9986	0.99904	0.99942	0.99961

	PC12	PC13	PC14	PC15	PC16	PC17	PC18	PC19	PC20	PC21	PC22
Standard deviation	0.22488	0.17236	0.12796	0.08467	0.07384	0.05176	0.04347	0.03974	0.03465	0.0335	0.02706
Proportion of Variance	0.00016	0.00009	0.00005	0.00002	0.00002	0.00001	0.00001	0.00000	0.00000	0.0000	0.00000
Cumulative Proportion	0.99977	0.99986	0.99991	0.99994	0.99995	0.99996	0.99997	0.99997	0.99998	1.0000	0.99998

	PC23	PC24	PC25	PC26	PC27	PC28	PC29	PC30	PC31	PC32	PC33
Standard deviation	0.02677	0.02279	0.02034	0.01753	0.01597	0.01545	0.0144	0.01356	0.01319	0.01307	0.01237
Proportion of Variance	0.00000	0.00000	0.00000	0.00000	0.00000	0.00000	0.0000	0.00000	0.00000	0.00000	0.00000
Cumulative Proportion	0.99998	0.99999	0.99999	0.99999	0.99999	0.99999	1.0000	0.99999	0.99999	0.99999	0.99999

	PC34	PC35	PC36	PC37	PC38	PC39	PC40	PC41	PC42	PC43	PC44
Standard deviation	0.01189	0.01152	0.01115	0.01107	0.01053	0.01009	0.01003	0.009869	0.009604	0.009284	0.009052
Proportion of Variance	0.00000	0.00000	0.00000	0.00000	0.00000	0.00000	0.00000	0.000000	0.000000	0.000000	0.000000
Cumulative Proportion	0.99999	0.99999	0.99999	0.99999	0.99999	0.99999	0.99999	0.999990	0.999990	0.999990	1.000000

	PC45	PC46	PC47	PC48	PC49	PC50	PC51	PC52	PC53	PC54
Standard deviation	0.008694	0.008397	0.008216	0.008175	0.007817	0.007752	0.007486	0.007432	0.007109	0.00697
Proportion of Variance	0.000000	0.000000	0.000000	0.000000	0.000000	0.000000	0.000000	0.000000	0.000000	0.00000
Cumulative Proportion	1.000000	1.000000	1.000000	1.000000	1.000000	1.000000	1.000000	1.000000	1.000000	1.00000

	PC55	PC56	PC57	PC58	PC59	PC60	PC61	PC62	PC63	PC64
Standard deviation	0.006852	0.006663	0.006541	0.006379	0.006175	0.006135	0.006035	0.005806	0.00577	0.005565
Proportion of Variance	0.000000	0.000000	0.000000	0.000000	0.000000	0.000000	0.000000	0.000000	0.00000	0.000000
Cumulative Proportion	1.000000	1.000000	1.000000	1.000000	1.000000	1.000000	1.000000	1.000000	1.00000	1.000000

	PC65	PC66	PC67	PC68	PC69	PC70	PC71	PC72	PC73	PC74
Standard deviation	0.005485	0.00542	0.005278	0.005205	0.005129	0.005051	0.004951	0.004861	0.004651	0.004471
Proportion of Variance	0.000000	0.00000	0.000000	0.000000	0.000000	0.000000	0.000000	0.000000	0.000000	0.000000
Cumulative Proportion	1.000000	1.00000	1.000000	1.000000	1.000000	1.000000	1.000000	1.000000	1.000000	1.000000

	PC75	PC76	PC77	PC78	PC79	PC80	PC81	PC82	PC83	PC84
Standard deviation	0.004413	0.004302	0.004192	0.004111	0.004036	0.004011	0.003886	0.003822	0.003757	0.003591
Proportion of Variance	0.000000	0.000000	0.000000	0.000000	0.000000	0.000000	0.000000	0.000000	0.000000	0.000000
Cumulative Proportion	1.000000	1.000000	1.000000	1.000000	1.000000	1.000000	1.000000	1.000000	1.000000	1.000000

	PC85	PC86	PC87	PC88	PC89	PC90	PC91	PC92	PC93	PC94
Standard deviation	0.003501	0.003401	0.003333	0.003120	0.003061	0.002993	0.002928	0.002844	0.002767	0.002694
Proportion of Variance	0.000000	0.000000	0.000000	0.000000	0.000000	0.000000	0.000000	0.000000	0.000000	0.000000
Cumulative Proportion	1.000000	1.000000	1.000000	1.000000	1.000000	1.000000	1.000000	1.000000	1.000000	1.000000

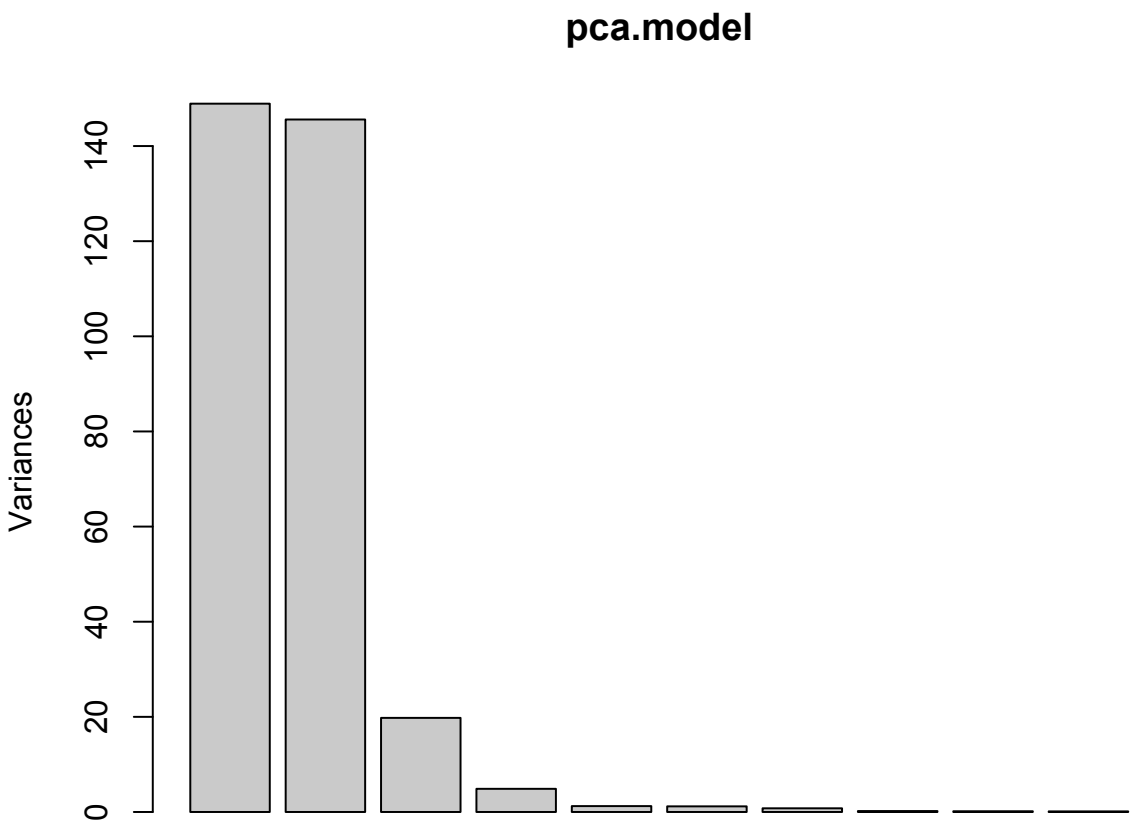


Figure 140: PCA scree plot for the first set of 10 container glass spectra (10 replicates), autoscaled.

B. PCA Results for the Peak Area Normalized Spectra

Table 152: PCA results for the first set of 30 normalized (peak area) glass spectra (10 replicates), no data pretreatment.

Importance of components:

	PC1	PC2	PC3	PC4	PC5	PC6	PC7	PC8
Standard deviation	0.06828	0.003136	0.001394	0.0009932	0.0005268	0.0004802	0.0002761	0.0002406
Proportion of Variance	0.99711	0.002100	0.000420	0.0002100	0.0000600	0.0000500	0.0000200	0.0000100
Cumulative Proportion	0.99711	0.999220	0.999630	0.9998400	0.9999000	0.9999500	0.9999700	0.9999800

	PC9	PC10	PC11	PC12	PC13	PC14	PC15
Standard deviation	0.0001893	0.0001793	9.227e-05	8.51e-05	5.254e-05	4.506e-05	4.096e-05
Proportion of Variance	0.0000100	0.0000100	0.000e+00	0.00e+00	0.000e+00	0.000e+00	0.000e+00
Cumulative Proportion	0.9999900	0.9999900	1.000e+00	1.00e+00	1.000e+00	1.000e+00	1.000e+00

	PC16	PC17	PC18	PC19	PC20	PC21	PC22	PC23
Standard deviation	3.221e-05	2.191e-05	1.898e-05	1.44e-05	1.336e-05	1.214e-05	9.59e-06	7.463e-06
Proportion of Variance	0.000e+00	0.000e+00	0.000e+00	0.00e+00	0.000e+00	0.000e+00	0.00e+00	0.000e+00
Cumulative Proportion	1.000e+00	1.000e+00	1.000e+00	1.00e+00	1.000e+00	1.000e+00	1.00e+00	1.000e+00

	PC24	PC25	PC26	PC27	PC28	PC29	PC30
Standard deviation	7.076e-06	6.627e-06	6.45e-06	6.038e-06	6.025e-06	5.574e-06	5.564e-06
Proportion of Variance	0.000e+00	0.000e+00	0.00e+00	0.000e+00	0.000e+00	0.000e+00	0.000e+00
Cumulative Proportion	1.000e+00	1.000e+00	1.00e+00	1.000e+00	1.000e+00	1.000e+00	1.000e+00

	PC31	PC32	PC33	PC34	PC35	PC36	PC37
Standard deviation	5.217e-06	5.099e-06	4.987e-06	4.859e-06	4.762e-06	4.611e-06	4.542e-06
Proportion of Variance	0.000e+00	0.000e+00	0.000e+00	0.000e+00	0.000e+00	0.000e+00	0.000e+00
Cumulative Proportion	1.000e+00	1.000e+00	1.000e+00	1.000e+00	1.000e+00	1.000e+00	1.000e+00

	PC38	PC39	PC40	PC41	PC42	PC43	PC44	PC45
Standard deviation	4.367e-06	4.316e-06	4.197e-06	4.09e-06	3.972e-06	3.930e-06	3.85e-06	3.738e-06
Proportion of Variance	0.000e+00	0.000e+00	0.000e+00	0.00e+00	0.000e+00	0.000e+00	0.00e+00	0.000e+00
Cumulative Proportion	1.000e+00	1.000e+00	1.000e+00	1.00e+00	1.000e+00	1.000e+00	1.00e+00	1.000e+00

	PC46	PC47	PC48	PC49	PC50	PC51	PC52
Standard deviation	3.655e-06	3.623e-06	3.535e-06	3.419e-06	3.315e-06	3.269e-06	3.150e-06
Proportion of Variance	0.000e+00	0.000e+00	0.000e+00	0.000e+00	0.000e+00	0.000e+00	0.000e+00
Cumulative Proportion	1.000e+00	1.000e+00	1.000e+00	1.000e+00	1.000e+00	1.000e+00	1.000e+00

	PC53	PC54	PC55	PC56	PC57	PC58	PC59
Standard deviation	3.132e-06	3.069e-06	2.995e-06	2.976e-06	2.922e-06	2.895e-06	2.853e-06
Proportion of Variance	0.000e+00	0.000e+00	0.000e+00	0.000e+00	0.000e+00	0.000e+00	0.000e+00
Cumulative Proportion	1.000e+00	1.000e+00	1.000e+00	1.000e+00	1.000e+00	1.000e+00	1.000e+00

	PC60	PC61	PC62	PC63	PC64	PC65	PC66
Standard deviation	2.766e-06	2.728e-06	2.635e-06	2.612e-06	2.552e-06	2.507e-06	2.441e-06
Proportion of Variance	0.000e+00	0.000e+00	0.000e+00	0.000e+00	0.000e+00	0.000e+00	0.000e+00
Cumulative Proportion	1.000e+00	1.000e+00	1.000e+00	1.000e+00	1.000e+00	1.000e+00	1.000e+00

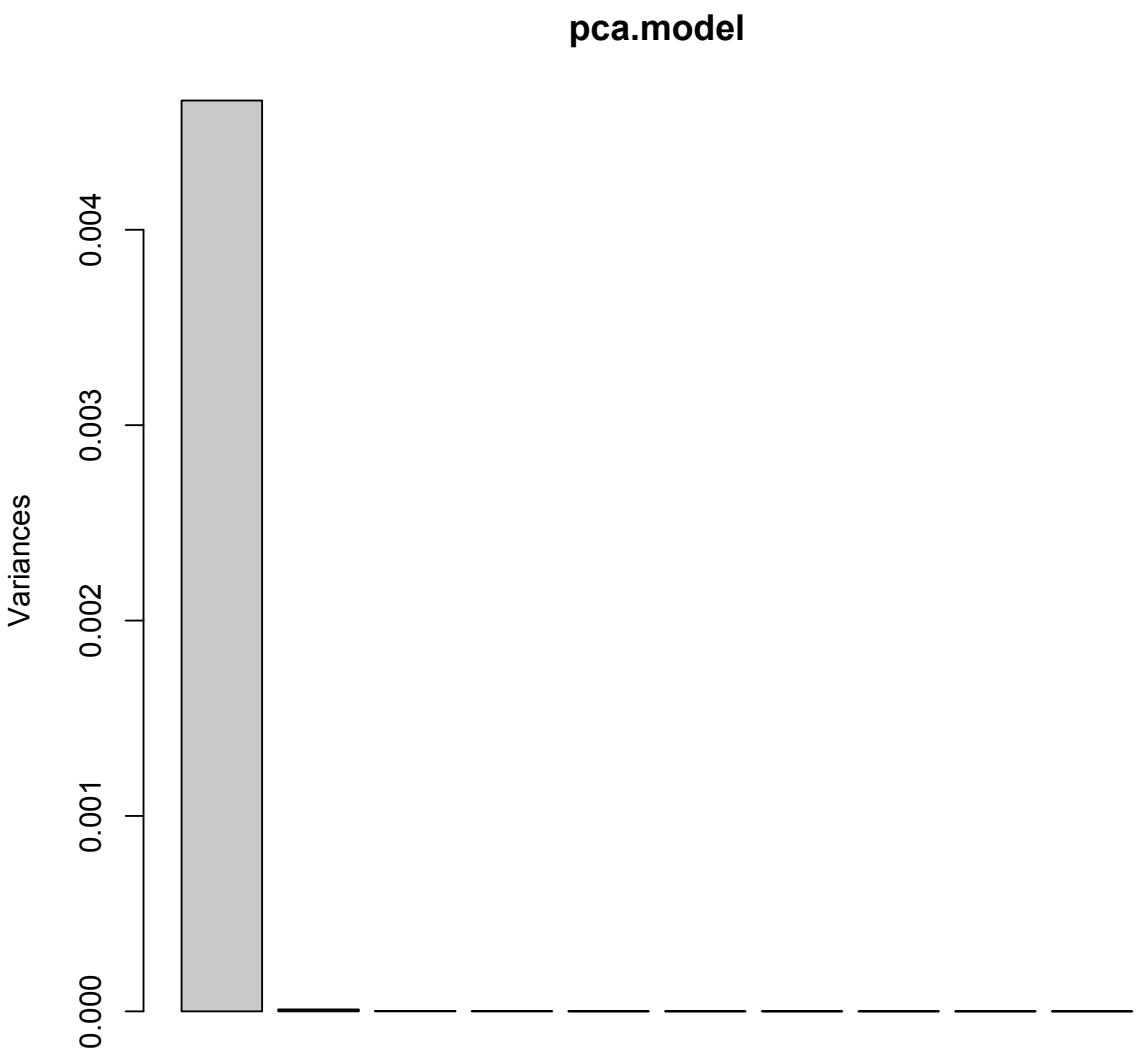


Figure 141: PCA scree plot for the first set of 30 normalized (peak area) glass spectra (10 replicates), no data pretreatment.

Table 153: PCA results for the first set of 30 normalized (peak area) glass spectra (10 replicates), centered.

Importance of components:

	PC1	PC2	PC3	PC4	PC5	PC6	PC7
Standard deviation	0.003179	0.001619	0.0009943	0.000527	0.0004969	0.0002767	0.0002408
Proportion of Variance	0.698510	0.181110	0.0683400	0.019200	0.0170700	0.0052900	0.0040100
Cumulative Proportion	0.698510	0.879620	0.9479500	0.967150	0.9842200	0.9895100	0.9935200

	PC8	PC9	PC10	PC11	PC12	PC13	PC14
Standard deviation	0.0001894	0.0001794	9.228e-05	8.511e-05	5.254e-05	4.506e-05	4.096e-05
Proportion of Variance	0.0024800	0.0022200	5.900e-04	5.000e-04	1.900e-04	1.400e-04	1.200e-04
Cumulative Proportion	0.9960000	0.9982200	9.988e-01	9.993e-01	9.995e-01	9.996e-01	9.998e-01

	PC15	PC16	PC17	PC18	PC19	PC20	PC21
Standard deviation	3.221e-05	2.191e-05	1.898e-05	0.0000144	1.336e-05	1.214e-05	9.59e-06
Proportion of Variance	7.000e-05	3.000e-05	2.000e-05	0.0000100	1.000e-05	1.000e-05	1.00e-05
Cumulative Proportion	9.998e-01	9.999e-01	9.999e-01	0.9999000	9.999e-01	9.999e-01	1.00e+00

	PC22	PC23	PC24	PC25	PC26	PC27	PC28
Standard deviation	7.463e-06	7.076e-06	6.627e-06	6.45e-06	6.038e-06	6.025e-06	5.574e-06
Proportion of Variance	0.000e+00	0.000e+00	0.000e+00	0.00e+00	0.000e+00	0.000e+00	0.000e+00
Cumulative Proportion	9.999e-01	9.999e-01	9.999e-01	1.00e+00	1.000e+00	1.000e+00	1.000e+00

	PC29	PC30	PC31	PC32	PC33	PC34	PC35
Standard deviation	5.564e-06	5.217e-06	5.099e-06	4.987e-06	4.859e-06	4.762e-06	4.611e-06
Proportion of Variance	0.000e+00	0.000e+00	0.000e+00	0.000e+00	0.000e+00	0.000e+00	0.000e+00
Cumulative Proportion	1.000e+00	1.000e+00	1.000e+00	1.000e+00	1.000e+00	1.000e+00	1.000e+00

	PC36	PC37	PC38	PC39	PC40	PC41	PC42
Standard deviation	4.542e-06	4.367e-06	4.316e-06	4.197e-06	4.09e-06	3.972e-06	3.930e-06
Proportion of Variance	0.000e+00	0.000e+00	0.000e+00	0.000e+00	0.00e+00	0.000e+00	0.000e+00
Cumulative Proportion	1.000e+00	1.000e+00	1.000e+00	1.000e+00	1.00e+00	1.000e+00	1.000e+00

	PC43	PC44	PC45	PC46	PC47	PC48	PC49
Standard deviation	3.85e-06	3.738e-06	3.655e-06	3.623e-06	3.535e-06	3.419e-06	3.315e-06
Proportion of Variance	0.00e+00	0.000e+00	0.000e+00	0.000e+00	0.000e+00	0.000e+00	0.000e+00
Cumulative Proportion	1.00e+00	1.000e+00	1.000e+00	1.000e+00	1.000e+00	1.000e+00	1.000e+00

	PC50	PC51	PC52	PC53	PC54	PC55	PC56
Standard deviation	3.269e-06	3.150e-06	3.132e-06	3.069e-06	2.995e-06	2.976e-06	2.922e-06
Proportion of Variance	0.000e+00	0.000e+00	0.000e+00	0.000e+00	0.000e+00	0.000e+00	0.000e+00
Cumulative Proportion	1.000e+00	1.000e+00	1.000e+00	1.000e+00	1.000e+00	1.000e+00	1.000e+00

	PC57	PC58	PC59	PC60	PC61	PC62	PC63
Standard deviation	2.895e-06	2.853e-06	2.766e-06	2.728e-06	2.635e-06	2.612e-06	2.552e-06
Proportion of Variance	0.000e+00	0.000e+00	0.000e+00	0.000e+00	0.000e+00	0.000e+00	0.000e+00
Cumulative Proportion	1.000e+00	1.000e+00	1.000e+00	1.000e+00	1.000e+00	1.000e+00	1.000e+00

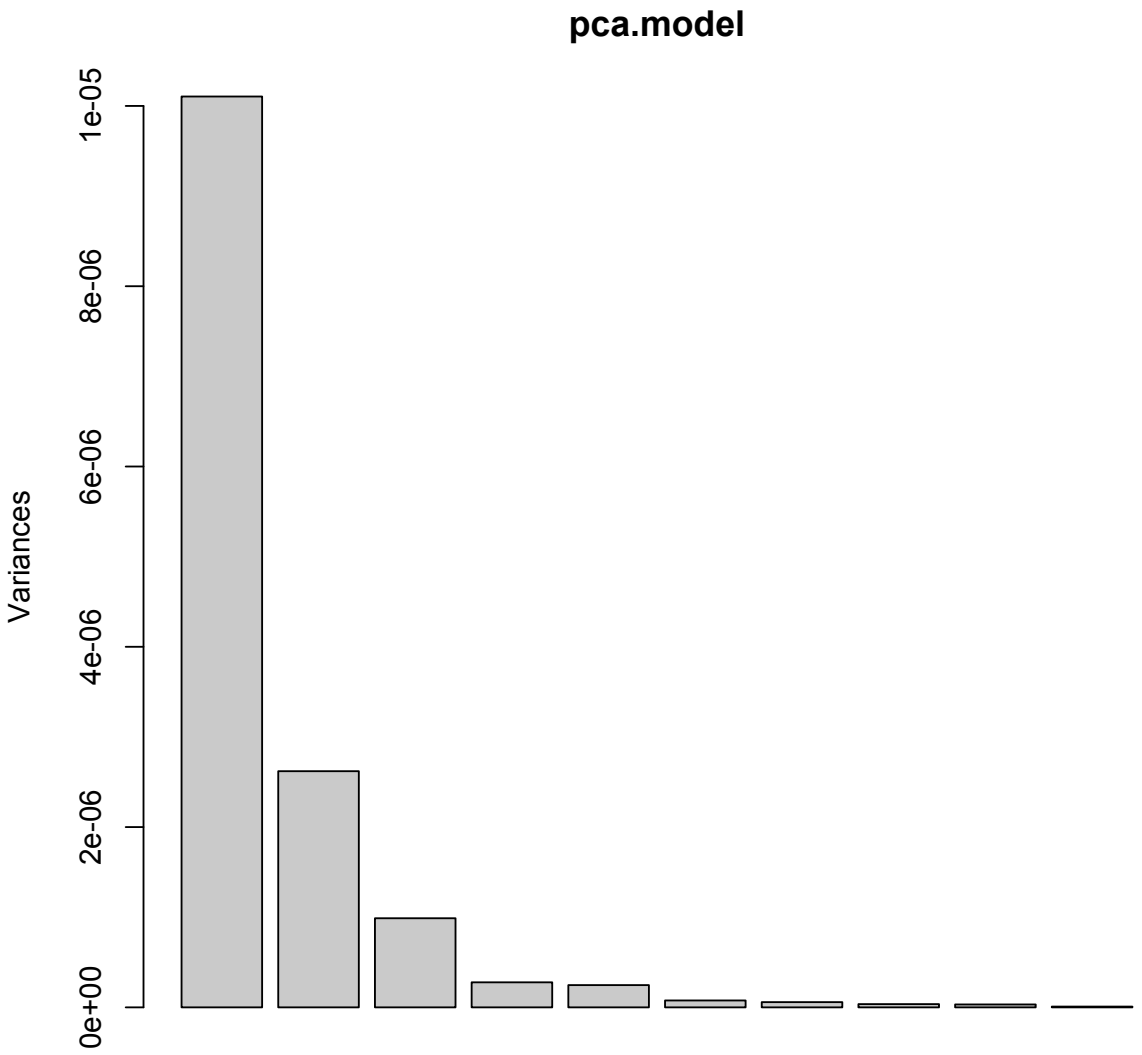


Figure 142: PCA scree plot for the first set of 30 normalized (peak area) glass spectra (10 replicates), centered.

Table 154: PCA results for the first set of 30 normalized (peak area) glass spectra (10 replicates), autoscaled.

Importance of components:

	PC1	PC2	PC3	PC4	PC5	PC6	PC7	PC8	PC9	PC10	PC11	PC12
Standard deviation	15.1450	7.7446	3.80950	2.76040	2.73897	1.23783	0.9837	0.77863	0.64218	0.38504	0.3123	0.29136
Proportion of Variance	0.7101	0.1857	0.04493	0.02359	0.02323	0.00474	0.0030	0.00188	0.00128	0.00046	0.0003	0.00026
Cumulative Proportion	0.7101	0.8958	0.94075	0.96434	0.98757	0.99231	0.9953	0.99719	0.99846	0.99892	0.9992	0.99949

	PC13	PC14	PC15	PC16	PC17	PC18	PC19	PC20	PC21	PC22	PC23
Standard deviation	0.24813	0.16831	0.13816	0.11040	0.09204	0.07394	0.05534	0.05297	0.04609	0.03983	0.03613
Proportion of Variance	0.00019	0.00009	0.00006	0.00004	0.00003	0.00002	0.00001	0.00001	0.00001	0.00000	0.00000
Cumulative Proportion	0.99968	0.99976	0.99982	0.99986	0.99989	0.99990	0.99991	0.99992	0.99993	0.99993	0.99994

	PC24	PC25	PC26	PC27	PC28	PC29	PC30	PC31	PC32	PC33	PC34
Standard deviation	0.03329	0.03007	0.02904	0.02787	0.02735	0.02679	0.02581	0.02482	0.02444	0.02416	0.02383
Proportion of Variance	0.00000	0.00000	0.00000	0.00000	0.00000	0.00000	0.00000	0.00000	0.00000	0.00000	0.00000
Cumulative Proportion	0.99994	0.99994	0.99995	0.99995	0.99995	0.99995	0.99996	0.99996	0.99996	0.99996	0.99996

	PC35	PC36	PC37	PC38	PC39	PC40	PC41	PC42	PC43	PC44	PC45
Standard deviation	0.02273	0.02189	0.02166	0.02112	0.02052	0.02018	0.01967	0.01894	0.01833	0.01797	0.01772
Proportion of Variance	0.00000	0.00000	0.00000	0.00000	0.00000	0.00000	0.00000	0.00000	0.00000	0.00000	0.00000
Cumulative Proportion	0.99996	0.99997	0.99997	0.99997	0.99997	0.99997	0.99997	0.99997	0.99997	0.99998	0.99998

	PC46	PC47	PC48	PC49	PC50	PC51	PC52	PC53	PC54	PC55	PC56
Standard deviation	0.01747	0.01719	0.01643	0.01611	0.01581	0.0155	0.01492	0.01466	0.01455	0.01409	0.01377
Proportion of Variance	0.00000	0.00000	0.00000	0.00000	0.00000	0.0000	0.00000	0.00000	0.00000	0.00000	0.00000
Cumulative Proportion	0.99998	0.99998	0.99998	0.99998	0.99998	1.0000	0.99998	0.99998	0.99998	0.99998	0.99998

	PC57	PC58	PC59	PC60	PC61	PC62	PC63	PC64	PC65	PC66	PC67
Standard deviation	0.01333	0.01317	0.01291	0.01276	0.01247	0.01202	0.01174	0.01171	0.01122	0.01113	0.01096
Proportion of Variance	0.00000	0.00000	0.00000	0.00000	0.00000	0.00000	0.00000	0.00000	0.00000	0.00000	0.00000
Cumulative Proportion	0.99999	0.99999	0.99999	0.99999	0.99999	0.99999	0.99999	0.99999	0.99999	0.99999	0.99999

	PC68	PC69	PC70	PC71	PC72	PC73	PC74	PC75	PC76	PC77	PC78
Standard deviation	0.01085	0.01065	0.01044	0.01029	0.01006	0.009833	0.00953	0.009254	0.009073	0.008798	0.008685
Proportion of Variance	0.00000	0.00000	0.00000	0.00000	0.00000	0.000000	0.00000	0.000000	0.000000	0.000000	0.000000
Cumulative Proportion	0.99999	0.99999	0.99999	0.99999	0.99999	0.999990	0.99999	0.999990	0.999990	0.999990	0.999990

	PC79	PC80	PC81	PC82	PC83	PC84	PC85	PC86	PC87	PC88
Standard deviation	0.008621	0.008263	0.008086	0.007906	0.007856	0.007825	0.007608	0.007308	0.007298	0.007204
Proportion of Variance	0.000000	0.000000	0.000000	0.000000	0.000000	0.000000	0.000000	0.000000	0.000000	0.000000
Cumulative Proportion	0.999990	0.999990	0.999990	0.999990	0.999990	0.999990	0.999990	0.999990	0.999990	1.000000

	PC89	PC90	PC91	PC92	PC93	PC94	PC95	PC96	PC97	PC98
Standard deviation	0.007096	0.006897	0.006687	0.006623	0.006447	0.006324	0.006206	0.006164	0.006132	0.005996
Proportion of Variance	0.000000	0.000000	0.000000	0.000000	0.000000	0.000000	0.000000	0.000000	0.000000	0.000000
Cumulative Proportion	1.000000	1.000000	1.000000	1.000000	1.000000	1.000000	1.000000	1.000000	1.000000	1.000000

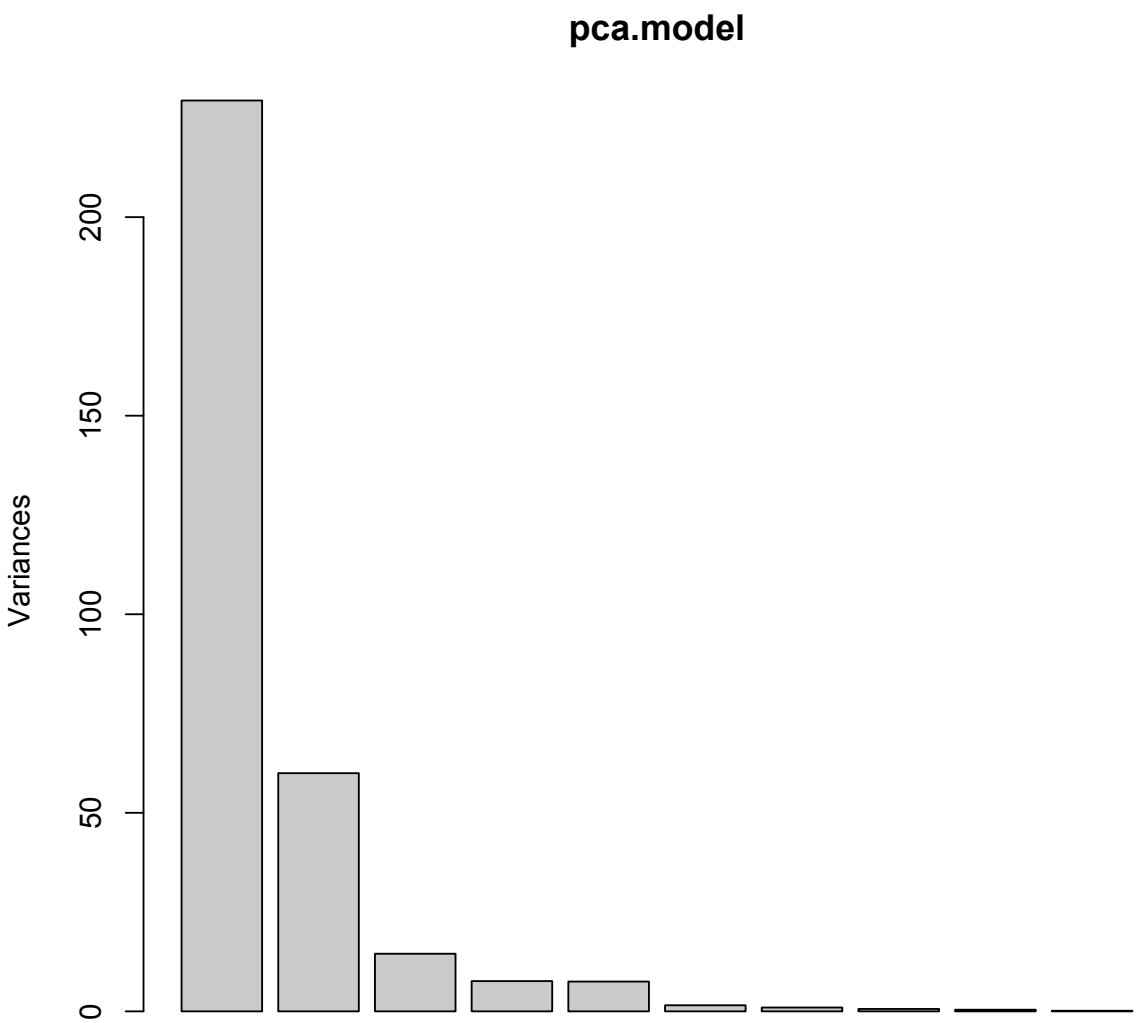


Figure 143: PCA scree plot for the first set of 30 normalized (peak area) glass spectra (10 replicates), autoscaled.

Table 155: PCA results for the first set of 20 normalized (peak area) window glass spectra (10 replicates), no data pretreatment.

Importance of components:

	PC1	PC2	PC3	PC4	PC5	PC6	PC7	PC8	PC9
Standard deviation	0.06831	0.002911	0.001354	0.0008725	0.0004617	0.0002716	0.0002385	0.0002070	0.0001849
Proportion of Variance	0.99754	0.001810	0.000390	0.0001600	0.0000500	0.0000200	0.0000100	0.0000100	0.0000100
Cumulative Proportion	0.99754	0.999350	0.999740	0.9999000	0.9999500	0.9999600	0.9999800	0.9999800	0.9999900

	PC10	PC11	PC12	PC13	PC14	PC15	PC16	PC17	PC18
Standard deviation	0.0001239	8.857e-05	8.022e-05	4.889e-05	4.376e-05	3.238e-05	3.050e-05	2.165e-05	1.613e-05
Proportion of Variance	0.0000000	0.000e+00	0.000e+00	0.000e+00	0.000e+00	0.000e+00	0.000e+00	0.000e+00	0.000e+00
Cumulative Proportion	1.0000000	1.000e+00	1.000e+00	1.000e+00	1.000e+00	1.000e+00	1.000e+00	1.000e+00	1.000e+00

	PC19	PC20	PC21	PC22	PC23	PC24	PC25	PC26	PC27
Standard deviation	1.243e-05	1.196e-05	1.024e-05	8.234e-06	7.37e-06	7.002e-06	6.494e-06	6.126e-06	5.884e-06
Proportion of Variance	0.000e+00	0.000e+00	0.000e+00	0.000e+00	0.00e+00	0.000e+00	0.000e+00	0.000e+00	0.000e+00
Cumulative Proportion	1.000e+00	1.000e+00	1.000e+00	1.000e+00	1.00e+00	1.000e+00	1.000e+00	1.000e+00	1.000e+00

	PC28	PC29	PC30	PC31	PC32	PC33	PC34	PC35	PC36
Standard deviation	5.725e-06	5.312e-06	5.275e-06	5.064e-06	5.013e-06	4.852e-06	4.688e-06	4.587e-06	4.551e-06
Proportion of Variance	0.000e+00	0.000e+00	0.000e+00	0.000e+00	0.000e+00	0.000e+00	0.000e+00	0.000e+00	0.000e+00
Cumulative Proportion	1.000e+00	1.000e+00	1.000e+00	1.000e+00	1.000e+00	1.000e+00	1.000e+00	1.000e+00	1.000e+00

	PC37	PC38	PC39	PC40	PC41	PC42	PC43	PC44	PC45
Standard deviation	4.456e-06	4.301e-06	4.134e-06	4.076e-06	4.03e-06	3.82e-06	3.641e-06	3.619e-06	3.548e-06
Proportion of Variance	0.000e+00	0.000e+00	0.000e+00	0.000e+00	0.00e+00	0.00e+00	0.000e+00	0.000e+00	0.000e+00
Cumulative Proportion	1.000e+00	1.000e+00	1.000e+00	1.000e+00	1.00e+00	1.00e+00	1.000e+00	1.000e+00	1.000e+00

	PC46	PC47	PC48	PC49	PC50	PC51	PC52	PC53	PC54
Standard deviation	3.459e-06	3.421e-06	3.385e-06	3.343e-06	3.217e-06	3.167e-06	3.117e-06	3.046e-06	2.938e-06
Proportion of Variance	0.000e+00	0.000e+00	0.000e+00	0.000e+00	0.000e+00	0.000e+00	0.000e+00	0.000e+00	0.000e+00
Cumulative Proportion	1.000e+00	1.000e+00	1.000e+00	1.000e+00	1.000e+00	1.000e+00	1.000e+00	1.000e+00	1.000e+00

	PC55	PC56	PC57	PC58	PC59	PC60	PC61	PC62	PC63
Standard deviation	2.898e-06	2.762e-06	2.741e-06	2.633e-06	2.601e-06	2.536e-06	2.501e-06	2.439e-06	2.42e-06
Proportion of Variance	0.000e+00	0.000e+00	0.000e+00	0.000e+00	0.000e+00	0.000e+00	0.000e+00	0.000e+00	0.00e+00
Cumulative Proportion	1.000e+00	1.000e+00	1.000e+00	1.000e+00	1.000e+00	1.000e+00	1.000e+00	1.000e+00	1.00e+00

	PC64	PC65	PC66	PC67	PC68	PC69	PC70	PC71	PC72
Standard deviation	2.357e-06	2.280e-06	2.270e-06	2.211e-06	2.175e-06	2.112e-06	2.061e-06	2.008e-06	1.975e-06
Proportion of Variance	0.000e+00	0.000e+00	0.000e+00	0.000e+00	0.000e+00	0.000e+00	0.000e+00	0.000e+00	0.000e+00
Cumulative Proportion	1.000e+00	1.000e+00	1.000e+00	1.000e+00	1.000e+00	1.000e+00	1.000e+00	1.000e+00	1.000e+00

	PC73	PC74	PC75	PC76	PC77	PC78	PC79	PC80	PC81
Standard deviation	1.921e-06	1.893e-06	1.808e-06	1.778e-06	1.743e-06	1.705e-06	1.688e-06	1.64e-06	1.577e-06
Proportion of Variance	0.000e+00	0.000e+00	0.000e+00	0.000e+00	0.000e+00	0.000e+00	0.000e+00	0.00e+00	0.000e+00
Cumulative Proportion	1.000e+00	1.000e+00	1.000e+00	1.000e+00	1.000e+00	1.000e+00	1.000e+00	1.00e+00	1.000e+00

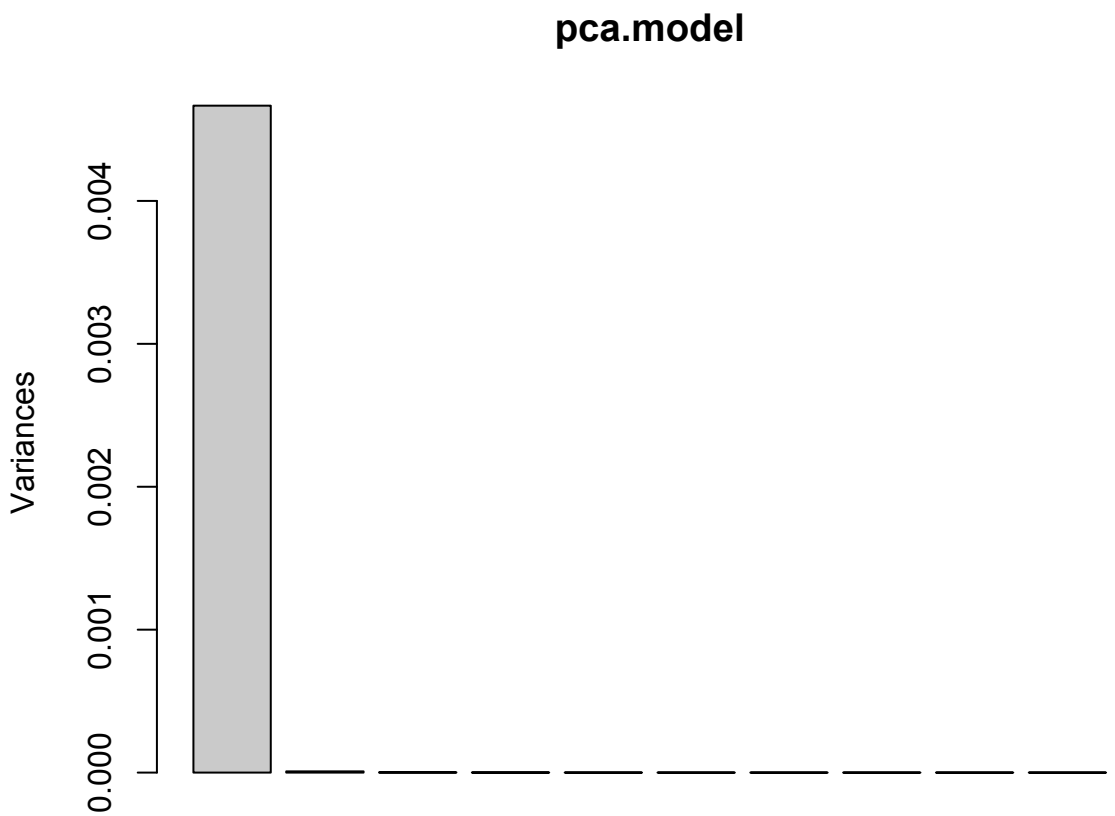


Figure 144: PCA scree plot for the first set of 20 normalized (peak area) window glass spectra (10 replicates), no data pretreatment.

Table 156: PCA results for the first set of 20 normalized (peak area) window glass spectra (10 replicates), centered.

Importance of components:

	PC1	PC2	PC3	PC4	PC5	PC6	PC7	PC8	PC9
Standard deviation	0.002938	0.001576	0.0008813	0.0004744	0.0002723	0.0002387	0.0002070	0.0001850	0.0001239
Proportion of Variance	0.698130	0.200910	0.0628300	0.0182100	0.0060000	0.0046100	0.0034700	0.0027700	0.0012400
Cumulative Proportion	0.698130	0.899040	0.9618700	0.9800800	0.9860800	0.9906900	0.9941600	0.9969300	0.9981700

	PC10	PC11	PC12	PC13	PC14	PC15	PC16	PC17	PC18
Standard deviation	8.857e-05	8.022e-05	4.889e-05	4.376e-05	3.238e-05	3.050e-05	2.165e-05	1.613e-05	1.243e-05
Proportion of Variance	6.300e-04	5.200e-04	1.900e-04	1.500e-04	8.000e-05	8.000e-05	4.000e-05	2.000e-05	1.000e-05
Cumulative Proportion	9.988e-01	9.993e-01	9.995e-01	9.997e-01	9.998e-01	9.998e-01	9.999e-01	9.999e-01	9.999e-01

	PC19	PC20	PC21	PC22	PC23	PC24	PC25	PC26	PC27
Standard deviation	1.196e-05	1.024e-05	8.234e-06	7.37e-06	7.002e-06	6.494e-06	6.126e-06	5.884e-06	5.725e-06
Proportion of Variance	1.000e-05	1.000e-05	1.000e-05	0.00e+00	0.000e+00	0.000e+00	0.000e+00	0.000e+00	0.000e+00
Cumulative Proportion	9.999e-01	9.999e-01	9.999e-01	1.00e+00	9.999e-01	9.999e-01	9.999e-01	1.000e+00	1.000e+00

	PC28	PC29	PC30	PC31	PC32	PC33	PC34	PC35	PC36
Standard deviation	5.312e-06	5.275e-06	5.064e-06	5.013e-06	4.852e-06	4.688e-06	4.587e-06	4.551e-06	4.456e-06
Proportion of Variance	0.000e+00	0.000e+00	0.000e+00	0.000e+00	0.000e+00	0.000e+00	0.000e+00	0.000e+00	0.000e+00
Cumulative Proportion	1.000e+00	1.000e+00	1.000e+00	1.000e+00	1.000e+00	1.000e+00	1.000e+00	1.000e+00	1.000e+00

	PC37	PC38	PC39	PC40	PC41	PC42	PC43	PC44	PC45
Standard deviation	4.301e-06	4.134e-06	4.076e-06	4.03e-06	3.82e-06	3.641e-06	3.619e-06	3.548e-06	3.459e-06
Proportion of Variance	0.000e+00	0.000e+00	0.000e+00	0.00e+00	0.00e+00	0.000e+00	0.000e+00	0.000e+00	0.000e+00
Cumulative Proportion	1.000e+00	1.000e+00	1.000e+00	1.00e+00	1.00e+00	1.000e+00	1.000e+00	1.000e+00	1.000e+00

	PC46	PC47	PC48	PC49	PC50	PC51	PC52	PC53	PC54
Standard deviation	3.421e-06	3.385e-06	3.343e-06	3.217e-06	3.167e-06	3.117e-06	3.046e-06	2.938e-06	2.898e-06
Proportion of Variance	0.000e+00	0.000e+00	0.000e+00	0.000e+00	0.000e+00	0.000e+00	0.000e+00	0.000e+00	0.000e+00
Cumulative Proportion	1.000e+00	1.000e+00	1.000e+00	1.000e+00	1.000e+00	1.000e+00	1.000e+00	1.000e+00	1.000e+00

	PC55	PC56	PC57	PC58	PC59	PC60	PC61	PC62	PC63
Standard deviation	2.762e-06	2.741e-06	2.633e-06	2.601e-06	2.536e-06	2.501e-06	2.439e-06	2.42e-06	2.357e-06
Proportion of Variance	0.000e+00	0.000e+00	0.000e+00	0.000e+00	0.000e+00	0.000e+00	0.000e+00	0.00e+00	0.000e+00
Cumulative Proportion	1.000e+00	1.000e+00	1.000e+00	1.000e+00	1.000e+00	1.000e+00	1.000e+00	1.00e+00	1.000e+00

	PC64	PC65	PC66	PC67	PC68	PC69	PC70	PC71	PC72
Standard deviation	2.280e-06	2.270e-06	2.211e-06	2.175e-06	2.112e-06	2.061e-06	2.008e-06	1.975e-06	1.921e-06
Proportion of Variance	0.000e+00	0.000e+00	0.000e+00	0.000e+00	0.000e+00	0.000e+00	0.000e+00	0.000e+00	0.000e+00
Cumulative Proportion	1.000e+00	1.000e+00	1.000e+00	1.000e+00	1.000e+00	1.000e+00	1.000e+00	1.000e+00	1.000e+00

	PC73	PC74	PC75	PC76	PC77	PC78	PC79	PC80	PC81
Standard deviation	1.893e-06	1.808e-06	1.778e-06	1.743e-06	1.705e-06	1.688e-06	1.64e-06	1.577e-06	1.563e-06
Proportion of Variance	0.000e+00	0.000e+00	0.000e+00	0.000e+00	0.000e+00	0.000e+00	0.00e+00	0.000e+00	0.000e+00
Cumulative Proportion	1.000e+00	1.000e+00	1.000e+00	1.000e+00	1.000e+00	1.000e+00	1.00e+00	1.000e+00	1.000e+00

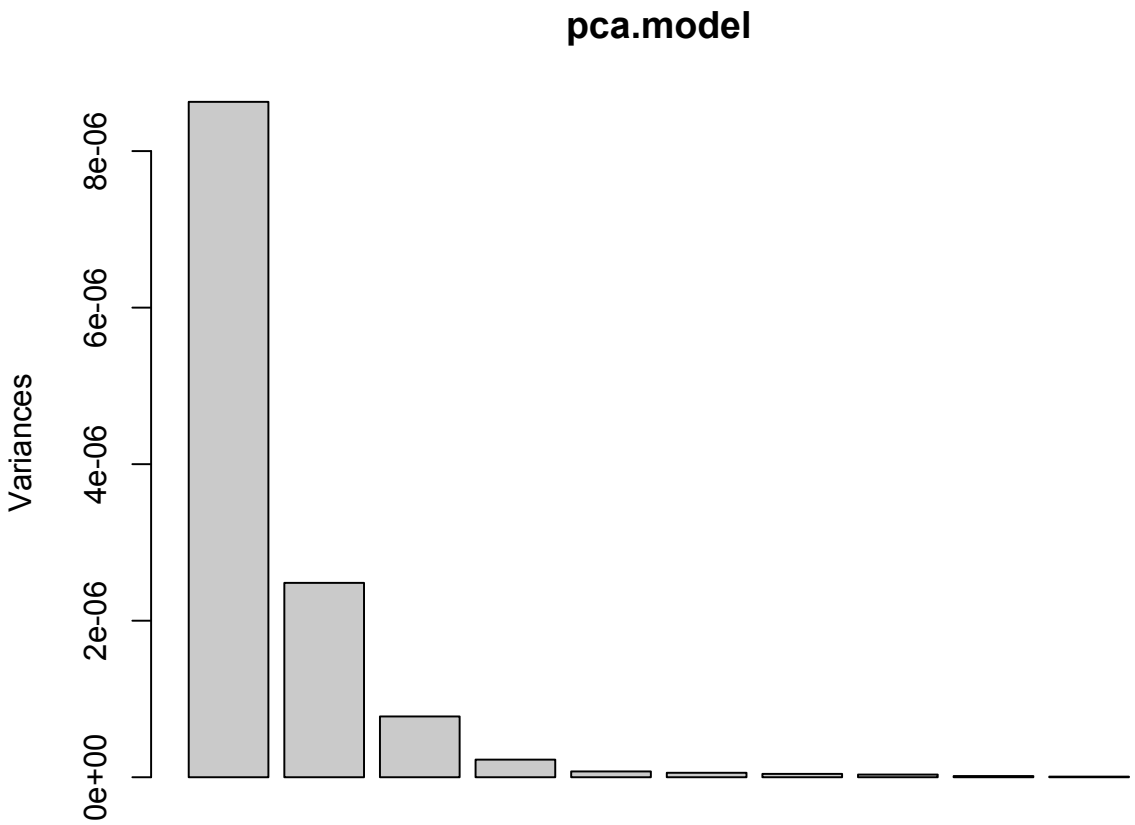


Figure 145: PCA scree plot for the first set of 20 normalized (peak area) window glass spectra (10 replicates), centered.

Table 157: PCA results for the first set of 20 normalized (peak area) window glass spectra (10 replicates), autoscaled.

Importance of components:

	PC1	PC2	PC3	PC4	PC5	PC6	PC7	PC8	PC9	PC10	PC11
Standard deviation	15.2652	8.0993	3.39269	2.72486	1.34017	1.20411	0.8619	0.73579	0.66210	0.37002	0.28540
Proportion of Variance	0.7214	0.2031	0.03564	0.02299	0.00556	0.00449	0.0023	0.00168	0.00136	0.00042	0.00025
Cumulative Proportion	0.7214	0.9245	0.96017	0.98316	0.98872	0.99321	0.9955	0.99718	0.99854	0.99896	0.99921

	PC12	PC13	PC14	PC15	PC16	PC17	PC18	PC19	PC20	PC21	PC22
Standard deviation	0.27427	0.2553	0.18624	0.15038	0.11269	0.08186	0.06283	0.05416	0.05203	0.04536	0.03991
Proportion of Variance	0.00023	0.0002	0.00011	0.00007	0.00004	0.00002	0.00001	0.00001	0.00001	0.00001	0.00000
Cumulative Proportion	0.99945	0.9997	0.99976	0.99983	0.99987	0.99989	0.99990	0.99991	0.99992	0.99992	0.99993

	PC23	PC24	PC25	PC26	PC27	PC28	PC29	PC30	PC31	PC32	PC33
Standard deviation	0.03604	0.03378	0.0335	0.03199	0.03122	0.03105	0.02939	0.02890	0.02755	0.02689	0.02601
Proportion of Variance	0.00000	0.00000	0.0000	0.00000	0.00000	0.00000	0.00000	0.00000	0.00000	0.00000	0.00000
Cumulative Proportion	0.99993	0.99994	0.9999	0.99994	0.99995	0.99995	0.99995	0.99995	0.99996	0.99996	0.99996

	PC34	PC35	PC36	PC37	PC38	PC39	PC40	PC41	PC42	PC43	PC44
Standard deviation	0.02484	0.02456	0.02371	0.02294	0.02226	0.0216	0.02103	0.02001	0.01979	0.01937	0.01927
Proportion of Variance	0.00000	0.00000	0.00000	0.00000	0.00000	0.0000	0.00000	0.00000	0.00000	0.00000	0.00000
Cumulative Proportion	0.99996	0.99996	0.99997	0.99997	0.99997	1.0000	0.99997	0.99997	0.99997	0.99998	0.99998

	PC45	PC46	PC47	PC48	PC49	PC50	PC51	PC52	PC53	PC54	PC55
Standard deviation	0.01855	0.0176	0.01733	0.01714	0.01678	0.01617	0.01607	0.01550	0.01516	0.01481	0.01426
Proportion of Variance	0.00000	0.0000	0.00000	0.00000	0.00000	0.00000	0.00000	0.00000	0.00000	0.00000	0.00000
Cumulative Proportion	0.99998	1.0000	0.99998	0.99998	0.99998	0.99998	0.99998	0.99998	0.99998	0.99998	0.99999

	PC56	PC57	PC58	PC59	PC60	PC61	PC62	PC63	PC64	PC65	PC66
Standard deviation	0.01391	0.01375	0.01305	0.01295	0.01247	0.01231	0.01200	0.01194	0.01134	0.01128	0.01104
Proportion of Variance	0.00000	0.00000	0.00000	0.00000	0.00000	0.00000	0.00000	0.00000	0.00000	0.00000	0.00000
Cumulative Proportion	0.99999	0.99999	0.99999	0.99999	0.99999	0.99999	0.99999	0.99999	0.99999	0.99999	0.99999

	PC67	PC68	PC69	PC70	PC71	PC72	PC73	PC74	PC75	PC76
Standard deviation	0.01085	0.01066	0.01042	0.01005	0.009906	0.009813	0.00921	0.008962	0.008923	0.008691
Proportion of Variance	0.00000	0.00000	0.00000	0.00000	0.000000	0.000000	0.00000	0.000000	0.000000	0.000000
Cumulative Proportion	0.99999	0.99999	0.99999	0.99999	0.999990	0.999990	0.99999	0.999990	0.999990	0.999990

	PC77	PC78	PC79	PC80	PC81	PC82	PC83	PC84	PC85	PC86
Standard deviation	0.008575	0.008443	0.008311	0.008127	0.007843	0.007759	0.00754	0.007496	0.007292	0.007134
Proportion of Variance	0.000000	0.000000	0.000000	0.000000	0.000000	0.000000	0.00000	0.000000	0.000000	0.000000
Cumulative Proportion	0.999990	0.999990	0.999990	0.999990	0.999990	1.000000	1.00000	1.000000	1.000000	1.000000

	PC87	PC88	PC89	PC90	PC91	PC92	PC93	PC94	PC95	PC96
Standard deviation	0.007076	0.006937	0.006788	0.006762	0.006605	0.006556	0.006342	0.00619	0.006097	0.005908
Proportion of Variance	0.000000	0.000000	0.000000	0.000000	0.000000	0.000000	0.000000	0.00000	0.000000	0.000000
Cumulative Proportion	1.000000	1.000000	1.000000	1.000000	1.000000	1.000000	1.000000	1.00000	1.000000	1.000000

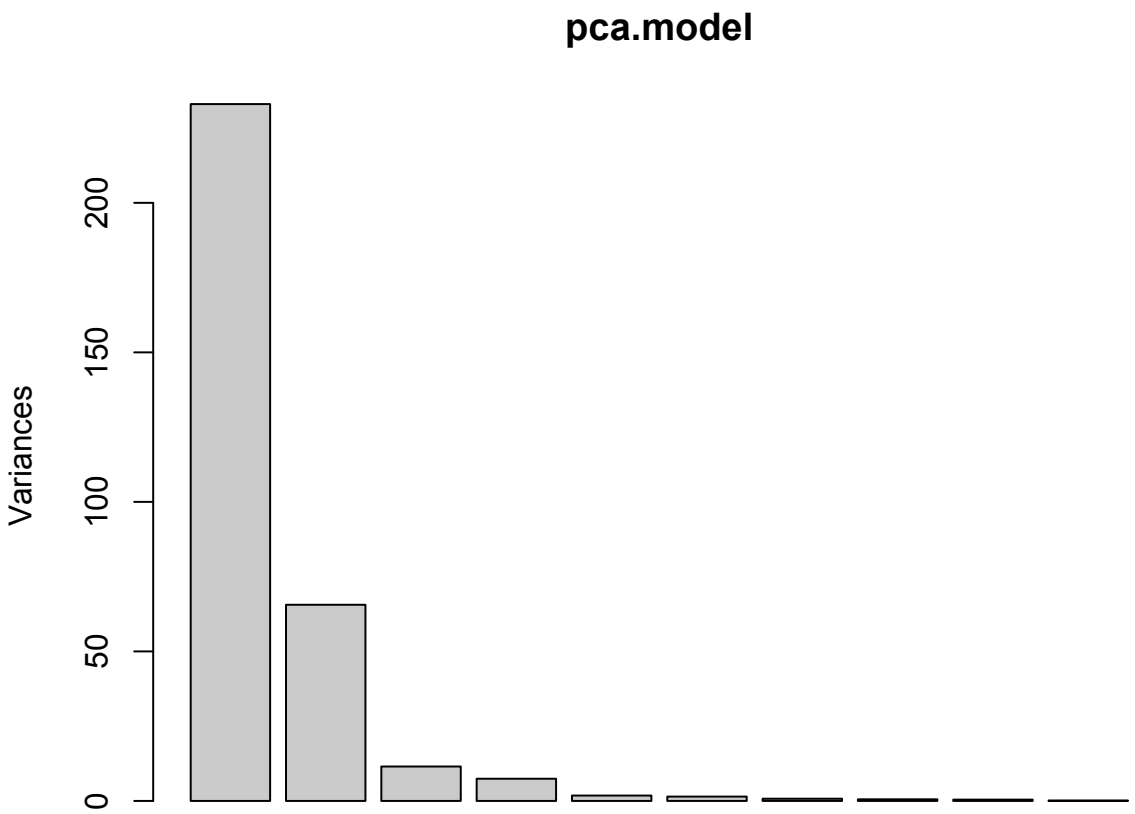


Figure 146: PCA scree plot for the first set of 20 normalized (peak area) window glass spectra (10 replicates), autoscaled.

Table 158: PCA results for the first set of 10 normalized (peak area) container glass spectra (10 replicates), no data pretreatment.

Importance of components:

	PC1	PC2	PC3	PC4	PC5	PC6	PC7	PC8	PC9
Standard deviation	0.06855	0.003556	0.001492	0.001155	0.0005131	0.0004301	0.0002598	0.0002368	0.0001601
Proportion of Variance	0.99643	0.002680	0.000470	0.000280	0.0000600	0.0000400	0.0000100	0.0000100	0.0000100
Cumulative Proportion	0.99643	0.999110	0.999580	0.999860	0.9999200	0.9999600	0.9999700	0.9999800	0.9999900

	PC10	PC11	PC12	PC13	PC14	PC15	PC16	PC17	PC18
Standard deviation	0.0001534	9.85e-05	8.346e-05	4.622e-05	4.097e-05	3.055e-05	2.374e-05	1.918e-05	1.493e-05
Proportion of Variance	0.0000000	0.00e+00	0.000e+00	0.000e+00	0.000e+00	0.000e+00	0.000e+00	0.000e+00	0.000e+00
Cumulative Proportion	0.9999900	1.00e+00	1.000e+00	1.000e+00	1.000e+00	1.000e+00	1.000e+00	1.000e+00	1.000e+00

	PC19	PC20	PC21	PC22	PC23	PC24	PC25	PC26	PC27
Standard deviation	1.407e-05	1.188e-05	1.046e-05	8.126e-06	7.43e-06	7.206e-06	6.685e-06	6.197e-06	6.081e-06
Proportion of Variance	0.000e+00	0.000e+00	0.000e+00	0.000e+00	0.00e+00	0.000e+00	0.000e+00	0.000e+00	0.000e+00
Cumulative Proportion	1.000e+00	1.000e+00	1.000e+00	1.000e+00	1.00e+00	1.000e+00	1.000e+00	1.000e+00	1.000e+00

	PC28	PC29	PC30	PC31	PC32	PC33	PC34	PC35	PC36
Standard deviation	5.908e-06	5.609e-06	5.475e-06	5.261e-06	5.106e-06	5.021e-06	4.828e-06	4.749e-06	4.421e-06
Proportion of Variance	0.000e+00	0.000e+00	0.000e+00	0.000e+00	0.000e+00	0.000e+00	0.000e+00	0.000e+00	0.000e+00
Cumulative Proportion	1.000e+00	1.000e+00	1.000e+00	1.000e+00	1.000e+00	1.000e+00	1.000e+00	1.000e+00	1.000e+00

	PC37	PC38	PC39	PC40	PC41	PC42	PC43	PC44	PC45
Standard deviation	4.323e-06	4.254e-06	4.027e-06	3.955e-06	3.871e-06	3.69e-06	3.454e-06	3.370e-06	3.26e-06
Proportion of Variance	0.000e+00	0.000e+00	0.000e+00	0.000e+00	0.000e+00	0.00e+00	0.000e+00	0.000e+00	0.00e+00
Cumulative Proportion	1.000e+00	1.000e+00	1.000e+00	1.000e+00	1.000e+00	1.00e+00	1.000e+00	1.000e+00	1.00e+00

	PC46	PC47	PC48	PC49	PC50	PC51	PC52	PC53	PC54
Standard deviation	3.243e-06	3.162e-06	2.99e-06	2.937e-06	2.862e-06	2.808e-06	2.712e-06	2.646e-06	2.52e-06
Proportion of Variance	0.000e+00	0.000e+00	0.00e+00	0.000e+00	0.000e+00	0.000e+00	0.000e+00	0.000e+00	0.00e+00
Cumulative Proportion	1.000e+00	1.000e+00	1.00e+00	1.000e+00	1.000e+00	1.000e+00	1.000e+00	1.000e+00	1.00e+00

	PC55	PC56	PC57	PC58	PC59	PC60	PC61	PC62	PC63
Standard deviation	2.503e-06	2.472e-06	2.377e-06	2.314e-06	2.258e-06	2.097e-06	2.06e-06	2.045e-06	1.986e-06
Proportion of Variance	0.000e+00	0.000e+00	0.000e+00	0.000e+00	0.000e+00	0.000e+00	0.00e+00	0.000e+00	0.000e+00
Cumulative Proportion	1.000e+00	1.000e+00	1.000e+00	1.000e+00	1.000e+00	1.000e+00	1.00e+00	1.000e+00	1.000e+00

	PC64	PC65	PC66	PC67	PC68	PC69	PC70	PC71	PC72
Standard deviation	1.944e-06	1.921e-06	1.842e-06	1.825e-06	1.792e-06	1.761e-06	1.726e-06	1.607e-06	1.542e-06
Proportion of Variance	0.000e+00	0.000e+00	0.000e+00	0.000e+00	0.000e+00	0.000e+00	0.000e+00	0.000e+00	0.000e+00
Cumulative Proportion	1.000e+00	1.000e+00	1.000e+00	1.000e+00	1.000e+00	1.000e+00	1.000e+00	1.000e+00	1.000e+00

	PC73	PC74	PC75	PC76	PC77	PC78	PC79	PC80	PC81
Standard deviation	1.509e-06	1.501e-06	1.450e-06	1.406e-06	1.294e-06	1.280e-06	1.249e-06	1.229e-06	1.183e-06
Proportion of Variance	0.000e+00	0.000e+00	0.000e+00	0.000e+00	0.000e+00	0.000e+00	0.000e+00	0.000e+00	0.000e+00
Cumulative Proportion	1.000e+00	1.000e+00	1.000e+00	1.000e+00	1.000e+00	1.000e+00	1.000e+00	1.000e+00	1.000e+00

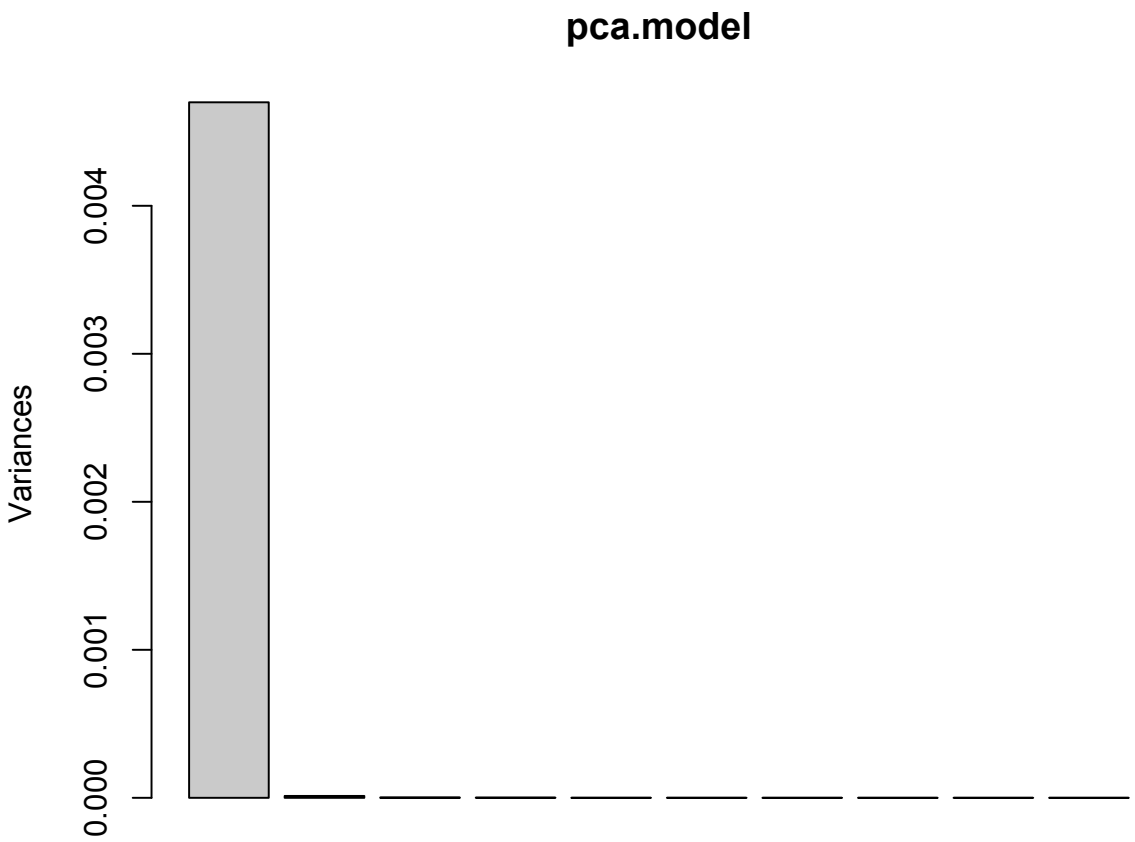


Figure 147: PCA scree plot for the first set of 10 normalized (peak area) container glass spectra (10 replicates), no data pretreatment.

Table 159: PCA results for the first set of 10 normalized (peak area) container glass spectra (10 replicates), centered.

Importance of components:

	PC1	PC2	PC3	PC4	PC5	PC6	PC7	PC8	PC9
Standard deviation	0.003630	0.001695	0.001165	0.000534	0.0004307	0.0002608	0.0002368	0.0001601	0.0001535
Proportion of Variance	0.729050	0.158890	0.075120	0.015770	0.0102600	0.0037600	0.0031000	0.0014200	0.0013000
Cumulative Proportion	0.729050	0.887950	0.963060	0.978830	0.9890900	0.9928600	0.9959600	0.9973800	0.9986800

	PC10	PC11	PC12	PC13	PC14	PC15	PC16	PC17	PC18
Standard deviation	9.853e-05	8.347e-05	4.622e-05	4.098e-05	3.055e-05	2.374e-05	1.918e-05	1.493e-05	1.407e-05
Proportion of Variance	5.400e-04	3.900e-04	1.200e-04	9.000e-05	5.000e-05	3.000e-05	2.000e-05	1.000e-05	1.000e-05
Cumulative Proportion	9.992e-01	9.996e-01	9.997e-01	9.998e-01	9.999e-01	9.999e-01	9.999e-01	9.999e-01	9.999e-01

	PC19	PC20	PC21	PC22	PC23	PC24	PC25	PC26	PC27
Standard deviation	1.188e-05	1.046e-05	8.126e-06	7.43e-06	7.206e-06	6.685e-06	6.197e-06	6.081e-06	5.908e-06
Proportion of Variance	1.000e-05	1.000e-05	0.000e+00	0.00e+00	0.000e+00	0.000e+00	0.000e+00	0.000e+00	0.000e+00
Cumulative Proportion	1.000e+00	1.000e+00	1.000e+00	1.00e+00	1.000e+00	1.000e+00	1.000e+00	1.000e+00	1.000e+00

	PC28	PC29	PC30	PC31	PC32	PC33	PC34	PC35	PC36
Standard deviation	5.609e-06	5.475e-06	5.261e-06	5.106e-06	5.021e-06	4.828e-06	4.749e-06	4.421e-06	4.323e-06
Proportion of Variance	0.000e+00	0.000e+00	0.000e+00	0.000e+00	0.000e+00	0.000e+00	0.000e+00	0.000e+00	0.000e+00
Cumulative Proportion	1.000e+00	1.000e+00	1.000e+00	1.000e+00	1.000e+00	1.000e+00	1.000e+00	1.000e+00	1.000e+00

	PC37	PC38	PC39	PC40	PC41	PC42	PC43	PC44	PC45
Standard deviation	4.254e-06	4.027e-06	3.955e-06	3.871e-06	3.69e-06	3.454e-06	3.370e-06	3.26e-06	3.243e-06
Proportion of Variance	0.000e+00	0.000e+00	0.000e+00	0.000e+00	0.00e+00	0.000e+00	0.000e+00	0.00e+00	0.000e+00
Cumulative Proportion	1.000e+00	1.000e+00	1.000e+00	1.000e+00	1.00e+00	1.000e+00	1.000e+00	1.00e+00	1.000e+00

	PC46	PC47	PC48	PC49	PC50	PC51	PC52	PC53	PC54
Standard deviation	3.162e-06	2.99e-06	2.937e-06	2.862e-06	2.808e-06	2.712e-06	2.646e-06	2.52e-06	2.503e-06
Proportion of Variance	0.000e+00	0.00e+00	0.000e+00	0.000e+00	0.000e+00	0.000e+00	0.000e+00	0.00e+00	0.000e+00
Cumulative Proportion	1.000e+00	1.00e+00	1.000e+00	1.000e+00	1.000e+00	1.000e+00	1.000e+00	1.00e+00	1.000e+00

	PC55	PC56	PC57	PC58	PC59	PC60	PC61	PC62	PC63
Standard deviation	2.472e-06	2.377e-06	2.314e-06	2.258e-06	2.097e-06	2.06e-06	2.045e-06	1.986e-06	1.944e-06
Proportion of Variance	0.000e+00	0.000e+00	0.000e+00	0.000e+00	0.000e+00	0.00e+00	0.000e+00	0.000e+00	0.000e+00
Cumulative Proportion	1.000e+00	1.000e+00	1.000e+00	1.000e+00	1.000e+00	1.00e+00	1.000e+00	1.000e+00	1.000e+00

	PC64	PC65	PC66	PC67	PC68	PC69	PC70	PC71	PC72
Standard deviation	1.921e-06	1.842e-06	1.825e-06	1.792e-06	1.761e-06	1.726e-06	1.607e-06	1.542e-06	1.509e-06
Proportion of Variance	0.000e+00	0.000e+00	0.000e+00	0.000e+00	0.000e+00	0.000e+00	0.000e+00	0.000e+00	0.000e+00
Cumulative Proportion	1.000e+00	1.000e+00	1.000e+00	1.000e+00	1.000e+00	1.000e+00	1.000e+00	1.000e+00	1.000e+00

	PC73	PC74	PC75	PC76	PC77	PC78	PC79	PC80	PC81
Standard deviation	1.501e-06	1.450e-06	1.406e-06	1.294e-06	1.280e-06	1.249e-06	1.229e-06	1.183e-06	1.132e-06
Proportion of Variance	0.000e+00	0.000e+00	0.000e+00	0.000e+00	0.000e+00	0.000e+00	0.000e+00	0.000e+00	0.000e+00
Cumulative Proportion	1.000e+00	1.000e+00	1.000e+00	1.000e+00	1.000e+00	1.000e+00	1.000e+00	1.000e+00	1.000e+00

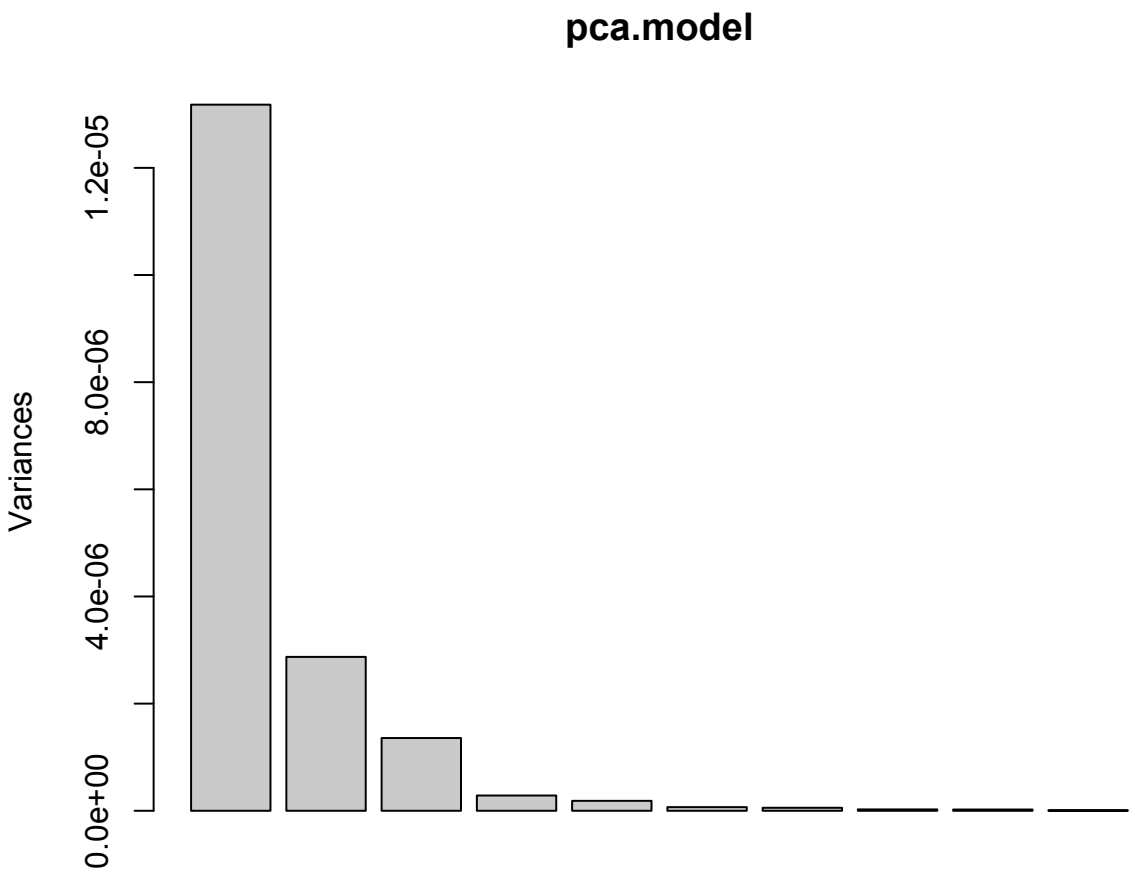


Figure 148: PCA scree plot for the first set of 10 normalized (peak area) container glass spectra (10 replicates), centered.

Table 160: PCA results for the first set of 10 normalized (peak area) container glass spectra (10 replicates), autoscaled.

Importance of components:

	PC1	PC2	PC3	PC4	PC5	PC6	PC7	PC8	PC9	PC10	PC11	PC12
Standard deviation	15.345	7.3891	4.41609	2.7077	1.7700	1.15281	0.76420	0.63542	0.55408	0.3596	0.28280	0.21932
Proportion of Variance	0.729	0.1690	0.06038	0.0227	0.0097	0.00411	0.00181	0.00125	0.00095	0.0004	0.00025	0.00015
Cumulative Proportion	0.729	0.8980	0.95838	0.9811	0.9908	0.99490	0.99670	0.99795	0.99890	0.9993	0.99955	0.99970

	PC13	PC14	PC15	PC16	PC17	PC18	PC19	PC20	PC21	PC22	PC23
Standard deviation	0.18990	0.12562	0.09429	0.08157	0.07139	0.05455	0.04837	0.04221	0.04008	0.03522	0.03155
Proportion of Variance	0.00011	0.00005	0.00003	0.00002	0.00002	0.00001	0.00001	0.00001	0.00000	0.00000	0.00000
Cumulative Proportion	0.99981	0.99986	0.99989	0.99991	0.99993	0.99994	0.99994	0.99995	0.99995	0.99996	0.99996

	PC24	PC25	PC26	PC27	PC28	PC29	PC30	PC31	PC32	PC33	PC34
Standard deviation	0.0307	0.02778	0.02667	0.02539	0.02521	0.02394	0.02316	0.02262	0.0215	0.02079	0.01973
Proportion of Variance	0.0000	0.00000	0.00000	0.00000	0.00000	0.00000	0.00000	0.00000	0.0000	0.00000	0.00000
Cumulative Proportion	1.0000	0.99997	0.99997	0.99997	0.99997	0.99997	0.99997	0.99998	1.0000	0.99998	0.99998

	PC35	PC36	PC37	PC38	PC39	PC40	PC41	PC42	PC43	PC44	PC45
Standard deviation	0.01951	0.01892	0.01871	0.0178	0.01695	0.01655	0.01585	0.01534	0.01517	0.01468	0.01432
Proportion of Variance	0.00000	0.00000	0.00000	0.0000	0.00000	0.00000	0.00000	0.00000	0.00000	0.00000	0.00000
Cumulative Proportion	0.99998	0.99998	0.99998	1.0000	0.99999	0.99999	0.99999	0.99999	0.99999	0.99999	0.99999

	PC46	PC47	PC48	PC49	PC50	PC51	PC52	PC53	PC54	PC55	PC56
Standard deviation	0.01394	0.01338	0.01287	0.01231	0.01195	0.01178	0.01130	0.01121	0.01093	0.01075	0.01013
Proportion of Variance	0.00000	0.00000	0.00000	0.00000	0.00000	0.00000	0.00000	0.00000	0.00000	0.00000	0.00000
Cumulative Proportion	0.99999	0.99999	0.99999	0.99999	0.99999	0.99999	0.99999	0.99999	0.99999	0.99999	0.99999

	PC57	PC58	PC59	PC60	PC61	PC62	PC63	PC64	PC65	PC66
Standard deviation	0.009807	0.0097	0.00965	0.009218	0.008835	0.008701	0.008506	0.00842	0.00818	0.008027
Proportion of Variance	0.000000	0.0000	0.00000	0.000000	0.000000	0.000000	0.000000	0.00000	0.00000	0.000000
Cumulative Proportion	1.000000	1.0000	1.00000	1.000000	1.000000	1.000000	1.000000	1.00000	1.00000	1.000000

	PC67	PC68	PC69	PC70	PC71	PC72	PC73	PC74	PC75	PC76
Standard deviation	0.007691	0.007425	0.007162	0.007129	0.00702	0.00662	0.006518	0.006283	0.006189	0.006094
Proportion of Variance	0.000000	0.000000	0.000000	0.000000	0.00000	0.00000	0.000000	0.000000	0.000000	0.000000
Cumulative Proportion	1.000000	1.000000	1.000000	1.000000	1.00000	1.00000	1.000000	1.000000	1.000000	1.000000

	PC77	PC78	PC79	PC80	PC81	PC82	PC83	PC84	PC85	PC86
Standard deviation	0.005688	0.005515	0.005387	0.005212	0.005102	0.004955	0.004865	0.004585	0.004371	0.004292
Proportion of Variance	0.000000	0.000000	0.000000	0.000000	0.000000	0.000000	0.000000	0.000000	0.000000	0.000000
Cumulative Proportion	1.000000	1.000000	1.000000	1.000000	1.000000	1.000000	1.000000	1.000000	1.000000	1.000000

	PC87	PC88	PC89	PC90	PC91	PC92	PC93	PC94	PC95	PC96
Standard deviation	0.004141	0.00403	0.003976	0.003777	0.003768	0.003613	0.003529	0.003433	0.003255	0.003078
Proportion of Variance	0.000000	0.00000	0.000000	0.000000	0.000000	0.000000	0.000000	0.000000	0.000000	0.000000
Cumulative Proportion	1.000000	1.00000	1.000000	1.000000	1.000000	1.000000	1.000000	1.000000	1.000000	1.000000

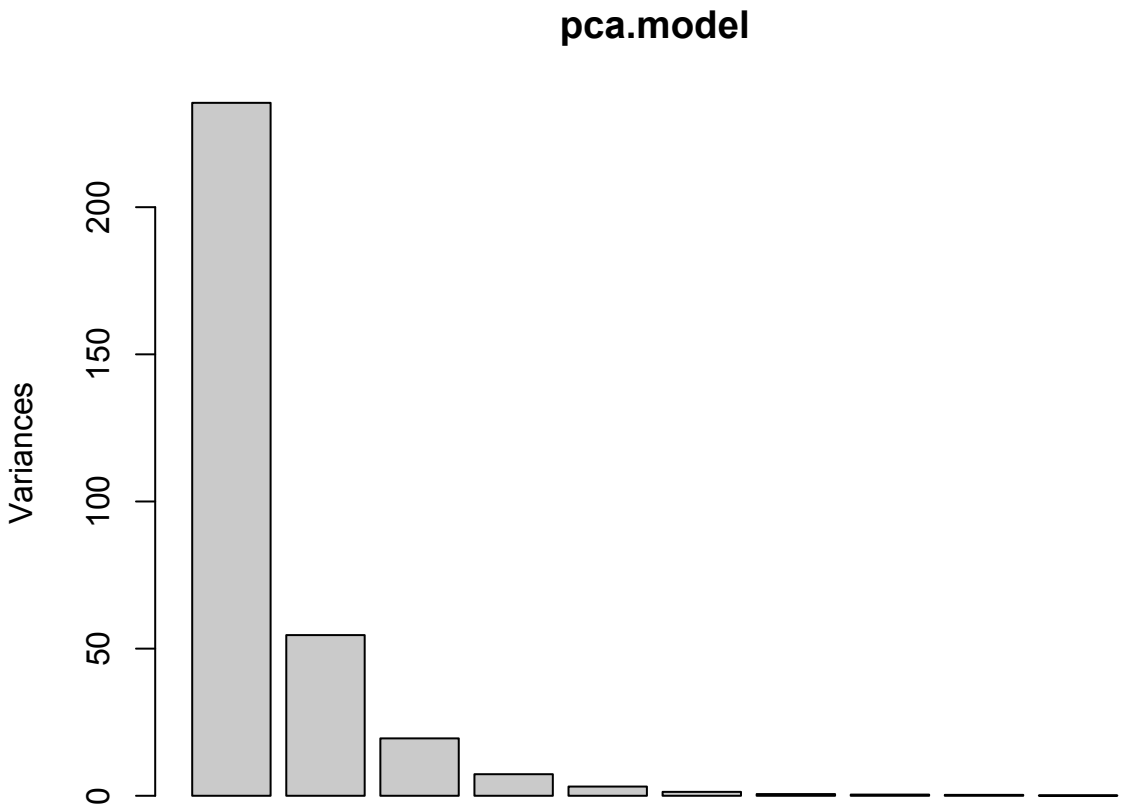


Figure 149: PCA scree plot for the first set of 10 normalized (peak area) container glass spectra (10 replicates), autoscaled.

C. PCA Results for the Peak Height Normalized Spectra

Table 161: PCA results for the first set of 30 normalized (peak height) glass spectra (10 replicates), no data pretreatment.

Importance of components:

	PC1	PC2	PC3	PC4	PC5	PC6	PC7	PC8	PC9	PC10	PC11	PC12
Standard deviation	8.383	0.38619	0.17418	0.1199	0.06384	0.05952	0.03368	0.02918	0.02315	0.02202	0.01130	0.01037
Proportion of Variance	0.997	0.00212	0.00043	0.0002	0.00006	0.00005	0.00002	0.00001	0.00001	0.00001	0.00000	0.00000
Cumulative Proportion	0.997	0.99921	0.99964	0.9998	0.99990	0.99995	0.99997	0.99998	0.99999	0.99999	1.00000	1.00000

	PC13	PC14	PC15	PC16	PC17	PC18	PC19	PC20	PC21	PC22
Standard deviation	0.006383	0.005488	0.004993	0.003869	0.002652	0.002335	0.001762	0.001632	0.001480	0.001174
Proportion of Variance	0.000000	0.000000	0.000000	0.000000	0.000000	0.000000	0.000000	0.000000	0.000000	0.000000
Cumulative Proportion	1.000000	1.000000	1.000000	1.000000	1.000000	1.000000	1.000000	1.000000	1.000000	1.000000

	PC23	PC24	PC25	PC26	PC27	PC28	PC29	PC30	PC31
Standard deviation	0.0009111	0.000861	0.0008083	0.0007857	0.0007457	0.0007357	0.0006786	0.000674	0.0006344
Proportion of Variance	0.0000000	0.000000	0.0000000	0.0000000	0.0000000	0.0000000	0.0000000	0.000000	0.0000000
Cumulative Proportion	1.0000000	1.000000	1.0000000	1.0000000	1.0000000	1.0000000	1.0000000	1.000000	1.0000000

	PC32	PC33	PC34	PC35	PC36	PC37	PC38	PC39	PC40
Standard deviation	0.0006253	0.0006116	0.0005924	0.0005838	0.000564	0.0005559	0.0005357	0.0005279	0.0005157
Proportion of Variance	0.0000000	0.0000000	0.0000000	0.0000000	0.000000	0.0000000	0.0000000	0.0000000	0.0000000
Cumulative Proportion	1.0000000	1.0000000	1.0000000	1.0000000	1.000000	1.0000000	1.0000000	1.0000000	1.0000000

	PC41	PC42	PC43	PC44	PC45	PC46	PC47	PC48	PC49
Standard deviation	0.0005007	0.0004884	0.0004814	0.0004711	0.0004577	0.0004477	0.0004437	0.0004352	0.0004203
Proportion of Variance	0.0000000	0.0000000	0.0000000	0.0000000	0.0000000	0.0000000	0.0000000	0.0000000	0.0000000
Cumulative Proportion	1.0000000	1.0000000	1.0000000	1.0000000	1.0000000	1.0000000	1.0000000	1.0000000	1.0000000

	PC50	PC51	PC52	PC53	PC54	PC55	PC56	PC57	PC58
Standard deviation	0.0004085	0.0004007	0.0003883	0.000386	0.000374	0.0003677	0.0003639	0.0003556	0.0003527
Proportion of Variance	0.0000000	0.0000000	0.0000000	0.000000	0.000000	0.0000000	0.0000000	0.0000000	0.0000000
Cumulative Proportion	1.0000000	1.0000000	1.0000000	1.000000	1.000000	1.0000000	1.0000000	1.0000000	1.0000000

	PC59	PC60	PC61	PC62	PC63	PC64	PC65	PC66	PC67
Standard deviation	0.0003522	0.000338	0.0003345	0.0003229	0.0003183	0.0003149	0.0003085	0.0002970	0.0002955
Proportion of Variance	0.0000000	0.000000	0.0000000	0.0000000	0.0000000	0.0000000	0.0000000	0.0000000	0.0000000
Cumulative Proportion	1.0000000	1.000000	1.0000000	1.0000000	1.0000000	1.0000000	1.0000000	1.0000000	1.0000000

	PC68	PC69	PC70	PC71	PC72	PC73	PC74	PC75	PC76
Standard deviation	0.0002864	0.0002795	0.0002750	0.0002706	0.0002658	0.000259	0.0002513	0.0002455	0.0002416
Proportion of Variance	0.0000000	0.0000000	0.0000000	0.0000000	0.0000000	0.000000	0.0000000	0.0000000	0.0000000
Cumulative Proportion	1.0000000	1.0000000	1.0000000	1.0000000	1.0000000	1.000000	1.0000000	1.0000000	1.0000000

	PC77	PC78	PC79	PC80	PC81	PC82	PC83	PC84	PC85
Standard deviation	0.0002394	0.0002313	0.0002284	0.0002201	0.0002187	0.0002168	0.0002137	0.0002084	0.0002011
Proportion of Variance	0.0000000	0.0000000	0.0000000	0.0000000	0.0000000	0.0000000	0.0000000	0.0000000	0.0000000
Cumulative Proportion	1.0000000	1.0000000	1.0000000	1.0000000	1.0000000	1.0000000	1.0000000	1.0000000	1.0000000

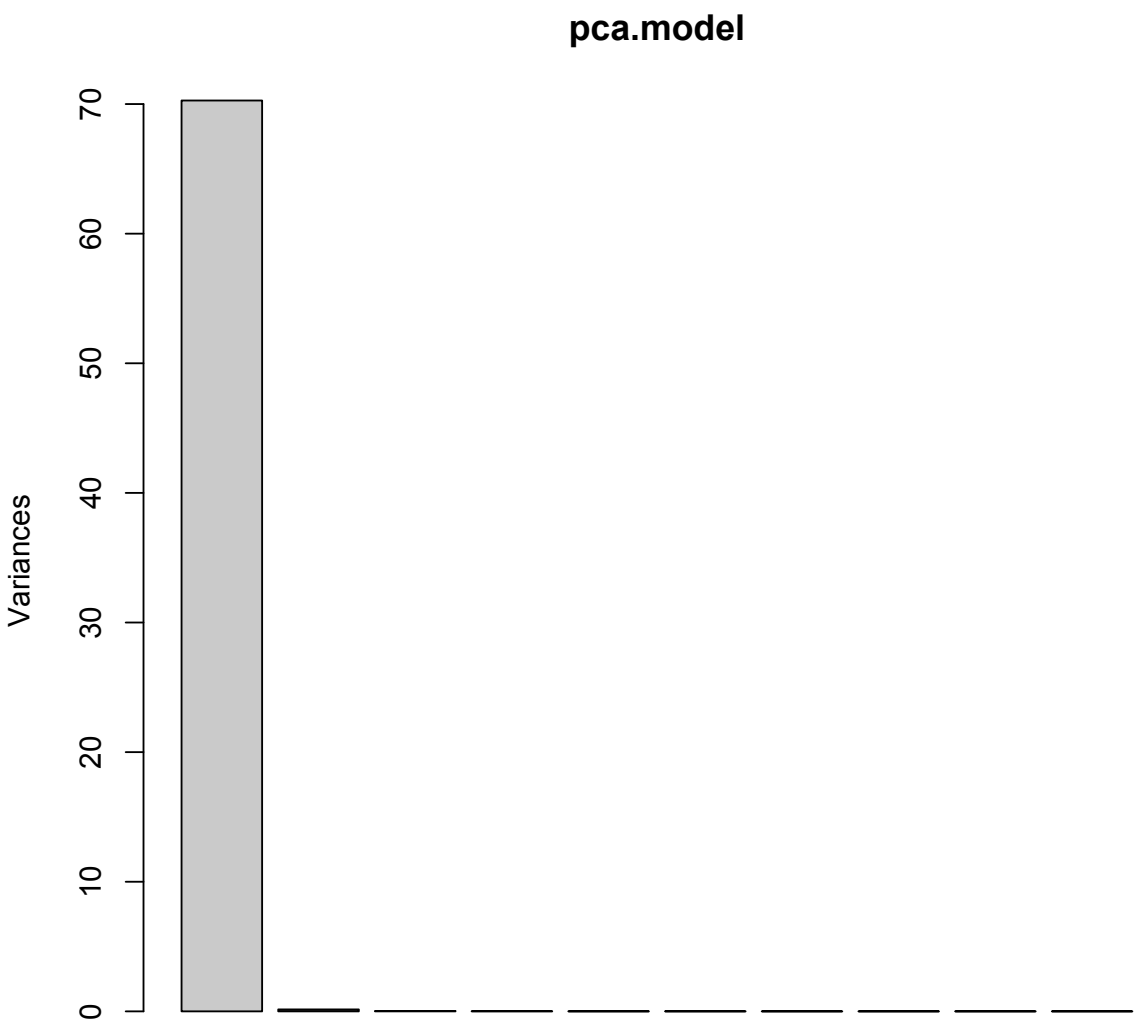


Figure 150: PCA scree plot for the first set of 30 normalized (peak height) glass spectra (10 replicates), no data pretreatment.

Table 162: PCA results for the first set of 30 normalized (peak height) glass spectra (10 replicates), centered.

Importance of components:

	PC1	PC2	PC3	PC4	PC5	PC6	PC7	PC8	PC9	PC10	PC11	PC12
Standard deviation	0.4538	0.2341	0.12623	0.06793	0.06383	0.03744	0.03055	0.02596	0.02266	0.01804	0.01097	0.009802
Proportion of Variance	0.7111	0.1893	0.05503	0.01593	0.01407	0.00484	0.00322	0.00233	0.00177	0.00112	0.00042	0.000330
Cumulative Proportion	0.7111	0.9004	0.95548	0.97141	0.98548	0.99032	0.99354	0.99587	0.99764	0.99877	0.99918	0.999510

	PC13	PC14	PC15	PC16	PC17	PC18	PC19	PC20	PC21	PC22
Standard deviation	0.006054	0.005484	0.004821	0.003826	0.002649	0.002335	0.001761	0.001631	0.001479	0.001157
Proportion of Variance	0.000130	0.000100	0.000080	0.000050	0.000020	0.000020	0.000010	0.000010	0.000010	0.000000
Cumulative Proportion	0.999640	0.999740	0.999820	0.999880	0.999900	0.999920	0.999930	0.999940	0.999950	0.999950

	PC23	PC24	PC25	PC26	PC27	PC28	PC29	PC30	PC31	PC32
Standard deviation	0.0009046	0.000857	0.000807	0.0007768	0.0007403	0.000735	0.0006785	0.000674	0.0006327	0.0006238
Proportion of Variance	0.0000000	0.000000	0.000000	0.0000000	0.0000000	0.000000	0.0000000	0.000000	0.0000000	0.0000000
Cumulative Proportion	0.9999500	0.999960	0.999960	0.9999600	0.9999600	0.999960	0.9999700	0.999970	0.9999700	0.9999700

	PC33	PC34	PC35	PC36	PC37	PC38	PC39	PC40	PC41
Standard deviation	0.0006116	0.0005924	0.0005815	0.0005593	0.0005559	0.0005302	0.0005254	0.0005112	0.0004976
Proportion of Variance	0.0000000	0.0000000	0.0000000	0.0000000	0.0000000	0.0000000	0.0000000	0.0000000	0.0000000
Cumulative Proportion	0.9999700	0.9999700	0.9999700	0.9999700	0.9999800	0.9999800	0.9999800	0.9999800	0.9999800

	PC42	PC43	PC44	PC45	PC46	PC47	PC48	PC49	PC50
Standard deviation	0.0004882	0.0004813	0.0004708	0.0004569	0.0004465	0.0004414	0.0004301	0.0004203	0.000405
Proportion of Variance	0.0000000	0.0000000	0.0000000	0.0000000	0.0000000	0.0000000	0.0000000	0.0000000	0.000000
Cumulative Proportion	0.9999800	0.9999800	0.9999800	0.9999800	0.9999800	0.9999800	0.9999800	0.9999800	0.999990

	PC51	PC52	PC53	PC54	PC55	PC56	PC57	PC58	PC59
Standard deviation	0.0003987	0.0003878	0.0003858	0.0003739	0.0003659	0.0003638	0.0003553	0.0003527	0.0003494
Proportion of Variance	0.0000000	0.0000000	0.0000000	0.0000000	0.0000000	0.0000000	0.0000000	0.0000000	0.0000000
Cumulative Proportion	0.9999900	0.9999900	0.9999900	0.9999900	0.9999900	0.9999900	0.9999900	0.9999900	0.9999900

	PC60	PC61	PC62	PC63	PC64	PC65	PC66	PC67	PC68
Standard deviation	0.0003378	0.0003335	0.0003206	0.0003177	0.0003129	0.0003073	0.0002969	0.000295	0.0002863
Proportion of Variance	0.0000000	0.0000000	0.0000000	0.0000000	0.0000000	0.0000000	0.0000000	0.000000	0.0000000
Cumulative Proportion	0.9999900	0.9999900	0.9999900	0.9999900	0.9999900	0.9999900	0.9999900	0.999990	0.9999900

	PC69	PC70	PC71	PC72	PC73	PC74	PC75	PC76	PC77
Standard deviation	0.0002777	0.0002748	0.0002702	0.0002656	0.0002579	0.0002512	0.0002454	0.0002416	0.0002387
Proportion of Variance	0.0000000	0.0000000	0.0000000	0.0000000	0.0000000	0.0000000	0.0000000	0.0000000	0.0000000
Cumulative Proportion	0.9999900	0.9999900	0.9999900	0.9999900	0.9999900	0.9999900	0.9999900	0.9999900	0.9999900

	PC78	PC79	PC80	PC81	PC82	PC83	PC84	PC85	PC86
Standard deviation	0.0002296	0.0002270	0.0002199	0.0002175	0.0002147	0.0002103	0.0002081	0.0001998	0.0001985
Proportion of Variance	0.0000000	0.0000000	0.0000000	0.0000000	0.0000000	0.0000000	0.0000000	0.0000000	0.0000000
Cumulative Proportion	1.0000000	1.0000000	1.0000000	1.0000000	1.0000000	1.0000000	1.0000000	1.0000000	1.0000000

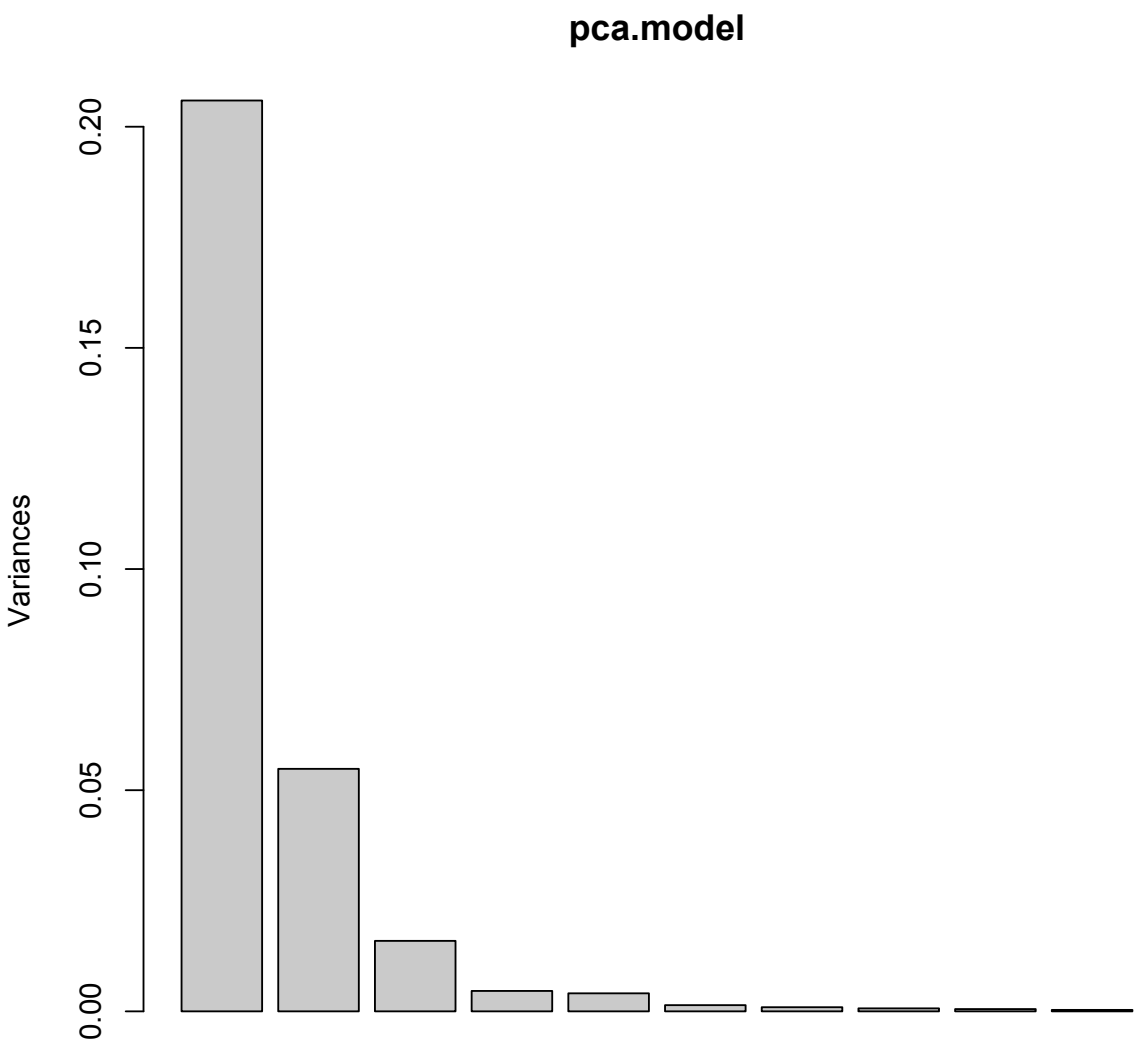


Figure 151: PCA scree plot for the first set of 30 normalized (peak height) glass spectra (10 replicates), centered.

Table 163: PCA results for the first set of 30 normalized (peak height) glass spectra (10 replicates), autoscaled.

Importance of components:

	PC1	PC2	PC3	PC4	PC5	PC6	PC7	PC8	PC9	PC10	PC11	PC12
Standard deviation	13.8854	9.3220	4.00484	3.39754	2.8529	1.82081	1.15377	1.00199	0.8800	0.73826	0.45757	0.38596
Proportion of Variance	0.5969	0.2690	0.04966	0.03574	0.0252	0.01026	0.00412	0.00311	0.0024	0.00169	0.00065	0.00046
Cumulative Proportion	0.5969	0.8659	0.91561	0.95135	0.9765	0.98681	0.99093	0.99404	0.9964	0.99812	0.99877	0.99923

	PC13	PC14	PC15	PC16	PC17	PC18	PC19	PC20	PC21	PC22	PC23	PC24
Standard deviation	0.26383	0.22060	0.1832	0.13164	0.11380	0.09456	0.08632	0.08065	0.07475	0.07221	0.06031	0.04652
Proportion of Variance	0.00022	0.00015	0.0001	0.00005	0.00004	0.00003	0.00002	0.00002	0.00002	0.00002	0.00001	0.00001
Cumulative Proportion	0.99945	0.99960	0.9997	0.99976	0.99980	0.99982	0.99985	0.99987	0.99988	0.99990	0.99991	0.99992

	PC25	PC26	PC27	PC28	PC29	PC30	PC31	PC32	PC33	PC34	PC35	PC36
Standard deviation	0.04448	0.04266	0.03843	0.03589	0.03279	0.03154	0.03077	0.02888	0.02758	0.02673	0.02655	0.02622
Proportion of Variance	0.00001	0.00001	0.00000	0.00000	0.00000	0.00000	0.00000	0.00000	0.00000	0.00000	0.00000	0.00000
Cumulative Proportion	0.99992	0.99993	0.99994	0.99994	0.99994	0.99995	0.99995	0.99995	0.99995	0.99996	0.99996	0.99996

	PC37	PC38	PC39	PC40	PC41	PC42	PC43	PC44	PC45	PC46	PC47	PC48
Standard deviation	0.02571	0.02470	0.02452	0.02385	0.02291	0.02228	0.02158	0.02097	0.02054	0.02011	0.01978	0.01905
Proportion of Variance	0.00000	0.00000	0.00000	0.00000	0.00000	0.00000	0.00000	0.00000	0.00000	0.00000	0.00000	0.00000
Cumulative Proportion	0.99996	0.99996	0.99997	0.99997	0.99997	0.99997	0.99997	0.99997	0.99997	0.99998	0.99998	0.99998

	PC49	PC50	PC51	PC52	PC53	PC54	PC55	PC56	PC57	PC58	PC59	PC60
Standard deviation	0.01832	0.01819	0.01740	0.01705	0.01667	0.01592	0.01574	0.01488	0.01459	0.01418	0.01361	0.01355
Proportion of Variance	0.00000	0.00000	0.00000	0.00000	0.00000	0.00000	0.00000	0.00000	0.00000	0.00000	0.00000	0.00000
Cumulative Proportion	0.99998	0.99998	0.99998	0.99998	0.99998	0.99998	0.99998	0.99999	0.99999	0.99999	0.99999	0.99999

	PC61	PC62	PC63	PC64	PC65	PC66	PC67	PC68	PC69	PC70	PC71
Standard deviation	0.01309	0.01289	0.01253	0.01242	0.01181	0.01153	0.01137	0.01131	0.01061	0.01041	0.01031
Proportion of Variance	0.00000	0.00000	0.00000	0.00000	0.00000	0.00000	0.00000	0.00000	0.00000	0.00000	0.00000
Cumulative Proportion	0.99999	0.99999	0.99999	0.99999	0.99999	0.99999	0.99999	0.99999	0.99999	0.99999	0.99999

	PC72	PC73	PC74	PC75	PC76	PC77	PC78	PC79	PC80	PC81
Standard deviation	0.009965	0.009823	0.009643	0.00943	0.009085	0.009076	0.008974	0.008553	0.008333	0.008193
Proportion of Variance	0.000000	0.000000	0.000000	0.00000	0.000000	0.000000	0.000000	0.000000	0.000000	0.000000
Cumulative Proportion	0.999990	0.999990	0.999990	0.99999	0.999990	0.999990	0.999990	0.999990	0.999990	1.000000

	PC82	PC83	PC84	PC85	PC86	PC87	PC88	PC89	PC90	PC91	PC92
Standard deviation	0.008067	0.007636	0.00751	0.00728	0.007154	0.00709	0.006931	0.006801	0.006623	0.006443	0.006363
Proportion of Variance	0.000000	0.000000	0.00000	0.00000	0.000000	0.00000	0.000000	0.000000	0.000000	0.000000	0.000000
Cumulative Proportion	1.000000	1.000000	1.00000	1.00000	1.000000	1.00000	1.000000	1.000000	1.000000	1.000000	1.000000

	PC93	PC94	PC95	PC96	PC97	PC98	PC99	PC100	PC101	PC102	PC103
Standard deviation	0.006288	0.006099	0.005988	0.005837	0.005715	0.0057	0.005471	0.005358	0.005274	0.00506	0.005001
Proportion of Variance	0.000000	0.000000	0.000000	0.000000	0.000000	0.0000	0.000000	0.000000	0.000000	0.00000	0.000000
Cumulative Proportion	1.000000	1.000000	1.000000	1.000000	1.000000	1.0000	1.000000	1.000000	1.000000	1.00000	1.000000

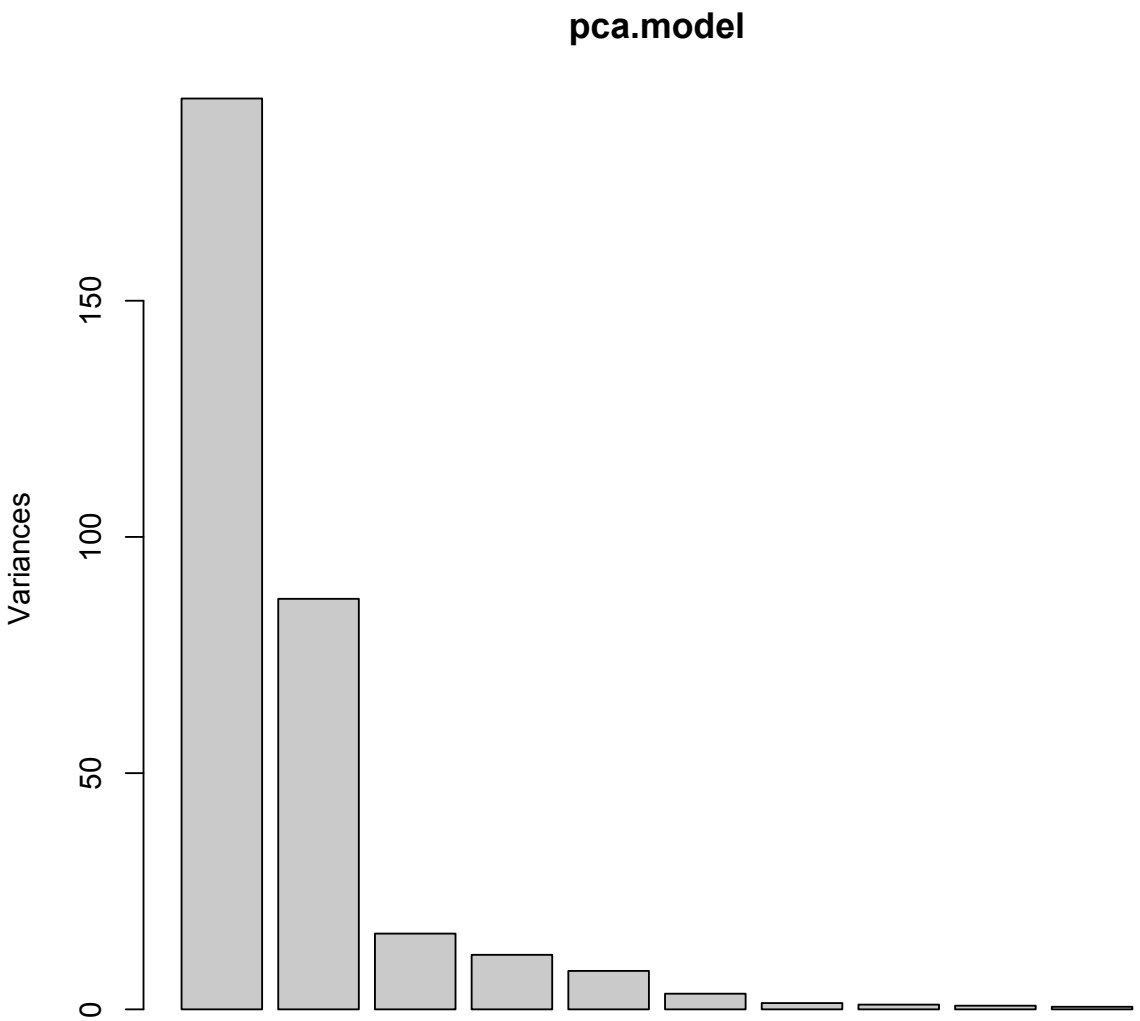


Figure 152: PCA scree plot for the first set of 30 normalized (peak height) glass spectra (10 replicates), autoscaled.

Table 164: PCA results for the first set of 20 normalized (peak height) window glass spectra (10 replicates), no data pretreatment.

Importance of components:

	PC1	PC2	PC3	PC4	PC5	PC6	PC7	PC8	PC9	PC10	PC11
Standard deviation	8.3905	0.35758	0.17012	0.10654	0.05719	0.03322	0.02913	0.02555	0.02259	0.01540	0.01084
Proportion of Variance	0.9975	0.00181	0.00041	0.00016	0.00005	0.00002	0.00001	0.00001	0.00001	0.00000	0.00000
Cumulative Proportion	0.9975	0.99933	0.99974	0.99990	0.99995	0.99996	0.99998	0.99998	0.99999	1.00000	1.00000

	PC12	PC13	PC14	PC15	PC16	PC17	PC18	PC19	PC20	PC21
Standard deviation	0.009758	0.005939	0.005183	0.003918	0.003768	0.002641	0.001988	0.001525	0.001458	0.001246
Proportion of Variance	0.000000	0.000000	0.000000	0.000000	0.000000	0.000000	0.000000	0.000000	0.000000	0.000000
Cumulative Proportion	1.000000	1.000000	1.000000	1.000000	1.000000	1.000000	1.000000	1.000000	1.000000	1.000000

	PC22	PC23	PC24	PC25	PC26	PC27	PC28	PC29	PC30
Standard deviation	0.001009	0.0009007	0.00085	0.000797	0.0007407	0.0007196	0.0007032	0.0006498	0.0006448
Proportion of Variance	0.000000	0.0000000	0.00000	0.000000	0.0000000	0.0000000	0.0000000	0.0000000	0.0000000
Cumulative Proportion	1.000000	1.0000000	1.00000	1.000000	1.0000000	1.0000000	1.0000000	1.0000000	1.0000000

	PC31	PC32	PC33	PC34	PC35	PC36	PC37	PC38	PC39
Standard deviation	0.0006219	0.0006112	0.0005937	0.0005774	0.0005648	0.0005601	0.0005471	0.0005225	0.0005074
Proportion of Variance	0.0000000	0.0000000	0.0000000	0.0000000	0.0000000	0.0000000	0.0000000	0.0000000	0.0000000
Cumulative Proportion	1.0000000	1.0000000	1.0000000	1.0000000	1.0000000	1.0000000	1.0000000	1.0000000	1.0000000

	PC40	PC41	PC42	PC43	PC44	PC45	PC46	PC47	PC48
Standard deviation	0.0005004	0.0004945	0.0004676	0.0004489	0.0004434	0.000435	0.0004204	0.0004182	0.0004156
Proportion of Variance	0.0000000	0.0000000	0.0000000	0.0000000	0.0000000	0.000000	0.0000000	0.0000000	0.0000000
Cumulative Proportion	1.0000000	1.0000000	1.0000000	1.0000000	1.0000000	1.000000	1.0000000	1.0000000	1.0000000

	PC49	PC50	PC51	PC52	PC53	PC54	PC55	PC56	PC57
Standard deviation	0.0004095	0.0003932	0.0003891	0.0003833	0.0003755	0.0003598	0.0003533	0.0003384	0.0003363
Proportion of Variance	0.0000000	0.0000000	0.0000000	0.0000000	0.0000000	0.0000000	0.0000000	0.0000000	0.0000000
Cumulative Proportion	1.0000000	1.0000000	1.0000000	1.0000000	1.0000000	1.0000000	1.0000000	1.0000000	1.0000000

	PC58	PC59	PC60	PC61	PC62	PC63	PC64	PC65	PC66
Standard deviation	0.0003203	0.0003184	0.0003128	0.0003085	0.0002986	0.0002979	0.0002877	0.0002811	0.0002786
Proportion of Variance	0.0000000	0.0000000	0.0000000	0.0000000	0.0000000	0.0000000	0.0000000	0.0000000	0.0000000
Cumulative Proportion	1.0000000	1.0000000	1.0000000	1.0000000	1.0000000	1.0000000	1.0000000	1.0000000	1.0000000

	PC67	PC68	PC69	PC70	PC71	PC72	PC73	PC74	PC75
Standard deviation	0.0002722	0.0002655	0.0002600	0.0002539	0.0002469	0.000244	0.0002352	0.0002322	0.0002215
Proportion of Variance	0.0000000	0.0000000	0.0000000	0.0000000	0.0000000	0.000000	0.0000000	0.0000000	0.0000000
Cumulative Proportion	1.0000000	1.0000000	1.0000000	1.0000000	1.0000000	1.000000	1.0000000	1.0000000	1.0000000

	PC76	PC77	PC78	PC79	PC80	PC81	PC82	PC83	PC84
Standard deviation	0.0002190	0.0002146	0.0002099	0.0002079	0.0002013	0.0001946	0.0001923	0.0001870	0.0001857
Proportion of Variance	0.0000000	0.0000000	0.0000000	0.0000000	0.0000000	0.0000000	0.0000000	0.0000000	0.0000000
Cumulative Proportion	1.0000000	1.0000000	1.0000000	1.0000000	1.0000000	1.0000000	1.0000000	1.0000000	1.0000000

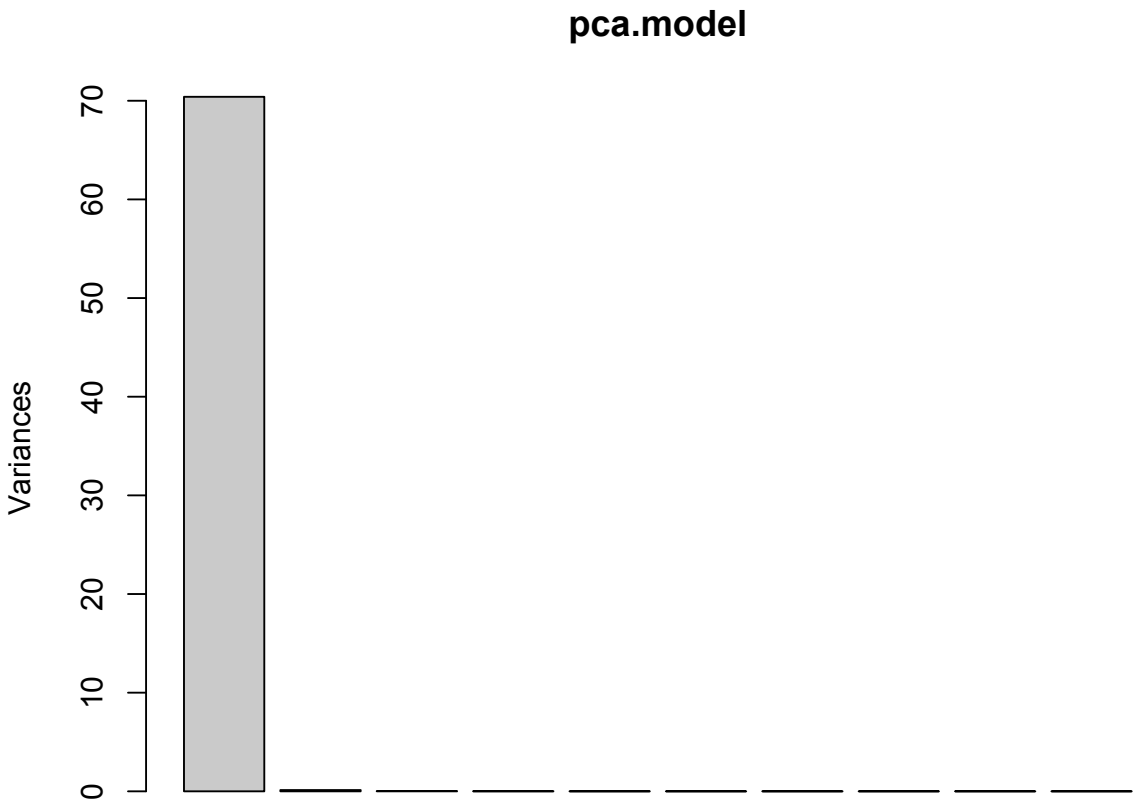


Figure 153: PCA scree plot for the first set of 20 normalized (peak height) window glass spectra (10 replicates), no data pretreatment.

Table 165: PCA results for the first set of 20 normalized (peak height) window glass spectra (10 replicates), centered.

Importance of components:

	PC1	PC2	PC3	PC4	PC5	PC6	PC7	PC8	PC9	PC10	PC11
Standard deviation	0.4150	0.2366	0.11093	0.06367	0.03808	0.02986	0.02578	0.02472	0.01754	0.01514	0.01073
Proportion of Variance	0.6915	0.2248	0.04942	0.01628	0.00582	0.00358	0.00267	0.00245	0.00124	0.00092	0.00046
Cumulative Proportion	0.6915	0.9164	0.96579	0.98207	0.98789	0.99147	0.99414	0.99659	0.99783	0.99875	0.99921

	PC12	PC13	PC14	PC15	PC16	PC17	PC18	PC19	PC20	PC21
Standard deviation	0.00889	0.005574	0.00518	0.003867	0.003674	0.002614	0.001988	0.001523	0.001458	0.001246
Proportion of Variance	0.00032	0.000120	0.00011	0.000060	0.000050	0.000030	0.000020	0.000010	0.000010	0.000010
Cumulative Proportion	0.99953	0.999650	0.99976	0.999820	0.999880	0.999900	0.999920	0.999930	0.999940	0.999940

	PC22	PC23	PC24	PC25	PC26	PC27	PC28	PC29	PC30
Standard deviation	0.000989	0.0009003	0.000849	0.0007957	0.0007326	0.0007192	0.0007032	0.0006485	0.0006448
Proportion of Variance	0.000000	0.0000000	0.000000	0.0000000	0.0000000	0.0000000	0.0000000	0.0000000	0.0000000
Cumulative Proportion	0.999950	0.9999500	0.999950	0.9999600	0.9999600	0.9999600	0.9999600	0.9999600	0.9999700

	PC31	PC32	PC33	PC34	PC35	PC36	PC37	PC38	PC39
Standard deviation	0.0006213	0.0006092	0.0005935	0.0005772	0.000564	0.0005585	0.000535	0.0005225	0.0005062
Proportion of Variance	0.0000000	0.0000000	0.0000000	0.0000000	0.000000	0.0000000	0.000000	0.0000000	0.0000000
Cumulative Proportion	0.9999700	0.9999700	0.9999700	0.9999700	0.999970	0.9999700	0.999980	0.9999800	0.9999800

	PC40	PC41	PC42	PC43	PC44	PC45	PC46	PC47	PC48
Standard deviation	0.0004997	0.0004945	0.0004598	0.0004484	0.0004423	0.0004346	0.0004203	0.0004178	0.0004154
Proportion of Variance	0.0000000	0.0000000	0.0000000	0.0000000	0.0000000	0.0000000	0.0000000	0.0000000	0.0000000
Cumulative Proportion	0.9999800	0.9999800	0.9999800	0.9999800	0.9999800	0.9999800	0.9999800	0.9999800	0.9999800

	PC49	PC50	PC51	PC52	PC53	PC54	PC55	PC56	PC57
Standard deviation	0.0004095	0.0003928	0.000389	0.000383	0.0003686	0.0003589	0.0003508	0.0003381	0.0003307
Proportion of Variance	0.0000000	0.0000000	0.000000	0.000000	0.0000000	0.0000000	0.0000000	0.0000000	0.0000000
Cumulative Proportion	0.9999900	0.9999900	0.999990	0.999990	0.9999900	0.9999900	0.9999900	0.9999900	0.9999900

	PC58	PC59	PC60	PC61	PC62	PC63	PC64	PC65	PC66
Standard deviation	0.0003202	0.0003174	0.0003112	0.0003082	0.0002981	0.0002925	0.0002877	0.0002803	0.0002783
Proportion of Variance	0.0000000	0.0000000	0.0000000	0.0000000	0.0000000	0.0000000	0.0000000	0.0000000	0.0000000
Cumulative Proportion	0.9999900	0.9999900	0.9999900	0.9999900	0.9999900	0.9999900	0.9999900	0.9999900	0.9999900

	PC67	PC68	PC69	PC70	PC71	PC72	PC73	PC74	PC75
Standard deviation	0.0002688	0.0002621	0.0002599	0.0002533	0.0002467	0.0002434	0.0002326	0.0002288	0.0002205
Proportion of Variance	0.0000000	0.0000000	0.0000000	0.0000000	0.0000000	0.0000000	0.0000000	0.0000000	0.0000000
Cumulative Proportion	0.9999900	0.9999900	0.9999900	0.9999900	0.9999900	0.9999900	0.9999900	1.0000000	1.0000000

	PC76	PC77	PC78	PC79	PC80	PC81	PC82	PC83	PC84
Standard deviation	0.0002184	0.0002112	0.0002088	0.0002049	0.0001978	0.0001946	0.0001905	0.0001870	0.0001815
Proportion of Variance	0.0000000	0.0000000	0.0000000	0.0000000	0.0000000	0.0000000	0.0000000	0.0000000	0.0000000
Cumulative Proportion	1.0000000	1.0000000	1.0000000	1.0000000	1.0000000	1.0000000	1.0000000	1.0000000	1.0000000

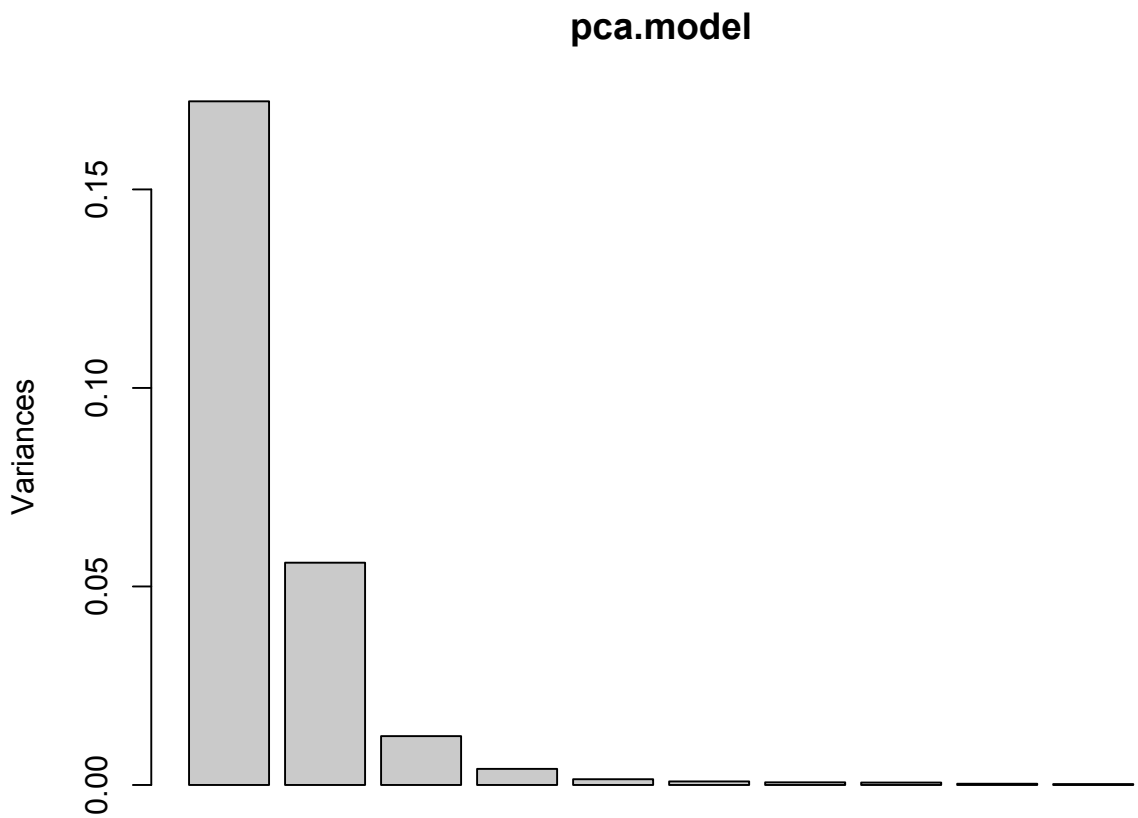


Figure 154: PCA scree plot for the first set of 20 normalized (peak height) window glass spectra (10 replicates), centered.

Table 166: PCA results for the first set of 20 normalized (peak height) window glass spectra (10 replicates), autoscaled.

Importance of components:

	PC1	PC2	PC3	PC4	PC5	PC6	PC7	PC8	PC9	PC10	PC11
Standard deviation	13.7568	9.9825	3.70877	3.33013	1.89850	1.30594	1.12535	1.0014	0.77527	0.69362	0.47078
Proportion of Variance	0.5859	0.3085	0.04259	0.03433	0.01116	0.00528	0.00392	0.0031	0.00186	0.00149	0.00069
Cumulative Proportion	0.5859	0.8944	0.93702	0.97135	0.98251	0.98779	0.99171	0.9948	0.99668	0.99817	0.99885

	PC12	PC13	PC14	PC15	PC16	PC17	PC18	PC19	PC20	PC21	PC22
Standard deviation	0.37387	0.23381	0.20303	0.1812	0.13698	0.12184	0.10073	0.08983	0.08720	0.07697	0.05846
Proportion of Variance	0.00043	0.00017	0.00013	0.0001	0.00006	0.00005	0.00003	0.00002	0.00002	0.00002	0.00001
Cumulative Proportion	0.99928	0.99945	0.99958	0.9997	0.99974	0.99979	0.99982	0.99984	0.99987	0.99989	0.99990

	PC23	PC24	PC25	PC26	PC27	PC28	PC29	PC30	PC31	PC32	PC33
Standard deviation	0.05771	0.05156	0.04571	0.04333	0.0395	0.03510	0.03437	0.03327	0.03215	0.03102	0.03041
Proportion of Variance	0.00001	0.00001	0.00001	0.00001	0.0000	0.00000	0.00000	0.00000	0.00000	0.00000	0.00000
Cumulative Proportion	0.99991	0.99991	0.99992	0.99993	0.9999	0.99994	0.99994	0.99994	0.99995	0.99995	0.99995

	PC34	PC35	PC36	PC37	PC38	PC39	PC40	PC41	PC42	PC43	PC44
Standard deviation	0.02895	0.02827	0.02815	0.02656	0.02604	0.02482	0.02453	0.02362	0.02273	0.02221	0.02171
Proportion of Variance	0.00000	0.00000	0.00000	0.00000	0.00000	0.00000	0.00000	0.00000	0.00000	0.00000	0.00000
Cumulative Proportion	0.99995	0.99996	0.99996	0.99996	0.99996	0.99997	0.99997	0.99997	0.99997	0.99997	0.99997

	PC45	PC46	PC47	PC48	PC49	PC50	PC51	PC52	PC53	PC54	PC55
Standard deviation	0.02114	0.02055	0.02029	0.01995	0.01898	0.01832	0.01803	0.01687	0.01644	0.0159	0.01558
Proportion of Variance	0.00000	0.00000	0.00000	0.00000	0.00000	0.00000	0.00000	0.00000	0.00000	0.0000	0.00000
Cumulative Proportion	0.99998	0.99998	0.99998	0.99998	0.99998	0.99998	0.99998	0.99998	0.99998	1.0000	0.99999

	PC56	PC57	PC58	PC59	PC60	PC61	PC62	PC63	PC64	PC65	PC66
Standard deviation	0.01493	0.01471	0.01430	0.01411	0.01381	0.01348	0.01324	0.01277	0.0125	0.01211	0.01179
Proportion of Variance	0.00000	0.00000	0.00000	0.00000	0.00000	0.00000	0.00000	0.00000	0.0000	0.00000	0.00000
Cumulative Proportion	0.99999	0.99999	0.99999	0.99999	0.99999	0.99999	0.99999	0.99999	1.0000	0.99999	0.99999

	PC67	PC68	PC69	PC70	PC71	PC72	PC73	PC74	PC75	PC76	PC77
Standard deviation	0.01158	0.01082	0.01064	0.01036	0.01025	0.009676	0.00943	0.009282	0.009221	0.009006	0.00863
Proportion of Variance	0.00000	0.00000	0.00000	0.00000	0.00000	0.000000	0.00000	0.000000	0.000000	0.000000	0.00000
Cumulative Proportion	0.99999	0.99999	0.99999	0.99999	0.99999	0.999990	0.99999	0.999990	0.999990	0.999990	1.00000

	PC78	PC79	PC80	PC81	PC82	PC83	PC84	PC85	PC86	PC87
Standard deviation	0.008511	0.008183	0.008063	0.007753	0.007467	0.007369	0.007233	0.007062	0.006852	0.006742
Proportion of Variance	0.000000	0.000000	0.000000	0.000000	0.000000	0.000000	0.000000	0.000000	0.000000	0.000000
Cumulative Proportion	1.000000	1.000000	1.000000	1.000000	1.000000	1.000000	1.000000	1.000000	1.000000	1.000000

	PC88	PC89	PC90	PC91	PC92	PC93	PC94	PC95	PC96	PC97
Standard deviation	0.006598	0.006499	0.00622	0.00604	0.005906	0.00581	0.005748	0.005549	0.005505	0.005467
Proportion of Variance	0.000000	0.000000	0.00000	0.00000	0.000000	0.00000	0.000000	0.000000	0.000000	0.000000
Cumulative Proportion	1.000000	1.000000	1.00000	1.00000	1.000000	1.00000	1.000000	1.000000	1.000000	1.000000

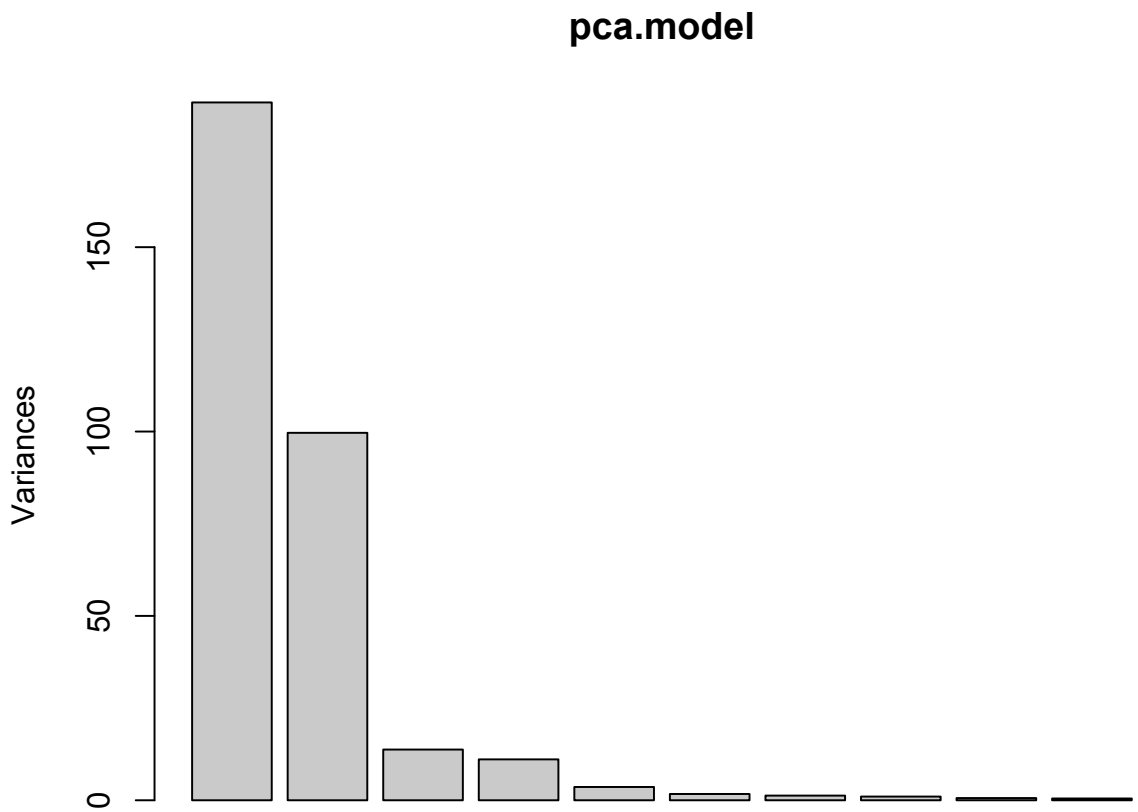


Figure 155: PCA scree plot for the first set of 20 normalized (peak height) window glass spectra (10 replicates), autoscaled.

Table 167: PCA results for the first set of 10 normalized (peak height) container glass spectra (10 replicates), no data pretreatment.

Importance of components:

	PC1	PC2	PC3	PC4	PC5	PC6	PC7	PC8	PC9	PC10	PC11
Standard deviation	8.4107	0.4376	0.18345	0.13896	0.06362	0.05194	0.03121	0.02855	0.01951	0.01868	0.01215
Proportion of Variance	0.9964	0.0027	0.00047	0.00027	0.00006	0.00004	0.00001	0.00001	0.00001	0.00000	0.00000
Cumulative Proportion	0.9964	0.9991	0.99959	0.99986	0.99992	0.99996	0.99997	0.99998	0.99999	0.99999	1.00000

	PC12	PC13	PC14	PC15	PC16	PC17	PC18	PC19	PC20	PC21
Standard deviation	0.01016	0.005596	0.005012	0.003731	0.002905	0.002361	0.00185	0.001719	0.001446	0.001274
Proportion of Variance	0.00000	0.000000	0.000000	0.000000	0.000000	0.000000	0.00000	0.000000	0.000000	0.000000
Cumulative Proportion	1.00000	1.000000	1.000000	1.000000	1.000000	1.000000	1.00000	1.000000	1.000000	1.000000

	PC22	PC23	PC24	PC25	PC26	PC27	PC28	PC29	PC30
Standard deviation	0.0009837	9e-04	0.0008832	0.0008165	0.0007541	0.0007387	0.0007099	0.0006918	0.0006692
Proportion of Variance	0.0000000	0e+00	0.0000000	0.0000000	0.0000000	0.0000000	0.0000000	0.0000000	0.0000000
Cumulative Proportion	1.0000000	1e+00	1.0000000	1.0000000	1.0000000	1.0000000	1.0000000	1.0000000	1.0000000

	PC31	PC32	PC33	PC34	PC35	PC36	PC37	PC38	PC39
Standard deviation	0.000639	0.0006288	0.0006182	0.0005924	0.000584	0.0005387	0.0005228	0.0005187	0.0004982
Proportion of Variance	0.000000	0.0000000	0.0000000	0.0000000	0.000000	0.0000000	0.0000000	0.0000000	0.0000000
Cumulative Proportion	1.000000	1.0000000	1.0000000	1.0000000	1.000000	1.0000000	1.0000000	1.0000000	1.0000000

	PC40	PC41	PC42	PC43	PC44	PC45	PC46	PC47	PC48
Standard deviation	0.0004943	0.0004739	0.000454	0.0004303	0.0004065	0.0004028	0.0003965	0.0003914	0.000373
Proportion of Variance	0.0000000	0.0000000	0.000000	0.0000000	0.0000000	0.0000000	0.0000000	0.0000000	0.000000
Cumulative Proportion	1.0000000	1.0000000	1.000000	1.0000000	1.0000000	1.0000000	1.0000000	1.0000000	1.000000

	PC49	PC50	PC51	PC52	PC53	PC54	PC55	PC56	PC57
Standard deviation	0.0003573	0.000355	0.0003441	0.0003331	0.0003216	0.0003142	0.0003084	0.0003025	0.0002907
Proportion of Variance	0.0000000	0.000000	0.0000000	0.0000000	0.0000000	0.0000000	0.0000000	0.0000000	0.0000000
Cumulative Proportion	1.0000000	1.000000	1.0000000	1.0000000	1.0000000	1.0000000	1.0000000	1.0000000	1.0000000

	PC58	PC59	PC60	PC61	PC62	PC63	PC64	PC65	PC66
Standard deviation	0.0002829	0.0002755	0.0002589	0.0002502	0.0002477	0.0002416	0.0002378	0.0002347	0.0002268
Proportion of Variance	0.0000000	0.0000000	0.0000000	0.0000000	0.0000000	0.0000000	0.0000000	0.0000000	0.0000000
Cumulative Proportion	1.0000000	1.0000000	1.0000000	1.0000000	1.0000000	1.0000000	1.0000000	1.0000000	1.0000000

	PC67	PC68	PC69	PC70	PC71	PC72	PC73	PC74	PC75
Standard deviation	0.0002239	0.0002211	0.0002175	0.0002127	0.0001971	0.0001896	0.0001850	0.0001823	0.0001778
Proportion of Variance	0.0000000	0.0000000	0.0000000	0.0000000	0.0000000	0.0000000	0.0000000	0.0000000	0.0000000
Cumulative Proportion	1.0000000	1.0000000	1.0000000	1.0000000	1.0000000	1.0000000	1.0000000	1.0000000	1.0000000

	PC76	PC77	PC78	PC79	PC80	PC81	PC82	PC83	PC84
Standard deviation	0.0001734	0.0001604	0.0001582	0.0001531	0.0001518	0.0001456	0.0001395	0.0001363	0.0001322
Proportion of Variance	0.0000000	0.0000000	0.0000000	0.0000000	0.0000000	0.0000000	0.0000000	0.0000000	0.0000000
Cumulative Proportion	1.0000000	1.0000000	1.0000000	1.0000000	1.0000000	1.0000000	1.0000000	1.0000000	1.0000000

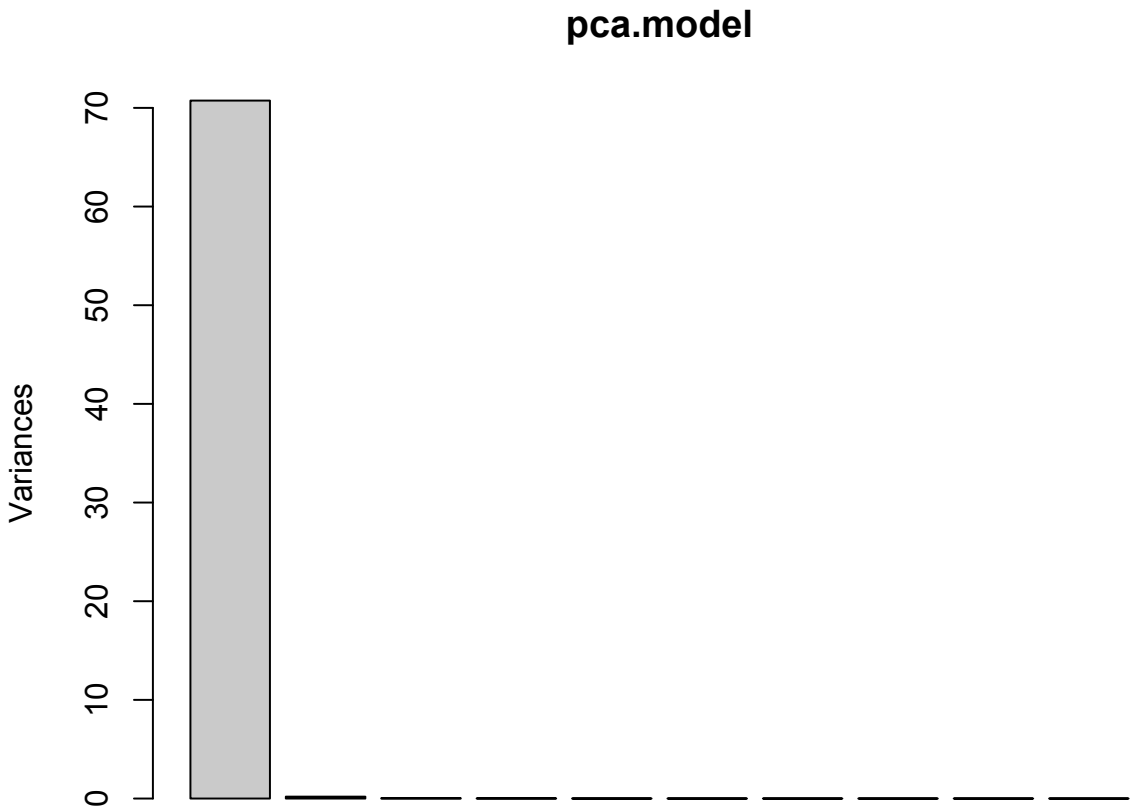


Figure 156: PCA scree plot for the first set of 10 normalized (peak height) container glass spectra (10 replicates), no data pretreatment.

Table 168: PCA results for the first set of 10 normalized (peak height) container glass spectra (10 replicates), centered.

Importance of components:

	PC1	PC2	PC3	PC4	PC5	PC6	PC7	PC8	PC9	PC10	PC11
Standard deviation	0.5244	0.2266	0.15323	0.07508	0.05197	0.03579	0.03111	0.02319	0.01870	0.01774	0.01087
Proportion of Variance	0.7598	0.1419	0.06486	0.01557	0.00746	0.00354	0.00267	0.00149	0.00097	0.00087	0.00033
Cumulative Proportion	0.7598	0.9017	0.96654	0.98211	0.98958	0.99312	0.99579	0.99728	0.99824	0.99911	0.99944

	PC12	PC13	PC14	PC15	PC16	PC17	PC18	PC19	PC20	PC21
Standard deviation	0.00995	0.005551	0.00488	0.00373	0.002841	0.00236	0.001821	0.001710	0.001415	0.001264
Proportion of Variance	0.00027	0.000090	0.00007	0.00004	0.000020	0.00002	0.000010	0.000010	0.000010	0.000000
Cumulative Proportion	0.99971	0.999800	0.99986	0.99990	0.999920	0.99994	0.999950	0.999960	0.999960	0.999970

	PC22	PC23	PC24	PC25	PC26	PC27	PC28	PC29	PC30
Standard deviation	0.0009814	9e-04	0.0008418	0.0008162	0.0007518	0.000724	0.0007093	0.0006917	0.0006489
Proportion of Variance	0.0000000	0e+00	0.0000000	0.0000000	0.0000000	0.000000	0.0000000	0.0000000	0.0000000
Cumulative Proportion	0.9999700	1e+00	0.9999700	0.9999700	0.9999800	0.999980	0.9999800	0.9999800	0.9999800

	PC31	PC32	PC33	PC34	PC35	PC36	PC37	PC38	PC39
Standard deviation	0.0006327	0.0006202	0.0006103	0.000592	0.000579	0.0005385	0.0005207	0.0005146	0.0004952
Proportion of Variance	0.0000000	0.0000000	0.0000000	0.000000	0.000000	0.0000000	0.0000000	0.0000000	0.0000000
Cumulative Proportion	0.9999800	0.9999800	0.9999800	0.999990	0.999990	0.9999900	0.9999900	0.9999900	0.9999900

	PC40	PC41	PC42	PC43	PC44	PC45	PC46	PC47	PC48
Standard deviation	0.0004866	0.000471	0.0004501	0.0004256	0.0004061	0.0004013	0.0003953	0.0003804	0.0003687
Proportion of Variance	0.0000000	0.000000	0.0000000	0.0000000	0.0000000	0.0000000	0.0000000	0.0000000	0.0000000
Cumulative Proportion	0.9999900	0.999990	0.9999900	0.9999900	0.9999900	0.9999900	0.9999900	0.9999900	0.9999900

	PC49	PC50	PC51	PC52	PC53	PC54	PC55	PC56	PC57
Standard deviation	0.0003557	0.0003490	0.0003441	0.0003267	0.0003203	0.0003141	0.0003073	0.0002956	0.0002837
Proportion of Variance	0.0000000	0.0000000	0.0000000	0.0000000	0.0000000	0.0000000	0.0000000	0.0000000	0.0000000
Cumulative Proportion	0.9999900	0.9999900	0.9999900	1.0000000	1.0000000	1.0000000	1.0000000	1.0000000	1.0000000

	PC58	PC59	PC60	PC61	PC62	PC63	PC64	PC65	PC66
Standard deviation	0.0002819	0.0002755	0.0002568	0.0002502	0.000247	0.0002398	0.0002378	0.0002312	0.0002249
Proportion of Variance	0.0000000	0.0000000	0.0000000	0.0000000	0.000000	0.0000000	0.0000000	0.0000000	0.0000000
Cumulative Proportion	1.0000000	1.0000000	1.0000000	1.0000000	1.000000	1.0000000	1.0000000	1.0000000	1.0000000

	PC67	PC68	PC69	PC70	PC71	PC72	PC73	PC74	PC75
Standard deviation	0.0002224	0.0002182	0.0002143	0.0002066	0.0001944	0.0001881	0.0001846	0.0001813	0.0001741
Proportion of Variance	0.0000000	0.0000000	0.0000000	0.0000000	0.0000000	0.0000000	0.0000000	0.0000000	0.0000000
Cumulative Proportion	1.0000000	1.0000000	1.0000000	1.0000000	1.0000000	1.0000000	1.0000000	1.0000000	1.0000000

	PC76	PC77	PC78	PC79	PC80	PC81	PC82	PC83	PC84
Standard deviation	0.0001719	0.0001594	0.0001579	0.0001529	0.0001473	0.0001455	0.0001367	0.0001355	0.0001321
Proportion of Variance	0.0000000	0.0000000	0.0000000	0.0000000	0.0000000	0.0000000	0.0000000	0.0000000	0.0000000
Cumulative Proportion	1.0000000	1.0000000	1.0000000	1.0000000	1.0000000	1.0000000	1.0000000	1.0000000	1.0000000

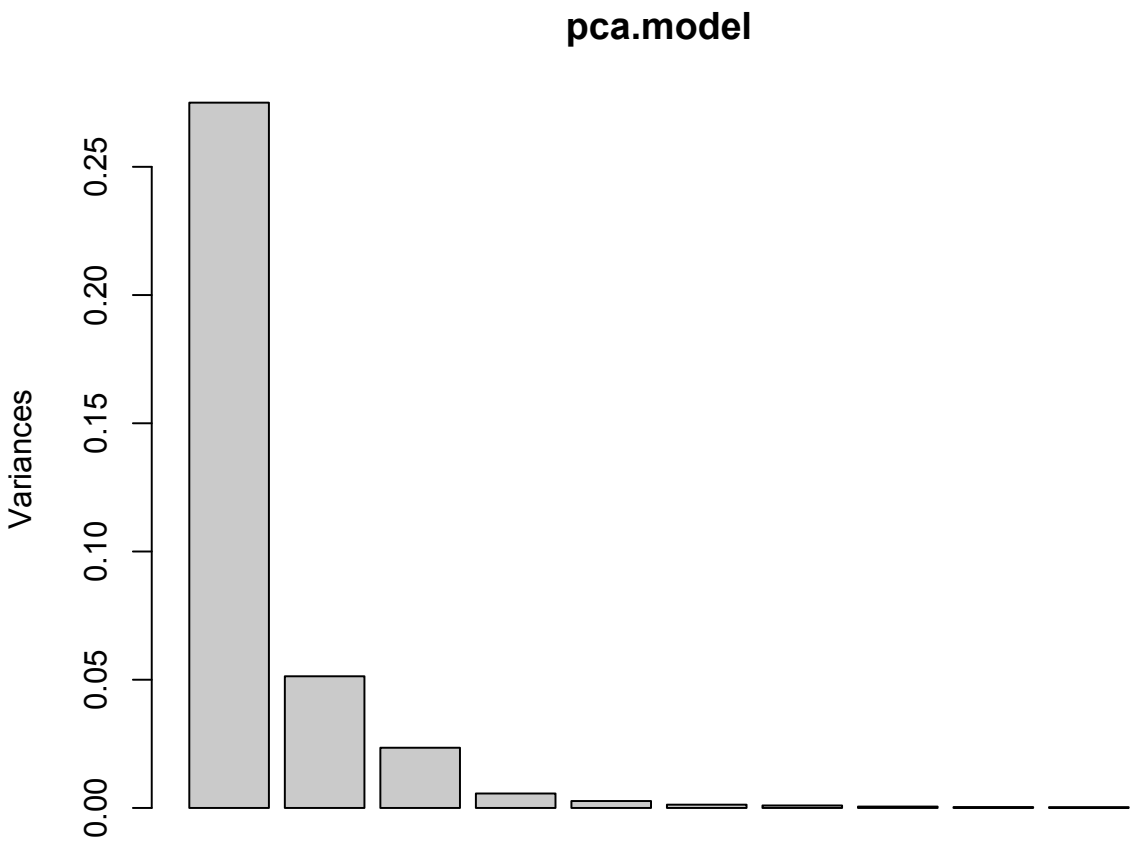


Figure 157: PCA scree plot for the first set of 10 normalized (peak height) container glass spectra (10 replicates), centered.

Table 169: PCA results for the first set of 10 normalized (peak height) container glass spectra (10 replicates), autoscaled.

Importance of components:

	PC1	PC2	PC3	PC4	PC5	PC6	PC7	PC8	PC9	PC10	PC11
Standard deviation	14.1374	8.9134	4.71497	3.34094	1.9771	1.77549	1.02278	0.87342	0.77586	0.61253	0.41462
Proportion of Variance	0.6188	0.2460	0.06883	0.03456	0.0121	0.00976	0.00324	0.00236	0.00186	0.00116	0.00053
Cumulative Proportion	0.6188	0.8648	0.93358	0.96814	0.9802	0.99000	0.99324	0.99560	0.99746	0.99862	0.99916

	PC12	PC13	PC14	PC15	PC16	PC17	PC18	PC19	PC20	PC21	PC22
Standard deviation	0.34082	0.19196	0.1756	0.15952	0.10209	0.09034	0.08575	0.07637	0.06409	0.05999	0.05182
Proportion of Variance	0.00036	0.00011	0.0001	0.00008	0.00003	0.00003	0.00002	0.00002	0.00001	0.00001	0.00001
Cumulative Proportion	0.99952	0.99963	0.9997	0.99980	0.99984	0.99986	0.99988	0.99990	0.99992	0.99993	0.99994

	PC23	PC24	PC25	PC26	PC27	PC28	PC29	PC30	PC31	PC32	PC33
Standard deviation	0.04583	0.04108	0.03752	0.03533	0.03341	0.03168	0.02983	0.02803	0.02753	0.02620	0.0258
Proportion of Variance	0.00001	0.00001	0.00000	0.00000	0.00000	0.00000	0.00000	0.00000	0.00000	0.00000	0.0000
Cumulative Proportion	0.99994	0.99995	0.99995	0.99996	0.99996	0.99996	0.99996	0.99997	0.99997	0.99997	1.0000

	PC34	PC35	PC36	PC37	PC38	PC39	PC40	PC41	PC42	PC43	PC44
Standard deviation	0.02438	0.0239	0.02331	0.0211	0.02097	0.02047	0.01977	0.01930	0.01875	0.01739	0.01701
Proportion of Variance	0.00000	0.0000	0.00000	0.0000	0.00000	0.00000	0.00000	0.00000	0.00000	0.00000	0.00000
Cumulative Proportion	0.99998	1.0000	0.99998	1.0000	0.99998	0.99998	0.99998	0.99999	0.99999	0.99999	0.99999

	PC45	PC46	PC47	PC48	PC49	PC50	PC51	PC52	PC53	PC54	PC55
Standard deviation	0.01661	0.01583	0.01531	0.0144	0.01429	0.01368	0.01300	0.01266	0.01225	0.01159	0.01084
Proportion of Variance	0.00000	0.00000	0.00000	0.0000	0.00000	0.00000	0.00000	0.00000	0.00000	0.00000	0.00000
Cumulative Proportion	0.99999	0.99999	0.99999	1.0000	0.99999	0.99999	0.99999	0.99999	0.99999	0.99999	0.99999

	PC56	PC57	PC58	PC59	PC60	PC61	PC62	PC63	PC64	PC65
Standard deviation	0.01071	0.01046	0.00993	0.009858	0.009537	0.00927	0.008924	0.008796	0.008587	0.008178
Proportion of Variance	0.00000	0.00000	0.00000	0.000000	0.000000	0.00000	0.000000	0.000000	0.000000	0.000000
Cumulative Proportion	0.99999	1.00000	1.00000	1.000000	1.000000	1.00000	1.000000	1.000000	1.000000	1.000000

	PC66	PC67	PC68	PC69	PC70	PC71	PC72	PC73	PC74	PC75
Standard deviation	0.007863	0.007788	0.007426	0.007209	0.006984	0.006915	0.006793	0.006699	0.006381	0.006059
Proportion of Variance	0.000000	0.000000	0.000000	0.000000	0.000000	0.000000	0.000000	0.000000	0.000000	0.000000
Cumulative Proportion	1.000000	1.000000	1.000000	1.000000	1.000000	1.000000	1.000000	1.000000	1.000000	1.000000

	PC76	PC77	PC78	PC79	PC80	PC81	PC82	PC83	PC84	PC85
Standard deviation	0.00594	0.005584	0.005493	0.005301	0.00516	0.004963	0.004791	0.004559	0.004286	0.00422
Proportion of Variance	0.00000	0.000000	0.000000	0.000000	0.00000	0.000000	0.000000	0.000000	0.000000	0.00000
Cumulative Proportion	1.00000	1.000000	1.000000	1.000000	1.00000	1.000000	1.000000	1.000000	1.000000	1.00000

	PC86	PC87	PC88	PC89	PC90	PC91	PC92	PC93	PC94	PC95
Standard deviation	0.003818	0.003793	0.003555	0.003501	0.003442	0.003324	0.003123	0.003016	0.002938	0.002865
Proportion of Variance	0.000000	0.000000	0.000000	0.000000	0.000000	0.000000	0.000000	0.000000	0.000000	0.000000
Cumulative Proportion	1.000000	1.000000	1.000000	1.000000	1.000000	1.000000	1.000000	1.000000	1.000000	1.000000

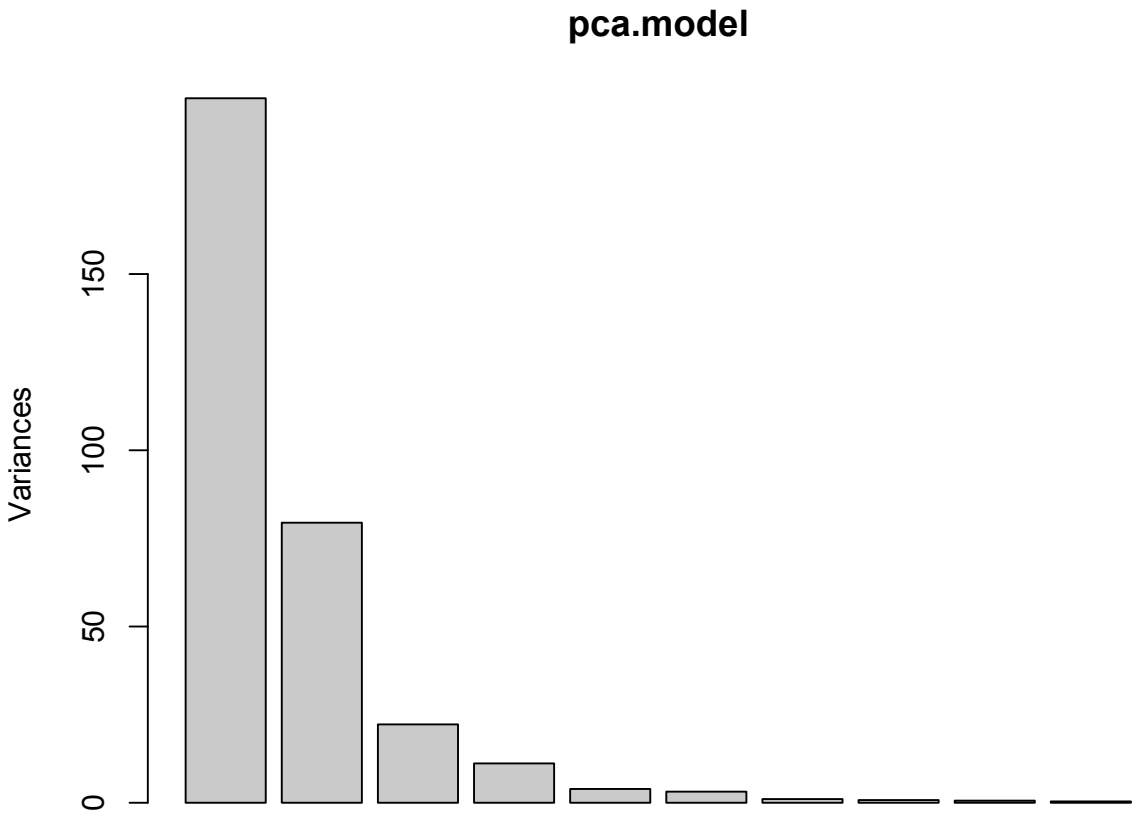


Figure 158: PCA scree plot for the first set of 10 normalized (peak height) container glass spectra (10 replicates), autoscaled.

D. PCA Results for the First Derivative Spectra (5-Point Smoothing)

Table 170: PCA results for the first set of 30 glass first derivative (5-point smoothing) spectra (10 replicates), no data pretreatment.

Importance of components:

	PC1	PC2	PC3	PC4	PC5	PC6	PC7	PC8	PC9	PC10	PC11
Standard deviation	0.1950	0.02141	0.01478	0.008242	0.00677	0.004828	0.003232	0.003048	0.002168	0.001779	0.001613
Proportion of Variance	0.9780	0.01179	0.00562	0.001750	0.00118	0.000600	0.000270	0.000240	0.000120	0.000080	0.000070
Cumulative Proportion	0.9780	0.98984	0.99546	0.997210	0.99839	0.998980	0.999250	0.999490	0.999610	0.999700	0.999760

	PC12	PC13	PC14	PC15	PC16	PC17	PC18	PC19	PC20
Standard deviation	0.001410	0.001150	0.0008062	0.000686	0.0006326	0.0006059	0.0005424	0.0004975	0.0004596
Proportion of Variance	0.000050	0.000030	0.0000200	0.000010	0.0000100	0.0000100	0.0000100	0.0000100	0.0000100
Cumulative Proportion	0.999810	0.999850	0.9998600	0.999880	0.9998900	0.9999000	0.9999000	0.9999100	0.9999200

	PC21	PC22	PC23	PC24	PC25	PC26	PC27	PC28	PC29
Standard deviation	0.0004479	0.0004358	0.0004156	0.0004098	0.0003828	0.0003583	0.0003469	0.0003368	0.0003324
Proportion of Variance	0.0000100	0.0000000	0.0000000	0.0000000	0.0000000	0.0000000	0.0000000	0.0000000	0.0000000
Cumulative Proportion	0.9999200	0.9999300	0.9999300	0.9999300	0.9999400	0.9999400	0.9999400	0.9999500	0.9999500

	PC30	PC31	PC32	PC33	PC34	PC35	PC36	PC37	PC38
Standard deviation	0.0003236	0.0003137	0.0003038	0.000296	0.0002847	0.0002713	0.0002585	0.0002557	0.0002486
Proportion of Variance	0.0000000	0.0000000	0.0000000	0.000000	0.0000000	0.0000000	0.0000000	0.0000000	0.0000000
Cumulative Proportion	0.9999500	0.9999600	0.9999600	0.999960	0.9999600	0.9999600	0.9999700	0.9999700	0.9999700

	PC39	PC40	PC41	PC42	PC43	PC44	PC45	PC46	PC47
Standard deviation	0.0002480	0.0002375	0.0002308	0.0002263	0.000215	0.0002135	0.0002114	0.0002022	0.0001965
Proportion of Variance	0.0000000	0.0000000	0.0000000	0.0000000	0.000000	0.0000000	0.0000000	0.0000000	0.0000000
Cumulative Proportion	0.9999700	0.9999700	0.9999700	0.9999700	0.999980	0.9999800	0.9999800	0.9999800	0.9999800

	PC48	PC49	PC50	PC51	PC52	PC53	PC54	PC55	PC56
Standard deviation	0.0001959	0.0001897	0.0001858	0.0001809	0.0001730	0.000169	0.0001639	0.0001618	0.0001548
Proportion of Variance	0.0000000	0.0000000	0.0000000	0.0000000	0.0000000	0.000000	0.0000000	0.0000000	0.0000000
Cumulative Proportion	0.9999800	0.9999800	0.9999800	0.9999800	0.9999800	0.999990	0.9999900	0.9999900	0.9999900

	PC57	PC58	PC59	PC60	PC61	PC62	PC63	PC64	PC65
Standard deviation	0.0001536	0.0001509	0.0001499	0.0001461	0.0001415	0.0001378	0.0001350	0.0001315	0.0001267
Proportion of Variance	0.0000000	0.0000000	0.0000000	0.0000000	0.0000000	0.0000000	0.0000000	0.0000000	0.0000000
Cumulative Proportion	0.9999900	0.9999900	0.9999900	0.9999900	0.9999900	0.9999900	0.9999900	0.9999900	0.9999900

	PC66	PC67	PC68	PC69	PC70	PC71	PC72	PC73	PC74
Standard deviation	0.0001239	0.0001216	0.0001170	0.0001117	0.0001114	0.0001092	0.0001071	0.0001047	0.0001019
Proportion of Variance	0.0000000	0.0000000	0.0000000	0.0000000	0.0000000	0.0000000	0.0000000	0.0000000	0.0000000
Cumulative Proportion	0.9999900	0.9999900	0.9999900	0.9999900	0.9999900	0.9999900	0.9999900	0.9999900	0.9999900

	PC75	PC76	PC77	PC78	PC79	PC80	PC81	PC82	PC83	PC84
Standard deviation	9.848e-05	9.706e-05	9.452e-05	9.162e-05	8.807e-05	8.656e-05	8.232e-05	7.9e-05	7.84e-05	7.66e-05
Proportion of Variance	0.000e+00	0.000e+00	0.000e+00	0.000e+00	0.000e+00	0.000e+00	0.000e+00	0.0e+00	0.00e+00	0.00e+00
Cumulative Proportion	1.000e+00	1.000e+00	1.000e+00	1.000e+00	1.000e+00	1.000e+00	1.000e+00	1.0e+00	1.00e+00	1.00e+00

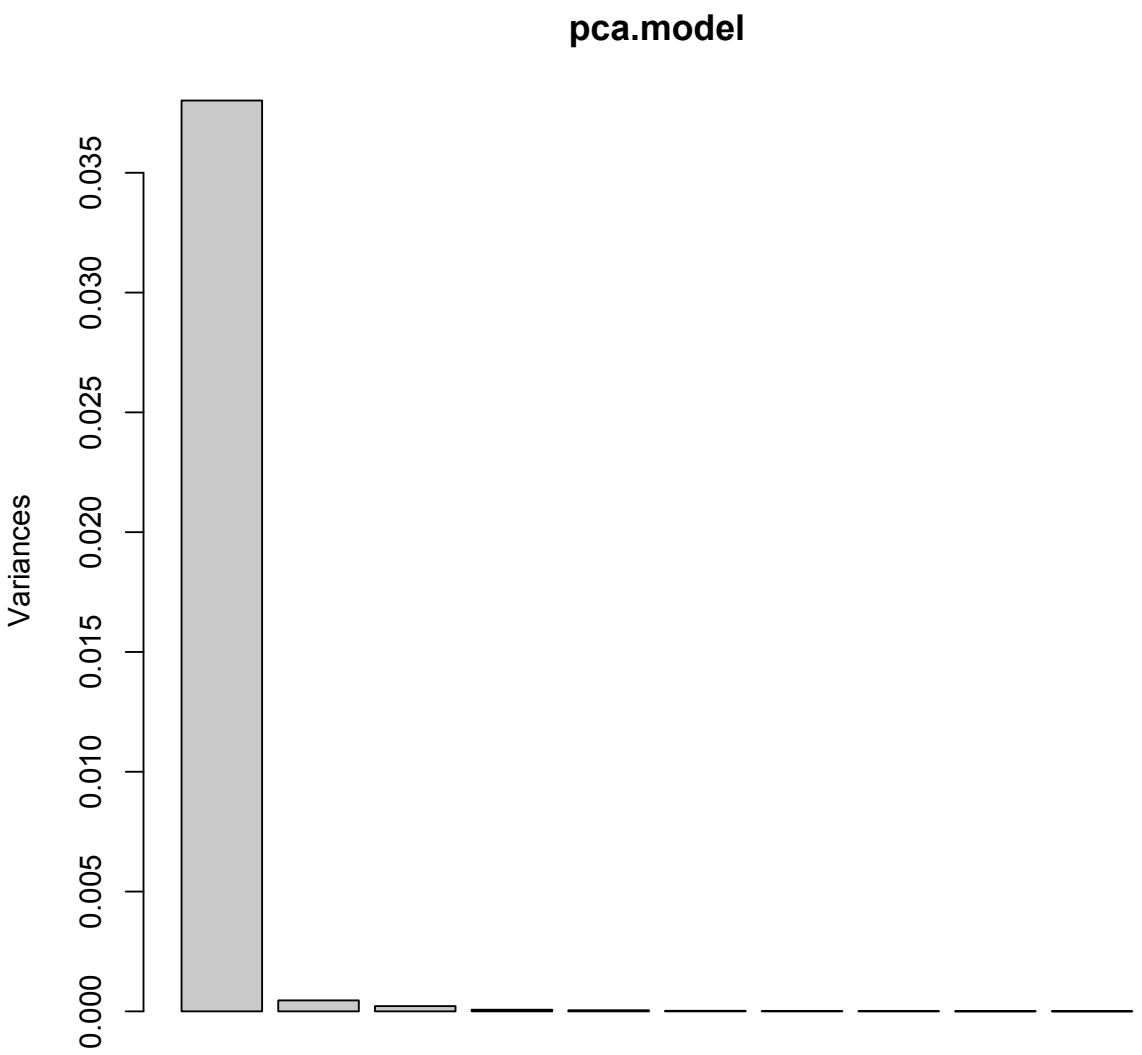


Figure 159: PCA scree plot for the first set of 30 glass first derivative (5-point smoothing) spectra (10 replicates), no data pretreatment.

Table 171: PCA results for the first set of 30 glass first derivative (5-point smoothing) spectra (10 replicates), centered.

Importance of components:

	PC1	PC2	PC3	PC4	PC5	PC6	PC7	PC8	PC9	PC10
Standard deviation	0.02827	0.01885	0.008617	0.007633	0.005063	0.004027	0.003227	0.002705	0.002119	0.001639
Proportion of Variance	0.58598	0.26048	0.054450	0.042730	0.018800	0.011890	0.007640	0.005370	0.003290	0.001970
Cumulative Proportion	0.58598	0.84646	0.900910	0.943640	0.962440	0.974330	0.981970	0.987330	0.990630	0.992600

	PC11	PC12	PC13	PC14	PC15	PC16	PC17	PC18	PC19
Standard deviation	0.001505	0.001246	0.0008086	0.0007133	0.0006777	0.0006326	0.0005488	0.000539	0.0004948
Proportion of Variance	0.001660	0.001140	0.0004800	0.0003700	0.0003400	0.0002900	0.0002200	0.000210	0.0001800
Cumulative Proportion	0.994260	0.995400	0.9958800	0.9962500	0.9965900	0.9968800	0.9971000	0.997310	0.9974900

	PC20	PC21	PC22	PC23	PC24	PC25	PC26	PC27	PC28
Standard deviation	0.0004508	0.0004432	0.0004261	0.000415	0.0003843	0.0003827	0.0003555	0.0003414	0.0003341
Proportion of Variance	0.0001500	0.0001400	0.0001300	0.000130	0.0001100	0.0001100	0.0000900	0.0000900	0.0000800
Cumulative Proportion	0.9976400	0.9977900	0.9979200	0.998040	0.9981500	0.9982600	0.9983500	0.9984400	0.9985200

	PC29	PC30	PC31	PC32	PC33	PC34	PC35	PC36	PC37
Standard deviation	0.0003275	0.0003139	0.000309	0.0003026	0.0002873	0.0002847	0.0002689	0.0002558	0.0002547
Proportion of Variance	0.0000800	0.0000700	0.000070	0.0000700	0.0000600	0.0000600	0.0000500	0.0000500	0.0000500
Cumulative Proportion	0.9986000	0.9986700	0.998740	0.9988100	0.9988700	0.9989300	0.9989800	0.9990300	0.9990800

	PC38	PC39	PC40	PC41	PC42	PC43	PC44	PC45	PC46
Standard deviation	0.0002484	0.0002380	0.0002311	0.0002307	0.0002261	0.0002141	0.0002127	0.0002082	0.0002019
Proportion of Variance	0.0000500	0.0000400	0.0000400	0.0000400	0.0000400	0.0000300	0.0000300	0.0000300	0.0000300
Cumulative Proportion	0.9991200	0.9991600	0.9992000	0.9992400	0.9992800	0.9993100	0.9993500	0.9993800	0.9994100

	PC47	PC48	PC49	PC50	PC51	PC52	PC53	PC54	PC55
Standard deviation	0.000196	0.0001937	0.0001882	0.0001842	0.0001804	0.0001723	0.0001690	0.0001637	0.0001607
Proportion of Variance	0.000030	0.0000300	0.0000300	0.0000200	0.0000200	0.0000200	0.0000200	0.0000200	0.0000200
Cumulative Proportion	0.999440	0.9994600	0.9994900	0.9995100	0.9995400	0.9995600	0.9995800	0.9996000	0.9996200

	PC56	PC57	PC58	PC59	PC60	PC61	PC62	PC63	PC64
Standard deviation	0.0001537	0.0001532	0.0001506	0.0001477	0.000145	0.0001405	0.0001375	0.0001333	0.0001305
Proportion of Variance	0.0000200	0.0000200	0.0000200	0.0000200	0.000020	0.0000100	0.0000100	0.0000100	0.0000100
Cumulative Proportion	0.9996400	0.9996500	0.9996700	0.9996900	0.999700	0.9997200	0.9997300	0.9997400	0.9997600

	PC65	PC66	PC67	PC68	PC69	PC70	PC71	PC72	PC73
Standard deviation	0.0001245	0.0001238	0.0001213	0.0001151	0.0001115	0.0001111	0.0001086	0.0001055	0.0001043
Proportion of Variance	0.0000100	0.0000100	0.0000100	0.0000100	0.0000100	0.0000100	0.0000100	0.0000100	0.0000100
Cumulative Proportion	0.9997700	0.9997800	0.9997900	0.9998000	0.9998100	0.9998200	0.9998300	0.9998300	0.9998400

	PC74	PC75	PC76	PC77	PC78	PC79	PC80	PC81	PC82
Standard deviation	0.0001019	9.707e-05	9.632e-05	9.446e-05	0.0000915	8.806e-05	0.0000863	0.0000822	7.894e-05
Proportion of Variance	0.0000100	1.000e-05	1.000e-05	1.000e-05	0.0000100	1.000e-05	0.0000100	0.0000000	0.000e+00
Cumulative Proportion	0.9998500	9.999e-01	9.999e-01	9.999e-01	0.9998800	9.999e-01	0.9998900	0.9998900	9.999e-01

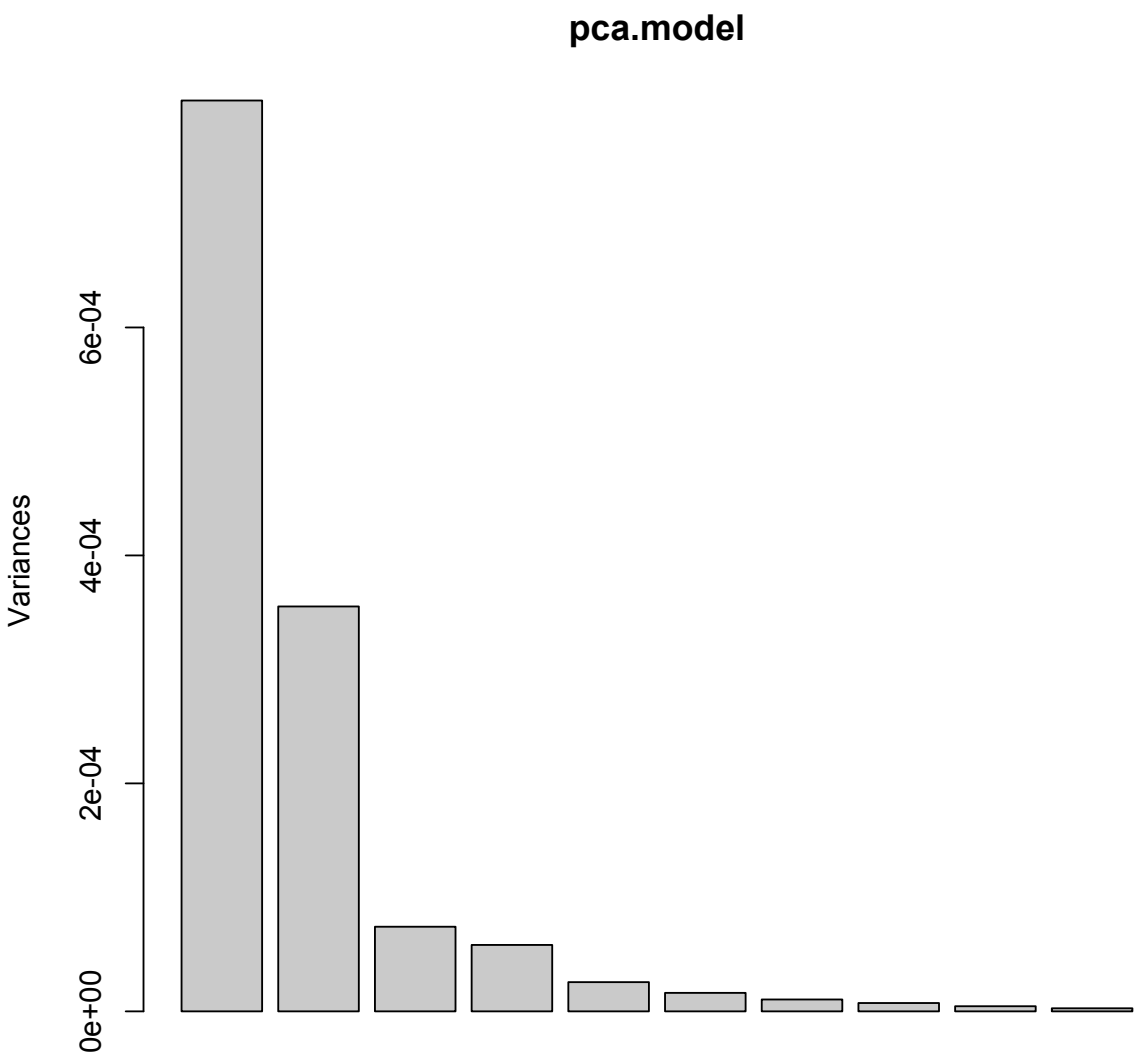


Figure 160. PCA scree plot for the first set of 30 glass first derivative (5-point smoothing) spectra (10 replicates), centered.

Table 172: PCA results for the first set of 30 glass first derivative (5-point smoothing) spectra (10 replicates), autoscaled.

Importance of components:

	PC1	PC2	PC3	PC4	PC5	PC6	PC7	PC8	PC9	PC10	PC11	PC12
Standard deviation	12.347	7.5640	5.8371	4.56036	3.65448	3.34845	3.02012	1.99838	1.8760	1.35926	1.28486	1.1924
Proportion of Variance	0.472	0.1771	0.1055	0.06439	0.04135	0.03471	0.02824	0.01236	0.0109	0.00572	0.00511	0.0044
Cumulative Proportion	0.472	0.6491	0.7546	0.81898	0.86032	0.89504	0.92328	0.93564	0.9465	0.95226	0.95737	0.9618

	PC13	PC14	PC15	PC16	PC17	PC18	PC19	PC20	PC21	PC22	PC23	PC24
Standard deviation	1.10188	0.98588	0.83176	0.78683	0.73775	0.71325	0.66079	0.61258	0.60552	0.59374	0.58511	0.5392
Proportion of Variance	0.00376	0.00301	0.00214	0.00192	0.00169	0.00157	0.00135	0.00116	0.00114	0.00109	0.00106	0.0009
Cumulative Proportion	0.96553	0.96854	0.97068	0.97260	0.97428	0.97586	0.97721	0.97837	0.97950	0.98060	0.98166	0.9826

	PC25	PC26	PC27	PC28	PC29	PC30	PC31	PC32	PC33	PC34	PC35	PC36
Standard deviation	0.51853	0.50127	0.47898	0.45917	0.4416	0.42974	0.41394	0.40715	0.4012	0.38880	0.38646	0.36847
Proportion of Variance	0.00083	0.00078	0.00071	0.00065	0.0006	0.00057	0.00053	0.00051	0.0005	0.00047	0.00046	0.00042
Cumulative Proportion	0.98339	0.98417	0.98488	0.98553	0.9861	0.98670	0.98723	0.98775	0.9882	0.98871	0.98918	0.98960

	PC37	PC38	PC39	PC40	PC41	PC42	PC43	PC44	PC45	PC46	PC47	PC48
Standard deviation	0.36188	0.35172	0.34287	0.33644	0.33503	0.31789	0.31690	0.3090	0.30357	0.29465	0.28504	0.27786
Proportion of Variance	0.00041	0.00038	0.00036	0.00035	0.00035	0.00031	0.00031	0.0003	0.00029	0.00027	0.00025	0.00024
Cumulative Proportion	0.99000	0.99039	0.99075	0.99110	0.99145	0.99176	0.99207	0.9924	0.99265	0.99292	0.99317	0.99341

	PC49	PC50	PC51	PC52	PC53	PC54	PC55	PC56	PC57	PC58	PC59	PC60
Standard deviation	0.27518	0.27232	0.26686	0.26019	0.2522	0.24886	0.24518	0.24006	0.23425	0.23230	0.22684	0.22604
Proportion of Variance	0.00023	0.00023	0.00022	0.00021	0.0002	0.00019	0.00019	0.00018	0.00017	0.00017	0.00016	0.00016
Cumulative Proportion	0.99365	0.99388	0.99410	0.99431	0.9945	0.99469	0.99488	0.99506	0.99523	0.99540	0.99556	0.99571

	PC61	PC62	PC63	PC64	PC65	PC66	PC67	PC68	PC69	PC70	PC71	PC72
Standard deviation	0.21876	0.21542	0.21087	0.20936	0.20829	0.20144	0.19812	0.19396	0.18981	0.18808	0.18569	0.1789
Proportion of Variance	0.00015	0.00014	0.00014	0.00014	0.00013	0.00013	0.00012	0.00012	0.00011	0.00011	0.00011	0.0001
Cumulative Proportion	0.99586	0.99601	0.99614	0.99628	0.99641	0.99654	0.99666	0.99678	0.99689	0.99700	0.99710	0.9972

	PC73	PC74	PC75	PC76	PC77	PC78	PC79	PC80	PC81	PC82	PC83	PC84
Standard deviation	0.1783	0.17510	0.17155	0.16669	0.16241	0.16147	0.15876	0.15578	0.15426	0.14749	0.14527	0.14333
Proportion of Variance	0.0001	0.00009	0.00009	0.00009	0.00008	0.00008	0.00008	0.00008	0.00007	0.00007	0.00007	0.00006
Cumulative Proportion	0.9973	0.99740	0.99749	0.99757	0.99766	0.99774	0.99781	0.99789	0.99796	0.99803	0.99810	0.99816

	PC85	PC86	PC87	PC88	PC89	PC90	PC91	PC92	PC93	PC94	PC95	PC96
Standard deviation	0.14189	0.13973	0.13741	0.13519	0.13261	0.13075	0.12848	0.12620	0.12470	0.12264	0.12149	0.11983
Proportion of Variance	0.00006	0.00006	0.00006	0.00006	0.00005	0.00005	0.00005	0.00005	0.00005	0.00005	0.00005	0.00004
Cumulative Proportion	0.99822	0.99828	0.99834	0.99840	0.99845	0.99850	0.99856	0.99860	0.99865	0.99870	0.99875	0.99879

	PC97	PC98	PC99	PC100	PC101	PC102	PC103	PC104	PC105	PC106	PC107	PC108
Standard deviation	0.11702	0.11397	0.11280	0.11071	0.10952	0.10808	0.10621	0.10459	0.10259	0.10171	0.10069	0.09874
Proportion of Variance	0.00004	0.00004	0.00004	0.00004	0.00004	0.00004	0.00003	0.00003	0.00003	0.00003	0.00003	0.00003
Cumulative Proportion	0.99883	0.99887	0.99891	0.99895	0.99899	0.99902	0.99906	0.99909	0.99912	0.99916	0.99919	0.99922

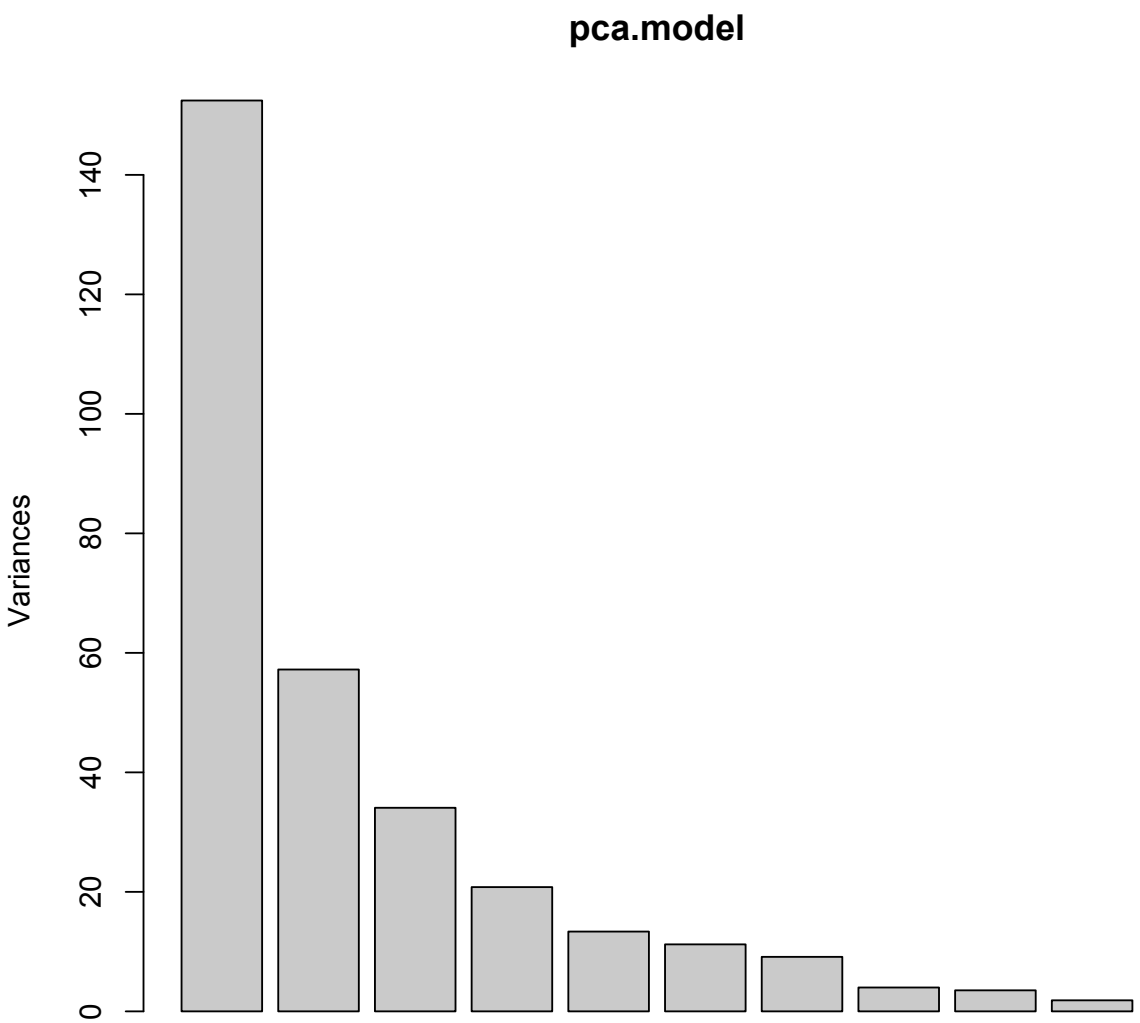


Figure 161: PCA scree plot for the first set of 30 glass first derivative (5-point smoothing) spectra (10 replicates), autoscaled.

Table 173: PCA results for the first set of 20 window glass first derivative (5-point smoothing) spectra (10 replicates), no data pretreatment.

Importance of components:

	PC1	PC2	PC3	PC4	PC5	PC6	PC7	PC8	PC9	PC10
Standard deviation	0.1948	0.02001	0.01373	0.008118	0.006944	0.003465	0.00312	0.002387	0.001845	0.001499
Proportion of Variance	0.9807	0.01034	0.00488	0.001700	0.001250	0.000310	0.00025	0.000150	0.000090	0.000060
Cumulative Proportion	0.9807	0.99108	0.99596	0.997660	0.998900	0.999210	0.99947	0.999610	0.999700	0.999760

	PC11	PC12	PC13	PC14	PC15	PC16	PC17	PC18	PC19
Standard deviation	0.001350	0.001143	0.0008622	0.0007972	0.0007051	0.0006147	0.0005403	0.0004824	0.0004658
Proportion of Variance	0.000050	0.000030	0.0000200	0.0000200	0.0000100	0.0000100	0.0000100	0.0000100	0.0000100
Cumulative Proportion	0.999810	0.999840	0.9998600	0.9998800	0.9998900	0.9999000	0.9999100	0.9999100	0.9999200

	PC20	PC21	PC22	PC23	PC24	PC25	PC26	PC27	PC28
Standard deviation	0.0004481	0.000431	0.0004207	0.0004033	0.0003910	0.0003815	0.0003518	0.000339	0.0003348
Proportion of Variance	0.0000100	0.000000	0.0000000	0.0000000	0.0000000	0.0000000	0.0000000	0.000000	0.0000000
Cumulative Proportion	0.9999200	0.999930	0.9999300	0.9999400	0.9999400	0.9999400	0.9999500	0.999950	0.9999500

	PC29	PC30	PC31	PC32	PC33	PC34	PC35	PC36	PC37
Standard deviation	0.0003205	0.0003047	0.0002974	0.000288	0.0002758	0.0002667	0.0002612	0.0002571	0.0002501
Proportion of Variance	0.0000000	0.0000000	0.0000000	0.000000	0.0000000	0.0000000	0.0000000	0.0000000	0.0000000
Cumulative Proportion	0.9999600	0.9999600	0.9999600	0.999960	0.9999700	0.9999700	0.9999700	0.9999700	0.9999700

	PC38	PC39	PC40	PC41	PC42	PC43	PC44	PC45	PC46
Standard deviation	0.0002406	0.0002261	0.0002248	0.0002154	0.0002118	0.0002072	0.0002007	0.0001938	0.0001857
Proportion of Variance	0.0000000	0.0000000	0.0000000	0.0000000	0.0000000	0.0000000	0.0000000	0.0000000	0.0000000
Cumulative Proportion	0.9999700	0.9999700	0.9999800	0.9999800	0.9999800	0.9999800	0.9999800	0.9999800	0.9999800

	PC47	PC48	PC49	PC50	PC51	PC52	PC53	PC54	PC55
Standard deviation	0.0001814	0.0001807	0.0001760	0.0001726	0.0001620	0.0001576	0.0001559	0.0001495	0.0001477
Proportion of Variance	0.0000000	0.0000000	0.0000000	0.0000000	0.0000000	0.0000000	0.0000000	0.0000000	0.0000000
Cumulative Proportion	0.9999800	0.9999800	0.9999900	0.9999900	0.9999900	0.9999900	0.9999900	0.9999900	0.9999900

	PC56	PC57	PC58	PC59	PC60	PC61	PC62	PC63	PC64
Standard deviation	0.0001464	0.0001453	0.0001397	0.0001330	0.0001318	0.0001293	0.0001288	0.0001243	0.0001221
Proportion of Variance	0.0000000	0.0000000	0.0000000	0.0000000	0.0000000	0.0000000	0.0000000	0.0000000	0.0000000
Cumulative Proportion	0.9999900	0.9999900	0.9999900	0.9999900	0.9999900	0.9999900	0.9999900	0.9999900	0.9999900

	PC65	PC66	PC67	PC68	PC69	PC70	PC71	PC72	PC73
Standard deviation	0.0001201	0.0001161	0.0001086	0.0001068	0.0001044	0.0001023	9.791e-05	9.677e-05	9.275e-05
Proportion of Variance	0.0000000	0.0000000	0.0000000	0.0000000	0.0000000	0.0000000	0.000e+00	0.000e+00	0.000e+00
Cumulative Proportion	0.9999900	0.9999900	0.9999900	0.9999900	0.9999900	1.0000000	1.000e+00	1.000e+00	1.000e+00

	PC74	PC75	PC76	PC77	PC78	PC79	PC80	PC81	PC82
Standard deviation	9.185e-05	9.024e-05	8.929e-05	8.367e-05	8.298e-05	8.096e-05	7.825e-05	7.715e-05	7.178e-05
Proportion of Variance	0.000e+00	0.000e+00	0.000e+00	0.000e+00	0.000e+00	0.000e+00	0.000e+00	0.000e+00	0.000e+00
Cumulative Proportion	1.000e+00	1.000e+00	1.000e+00	1.000e+00	1.000e+00	1.000e+00	1.000e+00	1.000e+00	1.000e+00

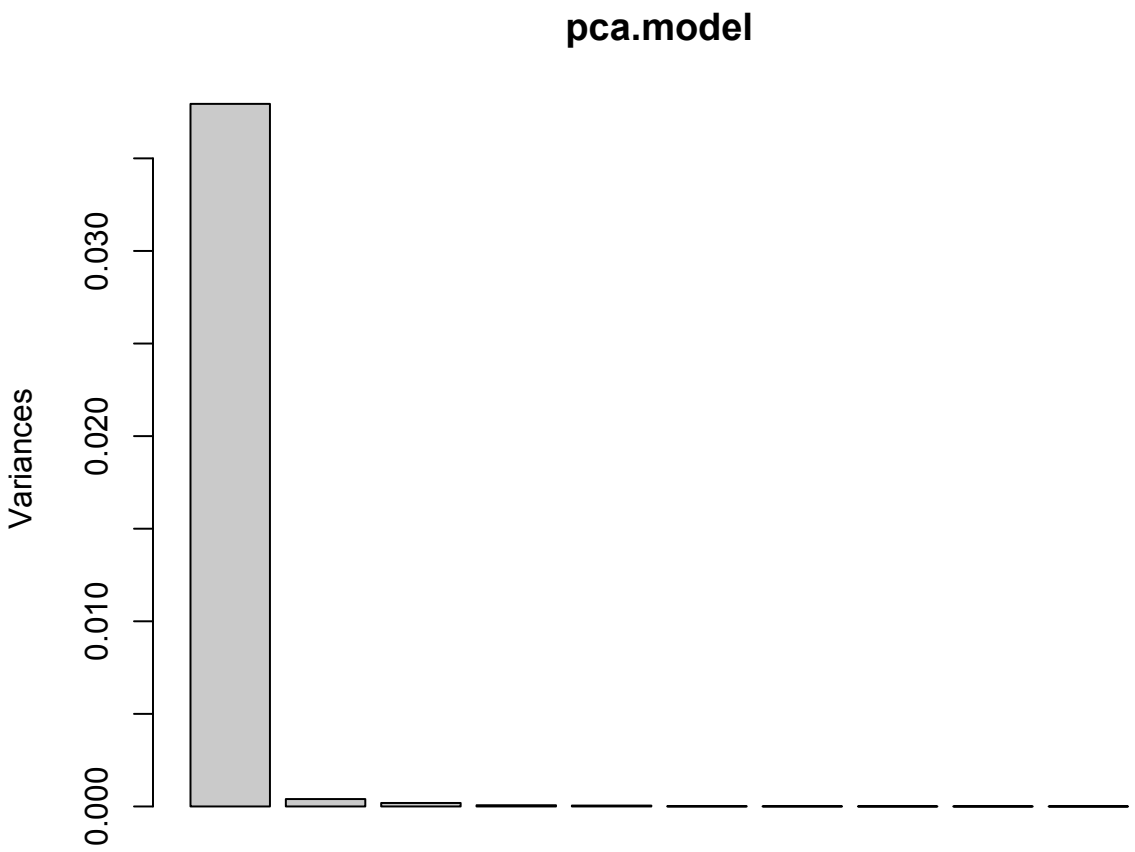


Figure 162: PCA scree plot for the first set of 20 window glass first derivative (5-point smoothing) spectra (10 replicates), no data pretreatment.

Table 174: PCA results for the first set of 20 window glass first derivative (5-point smoothing) spectra (10 replicates), centered.

Importance of components:

	PC1	PC2	PC3	PC4	PC5	PC6	PC7	PC8	PC9	PC10
Standard deviation	0.02637	0.01780	0.00825	0.007822	0.004002	0.003454	0.003101	0.002139	0.001576	0.00135
Proportion of Variance	0.58134	0.26494	0.05690	0.051140	0.013390	0.009970	0.008040	0.003820	0.002080	0.00152
Cumulative Proportion	0.58134	0.84628	0.90317	0.954320	0.967710	0.977680	0.985720	0.989540	0.991620	0.99314

	PC11	PC12	PC13	PC14	PC15	PC16	PC17	PC18	PC19
Standard deviation	0.001296	0.0008963	0.0008003	0.0007056	0.0006369	0.0006138	0.0005403	0.0004767	0.0004647
Proportion of Variance	0.001400	0.0006700	0.0005400	0.0004200	0.0003400	0.0003100	0.0002400	0.0001900	0.0001800
Cumulative Proportion	0.994540	0.9952200	0.9957500	0.9961700	0.9965100	0.9968200	0.9970700	0.9972600	0.9974400

	PC20	PC21	PC22	PC23	PC24	PC25	PC26	PC27	PC28
Standard deviation	0.0004371	0.0004277	0.0004109	0.0003995	0.0003857	0.0003659	0.0003438	0.0003376	0.0003207
Proportion of Variance	0.0001600	0.0001500	0.0001400	0.0001300	0.0001200	0.0001100	0.0001000	0.0001000	0.0000900
Cumulative Proportion	0.9976000	0.9977500	0.9978900	0.9980200	0.9981500	0.9982600	0.9983600	0.9984500	0.9985400

	PC29	PC30	PC31	PC32	PC33	PC34	PC35	PC36	PC37
Standard deviation	0.0003132	0.0003041	0.0002958	0.0002840	0.0002668	0.0002649	0.0002582	0.0002504	0.0002498
Proportion of Variance	0.0000800	0.0000800	0.0000700	0.0000700	0.0000600	0.0000600	0.0000600	0.0000500	0.0000500
Cumulative Proportion	0.9986200	0.9987000	0.9987700	0.9988400	0.9989000	0.9989600	0.9990100	0.9990700	0.9991200

	PC38	PC39	PC40	PC41	PC42	PC43	PC44	PC45	PC46
Standard deviation	0.0002311	0.0002255	0.0002236	0.0002154	0.0002079	0.0002028	0.0001962	0.0001938	0.0001852
Proportion of Variance	0.0000400	0.0000400	0.0000400	0.0000400	0.0000400	0.0000300	0.0000300	0.0000300	0.0000300
Cumulative Proportion	0.9991600	0.9992100	0.9992500	0.9992900	0.9993200	0.9993600	0.9993900	0.9994200	0.9994500

	PC47	PC48	PC49	PC50	PC51	PC52	PC53	PC54	PC55
Standard deviation	0.0001813	0.0001768	0.0001738	0.000163	0.0001609	0.0001562	0.0001530	0.0001486	0.0001477
Proportion of Variance	0.0000300	0.0000300	0.0000300	0.000020	0.0000200	0.0000200	0.0000200	0.0000200	0.0000200
Cumulative Proportion	0.9994800	0.9995000	0.9995300	0.999550	0.9995700	0.9995900	0.9996100	0.9996300	0.9996500

	PC56	PC57	PC58	PC59	PC60	PC61	PC62	PC63	PC64
Standard deviation	0.0001464	0.0001449	0.0001389	0.0001330	0.0001312	0.0001291	0.0001282	0.0001242	0.0001219
Proportion of Variance	0.0000200	0.0000200	0.0000200	0.0000100	0.0000100	0.0000100	0.0000100	0.0000100	0.0000100
Cumulative Proportion	0.9996700	0.9996800	0.9997000	0.9997100	0.9997300	0.9997400	0.9997600	0.9997700	0.9997800

	PC65	PC66	PC67	PC68	PC69	PC70	PC71	PC72	PC73
Standard deviation	0.0001162	0.0001089	0.0001081	0.0001061	0.0001039	0.0001023	0.0000973	0.0000953	9.272e-05
Proportion of Variance	0.0000100	0.0000100	0.0000100	0.0000100	0.0000100	0.0000100	0.0000100	0.0000100	1.000e-05
Cumulative Proportion	0.9997900	0.9998000	0.9998100	0.9998200	0.9998300	0.9998400	0.9998500	0.9998600	9.999e-01

	PC74	PC75	PC76	PC77	PC78	PC79	PC80	PC81	PC82
Standard deviation	9.182e-05	9.013e-05	8.845e-05	8.354e-05	8.298e-05	8.096e-05	7.794e-05	7.673e-05	7.177e-05
Proportion of Variance	1.000e-05	1.000e-05	1.000e-05	1.000e-05	1.000e-05	1.000e-05	1.000e-05	0.000e+00	0.000e+00
Cumulative Proportion	9.999e-01	9.999e-01	9.999e-01	9.999e-01	9.999e-01	9.999e-01	9.999e-01	9.999e-01	9.999e-01

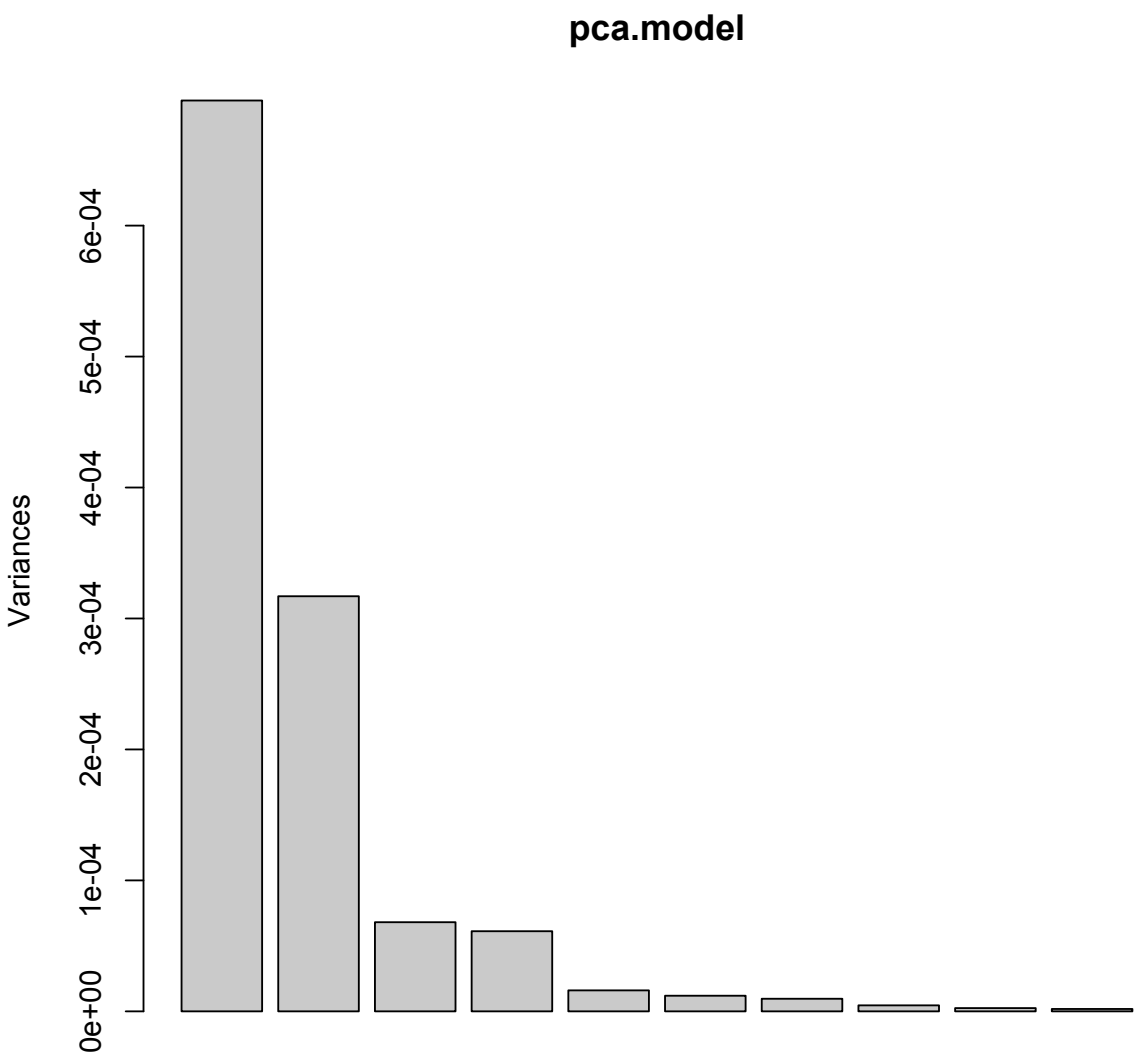


Figure 163: PCA scree plot for the first set of 20 window glass first derivative (5-point smoothing) spectra (10 replicates), centered.

Table 175: PCA results for the first set of 20 window glass first derivative (5-point smoothing) spectra (10 replicates), autoscaled.

Importance of components:

	PC1	PC2	PC3	PC4	PC5	PC6	PC7	PC8	PC9	PC10	PC11	PC12
Standard deviation	12.9109	6.7714	5.7617	4.60169	3.58452	2.85593	2.21930	2.01052	1.85294	1.5971	1.4926	1.32485
Proportion of Variance	0.5161	0.1420	0.1028	0.06556	0.03978	0.02525	0.01525	0.01251	0.01063	0.0079	0.0069	0.00543
Cumulative Proportion	0.5161	0.6580	0.7608	0.82636	0.86614	0.89139	0.90664	0.91916	0.92979	0.9377	0.9446	0.95002

	PC13	PC14	PC15	PC16	PC17	PC18	PC19	PC20	PC21	PC22	PC23
Standard deviation	1.25335	1.06565	1.01065	0.93118	0.8799	0.86618	0.83085	0.74520	0.7182	0.70224	0.62523
Proportion of Variance	0.00486	0.00352	0.00316	0.00268	0.0024	0.00232	0.00214	0.00172	0.0016	0.00153	0.00121
Cumulative Proportion	0.95488	0.95839	0.96156	0.96424	0.9666	0.96896	0.97110	0.97282	0.9744	0.97594	0.97715

	PC24	PC25	PC26	PC27	PC28	PC29	PC30	PC31	PC32	PC33	PC34
Standard deviation	0.61862	0.60947	0.57204	0.54285	0.52493	0.5079	0.49509	0.47851	0.47275	0.45827	0.44771
Proportion of Variance	0.00118	0.00115	0.00101	0.00091	0.00085	0.0008	0.00076	0.00071	0.00069	0.00065	0.00062
Cumulative Proportion	0.97834	0.97949	0.98050	0.98141	0.98227	0.9831	0.98382	0.98453	0.98522	0.98587	0.98649

	PC35	PC36	PC37	PC38	PC39	PC40	PC41	PC42	PC43	PC44	PC45
Standard deviation	0.4394	0.43070	0.41853	0.40410	0.39043	0.38475	0.37018	0.36607	0.34958	0.34389	0.33912
Proportion of Variance	0.0006	0.00057	0.00054	0.00051	0.00047	0.00046	0.00042	0.00041	0.00038	0.00037	0.00036
Cumulative Proportion	0.9871	0.98767	0.98821	0.98871	0.98919	0.98964	0.99007	0.99048	0.99086	0.99123	0.99158

	PC46	PC47	PC48	PC49	PC50	PC51	PC52	PC53	PC54	PC55	PC56
Standard deviation	0.33550	0.32393	0.31597	0.31559	0.3114	0.30013	0.29251	0.28479	0.27582	0.27328	0.26373
Proportion of Variance	0.00035	0.00032	0.00031	0.00031	0.0003	0.00028	0.00026	0.00025	0.00024	0.00023	0.00022
Cumulative Proportion	0.99193	0.99226	0.99257	0.99288	0.9932	0.99345	0.99372	0.99397	0.99421	0.99444	0.99465

	PC57	PC58	PC59	PC60	PC61	PC62	PC63	PC64	PC65	PC66	PC67
Standard deviation	0.25870	0.2524	0.24739	0.24264	0.23998	0.23332	0.23063	0.22265	0.22123	0.22008	0.21622
Proportion of Variance	0.00021	0.0002	0.00019	0.00018	0.00018	0.00017	0.00016	0.00015	0.00015	0.00015	0.00014
Cumulative Proportion	0.99486	0.9951	0.99525	0.99543	0.99561	0.99578	0.99594	0.99609	0.99624	0.99639	0.99654

	PC68	PC69	PC70	PC71	PC72	PC73	PC74	PC75	PC76	PC77	PC78
Standard deviation	0.21262	0.20421	0.20059	0.19698	0.19349	0.19305	0.18845	0.18653	0.1825	0.1803	0.17357
Proportion of Variance	0.00014	0.00013	0.00012	0.00012	0.00012	0.00012	0.00011	0.00011	0.0001	0.0001	0.00009
Cumulative Proportion	0.99668	0.99681	0.99693	0.99705	0.99717	0.99728	0.99739	0.99750	0.9976	0.9977	0.99780

	PC79	PC80	PC81	PC82	PC83	PC84	PC85	PC86	PC87	PC88	PC89
Standard deviation	0.16836	0.16539	0.16283	0.15910	0.15515	0.15271	0.14868	0.14646	0.14272	0.14066	0.13704
Proportion of Variance	0.00009	0.00008	0.00008	0.00008	0.00007	0.00007	0.00007	0.00007	0.00006	0.00006	0.00006
Cumulative Proportion	0.99789	0.99797	0.99805	0.99813	0.99821	0.99828	0.99835	0.99841	0.99848	0.99854	0.99860

	PC90	PC91	PC92	PC93	PC94	PC95	PC96	PC97	PC98	PC99	PC100
Standard deviation	0.13437	0.13181	0.13075	0.13012	0.12564	0.12424	0.12135	0.11787	0.11622	0.11170	0.11111
Proportion of Variance	0.00006	0.00005	0.00005	0.00005	0.00005	0.00005	0.00005	0.00004	0.00004	0.00004	0.00004
Cumulative Proportion	0.99865	0.99871	0.99876	0.99881	0.99886	0.99891	0.99895	0.99900	0.99904	0.99908	0.99912

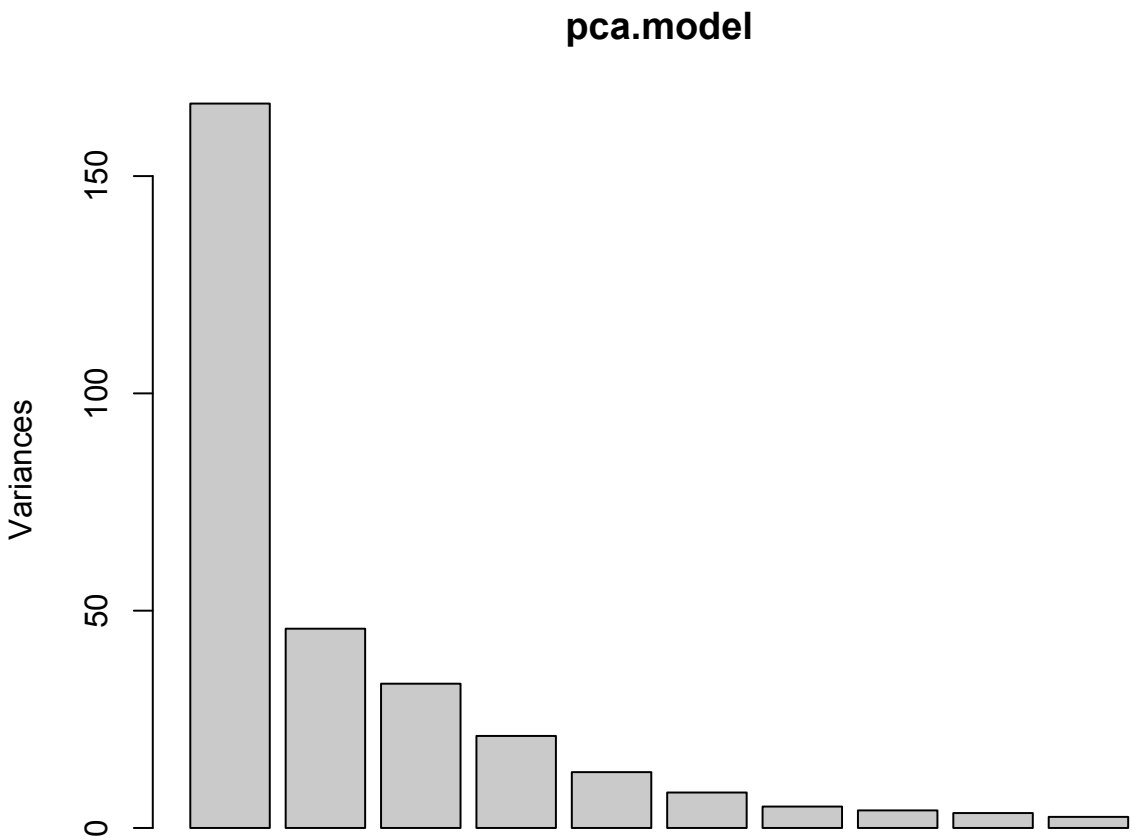


Figure 164: PCA scree plot for the first set of 20 window glass first derivative (5-point smoothing) spectra (10 replicates), autoscaled.

Table 176: PCA results for the first set of 10 container glass first derivative (5-point smoothing) spectra (10 replicates), no data pretreatment.

Importance of components:

	PC1	PC2	PC3	PC4	PC5	PC6	PC7	PC8	PC9	PC10
Standard deviation	0.1965	0.02410	0.01659	0.008261	0.006383	0.005321	0.003248	0.002769	0.001942	0.001751
Proportion of Variance	0.9740	0.01466	0.00695	0.001720	0.001030	0.000710	0.000270	0.000190	0.000100	0.000080
Cumulative Proportion	0.9740	0.98871	0.99566	0.997380	0.998410	0.999120	0.999390	0.999580	0.999680	0.999750

	PC11	PC12	PC13	PC14	PC15	PC16	PC17	PC18	PC19
Standard deviation	0.001497	0.001260	0.001039	0.0007655	0.0006386	0.000576	0.0005403	0.0005014	0.0004816
Proportion of Variance	0.000060	0.000040	0.000030	0.0000100	0.0000100	0.000010	0.0000100	0.0000100	0.0000100
Cumulative Proportion	0.999810	0.999850	0.999880	0.9998900	0.9999000	0.999910	0.9999200	0.9999200	0.9999300

	PC20	PC21	PC22	PC23	PC24	PC25	PC26	PC27	PC28
Standard deviation	0.0004668	0.0004533	0.0004173	0.0004056	0.0003668	0.0003593	0.0003508	0.0003349	0.0003220
Proportion of Variance	0.0000100	0.0000100	0.0000000	0.0000000	0.0000000	0.0000000	0.0000000	0.0000000	0.0000000
Cumulative Proportion	0.9999400	0.9999400	0.9999500	0.9999500	0.9999500	0.9999600	0.9999600	0.9999600	0.9999600

	PC29	PC30	PC31	PC32	PC33	PC34	PC35	PC36	PC37
Standard deviation	0.0003118	0.0002990	0.0002954	0.000279	0.0002665	0.0002587	0.0002501	0.0002342	0.0002285
Proportion of Variance	0.0000000	0.0000000	0.0000000	0.000000	0.0000000	0.0000000	0.0000000	0.0000000	0.0000000
Cumulative Proportion	0.9999700	0.9999700	0.9999700	0.999970	0.9999800	0.9999800	0.9999800	0.9999800	0.9999800

	PC38	PC39	PC40	PC41	PC42	PC43	PC44	PC45	PC46
Standard deviation	0.0002216	0.0002168	0.0002106	0.0002075	0.0001961	0.0001861	0.0001800	0.0001685	0.0001652
Proportion of Variance	0.0000000	0.0000000	0.0000000	0.0000000	0.0000000	0.0000000	0.0000000	0.0000000	0.0000000
Cumulative Proportion	0.9999800	0.9999800	0.9999800	0.9999900	0.9999900	0.9999900	0.9999900	0.9999900	0.9999900

	PC47	PC48	PC49	PC50	PC51	PC52	PC53	PC54	PC55
Standard deviation	0.0001619	0.0001591	0.0001553	0.0001491	0.0001369	0.0001337	0.0001308	0.0001299	0.0001235
Proportion of Variance	0.0000000	0.0000000	0.0000000	0.0000000	0.0000000	0.0000000	0.0000000	0.0000000	0.0000000
Cumulative Proportion	0.9999900	0.9999900	0.9999900	0.9999900	0.9999900	0.9999900	0.9999900	0.9999900	0.9999900

	PC56	PC57	PC58	PC59	PC60	PC61	PC62	PC63	PC64
Standard deviation	0.0001187	0.0001128	0.0001118	0.0001109	0.0001059	0.0001038	0.0001019	9.436e-05	9.142e-05
Proportion of Variance	0.0000000	0.0000000	0.0000000	0.0000000	0.0000000	0.0000000	0.0000000	0.000e+00	0.000e+00
Cumulative Proportion	1.0000000	1.0000000	1.0000000	1.0000000	1.0000000	1.0000000	1.0000000	1.000e+00	1.000e+00

	PC65	PC66	PC67	PC68	PC69	PC70	PC71	PC72	PC73
Standard deviation	8.737e-05	8.6e-05	8.303e-05	8.124e-05	7.714e-05	7.304e-05	7.268e-05	6.98e-05	6.931e-05
Proportion of Variance	0.000e+00	0.0e+00	0.000e+00	0.000e+00	0.000e+00	0.000e+00	0.000e+00	0.00e+00	0.000e+00
Cumulative Proportion	1.000e+00	1.0e+00	1.000e+00	1.000e+00	1.000e+00	1.000e+00	1.000e+00	1.00e+00	1.000e+00

	PC74	PC75	PC76	PC77	PC78	PC79	PC80	PC81	PC82
Standard deviation	6.642e-05	6.493e-05	6.164e-05	5.898e-05	5.758e-05	5.564e-05	5.319e-05	5.128e-05	4.892e-05
Proportion of Variance	0.000e+00	0.000e+00	0.000e+00	0.000e+00	0.000e+00	0.000e+00	0.000e+00	0.000e+00	0.000e+00
Cumulative Proportion	1.000e+00	1.000e+00	1.000e+00	1.000e+00	1.000e+00	1.000e+00	1.000e+00	1.000e+00	1.000e+00

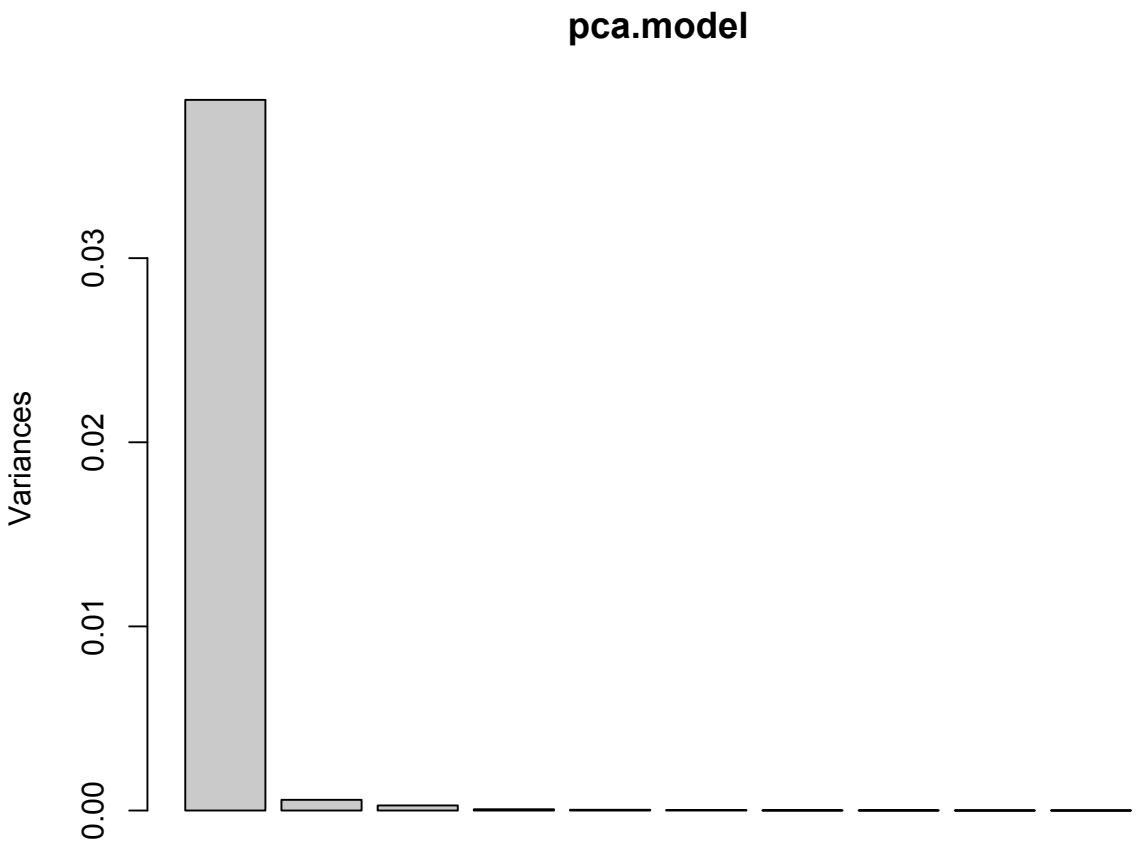


Figure 165: PCA scree plot for the first set of 10 container glass first derivative (5-point smoothing) spectra (10 replicates), no data pretreatment.

Table 177: PCA results for the first set of 10 container glass first derivative (5-point smoothing) spectra (10 replicates), centered.

Importance of components:

	PC1	PC2	PC3	PC4	PC5	PC6	PC7	PC8	PC9	PC10
Standard deviation	0.03196	0.02070	0.008934	0.00715	0.005957	0.004284	0.002779	0.002420	0.001817	0.001652
Proportion of Variance	0.61438	0.25773	0.048020	0.03075	0.021350	0.011040	0.004650	0.003520	0.001990	0.001640
Cumulative Proportion	0.61438	0.87211	0.920120	0.95088	0.972220	0.983260	0.987910	0.991430	0.993420	0.995060

	PC11	PC12	PC13	PC14	PC15	PC16	PC17	PC18	PC19
Standard deviation	0.001344	0.001081	0.0007842	0.0007378	0.0005837	0.0005649	0.00054	0.0004984	0.000478
Proportion of Variance	0.001090	0.000700	0.0003700	0.0003300	0.0002100	0.0001900	0.00018	0.0001500	0.000140
Cumulative Proportion	0.996150	0.996850	0.9972200	0.9975500	0.9977500	0.9979400	0.99812	0.9982700	0.998410

	PC20	PC21	PC22	PC23	PC24	PC25	PC26	PC27	PC28
Standard deviation	0.0004574	0.000425	0.0004136	0.0003837	0.0003658	0.0003554	0.0003508	0.0003346	0.0003218
Proportion of Variance	0.0001300	0.000110	0.0001000	0.0000900	0.0000800	0.0000800	0.0000700	0.0000700	0.0000600
Cumulative Proportion	0.9985300	0.998640	0.9987400	0.9988300	0.9989100	0.9989900	0.9990600	0.9991300	0.9991900

	PC29	PC30	PC31	PC32	PC33	PC34	PC35	PC36	PC37
Standard deviation	0.0003061	0.0002965	0.0002811	0.0002756	0.0002601	0.0002580	0.0002362	0.0002332	0.0002241
Proportion of Variance	0.0000600	0.0000500	0.0000500	0.0000500	0.0000400	0.0000400	0.0000300	0.0000300	0.0000300
Cumulative Proportion	0.9992500	0.9993000	0.9993500	0.9994000	0.9994400	0.9994800	0.9995100	0.9995400	0.9995700

	PC38	PC39	PC40	PC41	PC42	PC43	PC44	PC45	PC46
Standard deviation	0.0002178	0.0002132	0.0002093	0.0001971	0.0001869	0.0001830	0.0001786	0.0001679	0.0001620
Proportion of Variance	0.0000300	0.0000300	0.0000300	0.0000200	0.0000200	0.0000200	0.0000200	0.0000200	0.0000200
Cumulative Proportion	0.9996000	0.9996300	0.9996500	0.9996800	0.9997000	0.9997200	0.9997400	0.9997600	0.9997700

	PC47	PC48	PC49	PC50	PC51	PC52	PC53	PC54	PC55
Standard deviation	0.0001614	0.0001562	0.0001500	0.0001428	0.0001344	0.0001331	0.0001306	0.0001297	0.0001201
Proportion of Variance	0.0000200	0.0000100	0.0000100	0.0000100	0.0000100	0.0000100	0.0000100	0.0000100	0.0000100
Cumulative Proportion	0.9997900	0.9998000	0.9998200	0.9998300	0.9998400	0.9998500	0.9998600	0.9998700	0.9998800

	PC56	PC57	PC58	PC59	PC60	PC61	PC62	PC63	PC64
Standard deviation	0.0001186	0.0001120	0.0001117	0.000109	0.0001053	0.0001019	9.647e-05	9.436e-05	8.951e-05
Proportion of Variance	0.0000100	0.0000100	0.0000100	0.000010	0.0000100	0.0000100	1.000e-05	1.000e-05	0.000e+00
Cumulative Proportion	0.9998900	0.9998900	0.9999000	0.999910	0.9999200	0.9999200	9.999e-01	9.999e-01	9.999e-01

	PC65	PC66	PC67	PC68	PC69	PC70	PC71	PC72	PC73
Standard deviation	8.602e-05	8.482e-05	8.302e-05	8.057e-05	7.599e-05	7.274e-05	7.051e-05	6.951e-05	6.845e-05
Proportion of Variance	0.000e+00	0.000e+00	0.000e+00	0.000e+00	0.000e+00	0.000e+00	0.000e+00	0.000e+00	0.000e+00
Cumulative Proportion	9.999e-01	1.000e+00	1.000e+00	1.000e+00	1.000e+00	1.000e+00	1.000e+00	1.000e+00	1.000e+00

	PC74	PC75	PC76	PC77	PC78	PC79	PC80	PC81	PC82
Standard deviation	6.494e-05	6.462e-05	6.022e-05	5.82e-05	5.703e-05	5.32e-05	5.212e-05	5.071e-05	4.857e-05
Proportion of Variance	0.000e+00	0.000e+00	0.000e+00	0.00e+00	0.000e+00	0.00e+00	0.000e+00	0.000e+00	0.000e+00
Cumulative Proportion	1.000e+00	1.000e+00	1.000e+00	1.00e+00	1.000e+00	1.00e+00	1.000e+00	1.000e+00	1.000e+00

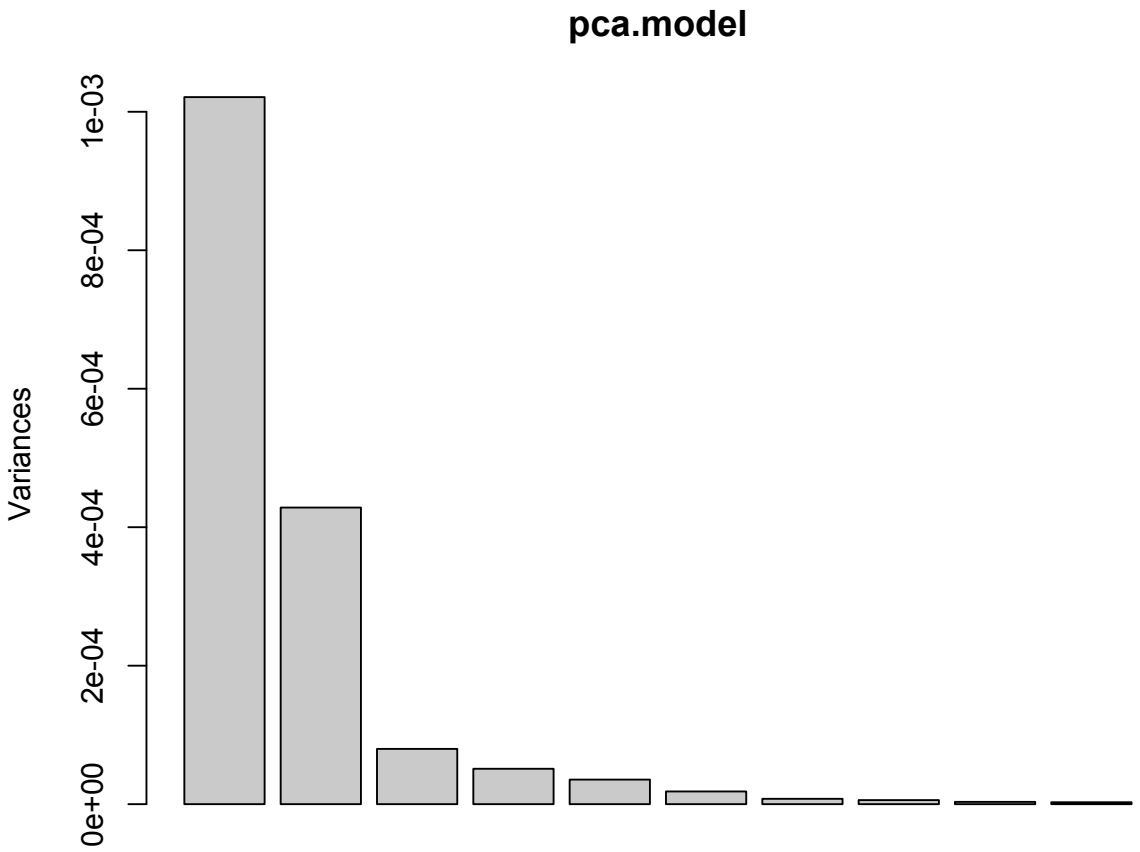


Figure 166: PCA scree plot for the first set of 10 container glass first derivative (5-point smoothing) spectra (10 replicates), centered.

Table 178: PCA results for the first set of 10 container glass first derivative (5-point smoothing) spectra (10 replicates), autoscaled.

Importance of components:

	PC1	PC2	PC3	PC4	PC5	PC6	PC7	PC8	PC9	PC10	PC11
Standard deviation	12.4073	8.9473	5.39995	4.33171	3.35664	2.64311	2.46009	1.79620	1.4715	1.20027	1.02665
Proportion of Variance	0.4766	0.2478	0.09028	0.05809	0.03488	0.02163	0.01874	0.00999	0.0067	0.00446	0.00326
Cumulative Proportion	0.4766	0.7244	0.81472	0.87281	0.90769	0.92932	0.94806	0.95805	0.9647	0.96921	0.97248

	PC12	PC13	PC14	PC15	PC16	PC17	PC18	PC19	PC20	PC21	PC22
Standard deviation	0.99381	0.86403	0.79673	0.72536	0.69132	0.62664	0.57390	0.55731	0.53607	0.53410	0.49520
Proportion of Variance	0.00306	0.00231	0.00197	0.00163	0.00148	0.00122	0.00102	0.00096	0.00089	0.00088	0.00076
Cumulative Proportion	0.97553	0.97784	0.97981	0.98144	0.98292	0.98413	0.98515	0.98611	0.98700	0.98789	0.98865

	PC23	PC24	PC25	PC26	PC27	PC28	PC29	PC30	PC31	PC32	PC33
Standard deviation	0.48233	0.46823	0.4406	0.40765	0.40431	0.39501	0.37746	0.37038	0.36364	0.3583	0.34396
Proportion of Variance	0.00072	0.00068	0.0006	0.00051	0.00051	0.00048	0.00044	0.00042	0.00041	0.0004	0.00037
Cumulative Proportion	0.98937	0.99005	0.9907	0.99116	0.99167	0.99215	0.99259	0.99302	0.99343	0.9938	0.99419

	PC34	PC35	PC36	PC37	PC38	PC39	PC40	PC41	PC42	PC43	PC44
Standard deviation	0.32932	0.32031	0.30221	0.29512	0.28653	0.27503	0.26892	0.26322	0.25785	0.2513	0.24172
Proportion of Variance	0.00034	0.00032	0.00028	0.00027	0.00025	0.00023	0.00022	0.00021	0.00021	0.0002	0.00018
Cumulative Proportion	0.99453	0.99484	0.99513	0.99540	0.99565	0.99588	0.99611	0.99632	0.99653	0.9967	0.99690

	PC45	PC46	PC47	PC48	PC49	PC50	PC51	PC52	PC53	PC54	PC55
Standard deviation	0.23603	0.23005	0.22757	0.21730	0.21304	0.20428	0.19735	0.19180	0.18908	0.18552	0.1806
Proportion of Variance	0.00017	0.00016	0.00016	0.00015	0.00014	0.00013	0.00012	0.00011	0.00011	0.00011	0.0001
Cumulative Proportion	0.99708	0.99724	0.99740	0.99755	0.99769	0.99782	0.99794	0.99805	0.99816	0.99827	0.9984

	PC56	PC57	PC58	PC59	PC60	PC61	PC62	PC63	PC64	PC65	PC66
Standard deviation	0.1755	0.17232	0.16620	0.16146	0.15890	0.15559	0.15186	0.14665	0.14373	0.13870	0.13113
Proportion of Variance	0.0001	0.00009	0.00009	0.00008	0.00008	0.00007	0.00007	0.00007	0.00006	0.00006	0.00005
Cumulative Proportion	0.9985	0.99856	0.99864	0.99872	0.99880	0.99888	0.99895	0.99901	0.99908	0.99914	0.99919

	PC67	PC68	PC69	PC70	PC71	PC72	PC73	PC74	PC75	PC76	PC77
Standard deviation	0.12983	0.12697	0.12308	0.12189	0.11773	0.11500	0.11209	0.11121	0.10741	0.10495	0.10124
Proportion of Variance	0.00005	0.00005	0.00005	0.00005	0.00004	0.00004	0.00004	0.00004	0.00004	0.00003	0.00003
Cumulative Proportion	0.99924	0.99929	0.99934	0.99939	0.99943	0.99947	0.99951	0.99955	0.99958	0.99962	0.99965

	PC78	PC79	PC80	PC81	PC82	PC83	PC84	PC85	PC86	PC87	PC88
Standard deviation	0.09892	0.09699	0.09180	0.08927	0.08757	0.08557	0.08390	0.07914	0.07438	0.07371	0.06996
Proportion of Variance	0.00003	0.00003	0.00003	0.00002	0.00002	0.00002	0.00002	0.00002	0.00002	0.00002	0.00002
Cumulative Proportion	0.99968	0.99971	0.99973	0.99976	0.99978	0.99981	0.99983	0.99985	0.99986	0.99988	0.99990

	PC89	PC90	PC91	PC92	PC93	PC94	PC95	PC96	PC97	PC98	PC99
Standard deviation	0.06799	0.06623	0.06124	0.06004	0.05810	0.05493	0.05178	0.04979	0.04918	0.04316	0.04027
Proportion of Variance	0.00001	0.00001	0.00001	0.00001	0.00001	0.00001	0.00001	0.00001	0.00001	0.00001	0.00001
Cumulative Proportion	0.99991	0.99992	0.99993	0.99995	0.99996	0.99997	0.99997	0.99998	0.99999	0.99999	1.00000

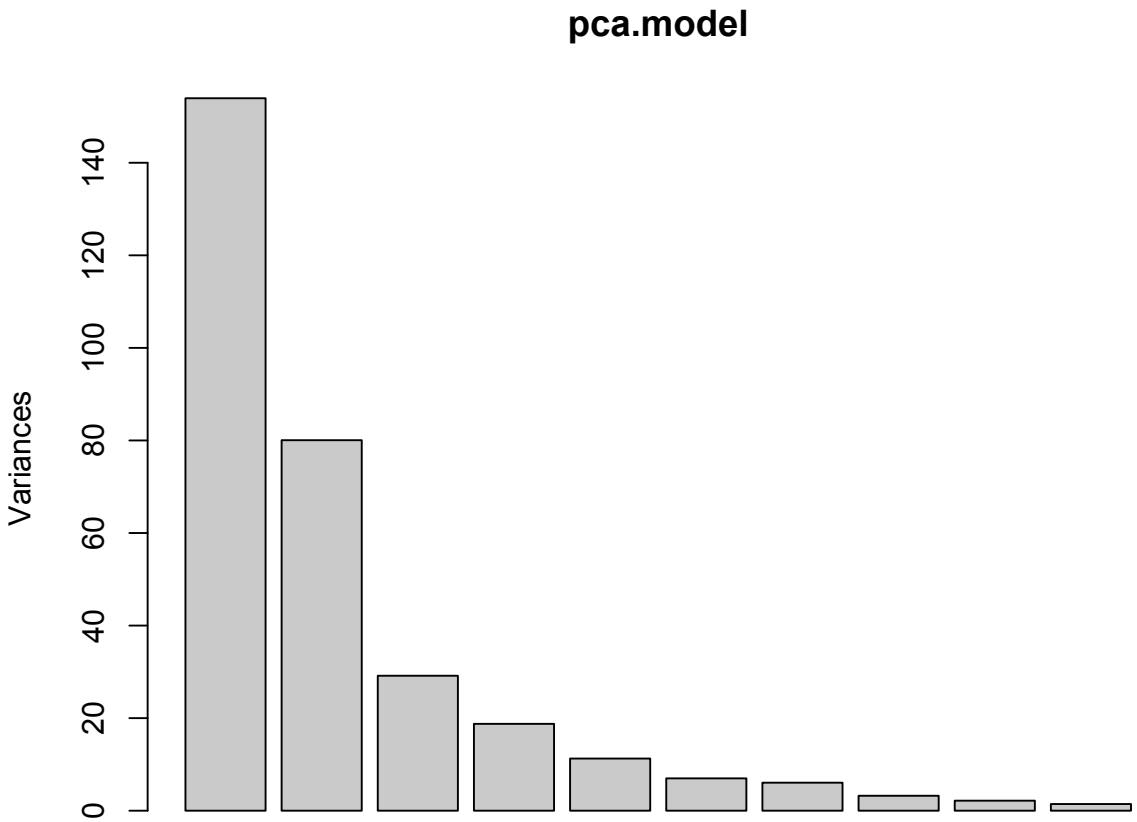


Figure 167: PCA scree plot for the first set of 10 container glass first derivative (5-point smoothing) spectra (10 replicates), autoscaled.

E. PCA Results for the First Derivative Spectra (9-Point Smoothing)

Table 179: PCA results for the first set of 30 glass first derivative (9-point smoothing) spectra (10 replicates), no data pretreatment.

Importance of components:

	PC1	PC2	PC3	PC4	PC5	PC6	PC7	PC8	PC9	PC10
Standard deviation	0.1914	0.02102	0.01413	0.007432	0.006256	0.004672	0.002769	0.002580	0.002063	0.00173
Proportion of Variance	0.9790	0.01181	0.00534	0.001480	0.001050	0.000580	0.000200	0.000180	0.000110	0.00008
Cumulative Proportion	0.9790	0.99080	0.99614	0.997610	0.998660	0.999240	0.999450	0.999620	0.999740	0.99982

	PC11	PC12	PC13	PC14	PC15	PC16	PC17	PC18	PC19
Standard deviation	0.001408	0.001330	0.0009536	0.0006344	0.0006123	0.0005649	0.0004438	0.0003412	0.000291
Proportion of Variance	0.000050	0.000050	0.0000200	0.0000100	0.0000100	0.0000100	0.0000100	0.0000000	0.000000
Cumulative Proportion	0.999870	0.999920	0.9999400	0.9999500	0.9999600	0.9999700	0.9999800	0.9999800	0.999980

	PC20	PC21	PC22	PC23	PC24	PC25	PC26	PC27	PC28
Standard deviation	0.0002502	0.0002333	0.0002240	0.00021	0.0001938	0.0001871	0.0001804	0.0001694	0.0001618
Proportion of Variance	0.0000000	0.0000000	0.0000000	0.00000	0.0000000	0.0000000	0.0000000	0.0000000	0.0000000
Cumulative Proportion	0.9999800	0.9999800	0.9999900	0.99999	0.9999900	0.9999900	0.9999900	0.9999900	0.9999900

	PC29	PC30	PC31	PC32	PC33	PC34	PC35	PC36	PC37
Standard deviation	0.0001549	0.0001502	0.0001447	0.0001425	0.0001330	0.0001242	0.0001211	0.0001162	0.0001114
Proportion of Variance	0.0000000	0.0000000	0.0000000	0.0000000	0.0000000	0.0000000	0.0000000	0.0000000	0.0000000
Cumulative Proportion	0.9999900	0.9999900	0.9999900	0.9999900	0.9999900	0.9999900	0.9999900	0.9999900	1.0000000

	PC38	PC39	PC40	PC41	PC42	PC43	PC44	PC45	PC46
Standard deviation	0.0001060	9.984e-05	9.735e-05	9.436e-05	9.242e-05	9.034e-05	8.417e-05	8.38e-05	7.936e-05
Proportion of Variance	0.0000000	0.000e+00	0.000e+00	0.000e+00	0.000e+00	0.000e+00	0.000e+00	0.00e+00	0.000e+00
Cumulative Proportion	1.0000000	1.000e+00	1.000e+00	1.000e+00	1.000e+00	1.000e+00	1.000e+00	1.00e+00	1.000e+00

	PC47	PC48	PC49	PC50	PC51	PC52	PC53	PC54	PC55
Standard deviation	7.489e-05	7.47e-05	7.283e-05	7.06e-05	6.698e-05	6.382e-05	6.014e-05	5.838e-05	5.77e-05
Proportion of Variance	0.000e+00	0.00e+00	0.000e+00	0.00e+00	0.000e+00	0.000e+00	0.000e+00	0.000e+00	0.00e+00
Cumulative Proportion	1.000e+00	1.00e+00	1.000e+00	1.00e+00	1.000e+00	1.000e+00	1.000e+00	1.000e+00	1.00e+00

	PC56	PC57	PC58	PC59	PC60	PC61	PC62	PC63	PC64
Standard deviation	5.66e-05	5.512e-05	5.464e-05	5.254e-05	4.93e-05	4.878e-05	4.537e-05	4.511e-05	4.32e-05
Proportion of Variance	0.00e+00	0.000e+00	0.000e+00	0.000e+00	0.00e+00	0.000e+00	0.000e+00	0.000e+00	0.00e+00
Cumulative Proportion	1.00e+00	1.000e+00	1.000e+00	1.000e+00	1.00e+00	1.000e+00	1.000e+00	1.000e+00	1.00e+00

	PC65	PC66	PC67	PC68	PC69	PC70	PC71	PC72	PC73
Standard deviation	4.245e-05	4.224e-05	3.835e-05	3.81e-05	3.710e-05	3.532e-05	3.441e-05	3.383e-05	3.35e-05
Proportion of Variance	0.000e+00	0.000e+00	0.000e+00	0.00e+00	0.000e+00	0.000e+00	0.000e+00	0.000e+00	0.00e+00
Cumulative Proportion	1.000e+00	1.000e+00	1.000e+00	1.00e+00	1.000e+00	1.000e+00	1.000e+00	1.000e+00	1.00e+00

	PC74	PC75	PC76	PC77	PC78	PC79	PC80	PC81	PC82
Standard deviation	3.138e-05	3.13e-05	3.103e-05	2.969e-05	2.897e-05	2.793e-05	2.707e-05	2.615e-05	2.573e-05
Proportion of Variance	0.000e+00	0.00e+00	0.000e+00	0.000e+00	0.000e+00	0.000e+00	0.000e+00	0.000e+00	0.000e+00
Cumulative Proportion	1.000e+00	1.00e+00	1.000e+00	1.000e+00	1.000e+00	1.000e+00	1.000e+00	1.000e+00	1.000e+00

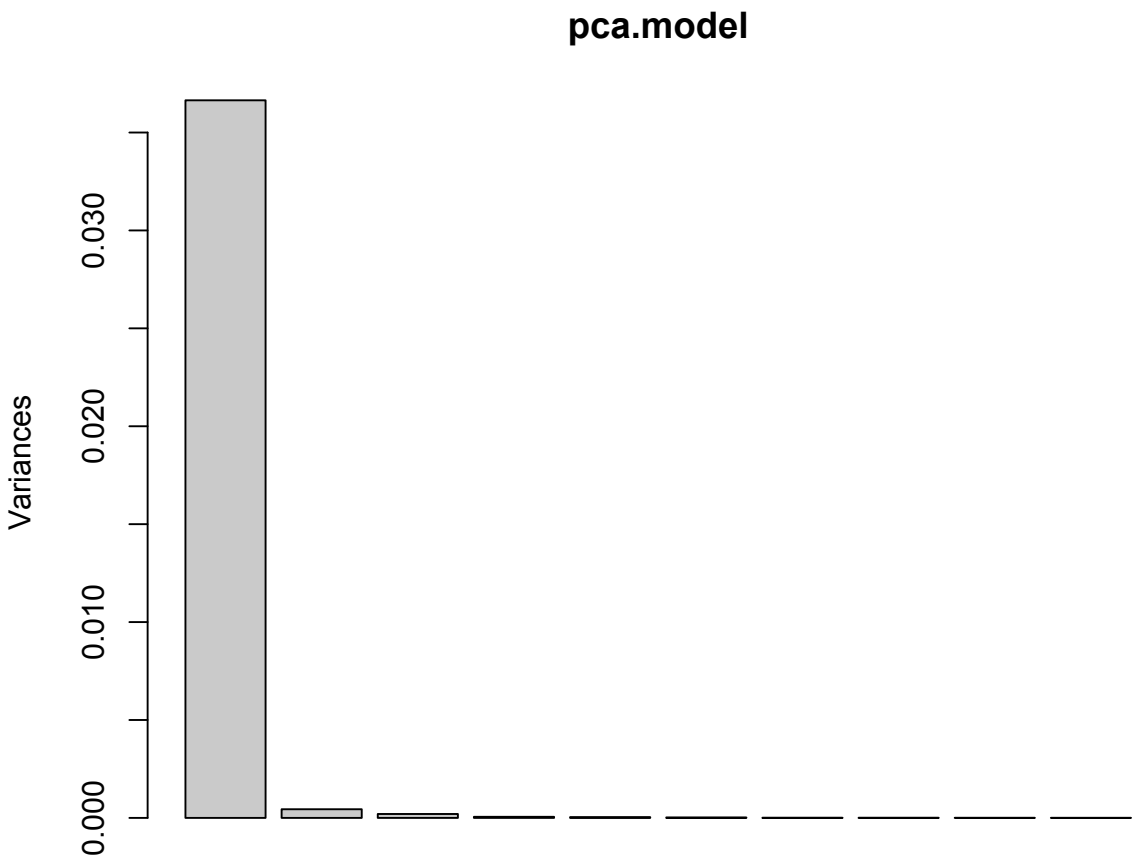


Figure 168: PCA scree plot for the first set of 30 glass first derivative (9-point smoothing) spectra (10 replicates), no data pretreatment.

Table 180: PCA results for the first set of 30 glass first derivative (9-point smoothing) spectra (10 replicates), centered.

Importance of components:

	PC1	PC2	PC3	PC4	PC5	PC6	PC7	PC8	PC9	PC10
Standard deviation	0.0358	0.02015	0.01193	0.007418	0.00601	0.004623	0.002749	0.002542	0.002061	0.001728
Proportion of Variance	0.6504	0.20602	0.07222	0.027920	0.01833	0.010840	0.003830	0.003280	0.002150	0.001520
Cumulative Proportion	0.6504	0.85645	0.92867	0.956600	0.97493	0.985770	0.989610	0.992880	0.995040	0.996550

	PC11	PC12	PC13	PC14	PC15	PC16	PC17	PC18	PC19
Standard deviation	0.001400	0.001328	0.0009496	0.0006319	0.0006121	0.0005602	0.0004359	0.000322	0.0002909
Proportion of Variance	0.000990	0.000900	0.0004600	0.0002000	0.0001900	0.0001600	0.0001000	0.000050	0.0000400
Cumulative Proportion	0.997550	0.998440	0.9989000	0.9991000	0.9992900	0.9994500	0.9995500	0.999600	0.9996500

	PC20	PC21	PC22	PC23	PC24	PC25	PC26	PC27	PC28
Standard deviation	0.0002449	0.0002321	0.0002237	0.0002100	0.000191	0.0001865	0.000179	0.0001691	0.0001605
Proportion of Variance	0.0000300	0.0000300	0.0000300	0.0000200	0.000020	0.0000200	0.000020	0.0000100	0.0000100
Cumulative Proportion	0.9996800	0.9997000	0.9997300	0.9997500	0.999770	0.9997900	0.999800	0.9998200	0.9998300

	PC29	PC30	PC31	PC32	PC33	PC34	PC35	PC36	PC37
Standard deviation	0.0001527	0.0001465	0.0001445	0.0001406	0.0001316	0.0001239	0.0001210	0.0001160	0.0001113
Proportion of Variance	0.0000100	0.0000100	0.0000100	0.0000100	0.0000100	0.0000100	0.0000100	0.0000100	0.0000100
Cumulative Proportion	0.9998400	0.9998500	0.9998600	0.9998700	0.9998800	0.9998900	0.9999000	0.9999100	0.9999100

	PC38	PC39	PC40	PC41	PC42	PC43	PC44	PC45	PC46
Standard deviation	0.0001057	9.952e-05	9.71e-05	9.423e-05	9.238e-05	9.034e-05	8.382e-05	8.325e-05	7.91e-05
Proportion of Variance	0.0000100	1.000e-05	0.00e+00	0.000e+00	0.000e+00	0.000e+00	0.000e+00	0.000e+00	0.00e+00
Cumulative Proportion	0.9999200	9.999e-01	1.00e+00	9.999e-01	9.999e-01	9.999e-01	9.999e-01	1.000e+00	1.00e+00

	PC47	PC48	PC49	PC50	PC51	PC52	PC53	PC54	PC55
Standard deviation	7.479e-05	7.44e-05	7.225e-05	7.05e-05	6.698e-05	6.382e-05	6.01e-05	5.823e-05	5.751e-05
Proportion of Variance	0.000e+00	0.00e+00	0.000e+00	0.00e+00	0.000e+00	0.000e+00	0.00e+00	0.000e+00	0.000e+00
Cumulative Proportion	1.000e+00	1.00e+00	1.000e+00	1.00e+00	1.000e+00	1.000e+00	1.00e+00	1.000e+00	1.000e+00

	PC56	PC57	PC58	PC59	PC60	PC61	PC62	PC63	PC64
Standard deviation	5.657e-05	5.504e-05	5.464e-05	5.252e-05	4.881e-05	4.847e-05	4.519e-05	4.503e-05	4.310e-05
Proportion of Variance	0.000e+00	0.000e+00	0.000e+00	0.000e+00	0.000e+00	0.000e+00	0.000e+00	0.000e+00	0.000e+00
Cumulative Proportion	1.000e+00	1.000e+00	1.000e+00	1.000e+00	1.000e+00	1.000e+00	1.000e+00	1.000e+00	1.000e+00

	PC65	PC66	PC67	PC68	PC69	PC70	PC71	PC72	PC73
Standard deviation	4.237e-05	4.197e-05	3.813e-05	3.784e-05	3.698e-05	3.531e-05	3.438e-05	3.382e-05	3.348e-05
Proportion of Variance	0.000e+00	0.000e+00	0.000e+00	0.000e+00	0.000e+00	0.000e+00	0.000e+00	0.000e+00	0.000e+00
Cumulative Proportion	1.000e+00	1.000e+00	1.000e+00	1.000e+00	1.000e+00	1.000e+00	1.000e+00	1.000e+00	1.000e+00

	PC74	PC75	PC76	PC77	PC78	PC79	PC80	PC81	PC82
Standard deviation	3.137e-05	3.128e-05	3.086e-05	2.963e-05	2.884e-05	2.790e-05	2.707e-05	2.615e-05	2.573e-05
Proportion of Variance	0.000e+00	0.000e+00	0.000e+00	0.000e+00	0.000e+00	0.000e+00	0.000e+00	0.000e+00	0.000e+00
Cumulative Proportion	1.000e+00	1.000e+00	1.000e+00	1.000e+00	1.000e+00	1.000e+00	1.000e+00	1.000e+00	1.000e+00

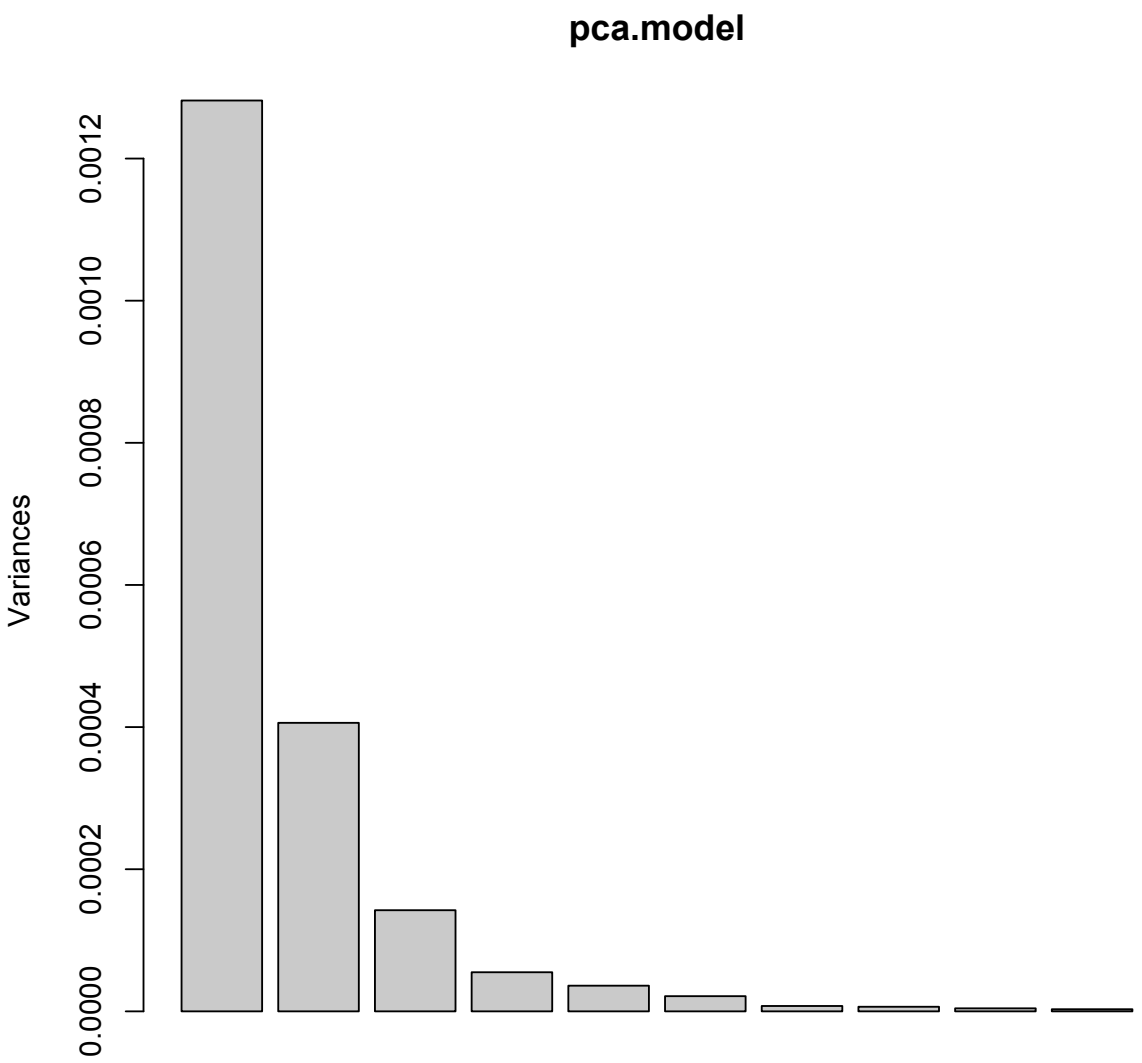


Figure 169: PCA scree plot for the first set of 30 glass first derivative (9-point smoothing) spectra (10 replicates), centered.

Table 181: PCA results for the first set of 30 glass first derivative (9-point smoothing) spectra (10 replicates), autoscaled.

Importance of components:

	PC1	PC2	PC3	PC4	PC5	PC6	PC7	PC8	PC9	PC10	PC11
Standard deviation	15.4302	5.61295	4.82672	3.03901	2.47658	2.17646	1.71039	1.38728	1.27985	0.87927	0.75795
Proportion of Variance	0.7371	0.09754	0.07213	0.02859	0.01899	0.01467	0.00906	0.00596	0.00507	0.00239	0.00178
Cumulative Proportion	0.7371	0.83466	0.90679	0.93539	0.95437	0.96904	0.97810	0.98406	0.98913	0.99152	0.99330

	PC12	PC13	PC14	PC15	PC16	PC17	PC18	PC19	PC20	PC21	PC22
Standard deviation	0.6480	0.51496	0.48100	0.46106	0.36914	0.32354	0.29146	0.27182	0.24941	0.23408	0.22494
Proportion of Variance	0.0013	0.00082	0.00072	0.00066	0.00042	0.00032	0.00026	0.00023	0.00019	0.00017	0.00016
Cumulative Proportion	0.9946	0.99542	0.99614	0.99679	0.99722	0.99754	0.99780	0.99803	0.99822	0.99839	0.99855

	PC23	PC24	PC25	PC26	PC27	PC28	PC29	PC30	PC31	PC32	PC33
Standard deviation	0.21365	0.18615	0.1826	0.16341	0.15962	0.14897	0.14623	0.14175	0.13472	0.13106	0.12619
Proportion of Variance	0.00014	0.00011	0.0001	0.00008	0.00008	0.00007	0.00007	0.00006	0.00006	0.00005	0.00005
Cumulative Proportion	0.99869	0.99880	0.9989	0.99898	0.99906	0.99913	0.99920	0.99926	0.99932	0.99937	0.99942

	PC34	PC35	PC36	PC37	PC38	PC39	PC40	PC41	PC42	PC43	PC44
Standard deviation	0.11951	0.11926	0.11119	0.09772	0.09391	0.08471	0.08288	0.08179	0.07715	0.07602	0.06954
Proportion of Variance	0.00004	0.00004	0.00004	0.00003	0.00003	0.00002	0.00002	0.00002	0.00002	0.00002	0.00001
Cumulative Proportion	0.99946	0.99951	0.99955	0.99958	0.99960	0.99963	0.99965	0.99967	0.99969	0.99970	0.99972

	PC45	PC46	PC47	PC48	PC49	PC50	PC51	PC52	PC53	PC54	PC55
Standard deviation	0.06822	0.06557	0.06493	0.06182	0.06104	0.05943	0.05817	0.05638	0.05373	0.05265	0.05086
Proportion of Variance	0.00001	0.00001	0.00001	0.00001	0.00001	0.00001	0.00001	0.00001	0.00001	0.00001	0.00001
Cumulative Proportion	0.99973	0.99975	0.99976	0.99977	0.99978	0.99979	0.99980	0.99981	0.99982	0.99983	0.99984

	PC56	PC57	PC58	PC59	PC60	PC61	PC62	PC63	PC64	PC65	PC66
Standard deviation	0.05064	0.04835	0.04766	0.04600	0.04463	0.04420	0.04253	0.04197	0.03922	0.03824	0.03762
Proportion of Variance	0.00001	0.00001	0.00001	0.00001	0.00001	0.00001	0.00001	0.00001	0.00000	0.00000	0.00000
Cumulative Proportion	0.99985	0.99985	0.99986	0.99987	0.99987	0.99988	0.99989	0.99989	0.99990	0.99990	0.99991

	PC67	PC68	PC69	PC70	PC71	PC72	PC73	PC74	PC75	PC76	PC77
Standard deviation	0.03694	0.03552	0.03484	0.03428	0.03342	0.03268	0.03142	0.03123	0.03092	0.02994	0.02893
Proportion of Variance	0.00000	0.00000	0.00000	0.00000	0.00000	0.00000	0.00000	0.00000	0.00000	0.00000	0.00000
Cumulative Proportion	0.99991	0.99991	0.99992	0.99992	0.99992	0.99993	0.99993	0.99993	0.99994	0.99994	0.99994

	PC78	PC79	PC80	PC81	PC82	PC83	PC84	PC85	PC86	PC87	PC88
Standard deviation	0.02859	0.02797	0.02727	0.02708	0.02678	0.02615	0.02454	0.02440	0.02376	0.02298	0.02258
Proportion of Variance	0.00000	0.00000	0.00000	0.00000	0.00000	0.00000	0.00000	0.00000	0.00000	0.00000	0.00000
Cumulative Proportion	0.99994	0.99995	0.99995	0.99995	0.99995	0.99996	0.99996	0.99996	0.99996	0.99996	0.99996

	PC89	PC90	PC91	PC92	PC93	PC94	PC95	PC96	PC97	PC98	PC99
Standard deviation	0.02189	0.02152	0.0213	0.02057	0.02027	0.02000	0.01966	0.01924	0.01852	0.01823	0.01789
Proportion of Variance	0.00000	0.00000	0.0000	0.00000	0.00000	0.00000	0.00000	0.00000	0.00000	0.00000	0.00000
Cumulative Proportion	0.99997	0.99997	1.0000	0.99997	0.99997	0.99997	0.99997	0.99997	0.99998	0.99998	0.99998

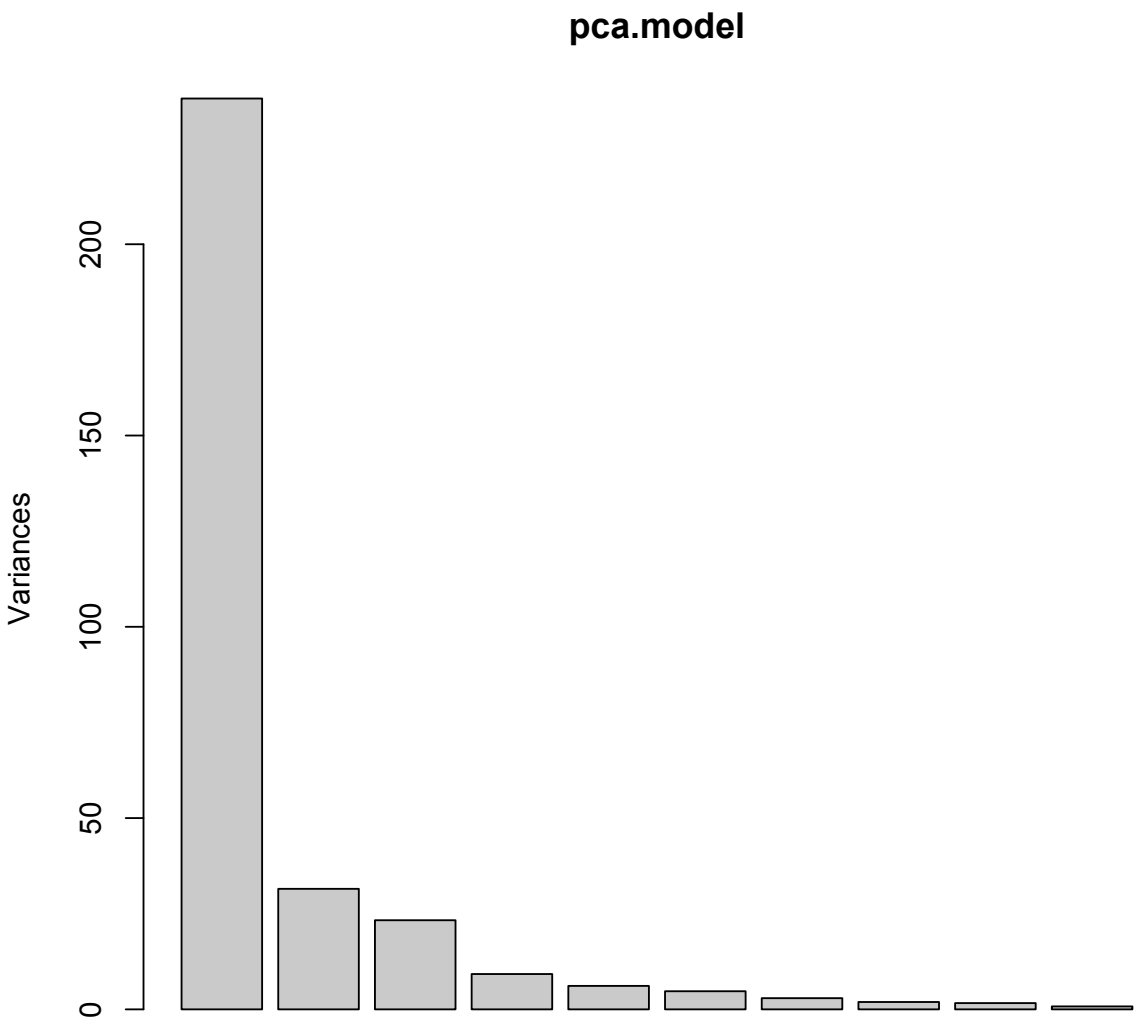


Figure 170: PCA scree plot for the first set of 30 glass first derivative (9-point smoothing) spectra (10 replicates), autoscaled.

Table 182: PCA results for the first set of 20 window glass first derivative (9-point smoothing) spectra (10 replicates), no data pretreatment.

Importance of components:

	PC1	PC2	PC3	PC4	PC5	PC6	PC7	PC8	PC9	PC10
Standard deviation	0.1902	0.01961	0.01315	0.00736	0.006316	0.002947	0.002667	0.002238	0.001775	0.001390
Proportion of Variance	0.9815	0.01044	0.00469	0.00147	0.001080	0.000240	0.000190	0.000140	0.000090	0.000050
Cumulative Proportion	0.9815	0.99192	0.99661	0.99808	0.999160	0.999400	0.999590	0.999730	0.999810	0.999870

	PC11	PC12	PC13	PC14	PC15	PC16	PC17	PC18	PC19
Standard deviation	0.001178	0.000944	0.000825	0.0007231	0.0005485	0.0004062	0.000393	0.0003261	0.0002666
Proportion of Variance	0.000040	0.000020	0.000020	0.0000100	0.0000100	0.0000000	0.000000	0.0000000	0.0000000
Cumulative Proportion	0.999900	0.999930	0.999950	0.9999600	0.9999700	0.9999700	0.999980	0.9999800	0.9999800

	PC20	PC21	PC22	PC23	PC24	PC25	PC26	PC27	PC28
Standard deviation	0.0002445	0.0002194	0.0002102	0.0001903	0.0001778	0.0001773	0.0001661	0.0001566	0.0001550
Proportion of Variance	0.0000000	0.0000000	0.0000000	0.0000000	0.0000000	0.0000000	0.0000000	0.0000000	0.0000000
Cumulative Proportion	0.9999800	0.9999900	0.9999900	0.9999900	0.9999900	0.9999900	0.9999900	0.9999900	0.9999900

	PC29	PC30	PC31	PC32	PC33	PC34	PC35	PC36	PC37
Standard deviation	0.0001474	0.0001410	0.0001341	0.0001329	0.0001257	0.0001221	0.0001166	0.0001074	0.0001016
Proportion of Variance	0.0000000	0.0000000	0.0000000	0.0000000	0.0000000	0.0000000	0.0000000	0.0000000	0.0000000
Cumulative Proportion	0.9999900	0.9999900	0.9999900	0.9999900	0.9999900	1.0000000	1.0000000	1.0000000	1.0000000

	PC38	PC39	PC40	PC41	PC42	PC43	PC44	PC45	PC46
Standard deviation	9.722e-05	9.28e-05	8.722e-05	8.523e-05	8.425e-05	8.008e-05	7.85e-05	7.696e-05	7.246e-05
Proportion of Variance	0.000e+00	0.00e+00	0.000e+00	0.000e+00	0.000e+00	0.000e+00	0.00e+00	0.000e+00	0.000e+00
Cumulative Proportion	1.000e+00	1.00e+00	1.000e+00	1.000e+00	1.000e+00	1.000e+00	1.00e+00	1.000e+00	1.000e+00

	PC47	PC48	PC49	PC50	PC51	PC52	PC53	PC54	PC55
Standard deviation	6.917e-05	6.9e-05	6.551e-05	6.336e-05	6.197e-05	5.731e-05	5.625e-05	5.539e-05	5.304e-05
Proportion of Variance	0.000e+00	0.0e+00	0.000e+00	0.000e+00	0.000e+00	0.000e+00	0.000e+00	0.000e+00	0.000e+00
Cumulative Proportion	1.000e+00	1.0e+00	1.000e+00	1.000e+00	1.000e+00	1.000e+00	1.000e+00	1.000e+00	1.000e+00

	PC56	PC57	PC58	PC59	PC60	PC61	PC62	PC63	PC64
Standard deviation	5.153e-05	5.056e-05	5.026e-05	4.731e-05	4.484e-05	4.39e-05	4.248e-05	4.064e-05	3.88e-05
Proportion of Variance	0.000e+00	0.000e+00	0.000e+00	0.000e+00	0.000e+00	0.00e+00	0.000e+00	0.000e+00	0.00e+00
Cumulative Proportion	1.000e+00	1.000e+00	1.000e+00	1.000e+00	1.000e+00	1.00e+00	1.000e+00	1.000e+00	1.00e+00

	PC65	PC66	PC67	PC68	PC69	PC70	PC71	PC72	PC73
Standard deviation	3.845e-05	3.66e-05	3.554e-05	3.509e-05	3.366e-05	3.291e-05	3.192e-05	3.067e-05	2.978e-05
Proportion of Variance	0.000e+00	0.00e+00	0.000e+00	0.000e+00	0.000e+00	0.000e+00	0.000e+00	0.000e+00	0.000e+00
Cumulative Proportion	1.000e+00	1.00e+00	1.000e+00	1.000e+00	1.000e+00	1.000e+00	1.000e+00	1.000e+00	1.000e+00

	PC74	PC75	PC76	PC77	PC78	PC79	PC80	PC81	PC82
Standard deviation	2.867e-05	2.803e-05	2.752e-05	2.672e-05	2.593e-05	2.514e-05	2.471e-05	2.338e-05	2.259e-05
Proportion of Variance	0.000e+00	0.000e+00	0.000e+00	0.000e+00	0.000e+00	0.000e+00	0.000e+00	0.000e+00	0.000e+00
Cumulative Proportion	1.000e+00	1.000e+00	1.000e+00	1.000e+00	1.000e+00	1.000e+00	1.000e+00	1.000e+00	1.000e+00

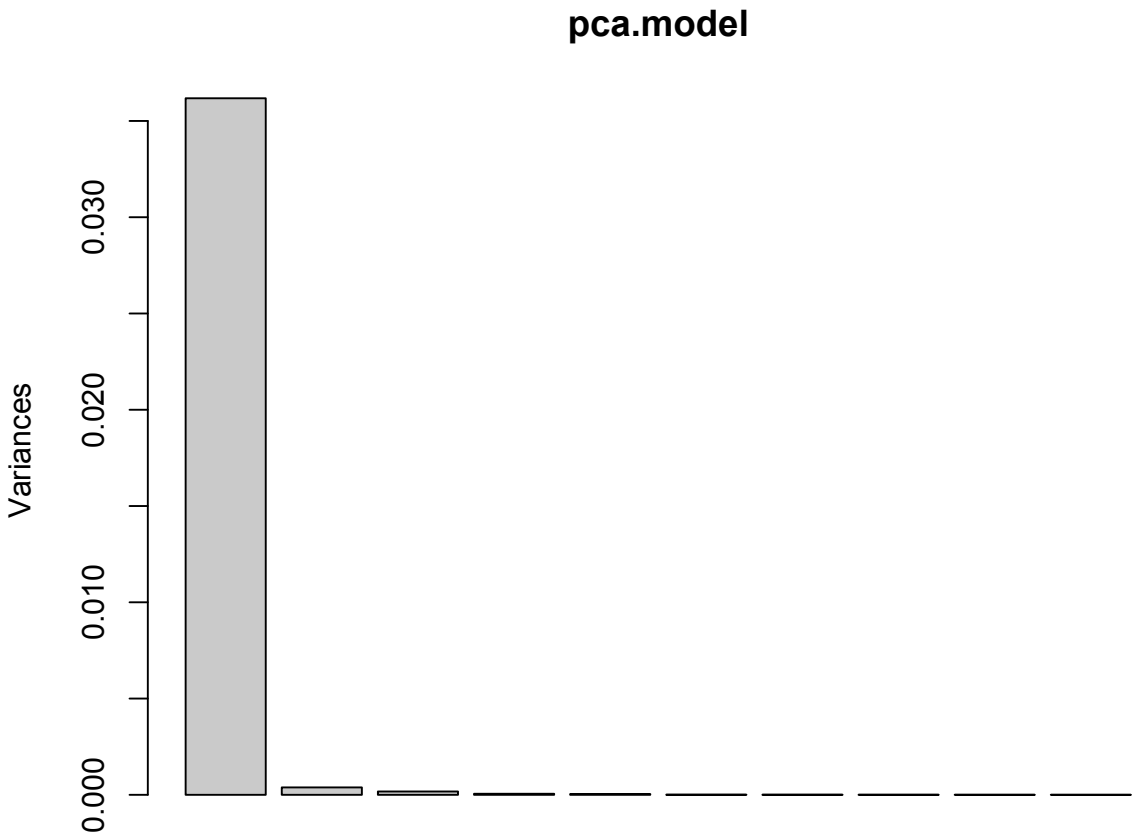


Figure 171: PCA scree plot for the first set of 20 window glass first derivative (9-point smoothing) spectra (10 replicates), no data pretreatment.

Table 183: PCA results for the first set of 20 window glass first derivative (9-point smoothing) spectra (10 replicates), centered.

Importance of components:

	PC1	PC2	PC3	PC4	PC5	PC6	PC7	PC8	PC9	PC10
Standard deviation	0.03886	0.01929	0.01178	0.007358	0.006079	0.002943	0.002649	0.002214	0.001766	0.001367
Proportion of Variance	0.70480	0.17376	0.06475	0.025270	0.017250	0.004040	0.003280	0.002290	0.001460	0.000870
Cumulative Proportion	0.70480	0.87856	0.94331	0.968580	0.985830	0.989870	0.993140	0.995430	0.996890	0.997760

	PC11	PC12	PC13	PC14	PC15	PC16	PC17	PC18	PC19
Standard deviation	0.001178	0.0009418	0.0007965	0.0007172	0.0005433	0.0003983	0.0003924	0.0003073	0.0002513
Proportion of Variance	0.000650	0.0004100	0.0003000	0.0002400	0.0001400	0.0000700	0.0000700	0.0000400	0.0000300
Cumulative Proportion	0.998410	0.9988200	0.9991200	0.9993600	0.9995000	0.9995700	0.9996400	0.9996900	0.9997200

	PC20	PC21	PC22	PC23	PC24	PC25	PC26	PC27	PC28
Standard deviation	0.0002422	0.0002177	0.0002102	0.0001885	0.0001778	0.0001746	0.0001655	0.0001556	0.0001486
Proportion of Variance	0.0000300	0.0000200	0.0000200	0.0000200	0.0000100	0.0000100	0.0000100	0.0000100	0.0000100
Cumulative Proportion	0.9997500	0.9997700	0.9997900	0.9998000	0.9998200	0.9998300	0.9998500	0.9998600	0.9998700

	PC29	PC30	PC31	PC32	PC33	PC34	PC35	PC36	PC37
Standard deviation	0.0001470	0.0001368	0.0001340	0.0001329	0.0001243	0.0001193	0.0001164	0.0001070	0.0001016
Proportion of Variance	0.0000100	0.0000100	0.0000100	0.0000100	0.0000100	0.0000100	0.0000100	0.0000100	0.0000000
Cumulative Proportion	0.9998800	0.9998900	0.9998900	0.9999000	0.9999100	0.9999200	0.9999200	0.9999300	0.9999300

	PC38	PC39	PC40	PC41	PC42	PC43	PC44	PC45	PC46
Standard deviation	9.668e-05	9.28e-05	8.699e-05	8.522e-05	8.322e-05	7.986e-05	7.784e-05	7.69e-05	7.092e-05
Proportion of Variance	0.000e+00	0.00e+00	0.000e+00	0.000e+00	0.000e+00	0.000e+00	0.000e+00	0.00e+00	0.000e+00
Cumulative Proportion	9.999e-01	1.00e+00	1.000e+00	1.000e+00	1.000e+00	1.000e+00	1.000e+00	1.00e+00	1.000e+00

	PC47	PC48	PC49	PC50	PC51	PC52	PC53	PC54	PC55
Standard deviation	6.91e-05	6.822e-05	6.483e-05	6.333e-05	6.132e-05	5.679e-05	5.61e-05	5.522e-05	5.291e-05
Proportion of Variance	0.00e+00	0.000e+00	0.000e+00	0.000e+00	0.000e+00	0.000e+00	0.00e+00	0.000e+00	0.000e+00
Cumulative Proportion	1.00e+00	1.000e+00	1.000e+00	1.000e+00	1.000e+00	1.000e+00	1.00e+00	1.000e+00	1.000e+00

	PC56	PC57	PC58	PC59	PC60	PC61	PC62	PC63	PC64
Standard deviation	5.112e-05	5.041e-05	4.981e-05	4.691e-05	4.48e-05	4.385e-05	4.248e-05	4.041e-05	3.878e-05
Proportion of Variance	0.000e+00	0.000e+00	0.000e+00	0.000e+00	0.00e+00	0.000e+00	0.000e+00	0.000e+00	0.000e+00
Cumulative Proportion	1.000e+00	1.000e+00	1.000e+00	1.000e+00	1.00e+00	1.000e+00	1.000e+00	1.000e+00	1.000e+00

	PC65	PC66	PC67	PC68	PC69	PC70	PC71	PC72	PC73
Standard deviation	3.843e-05	3.649e-05	3.553e-05	3.506e-05	3.366e-05	3.291e-05	3.164e-05	3.067e-05	2.971e-05
Proportion of Variance	0.000e+00	0.000e+00	0.000e+00	0.000e+00	0.000e+00	0.000e+00	0.000e+00	0.000e+00	0.000e+00
Cumulative Proportion	1.000e+00	1.000e+00	1.000e+00	1.000e+00	1.000e+00	1.000e+00	1.000e+00	1.000e+00	1.000e+00

	PC74	PC75	PC76	PC77	PC78	PC79	PC80	PC81	PC82
Standard deviation	2.867e-05	2.801e-05	2.751e-05	2.635e-05	2.591e-05	2.512e-05	2.469e-05	2.316e-05	2.236e-05
Proportion of Variance	0.000e+00	0.000e+00	0.000e+00	0.000e+00	0.000e+00	0.000e+00	0.000e+00	0.000e+00	0.000e+00
Cumulative Proportion	1.000e+00	1.000e+00	1.000e+00	1.000e+00	1.000e+00	1.000e+00	1.000e+00	1.000e+00	1.000e+00

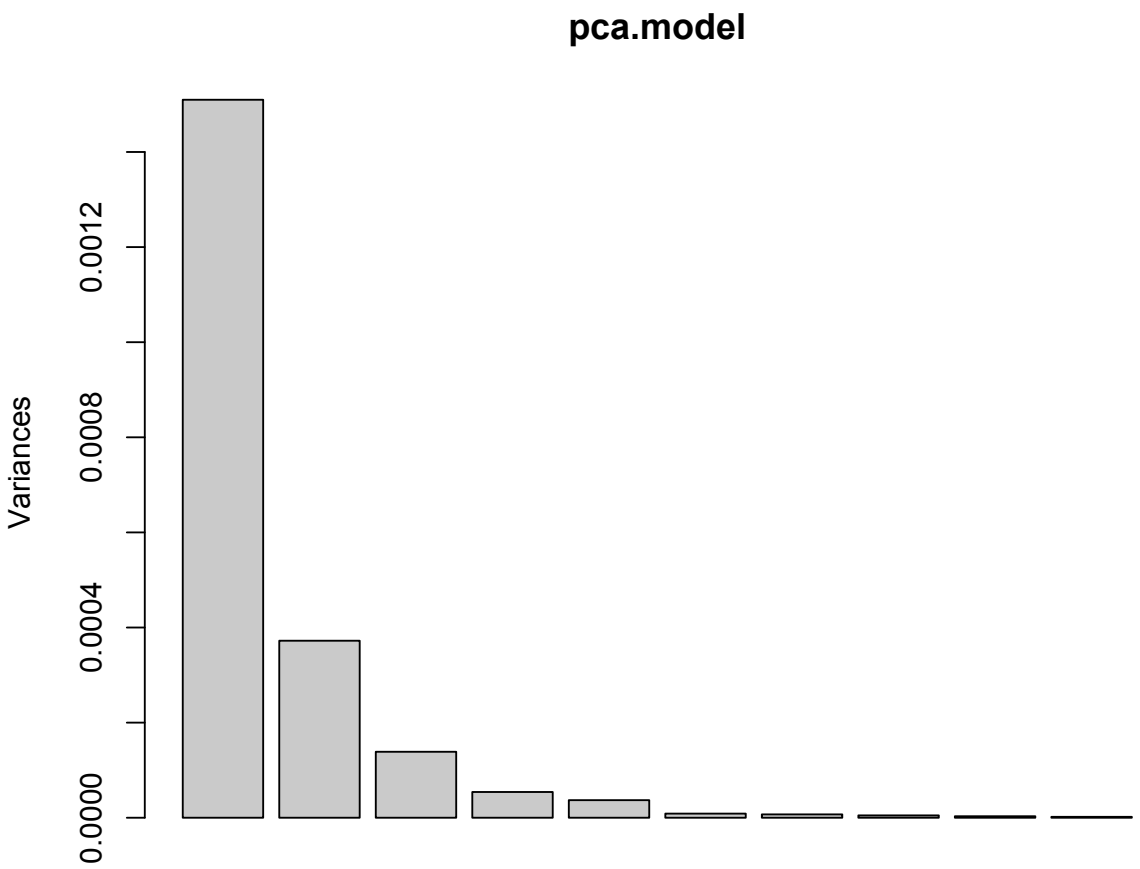


Figure 172: PCA scree plot for the first set of 20 window glass first derivative (9-point smoothing) spectra (10 replicates), centered.

Table 184: PCA results for the first set of 20 window glass first derivative (9-point smoothing) spectra (10 replicates), autoscaled.

Importance of components:

	PC1	PC2	PC3	PC4	PC5	PC6	PC7	PC8	PC9	PC10	PC11	PC12
Standard deviation	16.205	4.8758	4.30484	2.38803	1.66173	1.51854	1.34134	1.19501	1.12945	0.78952	0.65475	0.5671
Proportion of Variance	0.813	0.0736	0.05737	0.01766	0.00855	0.00714	0.00557	0.00442	0.00395	0.00193	0.00133	0.0010
Cumulative Proportion	0.813	0.8866	0.94398	0.96164	0.97019	0.97733	0.98290	0.98732	0.99127	0.99320	0.99452	0.9955

	PC13	PC14	PC15	PC16	PC17	PC18	PC19	PC20	PC21	PC22	PC23
Standard deviation	0.52128	0.42310	0.40792	0.32755	0.3098	0.28105	0.23521	0.22610	0.21036	0.19191	0.1765
Proportion of Variance	0.00084	0.00055	0.00052	0.00033	0.0003	0.00024	0.00017	0.00016	0.00014	0.00011	0.0001
Cumulative Proportion	0.99636	0.99692	0.99743	0.99776	0.9981	0.99830	0.99848	0.99863	0.99877	0.99888	0.9990

	PC24	PC25	PC26	PC27	PC28	PC29	PC30	PC31	PC32	PC33	PC34
Standard deviation	0.16946	0.15648	0.15197	0.14638	0.14202	0.13049	0.12409	0.12332	0.11464	0.10623	0.10315
Proportion of Variance	0.00009	0.00008	0.00007	0.00007	0.00006	0.00005	0.00005	0.00005	0.00004	0.00003	0.00003
Cumulative Proportion	0.99907	0.99915	0.99922	0.99928	0.99935	0.99940	0.99945	0.99949	0.99953	0.99957	0.99960

	PC35	PC36	PC37	PC38	PC39	PC40	PC41	PC42	PC43	PC44	PC45
Standard deviation	0.09368	0.09143	0.08670	0.08432	0.07987	0.07859	0.07308	0.06953	0.06453	0.06424	0.06241
Proportion of Variance	0.00003	0.00003	0.00002	0.00002	0.00002	0.00002	0.00002	0.00001	0.00001	0.00001	0.00001
Cumulative Proportion	0.99963	0.99966	0.99968	0.99970	0.99972	0.99974	0.99976	0.99977	0.99978	0.99980	0.99981

	PC46	PC47	PC48	PC49	PC50	PC51	PC52	PC53	PC54	PC55	PC56
Standard deviation	0.06011	0.05757	0.05563	0.05399	0.05304	0.05102	0.05052	0.04782	0.04573	0.04344	0.04277
Proportion of Variance	0.00001	0.00001	0.00001	0.00001	0.00001	0.00001	0.00001	0.00001	0.00001	0.00001	0.00001
Cumulative Proportion	0.99982	0.99983	0.99984	0.99985	0.99986	0.99987	0.99987	0.99988	0.99989	0.99989	0.99990

	PC57	PC58	PC59	PC60	PC61	PC62	PC63	PC64	PC65	PC66	PC67
Standard deviation	0.04210	0.04088	0.03878	0.03762	0.03645	0.03602	0.03556	0.03294	0.03259	0.0319	0.03151
Proportion of Variance	0.00001	0.00001	0.00000	0.00000	0.00000	0.00000	0.00000	0.00000	0.00000	0.0000	0.00000
Cumulative Proportion	0.99990	0.99991	0.99991	0.99992	0.99992	0.99993	0.99993	0.99993	0.99994	0.9999	0.99994

	PC68	PC69	PC70	PC71	PC72	PC73	PC74	PC75	PC76	PC77	PC78
Standard deviation	0.02968	0.02904	0.02781	0.0274	0.02685	0.02639	0.02511	0.02437	0.02395	0.02379	0.02290
Proportion of Variance	0.00000	0.00000	0.00000	0.0000	0.00000	0.00000	0.00000	0.00000	0.00000	0.00000	0.00000
Cumulative Proportion	0.99995	0.99995	0.99995	1.0000	0.99996	0.99996	0.99996	0.99996	0.99996	0.99996	0.99997

	PC79	PC80	PC81	PC82	PC83	PC84	PC85	PC86	PC87	PC88	PC89
Standard deviation	0.02188	0.02142	0.02115	0.02046	0.02012	0.01976	0.01941	0.01883	0.01875	0.01824	0.01803
Proportion of Variance	0.00000	0.00000	0.00000	0.00000	0.00000	0.00000	0.00000	0.00000	0.00000	0.00000	0.00000
Cumulative Proportion	0.99997	0.99997	0.99997	0.99997	0.99997	0.99997	0.99998	0.99998	0.99998	0.99998	0.99998

	PC90	PC91	PC92	PC93	PC94	PC95	PC96	PC97	PC98	PC99	PC100
Standard deviation	0.0175	0.01721	0.01689	0.01657	0.01619	0.01541	0.0152	0.01505	0.01449	0.01437	0.01427
Proportion of Variance	0.0000	0.00000	0.00000	0.00000	0.00000	0.00000	0.0000	0.00000	0.00000	0.00000	0.00000
Cumulative Proportion	1.0000	0.99998	0.99998	0.99998	0.99998	0.99999	1.0000	0.99999	0.99999	0.99999	0.99999

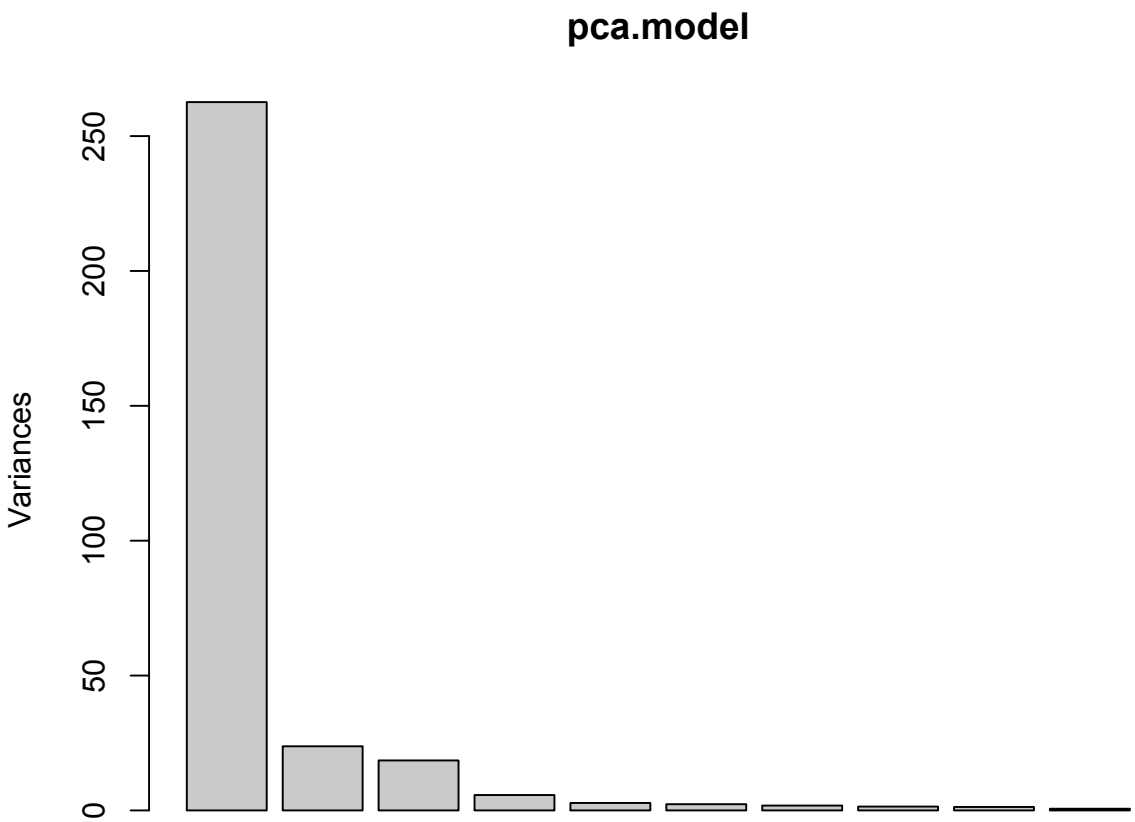


Figure 173: PCA scree plot for the first set of 20 window glass first derivative (9-point smoothing) spectra (10 replicates), autoscaled.

Table 185: PCA results for the first set of 10 container glass first derivative (9-point smoothing) spectra (10 replicates), no data pretreatment.

Importance of components:

	PC1	PC2	PC3	PC4	PC5	PC6	PC7	PC8	PC9	PC10
Standard deviation	0.1949	0.02372	0.01586	0.007397	0.00620	0.004949	0.002841	0.002343	0.001783	0.001611
Proportion of Variance	0.9754	0.01445	0.00646	0.001400	0.00099	0.000630	0.000210	0.000140	0.000080	0.000070
Cumulative Proportion	0.9754	0.98988	0.99634	0.997750	0.99873	0.999360	0.999570	0.999710	0.999790	0.999860

	PC11	PC12	PC13	PC14	PC15	PC16	PC17	PC18	PC19
Standard deviation	0.001364	0.001172	0.0008572	0.0005705	0.0004754	0.0003967	0.0003356	0.0003082	0.0002596
Proportion of Variance	0.000050	0.000040	0.0000200	0.0000100	0.0000100	0.0000000	0.0000000	0.0000000	0.0000000
Cumulative Proportion	0.999910	0.999940	0.9999600	0.9999700	0.9999700	0.9999800	0.9999800	0.9999800	0.9999900

	PC20	PC21	PC22	PC23	PC24	PC25	PC26	PC27	PC28
Standard deviation	0.0002374	0.0002246	0.0002013	0.0001936	0.0001872	0.0001662	0.0001637	0.0001559	0.0001454
Proportion of Variance	0.0000000	0.0000000	0.0000000	0.0000000	0.0000000	0.0000000	0.0000000	0.0000000	0.0000000
Cumulative Proportion	0.9999900	0.9999900	0.9999900	0.9999900	0.9999900	0.9999900	0.9999900	0.9999900	0.9999900

	PC29	PC30	PC31	PC32	PC33	PC34	PC35	PC36	PC37
Standard deviation	0.0001414	0.0001388	0.0001325	0.0001250	0.0001140	0.0001129	0.0001075	0.0001016	9.524e-05
Proportion of Variance	0.0000000	0.0000000	0.0000000	0.0000000	0.0000000	0.0000000	0.0000000	0.0000000	0.000e+00
Cumulative Proportion	0.9999900	1.0000000	1.0000000	1.0000000	1.0000000	1.0000000	1.0000000	1.0000000	1.000e+00

	PC38	PC39	PC40	PC41	PC42	PC43	PC44	PC45	PC46
Standard deviation	9.185e-05	9.044e-05	8.513e-05	8.158e-05	7.393e-05	6.957e-05	6.738e-05	6.478e-05	6.266e-05
Proportion of Variance	0.000e+00	0.000e+00	0.000e+00	0.000e+00	0.000e+00	0.000e+00	0.000e+00	0.000e+00	0.000e+00
Cumulative Proportion	1.000e+00	1.000e+00	1.000e+00	1.000e+00	1.000e+00	1.000e+00	1.000e+00	1.000e+00	1.000e+00

	PC47	PC48	PC49	PC50	PC51	PC52	PC53	PC54	PC55
Standard deviation	5.915e-05	5.845e-05	5.707e-05	5.44e-05	5.228e-05	4.978e-05	4.801e-05	4.665e-05	4.313e-05
Proportion of Variance	0.000e+00	0.000e+00	0.000e+00	0.00e+00	0.000e+00	0.000e+00	0.000e+00	0.000e+00	0.000e+00
Cumulative Proportion	1.000e+00	1.000e+00	1.000e+00	1.00e+00	1.000e+00	1.000e+00	1.000e+00	1.000e+00	1.000e+00

	PC56	PC57	PC58	PC59	PC60	PC61	PC62	PC63	PC64
Standard deviation	4.211e-05	4.163e-05	4.015e-05	3.91e-05	3.689e-05	3.581e-05	3.419e-05	3.307e-05	3.186e-05
Proportion of Variance	0.000e+00	0.000e+00	0.000e+00	0.00e+00	0.000e+00	0.000e+00	0.000e+00	0.000e+00	0.000e+00
Cumulative Proportion	1.000e+00	1.000e+00	1.000e+00	1.00e+00	1.000e+00	1.000e+00	1.000e+00	1.000e+00	1.000e+00

	PC65	PC66	PC67	PC68	PC69	PC70	PC71	PC72	PC73
Standard deviation	3.093e-05	3.053e-05	2.889e-05	2.768e-05	2.689e-05	2.567e-05	2.455e-05	2.323e-05	2.254e-05
Proportion of Variance	0.000e+00	0.000e+00	0.000e+00	0.000e+00	0.000e+00	0.000e+00	0.000e+00	0.000e+00	0.000e+00
Cumulative Proportion	1.000e+00	1.000e+00	1.000e+00	1.000e+00	1.000e+00	1.000e+00	1.000e+00	1.000e+00	1.000e+00

	PC74	PC75	PC76	PC77	PC78	PC79	PC80	PC81	PC82
Standard deviation	2.109e-05	2.085e-05	2.078e-05	2.03e-05	1.902e-05	1.849e-05	1.773e-05	1.735e-05	1.709e-05
Proportion of Variance	0.000e+00	0.000e+00	0.000e+00	0.00e+00	0.000e+00	0.000e+00	0.000e+00	0.000e+00	0.000e+00
Cumulative Proportion	1.000e+00	1.000e+00	1.000e+00	1.00e+00	1.000e+00	1.000e+00	1.000e+00	1.000e+00	1.000e+00

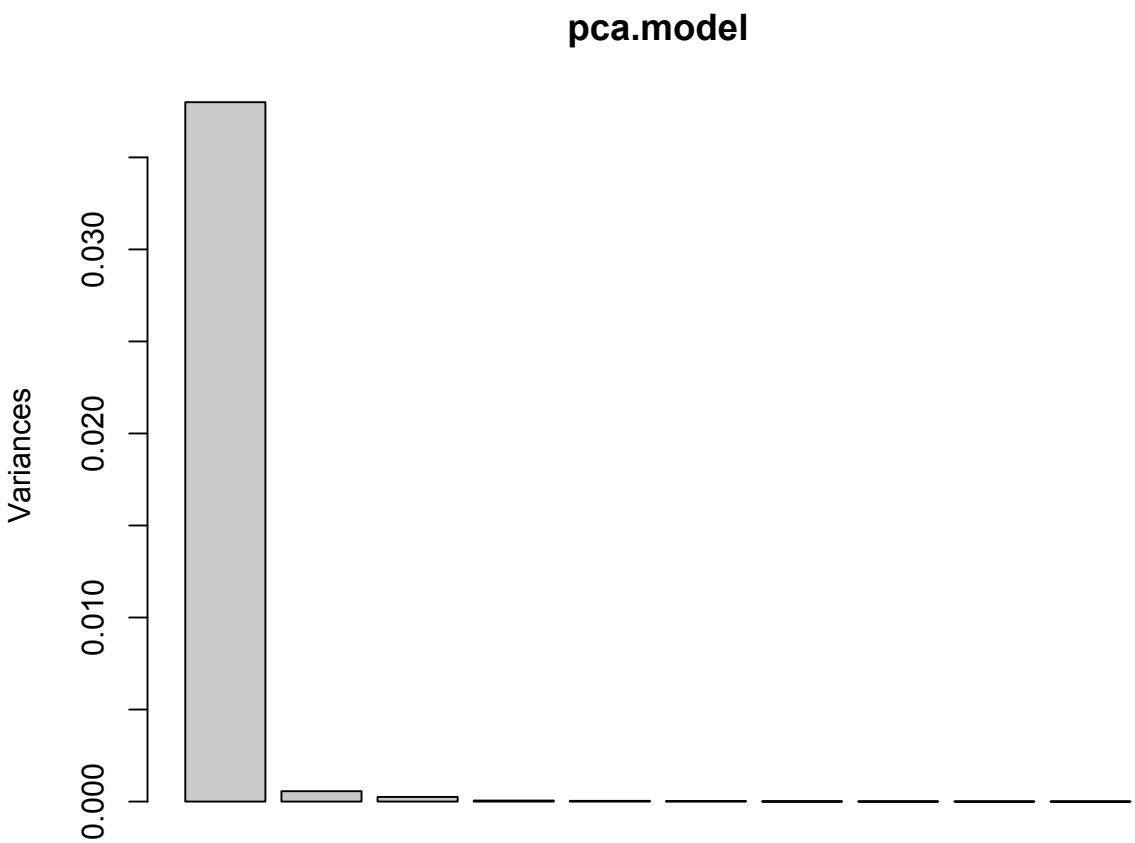


Figure 174: PCA scree plot for the first set of 10 container glass first derivative (9-point smoothing) spectra (10 replicates), no data pretreatment.

Table 186: PCA results for the first set of 10 container glass first derivative (9-point smoothing) spectra (10 replicates), centered.

Importance of components:

	PC1	PC2	PC3	PC4	PC5	PC6	PC7	PC8	PC9	PC10
Standard deviation	0.03142	0.02006	0.008166	0.006663	0.005845	0.003794	0.002374	0.002247	0.001638	0.001488
Proportion of Variance	0.62914	0.25657	0.042490	0.028290	0.021770	0.009170	0.003590	0.003220	0.001710	0.001410
Cumulative Proportion	0.62914	0.88571	0.928200	0.956490	0.978260	0.987430	0.991020	0.994240	0.995950	0.997360

	PC11	PC12	PC13	PC14	PC15	PC16	PC17	PC18	PC19
Standard deviation	0.001183	0.0009242	0.0006964	0.0005342	0.0004514	0.0003666	0.0003087	0.0002875	0.0002577
Proportion of Variance	0.000890	0.0005400	0.0003100	0.0001800	0.0001300	0.0000900	0.0000600	0.0000500	0.0000400
Cumulative Proportion	0.998250	0.9988000	0.9991100	0.9992900	0.9994200	0.9995000	0.9995700	0.9996200	0.9996600

	PC20	PC21	PC22	PC23	PC24	PC25	PC26	PC27	PC28
Standard deviation	0.0002278	0.0002178	0.0002000	0.0001919	0.0001841	0.0001662	0.0001621	0.0001504	0.0001425
Proportion of Variance	0.0000300	0.0000300	0.0000300	0.0000200	0.0000200	0.0000200	0.0000200	0.0000100	0.0000100
Cumulative Proportion	0.9996900	0.9997200	0.9997500	0.9997700	0.9997900	0.9998100	0.9998300	0.9998400	0.9998600

	PC29	PC30	PC31	PC32	PC33	PC34	PC35	PC36	PC37
Standard deviation	0.0001414	0.0001385	0.0001285	0.0001245	0.0001140	0.0001111	0.0001064	0.0001007	9.494e-05
Proportion of Variance	0.0000100	0.0000100	0.0000100	0.0000100	0.0000100	0.0000100	0.0000100	0.0000100	1.000e-05
Cumulative Proportion	0.9998700	0.9998800	0.9998900	0.9999000	0.9999100	0.9999200	0.9999200	0.9999300	9.999e-01

	PC38	PC39	PC40	PC41	PC42	PC43	PC44	PC45	PC46
Standard deviation	9.066e-05	8.962e-05	8.263e-05	7.909e-05	7.292e-05	6.766e-05	6.537e-05	6.306e-05	6.266e-05
Proportion of Variance	1.000e-05	1.000e-05	0.000e+00	0.000e+00	0.000e+00	0.000e+00	0.000e+00	0.000e+00	0.000e+00
Cumulative Proportion	9.999e-01	1.000e+00	1.000e+00	1.000e+00	1.000e+00	1.000e+00	1.000e+00	1.000e+00	1.000e+00

	PC47	PC48	PC49	PC50	PC51	PC52	PC53	PC54	PC55
Standard deviation	5.882e-05	5.806e-05	5.692e-05	5.347e-05	5.026e-05	4.839e-05	4.745e-05	4.665e-05	4.292e-05
Proportion of Variance	0.000e+00	0.000e+00	0.000e+00	0.000e+00	0.000e+00	0.000e+00	0.000e+00	0.000e+00	0.000e+00
Cumulative Proportion	1.000e+00	1.000e+00	1.000e+00	1.000e+00	1.000e+00	1.000e+00	1.000e+00	1.000e+00	1.000e+00

	PC56	PC57	PC58	PC59	PC60	PC61	PC62	PC63	PC64
Standard deviation	4.189e-05	4.038e-05	3.984e-05	3.91e-05	3.659e-05	3.482e-05	3.400e-05	3.187e-05	3.143e-05
Proportion of Variance	0.000e+00	0.000e+00	0.000e+00	0.00e+00	0.000e+00	0.000e+00	0.000e+00	0.000e+00	0.000e+00
Cumulative Proportion	1.000e+00	1.000e+00	1.000e+00	1.00e+00	1.000e+00	1.000e+00	1.000e+00	1.000e+00	1.000e+00

	PC65	PC66	PC67	PC68	PC69	PC70	PC71	PC72	PC73
Standard deviation	3.092e-05	3.05e-05	2.781e-05	2.689e-05	2.671e-05	2.555e-05	2.345e-05	2.276e-05	2.218e-05
Proportion of Variance	0.000e+00	0.00e+00	0.000e+00	0.000e+00	0.000e+00	0.000e+00	0.000e+00	0.000e+00	0.000e+00
Cumulative Proportion	1.000e+00	1.00e+00	1.000e+00	1.000e+00	1.000e+00	1.000e+00	1.000e+00	1.000e+00	1.000e+00

	PC74	PC75	PC76	PC77	PC78	PC79	PC80	PC81	PC82
Standard deviation	2.092e-05	2.080e-05	2.070e-05	1.952e-05	1.851e-05	1.78e-05	1.742e-05	1.718e-05	1.546e-05
Proportion of Variance	0.000e+00	0.000e+00	0.000e+00	0.000e+00	0.000e+00	0.00e+00	0.000e+00	0.000e+00	0.000e+00
Cumulative Proportion	1.000e+00	1.000e+00	1.000e+00	1.000e+00	1.000e+00	1.00e+00	1.000e+00	1.000e+00	1.000e+00

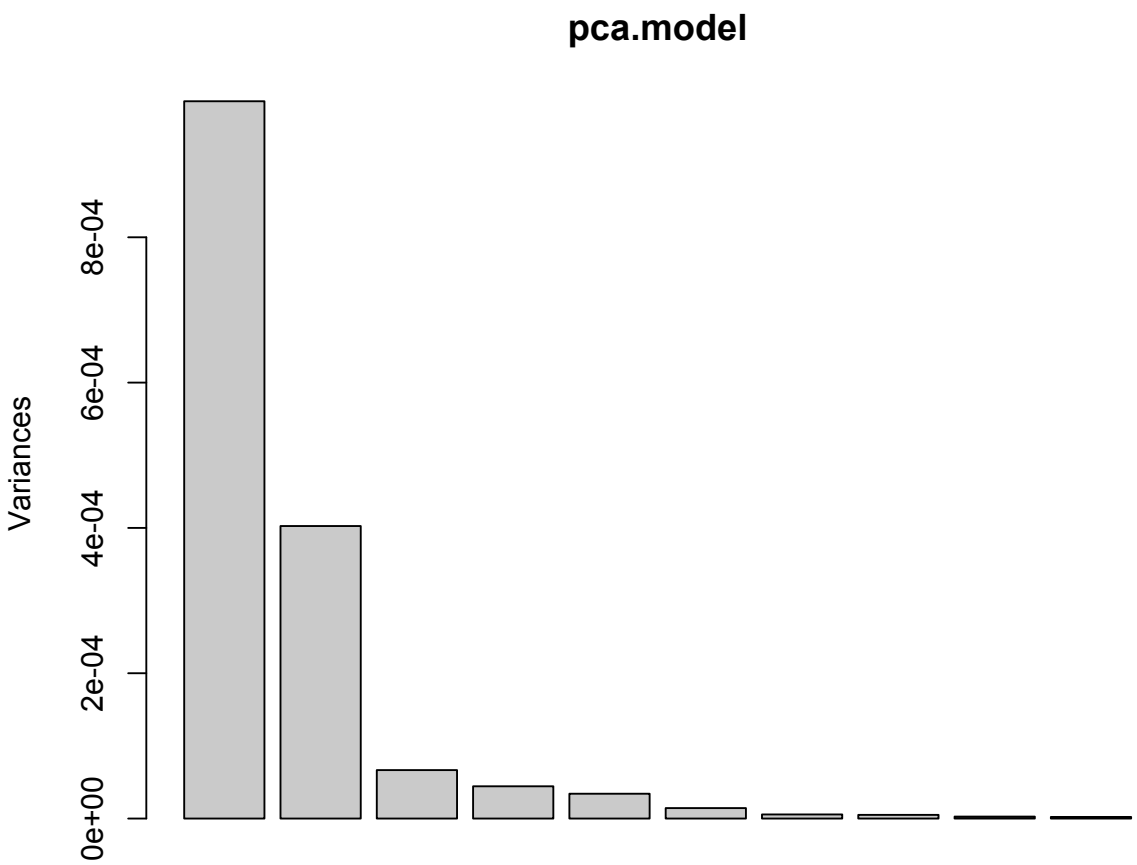


Figure 175: PCA scree plot for the first set of 10 container glass first derivative (9-point smoothing) spectra (10 replicates), centered.

Table 187: PCA results for the first set of 10 container glass first derivative (9-point smoothing) spectra (10 replicates), autoscaled.

	PC1	PC2	PC3	PC4	PC5	PC6	PC7	PC8	PC9	PC10	PC11	PC12
Standard deviation	12.542	9.0279	5.42829	4.35483	3.39834	2.64477	2.4774	1.70839	1.37422	1.17430	0.96042	0.92952
Proportion of Variance	0.487	0.2523	0.09123	0.05871	0.03575	0.02166	0.0190	0.00904	0.00585	0.00427	0.00286	0.00267
Cumulative Proportion	0.487	0.7393	0.83056	0.88928	0.92503	0.94669	0.9657	0.97473	0.98057	0.98484	0.98770	0.99037

	PC13	PC14	PC15	PC16	PC17	PC18	PC19	PC20	PC21	PC22	PC23
Standard deviation	0.77814	0.58869	0.53313	0.49056	0.42776	0.41173	0.36820	0.3114	0.29194	0.28686	0.26344
Proportion of Variance	0.00187	0.00107	0.00088	0.00075	0.00057	0.00052	0.00042	0.0003	0.00026	0.00025	0.00021
Cumulative Proportion	0.99225	0.99332	0.99420	0.99494	0.99551	0.99604	0.99646	0.9968	0.99702	0.99727	0.99749

	PC24	PC25	PC26	PC27	PC28	PC29	PC30	PC31	PC32	PC33	PC34
Standard deviation	0.24955	0.24350	0.23767	0.22950	0.21885	0.20562	0.18918	0.18715	0.1811	0.16535	0.15940
Proportion of Variance	0.00019	0.00018	0.00017	0.00016	0.00015	0.00013	0.00011	0.00011	0.0001	0.00008	0.00008
Cumulative Proportion	0.99768	0.99787	0.99804	0.99820	0.99835	0.99848	0.99859	0.99870	0.9988	0.99889	0.99897

	PC35	PC36	PC37	PC38	PC39	PC40	PC41	PC42	PC43	PC44	PC45
Standard deviation	0.15775	0.15529	0.14378	0.13294	0.13099	0.12530	0.12345	0.12245	0.11736	0.11129	0.10294
Proportion of Variance	0.00008	0.00007	0.00006	0.00005	0.00005	0.00005	0.00005	0.00005	0.00004	0.00004	0.00003
Cumulative Proportion	0.99904	0.99912	0.99918	0.99924	0.99929	0.99934	0.99939	0.99943	0.99948	0.99951	0.99955

	PC46	PC47	PC48	PC49	PC50	PC51	PC52	PC53	PC54	PC55	PC56
Standard deviation	0.10246	0.09771	0.09113	0.08932	0.08618	0.08316	0.07856	0.07516	0.07356	0.07215	0.07141
Proportion of Variance	0.00003	0.00003	0.00003	0.00002	0.00002	0.00002	0.00002	0.00002	0.00002	0.00002	0.00002
Cumulative Proportion	0.99958	0.99961	0.99963	0.99966	0.99968	0.99970	0.99972	0.99974	0.99976	0.99977	0.99979

	PC57	PC58	PC59	PC60	PC61	PC62	PC63	PC64	PC65	PC66	PC67
Standard deviation	0.06987	0.06864	0.06544	0.06175	0.06097	0.05658	0.05551	0.05455	0.05203	0.05067	0.05027
Proportion of Variance	0.00002	0.00001	0.00001	0.00001	0.00001	0.00001	0.00001	0.00001	0.00001	0.00001	0.00001
Cumulative Proportion	0.99980	0.99982	0.99983	0.99984	0.99985	0.99986	0.99987	0.99988	0.99989	0.99990	0.99991

	PC68	PC69	PC70	PC71	PC72	PC73	PC74	PC75	PC76	PC77	PC78
Standard deviation	0.04922	0.04783	0.04501	0.04493	0.04333	0.04110	0.03913	0.03799	0.03662	0.03525	0.03482
Proportion of Variance	0.00001	0.00001	0.00001	0.00001	0.00001	0.00001	0.00000	0.00000	0.00000	0.00000	0.00000
Cumulative Proportion	0.99992	0.99992	0.99993	0.99993	0.99994	0.99995	0.99995	0.99996	0.99996	0.99996	0.99997

	PC79	PC80	PC81	PC82	PC83	PC84	PC85	PC86	PC87	PC88	PC89
Standard deviation	0.03350	0.03132	0.03079	0.02951	0.02788	0.02667	0.02463	0.02333	0.02252	0.02157	0.02099
Proportion of Variance	0.00000	0.00000	0.00000	0.00000	0.00000	0.00000	0.00000	0.00000	0.00000	0.00000	0.00000
Cumulative Proportion	0.99997	0.99997	0.99998	0.99998	0.99998	0.99998	0.99999	0.99999	0.99999	0.99999	0.99999

	PC90	PC91	PC92	PC93	PC94	PC95	PC96	PC97	PC98	PC99	PC100
Standard deviation	0.02014	0.01923	0.01824	0.01776	0.0171	0.01647	0.01476	0.01426	0.01347	0.01279	1.035e-14
Proportion of Variance	0.00000	0.00000	0.00000	0.00000	0.0000	0.00000	0.00000	0.00000	0.00000	0.00000	0.000e+00
Cumulative Proportion	0.99999	0.99999	0.99999	1.00000	1.0000	1.00000	1.00000	1.00000	1.00000	1.00000	1.000e+00

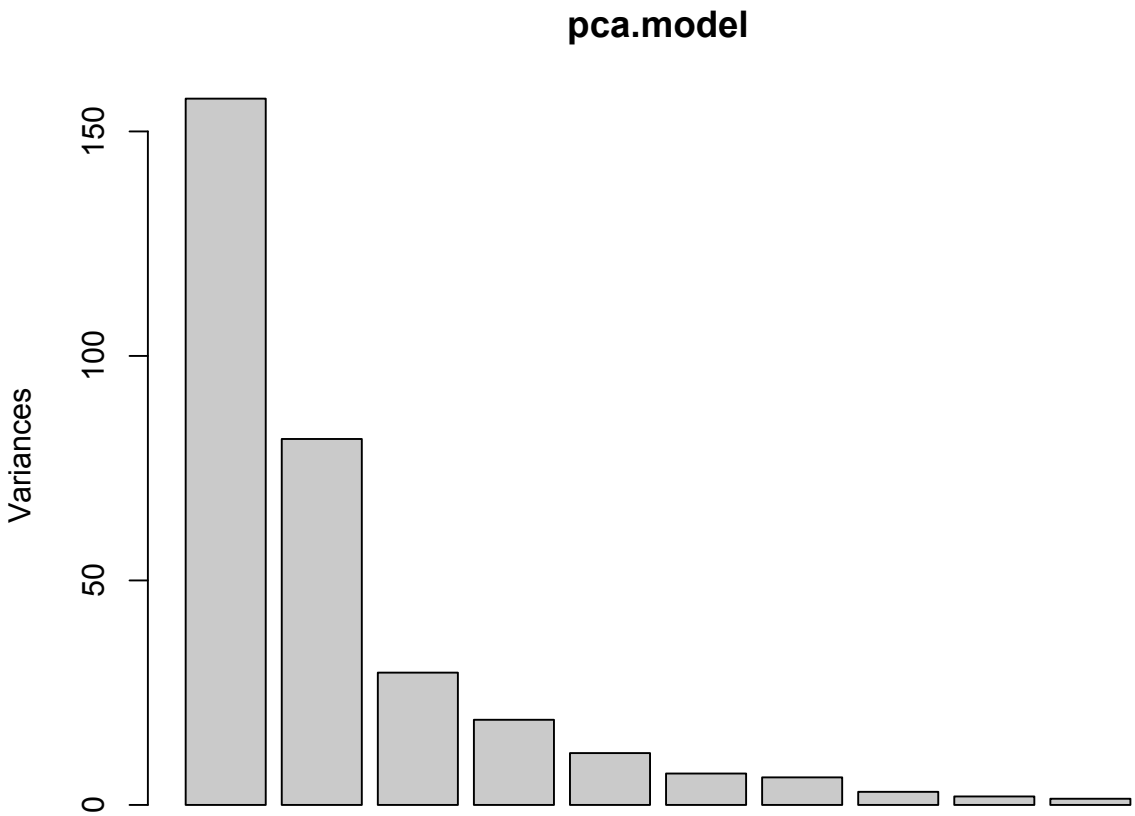


Figure 176: PCA scree plot for the first set of 10 container glass first derivative (9-point smoothing) spectra (10 replicates), autoscaled.

F. PCA Results for the Second Derivative Spectra (5-Point Smoothing)

Table 188: PCA results for the first set of 30 glass second derivative (5-point smoothing) spectra (10 replicates), no data pretreatment.

Importance of components:

	PC1	PC2	PC3	PC4	PC5	PC6	PC7	PC8	PC9	PC10
Standard deviation	0.01539	0.003055	0.002545	0.001765	0.001480	0.001176	0.0009787	0.0008727	0.0007437	0.0007032
Proportion of Variance	0.88119	0.034730	0.024090	0.011590	0.008150	0.005150	0.0035600	0.0028300	0.0020600	0.0018400
Cumulative Proportion	0.88119	0.915920	0.940010	0.951590	0.959740	0.964890	0.9684500	0.9712800	0.9733400	0.9751800

	PC11	PC12	PC13	PC14	PC15	PC16	PC17	PC18	PC19
Standard deviation	0.000604	0.0005799	0.0005565	0.0005464	0.000529	0.0005053	0.0004817	0.0004617	0.0004512
Proportion of Variance	0.001360	0.0012500	0.0011500	0.0011100	0.001040	0.0009500	0.0008600	0.0007900	0.0007600
Cumulative Proportion	0.976540	0.9777900	0.9789400	0.9800500	0.981090	0.9820400	0.9829100	0.9837000	0.9844600

	PC20	PC21	PC22	PC23	PC24	PC25	PC26	PC27	PC28
Standard deviation	0.0004392	0.000432	0.0004289	0.0004021	0.0004003	0.0003904	0.0003822	0.0003742	0.0003567
Proportion of Variance	0.0007200	0.000690	0.0006800	0.0006000	0.0006000	0.0005700	0.0005400	0.0005200	0.0004700
Cumulative Proportion	0.9851800	0.985870	0.9865500	0.9871600	0.9877500	0.9883200	0.9888600	0.9893800	0.9898600

	PC29	PC30	PC31	PC32	PC33	PC34	PC35	PC36	PC37
Standard deviation	0.0003503	0.0003405	0.0003323	0.0003264	0.0003159	0.0003126	0.0003018	0.0002920	0.0002875
Proportion of Variance	0.0004600	0.0004300	0.0004100	0.0004000	0.0003700	0.0003600	0.0003400	0.0003200	0.0003100
Cumulative Proportion	0.9903100	0.9907400	0.9911600	0.9915500	0.9919200	0.9922900	0.9926300	0.9929400	0.9932500

	PC38	PC39	PC40	PC41	PC42	PC43	PC44	PC45	PC46
Standard deviation	0.0002825	0.0002693	0.0002661	0.0002571	0.0002547	0.0002537	0.0002426	0.0002362	0.0002321
Proportion of Variance	0.0003000	0.0002700	0.0002600	0.0002500	0.0002400	0.0002400	0.0002200	0.0002100	0.0002000
Cumulative Proportion	0.9935500	0.9938200	0.9940800	0.9943300	0.9945700	0.9948100	0.9950300	0.9952300	0.9954300

	PC47	PC48	PC49	PC50	PC51	PC52	PC53	PC54	PC55
Standard deviation	0.0002247	0.0002188	0.0002108	0.0002083	0.0002066	0.0001965	0.0001931	0.0001921	0.0001872
Proportion of Variance	0.0001900	0.0001800	0.0001700	0.0001600	0.0001600	0.0001400	0.0001400	0.0001400	0.0001300
Cumulative Proportion	0.9956200	0.9958000	0.9959700	0.9961300	0.9962900	0.9964300	0.9965700	0.9967100	0.9968400

	PC56	PC57	PC58	PC59	PC60	PC61	PC62	PC63	PC64
Standard deviation	0.0001839	0.0001821	0.0001770	0.0001756	0.0001660	0.0001654	0.0001629	0.0001612	0.0001574
Proportion of Variance	0.0001300	0.0001200	0.0001200	0.0001100	0.0001000	0.0001000	0.0001000	0.0001000	0.0000900
Cumulative Proportion	0.9969600	0.9970800	0.9972000	0.9973200	0.9974200	0.9975200	0.9976200	0.9977200	0.9978100

	PC65	PC66	PC67	PC68	PC69	PC70	PC71	PC72	PC73
Standard deviation	0.0001559	0.0001531	0.0001462	0.0001420	0.0001390	0.0001374	0.0001335	0.0001296	0.0001286
Proportion of Variance	0.0000900	0.0000900	0.0000800	0.0000800	0.0000700	0.0000700	0.0000700	0.0000600	0.0000600
Cumulative Proportion	0.9979000	0.9979900	0.9980700	0.9981400	0.9982100	0.9982800	0.9983500	0.9984100	0.9984700

	PC74	PC75	PC76	PC77	PC78	PC79	PC80	PC81	PC82
Standard deviation	0.0001256	0.0001219	0.0001199	0.0001189	0.0001152	0.0001139	0.0001113	0.0001102	0.0001080
Proportion of Variance	0.0000600	0.0000600	0.0000500	0.0000500	0.0000500	0.0000500	0.0000500	0.0000500	0.0000400
Cumulative Proportion	0.9985300	0.9985900	0.9986400	0.9986900	0.9987400	0.9987900	0.9988400	0.9988800	0.9989200

	PC83	PC84	PC85	PC86	PC87	PC88	PC89	PC90	PC91
Standard deviation	0.0001072	0.0001067	0.0001028	0.0001004	9.942e-05	9.657e-05	9.556e-05	0.0000929	9.197e-05
Proportion of Variance	0.0000400	0.0000400	0.0000400	0.0000400	4.000e-05	3.000e-05	3.000e-05	0.0000300	3.000e-05
Cumulative Proportion	0.9989700	0.9990100	0.9990500	0.9990900	9.991e-01	9.992e-01	9.992e-01	0.9992200	9.993e-01

	PC92	PC93	PC94	PC95	PC96	PC97	PC98	PC99	PC100
Standard deviation	8.955e-05	8.825e-05	8.772e-05	8.579e-05	8.288e-05	8.031e-05	7.928e-05	0.0000778	0.0000757
Proportion of Variance	3.000e-05	3.000e-05	3.000e-05	3.000e-05	3.000e-05	2.000e-05	2.000e-05	0.0000200	0.0000200
Cumulative Proportion	9.993e-01	9.993e-01	9.993e-01	9.994e-01	9.994e-01	9.994e-01	9.994e-01	0.9994700	0.9994900

	PC101	PC102	PC103	PC104	PC105	PC106	PC107	PC108	PC109
Standard deviation	7.306e-05	7.228e-05	7.156e-05	7.045e-05	6.914e-05	6.609e-05	6.429e-05	6.249e-05	6.089e-05
Proportion of Variance	2.000e-05	2.000e-05	2.000e-05	2.000e-05	2.000e-05	2.000e-05	2.000e-05	1.000e-05	1.000e-05
Cumulative Proportion	9.995e-01	9.995e-01	9.996e-01	9.996e-01	9.996e-01	9.996e-01	9.996e-01	9.996e-01	9.996e-01

	PC110	PC111	PC112	PC113	PC114	PC115	PC116	PC117	PC118
Standard deviation	5.999e-05	5.882e-05	5.773e-05	0.0000561	5.546e-05	5.494e-05	5.203e-05	5.175e-05	5.018e-05
Proportion of Variance	1.000e-05	1.000e-05	1.000e-05	0.0000100	1.000e-05	1.000e-05	1.000e-05	1.000e-05	1.000e-05
Cumulative Proportion	9.997e-01	9.997e-01	9.997e-01	0.9996900	9.997e-01	9.997e-01	9.997e-01	9.997e-01	9.997e-01

	PC119	PC120	PC121	PC122	PC123	PC124	PC125	PC126	PC127
Standard deviation	4.938e-05	4.864e-05	4.759e-05	4.674e-05	4.562e-05	4.532e-05	4.474e-05	4.409e-05	4.314e-05
Proportion of Variance	1.000e-05	1.000e-05	1.000e-05	1.000e-05	1.000e-05	1.000e-05	1.000e-05	1.000e-05	1.000e-05
Cumulative Proportion	9.998e-01	9.998e-01	9.998e-01	9.998e-01	9.998e-01	9.998e-01	9.998e-01	9.998e-01	9.998e-01

	PC128	PC129	PC130	PC131	PC132	PC133	PC134	PC135	PC136
Standard deviation	4.208e-05	4.154e-05	4.084e-05	3.983e-05	3.949e-05	3.852e-05	0.0000381	3.741e-05	3.646e-05
Proportion of Variance	1.000e-05	1.000e-05	1.000e-05	1.000e-05	1.000e-05	1.000e-05	0.0000100	1.000e-05	0.000e+00
Cumulative Proportion	9.998e-01	9.998e-01	9.998e-01	9.998e-01	9.999e-01	9.999e-01	0.9998600	9.999e-01	9.999e-01

	PC137	PC138	PC139	PC140	PC141	PC142	PC143	PC144	PC145
Standard deviation	3.615e-05	3.471e-05	3.442e-05	3.413e-05	3.358e-05	3.299e-05	3.237e-05	3.191e-05	3.147e-05
Proportion of Variance	0.000e+00	0.000e+00	0.000e+00	0.000e+00	0.000e+00	0.000e+00	0.000e+00	0.000e+00	0.000e+00
Cumulative Proportion	9.999e-01	9.999e-01	9.999e-01	9.999e-01	9.999e-01	9.999e-01	9.999e-01	9.999e-01	9.999e-01

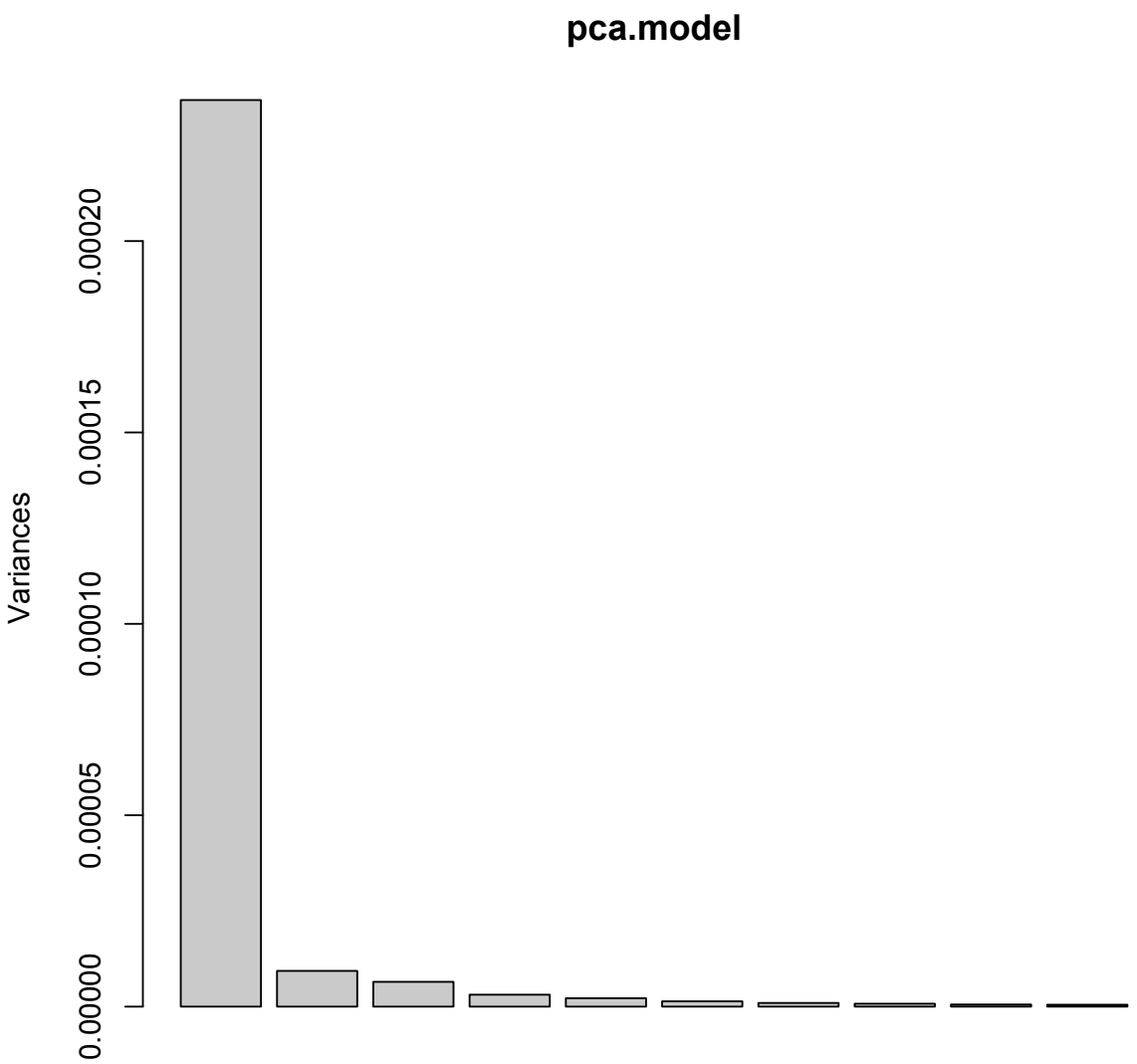


Figure 177: PCA scree plot for the first set of 30 glass second derivative (5-point smoothing) spectra (10 replicates), no data pretreatment.

Table 189: PCA results for the first set of 30 glass second derivative (5-point smoothing) spectra (10 replicates), centered.

Importance of components:

	PC1	PC2	PC3	PC4	PC5	PC6	PC7	PC8	PC9	PC10
Standard deviation	0.003618	0.003030	0.002262	0.001578	0.001182	0.001011	0.0009753	0.00075	0.0007044	0.000604
Proportion of Variance	0.318630	0.223600	0.124590	0.060650	0.034030	0.024890	0.0231600	0.01369	0.0120800	0.008880
Cumulative Proportion	0.318630	0.542230	0.666820	0.727470	0.761500	0.786390	0.8095500	0.82325	0.8353300	0.844210

	PC11	PC12	PC13	PC14	PC15	PC16	PC17	PC18	PC19
Standard deviation	0.0005858	0.0005596	0.0005474	0.0005302	0.0005057	0.0004819	0.0004618	0.000459	0.0004396
Proportion of Variance	0.0083600	0.0076300	0.0073000	0.0068500	0.0062300	0.0056500	0.0051900	0.005130	0.0047100
Cumulative Proportion	0.8525600	0.8601900	0.8674900	0.8743300	0.8805600	0.8862100	0.8914000	0.896530	0.9012400

	PC20	PC21	PC22	PC23	PC24	PC25	PC26	PC27	PC28
Standard deviation	0.0004388	0.0004294	0.0004102	0.000401	0.0003969	0.0003902	0.0003742	0.0003572	0.0003525
Proportion of Variance	0.0046900	0.0044900	0.0041000	0.003920	0.0038300	0.0037100	0.0034100	0.0031100	0.0030300
Cumulative Proportion	0.9059300	0.9104200	0.9145100	0.918430	0.9222600	0.9259700	0.9293800	0.9324900	0.9355100

	PC29	PC30	PC31	PC32	PC33	PC34	PC35	PC36	PC37
Standard deviation	0.0003419	0.0003325	0.0003265	0.0003192	0.0003138	0.0003068	0.0002966	0.0002919	0.0002826
Proportion of Variance	0.0028500	0.0026900	0.0026000	0.0024800	0.0024000	0.0022900	0.0021400	0.0020700	0.0019400
Cumulative Proportion	0.9383600	0.9410500	0.9436500	0.9461300	0.9485200	0.9508200	0.9529600	0.9550300	0.9569800

	PC38	PC39	PC40	PC41	PC42	PC43	PC44	PC45	PC46
Standard deviation	0.0002704	0.0002661	0.0002646	0.0002564	0.0002545	0.0002430	0.0002398	0.0002345	0.0002248
Proportion of Variance	0.0017800	0.0017200	0.0017000	0.0016000	0.0015800	0.0014400	0.0014000	0.0013400	0.0012300
Cumulative Proportion	0.9587600	0.9604800	0.9621900	0.9637900	0.9653600	0.9668000	0.9682000	0.9695400	0.9707700

	PC47	PC48	PC49	PC50	PC51	PC52	PC53	PC54	PC55
Standard deviation	0.0002188	0.0002126	0.0002103	0.0002071	0.0002028	0.0001953	0.0001931	0.0001906	0.0001856
Proportion of Variance	0.0011700	0.0011000	0.0010800	0.0010400	0.0010000	0.0009300	0.0009100	0.0008800	0.0008400
Cumulative Proportion	0.9719300	0.9730300	0.9741100	0.9751600	0.9761600	0.9770900	0.9779900	0.9788800	0.9797200

	PC56	PC57	PC58	PC59	PC60	PC61	PC62	PC63	PC64
Standard deviation	0.0001837	0.0001814	0.0001758	0.0001702	0.0001657	0.0001629	0.0001619	0.0001611	0.0001559
Proportion of Variance	0.0008200	0.0008000	0.0007500	0.0007100	0.0006700	0.0006500	0.0006400	0.0006300	0.0005900
Cumulative Proportion	0.9805400	0.9813400	0.9820900	0.9828000	0.9834700	0.9841100	0.9847500	0.9853800	0.9859700

	PC65	PC66	PC67	PC68	PC69	PC70	PC71	PC72	PC73
Standard deviation	0.0001534	0.0001467	0.0001453	0.0001409	0.0001385	0.0001373	0.0001334	0.0001286	0.0001258
Proportion of Variance	0.0005700	0.0005200	0.0005100	0.0004800	0.0004700	0.0004600	0.0004300	0.0004000	0.0003900
Cumulative Proportion	0.9865500	0.9870700	0.9875800	0.9880700	0.9885300	0.9889900	0.9894300	0.9898300	0.9902200

	PC74	PC75	PC76	PC77	PC78	PC79	PC80	PC81	PC82
Standard deviation	0.0001223	0.0001209	0.0001199	0.0001185	0.0001150	0.0001113	0.0001108	0.0001094	0.0001073
Proportion of Variance	0.0003600	0.0003600	0.0003500	0.0003400	0.0003200	0.0003000	0.0003000	0.0002900	0.0002800
Cumulative Proportion	0.9905800	0.9909400	0.9912900	0.9916300	0.9919500	0.9922500	0.9925500	0.9928400	0.9931200

	PC83	PC84	PC85	PC86	PC87	PC88	PC89	PC90	PC91
Standard deviation	0.0001067	0.0001036	0.0001024	0.0000996	9.661e-05	9.575e-05	9.507e-05	9.243e-05	8.955e-05
Proportion of Variance	0.0002800	0.0002600	0.0002600	0.0002400	2.300e-04	2.200e-04	2.200e-04	2.100e-04	2.000e-04
Cumulative Proportion	0.9934000	0.9936600	0.9939100	0.9941600	9.944e-01	9.946e-01	9.948e-01	9.950e-01	9.952e-01

	PC92	PC93	PC94	PC95	PC96	PC97	PC98	PC99	PC100
Standard deviation	8.825e-05	8.787e-05	0.0000858	8.396e-05	0.0000817	7.992e-05	7.854e-05	7.582e-05	7.478e-05
Proportion of Variance	1.900e-04	1.900e-04	0.0001800	1.700e-04	0.0001600	1.600e-04	1.500e-04	1.400e-04	1.400e-04
Cumulative Proportion	9.954e-01	9.956e-01	0.9957900	9.960e-01	0.9961200	9.963e-01	9.964e-01	9.966e-01	9.967e-01

	PC101	PC102	PC103	PC104	PC105	PC106	PC107	PC108	PC109
Standard deviation	7.282e-05	7.187e-05	7.107e-05	6.964e-05	6.911e-05	6.511e-05	6.401e-05	6.169e-05	6.055e-05
Proportion of Variance	1.300e-04	1.300e-04	1.200e-04	1.200e-04	1.200e-04	1.000e-04	1.000e-04	9.000e-05	9.000e-05
Cumulative Proportion	9.968e-01	9.970e-01	9.971e-01	9.972e-01	9.973e-01	9.974e-01	9.975e-01	9.976e-01	9.977e-01

	PC110	PC111	PC112	PC113	PC114	PC115	PC116	PC117	PC118
Standard deviation	5.893e-05	5.801e-05	5.768e-05	5.586e-05	5.534e-05	5.386e-05	0.0000519	5.174e-05	5.017e-05
Proportion of Variance	8.000e-05	8.000e-05	8.000e-05	8.000e-05	7.000e-05	7.000e-05	0.0000700	7.000e-05	6.000e-05
Cumulative Proportion	9.978e-01	9.979e-01	9.980e-01	9.980e-01	9.981e-01	9.982e-01	0.9982300	9.983e-01	9.984e-01

	PC119	PC120	PC121	PC122	PC123	PC124	PC125	PC126	PC127
Standard deviation	4.933e-05	4.824e-05	4.674e-05	4.627e-05	4.543e-05	4.492e-05	4.424e-05	4.349e-05	4.292e-05
Proportion of Variance	6.000e-05	6.000e-05	5.000e-05	5.000e-05	5.000e-05	5.000e-05	5.000e-05	5.000e-05	4.000e-05
Cumulative Proportion	9.984e-01	9.985e-01	9.985e-01	9.986e-01	9.986e-01	9.987e-01	9.987e-01	9.988e-01	9.988e-01

	PC128	PC129	PC130	PC131	PC132	PC133	PC134	PC135	PC136
Standard deviation	4.207e-05	4.113e-05	3.994e-05	3.976e-05	3.932e-05	3.845e-05	3.773e-05	3.723e-05	3.616e-05
Proportion of Variance	4.000e-05	4.000e-05	4.000e-05	4.000e-05	4.000e-05	4.000e-05	3.000e-05	3.000e-05	3.000e-05
Cumulative Proportion	9.989e-01	9.989e-01	9.989e-01	9.990e-01	9.990e-01	9.991e-01	9.991e-01	9.991e-01	9.992e-01

	PC137	PC138	PC139	PC140	PC141	PC142	PC143	PC144	PC145
Standard deviation	3.478e-05	3.469e-05	0.0000342	3.361e-05	3.348e-05	3.268e-05	3.205e-05	3.147e-05	0.0000309
Proportion of Variance	3.000e-05	3.000e-05	0.0000300	3.000e-05	3.000e-05	3.000e-05	3.000e-05	2.000e-05	0.0000200
Cumulative Proportion	9.992e-01	9.992e-01	0.9992400	9.993e-01	9.993e-01	9.993e-01	9.993e-01	9.994e-01	0.9994000

	PC146	PC147	PC148	PC149	PC150	PC151	PC152	PC153	PC154
Standard deviation	2.999e-05	2.938e-05	2.906e-05	2.858e-05	2.811e-05	2.732e-05	2.688e-05	2.658e-05	2.604e-05
Proportion of Variance	2.000e-05	2.000e-05	2.000e-05	2.000e-05	2.000e-05	2.000e-05	2.000e-05	2.000e-05	2.000e-05
Cumulative Proportion	9.994e-01	9.994e-01	9.995e-01	9.995e-01	9.995e-01	9.995e-01	9.995e-01	9.996e-01	9.996e-01

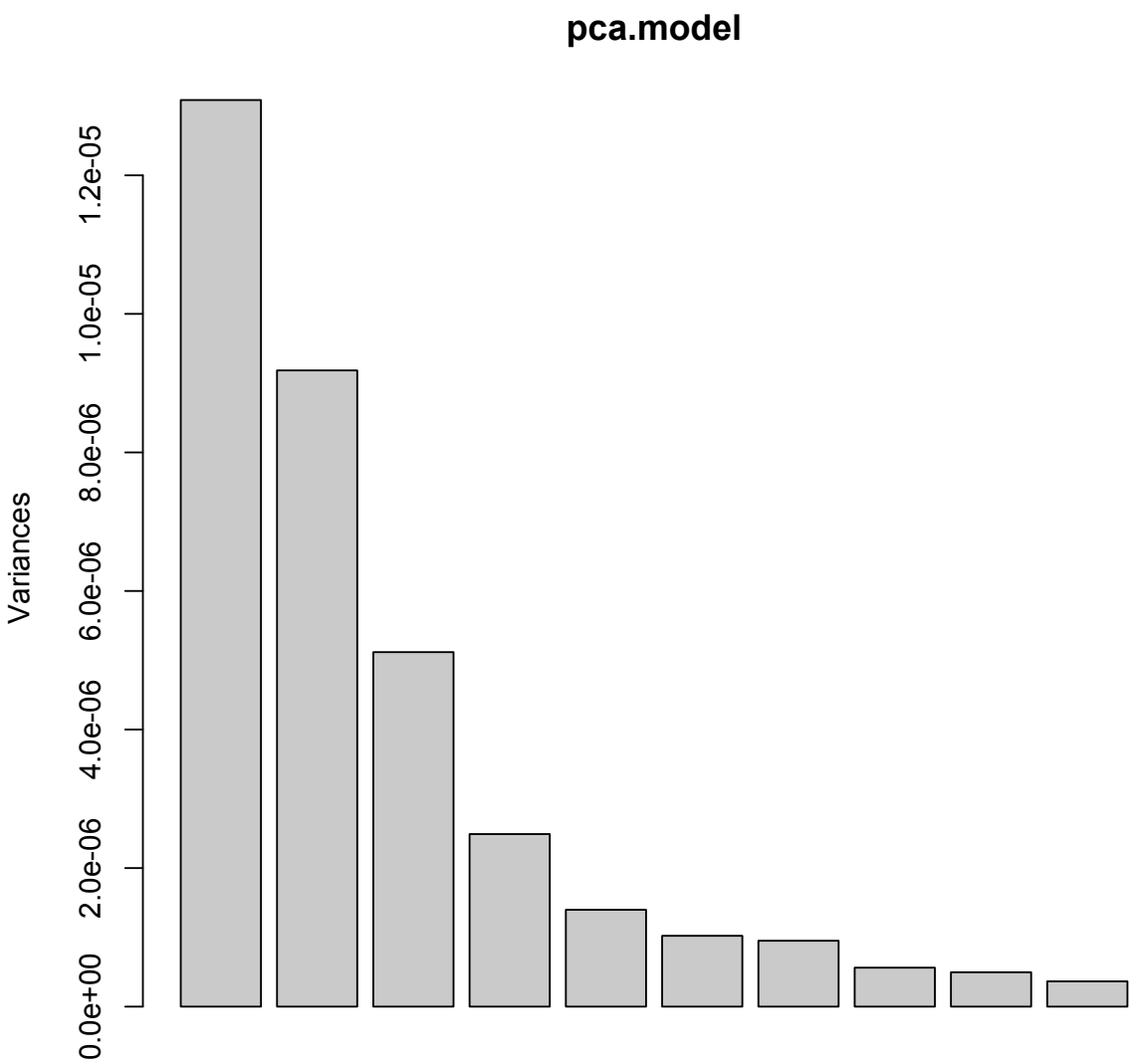


Figure 178. PCA scree plot for the first set of 30 glass second derivative (5-point smoothing) spectra (10 replicates), centered.

Table 190: PCA results for the first set of 30 glass second derivative (5-point smoothing) spectra (10 replicates), autoscaled.

Importance of components:

	PC1	PC2	PC3	PC4	PC5	PC6	PC7	PC8	PC9	PC10	PC11	PC12
Standard deviation	6.2199	4.74565	4.13423	3.29749	3.21165	2.94869	2.87298	2.60711	2.43314	2.3980	2.30990	2.22111
Proportion of Variance	0.1198	0.06973	0.05292	0.03366	0.03193	0.02692	0.02555	0.02104	0.01833	0.0178	0.01652	0.01527
Cumulative Proportion	0.1198	0.18950	0.24241	0.27608	0.30801	0.33493	0.36049	0.38153	0.39986	0.4177	0.43418	0.44945

	PC13	PC14	PC15	PC16	PC17	PC18	PC19	PC20	PC21	PC22	PC23	PC24
Standard deviation	2.15769	2.12150	2.0956	2.08352	1.99895	1.98231	1.94772	1.90441	1.88408	1.85466	1.81451	1.79052
Proportion of Variance	0.01441	0.01393	0.0136	0.01344	0.01237	0.01217	0.01174	0.01123	0.01099	0.01065	0.01019	0.00993
Cumulative Proportion	0.46387	0.47780	0.4914	0.50484	0.51721	0.52937	0.54112	0.55235	0.56334	0.57399	0.58418	0.59411

	PC25	PC26	PC27	PC28	PC29	PC30	PC31	PC32	PC33	PC34	PC35	PC36
Standard deviation	1.77829	1.7519	1.74719	1.70022	1.67830	1.66393	1.65887	1.62533	1.60933	1.58545	1.57625	1.55794
Proportion of Variance	0.00979	0.0095	0.00945	0.00895	0.00872	0.00857	0.00852	0.00818	0.00802	0.00778	0.00769	0.00751
Cumulative Proportion	0.60390	0.6134	0.62285	0.63180	0.64052	0.64909	0.65761	0.66579	0.67381	0.68159	0.68928	0.69680

	PC37	PC38	PC39	PC40	PC41	PC42	PC43	PC44	PC45	PC46	PC47	PC48
Standard deviation	1.54162	1.5245	1.51021	1.48648	1.46631	1.45851	1.44106	1.40186	1.38929	1.37244	1.36748	1.35815
Proportion of Variance	0.00736	0.0072	0.00706	0.00684	0.00666	0.00659	0.00643	0.00608	0.00598	0.00583	0.00579	0.00571
Cumulative Proportion	0.70415	0.7114	0.71841	0.72525	0.73191	0.73849	0.74492	0.75101	0.75698	0.76282	0.76860	0.77432

	PC49	PC50	PC51	PC52	PC53	PC54	PC55	PC56	PC57	PC58	PC59	PC60
Standard deviation	1.34835	1.32656	1.31138	1.29426	1.27879	1.26227	1.24392	1.23021	1.21693	1.19937	1.18718	1.17416
Proportion of Variance	0.00563	0.00545	0.00532	0.00519	0.00506	0.00493	0.00479	0.00469	0.00458	0.00445	0.00436	0.00427
Cumulative Proportion	0.77994	0.78539	0.79072	0.79590	0.80097	0.80590	0.81069	0.81537	0.81996	0.82441	0.82878	0.83304

	PC61	PC62	PC63	PC64	PC65	PC66	PC67	PC68	PC69	PC70	PC71	PC72
Standard deviation	1.1511	1.14752	1.13040	1.11457	1.11255	1.09654	1.09039	1.0781	1.07578	1.06081	1.04872	1.02099
Proportion of Variance	0.0041	0.00408	0.00396	0.00385	0.00383	0.00372	0.00368	0.0036	0.00358	0.00348	0.00341	0.00323
Cumulative Proportion	0.8371	0.84122	0.84518	0.84903	0.85286	0.85658	0.86026	0.8639	0.86744	0.87093	0.87433	0.87756

	PC73	PC74	PC75	PC76	PC77	PC78	PC79	PC80	PC81	PC82	PC83	PC84
Standard deviation	1.01253	1.00513	0.99316	0.98941	0.97321	0.96187	0.94325	0.93758	0.9330	0.91447	0.90407	0.8983
Proportion of Variance	0.00317	0.00313	0.00305	0.00303	0.00293	0.00286	0.00275	0.00272	0.0027	0.00259	0.00253	0.0025
Cumulative Proportion	0.88073	0.88386	0.88691	0.88994	0.89288	0.89574	0.89850	0.90122	0.9039	0.90650	0.90903	0.9115

	PC85	PC86	PC87	PC88	PC89	PC90	PC91	PC92	PC93	PC94	PC95	PC96
Standard deviation	0.88969	0.87766	0.87236	0.85187	0.83489	0.83207	0.81382	0.80642	0.80485	0.79951	0.78075	0.77120
Proportion of Variance	0.00245	0.00238	0.00236	0.00225	0.00216	0.00214	0.00205	0.00201	0.00201	0.00198	0.00189	0.00184
Cumulative Proportion	0.91398	0.91637	0.91872	0.92097	0.92313	0.92527	0.92732	0.92933	0.93134	0.93332	0.93521	0.93705

	PC97	PC98	PC99	PC100	PC101	PC102	PC103	PC104	PC105	PC106	PC107	PC108
Standard deviation	0.76060	0.75687	0.74814	0.73504	0.73174	0.72883	0.71315	0.70095	0.69310	0.68653	0.67824	0.67058
Proportion of Variance	0.00179	0.00177	0.00173	0.00167	0.00166	0.00164	0.00157	0.00152	0.00149	0.00146	0.00142	0.00139
Cumulative Proportion	0.93884	0.94061	0.94234	0.94402	0.94567	0.94732	0.94889	0.95042	0.95190	0.95336	0.95479	0.95618

	PC109	PC110	PC111	PC112	PC113	PC114	PC115	PC116	PC117	PC118	PC119	PC120
Standard deviation	0.65971	0.65747	0.64284	0.63504	0.62856	0.62657	0.61674	0.60807	0.60351	0.5971	0.58549	0.5684
Proportion of Variance	0.00135	0.00134	0.00128	0.00125	0.00122	0.00122	0.00118	0.00114	0.00113	0.0011	0.00106	0.0010
Cumulative Proportion	0.95753	0.95886	0.96014	0.96139	0.96261	0.96383	0.96501	0.96615	0.96728	0.9684	0.96945	0.9705

	PC121	PC122	PC123	PC124	PC125	PC126	PC127	PC128	PC129	PC130	PC131	PC132
Standard deviation	0.56364	0.55899	0.54307	0.53557	0.53203	0.52310	0.52103	0.51588	0.50437	0.49034	0.48589	0.4772
Proportion of Variance	0.00098	0.00097	0.00091	0.00089	0.00088	0.00085	0.00084	0.00082	0.00079	0.00074	0.00073	0.0007
Cumulative Proportion	0.97143	0.97240	0.97331	0.97420	0.97507	0.97592	0.97676	0.97759	0.97837	0.97912	0.97985	0.9806

	PC133	PC134	PC135	PC136	PC137	PC138	PC139	PC140	PC141	PC142	PC143	PC144
Standard deviation	0.46253	0.46026	0.45341	0.44815	0.43670	0.43462	0.42926	0.42318	0.41872	0.40465	0.39754	0.39009
Proportion of Variance	0.00066	0.00066	0.00064	0.00062	0.00059	0.00058	0.00057	0.00055	0.00054	0.00051	0.00049	0.00047
Cumulative Proportion	0.98122	0.98187	0.98251	0.98313	0.98372	0.98431	0.98488	0.98543	0.98597	0.98648	0.98697	0.98744

	PC145	PC146	PC147	PC148	PC149	PC150	PC151	PC152	PC153	PC154	PC155	PC156
Standard deviation	0.38816	0.38259	0.37466	0.36473	0.3610	0.35323	0.34970	0.34176	0.33417	0.32822	0.32192	0.31790
Proportion of Variance	0.00047	0.00045	0.00043	0.00041	0.0004	0.00039	0.00038	0.00036	0.00035	0.00033	0.00032	0.00031
Cumulative Proportion	0.98791	0.98836	0.98879	0.98921	0.9896	0.99000	0.99037	0.99074	0.99108	0.99142	0.99174	0.99205

	PC157	PC158	PC159	PC160	PC161	PC162	PC163	PC164	PC165	PC166	PC167	PC168
Standard deviation	0.31479	0.3123	0.30231	0.29672	0.29334	0.29137	0.28996	0.28413	0.27623	0.26810	0.26293	0.25950
Proportion of Variance	0.00031	0.0003	0.00028	0.00027	0.00027	0.00026	0.00026	0.00025	0.00024	0.00022	0.00021	0.00021
Cumulative Proportion	0.99236	0.9927	0.99294	0.99321	0.99348	0.99374	0.99400	0.99425	0.99449	0.99471	0.99493	0.99513

	PC169	PC170	PC171	PC172	PC173	PC174	PC175	PC176	PC177	PC178	PC179	PC180
Standard deviation	0.25833	0.2538	0.24755	0.24469	0.23441	0.23040	0.22678	0.22004	0.21571	0.21172	0.20648	0.20150
Proportion of Variance	0.00021	0.0002	0.00019	0.00019	0.00017	0.00016	0.00016	0.00015	0.00014	0.00014	0.00013	0.00013
Cumulative Proportion	0.99534	0.9955	0.99573	0.99592	0.99609	0.99625	0.99641	0.99656	0.99670	0.99684	0.99697	0.99710

	PC181	PC182	PC183	PC184	PC185	PC186	PC187	PC188	PC189	PC190	PC191	PC192
Standard deviation	0.19758	0.19325	0.19269	0.18844	0.18520	0.1819	0.1777	0.1753	0.17035	0.16709	0.16631	0.16061
Proportion of Variance	0.00012	0.00012	0.00011	0.00011	0.00011	0.0001	0.0001	0.0001	0.00009	0.00009	0.00009	0.00008
Cumulative Proportion	0.99722	0.99734	0.99745	0.99756	0.99767	0.9978	0.9979	0.9980	0.99805	0.99814	0.99822	0.99830

	PC193	PC194	PC195	PC196	PC197	PC198	PC199	PC200	PC201	PC202	PC203	PC204
Standard deviation	0.15699	0.15400	0.14966	0.14783	0.14569	0.14151	0.13868	0.13608	0.13285	0.13057	0.12688	0.12534
Proportion of Variance	0.00008	0.00007	0.00007	0.00007	0.00007	0.00006	0.00006	0.00006	0.00005	0.00005	0.00005	0.00005
Cumulative Proportion	0.99838	0.99845	0.99852	0.99859	0.99866	0.99872	0.99878	0.99884	0.99889	0.99894	0.99899	0.99904

	PC205	PC206	PC207	PC208	PC209	PC210	PC211	PC212	PC213	PC214	PC215	PC216
Standard deviation	0.12258	0.12050	0.11439	0.11327	0.11041	0.10935	0.10678	0.10293	0.10143	0.09936	0.09798	0.09621
Proportion of Variance	0.00005	0.00004	0.00004	0.00004	0.00004	0.00004	0.00004	0.00003	0.00003	0.00003	0.00003	0.00003
Cumulative Proportion	0.99909	0.99913	0.99917	0.99921	0.99925	0.99929	0.99932	0.99936	0.99939	0.99942	0.99945	0.99948

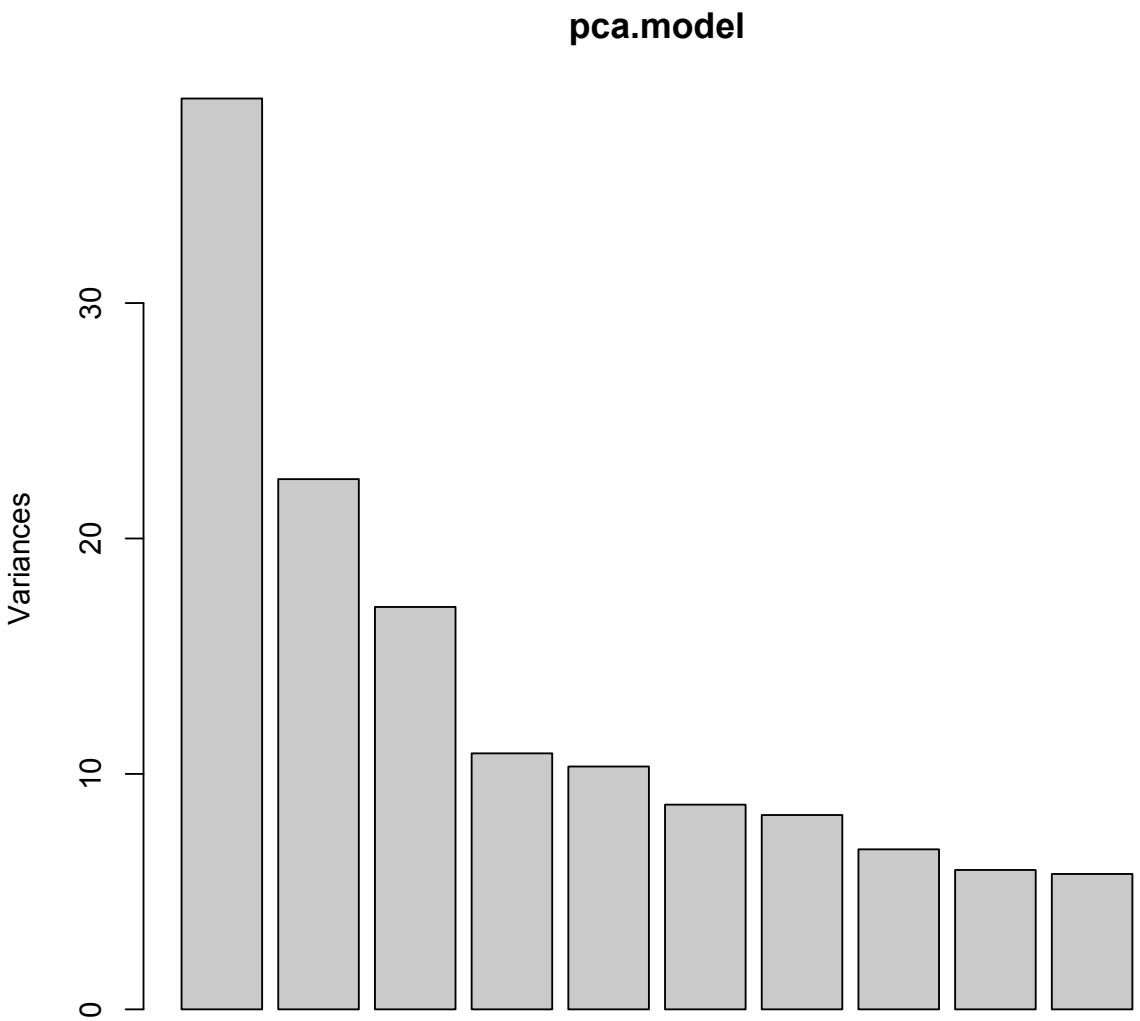


Figure 179: PCA scree plot for the first set of 30 glass second derivative (5-point smoothing) spectra (10 replicates), autoscaled.

Table 191: PCA results for the first set of 20 window glass second derivative (5-point smoothing) spectra (10 replicates), no data pretreatment.

Importance of components:

	PC1	PC2	PC3	PC4	PC5	PC6	PC7	PC8	PC9	PC10
Standard deviation	0.01532	0.002961	0.002387	0.001735	0.001543	0.001128	0.000945	0.0008921	0.0007513	0.0007152
Proportion of Variance	0.88629	0.033080	0.021500	0.011360	0.008990	0.004800	0.003370	0.0030000	0.0021300	0.0019300
Cumulative Proportion	0.88629	0.919370	0.940870	0.952230	0.961220	0.966020	0.969390	0.9723900	0.9745300	0.9764600

	PC11	PC12	PC13	PC14	PC15	PC16	PC17	PC18	PC19
Standard deviation	0.0006121	0.0005901	0.0005473	0.0005387	0.0005267	0.00050	0.000473	0.0004564	0.0004428
Proportion of Variance	0.0014100	0.0013100	0.0011300	0.0011000	0.0010500	0.00094	0.000840	0.0007900	0.0007400
Cumulative Proportion	0.9778700	0.9791800	0.9803100	0.9814100	0.9824600	0.98340	0.984250	0.9850300	0.9857700

	PC20	PC21	PC22	PC23	PC24	PC25	PC26	PC27	PC28
Standard deviation	0.000432	0.0004243	0.0004183	0.0003896	0.0003894	0.0003875	0.0003808	0.0003642	0.0003446
Proportion of Variance	0.000700	0.0006800	0.0006600	0.0005700	0.0005700	0.0005700	0.0005500	0.0005000	0.0004500
Cumulative Proportion	0.986480	0.9871500	0.9878200	0.9883900	0.9889600	0.9895300	0.9900700	0.9905800	0.9910200

	PC29	PC30	PC31	PC32	PC33	PC34	PC35	PC36	PC37
Standard deviation	0.0003383	0.0003349	0.0003277	0.0003129	0.0003018	0.0002941	0.0002839	0.0002819	0.0002792
Proportion of Variance	0.0004300	0.0004200	0.0004100	0.0003700	0.0003400	0.0003300	0.0003000	0.0003000	0.0002900
Cumulative Proportion	0.9914600	0.9918800	0.9922800	0.9926500	0.9930000	0.9933200	0.9936300	0.9939300	0.9942200

	PC38	PC39	PC40	PC41	PC42	PC43	PC44	PC45	PC46
Standard deviation	0.0002691	0.0002627	0.0002558	0.0002420	0.0002387	0.0002371	0.0002330	0.0002255	0.0002163
Proportion of Variance	0.0002700	0.0002600	0.0002500	0.0002200	0.0002200	0.0002100	0.0002000	0.0001900	0.0001800
Cumulative Proportion	0.9945000	0.9947600	0.9950000	0.9952200	0.9954400	0.9956500	0.9958600	0.9960500	0.9962200

	PC47	PC48	PC49	PC50	PC51	PC52	PC53	PC54	PC55
Standard deviation	0.0002143	0.0002089	0.0001998	0.0001959	0.0001853	0.0001845	0.0001774	0.0001768	0.0001716
Proportion of Variance	0.0001700	0.0001600	0.0001500	0.0001400	0.0001300	0.0001300	0.0001200	0.0001200	0.0001100
Cumulative Proportion	0.9964000	0.9965600	0.9967100	0.9968600	0.9969900	0.9971200	0.9972400	0.9973500	0.9974600

	PC56	PC57	PC58	PC59	PC60	PC61	PC62	PC63	PC64
Standard deviation	0.0001712	0.0001639	0.0001591	0.0001585	0.0001531	0.0001510	0.0001490	0.0001462	0.0001435
Proportion of Variance	0.0001100	0.0001000	0.0001000	0.0000900	0.0000900	0.0000900	0.0000800	0.0000800	0.0000800
Cumulative Proportion	0.9975700	0.9976800	0.9977700	0.9978700	0.9979500	0.9980400	0.9981200	0.9982100	0.9982800

	PC65	PC66	PC67	PC68	PC69	PC70	PC71	PC72	PC73
Standard deviation	0.0001399	0.0001361	0.0001344	0.0001332	0.0001292	0.0001224	0.0001218	0.0001203	0.0001151
Proportion of Variance	0.0000700	0.0000700	0.0000700	0.0000700	0.0000600	0.0000600	0.0000600	0.0000500	0.0000500
Cumulative Proportion	0.9983600	0.9984300	0.9985000	0.9985600	0.9986300	0.9986800	0.9987400	0.9987900	0.9988400

	PC74	PC75	PC76	PC77	PC78	PC79	PC80	PC81	PC82
Standard deviation	0.0001148	0.0001140	0.0001113	0.0001097	0.0001072	0.0001051	0.0001032	0.0001002	9.822e-05
Proportion of Variance	0.0000500	0.0000500	0.0000500	0.0000500	0.0000400	0.0000400	0.0000400	0.0000400	4.000e-05
Cumulative Proportion	0.9988900	0.9989400	0.9989900	0.9990300	0.9990800	0.9991200	0.9991600	0.9992000	9.992e-01

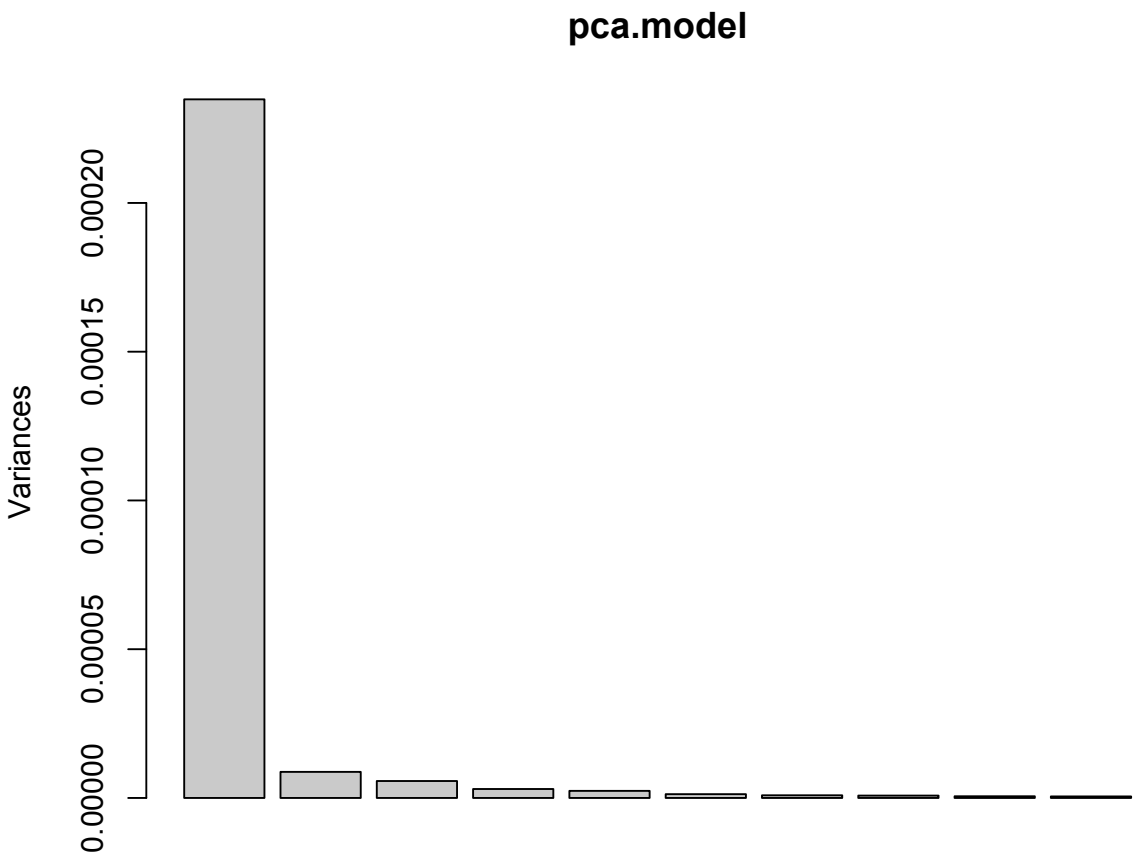


Figure 180: PCA scree plot for the first set of 20 window glass second derivative (5-point smoothing) spectra (10 replicates), no data pretreatment.

Table 192: PCA results for the first set of 20 window glass second derivative (5-point smoothing) spectra (10 replicates), centered.

Importance of components:

	PC1	PC2	PC3	PC4	PC5	PC6	PC7	PC8	PC9
Standard deviation	0.003332	0.002961	0.002186	0.001645	0.001141	0.001035	0.0009264	0.0007577	0.0007188
Proportion of Variance	0.292110	0.230630	0.125740	0.071240	0.034280	0.028200	0.0225800	0.0151100	0.0135900
Cumulative Proportion	0.292110	0.522730	0.648470	0.719710	0.753990	0.782190	0.8047700	0.8198800	0.8334700

	PC10	PC11	PC12	PC13	PC14	PC15	PC16	PC17	PC18
Standard deviation	0.0006203	0.0005909	0.0005496	0.0005391	0.0005272	0.0005008	0.0004731	0.0004569	0.0004517
Proportion of Variance	0.0101200	0.0091900	0.0079500	0.0076500	0.0073100	0.0066000	0.0058900	0.0054900	0.0053700
Cumulative Proportion	0.8436000	0.8527800	0.8607300	0.8683700	0.8756900	0.8822900	0.8881700	0.8936700	0.8990300

	PC19	PC20	PC21	PC22	PC23	PC24	PC25	PC26	PC27
Standard deviation	0.0004372	0.0004319	0.0004233	0.0004003	0.0003895	0.000388	0.0003836	0.0003662	0.0003452
Proportion of Variance	0.0050300	0.0049100	0.0047200	0.0042200	0.0039900	0.003960	0.0038700	0.0035300	0.0031400
Cumulative Proportion	0.9040600	0.9089700	0.9136900	0.9179000	0.9219000	0.925860	0.9297300	0.9332600	0.9363900

	PC28	PC29	PC30	PC31	PC32	PC33	PC34	PC35	PC36
Standard deviation	0.0003385	0.0003357	0.0003293	0.000313	0.0003048	0.0002973	0.0002847	0.0002839	0.0002794
Proportion of Variance	0.0030200	0.0029700	0.0028500	0.002580	0.0024400	0.0023200	0.0021300	0.0021200	0.0020500
Cumulative Proportion	0.9394100	0.9423700	0.9452300	0.947800	0.9502500	0.9525700	0.9547000	0.9568200	0.9588800

	PC37	PC38	PC39	PC40	PC41	PC42	PC43	PC44	PC45
Standard deviation	0.0002708	0.0002643	0.0002567	0.0002529	0.0002389	0.000238	0.0002335	0.0002256	0.0002191
Proportion of Variance	0.0019300	0.0018400	0.0017300	0.0016800	0.0015000	0.001490	0.0014300	0.0013400	0.0012600
Cumulative Proportion	0.9608100	0.9626500	0.9643800	0.9660600	0.9675600	0.969060	0.9704900	0.9718300	0.9730900

	PC46	PC47	PC48	PC49	PC50	PC51	PC52	PC53	PC54
Standard deviation	0.0002148	0.0002092	0.0002026	0.0001966	0.0001904	0.0001852	0.0001832	0.0001774	0.0001761
Proportion of Variance	0.0012100	0.0011500	0.0010800	0.0010200	0.0009500	0.0009000	0.0008800	0.0008300	0.0008200
Cumulative Proportion	0.9743100	0.9754600	0.9765400	0.9775500	0.9785100	0.9794100	0.9802900	0.9811200	0.9819400

	PC55	PC56	PC57	PC58	PC59	PC60	PC61	PC62	PC63
Standard deviation	0.0001715	0.0001679	0.0001635	0.0001585	0.0001564	0.0001522	0.00015	0.0001462	0.0001461
Proportion of Variance	0.0007700	0.0007400	0.0007000	0.0006600	0.0006400	0.0006100	0.00059	0.0005600	0.0005600
Cumulative Proportion	0.9827100	0.9834500	0.9841600	0.9848200	0.9854600	0.9860700	0.98666	0.9872300	0.9877900

	PC64	PC65	PC66	PC67	PC68	PC69	PC70	PC71	PC72
Standard deviation	0.0001421	0.0001395	0.0001347	0.0001342	0.0001306	0.0001230	0.0001222	0.0001212	0.0001191
Proportion of Variance	0.0005300	0.0005100	0.0004800	0.0004700	0.0004500	0.0004000	0.0003900	0.0003900	0.0003700
Cumulative Proportion	0.9883200	0.9888300	0.9893100	0.9897800	0.9902300	0.9906300	0.9910200	0.9914100	0.9917800

	PC73	PC74	PC75	PC76	PC77	PC78	PC79	PC80	PC81
Standard deviation	0.0001150	0.0001145	0.0001121	0.0001098	0.0001083	0.0001055	0.0001033	0.0001011	9.875e-05
Proportion of Variance	0.0003500	0.0003500	0.0003300	0.0003200	0.0003100	0.0002900	0.0002800	0.0002700	2.600e-04
Cumulative Proportion	0.9921300	0.9924700	0.9928100	0.9931200	0.9934300	0.9937200	0.9940000	0.9942700	9.945e-01

	PC82	PC83	PC84	PC85	PC86	PC87	PC88	PC89	PC90
Standard deviation	9.664e-05	9.42e-05	9.248e-05	0.0000913	8.973e-05	8.677e-05	8.49e-05	8.305e-05	8.244e-05
Proportion of Variance	2.500e-04	2.30e-04	2.300e-04	0.0002200	2.100e-04	2.000e-04	1.90e-04	1.800e-04	1.800e-04
Cumulative Proportion	9.948e-01	9.95e-01	9.952e-01	0.9954500	9.957e-01	9.959e-01	9.96e-01	9.962e-01	9.964e-01

	PC91	PC92	PC93	PC94	PC95	PC96	PC97	PC98	PC99
Standard deviation	8.044e-05	7.826e-05	7.521e-05	7.359e-05	7.167e-05	6.957e-05	6.791e-05	6.667e-05	6.627e-05
Proportion of Variance	1.700e-04	1.600e-04	1.500e-04	1.400e-04	1.400e-04	1.300e-04	1.200e-04	1.200e-04	1.200e-04
Cumulative Proportion	9.966e-01	9.968e-01	9.969e-01	9.970e-01	9.972e-01	9.973e-01	9.974e-01	9.975e-01	9.977e-01

	PC100	PC101	PC102	PC103	PC104	PC105	PC106	PC107	PC108
Standard deviation	6.314e-05	6.033e-05	5.987e-05	5.715e-05	5.671e-05	5.559e-05	5.394e-05	5.315e-05	5.174e-05
Proportion of Variance	1.000e-04	1.000e-04	9.000e-05	9.000e-05	8.000e-05	8.000e-05	8.000e-05	7.000e-05	7.000e-05
Cumulative Proportion	9.978e-01	9.979e-01	9.980e-01	9.980e-01	9.981e-01	9.982e-01	9.983e-01	9.983e-01	9.984e-01

	PC109	PC110	PC111	PC112	PC113	PC114	PC115	PC116	PC117
Standard deviation	5.138e-05	4.993e-05	4.931e-05	4.694e-05	4.583e-05	4.565e-05	4.465e-05	4.388e-05	4.374e-05
Proportion of Variance	7.000e-05	7.000e-05	6.000e-05	6.000e-05	6.000e-05	5.000e-05	5.000e-05	5.000e-05	5.000e-05
Cumulative Proportion	9.985e-01	9.986e-01	9.986e-01	9.987e-01	9.987e-01	9.988e-01	9.988e-01	9.989e-01	9.989e-01

	PC118	PC119	PC120	PC121	PC122	PC123	PC124	PC125	PC126
Standard deviation	4.199e-05	4.116e-05	4.056e-05	3.968e-05	3.889e-05	0.000038	3.756e-05	3.678e-05	3.537e-05
Proportion of Variance	5.000e-05	4.000e-05	4.000e-05	4.000e-05	4.000e-05	0.000040	4.000e-05	4.000e-05	3.000e-05
Cumulative Proportion	9.990e-01	9.990e-01	9.991e-01	9.991e-01	9.992e-01	0.999200	9.992e-01	9.993e-01	9.993e-01

	PC127	PC128	PC129	PC130	PC131	PC132	PC133	PC134	PC135
Standard deviation	3.494e-05	3.408e-05	3.368e-05	3.294e-05	3.210e-05	3.123e-05	3.048e-05	3.023e-05	2.933e-05
Proportion of Variance	3.000e-05	3.000e-05	3.000e-05	3.000e-05	3.000e-05	3.000e-05	2.000e-05	2.000e-05	2.000e-05
Cumulative Proportion	9.993e-01	9.994e-01	9.994e-01	9.994e-01	9.994e-01	9.995e-01	9.995e-01	9.995e-01	9.996e-01

	PC136	PC137	PC138	PC139	PC140	PC141	PC142	PC143	PC144
Standard deviation	2.911e-05	2.872e-05	2.776e-05	2.677e-05	2.643e-05	2.590e-05	2.533e-05	2.450e-05	2.437e-05
Proportion of Variance	2.000e-05	2.000e-05	2.000e-05	2.000e-05	2.000e-05	2.000e-05	2.000e-05	2.000e-05	2.000e-05
Cumulative Proportion	9.996e-01	9.996e-01	9.996e-01	9.996e-01	9.997e-01	9.997e-01	9.997e-01	9.997e-01	9.997e-01

	PC145	PC146	PC147	PC148	PC149	PC150	PC151	PC152	PC153
Standard deviation	2.372e-05	0.000023	2.271e-05	2.226e-05	2.173e-05	2.130e-05	2.112e-05	2.064e-05	2.032e-05
Proportion of Variance	1.000e-05	0.000010	1.000e-05	1.000e-05	1.000e-05	1.000e-05	1.000e-05	1.000e-05	1.000e-05
Cumulative Proportion	9.997e-01	0.999740	9.998e-01	9.998e-01	9.998e-01	9.998e-01	9.998e-01	9.998e-01	9.998e-01

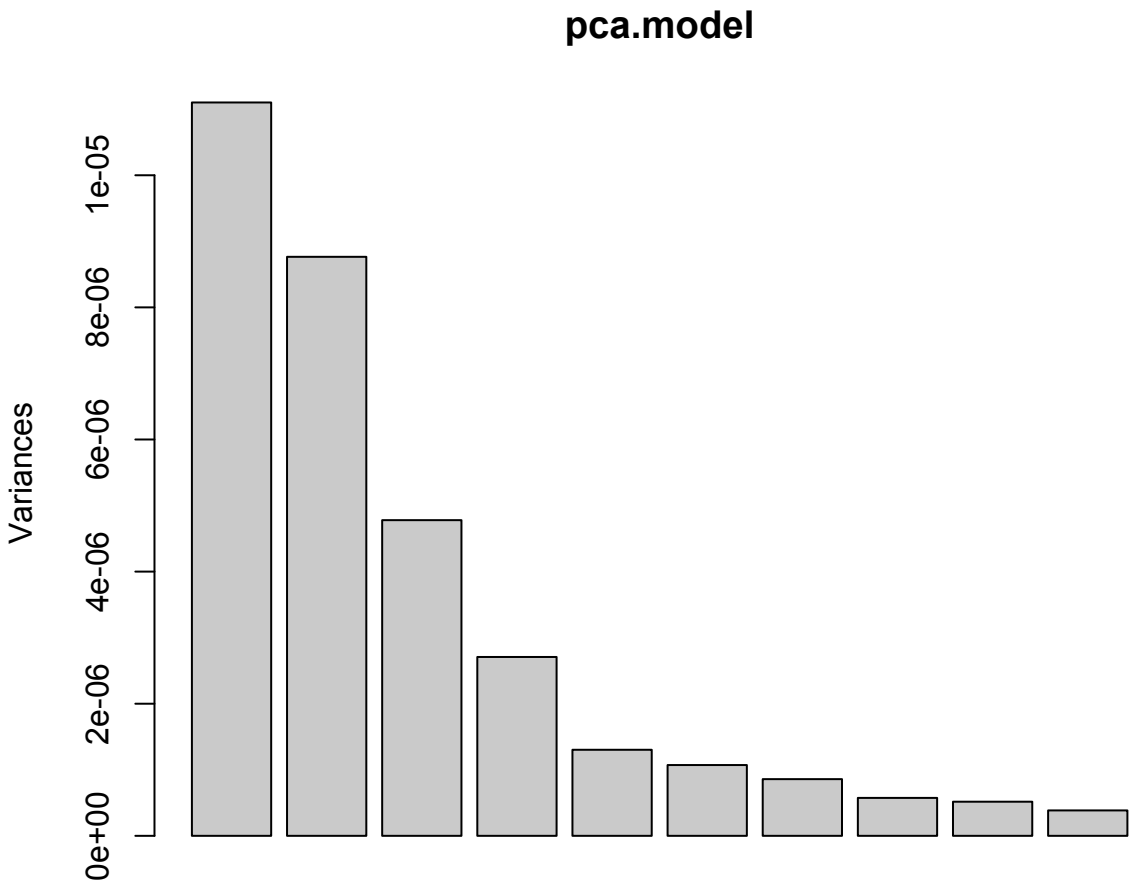


Figure 181: PCA scree plot for the first set of 20 window glass second derivative (5-point smoothing) spectra (10 replicates), centered.

Table 193: PCA results for the first set of 20 window glass second derivative (5-point smoothing) spectra (10 replicates), autoscaled.

Importance of components:

	PC1	PC2	PC3	PC4	PC5	PC6	PC7	PC8	PC9	PC10	PC11
Standard deviation	6.2187	4.47199	3.79180	3.35654	3.14997	3.06266	2.94959	2.73469	2.59266	2.55709	2.46556
Proportion of Variance	0.1197	0.06192	0.04451	0.03488	0.03072	0.02904	0.02694	0.02315	0.02081	0.02024	0.01882
Cumulative Proportion	0.1197	0.18165	0.22616	0.26104	0.29176	0.32080	0.34773	0.37089	0.39170	0.41194	0.43076

	PC12	PC13	PC14	PC15	PC16	PC17	PC18	PC19	PC20	PC21	PC22
Standard deviation	2.34860	2.33748	2.27261	2.20569	2.19039	2.12536	2.06300	2.03266	2.0012	1.98097	1.95778
Proportion of Variance	0.01708	0.01692	0.01599	0.01506	0.01485	0.01398	0.01318	0.01279	0.0124	0.01215	0.01187
Cumulative Proportion	0.44784	0.46475	0.48074	0.49581	0.51066	0.52465	0.53782	0.55061	0.5630	0.57516	0.58703

	PC23	PC24	PC25	PC26	PC27	PC28	PC29	PC30	PC31	PC32	PC33
Standard deviation	1.91653	1.90130	1.88378	1.84452	1.82996	1.79512	1.78014	1.72481	1.71303	1.70415	1.67536
Proportion of Variance	0.01137	0.01119	0.01099	0.01053	0.01037	0.00998	0.00981	0.00921	0.00909	0.00899	0.00869
Cumulative Proportion	0.59840	0.60959	0.62058	0.63111	0.64148	0.65146	0.66127	0.67048	0.67956	0.68855	0.69724

	PC34	PC35	PC36	PC37	PC38	PC39	PC40	PC41	PC42	PC43	PC44
Standard deviation	1.64066	1.63311	1.60334	1.58985	1.56609	1.54815	1.53017	1.49984	1.49770	1.44825	1.43486
Proportion of Variance	0.00833	0.00826	0.00796	0.00783	0.00759	0.00742	0.00725	0.00696	0.00694	0.00649	0.00637
Cumulative Proportion	0.70558	0.71383	0.72179	0.72962	0.73721	0.74463	0.75188	0.75885	0.76579	0.77228	0.77866

	PC45	PC46	PC47	PC48	PC49	PC50	PC51	PC52	PC53	PC54	PC55
Standard deviation	1.41843	1.41007	1.37646	1.37088	1.3572	1.3454	1.32335	1.29707	1.28067	1.26896	1.24355
Proportion of Variance	0.00623	0.00616	0.00587	0.00582	0.0057	0.0056	0.00542	0.00521	0.00508	0.00499	0.00479
Cumulative Proportion	0.78489	0.79104	0.79691	0.80273	0.8084	0.8140	0.81945	0.82466	0.82974	0.83473	0.83951

	PC56	PC57	PC58	PC59	PC60	PC61	PC62	PC63	PC64	PC65	PC66
Standard deviation	1.22708	1.21157	1.20952	1.19809	1.15907	1.14959	1.11928	1.11447	1.10283	1.08664	1.0790
Proportion of Variance	0.00466	0.00454	0.00453	0.00444	0.00416	0.00409	0.00388	0.00385	0.00377	0.00366	0.0036
Cumulative Proportion	0.84418	0.84872	0.85325	0.85769	0.86185	0.86594	0.86982	0.87367	0.87743	0.88109	0.8847

	PC67	PC68	PC69	PC70	PC71	PC72	PC73	PC74	PC75	PC76	PC77
Standard deviation	1.07506	1.06712	1.0477	1.02637	0.99968	0.98954	0.96886	0.95986	0.95002	0.93802	0.92424
Proportion of Variance	0.00358	0.00353	0.0034	0.00326	0.00309	0.00303	0.00291	0.00285	0.00279	0.00272	0.00264
Cumulative Proportion	0.88827	0.89180	0.8952	0.89846	0.90155	0.90458	0.90749	0.91034	0.91313	0.91586	0.91850

	PC78	PC79	PC80	PC81	PC82	PC83	PC84	PC85	PC86	PC87	PC88
Standard deviation	0.9170	0.89474	0.89032	0.87349	0.86562	0.85445	0.84622	0.83791	0.82985	0.81285	0.8042
Proportion of Variance	0.0026	0.00248	0.00245	0.00236	0.00232	0.00226	0.00222	0.00217	0.00213	0.00205	0.0020
Cumulative Proportion	0.9211	0.92359	0.92604	0.92840	0.93072	0.93298	0.93520	0.93737	0.93950	0.94155	0.9435

	PC89	PC90	PC91	PC92	PC93	PC94	PC95	PC96	PC97	PC98	PC99
Standard deviation	0.79460	0.78631	0.75772	0.74969	0.74430	0.73722	0.72220	0.71480	0.70447	0.68110	0.67919
Proportion of Variance	0.00195	0.00191	0.00178	0.00174	0.00172	0.00168	0.00161	0.00158	0.00154	0.00144	0.00143
Cumulative Proportion	0.94551	0.94742	0.94920	0.95094	0.95265	0.95434	0.95595	0.95753	0.95907	0.96051	0.96193

	PC100	PC101	PC102	PC103	PC104	PC105	PC106	PC107	PC108	PC109	PC110
Standard deviation	0.66772	0.65870	0.65553	0.63992	0.62711	0.61856	0.60695	0.59791	0.5966	0.57661	0.57284
Proportion of Variance	0.00138	0.00134	0.00133	0.00127	0.00122	0.00118	0.00114	0.00111	0.0011	0.00103	0.00102
Cumulative Proportion	0.96331	0.96466	0.96599	0.96726	0.96847	0.96966	0.97080	0.97191	0.9730	0.97404	0.97505

	PC111	PC112	PC113	PC114	PC115	PC116	PC117	PC118	PC119	PC120	PC121
Standard deviation	0.55873	0.54173	0.53431	0.53119	0.51914	0.51625	0.5095	0.49846	0.49126	0.48569	0.46799
Proportion of Variance	0.00097	0.00091	0.00088	0.00087	0.00083	0.00083	0.0008	0.00077	0.00075	0.00073	0.00068
Cumulative Proportion	0.97602	0.97693	0.97781	0.97869	0.97952	0.98034	0.9811	0.98192	0.98266	0.98339	0.98407

	PC122	PC123	PC124	PC125	PC126	PC127	PC128	PC129	PC130	PC131	PC132
Standard deviation	0.46160	0.45865	0.45211	0.4387	0.43212	0.42793	0.41002	0.4012	0.4006	0.38892	0.38419
Proportion of Variance	0.00066	0.00065	0.00063	0.0006	0.00058	0.00057	0.00052	0.0005	0.0005	0.00047	0.00046
Cumulative Proportion	0.98473	0.98538	0.98602	0.9866	0.98719	0.98776	0.98828	0.9888	0.9893	0.98974	0.99020

	PC133	PC134	PC135	PC136	PC137	PC138	PC139	PC140	PC141	PC142	PC143
Standard deviation	0.37886	0.37636	0.37201	0.35233	0.34741	0.33797	0.33104	0.32849	0.31910	0.31892	0.3118
Proportion of Variance	0.00044	0.00044	0.00043	0.00038	0.00037	0.00035	0.00034	0.00033	0.00032	0.00031	0.0003
Cumulative Proportion	0.99064	0.99108	0.99151	0.99189	0.99227	0.99262	0.99296	0.99330	0.99361	0.99393	0.9942

	PC144	PC145	PC146	PC147	PC148	PC149	PC150	PC151	PC152	PC153	PC154
Standard deviation	0.30758	0.30006	0.29288	0.29067	0.28790	0.27888	0.26715	0.2571	0.2547	0.24769	0.24523
Proportion of Variance	0.00029	0.00028	0.00027	0.00026	0.00026	0.00024	0.00022	0.0002	0.0002	0.00019	0.00019
Cumulative Proportion	0.99452	0.99480	0.99506	0.99532	0.99558	0.99582	0.99604	0.9962	0.9964	0.99664	0.99682

	PC155	PC156	PC157	PC158	PC159	PC160	PC161	PC162	PC163	PC164	PC165
Standard deviation	0.23711	0.23481	0.23054	0.22435	0.22260	0.21468	0.21171	0.21030	0.20007	0.19529	0.19377
Proportion of Variance	0.00017	0.00017	0.00016	0.00016	0.00015	0.00014	0.00014	0.00014	0.00012	0.00012	0.00012
Cumulative Proportion	0.99700	0.99717	0.99733	0.99749	0.99764	0.99779	0.99792	0.99806	0.99819	0.99830	0.99842

	PC166	PC167	PC168	PC169	PC170	PC171	PC172	PC173	PC174	PC175	PC176
Standard deviation	0.18566	0.1778	0.17425	0.16904	0.16631	0.15927	0.15443	0.15390	0.14930	0.14709	0.14057
Proportion of Variance	0.00011	0.0001	0.00009	0.00009	0.00009	0.00008	0.00007	0.00007	0.00007	0.00007	0.00006
Cumulative Proportion	0.99853	0.9986	0.99872	0.99881	0.99889	0.99897	0.99905	0.99912	0.99919	0.99925	0.99932

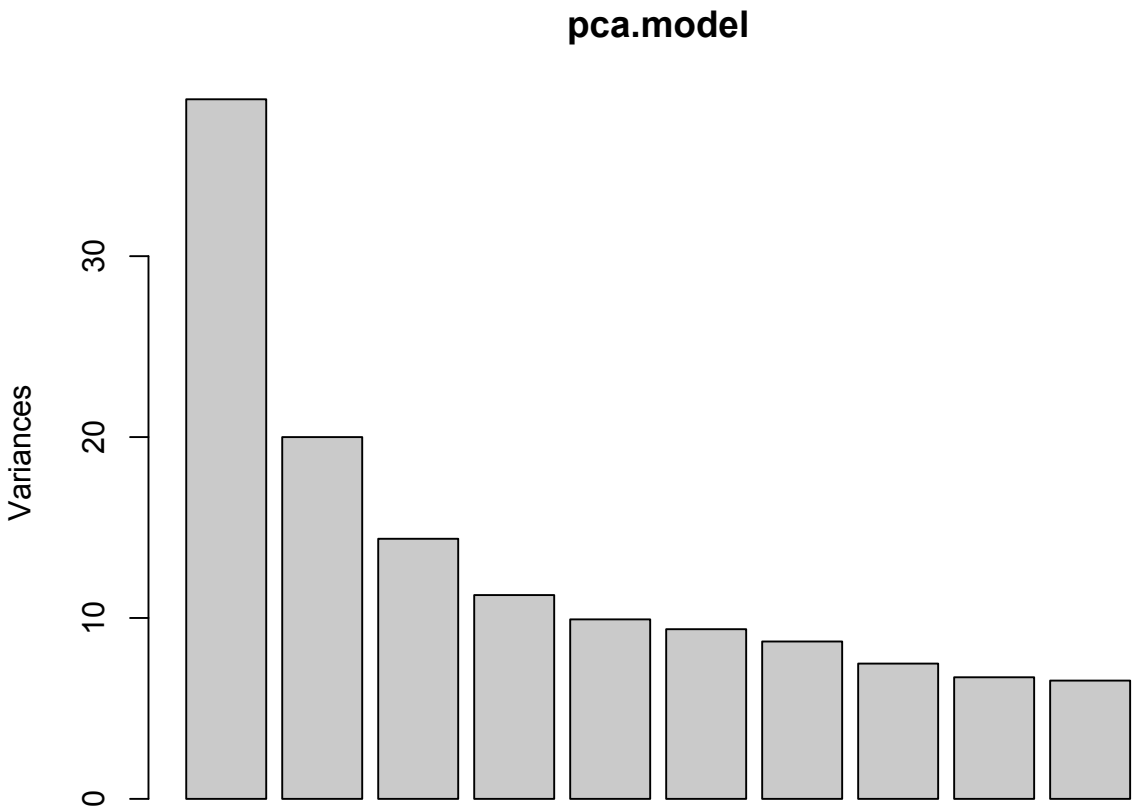


Figure 182: PCA scree plot for the first set of 20 window glass second derivative (5-point smoothing) spectra (10 replicates), autoscaled.

Table 194: PCA results for the first set of 10 container glass second derivative (5-point smoothing) spectra (10 replicates), no data pretreatment.

Importance of components:

	PC1	PC2	PC3	PC4	PC5	PC6	PC7	PC8	PC9	PC10
Standard deviation	0.01565	0.003234	0.002753	0.001867	0.001388	0.001281	0.001102	0.0008225	0.0007685	0.0007426
Proportion of Variance	0.87687	0.037450	0.027140	0.012490	0.006900	0.005880	0.004350	0.0024200	0.0021200	0.0019800
Cumulative Proportion	0.87687	0.914320	0.941460	0.953950	0.960850	0.966730	0.971080	0.9735000	0.9756200	0.9775900

	PC11	PC12	PC13	PC14	PC15	PC16	PC17	PC18	PC19
Standard deviation	0.0006807	0.0006638	0.0006378	0.0005803	0.0005495	0.0005145	0.000501	0.0004865	0.0004694
Proportion of Variance	0.0016600	0.0015800	0.0014600	0.0012100	0.0010800	0.0009500	0.000900	0.0008500	0.0007900
Cumulative Proportion	0.9792500	0.9808300	0.9822900	0.9835000	0.9845800	0.9855300	0.986420	0.9872700	0.9880600

	PC20	PC21	PC22	PC23	PC24	PC25	PC26	PC27	PC28
Standard deviation	0.0004605	0.0004458	0.0004346	0.0004217	0.0003846	0.0003818	0.0003619	0.0003533	0.0003460
Proportion of Variance	0.0007600	0.0007100	0.0006800	0.0006400	0.0005300	0.0005200	0.0004700	0.0004500	0.0004300
Cumulative Proportion	0.9888200	0.9895300	0.9902100	0.9908500	0.9913800	0.9919000	0.9923700	0.9928100	0.9932400

	PC29	PC30	PC31	PC32	PC33	PC34	PC35	PC36	PC37
Standard deviation	0.0003377	0.0003203	0.0003196	0.0003003	0.0002963	0.0002878	0.0002818	0.0002699	0.0002662
Proportion of Variance	0.0004100	0.0003700	0.0003700	0.0003200	0.0003100	0.0003000	0.0002800	0.0002600	0.0002500
Cumulative Proportion	0.9936500	0.9940200	0.9943900	0.9947100	0.9950200	0.9953200	0.9956000	0.9958600	0.9961200

	PC38	PC39	PC40	PC41	PC42	PC43	PC44	PC45	PC46
Standard deviation	0.0002533	0.0002462	0.0002385	0.0002314	0.0002260	0.0002203	0.0002171	0.0002030	0.0001993
Proportion of Variance	0.0002300	0.0002200	0.0002000	0.0001900	0.0001800	0.0001700	0.0001700	0.0001500	0.0001400
Cumulative Proportion	0.9963500	0.9965700	0.9967700	0.9969600	0.9971400	0.9973200	0.9974900	0.9976300	0.9977800

	PC47	PC48	PC49	PC50	PC51	PC52	PC53	PC54	PC55
Standard deviation	0.0001944	0.0001868	0.000182	0.0001738	0.0001712	0.0001690	0.0001616	0.0001549	0.0001507
Proportion of Variance	0.0001400	0.0001200	0.000120	0.0001100	0.0001100	0.0001000	0.0000900	0.0000900	0.0000800
Cumulative Proportion	0.9979100	0.9980400	0.998160	0.9982600	0.9983700	0.9984700	0.9985600	0.9986500	0.9987300

	PC56	PC57	PC58	PC59	PC60	PC61	PC62	PC63	PC64
Standard deviation	0.0001490	0.000145	0.0001434	0.0001338	0.0001312	0.0001302	0.0001272	0.0001238	0.0001195
Proportion of Variance	0.0000800	0.000080	0.0000700	0.0000600	0.0000600	0.0000600	0.0000600	0.0000500	0.0000500
Cumulative Proportion	0.9988100	0.998890	0.9989600	0.9990200	0.9990900	0.9991500	0.9992000	0.9992600	0.9993100

	PC65	PC66	PC67	PC68	PC69	PC70	PC71	PC72	PC73
Standard deviation	0.0001163	0.0001129	0.0001112	0.0001051	0.0001019	9.773e-05	9.404e-05	0.0000929	9.062e-05
Proportion of Variance	0.0000500	0.0000500	0.0000400	0.0000400	0.0000400	3.000e-05	3.000e-05	0.0000300	3.000e-05
Cumulative Proportion	0.9993600	0.9994000	0.9994500	0.9994900	0.9995300	9.996e-01	9.996e-01	0.9996200	9.997e-01

	PC74	PC75	PC76	PC77	PC78	PC79	PC80	PC81	PC82
Standard deviation	8.545e-05	8.247e-05	0.0000809	7.907e-05	7.877e-05	7.564e-05	6.928e-05	6.806e-05	6.767e-05
Proportion of Variance	3.000e-05	2.000e-05	0.0000200	2.000e-05	2.000e-05	2.000e-05	2.000e-05	2.000e-05	2.000e-05
Cumulative Proportion	9.997e-01	9.997e-01	0.9997300	9.998e-01	9.998e-01	9.998e-01	9.998e-01	9.998e-01	9.998e-01

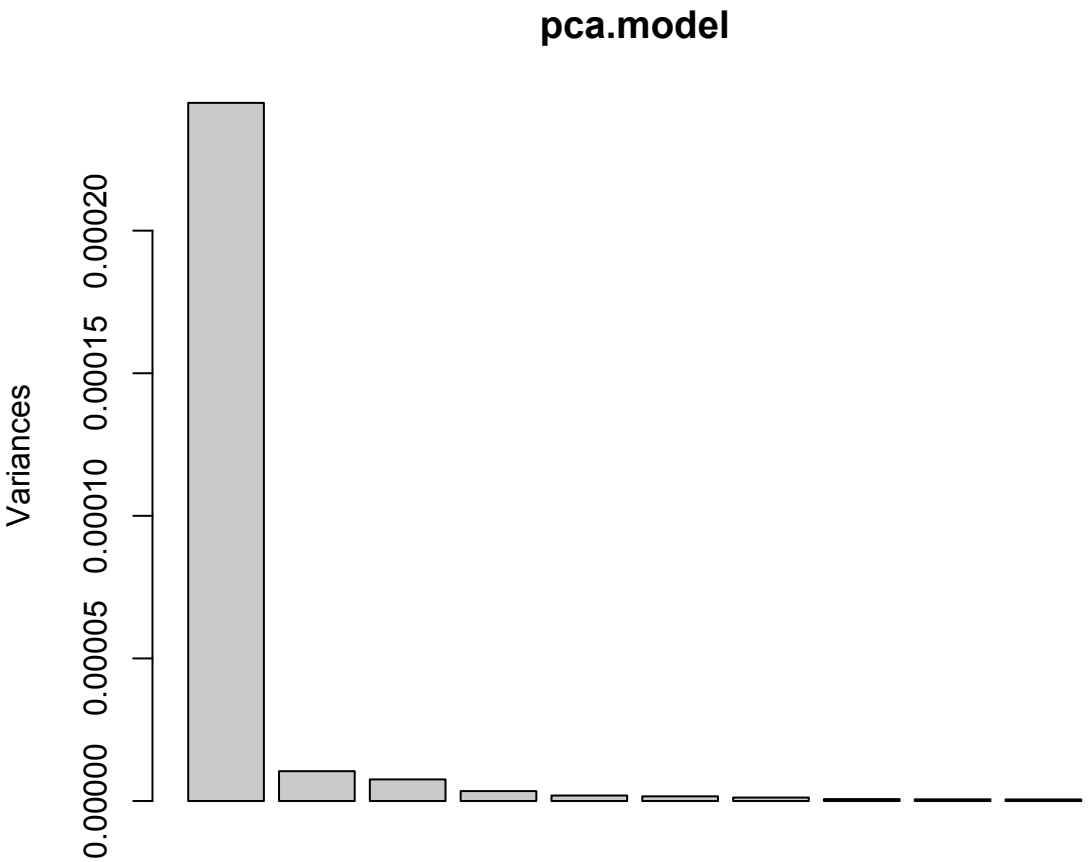


Figure 183: PCA scree plot for the first set of 10 container glass second derivative (5-point smoothing) spectra (10 replicates), no data pretreatment.

Table 195: PCA results for the first set of 10 container glass second derivative (5-point smoothing) spectra (10 replicates), centered.

Importance of components:

	PC1	PC2	PC3	PC4	PC5	PC6	PC7	PC8	PC9
Standard deviation	0.004178	0.003189	0.00232	0.001458	0.001285	0.001102	0.0009362	0.00078	0.0007598
Proportion of Variance	0.376080	0.219070	0.11597	0.045780	0.035550	0.026170	0.0188800	0.01311	0.0124400
Cumulative Proportion	0.376080	0.595140	0.71111	0.756890	0.792440	0.818610	0.8374900	0.85060	0.8630400

	PC10	PC11	PC12	PC13	PC14	PC15	PC16	PC17	PC18
Standard deviation	0.0006996	0.000664	0.0006391	0.0005803	0.0005496	0.0005145	0.0005012	0.0004876	0.0004725
Proportion of Variance	0.0105400	0.009500	0.0088000	0.0072500	0.0065100	0.0057000	0.0054100	0.0051200	0.0048100
Cumulative Proportion	0.8735800	0.883080	0.8918800	0.8991300	0.9056400	0.9113400	0.9167500	0.9218800	0.9266900

	PC19	PC20	PC21	PC22	PC23	PC24	PC25	PC26	PC27
Standard deviation	0.0004627	0.0004597	0.0004349	0.0004233	0.0003895	0.0003845	0.0003665	0.0003619	0.0003473
Proportion of Variance	0.0046100	0.0045500	0.0040700	0.0038600	0.0032700	0.0031800	0.0028900	0.0028200	0.0026000
Cumulative Proportion	0.9313000	0.9358500	0.9399300	0.9437900	0.9470600	0.9502400	0.9531300	0.9559600	0.9585500

	PC28	PC29	PC30	PC31	PC32	PC33	PC34	PC35	PC36
Standard deviation	0.0003390	0.0003242	0.0003203	0.0003167	0.0003001	0.0002935	0.000282	0.0002738	0.0002667
Proportion of Variance	0.0024800	0.0022600	0.0022100	0.0021600	0.0019400	0.0018600	0.001710	0.0016100	0.0015300
Cumulative Proportion	0.9610300	0.9632900	0.9655000	0.9676600	0.9696000	0.9714600	0.973170	0.9747900	0.9763200

	PC37	PC38	PC39	PC40	PC41	PC42	PC43	PC44	PC45
Standard deviation	0.0002540	0.0002467	0.0002403	0.0002326	0.0002314	0.0002208	0.0002174	0.0002057	0.0002021
Proportion of Variance	0.0013900	0.0013100	0.0012400	0.0011700	0.0011500	0.0010500	0.0010200	0.0009100	0.0008800
Cumulative Proportion	0.9777100	0.9790200	0.9802600	0.9814300	0.9825800	0.9836300	0.9846500	0.9855600	0.9864400

	PC46	PC47	PC48	PC49	PC50	PC51	PC52	PC53	PC54
Standard deviation	0.0001944	0.0001874	0.0001831	0.0001787	0.0001719	0.0001699	0.0001616	0.0001567	0.0001515
Proportion of Variance	0.0008100	0.0007600	0.0007200	0.0006900	0.0006400	0.0006200	0.0005600	0.0005300	0.0004900
Cumulative Proportion	0.9872600	0.9880100	0.9887400	0.9894200	0.9900600	0.9906800	0.9912500	0.9917700	0.9922700

	PC55	PC56	PC57	PC58	PC59	PC60	PC61	PC62	PC63
Standard deviation	0.0001493	0.0001465	0.0001437	0.0001345	0.0001316	0.0001302	0.0001281	0.0001240	0.0001195
Proportion of Variance	0.0004800	0.0004600	0.0004400	0.0003900	0.0003700	0.0003700	0.0003500	0.0003300	0.0003100
Cumulative Proportion	0.9927500	0.9932100	0.9936600	0.9940500	0.9944200	0.9947800	0.9951400	0.9954700	0.9957800

	PC64	PC65	PC66	PC67	PC68	PC69	PC70	PC71	PC72
Standard deviation	0.0001178	0.0001136	0.0001128	0.0001057	0.0001039	9.788e-05	9.424e-05	9.339e-05	9.069e-05
Proportion of Variance	0.0003000	0.0002800	0.0002700	0.0002400	0.0002300	2.100e-04	1.900e-04	1.900e-04	1.800e-04
Cumulative Proportion	0.9960800	0.9963500	0.9966300	0.9968700	0.9971000	9.973e-01	9.975e-01	9.977e-01	9.979e-01

	PC73	PC74	PC75	PC76	PC77	PC78	PC79	PC80	PC81
Standard deviation	8.603e-05	8.403e-05	8.148e-05	7.998e-05	7.897e-05	7.567e-05	7.138e-05	6.857e-05	6.782e-05
Proportion of Variance	1.600e-04	1.500e-04	1.400e-04	1.400e-04	1.300e-04	1.200e-04	1.100e-04	1.000e-04	1.000e-04
Cumulative Proportion	9.980e-01	9.982e-01	9.983e-01	9.985e-01	9.986e-01	9.987e-01	9.988e-01	9.989e-01	9.990e-01

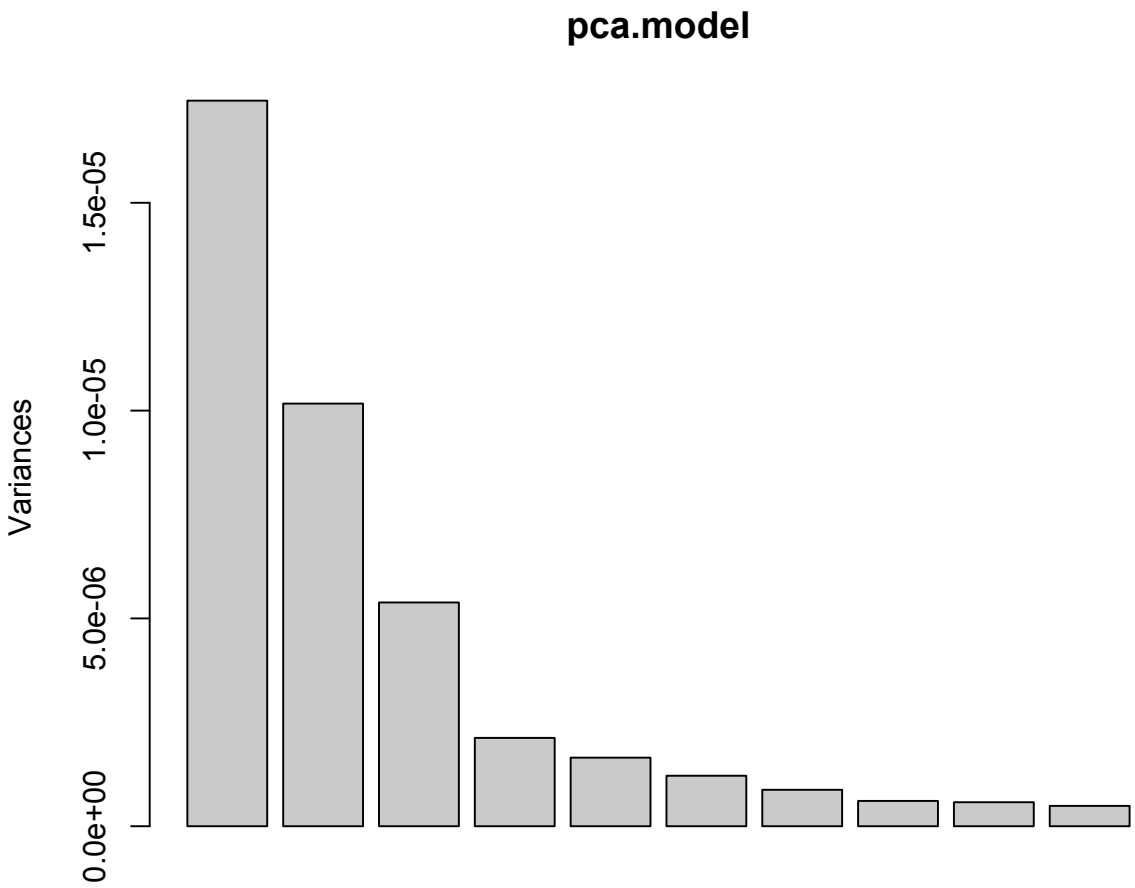


Figure 184: PCA scree plot for the first set of 10 container glass second derivative (5-point smoothing) spectra (10 replicates), centered.

Table 196: PCA results for the first set of 10 container glass second derivative (5-point smoothing) spectra (10 replicates), autoscaled.

Importance of components:

	PC1	PC2	PC3	PC4	PC5	PC6	PC7	PC8	PC9	PC10	PC11
Standard deviation	6.8024	5.7190	4.94206	4.01973	3.40236	3.19196	3.03444	2.85475	2.81564	2.59495	2.52649
Proportion of Variance	0.1433	0.1013	0.07562	0.05003	0.03584	0.03154	0.02851	0.02523	0.02454	0.02085	0.01976
Cumulative Proportion	0.1433	0.2445	0.32014	0.37016	0.40600	0.43754	0.46605	0.49128	0.51583	0.53667	0.55644

	PC12	PC13	PC14	PC15	PC16	PC17	PC18	PC19	PC20	PC21	PC22
Standard deviation	2.49076	2.3504	2.32816	2.24897	2.23308	2.19881	2.11206	2.09126	2.04762	1.98005	1.94336
Proportion of Variance	0.01921	0.0171	0.01678	0.01566	0.01544	0.01497	0.01381	0.01354	0.01298	0.01214	0.01169
Cumulative Proportion	0.57564	0.5927	0.60953	0.62519	0.64063	0.65559	0.66940	0.68294	0.69593	0.70806	0.71976

	PC23	PC24	PC25	PC26	PC27	PC28	PC29	PC30	PC31	PC32	PC33
Standard deviation	1.91353	1.82019	1.81422	1.79367	1.7331	1.7144	1.67577	1.66312	1.62030	1.56995	1.53732
Proportion of Variance	0.01134	0.01026	0.01019	0.00996	0.0093	0.0091	0.00869	0.00856	0.00813	0.00763	0.00732
Cumulative Proportion	0.73109	0.74135	0.75154	0.76150	0.7708	0.7799	0.78859	0.79716	0.80528	0.81291	0.82023

	PC34	PC35	PC36	PC37	PC38	PC39	PC40	PC41	PC42	PC43	PC44
Standard deviation	1.50118	1.47734	1.46425	1.42848	1.41347	1.40910	1.38162	1.34700	1.3453	1.31906	1.29257
Proportion of Variance	0.00698	0.00676	0.00664	0.00632	0.00619	0.00615	0.00591	0.00562	0.0056	0.00539	0.00517
Cumulative Proportion	0.82721	0.83396	0.84060	0.84692	0.85311	0.85925	0.86516	0.87078	0.8764	0.88177	0.88694

	PC45	PC46	PC47	PC48	PC49	PC50	PC51	PC52	PC53	PC54	PC55
Standard deviation	1.25690	1.24589	1.2316	1.21337	1.17623	1.15740	1.12798	1.11917	1.09152	1.08220	1.06176
Proportion of Variance	0.00489	0.00481	0.0047	0.00456	0.00428	0.00415	0.00394	0.00388	0.00369	0.00363	0.00349
Cumulative Proportion	0.89183	0.89664	0.9013	0.90589	0.91018	0.91432	0.91826	0.92214	0.92583	0.92946	0.93295

	PC56	PC57	PC58	PC59	PC60	PC61	PC62	PC63	PC64	PC65	PC66
Standard deviation	1.03634	1.00579	0.99822	0.97916	0.95802	0.94944	0.94456	0.91182	0.89600	0.87903	0.86829
Proportion of Variance	0.00333	0.00313	0.00308	0.00297	0.00284	0.00279	0.00276	0.00257	0.00249	0.00239	0.00233
Cumulative Proportion	0.93627	0.93940	0.94249	0.94546	0.94830	0.95109	0.95385	0.95642	0.95891	0.96130	0.96364

	PC67	PC68	PC69	PC70	PC71	PC72	PC73	PC74	PC75	PC76	PC77
Standard deviation	0.85877	0.83592	0.81184	0.79158	0.76828	0.74353	0.73193	0.71762	0.70203	0.68132	0.66155
Proportion of Variance	0.00228	0.00216	0.00204	0.00194	0.00183	0.00171	0.00166	0.00159	0.00153	0.00144	0.00135
Cumulative Proportion	0.96592	0.96808	0.97012	0.97206	0.97389	0.97560	0.97726	0.97886	0.98038	0.98182	0.98317

	PC78	PC79	PC80	PC81	PC82	PC83	PC84	PC85	PC86	PC87	PC88
Standard deviation	0.6480	0.63808	0.61844	0.61255	0.60431	0.58546	0.55109	0.53606	0.52483	0.49858	0.49238
Proportion of Variance	0.0013	0.00126	0.00118	0.00116	0.00113	0.00106	0.00094	0.00089	0.00085	0.00077	0.00075
Cumulative Proportion	0.9845	0.98573	0.98692	0.98808	0.98921	0.99027	0.99121	0.99210	0.99295	0.99372	0.99447

	PC89	PC90	PC91	PC92	PC93	PC94	PC95	PC96	PC97	PC98	PC99
Standard deviation	0.48727	0.45661	0.4419	0.42475	0.41254	0.40761	0.38969	0.37657	0.3604	0.32363	0.3137
Proportion of Variance	0.00074	0.00065	0.0006	0.00056	0.00053	0.00051	0.00047	0.00044	0.0004	0.00032	0.0003
Cumulative Proportion	0.99521	0.99586	0.9965	0.99702	0.99755	0.99806	0.99853	0.99897	0.9994	0.99970	1.0000

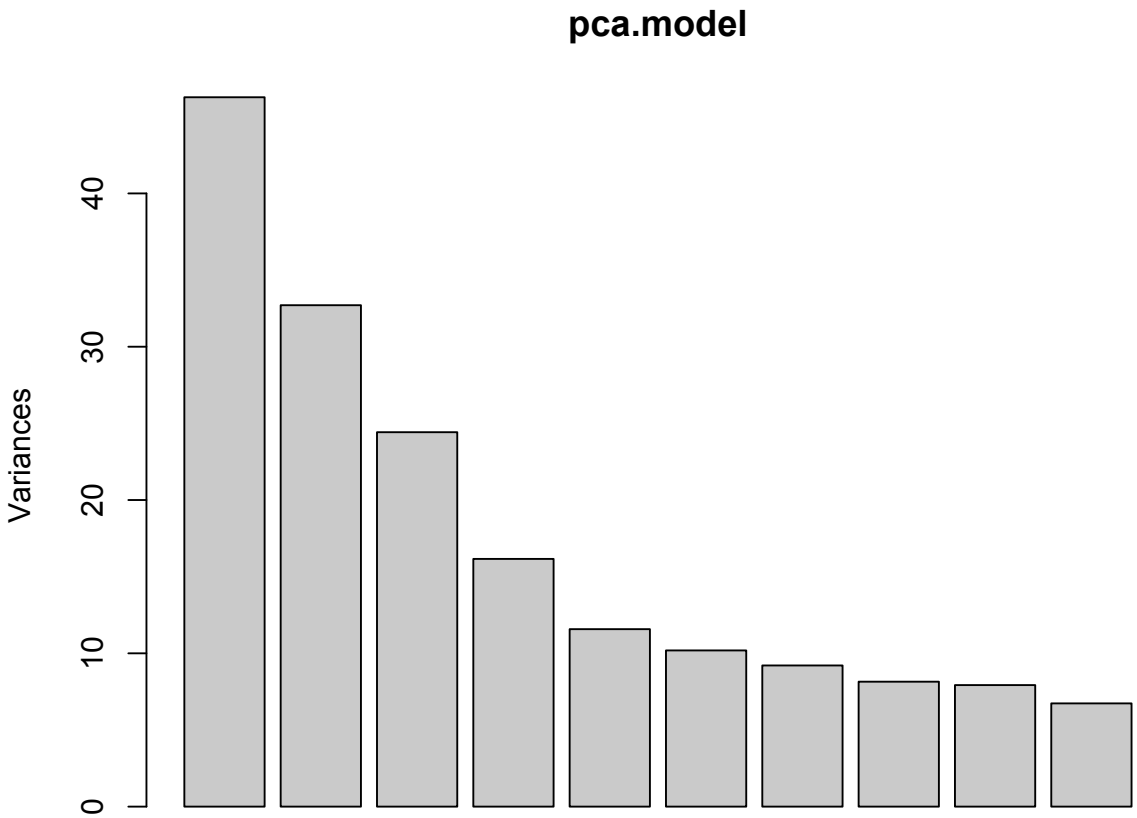


Figure 185: PCA scree plot for the first set of 10 container glass second derivative (5-point smoothing) spectra (10 replicates), autoscaled.

G. PCA Results for the Second Derivative Spectra (9-Point Smoothing)

Table 197: PCA results for the first set of 30 glass second derivative (9-point smoothing) spectra (10 replicates), no data pretreatment.

Importance of components:

	PC1	PC2	PC3	PC4	PC5	PC6	PC7	PC8	PC9
Standard deviation	0.01430	0.002859	0.002308	0.001561	0.001250	0.0008474	0.0007533	0.0004301	0.0003319
Proportion of Variance	0.91158	0.036460	0.023770	0.010870	0.006970	0.0032000	0.0025300	0.0008300	0.0004900
Cumulative Proportion	0.91158	0.948040	0.971810	0.982680	0.989650	0.9928500	0.9953800	0.9962100	0.9967000

	PC10	PC11	PC12	PC13	PC14	PC15	PC16	PC17	PC18
Standard deviation	0.0002944	0.0002689	0.0002319	0.0002040	0.0001863	0.0001794	0.0001730	0.0001608	0.0001585
Proportion of Variance	0.0003900	0.0003200	0.0002400	0.0001900	0.0001500	0.0001400	0.0001300	0.0001200	0.0001100
Cumulative Proportion	0.9970900	0.9974100	0.9976500	0.9978300	0.9979900	0.9981300	0.9982700	0.9983800	0.9984900

	PC19	PC20	PC21	PC22	PC23	PC24	PC25	PC26	PC27
Standard deviation	0.0001531	0.0001440	0.0001385	0.0001294	0.0001267	0.0001231	0.0001205	0.0001147	0.0001089
Proportion of Variance	0.0001000	0.0000900	0.0000900	0.0000700	0.0000700	0.0000700	0.0000600	0.0000600	0.0000500
Cumulative Proportion	0.9986000	0.9986900	0.9987800	0.9988500	0.9989200	0.9989900	0.9990600	0.9991100	0.9991700

	PC28	PC29	PC30	PC31	PC32	PC33	PC34	PC35	PC36
Standard deviation	0.0001080	0.0001043	9.917e-05	9.465e-05	9.074e-05	8.566e-05	8.333e-05	8.142e-05	7.717e-05
Proportion of Variance	0.0000500	0.0000500	4.000e-05	4.000e-05	4.000e-05	3.000e-05	3.000e-05	3.000e-05	3.000e-05
Cumulative Proportion	0.9992200	0.9992700	9.993e-01	9.993e-01	9.994e-01	9.994e-01	9.994e-01	9.995e-01	9.995e-01

	PC37	PC38	PC39	PC40	PC41	PC42	PC43	PC44	PC45
Standard deviation	7.653e-05	7.189e-05	6.999e-05	6.831e-05	6.647e-05	0.0000646	6.333e-05	0.0000612	5.963e-05
Proportion of Variance	3.000e-05	2.000e-05	2.000e-05	2.000e-05	2.000e-05	0.0000200	2.000e-05	0.0000200	2.000e-05
Cumulative Proportion	9.995e-01	9.996e-01	9.996e-01	9.996e-01	9.996e-01	0.9996400	9.997e-01	0.9996700	9.997e-01

	PC46	PC47	PC48	PC49	PC50	PC51	PC52	PC53	PC54
Standard deviation	5.821e-05	5.684e-05	5.594e-05	5.355e-05	5.305e-05	5.121e-05	4.985e-05	4.878e-05	4.668e-05
Proportion of Variance	2.000e-05	1.000e-05	1.000e-05	1.000e-05	1.000e-05	1.000e-05	1.000e-05	1.000e-05	1.000e-05
Cumulative Proportion	9.997e-01	9.997e-01	9.997e-01	9.997e-01	9.998e-01	9.998e-01	9.998e-01	9.998e-01	9.998e-01

	PC55	PC56	PC57	PC58	PC59	PC60	PC61	PC62	PC63
Standard deviation	4.609e-05	0.0000436	4.196e-05	4.168e-05	4.092e-05	3.942e-05	3.811e-05	3.763e-05	3.673e-05
Proportion of Variance	1.000e-05	0.0000100	1.000e-05	1.000e-05	1.000e-05	1.000e-05	1.000e-05	1.000e-05	1.000e-05
Cumulative Proportion	9.998e-01	0.9998200	9.998e-01	9.998e-01	9.998e-01	9.999e-01	9.999e-01	9.999e-01	9.999e-01

	PC64	PC65	PC66	PC67	PC68	PC69	PC70	PC71	PC72
Standard deviation	3.572e-05	0.0000351	3.358e-05	3.268e-05	3.244e-05	3.195e-05	3.158e-05	3.129e-05	3.072e-05
Proportion of Variance	1.000e-05	0.0000100	1.000e-05	0.000e+00	0.000e+00	0.000e+00	0.000e+00	0.000e+00	0.000e+00
Cumulative Proportion	9.999e-01	0.9998800	9.999e-01	9.999e-01	9.999e-01	9.999e-01	9.999e-01	9.999e-01	9.999e-01

	PC73	PC74	PC75	PC76	PC77	PC78	PC79	PC80	PC81
Standard deviation	2.881e-05	2.794e-05	2.730e-05	2.657e-05	2.625e-05	2.577e-05	2.528e-05	2.479e-05	2.4e-05
Proportion of Variance	0.000e+00	0.000e+00	0.000e+00	0.000e+00	0.000e+00	0.000e+00	0.000e+00	0.000e+00	0.0e+00
Cumulative Proportion	9.999e-01	9.999e-01	9.999e-01	9.999e-01	9.999e-01	9.999e-01	9.999e-01	9.999e-01	1.0e+00

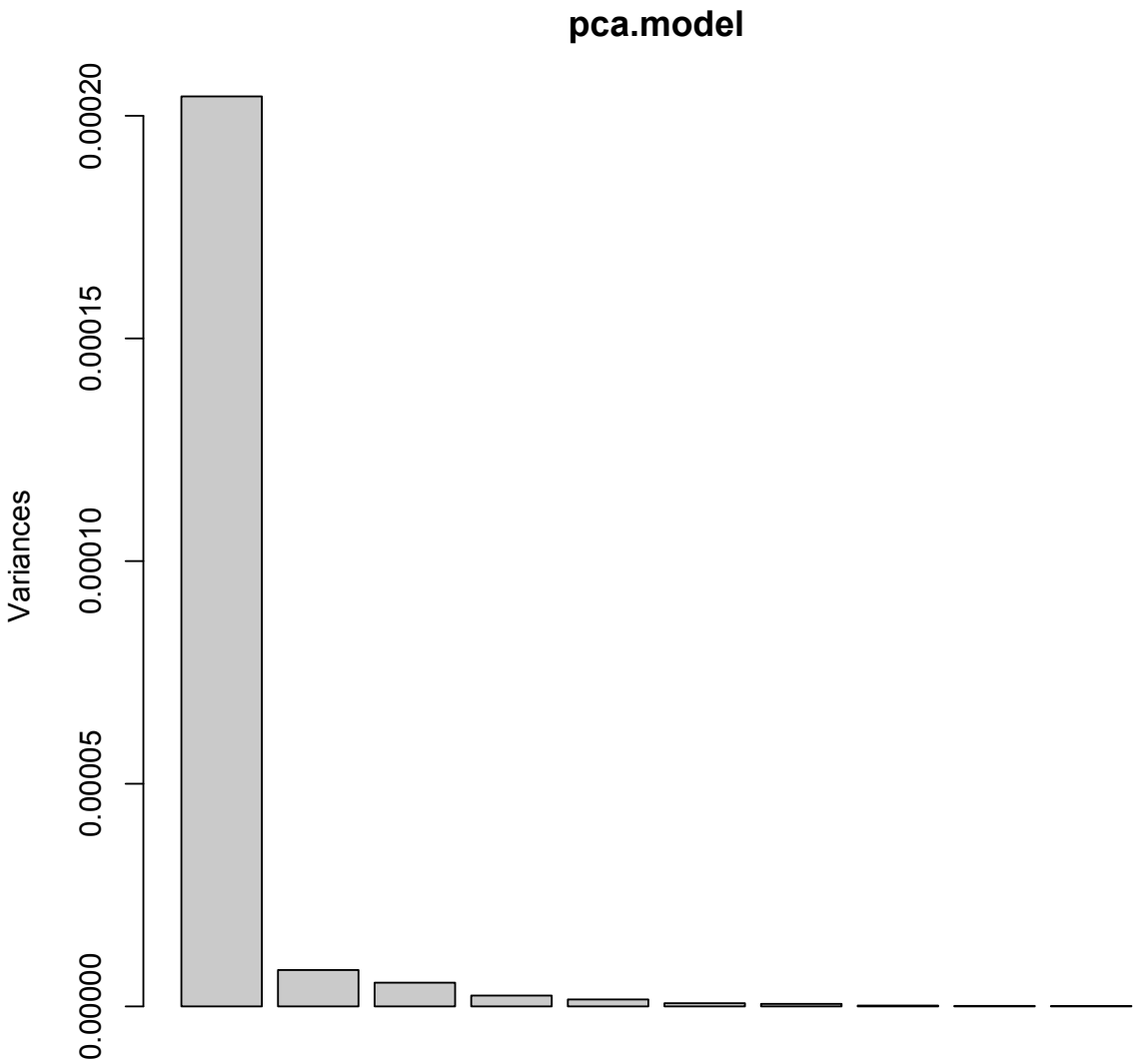


Figure 186: PCA scree plot for the first set of 30 glass second derivative (9-point smoothing) spectra (10 replicates), no data pretreatment.

Table 198: PCA results for the first set of 30 glass second derivative (9-point smoothing) spectra (10 replicates), centered.

Importance of components:

	PC1	PC2	PC3	PC4	PC5	PC6	PC7	PC8	PC9
Standard deviation	0.003266	0.002830	0.001946	0.001393	0.000913	0.0008307	0.0004302	0.000363	0.0003053
Proportion of Variance	0.394430	0.296310	0.140040	0.071780	0.030830	0.0255200	0.0068500	0.004870	0.0034500
Cumulative Proportion	0.394430	0.690740	0.830780	0.902560	0.933390	0.9589200	0.9657600	0.970640	0.9740800

	PC10	PC11	PC12	PC13	PC14	PC15	PC16	PC17	PC18
Standard deviation	0.0002806	0.0002343	0.0002270	0.0002039	0.0001862	0.0001787	0.0001729	0.0001592	0.0001564
Proportion of Variance	0.0029100	0.0020300	0.0019100	0.0015400	0.0012800	0.0011800	0.0011100	0.0009400	0.0009100
Cumulative Proportion	0.9770000	0.9790300	0.9809300	0.9824700	0.9837500	0.9849300	0.9860400	0.9869800	0.9878800

	PC19	PC20	PC21	PC22	PC23	PC24	PC25	PC26	PC27
Standard deviation	0.0001488	0.0001415	0.0001365	0.0001269	0.0001266	0.0001229	0.0001188	0.0001116	0.0001088
Proportion of Variance	0.0008200	0.0007400	0.0006900	0.0006000	0.0005900	0.0005600	0.0005200	0.0004600	0.0004400
Cumulative Proportion	0.9887000	0.9894400	0.9901300	0.9907300	0.9913200	0.9918800	0.9924000	0.9928600	0.9933000

	PC28	PC29	PC30	PC31	PC32	PC33	PC34	PC35	PC36
Standard deviation	0.0001068	9.986e-05	9.584e-05	9.444e-05	8.974e-05	8.565e-05	0.0000824	8.052e-05	7.66e-05
Proportion of Variance	0.0004200	3.700e-04	3.400e-04	3.300e-04	3.000e-04	2.700e-04	0.0002500	2.400e-04	2.20e-04
Cumulative Proportion	0.9937200	9.941e-01	9.944e-01	9.948e-01	9.951e-01	9.953e-01	0.9955800	9.958e-01	9.96e-01

	PC37	PC38	PC39	PC40	PC41	PC42	PC43	PC44	PC45
Standard deviation	7.416e-05	7.188e-05	6.914e-05	6.674e-05	6.578e-05	6.388e-05	6.253e-05	6.017e-05	5.821e-05
Proportion of Variance	2.000e-04	1.900e-04	1.800e-04	1.600e-04	1.600e-04	1.500e-04	1.400e-04	1.300e-04	1.300e-04
Cumulative Proportion	9.962e-01	9.964e-01	9.966e-01	9.968e-01	9.969e-01	9.971e-01	9.972e-01	9.974e-01	9.975e-01

	PC46	PC47	PC48	PC49	PC50	PC51	PC52	PC53	PC54
Standard deviation	5.684e-05	5.609e-05	5.431e-05	5.34e-05	5.197e-05	0.0000512	4.965e-05	4.793e-05	4.649e-05
Proportion of Variance	1.200e-04	1.200e-04	1.100e-04	1.10e-04	1.000e-04	0.0001000	9.000e-05	8.000e-05	8.000e-05
Cumulative Proportion	9.976e-01	9.977e-01	9.978e-01	9.98e-01	9.980e-01	0.9981300	9.982e-01	9.983e-01	9.984e-01

	PC55	PC56	PC57	PC58	PC59	PC60	PC61	PC62	PC63
Standard deviation	4.372e-05	4.246e-05	4.195e-05	0.0000411	4.050e-05	3.812e-05	3.763e-05	0.0000374	3.586e-05
Proportion of Variance	7.000e-05	7.000e-05	7.000e-05	0.0000600	6.000e-05	5.000e-05	5.000e-05	0.0000500	5.000e-05
Cumulative Proportion	9.985e-01	9.985e-01	9.986e-01	0.9986500	9.987e-01	9.988e-01	9.988e-01	0.9988700	9.989e-01

	PC64	PC65	PC66	PC67	PC68	PC69	PC70	PC71	PC72
Standard deviation	3.564e-05	3.438e-05	3.341e-05	3.267e-05	3.244e-05	3.182e-05	3.146e-05	3.072e-05	2.949e-05
Proportion of Variance	5.000e-05	4.000e-05	4.000e-05	4.000e-05	4.000e-05	4.000e-05	4.000e-05	3.000e-05	3.000e-05
Cumulative Proportion	9.990e-01	9.990e-01	9.990e-01	9.991e-01	9.991e-01	9.992e-01	9.992e-01	9.992e-01	9.993e-01

	PC73	PC74	PC75	PC76	PC77	PC78	PC79	PC80	PC81
Standard deviation	2.858e-05	2.738e-05	2.674e-05	2.655e-05	2.617e-05	2.551e-05	2.489e-05	2.455e-05	2.391e-05
Proportion of Variance	3.000e-05	3.000e-05	3.000e-05	3.000e-05	3.000e-05	2.000e-05	2.000e-05	2.000e-05	2.000e-05
Cumulative Proportion	9.993e-01	9.993e-01	9.994e-01	9.994e-01	9.994e-01	9.994e-01	9.994e-01	9.995e-01	9.995e-01

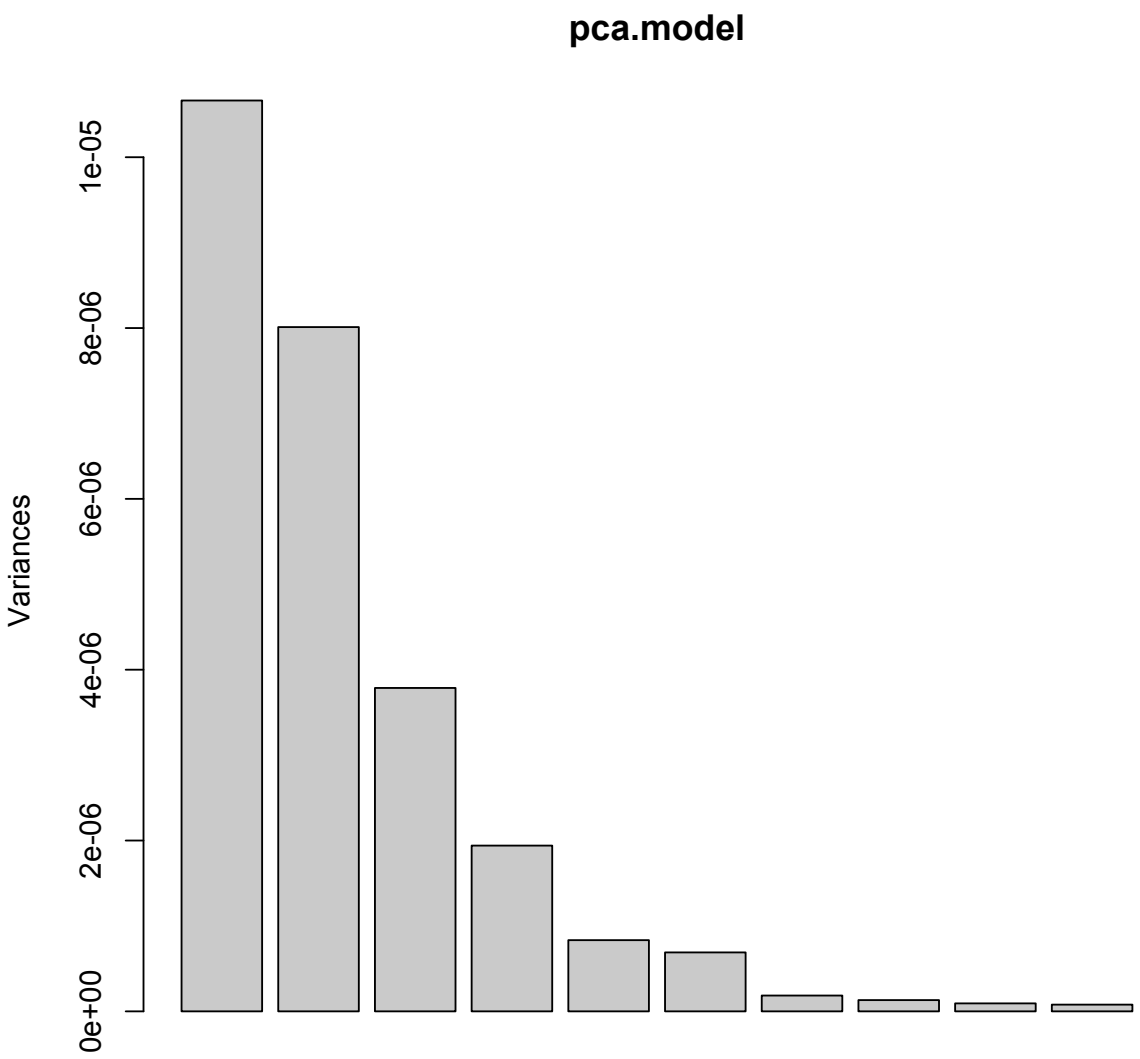


Figure 187. PCA scree plot for the first set of 30 glass second derivative (9-point smoothing) spectra (10 replicates), centered.

Table 199: PCA results for the first set of 30 glass second derivative (9-point smoothing) spectra (10 replicates), autoscaled.

Importance of components:

	PC1	PC2	PC3	PC4	PC5	PC6	PC7	PC8	PC9	PC10	PC11
Standard deviation	8.4312	7.3792	4.40436	4.15809	3.43700	3.22931	3.14316	2.72149	2.59556	2.37614	2.14222
Proportion of Variance	0.2201	0.1686	0.06006	0.05353	0.03657	0.03229	0.03059	0.02293	0.02086	0.01748	0.01421
Cumulative Proportion	0.2201	0.3887	0.44872	0.50225	0.53882	0.57111	0.60169	0.62462	0.64548	0.66296	0.67717

	PC12	PC13	PC14	PC15	PC16	PC17	PC18	PC19	PC20	PC21	PC22
Standard deviation	2.08260	2.05286	2.01785	1.95977	1.91401	1.88302	1.7795	1.76211	1.7052	1.69287	1.67299
Proportion of Variance	0.01343	0.01305	0.01261	0.01189	0.01134	0.01098	0.0098	0.00961	0.0090	0.00887	0.00867
Cumulative Proportion	0.69060	0.70364	0.71625	0.72814	0.73948	0.75046	0.7603	0.76988	0.7789	0.78775	0.79642

	PC23	PC24	PC25	PC26	PC27	PC28	PC29	PC30	PC31	PC32	PC33
Standard deviation	1.63458	1.5566	1.5351	1.50155	1.49078	1.43196	1.38449	1.3682	1.35300	1.31370	1.28836
Proportion of Variance	0.00827	0.0075	0.0073	0.00698	0.00688	0.00635	0.00593	0.0058	0.00567	0.00534	0.00514
Cumulative Proportion	0.80469	0.8122	0.8195	0.82647	0.83335	0.83969	0.84563	0.8514	0.85709	0.86243	0.86757

	PC34	PC35	PC36	PC37	PC38	PC39	PC40	PC41	PC42	PC43	PC44
Standard deviation	1.25637	1.24028	1.22573	1.19845	1.14814	1.12981	1.11589	1.07370	1.04710	1.02311	1.01555
Proportion of Variance	0.00489	0.00476	0.00465	0.00445	0.00408	0.00395	0.00386	0.00357	0.00339	0.00324	0.00319
Cumulative Proportion	0.87246	0.87722	0.88187	0.88632	0.89040	0.89435	0.89821	0.90178	0.90517	0.90841	0.91161

	PC45	PC46	PC47	PC48	PC49	PC50	PC51	PC52	PC53	PC54	PC55
Standard deviation	1.00498	0.9851	0.96448	0.96256	0.93687	0.92759	0.92190	0.89005	0.87173	0.8432	0.83085
Proportion of Variance	0.00313	0.0030	0.00288	0.00287	0.00272	0.00266	0.00263	0.00245	0.00235	0.0022	0.00214
Cumulative Proportion	0.91473	0.9177	0.92062	0.92349	0.92620	0.92887	0.93150	0.93395	0.93630	0.9385	0.94064

	PC56	PC57	PC58	PC59	PC60	PC61	PC62	PC63	PC64	PC65	PC66
Standard deviation	0.81689	0.79906	0.78910	0.77671	0.76839	0.76064	0.73620	0.72975	0.71501	0.71280	0.70531
Proportion of Variance	0.00207	0.00198	0.00193	0.00187	0.00183	0.00179	0.00168	0.00165	0.00158	0.00157	0.00154
Cumulative Proportion	0.94271	0.94469	0.94661	0.94848	0.95031	0.95210	0.95378	0.95543	0.95701	0.95858	0.96012

	PC67	PC68	PC69	PC70	PC71	PC72	PC73	PC74	PC75	PC76	PC77
Standard deviation	0.69057	0.68001	0.66038	0.65135	0.63293	0.61768	0.60941	0.58886	0.5684	0.55597	0.55417
Proportion of Variance	0.00148	0.00143	0.00135	0.00131	0.00124	0.00118	0.00115	0.00107	0.0010	0.00096	0.00095
Cumulative Proportion	0.96160	0.96303	0.96438	0.96569	0.96693	0.96812	0.96927	0.97034	0.9713	0.97230	0.97325

	PC78	PC79	PC80	PC81	PC82	PC83	PC84	PC85	PC86	PC87	PC88
Standard deviation	0.54121	0.53714	0.52263	0.51811	0.5069	0.49959	0.48902	0.48549	0.47246	0.46856	0.45135
Proportion of Variance	0.00091	0.00089	0.00085	0.00083	0.0008	0.00077	0.00074	0.00073	0.00069	0.00068	0.00063
Cumulative Proportion	0.97415	0.97505	0.97589	0.97672	0.9775	0.97829	0.97903	0.97976	0.98045	0.98113	0.98176

	PC89	PC90	PC91	PC92	PC93	PC94	PC95	PC96	PC97	PC98	PC99
Standard deviation	0.44345	0.43655	0.42660	0.42514	0.42160	0.41402	0.4004	0.39944	0.39218	0.38478	0.38288
Proportion of Variance	0.00061	0.00059	0.00056	0.00056	0.00055	0.00053	0.0005	0.00049	0.00048	0.00046	0.00045
Cumulative Proportion	0.98237	0.98296	0.98353	0.98409	0.98464	0.98517	0.9857	0.98616	0.98663	0.98709	0.98755

	PC100	PC101	PC102	PC103	PC104	PC105	PC106	PC107	PC108	PC109	PC110
Standard deviation	0.37546	0.36500	0.36250	0.35671	0.34744	0.34085	0.33910	0.32869	0.32432	0.31820	0.31738
Proportion of Variance	0.00044	0.00041	0.00041	0.00039	0.00037	0.00036	0.00036	0.00033	0.00033	0.00031	0.00031
Cumulative Proportion	0.98798	0.98839	0.98880	0.98919	0.98957	0.98993	0.99028	0.99062	0.99094	0.99126	0.99157

	PC111	PC112	PC113	PC114	PC115	PC116	PC117	PC118	PC119	PC120	PC121
Standard deviation	0.31543	0.3106	0.29943	0.29782	0.29345	0.28872	0.28361	0.27762	0.27742	0.27017	0.26386
Proportion of Variance	0.00031	0.0003	0.00028	0.00027	0.00027	0.00026	0.00025	0.00024	0.00024	0.00023	0.00022
Cumulative Proportion	0.99188	0.9922	0.99245	0.99273	0.99300	0.99325	0.99350	0.99374	0.99398	0.99421	0.99442

	PC122	PC123	PC124	PC125	PC126	PC127	PC128	PC129	PC130	PC131	PC132
Standard deviation	0.2563	0.2520	0.24876	0.24233	0.24125	0.23826	0.23495	0.23134	0.22941	0.22649	0.22104
Proportion of Variance	0.0002	0.0002	0.00019	0.00018	0.00018	0.00018	0.00017	0.00017	0.00016	0.00016	0.00015
Cumulative Proportion	0.9946	0.9948	0.99501	0.99519	0.99537	0.99555	0.99572	0.99589	0.99605	0.99621	0.99636

	PC133	PC134	PC135	PC136	PC137	PC138	PC139	PC140	PC141	PC142	PC143
Standard deviation	0.21368	0.21061	0.20351	0.19685	0.19564	0.19232	0.19132	0.18662	0.18521	0.1824	0.1789
Proportion of Variance	0.00014	0.00014	0.00013	0.00012	0.00012	0.00011	0.00011	0.00011	0.00011	0.0001	0.0001
Cumulative Proportion	0.99650	0.99664	0.99677	0.99689	0.99700	0.99712	0.99723	0.99734	0.99745	0.9976	0.9977

	PC144	PC145	PC146	PC147	PC148	PC149	PC150	PC151	PC152	PC153	PC154
Standard deviation	0.17346	0.17312	0.17100	0.16061	0.16028	0.15862	0.15379	0.15275	0.14946	0.14623	0.14475
Proportion of Variance	0.00009	0.00009	0.00009	0.00008	0.00008	0.00008	0.00007	0.00007	0.00007	0.00007	0.00006
Cumulative Proportion	0.99774	0.99783	0.99793	0.99801	0.99808	0.99816	0.99824	0.99831	0.99838	0.99844	0.99851

	PC155	PC156	PC157	PC158	PC159	PC160	PC161	PC162	PC163	PC164	PC165
Standard deviation	0.14000	0.13776	0.13271	0.13040	0.12766	0.12675	0.12487	0.12190	0.12164	0.11970	0.11782
Proportion of Variance	0.00006	0.00006	0.00005	0.00005	0.00005	0.00005	0.00005	0.00005	0.00005	0.00004	0.00004
Cumulative Proportion	0.99857	0.99863	0.99868	0.99873	0.99879	0.99884	0.99888	0.99893	0.99898	0.99902	0.99906

	PC166	PC167	PC168	PC169	PC170	PC171	PC172	PC173	PC174	PC175	PC176
Standard deviation	0.11742	0.11140	0.11056	0.10862	0.10543	0.10135	0.09997	0.09961	0.09596	0.09472	0.09315
Proportion of Variance	0.00004	0.00004	0.00004	0.00004	0.00003	0.00003	0.00003	0.00003	0.00003	0.00003	0.00003
Cumulative Proportion	0.99911	0.99914	0.99918	0.99922	0.99925	0.99928	0.99932	0.99935	0.99937	0.99940	0.99943

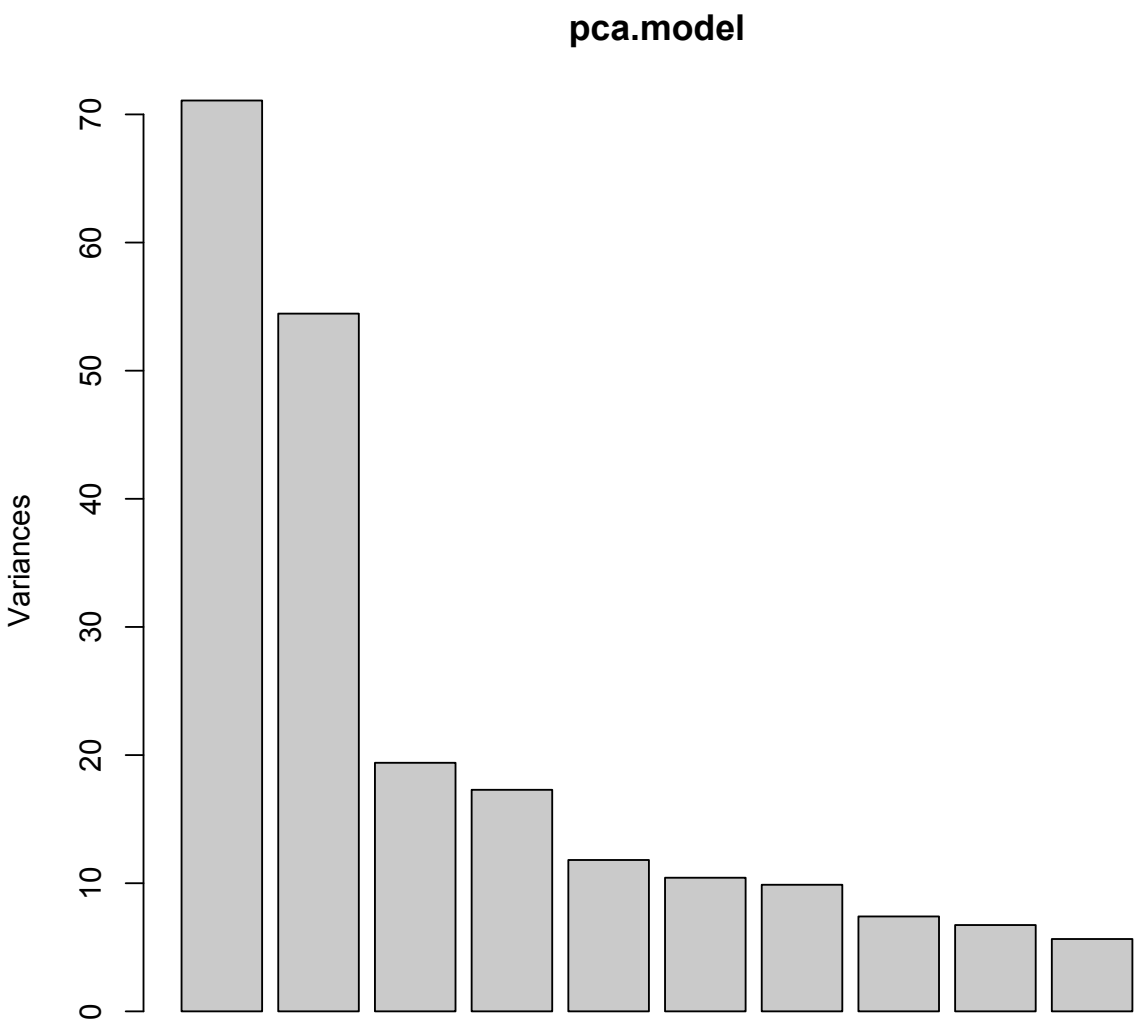


Figure 188: PCA scree plot for the first set of 30 glass second derivative (9-point smoothing) spectra (10 replicates), autoscaled.

Table 200: PCA results for the first set of 20 window glass second derivative (9-point smoothing) spectra (10 replicates), no data pretreatment.

Importance of components:

	PC1	PC2	PC3	PC4	PC5	PC6	PC7	PC8	PC9
Standard deviation	0.01421	0.002760	0.002166	0.001535	0.001298	0.0008326	0.0007648	0.0003464	0.0003049
Proportion of Variance	0.91608	0.034570	0.021300	0.010700	0.007650	0.0031500	0.0026600	0.0005400	0.0004200
Cumulative Proportion	0.91608	0.950650	0.971950	0.982650	0.990300	0.9934500	0.9961000	0.9966500	0.9970700

	PC10	PC11	PC12	PC13	PC14	PC15	PC16	PC17	PC18
Standard deviation	0.0002776	0.0002344	0.0002098	0.0001959	0.0001802	0.0001750	0.0001719	0.0001639	0.0001459
Proportion of Variance	0.0003500	0.0002500	0.0002000	0.0001700	0.0001500	0.0001400	0.0001300	0.0001200	0.0001000
Cumulative Proportion	0.9974200	0.9976700	0.9978700	0.9980400	0.9981900	0.9983300	0.9984600	0.9985900	0.9986800

	PC19	PC20	PC21	PC22	PC23	PC24	PC25	PC26	PC27
Standard deviation	0.0001410	0.0001306	0.0001292	0.0001238	0.0001182	0.0001143	0.0001116	0.0001072	0.0001025
Proportion of Variance	0.0000900	0.0000800	0.0000800	0.0000700	0.0000600	0.0000600	0.0000600	0.0000500	0.0000500
Cumulative Proportion	0.9987700	0.9988500	0.9989300	0.9990000	0.9990600	0.9991200	0.9991700	0.9992300	0.9992700

	PC28	PC29	PC30	PC31	PC32	PC33	PC34	PC35	PC36
Standard deviation	9.797e-05	9.283e-05	8.994e-05	8.818e-05	8.741e-05	8.458e-05	7.875e-05	7.809e-05	7.324e-05
Proportion of Variance	4.000e-05	4.000e-05	4.000e-05	4.000e-05	3.000e-05	3.000e-05	3.000e-05	3.000e-05	2.000e-05
Cumulative Proportion	9.993e-01	9.994e-01	9.994e-01	9.994e-01	9.995e-01	9.995e-01	9.995e-01	9.996e-01	9.996e-01

	PC37	PC38	PC39	PC40	PC41	PC42	PC43	PC44	PC45
Standard deviation	0.0000713	6.755e-05	6.549e-05	6.318e-05	6.168e-05	6.066e-05	5.853e-05	5.625e-05	5.588e-05
Proportion of Variance	0.0000200	2.000e-05	2.000e-05	2.000e-05	2.000e-05	2.000e-05	2.000e-05	1.000e-05	1.000e-05
Cumulative Proportion	0.9996000	9.996e-01	9.996e-01	9.997e-01	9.997e-01	9.997e-01	9.997e-01	9.997e-01	9.997e-01

	PC46	PC47	PC48	PC49	PC50	PC51	PC52	PC53	PC54
Standard deviation	5.421e-05	5.352e-05	5.203e-05	5.075e-05	4.945e-05	4.683e-05	4.601e-05	0.0000443	4.334e-05
Proportion of Variance	1.000e-05	1.000e-05	1.000e-05	1.000e-05	1.000e-05	1.000e-05	1.000e-05	0.0000100	1.000e-05
Cumulative Proportion	9.998e-01	9.998e-01	9.998e-01	9.998e-01	9.998e-01	9.998e-01	9.998e-01	0.9998300	9.998e-01

	PC55	PC56	PC57	PC58	PC59	PC60	PC61	PC62	PC63
Standard deviation	4.197e-05	4.011e-05	3.917e-05	3.846e-05	3.778e-05	3.701e-05	3.603e-05	3.481e-05	3.415e-05
Proportion of Variance	1.000e-05	1.000e-05	1.000e-05	1.000e-05	1.000e-05	1.000e-05	1.000e-05	1.000e-05	1.000e-05
Cumulative Proportion	9.998e-01	9.999e-01	9.999e-01	9.999e-01	9.999e-01	9.999e-01	9.999e-01	9.999e-01	9.999e-01

	PC64	PC65	PC66	PC67	PC68	PC69	PC70	PC71	PC72
Standard deviation	3.362e-05	3.274e-05	3.124e-05	3.087e-05	3.035e-05	2.933e-05	2.903e-05	2.846e-05	2.736e-05
Proportion of Variance	1.000e-05	0.000e+00	0.000e+00	0.000e+00	0.000e+00	0.000e+00	0.000e+00	0.000e+00	0.000e+00
Cumulative Proportion	9.999e-01	9.999e-01	9.999e-01	9.999e-01	9.999e-01	9.999e-01	9.999e-01	9.999e-01	9.999e-01

	PC73	PC74	PC75	PC76	PC77	PC78	PC79	PC80	PC81
Standard deviation	2.642e-05	2.519e-05	2.482e-05	2.403e-05	2.38e-05	2.303e-05	2.265e-05	2.263e-05	2.164e-05
Proportion of Variance	0.000e+00	0.000e+00	0.000e+00	0.000e+00	0.00e+00	0.000e+00	0.000e+00	0.000e+00	0.000e+00
Cumulative Proportion	9.999e-01	9.999e-01	9.999e-01	9.999e-01	1.00e+00	1.000e+00	1.000e+00	1.000e+00	1.000e+00

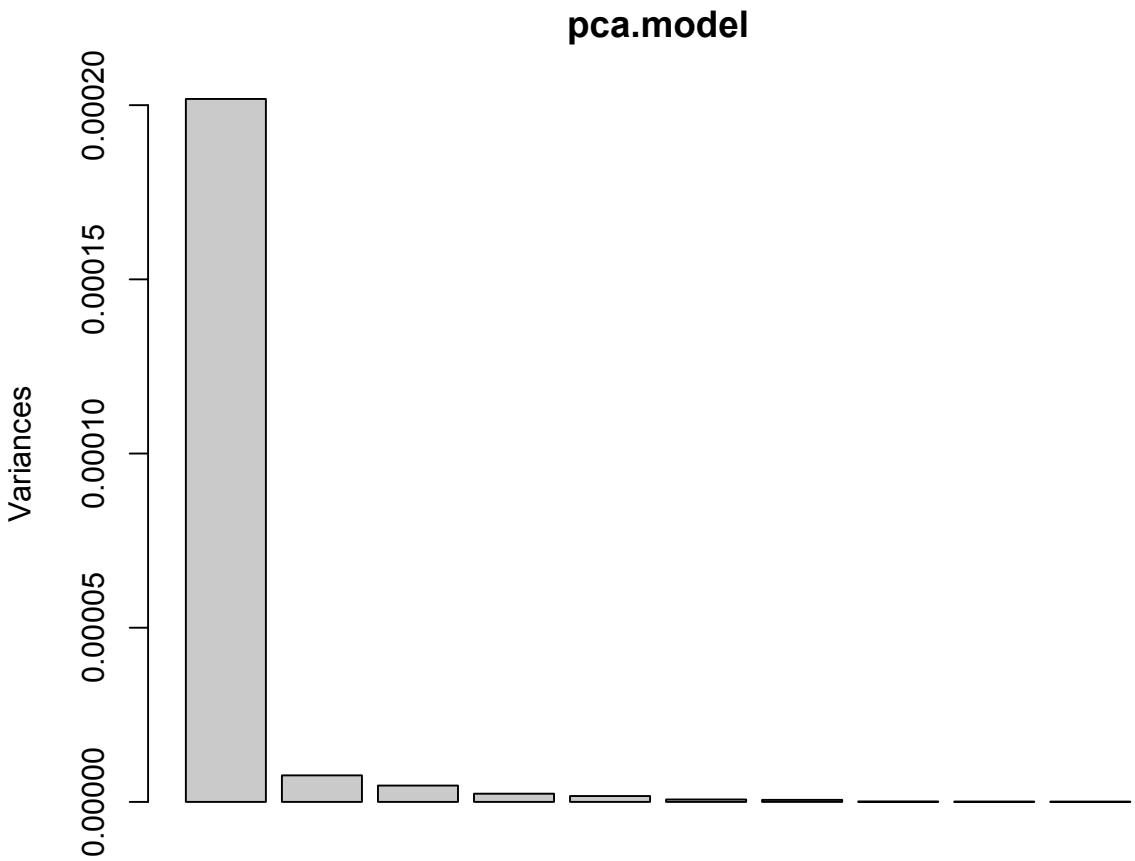


Figure 189: PCA scree plot for the first set of 20 window glass second derivative (9-point smoothing) spectra (10 replicates), no data pretreatment.

Table 201: PCA results for the first set of 20 window glass second derivative (9-point smoothing) spectra (10 replicates), centered.

Importance of components:

	PC1	PC2	PC3	PC4	PC5	PC6	PC7	PC8	PC9
Standard deviation	0.002973	0.002758	0.001889	0.001468	0.000901	0.000823	0.0003466	0.0003435	0.0002842
Proportion of Variance	0.359440	0.309340	0.145180	0.087580	0.033010	0.027540	0.0048800	0.0048000	0.0032800
Cumulative Proportion	0.359440	0.668780	0.813950	0.901540	0.934550	0.962090	0.9669700	0.9717700	0.9750600

	PC10	PC11	PC12	PC13	PC14	PC15	PC16	PC17	PC18
Standard deviation	0.0002537	0.0002168	0.0002087	0.0001906	0.0001793	0.0001733	0.0001716	0.0001638	0.0001457
Proportion of Variance	0.0026200	0.0019100	0.0017700	0.0014800	0.0013100	0.0012200	0.0012000	0.0010900	0.0008600
Cumulative Proportion	0.9776700	0.9795800	0.9813600	0.9828300	0.9841400	0.9853600	0.9865600	0.9876500	0.9885100

	PC19	PC20	PC21	PC22	PC23	PC24	PC25	PC26	PC27
Standard deviation	0.0001381	0.0001304	0.0001283	0.0001198	0.0001165	0.0001135	0.0001107	0.000106	0.0001001
Proportion of Variance	0.0007800	0.0006900	0.0006700	0.0005800	0.0005500	0.0005200	0.0005000	0.000460	0.0004100
Cumulative Proportion	0.9892900	0.9899800	0.9906500	0.9912300	0.9917900	0.9923100	0.9928100	0.993270	0.9936700

	PC28	PC29	PC30	PC31	PC32	PC33	PC34	PC35	PC36
Standard deviation	9.71e-05	0.0000907	8.904e-05	8.817e-05	8.733e-05	8.354e-05	7.833e-05	7.696e-05	7.309e-05
Proportion of Variance	3.80e-04	0.0003300	3.200e-04	3.200e-04	3.100e-04	2.800e-04	2.500e-04	2.400e-04	2.200e-04
Cumulative Proportion	9.94e-01	0.9943900	9.947e-01	9.950e-01	9.953e-01	9.956e-01	9.959e-01	9.961e-01	9.963e-01

	PC37	PC38	PC39	PC40	PC41	PC42	PC43	PC44	PC45
Standard deviation	7.122e-05	6.577e-05	6.362e-05	6.224e-05	0.0000616	5.869e-05	5.739e-05	5.623e-05	5.445e-05
Proportion of Variance	2.100e-04	1.800e-04	1.600e-04	1.600e-04	0.0001500	1.400e-04	1.300e-04	1.300e-04	1.200e-04
Cumulative Proportion	9.965e-01	9.967e-01	9.969e-01	9.970e-01	0.9971900	9.973e-01	9.975e-01	9.976e-01	9.977e-01

	PC46	PC47	PC48	PC49	PC50	PC51	PC52	PC53	PC54
Standard deviation	5.362e-05	5.27e-05	5.135e-05	4.978e-05	4.861e-05	4.648e-05	4.478e-05	4.334e-05	4.232e-05
Proportion of Variance	1.200e-04	1.10e-04	1.100e-04	1.000e-04	1.000e-04	9.000e-05	8.000e-05	8.000e-05	7.000e-05
Cumulative Proportion	9.978e-01	9.98e-01	9.980e-01	9.981e-01	9.982e-01	9.983e-01	9.984e-01	9.985e-01	9.986e-01

	PC55	PC56	PC57	PC58	PC59	PC60	PC61	PC62	PC63
Standard deviation	4.011e-05	3.932e-05	3.907e-05	3.846e-05	3.737e-05	3.606e-05	3.491e-05	3.454e-05	3.392e-05
Proportion of Variance	7.000e-05	6.000e-05	6.000e-05	6.000e-05	6.000e-05	5.000e-05	5.000e-05	5.000e-05	5.000e-05
Cumulative Proportion	9.986e-01	9.987e-01	9.988e-01	9.988e-01	9.989e-01	9.989e-01	9.990e-01	9.990e-01	9.991e-01

	PC64	PC65	PC66	PC67	PC68	PC69	PC70	PC71	PC72
Standard deviation	3.302e-05	3.195e-05	3.120e-05	3.047e-05	0.0000294	2.904e-05	2.848e-05	2.763e-05	2.643e-05
Proportion of Variance	4.000e-05	4.000e-05	4.000e-05	4.000e-05	0.0000400	3.000e-05	3.000e-05	3.000e-05	3.000e-05
Cumulative Proportion	9.991e-01	9.992e-01	9.992e-01	9.992e-01	0.9992700	9.993e-01	9.993e-01	9.994e-01	9.994e-01

	PC73	PC74	PC75	PC76	PC77	PC78	PC79	PC80	PC81
Standard deviation	0.0000253	2.507e-05	2.403e-05	2.380e-05	2.324e-05	2.299e-05	2.265e-05	0.000022	2.162e-05
Proportion of Variance	0.0000300	3.000e-05	2.000e-05	2.000e-05	2.000e-05	2.000e-05	2.000e-05	0.000020	2.000e-05
Cumulative Proportion	0.9994200	9.994e-01	9.995e-01	9.995e-01	9.995e-01	9.995e-01	9.996e-01	0.999580	9.996e-01

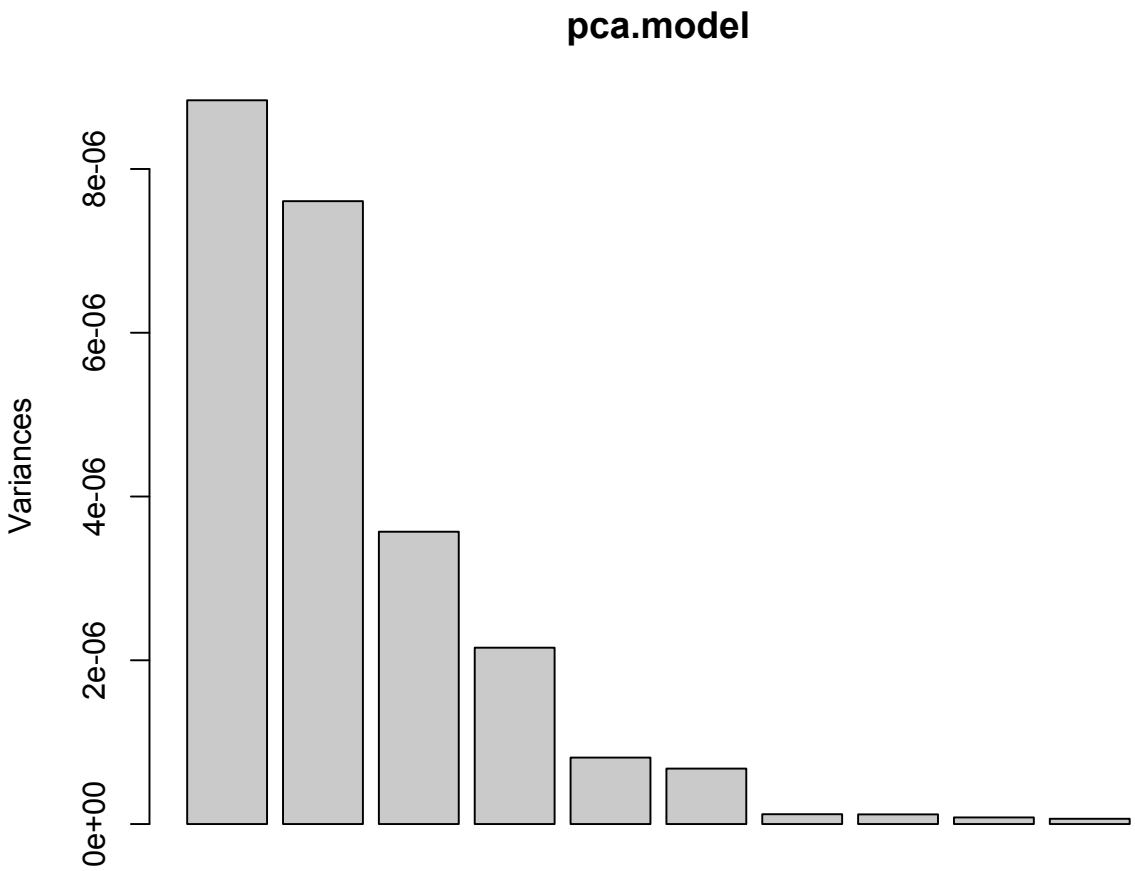


Figure 190: PCA scree plot for the first set of 20 window glass second derivative (9-point smoothing) spectra (10 replicates), centered.

Table 202: PCA results for the first set of 20 window glass second derivative (9-point smoothing) spectra (10 replicates), autoscaled.

Importance of components:

	PC1	PC2	PC3	PC4	PC5	PC6	PC7	PC8	PC9	PC10	PC11
Standard deviation	8.6336	6.1177	4.94564	3.88864	3.59654	3.24442	3.15019	2.83121	2.54937	2.39668	2.31177
Proportion of Variance	0.2308	0.1159	0.07573	0.04682	0.04005	0.03259	0.03072	0.02482	0.02012	0.01778	0.01655
Cumulative Proportion	0.2308	0.3466	0.42237	0.46918	0.50923	0.54182	0.57254	0.59736	0.61748	0.63527	0.65181

	PC12	PC13	PC14	PC15	PC16	PC17	PC18	PC19	PC20	PC21	PC22
Standard deviation	2.27707	2.2086	2.08985	2.06360	2.05074	2.00029	1.91111	1.86959	1.84309	1.77802	1.72464
Proportion of Variance	0.01605	0.0151	0.01352	0.01318	0.01302	0.01239	0.01131	0.01082	0.01052	0.00979	0.00921
Cumulative Proportion	0.66786	0.6830	0.69649	0.70967	0.72269	0.73508	0.74639	0.75721	0.76773	0.77751	0.78672

	PC23	PC24	PC25	PC26	PC27	PC28	PC29	PC30	PC31	PC32	PC33
Standard deviation	1.67915	1.65173	1.60925	1.54104	1.53771	1.49184	1.46238	1.43569	1.4042	1.37791	1.35234
Proportion of Variance	0.00873	0.00845	0.00802	0.00735	0.00732	0.00689	0.00662	0.00638	0.0061	0.00588	0.00566
Cumulative Proportion	0.79545	0.80390	0.81191	0.81927	0.82659	0.83348	0.84010	0.84648	0.8526	0.85846	0.86412

	PC34	PC35	PC36	PC37	PC38	PC39	PC40	PC41	PC42	PC43	PC44
Standard deviation	1.33118	1.31862	1.27831	1.24238	1.21086	1.19332	1.14691	1.14429	1.12383	1.11666	1.08658
Proportion of Variance	0.00549	0.00538	0.00506	0.00478	0.00454	0.00441	0.00407	0.00405	0.00391	0.00386	0.00366
Cumulative Proportion	0.86961	0.87499	0.88005	0.88483	0.88937	0.89378	0.89785	0.90191	0.90582	0.90968	0.91333

	PC45	PC46	PC47	PC48	PC49	PC50	PC51	PC52	PC53	PC54	PC55	PC56
Standard deviation	1.05687	1.04134	0.9838	0.97205	0.95672	0.9515	0.92079	0.90639	0.87874	0.86598	0.8611	0.83157
Proportion of Variance	0.00346	0.00336	0.0030	0.00293	0.00283	0.0028	0.00262	0.00254	0.00239	0.00232	0.0023	0.00214
Cumulative Proportion	0.91679	0.92015	0.9231	0.92607	0.92890	0.9317	0.93433	0.93687	0.93927	0.94159	0.9439	0.94602

	PC57	PC58	PC59	PC60	PC61	PC62	PC63	PC64	PC65	PC66	PC67
Standard deviation	0.81261	0.79884	0.79138	0.77203	0.7627	0.74295	0.72946	0.72156	0.70477	0.69864	0.68142
Proportion of Variance	0.00204	0.00198	0.00194	0.00185	0.0018	0.00171	0.00165	0.00161	0.00154	0.00151	0.00144
Cumulative Proportion	0.94807	0.95004	0.95198	0.95383	0.9556	0.95734	0.95898	0.96060	0.96213	0.96365	0.96508

	PC68	PC69	PC70	PC71	PC72	PC73	PC74	PC75	PC76	PC77	PC78
Standard deviation	0.6731	0.64339	0.63697	0.61456	0.60985	0.5972	0.57833	0.57051	0.56121	0.54942	0.54243
Proportion of Variance	0.0014	0.00128	0.00126	0.00117	0.00115	0.0011	0.00104	0.00101	0.00098	0.00093	0.00091
Cumulative Proportion	0.9665	0.96777	0.96902	0.97019	0.97134	0.9725	0.97348	0.97449	0.97547	0.97640	0.97731

	PC79	PC80	PC81	PC82	PC83	PC84	PC85	PC86	PC87	PC88	PC89
Standard deviation	0.52738	0.52637	0.51005	0.50220	0.49389	0.48813	0.4752	0.45725	0.45205	0.45100	0.4401
Proportion of Variance	0.00086	0.00086	0.00081	0.00078	0.00076	0.00074	0.0007	0.00065	0.00063	0.00063	0.0006
Cumulative Proportion	0.97817	0.97903	0.97984	0.98062	0.98137	0.98211	0.9828	0.98346	0.98409	0.98472	0.9853

	PC90	PC91	PC92	PC93	PC94	PC95	PC96	PC97	PC98	PC99	PC100
Standard deviation	0.42922	0.42400	0.41129	0.4033	0.39708	0.39240	0.38402	0.38268	0.37305	0.36747	0.3601
Proportion of Variance	0.00057	0.00056	0.00052	0.0005	0.00049	0.00048	0.00046	0.00045	0.00043	0.00042	0.0004
Cumulative Proportion	0.98589	0.98645	0.98697	0.9875	0.98796	0.98844	0.98889	0.98935	0.98978	0.99020	0.9906

	PC101	PC102	PC103	PC104	PC105	PC106	PC107	PC108	PC109	PC110	PC111
Standard deviation	0.35667	0.34572	0.33446	0.33248	0.32786	0.32464	0.31597	0.3123	0.30749	0.29998	0.29477
Proportion of Variance	0.00039	0.00037	0.00035	0.00034	0.00033	0.00033	0.00031	0.0003	0.00029	0.00028	0.00027
Cumulative Proportion	0.99099	0.99136	0.99171	0.99205	0.99238	0.99271	0.99302	0.9933	0.99361	0.99389	0.99416

	PC112	PC113	PC114	PC115	PC116	PC117	PC118	PC119	PC120	PC121	PC122
Standard deviation	0.29001	0.28583	0.27899	0.26897	0.26762	0.26478	0.25847	0.2514	0.24609	0.23933	0.23672
Proportion of Variance	0.00026	0.00025	0.00024	0.00022	0.00022	0.00022	0.00021	0.0002	0.00019	0.00018	0.00017
Cumulative Proportion	0.99442	0.99467	0.99492	0.99514	0.99536	0.99558	0.99578	0.9960	0.99617	0.99635	0.99652

	PC123	PC124	PC125	PC126	PC127	PC128	PC129	PC130	PC131	PC132	PC133
Standard deviation	0.23564	0.23107	0.21829	0.21595	0.21505	0.20092	0.19989	0.19441	0.19242	0.18968	0.1817
Proportion of Variance	0.00017	0.00017	0.00015	0.00014	0.00014	0.00012	0.00012	0.00012	0.00011	0.00011	0.0001
Cumulative Proportion	0.99669	0.99686	0.99700	0.99715	0.99729	0.99742	0.99754	0.99766	0.99777	0.99788	0.9980

	PC134	PC135	PC136	PC137	PC138	PC139	PC140	PC141	PC142	PC143	PC144
Standard deviation	0.1787	0.1779	0.17478	0.17066	0.16631	0.16192	0.15956	0.15680	0.14959	0.14418	0.14068
Proportion of Variance	0.0001	0.0001	0.00009	0.00009	0.00009	0.00008	0.00008	0.00008	0.00007	0.00006	0.00006
Cumulative Proportion	0.9981	0.9982	0.99828	0.99837	0.99845	0.99853	0.99861	0.99869	0.99876	0.99882	0.99888

	PC145	PC146	PC147	PC148	PC149	PC150	PC151	PC152	PC153	PC154	PC155
Standard deviation	0.13800	0.13474	0.13286	0.13148	0.12756	0.12505	0.12370	0.12098	0.11737	0.11333	0.11028
Proportion of Variance	0.00006	0.00006	0.00005	0.00005	0.00005	0.00005	0.00005	0.00005	0.00004	0.00004	0.00004
Cumulative Proportion	0.99894	0.99900	0.99905	0.99911	0.99916	0.99921	0.99925	0.99930	0.99934	0.99938	0.99942

	PC156	PC157	PC158	PC159	PC160	PC161	PC162	PC163	PC164	PC165	PC166
Standard deviation	0.10806	0.10265	0.10163	0.09865	0.09493	0.09364	0.08981	0.08797	0.08562	0.08373	0.08251
Proportion of Variance	0.00004	0.00003	0.00003	0.00003	0.00003	0.00003	0.00002	0.00002	0.00002	0.00002	0.00002
Cumulative Proportion	0.99945	0.99949	0.99952	0.99955	0.99958	0.99960	0.99963	0.99965	0.99968	0.99970	0.99972

	PC167	PC168	PC169	PC170	PC171	PC172	PC173	PC174	PC175	PC176	PC177
Standard deviation	0.07900	0.07588	0.07563	0.07225	0.07087	0.06858	0.06609	0.06541	0.06346	0.06139	0.06137
Proportion of Variance	0.00002	0.00002	0.00002	0.00002	0.00002	0.00001	0.00001	0.00001	0.00001	0.00001	0.00001
Cumulative Proportion	0.99974	0.99976	0.99977	0.99979	0.99980	0.99982	0.99983	0.99985	0.99986	0.99987	0.99988

	PC178	PC179	PC180	PC181	PC182	PC183	PC184	PC185	PC186	PC187	PC188
Standard deviation	0.06053	0.05706	0.05434	0.05401	0.05138	0.04983	0.04651	0.04532	0.04323	0.04161	0.04076
Proportion of Variance	0.00001	0.00001	0.00001	0.00001	0.00001	0.00001	0.00001	0.00001	0.00001	0.00001	0.00001
Cumulative Proportion	0.99989	0.99990	0.99991	0.99992	0.99993	0.99994	0.99994	0.99995	0.99996	0.99996	0.99997

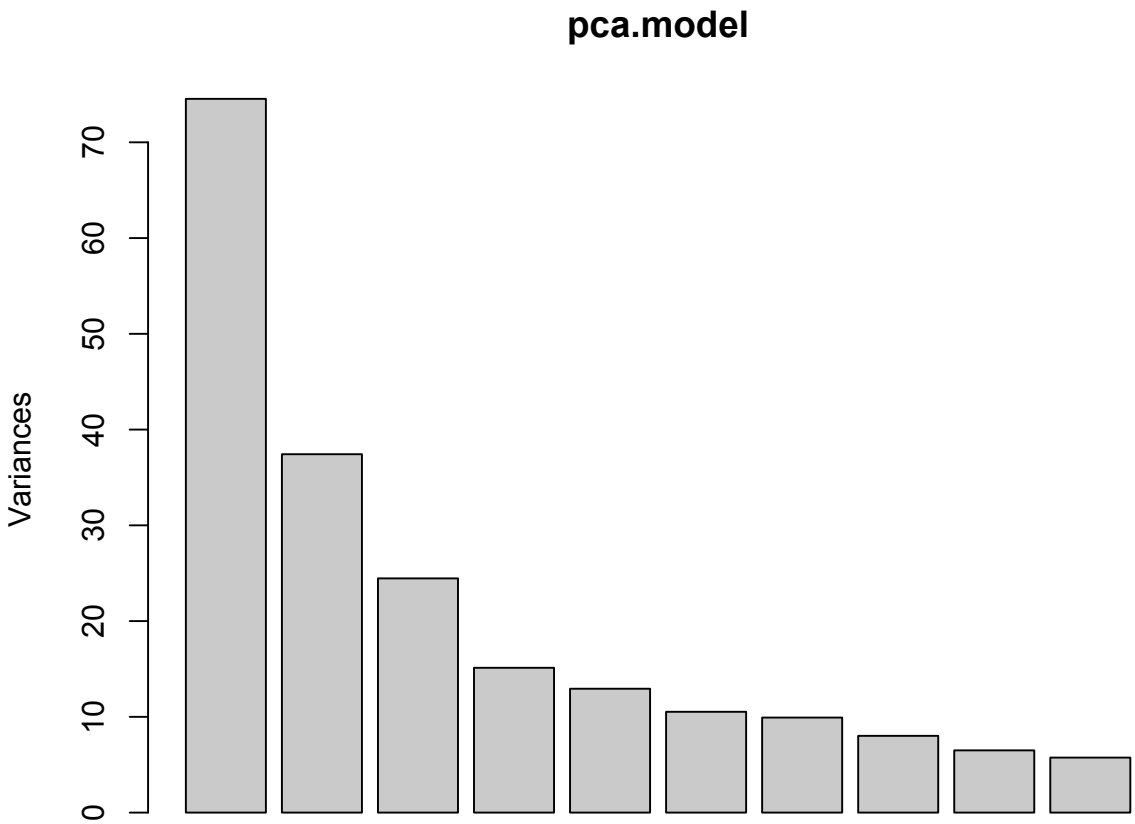


Figure 191: PCA scree plot for the first set of 20 window glass second derivative (9-point smoothing) spectra (10 replicates), autoscaled.

Table 203: PCA results for the first set of 10 container glass second derivative (9-point smoothing) spectra (10 replicates), no data pretreatment.

Importance of components:

	PC1	PC2	PC3	PC4	PC5	PC6	PC7	PC8	PC9	PC10
Standard deviation	0.01458	0.00303	0.002477	0.001641	0.001131	0.0008633	0.0006912	0.0005253	0.0003508	0.0003351
Proportion of Variance	0.90782	0.03919	0.026190	0.011490	0.005460	0.0031800	0.0020400	0.0011800	0.0005300	0.0004800
Cumulative Proportion	0.90782	0.94701	0.973200	0.984690	0.990150	0.9933300	0.9953700	0.9965500	0.9970800	0.9975600

	PC11	PC12	PC13	PC14	PC15	PC16	PC17	PC18	PC19
Standard deviation	0.0002628	0.0002152	0.0002012	0.0002000	0.0001767	0.0001728	0.0001645	0.000159	0.000148
Proportion of Variance	0.0002900	0.0002000	0.0001700	0.0001700	0.0001300	0.0001300	0.0001200	0.000110	0.000090
Cumulative Proportion	0.9978500	0.9980500	0.9982200	0.9983900	0.9985200	0.9986500	0.9987700	0.998880	0.998970

	PC20	PC21	PC22	PC23	PC24	PC25	PC26	PC27	PC28
Standard deviation	0.0001412	0.0001379	0.0001279	0.0001211	0.0001156	0.0001078	0.0001013	9.933e-05	9.411e-05
Proportion of Variance	0.0000900	0.0000800	0.0000700	0.0000600	0.0000600	0.0000500	0.0000400	4.000e-05	4.000e-05
Cumulative Proportion	0.9990500	0.9991300	0.9992000	0.9992700	0.9993200	0.9993700	0.9994200	9.995e-01	9.995e-01

	PC29	PC30	PC31	PC32	PC33	PC34	PC35	PC36	PC37
Standard deviation	0.0000909	8.907e-05	8.473e-05	8.209e-05	7.544e-05	7.403e-05	7.287e-05	7.148e-05	6.845e-05
Proportion of Variance	0.0000400	3.000e-05	3.000e-05	3.000e-05	2.000e-05	2.000e-05	2.000e-05	2.000e-05	2.000e-05
Cumulative Proportion	0.9995300	9.996e-01	9.996e-01	9.996e-01	9.997e-01	9.997e-01	9.997e-01	9.997e-01	9.997e-01

	PC38	PC39	PC40	PC41	PC42	PC43	PC44	PC45	PC46
Standard deviation	0.0000656	6.244e-05	6.046e-05	5.665e-05	5.554e-05	5.336e-05	5.175e-05	5.039e-05	4.757e-05
Proportion of Variance	0.0000200	2.000e-05	2.000e-05	1.000e-05	1.000e-05	1.000e-05	1.000e-05	1.000e-05	1.000e-05
Cumulative Proportion	0.9997600	9.998e-01	9.998e-01	9.998e-01	9.998e-01	9.998e-01	9.998e-01	9.999e-01	9.999e-01

	PC47	PC48	PC49	PC50	PC51	PC52	PC53	PC54	PC55
Standard deviation	4.593e-05	4.566e-05	0.0000433	4.209e-05	3.972e-05	3.834e-05	3.743e-05	3.669e-05	3.574e-05
Proportion of Variance	1.000e-05	1.000e-05	0.0000100	1.000e-05	1.000e-05	1.000e-05	1.000e-05	1.000e-05	1.000e-05
Cumulative Proportion	9.999e-01	9.999e-01	0.9998900	9.999e-01	9.999e-01	9.999e-01	9.999e-01	9.999e-01	9.999e-01

	PC56	PC57	PC58	PC59	PC60	PC61	PC62	PC63	PC64
Standard deviation	3.491e-05	3.305e-05	3.219e-05	3.143e-05	3.012e-05	2.873e-05	2.815e-05	2.752e-05	2.656e-05
Proportion of Variance	1.000e-05	0.000e+00	0.000e+00	0.000e+00	0.000e+00	0.000e+00	0.000e+00	0.000e+00	0.000e+00
Cumulative Proportion	9.999e-01	9.999e-01	9.999e-01	9.999e-01	1.000e+00	1.000e+00	1.000e+00	1.000e+00	1.000e+00

	PC65	PC66	PC67	PC68	PC69	PC70	PC71	PC72	PC73
Standard deviation	2.576e-05	2.500e-05	2.416e-05	2.333e-05	2.283e-05	2.266e-05	2.138e-05	2.098e-05	2.048e-05
Proportion of Variance	0.000e+00	0.000e+00	0.000e+00	0.000e+00	0.000e+00	0.000e+00	0.000e+00	0.000e+00	0.000e+00
Cumulative Proportion	1.000e+00	1.000e+00	1.000e+00	1.000e+00	1.000e+00	1.000e+00	1.000e+00	1.000e+00	1.000e+00

	PC74	PC75	PC76	PC77	PC78	PC79	PC80	PC81	PC82
Standard deviation	2.003e-05	1.933e-05	1.881e-05	1.816e-05	1.754e-05	1.642e-05	1.590e-05	1.574e-05	1.561e-05
Proportion of Variance	0.000e+00	0.000e+00	0.000e+00	0.000e+00	0.000e+00	0.000e+00	0.000e+00	0.000e+00	0.000e+00
Cumulative Proportion	1.000e+00	1.000e+00	1.000e+00	1.000e+00	1.000e+00	1.000e+00	1.000e+00	1.000e+00	1.000e+00

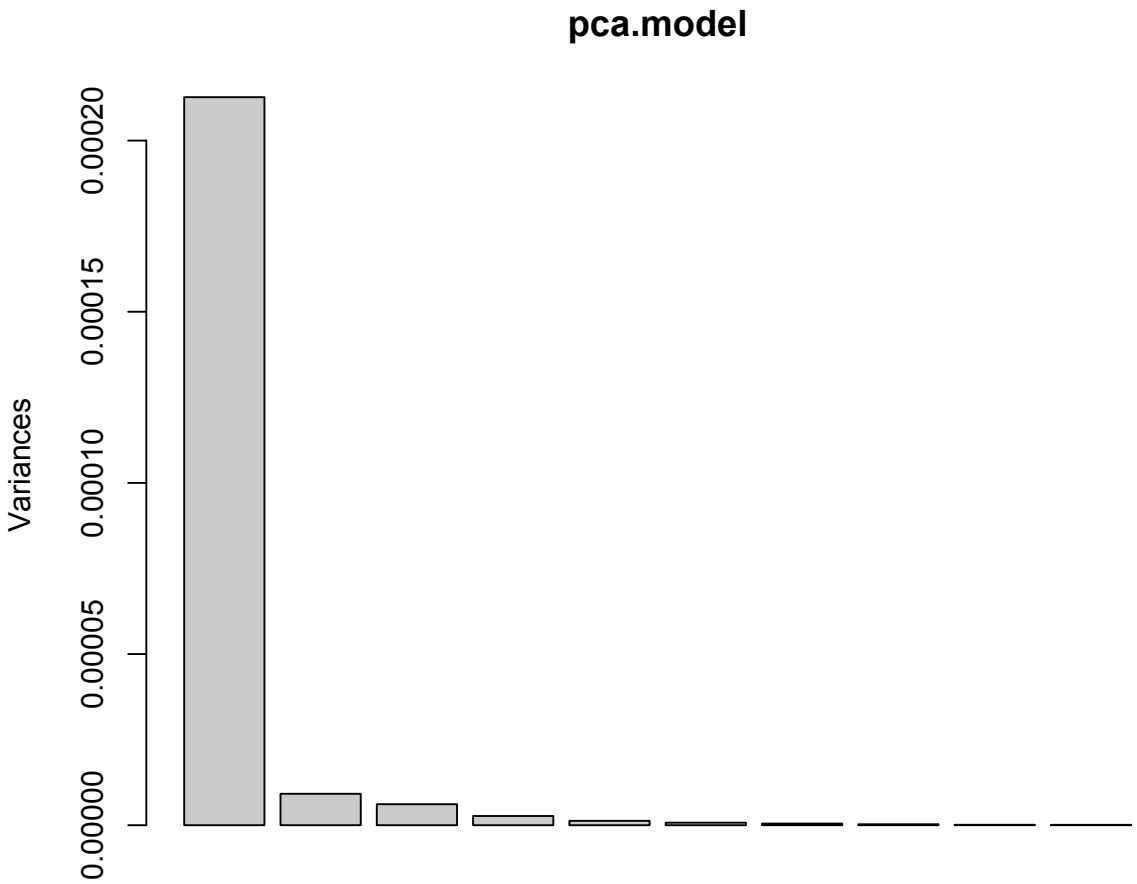


Figure 192: PCA scree plot for the first set of 10 container glass second derivative (9-point smoothing) spectra (10 replicates), no data pretreatment.

Table 204: PCA results for the first set of 10 container glass second derivative (9-point smoothing) spectra (10 replicates), centered.

Importance of components:

	PC1	PC2	PC3	PC4	PC5	PC6	PC7	PC8	PC9	PC10
Standard deviation	0.003779	0.002985	0.001992	0.001204	0.000896	0.0008532	0.00053	0.0003800	0.0003405	0.000279
Proportion of Variance	0.456290	0.284700	0.126820	0.046320	0.025660	0.0232600	0.00898	0.0046200	0.0037100	0.002490
Cumulative Proportion	0.456290	0.740990	0.867820	0.914140	0.939790	0.9630600	0.97203	0.9766500	0.9803600	0.982840

	PC11	PC12	PC13	PC14	PC15	PC16	PC17	PC18	PC19
Standard deviation	0.0002410	0.0002064	0.0002006	0.000186	0.0001740	0.0001688	0.0001593	0.0001556	0.0001469
Proportion of Variance	0.0018600	0.0013600	0.0012900	0.001110	0.0009700	0.0009100	0.0008100	0.0007700	0.0006900
Cumulative Proportion	0.9847000	0.9860600	0.9873500	0.988450	0.9894200	0.9903300	0.9911400	0.9919200	0.9926000

	PC20	PC21	PC22	PC23	PC24	PC25	PC26	PC27	PC28
Standard deviation	0.0001409	0.0001356	0.000124	0.0001185	0.0001131	0.0001013	9.977e-05	9.412e-05	9.115e-05
Proportion of Variance	0.0006300	0.0005900	0.000490	0.0004500	0.0004100	0.0003300	3.200e-04	2.800e-04	2.700e-04
Cumulative Proportion	0.9932400	0.9938300	0.994320	0.9947700	0.9951800	0.9955000	9.958e-01	9.961e-01	9.964e-01

	PC29	PC30	PC31	PC32	PC33	PC34	PC35	PC36	PC37
Standard deviation	8.917e-05	8.483e-05	8.33e-05	8.159e-05	7.498e-05	7.398e-05	0.0000715	6.974e-05	6.842e-05
Proportion of Variance	2.500e-04	2.300e-04	2.20e-04	2.100e-04	1.800e-04	1.700e-04	0.0001600	1.600e-04	1.500e-04
Cumulative Proportion	9.966e-01	9.969e-01	9.97e-01	9.973e-01	9.975e-01	9.976e-01	0.9978100	9.980e-01	9.981e-01

	PC38	PC39	PC40	PC41	PC42	PC43	PC44	PC45	PC46
Standard deviation	6.558e-05	6.046e-05	5.666e-05	5.608e-05	5.541e-05	5.335e-05	5.163e-05	5.018e-05	4.596e-05
Proportion of Variance	1.400e-04	1.200e-04	1.000e-04	1.000e-04	1.000e-04	9.000e-05	9.000e-05	8.000e-05	7.000e-05
Cumulative Proportion	9.982e-01	9.984e-01	9.985e-01	9.986e-01	9.987e-01	9.988e-01	9.988e-01	9.989e-01	9.990e-01

	PC47	PC48	PC49	PC50	PC51	PC52	PC53	PC54	PC55
Standard deviation	4.569e-05	4.436e-05	4.324e-05	4.078e-05	3.971e-05	3.758e-05	3.694e-05	3.597e-05	3.516e-05
Proportion of Variance	7.000e-05	6.000e-05	6.000e-05	5.000e-05	5.000e-05	5.000e-05	4.000e-05	4.000e-05	4.000e-05
Cumulative Proportion	9.991e-01	9.991e-01	9.992e-01	9.992e-01	9.993e-01	9.993e-01	9.994e-01	9.994e-01	9.994e-01

	PC56	PC57	PC58	PC59	PC60	PC61	PC62	PC63	PC64
Standard deviation	3.396e-05	3.253e-05	3.145e-05	3.078e-05	2.873e-05	2.825e-05	2.768e-05	2.673e-05	2.636e-05
Proportion of Variance	4.000e-05	3.000e-05	3.000e-05	3.000e-05	3.000e-05	3.000e-05	2.000e-05	2.000e-05	2.000e-05
Cumulative Proportion	9.995e-01	9.995e-01	9.996e-01	9.996e-01	9.996e-01	9.996e-01	9.997e-01	9.997e-01	9.997e-01

	PC65	PC66	PC67	PC68	PC69	PC70	PC71	PC72	PC73
Standard deviation	2.531e-05	2.444e-05	0.000024	2.287e-05	2.276e-05	2.177e-05	2.122e-05	0.0000206	2.004e-05
Proportion of Variance	2.000e-05	2.000e-05	0.000020	2.000e-05	2.000e-05	2.000e-05	1.000e-05	0.0000100	1.000e-05
Cumulative Proportion	9.997e-01	9.998e-01	0.999770	9.998e-01	9.998e-01	9.998e-01	9.998e-01	0.9998400	9.999e-01

	PC74	PC75	PC76	PC77	PC78	PC79	PC80	PC81	PC82
Standard deviation	1.944e-05	1.928e-05	1.875e-05	1.762e-05	1.687e-05	1.595e-05	1.584e-05	1.562e-05	1.475e-05
Proportion of Variance	1.000e-05	1.000e-05	1.000e-05	1.000e-05	1.000e-05	1.000e-05	1.000e-05	1.000e-05	1.000e-05
Cumulative Proportion	9.999e-01	9.999e-01	9.999e-01	9.999e-01	9.999e-01	9.999e-01	9.999e-01	9.999e-01	9.999e-01

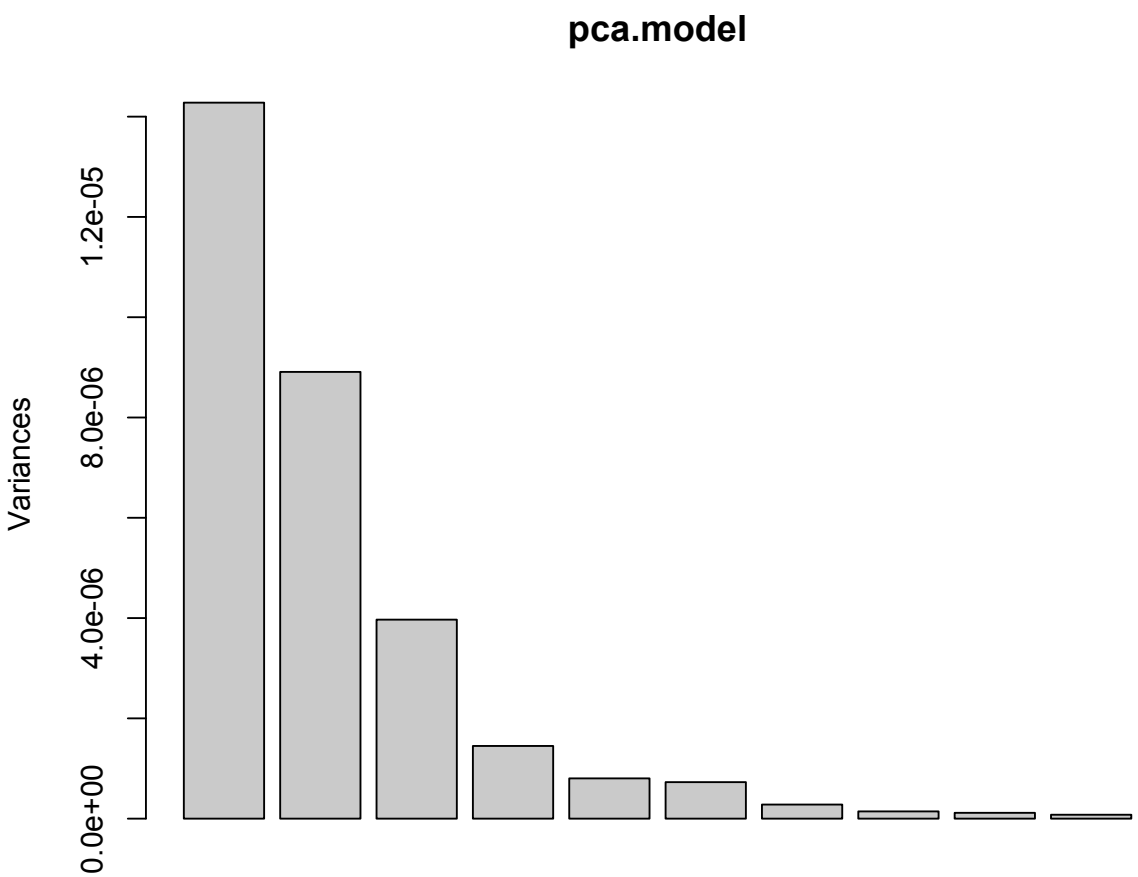


Figure 193: PCA scree plot for the first set of 10 container glass second derivative (9-point smoothing) spectra (10 replicates), centered.

Table 205: PCA results for the first set of 10 container glass second derivative (9-point smoothing) spectra (10 replicates), autoscaled.

Importance of components:

	PC1	PC2	PC3	PC4	PC5	PC6	PC7	PC8	PC9	PC10	PC11	PC12
Standard deviation	9.1059	8.7459	4.52998	3.71616	3.43484	3.3187	2.88006	2.69880	2.34126	2.31792	2.13991	2.00509
Proportion of Variance	0.2567	0.2368	0.06353	0.04276	0.03653	0.0341	0.02568	0.02255	0.01697	0.01663	0.01418	0.01245
Cumulative Proportion	0.2567	0.4935	0.55706	0.59981	0.63634	0.6704	0.69612	0.71867	0.73564	0.75227	0.76645	0.77890

	PC13	PC14	PC15	PC16	PC17	PC18	PC19	PC20	PC21	PC22	PC23
Standard deviation	1.96611	1.92634	1.86949	1.83781	1.74579	1.72592	1.66758	1.6072	1.56735	1.53943	1.49613
Proportion of Variance	0.01197	0.01149	0.01082	0.01046	0.00944	0.00922	0.00861	0.0080	0.00761	0.00734	0.00693
Cumulative Proportion	0.79086	0.80235	0.81317	0.82363	0.83307	0.84229	0.85090	0.8589	0.86650	0.87384	0.88077

	PC24	PC25	PC26	PC27	PC28	PC29	PC30	PC31	PC32	PC33	PC34
Standard deviation	1.41081	1.4041	1.37931	1.33636	1.29024	1.26546	1.16990	1.16280	1.15161	1.1072	1.08954
Proportion of Variance	0.00616	0.0061	0.00589	0.00553	0.00515	0.00496	0.00424	0.00419	0.00411	0.0038	0.00368
Cumulative Proportion	0.88693	0.8930	0.89892	0.90445	0.90961	0.91456	0.91880	0.92299	0.92709	0.9309	0.93456

	PC35	PC36	PC37	PC38	PC39	PC40	PC41	PC42	PC43	PC44	PC45
Standard deviation	1.07265	1.05057	1.02650	1.00917	0.96667	0.92955	0.8987	0.8804	0.83561	0.83141	0.79289
Proportion of Variance	0.00356	0.00342	0.00326	0.00315	0.00289	0.00268	0.0025	0.0024	0.00216	0.00214	0.00195
Cumulative Proportion	0.93813	0.94154	0.94481	0.94796	0.95085	0.95353	0.9560	0.9584	0.96059	0.96273	0.96467

	PC46	PC47	PC48	PC49	PC50	PC51	PC52	PC53	PC54	PC55	PC56
Standard deviation	0.77843	0.75737	0.73458	0.72342	0.70179	0.6965	0.67972	0.65858	0.63251	0.62472	0.61230
Proportion of Variance	0.00188	0.00178	0.00167	0.00162	0.00152	0.0015	0.00143	0.00134	0.00124	0.00121	0.00116
Cumulative Proportion	0.96655	0.96833	0.97000	0.97162	0.97314	0.9746	0.97607	0.97742	0.97866	0.97986	0.98103

	PC57	PC58	PC59	PC60	PC61	PC62	PC63	PC64	PC65	PC66	PC67	PC68
Standard deviation	0.60190	0.57637	0.56200	0.5400	0.53468	0.51948	0.5074	0.50450	0.49221	0.48237	0.4751	0.46052
Proportion of Variance	0.00112	0.00103	0.00098	0.0009	0.00089	0.00084	0.0008	0.00079	0.00075	0.00072	0.0007	0.00066
Cumulative Proportion	0.98215	0.98318	0.98415	0.9851	0.98594	0.98678	0.9876	0.98836	0.98911	0.98983	0.9905	0.99119

	PC69	PC70	PC71	PC72	PC73	PC74	PC75	PC76	PC77	PC78	PC79
Standard deviation	0.44867	0.42836	0.42241	0.40878	0.39971	0.38738	0.38535	0.36495	0.36416	0.34456	0.33741
Proportion of Variance	0.00062	0.00057	0.00055	0.00052	0.00049	0.00046	0.00046	0.00041	0.00041	0.00037	0.00035
Cumulative Proportion	0.99181	0.99238	0.99293	0.99345	0.99394	0.99441	0.99487	0.99528	0.99569	0.99606	0.99641

	PC80	PC81	PC82	PC83	PC84	PC85	PC86	PC87	PC88	PC89	PC90
Standard deviation	0.32515	0.3092	0.29878	0.28863	0.27414	0.26669	0.26265	0.25992	0.24759	0.23632	0.23446
Proportion of Variance	0.00033	0.0003	0.00028	0.00026	0.00023	0.00022	0.00021	0.00021	0.00019	0.00017	0.00017
Cumulative Proportion	0.99674	0.9970	0.99731	0.99757	0.99780	0.99802	0.99823	0.99844	0.99863	0.99881	0.99898

	PC91	PC92	PC93	PC94	PC95	PC96	PC97	PC98	PC99	PC100
Standard deviation	0.22507	0.22141	0.21031	0.19797	0.18979	0.18708	0.16938	0.16001	0.14883	4.044e-15
Proportion of Variance	0.00016	0.00015	0.00014	0.00012	0.00011	0.00011	0.00009	0.00008	0.00007	0.000e+00
Cumulative Proportion	0.99913	0.99929	0.99942	0.99954	0.99965	0.99976	0.99985	0.99993	1.00000	1.000e+00

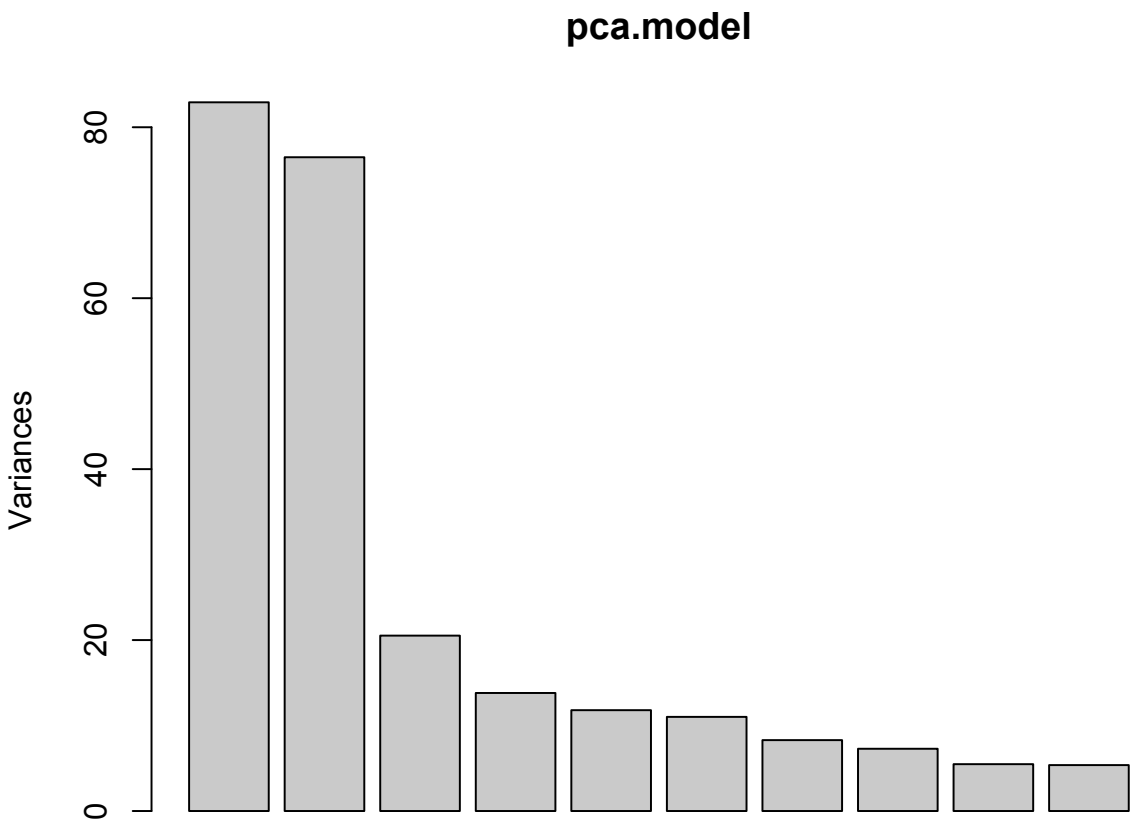


Figure 194: PCA scree plot for the first set of 10 container glass second derivative (9-point smoothing) spectra (10 replicates), autoscaled.

A STUDY OF THE MOLECULAR CHEMISTRY OF GLASSES BY INFRARED MICROSPECTROSCOPYAND ITS USE IN FORENSIC GLASS DISCRIMINATION AND CLASSIFICATION

by

BROOKE WEINGER KAMMRATH

VOLUME III

A dissertation submitted to the Graduate Faculty in Criminal Justice in partial fulfillment of the requirements for the degree of Doctor of Philosophy, The City University of New York

2012

APPENDIX XI: HOO-CV PCA-CVA RESULTS FOR CHEMOMETRIC ANALYSIS OF THE FIRST SET OF 30 GLASSES

A. HOO-CV PCA-CVA Results for the Unprocessed Spectra

First Set - Discrimination

Table 206: Discrimination error rates for HOO-CV with PCA reduced CVA for the first set of 30 glass spectra (10 replicates), no data pretreatment. The smallest PC dimension with the minimum error rate is highlighted in yellow.

PCs	Error Rate (%)	PCs	Error Rate (%)	PCs	Error Rate (%)	PCs	Error Rate (%)	PCs	Error Rate (%)
2	93.67	29	15.67	56	14.67	83	12.33	110	13.67
3	90.00	30	15.67	57	14.33	84	13.33	111	12.67
4	89.67	31	16.33	58	15.00	85	13.33	112	11.67
5	72.33	32	15.67	59	14.67	86	14.33	113	12.67
6	62.67	33	15.33	60	14.67	87	13.67	114	12.67
7	61.67	34	15.00	61	15.00	88	12.00	115	13.67
8	55.00	35	16.33	62	15.33	89	12.00	116	13.33
9	52.67	36	15.00	63	15.33	90	12.67	117	14.33
10	46.33	37	14.67	64	15.00	91	12.67	118	14.00
11	47.00	38	14.67	65	14.67	92	13.33	119	14.33
12	45.33	39	14.67	66	14.67	93	14.00	120	13.00
13	43.67	40	15.00	67	15.00	94	13.33	121	13.33
14	42.00	41	15.67	68	14.00	95	13.00	122	13.33
15	35.33	42	15.67	69	12.67	96	12.67	123	14.33
16	32.00	43	14.67	70	12.67	97	12.33	124	14.33
17	31.67	44	14.67	71	13.00	98	11.67	125	13.33
18	32.67	45	14.33	72	14.33	99	11.67	126	12.67
19	27.67	46	13.67	73	12.67	100	11.33	127	12.67
20	23.33	47	15.00	74	14.00	101	11.33	128	12.33
21	19.00	48	15.00	75	14.00	102	11.33	129	12.67
22	17.00	49	15.67	76	13.67	103	12.00	130	12.33
23	16.67	50	15.00	77	12.00	104	11.33	131	13.33
24	17.67	51	15.33	78	12.33	105	11.67	132	13.00
25	17.00	52	15.00	79	12.67	106	12.00	133	11.67
26	17.00	53	15.00	80	12.67	107	12.67		
27	16.00	54	14.00	81	13.00	108	13.33		
28	16.00	55	14.00	82	13.67	109	13.00		

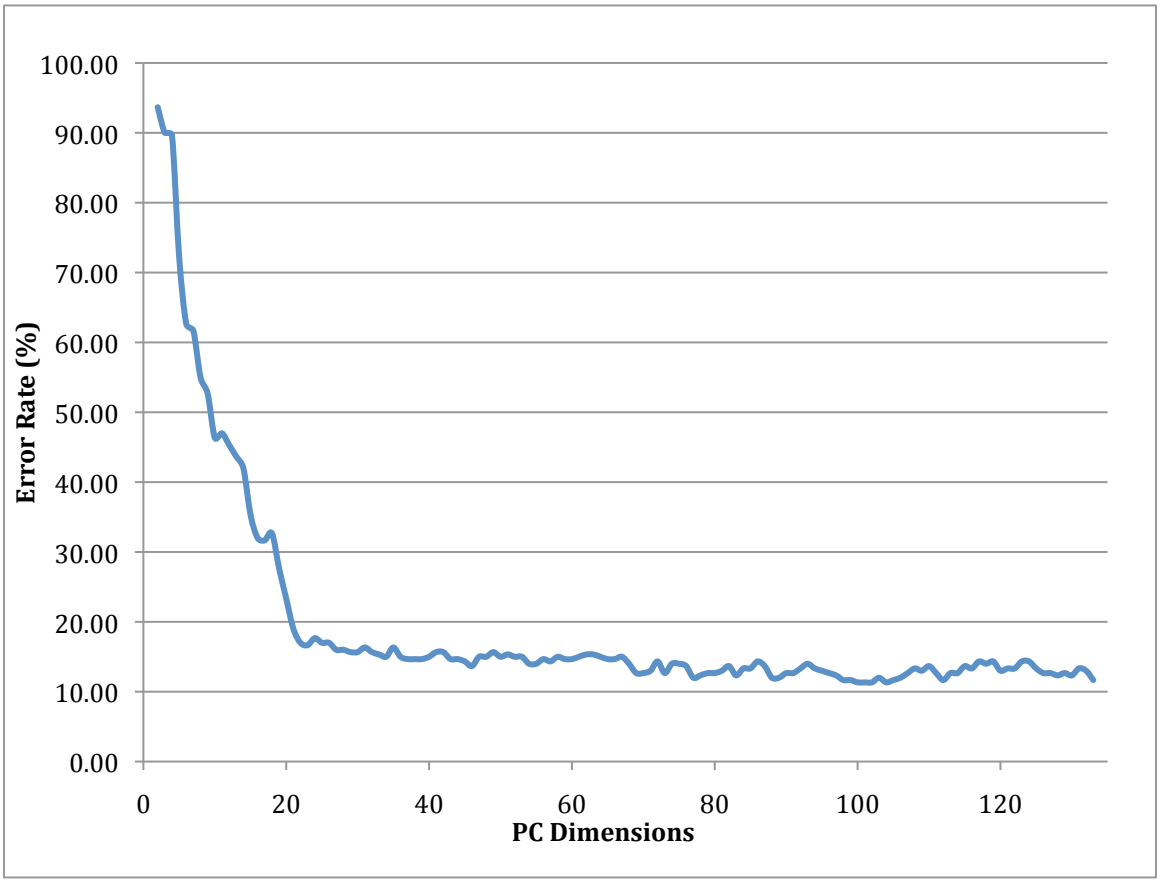


Figure 195: Graph of the discrimination error rate versus PC dimensions for HOO-CV with PCA reduced CVA for the first set of 30 glass spectra (10 replicates), no data pretreatment.

Table 207: Discrimination error rates for HOO-CV with PCA reduced CVA for the first set of 30 glass spectra (10 replicates), centered data. The smallest PC dimension with the minimum error rate is highlighted in yellow.

PCs	Error Rate (%)	PCs	Error Rate (%)	PCs	Error Rate (%)	PCs	Error Rate (%)	PCs	Error Rate (%)
2	93.00	29	15.33	56	14.33	83	12.67	110	14.00
3	90.67	30	16.00	57	14.33	84	13.00	111	12.33
4	89.33	31	15.00	58	14.67	85	14.33	112	12.00
5	70.00	32	15.33	59	15.00	86	14.33	113	12.33
6	61.00	33	15.00	60	14.67	87	14.67	114	13.67
7	61.00	34	15.67	61	15.00	88	12.33	115	13.33
8	56.67	35	13.33	62	15.67	89	12.33	116	14.00
9	47.00	36	15.00	63	15.33	90	12.33	117	14.00
10	46.00	37	15.33	64	15.33	91	12.67	118	14.67
11	46.00	38	15.67	65	15.33	92	13.33	119	14.00
12	45.00	39	15.33	66	14.33	93	14.00	120	12.67
13	42.00	40	15.00	67	15.00	94	13.00	121	13.00
14	42.33	41	15.67	68	14.67	95	12.67	122	13.00
15	34.33	42	15.67	69	12.67	96	12.67	123	14.00
16	32.33	43	14.33	70	13.00	97	11.00	124	14.33
17	33.00	44	14.33	71	14.33	98	12.33	125	13.67
18	33.33	45	14.00	72	14.67	99	11.67	126	12.67
19	27.33	46	14.00	73	15.00	100	11.33	127	13.00
20	21.00	47	14.33	74	15.00	101	11.67	128	12.33
21	19.33	48	14.33	75	14.67	102	11.67	129	12.67
22	17.33	49	15.67	76	13.67	103	11.67	130	13.00
23	15.67	50	14.67	77	11.67	104	10.67	131	13.33
24	15.33	51	15.67	78	12.00	105	11.00	132	13.00
25	17.33	52	14.33	79	12.67	106	12.00	133	12.33
26	18.00	53	14.00	80	13.00	107	12.67		
27	17.33	54	14.00	81	13.33	108	13.33		
28	16.33	55	14.00	82	13.00	109	13.00		

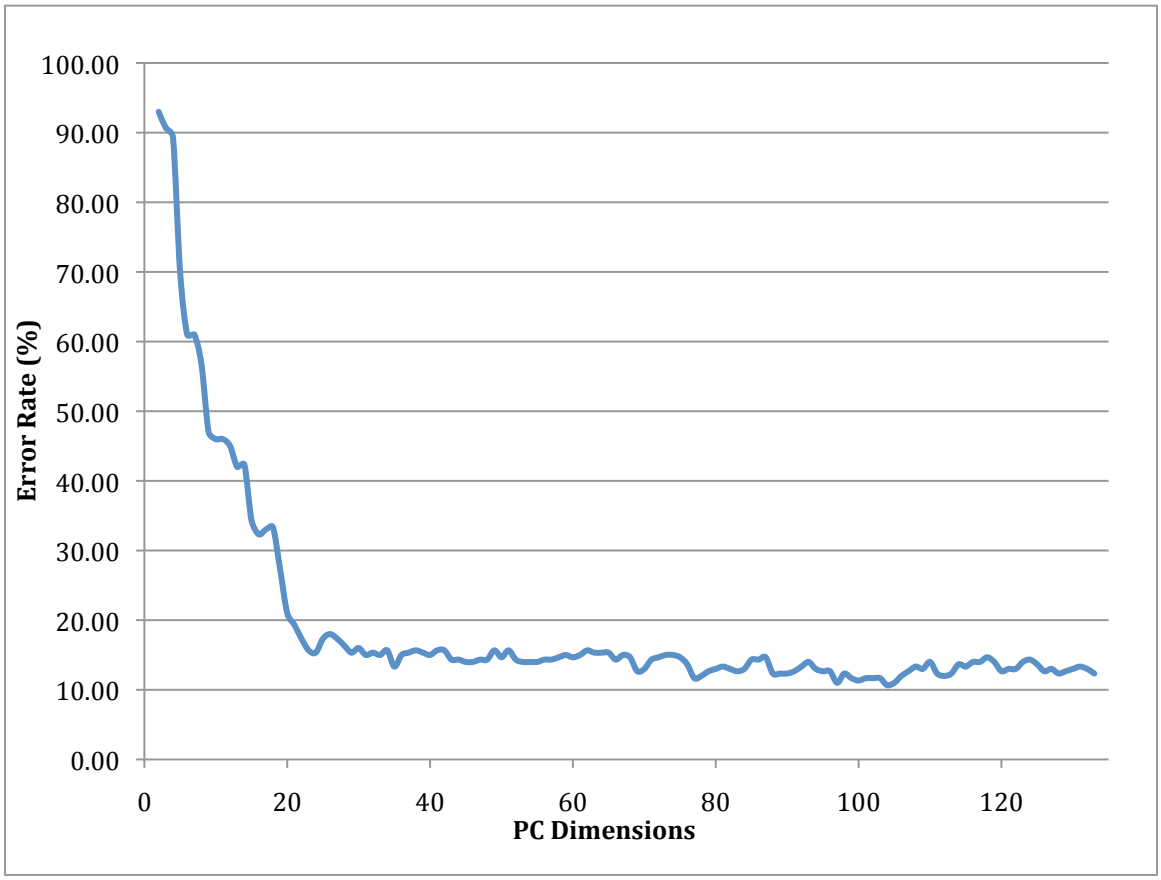


Figure 196: Graph of the discrimination error rate versus PC dimensions for HOO-CV with PCA reduced CVA for the first set of 30 glass spectra (10 replicates), centered data.

Table 208: Discrimination error rates for HOO-CV with PCA reduced CVA for the first set of 30 glass spectra (10 replicates), autoscaled data. The smallest PC dimension with the minimum error rate is highlighted in yellow.

PCs	Error Rate (%)	PCs	Error Rate (%)	PCs	Error Rate (%)	PCs	Error Rate (%)	PCs	Error Rate (%)
2	96.00	56	11.33	110	9.33	164	8.33	218	13.33
3	92.00	57	10.33	111	8.67	165	8.00	219	14.00
4	84.67	58	10.67	112	9.00	166	7.33	220	16.00
5	70.67	59	10.67	113	9.00	167	8.00	221	14.67
6	57.67	60	11.33	114	8.33	168	8.67	222	15.00
7	51.67	61	11.33	115	8.33	169	8.67	223	17.00
8	48.00	62	10.67	116	9.00	170	9.33	224	17.33
9	47.00	63	11.33	117	9.00	171	10.00	225	17.67
10	44.33	64	11.33	118	9.33	172	10.33	226	17.67
11	36.33	65	12.00	119	9.00	173	10.33	227	18.00
12	32.67	66	12.33	120	9.00	174	10.67	228	16.33
13	31.33	67	12.00	121	8.67	175	10.67	229	16.00
14	32.67	68	11.33	122	9.33	176	10.00	230	17.67
15	32.33	69	12.33	123	9.67	177	10.67	231	17.67
16	30.67	70	12.33	124	8.33	178	10.33	232	18.33
17	30.67	71	11.33	125	8.00	179	10.33	233	19.00
18	29.00	72	11.67	126	7.67	180	11.33	234	18.67
19	26.00	73	12.67	127	8.00	181	12.00	235	19.00
20	24.67	74	12.67	128	8.33	182	11.33	236	19.67
21	23.33	75	11.67	129	8.33	183	11.00	237	19.67
22	22.33	76	9.67	130	8.67	184	11.33	238	21.00
23	16.67	77	10.33	131	9.33	185	11.00	239	20.67
24	16.33	78	10.67	132	9.33	186	10.67	240	21.33
25	16.00	79	10.67	133	8.67	187	10.33	241	24.33
26	14.00	80	10.33	134	8.33	188	11.33	242	24.00
27	13.33	81	10.00	135	7.67	189	11.67	243	26.33
28	12.00	82	10.67	136	8.00	190	11.00	244	27.33
29	13.00	83	10.00	137	7.33	191	11.67	245	27.33
30	13.00	84	10.33	138	8.33	192	12.00	246	29.67
31	13.00	85	10.00	139	8.67	193	12.00	247	29.00
32	11.33	86	11.00	140	8.33	194	12.00	248	30.67
33	11.33	87	11.33	141	7.67	195	11.67	249	31.33
34	12.33	88	11.00	142	8.00	196	12.33	250	32.33

35	12.00	89	10.67	143	8.00	197	12.33	251	34.33
36	12.33	90	10.33	144	8.00	198	12.33	252	34.33
37	12.67	91	10.00	145	8.00	199	13.33	253	35.00
38	12.67	92	9.67	146	7.67	200	13.33	254	36.67
39	11.33	93	9.67	147	7.33	201	14.00	255	38.67
40	11.33	94	10.33	148	7.33	202	14.00	256	40.00
41	12.00	95	10.00	149	8.00	203	14.67	257	42.67
42	12.33	96	10.00	150	8.00	204	14.33	258	44.33
43	12.00	97	10.33	151	7.67	205	13.33	259	44.67
44	11.67	98	9.67	152	8.00	206	13.33	260	50.33
45	11.67	99	9.33	153	7.67	207	14.33	261	53.33
46	11.67	100	9.67	154	8.00	208	14.00	262	53.67
47	11.67	101	10.00	155	8.67	209	13.67	263	54.00
48	11.33	102	10.00	156	9.00	210	13.67	264	58.33
49	11.33	103	10.33	157	9.00	211	15.67	265	56.67
50	11.67	104	10.00	158	8.33	212	15.00	266	55.67
51	11.67	105	10.00	159	8.33	213	14.67	267	55.00
52	11.33	106	10.33	160	8.33	214	15.00	268	59.00
53	10.67	107	9.33	161	8.67	215	15.00	269	74.33
54	11.67	108	9.33	162	9.00	216	15.00	270	72.00
55	11.33	109	9.33	163	8.33	217	14.33	271	76.33

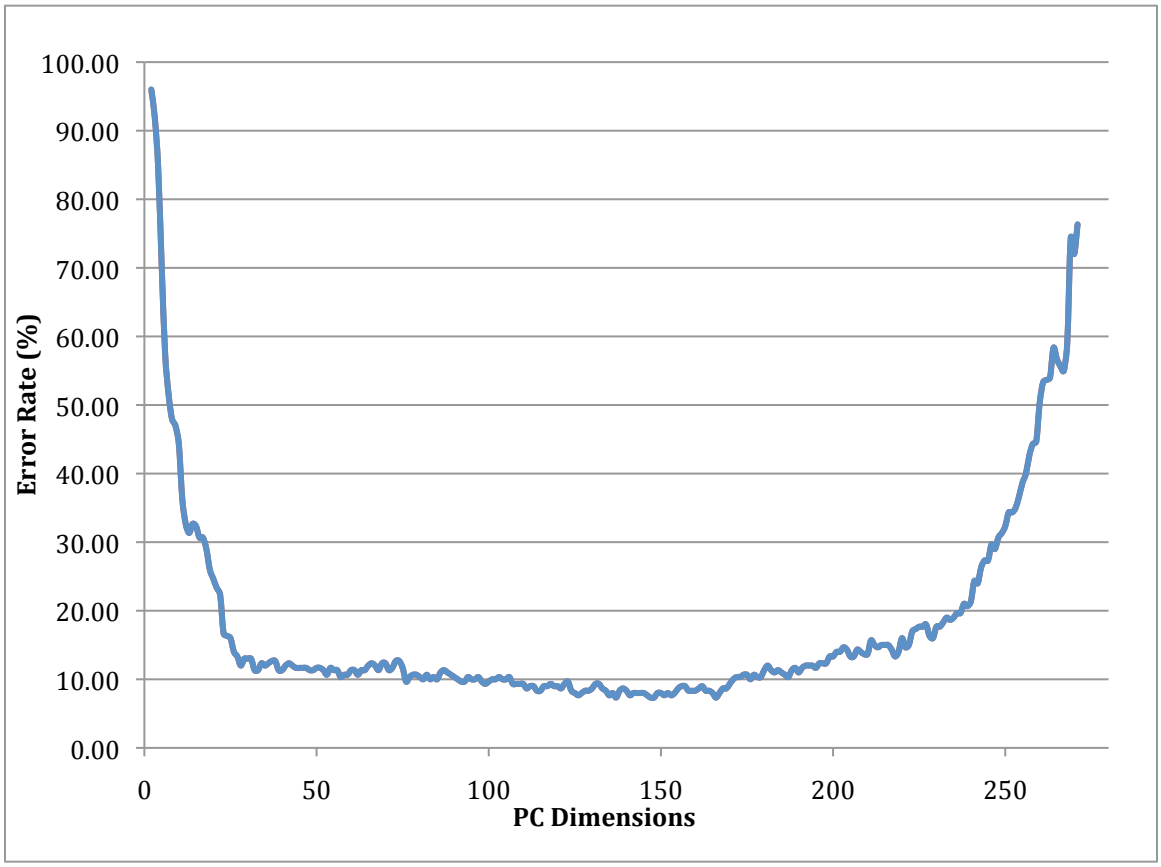


Figure 197: Graph of the discrimination error rate versus PC dimensions for HOO-CV with PCA reduced CVA for the first set of 30 glass spectra (10 replicates), autoscaled data.

First Set – Classification (automotive, architectural or container)

Table 209: Classification (automotive, architectural or container) error rates for HOO-CV with PCA reduced CVA for the first set of 30 glass spectra (10 replicates), no data pretreatment. The smallest PC dimension with the minimum error rate is highlighted in yellow.

PCs	Error Rate (%)	PCs	Error Rate (%)	PCs	Error Rate (%)	PCs	Error Rate (%)	PCs	Error Rate (%)
3	66.00	30	16.00	57	16.67	84	20.33	111	20.67
4	65.00	31	16.33	58	17.67	85	20.67	112	20.33
5	31.67	32	17.00	59	18.33	86	19.00	113	21.33
6	33.00	33	17.33	60	18.67	87	19.33	114	21.00
7	28.67	34	17.00	61	18.00	88	19.33	115	21.67
8	29.33	35	17.67	62	18.67	89	19.67	116	22.33
9	25.33	36	18.33	63	18.33	90	20.00	117	22.67
10	23.67	37	17.33	64	19.00	91	20.00	118	23.00
11	24.00	38	16.33	65	18.33	92	20.00	119	21.67
12	25.67	39	16.67	66	17.33	93	20.33	120	22.33
13	23.33	40	17.33	67	18.00	94	22.00	121	21.33
14	23.67	41	16.67	68	18.33	95	21.67	122	22.33
15	24.00	42	17.00	69	18.67	96	22.33	123	22.67
16	24.00	43	16.67	70	18.00	97	21.67	124	21.33
17	23.67	44	16.33	71	16.67	98	20.33	125	21.67
18	20.67	45	18.00	72	17.00	99	21.33	126	22.33
19	15.67	46	17.00	73	18.00	100	20.00	127	22.00
20	16.00	47	17.33	74	18.67	101	21.00	128	22.33
21	16.33	48	17.67	75	19.00	102	21.33	129	21.33
22	17.33	49	19.33	76	18.33	103	20.33	130	21.00
23	17.33	50	18.33	77	18.67	104	21.00	131	21.33
24	17.00	51	18.00	78	18.67	105	21.00	132	20.00
25	17.33	52	17.33	79	18.67	106	21.00	133	20.33
26	17.00	53	17.00	80	18.00	107	21.00	134	19.67
27	16.33	54	16.00	81	19.33	108	22.00	135	19.67
28	16.00	55	16.33	82	19.33	109	20.33		
29	15.33	56	16.67	83	18.33	110	20.67		

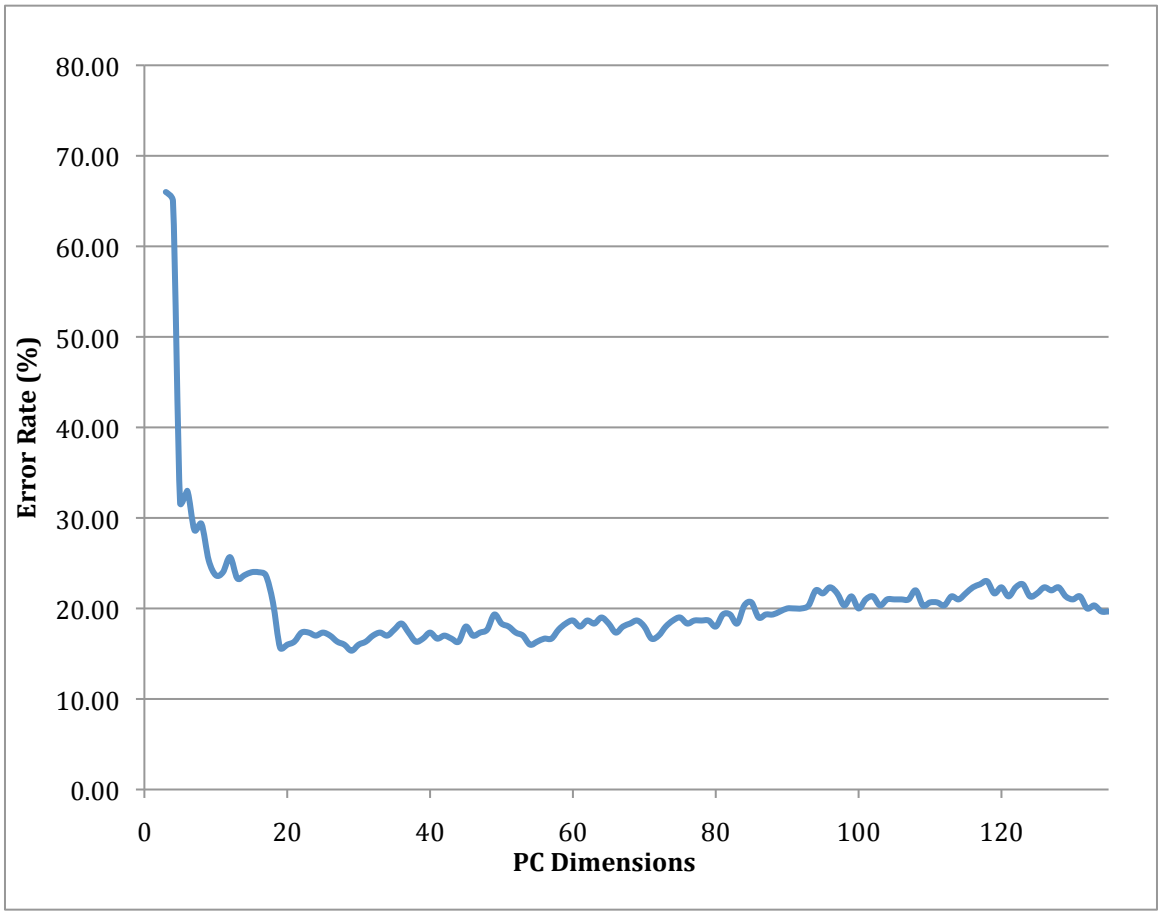


Figure 198: Graph of the classification (automotive, architectural or container) error rate versus PC dimensions for HOO-CV with PCA reduced CVA for the first set of 30 glass spectra (10 replicates), no data pretreatment.

Table 210: Classification (automotive, architectural or container) error rates for HOO-CV with PCA reduced CVA for the first set of 30 glass spectra (10 replicates), centered data. The smallest PC dimension with the minimum error rate is highlighted in yellow.

PCs	Error Rate (%)	PCs	Error Rate (%)	PCs	Error Rate (%)	PCs	Error Rate (%)	PCs	Error Rate (%)
3	65.33	30	17.67	57	17.00	84	20.33	111	20.67
4	66.33	31	17.67	58	18.00	85	20.33	112	20.33
5	30.67	32	16.67	59	17.67	86	19.00	113	20.67
6	33.33	33	17.33	60	17.67	87	19.33	114	21.33
7	29.00	34	16.67	61	17.33	88	19.33	115	22.33
8	28.67	35	17.00	62	18.00	89	20.00	116	22.00
9	26.33	36	17.67	63	18.67	90	20.00	117	22.33
10	23.33	37	17.33	64	19.00	91	20.00	118	22.67
11	24.33	38	14.67	65	17.00	92	20.00	119	22.00
12	25.33	39	16.33	66	17.67	93	20.00	120	22.00
13	23.33	40	17.00	67	17.67	94	20.33	121	22.00
14	23.33	41	16.67	68	18.00	95	21.67	122	22.00
15	22.67	42	16.67	69	18.33	96	21.67	123	22.33
16	23.67	43	16.67	70	18.67	97	20.67	124	22.00
17	23.33	44	16.33	71	16.00	98	21.00	125	21.33
18	21.33	45	18.00	72	16.67	99	20.00	126	22.33
19	17.33	46	17.67	73	18.67	100	20.00	127	22.00
20	18.00	47	17.67	74	19.00	101	20.67	128	22.00
21	17.67	48	17.67	75	17.67	102	21.33	129	21.33
22	17.67	49	19.00	76	18.00	103	20.67	130	21.00
23	18.00	50	19.00	77	18.67	104	20.67	131	20.67
24	17.33	51	18.00	78	18.33	105	20.67	132	21.33
25	17.33	52	18.00	79	18.67	106	21.67	133	20.00
26	16.67	53	18.33	80	18.67	107	21.00	134	20.33
27	17.33	54	17.33	81	19.67	108	21.67		
28	17.67	55	17.00	82	19.67	109	20.33		
29	17.33	56	16.33	83	19.00	110	20.67		

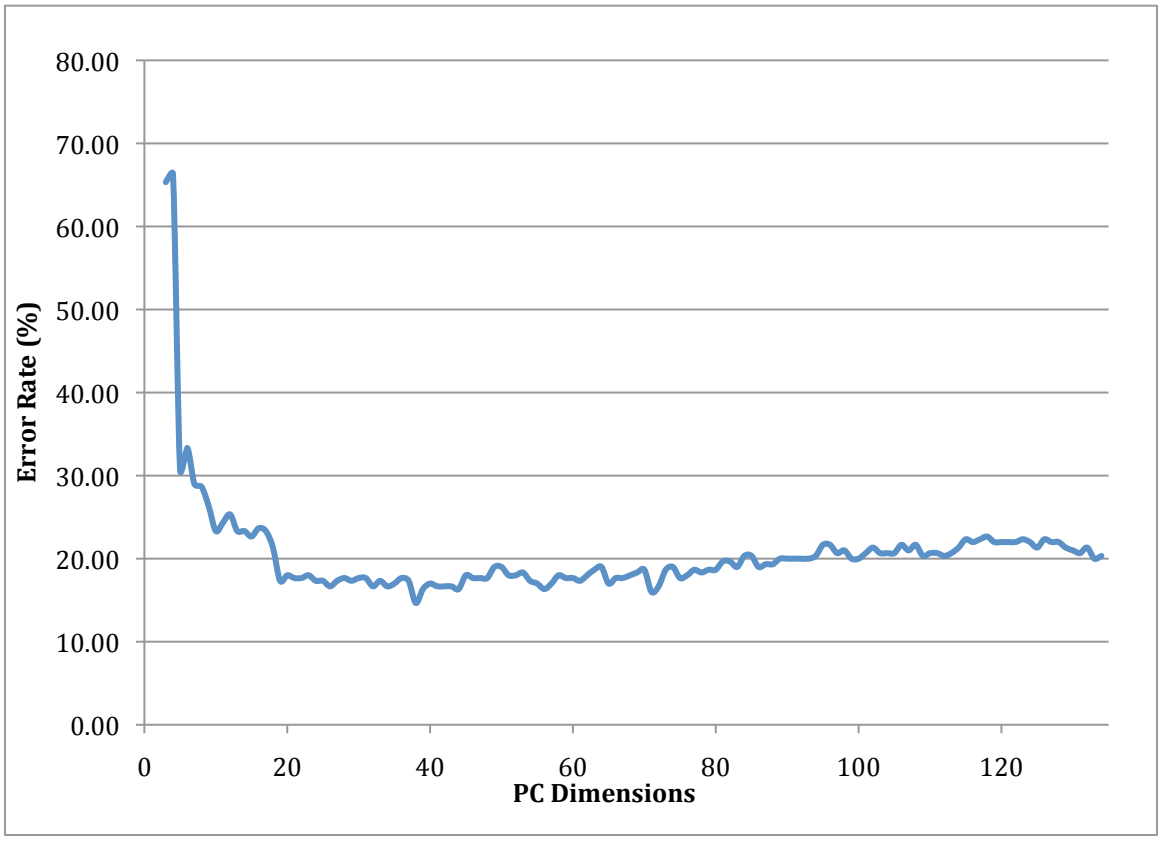


Figure 199: Graph of the classification (automotive, architectural or container) error rate versus PC dimensions for HOO-CV with PCA reduced CVA for the first set of 30 glass spectra (10 replicates), centered data.

Table 211: Classification (automotive, architectural or container) error rates for HOO-CV with PCA reduced CVA for the first set of 30 glass spectra (10 replicates), autoscaled data. The smallest PC dimension with the minimum error rate is highlighted in yellow.

PCs	Error Rate (%)	PCs	Error Rate (%)	PCs	Error Rate (%)	PCs	Error Rate (%)	PCs	Error Rate (%)
3	67.33	61	17.33	119	18.00	177	22.33	235	26.33
4	61.33	62	17.67	120	18.00	178	21.67	236	26.00
5	29.67	63	17.00	121	18.67	179	21.67	237	27.00
6	26.67	64	17.33	122	17.67	180	21.67	238	25.67
7	26.33	65	17.33	123	17.33	181	21.67	239	26.00
8	21.67	66	17.67	124	18.00	182	21.67	240	26.33
9	21.33	67	18.00	125	18.00	183	21.00	241	27.00
10	21.33	68	17.67	126	17.67	184	21.00	242	25.67
11	23.00	69	17.67	127	18.33	185	22.33	243	27.33
12	23.00	70	19.33	128	17.67	186	22.33	244	27.67
13	22.00	71	19.33	129	18.00	187	22.00	245	28.67
14	21.33	72	19.33	130	18.67	188	23.00	246	29.33
15	22.00	73	19.00	131	18.00	189	23.67	247	30.33
16	20.33	74	18.33	132	19.00	190	21.67	248	31.00
17	21.67	75	18.00	133	19.33	191	22.00	249	31.33
18	20.33	76	17.33	134	20.33	192	21.33	250	32.67
19	19.67	77	19.00	135	20.00	193	22.00	251	33.67
20	16.67	78	19.00	136	19.67	194	21.33	252	34.67
21	15.33	79	19.00	137	19.00	195	21.67	253	36.00
22	15.33	80	18.33	138	17.67	196	22.00	254	36.00
23	17.00	81	18.67	139	18.67	197	22.00	255	35.67
24	17.33	82	18.67	140	18.33	198	22.00	256	33.00
25	17.33	83	18.67	141	18.00	199	21.00	257	32.33
26	18.33	84	19.00	142	17.67	200	21.00	258	35.00
27	17.67	85	19.00	143	17.67	201	20.67	259	34.00
28	17.00	86	19.33	144	18.00	202	21.00	260	34.33
29	17.00	87	19.33	145	18.67	203	21.33	261	34.33
30	15.67	88	20.00	146	18.67	204	22.67	262	30.67
31	16.33	89	19.67	147	18.67	205	21.67	263	31.67
32	16.67	90	19.67	148	19.67	206	22.00	264	31.67
33	16.00	91	20.00	149	18.00	207	23.00	265	32.33
34	16.33	92	19.33	150	19.00	208	21.67	266	31.00
35	15.67	93	20.00	151	18.67	209	22.00	267	33.00
36	16.67	94	20.00	152	18.67	210	22.67	268	34.00
37	17.00	95	19.67	153	18.33	211	24.00	269	34.00
38	16.67	96	20.33	154	20.67	212	23.67	270	35.33
39	16.33	97	19.33	155	20.67	213	23.00	271	33.33

40	15.67	98	19.33	156	19.00	214	23.00	272	35.00
41	14.67	99	20.67	157	19.33	215	23.00	273	36.00
42	14.00	100	21.00	158	20.33	216	23.67	274	35.67
43	15.00	101	20.67	159	20.67	217	23.00	275	35.67
44	14.33	102	20.33	160	20.67	218	23.33	276	37.67
45	14.67	103	20.33	161	19.33	219	23.33	277	39.00
46	16.33	104	20.33	162	19.33	220	24.67	278	38.67
47	15.33	105	19.00	163	20.33	221	23.67	279	38.33
48	15.00	106	19.33	164	21.00	222	23.00	280	42.00
49	16.00	107	18.67	165	21.00	223	24.00	281	39.33
50	16.33	108	19.00	166	21.00	224	25.33	282	41.00
51	16.00	109	19.67	167	20.67	225	25.33	283	41.67
52	16.33	110	19.00	168	19.67	226	25.33	284	43.33
53	16.67	111	19.00	169	20.33	227	25.33	285	46.00
54	16.00	112	18.33	170	19.00	228	26.00	286	45.33
55	16.33	113	18.67	171	19.33	229	24.67	287	46.67
56	16.00	114	18.33	172	20.00	230	24.67	288	50.33
57	16.00	115	18.33	173	20.00	231	24.67	289	50.00
58	16.67	116	18.00	174	20.33	232	25.33	290	69.33
59	16.67	117	18.00	175	20.33	233	25.67		
60	17.00	118	17.67	176	22.00	234	26.33		

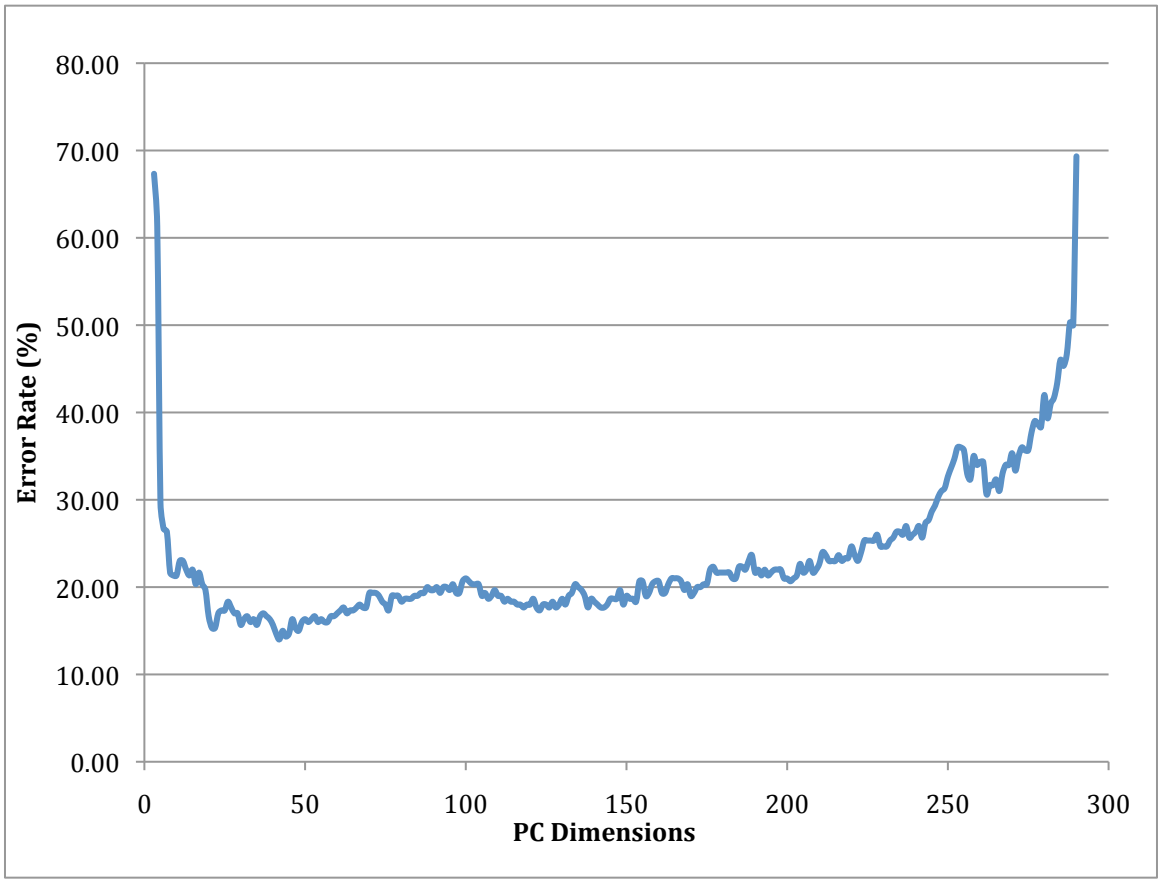


Figure 200: Graph of the classification (automotive, architectural or container) error rate versus PC dimensions for HOO-CV with PCA reduced CVA for the first set of 30 glass spectra (10 replicates), autoscaled data.

First Set – Classification (window or container)

Table 212: Classification (window or container) error rates for HOO-CV with PCA reduced CVA for the first set of 30 glass spectra (10 replicates), no data pretreatment. The smallest PC dimension with the minimum error rate is highlighted in yellow.

PCs	Error Rate (%)	PCs	Error Rate (%)	PCs	Error Rate (%)	PCs	Error Rate (%)	PCs	Error Rate (%)
3	33.33	30	3.33	57	4.00	84	4.67	111	4.67
4	33.33	31	4.00	58	3.67	85	4.67	112	4.67
5	6.33	32	4.00	59	3.67	86	3.67	113	5.00
6	7.33	33	4.00	60	3.67	87	3.67	114	5.00
7	6.33	34	4.00	61	3.67	88	4.00	115	5.33
8	5.33	35	4.00	62	3.67	89	3.67	116	6.00
9	5.33	36	4.00	63	4.00	90	3.67	117	6.00
10	3.67	37	4.00	64	4.67	91	3.67	118	5.67
11	3.67	38	4.00	65	4.67	92	4.33	119	5.33
12	4.00	39	4.00	66	4.00	93	5.00	120	5.33
13	4.00	40	4.00	67	4.33	94	4.67	121	5.67
14	4.00	41	3.67	68	4.33	95	4.67	122	6.00
15	4.00	42	3.67	69	4.33	96	5.00	123	5.67
16	4.00	43	3.67	70	4.33	97	4.67	124	6.33
17	4.00	44	3.67	71	4.33	98	5.00	125	6.33
18	4.00	45	3.67	72	4.33	99	5.00	126	6.33
19	3.67	46	3.67	73	4.67	100	4.67	127	6.33
20	3.67	47	4.00	74	4.67	101	4.67	128	6.33
21	4.00	48	4.00	75	4.33	102	4.67	129	6.33
22	4.00	49	4.00	76	4.33	103	4.67	130	6.00
23	4.00	50	4.00	77	4.33	104	4.33	131	6.00
24	4.00	51	4.00	78	4.00	105	4.33	132	5.67
25	4.00	52	4.00	79	4.33	106	4.33	133	6.00
26	4.00	53	4.00	80	4.00	107	5.00	134	6.33
27	3.67	54	3.67	81	4.33	108	5.00	135	6.00
28	3.33	55	3.67	82	4.33	109	4.33		
29	3.33	56	3.67	83	3.33	110	4.67		

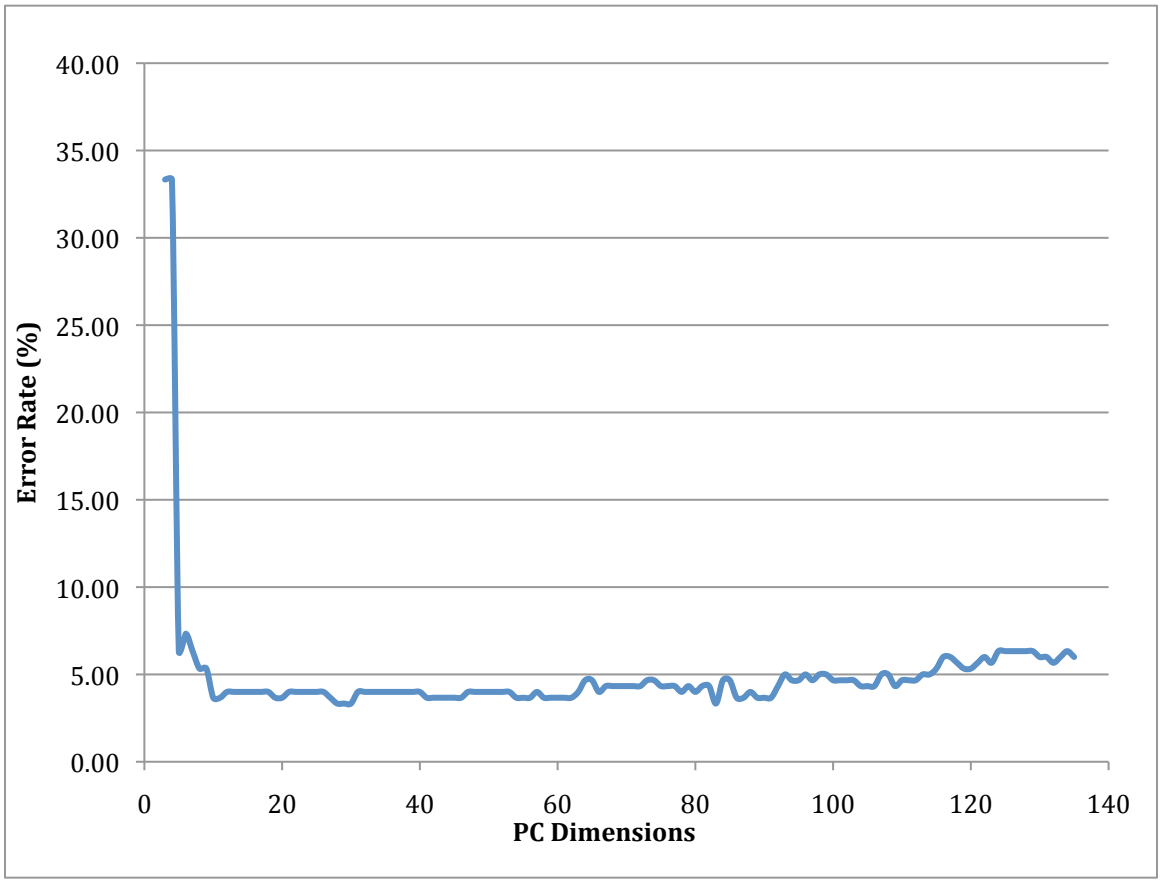


Figure 201: Graph of the classification (window or container) error rate versus PC dimensions for HOO-CV with PCA reduced CVA for the first set of 30 glass spectra (10 replicates), no data pretreatment.

Table 213: Classification (window or container) error rates for HOO-CV with PCA reduced CVA for the first set of 30 glass spectra (10 replicates), centered data. The smallest PC dimension with the minimum error rate is highlighted in yellow.

PCs	Error Rate (%)	PCs	Error Rate (%)	PCs	Error Rate (%)	PCs	Error Rate (%)	PCs	Error Rate (%)
3	33.33	30	4.00	57	3.67	84	4.33	111	4.33
4	33.67	31	4.00	58	3.67	85	4.67	112	4.67
5	6.00	32	4.00	59	3.67	86	3.67	113	5.00
6	7.00	33	4.00	60	3.67	87	3.67	114	5.00
7	6.67	34	4.00	61	3.67	88	3.67	115	5.33
8	4.67	35	4.00	62	3.67	89	3.67	116	5.67
9	4.00	36	4.00	63	4.00	90	3.67	117	5.67
10	3.67	37	4.00	64	4.00	91	3.67	118	5.33
11	3.67	38	4.00	65	4.00	92	4.33	119	5.67
12	4.00	39	4.00	66	4.00	93	4.67	120	5.33
13	4.00	40	4.33	67	4.33	94	4.00	121	5.67
14	4.00	41	3.67	68	4.33	95	4.33	122	6.00
15	3.67	42	3.67	69	4.33	96	5.00	123	6.00
16	3.67	43	3.33	70	4.33	97	4.67	124	6.33
17	4.00	44	4.00	71	4.33	98	4.33	125	6.33
18	4.00	45	4.00	72	4.33	99	4.67	126	6.33
19	4.00	46	4.00	73	4.67	100	4.67	127	6.33
20	4.00	47	4.00	74	4.33	101	4.67	128	6.33
21	4.00	48	4.00	75	4.33	102	4.67	129	6.33
22	4.00	49	4.00	76	4.67	103	4.67	130	6.00
23	4.00	50	4.33	77	4.33	104	4.33	131	6.33
24	4.00	51	4.33	78	4.00	105	4.33	132	6.00
25	4.00	52	4.33	79	4.33	106	4.67	133	6.00
26	4.00	53	4.00	80	4.00	107	4.67	134	6.33
27	3.67	54	4.33	81	4.33	108	5.00		
28	3.33	55	4.33	82	4.33	109	4.33		
29	3.33	56	3.67	83	3.33	110	4.33		

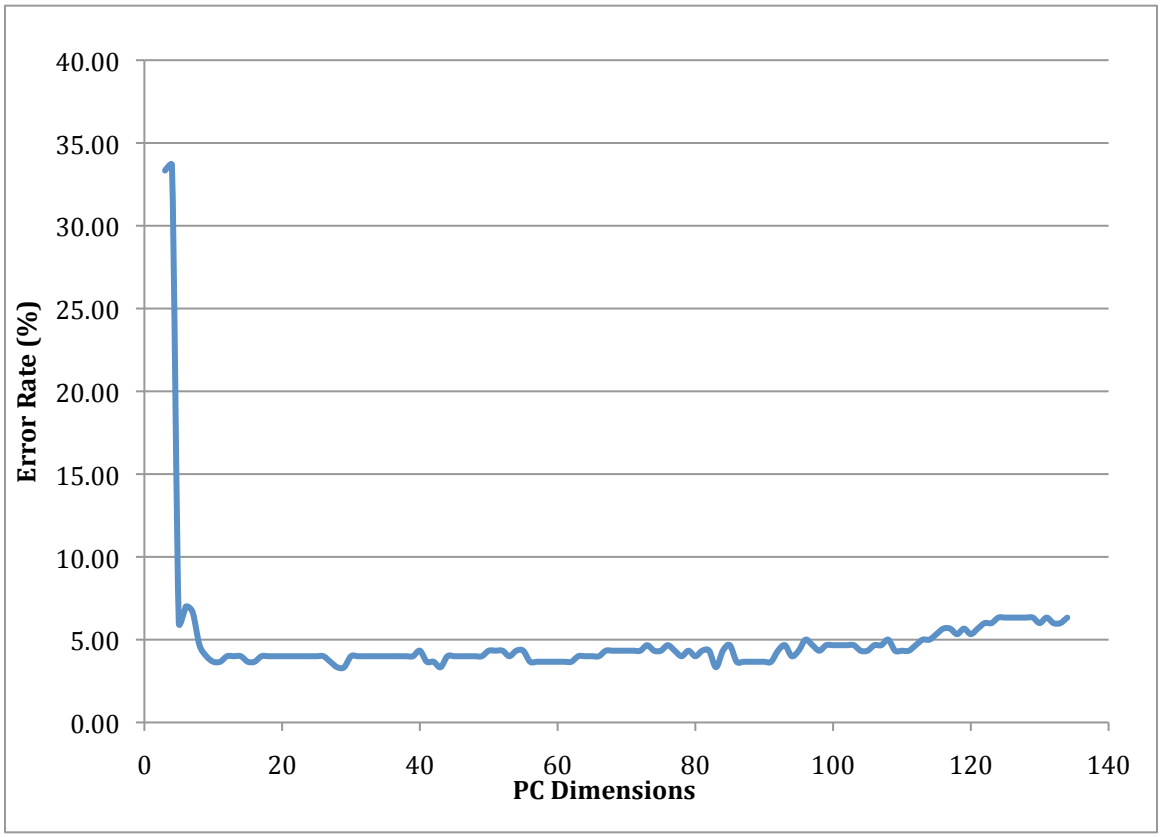


Figure 202: Graph of the classification (window or container) error rate versus PC dimensions for HOO-CV with PCA reduced CVA for the first set of 30 glass spectra (10 replicates), centered data.

Table 214: Classification (window or container) error rates for HOO-CV with PCA reduced CVA for the first set of 30 glass spectra (10 replicates), autoscaled data. The smallest PC dimension with the minimum error rate is highlighted in yellow.

PCs	Error Rate (%)	PCs	Error Rate (%)	PCs	Error Rate (%)	PCs	Error Rate (%)	PCs	Error Rate (%)
3	33.67	61	4.00	119	3.33	177	4.00	235	7.00
4	32.67	62	4.00	120	3.00	178	4.33	236	8.33
5	6.67	63	4.00	121	3.00	179	4.67	237	8.67
6	6.67	64	4.00	122	3.00	180	4.00	238	9.00
7	5.67	65	4.00	123	3.00	181	4.00	239	9.67
8	4.00	66	4.33	124	3.00	182	4.33	240	9.67
9	4.00	67	4.00	125	3.00	183	4.33	241	9.67
10	4.00	68	4.33	126	3.00	184	4.00	242	9.33
11	4.00	69	4.33	127	3.33	185	4.00	243	11.00
12	4.00	70	4.33	128	3.00	186	3.67	244	11.00
13	4.00	71	4.33	129	3.67	187	4.67	245	10.67
14	4.33	72	4.33	130	3.33	188	4.00	246	11.00
15	4.33	73	4.33	131	3.00	189	4.67	247	10.67
16	4.33	74	4.33	132	3.67	190	4.67	248	11.00
17	4.00	75	4.33	133	3.67	191	4.67	249	12.33
18	3.67	76	4.33	134	3.33	192	3.67	250	12.33
19	3.67	77	4.33	135	3.67	193	4.00	251	13.00
20	3.67	78	4.33	136	3.67	194	4.67	252	14.00
21	3.33	79	4.33	137	3.67	195	4.67	253	14.33
22	3.67	80	4.33	138	3.67	196	5.00	254	15.33
23	3.33	81	4.33	139	3.67	197	5.33	255	15.67
24	3.67	82	4.33	140	3.67	198	5.33	256	12.67
25	3.67	83	4.33	141	3.67	199	5.33	257	12.33
26	3.67	84	4.33	142	3.00	200	5.67	258	12.33
27	3.67	85	4.33	143	3.00	201	6.33	259	14.33
28	3.67	86	4.00	144	4.00	202	6.33	260	13.67
29	3.33	87	4.33	145	4.00	203	7.00	261	15.00
30	3.33	88	4.00	146	4.00	204	7.00	262	14.33
31	3.33	89	4.00	147	3.33	205	7.33	263	12.67
32	3.33	90	4.00	148	3.33	206	7.33	264	12.67
33	3.33	91	4.33	149	2.67	207	7.67	265	14.00
34	3.33	92	4.00	150	3.00	208	7.67	266	14.67
35	3.67	93	4.00	151	3.00	209	8.00	267	14.33
36	3.67	94	4.00	152	3.00	210	8.00	268	15.33
37	3.67	95	3.67	153	3.33	211	8.33	269	13.00
38	3.67	96	4.00	154	3.33	212	8.33	270	14.33
39	3.67	97	4.00	155	3.67	213	6.67	271	14.00

40	3.33	98	4.00	156	3.33	214	7.33	272	14.67
41	3.67	99	4.33	157	3.67	215	8.00	273	15.33
42	3.33	100	4.33	158	3.33	216	8.00	274	16.67
43	4.00	101	4.67	159	3.00	217	8.00	275	18.00
44	3.67	102	4.00	160	3.00	218	8.33	276	18.00
45	3.67	103	3.67	161	3.33	219	7.67	277	18.67
46	3.67	104	4.00	162	3.33	220	8.67	278	16.00
47	4.00	105	2.67	163	3.67	221	8.00	279	15.33
48	4.00	106	3.00	164	3.33	222	8.67	280	17.33
49	4.00	107	3.33	165	3.33	223	8.67	281	18.67
50	4.00	108	3.33	166	3.33	224	9.33	282	20.00
51	3.67	109	3.33	167	2.67	225	10.00	283	19.67
52	3.67	110	3.67	168	2.67	226	10.33	284	23.00
53	3.67	111	3.33	169	3.67	227	10.33	285	24.00
54	3.67	112	3.00	170	3.33	228	10.00	286	25.67
55	3.67	113	3.33	171	3.33	229	10.00	287	27.33
56	3.67	114	3.33	172	3.67	230	9.67	288	28.33
57	3.67	115	3.33	173	3.33	231	9.67	289	29.00
58	3.67	116	3.00	174	3.33	232	8.67		
59	3.67	117	3.33	175	4.00	233	6.67		
60	3.67	118	3.33	176	4.00	234	7.33		

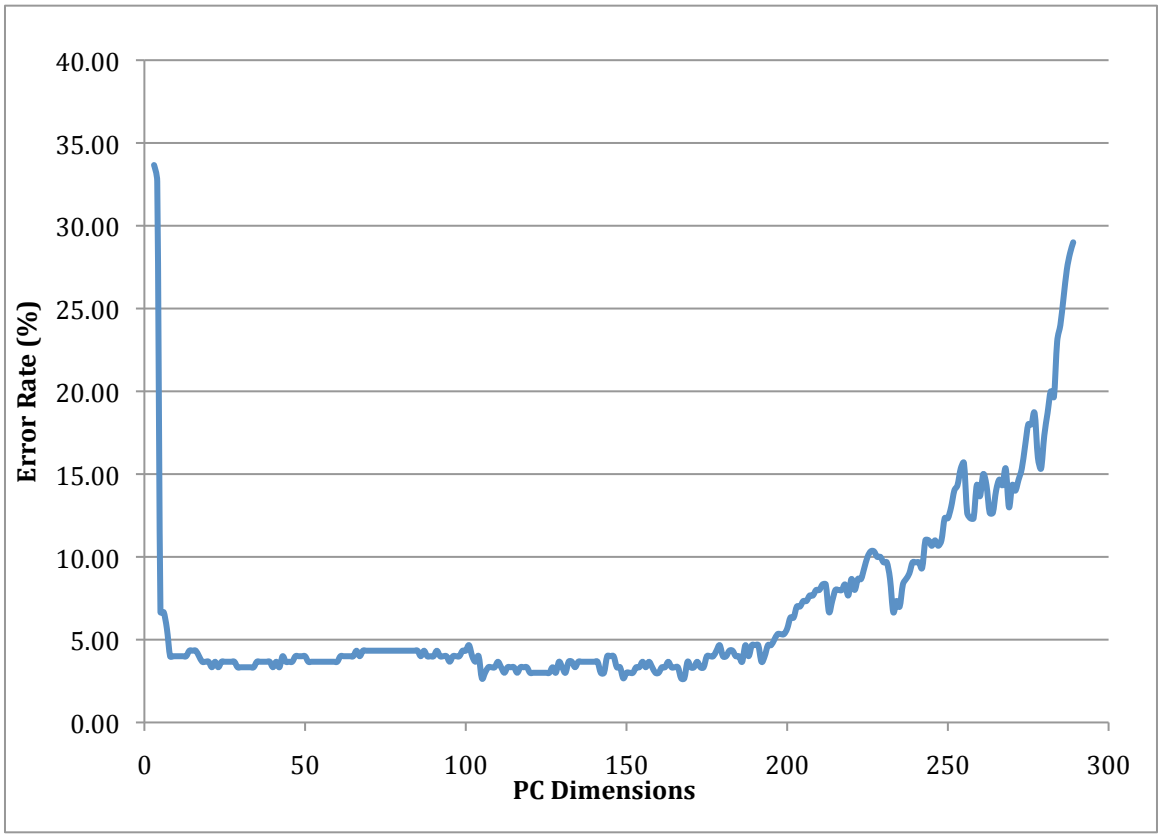


Figure 203: Graph of the classification (window or container) error rate versus PC dimensions for HOO-CV with PCA reduced CVA for the first set of 30 glass spectra (10 replicates), autoscaled data.

First Set – Window Discrimination

Table 215: Discrimination error rates for HOO-CV with PCA reduced CVA for the first set of 20 window glass spectra (10 replicates), no data pretreatment. The smallest PC dimension with the minimum error rate is highlighted in yellow.

PCs	Error Rate (%)	PCs	Error Rate (%)	PCs	Error Rate (%)	PCs	Error Rate (%)	PCs	Error Rate (%)
3	92.50	28	15.50	53	15.50	78	13.00	103	15.50
4	89.00	29	15.50	54	14.00	79	12.00	104	18.00
5	82.00	30	15.00	55	14.50	80	11.50	105	17.00
6	79.00	31	16.00	56	13.00	81	13.50	106	17.00
7	71.00	32	15.00	57	13.50	82	12.00	107	17.00
8	57.50	33	14.50	58	13.00	83	13.50	108	17.50
9	53.50	34	14.50	59	13.00	84	15.00	109	19.00
10	45.50	35	13.00	60	14.00	85	13.50	110	16.50
11	46.50	36	13.00	61	11.50	86	14.00	111	16.50
12	46.00	37	14.50	62	13.50	87	14.00	112	16.00
13	43.00	38	14.00	63	13.00	88	14.00	113	16.00
14	44.00	39	10.00	64	13.50	89	16.50	114	16.50
15	39.50	40	13.00	65	14.00	90	18.00	115	16.50
16	32.50	41	12.50	66	14.00	91	16.50	116	18.00
17	29.00	42	12.50	67	13.50	92	16.00	117	17.50
18	28.00	43	13.50	68	15.00	93	15.00	118	18.00
19	22.00	44	13.00	69	13.50	94	15.00	119	18.50
20	17.00	45	13.00	70	15.00	95	15.00	120	20.00
21	16.00	46	13.00	71	13.50	96	14.00	121	20.00
22	15.00	47	15.00	72	13.00	97	13.50	122	21.00
23	15.00	48	14.50	73	13.50	98	15.50	123	18.00
24	13.50	49	15.50	74	12.50	99	16.00		
25	11.50	50	15.50	75	12.00	100	15.50		
26	13.50	51	15.50	76	11.50	101	15.00		
27	15.50	52	15.50	77	12.00	102	15.50		

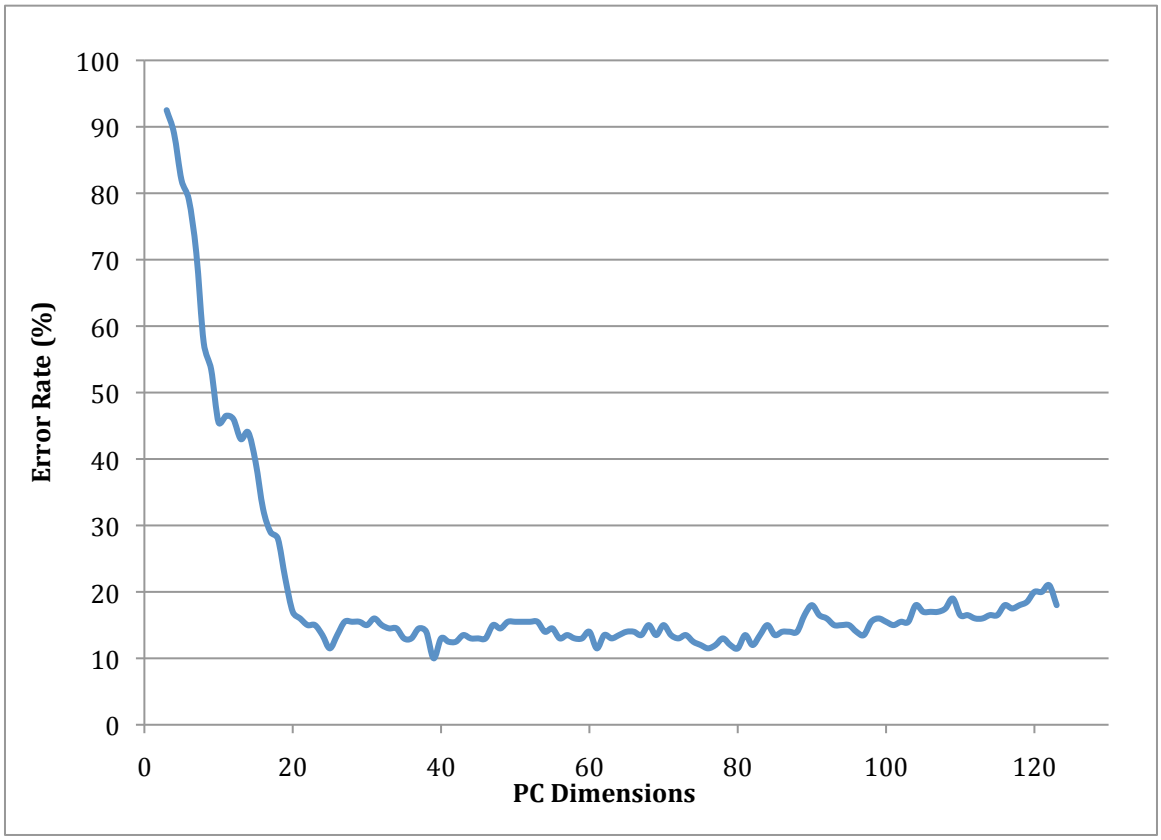


Figure 204: Graph of the discrimination error rate versus PC dimensions for HOO-CV with PCA reduced CVA for the first set of 20 window glass spectra (10 replicates), no data pretreatment.

Table 216: Discrimination error rates for HOO-CV with PCA reduced CVA for the first set of 20 window glass spectra (10 replicates), centered data. The smallest PC dimension with the minimum error rate is highlighted in yellow.

PCs	Error Rate (%)	PCs	Error Rate (%)	PCs	Error Rate (%)	PCs	Error Rate (%)	PCs	Error Rate (%)
3	94.00	28	15.50	53	15.50	78	12.50	103	16.00
4	88.50	29	15.00	54	14.50	79	12.50	104	16.00
5	80.50	30	15.50	55	15.00	80	11.50	105	18.00
6	77.00	31	14.50	56	13.50	81	13.00	106	17.00
7	66.50	32	15.00	57	13.00	82	12.00	107	17.50
8	63.00	33	15.00	58	12.50	83	13.50	108	17.50
9	52.50	34	14.50	59	13.00	84	15.50	109	18.00
10	46.50	35	14.00	60	14.00	85	13.50	110	16.00
11	47.00	36	13.50	61	13.00	86	14.00	111	16.00
12	47.00	37	16.00	62	12.50	87	15.00	112	15.00
13	43.00	38	14.00	63	13.50	88	17.00	113	15.50
14	44.00	39	12.50	64	13.50	89	17.00	114	16.00
15	38.00	40	12.50	65	13.00	90	15.00	115	17.00
16	32.50	41	13.00	66	13.50	91	14.50	116	18.00
17	30.00	42	13.00	67	13.00	92	15.00	117	19.00
18	28.00	43	14.00	68	14.00	93	14.00	118	18.00
19	19.00	44	13.00	69	13.50	94	15.00	119	17.50
20	18.50	45	13.00	70	15.00	95	16.00	120	19.00
21	16.00	46	14.00	71	13.50	96	14.50	121	19.50
22	15.00	47	14.50	72	13.00	97	14.50	122	20.50
23	16.00	48	14.50	73	12.50	98	15.00	123	20.00
24	13.00	49	14.00	74	12.50	99	15.00		
25	12.00	50	14.50	75	11.50	100	15.00		
26	14.50	51	16.00	76	11.50	101	15.00		
27	15.00	52	15.50	77	11.50	102	15.50		

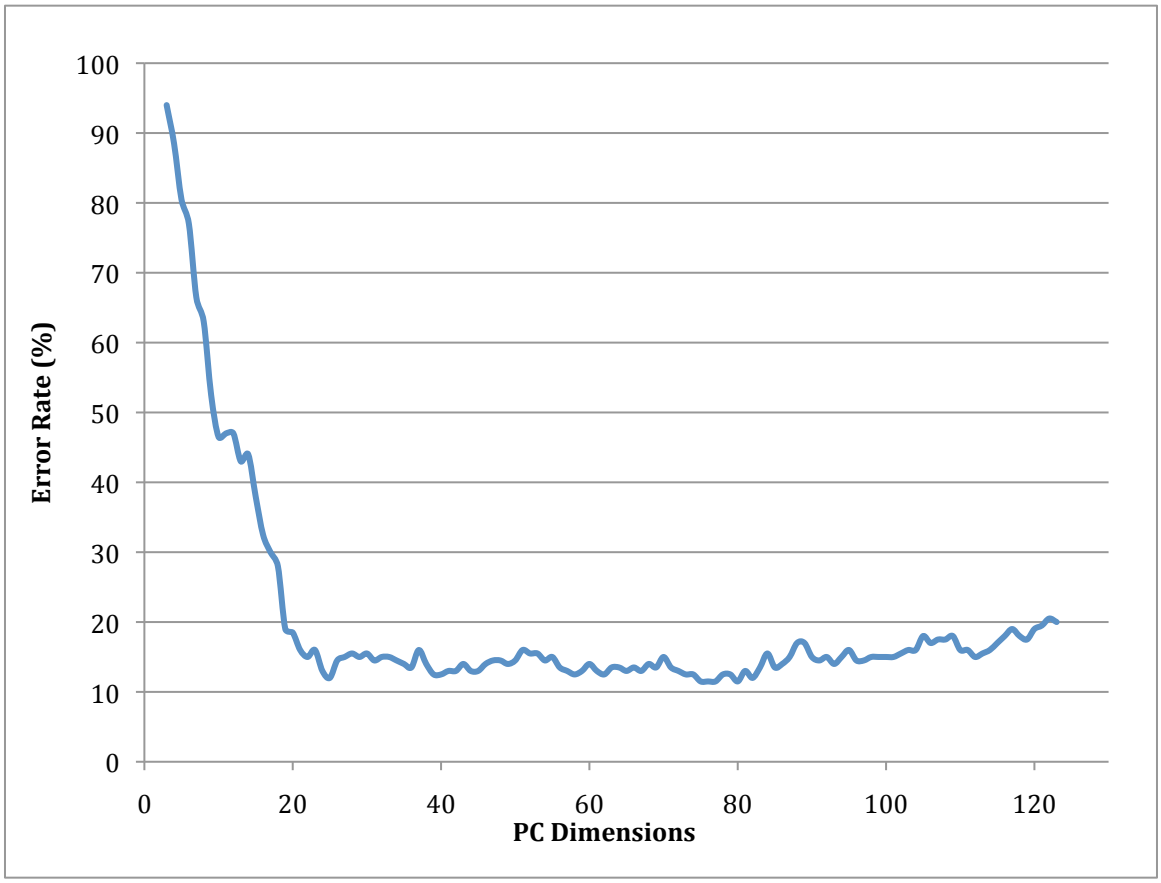


Figure 205: Graph of the discrimination error rate versus PC dimensions for HOO-CV with PCA reduced CVA for the first set of 20 window glass spectra (10 replicates), centered data.

Table 217: Discrimination error rates for HOO-CV with PCA reduced CVA for the first set of 20 window glass spectra (10 replicates), autoscaled data. The smallest PC dimension with the minimum error rate is highlighted in yellow.

PCs	Error Rate (%)	PCs	Error Rate (%)	PCs	Error Rate (%)	PCs	Error Rate (%)	PCs	Error Rate (%)
3	90.50	43	13.00	83	11.50	123	12.00	163	30.50
4	85.50	44	11.00	84	11.50	124	13.50	164	31.50
5	74.50	45	10.00	85	10.50	125	13.50	165	35.00
6	69.50	46	11.50	86	11.00	126	12.50	166	36.00
7	52.50	47	11.50	87	10.00	127	14.00	167	36.50
8	50.00	48	11.50	88	10.00	128	14.00	168	37.50
9	49.50	49	11.00	89	10.00	129	14.00	169	40.00
10	46.50	50	11.50	90	10.00	130	15.50	170	45.00
11	39.50	51	10.50	91	10.00	131	15.50	171	46.50
12	33.00	52	10.50	92	9.50	132	15.00	172	51.50
13	31.50	53	10.50	93	9.50	133	16.50	173	55.00
14	33.00	54	11.00	94	9.50	134	16.50	174	60.00
15	28.50	55	10.00	95	9.50	135	17.00	175	69.00
16	24.50	56	10.50	96	10.00	136	16.00	176	64.50
17	26.50	57	11.50	97	10.00	137	15.50	177	70.50
18	25.00	58	12.00	98	10.50	138	16.50	178	74.00
19	21.00	59	13.00	99	9.50	139	17.00	179	72.00
20	21.50	60	12.00	100	10.50	140	16.00	180	81.50
21	20.50	61	11.00	101	11.50	141	17.50	181	89.00
22	18.00	62	11.50	102	11.00	142	18.50	182	83.00
23	13.00	63	12.50	103	11.50	143	18.50	183	73.00
24	10.50	64	11.00	104	12.00	144	17.50	184	76.00
25	11.50	65	11.50	105	11.00	145	18.00	185	80.50
26	11.00	66	11.50	106	12.00	146	19.50	186	86.50
27	8.50	67	11.00	107	12.00	147	20.50	187	90.00
28	9.50	68	11.00	108	9.50	148	21.00	188	93.00
29	10.50	69	11.50	109	8.50	149	22.00	189	95.50
30	8.00	70	11.00	110	9.50	150	21.50	190	94.00
31	10.50	71	11.50	111	9.50	151	21.00	191	90.50
32	8.50	72	11.00	112	10.50	152	22.00	192	92.00
33	9.50	73	11.00	113	10.00	153	22.00	193	96.00
34	10.00	74	11.50	114	9.00	154	24.50	194	97.00
35	10.00	75	11.50	115	9.00	155	24.50	195	96.50
36	11.00	76	11.00	116	10.00	156	24.00	196	98.50
37	11.50	77	11.00	117	10.50	157	24.50	197	96.00
38	12.00	78	11.00	118	11.00	158	26.00	198	94.00
39	12.00	79	9.50	119	11.50	159	27.50	199	81.00

40	12.00	80	10.50	120	12.00	160	23.00	
41	13.00	81	10.00	121	11.00	161	26.50	
42	13.50	82	11.50	122	11.50	162	27.50	

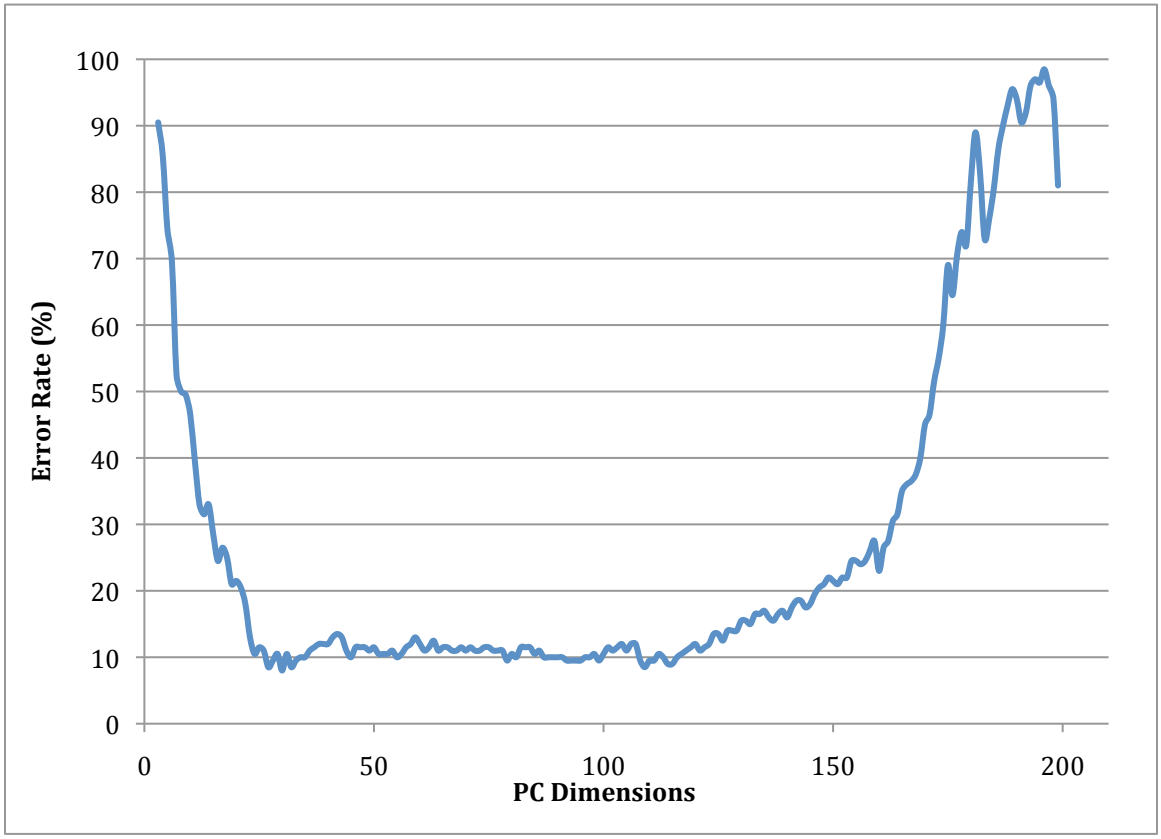


Figure 206: Graph of the discrimination error rate versus PC dimensions for HOO-CV with PCA reduced CVA for the first set of 20 window glass spectra (10 replicates), autoscaled data.

First Set – Container Discrimination

Table 218: Discrimination error rates for HOO-CV with PCA reduced CVA for the first set of 10 container glass spectra (10 replicates), no data pretreatment. The smallest PC dimension with the minimum error rate is highlighted in yellow.

PCs	Error Rate (%)	PCs	Error Rate (%)	PCs	Error Rate (%)	PCs	Error Rate (%)	PCs	Error Rate (%)
3	72.00	22	15.00	41	15.00	60	17.00	79	20.00
4	69.00	23	16.00	42	14.00	61	17.00	80	20.00
5	62.00	24	18.00	43	14.00	62	16.00	81	22.00
6	49.00	25	17.00	44	15.00	63	17.00	82	25.00
7	49.00	26	16.00	45	14.00	64	19.00	83	26.00
8	52.00	27	16.00	46	13.00	65	21.00	84	30.00
9	43.00	28	15.00	47	13.00	66	23.00	85	36.00
10	46.00	29	14.00	48	11.00	67	23.00	86	37.00
11	43.00	30	13.00	49	11.00	68	20.00	87	45.00
12	42.00	31	13.00	50	13.00	69	22.00	88	57.00
13	43.00	32	13.00	51	12.00	70	22.00	89	64.00
14	43.00	33	14.00	52	12.00	71	21.00	90	59.00
15	32.00	34	14.00	53	12.00	72	19.00	91	64.00
16	28.00	35	12.00	54	12.00	73	21.00	92	76.00
17	27.00	36	15.00	55	13.00	74	20.00	93	78.00
18	30.00	37	15.00	56	11.00	75	20.00	94	81.00
19	18.00	38	17.00	57	13.00	76	21.00	95	91.00
20	15.00	39	16.00	58	16.00	77	22.00	96	91.00
21	14.00	40	14.00	59	17.00	78	21.00		

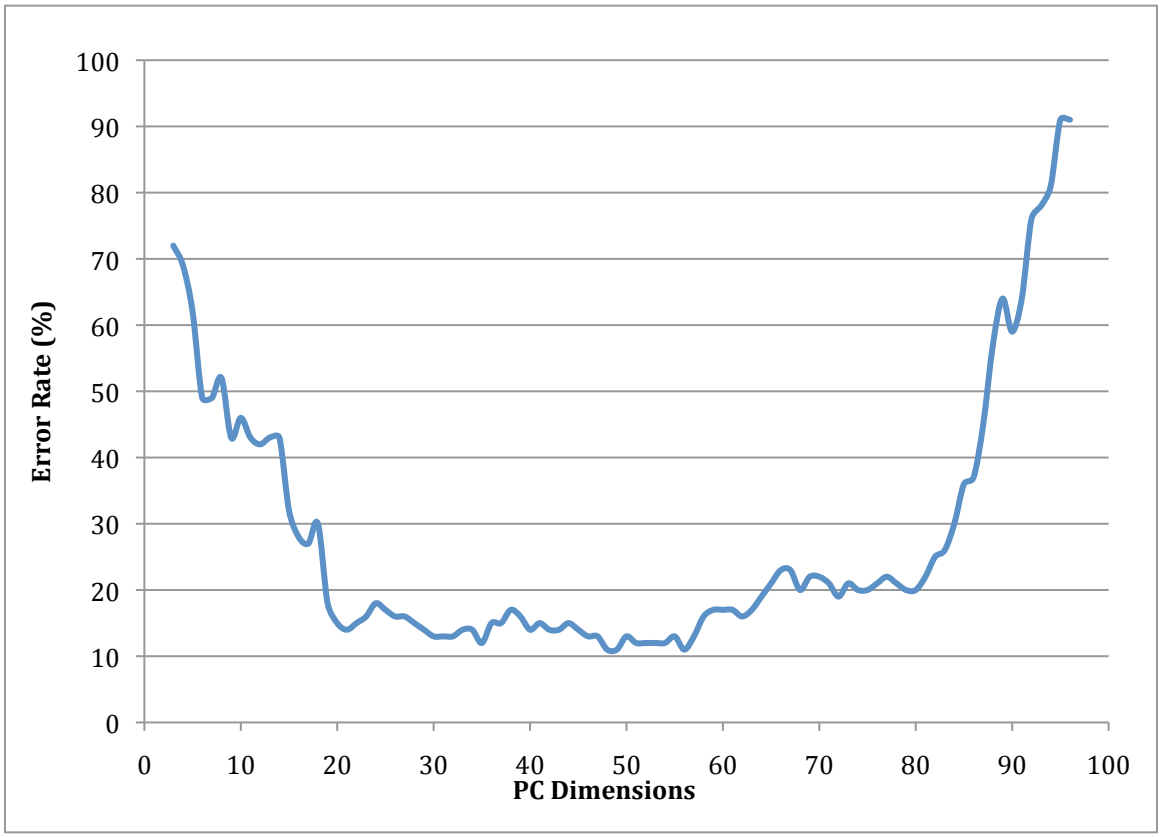


Figure 207: Graph of the discrimination error rate versus PC dimensions for HOO-CV with PCA reduced CVA for the first set of 10 container glass spectra (10 replicates), no data pretreatment.

Table 219: Discrimination error rates for HOO-CV with PCA reduced CVA for the first set of 10 container glass spectra (10 replicates), centered data. The smallest PC dimension with the minimum error rate is highlighted in yellow.

PCs	Error Rate (%)	PCs	Error Rate (%)	PCs	Error Rate (%)	PCs	Error Rate (%)	PCs	Error Rate (%)
3	69.00	22	15.00	41	14.00	60	14.00	79	20.00
4	70.00	23	16.00	42	14.00	61	16.00	80	20.00
5	63.00	24	18.00	43	14.00	62	17.00	81	21.00
6	50.00	25	18.00	44	12.00	63	18.00	82	24.00
7	53.00	26	14.00	45	13.00	64	21.00	83	24.00
8	51.00	27	13.00	46	12.00	65	19.00	84	31.00
9	48.00	28	15.00	47	10.00	66	20.00	85	35.00
10	44.00	29	13.00	48	10.00	67	22.00	86	42.00
11	43.00	30	13.00	49	11.00	68	20.00	87	48.00
12	43.00	31	13.00	50	9.00	69	21.00	88	49.00
13	42.00	32	13.00	51	12.00	70	19.00	89	67.00
14	36.00	33	14.00	52	12.00	71	19.00	90	63.00
15	34.00	34	14.00	53	12.00	72	18.00	91	75.00
16	27.00	35	13.00	54	12.00	73	19.00	92	77.00
17	28.00	36	13.00	55	11.00	74	17.00	93	83.00
18	22.00	37	13.00	56	13.00	75	16.00	94	90.00
19	17.00	38	14.00	57	15.00	76	19.00	95	86.00
20	15.00	39	14.00	58	15.00	77	19.00		
21	14.00	40	11.00	59	14.00	78	21.00		

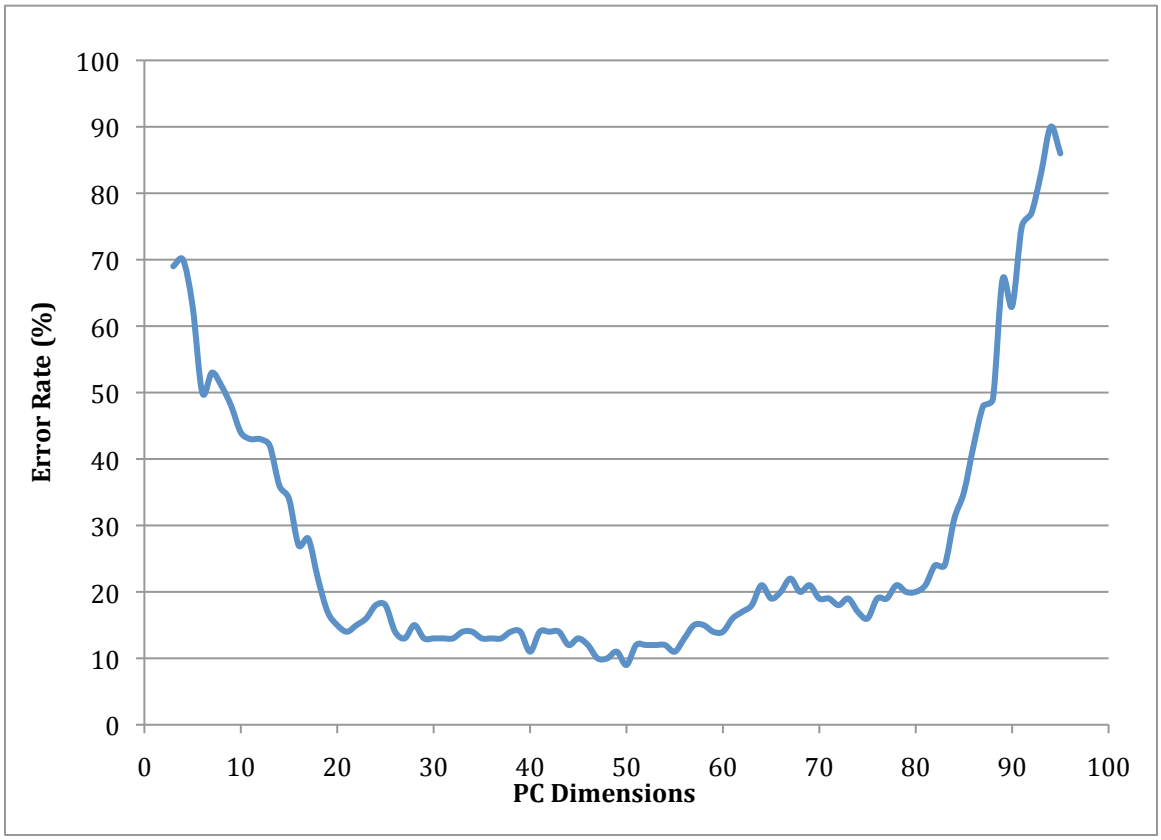


Figure 208: Graph of the discrimination error rate versus PC dimensions for HOO-CV with PCA reduced CVA for the first set of 10 container glass spectra (10 replicates), centered data.

Table 220: Discrimination error rates for HOO-CV with PCA reduced CVA for the first set of 10 container glass spectra (10 replicates), autoscaled data. The smallest PC dimension with the minimum error rate is highlighted in yellow.

PCs	Error Rate (%)	PCs	Error Rate (%)	PCs	Error Rate (%)	PCs	Error Rate (%)	PCs	Error Rate (%)
3	74.00	23	12.00	43	9.00	63	12.00	83	20.00
4	62.00	24	11.00	44	10.00	64	14.00	84	20.00
5	64.00	25	8.00	45	10.00	65	12.00	85	23.00
6	59.00	26	10.00	46	10.00	66	12.00	86	32.00
7	46.00	27	9.00	47	10.00	67	10.00	87	38.00
8	43.00	28	8.00	48	9.00	68	11.00	88	49.00
9	45.00	29	8.00	49	9.00	69	9.00	89	56.00
10	37.00	30	8.00	50	10.00	70	9.00	90	57.00
11	34.00	31	9.00	51	10.00	71	9.00	91	68.00
12	30.00	32	6.00	52	10.00	72	12.00	92	74.00
13	26.00	33	7.00	53	9.00	73	13.00	93	87.00
14	24.00	34	8.00	54	11.00	74	14.00	94	94.00
15	27.00	35	7.00	55	10.00	75	16.00	95	84.00
16	27.00	36	6.00	56	8.00	76	16.00	96	96.00
17	23.00	37	7.00	57	9.00	77	17.00	97	98.00
18	25.00	38	8.00	58	10.00	78	19.00	98	96.00
19	25.00	39	9.00	59	10.00	79	17.00	99	85.00
20	18.00	40	10.00	60	12.00	80	16.00		
21	14.00	41	10.00	61	12.00	81	18.00		
22	13.00	42	9.00	62	13.00	82	20.00		

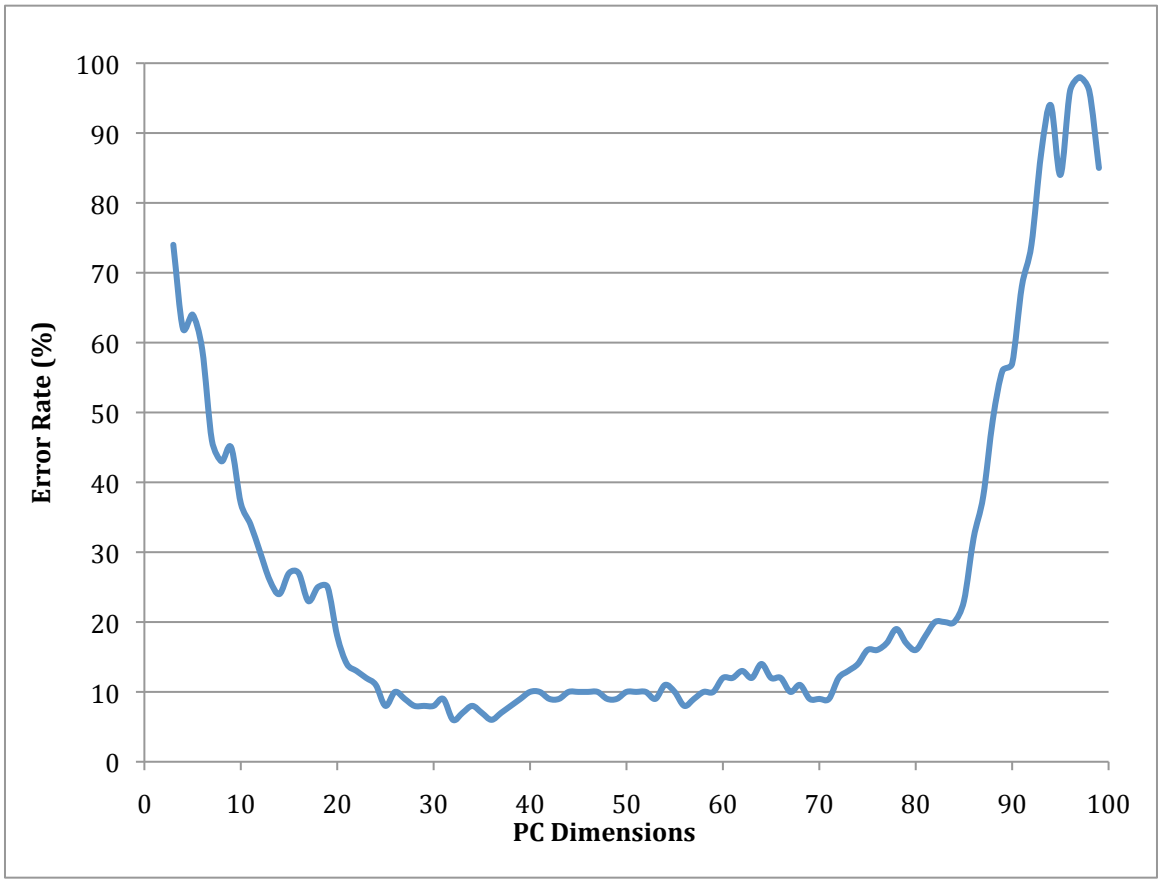


Figure 209: Graph of the discrimination error rate versus PC dimensions for HOO-CV with PCA reduced CVA for the first set of 10 container glass spectra (10 replicates), autoscaled data.

First Set – Float Classification

Table 221: Float classification error rates for HOO-CV with PCA reduced CVA for the first set of 20 window glass spectra (10 replicates), no data pretreatment. The smallest PC dimension with the minimum error rate is highlighted in yellow.

PCs	Error Rate (%)	PCs	Error Rate (%)	PCs	Error Rate (%)	PCs	Error Rate (%)	PCs	Error Rate (%)
3	37.00	28	19.50	53	24.00	78	19.50	103	27.00
4	33.00	29	21.00	54	24.00	79	20.50	104	28.00
5	32.50	30	21.50	55	24.50	80	20.00	105	29.00
6	29.50	31	21.50	56	24.00	81	20.00	106	29.00
7	29.00	32	20.50	57	24.00	82	20.00	107	28.50
8	28.50	33	19.50	58	25.50	83	21.50	108	27.00
9	22.00	34	19.50	59	25.50	84	20.50	109	25.00
10	21.00	35	20.50	60	23.50	85	20.50	110	27.50
11	21.00	36	22.00	61	25.00	86	20.50	111	28.50
12	21.00	37	21.00	62	20.50	87	21.00	112	27.00
13	21.50	38	20.00	63	19.00	88	21.50	113	26.50
14	20.50	39	21.00	64	18.50	89	21.50	114	27.50
15	20.50	40	21.00	65	17.00	90	24.00	115	27.50
16	20.50	41	20.00	66	16.50	91	24.50	116	28.50
17	19.50	42	21.50	67	16.50	92	25.00	117	30.00
18	20.50	43	22.00	68	17.50	93	25.00	118	31.00
19	21.00	44	23.00	69	18.00	94	24.00	119	30.50
20	20.00	45	23.00	70	18.50	95	25.50	120	28.00
21	21.50	46	24.50	71	21.00	96	25.50	121	32.50
22	20.00	47	24.00	72	19.50	97	25.00	122	32.50
23	19.00	48	23.50	73	20.50	98	25.00	123	31.50
24	18.50	49	21.50	74	19.50	99	25.00	124	32.00
25	19.00	50	22.50	75	20.50	100	25.50		
26	19.50	51	22.50	76	20.50	101	28.00		
27	19.50	52	24.00	77	20.50	102	28.00		

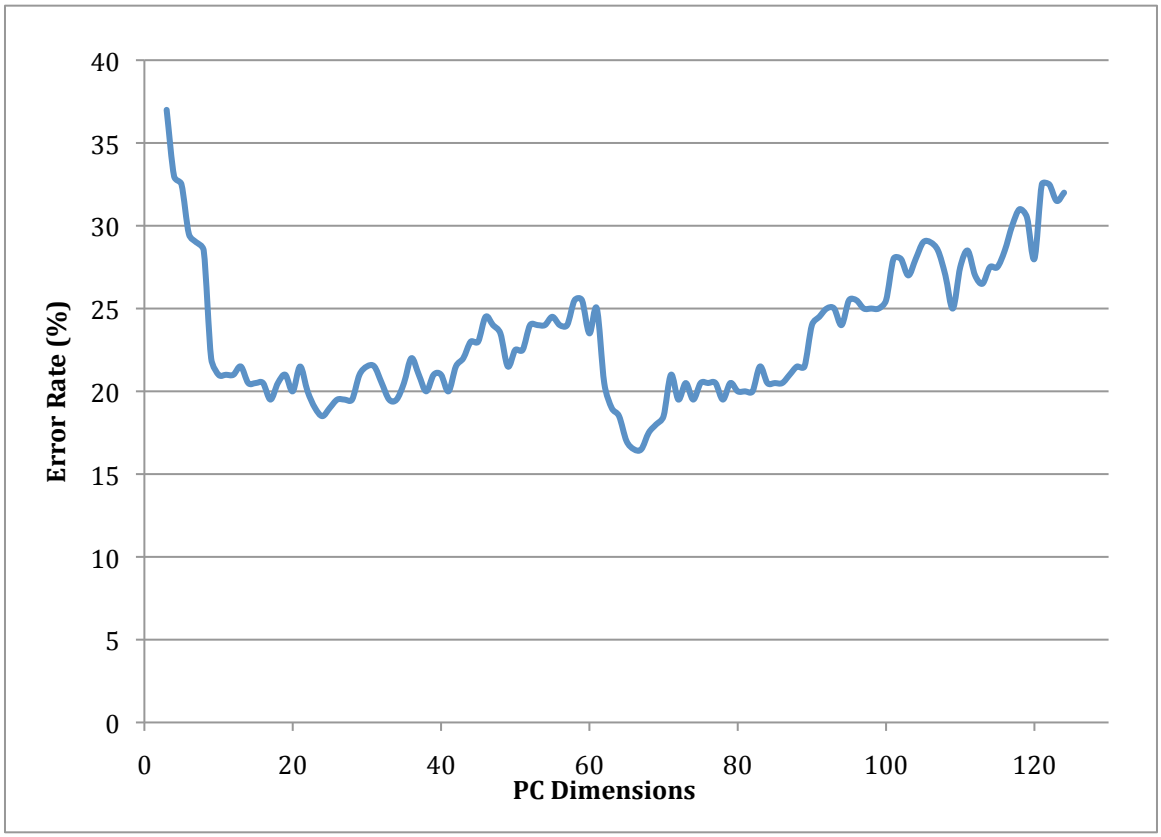


Figure 210: Graph of the float classification error rate versus PC dimensions for HOO-CV with PCA reduced CVA for the first set of 20 window glass spectra (10 replicates), no data pretreatment.

Table 222: Float classification error rates for HOO-CV with PCA reduced CVA for the first set of 20 window glass spectra (10 replicates), centered data. The smallest PC dimension with the minimum error rate is highlighted in yellow.

PCs	Error Rate (%)	PCs	Error Rate (%)	PCs	Error Rate (%)	PCs	Error Rate (%)	PCs	Error Rate (%)
3	35.50	28	20.00	53	23.50	78	20.00	103	26.50
4	33.00	29	20.50	54	24.00	79	18.50	104	29.00
5	33.00	30	20.50	55	24.00	80	18.50	105	28.50
6	30.00	31	21.00	56	24.50	81	18.50	106	29.00
7	29.50	32	21.00	57	24.50	82	19.50	107	29.50
8	28.00	33	21.00	58	25.50	83	21.50	108	27.50
9	21.50	34	21.00	59	25.50	84	20.00	109	25.50
10	21.00	35	21.00	60	23.50	85	21.50	110	28.00
11	20.50	36	21.00	61	25.00	86	20.50	111	28.00
12	21.00	37	21.50	62	18.50	87	21.50	112	27.50
13	21.00	38	20.50	63	17.50	88	22.50	113	27.00
14	20.50	39	20.00	64	18.50	89	23.00	114	26.50
15	20.50	40	21.00	65	17.00	90	24.50	115	28.00
16	20.50	41	19.00	66	16.50	91	24.50	116	28.00
17	20.00	42	21.50	67	17.00	92	25.00	117	29.00
18	21.50	43	21.50	68	17.50	93	25.00	118	30.50
19	20.00	44	23.00	69	18.50	94	24.00	119	30.50
20	19.50	45	23.50	70	19.00	95	26.00	120	29.50
21	21.50	46	23.50	71	20.00	96	26.00	121	32.00
22	20.00	47	23.00	72	19.50	97	25.00	122	33.00
23	19.50	48	22.50	73	20.50	98	26.50	123	31.00
24	18.50	49	23.00	74	19.50	99	25.50	124	31.50
25	19.00	50	23.00	75	20.50	100	25.50		
26	18.00	51	23.50	76	20.50	101	27.50		
27	18.00	52	24.50	77	20.50	102	27.50		

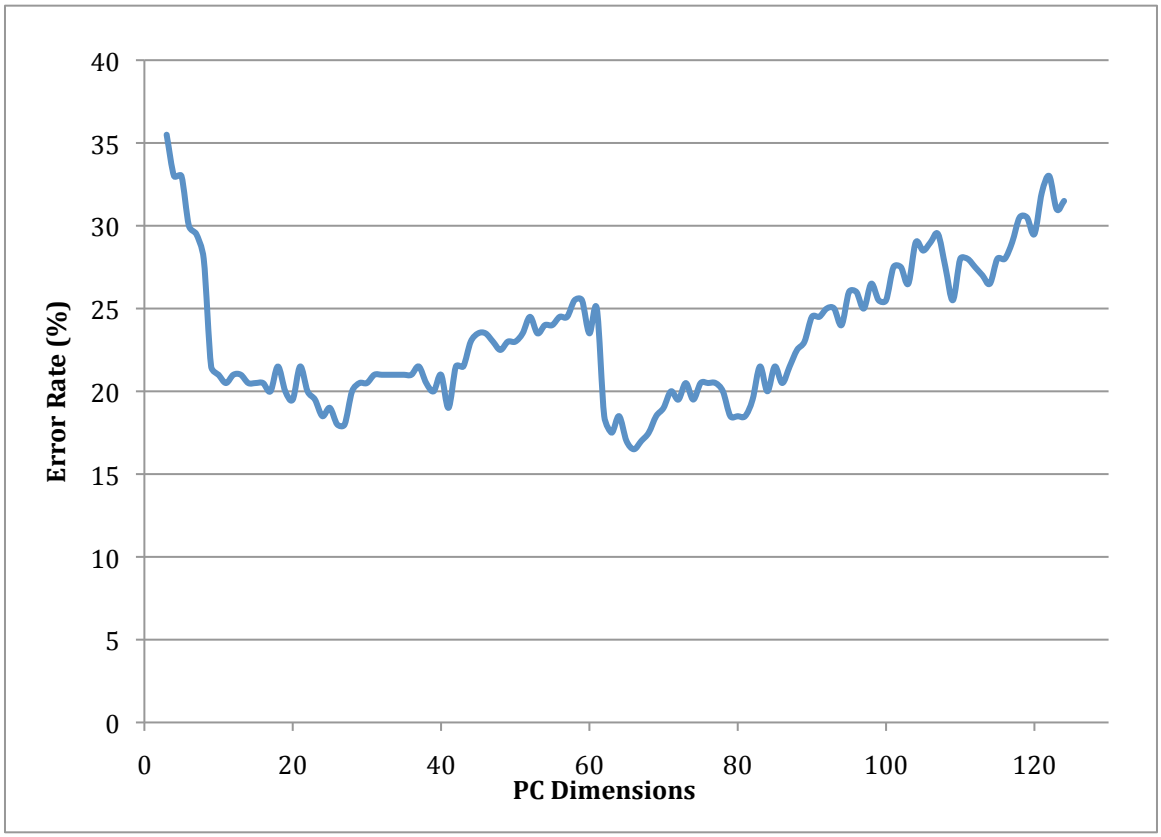


Figure 211: Graph of the float classification error rate versus PC dimensions for HOO-CV with PCA reduced CVA for the first set of 20 window glass spectra (10 replicates), centered data.

Table 223: Float classification error rates for HOO-CV with PCA reduced CVA for the first set of 20 window glass spectra (10 replicates), autoscaled data. The smallest PC dimension with the minimum error rate is highlighted in yellow.

PCs	Error Rate (%)	PCs	Error Rate (%)	PCs	Error Rate (%)	PCs	Error Rate (%)	PCs	Error Rate (%)
3	39.00	43	19.00	83	20.00	123	26.00	163	33.00
4	21.50	44	22.00	84	20.00	124	26.00	164	34.00
5	21.00	45	22.50	85	22.50	125	28.00	165	34.50
6	21.50	46	22.00	86	21.00	126	28.00	166	33.00
7	23.00	47	22.50	87	21.50	127	28.00	167	33.50
8	20.00	48	22.50	88	21.00	128	26.00	168	35.00
9	21.00	49	23.50	89	20.50	129	27.00	169	35.50
10	20.00	50	23.50	90	20.50	130	27.00	170	38.00
11	21.00	51	22.00	91	20.50	131	27.00	171	39.00
12	21.00	52	21.00	92	21.00	132	26.50	172	37.00
13	20.50	53	22.00	93	22.00	133	27.50	173	36.00
14	20.50	54	18.50	94	22.50	134	26.50	174	37.50
15	19.50	55	19.50	95	23.00	135	28.00	175	38.00
16	19.50	56	18.00	96	23.00	136	26.50	176	39.50
17	19.50	57	19.00	97	22.50	137	26.00	177	40.00
18	19.00	58	18.00	98	22.00	138	25.50	178	40.00
19	19.50	59	20.50	99	23.00	139	26.50	179	40.00
20	20.50	60	19.50	100	25.00	140	26.50	180	40.00
21	19.50	61	20.00	101	25.50	141	26.00	181	41.50
22	19.50	62	20.50	102	24.00	142	28.50	182	41.00
23	20.50	63	19.50	103	24.50	143	29.00	183	42.00
24	21.00	64	20.00	104	25.00	144	30.50	184	42.50
25	21.00	65	19.00	105	25.00	145	31.00	185	43.50
26	18.50	66	18.50	106	24.50	146	30.50	186	43.50
27	18.00	67	19.00	107	25.00	147	31.00	187	42.50
28	20.00	68	19.00	108	25.00	148	27.00	188	36.50
29	20.50	69	21.00	109	25.00	149	28.50	189	37.00
30	20.50	70	21.50	110	25.00	150	29.00	190	38.00
31	20.50	71	18.50	111	25.50	151	30.00	191	39.00
32	21.50	72	19.50	112	25.00	152	31.00	192	43.00
33	21.00	73	18.00	113	26.50	153	30.50	193	45.50
34	22.00	74	18.50	114	26.00	154	30.50	194	40.50
35	21.50	75	19.00	115	23.50	155	32.00	195	43.00
36	19.50	76	19.00	116	23.50	156	33.50	196	42.50
37	20.50	77	19.00	117	24.00	157	33.50	197	47.00
38	20.50	78	20.00	118	26.00	158	34.50	198	46.50
39	20.00	79	19.00	119	27.00	159	35.00	199	45.50

40	20.50	80	20.00	120	25.50	160	34.50	
41	20.50	81	20.00	121	25.50	161	31.00	
42	20.50	82	21.00	122	26.00	162	31.50	

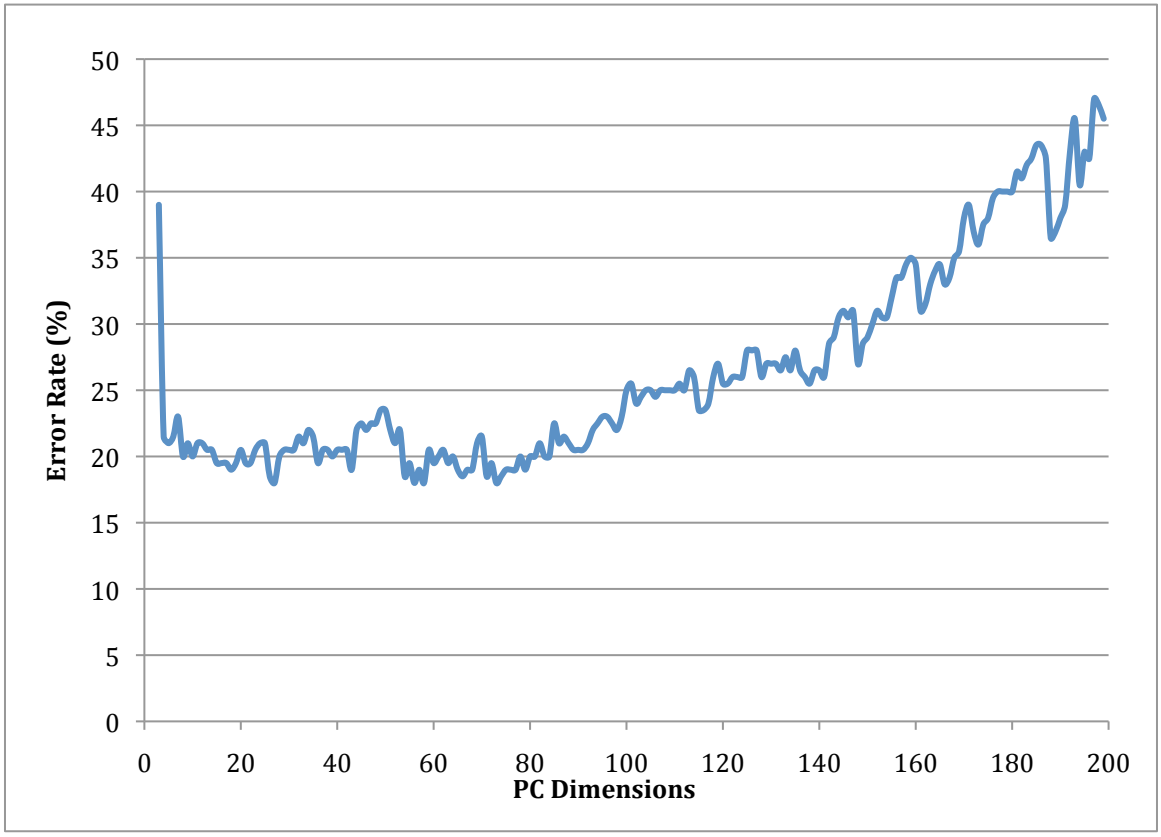


Figure 212: Graph of the float classification error rate versus PC dimensions for HOO-CV with PCA reduced CVA for the first set of 20 window glass spectra (10 replicates), autoscaled data.

First Set – Tempered Classification

Table 224: Tempered classification error rates for HOO-CV with PCA reduced CVA for the first set of 20 window glass spectra (10 replicates), no data pretreatment. The smallest PC dimension with the minimum error rate is highlighted in yellow.

PCs	Error Rate (%)	PCs	Error Rate (%)	PCs	Error Rate (%)	PCs	Error Rate (%)	PCs	Error Rate (%)
3	31.50	28	18.50	53	19.50	78	18.50	103	24.00
4	30.50	29	18.50	54	20.00	79	19.00	104	22.50
5	32.00	30	18.00	55	20.50	80	19.00	105	22.50
6	30.00	31	19.00	56	19.00	81	19.50	106	23.00
7	31.00	32	16.50	57	17.00	82	18.50	107	24.00
8	29.00	33	19.50	58	17.50	83	17.50	108	24.00
9	30.00	34	19.00	59	17.50	84	19.50	109	24.00
10	27.00	35	16.50	60	16.50	85	20.50	110	25.00
11	28.00	36	17.00	61	16.00	86	21.00	111	25.50
12	28.00	37	18.00	62	17.00	87	21.50	112	24.50
13	30.00	38	18.00	63	19.00	88	19.00	113	26.00
14	30.00	39	17.50	64	18.00	89	19.50	114	26.00
15	26.00	40	18.50	65	18.50	90	17.00	115	25.00
16	25.50	41	17.50	66	19.00	91	20.00	116	25.50
17	26.50	42	18.50	67	17.50	92	21.00	117	26.00
18	25.50	43	17.00	68	18.00	93	19.50	118	27.00
19	22.50	44	16.00	69	18.00	94	19.50	119	24.00
20	21.00	45	18.50	70	17.50	95	20.50	120	24.50
21	19.00	46	19.00	71	16.50	96	20.50	121	24.50
22	21.00	47	19.00	72	17.00	97	21.50	122	25.00
23	19.00	48	17.00	73	17.50	98	20.50	123	22.00
24	19.00	49	17.50	74	19.00	99	22.00	124	20.50
25	18.00	50	18.00	75	18.50	100	21.50		
26	18.50	51	17.50	76	19.00	101	22.00		
27	18.50	52	20.00	77	19.50	102	24.00		

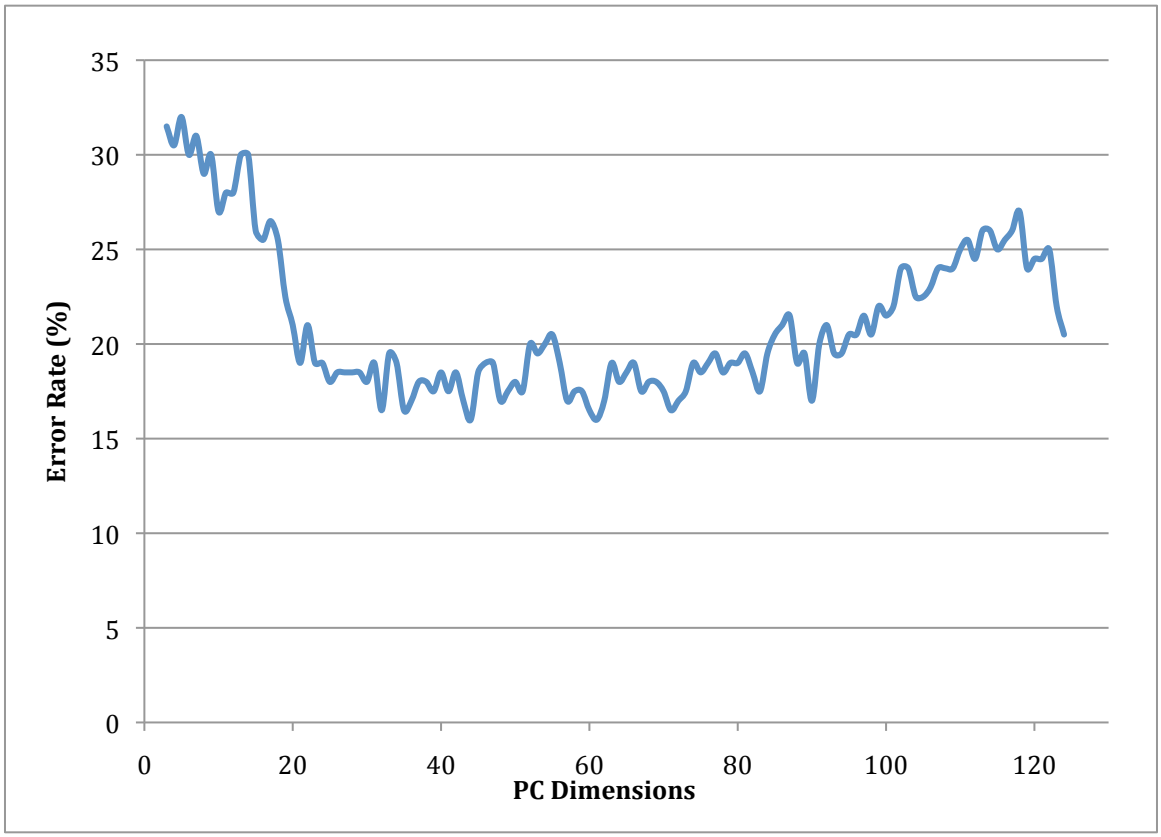


Figure 213: Graph of the tempered classification error rate versus PC dimensions for HOO-CV with PCA reduced CVA for the first set of 20 window glass spectra (10 replicates), no data pretreatment.

Table 225: Tempered classification error rates for HOO-CV with PCA reduced CVA for the first set of 20 window glass spectra (10 replicates), centered data. The smallest PC dimension with the minimum error rate is highlighted in yellow.

PCs	Error Rate (%)	PCs	Error Rate (%)	PCs	Error Rate (%)	PCs	Error Rate (%)	PCs	Error Rate (%)
3	33.00	28	18.50	53	17.00	78	19.50	103	22.50
4	30.50	29	18.50	54	19.50	79	17.50	104	23.50
5	32.50	30	19.50	55	20.00	80	19.00	105	24.50
6	30.00	31	18.00	56	20.00	81	19.00	106	22.00
7	29.50	32	18.50	57	17.50	82	18.50	107	24.00
8	31.50	33	19.50	58	16.00	83	18.50	108	24.00
9	30.00	34	18.50	59	17.00	84	18.50	109	24.50
10	27.00	35	17.00	60	16.50	85	19.50	110	24.50
11	27.50	36	17.00	61	17.00	86	20.00	111	24.50
12	27.50	37	18.00	62	17.50	87	19.50	112	24.00
13	29.50	38	18.00	63	18.00	88	20.00	113	25.00
14	30.00	39	18.50	64	18.00	89	19.00	114	24.50
15	26.50	40	18.00	65	18.50	90	20.00	115	25.00
16	25.50	41	17.00	66	18.00	91	19.50	116	24.50
17	26.50	42	17.00	67	17.50	92	19.00	117	25.00
18	25.50	43	16.00	68	17.50	93	19.00	118	27.50
19	20.50	44	16.00	69	17.50	94	19.00	119	25.00
20	19.50	45	17.50	70	18.00	95	20.50	120	24.00
21	19.50	46	18.50	71	17.50	96	21.00	121	24.00
22	20.50	47	19.50	72	18.00	97	21.50	122	21.00
23	20.00	48	16.50	73	19.50	98	20.50	123	22.00
24	19.50	49	16.50	74	19.00	99	21.00	124	21.00
25	18.50	50	16.00	75	18.50	100	21.50		
26	18.50	51	16.50	76	19.50	101	22.00		
27	19.00	52	17.00	77	19.50	102	22.00		

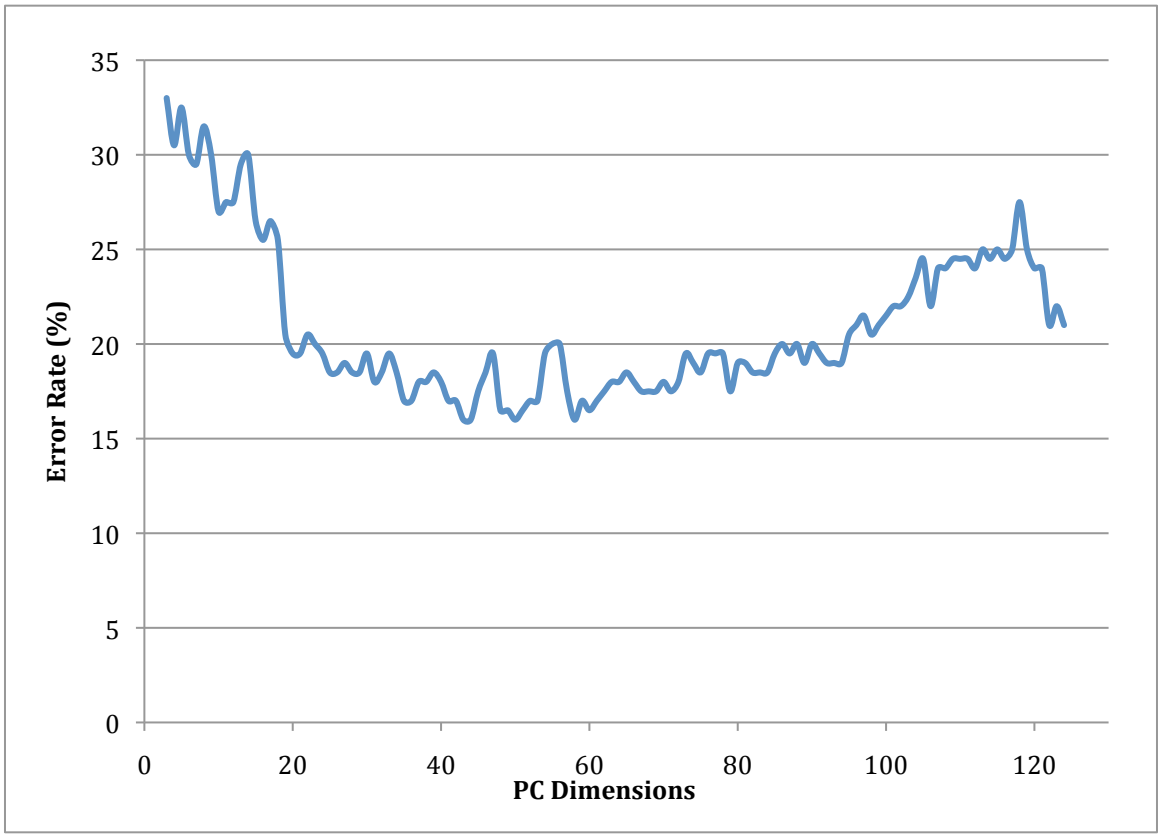


Figure 214: Graph of the tempered classification error rate versus PC dimensions for HOO-CV with PCA reduced CVA for the first set of 20 window glass spectra (10 replicates), centered data.

Table 226: Tempered classification error rates for HOO-CV with PCA reduced CVA for the first set of 20 window glass spectra (10 replicates), autoscaled data. The smallest PC dimension with the minimum error rate is highlighted in yellow.

PCs	Error Rate (%)	PCs	Error Rate (%)	PCs	Error Rate (%)	PCs	Error Rate (%)	PCs	Error Rate (%)
3	32.50	43	13.00	83	19.50	123	14.50	163	19.50
4	32.50	44	11.50	84	18.50	124	14.50	164	20.00
5	31.00	45	12.00	85	18.50	125	14.00	165	19.50
6	30.50	46	14.00	86	18.50	126	14.00	166	18.00
7	28.50	47	14.50	87	16.00	127	14.50	167	19.50
8	29.50	48	15.00	88	16.00	128	13.50	168	17.00
9	27.00	49	16.00	89	16.00	129	15.00	169	19.50
10	28.50	50	16.50	90	16.50	130	12.00	170	20.00
11	27.00	51	15.50	91	16.50	131	13.50	171	21.00
12	27.00	52	15.50	92	16.50	132	12.50	172	20.00
13	28.50	53	15.50	93	14.50	133	13.00	173	23.50
14	29.50	54	17.00	94	15.50	134	13.00	174	26.00
15	29.00	55	17.00	95	16.00	135	14.00	175	25.00
16	30.50	56	16.00	96	14.50	136	15.50	176	26.00
17	29.00	57	17.00	97	15.00	137	11.50	177	28.00
18	27.00	58	15.50	98	15.00	138	11.00	178	28.50
19	25.00	59	17.50	99	13.00	139	11.50	179	24.00
20	19.00	60	16.00	100	16.00	140	12.00	180	24.50
21	20.00	61	16.50	101	14.50	141	12.50	181	22.00
22	20.00	62	17.00	102	14.50	142	12.50	182	23.00
23	20.00	63	18.50	103	15.00	143	11.00	183	25.00
24	18.50	64	19.50	104	15.50	144	11.50	184	27.00
25	17.00	65	19.50	105	16.00	145	12.50	185	24.00
26	17.00	66	18.00	106	15.50	146	13.50	186	23.50
27	16.00	67	18.00	107	17.00	147	15.00	187	21.00
28	17.00	68	20.00	108	13.00	148	15.50	188	23.50
29	16.50	69	19.50	109	14.00	149	13.00	189	26.00
30	15.50	70	20.00	110	12.50	150	13.00	190	28.50
31	16.50	71	20.00	111	13.50	151	13.50	191	21.50
32	15.00	72	19.50	112	13.00	152	14.00	192	23.00
33	14.00	73	19.00	113	14.50	153	15.50	193	23.50
34	15.00	74	19.50	114	11.50	154	15.00	194	30.50
35	15.50	75	21.00	115	13.50	155	16.00	195	30.00
36	14.00	76	24.00	116	13.00	156	16.00	196	35.00
37	14.00	77	22.00	117	13.00	157	17.50	197	35.00
38	14.00	78	22.50	118	15.00	158	16.00	198	53.50
39	14.50	79	23.00	119	15.00	159	17.50	199	40.00

40	15.50	80	22.00	120	15.50	160	17.50	
41	12.00	81	21.50	121	16.00	161	19.50	
42	12.00	82	22.00	122	12.50	162	21.50	

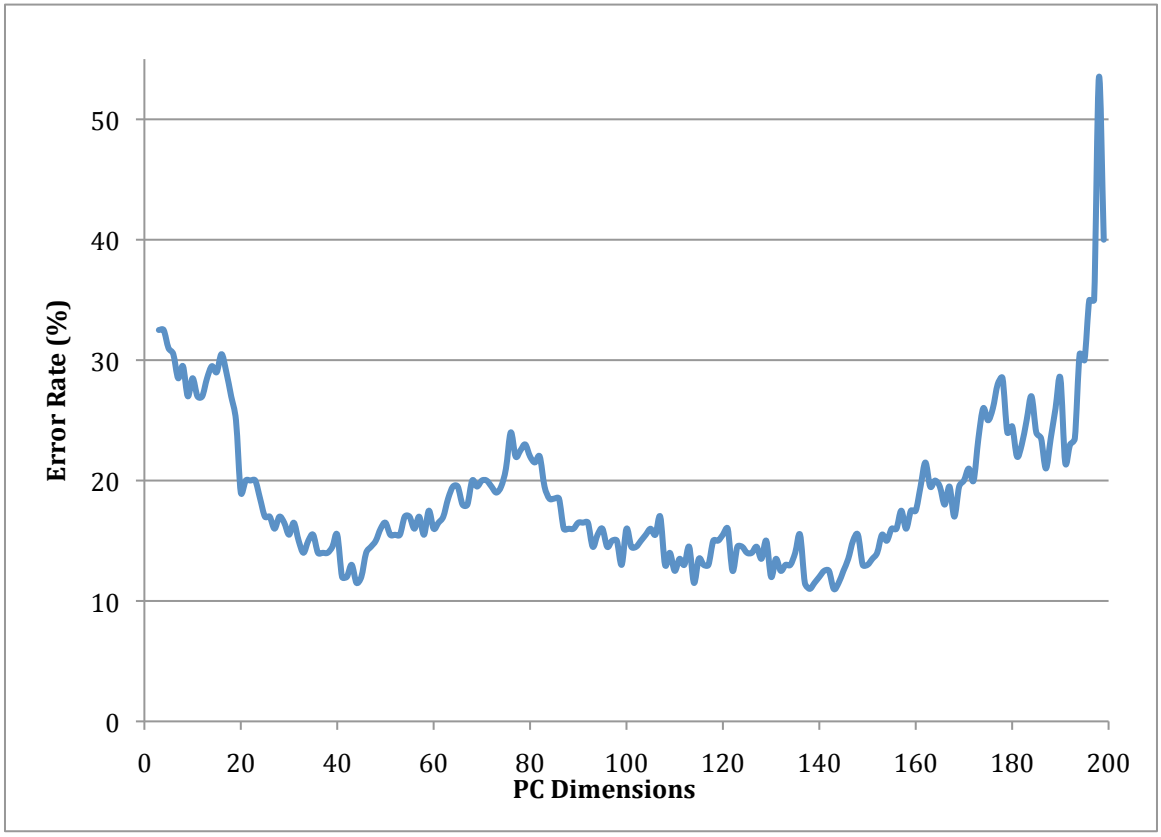


Figure 215: Graph of the tempered classification error rate versus PC dimensions for HOO-CV with PCA reduced CVA for the first set of 20 window glass spectra (10 replicates), autoscaled data.

B. HOO-CV PCA-CVA Results for the Peak Area Normalized Spectra

First Set, Normalized (Peak Area) - Discrimination

Table 227: Discrimination error rates for HOO-CV with PCA reduced CVA for the first set of 30 normalized (peak area) glass spectra (10 replicates), no data pretreatment. The smallest PC dimension with the minimum error rate is highlighted in yellow.

PCs	Error Rate (%)	PCs	Error Rate (%)	PCs	Error Rate (%)	PCs	Error Rate (%)	PCs	Error Rate (%)
2	96.00	4	88.33	6	61.33	8	57.33	10	49.33
3	93.33	5	65.00	7	58.67	9	50.67		

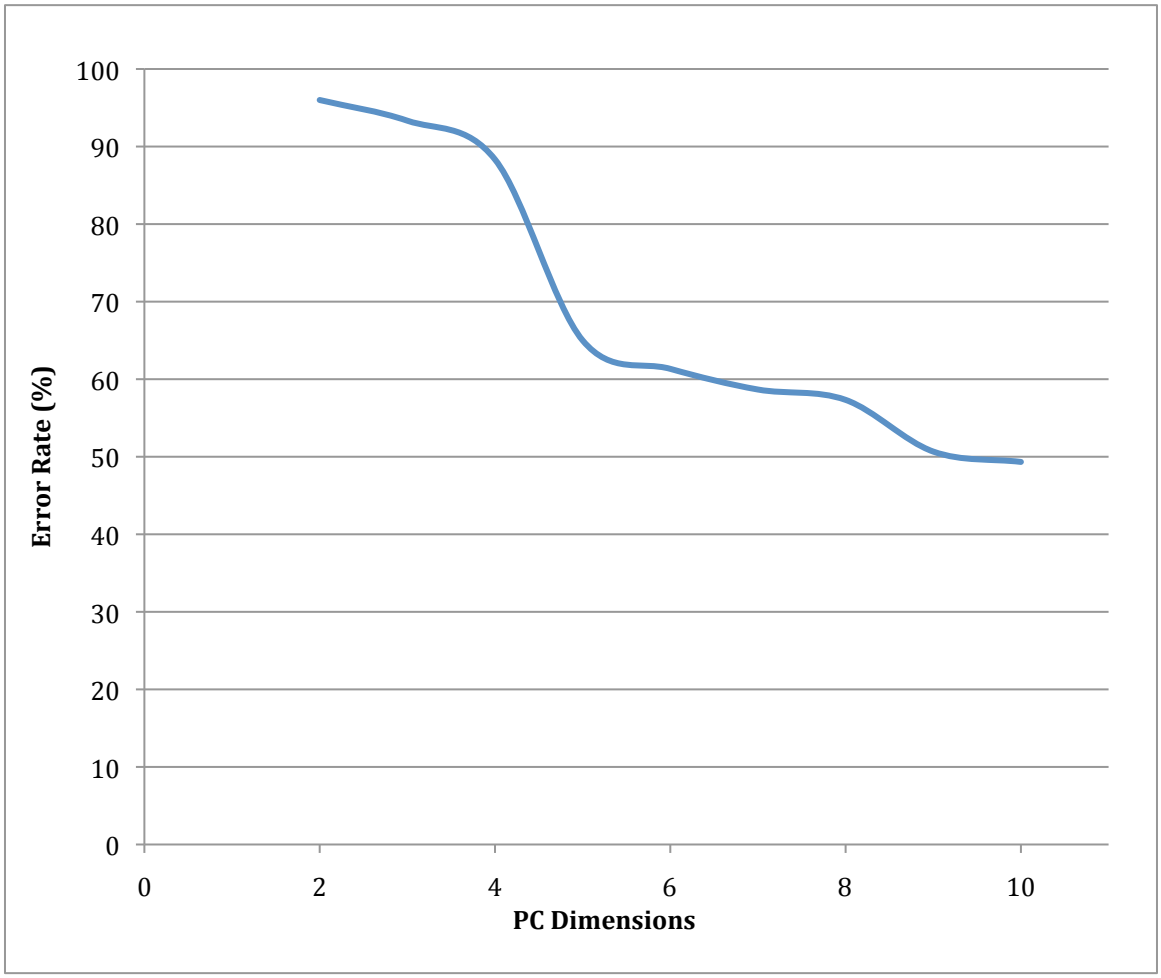


Figure 216: Graph of the discrimination error rate versus PC dimensions for HOO-CV with PCA reduced CVA for the first set of 30 normalized (peak area) glass spectra (10 replicates), no data pretreatment.

Table 228: Discrimination error rates for HOO-CV with PCA reduced CVA for the first set of 30 normalized (peak area) glass spectra (10 replicates), centered data. The smallest PC dimension with the minimum error rate is highlighted in yellow.

PCs	Error Rate (%)	PCs	Error Rate (%)	PCs	Error Rate (%)	PCs	Error Rate (%)	PCs	Error Rate (%)
2	96.00	4	68.33	6	63.33	8	55.67	9	50.33
3	89.00	5	64.33	7	58.33				

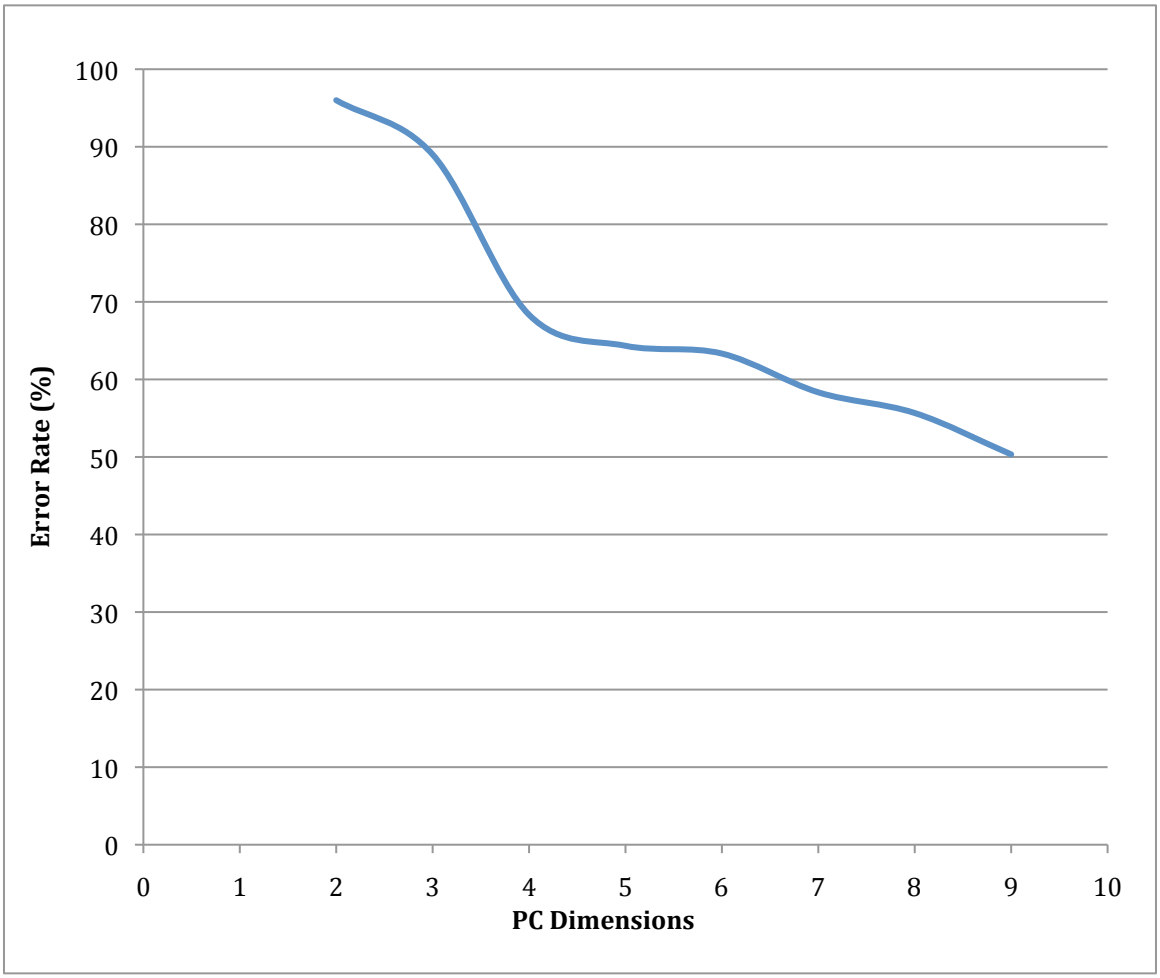


Figure 217: Graph of the discrimination error rate versus PC dimensions for HOO-CV with PCA reduced CVA for the first set of 30 normalized (peak area) glass spectra (10 replicates), centered data.

Table 229: Discrimination error rates for HOO-CV with PCA reduced CVA for the first set of 30 normalized (peak area) glass spectra (10 replicates), autoscaled data. The smallest PC dimension with the minimum error rate is highlighted in yellow.

PCs	Error Rate (%)	PCs	Error Rate (%)	PCs	Error Rate (%)	PCs	Error Rate (%)	PCs	Error Rate (%)
2	96.33	60	14.00	118	8.00	176	9.67	234	18.33
3	87.67	61	14.33	119	8.00	177	9.33	235	19.67
4	77.33	62	14.33	120	7.67	178	9.33	236	20.67
5	60.00	63	14.00	121	7.67	179	8.67	237	19.33
6	53.00	64	14.67	122	7.33	180	9.67	238	19.00
7	50.00	65	13.67	123	7.67	181	9.67	239	19.00
8	51.00	66	14.33	124	7.67	182	10.67	240	21.00
9	46.67	67	14.33	125	8.67	183	10.67	241	21.33
10	44.67	68	14.67	126	8.67	184	10.67	242	21.00
11	35.67	69	15.00	127	7.67	185	11.33	243	21.00
12	35.67	70	14.33	128	8.00	186	11.00	244	23.33
13	33.33	71	14.33	129	7.67	187	11.00	245	27.33
14	32.00	72	15.00	130	7.33	188	11.00	246	27.00
15	30.67	73	14.67	131	7.33	189	10.33	247	27.67
16	31.00	74	13.33	132	8.00	190	11.00	248	28.67
17	29.33	75	14.00	133	6.67	191	12.33	249	28.67
18	29.33	76	14.33	134	6.67	192	12.33	250	31.67
19	27.00	77	13.33	135	7.00	193	12.00	251	34.67
20	19.67	78	13.33	136	7.00	194	11.33	252	33.33
21	19.00	79	13.33	137	7.00	195	11.33	253	37.00
22	19.00	80	13.33	138	7.67	196	11.67	254	38.33
23	18.33	81	13.00	139	7.00	197	12.33	255	41.33
24	16.67	82	12.00	140	8.00	198	12.00	256	41.00
25	17.67	83	11.67	141	8.33	199	11.67	257	43.67
26	16.33	84	11.67	142	8.67	200	12.00	258	47.33
27	16.67	85	11.67	143	8.33	201	12.67	259	52.33
28	16.67	86	12.00	144	8.67	202	13.00	260	55.33
29	17.00	87	11.33	145	8.33	203	12.67	261	56.33
30	13.67	88	11.00	146	9.00	204	12.67	262	58.33
31	14.00	89	10.67	147	8.67	205	12.67	263	61.00
32	14.00	90	9.33	148	8.33	206	13.00	264	54.00
33	13.33	91	10.67	149	9.33	207	14.00	265	62.33
34	13.33	92	10.67	150	8.67	208	13.00	266	62.33
35	13.33	93	9.67	151	9.67	209	13.00	267	69.67
36	13.67	94	9.67	152	8.67	210	13.67	268	66.33
37	15.00	95	9.67	153	8.67	211	13.67	269	65.67
38	14.67	96	9.67	154	8.67	212	14.67	270	80.33

39	15.00	97	9.67	155	8.00	213	14.67	271	89.00
40	17.00	98	9.33	156	8.33	214	16.00	272	89.33
41	16.67	99	9.33	157	8.33	215	15.33	273	94.67
42	16.67	100	9.67	158	9.00	216	16.33	274	96.00
43	16.00	101	10.67	159	9.33	217	16.33	275	87.00
44	14.67	102	10.67	160	10.33	218	17.00	276	89.33
45	16.33	103	10.00	161	10.00	219	16.00	277	91.33
46	14.67	104	9.67	162	10.67	220	17.00	278	85.67
47	15.33	105	10.00	163	10.67	221	18.00	279	89.00
48	14.67	106	9.33	164	11.00	222	18.00	280	79.33
49	14.67	107	9.00	165	10.00	223	18.33	281	86.33
50	13.67	108	9.33	166	9.33	224	18.00	282	89.00
51	13.67	109	9.00	167	8.67	225	18.33	283	90.67
52	13.33	110	8.67	168	9.67	226	17.00	284	91.33
53	13.33	111	7.67	169	8.33	227	17.00	285	92.67
54	14.00	112	8.00	170	8.67	228	14.67	286	93.67
55	14.00	113	8.00	171	8.67	229	15.00	287	95.33
56	14.00	114	7.33	172	8.67	230	15.33	288	96.00
57	14.33	115	8.00	173	9.00	231	16.00	289	96.67
58	14.33	116	9.00	174	9.33	232	18.00		
59	14.33	117	7.00	175	9.33	233	19.00		

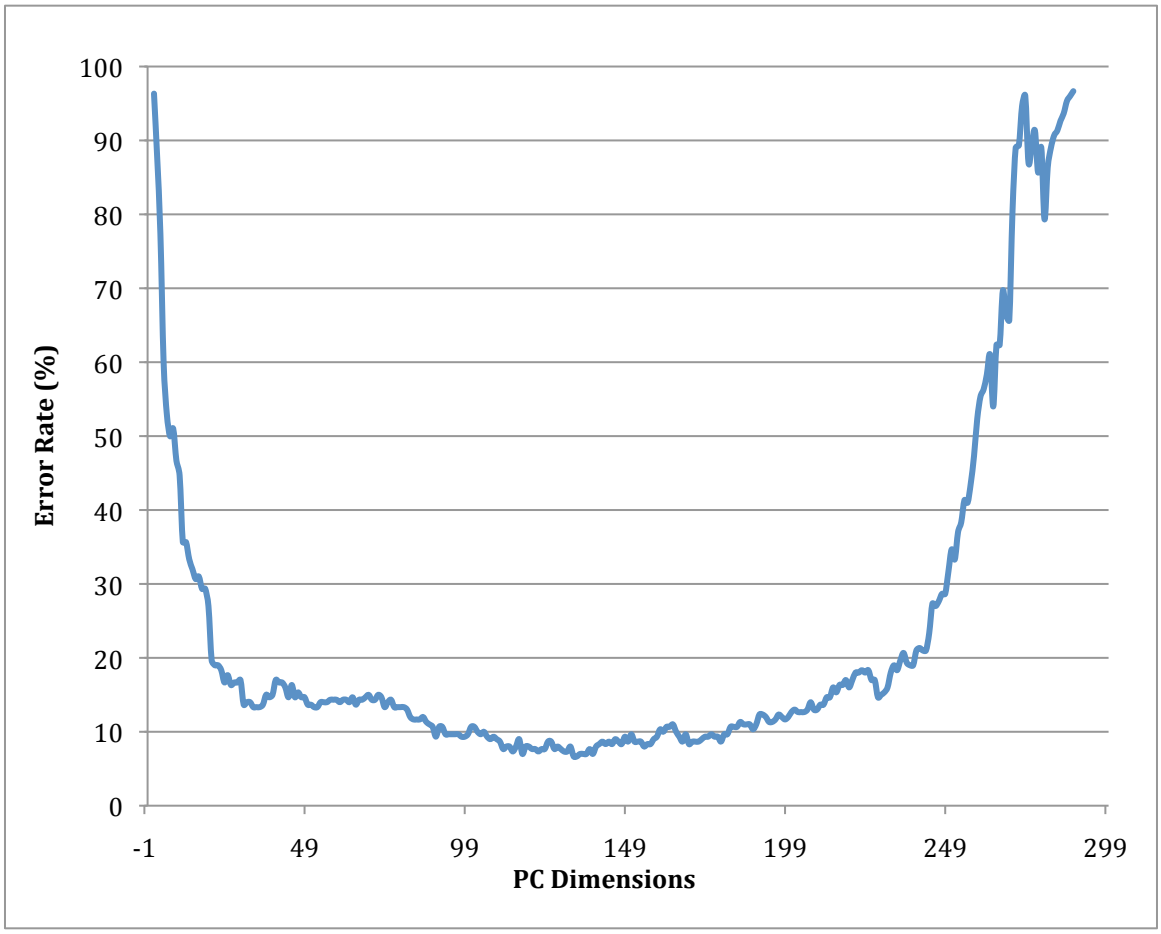


Figure 218: Graph of the discrimination error rate versus PC dimensions for HOO-CV with PCA reduced CVA for the first set of 30 normalized (peak area) glass spectra (10 replicates), autoscaled data.

First Set, Normalized (Peak Area) – Classification (automotive, architectural or container)

Table 230: Classification (automotive, architectural or container) error rates for HOO-CV with PCA reduced CVA for the first set of 30 normalized (peak area) glass spectra (10 replicates), no data pretreatment. The smallest PC dimension with the minimum error rate is highlighted in yellow.

PCs	Error Rate (%)	PCs	Error Rate (%)	PCs	Error Rate (%)	PCs	Error Rate (%)	PCs	Error Rate (%)
2	66.00	4	64.33	6	29.67	8	27.67	10	26.67
3	68.00	5	30.33	7	28.00	9	27.00		

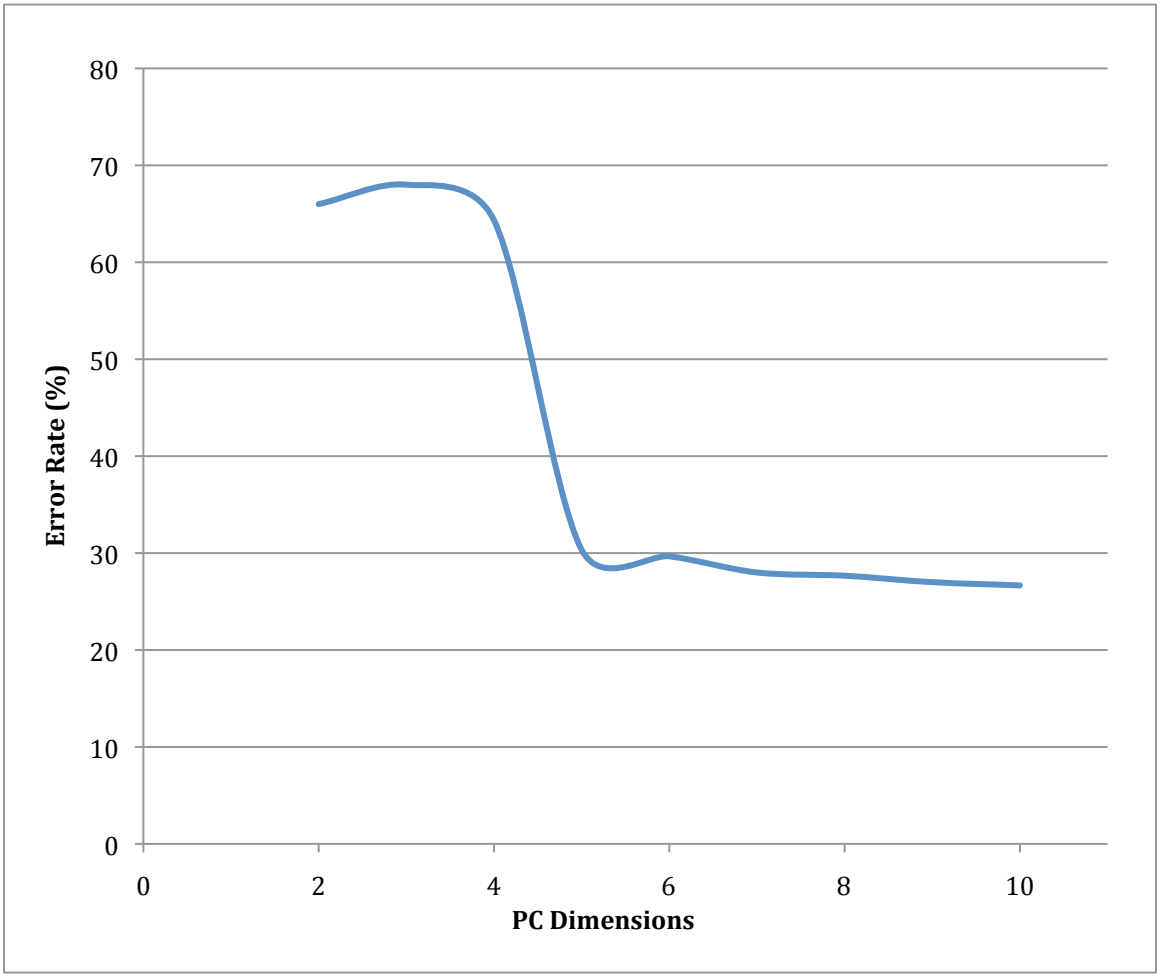


Figure 219: Graph of the classification (automotive, architectural or container) error rate versus PC dimensions for HOO-CV with PCA reduced CVA for the first set of 30 normalized (peak area) glass spectra (10 replicates), no data pretreatment.

Table 231: Classification (automotive, architectural or container) error rates for HOO-CV with PCA reduced CVA for the first set of 30 normalized (peak area) glass spectra (10 replicates), centered data. The smallest PC dimension with the minimum error rate is highlighted in yellow.

PCs	Error Rate (%)	PCs	Error Rate (%)	PCs	Error Rate (%)	PCs	Error Rate (%)	PCs	Error Rate (%)
2	66.67	4	30.33	6	29.33	8	29.00	9	26.67
3	61.33	5	30.67	7	29.33				

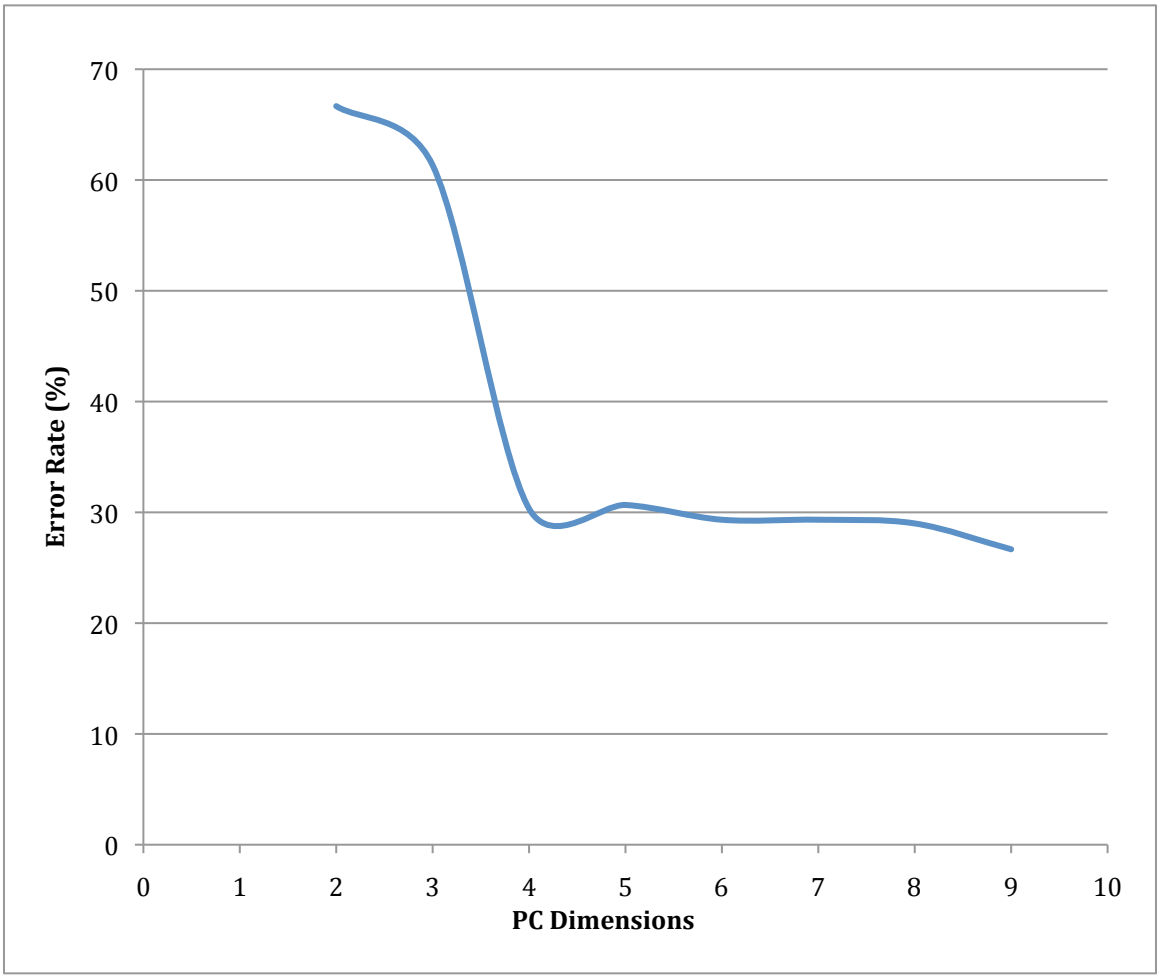


Figure 220: Graph of the classification (automotive, architectural or container) error rate versus PC dimensions for HOO-CV with PCA reduced CVA for the first set of 30 normalized (peak area) glass spectra (10 replicates), centered data.

Table 232: Classification (automotive, architectural or container) error rates for HOO-CV with PCA reduced CVA for the first set of 30 normalized (peak area) glass spectra (10 replicates), autoscaled data. The smallest PC dimension with the minimum error rate is highlighted in yellow.

PCs	Error Rate (%)	PCs	Error Rate (%)	PCs	Error Rate (%)	PCs	Error Rate (%)	PCs	Error Rate (%)
2	64.67	60	16.00	118	19.33	176	22.00	234	23.33
3	63.00	61	16.33	119	19.67	177	22.33	235	24.33
4	34.33	62	16.00	120	19.33	178	23.33	236	24.33
5	29.33	63	16.67	121	18.33	179	23.67	237	24.33
6	27.33	64	16.67	122	20.33	180	23.33	238	25.00
7	26.33	65	16.67	123	20.00	181	22.00	239	25.67
8	26.67	66	16.67	124	18.67	182	22.33	240	26.00
9	27.67	67	18.00	125	19.00	183	23.67	241	26.67
10	27.00	68	17.67	126	18.67	184	24.00	242	25.67
11	25.67	69	18.00	127	18.33	185	23.00	243	26.00
12	26.00	70	17.67	128	18.67	186	21.67	244	27.00
13	22.33	71	17.67	129	18.67	187	21.00	245	27.00
14	23.33	72	18.00	130	19.33	188	21.00	246	28.00
15	24.00	73	18.00	131	20.00	189	21.00	247	28.67
16	23.33	74	18.33	132	20.67	190	21.33	248	30.00
17	17.67	75	18.33	133	20.67	191	21.67	249	30.00
18	15.67	76	18.33	134	21.33	192	21.67	250	28.33
19	15.67	77	18.67	135	21.33	193	20.33	251	31.33
20	15.00	78	19.00	136	21.33	194	19.00	252	32.33
21	17.00	79	19.33	137	21.00	195	19.67	253	32.67
22	16.67	80	18.67	138	22.33	196	20.00	254	33.00
23	16.67	81	19.00	139	21.67	197	19.00	255	33.33
24	16.67	82	19.67	140	22.00	198	19.33	256	32.33
25	16.67	83	19.67	141	21.67	199	20.67	257	32.67
26	16.67	84	20.33	142	18.00	200	20.67	258	32.67
27	15.67	85	20.33	143	18.33	201	20.67	259	33.33
28	16.00	86	20.00	144	18.67	202	21.33	260	36.33
29	15.33	87	19.67	145	20.67	203	20.67	261	36.33
30	16.00	88	20.33	146	20.33	204	22.33	262	35.33
31	16.33	89	20.00	147	18.33	205	21.67	263	35.00
32	17.33	90	20.00	148	18.00	206	22.33	264	32.33
33	17.33	91	19.33	149	16.00	207	23.33	265	32.33
34	17.33	92	19.00	150	16.33	208	22.67	266	30.67
35	17.00	93	19.67	151	17.00	209	20.33	267	31.00
36	18.00	94	19.67	152	18.00	210	20.00	268	31.67
37	17.00	95	19.33	153	18.33	211	20.00	269	33.00

38	17.00	96	19.67	154	19.00	212	18.67	270	33.33
39	17.33	97	20.33	155	18.67	213	19.67	271	33.67
40	17.33	98	20.00	156	19.00	214	20.67	272	32.00
41	18.00	99	19.67	157	20.00	215	21.33	273	33.67
42	16.67	100	19.67	158	19.33	216	22.67	274	34.67
43	15.67	101	20.67	159	19.67	217	22.33	275	37.33
44	16.00	102	19.67	160	19.67	218	23.00	276	36.67
45	15.67	103	19.33	161	19.67	219	22.67	277	38.00
46	16.00	104	19.00	162	18.67	220	25.00	278	40.00
47	15.33	105	20.33	163	20.33	221	25.00	279	37.67
48	15.67	106	20.33	164	18.67	222	25.33	280	38.00
49	16.67	107	20.67	165	19.33	223	23.00	281	38.00
50	18.00	108	20.67	166	20.00	224	23.67	282	38.00
51	18.33	109	19.67	167	21.00	225	24.33	283	40.33
52	17.67	110	21.00	168	19.67	226	24.33	284	43.00
53	17.67	111	18.67	169	19.67	227	24.00	285	45.67
54	16.00	112	19.00	170	19.67	228	22.00	286	44.33
55	16.67	113	21.00	171	19.67	229	23.00	287	44.33
56	16.33	114	21.00	172	20.33	230	24.33	288	45.00
57	16.00	115	19.33	173	21.00	231	25.00	289	47.33
58	16.67	116	19.00	174	21.00	232	24.33		
59	16.33	117	18.67	175	22.00	233	23.00		

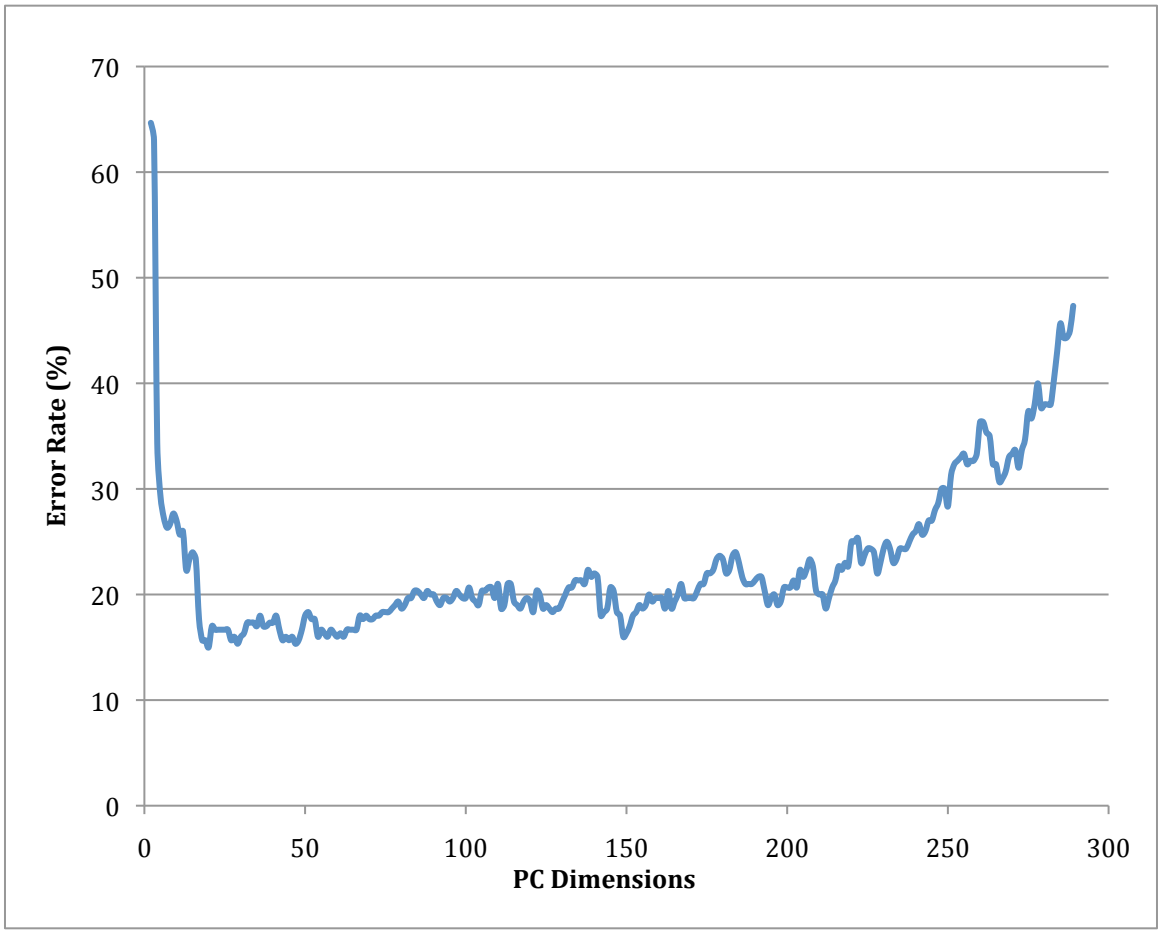


Figure 221: Graph of the classification (automotive, architectural or container) error rate versus PC dimensions for HOO-CV with PCA reduced CVA for the first set of 30 normalized (peak area) glass spectra (10 replicates), autoscaled data.

First Set, Normalized (Peak Area) – Classification (window or container)

Table 233: Classification (window or container) error rates for HOO-CV with PCA reduced CVA for the first set of 30 normalized (peak area) glass spectra (10 replicates), no data pretreatment. The smallest PC dimension with the minimum error rate is highlighted in yellow.

PCs	Error Rate (%)	PCs	Error Rate (%)	PCs	Error Rate (%)	PCs	Error Rate (%)	PCs	Error Rate (%)
2	33.33	4	33.33	6	7.00	8	4.33	10	4.00
3	33.33	5	6.67	7	6.33	9	4.00		

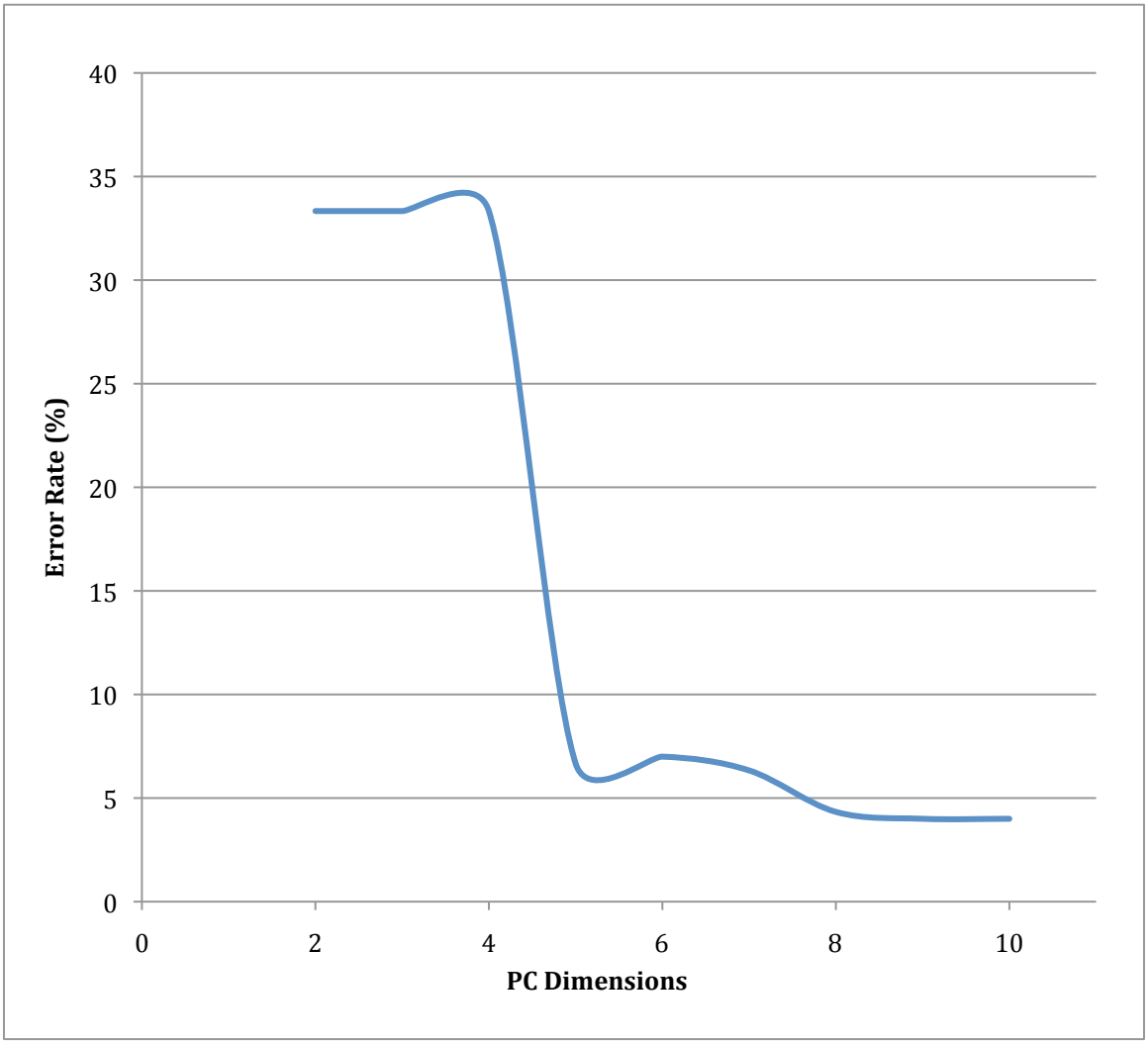


Figure 222: Graph of the classification (window or container) error rate versus PC dimensions for HOO-CV with PCA reduced CVA for the first set of 30 normalized (peak area) glass spectra (10 replicates), no data pretreatment.

Table 234: Classification (window or container) error rates for HOO-CV with PCA reduced CVA for the first set of 30 normalized (peak area) glass spectra (10 replicates), centered data. The smallest PC dimension with the minimum error rate is highlighted in yellow.

PCs	Error Rate (%)	PCs	Error Rate (%)	PCs	Error Rate (%)	PCs	Error Rate (%)	PCs	Error Rate (%)
2	33.33	4	6.00	6	5.67	8	5.33	9	4.00
3	33.33	5	7.00	7	5.33				

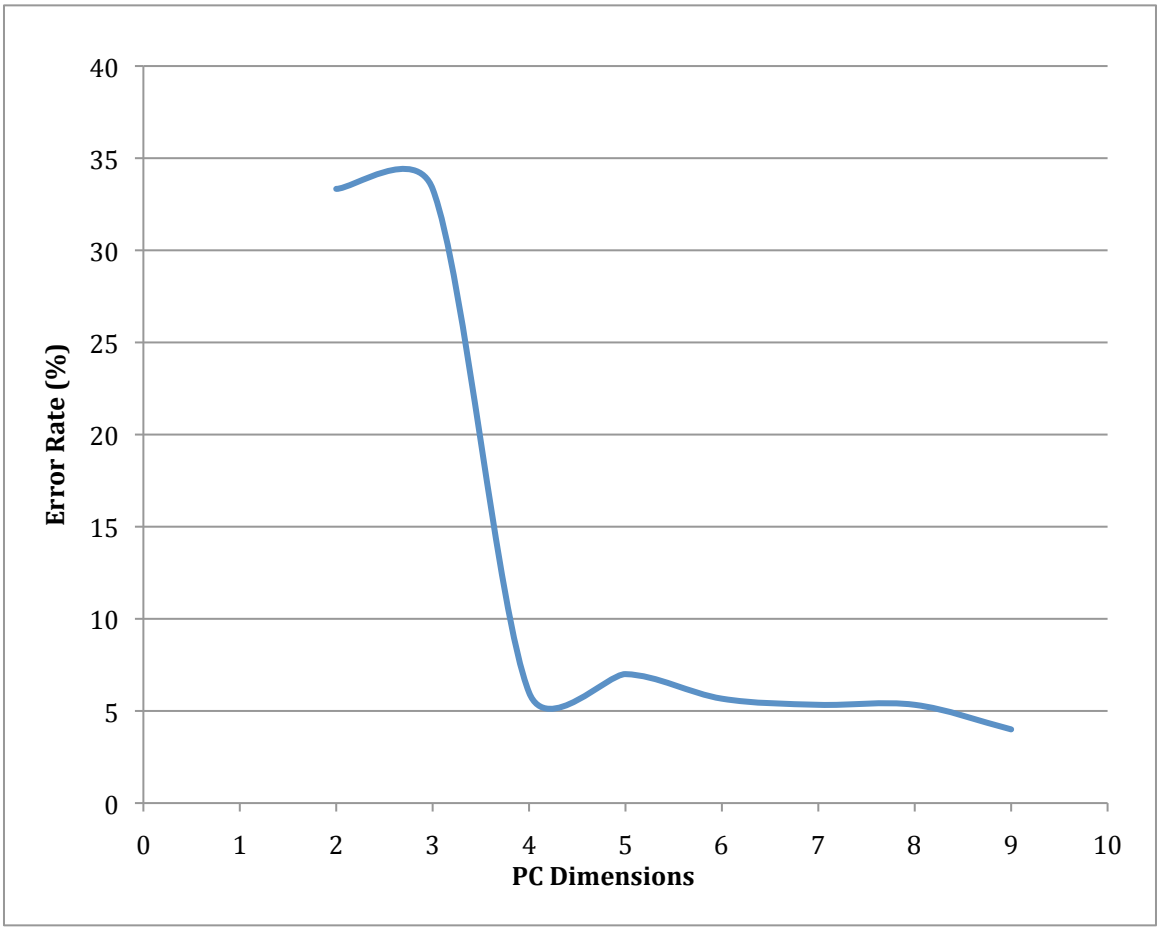


Figure 223: Graph of the classification (window or container) error rate versus PC dimensions for HOO-CV with PCA reduced CVA for the first set of 30 normalized (peak area) glass spectra (10 replicates), centered data.

Table 235: Classification (window or container) error rates for HOO-CV with PCA reduced CVA for the first set of 30 normalized (peak area) glass spectra (10 replicates), autoscaled data. The smallest PC dimension with the minimum error rate is highlighted in yellow.

PCs	Error Rate (%)	PCs	Error Rate (%)	PCs	Error Rate (%)	PCs	Error Rate (%)	PCs	Error Rate (%)
2	33.33	60	4.33	118	4.00	176	4.00	234	8.00
3	31.00	61	4.00	119	4.33	177	4.00	235	8.33
4	9.33	62	3.67	120	5.00	178	4.33	236	6.33
5	7.67	63	4.33	121	3.67	179	4.33	237	6.33
6	7.33	64	4.67	122	4.67	180	4.67	238	6.67
7	3.67	65	4.33	123	4.33	181	4.67	239	6.33
8	3.67	66	4.67	124	4.00	182	4.67	240	8.00
9	3.67	67	4.67	125	4.33	183	5.33	241	8.33
10	4.33	68	4.67	126	4.67	184	5.33	242	8.33
11	4.00	69	4.00	127	4.67	185	4.67	243	8.33
12	3.67	70	4.00	128	3.67	186	5.00	244	8.33
13	4.00	71	4.00	129	4.33	187	4.00	245	8.33
14	4.00	72	4.00	130	4.67	188	4.00	246	9.00
15	4.00	73	4.33	131	5.00	189	4.33	247	10.00
16	4.00	74	4.33	132	5.33	190	5.00	248	10.67
17	3.67	75	4.33	133	5.33	191	5.00	249	11.00
18	3.67	76	4.33	134	5.33	192	5.33	250	8.00
19	4.00	77	4.33	135	5.33	193	5.33	251	8.33
20	4.00	78	4.33	136	5.00	194	5.00	252	9.00
21	4.00	79	4.33	137	5.00	195	5.67	253	9.33
22	4.00	80	4.67	138	5.33	196	5.67	254	10.67
23	4.00	81	4.67	139	5.33	197	5.33	255	11.33
24	3.33	82	4.67	140	5.67	198	6.00	256	11.33
25	3.33	83	4.67	141	4.67	199	6.00	257	10.67
26	3.33	84	4.67	142	3.00	200	6.67	258	11.00
27	3.33	85	4.67	143	3.00	201	6.33	259	11.33
28	3.33	86	4.67	144	3.33	202	6.67	260	12.33
29	3.00	87	4.67	145	3.33	203	6.00	261	13.33
30	3.33	88	4.67	146	3.00	204	6.00	262	14.33
31	3.33	89	4.33	147	3.00	205	6.67	263	14.33
32	3.33	90	4.33	148	3.00	206	7.00	264	11.00
33	3.33	91	4.33	149	3.00	207	7.00	265	12.00
34	3.33	92	5.00	150	3.33	208	5.67	266	13.00
35	3.33	93	5.00	151	3.67	209	6.00	267	12.67
36	3.33	94	5.00	152	3.67	210	5.33	268	13.67
37	3.67	95	5.00	153	3.33	211	5.67	269	14.00
38	3.67	96	5.00	154	3.33	212	6.33	270	14.00

39	3.67	97	5.00	155	3.33	213	6.67	271	14.67
40	4.00	98	5.00	156	3.67	214	7.00	272	14.67
41	3.67	99	5.00	157	3.67	215	7.00	273	15.33
42	3.67	100	5.00	158	3.67	216	7.00	274	16.33
43	3.67	101	5.00	159	3.67	217	6.67	275	16.33
44	3.67	102	5.00	160	3.67	218	6.67	276	17.00
45	3.67	103	4.33	161	3.33	219	7.00	277	15.67
46	3.67	104	4.33	162	3.33	220	7.33	278	16.67
47	3.67	105	4.33	163	3.33	221	8.33	279	16.67
48	3.67	106	4.00	164	3.33	222	8.33	280	15.00
49	3.67	107	4.00	165	3.33	223	6.33	281	15.67
50	4.00	108	4.00	166	3.33	224	6.67	282	16.67
51	3.33	109	4.33	167	3.33	225	7.00	283	17.67
52	4.00	110	4.33	168	3.67	226	7.33	284	19.67
53	4.00	111	3.67	169	3.00	227	8.33	285	20.67
54	4.00	112	3.67	170	3.00	228	8.33	286	22.00
55	4.00	113	4.67	171	3.33	229	8.33	287	21.00
56	4.33	114	4.33	172	3.67	230	7.33	288	21.33
57	4.33	115	5.00	173	3.67	231	7.67	289	24.67
58	4.33	116	4.67	174	3.67	232	7.33		
59	4.33	117	4.67	175	4.33	233	7.67		

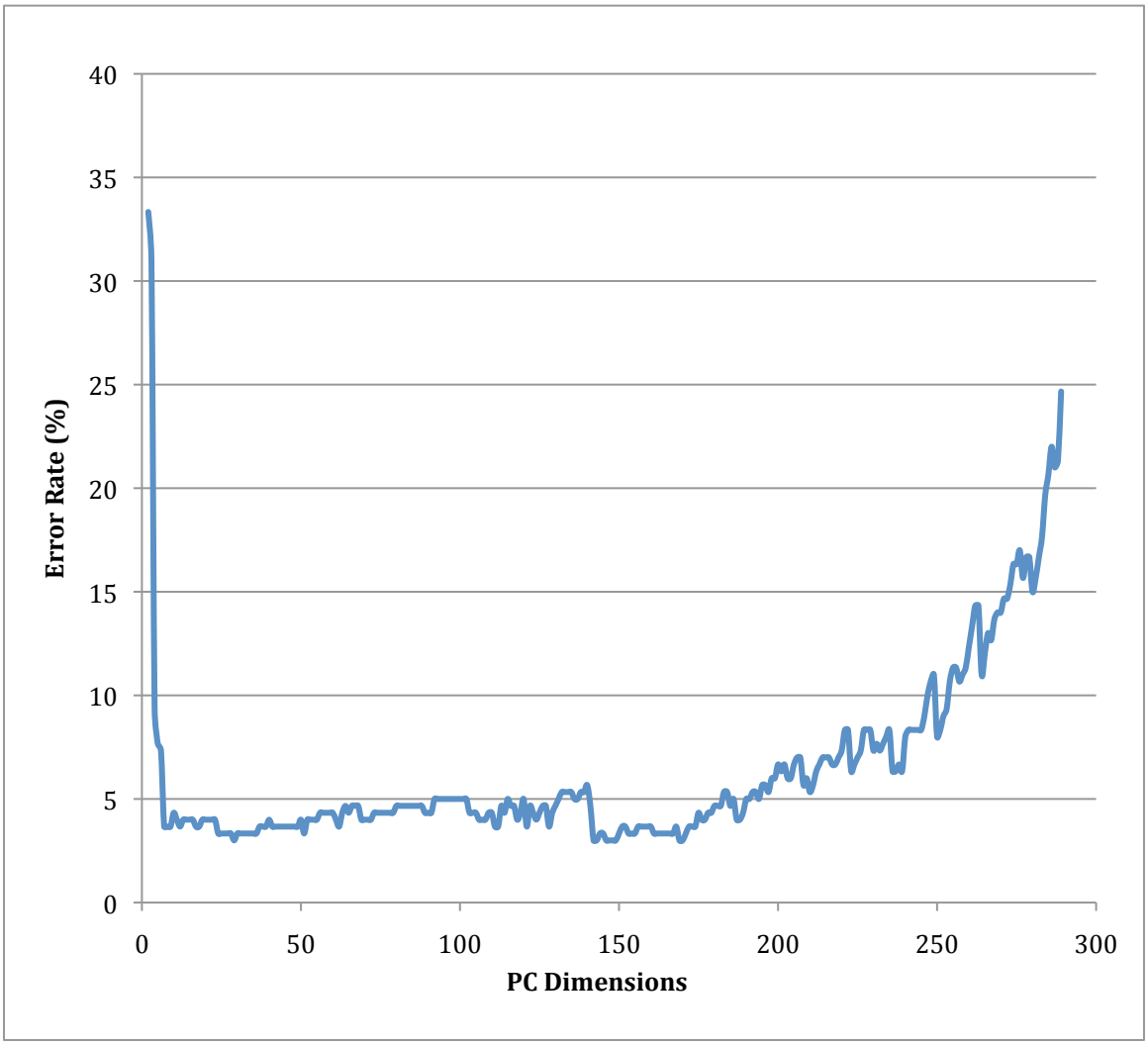


Figure 224: Graph of the classification (window or container) error rate versus PC dimensions for HOO-CV with PCA reduced CVA for the first set of 30 normalized (peak area) glass spectra (10 replicates), autoscaled data.

First Set, Normalized (Peak Area) – Window Discrimination

Table 236: Discrimination error rates for HOO-CV with PCA reduced CVA for the first set of 20 window normalized (peak area) glass spectra (10 replicates), no data pretreatment. The smallest PC dimension with the minimum error rate is highlighted in yellow.

PCs	Error Rate (%)	PCs	Error Rate (%)	PCs	Error Rate (%)	PCs	Error Rate (%)	PCs	Error Rate (%)
2	94.00	4	86.00	6	78.50	8	57.50	9	53.00
3	92.00	5	80.50	7	75.50				

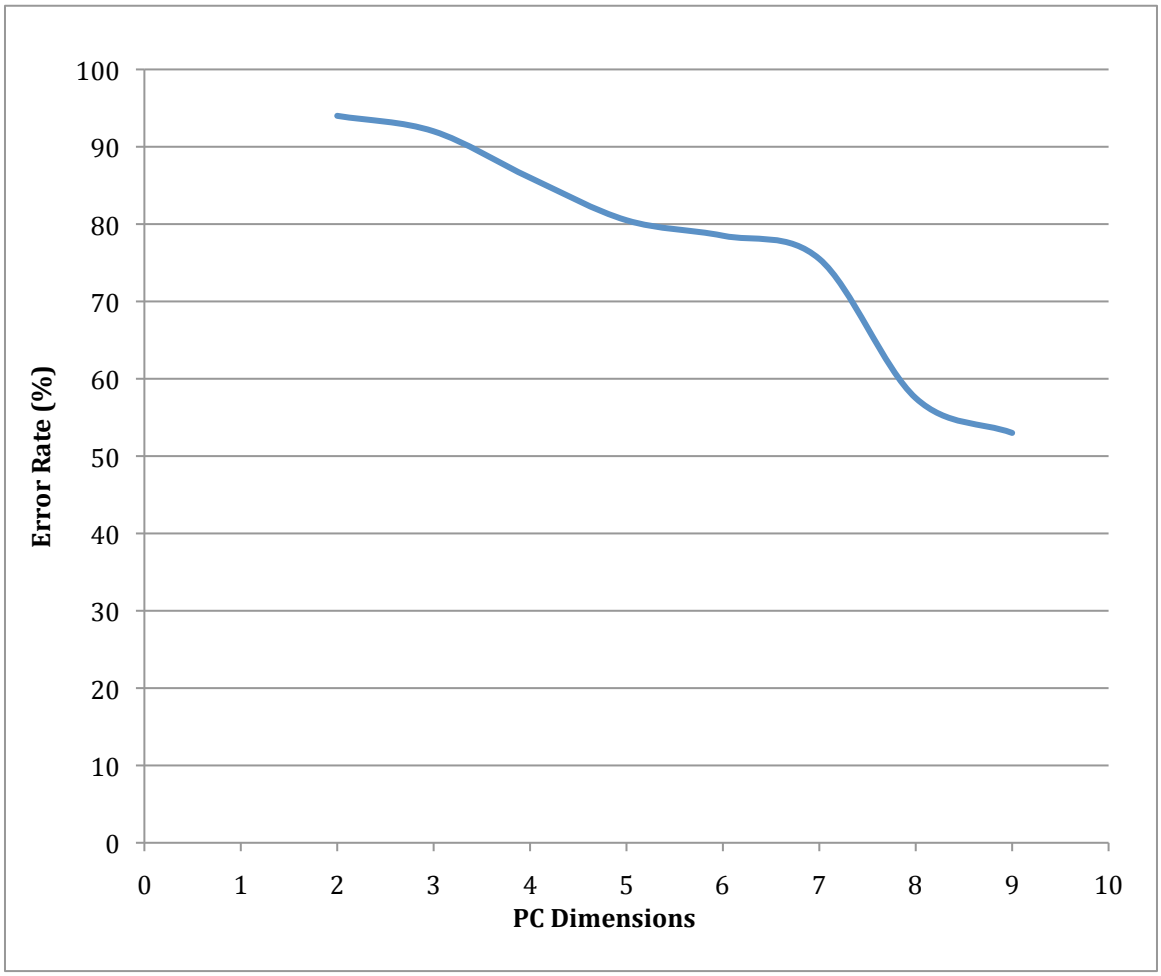


Figure 225: Graph of the discrimination error rate versus PC dimensions for HOO-CV with PCA reduced CVA for the first set of 20 window normalized (peak area) glass spectra (10 replicates), no data pretreatment.

Table 237: Discrimination error rates for HOO-CV with PCA reduced CVA for the first set of 20 window normalized (peak area) glass spectra (10 replicates), centered data. The smallest PC dimension with the minimum error rate is highlighted in yellow.

PCs	Error Rate (%)	PCs	Error Rate (%)	PCs	Error Rate (%)	PCs	Error Rate (%)	PCs	Error Rate (%)
2	92.00	4	83.50	6	79.50	7	65.50	8	56.50
3	90.00	5	85.00						

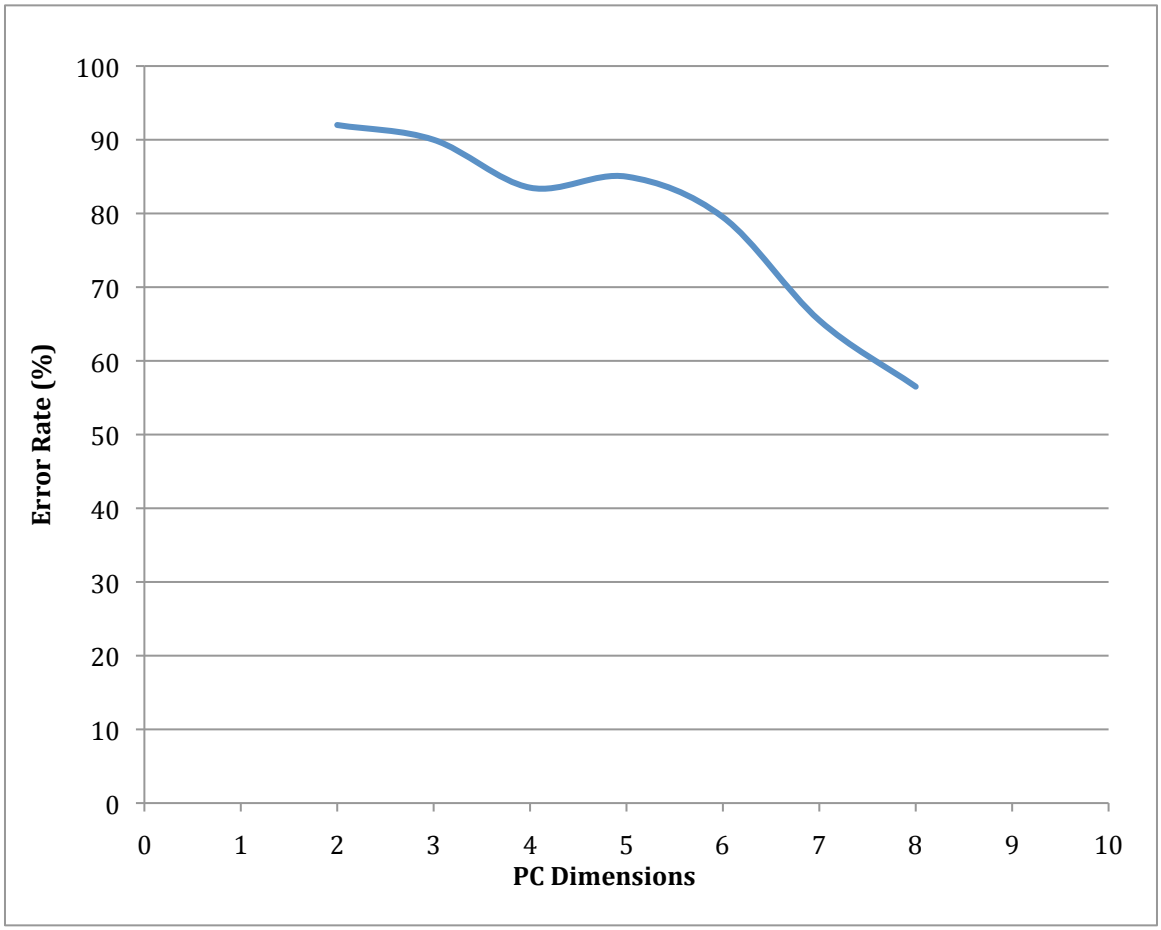


Figure 226: Graph of the discrimination error rate versus PC dimensions for HOO-CV with PCA reduced CVA for the first set of 20 window normalized (peak area) glass spectra (10 replicates), centered data.

Table 238: Discrimination error rates for HOO-CV with PCA reduced CVA for the first set of 20 window normalized (peak area) glass spectra (10 replicates), autoscaled data. The smallest PC dimension with the minimum error rate is highlighted in yellow.

PCs	Error Rate (%)	PCs	Error Rate (%)	PCs	Error Rate (%)	PCs	Error Rate (%)	PCs	Error Rate (%)
2	93.50	38	16.00	74	13.50	110	13.50	146	18.50
3	90.50	39	17.50	75	13.00	111	14.00	147	21.50
4	85.00	40	15.50	76	13.50	112	14.00	148	20.50
5	63.00	41	16.00	77	12.00	113	13.50	149	20.00
6	54.00	42	16.50	78	15.00	114	14.00	150	20.00
7	52.50	43	14.00	79	13.50	115	14.50	151	21.50
8	55.50	44	14.50	80	13.00	116	15.00	152	23.50
9	49.50	45	16.50	81	12.50	117	15.00	153	22.50
10	49.50	46	17.50	82	13.00	118	13.50	154	23.50
11	48.00	47	16.00	83	13.00	119	14.00	155	23.50
12	48.00	48	15.00	84	14.50	120	14.00	156	25.50
13	34.50	49	15.00	85	13.50	121	15.50	157	22.00
14	34.00	50	16.50	86	13.50	122	14.50	158	24.00
15	28.50	51	17.00	87	13.50	123	14.00	159	26.00
16	26.50	52	17.00	88	13.50	124	14.00	160	27.00
17	27.00	53	17.00	89	12.50	125	15.00	161	27.00
18	27.00	54	16.50	90	14.50	126	15.00	162	29.50
19	22.00	55	16.50	91	13.50	127	17.50	163	24.50
20	17.50	56	15.00	92	13.00	128	16.50	164	30.00
21	16.50	57	16.00	93	14.00	129	17.50	165	31.00
22	16.00	58	16.50	94	14.00	130	19.50	166	34.00
23	17.00	59	16.50	95	13.50	131	20.00	167	35.00
24	17.50	60	17.00	96	13.00	132	20.00	168	37.00
25	15.50	61	17.50	97	13.00	133	20.00	169	36.00
26	16.50	62	16.00	98	13.50	134	19.00	170	38.50
27	16.50	63	15.00	99	12.50	135	18.00	171	42.50
28	16.50	64	13.00	100	13.50	136	18.50	172	49.00
29	15.50	65	14.00	101	13.00	137	18.00	173	50.50
30	15.50	66	14.00	102	13.00	138	18.00	174	52.50
31	14.50	67	13.50	103	13.00	139	19.50	175	54.50
32	17.00	68	13.00	104	14.50	140	18.00	176	53.00
33	17.00	69	13.00	105	12.50	141	20.00	177	56.50
34	17.00	70	13.50	106	14.00	142	20.50	178	63.00
35	16.50	71	12.50	107	12.50	143	20.00	179	74.00
36	16.00	72	13.00	108	12.50	144	20.50	180	61.00
37	16.50	73	14.00	109	13.50	145	19.50		

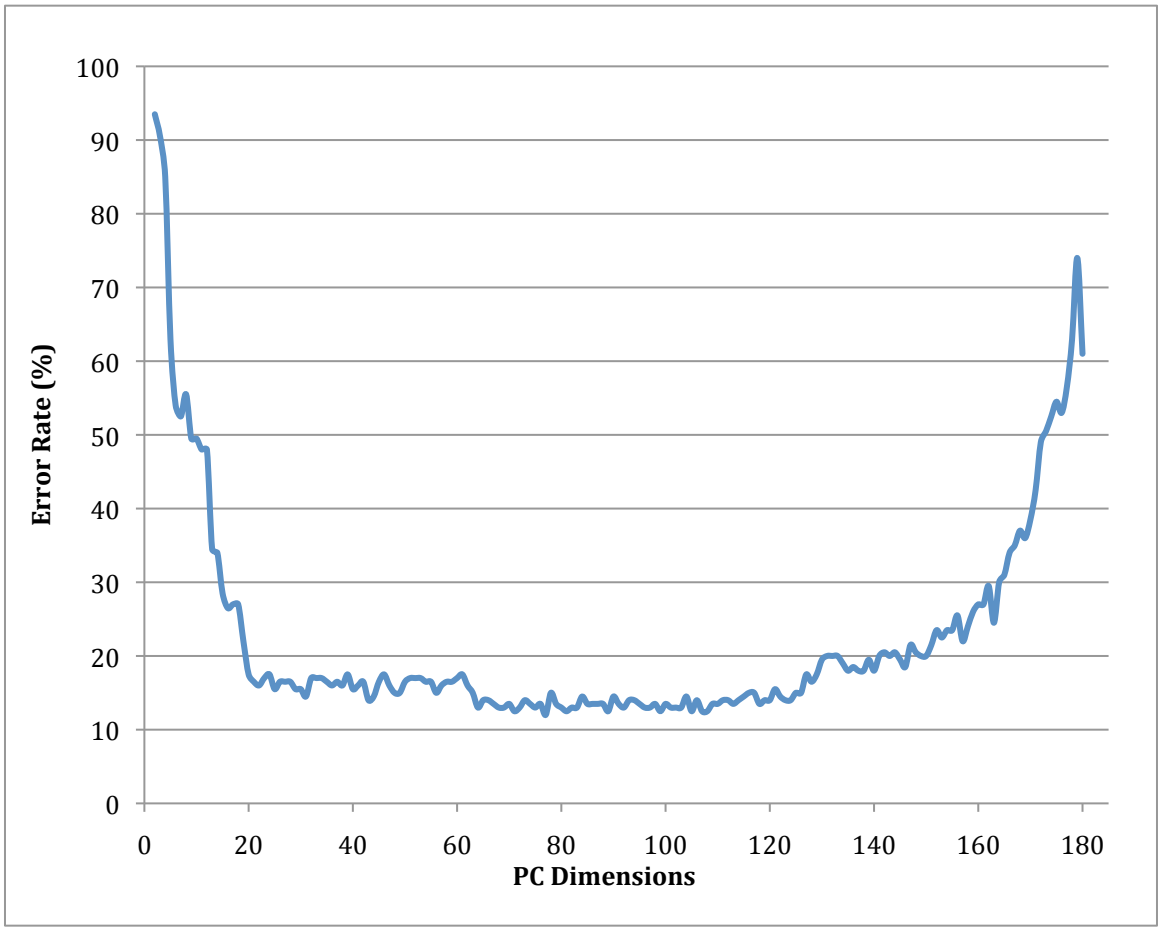


Figure 227: Graph of the discrimination error rate versus PC dimensions for HOO-CV with PCA reduced CVA for the first set of 20 window normalized (peak area) glass spectra (10 replicates), autoscaled data.

First Set, Normalized (Peak Area) – Container Discrimination

Table 239: Discrimination error rates for HOO-CV with PCA reduced CVA for the first set of 10 container normalized (peak area) glass spectra (10 replicates), no data pretreatment. The smallest PC dimension with the minimum error rate is highlighted in yellow.

PCs	Error Rate (%)	PCs	Error Rate (%)	PCs	Error Rate (%)	PCs	Error Rate (%)	PCs	Error Rate (%)
2	86.00	4	64.00	6	50.00	8	53.00	10	46.00
3	73.00	5	64.00	7	53.00	9	42.00		

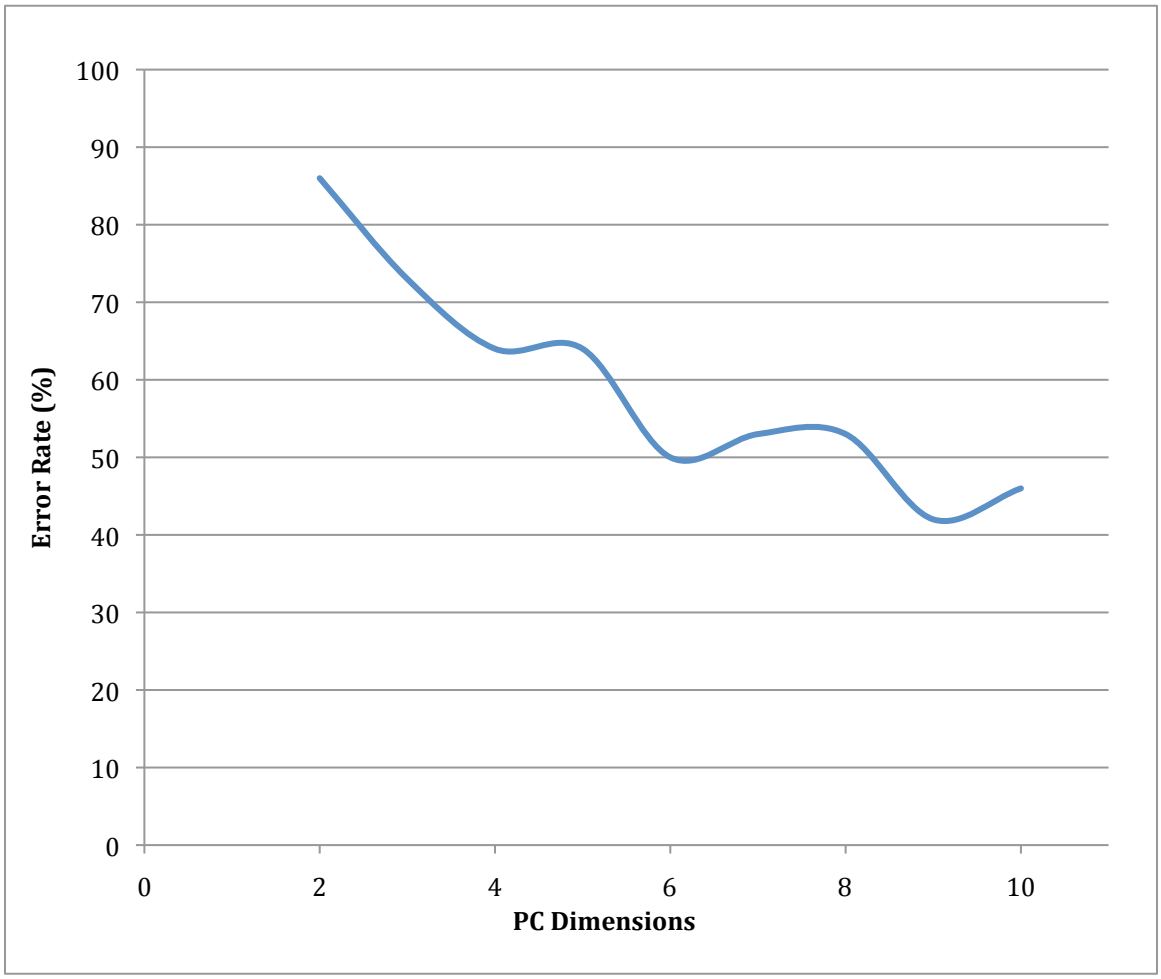


Figure 228: Graph of the discrimination error rate versus PC dimensions for HOO-CV with PCA reduced CVA for the first set of 10 container normalized (peak area) glass spectra (10 replicates), no data pretreatment.

Table 240: Discrimination error rates for HOO-CV with PCA reduced CVA for the first set of 10 container normalized (peak area) glass spectra (10 replicates), centered data. The smallest PC dimension with the minimum error rate is highlighted in yellow.

PCs	Error Rate (%)	PCs	Error Rate (%)	PCs	Error Rate (%)	PCs	Error Rate (%)	PCs	Error Rate (%)
2	85.00	4	65.00	6	52.00	8	47.00	9	42.00
3	69.00	5	55.00	7	51.00				

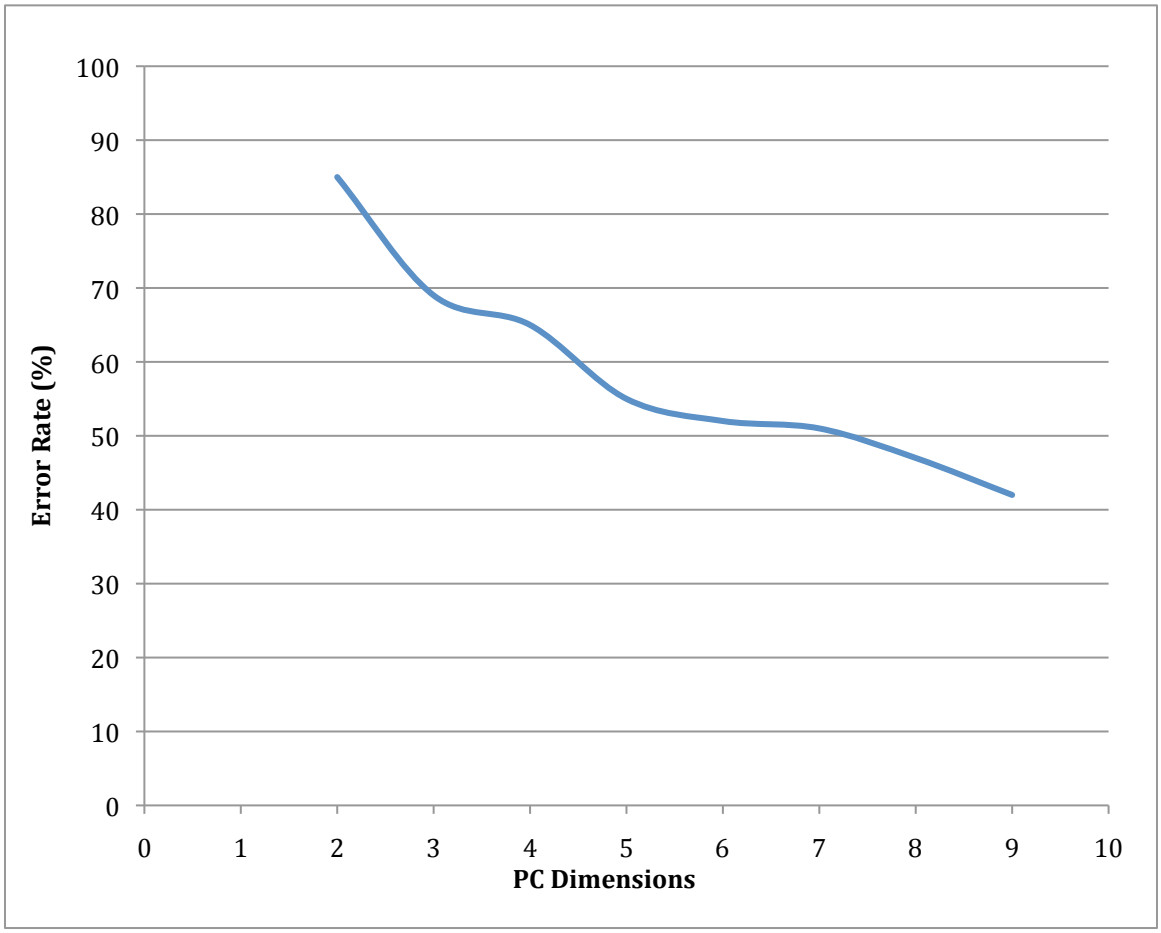


Figure 229: Graph of the discrimination error rate versus PC dimensions for HOO-CV with PCA reduced CVA for the first set of 10 container normalized (peak area) glass spectra (10 replicates), centered data.

Table 241: Discrimination error rates for HOO-CV with PCA reduced CVA for the first set of 10 container normalized (peak area) glass spectra (10 replicates), autoscaled data. The smallest PC dimension with the minimum error rate is highlighted in yellow.

PCs	Error Rate (%)	PCs	Error Rate (%)	PCs	Error Rate (%)	PCs	Error Rate (%)	PCs	Error Rate (%)
2	92.00	22	14.00	42	13.00	62	18.00	82	22.00
3	65.00	23	12.00	43	14.00	63	17.00	83	25.00
4	63.00	24	11.00	44	14.00	64	19.00	84	24.00
5	55.00	25	11.00	45	10.00	65	19.00	85	33.00
6	49.00	26	10.00	46	11.00	66	23.00	86	33.00
7	38.00	27	11.00	47	11.00	67	22.00	87	40.00
8	40.00	28	11.00	48	13.00	68	23.00	88	49.00
9	37.00	29	10.00	49	11.00	69	20.00	89	69.00
10	38.00	30	10.00	50	12.00	70	20.00	90	75.00
11	35.00	31	10.00	51	13.00	71	22.00	91	55.00
12	34.00	32	11.00	52	16.00	72	24.00	92	75.00
13	26.00	33	11.00	53	16.00	73	21.00	93	69.00
14	30.00	34	10.00	54	16.00	74	21.00	94	74.00
15	27.00	35	10.00	55	16.00	75	17.00	95	86.00
16	29.00	36	11.00	56	13.00	76	20.00	96	95.00
17	29.00	37	11.00	57	15.00	77	21.00	97	93.00
18	23.00	38	13.00	58	15.00	78	26.00	98	88.00
19	21.00	39	14.00	59	16.00	79	27.00	99	70.00
20	15.00	40	11.00	60	18.00	80	29.00		
21	11.00	41	13.00	61	19.00	81	27.00		

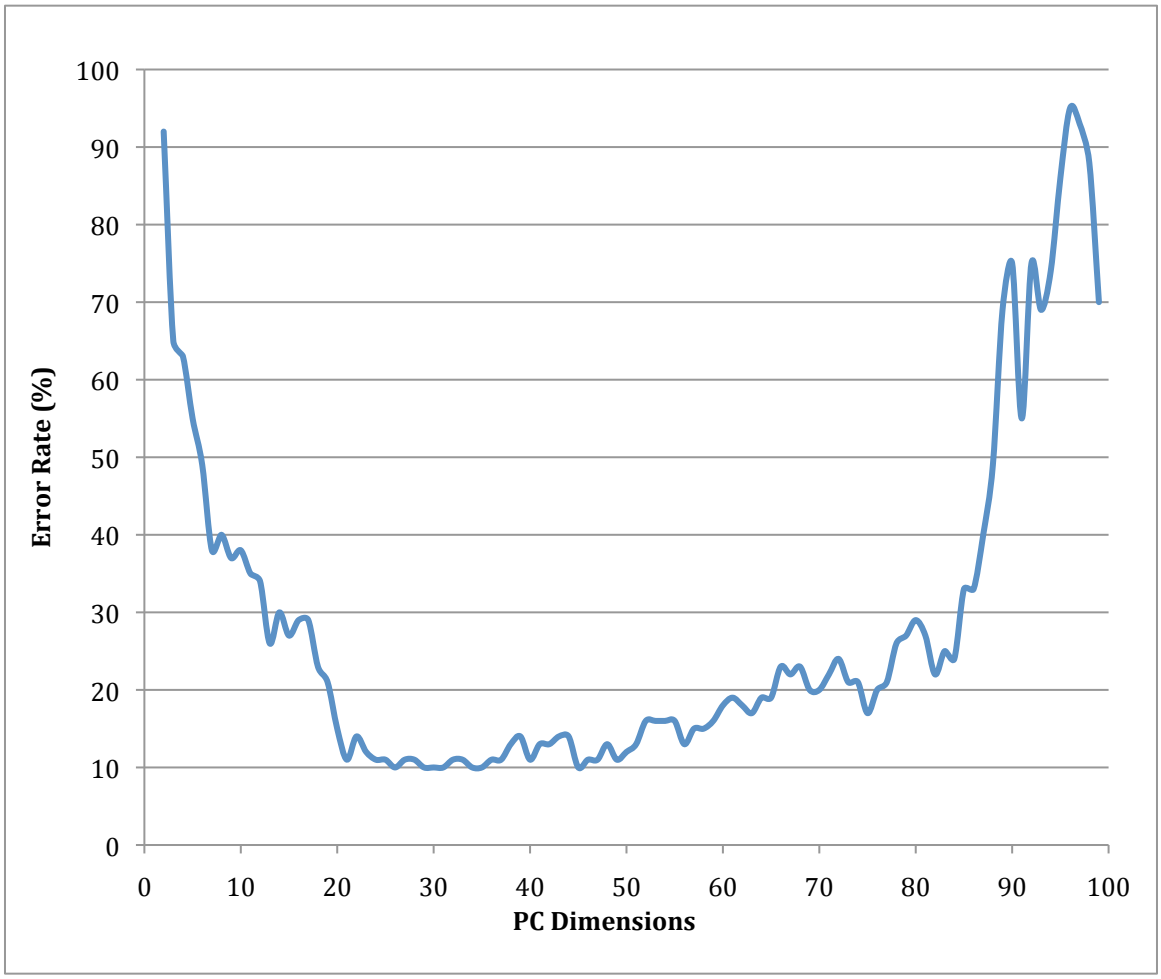


Figure 230: Graph of the discrimination error rate versus PC dimensions for HOO-CV with PCA reduced CVA for the first set of 10 container normalized (peak area) glass spectra (10 replicates), autoscaled data.

First Set, Normalized (Peak Area) – Float Classification

Table 242: Float classification error rates for HOO-CV with PCA reduced CVA for the first set of 20 window normalized (peak area) glass spectra (10 replicates), no data pretreatment. The smallest PC dimension with the minimum error rate is highlighted in yellow.

PCs	Error Rate (%)	PCs	Error Rate (%)	PCs	Error Rate (%)	PCs	Error Rate (%)	PCs	Error Rate (%)
2	48.50	4	33.50	6	33.00	8	26.50	10	22.50
3	38.50	5	32.50	7	26.00	9	26.50		

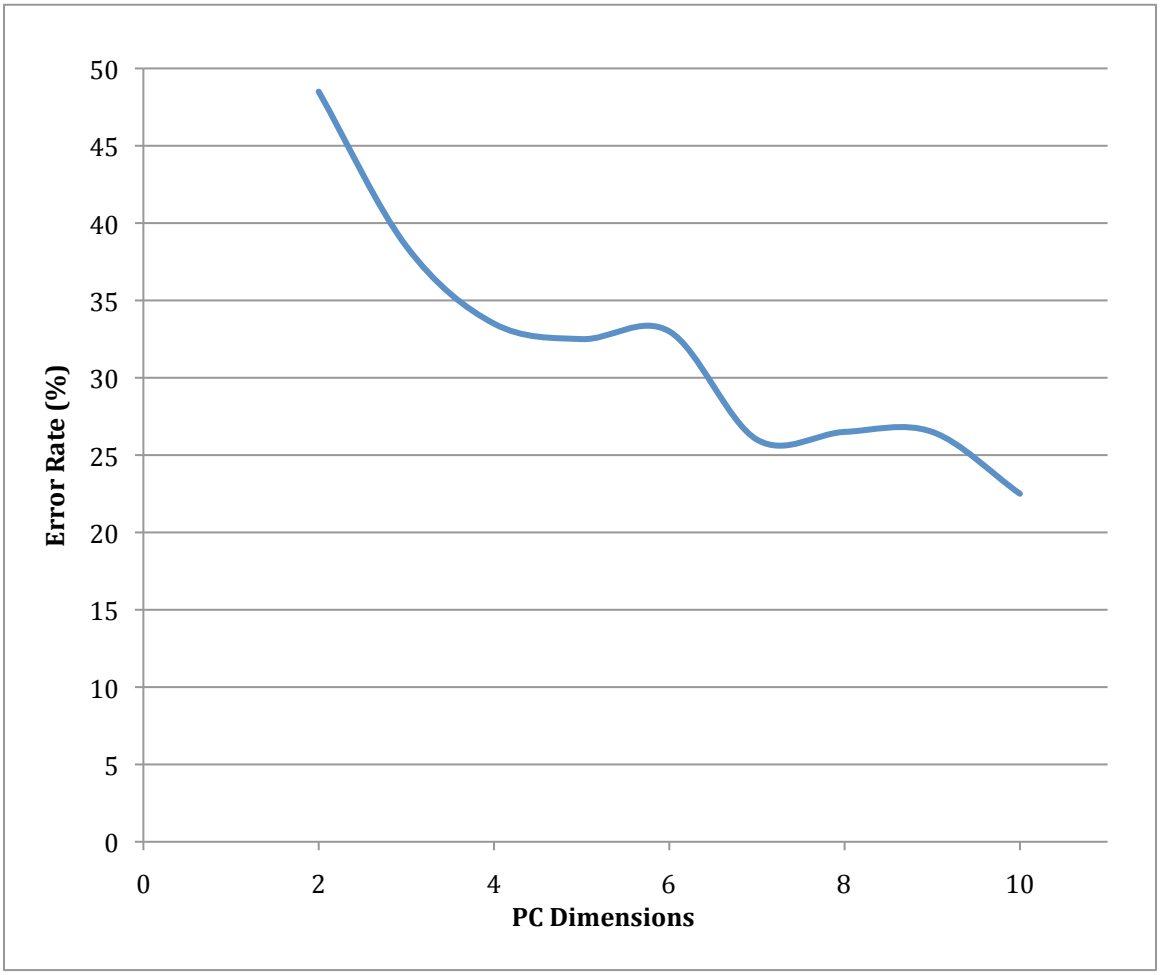


Figure 231: Graph of the float classification error rate versus PC dimensions for HOO-CV with PCA reduced CVA for the first set of 20 window normalized (peak area) glass spectra (10 replicates), no data pretreatment.

Table 243: Float classification error rates for HOO-CV with PCA reduced CVA for the first set of 20 window normalized (peak area) glass spectra (10 replicates), centered data. The smallest PC dimension with the minimum error rate is highlighted in yellow.

PCs	Error Rate (%)	PCs	Error Rate (%)	PCs	Error Rate (%)	PCs	Error Rate (%)	PCs	Error Rate (%)
2	50.00	4	33.00	6	31.50	8	25.50	9	23.50
3	33.00	5	30.50	7	32.50				

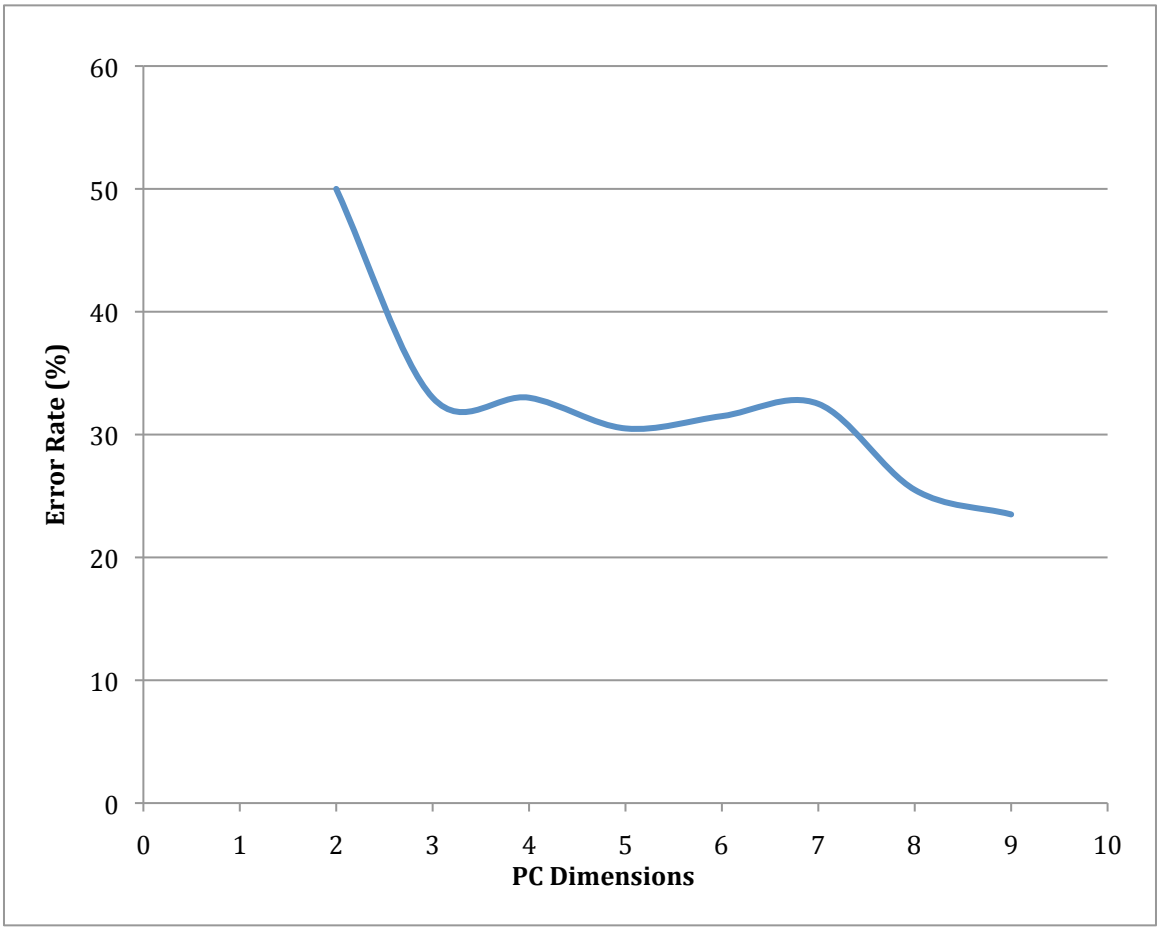


Figure 232: Graph of the float classification error rate versus PC dimensions for HOO-CV with PCA reduced CVA for the first set of 20 window normalized (peak area) glass spectra (10 replicates), centered data.

Table 244: Float classification error rates for HOO-CV with PCA reduced CVA for the first set of 20 window normalized (peak area) glass spectra (10 replicates), autoscaled data. The smallest PC dimension with the minimum error rate is highlighted in yellow.

PCs	Error Rate (%)	PCs	Error Rate (%)	PCs	Error Rate (%)	PCs	Error Rate (%)	PCs	Error Rate (%)
2	45.50	42	20.00	82	20.00	122	25.50	162	28.50
3	34.00	43	20.00	83	20.50	123	27.00	163	29.50
4	33.50	44	21.00	84	21.50	124	27.00	164	30.50
5	33.00	45	20.50	85	22.00	125	26.50	165	31.50
6	32.00	46	21.50	86	22.00	126	27.50	166	31.00
7	24.00	47	21.00	87	22.50	127	27.00	167	30.00
8	24.00	48	20.50	88	21.50	128	27.00	168	31.00
9	23.00	49	21.00	89	22.00	129	26.00	169	32.50
10	22.50	50	22.50	90	22.00	130	27.00	170	33.50
11	22.50	51	20.00	91	23.00	131	27.00	171	33.50
12	21.00	52	23.50	92	23.00	132	27.50	172	34.00
13	21.50	53	21.00	93	24.00	133	28.00	173	34.50
14	21.50	54	20.50	94	22.00	134	26.50	174	35.50
15	20.00	55	21.50	95	23.00	135	28.00	175	36.50
16	20.00	56	18.50	96	22.50	136	25.50	176	38.00
17	21.50	57	19.50	97	23.00	137	25.00	177	38.00
18	20.50	58	20.50	98	23.50	138	26.50	178	39.00
19	22.00	59	19.50	99	23.00	139	27.50	179	33.50
20	19.50	60	19.00	100	24.00	140	27.00	180	34.50
21	19.50	61	18.50	101	25.00	141	23.50	181	32.50
22	21.00	62	18.50	102	26.50	142	24.50	182	33.50
23	19.50	63	18.50	103	23.00	143	26.00	183	34.00
24	19.50	64	17.00	104	24.00	144	25.00	184	38.50
25	20.00	65	17.50	105	24.50	145	25.50	185	38.00
26	21.00	66	16.50	106	26.50	146	25.50	186	39.00
27	20.00	67	16.50	107	26.00	147	26.00	187	38.00
28	21.00	68	19.50	108	26.00	148	28.00	188	40.00
29	21.00	69	20.00	109	27.00	149	28.00	189	42.50
30	18.00	70	20.00	110	25.50	150	29.00	190	43.50
31	17.50	71	20.50	111	25.00	151	28.50	191	43.00
32	17.00	72	20.50	112	26.00	152	30.00	192	41.00
33	16.50	73	19.00	113	27.50	153	31.00	193	46.00
34	19.50	74	19.50	114	28.50	154	29.00	194	40.00
35	18.00	75	19.00	115	27.50	155	29.50	195	43.50
36	18.00	76	19.00	116	28.50	156	29.00	196	46.50
37	17.50	77	19.50	117	28.00	157	29.50	197	49.50
38	19.00	78	20.50	118	27.00	158	29.00	198	48.50

39	20.00	79	20.50	119	28.00	159	28.50	199	45.00
40	21.50	80	19.50	120	26.00	160	29.50		
41	21.50	81	19.00	121	27.00	161	28.50		

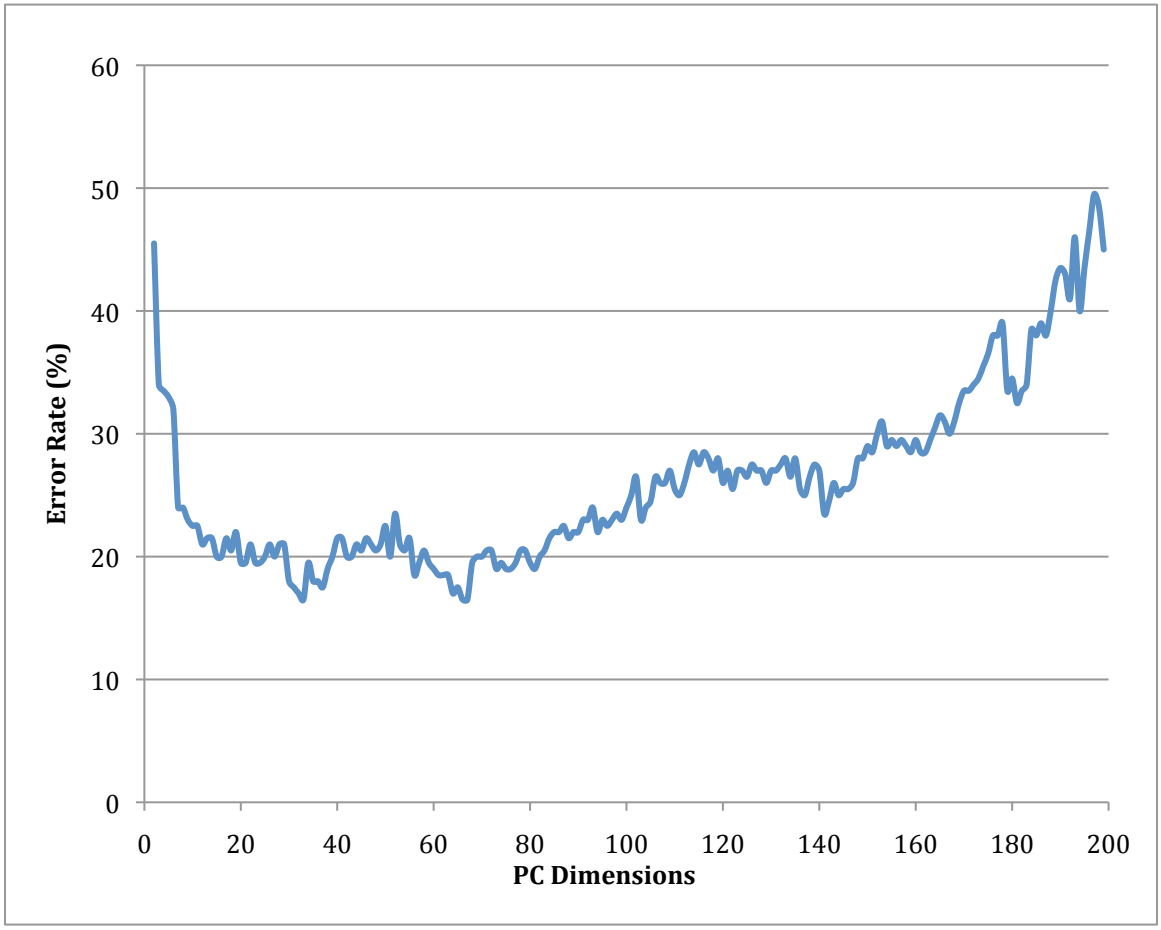


Figure 233: Graph of the float classification error rate versus PC dimensions for HOO-CV with PCA reduced CVA for the first set of 20 window normalized (peak area) glass spectra (10 replicates), autoscaled data.

First Set, Normalized (Peak Area) – Tempered Classification

Table 245: Tempered classification error rates for HOO-CV with PCA reduced CVA for the first set of 20 window normalized (peak area) glass spectra (10 replicates), no data pretreatment. The smallest PC dimension with the minimum error rate is highlighted in yellow.

PCs	Error Rate (%)	PCs	Error Rate (%)	PCs	Error Rate (%)	PCs	Error Rate (%)	PCs	Error Rate (%)
2	37.50	4	30.00	6	29.00	8	31.50	10	28.50
3	31.50	5	29.50	7	28.00	9	28.50		

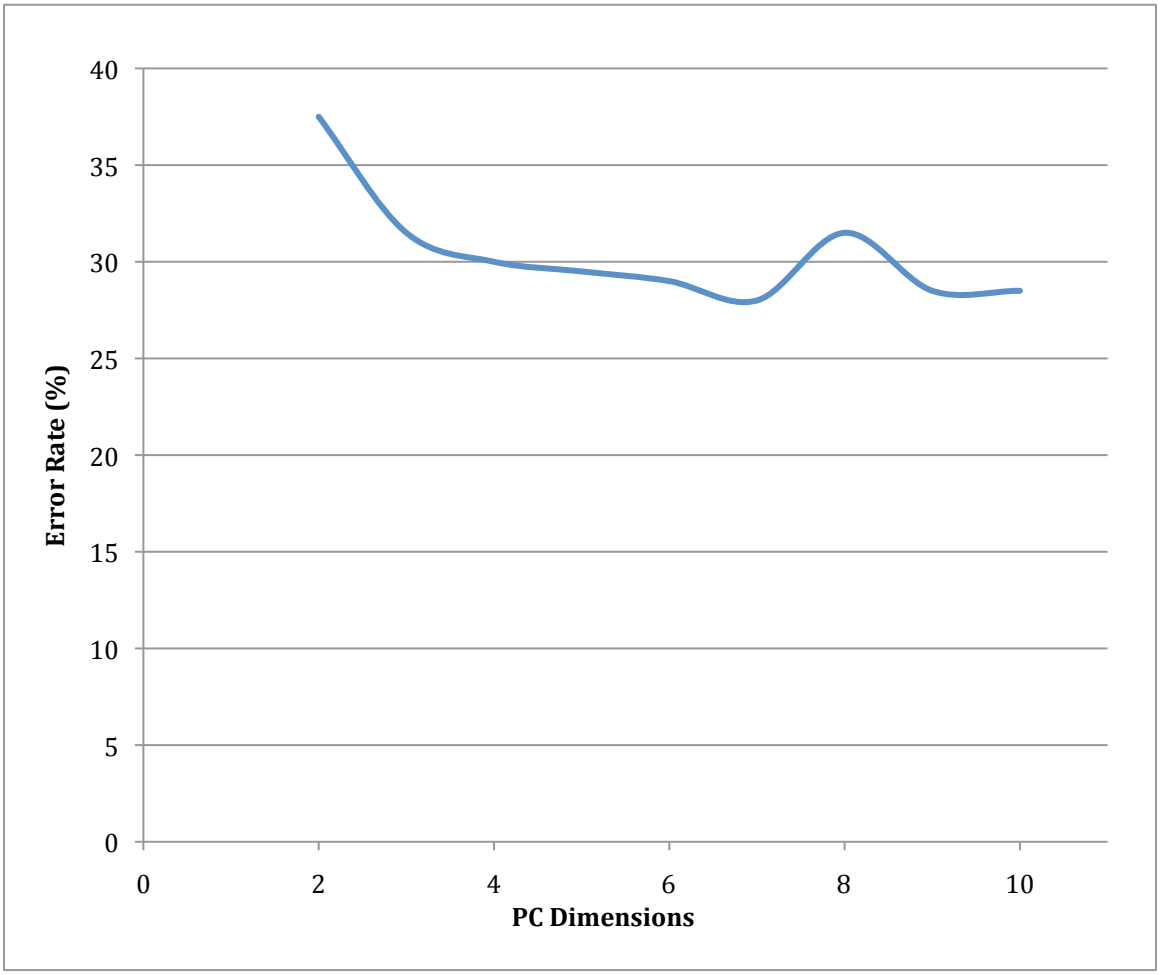


Figure 234: Graph of the tempered classification error rate versus PC dimensions for HOO-CV with PCA reduced CVA for the first set of 20 window normalized (peak area) glass spectra (10 replicates), no data pretreatment.

Table 246: Tempered classification error rates for HOO-CV with PCA reduced CVA for the first set of 20 window normalized (peak area) glass spectra (10 replicates), centered data. The smallest PC dimension with the minimum error rate is highlighted in yellow.

PCs	Error Rate (%)	PCs	Error Rate (%)	PCs	Error Rate (%)	PCs	Error Rate (%)	PCs	Error Rate (%)
2	33.00	4	31.00	6	29.00	8	32.00	9	25.50
3	27.00	5	29.00	7	28.50				

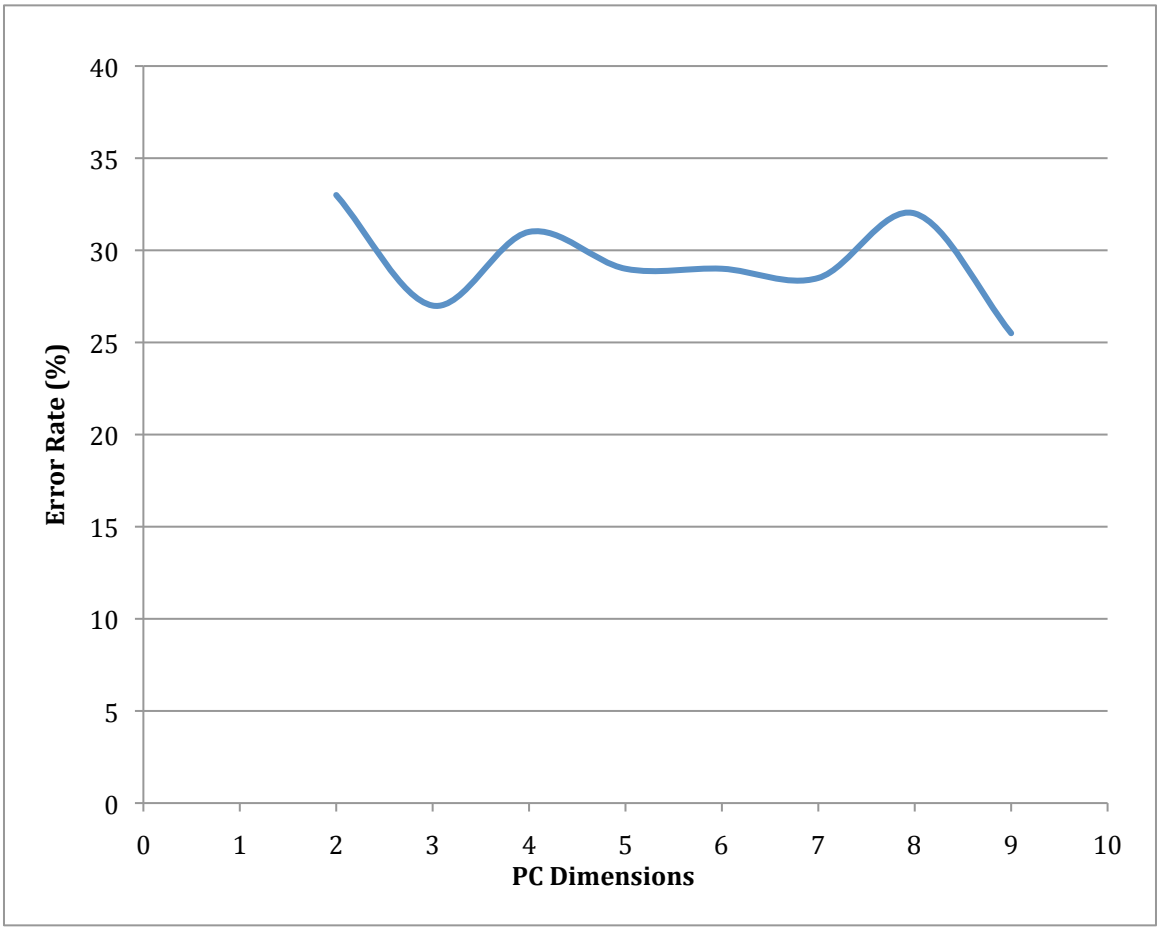


Figure 235: Graph of the tempered classification error rate versus PC dimensions for HOO-CV with PCA reduced CVA for the first set of 20 window normalized (peak area) glass spectra (10 replicates), centered data.

Table 247: Tempered classification error rates for HOO-CV with PCA reduced CVA for the first set of 20 window normalized (peak area) glass spectra (10 replicates), autoscaled data. The smallest PC dimension with the minimum error rate is highlighted in yellow.

PCs	Error Rate (%)	PCs	Error Rate (%)	PCs	Error Rate (%)	PCs	Error Rate (%)	PCs	Error Rate (%)
2	38.00	42	16.00	82	19.50	122	19.00	162	17.00
3	28.00	43	14.50	83	18.00	123	17.00	163	18.00
4	28.00	44	16.00	84	18.50	124	17.50	164	21.50
5	30.00	45	17.00	85	19.50	125	18.50	165	20.00
6	30.50	46	17.00	86	20.50	126	18.50	166	18.00
7	29.00	47	17.00	87	21.00	127	19.50	167	17.50
8	25.00	48	16.50	88	20.50	128	20.00	168	19.00
9	26.00	49	16.00	89	21.00	129	20.00	169	20.50
10	27.00	50	17.00	90	21.00	130	20.50	170	20.50
11	27.50	51	16.50	91	20.00	131	20.50	171	21.00
12	28.50	52	17.00	92	23.00	132	20.50	172	21.00
13	28.50	53	17.00	93	22.00	133	19.50	173	22.50
14	28.00	54	17.50	94	22.00	134	21.50	174	20.00
15	28.00	55	18.00	95	22.00	135	21.50	175	21.00
16	26.00	56	19.50	96	20.50	136	21.50	176	20.00
17	23.00	57	19.50	97	19.50	137	23.00	177	20.00
18	23.50	58	18.00	98	19.50	138	20.00	178	22.00
19	20.50	59	18.00	99	19.50	139	20.50	179	24.50
20	19.50	60	18.50	100	19.00	140	21.00	180	24.50
21	19.50	61	20.00	101	19.00	141	21.50	181	27.00
22	19.00	62	20.00	102	18.00	142	21.50	182	29.00
23	19.50	63	20.00	103	19.50	143	23.50	183	29.50
24	18.50	64	20.50	104	19.00	144	22.00	184	30.50
25	20.50	65	20.50	105	18.00	145	19.50	185	29.00
26	20.00	66	21.00	106	18.50	146	21.00	186	30.50
27	19.50	67	19.00	107	20.00	147	21.50	187	31.00
28	18.50	68	19.00	108	21.50	148	14.50	188	25.00
29	16.00	69	19.00	109	19.00	149	14.50	189	25.50
30	17.00	70	18.50	110	19.50	150	16.00	190	28.50
31	14.50	71	18.50	111	20.50	151	17.00	191	30.00
32	14.50	72	19.50	112	17.00	152	18.00	192	29.50
33	16.50	73	18.50	113	18.00	153	17.00	193	35.00
34	15.00	74	19.50	114	19.50	154	17.00	194	36.50
35	13.50	75	17.50	115	16.50	155	16.00	195	40.00
36	16.00	76	16.50	116	17.00	156	16.00	196	36.00
37	16.00	77	17.50	117	18.50	157	15.50	197	43.50
38	16.00	78	16.50	118	19.50	158	15.50	198	53.00

39	16.00	79	18.50	119	19.50	159	15.50	199	40.00
40	16.50	80	19.50	120	18.00	160	15.00		
41	15.50	81	17.50	121	19.50	161	15.50		

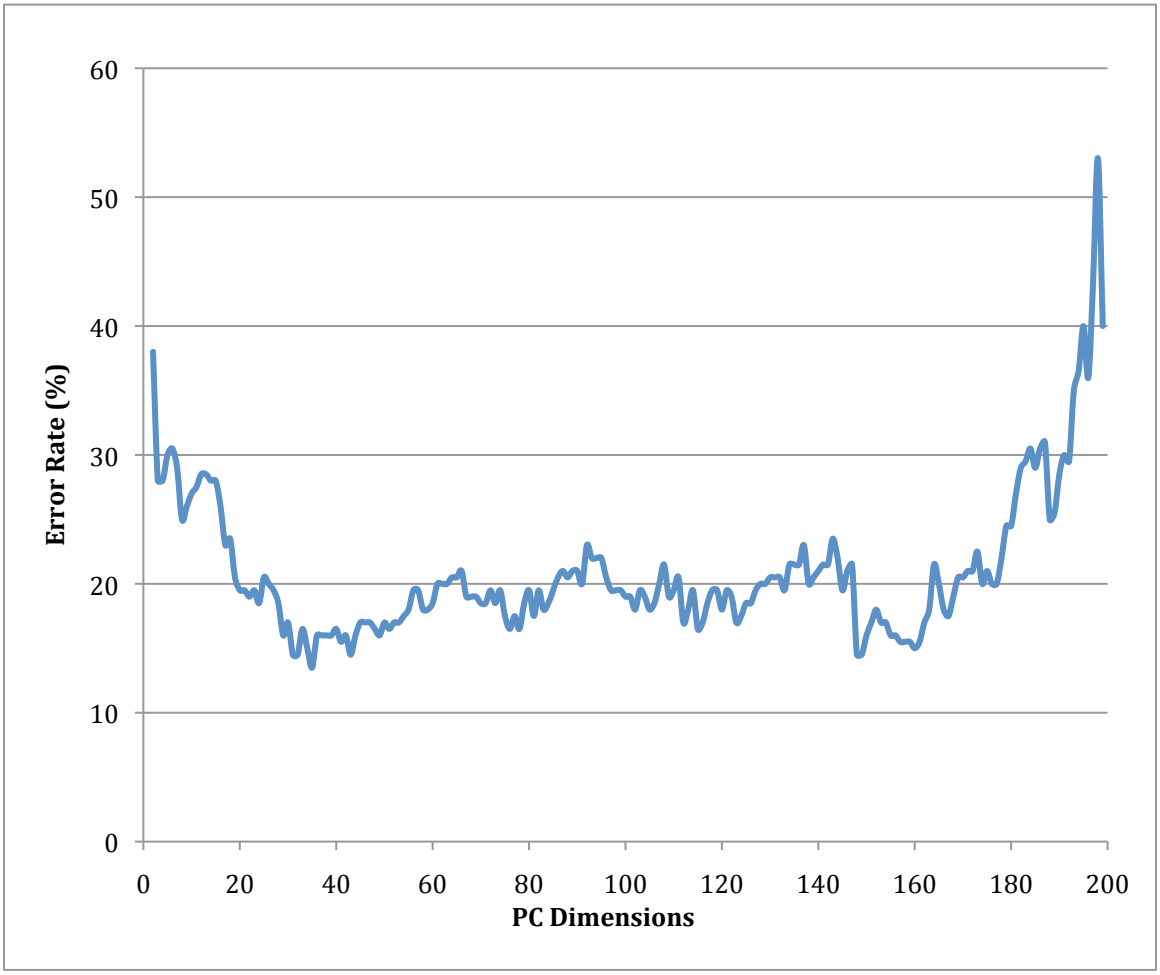


Figure 236: Graph of the tempered classification error rate versus PC dimensions for HOO-CV with PCA reduced CVA for the first set of 20 window normalized (peak area) glass spectra (10 replicates), autoscaled data.

C. HOO-CV PCA-CVA Results for the Peak Height Normalized Spectra

First Set, Normalized (Peak Height) - Discrimination

Table 248: Discrimination error rates for HOO-CV with PCA reduced CVA for the first set of 30 normalized (peak height) glass spectra (10 replicates), no data pretreatment. The smallest PC dimension with the minimum error rate is highlighted in yellow.

PCs	Error Rate (%)	PCs	Error Rate (%)	PCs	Error Rate (%)	PCs	Error Rate (%)	PCs	Error Rate (%)
2	94.00	26	17.00	50	15.00	74	14.67	98	12.67
3	91.00	27	15.33	51	15.00	75	14.33	99	13.33
4	89.00	28	15.33	52	15.33	76	14.00	100	13.00
5	63.00	29	15.67	53	15.00	77	13.67	101	12.33
6	62.00	30	15.67	54	15.00	78	13.33	102	12.33
7	63.67	31	16.00	55	14.33	79	13.33	103	12.00
8	60.00	32	16.67	56	13.33	80	14.00	104	12.33
9	57.00	33	16.33	57	13.67	81	13.00	105	12.33
10	52.67	34	15.67	58	14.67	82	14.33	106	12.67
11	49.33	35	15.67	59	15.00	83	14.33	107	13.00
12	48.33	36	15.67	60	15.33	84	14.33	108	13.33
13	45.67	37	16.00	61	16.00	85	15.00	109	12.67
14	43.67	38	17.00	62	16.67	86	14.67	110	12.33
15	36.67	39	17.00	63	15.67	87	14.33	111	12.00
16	37.33	40	17.00	64	15.33	88	14.33	112	13.33
17	35.33	41	17.00	65	15.33	89	14.33	113	13.33
18	35.00	42	17.67	66	15.33	90	14.33	114	14.33
19	28.67	43	16.00	67	15.00	91	13.33	115	14.00
20	24.33	44	16.67	68	16.00	92	13.67	116	14.00
21	18.33	45	17.33	69	15.00	93	13.33	117	14.00
22	19.00	46	15.33	70	15.33	94	13.00	118	13.00
23	16.67	47	15.67	71	14.00	95	12.67	119	12.67
24	17.33	48	16.00	72	14.00	96	13.00	120	12.33
25	18.00	49	16.00	73	14.33	97	12.00		

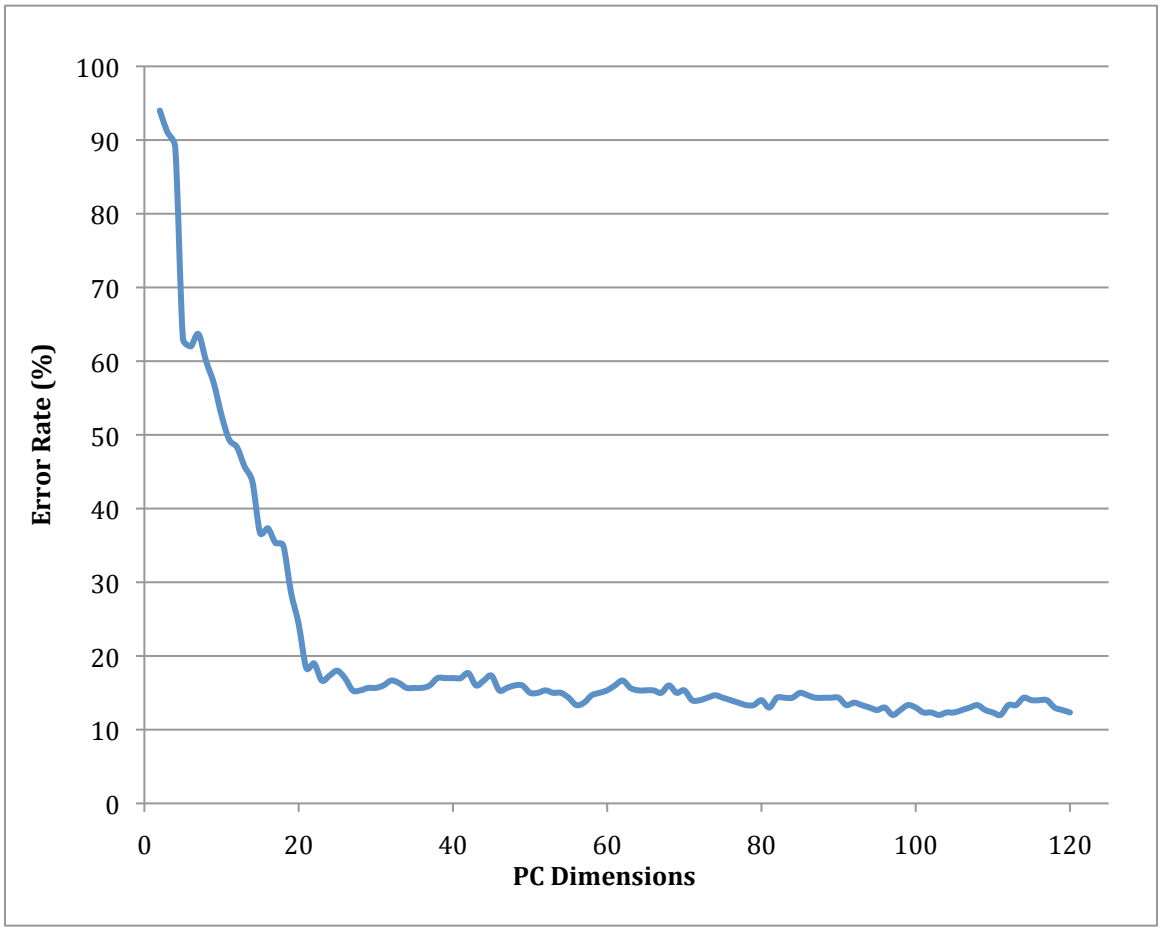


Figure 237: Graph of the discrimination error rate versus PC dimensions for HOO-CV with PCA reduced CVA for the first set of 30 normalized (peak height) glass spectra (10 replicates), no data pretreatment.

Table 249: Discrimination error rates for HOO-CV with PCA reduced CVA for the first set of 30 normalized (peak height) glass spectra (10 replicates), centered data. The smallest PC dimension with the minimum error rate is highlighted in yellow.

PCs	Error Rate (%)	PCs	Error Rate (%)	PCs	Error Rate (%)	PCs	Error Rate (%)	PCs	Error Rate (%)
2	95.00	26	17.33	50	15.33	74	15.00	98	12.00
3	89.00	27	15.67	51	15.33	75	14.67	99	13.00
4	89.33	28	15.67	52	15.33	76	14.00	100	13.00
5	61.00	29	15.67	53	14.67	77	12.00	101	12.33
6	62.67	30	15.33	54	14.67	78	13.33	102	13.00
7	60.33	31	17.00	55	14.00	79	13.33	103	12.33
8	58.00	32	16.67	56	14.00	80	13.33	104	12.33
9	53.33	33	16.33	57	14.00	81	14.00	105	12.67
10	50.67	34	16.00	58	14.67	82	14.33	106	12.67
11	48.00	35	17.67	59	15.00	83	13.67	107	14.33
12	49.67	36	16.00	60	16.00	84	14.33	108	14.00
13	46.00	37	16.33	61	15.67	85	14.67	109	13.33
14	43.33	38	16.67	62	16.67	86	14.33	110	12.67
15	36.33	39	17.33	63	16.33	87	13.33	111	12.67
16	37.33	40	16.67	64	16.00	88	13.33	112	13.33
17	35.33	41	16.67	65	16.00	89	14.33	113	13.00
18	35.00	42	17.33	66	15.67	90	13.33	114	14.33
19	28.33	43	16.00	67	15.00	91	13.00	115	14.33
20	24.33	44	16.33	68	16.00	92	13.33	116	14.33
21	18.33	45	16.67	69	14.67	93	12.00	117	14.33
22	18.67	46	15.00	70	14.00	94	12.67	118	12.67
23	17.33	47	15.00	71	13.67	95	13.00	119	11.33
24	18.00	48	15.67	72	14.00	96	13.00	120	12.67
25	18.67	49	15.67	73	14.00	97	11.33		

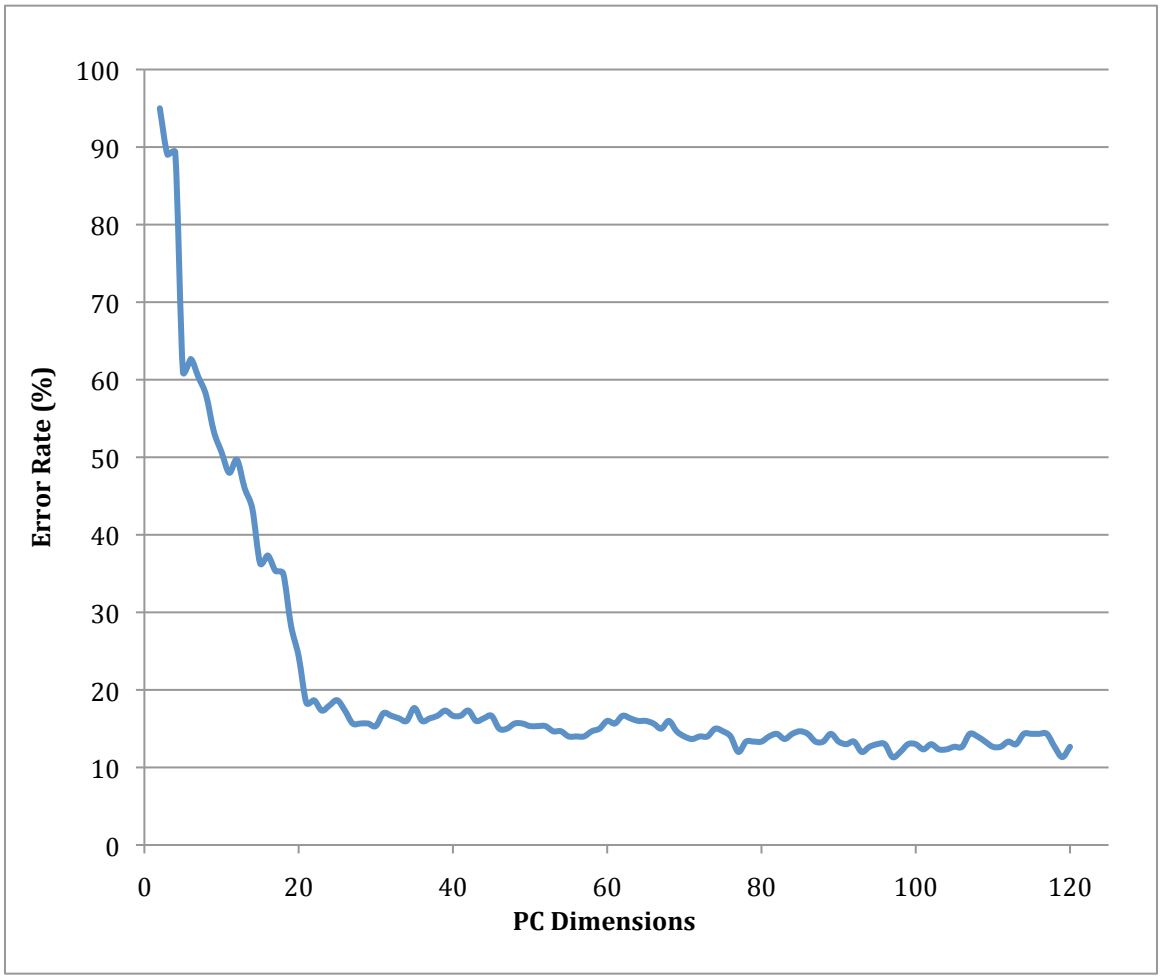


Figure 238: Graph of the discrimination error rate versus PC dimensions for HOO-CV with PCA reduced CVA for the first set of 30 normalized (peak height) glass spectra (10 replicates), centered data.

Table 250: Discrimination error rates for HOO-CV with PCA reduced CVA for the first set of 30 normalized (peak height) glass spectra (10 replicates), autoscaled data. The smallest PC dimension with the minimum error rate is highlighted in yellow.

PCs	Error Rate (%)	PCs	Error Rate (%)	PCs	Error Rate (%)	PCs	Error Rate (%)	PCs	Error Rate (%)
2	95.67	59	14.33	116	8.67	173	8.67	230	17.00
3	87.33	60	14.33	117	8.00	174	8.67	231	16.00
4	84.67	61	14.67	118	8.33	175	9.33	232	18.33
5	63.33	62	15.67	119	8.67	176	9.33	233	19.67
6	62.67	63	15.00	120	8.67	177	9.33	234	20.00
7	61.00	64	15.00	121	8.67	178	9.33	235	19.33
8	54.67	65	15.00	122	9.67	179	9.33	236	20.00
9	56.00	66	13.33	123	9.00	180	10.00	237	19.33
10	52.33	67	13.33	124	8.67	181	10.33	238	20.33
11	50.33	68	13.67	125	8.67	182	10.67	239	20.33
12	50.00	69	13.67	126	9.00	183	11.00	240	20.00
13	41.00	70	13.33	127	9.33	184	11.00	241	22.00
14	39.00	71	13.00	128	9.00	185	10.67	242	20.67
15	35.67	72	14.00	129	8.00	186	10.33	243	22.00
16	33.33	73	14.00	130	8.67	187	11.00	244	21.33
17	32.33	74	13.33	131	8.00	188	11.00	245	23.00
18	26.00	75	13.33	132	7.67	189	10.33	246	24.00
19	21.67	76	13.33	133	7.33	190	11.00	247	26.33
20	21.00	77	13.33	134	7.67	191	12.00	248	27.33
21	20.00	78	12.67	135	8.33	192	11.00	249	30.67
22	17.67	79	12.33	136	7.33	193	11.33	250	33.67
23	17.00	80	11.67	137	7.33	194	11.67	251	33.33
24	16.67	81	11.33	138	8.67	195	11.00	252	35.67
25	16.00	82	11.00	139	8.00	196	11.67	253	34.00
26	17.33	83	10.67	140	7.67	197	12.67	254	36.33
27	17.33	84	11.33	141	8.00	198	13.00	255	38.00
28	17.33	85	10.33	142	8.33	199	14.00	256	40.67
29	17.33	86	11.00	143	7.67	200	12.67	257	43.67
30	16.67	87	11.00	144	8.00	201	12.67	258	45.00
31	16.67	88	10.67	145	8.00	202	11.00	259	48.00
32	16.67	89	9.67	146	7.33	203	12.00	260	48.67
33	16.00	90	9.00	147	7.33	204	13.00	261	53.00
34	15.67	91	9.67	148	7.33	205	13.00	262	58.67
35	16.00	92	9.33	149	8.00	206	11.33	263	60.67
36	16.67	93	9.67	150	8.00	207	12.00	264	60.33
37	15.00	94	9.33	151	8.00	208	13.33	265	66.00
38	15.67	95	10.00	152	8.00	209	14.00	266	70.67

39	15.00	96	9.33	153	7.67	210	14.00	267	75.33
40	14.67	97	8.67	154	7.67	211	14.00	268	75.00
41	15.00	98	8.33	155	8.67	212	13.67	269	75.00
42	15.67	99	8.00	156	8.33	213	14.33	270	60.00
43	15.67	100	7.67	157	8.33	214	15.00	271	71.33
44	16.67	101	8.67	158	9.00	215	13.00	272	95.00
45	16.33	102	9.67	159	7.67	216	15.33	273	92.00
46	16.67	103	9.00	160	8.33	217	15.33	274	91.00
47	15.33	104	9.00	161	8.67	218	15.33	275	94.33
48	15.67	105	9.67	162	8.67	219	15.67	276	81.33
49	15.67	106	10.00	163	8.00	220	16.00	277	86.67
50	16.67	107	10.67	164	8.67	221	16.33	278	87.33
51	16.33	108	10.33	165	9.00	222	16.33	279	87.67
52	17.00	109	10.33	166	9.00	223	16.67	280	89.67
53	16.67	110	10.00	167	9.33	224	17.67	281	91.33
54	16.33	111	10.67	168	9.67	225	16.67	282	88.00
55	15.67	112	9.33	169	9.00	226	17.00	283	90.67
56	14.67	113	9.33	170	9.00	227	17.67	284	93.67
57	13.67	114	8.00	171	9.33	228	18.00		
58	13.33	115	8.67	172	9.00	229	17.00		

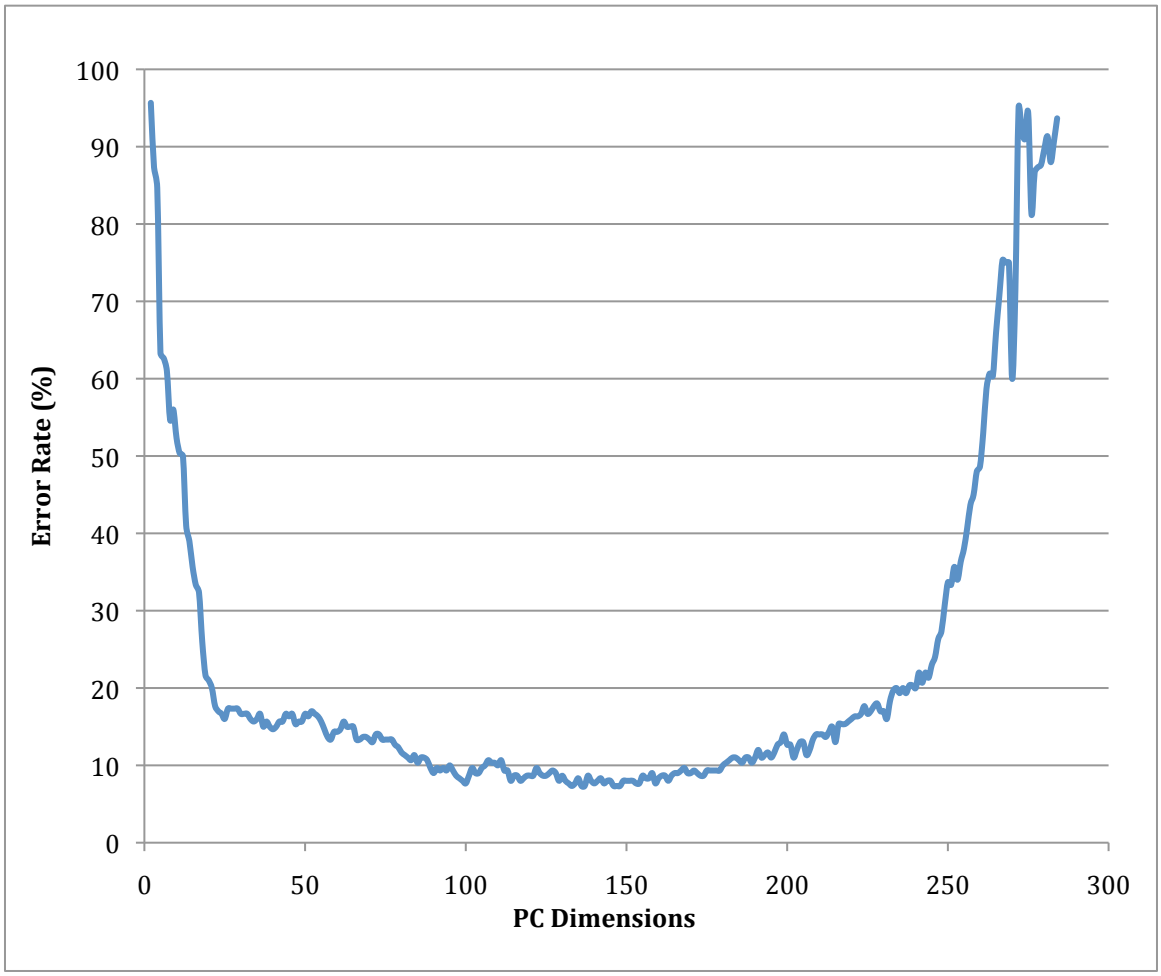


Figure 239: Graph of the discrimination error rate versus PC dimensions for HOO-CV with PCA reduced CVA for the first set of 30 normalized (peak height) glass spectra (10 replicates), autoscaled data.

First Set, Normalized (Peak Height) – Classification (automotive, architectural or container)

Table 251: Classification (automotive, architectural or container) error rates for HOO-CV with PCA reduced CVA for the first set of 30 normalized (peak height) glass spectra (10 replicates), no data pretreatment. The smallest PC dimension with the minimum error rate is highlighted in yellow.

PCs	Error Rate (%)	PCs	Error Rate (%)	PCs	Error Rate (%)	PCs	Error Rate (%)	PCs	Error Rate (%)
2	63.33	27	14.33	52	16.67	77	18.33	102	20.33
3	61.00	28	15.00	53	15.67	78	18.67	103	20.00
4	63.00	29	14.67	54	16.00	79	18.33	104	19.67
5	30.33	30	15.33	55	15.67	80	19.00	105	20.33
6	29.67	31	15.00	56	16.00	81	21.00	106	20.00
7	30.33	32	15.00	57	16.00	82	20.33	107	21.33
8	29.33	33	14.67	58	17.33	83	20.33	108	21.67
9	29.67	34	15.67	59	16.33	84	19.33	109	20.67
10	27.00	35	16.00	60	16.00	85	18.67	110	19.33
11	26.67	36	16.33	61	16.67	86	20.00	111	19.67
12	27.67	37	16.33	62	16.67	87	19.67	112	19.67
13	23.33	38	16.33	63	17.67	88	19.33	113	20.00
14	22.33	39	16.67	64	18.33	89	19.67	114	19.67
15	21.67	40	17.67	65	17.33	90	19.33	115	20.67
16	22.00	41	17.00	66	17.33	91	19.33	116	21.33
17	23.00	42	17.00	67	17.33	92	19.33	117	21.00
18	20.33	43	16.67	68	17.33	93	20.33	118	22.00
19	14.00	44	16.33	69	17.00	94	20.33	119	20.33
20	14.33	45	16.67	70	16.67	95	20.33	120	19.67
21	14.67	46	16.67	71	16.33	96	21.33	121	19.33
22	16.00	47	16.33	72	16.67	97	21.33	122	19.33
23	16.00	48	16.67	73	18.00	98	19.67	123	19.67
24	15.33	49	17.33	74	18.00	99	20.00		
25	15.67	50	18.00	75	18.00	100	19.67		
26	14.00	51	17.00	76	18.33	101	19.67		

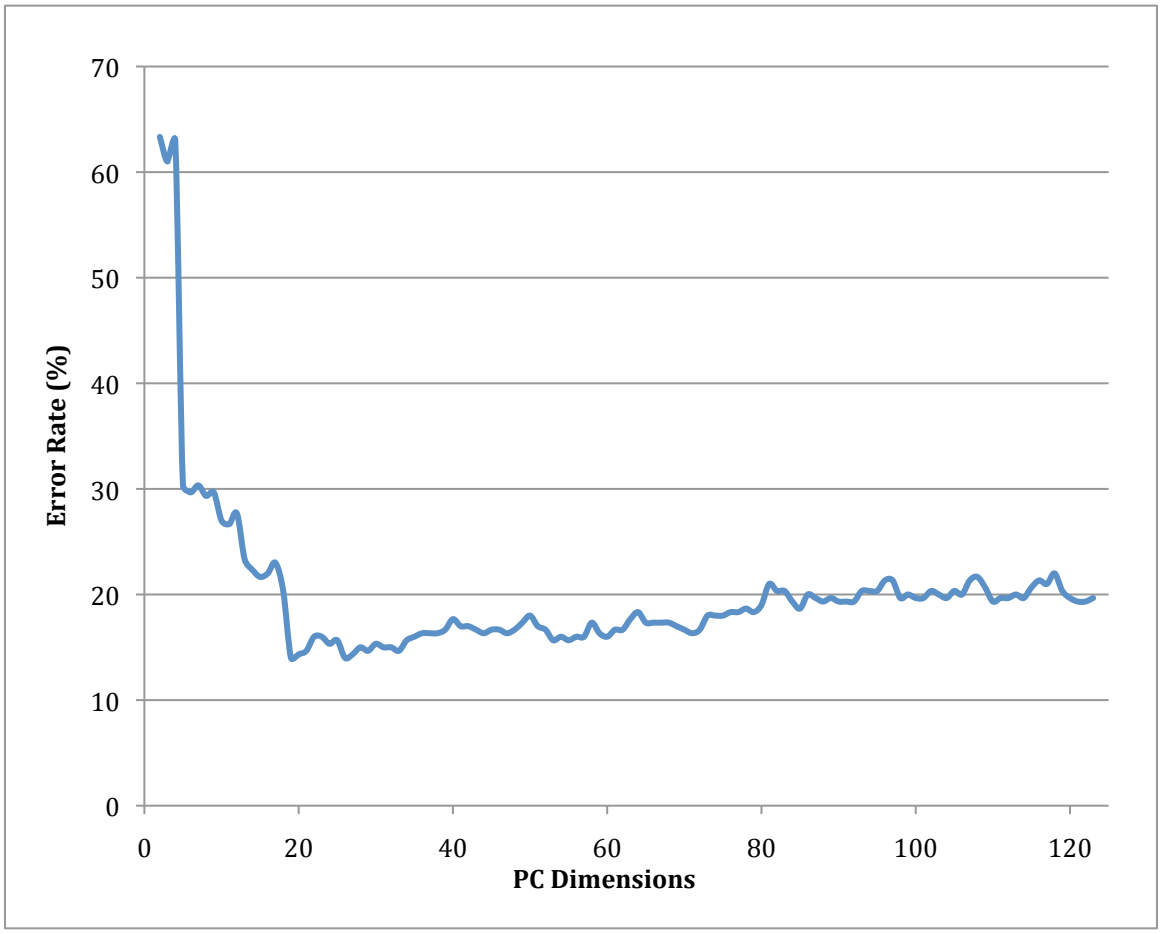


Figure 240: Graph of the classification (automotive, architectural or container) error rate versus PC dimensions for HOO-CV with PCA reduced CVA for the first set of 30 normalized (peak height) glass spectra (10 replicates), no data pretreatment.

Table 252: Classification (automotive, architectural or container) error rates for HOO-CV with PCA reduced CVA for the first set of 30 normalized (peak height) glass spectra (10 replicates), centered data. The smallest PC dimension with the minimum error rate is highlighted in yellow.

PCs	Error Rate (%)	PCs	Error Rate (%)	PCs	Error Rate (%)	PCs	Error Rate (%)	PCs	Error Rate (%)
2	64.00	27	14.00	52	17.00	77	18.33	102	19.33
3	60.00	28	15.00	53	15.67	78	18.33	103	19.33
4	62.33	29	15.00	54	16.00	79	18.33	104	19.00
5	30.00	30	15.33	55	15.67	80	19.00	105	19.33
6	30.00	31	14.67	56	16.00	81	19.67	106	19.33
7	28.33	32	15.00	57	16.00	82	20.00	107	20.67
8	27.33	33	14.67	58	17.67	83	20.33	108	21.67
9	29.00	34	15.67	59	16.33	84	19.67	109	21.00
10	27.00	35	16.67	60	16.33	85	18.67	110	19.67
11	27.00	36	16.67	61	16.33	86	19.33	111	19.33
12	28.00	37	16.33	62	17.00	87	19.67	112	20.00
13	22.00	38	17.00	63	18.00	88	20.00	113	20.33
14	21.67	39	16.33	64	17.67	89	20.00	114	19.67
15	21.67	40	17.00	65	17.33	90	19.33	115	21.67
16	22.00	41	17.00	66	17.33	91	20.00	116	21.67
17	23.00	42	17.00	67	17.67	92	19.33	117	21.00
18	20.33	43	16.33	68	17.67	93	20.67	118	22.00
19	14.00	44	16.33	69	18.00	94	21.00	119	19.67
20	14.33	45	16.33	70	16.67	95	21.00	120	19.33
21	14.67	46	17.00	71	16.33	96	21.33	121	20.67
22	16.00	47	16.67	72	16.33	97	21.33	122	18.67
23	16.00	48	16.67	73	17.33	98	20.67	123	19.33
24	15.67	49	17.33	74	17.33	99	20.33		
25	15.00	50	16.33	75	18.00	100	19.33		
26	15.00	51	17.00	76	18.33	101	20.33		

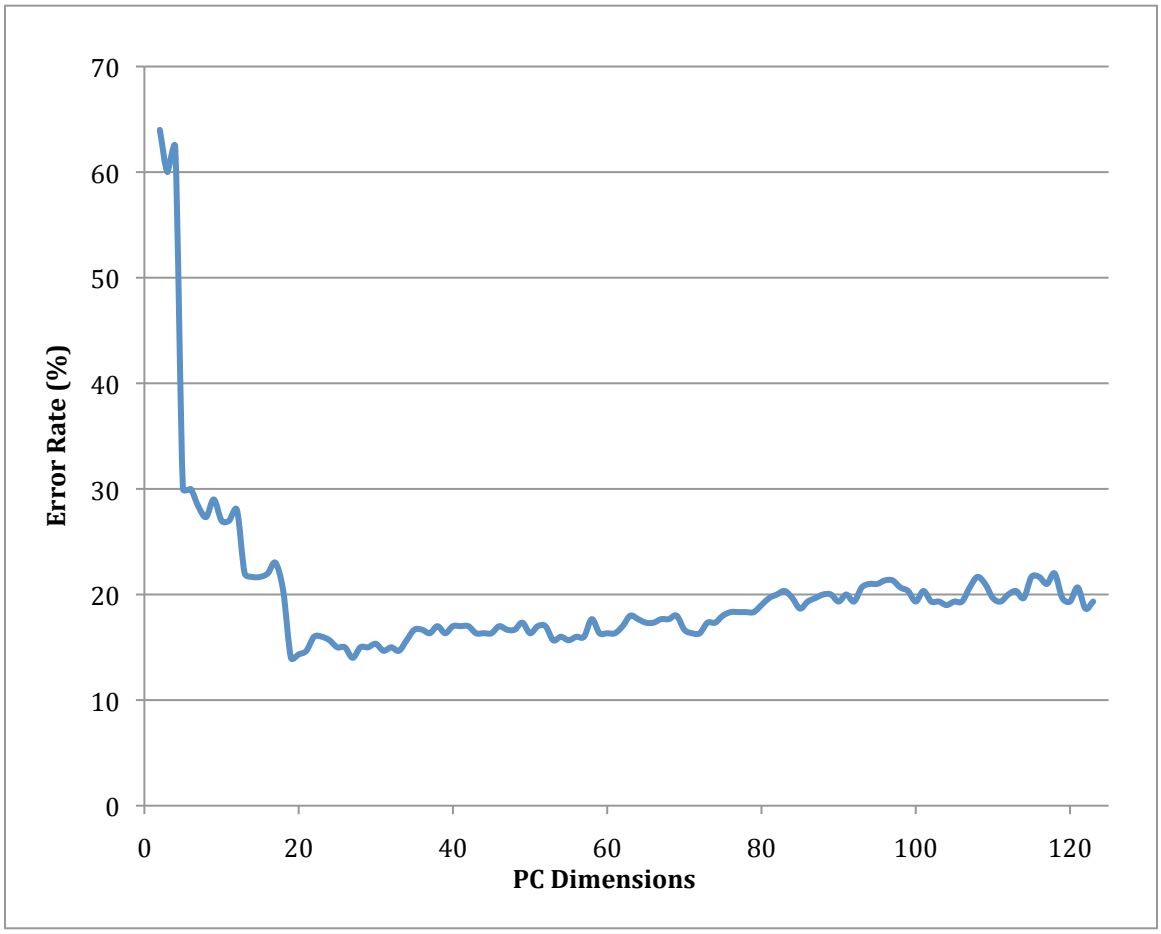


Figure 241: Graph of the classification (automotive, architectural or container) error rate versus PC dimensions for HOO-CV with PCA reduced CVA for the first set of 30 normalized (peak height) glass spectra (10 replicates), centered data.

Table 253: Classification (automotive, architectural or container) error rates for HOO-CV with PCA reduced CVA for the first set of 30 normalized (peak height) glass spectra (10 replicates), autoscaled data. The smallest PC dimension with the minimum error rate is highlighted in yellow.

PCs	Error Rate (%)	PCs	Error Rate (%)	PCs	Error Rate (%)	PCs	Error Rate (%)	PCs	Error Rate (%)
2	67.67	59	17.00	116	22.00	173	19.00	230	22.67
3	64.67	60	17.67	117	18.67	174	19.00	231	24.00
4	66.33	61	17.00	118	18.67	175	19.00	232	24.67
5	32.00	62	16.67	119	19.33	176	19.67	233	25.00
6	31.00	63	16.33	120	19.67	177	20.67	234	26.33
7	28.00	64	16.00	121	20.00	178	20.33	235	25.67
8	27.33	65	16.67	122	21.00	179	19.67	236	26.67
9	26.67	66	16.67	123	19.67	180	19.67	237	26.00
10	28.33	67	17.00	124	20.00	181	18.00	238	27.00
11	27.67	68	17.00	125	18.33	182	18.00	239	27.67
12	27.67	69	17.33	126	19.67	183	17.33	240	27.67
13	27.67	70	17.00	127	19.67	184	18.00	241	28.67
14	26.33	71	16.67	128	19.00	185	18.67	242	26.67
15	23.33	72	16.00	129	18.33	186	20.00	243	26.33
16	26.00	73	16.00	130	18.33	187	20.67	244	28.00
17	25.33	74	16.67	131	18.00	188	19.67	245	29.00
18	20.00	75	17.00	132	19.00	189	19.00	246	29.33
19	20.33	76	17.33	133	18.00	190	20.67	247	30.00
20	18.67	77	17.67	134	18.33	191	21.00	248	31.67
21	19.33	78	18.00	135	18.00	192	22.00	249	32.67
22	16.33	79	18.00	136	19.67	193	21.67	250	31.67
23	16.33	80	18.00	137	19.00	194	22.67	251	28.67
24	16.67	81	18.33	138	19.67	195	23.00	252	29.33
25	16.67	82	18.33	139	19.00	196	22.67	253	30.33
26	17.33	83	18.67	140	19.00	197	22.00	254	29.00
27	17.00	84	19.67	141	19.33	198	21.67	255	30.67
28	17.33	85	20.00	142	19.33	199	20.67	256	32.33
29	18.00	86	20.00	143	19.33	200	21.00	257	30.33
30	18.33	87	20.00	144	17.00	201	21.00	258	31.00
31	16.67	88	20.00	145	17.33	202	21.67	259	32.00
32	16.67	89	20.67	146	17.67	203	20.67	260	30.67
33	16.00	90	19.67	147	18.00	204	21.33	261	32.00
34	16.67	91	19.67	148	18.67	205	21.67	262	32.33
35	16.33	92	20.00	149	19.67	206	21.00	263	33.00
36	16.33	93	19.00	150	19.00	207	22.00	264	33.00
37	16.33	94	20.33	151	19.00	208	21.00	265	32.33

38	16.33	95	19.00	152	18.33	209	22.00	266	32.33
39	16.67	96	19.00	153	17.33	210	21.67	267	32.00
40	17.67	97	19.33	154	18.00	211	20.33	268	34.00
41	16.00	98	19.00	155	18.67	212	21.00	269	34.00
42	15.67	99	19.33	156	18.33	213	21.67	270	33.00
43	16.00	100	20.00	157	19.33	214	20.33	271	35.33
44	16.67	101	20.67	158	19.33	215	21.67	272	34.33
45	16.33	102	20.67	159	17.33	216	22.33	273	34.00
46	16.33	103	20.00	160	18.67	217	23.00	274	36.00
47	16.00	104	19.67	161	17.33	218	23.33	275	33.00
48	15.00	105	20.00	162	17.00	219	24.00	276	33.33
49	16.00	106	20.33	163	17.00	220	21.33	277	35.00
50	15.33	107	21.67	164	16.00	221	22.33	278	35.00
51	16.00	108	21.33	165	17.00	222	20.67	279	35.67
52	16.00	109	21.33	166	17.67	223	21.00	280	37.00
53	16.33	110	22.00	167	16.67	224	21.33	281	37.33
54	16.67	111	21.33	168	17.00	225	21.67	282	37.67
55	17.00	112	22.67	169	19.00	226	22.67	283	39.00
56	17.00	113	22.00	170	19.33	227	23.33	284	41.67
57	16.67	114	22.33	171	19.00	228	23.33		
58	16.67	115	22.00	172	19.00	229	22.33		

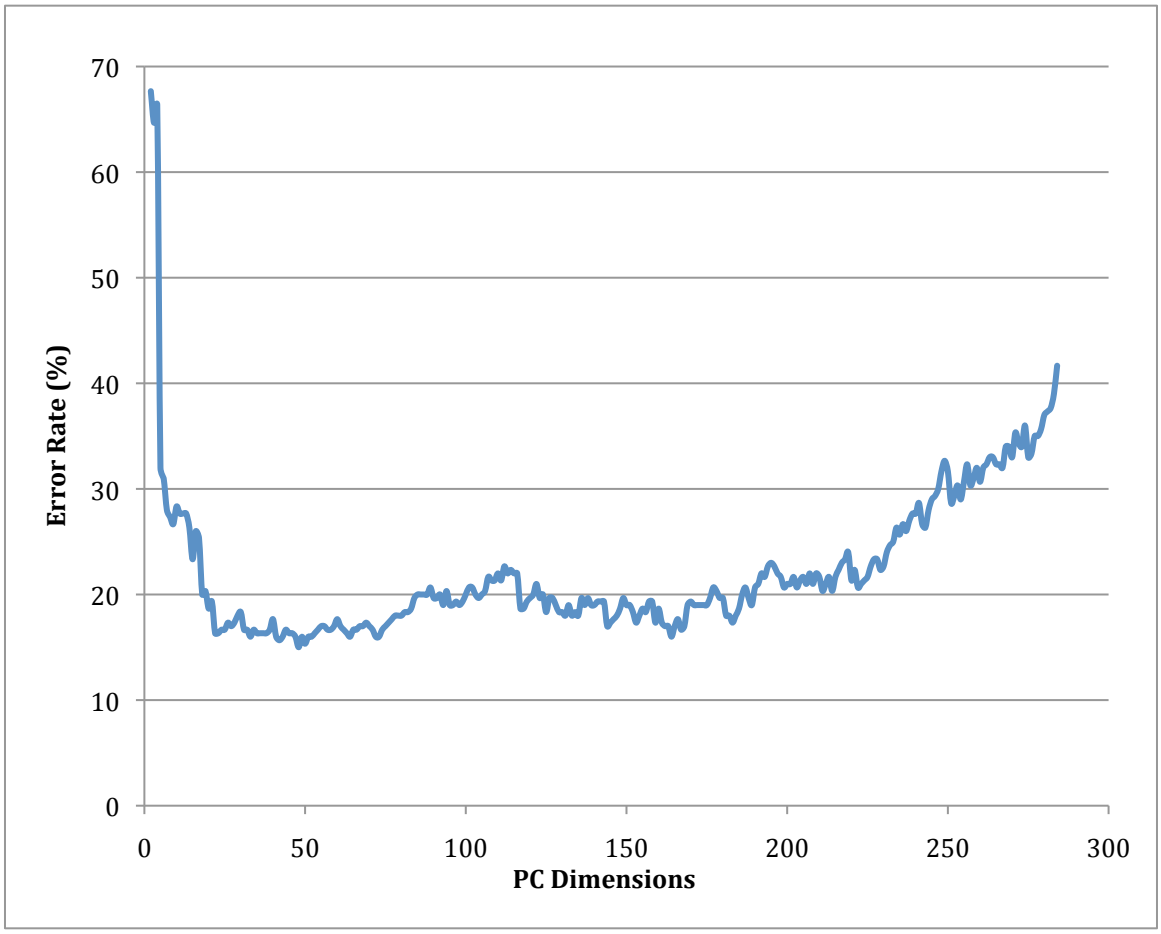


Figure 242: Graph of the classification (automotive, architectural or container) error rate versus PC dimensions for HOO-CV with PCA reduced CVA for the first set of 30 normalized (peak height) glass spectra (10 replicates), autoscaled data.

First Set, Normalized (Peak Height) – Classification (window or container)

Table 254: Classification (window or container) error rates for HOO-CV with PCA reduced CVA for the first set of 30 normalized (peak height) glass spectra (10 replicates), no data pretreatment. The smallest PC dimension with the minimum error rate is highlighted in yellow.

PCs	Error Rate (%)	PCs	Error Rate (%)	PCs	Error Rate (%)	PCs	Error Rate (%)	PCs	Error Rate (%)
2	33.33	27	4.00	52	4.67	77	4.67	102	5.33
3	34.00	28	3.67	53	4.67	78	4.33	103	5.00
4	34.00	29	4.00	54	4.67	79	4.33	104	5.00
5	6.67	30	4.00	55	4.67	80	4.33	105	5.33
6	7.00	31	4.00	56	4.67	81	4.67	106	5.67
7	5.67	32	4.00	57	4.67	82	5.00	107	6.00
8	7.00	33	3.67	58	4.67	83	5.00	108	6.00
9	5.67	34	4.00	59	5.00	84	4.67	109	5.00
10	4.00	35	4.00	60	4.67	85	4.67	110	5.00
11	4.00	36	4.00	61	5.00	86	5.00	111	5.00
12	4.00	37	4.00	62	4.67	87	5.00	112	5.00
13	4.00	38	4.00	63	5.00	88	5.33	113	5.00
14	3.67	39	4.00	64	5.00	89	5.00	114	5.67
15	3.67	40	4.00	65	5.00	90	5.00	115	5.33
16	3.67	41	4.33	66	5.00	91	5.00	116	5.33
17	4.00	42	4.67	67	5.00	92	5.00	117	5.33
18	4.00	43	4.67	68	5.00	93	5.00	118	5.67
19	3.67	44	4.33	69	5.00	94	5.00	119	5.67
20	3.67	45	3.67	70	5.00	95	5.00	120	5.33
21	4.00	46	4.00	71	5.00	96	5.00	121	5.33
22	4.00	47	4.33	72	5.00	97	5.00	122	5.33
23	4.00	48	4.67	73	5.00	98	5.00	123	5.33
24	4.00	49	4.67	74	5.00	99	5.00		
25	4.00	50	4.67	75	5.00	100	5.33		
26	4.00	51	4.67	76	4.67	101	5.00		

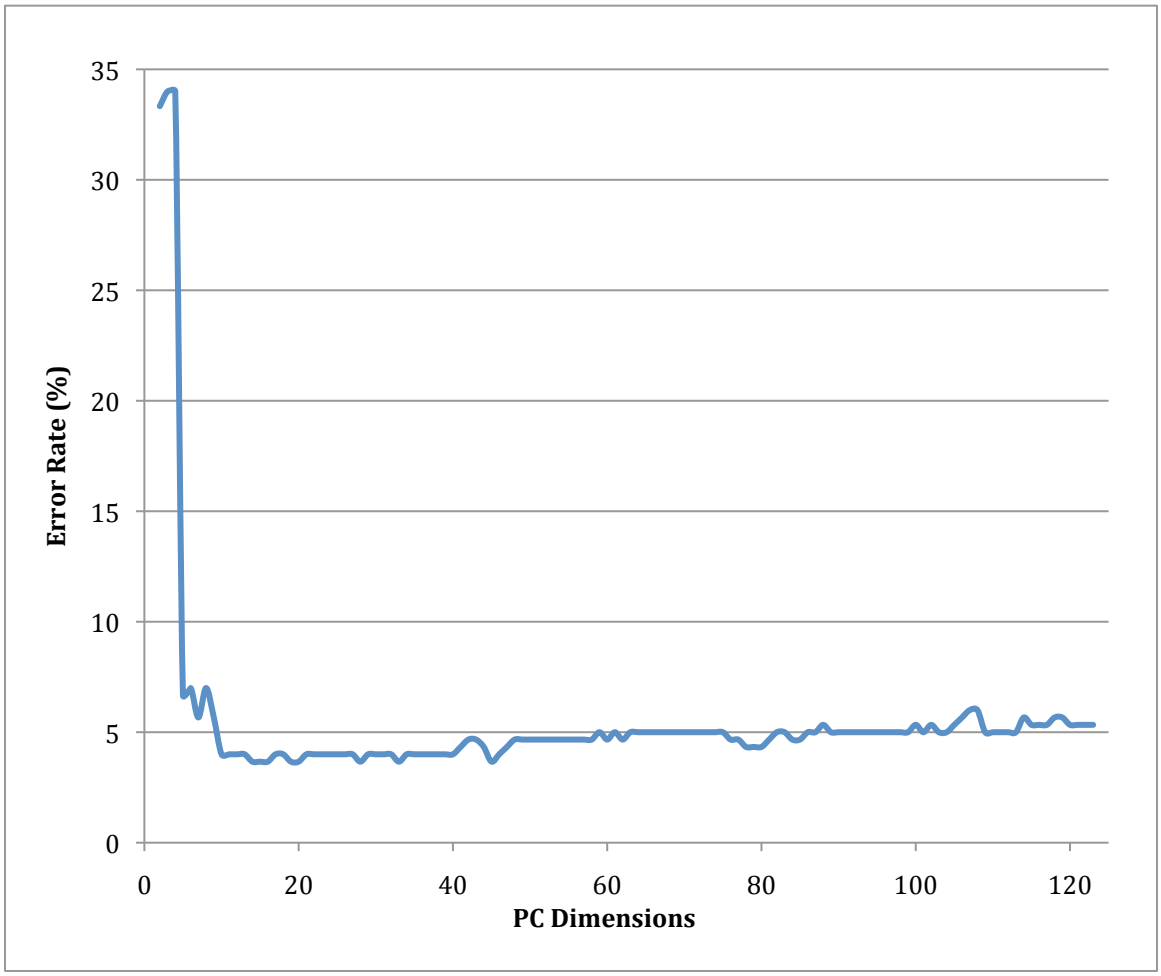


Figure 243: Graph of the classification (window or container) error rate versus PC dimensions for HOO-CV with PCA reduced CVA for the first set of 30 normalized (peak height) glass spectra (10 replicates), no data pretreatment.

Table 255: Classification (window or container) error rates for HOO-CV with PCA reduced CVA for the first set of 30 normalized (peak height) glass spectra (10 replicates), centered data. The smallest PC dimension with the minimum error rate is highlighted in yellow.

PCs	Error Rate (%)	PCs	Error Rate (%)	PCs	Error Rate (%)	PCs	Error Rate (%)	PCs	Error Rate (%)
2	33.33	27	4.00	52	4.67	77	4.67	102	5.00
3	33.33	28	3.67	53	4.67	78	4.67	103	4.67
4	33.67	29	4.00	54	4.67	79	4.33	104	5.00
5	7.00	30	4.00	55	4.67	80	4.33	105	5.33
6	5.33	31	4.00	56	4.67	81	5.00	106	5.33
7	5.67	32	4.00	57	4.67	82	5.00	107	5.67
8	6.00	33	4.00	58	4.67	83	5.00	108	5.67
9	4.67	34	4.00	59	4.67	84	5.00	109	4.67
10	4.00	35	4.00	60	4.67	85	4.67	110	4.67
11	4.00	36	4.00	61	5.00	86	5.00	111	5.00
12	4.00	37	4.00	62	5.00	87	5.33	112	5.33
13	3.67	38	4.00	63	5.00	88	5.33	113	5.33
14	3.67	39	4.00	64	4.67	89	5.33	114	5.00
15	3.67	40	4.00	65	5.00	90	5.00	115	5.33
16	3.67	41	4.33	66	5.00	91	5.33	116	5.33
17	4.00	42	4.67	67	5.00	92	5.00	117	5.33
18	4.00	43	4.67	68	5.00	93	5.00	118	5.67
19	3.67	44	4.33	69	5.00	94	5.00	119	5.67
20	3.67	45	3.67	70	5.00	95	5.00	120	5.00
21	4.00	46	3.67	71	5.00	96	5.00	121	5.67
22	4.00	47	3.67	72	5.00	97	5.00	122	5.33
23	4.00	48	4.67	73	5.00	98	5.00	123	5.33
24	4.00	49	4.67	74	5.00	99	5.00		
25	4.00	50	4.67	75	5.00	100	5.00		
26	4.00	51	4.67	76	4.67	101	5.00		

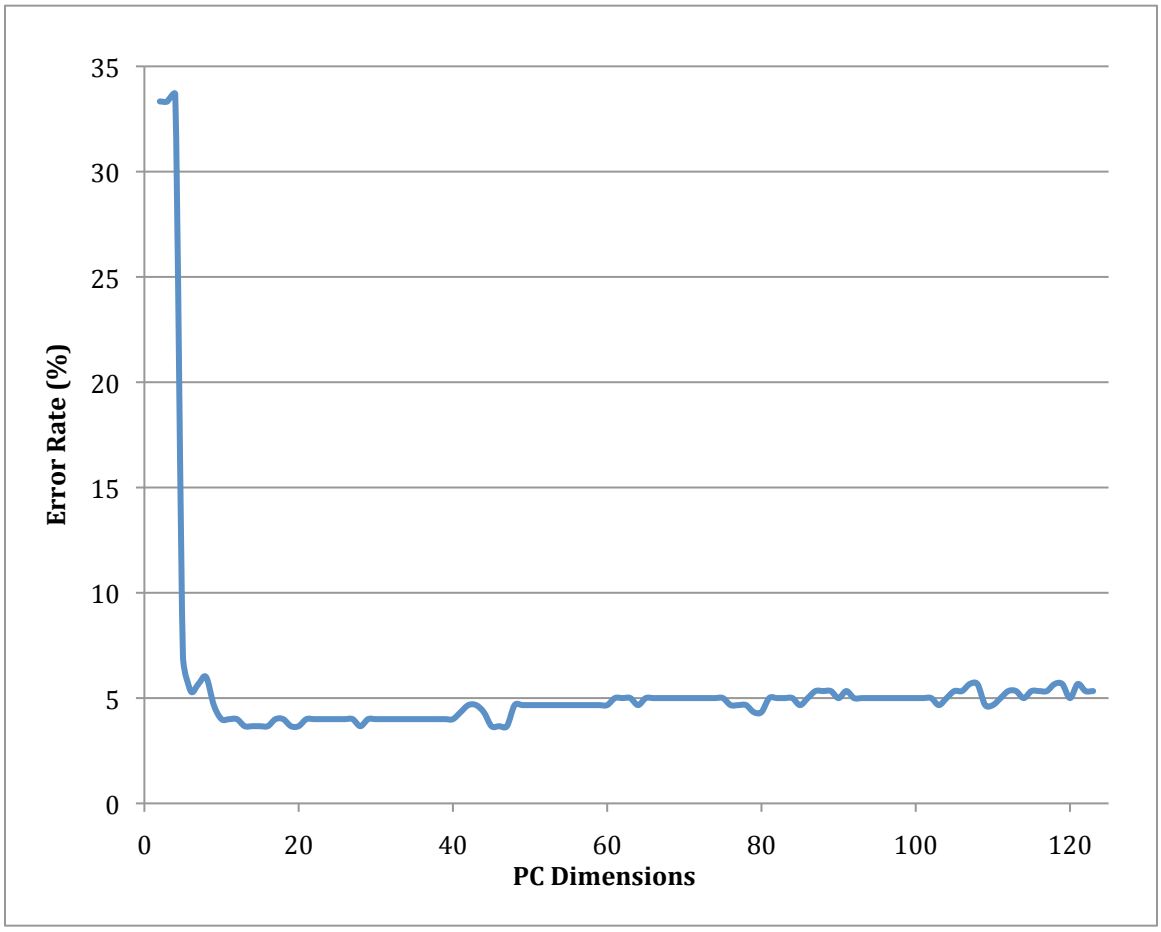


Figure 244: Graph of the classification (window or container) error rate versus PC dimensions for HOO-CV with PCA reduced CVA for the first set of 30 normalized (peak height) glass spectra (10 replicates), centered data.

Table 256: Classification (window or container) error rates for HOO-CV with PCA reduced CVA for the first set of 30 normalized (peak height) glass spectra (10 replicates), autoscaled data. The smallest PC dimension with the minimum error rate is highlighted in yellow.

PCs	Error Rate (%)	PCs	Error Rate (%)	PCs	Error Rate (%)	PCs	Error Rate (%)	PCs	Error Rate (%)
2	33.33	59	4.67	116	5.33	173	3.00	230	8.00
3	30.67	60	4.33	117	5.00	174	3.67	231	7.67
4	30.00	61	4.33	118	5.00	175	3.67	232	8.67
5	7.67	62	4.33	119	5.67	176	4.00	233	8.67
6	7.33	63	4.33	120	5.33	177	3.33	234	7.33
7	5.67	64	4.33	121	5.33	178	3.67	235	7.00
8	4.67	65	4.33	122	6.00	179	3.33	236	7.67
9	4.00	66	4.33	123	5.67	180	3.33	237	8.00
10	4.00	67	4.33	124	5.33	181	3.33	238	8.00
11	4.00	68	4.33	125	5.33	182	3.33	239	8.67
12	3.67	69	4.00	126	6.00	183	3.33	240	7.33
13	4.33	70	4.00	127	6.00	184	3.33	241	7.67
14	4.33	71	4.33	128	6.00	185	3.00	242	7.67
15	4.00	72	4.33	129	6.00	186	3.00	243	8.00
16	4.00	73	4.33	130	6.00	187	3.67	244	8.67
17	4.00	74	4.33	131	5.33	188	3.33	245	8.33
18	3.67	75	4.67	132	5.67	189	4.00	246	8.67
19	3.67	76	4.33	133	5.00	190	3.67	247	8.67
20	3.67	77	4.33	134	5.00	191	4.00	248	9.00
21	3.67	78	3.67	135	5.00	192	4.67	249	10.00
22	3.67	79	4.00	136	5.33	193	5.00	250	8.33
23	4.00	80	4.33	137	3.67	194	5.00	251	9.33
24	4.00	81	4.33	138	4.33	195	4.67	252	9.67
25	4.00	82	4.33	139	4.33	196	4.33	253	9.67
26	4.00	83	4.33	140	5.00	197	4.00	254	10.33
27	4.00	84	4.67	141	4.67	198	3.67	255	10.00
28	4.33	85	4.67	142	3.33	199	3.67	256	11.00
29	4.33	86	4.67	143	4.67	200	3.67	257	9.67
30	3.67	87	4.67	144	5.33	201	4.33	258	10.33
31	3.67	88	4.67	145	5.33	202	4.33	259	11.00
32	4.00	89	4.67	146	5.33	203	4.00	260	11.67
33	4.00	90	4.00	147	5.00	204	4.33	261	13.33
34	4.33	91	4.00	148	5.33	205	4.33	262	13.33
35	4.33	92	4.00	149	6.00	206	4.67	263	13.33
36	4.00	93	4.00	150	6.00	207	5.67	264	11.00
37	4.00	94	3.67	151	4.67	208	4.67	265	11.67
38	3.67	95	4.00	152	4.67	209	5.00	266	12.67

39	3.67	96	4.33	153	4.33	210	4.67	267	13.67
40	3.67	97	4.00	154	4.33	211	5.33	268	12.67
41	3.67	98	4.00	155	4.33	212	5.33	269	13.33
42	3.67	99	4.33	156	4.33	213	5.67	270	14.00
43	4.00	100	4.33	157	4.33	214	5.00	271	15.00
44	4.00	101	5.00	158	4.67	215	6.67	272	12.00
45	4.00	102	4.33	159	4.67	216	5.67	273	12.00
46	3.67	103	4.67	160	4.67	217	6.33	274	12.33
47	3.67	104	5.00	161	3.33	218	6.33	275	12.67
48	3.67	105	5.00	162	3.00	219	6.67	276	14.00
49	3.67	106	5.00	163	3.00	220	6.67	277	14.67
50	3.67	107	5.00	164	3.33	221	7.33	278	14.33
51	3.67	108	4.33	165	3.67	222	7.00	279	15.00
52	4.00	109	4.67	166	3.67	223	7.00	280	16.33
53	4.00	110	5.33	167	3.67	224	7.00	281	16.00
54	4.00	111	5.00	168	3.33	225	7.00	282	17.67
55	4.33	112	5.33	169	3.33	226	7.67	283	18.33
56	4.00	113	5.33	170	3.00	227	7.67	284	19.00
57	4.00	114	5.33	171	2.67	228	8.00		
58	4.33	115	5.33	172	3.00	229	7.33		

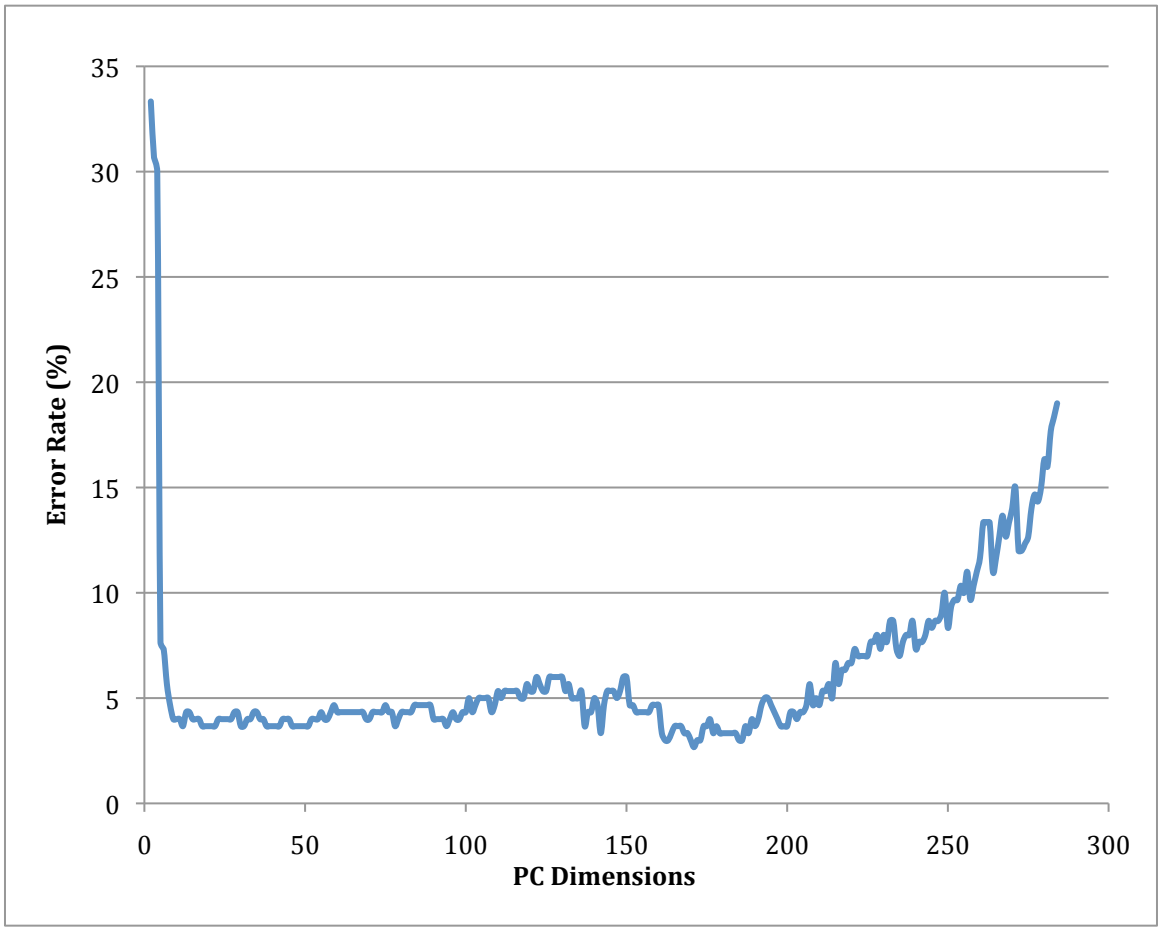


Figure 245: Graph of the classification (window or container) error rate versus PC dimensions for HOO-CV with PCA reduced CVA for the first set of 30 normalized (peak height) glass spectra (10 replicates), autoscaled data.

First Set, Normalized (Peak Height) – Window Discrimination

Table 257: Discrimination error rates for HOO-CV with PCA reduced CVA for the first set of 20 window normalized (peak height) glass spectra (10 replicates), no data pretreatment. The smallest PC dimension with the minimum error rate is highlighted in yellow.

PCs	Error Rate (%)	PCs	Error Rate (%)	PCs	Error Rate (%)	PCs	Error Rate (%)	PCs	Error Rate (%)
2	93.50	25	15.50	48	15.50	71	15.50	94	14.50
3	91.00	26	16.00	49	17.00	72	15.50	95	14.50
4	84.00	27	17.50	50	16.00	73	14.50	96	14.50
5	86.00	28	16.50	51	16.50	74	15.50	97	14.50
6	83.50	29	16.00	52	17.50	75	15.50	98	14.50
7	81.50	30	15.50	53	16.50	76	15.50	99	13.50
8	62.50	31	16.00	54	18.00	77	14.50	100	14.00
9	58.00	32	16.50	55	18.00	78	16.50	101	14.00
10	53.00	33	16.00	56	15.50	79	14.50	102	14.00
11	50.00	34	17.00	57	15.50	80	14.00	103	14.00
12	53.50	35	16.50	58	15.50	81	15.50	104	14.50
13	46.00	36	15.50	59	15.00	82	16.50	105	14.00
14	47.50	37	16.00	60	17.00	83	15.50	106	15.00
15	44.50	38	15.50	61	16.50	84	15.00	107	15.50
16	35.00	39	16.50	62	16.50	85	15.00	108	16.50
17	28.50	40	15.50	63	16.00	86	13.50	109	16.50
18	29.50	41	15.50	64	17.50	87	14.00	110	16.50
19	25.50	42	15.50	65	17.50	88	15.50	111	15.50
20	19.50	43	16.00	66	15.50	89	14.00	112	15.50
21	19.00	44	16.00	67	15.50	90	14.00		
22	19.50	45	16.00	68	16.00	91	14.00		
23	17.50	46	15.50	69	15.50	92	13.50		
24	15.50	47	14.00	70	16.00	93	14.50		

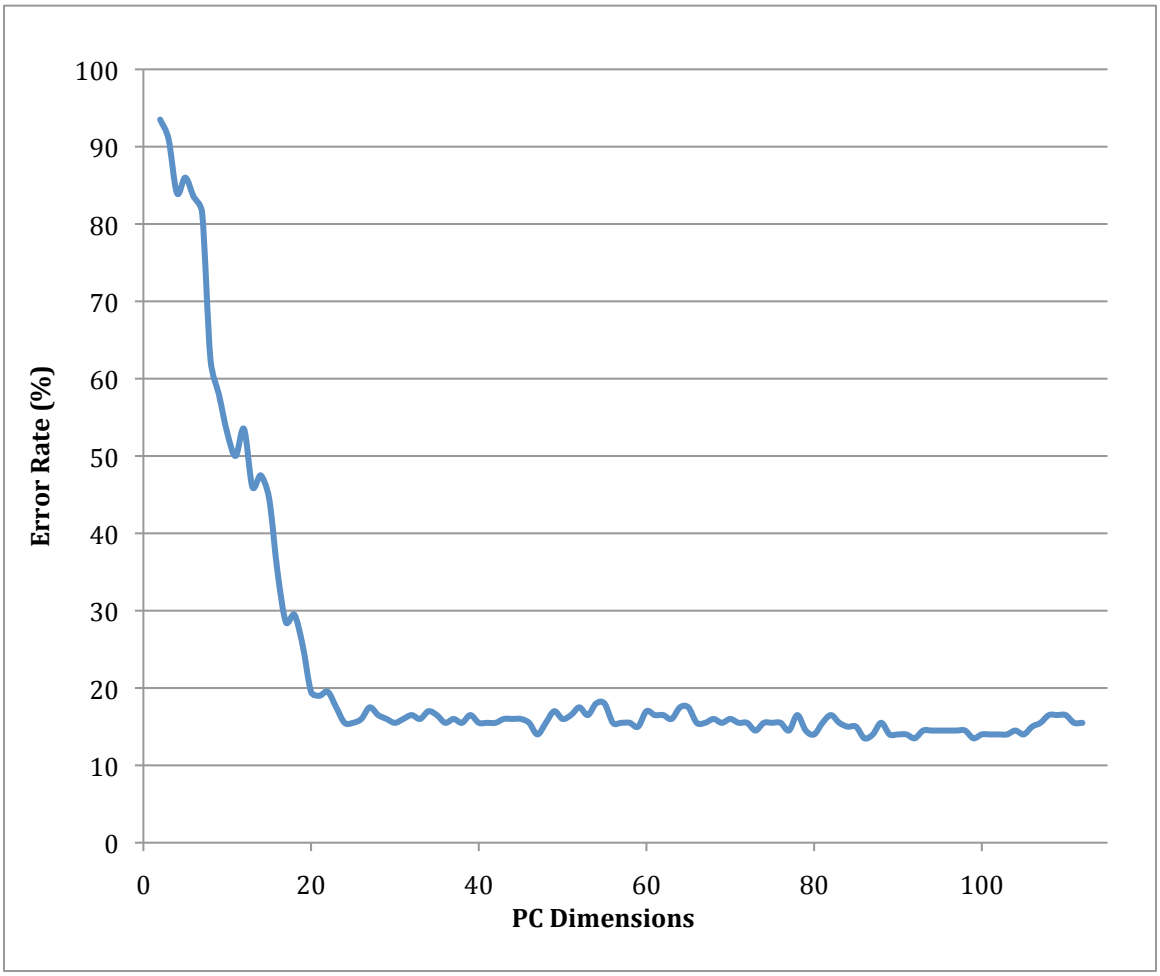


Figure 246: Graph of the discrimination error rate versus PC dimensions for HOO-CV with PCA reduced CVA for the first set of 20 window normalized (peak height) glass spectra (10 replicates), no data pretreatment.

Table 258: Discrimination error rates for HOO-CV with PCA reduced CVA for the first set of 20 window normalized (peak height) glass spectra (10 replicates), centered data. The smallest PC dimension with the minimum error rate is highlighted in yellow.

PCs	Error Rate (%)	PCs	Error Rate (%)	PCs	Error Rate (%)	PCs	Error Rate (%)	PCs	Error Rate (%)
2	92.50	25	15.50	48	16.00	71	15.50	94	14.50
3	89.00	26	16.50	49	17.00	72	16.50	95	13.50
4	83.00	27	17.50	50	16.50	73	16.00	96	13.50
5	84.00	28	17.00	51	17.00	74	15.00	97	15.00
6	81.00	29	16.00	52	17.50	75	14.50	98	16.00
7	63.50	30	15.50	53	17.00	76	15.00	99	14.50
8	62.00	31	15.50	54	17.00	77	14.50	100	13.50
9	58.00	32	16.50	55	17.00	78	15.00	101	13.50
10	53.50	33	16.50	56	16.00	79	14.00	102	15.00
11	50.00	34	17.00	57	15.50	80	14.50	103	15.00
12	51.00	35	15.00	58	15.00	81	15.00	104	14.50
13	46.00	36	15.50	59	14.50	82	16.00	105	14.00
14	46.50	37	15.50	60	16.00	83	15.50	106	15.50
15	44.50	38	15.50	61	16.00	84	16.00	107	16.00
16	35.00	39	15.50	62	15.50	85	15.50	108	15.50
17	28.50	40	15.50	63	16.00	86	15.00	109	15.50
18	29.50	41	15.00	64	16.50	87	14.50	110	15.50
19	25.50	42	15.50	65	16.50	88	13.50	111	16.00
20	19.50	43	16.50	66	15.50	89	13.50	112	16.50
21	19.00	44	16.00	67	16.00	90	14.50		
22	19.50	45	15.50	68	15.50	91	14.00		
23	17.50	46	14.50	69	14.50	92	14.00		
24	15.50	47	14.00	70	15.50	93	14.00		

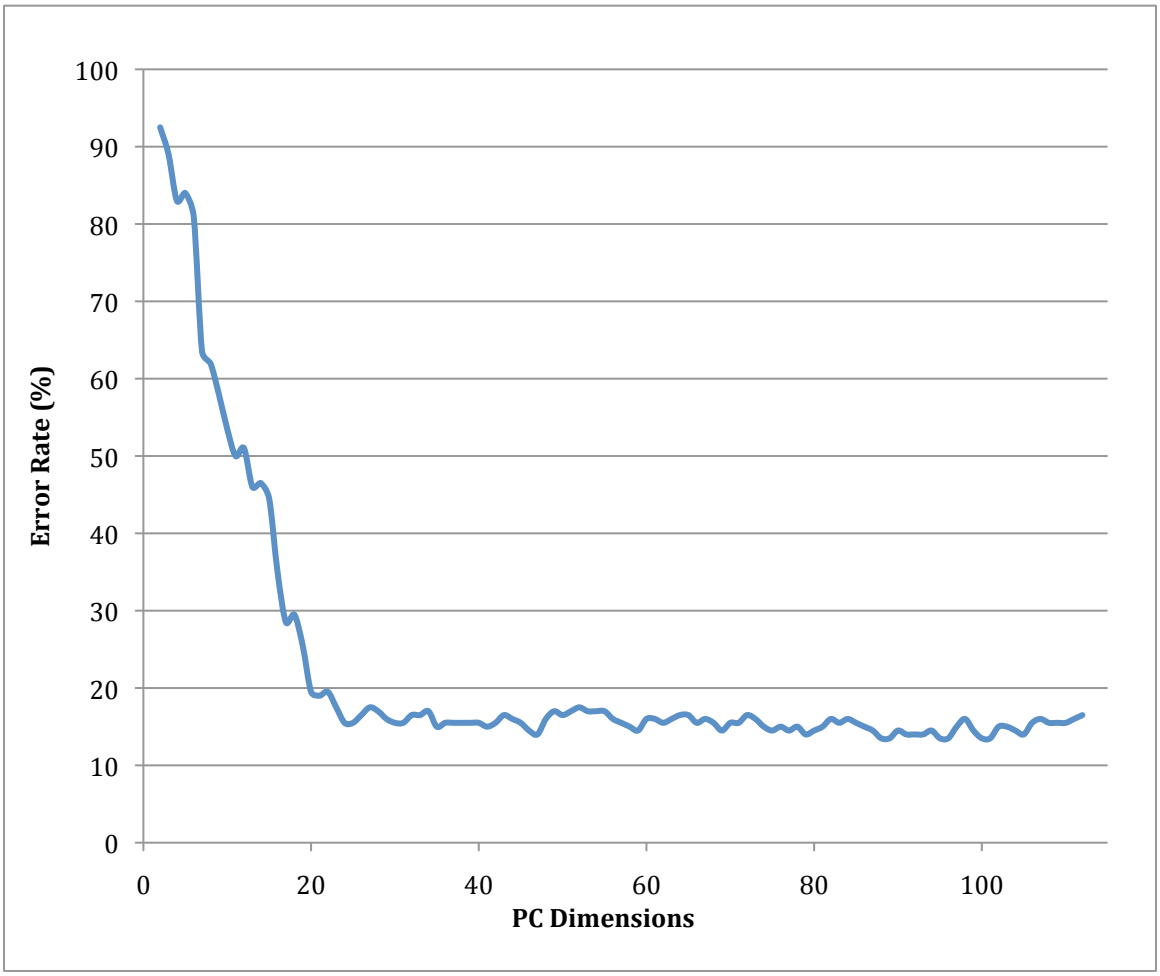


Figure 247: Graph of the discrimination error rate versus PC dimensions for HOO-CV with PCA reduced CVA for the first set of 20 window normalized (peak height) glass spectra (10 replicates), centered data.

Table 259: Discrimination error rates for HOO-CV with PCA reduced CVA for the first set of 20 window normalized (peak height) glass spectra (10 replicates), autoscaled data. The smallest PC dimension with the minimum error rate is highlighted in yellow.

PCs	Error Rate (%)	PCs	Error Rate (%)	PCs	Error Rate (%)	PCs	Error Rate (%)	PCs	Error Rate (%)
2	93.00	42	15.00	82	13.00	122	14.00	162	32.50
3	90.00	43	15.50	83	12.50	123	12.50	163	35.00
4	81.00	44	15.00	84	13.50	124	13.50	164	36.50
5	82.00	45	15.50	85	13.50	125	12.00	165	35.00
6	69.00	46	15.00	86	12.00	126	12.50	166	35.50
7	62.50	47	15.50	87	11.00	127	13.00	167	38.00
8	61.00	48	16.00	88	11.00	128	15.00	168	39.50
9	56.00	49	16.50	89	11.50	129	15.50	169	38.50
10	54.00	50	16.00	90	12.00	130	14.50	170	37.50
11	55.00	51	16.50	91	12.00	131	13.50	171	42.50
12	52.00	52	16.50	92	12.00	132	15.00	172	48.50
13	49.00	53	16.00	93	12.00	133	16.50	173	52.00
14	38.00	54	16.50	94	12.00	134	15.50	174	58.00
15	36.00	55	16.00	95	11.50	135	16.50	175	56.00
16	33.00	56	16.00	96	10.00	136	16.00	176	57.50
17	33.00	57	15.50	97	10.50	137	14.50	177	62.00
18	30.00	58	15.00	98	11.00	138	16.50	178	66.50
19	25.50	59	15.00	99	12.00	139	17.00	179	67.50
20	21.50	60	16.00	100	12.00	140	17.50	180	78.50
21	21.00	61	15.00	101	13.00	141	17.50	181	78.50
22	18.50	62	15.50	102	12.50	142	19.50	182	77.50
23	16.50	63	15.50	103	13.00	143	19.00	183	84.50
24	16.50	64	16.00	104	13.50	144	18.00	184	88.50
25	15.00	65	14.00	105	13.00	145	19.50	185	87.50
26	15.00	66	15.00	106	13.00	146	20.50	186	75.50
27	16.50	67	12.00	107	14.00	147	21.00	187	84.00
28	18.50	68	13.00	108	13.50	148	19.50	188	90.00
29	17.00	69	14.00	109	13.00	149	18.50	189	88.50
30	17.00	70	13.00	110	13.50	150	17.00	190	93.00
31	18.00	71	12.50	111	12.00	151	19.50	191	96.50
32	17.00	72	13.00	112	13.00	152	20.00	192	96.00
33	17.50	73	13.00	113	13.00	153	20.50	193	97.50
34	19.50	74	13.00	114	11.50	154	21.50	194	98.50
35	18.50	75	12.00	115	12.00	155	20.50	195	98.00
36	15.50	76	11.50	116	12.50	156	22.00	196	97.50
37	16.00	77	11.00	117	13.50	157	24.50	197	95.50
38	15.50	78	13.00	118	15.00	158	26.50	198	95.50

39	15.50	79	13.50	119	14.50	159	27.50	199	90.00
40	15.50	80	12.00	120	13.50	160	30.50		
41	16.50	81	12.50	121	13.50	161	32.50		

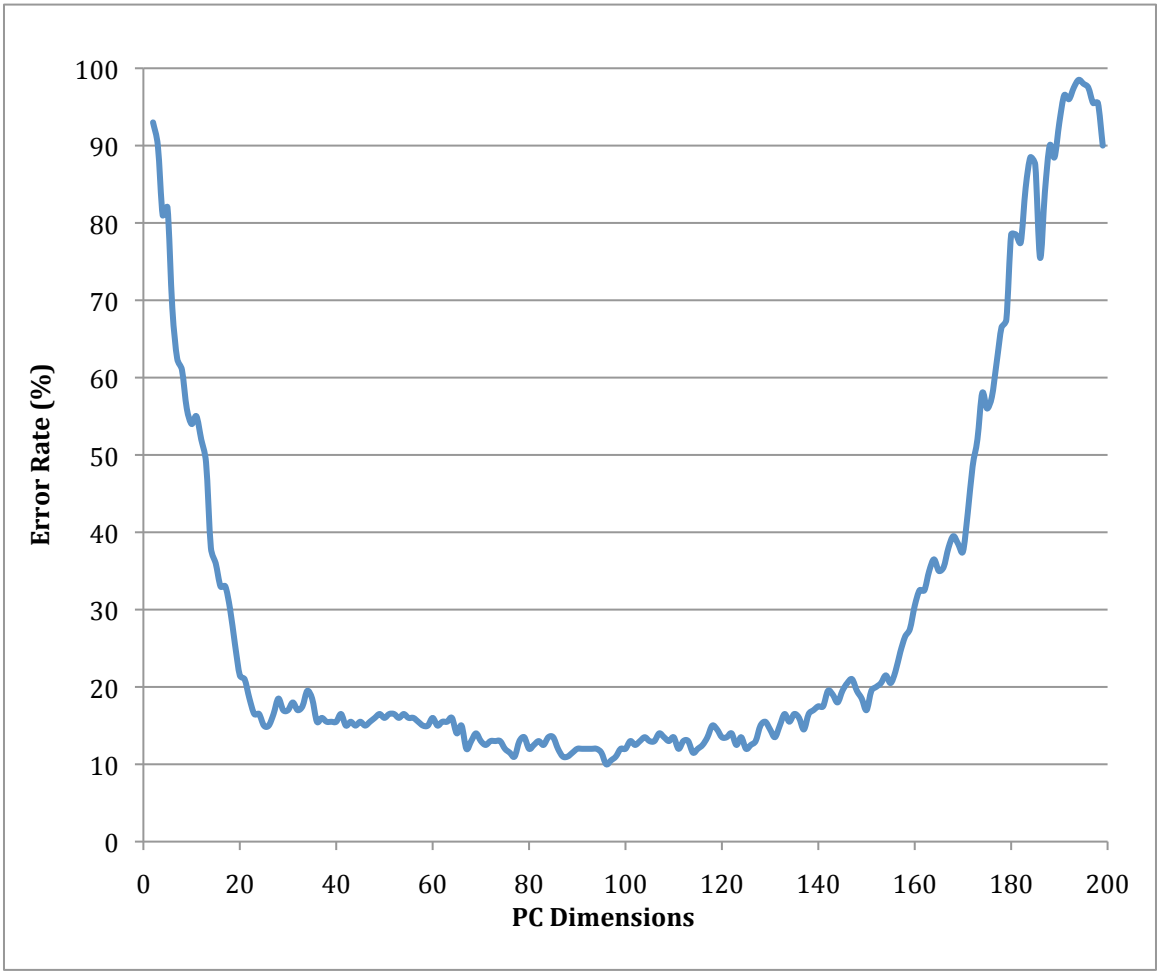


Figure 248: Graph of the discrimination error rate versus PC dimensions for HOO-CV with PCA reduced CVA for the first set of 20 window normalized (peak height) glass spectra (10 replicates), autoscaled data.

First Set, Normalized (Peak Height) – Container Discrimination

Table 260: Discrimination error rates for HOO-CV with PCA reduced CVA for the first set of 10 container normalized (peak height) glass spectra (10 replicates), no data pretreatment. The smallest PC dimension with the minimum error rate is highlighted in yellow.

PCs	Error Rate (%)	PCs	Error Rate (%)	PCs	Error Rate (%)	PCs	Error Rate (%)	PCs	Error Rate (%)
2	80.00	20	17.00	38	13.00	56	16.00	74	22.00
3	76.00	21	16.00	39	14.00	57	17.00	75	21.00
4	69.00	22	18.00	40	13.00	58	16.00	76	20.00
5	65.00	23	20.00	41	11.00	59	15.00	77	26.00
6	58.00	24	14.00	42	12.00	60	16.00	78	29.00
7	56.00	25	16.00	43	11.00	61	18.00	79	29.00
8	54.00	26	17.00	44	11.00	62	16.00	80	30.00
9	47.00	27	13.00	45	11.00	63	17.00	81	31.00
10	42.00	28	11.00	46	14.00	64	17.00	82	29.00
11	46.00	29	12.00	47	15.00	65	19.00	83	23.00
12	43.00	30	11.00	48	15.00	66	14.00	84	27.00
13	41.00	31	13.00	49	16.00	67	18.00	85	30.00
14	40.00	32	13.00	50	15.00	68	18.00	86	39.00
15	37.00	33	13.00	51	15.00	69	18.00	87	44.00
16	34.00	34	11.00	52	13.00	70	19.00	88	52.00
17	32.00	35	12.00	53	14.00	71	19.00	89	52.00
18	32.00	36	13.00	54	12.00	72	19.00	90	43.00
19	25.00	37	14.00	55	16.00	73	20.00		

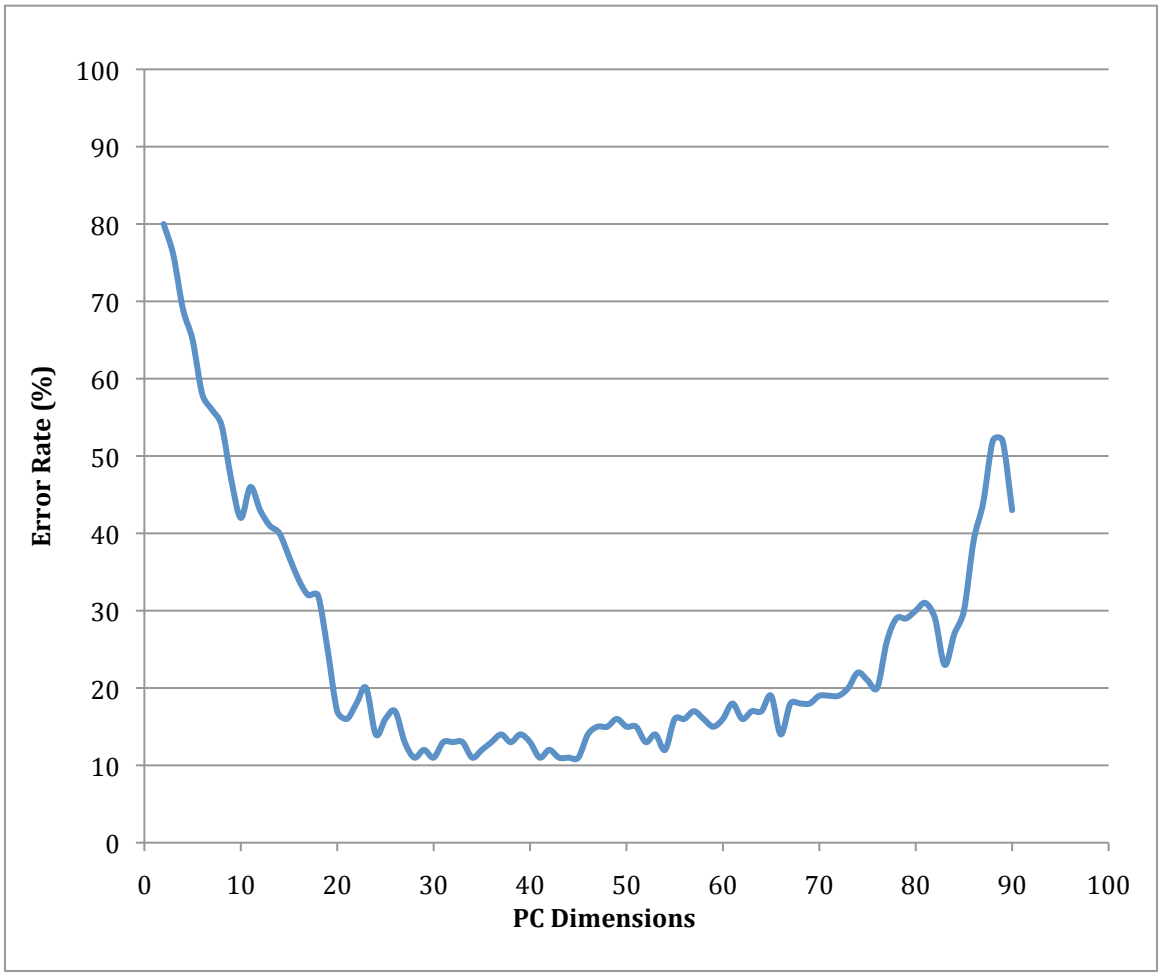


Figure 249: Graph of the discrimination error rate versus PC dimensions for HOO-CV with PCA reduced CVA for the first set of 10 container normalized (peak height) glass spectra (10 replicates), no data pretreatment.

Table 261: Discrimination error rates for HOO-CV with PCA reduced CVA for the first set of 10 container normalized (peak height) glass spectra (10 replicates), centered data. The smallest PC dimension with the minimum error rate is highlighted in yellow.

PCs	Error Rate (%)	PCs	Error Rate (%)	PCs	Error Rate (%)	PCs	Error Rate (%)	PCs	Error Rate (%)
2	83.00	20	17.00	38	14.00	56	16.00	74	23.00
3	70.00	21	16.00	39	13.00	57	16.00	75	24.00
4	63.00	22	18.00	40	14.00	58	17.00	76	22.00
5	57.00	23	20.00	41	12.00	59	17.00	77	26.00
6	59.00	24	14.00	42	12.00	60	16.00	78	29.00
7	53.00	25	18.00	43	13.00	61	16.00	79	26.00
8	52.00	26	17.00	44	11.00	62	15.00	80	28.00
9	53.00	27	15.00	45	11.00	63	18.00	81	29.00
10	40.00	28	13.00	46	15.00	64	17.00	82	30.00
11	46.00	29	13.00	47	16.00	65	17.00	83	25.00
12	43.00	30	14.00	48	16.00	66	18.00	84	27.00
13	42.00	31	12.00	49	17.00	67	19.00	85	30.00
14	40.00	32	13.00	50	15.00	68	22.00	86	37.00
15	37.00	33	13.00	51	12.00	69	23.00	87	46.00
16	35.00	34	10.00	52	14.00	70	17.00	88	35.00
17	33.00	35	12.00	53	15.00	71	19.00	89	54.00
18	33.00	36	13.00	54	14.00	72	16.00		
19	24.00	37	14.00	55	15.00	73	19.00		

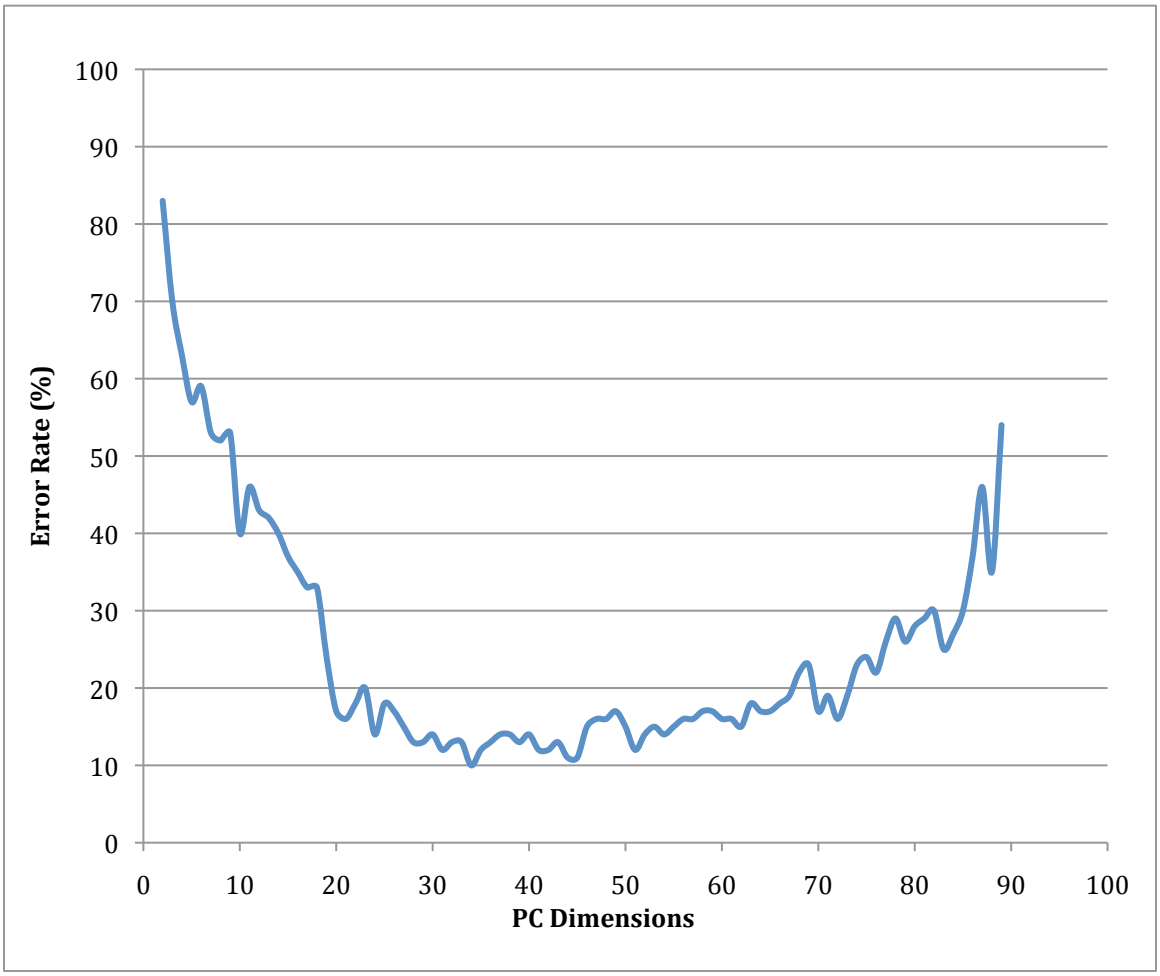


Figure 250: Graph of the discrimination error rate versus PC dimensions for HOO-CV with PCA reduced CVA for the first set of 10 container normalized (peak height) glass spectra (10 replicates), centered data.

Table 262: Discrimination error rates for HOO-CV with PCA reduced CVA for the first set of 10 container normalized (peak height) glass spectra (10 replicates), autoscaled data. The smallest PC dimension with the minimum error rate is highlighted in yellow.

PCs	Error Rate (%)	PCs	Error Rate (%)	PCs	Error Rate (%)	PCs	Error Rate (%)	PCs	Error Rate (%)
2	85.00	22	12.00	42	14.00	62	19.00	82	29.00
3	69.00	23	11.00	43	13.00	63	17.00	83	27.00
4	66.00	24	11.00	44	14.00	64	15.00	84	24.00
5	53.00	25	12.00	45	14.00	65	18.00	85	32.00
6	55.00	26	9.00	46	15.00	66	19.00	86	29.00
7	54.00	27	10.00	47	15.00	67	20.00	87	37.00
8	55.00	28	9.00	48	15.00	68	21.00	88	33.00
9	47.00	29	11.00	49	12.00	69	23.00	89	40.00
10	43.00	30	10.00	50	12.00	70	23.00	90	59.00
11	49.00	31	10.00	51	12.00	71	24.00	91	83.00
12	44.00	32	11.00	52	12.00	72	27.00	92	81.00
13	39.00	33	12.00	53	11.00	73	22.00	93	80.00
14	39.00	34	10.00	54	12.00	74	22.00	94	88.00
15	33.00	35	10.00	55	11.00	75	25.00	95	87.00
16	33.00	36	13.00	56	11.00	76	25.00	96	93.00
17	35.00	37	13.00	57	11.00	77	23.00	97	91.00
18	32.00	38	13.00	58	12.00	78	21.00	98	88.00
19	13.00	39	13.00	59	15.00	79	23.00	99	81.00
20	13.00	40	14.00	60	17.00	80	27.00		
21	11.00	41	17.00	61	17.00	81	28.00		

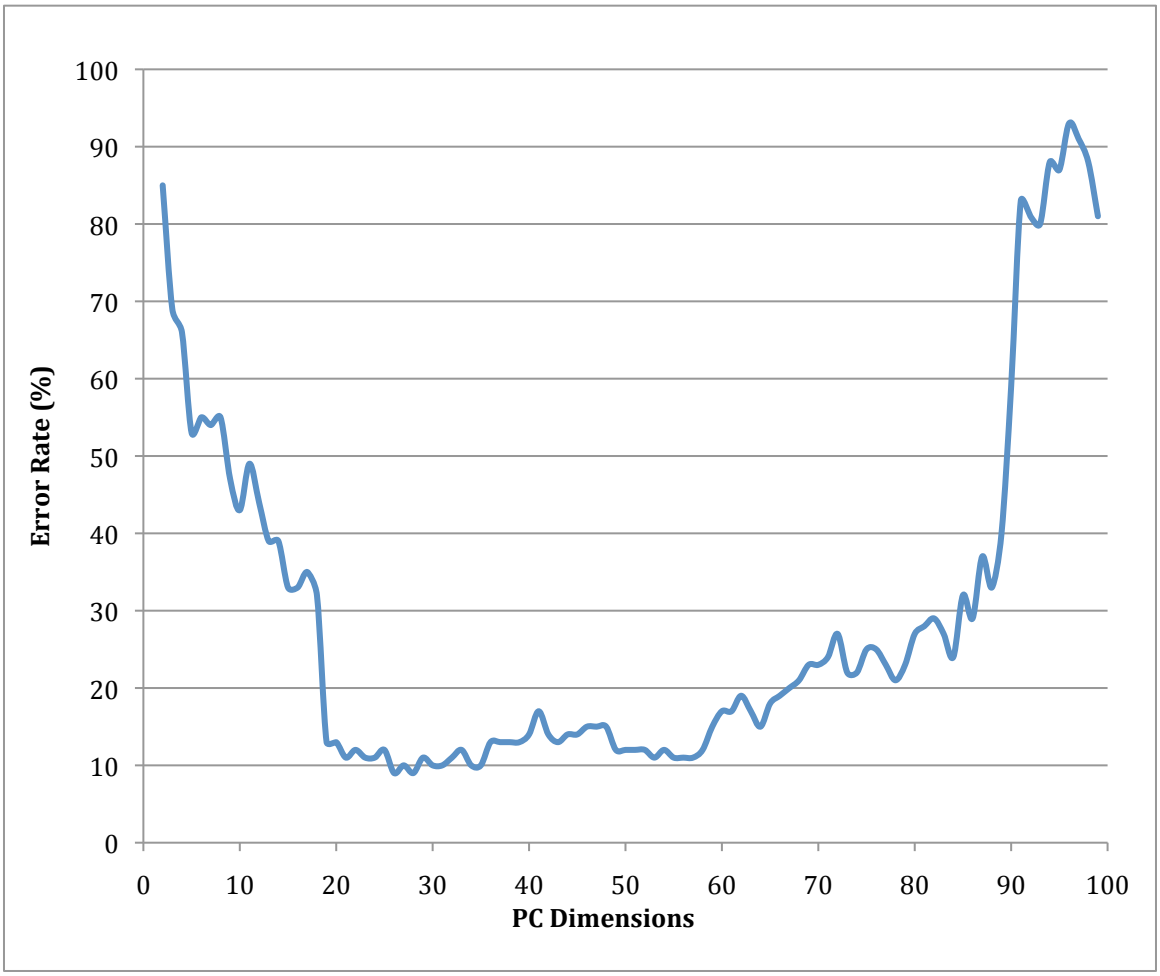


Figure 251: Graph of the discrimination error rate versus PC dimensions for HOO-CV with PCA reduced CVA for the first set of 10 container normalized (peak height) glass spectra (10 replicates), autoscaled data.

First Set, Normalized (Peak Height) – Float Classification

Table 263: Float classification error rates for HOO-CV with PCA reduced CVA for the first set of 20 window normalized (peak height) glass spectra (10 replicates), no data pretreatment. The smallest PC dimension with the minimum error rate is highlighted in yellow.

PCs	Error Rate (%)	PCs	Error Rate (%)	PCs	Error Rate (%)	PCs	Error Rate (%)	PCs	Error Rate (%)
2	41.00	25	20.00	48	23.50	71	20.00	94	24.00
3	37.50	26	21.00	49	25.00	72	20.50	95	26.00
4	33.50	27	22.50	50	23.50	73	20.50	96	26.00
5	33.50	28	21.50	51	23.50	74	21.00	97	26.00
6	31.50	29	22.00	52	24.00	75	20.50	98	25.50
7	31.00	30	22.00	53	24.00	76	20.50	99	26.00
8	31.00	31	22.50	54	24.50	77	21.00	100	25.50
9	26.50	32	20.00	55	24.50	78	20.50	101	27.00
10	23.50	33	19.00	56	24.50	79	21.00	102	27.50
11	23.50	34	19.00	57	25.00	80	21.00	103	27.50
12	24.50	35	20.50	58	27.00	81	21.00	104	27.50
13	24.50	36	22.00	59	27.00	82	21.50	105	28.50
14	21.50	37	22.50	60	25.00	83	21.00	106	28.00
15	20.50	38	21.00	61	24.00	84	22.00	107	28.50
16	21.00	39	22.50	62	20.00	85	23.50	108	28.00
17	21.00	40	20.00	63	20.50	86	23.50	109	31.00
18	21.00	41	20.00	64	21.00	87	22.50	110	30.50
19	21.00	42	21.00	65	22.00	88	23.00	111	30.50
20	21.00	43	21.00	66	17.50	89	23.50	112	29.50
21	20.50	44	22.00	67	20.50	90	23.00	113	29.00
22	20.50	45	21.00	68	21.00	91	23.50		
23	20.00	46	23.00	69	19.50	92	23.00		
24	19.50	47	23.00	70	20.00	93	23.50		

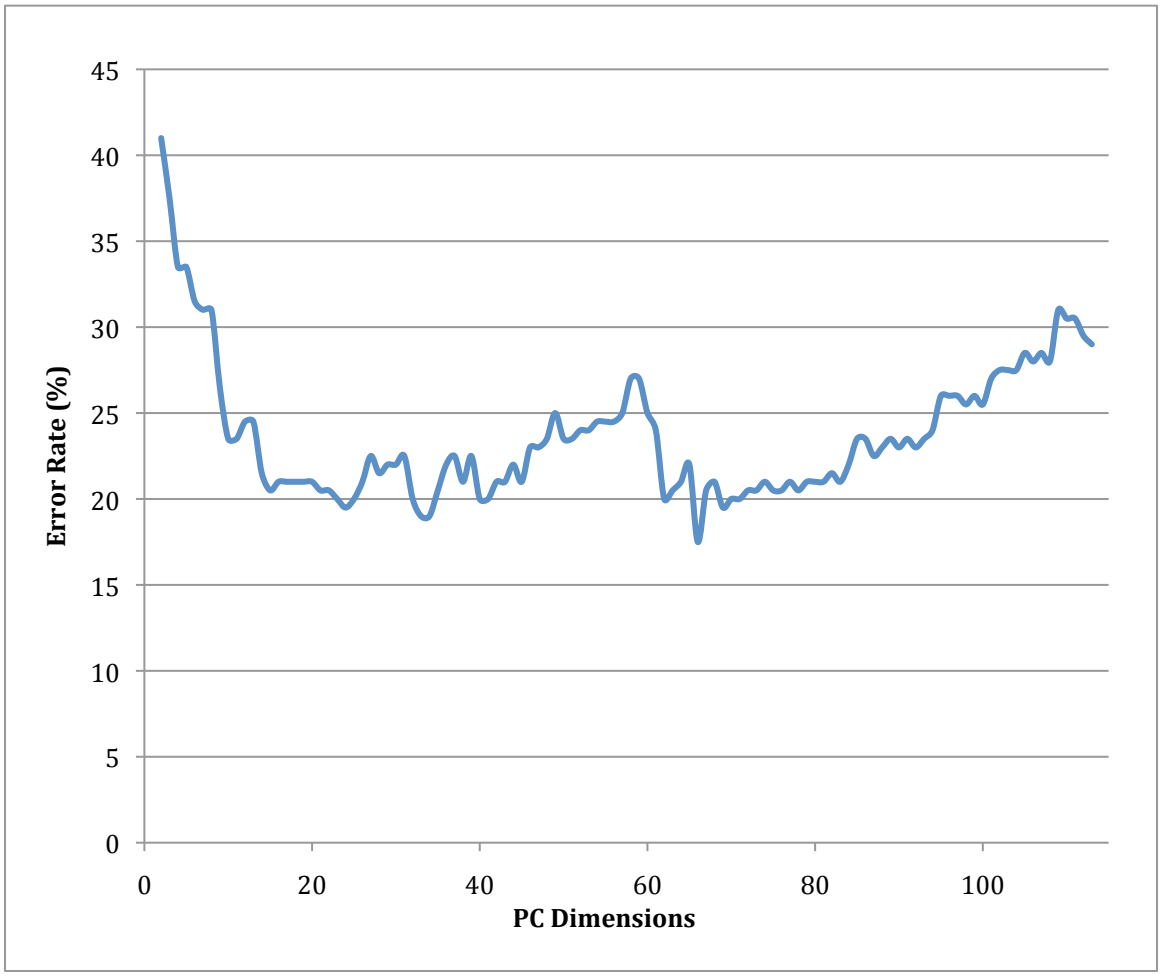


Figure 252: Graph of the float classification error rate versus PC dimensions for HOO-CV with PCA reduced CVA for the first set of 20 window normalized (peak height) glass spectra (10 replicates), no data pretreatment.

Table 264: Float classification error rates for HOO-CV with PCA reduced CVA for the first set of 20 window normalized (peak height) glass spectra (10 replicates), centered data. The smallest PC dimension with the minimum error rate is highlighted in yellow.

PCs	Error Rate (%)	PCs	Error Rate (%)	PCs	Error Rate (%)	PCs	Error Rate (%)	PCs	Error Rate (%)
2	43.50	25	19.00	48	23.50	71	20.50	94	24.00
3	33.50	26	21.50	49	24.50	72	21.00	95	25.50
4	33.50	27	22.50	50	23.50	73	20.50	96	24.00
5	32.50	28	21.50	51	23.50	74	20.00	97	25.00
6	33.00	29	21.50	52	24.50	75	19.50	98	25.50
7	34.50	30	22.50	53	23.50	76	20.00	99	26.00
8	23.50	31	22.00	54	24.50	77	20.00	100	26.50
9	26.00	32	20.00	55	24.50	78	21.00	101	27.00
10	23.50	33	19.00	56	24.00	79	20.50	102	27.50
11	22.50	34	19.50	57	25.00	80	21.50	103	29.00
12	23.50	35	20.00	58	26.00	81	21.50	104	29.00
13	24.00	36	22.00	59	25.50	82	21.00	105	29.50
14	21.50	37	22.50	60	25.00	83	20.50	106	28.50
15	19.50	38	21.00	61	22.00	84	22.00	107	28.50
16	21.50	39	21.00	62	19.00	85	22.50	108	28.50
17	21.00	40	20.50	63	19.50	86	21.50	109	30.00
18	21.00	41	20.50	64	21.50	87	22.50	110	30.50
19	21.00	42	21.50	65	21.00	88	23.00	111	29.00
20	21.00	43	21.00	66	18.00	89	23.00	112	30.00
21	20.50	44	22.00	67	20.50	90	23.50	113	30.00
22	20.00	45	21.00	68	20.00	91	24.00		
23	19.50	46	23.00	69	20.00	92	23.00		
24	19.50	47	22.50	70	20.50	93	24.00		

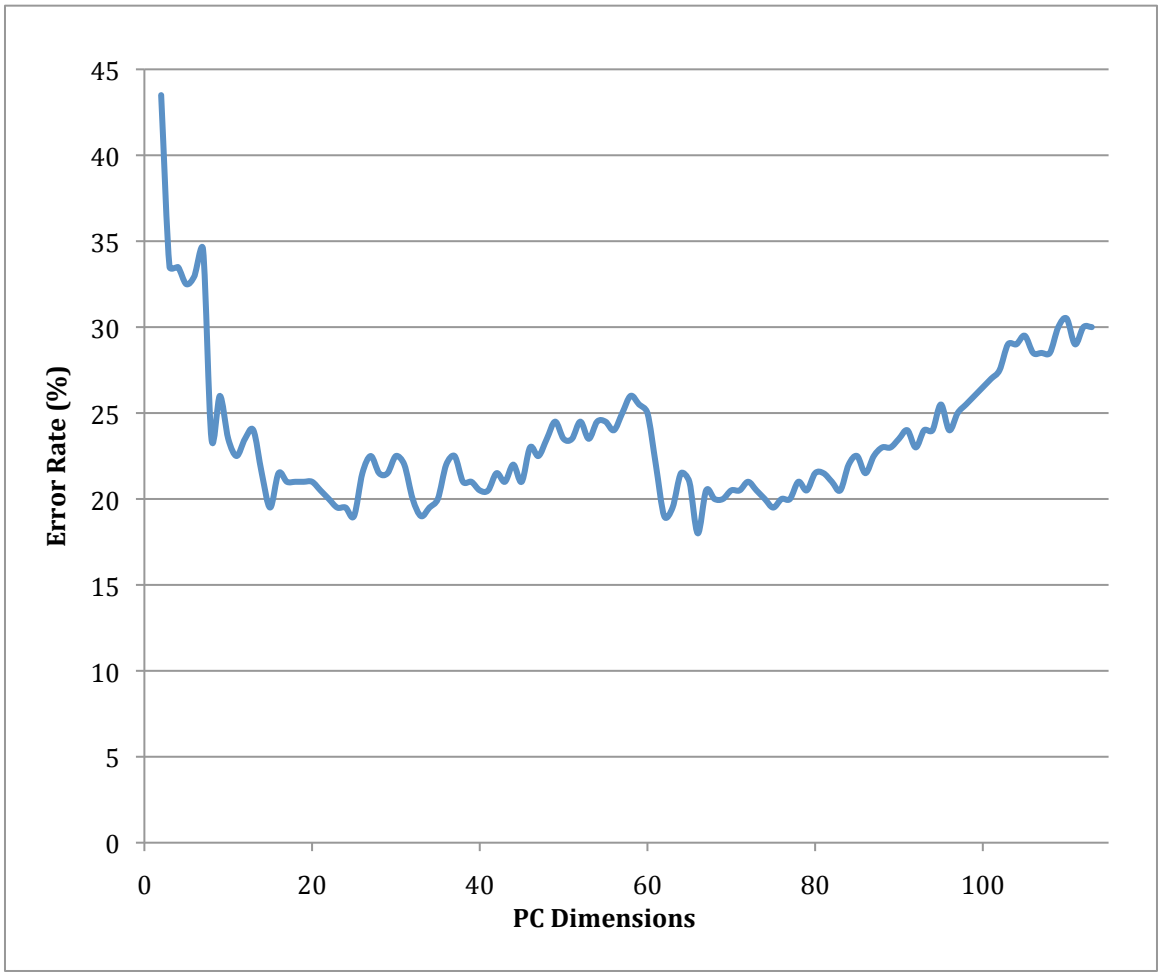


Figure 253: Graph of the float classification error rate versus PC dimensions for HOO-CV with PCA reduced CVA for the first set of 20 window normalized (peak height) glass spectra (10 replicates), centered data.

Table 265: Float classification error rates for HOO-CV with PCA reduced CVA for the first set of 20 window normalized (peak height) glass spectra (10 replicates), autoscaled data. The smallest PC dimension with the minimum error rate is highlighted in yellow.

PCs	Error Rate (%)	PCs	Error Rate (%)	PCs	Error Rate (%)	PCs	Error Rate (%)	PCs	Error Rate (%)
2	52.00	42	20.00	82	23.00	122	26.00	162	29.00
3	37.00	43	19.50	83	23.50	123	25.50	163	29.00
4	32.00	44	20.00	84	24.00	124	27.00	164	30.50
5	32.00	45	21.00	85	23.50	125	26.00	165	29.50
6	32.00	46	20.50	86	24.50	126	26.50	166	30.00
7	32.00	47	20.00	87	25.00	127	27.00	167	30.00
8	31.50	48	21.50	88	26.00	128	27.00	168	30.50
9	29.00	49	20.50	89	27.00	129	25.50	169	32.50
10	23.50	50	20.50	90	27.00	130	25.00	170	34.50
11	25.00	51	20.50	91	28.00	131	26.50	171	35.50
12	26.50	52	21.50	92	24.50	132	27.00	172	36.00
13	26.00	53	22.00	93	26.00	133	26.00	173	35.50
14	28.00	54	22.00	94	26.00	134	27.00	174	35.50
15	17.50	55	22.00	95	26.00	135	26.00	175	34.00
16	18.50	56	19.50	96	26.00	136	25.00	176	35.50
17	21.50	57	21.50	97	27.00	137	25.00	177	36.00
18	22.00	58	22.00	98	25.50	138	25.00	178	35.50
19	20.50	59	22.00	99	25.50	139	26.00	179	38.00
20	18.50	60	22.00	100	26.00	140	28.00	180	35.00
21	19.50	61	22.50	101	26.50	141	28.00	181	36.00
22	19.50	62	22.00	102	24.50	142	28.00	182	37.50
23	22.00	63	20.50	103	24.00	143	28.00	183	37.50
24	21.50	64	20.00	104	24.00	144	27.00	184	36.00
25	21.00	65	21.00	105	24.50	145	23.50	185	39.00
26	22.00	66	21.00	106	26.00	146	25.00	186	37.50
27	21.50	67	19.00	107	21.50	147	26.00	187	40.00
28	22.00	68	20.00	108	23.00	148	25.00	188	41.00
29	21.00	69	19.50	109	24.00	149	22.50	189	43.00
30	21.50	70	20.50	110	25.50	150	23.50	190	45.50
31	20.00	71	19.50	111	25.00	151	24.50	191	46.50
32	19.50	72	20.50	112	26.00	152	23.50	192	45.00
33	19.50	73	20.50	113	22.00	153	24.00	193	47.50
34	19.50	74	21.00	114	22.00	154	22.50	194	48.50
35	19.50	75	21.50	115	23.00	155	22.00	195	46.50
36	18.50	76	21.50	116	24.00	156	23.50	196	49.00
37	19.00	77	20.50	117	24.00	157	23.50	197	50.50
38	19.50	78	20.50	118	25.00	158	26.50	198	50.50

39	20.00	79	21.00	119	24.00	159	27.50	199	45.00
40	20.00	80	23.00	120	25.50	160	28.00		
41	20.00	81	23.00	121	26.00	161	28.50		

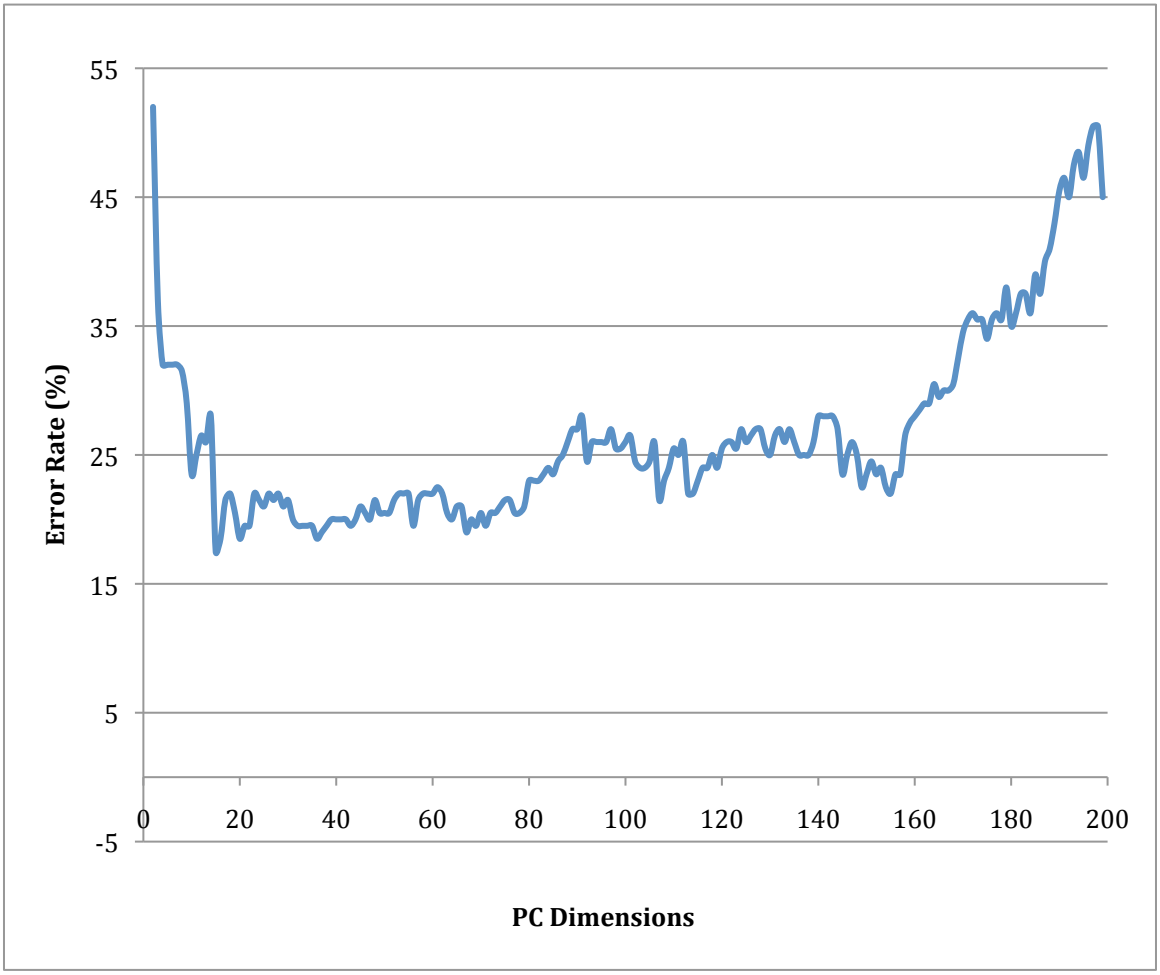


Figure 254: Graph of the float classification error rate versus PC dimensions for HOO-CV with PCA reduced CVA for the first set of 20 window normalized (peak height) glass spectra (10 replicates), autoscaled data.

First Set, Normalized (Peak Height) – Tempered Classification

Table 266: Tempered classification error rates for HOO-CV with PCA reduced CVA for the first set of 20 window normalized (peak height) glass spectra (10 replicates), no data pretreatment. The smallest PC dimension with the minimum error rate is highlighted in yellow.

PCs	Error Rate (%)	PCs	Error Rate (%)	PCs	Error Rate (%)	PCs	Error Rate (%)	PCs	Error Rate (%)
2	29.50	25	20.50	48	21.00	71	17.00	94	20.00
3	29.50	26	21.00	49	20.50	72	16.00	95	21.00
4	27.50	27	18.50	50	19.50	73	17.00	96	20.50
5	32.00	28	18.00	51	20.50	74	18.00	97	21.00
6	29.00	29	20.00	52	20.00	75	19.50	98	21.00
7	29.50	30	21.50	53	19.50	76	19.50	99	22.00
8	28.00	31	19.50	54	20.00	77	19.00	100	22.00
9	32.50	32	18.50	55	20.00	78	19.00	101	23.50
10	25.50	33	20.00	56	20.00	79	17.50	102	24.50
11	28.00	34	19.50	57	17.50	80	19.00	103	24.50
12	28.50	35	19.50	58	17.50	81	18.50	104	24.00
13	28.50	36	17.50	59	16.50	82	17.50	105	22.50
14	28.50	37	17.50	60	18.00	83	18.00	106	24.50
15	25.00	38	18.00	61	18.50	84	18.50	107	25.50
16	26.50	39	19.00	62	18.50	85	19.00	108	25.00
17	26.00	40	19.50	63	17.50	86	20.00	109	25.50
18	24.00	41	21.50	64	17.50	87	21.50	110	23.00
19	26.00	42	20.50	65	18.00	88	20.00	111	24.50
20	19.50	43	17.50	66	18.50	89	19.00	112	25.50
21	18.00	44	17.50	67	16.50	90	20.50	113	24.50
22	19.50	45	19.50	68	18.00	91	21.50		
23	17.50	46	19.50	69	18.00	92	20.00		
24	19.50	47	20.00	70	18.50	93	20.50		

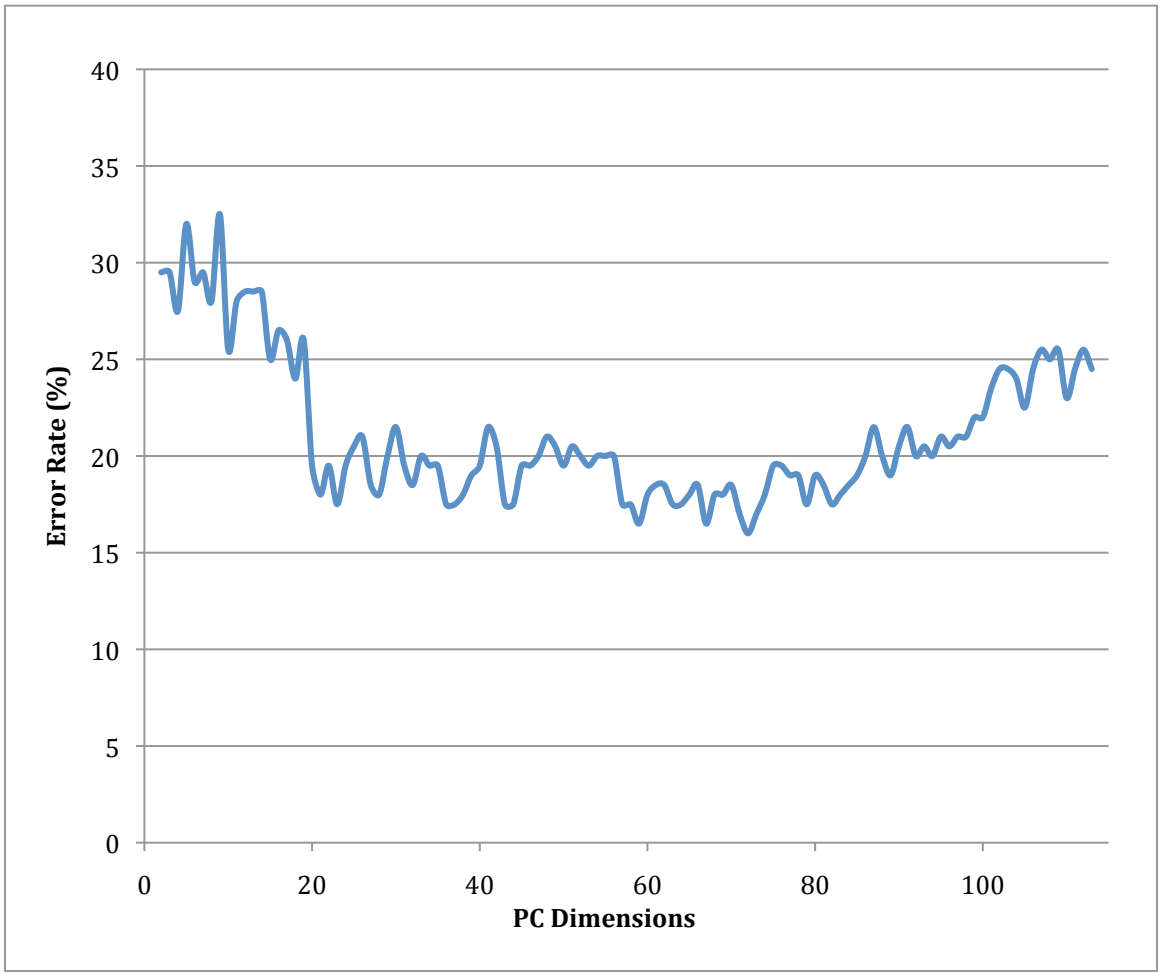


Figure 255: Graph of the tempered classification error rate versus PC dimensions for HOO-CV with PCA reduced CVA for the first set of 20 window normalized (peak height) glass spectra (10 replicates), no data pretreatment.

Table 267: Tempered classification error rates for HOO-CV with PCA reduced CVA for the first set of 20 window normalized (peak height) glass spectra (10 replicates), centered data. The smallest PC dimension with the minimum error rate is highlighted in yellow.

PCs	Error Rate (%)	PCs	Error Rate (%)	PCs	Error Rate (%)	PCs	Error Rate (%)	PCs	Error Rate (%)
2	29.50	25	21.00	48	20.00	71	18.50	94	19.50
3	27.50	26	21.00	49	20.50	72	16.50	95	21.00
4	28.00	27	18.50	50	20.00	73	17.00	96	21.50
5	29.00	28	18.00	51	20.50	74	17.00	97	20.50
6	29.50	29	19.50	52	21.00	75	19.50	98	21.00
7	29.00	30	20.50	53	20.00	76	20.50	99	21.50
8	29.00	31	19.50	54	20.50	77	20.50	100	24.00
9	31.00	32	18.50	55	19.00	78	19.50	101	24.00
10	25.00	33	19.50	56	21.50	79	19.00	102	25.00
11	28.50	34	19.50	57	18.00	80	18.00	103	24.50
12	28.50	35	19.00	58	17.00	81	18.00	104	23.50
13	28.00	36	18.00	59	17.00	82	18.00	105	24.00
14	28.50	37	17.50	60	18.50	83	17.50	106	24.00
15	28.00	38	17.50	61	18.00	84	19.00	107	24.50
16	27.00	39	18.50	62	18.50	85	19.00	108	25.00
17	26.00	40	18.50	63	18.50	86	20.00	109	25.50
18	24.00	41	21.00	64	18.50	87	17.00	110	26.00
19	26.00	42	21.00	65	19.00	88	18.50	111	26.00
20	19.50	43	17.00	66	18.50	89	21.50	112	23.00
21	18.00	44	18.00	67	17.50	90	19.50	113	23.50
22	19.00	45	18.50	68	17.50	91	21.00		
23	18.50	46	18.50	69	18.50	92	19.50		
24	19.50	47	20.00	70	18.50	93	19.50		

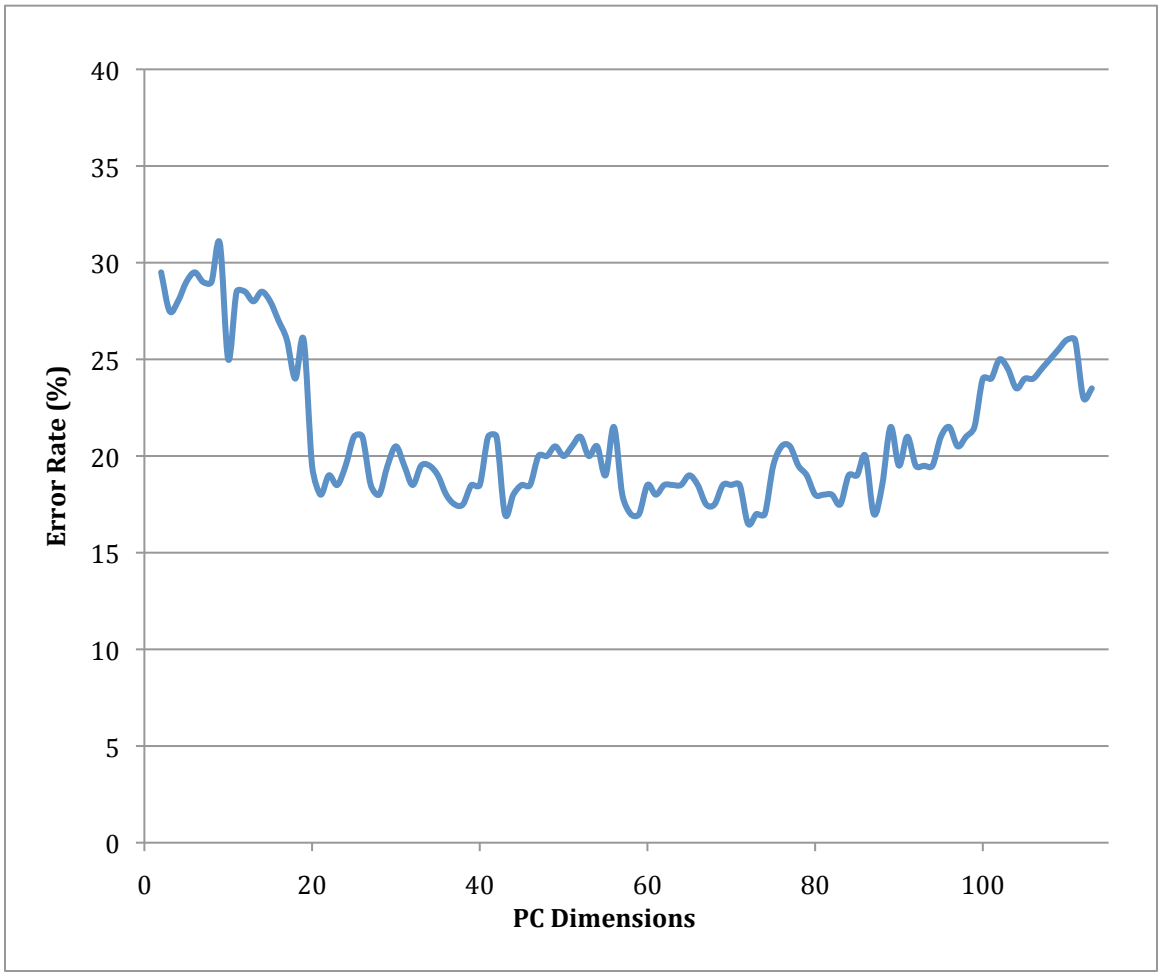


Figure 256: Graph of the tempered classification error rate versus PC dimensions for HOO-CV with PCA reduced CVA for the first set of 20 window normalized (peak height) glass spectra (10 replicates), centered data.

Table 268: Tempered classification error rates for HOO-CV with PCA reduced CVA for the first set of 20 window normalized (peak height) glass spectra (10 replicates), autoscaled data. The smallest PC dimension with the minimum error rate is highlighted in yellow.

PCs	Error Rate (%)	PCs	Error Rate (%)	PCs	Error Rate (%)	PCs	Error Rate (%)	PCs	Error Rate (%)
2	33.50	42	18.50	82	20.00	122	22.00	162	19.50
3	31.00	43	18.00	83	23.00	123	23.00	163	21.00
4	28.50	44	18.00	84	24.00	124	24.00	164	21.00
5	29.00	45	18.00	85	23.00	125	21.00	165	21.00
6	31.00	46	18.00	86	24.50	126	21.50	166	18.00
7	30.50	47	18.50	87	23.50	127	22.00	167	19.00
8	29.50	48	19.00	88	21.50	128	22.00	168	20.50
9	30.00	49	17.00	89	22.00	129	21.00	169	19.00
10	26.00	50	17.50	90	22.50	130	19.50	170	20.00
11	27.50	51	17.00	91	23.50	131	21.00	171	21.00
12	27.50	52	17.50	92	21.00	132	21.50	172	22.50
13	28.00	53	17.00	93	22.00	133	23.00	173	21.50
14	27.50	54	17.50	94	19.00	134	22.50	174	22.00
15	26.00	55	18.00	95	20.00	135	25.00	175	22.50
16	24.00	56	19.50	96	21.00	136	25.50	176	24.50
17	23.50	57	18.50	97	21.00	137	23.00	177	27.50
18	24.00	58	19.00	98	22.50	138	21.50	178	26.50
19	24.00	59	19.50	99	21.50	139	21.50	179	26.50
20	22.50	60	17.00	100	22.00	140	23.00	180	28.50
21	21.50	61	18.00	101	23.00	141	23.50	181	28.00
22	23.50	62	18.00	102	23.50	142	23.00	182	27.50
23	22.00	63	18.50	103	22.50	143	22.50	183	27.00
24	22.50	64	19.00	104	21.50	144	20.00	184	28.00
25	23.00	65	18.50	105	22.00	145	20.50	185	28.50
26	23.00	66	18.50	106	23.00	146	19.50	186	30.00
27	19.00	67	20.00	107	22.00	147	19.50	187	30.50
28	21.00	68	19.00	108	22.00	148	18.50	188	32.50
29	22.50	69	19.00	109	23.00	149	17.50	189	33.00
30	21.00	70	20.00	110	23.00	150	19.00	190	33.50
31	20.00	71	21.00	111	23.00	151	18.50	191	34.50
32	20.50	72	21.50	112	22.50	152	20.00	192	30.50
33	19.50	73	21.50	113	25.50	153	22.00	193	32.50
34	19.50	74	22.00	114	24.00	154	23.50	194	36.50
35	19.00	75	19.50	115	22.00	155	22.00	195	39.00
36	17.00	76	21.50	116	22.50	156	22.00	196	43.00
37	17.00	77	19.50	117	22.50	157	21.00	197	47.50
38	19.00	78	20.00	118	22.50	158	20.50	198	58.00

39	18.00	79	20.00	119	23.50	159	19.50	199	40.00
40	19.00	80	20.50	120	23.00	160	20.00		
41	17.50	81	22.50	121	21.50	161	20.00		

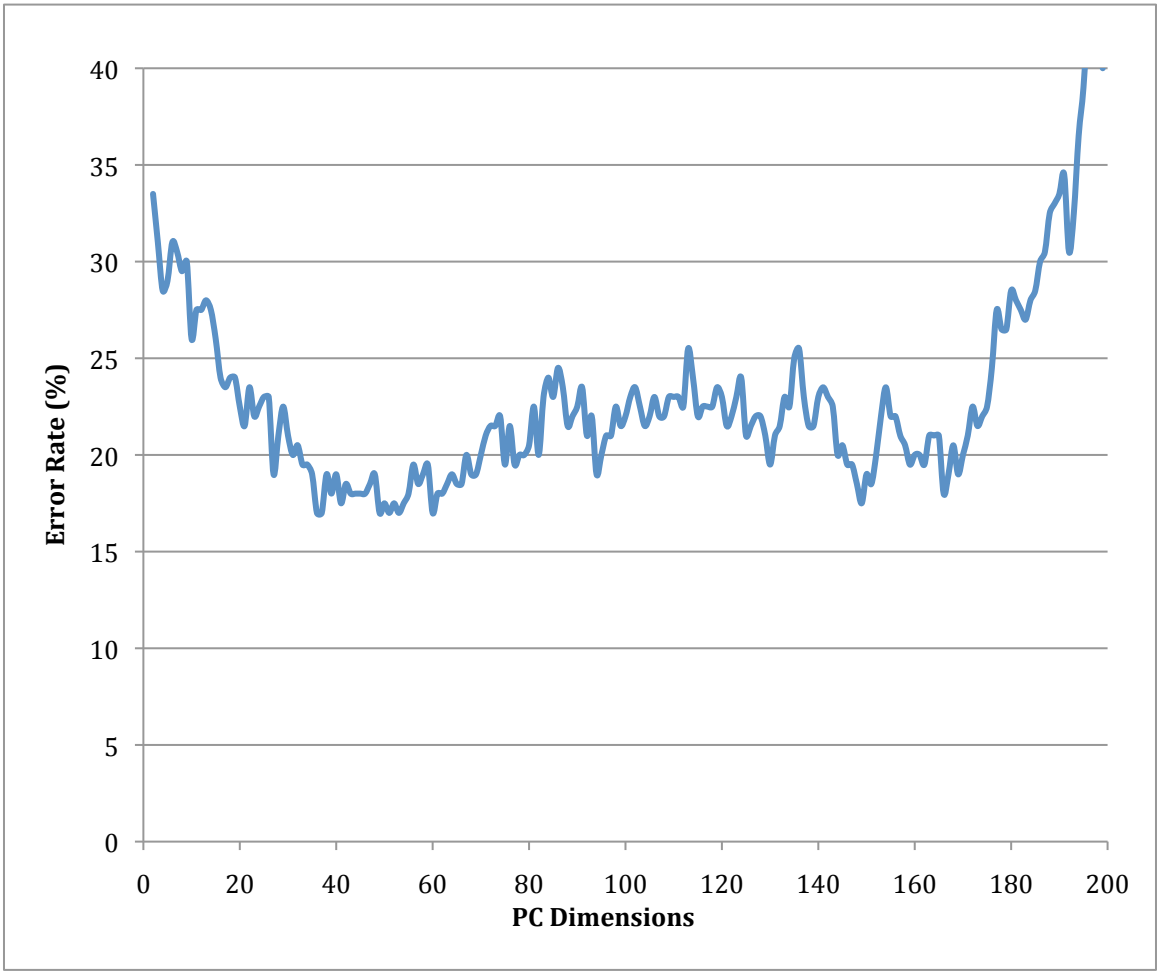


Figure 257: Graph of the tempered classification error rate versus PC dimensions for HOO-CV with PCA reduced CVA for the first set of 20 window normalized (peak height) glass spectra (10 replicates), autoscaled data.

D. HOO-CV PCA-CVA Results for the First Derivative Spectra (5-Point Smoothing)

First Set, First Derivative (5-point smoothing) - Discrimination

Table 269: Discrimination error rates for HOO-CV with PCA reduced CVA for the first set of 30 glass first derivative (5-point smoothing) spectra (10 replicates), no data pretreatment. The smallest PC dimension with the minimum error rate is highlighted in yellow.

PCs	Error Rate (%)	PCs	Error Rate (%)	PCs	Error Rate (%)	PCs	Error Rate (%)	PCs	Error Rate (%)
2	95.33	16	41.67	30	31.67	44	24.67	58	20.00
3	94.33	17	42.67	31	30.33	45	23.00	59	20.33
4	92.67	18	38.67	32	30.00	46	21.00	60	20.00
5	91.67	19	38.00	33	29.33	47	21.00	61	19.33
6	80.67	20	38.00	34	30.00	48	21.33	62	21.33
7	83.67	21	38.00	35	29.33	49	22.33	63	20.33
8	74.67	22	35.67	36	25.33	50	20.67	64	21.67
9	58.33	23	36.00	37	26.33	51	21.33	65	21.33
10	59.00	24	35.00	38	25.67	52	19.00	66	21.00
11	58.00	25	34.00	39	24.33	53	20.33	67	20.00
12	50.00	26	33.00	40	26.00	54	22.00	68	20.67
13	44.33	27	33.00	41	26.00	55	19.33	69	21.00
14	45.33	28	33.00	42	23.67	56	19.33	70	19.67
15	44.33	29	30.33	43	24.00	57	20.67	71	21.00

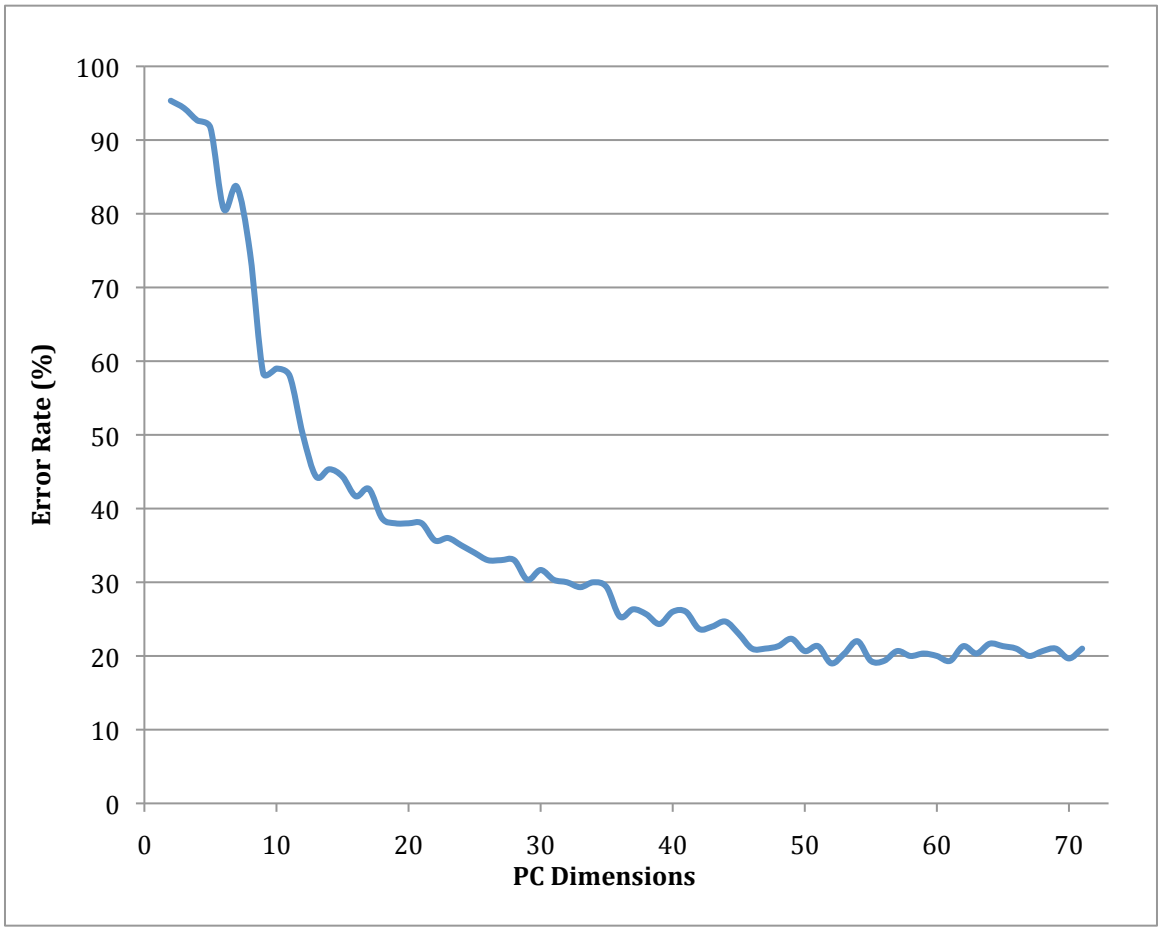


Figure 258: Graph of the discrimination error rate versus PC dimensions for HOO-CV with PCA reduced CVA for the first set of 30 glass first derivative (5-point smoothing) spectra (10 replicates), no data pretreatment.

Table 270: Discrimination error rates for HOO-CV with PCA reduced CVA for the first set of 30 glass first derivative (5-point smoothing) spectra (10 replicates), centered data. The smallest PC dimension with the minimum error rate is highlighted in yellow.

PCs	Error Rate (%)	PCs	Error Rate (%)	PCs	Error Rate (%)	PCs	Error Rate (%)	PCs	Error Rate (%)
2	95.67	16	43.00	30	30.67	44	24.33	58	21.00
3	95.33	17	41.33	31	31.00	45	22.33	59	20.00
4	94.00	18	38.67	32	31.00	46	20.67	60	21.33
5	84.33	19	38.67	33	29.67	47	19.33	61	20.00
6	82.00	20	36.00	34	30.00	48	21.00	62	20.67
7	84.67	21	36.00	35	28.00	49	20.67	63	21.00
8	74.67	22	36.67	36	27.67	50	20.67	64	21.33
9	57.33	23	37.67	37	26.33	51	20.67	65	20.00
10	57.33	24	34.33	38	25.67	52	20.33	66	20.67
11	52.00	25	32.67	39	27.00	53	21.33	67	20.33
12	49.33	26	33.00	40	27.33	54	21.67	68	21.00
13	47.67	27	30.00	41	25.33	55	20.67	69	20.67
14	45.67	28	31.00	42	23.00	56	20.67		
15	45.00	29	30.00	43	24.67	57	20.67		

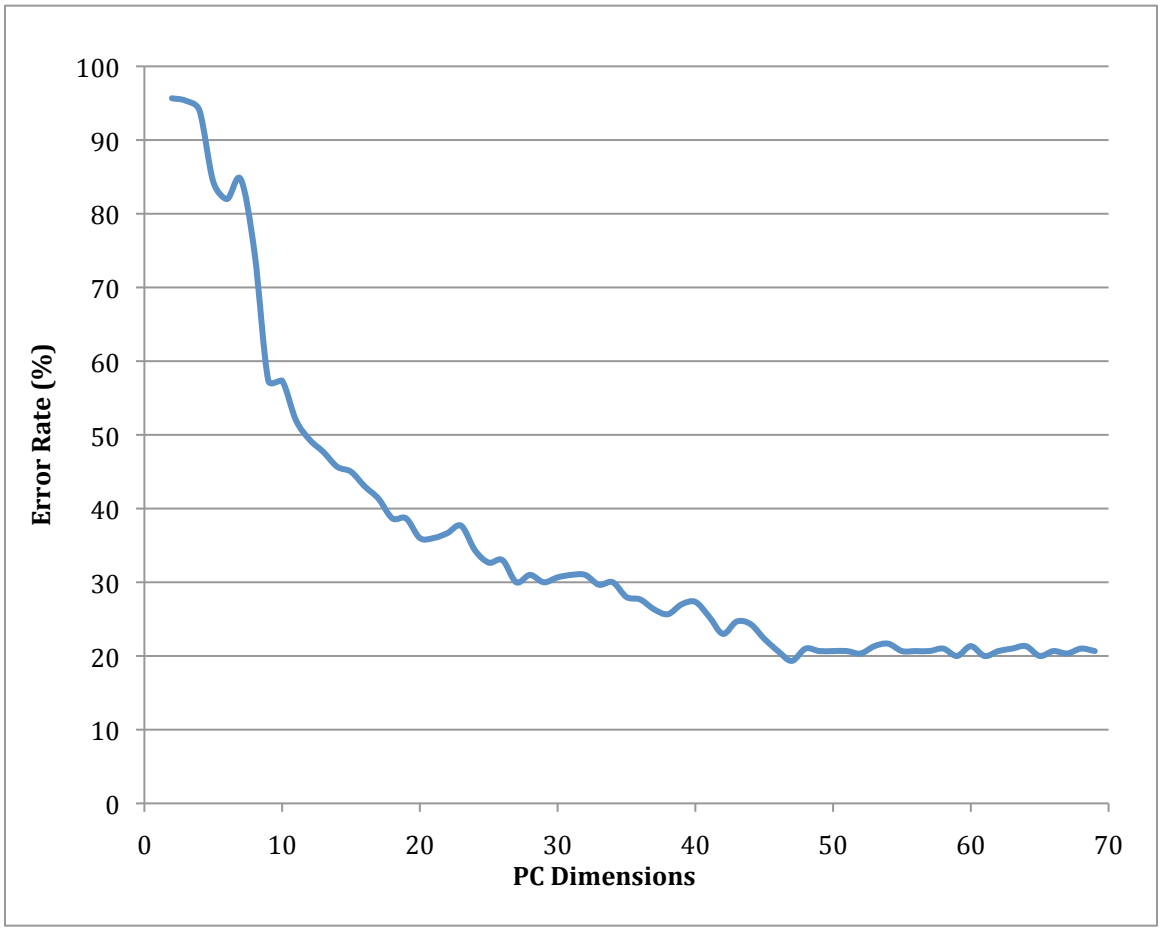


Figure 259: Graph of the discrimination error rate versus PC dimensions for HOO-CV with PCA reduced CVA for the first set of 30 glass first derivative (5-point smoothing) spectra (10 replicates), centered data.

Table 271: Discrimination error rates for HOO-CV with PCA reduced CVA for the first set of 30 glass first derivative (5-point smoothing) spectra (10 replicates), autoscaled data. The smallest PC dimension with the minimum error rate is highlighted in yellow.

PCs	Error Rate (%)	PCs	Error Rate (%)	PCs	Error Rate (%)	PCs	Error Rate (%)	PCs	Error Rate (%)
2	88.33	62	8.67	122	7.67	182	13.00	242	21.00
3	84.33	63	7.67	123	8.00	183	12.33	243	22.00
4	78.00	64	7.33	124	8.00	184	13.00	244	22.67
5	60.33	65	7.00	125	8.33	185	13.33	245	26.67
6	52.67	66	6.33	126	8.00	186	13.33	246	25.67
7	49.33	67	7.00	127	7.33	187	13.33	247	27.33
8	47.00	68	7.33	128	7.67	188	14.00	248	30.67
9	47.00	69	8.00	129	8.33	189	14.00	249	29.00
10	40.33	70	7.67	130	8.33	190	13.67	250	30.33
11	41.00	71	7.33	131	7.67	191	15.00	251	30.33
12	39.33	72	7.33	132	7.33	192	15.00	252	31.67
13	33.67	73	7.00	133	7.33	193	14.00	253	31.67
14	31.33	74	7.00	134	8.00	194	12.67	254	35.00
15	28.00	75	7.00	135	8.33	195	13.33	255	35.33
16	24.67	76	6.67	136	8.33	196	13.33	256	37.33
17	23.67	77	6.67	137	8.00	197	13.33	257	40.33
18	23.33	78	6.00	138	8.33	198	13.33	258	44.33
19	22.00	79	5.67	139	8.33	199	13.00	259	45.00
20	22.67	80	6.33	140	8.67	200	14.00	260	46.33
21	23.33	81	5.33	141	9.00	201	14.67	261	45.00
22	22.00	82	5.00	142	9.33	202	14.33	262	47.00
23	20.33	83	5.00	143	9.00	203	14.33	263	47.67
24	19.67	84	5.33	144	9.33	204	16.00	264	53.33
25	20.67	85	6.00	145	9.33	205	15.33	265	58.67
26	19.67	86	6.33	146	9.67	206	14.00	266	64.67
27	20.00	87	6.33	147	10.33	207	14.33	267	65.67
28	21.00	88	6.33	148	10.33	208	14.00	268	74.00
29	20.33	89	6.00	149	10.67	209	13.67	269	67.67
30	19.00	90	6.00	150	11.00	210	15.33	270	89.00
31	16.00	91	5.33	151	11.00	211	15.00	271	92.67
32	16.33	92	6.33	152	9.67	212	15.00	272	87.67
33	16.33	93	5.33	153	10.33	213	15.33	273	91.67
34	15.67	94	5.33	154	10.67	214	14.00	274	91.67
35	14.33	95	5.67	155	11.00	215	13.33	275	83.00
36	14.00	96	4.67	156	11.67	216	14.33	276	83.33
37	13.00	97	5.33	157	10.67	217	13.67	277	86.00
38	12.67	98	5.67	158	11.00	218	13.67	278	91.67

39	12.67	99	5.67	159	11.00	219	13.33	279	91.33
40	12.33	100	5.67	160	11.00	220	13.33	280	93.67
41	11.67	101	6.00	161	11.33	221	15.00	281	94.00
42	10.67	102	6.67	162	12.00	222	16.33	282	89.33
43	11.00	103	6.33	163	11.00	223	17.67	283	92.67
44	10.33	104	6.00	164	11.00	224	16.00	284	93.33
45	10.33	105	6.67	165	10.67	225	18.00	285	93.00
46	10.33	106	6.33	166	10.67	226	18.67	286	95.00
47	9.33	107	6.33	167	11.33	227	18.00	287	96.33
48	9.67	108	6.67	168	12.00	228	16.67	288	97.67
49	10.67	109	7.00	169	11.67	229	19.00	289	98.33
50	9.67	110	7.00	170	12.67	230	16.67	290	98.00
51	8.67	111	7.33	171	12.33	231	18.00	291	97.67
52	9.33	112	7.67	172	12.67	232	18.33	292	98.33
53	9.33	113	7.67	173	11.67	233	19.00	293	98.67
54	9.00	114	8.00	174	12.67	234	18.33	294	98.00
55	9.33	115	7.67	175	13.67	235	19.33	295	99.33
56	10.33	116	8.00	176	13.33	236	20.33	296	99.00
57	10.33	117	8.00	177	13.67	237	21.00	297	97.33
58	9.33	118	8.33	178	12.33	238	19.00	298	94.33
59	8.00	119	8.33	179	10.33	239	19.67	299	84.00
60	8.67	120	8.67	180	10.33	240	20.33		
61	8.33	121	8.33	181	12.00	241	20.33		

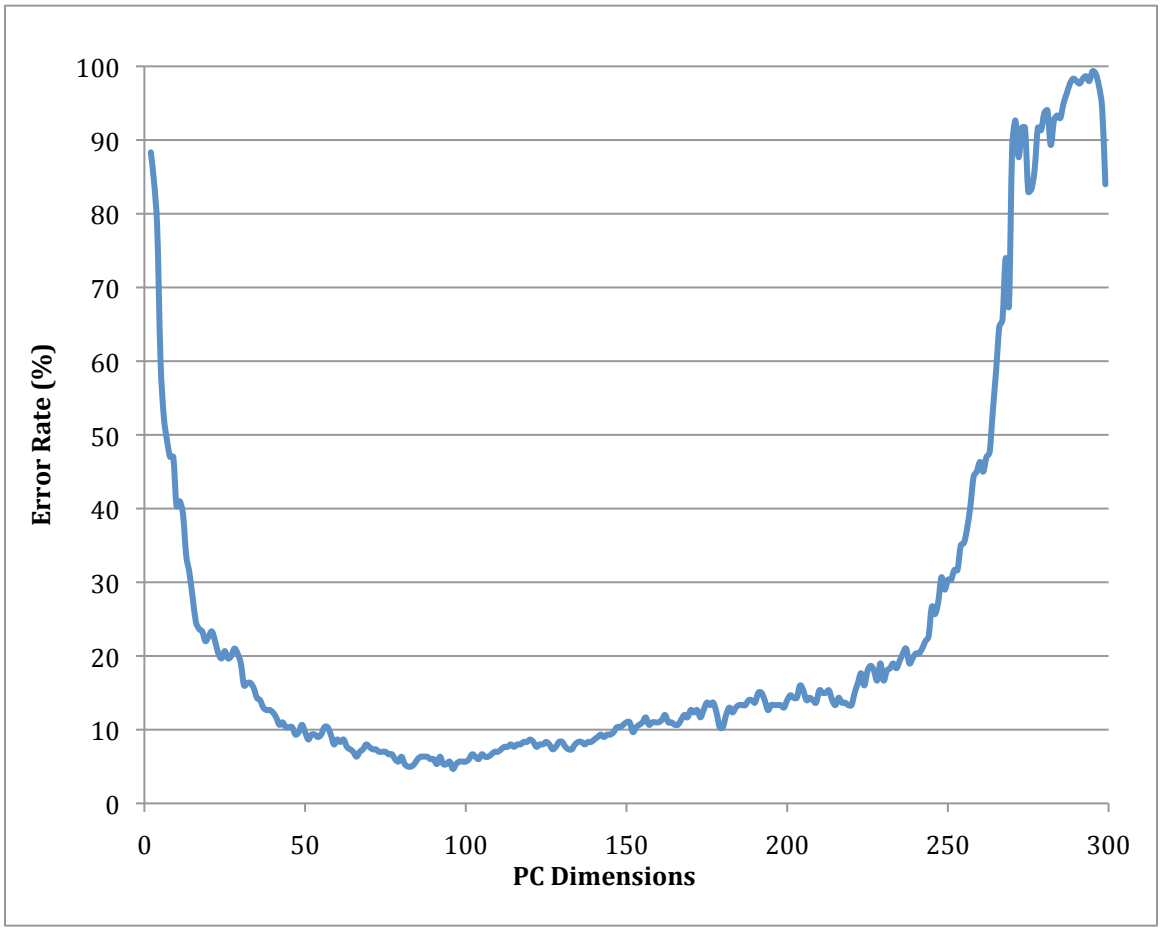


Figure 260: Graph of the discrimination error rate versus PC dimensions for HOO-CV with PCA reduced CVA for the first set of 30 glass first derivative (5-point smoothing) spectra (10 replicates), autoscaled data.

First Set, First Derivative (5-point smoothing) – Classification (automotive, architectural or container)

Table 272: Classification (automotive, architectural or container) error rates for HOO-CV with PCA reduced CVA for the first set of 30 glass first derivative (5-point smoothing) spectra (10 replicates), no data pretreatment. The smallest PC dimension with the minimum error rate is highlighted in yellow.

PCs	Error Rate (%)	PCs	Error Rate (%)	PCs	Error Rate (%)	PCs	Error Rate (%)	PCs	Error Rate (%)
2	66.00	17	21.67	32	21.33	47	14.33	62	17.67
3	64.67	18	21.67	33	18.67	48	16.33	63	17.67
4	62.67	19	21.33	34	19.33	49	17.67	64	17.33
5	56.33	20	22.33	35	19.67	50	17.00	65	17.33
6	47.00	21	24.33	36	18.00	51	18.00	66	17.67
7	44.67	22	23.33	37	17.67	52	17.67	67	17.00
8	45.00	23	23.67	38	18.67	53	15.67	68	17.67
9	25.67	24	24.33	39	18.67	54	17.00	69	17.67
10	28.00	25	25.67	40	16.67	55	16.67	70	18.33
11	28.00	26	26.00	41	17.00	56	17.00	71	17.33
12	26.67	27	25.67	42	16.67	57	17.00	72	17.67
13	27.33	28	25.00	43	16.67	58	15.00	73	18.33
14	23.33	29	23.00	44	17.33	59	16.33	74	18.33
15	24.67	30	22.33	45	17.33	60	16.67		
16	21.00	31	23.67	46	17.33	61	16.67		

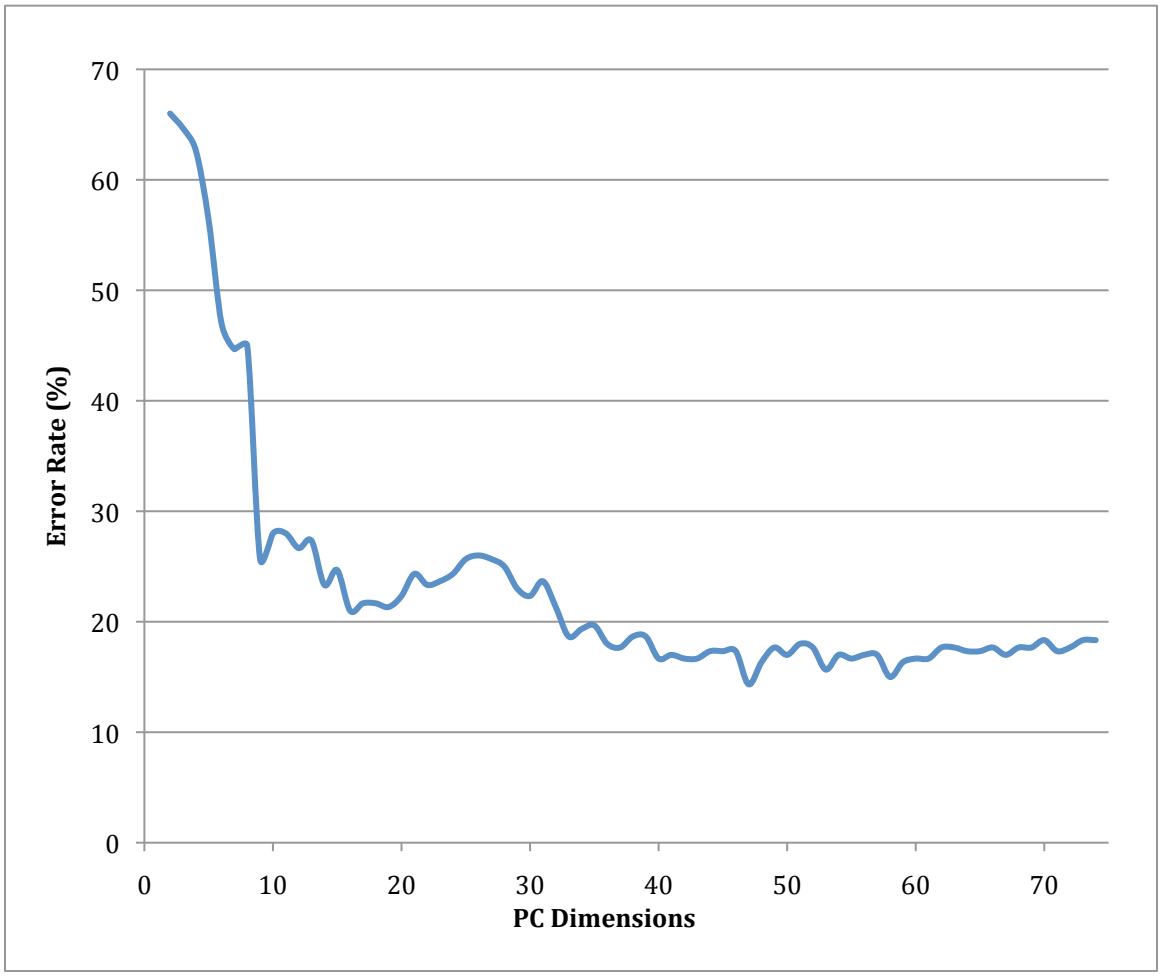


Figure 261: Graph of the classification (automotive, architectural or container) error rate versus PC dimensions for HOO-CV with PCA reduced CVA for the first set of 30 glass first derivative (5-point smoothing) spectra (10 replicates), no data pretreatment.

Table 273: Classification (automotive, architectural or container) error rates for HOO-CV with PCA reduced CVA for the first set of 30 glass first derivative (5-point smoothing) spectra (10 replicates), centered data. The smallest PC dimension with the minimum error rate is highlighted in yellow.

PCs	Error Rate (%)	PCs	Error Rate (%)	PCs	Error Rate (%)	PCs	Error Rate (%)	PCs	Error Rate (%)
2	65.67	17	21.67	32	24.67	47	16.33	62	18.00
3	61.00	18	21.67	33	19.67	48	16.00	63	18.33
4	61.33	19	21.00	34	19.33	49	18.00	64	16.67
5	50.33	20	22.67	35	17.00	50	17.33	65	17.33
6	47.33	21	24.00	36	17.00	51	17.67	66	17.67
7	45.00	22	25.00	37	17.33	52	17.67	67	17.33
8	46.00	23	23.67	38	17.67	53	16.33	68	17.67
9	26.67	24	24.00	39	16.67	54	16.67	69	17.67
10	28.33	25	24.33	40	16.67	55	17.00	70	18.33
11	26.67	26	25.00	41	16.67	56	16.67	71	17.00
12	27.67	27	24.67	42	16.33	57	17.33	72	18.00
13	26.67	28	24.67	43	17.67	58	18.33	73	18.33
14	25.00	29	24.67	44	17.67	59	16.67	74	18.67
15	25.00	30	25.33	45	16.67	60	17.67		
16	21.33	31	25.33	46	16.67	61	17.33		

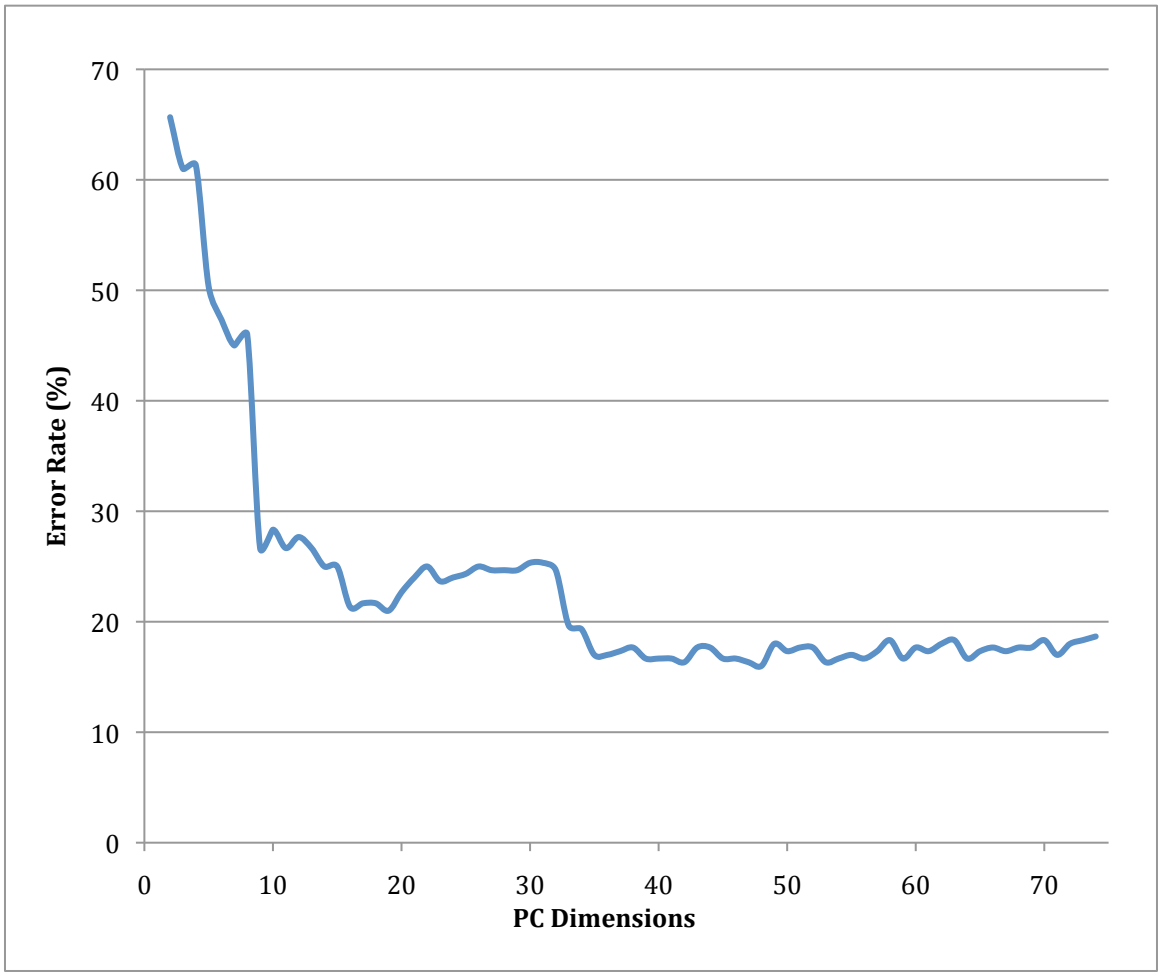


Figure 262: Graph of the classification (automotive, architectural or container) error rate versus PC dimensions for HOO-CV with PCA reduced CVA for the first set of 30 glass first derivative (5-point smoothing) spectra (10 replicates), centered data.

Table 274: Classification (automotive, architectural or container) error rates for HOO-CV with PCA reduced CVA for the first set of 30 glass first derivative (5-point smoothing) spectra (10 replicates), autoscaled data. The smallest PC dimension with the minimum error rate is highlighted in yellow.

PCs	Error Rate (%)	PCs	Error Rate (%)	PCs	Error Rate (%)	PCs	Error Rate (%)	PCs	Error Rate (%)
2	69.33	62	17.33	122	19.67	182	20.67	242	31.00
3	49.00	63	18.33	123	20.67	183	20.33	243	31.33
4	39.33	64	18.67	124	20.33	184	21.00	244	32.33
5	24.00	65	19.00	125	20.00	185	20.00	245	33.00
6	24.33	66	19.00	126	19.33	186	21.67	246	32.33
7	27.00	67	19.00	127	20.00	187	21.67	247	32.00
8	25.67	68	18.67	128	20.33	188	22.00	248	32.67
9	25.33	69	19.00	129	20.00	189	22.33	249	33.67
10	26.67	70	18.00	130	20.33	190	22.33	250	33.33
11	26.67	71	19.00	131	21.00	191	22.33	251	33.33
12	26.67	72	18.67	132	21.00	192	23.67	252	33.67
13	28.00	73	19.00	133	20.67	193	25.00	253	34.33
14	22.00	74	18.67	134	20.67	194	26.00	254	36.00
15	23.67	75	19.00	135	21.00	195	23.00	255	37.33
16	24.00	76	19.00	136	21.67	196	23.67	256	37.33
17	25.67	77	18.33	137	20.00	197	22.67	257	34.00
18	25.33	78	17.67	138	20.33	198	23.67	258	33.67
19	26.33	79	18.67	139	21.00	199	23.00	259	35.00
20	23.67	80	18.33	140	21.00	200	23.67	260	35.00
21	23.33	81	18.33	141	21.00	201	25.33	261	35.67
22	21.33	82	18.67	142	21.00	202	25.33	262	37.33
23	21.00	83	17.00	143	21.00	203	25.00	263	36.00
24	21.00	84	15.33	144	21.00	204	24.67	264	38.00
25	21.33	85	16.33	145	21.00	205	25.33	265	36.33
26	21.33	86	16.33	146	20.00	206	25.33	266	38.00
27	22.33	87	15.67	147	19.67	207	25.67	267	38.00
28	22.67	88	15.33	148	20.67	208	25.67	268	36.67
29	22.33	89	15.67	149	20.33	209	25.67	269	37.33
30	22.33	90	15.33	150	20.67	210	25.67	270	40.00
31	21.33	91	15.33	151	20.33	211	26.00	271	41.67
32	21.00	92	16.33	152	20.33	212	26.00	272	42.00
33	21.67	93	16.33	153	21.33	213	25.67	273	42.00
34	20.00	94	17.00	154	20.00	214	26.33	274	41.00
35	20.00	95	17.67	155	20.00	215	26.67	275	42.00
36	18.00	96	17.33	156	19.33	216	26.67	276	45.00
37	18.00	97	17.00	157	20.00	217	27.33	277	44.33

38	16.67	98	17.33	158	20.00	218	28.67	278	45.33
39	17.33	99	17.33	159	19.33	219	29.67	279	44.67
40	16.33	100	17.67	160	18.67	220	30.33	280	42.00
41	17.67	101	17.67	161	19.33	221	29.33	281	41.33
42	17.67	102	17.67	162	19.33	222	30.00	282	43.67
43	17.67	103	18.00	163	17.67	223	29.33	283	44.67
44	17.00	104	17.00	164	18.67	224	29.00	284	45.67
45	17.00	105	17.33	165	19.33	225	28.00	285	46.33
46	17.33	106	19.67	166	20.00	226	28.00	286	44.33
47	17.00	107	19.33	167	20.67	227	27.67	287	48.00
48	18.00	108	17.33	168	19.00	228	27.67	288	48.33
49	18.33	109	17.33	169	20.33	229	26.00	289	46.33
50	17.67	110	17.67	170	19.67	230	26.33	290	51.00
51	18.00	111	17.33	171	19.67	231	26.33	291	50.33
52	18.00	112	18.00	172	20.33	232	28.67	292	53.67
53	19.00	113	18.00	173	20.67	233	28.33	293	56.67
54	18.00	114	18.00	174	19.67	234	28.67	294	61.00
55	18.67	115	18.00	175	20.33	235	28.33	295	55.33
56	18.33	116	18.33	176	20.00	236	29.33	296	62.00
57	19.00	117	19.33	177	20.00	237	27.67	297	61.33
58	16.67	118	19.33	178	21.67	238	27.67	298	63.33
59	18.00	119	19.33	179	21.67	239	28.33	299	45.33
60	17.33	120	20.00	180	22.00	240	29.00		
61	17.67	121	19.67	181	21.00	241	30.33		

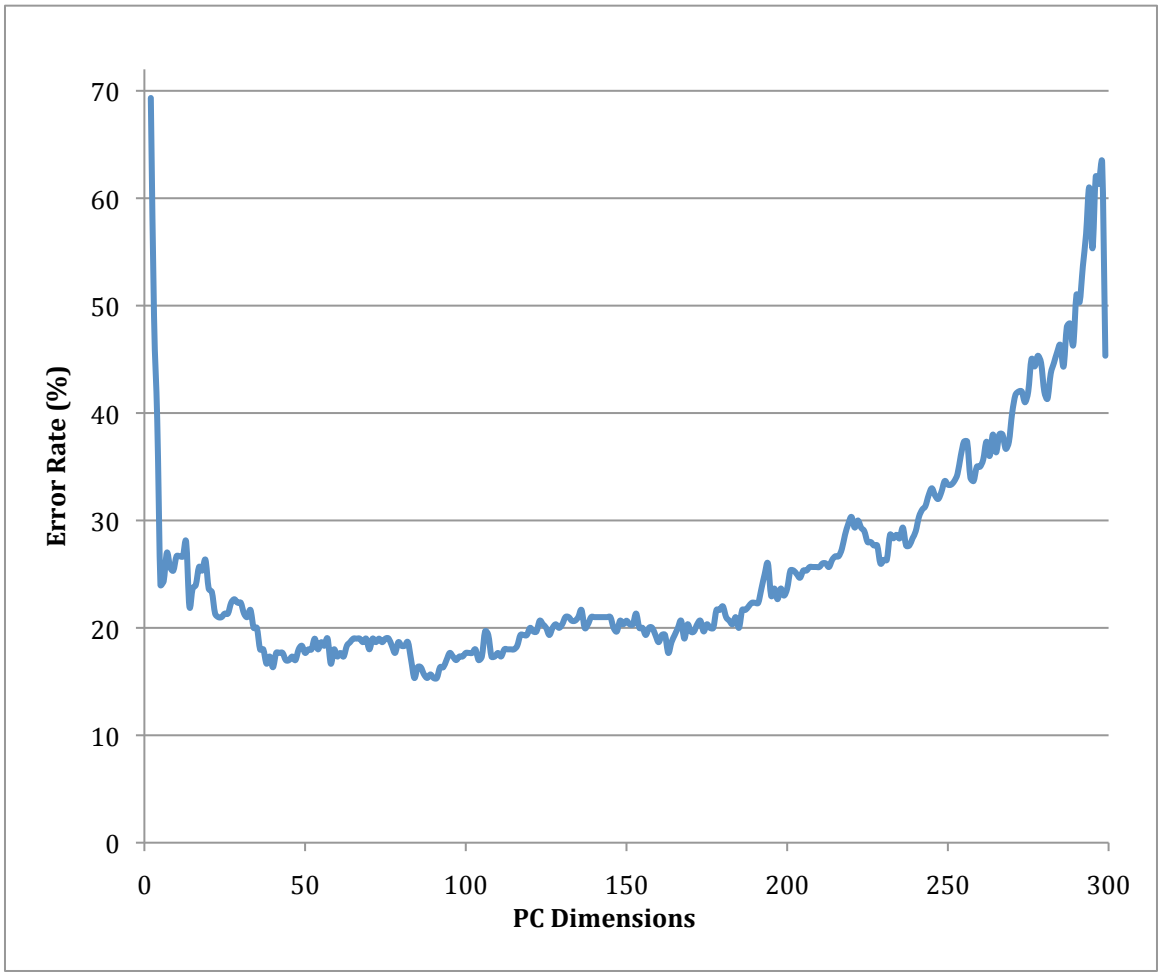


Figure 263: Graph of the classification (automotive, architectural or container) error rate versus PC dimensions for HOO-CV with PCA reduced CVA for the first set of 30 glass first derivative (5-point smoothing) spectra (10 replicates), autoscaled data.

First Set, First Derivative (5-point smoothing) – Classification (window or container)

Table 275: Classification (window or container) error rates for HOO-CV with PCA reduced CVA for the first set of 30 glass first derivative (5-point smoothing) spectra (10 replicates), no data pretreatment. The smallest PC dimension with the minimum error rate is highlighted in yellow.

PCs	Error Rate (%)	PCs	Error Rate (%)	PCs	Error Rate (%)	PCs	Error Rate (%)	PCs	Error Rate (%)
2	33.33	17	3.67	32	4.33	47	4.00	62	3.67
3	33.67	18	3.67	33	4.00	48	4.00	63	3.67
4	35.67	19	3.67	34	4.33	49	4.00	64	4.00
5	29.00	20	4.33	35	4.33	50	4.00	65	4.00
6	23.00	21	4.00	36	5.00	51	4.33	66	4.00
7	19.67	22	4.00	37	5.00	52	4.33	67	4.00
8	19.67	23	4.00	38	4.67	53	4.33	68	4.00
9	3.67	24	4.33	39	4.67	54	4.67	69	4.33
10	3.67	25	4.33	40	4.67	55	4.00	70	4.00
11	3.67	26	4.67	41	4.67	56	4.00	71	3.67
12	3.67	27	4.67	42	4.33	57	3.33	72	3.67
13	3.67	28	4.67	43	4.67	58	3.00	73	4.00
14	3.67	29	4.33	44	4.67	59	3.00	74	4.00
15	3.67	30	4.00	45	4.67	60	3.33		
16	3.67	31	4.33	46	4.00	61	3.67		

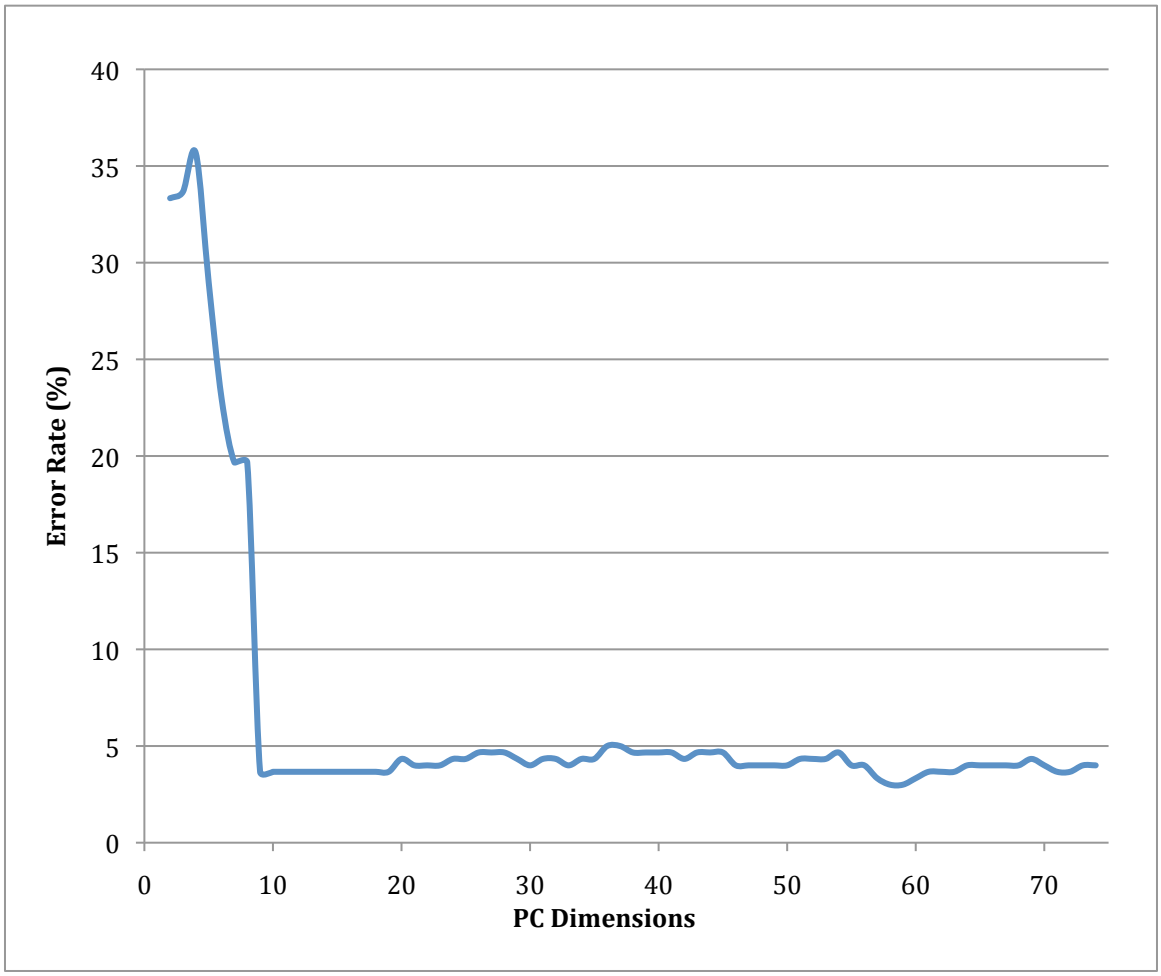


Figure 264: Graph of the classification (window or container) error rate versus PC dimensions for HOO-CV with PCA reduced CVA for the first set of 30 glass first derivative (5-point smoothing) spectra (10 replicates), no data pretreatment.

Table 276: Classification (window or container) error rates for HOO-CV with PCA reduced CVA for the first set of 30 glass first derivative (5-point smoothing) spectra (10 replicates), centered data. The smallest PC dimension with the minimum error rate is highlighted in yellow.

PCs	Error Rate (%)	PCs	Error Rate (%)	PCs	Error Rate (%)	PCs	Error Rate (%)	PCs	Error Rate (%)
2	33.33	17	3.67	32	4.67	47	4.00	62	3.67
3	32.67	18	3.67	33	4.00	48	4.33	63	4.00
4	33.67	19	3.67	34	4.33	49	4.67	64	4.00
5	22.67	20	4.00	35	4.33	50	4.33	65	4.33
6	22.33	21	4.00	36	4.33	51	4.33	66	4.33
7	19.33	22	4.00	37	5.00	52	4.67	67	4.00
8	19.67	23	4.00	38	4.67	53	4.33	68	4.33
9	3.67	24	4.00	39	4.67	54	4.67	69	4.33
10	3.67	25	4.00	40	4.67	55	4.33	70	4.00
11	3.67	26	4.67	41	5.00	56	4.33	71	3.67
12	3.67	27	4.67	42	4.67	57	4.33	72	4.00
13	3.67	28	4.67	43	5.00	58	4.33	73	4.00
14	3.67	29	4.67	44	4.33	59	4.00	74	4.00
15	3.67	30	4.67	45	4.67	60	4.00		
16	3.67	31	4.67	46	4.00	61	4.00		

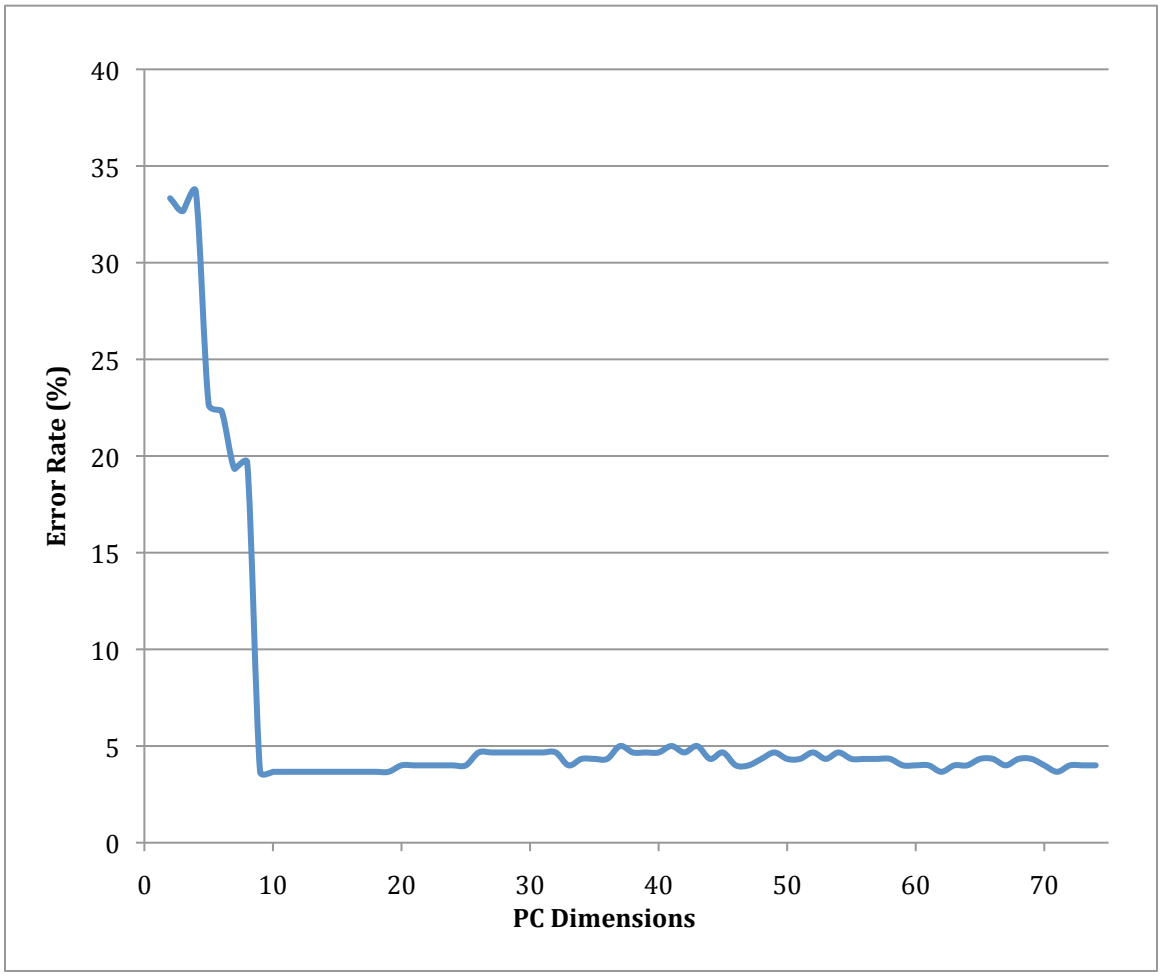


Figure 265: Graph of the classification (window or container) error rate versus PC dimensions for HOO-CV with PCA reduced CVA for the first set of 30 glass first derivative (5-point smoothing) spectra (10 replicates), centered data.

Table 277: Classification (window or container) error rates for HOO-CV with PCA reduced CVA for the first set of 30 glass first derivative (5-point smoothing) spectra (10 replicates), autoscaled data. The smallest PC dimension with the minimum error rate is highlighted in yellow.

PCs	Error Rate (%)	PCs	Error Rate (%)	PCs	Error Rate (%)	PCs	Error Rate (%)	PCs	Error Rate (%)
2	33.33	62	3.33	122	3.67	182	4.67	242	11.00
3	27.67	63	3.33	123	3.67	183	4.00	243	11.33
4	15.67	64	3.33	124	4.00	184	4.00	244	12.00
5	3.67	65	3.33	125	3.33	185	4.33	245	13.33
6	3.67	66	3.33	126	3.33	186	5.33	246	13.67
7	3.67	67	3.33	127	3.33	187	5.33	247	13.33
8	3.67	68	3.67	128	3.67	188	5.33	248	14.00
9	3.67	69	3.67	129	3.67	189	5.33	249	14.33
10	3.67	70	3.67	130	3.67	190	5.33	250	14.67
11	3.67	71	3.67	131	3.67	191	5.33	251	14.33
12	3.67	72	3.67	132	3.67	192	5.00	252	14.33
13	3.67	73	3.67	133	3.33	193	5.67	253	15.33
14	4.00	74	3.33	134	3.67	194	6.00	254	17.00
15	4.00	75	3.33	135	3.67	195	5.33	255	15.33
16	4.00	76	3.33	136	3.67	196	6.00	256	14.67
17	4.33	77	3.33	137	3.67	197	5.00	257	15.67
18	4.00	78	3.67	138	3.67	198	5.33	258	16.33
19	4.33	79	2.67	139	3.67	199	5.67	259	16.67
20	4.00	80	2.67	140	3.33	200	6.00	260	17.00
21	3.67	81	2.33	141	3.33	201	6.00	261	17.67
22	3.67	82	2.67	142	3.33	202	6.33	262	17.67
23	3.67	83	2.67	143	3.67	203	6.67	263	18.00
24	3.67	84	3.00	144	3.67	204	5.67	264	19.00
25	3.67	85	3.00	145	3.67	205	6.33	265	19.67
26	3.67	86	2.67	146	3.67	206	6.67	266	18.67
27	3.67	87	2.67	147	3.67	207	7.00	267	18.33
28	3.67	88	3.00	148	4.00	208	7.00	268	19.33
29	3.67	89	3.00	149	4.00	209	7.00	269	21.00
30	3.67	90	3.00	150	4.00	210	6.67	270	21.67
31	3.67	91	3.00	151	4.00	211	8.00	271	21.33
32	3.67	92	3.00	152	4.00	212	7.33	272	22.33
33	3.67	93	3.00	153	4.00	213	7.33	273	23.33
34	3.67	94	3.00	154	4.00	214	7.67	274	21.67
35	3.67	95	3.00	155	4.00	215	7.67	275	23.00
36	3.67	96	3.00	156	4.00	216	8.00	276	24.33
37	3.33	97	3.00	157	4.33	217	8.33	277	25.67

38	3.33	98	2.67	158	4.00	218	8.67	278	25.33
39	3.33	99	2.67	159	4.00	219	8.33	279	22.67
40	3.33	100	2.67	160	4.67	220	8.33	280	23.67
41	3.33	101	2.67	161	5.00	221	8.33	281	21.67
42	3.33	102	2.67	162	5.00	222	8.33	282	22.67
43	3.33	103	2.67	163	4.67	223	8.00	283	24.67
44	3.33	104	2.67	164	4.00	224	8.67	284	24.67
45	3.33	105	2.67	165	5.33	225	8.67	285	25.00
46	3.33	106	3.00	166	5.67	226	9.00	286	24.33
47	3.33	107	3.33	167	6.00	227	9.33	287	26.00
48	3.33	108	2.33	168	5.00	228	9.67	288	28.33
49	3.33	109	2.33	169	4.67	229	9.00	289	25.33
50	3.33	110	2.67	170	4.33	230	9.00	290	29.33
51	3.67	111	3.00	171	4.00	231	9.00	291	30.67
52	3.67	112	3.33	172	4.67	232	9.00	292	32.33
53	3.67	113	3.33	173	4.00	233	10.00	293	33.67
54	3.33	114	3.33	174	4.00	234	9.67	294	38.00
55	3.67	115	3.33	175	4.33	235	10.00	295	41.33
56	3.67	116	3.67	176	4.33	236	11.33	296	43.67
57	3.67	117	3.67	177	4.00	237	11.67	297	46.00
58	3.67	118	3.67	178	5.33	238	11.33	298	48.33
59	3.67	119	3.67	179	4.67	239	11.67		
60	3.33	120	4.00	180	4.67	240	11.00		
61	3.00	121	4.00	181	4.67	241	11.33		

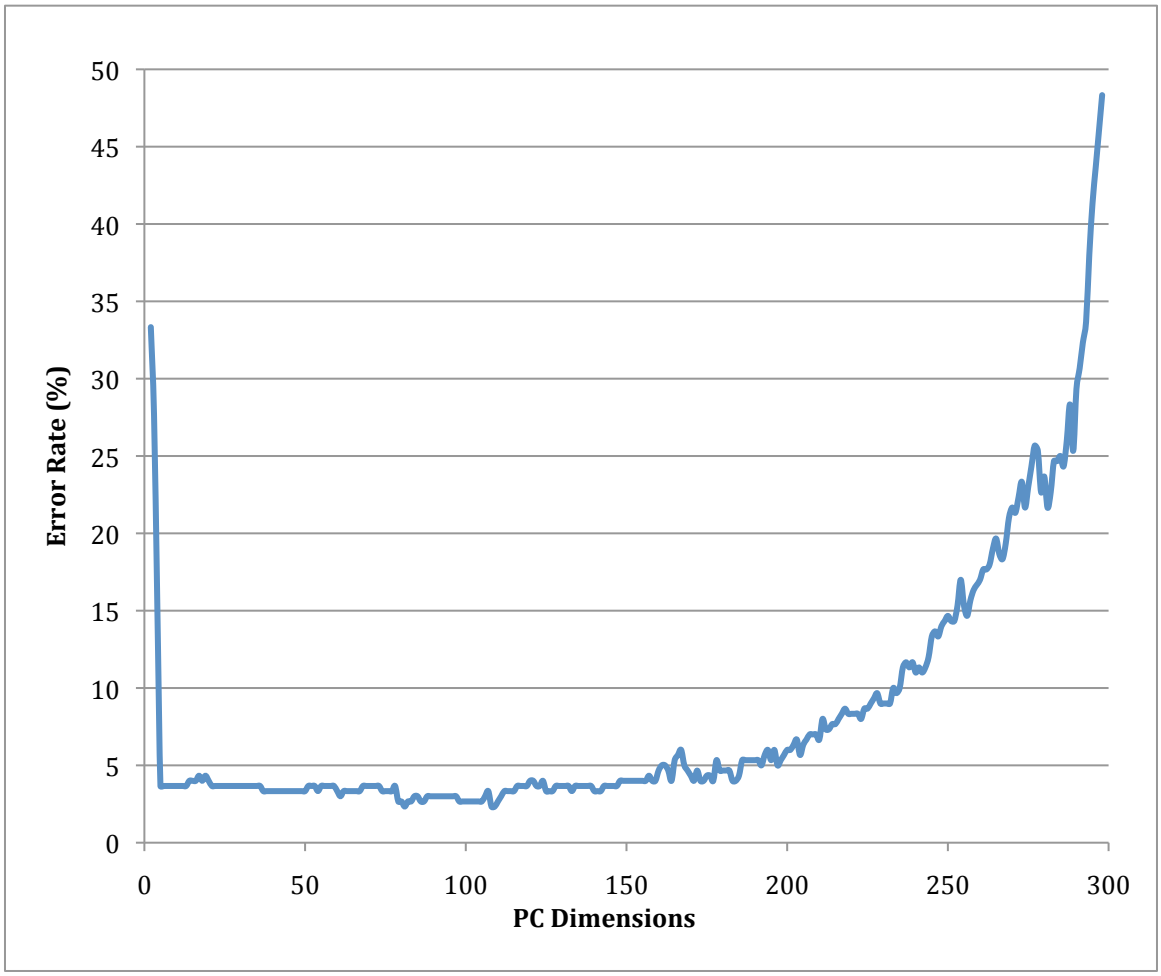


Figure 266: Graph of the classification (window or container) error rate versus PC dimensions for HOO-CV with PCA reduced CVA for the first set of 30 glass first derivative (5-point smoothing) spectra (10 replicates), autoscaled data.

First Set, First Derivative (5-point smoothing) – Window Discrimination

Table 278: Discrimination error rates for HOO-CV with PCA reduced CVA for the first set of 20 window glass first derivative (5-point smoothing) spectra (10 replicates), no data pretreatment. The smallest PC dimension with the minimum error rate is highlighted in yellow.

PCs	Error Rate (%)	PCs	Error Rate (%)	PCs	Error Rate (%)	PCs	Error Rate (%)	PCs	Error Rate (%)
2	93.50	15	42.00	28	31.00	41	26.00	54	20.50
3	90.50	16	41.50	29	29.50	42	25.00	55	17.50
4	90.50	17	41.00	30	29.50	43	24.00	56	18.00
5	88.50	18	38.50	31	29.00	44	23.00	57	19.00
6	87.00	19	41.50	32	30.00	45	23.00	58	21.00
7	86.50	20	36.50	33	30.00	46	21.50	59	21.50
8	72.00	21	38.00	34	31.50	47	22.50	60	22.50
9	68.00	22	34.50	35	32.00	48	22.00	61	21.00
10	68.50	23	35.00	36	29.50	49	21.50	62	20.50
11	61.50	24	35.00	37	29.50	50	21.50	63	22.50
12	54.50	25	33.50	38	28.00	51	19.50	64	22.00
13	51.50	26	35.50	39	29.50	52	21.50	65	19.00
14	44.50	27	33.50	40	26.50	53	21.00	66	19.50

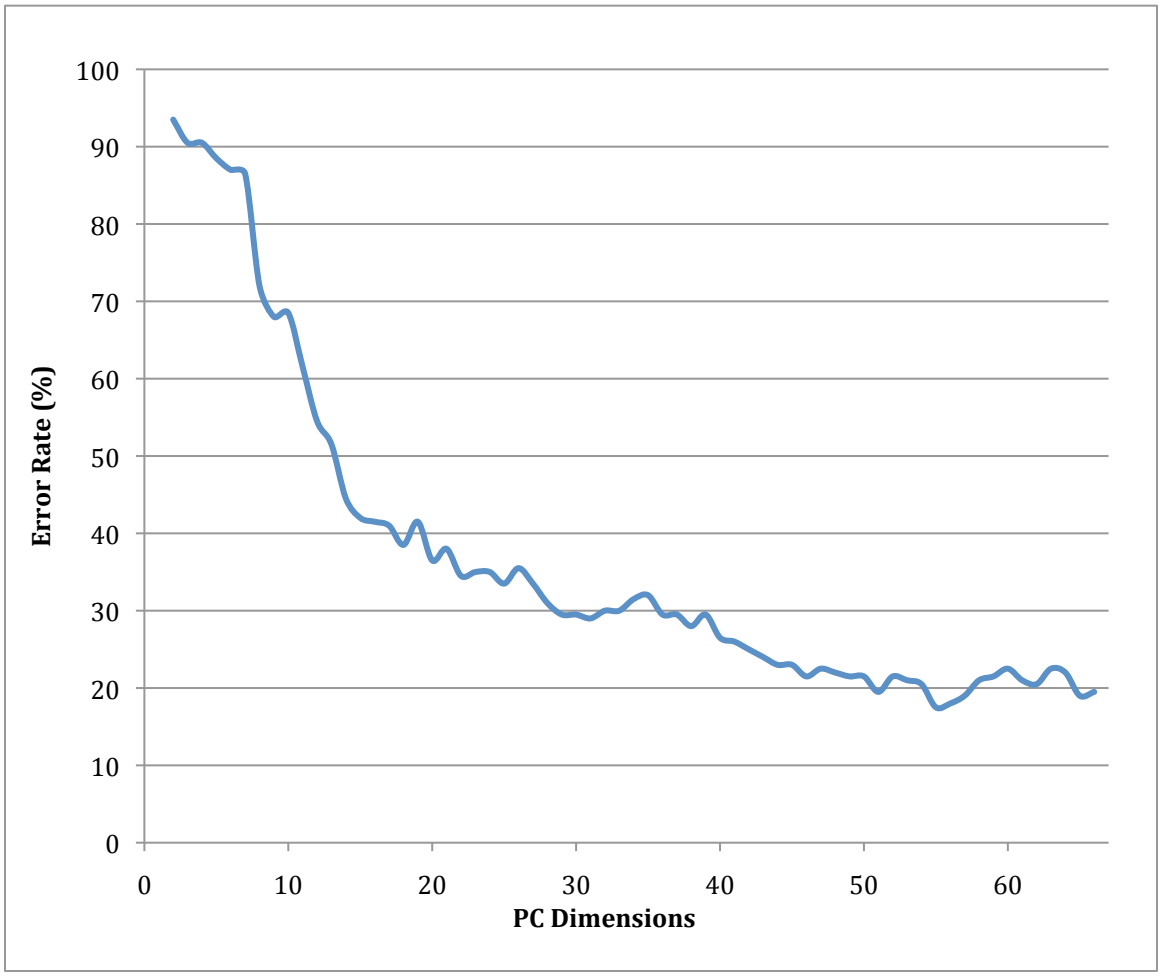


Figure 267: Graph of the discrimination error rate versus PC dimensions for HOO-CV with PCA reduced CVA for the first set of 20 window glass first derivative (5-point smoothing) spectra (10 replicates), no data pretreatment.

Table 279: Discrimination error rates for HOO-CV with PCA reduced CVA for the first set of 20 window glass first derivative (5-point smoothing) spectra (10 replicates), centered data. The smallest PC dimension with the minimum error rate is highlighted in yellow.

PCs	Error Rate (%)	PCs	Error Rate (%)	PCs	Error Rate (%)	PCs	Error Rate (%)	PCs	Error Rate (%)
2	94.50	15	42.50	28	30.50	41	26.50	54	20.50
3	94.50	16	40.00	29	29.50	42	25.50	55	17.50
4	90.00	17	41.50	30	29.50	43	25.00	56	18.00
5	90.50	18	39.50	31	29.50	44	24.50	57	18.50
6	87.00	19	39.50	32	29.50	45	23.50	58	20.50
7	86.00	20	38.50	33	29.00	46	22.50	59	21.00
8	68.50	21	36.50	34	29.00	47	20.50	60	21.00
9	70.00	22	33.50	35	27.50	48	20.00	61	21.00
10	64.00	23	34.00	36	28.00	49	20.50	62	21.00
11	60.50	24	36.50	37	29.00	50	21.50	63	20.50
12	55.00	25	34.50	38	28.50	51	20.50	64	20.50
13	51.00	26	33.00	39	29.00	52	22.00	65	19.00
14	46.50	27	31.50	40	27.50	53	20.50		

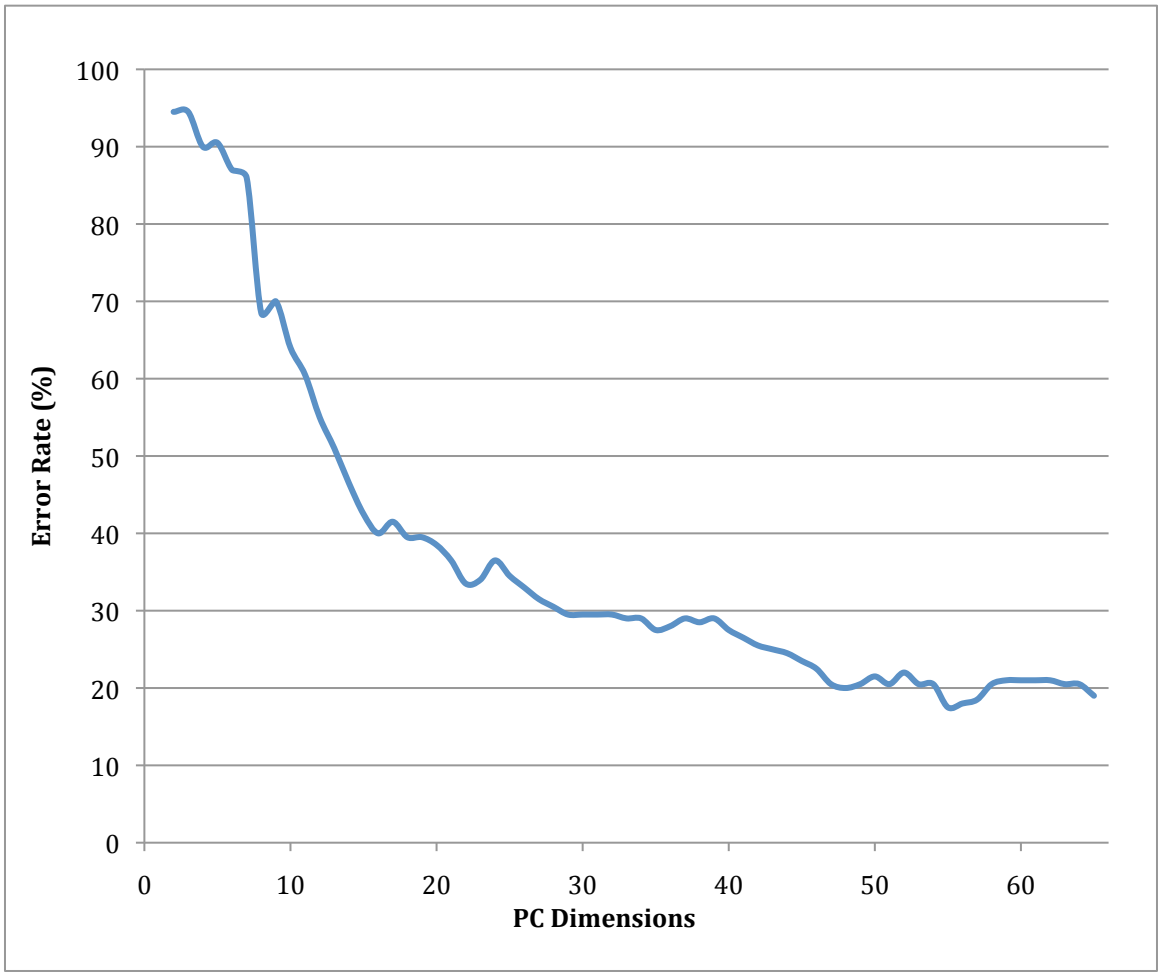


Figure 268: Graph of the discrimination error rate versus PC dimensions for HOO-CV with PCA reduced CVA for the first set of 20 window glass first derivative (5-point smoothing) spectra (10 replicates), centered data.

Table 280: Discrimination error rates for HOO-CV with PCA reduced CVA for the first set of 20 window glass first derivative (5-point smoothing) spectra (10 replicates), autoscaled data. The smallest PC dimension with the minimum error rate is highlighted in yellow.

PCs	Error Rate (%)	PCs	Error Rate (%)	PCs	Error Rate (%)	PCs	Error Rate (%)	PCs	Error Rate (%)
2	92.50	42	11.50	82	8.00	122	13.00	162	37.00
3	85.00	43	10.50	83	7.50	123	14.00	163	37.50
4	78.50	44	10.50	84	8.50	124	15.00	164	40.50
5	67.50	45	10.00	85	6.00	125	15.50	165	43.00
6	55.00	46	11.00	86	7.00	126	17.00	166	45.50
7	55.00	47	11.00	87	8.00	127	18.00	167	49.00
8	55.50	48	11.00	88	8.50	128	19.50	168	52.00
9	43.00	49	9.00	89	9.00	129	18.50	169	52.00
10	39.00	50	9.50	90	9.50	130	17.50	170	57.50
11	33.50	51	9.00	91	9.50	131	16.50	171	55.50
12	31.00	52	9.00	92	9.00	132	16.50	172	60.50
13	27.00	53	9.00	93	10.00	133	17.50	173	65.00
14	25.00	54	9.00	94	10.00	134	19.00	174	61.50
15	23.00	55	9.00	95	9.50	135	21.00	175	67.00
16	20.50	56	10.50	96	11.00	136	21.00	176	70.00
17	21.00	57	9.00	97	10.50	137	21.50	177	75.50
18	19.00	58	8.50	98	10.00	138	21.50	178	81.00
19	19.50	59	7.50	99	10.50	139	21.50	179	87.00
20	20.00	60	6.50	100	9.50	140	21.50	180	57.00
21	19.00	61	6.00	101	9.50	141	22.50	181	66.00
22	20.50	62	7.00	102	10.00	142	22.50	182	80.50
23	20.50	63	6.00	103	11.00	143	24.00	183	80.50
24	20.00	64	6.00	104	11.00	144	24.50	184	82.00
25	19.00	65	6.00	105	11.00	145	26.00	185	81.50
26	21.00	66	6.00	106	11.00	146	27.00	186	67.00
27	18.50	67	6.50	107	12.00	147	27.00	187	82.50
28	16.50	68	6.50	108	12.50	148	25.50	188	88.00
29	15.00	69	7.00	109	12.50	149	26.50	189	88.50
30	16.00	70	7.00	110	12.00	150	29.50	190	93.00
31	14.50	71	6.50	111	13.00	151	29.50	191	96.00
32	14.00	72	7.50	112	12.00	152	30.00	192	96.00
33	12.50	73	8.50	113	13.00	153	30.50	193	96.50
34	10.50	74	8.00	114	13.50	154	29.50	194	96.00
35	12.00	75	8.00	115	14.00	155	30.50	195	96.50
36	12.50	76	7.00	116	13.00	156	34.00	196	96.00
37	12.00	77	8.00	117	12.50	157	36.00	197	95.00
38	10.50	78	8.00	118	12.00	158	35.00	198	93.50

39	11.50	79	8.50	119	12.50	159	37.00	199	89.50
40	11.00	80	8.50	120	12.50	160	38.00		
41	11.00	81	9.00	121	13.00	161	37.00		

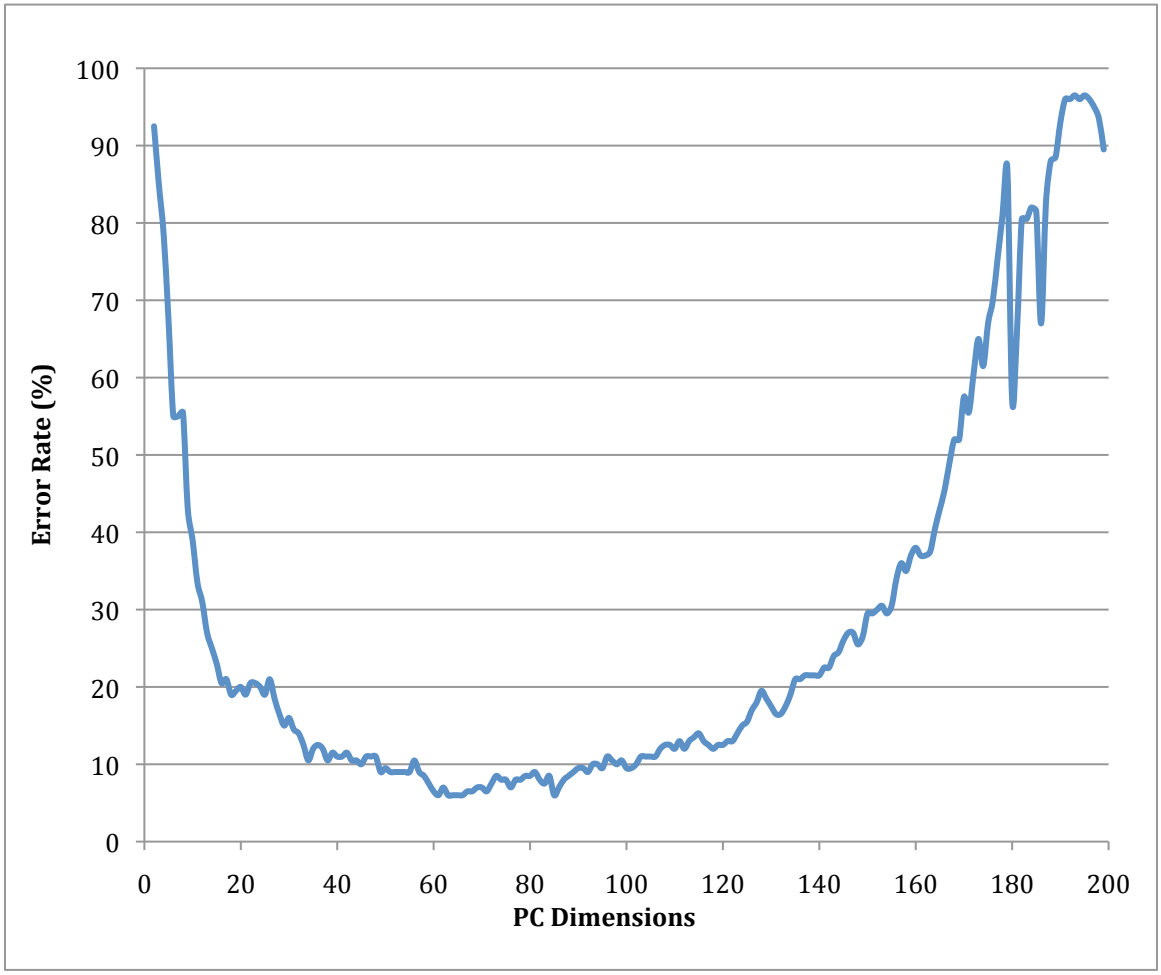


Figure 269: Graph of the discrimination error rate versus PC dimensions for HOO-CV with PCA reduced CVA for the first set of 20 window glass first derivative (5-point smoothing) spectra (10 replicates), autoscaled data.

First Set, First Derivative (5-point smoothing) – Container Discrimination

Table 281: Discrimination error rates for HOO-CV with PCA reduced CVA for the first set of 10 container glass first derivative (5-point smoothing) spectra (10 replicates), no data pretreatment. The smallest PC dimension with the minimum error rate is highlighted in yellow.

PCs	Error Rate (%)	PCs	Error Rate (%)	PCs	Error Rate (%)	PCs	Error Rate (%)	PCs	Error Rate (%)
2	77.00	14	40.00	26	26.00	38	19.00	50	21.00
3	81.00	15	40.00	27	26.00	39	20.00	51	21.00
4	80.00	16	38.00	28	29.00	40	21.00	52	18.00
5	73.00	17	31.00	29	30.00	41	20.00	53	20.00
6	67.00	18	33.00	30	32.00	42	20.00	54	19.00
7	58.00	19	32.00	31	27.00	43	21.00	55	20.00
8	59.00	20	30.00	32	27.00	44	19.00	56	21.00
9	60.00	21	32.00	33	29.00	45	19.00	57	21.00
10	53.00	22	33.00	34	23.00	46	20.00	58	19.00
11	51.00	23	28.00	35	23.00	47	20.00	59	18.00
12	41.00	24	28.00	36	18.00	48	19.00	60	18.00
13	37.00	25	29.00	37	19.00	49	22.00		

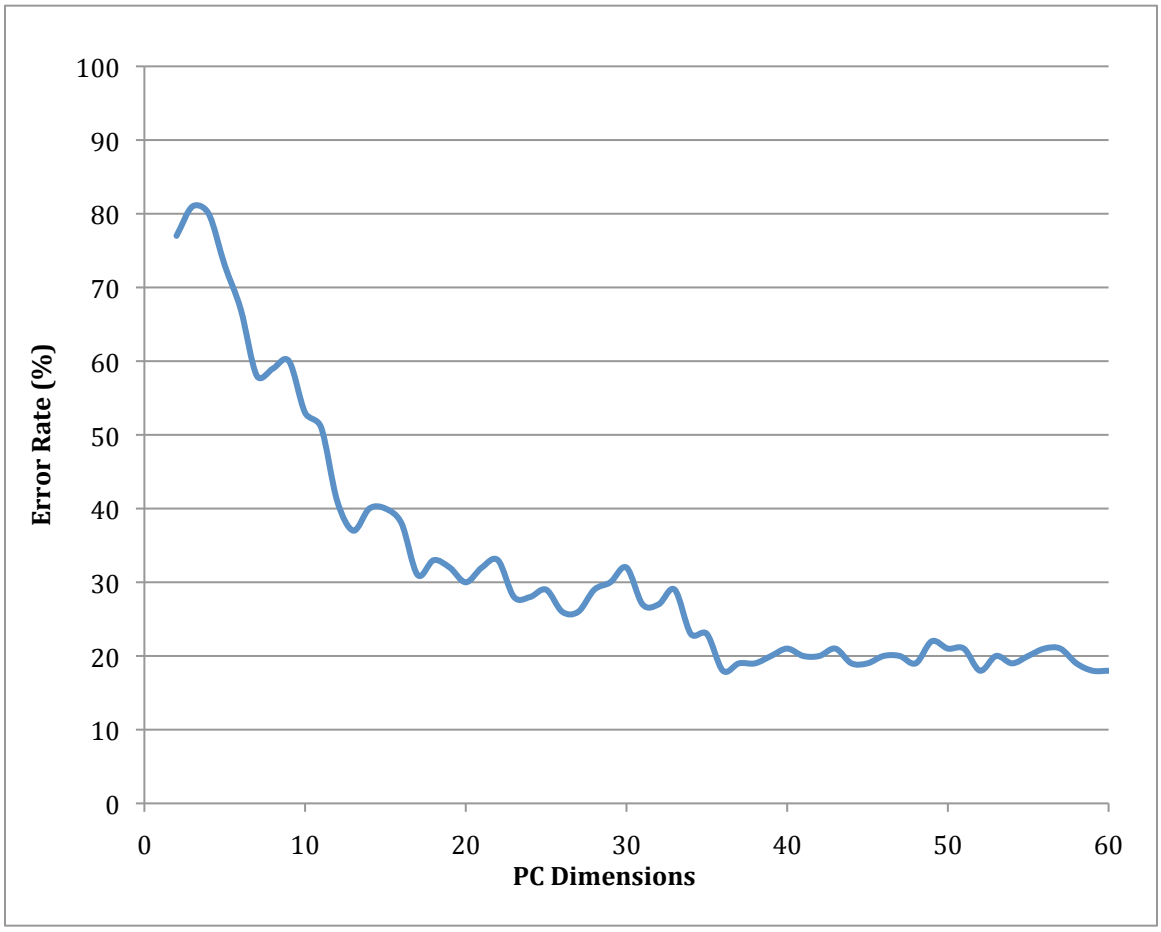


Figure 270: Graph of the discrimination error rate versus PC dimensions for HOO-CV with PCA reduced CVA for the first set of 10 container glass first derivative (5-point smoothing) spectra (10 replicates), no data pretreatment.

Table 282: Discrimination error rates for HOO-CV with PCA reduced CVA for the first set of 10 container glass first derivative (5-point smoothing) spectra (10 replicates), centered data. The smallest PC dimension with the minimum error rate is highlighted in yellow.

PCs	Error Rate (%)	PCs	Error Rate (%)	PCs	Error Rate (%)	PCs	Error Rate (%)	PCs	Error Rate (%)
2	80.00	14	40.00	26	27.00	38	22.00	50	22.00
3	79.00	15	40.00	27	27.00	39	20.00	51	20.00
4	79.00	16	39.00	28	29.00	40	19.00	52	20.00
5	67.00	17	33.00	29	31.00	41	19.00	53	20.00
6	67.00	18	34.00	30	29.00	42	22.00	54	18.00
7	71.00	19	31.00	31	30.00	43	19.00	55	19.00
8	59.00	20	29.00	32	27.00	44	17.00	56	21.00
9	61.00	21	32.00	33	26.00	45	19.00	57	18.00
10	44.00	22	32.00	34	23.00	46	19.00	58	18.00
11	42.00	23	28.00	35	25.00	47	19.00	59	15.00
12	39.00	24	28.00	36	17.00	48	20.00		
13	38.00	25	29.00	37	20.00	49	22.00		

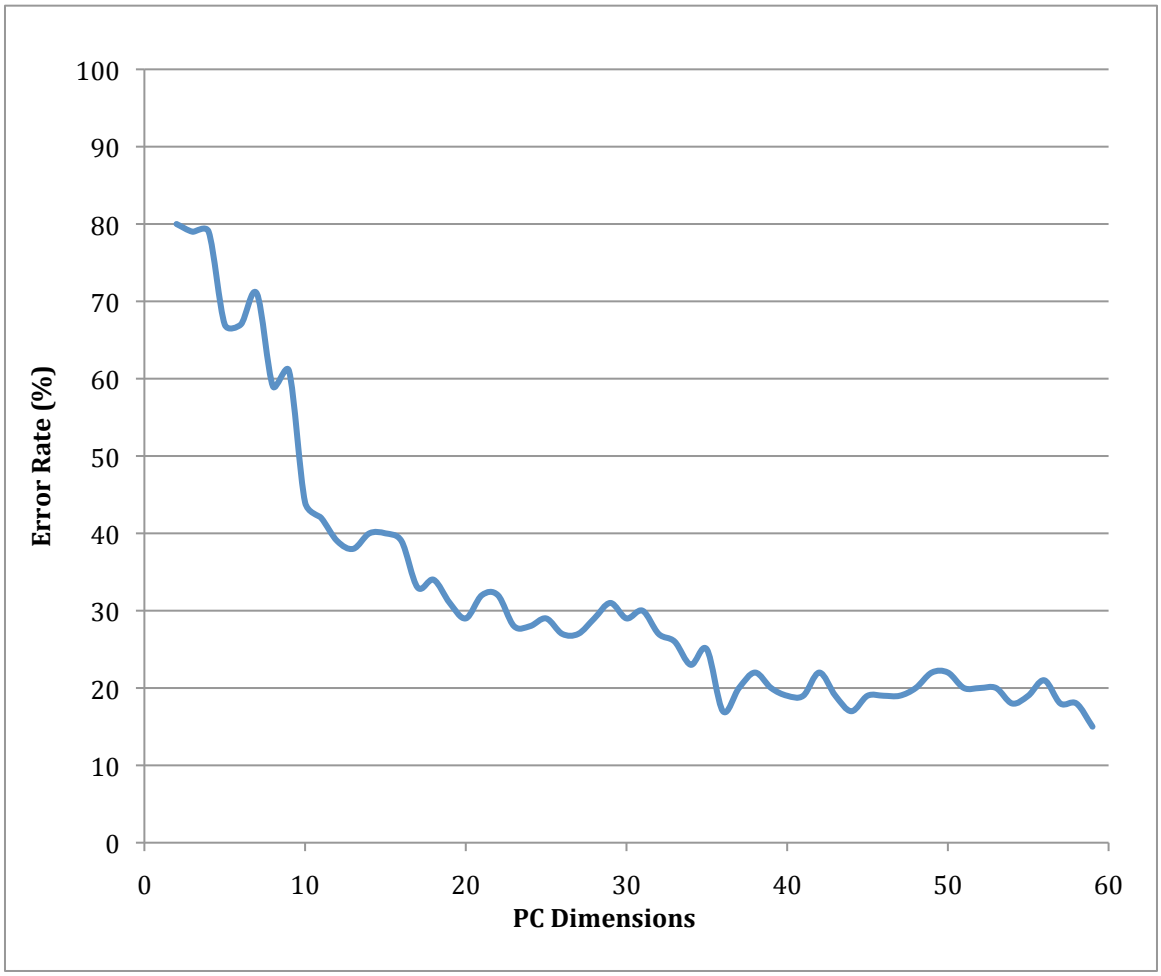


Figure 271: Graph of the discrimination error rate versus PC dimensions for HOO-CV with PCA reduced CVA for the first set of 10 container glass first derivative (5-point smoothing) spectra (10 replicates), centered data.

Table 283: Discrimination error rates for HOO-CV with PCA reduced CVA for the first set of 10 container glass first derivative (5-point smoothing) spectra (10 replicates), autoscaled data. The smallest PC dimension with the minimum error rate is highlighted in yellow.

PCs	Error Rate (%)	PCs	Error Rate (%)	PCs	Error Rate (%)	PCs	Error Rate (%)	PCs	Error Rate (%)
2	74.00	22	8.00	42	4.00	62	5.00	82	33.00
3	60.00	23	9.00	43	3.00	63	6.00	83	39.00
4	62.00	24	8.00	44	5.00	64	6.00	84	25.00
5	44.00	25	9.00	45	5.00	65	6.00	85	36.00
6	46.00	26	8.00	46	7.00	66	8.00	86	46.00
7	44.00	27	9.00	47	8.00	67	9.00	87	57.00
8	41.00	28	8.00	48	6.00	68	9.00	88	61.00
9	37.00	29	8.00	49	5.00	69	10.00	89	61.00
10	37.00	30	9.00	50	4.00	70	10.00	90	48.00
11	39.00	31	11.00	51	4.00	71	13.00	91	62.00
12	37.00	32	11.00	52	5.00	72	15.00	92	81.00
13	31.00	33	10.00	53	4.00	73	16.00	93	71.00
14	21.00	34	5.00	54	4.00	74	20.00	94	84.00
15	16.00	35	4.00	55	2.00	75	17.00	95	84.00
16	19.00	36	5.00	56	2.00	76	18.00	96	88.00
17	18.00	37	5.00	57	3.00	77	20.00	97	88.00
18	9.00	38	6.00	58	3.00	78	21.00	98	91.00
19	11.00	39	4.00	59	4.00	79	21.00	99	82.00
20	8.00	40	5.00	60	5.00	80	25.00		
21	8.00	41	4.00	61	4.00	81	26.00		

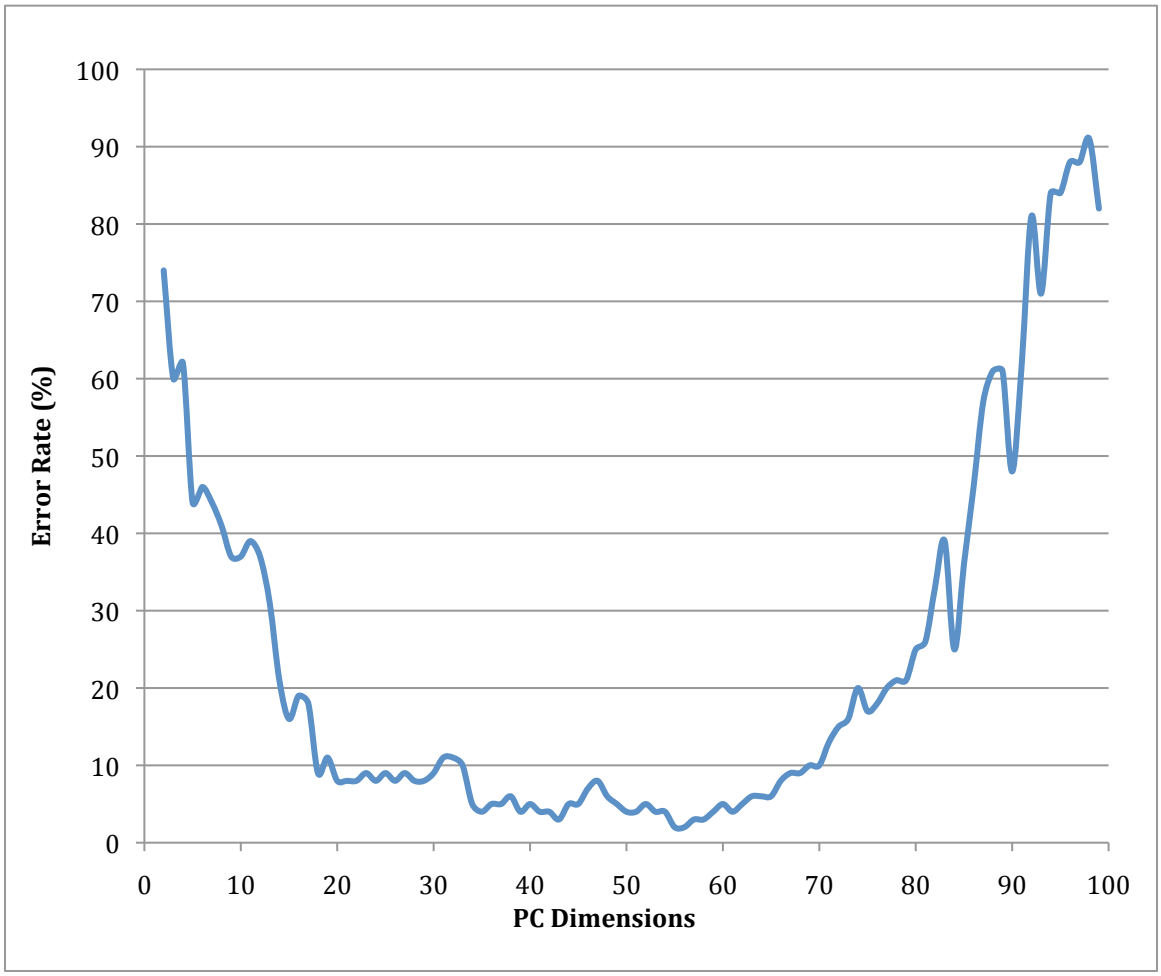


Figure 272: Graph of the discrimination error rate versus PC dimensions for HOO-CV with PCA reduced CVA for the first set of 10 container glass first derivative (5-point smoothing) spectra (10 replicates), autoscaled data.

First Set, First Derivative (5-point smoothing) – Float Classification

Table 284: Float classification error rates for HOO-CV with PCA reduced CVA for the first set of 20 window glass first derivative (5-point smoothing) spectra (10 replicates), no data pretreatment. The smallest PC dimension with the minimum error rate is highlighted in yellow.

PCs	Error Rate (%)	PCs	Error Rate (%)	PCs	Error Rate (%)	PCs	Error Rate (%)	PCs	Error Rate (%)
2	33.50	16	20.00	30	20.00	44	24.50	58	24.50
3	33.00	17	20.50	31	19.50	45	25.00	59	23.00
4	35.50	18	21.00	32	22.00	46	22.50	60	22.50
5	36.50	19	22.00	33	22.50	47	23.00	61	22.50
6	31.00	20	20.50	34	22.50	48	23.00	62	22.00
7	28.00	21	19.50	35	22.50	49	23.00	63	23.00
8	30.50	22	21.00	36	24.00	50	23.00	64	23.00
9	26.00	23	21.50	37	22.50	51	23.00	65	23.50
10	23.00	24	18.00	38	22.50	52	24.00	66	24.50
11	21.00	25	19.50	39	22.00	53	23.50	67	20.50
12	23.50	26	19.50	40	22.50	54	24.00	68	22.00
13	22.00	27	22.50	41	23.00	55	24.00	69	21.50
14	19.00	28	20.50	42	23.00	56	24.00		
15	21.00	29	19.50	43	23.50	57	24.00		

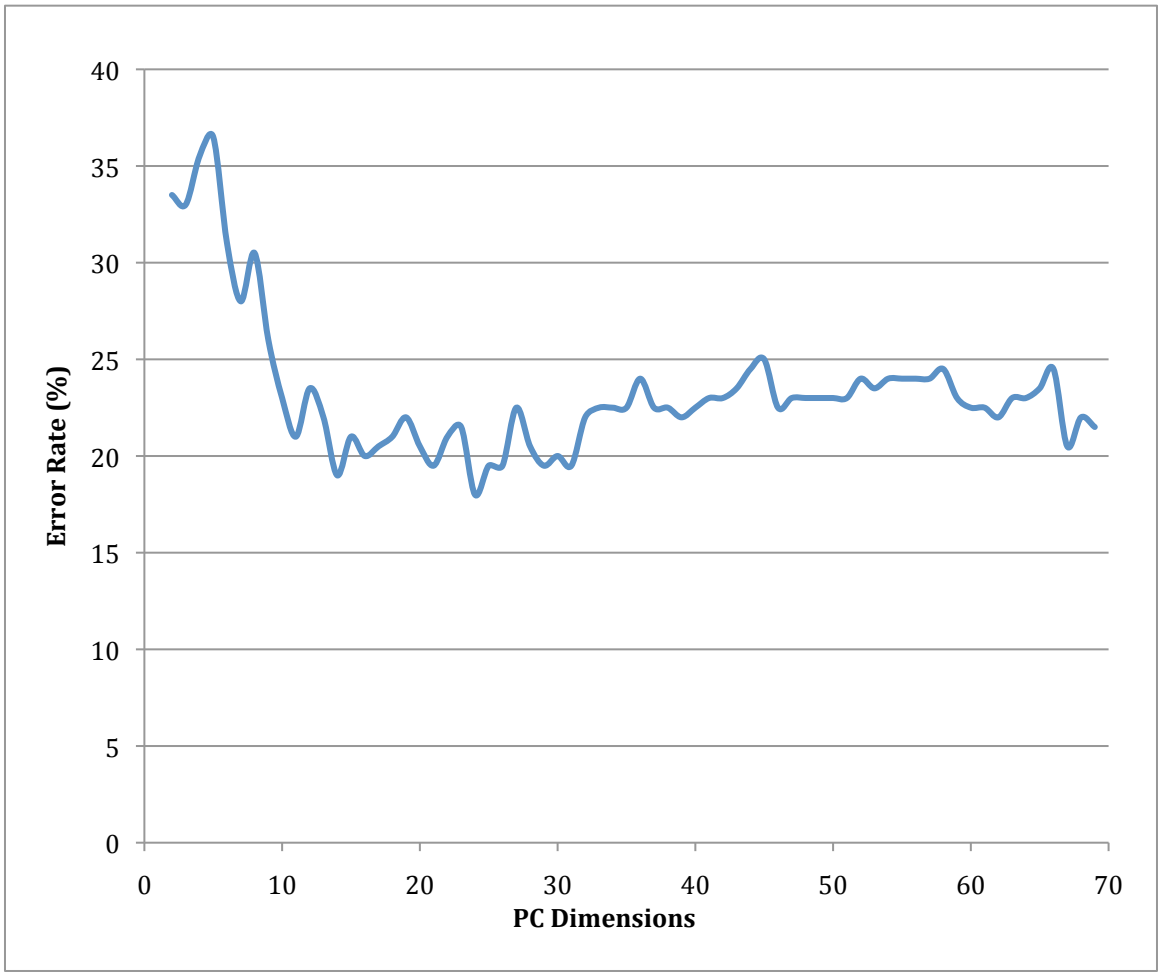


Figure 273: Graph of the float classification error rate versus PC dimensions for HOO-CV with PCA reduced CVA for the first set of 20 window glass first derivative (5-point smoothing) spectra (10 replicates), no data pretreatment.

Table 285: Float classification error rates for HOO-CV with PCA reduced CVA for the first set of 20 window glass first derivative (5-point smoothing) spectra (10 replicates), centered data. The smallest PC dimension with the minimum error rate is highlighted in yellow.

PCs	Error Rate (%)	PCs	Error Rate (%)	PCs	Error Rate (%)	PCs	Error Rate (%)	PCs	Error Rate (%)
2	34.50	16	19.00	30	20.00	44	22.50	58	24.00
3	33.50	17	19.00	31	20.50	45	23.50	59	23.50
4	34.00	18	20.50	32	21.50	46	24.50	60	22.00
5	34.00	19	21.00	33	20.50	47	23.50	61	22.00
6	31.00	20	21.00	34	21.50	48	23.50	62	23.00
7	28.00	21	21.50	35	22.00	49	23.50	63	23.50
8	28.50	22	21.50	36	22.00	50	23.50	64	23.00
9	28.00	23	23.50	37	22.50	51	23.50	65	24.00
10	27.00	24	22.00	38	22.50	52	24.00	66	22.50
11	23.50	25	19.50	39	23.50	53	24.00	67	21.50
12	22.50	26	19.00	40	22.00	54	24.00	68	23.00
13	20.00	27	19.50	41	22.00	55	24.00	69	22.00
14	19.50	28	18.00	42	22.50	56	23.00		
15	18.50	29	18.00	43	22.50	57	23.00		

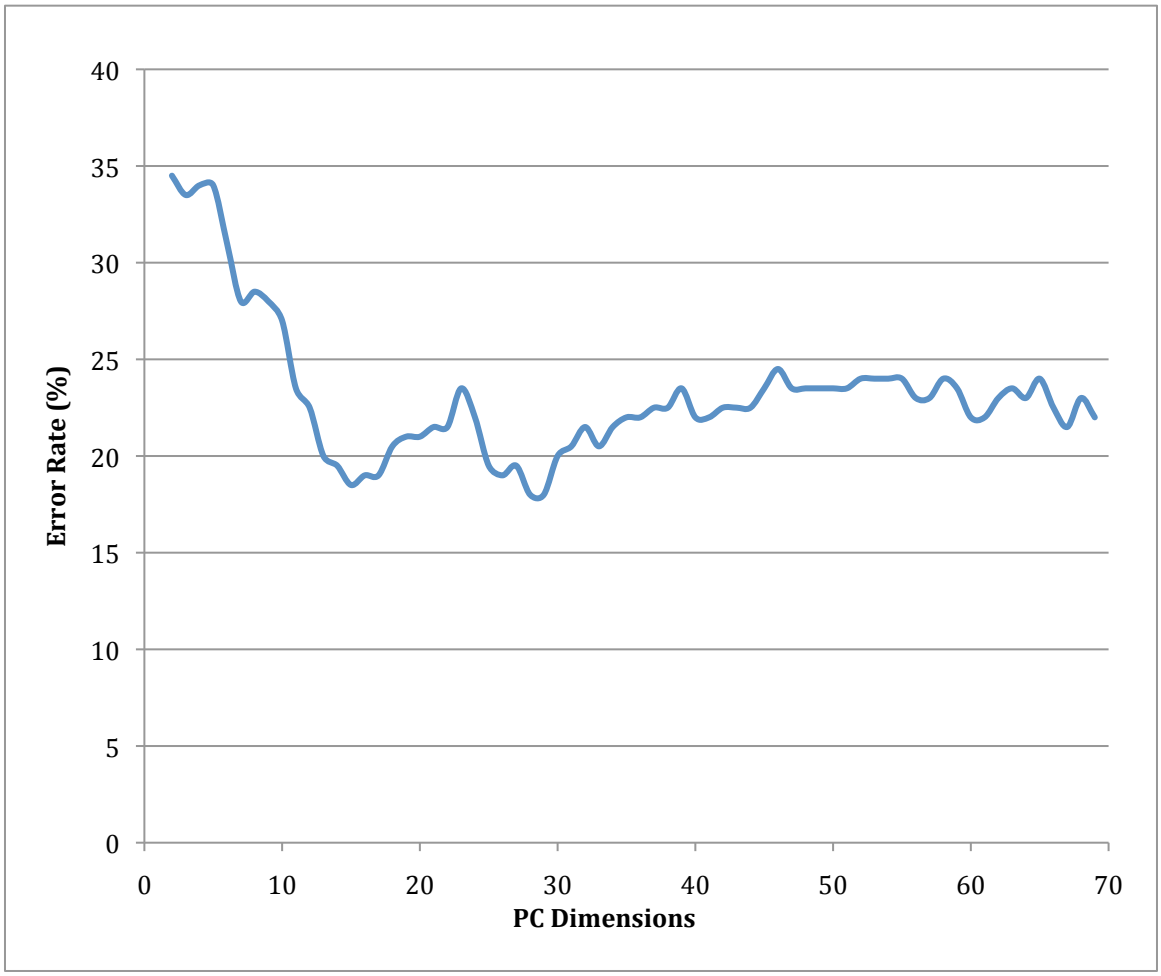


Figure 274: Graph of the float classification error rate versus PC dimensions for HOO-CV with PCA reduced CVA for the first set of 20 window glass first derivative (5-point smoothing) spectra (10 replicates), centered data.

Table 286: Float classification error rates for HOO-CV with PCA reduced CVA for the first set of 20 window glass first derivative (5-point smoothing) spectra (10 replicates), autoscaled data. The smallest PC dimension with the minimum error rate is highlighted in yellow.

PCs	Error Rate (%)	PCs	Error Rate (%)	PCs	Error Rate (%)	PCs	Error Rate (%)	PCs	Error Rate (%)
2	34.50	42	17.50	82	21.50	122	26.50	162	31.50
3	27.00	43	17.50	83	21.50	123	25.00	163	30.50
4	27.50	44	15.50	84	21.50	124	26.00	164	33.50
5	28.50	45	16.00	85	21.50	125	26.00	165	33.00
6	25.50	46	15.50	86	22.50	126	27.50	166	33.50
7	24.50	47	17.00	87	21.50	127	27.00	167	34.00
8	22.50	48	17.50	88	21.50	128	26.50	168	36.00
9	18.50	49	16.50	89	23.00	129	27.50	169	36.50
10	20.00	50	16.00	90	23.00	130	23.50	170	36.50
11	20.00	51	17.00	91	22.50	131	23.00	171	38.50
12	20.50	52	17.50	92	20.00	132	23.00	172	39.00
13	20.50	53	17.50	93	21.00	133	21.50	173	40.00
14	17.00	54	17.00	94	22.00	134	22.50	174	38.50
15	19.00	55	16.50	95	23.00	135	23.00	175	38.50
16	17.00	56	16.50	96	23.00	136	21.00	176	34.50
17	18.50	57	17.00	97	22.50	137	22.50	177	35.00
18	19.00	58	16.00	98	22.00	138	21.50	178	38.00
19	18.50	59	18.00	99	24.50	139	21.50	179	36.00
20	16.50	60	17.00	100	24.50	140	21.50	180	37.50
21	17.50	61	17.00	101	25.00	141	22.00	181	31.50
22	15.50	62	16.50	102	25.00	142	22.50	182	33.50
23	17.00	63	16.50	103	24.00	143	23.00	183	23.00
24	14.00	64	17.50	104	25.50	144	23.00	184	23.50
25	14.50	65	18.00	105	25.50	145	23.00	185	29.00
26	14.00	66	15.50	106	26.00	146	25.00	186	29.00
27	13.50	67	14.50	107	25.00	147	25.00	187	32.00
28	14.50	68	15.50	108	24.00	148	26.00	188	34.00
29	14.50	69	16.00	109	26.00	149	27.50	189	35.50
30	15.00	70	16.00	110	28.00	150	24.00	190	32.00
31	16.00	71	16.00	111	27.00	151	25.50	191	33.50
32	14.50	72	18.00	112	27.00	152	28.00	192	34.00
33	14.00	73	16.50	113	25.00	153	27.00	193	37.00
34	14.00	74	18.00	114	24.50	154	26.50	194	40.50
35	17.50	75	18.00	115	26.00	155	28.50	195	44.50
36	15.00	76	18.50	116	25.00	156	28.50	196	45.00
37	14.50	77	18.50	117	25.00	157	31.00	197	45.00
38	15.50	78	19.50	118	25.00	158	32.00	198	49.00

39	15.00	79	19.00	119	24.50	159	31.00	199	45.00
40	16.50	80	19.50	120	25.50	160	28.50		
41	17.50	81	19.50	121	26.00	161	28.50		

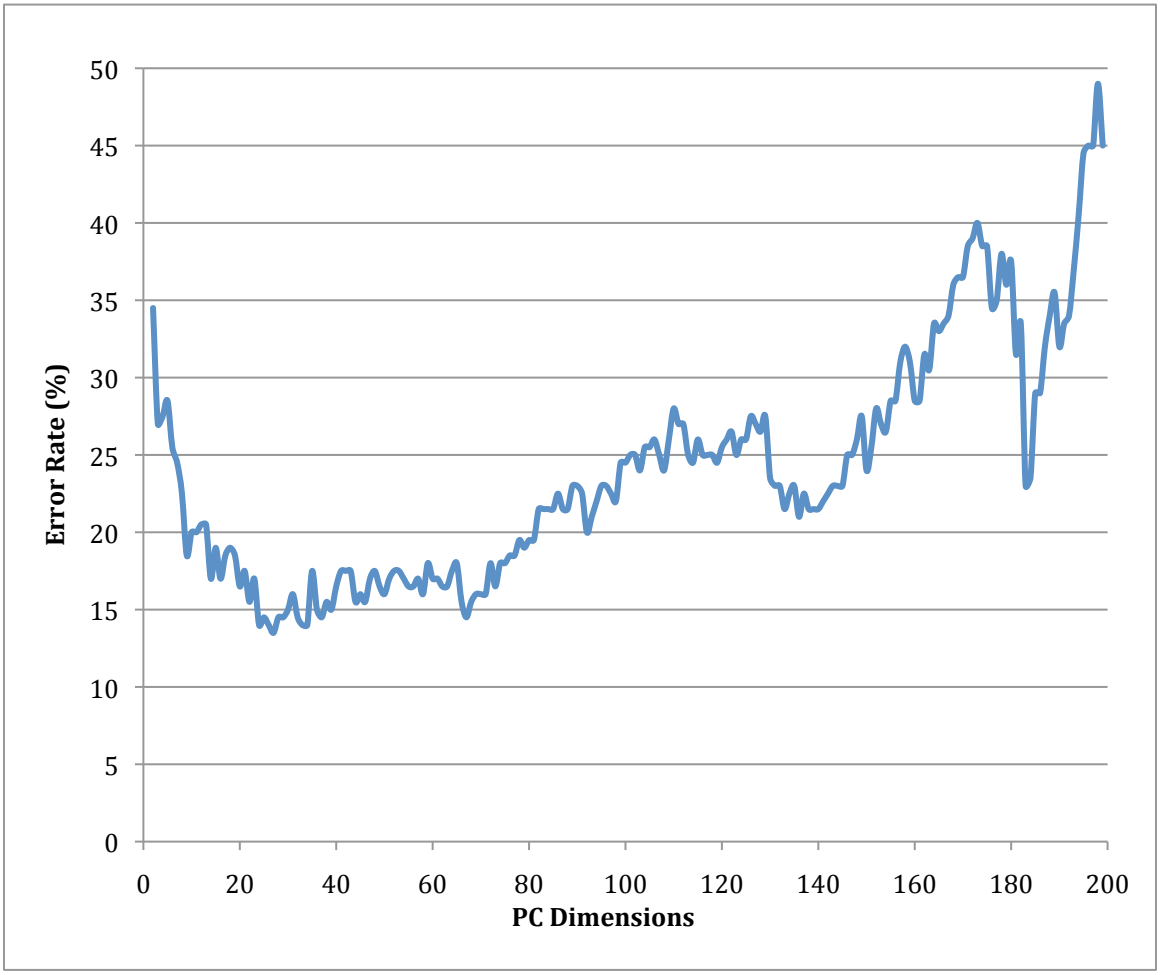


Figure 275: Graph of the float classification error rate versus PC dimensions for HOO-CV with PCA reduced CVA for the first set of 20 window glass first derivative (5-point smoothing) spectra (10 replicates), autoscaled data.

First Set, First Derivative (5-point smoothing) – Tempered Classification

Table 287: Tempered classification error rates for HOO-CV with PCA reduced CVA for the first set of 20 window glass first derivative (5-point smoothing) spectra (10 replicates), no data pretreatment. The smallest PC dimension with the minimum error rate is highlighted in yellow.

PCs	Error Rate (%)	PCs	Error Rate (%)	PCs	Error Rate (%)	PCs	Error Rate (%)	PCs	Error Rate (%)
2	28.50	16	27.00	30	23.50	44	24.50	58	20.50
3	28.50	17	29.50	31	24.50	45	18.00	59	18.50
4	28.50	18	28.50	32	24.50	46	17.50	60	19.00
5	29.50	19	24.00	33	25.00	47	17.50	61	18.00
6	31.00	20	24.00	34	25.00	48	18.00	62	18.50
7	30.50	21	24.50	35	25.00	49	18.00	63	18.50
8	29.50	22	23.50	36	26.00	50	18.00	64	18.00
9	30.00	23	25.00	37	26.00	51	17.50	65	16.50
10	31.50	24	24.00	38	25.50	52	19.00	66	16.50
11	25.00	25	23.00	39	26.00	53	17.50	67	17.50
12	25.50	26	20.50	40	26.00	54	17.50	68	17.00
13	25.00	27	21.00	41	22.00	55	17.50	69	18.50
14	25.50	28	23.00	42	23.50	56	19.00		
15	26.00	29	23.50	43	22.50	57	20.50		

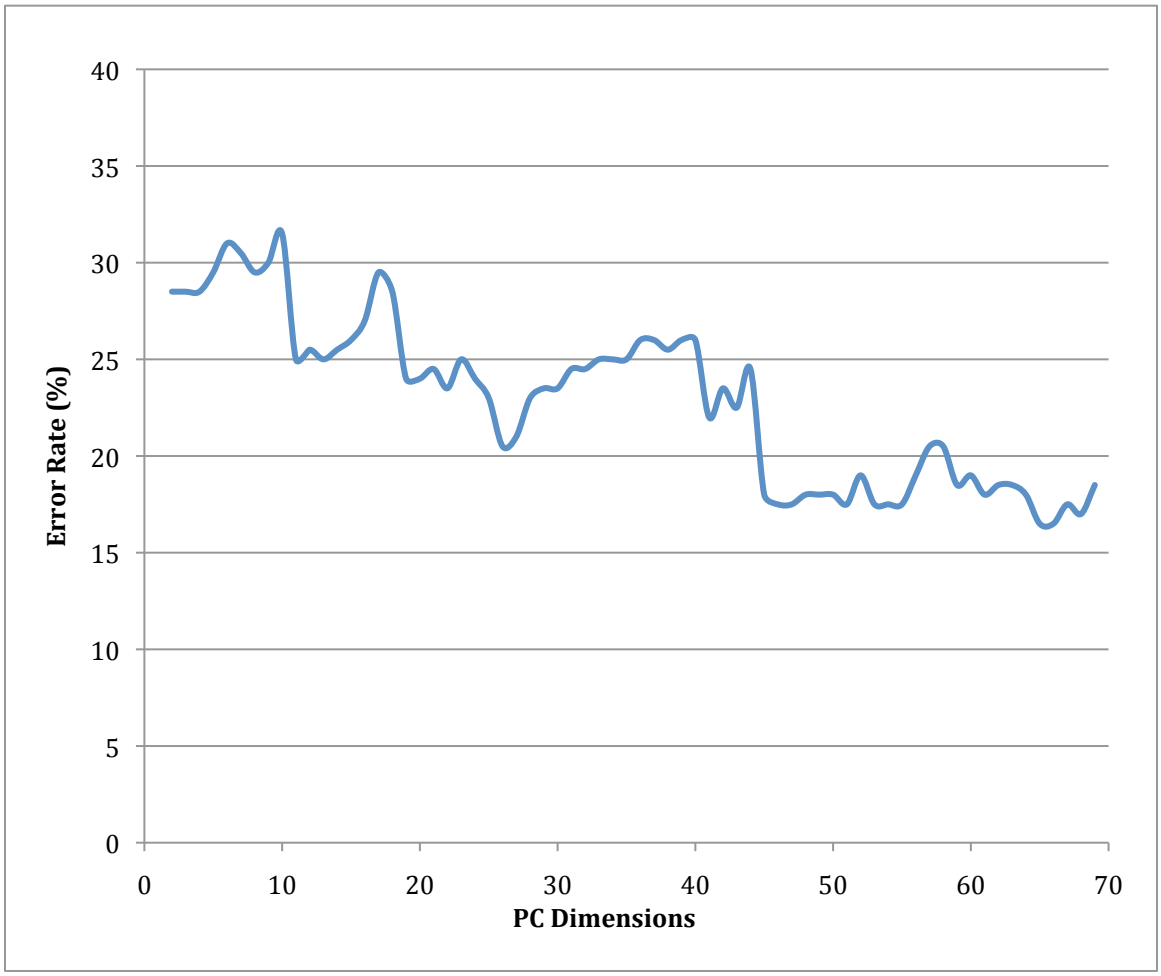


Figure 276: Graph of the tempered classification error rate versus PC dimensions for HOO-CV with PCA reduced CVA for the first set of 20 window glass first derivative (5-point smoothing) spectra (10 replicates), no data pretreatment.

Table 288: Tempered classification error rates for HOO-CV with PCA reduced CVA for the first set of 20 window glass first derivative (5-point smoothing) spectra (10 replicates), centered data. The smallest PC dimension with the minimum error rate is highlighted in yellow.

PCs	Error Rate (%)	PCs	Error Rate (%)	PCs	Error Rate (%)	PCs	Error Rate (%)	PCs	Error Rate (%)
2	27.00	16	27.50	30	25.00	44	22.50	58	19.50
3	29.00	17	30.00	31	24.50	45	18.50	59	19.00
4	31.00	18	30.50	32	24.50	46	18.00	60	20.00
5	29.50	19	23.50	33	24.50	47	18.00	61	19.50
6	28.00	20	23.50	34	24.50	48	17.50	62	21.00
7	30.00	21	23.00	35	25.50	49	17.50	63	19.00
8	30.50	22	25.50	36	25.50	50	17.50	64	20.00
9	32.50	23	25.00	37	25.50	51	17.50	65	19.00
10	25.00	24	20.50	38	26.00	52	18.00	66	18.00
11	25.00	25	20.00	39	26.00	53	18.00	67	18.50
12	23.50	26	23.00	40	26.00	54	17.50	68	18.50
13	24.50	27	24.00	41	23.50	55	17.50	69	18.50
14	25.00	28	23.50	42	24.50	56	18.00		
15	27.00	29	24.00	43	24.50	57	19.50		

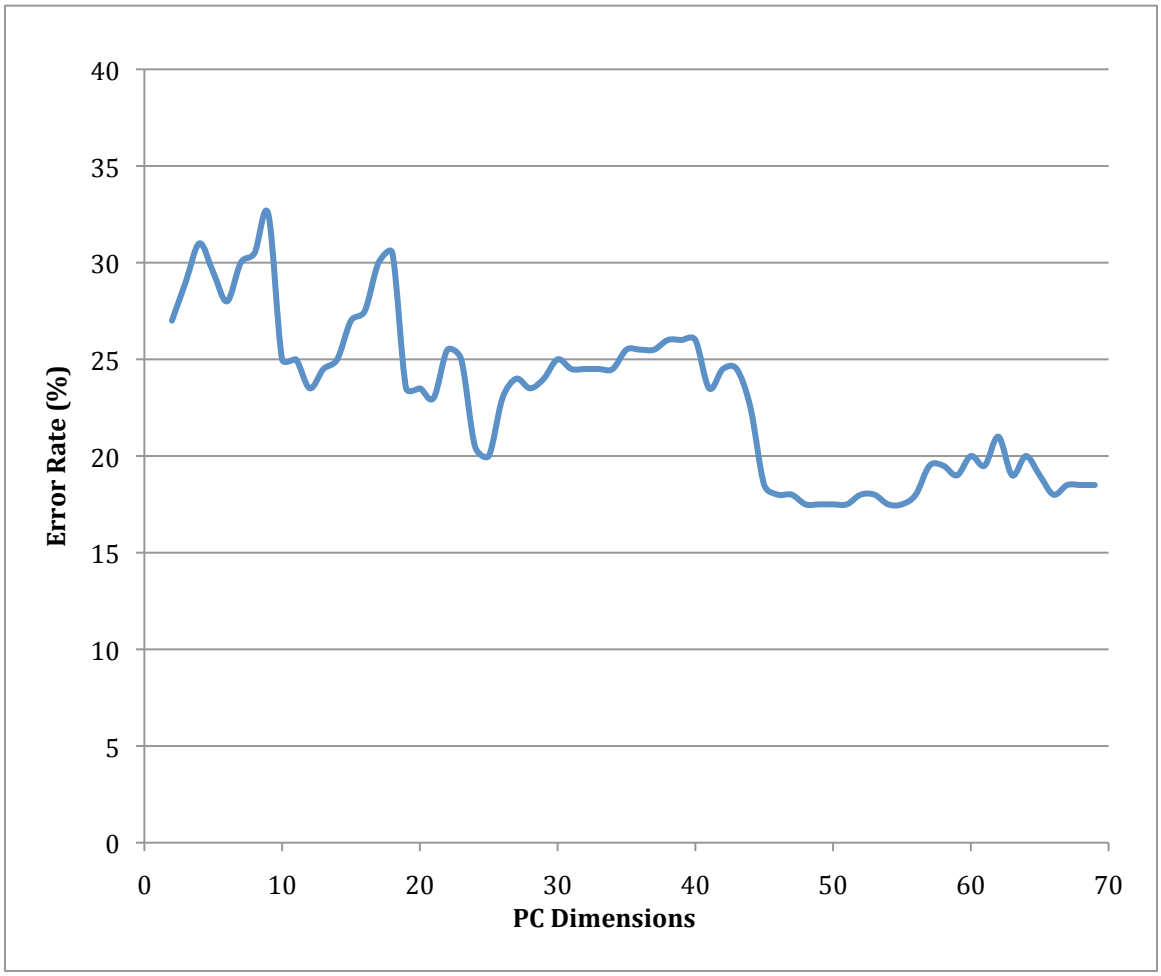


Figure 277: Graph of the tempered classification error rate versus PC dimensions for HOO-CV with PCA reduced CVA for the first set of 20 window glass first derivative (5-point smoothing) spectra (10 replicates), centered data.

Table 289: Tempered classification error rates for HOO-CV with PCA reduced CVA for the first set of 20 window glass first derivative (5-point smoothing) spectra (10 replicates), autoscaled data. The smallest PC dimension with the minimum error rate is highlighted in yellow.

PCs	Error Rate (%)	PCs	Error Rate (%)	PCs	Error Rate (%)	PCs	Error Rate (%)	PCs	Error Rate (%)
2	30.00	42	20.00	82	12.00	122	17.50	162	19.00
3	29.50	43	19.50	83	12.50	123	17.50	163	18.00
4	30.00	44	19.50	84	13.50	124	16.00	164	20.50
5	28.00	45	19.00	85	15.00	125	16.00	165	21.50
6	26.50	46	19.50	86	15.00	126	16.00	166	22.00
7	25.00	47	16.50	87	15.00	127	17.50	167	21.50
8	26.00	48	18.00	88	15.50	128	17.50	168	19.50
9	26.00	49	18.00	89	15.50	129	15.50	169	20.00
10	26.50	50	15.00	90	15.50	130	17.00	170	21.00
11	29.00	51	15.00	91	16.50	131	14.00	171	23.00
12	25.00	52	15.50	92	11.50	132	16.00	172	23.50
13	24.50	53	15.00	93	12.50	133	16.00	173	21.00
14	25.50	54	13.00	94	12.50	134	16.50	174	22.00
15	25.00	55	14.00	95	12.50	135	18.00	175	21.50
16	23.50	56	13.50	96	13.50	136	18.00	176	21.50
17	19.00	57	13.50	97	13.50	137	18.50	177	20.00
18	20.00	58	13.00	98	13.50	138	17.00	178	21.00
19	20.00	59	13.00	99	13.50	139	16.00	179	22.00
20	21.00	60	13.00	100	14.00	140	16.50	180	24.50
21	21.00	61	13.50	101	14.00	141	16.50	181	23.50
22	21.50	62	14.00	102	14.00	142	15.50	182	26.00
23	21.50	63	14.00	103	15.50	143	15.50	183	25.00
24	23.50	64	13.50	104	15.00	144	15.00	184	26.00
25	22.50	65	13.50	105	16.00	145	15.50	185	27.50
26	23.00	66	12.50	106	15.00	146	13.00	186	30.50
27	18.50	67	12.50	107	15.50	147	13.50	187	27.00
28	18.50	68	13.00	108	17.00	148	14.00	188	29.00
29	19.50	69	13.00	109	17.00	149	14.00	189	32.50
30	17.50	70	14.00	110	16.00	150	14.50	190	35.00
31	16.50	71	15.00	111	16.50	151	14.50	191	37.50
32	16.50	72	14.50	112	16.00	152	15.50	192	37.00
33	17.50	73	14.50	113	15.00	153	17.50	193	37.00
34	18.50	74	14.50	114	16.00	154	18.50	194	39.50
35	18.00	75	13.00	115	17.00	155	19.00	195	41.50
36	17.50	76	13.50	116	17.00	156	20.00	196	41.00
37	18.00	77	12.50	117	17.00	157	14.50	197	47.50

38	18.00	78	12.50	118	16.00	158	15.50	198	51.00
39	18.00	79	14.50	119	17.00	159	16.00	199	40.00
40	18.00	80	12.50	120	17.50	160	15.00		
41	19.00	81	12.50	121	17.00	161	16.50		

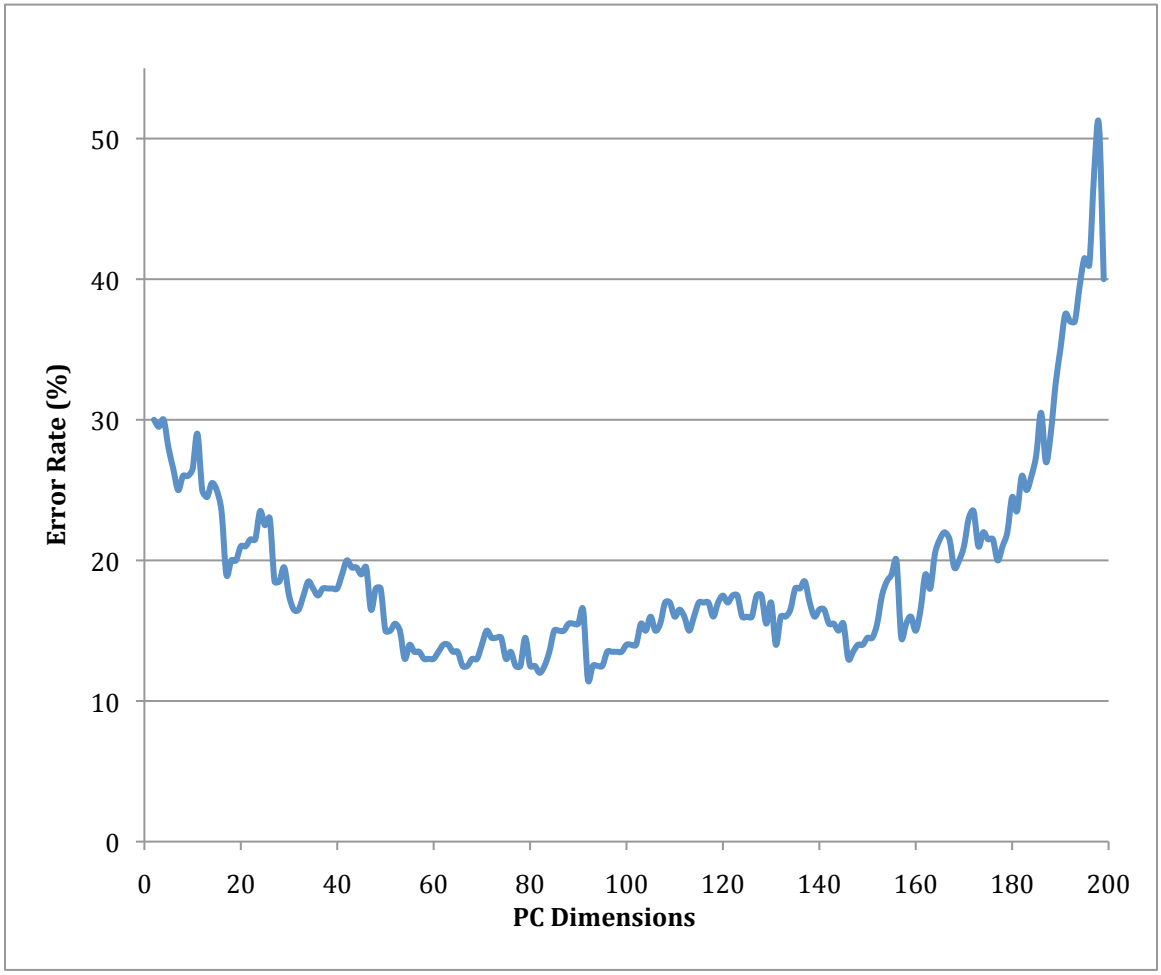


Figure 278: Graph of the tempered classification error rate versus PC dimensions for HOO-CV with PCA reduced CVA for the first set of 20 window glass first derivative (5-point smoothing) spectra (10 replicates), autoscaled data.

E. HOO-CV PCA-CVA Results for the First Derivative Spectra (9-Point Smoothing)

First Set, First Derivative (9-point smoothing) - Discrimination

Table 290: Discrimination error rates for HOO-CV with PCA reduced CVA for the first set of 30 glass first derivative (9-point smoothing) spectra (10 replicates), no data pretreatment. The smallest PC dimension with the minimum error rate is highlighted in yellow.

PCs	Error Rate (%)	PCs	Error Rate (%)	PCs	Error Rate (%)	PCs	Error Rate (%)	PCs	Error Rate (%)
2	94.67	9	64.00	16	42.67	23	28.00	30	23.00
3	94.33	10	59.00	17	38.67	24	26.67	31	21.00
4	93.67	11	57.00	18	39.00	25	25.00	32	18.67
5	90.67	12	50.00	19	35.00	26	24.33	33	18.33
6	80.67	13	44.33	20	33.33	27	23.67	34	18.33
7	78.67	14	42.67	21	31.33	28	22.33	35	16.67
8	78.00	15	44.00	22	30.33	29	22.00	36	16.00

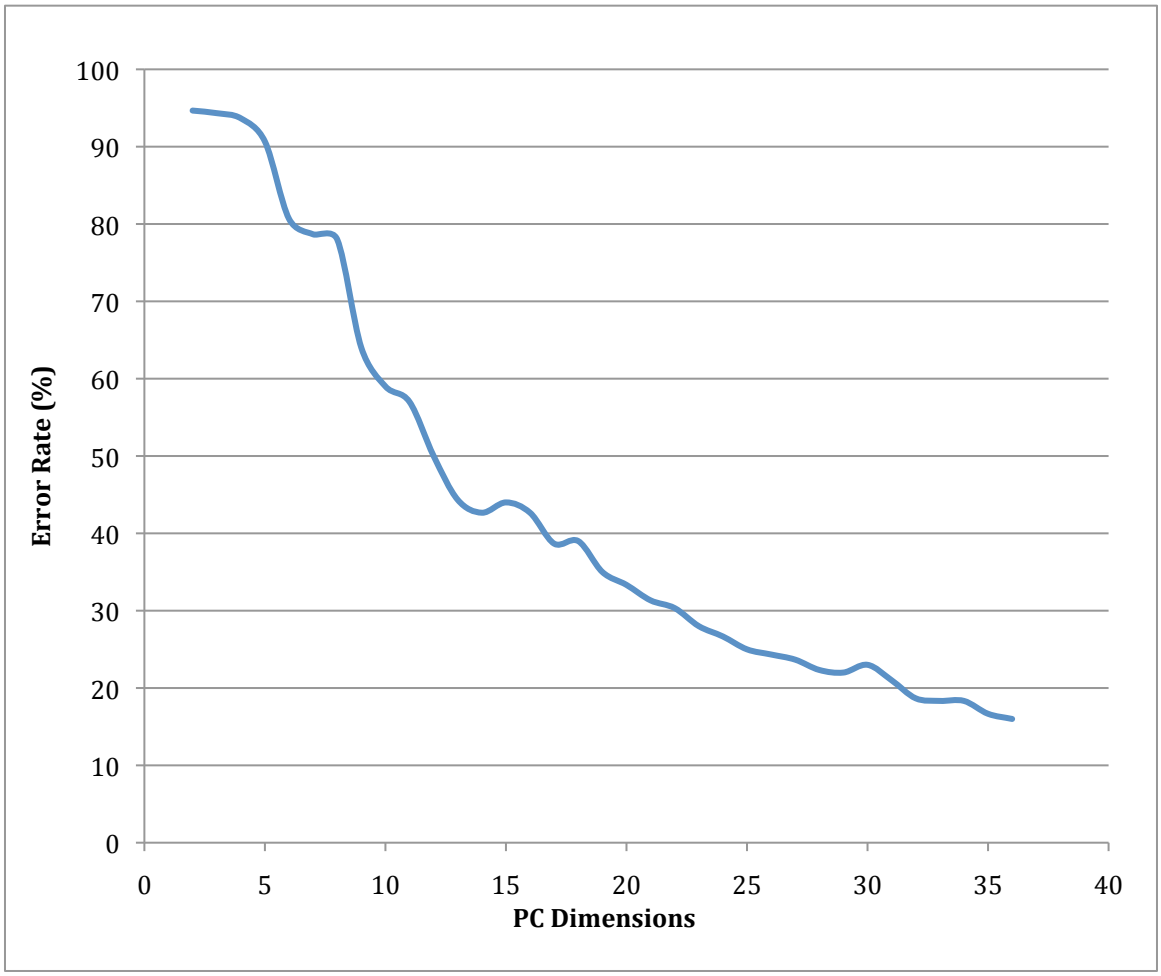


Figure 279: Graph of the discrimination error rate versus PC dimensions for HOO-CV with PCA reduced CVA for the first set of 30 glass first derivative (9-point smoothing) spectra (10 replicates), no data pretreatment.

Table 291: Discrimination error rates for HOO-CV with PCA reduced CVA for the first set of 30 glass first derivative (9-point smoothing) spectra (10 replicates), centered data. The smallest PC dimension with the minimum error rate is highlighted in yellow.

PCs	Error Rate (%)	PCs	Error Rate (%)	PCs	Error Rate (%)	PCs	Error Rate (%)	PCs	Error Rate (%)
2	93.33	9	64.33	16	43.00	23	27.33	30	24.00
3	94.33	10	59.00	17	39.33	24	24.67	31	19.67
4	93.67	11	56.67	18	38.33	25	24.00	32	18.33
5	90.33	12	49.33	19	34.00	26	23.33	33	17.67
6	80.67	13	44.33	20	32.67	27	23.00	34	18.33
7	80.67	14	43.00	21	31.33	28	22.67	35	16.67
8	77.67	15	44.00	22	29.67	29	22.33	36	16.00

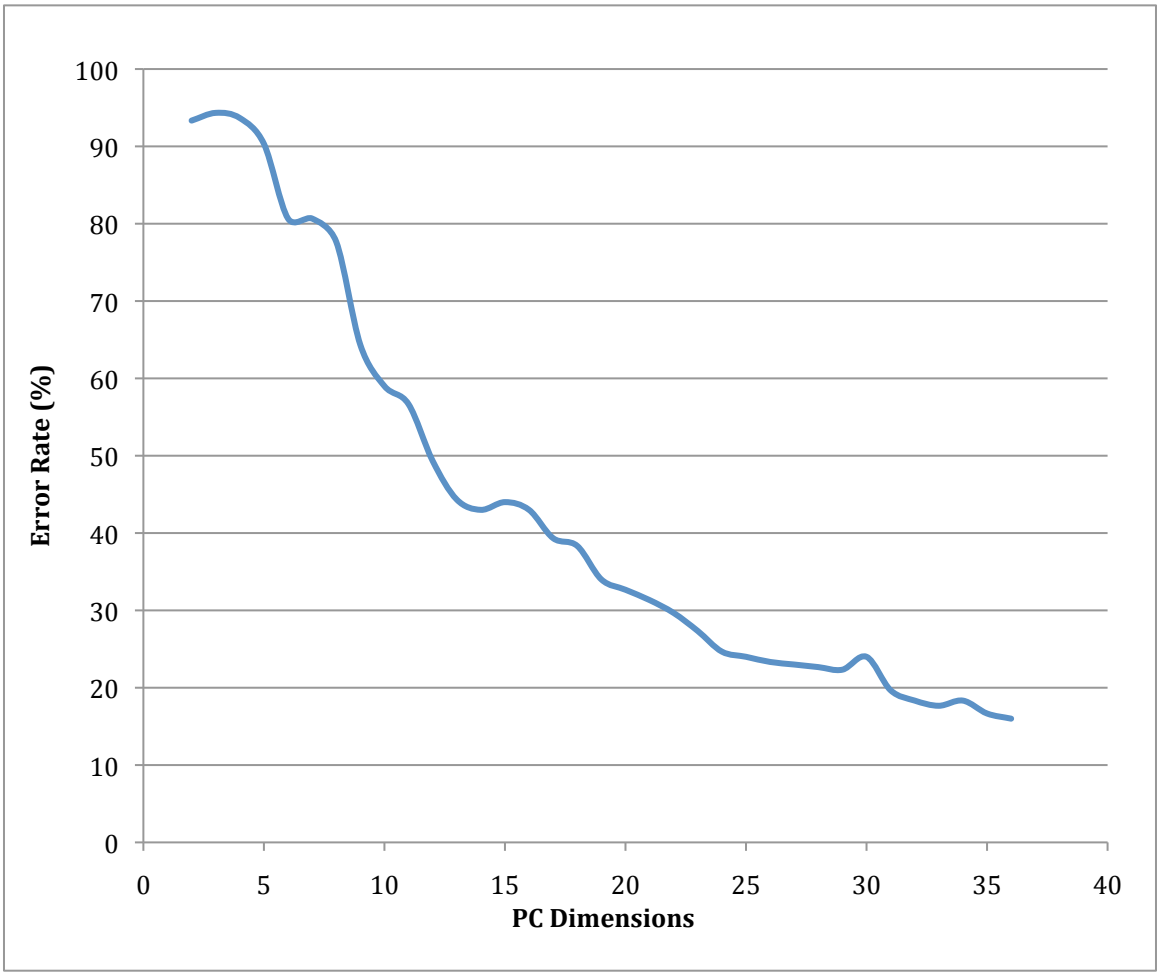


Figure 280: Graph of the discrimination error rate versus PC dimensions for HOO-CV with PCA reduced CVA for the first set of 30 glass first derivative (9-point smoothing) spectra (10 replicates), centered data.

Table 292: Discrimination error rates for HOO-CV with PCA reduced CVA for the first set of 30 glass first derivative (9-point smoothing) spectra (10 replicates), autoscaled data. The smallest PC dimension with the minimum error rate is highlighted in yellow.

PCs	Error Rate (%)	PCs	Error Rate (%)	PCs	Error Rate (%)	PCs	Error Rate (%)	PCs	Error Rate (%)
2	94.33	57	9.33	112	5.67	167	8.67	222	13.00
3	87.67	58	10.00	113	6.00	168	9.00	223	12.67
4	78.33	59	8.33	114	6.67	169	9.00	224	14.00
5	67.33	60	8.33	115	7.00	170	8.67	225	14.00
6	57.33	61	8.67	116	6.33	171	9.33	226	14.33
7	53.00	62	8.33	117	6.33	172	8.67	227	14.33
8	51.67	63	8.67	118	6.00	173	8.67	228	14.00
9	44.00	64	8.00	119	5.67	174	9.33	229	15.00
10	41.33	65	8.00	120	5.67	175	10.33	230	15.67
11	36.67	66	8.67	121	5.67	176	10.00	231	16.67
12	37.33	67	8.67	122	5.33	177	8.33	232	19.00
13	37.00	68	9.00	123	5.00	178	8.67	233	17.67
14	36.00	69	9.00	124	6.00	179	8.33	234	17.33
15	34.67	70	8.67	125	6.33	180	8.00	235	18.67
16	32.00	71	8.00	126	6.00	181	7.67	236	20.00
17	26.33	72	7.67	127	5.67	182	8.33	237	20.33
18	26.67	73	7.00	128	5.00	183	8.33	238	20.33
19	24.67	74	6.67	129	5.33	184	9.33	239	22.33
20	24.33	75	6.67	130	5.33	185	9.00	240	20.00
21	24.67	76	6.67	131	5.67	186	9.00	241	20.67
22	21.00	77	7.00	132	5.33	187	8.33	242	22.00
23	21.00	78	7.00	133	5.33	188	8.33	243	23.33
24	19.67	79	7.67	134	6.00	189	8.67	244	25.67
25	21.33	80	7.33	135	6.33	190	9.00	245	24.67
26	20.67	81	7.67	136	6.00	191	9.67	246	25.33
27	20.00	82	8.00	137	6.00	192	10.00	247	28.00
28	21.33	83	7.67	138	6.00	193	9.67	248	28.67
29	20.33	84	7.67	139	5.67	194	10.00	249	31.67
30	20.33	85	8.00	140	6.33	195	9.33	250	33.67
31	18.33	86	8.67	141	6.00	196	8.00	251	32.67
32	16.67	87	8.33	142	7.33	197	8.33	252	33.67
33	15.33	88	8.00	143	8.33	198	8.67	253	37.33
34	18.00	89	7.33	144	8.33	199	9.33	254	39.33
35	17.00	90	7.67	145	8.33	200	9.33	255	36.00
36	15.67	91	7.67	146	8.00	201	9.67	256	38.00
37	14.67	92	8.00	147	8.33	202	9.67	257	39.00
38	15.00	93	8.33	148	8.67	203	10.33	258	41.33

39	14.33	94	8.33	149	8.33	204	12.00	259	39.67
40	13.33	95	8.33	150	7.67	205	12.00	260	44.67
41	12.67	96	8.67	151	8.00	206	11.00	261	48.67
42	12.00	97	8.67	152	8.33	207	11.33	262	52.33
43	12.33	98	8.00	153	7.67	208	13.00	263	55.33
44	11.67	99	8.67	154	8.00	209	11.67	264	57.67
45	10.33	100	8.67	155	8.00	210	11.33	265	60.00
46	11.00	101	8.33	156	7.67	211	11.00	266	70.00
47	9.67	102	8.00	157	8.33	212	11.33	267	74.33
48	10.00	103	8.00	158	8.33	213	12.00	268	81.00
49	10.33	104	8.00	159	8.67	214	10.67	269	89.67
50	11.33	105	8.67	160	8.33	215	10.67	270	83.33
51	11.00	106	8.33	161	8.67	216	9.00	271	88.67
52	11.33	107	8.00	162	9.00	217	10.33	272	71.67
53	10.67	108	7.33	163	8.67	218	10.67	273	82.33
54	10.00	109	7.67	164	8.00	219	10.33		
55	9.33	110	7.00	165	9.00	220	11.00		
56	9.67	111	6.67	166	8.67	221	12.00		

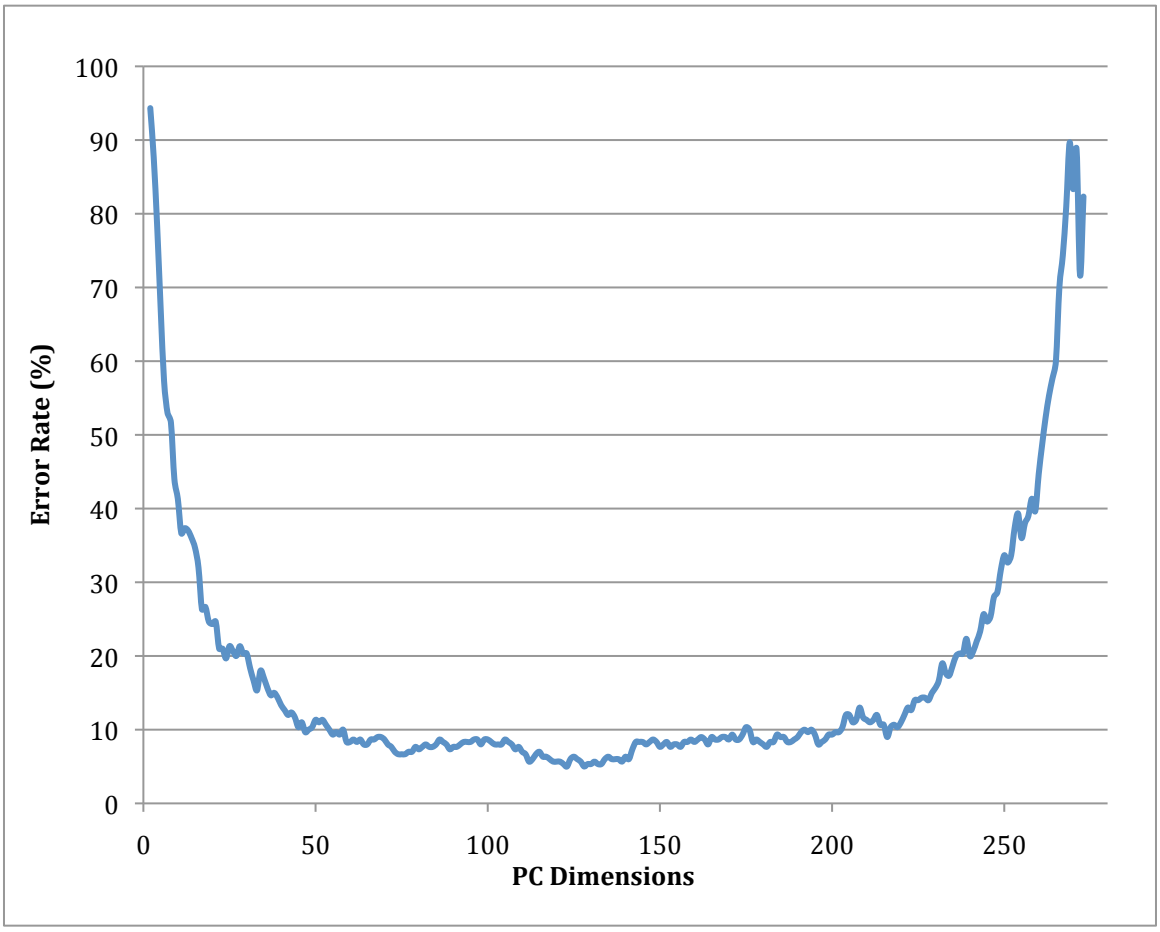


Figure 281: Graph of the discrimination error rate versus PC dimensions for HOO-CV with PCA reduced CVA for the first set of 30 glass first derivative (9-point smoothing) spectra (10 replicates), autoscaled data.

First Set, First Derivative (9-point smoothing) – Classification (automotive, architectural or container)

Table 293: Classification (automotive, architectural or container) error rates for HOO-CV with PCA reduced CVA for the first set of 30 glass first derivative (9-point smoothing) spectra (10 replicates), no data pretreatment. The smallest PC dimension with the minimum error rate is highlighted in yellow.

PCs	Error Rate (%)	PCs	Error Rate (%)	PCs	Error Rate (%)	PCs	Error Rate (%)	PCs	Error Rate (%)
2	63.67	10	28.67	18	21.00	26	14.67	34	17.00
3	64.67	11	26.33	19	18.67	27	15.67	35	17.33
4	57.67	12	25.67	20	17.67	28	15.00	36	16.67
5	54.00	13	27.67	21	17.00	29	14.33	37	16.67
6	46.67	14	26.33	22	16.00	30	14.67	38	16.67
7	44.33	15	23.67	23	17.00	31	14.33		
8	45.67	16	24.33	24	15.33	32	16.33		
9	26.33	17	21.33	25	15.67	33	16.67		

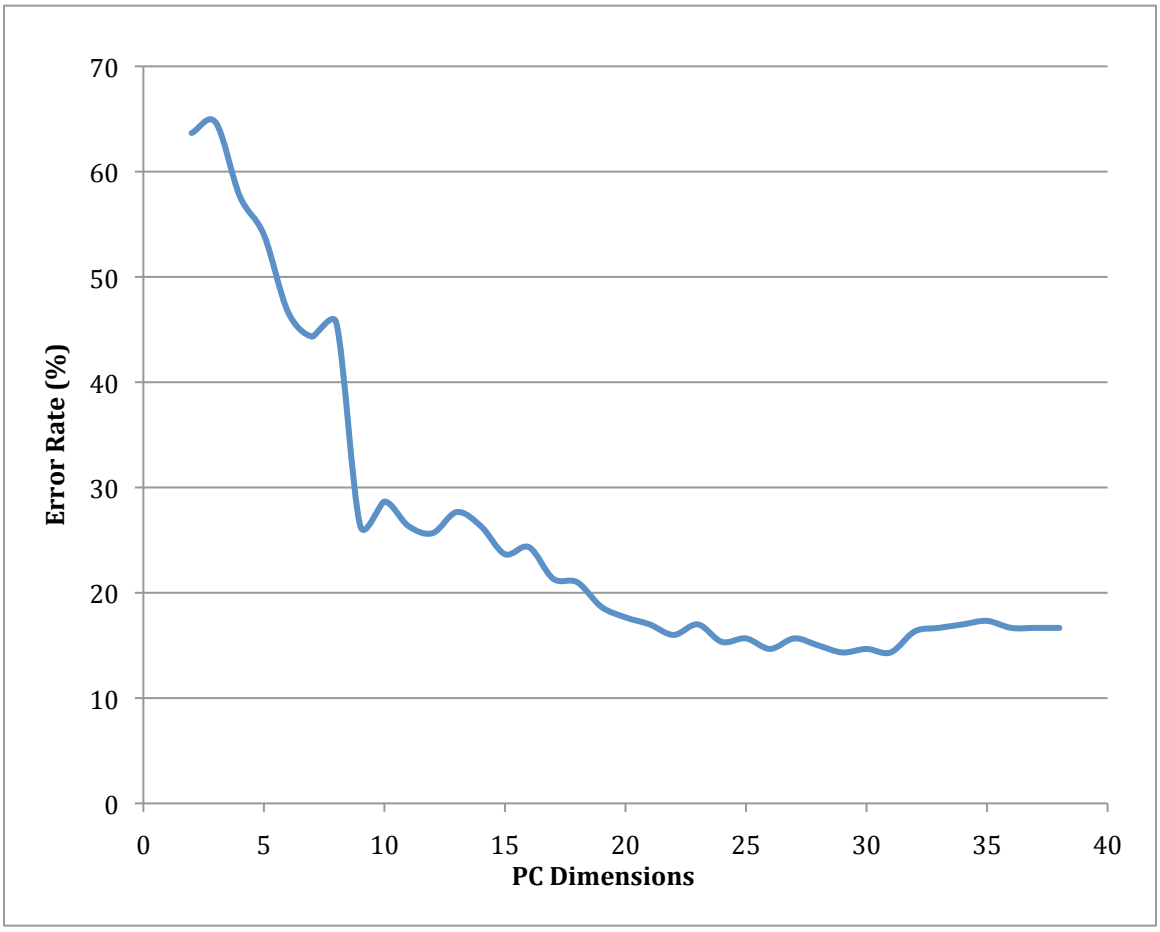


Figure 282: Graph of the classification (automotive, architectural or container) error rate versus PC dimensions for HOO-CV with PCA reduced CVA for the first set of 30 glass first derivative (9-point smoothing) spectra (10 replicates), no data pretreatment.

Table 294: Classification (automotive, architectural or container) error rates for HOO-CV with PCA reduced CVA for the first set of 30 glass first derivative (9-point smoothing) spectra (10 replicates), centered data. The smallest PC dimension with the minimum error rate is highlighted in yellow.

PCs	Error Rate (%)	PCs	Error Rate (%)	PCs	Error Rate (%)	PCs	Error Rate (%)	PCs	Error Rate (%)
2	64.00	10	28.67	18	21.00	26	14.67	34	17.33
3	62.67	11	26.67	19	19.67	27	16.00	35	17.67
4	58.67	12	25.67	20	17.67	28	15.00	36	16.67
5	53.67	13	27.67	21	16.67	29	15.00	37	16.67
6	47.33	14	26.67	22	15.33	30	15.67	38	16.67
7	44.67	15	23.33	23	15.67	31	15.67		
8	45.00	16	24.67	24	14.67	32	16.33		
9	27.00	17	21.33	25	15.33	33	16.33		

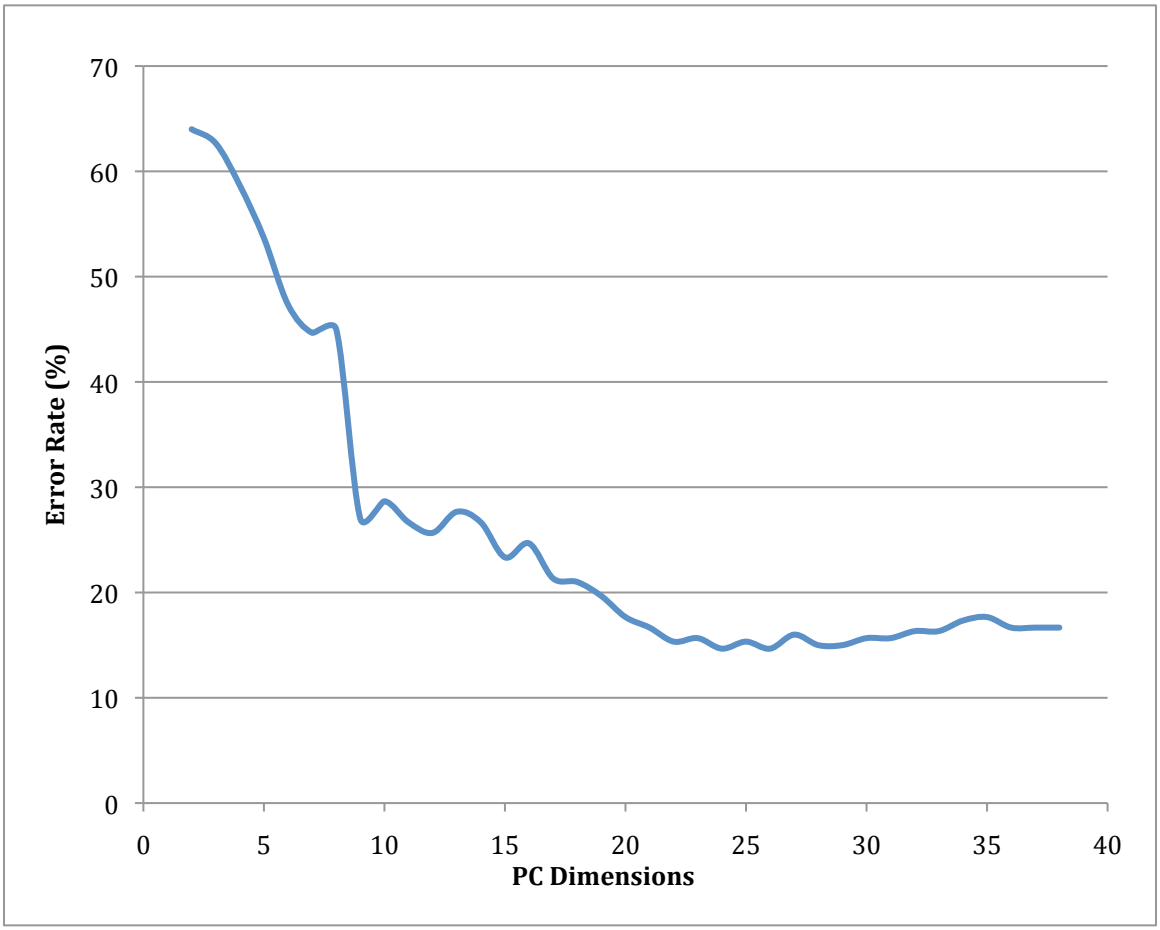


Figure 283: Graph of the classification (automotive, architectural or container) error rate versus PC dimensions for HOO-CV with PCA reduced CVA for the first set of 30 glass first derivative (9-point smoothing) spectra (10 replicates), centered data.

Table 295: Classification (automotive, architectural or container) error rates for HOO-CV with PCA reduced CVA for the first set of 30 glass first derivative (9-point smoothing) spectra (10 replicates), autoscaled data. The smallest PC dimension with the minimum error rate is highlighted in yellow.

PCs	Error Rate (%)	PCs	Error Rate (%)	PCs	Error Rate (%)	PCs	Error Rate (%)	PCs	Error Rate (%)
2	60.67	60	14.67	118	16.67	176	19.33	234	23.33
3	54.00	61	14.33	119	16.33	177	19.33	235	23.67
4	37.00	62	15.33	120	16.67	178	19.67	236	23.67
5	29.67	63	15.00	121	16.00	179	18.00	237	24.00
6	28.00	64	15.67	122	16.00	180	18.67	238	24.33
7	28.33	65	15.00	123	16.33	181	17.00	239	24.33
8	29.00	66	15.33	124	16.33	182	17.33	240	25.00
9	25.67	67	15.67	125	16.67	183	18.33	241	23.67
10	26.00	68	16.00	126	16.67	184	18.67	242	23.00
11	26.33	69	15.33	127	16.67	185	19.33	243	24.67
12	25.33	70	15.33	128	17.00	186	20.33	244	25.00
13	26.00	71	16.00	129	17.33	187	20.33	245	26.33
14	27.33	72	15.33	130	17.67	188	20.67	246	25.67
15	27.33	73	15.67	131	17.00	189	20.33	247	27.67
16	25.67	74	17.00	132	17.00	190	20.00	248	27.33
17	22.33	75	17.00	133	17.33	191	21.67	249	29.00
18	18.33	76	16.33	134	17.67	192	21.67	250	29.00
19	16.67	77	15.67	135	18.00	193	21.67	251	27.33
20	17.33	78	16.00	136	17.67	194	21.67	252	27.33
21	17.00	79	16.33	137	17.67	195	19.67	253	28.33
22	17.00	80	16.00	138	17.67	196	19.33	254	27.67
23	19.00	81	16.67	139	18.00	197	19.67	255	25.67
24	18.67	82	17.00	140	17.67	198	20.00	256	27.33
25	18.67	83	17.00	141	17.33	199	20.33	257	28.33
26	17.33	84	18.00	142	16.33	200	19.67	258	29.67
27	17.67	85	18.67	143	17.00	201	19.00	259	29.67
28	18.00	86	17.33	144	17.67	202	17.67	260	28.67
29	18.00	87	17.67	145	16.67	203	18.00	261	29.33
30	17.67	88	18.00	146	17.67	204	19.00	262	29.67
31	16.67	89	18.67	147	17.33	205	19.00	263	31.67
32	16.33	90	16.00	148	17.00	206	18.00	264	31.67
33	16.33	91	16.33	149	18.00	207	18.33	265	31.33
34	15.00	92	15.33	150	18.00	208	18.33	266	31.33
35	15.00	93	15.33	151	16.67	209	17.67	267	32.33
36	15.67	94	14.67	152	16.67	210	18.67	268	33.33
37	16.67	95	15.67	153	17.67	211	18.67	269	35.00

38	17.67	96	15.00	154	17.33	212	20.00	270	31.33
39	18.00	97	15.33	155	17.67	213	20.00	271	33.67
40	18.00	98	15.67	156	18.67	214	21.67	272	32.67
41	17.67	99	15.33	157	18.33	215	22.00	273	34.67
42	17.33	100	16.33	158	17.67	216	22.33	274	38.00
43	17.33	101	16.33	159	18.67	217	23.00	275	35.00
44	16.67	102	16.33	160	18.33	218	23.33	276	36.00
45	17.33	103	16.00	161	18.33	219	24.33	277	40.33
46	16.67	104	16.33	162	18.33	220	24.33	278	40.67
47	16.00	105	16.67	163	18.00	221	24.67	279	41.67
48	16.00	106	16.33	164	17.00	222	24.00	280	41.00
49	17.33	107	16.67	165	17.00	223	23.00	281	43.00
50	17.00	108	15.67	166	18.00	224	23.67	282	44.67
51	16.67	109	17.00	167	18.33	225	24.33	283	41.67
52	17.67	110	16.33	168	18.00	226	24.33	284	42.67
53	17.00	111	16.00	169	20.00	227	25.67	285	42.33
54	16.67	112	16.00	170	17.33	228	24.67	286	41.33
55	18.00	113	16.67	171	17.00	229	25.67	287	44.33
56	18.33	114	17.00	172	18.67	230	23.67		
57	13.33	115	16.33	173	18.67	231	22.00		
58	14.33	116	16.33	174	20.33	232	23.33		
59	15.00	117	16.67	175	20.33	233	22.67		

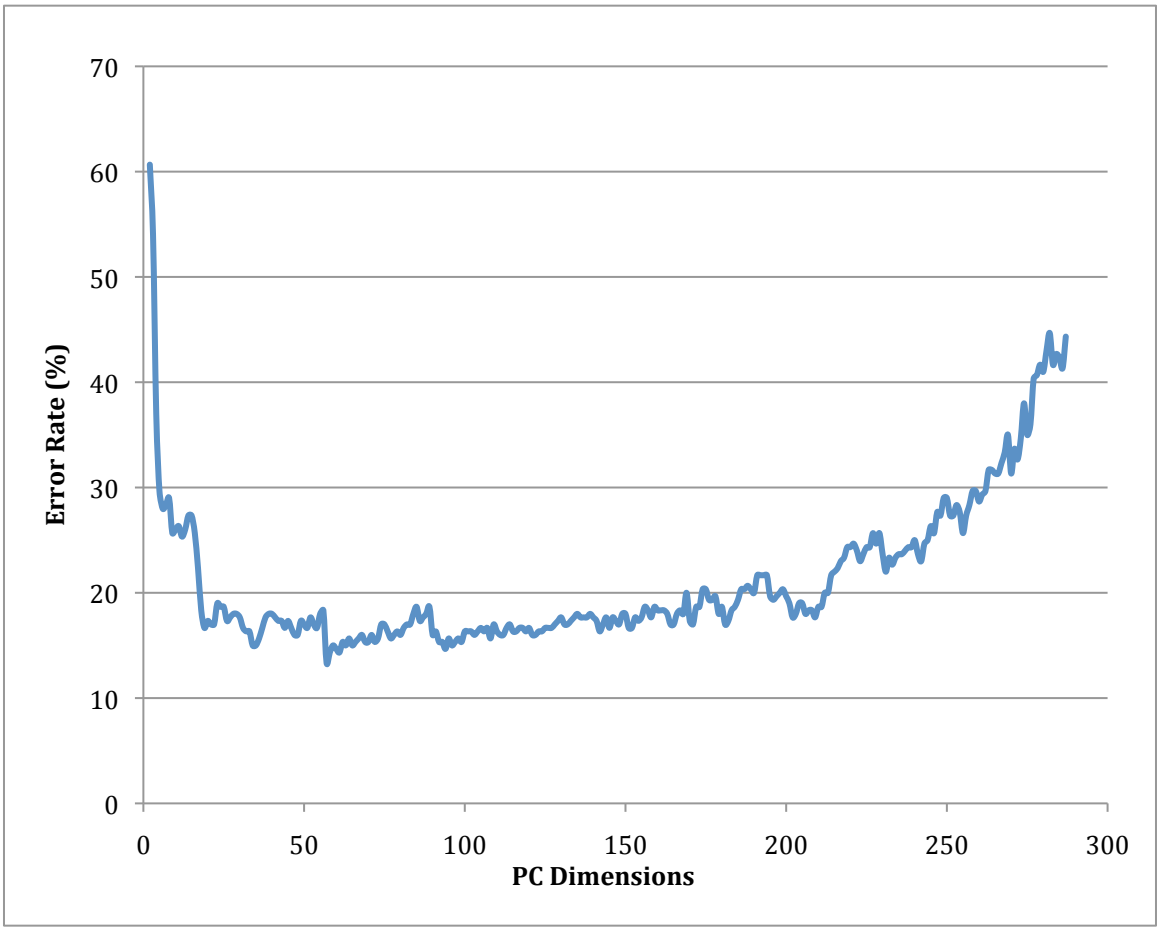


Figure 284: Graph of the classification (automotive, architectural or container) error rate versus PC dimensions for HOO-CV with PCA reduced CVA for the first set of 30 glass first derivative (9-point smoothing) spectra (10 replicates), autoscaled data.

First Set, First Derivative (9-point smoothing) – Classification (window or container)

Table 296: Classification (window or container) error rates for HOO-CV with PCA reduced CVA for the first set of 30 glass first derivative (9-point smoothing) spectra (10 replicates), no data pretreatment. The smallest PC dimension with the minimum error rate is highlighted in yellow.

PCs	Error Rate (%)	PCs	Error Rate (%)	PCs	Error Rate (%)	PCs	Error Rate (%)	PCs	Error Rate (%)
2	33.33	10	3.67	18	4.00	26	4.00	34	3.67
3	33.67	11	3.67	19	4.00	27	4.00	35	3.67
4	35.00	12	3.67	20	3.67	28	3.67	36	3.67
5	30.00	13	3.67	21	4.00	29	3.67	37	4.00
6	23.67	14	3.67	22	4.00	30	3.67	38	3.67
7	16.00	15	3.67	23	4.00	31	3.67		
8	17.00	16	3.67	24	4.00	32	3.33		
9	4.33	17	4.00	25	4.00	33	3.33		

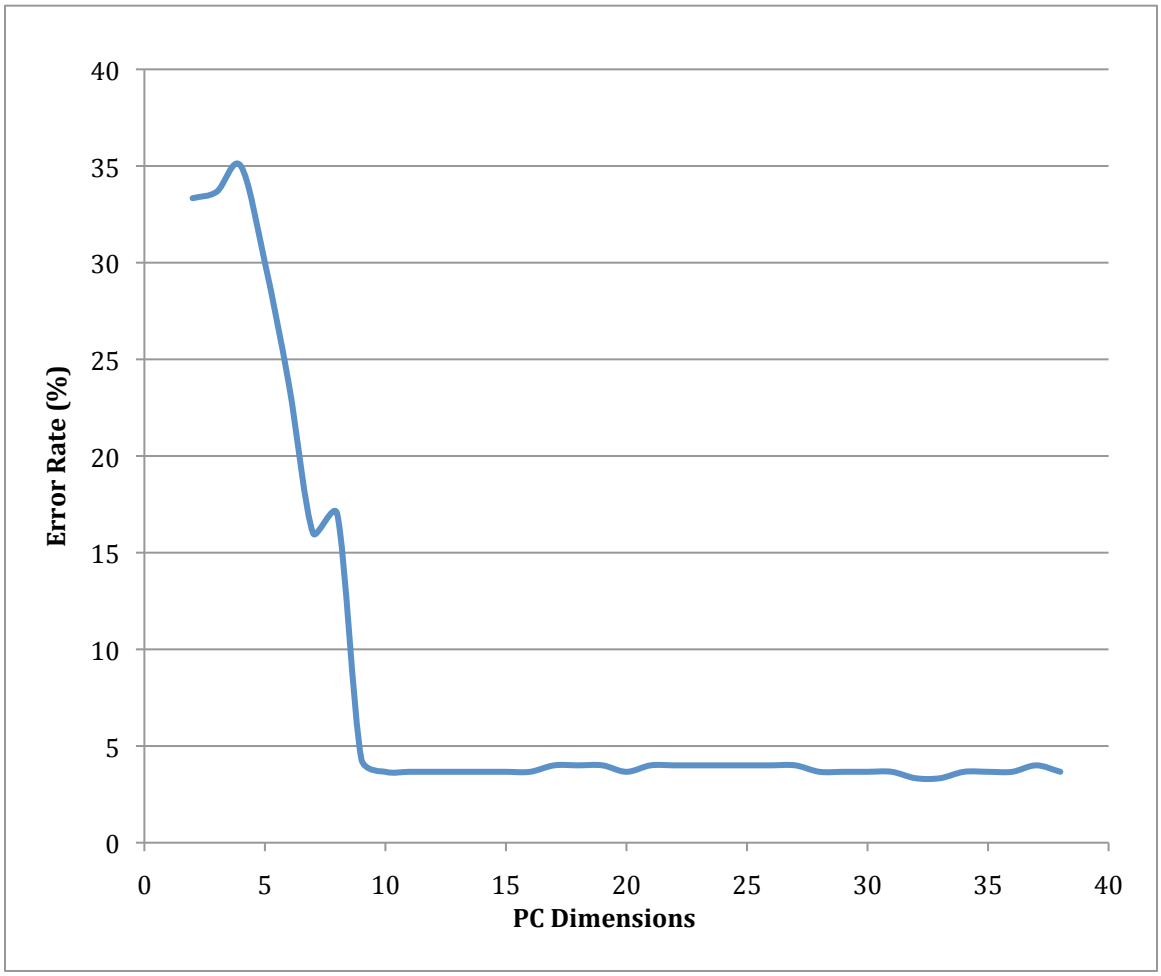


Figure 285: Graph of the classification (window or container) error rate versus PC dimensions for HOO-CV with PCA reduced CVA for the first set of 30 glass first derivative (9-point smoothing) spectra (10 replicates), no data pretreatment.

Table 297: Classification (window or container) error rates for HOO-CV with PCA reduced CVA for the first set of 30 glass first derivative (9-point smoothing) spectra (10 replicates), centered data. The smallest PC dimension with the minimum error rate is highlighted in yellow.

PCs	Error Rate (%)	PCs	Error Rate (%)	PCs	Error Rate (%)	PCs	Error Rate (%)	PCs	Error Rate (%)
2	33.33	10	3.67	18	4.00	26	4.00	34	3.67
3	34.00	11	3.67	19	4.00	27	4.00	35	3.67
4	35.00	12	3.67	20	3.67	28	3.67	36	4.00
5	29.67	13	3.67	21	4.00	29	4.00	37	4.00
6	23.00	14	3.67	22	4.00	30	3.67	38	3.67
7	17.00	15	3.67	23	4.00	31	3.67		
8	17.00	16	3.67	24	4.00	32	3.33		
9	4.33	17	3.67	25	4.00	33	3.33		

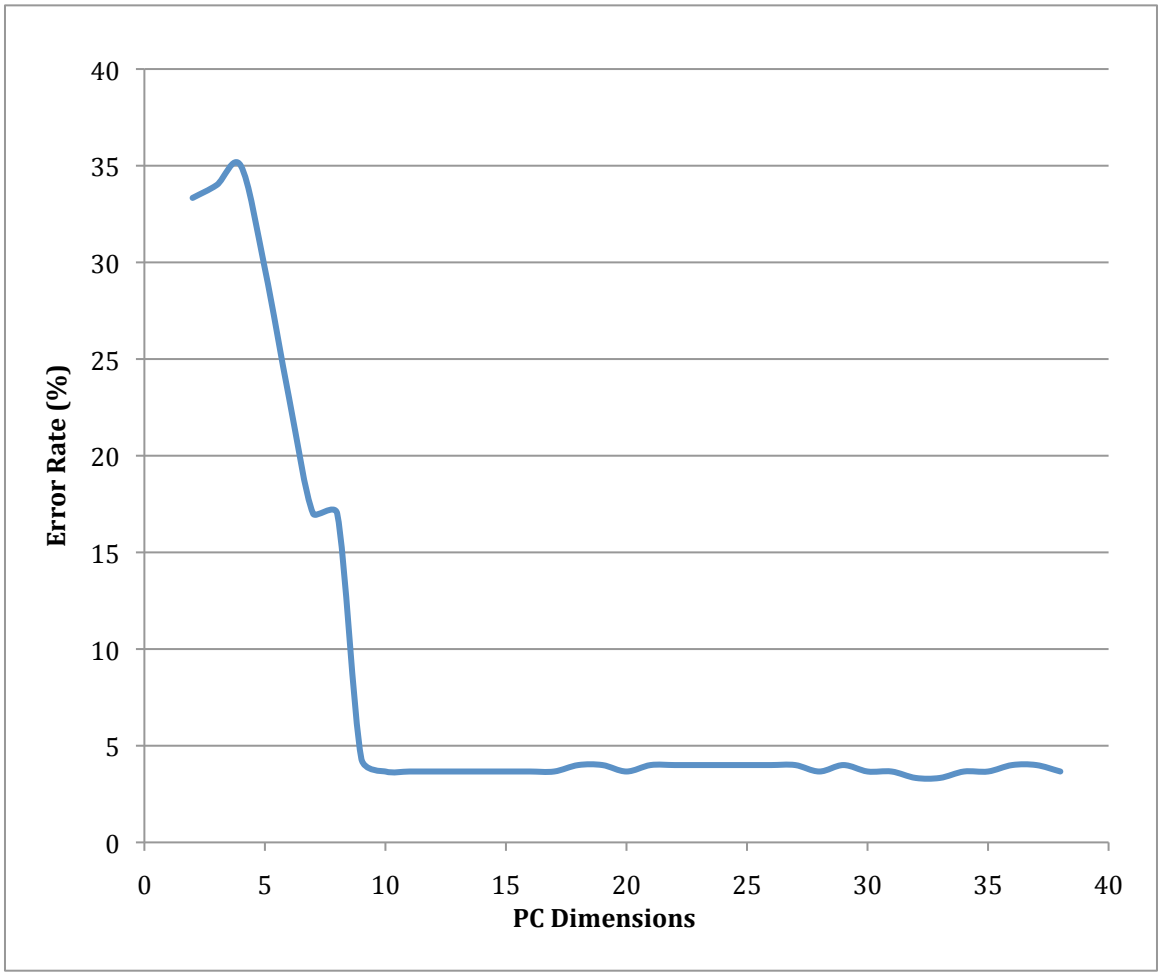


Figure 286: Graph of the classification (window or container) error rate versus PC dimensions for HOO-CV with PCA reduced CVA for the first set of 30 glass first derivative (9-point smoothing) spectra (10 replicates), centered data.

Table 298: Classification (window or container) error rates for HOO-CV with PCA reduced CVA for the first set of 30 glass first derivative (9-point smoothing) spectra (10 replicates), autoscaled data. The smallest PC dimension with the minimum error rate is highlighted in yellow.

PCs	Error Rate (%)	PCs	Error Rate (%)	PCs	Error Rate (%)	PCs	Error Rate (%)	PCs	Error Rate (%)
2	32.33	60	3.33	118	2.33	176	5.33	234	8.00
3	28.67	61	2.67	119	2.33	177	5.67	235	9.00
4	9.67	62	3.67	120	2.33	178	6.00	236	8.33
5	3.67	63	3.67	121	2.67	179	5.67	237	8.00
6	4.33	64	3.67	122	2.67	180	5.67	238	10.00
7	4.33	65	3.67	123	2.00	181	6.33	239	8.33
8	4.00	66	3.67	124	2.00	182	6.33	240	8.33
9	4.00	67	3.33	125	2.00	183	6.00	241	8.67
10	3.67	68	3.67	126	2.00	184	5.33	242	8.67
11	4.00	69	3.00	127	2.00	185	6.00	243	8.33
12	4.00	70	4.00	128	2.00	186	6.00	244	8.33
13	3.67	71	4.00	129	2.33	187	6.00	245	9.67
14	3.67	72	3.67	130	2.33	188	6.00	246	9.00
15	4.00	73	3.00	131	2.33	189	6.00	247	10.33
16	4.00	74	3.33	132	2.00	190	6.00	248	10.33
17	4.00	75	4.00	133	2.00	191	5.67	249	11.67
18	4.00	76	4.00	134	2.00	192	4.67	250	11.33
19	4.00	77	3.33	135	2.00	193	5.33	251	11.00
20	4.33	78	3.00	136	2.33	194	5.33	252	10.33
21	4.33	79	3.33	137	2.33	195	5.67	253	11.33
22	4.33	80	3.33	138	2.33	196	5.00	254	10.33
23	4.33	81	4.00	139	2.33	197	5.33	255	9.00
24	4.00	82	4.00	140	2.67	198	5.33	256	10.00
25	4.33	83	3.33	141	3.00	199	4.67	257	11.00
26	4.33	84	3.67	142	2.67	200	5.00	258	11.67
27	4.33	85	4.00	143	2.67	201	5.33	259	11.33
28	4.33	86	4.33	144	2.67	202	5.33	260	10.67
29	4.33	87	4.33	145	3.00	203	4.33	261	11.00
30	3.67	88	4.33	146	3.00	204	5.00	262	11.67
31	3.33	89	4.33	147	3.00	205	4.67	263	11.67
32	3.33	90	4.00	148	2.67	206	5.67	264	13.00
33	3.00	91	3.67	149	2.67	207	5.67	265	11.67
34	3.33	92	4.33	150	2.67	208	5.33	266	13.33
35	3.00	93	4.00	151	2.33	209	5.00	267	13.67
36	3.00	94	3.00	152	2.00	210	5.00	268	13.67
37	3.33	95	3.67	153	3.00	211	5.33	269	16.33

38	3.33	96	3.67	154	2.33	212	5.33	270	13.67
39	3.33	97	3.67	155	2.33	213	6.00	271	15.00
40	3.33	98	3.67	156	3.33	214	7.33	272	11.33
41	3.00	99	3.67	157	3.33	215	7.67	273	13.00
42	3.33	100	3.67	158	3.33	216	7.00	274	14.67
43	3.00	101	3.67	159	3.33	217	7.33	275	15.00
44	2.67	102	3.67	160	3.00	218	7.67	276	16.33
45	2.67	103	3.67	161	3.33	219	8.67	277	17.67
46	2.67	104	3.00	162	3.33	220	8.67	278	17.67
47	2.67	105	3.00	163	3.67	221	9.33	279	19.33
48	2.33	106	3.00	164	4.00	222	8.00	280	18.33
49	2.67	107	3.00	165	3.67	223	7.67	281	18.00
50	2.67	108	2.67	166	4.33	224	8.00	282	17.67
51	2.67	109	3.00	167	3.67	225	8.00	283	18.33
52	2.67	110	2.33	168	4.00	226	8.00	284	17.33
53	2.33	111	2.33	169	4.00	227	9.33	285	16.00
54	2.33	112	2.33	170	5.00	228	9.33	286	18.67
55	2.33	113	2.33	171	5.00	229	9.33	287	20.33
56	2.33	114	2.33	172	5.00	230	9.33		
57	2.33	115	2.33	173	5.00	231	7.33		
58	3.00	116	2.33	174	5.00	232	7.67		
59	3.33	117	2.33	175	5.00	233	8.00		

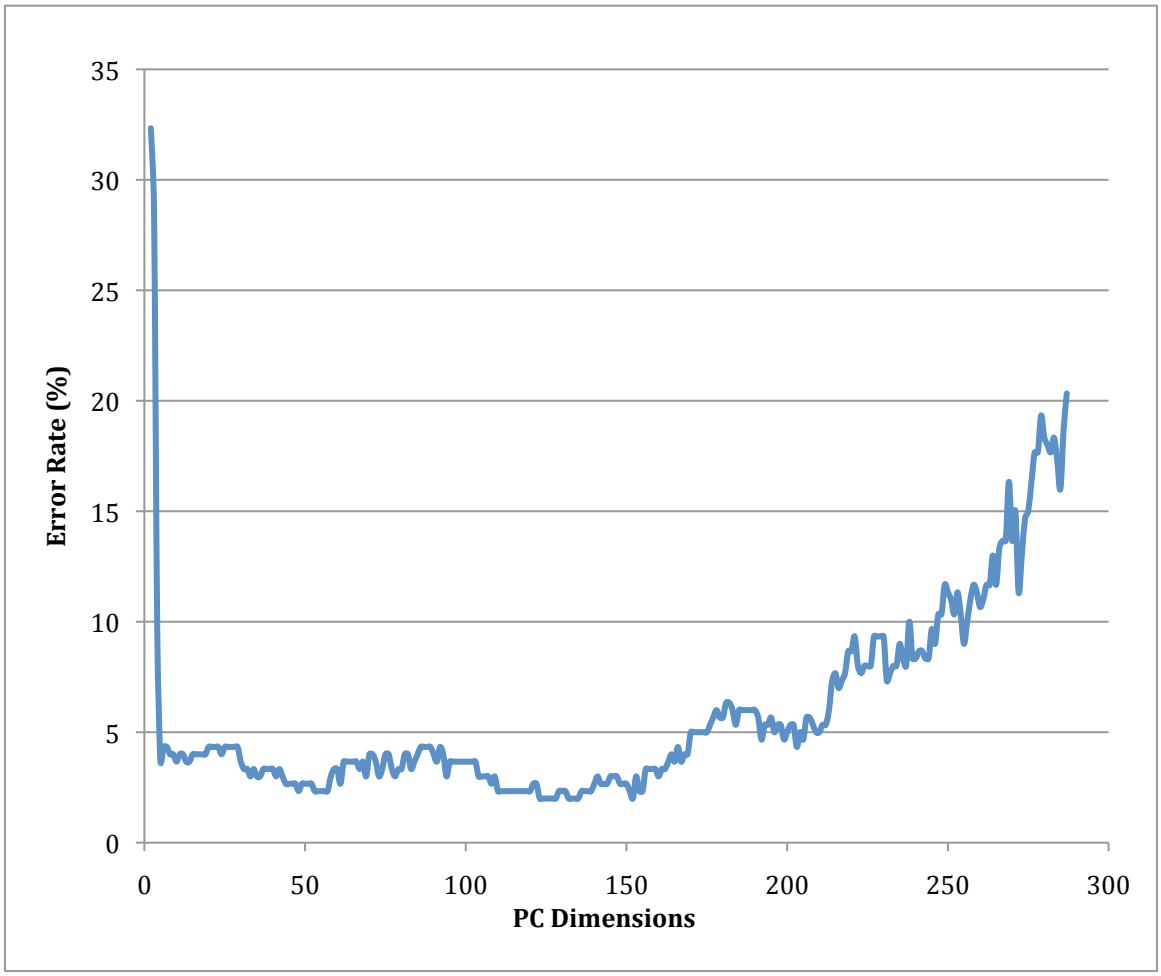


Figure 287: Graph of the classification (window or container) error rate versus PC dimensions for HOO-CV with PCA reduced CVA for the first set of 30 glass first derivative (9-point smoothing) spectra (10 replicates), autoscaled data.

First Set, First Derivative (9-point smoothing) – Window Discrimination

Table 299: Discrimination error rates for HOO-CV with PCA reduced CVA for the first set of 20 window glass first derivative (9-point smoothing) spectra (10 replicates), no data pretreatment. The smallest PC dimension with the minimum error rate is highlighted in yellow.

PCs	Error Rate (%)	PCs	Error Rate (%)	PCs	Error Rate (%)	PCs	Error Rate (%)	PCs	Error Rate (%)
2	93.00	9	68.00	16	34.00	23	26.00	30	21.00
3	90.00	10	63.50	17	33.50	24	25.50	31	19.50
4	90.50	11	57.50	18	32.50	25	22.00	32	19.50
5	88.50	12	52.00	19	31.50	26	21.00	33	20.00
6	87.00	13	45.50	20	28.50	27	21.50	34	19.50
7	84.00	14	42.00	21	30.50	28	21.00		
8	75.50	15	39.50	22	26.50	29	21.50		

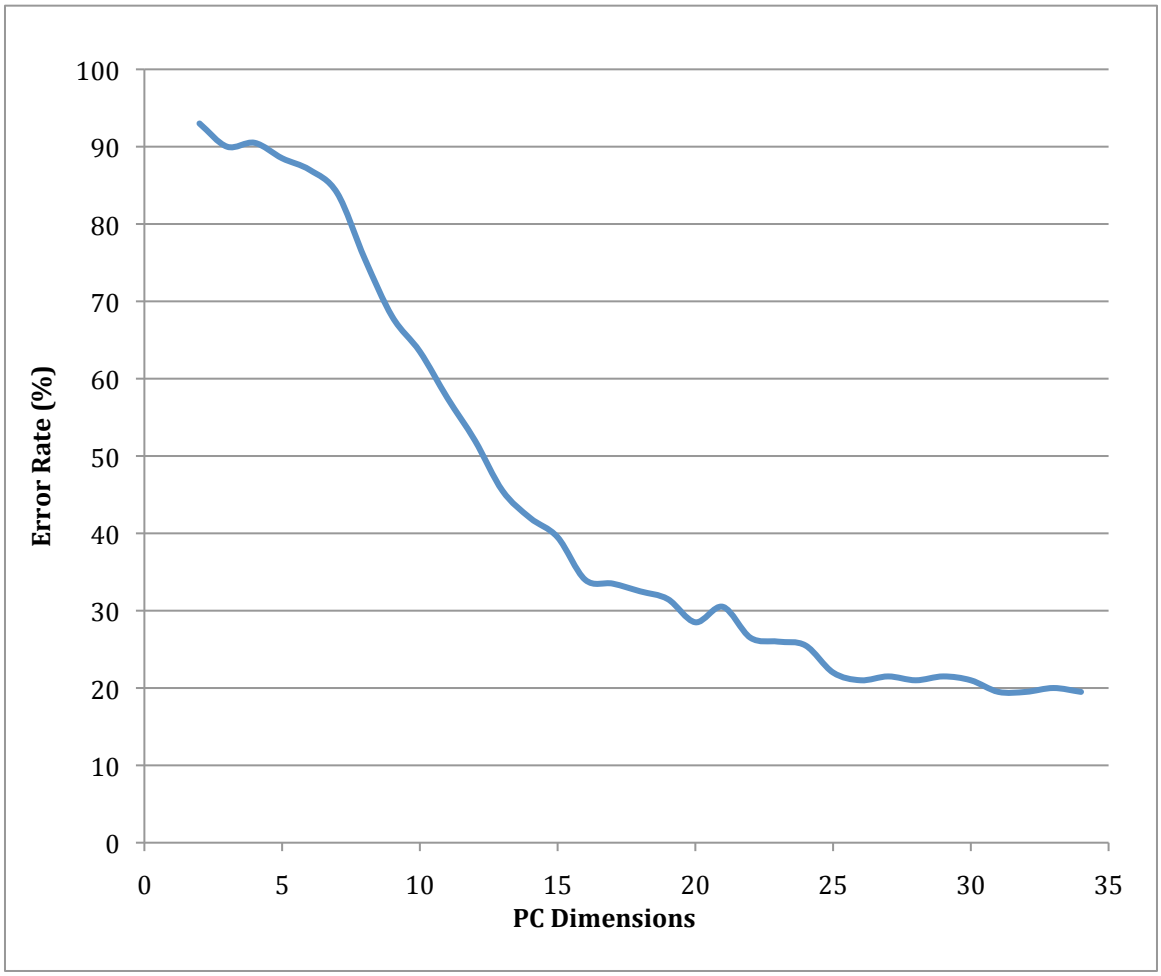


Figure 288: Graph of the discrimination error rate versus PC dimensions for HOO-CV with PCA reduced CVA for the first set of 20 window glass first derivative (9-point smoothing) spectra (10 replicates), no data pretreatment.

Table 300: Discrimination error rates for HOO-CV with PCA reduced CVA for the first set of 20 window glass first derivative (9-point smoothing) spectra (10 replicates), centered data. The smallest PC dimension with the minimum error rate is highlighted in yellow.

PCs	Error Rate (%)	PCs	Error Rate (%)	PCs	Error Rate (%)	PCs	Error Rate (%)	PCs	Error Rate (%)
2	93.00	9	68.50	16	34.50	23	25.00	30	21.00
3	89.50	10	64.50	17	33.00	24	24.50	31	19.00
4	91.00	11	57.00	18	31.00	25	21.50	32	19.50
5	88.50	12	52.00	19	30.50	26	20.00	33	21.00
6	88.00	13	47.00	20	29.50	27	19.50	34	20.50
7	84.50	14	42.00	21	29.00	28	22.00		
8	76.00	15	39.50	22	27.00	29	21.00		

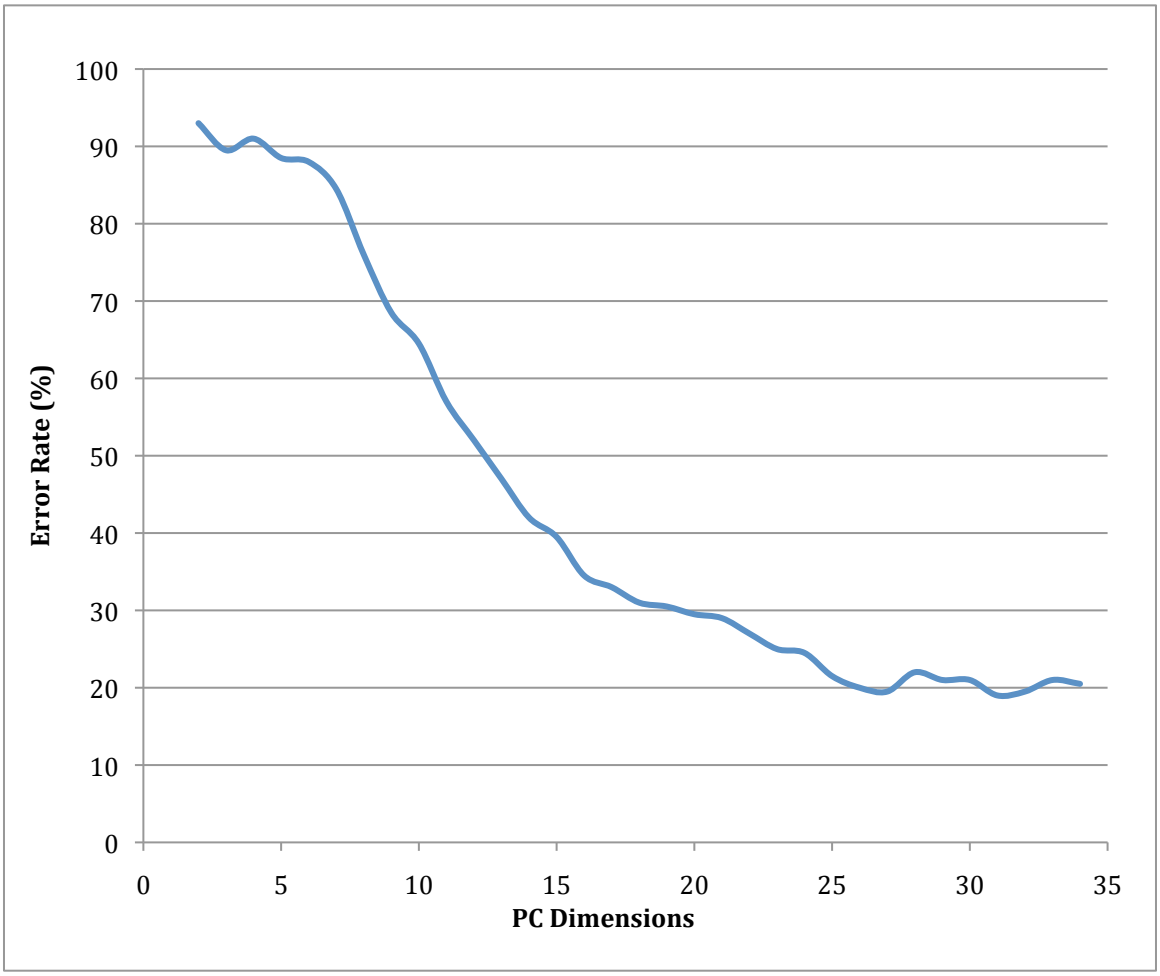


Figure 289: Graph of the discrimination error rate versus PC dimensions for HOO-CV with PCA reduced CVA for the first set of 20 window glass first derivative (9-point smoothing) spectra (10 replicates), centered data.

Table 301: Discrimination error rates for HOO-CV with PCA reduced CVA for the first set of 20 window glass first derivative (9-point smoothing) spectra (10 replicates), autoscaled data. The smallest PC dimension with the minimum error rate is highlighted in yellow.

PCs	Error Rate (%)	PCs	Error Rate (%)	PCs	Error Rate (%)	PCs	Error Rate (%)	PCs	Error Rate (%)
2	94.00	39	11.50	76	10.50	113	14.00	150	23.50
3	86.00	40	11.00	77	9.50	114	14.00	151	25.00
4	81.00	41	11.00	78	11.50	115	14.50	152	27.00
5	66.50	42	10.50	79	11.00	116	15.00	153	25.50
6	65.00	43	10.50	80	11.50	117	14.50	154	27.00
7	61.50	44	9.50	81	12.00	118	14.50	155	27.00
8	50.00	45	10.50	82	11.00	119	14.50	156	26.50
9	44.50	46	10.50	83	10.50	120	14.50	157	28.00
10	42.00	47	12.00	84	10.50	121	14.00	158	27.00
11	39.50	48	12.00	85	10.50	122	13.50	159	26.00
12	35.00	49	10.50	86	9.50	123	13.50	160	28.00
13	32.50	50	9.00	87	10.00	124	15.00	161	32.00
14	31.00	51	9.50	88	9.00	125	16.00	162	37.00
15	32.00	52	10.00	89	9.50	126	16.50	163	40.50
16	28.00	53	9.00	90	10.00	127	15.00	164	42.00
17	26.00	54	9.00	91	9.50	128	14.00	165	42.50
18	26.50	55	10.50	92	9.00	129	16.00	166	44.50
19	26.00	56	11.50	93	9.50	130	15.50	167	43.50
20	25.00	57	10.00	94	9.00	131	16.50	168	45.50
21	20.00	58	10.00	95	10.00	132	15.50	169	42.00
22	20.00	59	9.00	96	10.00	133	15.50	170	45.50
23	21.50	60	8.50	97	10.00	134	16.50	171	47.00
24	21.00	61	8.00	98	8.50	135	17.00	172	42.50
25	20.00	62	8.00	99	8.50	136	16.00	173	42.00
26	18.00	63	8.50	100	9.00	137	15.00	174	49.50
27	18.50	64	9.00	101	9.00	138	15.50	175	54.50
28	18.00	65	9.00	102	8.50	139	16.50	176	54.00
29	16.50	66	9.00	103	9.00	140	17.00	177	59.00
30	17.50	67	10.50	104	9.00	141	20.00	178	66.00
31	16.50	68	11.00	105	9.50	142	18.50	179	79.00
32	17.00	69	10.50	106	10.50	143	18.50	180	46.00
33	18.00	70	11.00	107	11.50	144	21.00	181	71.00
34	16.50	71	9.50	108	10.50	145	20.50	182	82.50
35	15.50	72	10.50	109	11.50	146	21.00		
36	13.00	73	10.00	110	12.00	147	21.00		
37	12.50	74	11.00	111	11.00	148	20.50		
38	12.00	75	11.50	112	12.50	149	23.00		

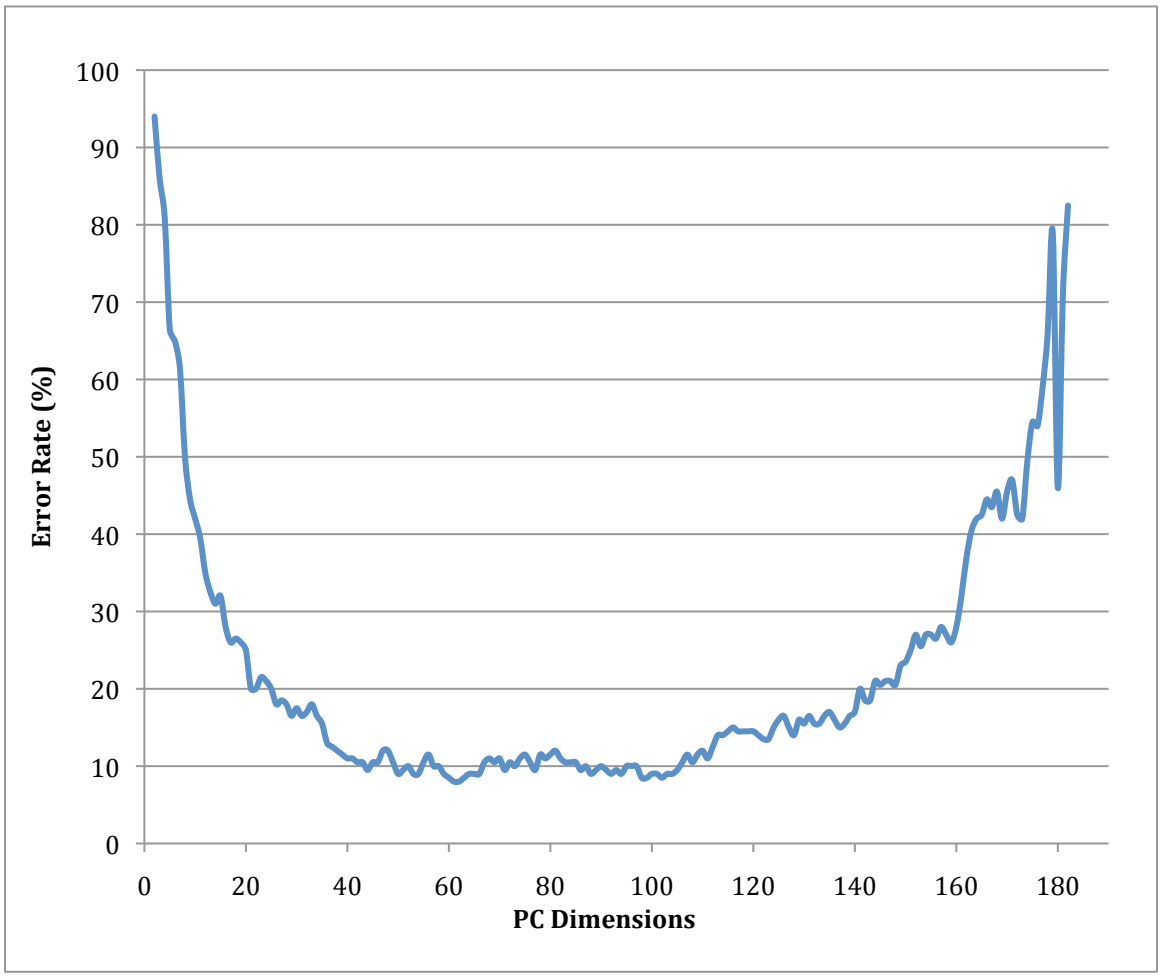


Figure 290: Graph of the discrimination error rate versus PC dimensions for HOO-CV with PCA reduced CVA for the first set of 20 window glass first derivative (9-point smoothing) spectra (10 replicates), autoscaled data.

First Set, First Derivative (9-point smoothing) – Container Discrimination

Table 302: Discrimination error rates for HOO-CV with PCA reduced CVA for the first set of 10 container glass first derivative (9-point smoothing) spectra (10 replicates), no data pretreatment. The smallest PC dimension with the minimum error rate is highlighted in yellow.

PCs	Error Rate (%)	PCs	Error Rate (%)	PCs	Error Rate (%)	PCs	Error Rate (%)	PCs	Error Rate (%)
2	77.00	9	56.00	16	39.00	23	20.00	30	18.00
3	80.00	10	51.00	17	36.00	24	21.00	31	18.00
4	80.00	11	46.00	18	35.00	25	24.00	32	18.00
5	72.00	12	37.00	19	33.00	26	22.00	33	17.00
6	65.00	13	35.00	20	30.00	27	22.00	34	17.00
7	56.00	14	41.00	21	29.00	28	23.00	35	16.00
8	58.00	15	38.00	22	25.00	29	20.00		

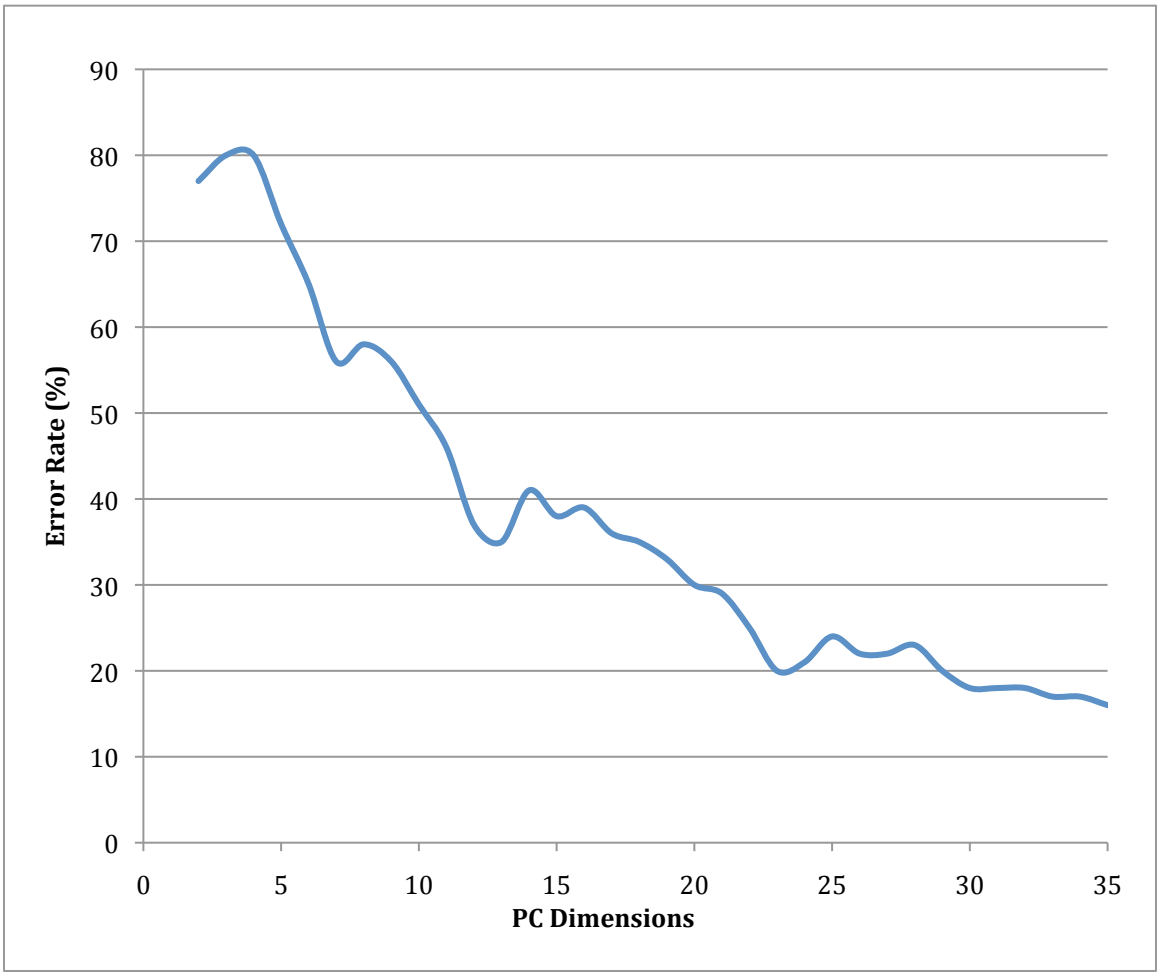


Figure 291: Graph of the discrimination error rate versus PC dimensions for HOO-CV with PCA reduced CVA for the first set of 10 container glass first derivative (9-point smoothing) spectra (10 replicates), no data pretreatment.

Table 303: Discrimination error rates for HOO-CV with PCA reduced CVA for the first set of 10 container glass first derivative (9-point smoothing) spectra (10 replicates), centered data. The smallest PC dimension with the minimum error rate is highlighted in yellow.

PCs	Error Rate (%)	PCs	Error Rate (%)	PCs	Error Rate (%)	PCs	Error Rate (%)	PCs	Error Rate (%)
2	77.00	9	51.00	16	35.00	23	26.00	30	20.00
3	79.00	10	47.00	17	36.00	24	22.00	31	20.00
4	78.00	11	41.00	18	29.00	25	25.00	32	18.00
5	68.00	12	42.00	19	35.00	26	23.00	33	18.00
6	68.00	13	38.00	20	25.00	27	25.00		
7	68.00	14	39.00	21	31.00	28	23.00		
8	59.00	15	38.00	22	26.00	29	21.00		

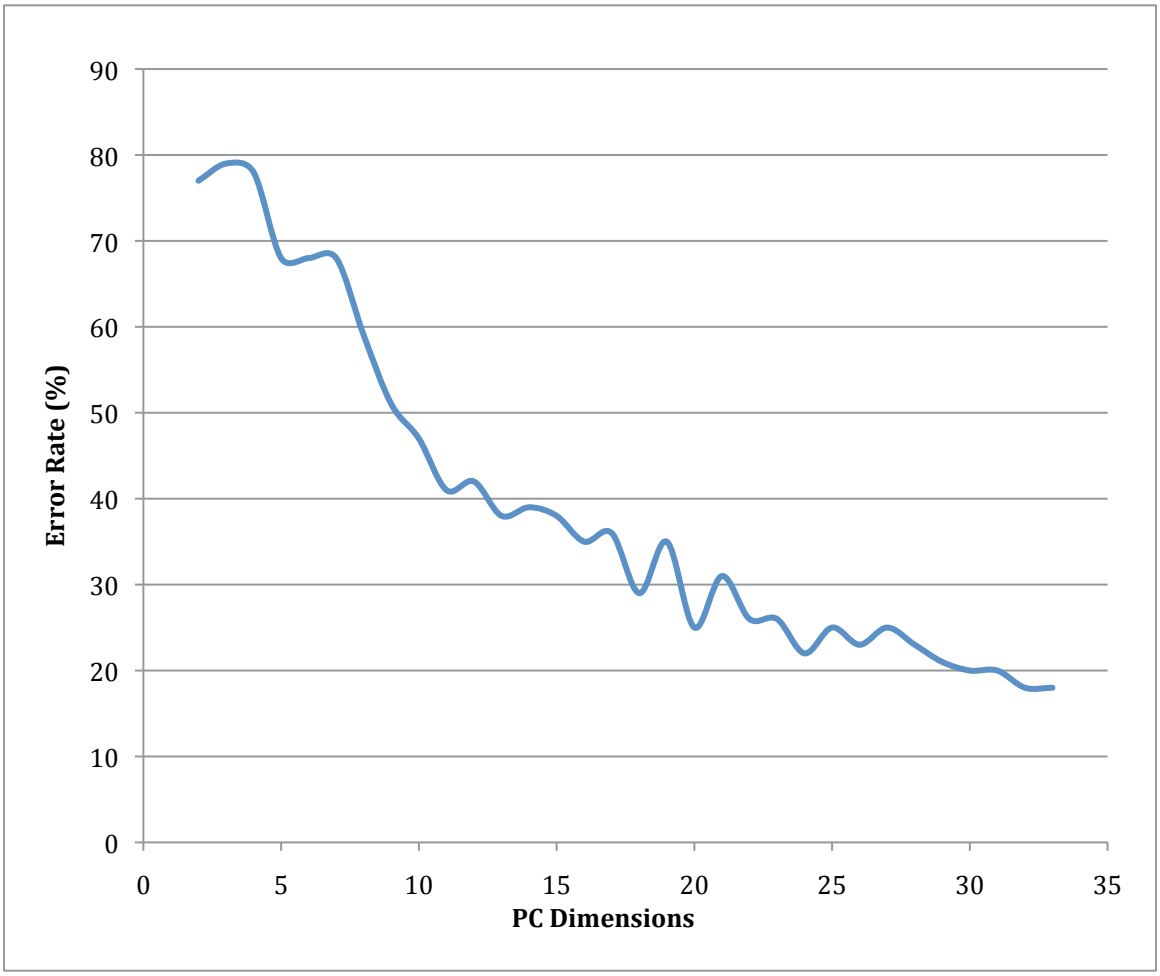


Figure 292: Graph of the discrimination error rate versus PC dimensions for HOO-CV with PCA reduced CVA for the first set of 10 container glass first derivative (9-point smoothing) spectra (10 replicates), centered data.

Table 304: Discrimination error rates for HOO-CV with PCA reduced CVA for the first set of 10 container glass first derivative (9-point smoothing) spectra (10 replicates), autoscaled data. The smallest PC dimension with the minimum error rate is highlighted in yellow.

PCs	Error Rate (%)	PCs	Error Rate (%)	PCs	Error Rate (%)	PCs	Error Rate (%)	PCs	Error Rate (%)
2	74.00	22	16.00	42	10.00	62	13.00	82	22.00
3	60.00	23	13.00	43	10.00	63	13.00	83	24.00
4	62.00	24	12.00	44	9.00	64	12.00	84	29.00
5	44.00	25	13.00	45	9.00	65	13.00	85	30.00
6	46.00	26	12.00	46	9.00	66	16.00	86	37.00
7	43.00	27	13.00	47	9.00	67	15.00	87	46.00
8	42.00	28	11.00	48	9.00	68	16.00	88	30.00
9	36.00	29	9.00	49	9.00	69	16.00	89	43.00
10	35.00	30	8.00	50	9.00	70	17.00	90	62.00
11	39.00	31	7.00	51	10.00	71	20.00	91	53.00
12	38.00	32	7.00	52	11.00	72	17.00	92	59.00
13	32.00	33	6.00	53	9.00	73	17.00	93	76.00
14	26.00	34	7.00	54	10.00	74	21.00	94	88.00
15	21.00	35	7.00	55	10.00	75	22.00	95	94.00
16	21.00	36	10.00	56	9.00	76	21.00	96	91.00
17	23.00	37	10.00	57	9.00	77	24.00	97	95.00
18	16.00	38	8.00	58	12.00	78	22.00	98	95.00
19	16.00	39	9.00	59	12.00	79	23.00	99	86.00
20	16.00	40	8.00	60	11.00	80	25.00		
21	17.00	41	10.00	61	12.00	81	30.00		

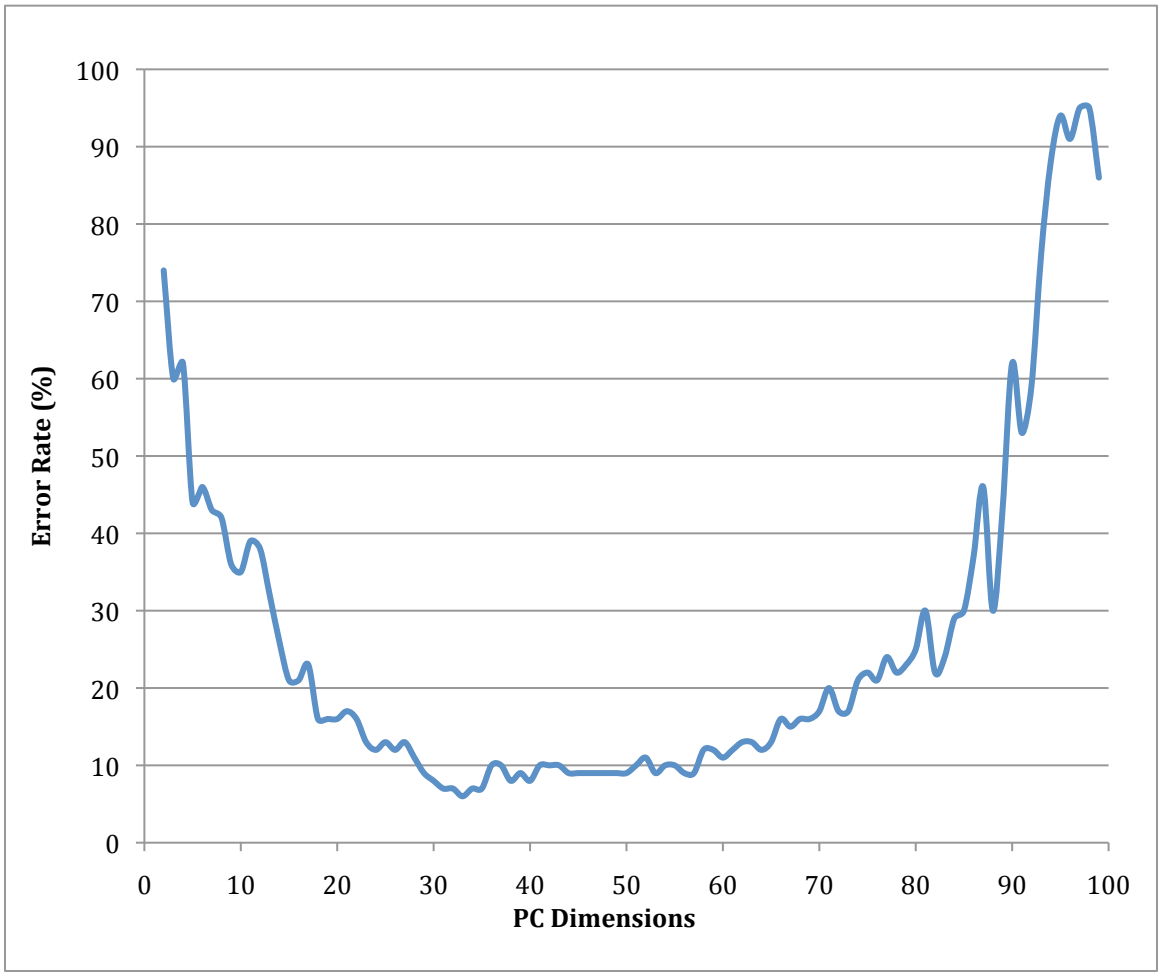


Figure 293: Graph of the discrimination error rate versus PC dimensions for HOO-CV with PCA reduced CVA for the first set of 10 container glass first derivative (9-point smoothing) spectra (10 replicates), autoscaled data.

First Set, First Derivative (9-point smoothing) – Float Classification

Table 305: Float classification error rates for HOO-CV with PCA reduced CVA for the first set of 20 window glass first derivative (9-point smoothing) spectra (10 replicates), no data pretreatment. The smallest PC dimension with the minimum error rate is highlighted in yellow.

PCs	Error Rate (%)	PCs	Error Rate (%)	PCs	Error Rate (%)	PCs	Error Rate (%)	PCs	Error Rate (%)
2	42.50	9	26.00	16	18.00	23	18.00	30	18.50
3	37.50	10	22.00	17	16.50	24	18.50	31	20.00
4	38.00	11	22.00	18	16.50	25	19.50	32	18.00
5	33.00	12	22.50	19	17.50	26	19.00	33	16.50
6	27.50	13	21.00	20	19.00	27	17.00	34	18.00
7	26.50	14	24.00	21	20.50	28	19.00	35	18.50
8	26.00	15	24.00	22	20.50	29	18.50		

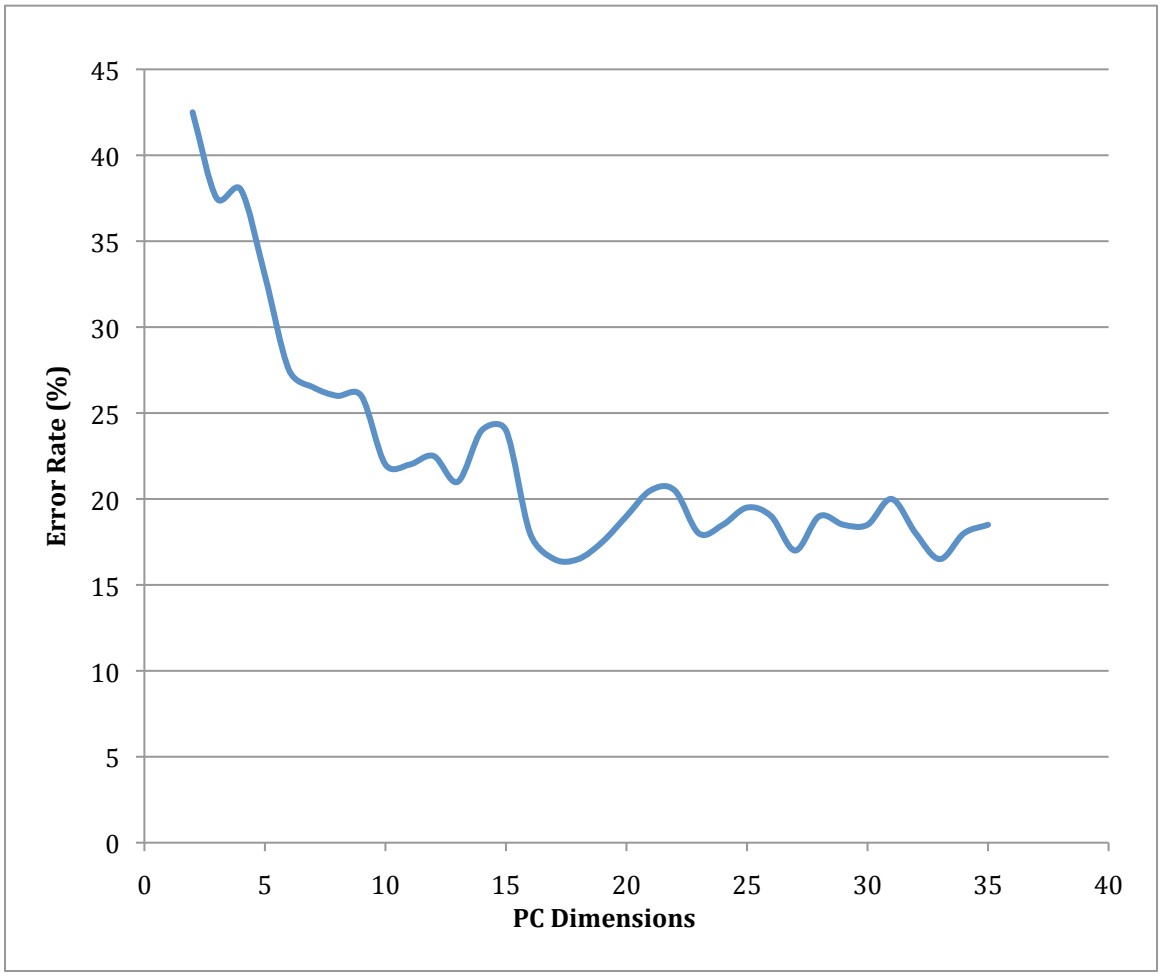


Figure 294: Graph of the float classification error rate versus PC dimensions for HOO-CV with PCA reduced CVA for the first set of 20 window glass first derivative (9-point smoothing) spectra (10 replicates), no data pretreatment.

Table 306: Float classification error rates for HOO-CV with PCA reduced CVA for the first set of 20 window glass first derivative (9-point smoothing) spectra (10 replicates), centered data. The smallest PC dimension with the minimum error rate is highlighted in yellow.

PCs	Error Rate (%)	PCs	Error Rate (%)	PCs	Error Rate (%)	PCs	Error Rate (%)	PCs	Error Rate (%)
2	41.50	9	26.00	16	19.00	23	19.00	30	18.00
3	37.50	10	22.50	17	17.50	24	19.50	31	18.00
4	37.00	11	22.00	18	17.50	25	19.50	32	18.50
5	33.00	12	23.00	19	18.50	26	20.50	33	17.50
6	27.50	13	20.50	20	20.00	27	18.50	34	18.00
7	26.50	14	23.50	21	20.50	28	18.00	35	18.50
8	26.00	15	24.00	22	19.50	29	18.50		

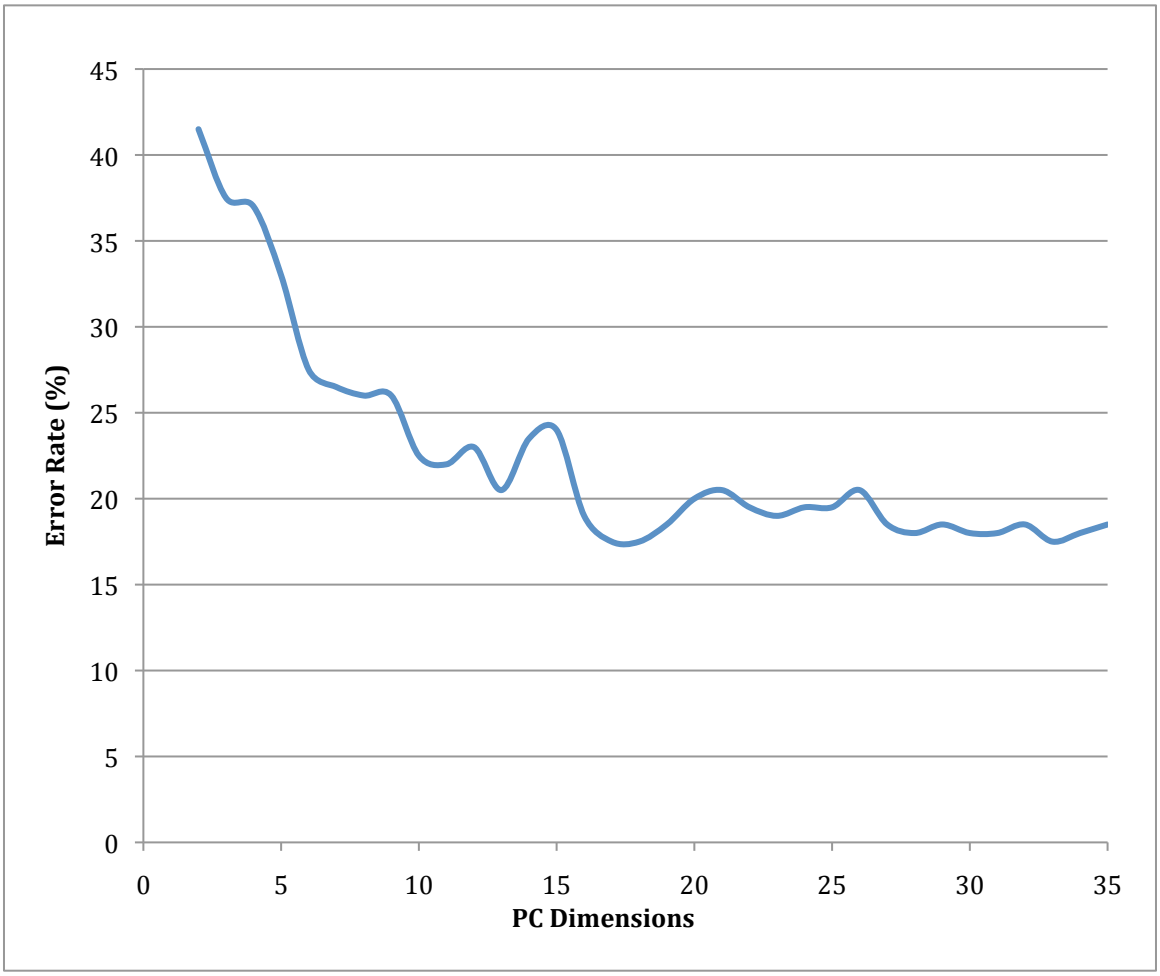


Figure 295: Graph of the float classification error rate versus PC dimensions for HOO-CV with PCA reduced CVA for the first set of 20 window glass first derivative (9-point smoothing) spectra (10 replicates), centered data.

Table 307: Float classification error rates for HOO-CV with PCA reduced CVA for the first set of 20 window glass first derivative (9-point smoothing) spectra (10 replicates), autoscaled data. The smallest PC dimension with the minimum error rate is highlighted in yellow.

PCs	Error Rate (%)	PCs	Error Rate (%)	PCs	Error Rate (%)	PCs	Error Rate (%)	PCs	Error Rate (%)
2	40.50	42	15.00	82	18.00	122	24.00	162	24.00
3	31.50	43	15.00	83	16.00	123	25.50	163	24.00
4	32.00	44	14.50	84	16.00	124	25.50	164	25.50
5	32.00	45	16.50	85	16.00	125	25.00	165	26.50
6	28.50	46	15.00	86	17.00	126	25.50	166	28.50
7	30.00	47	13.50	87	16.50	127	25.00	167	30.00
8	19.00	48	14.00	88	18.50	128	22.00	168	30.50
9	19.00	49	15.00	89	19.50	129	22.00	169	30.50
10	19.50	50	15.50	90	21.00	130	22.50	170	31.00
11	20.00	51	16.00	91	21.50	131	21.50	171	31.00
12	19.50	52	15.00	92	21.50	132	22.00	172	32.50
13	19.50	53	15.00	93	22.00	133	22.50	173	32.00
14	21.00	54	15.50	94	20.00	134	23.50	174	33.50
15	18.50	55	14.50	95	18.50	135	23.50	175	34.00
16	18.00	56	14.50	96	18.00	136	24.50	176	30.00
17	15.50	57	15.00	97	19.00	137	24.00	177	31.50
18	15.50	58	15.50	98	19.00	138	25.00	178	32.50
19	15.00	59	16.00	99	19.00	139	25.50	179	29.50
20	15.00	60	16.00	100	20.00	140	25.00	180	31.50
21	16.00	61	14.50	101	20.50	141	28.00	181	32.50
22	15.00	62	14.50	102	20.50	142	27.50	182	32.50
23	14.00	63	16.50	103	20.50	143	28.00	183	32.50
24	15.00	64	16.00	104	21.50	144	24.00	184	35.50
25	14.00	65	16.00	105	20.00	145	25.00	185	37.00
26	14.50	66	16.00	106	20.50	146	27.00	186	35.50
27	15.00	67	16.00	107	20.50	147	25.50	187	37.50
28	13.50	68	16.00	108	21.00	148	26.50	188	38.50
29	13.00	69	16.50	109	20.50	149	27.50	189	33.00
30	13.50	70	16.50	110	21.00	150	27.50	190	36.00
31	13.50	71	15.00	111	20.50	151	24.50	191	39.50
32	14.50	72	15.50	112	20.50	152	24.00	192	43.00
33	14.50	73	15.00	113	22.00	153	22.50	193	42.00
34	14.50	74	15.50	114	22.50	154	23.50	194	45.50
35	13.00	75	15.50	115	20.50	155	24.50	195	47.00
36	14.50	76	15.50	116	21.00	156	24.50	196	43.00
37	14.50	77	15.50	117	20.00	157	25.50	197	47.50
38	15.50	78	16.50	118	21.00	158	25.00	198	50.00

39	14.50	79	16.50	119	21.00	159	25.50	199	45.00
40	15.00	80	17.00	120	24.00	160	26.00		
41	15.50	81	15.00	121	24.00	161	27.50		

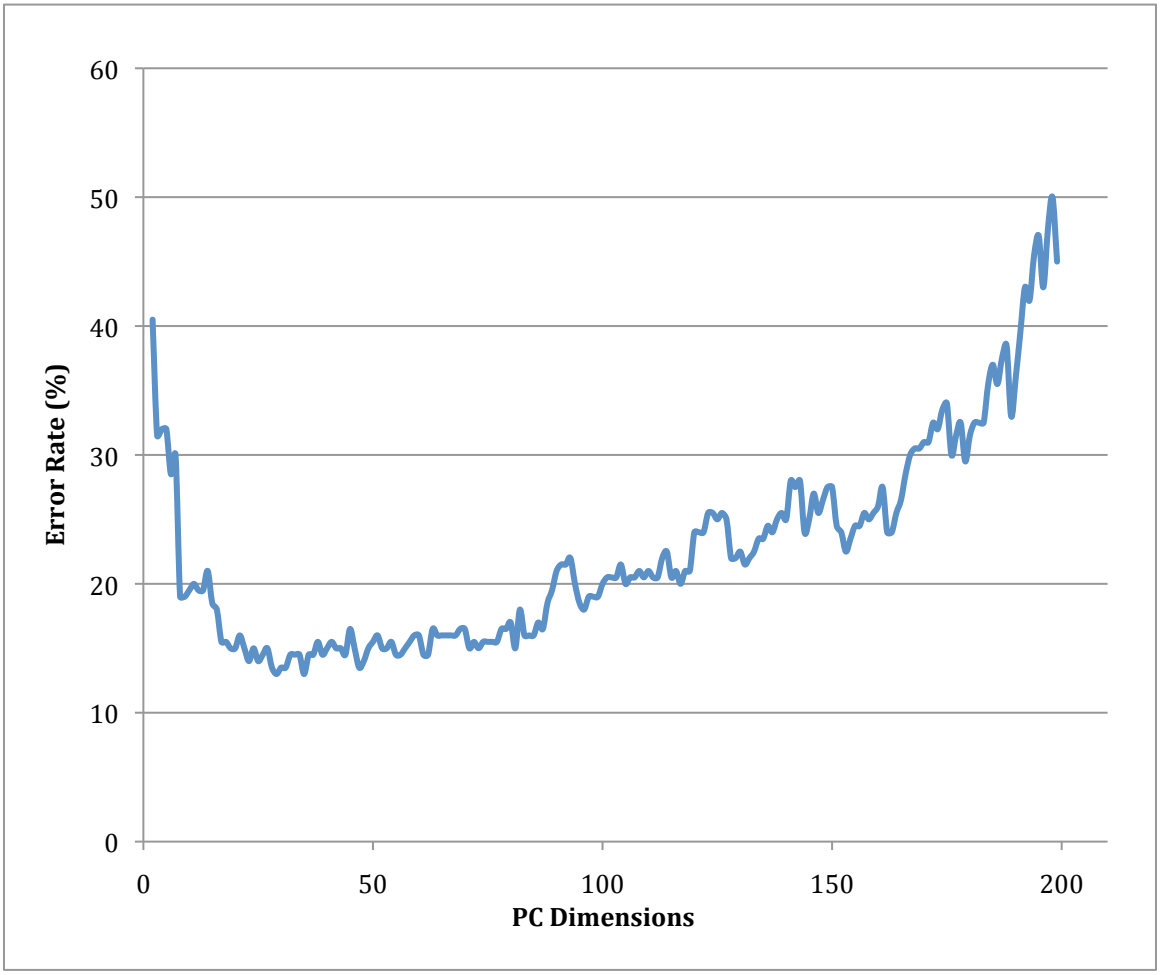


Figure 296: Graph of the float classification error rate versus PC dimensions for HOO-CV with PCA reduced CVA for the first set of 20 window glass first derivative (9-point smoothing) spectra (10 replicates), autoscaled data.

First Set, First Derivative (9-point smoothing) – Tempered Classification

Table 308: Tempered classification error rates for HOO-CV with PCA reduced CVA for the first set of 20 window glass first derivative (9-point smoothing) spectra (10 replicates), no data pretreatment. The smallest PC dimension with the minimum error rate is highlighted in yellow.

PCs	Error Rate (%)	PCs	Error Rate (%)	PCs	Error Rate (%)	PCs	Error Rate (%)	PCs	Error Rate (%)
2	42.00	9	30.00	16	25.00	23	22.50	30	22.00
3	29.50	10	29.00	17	25.00	24	22.50	31	20.00
4	30.00	11	28.00	18	24.50	25	23.50	32	19.50
5	30.50	12	28.00	19	25.50	26	21.00	33	19.50
6	30.00	13	29.00	20	25.00	27	22.50	34	21.00
7	30.50	14	27.00	21	26.00	28	19.00	35	21.00
8	32.00	15	28.00	22	25.00	29	20.00		

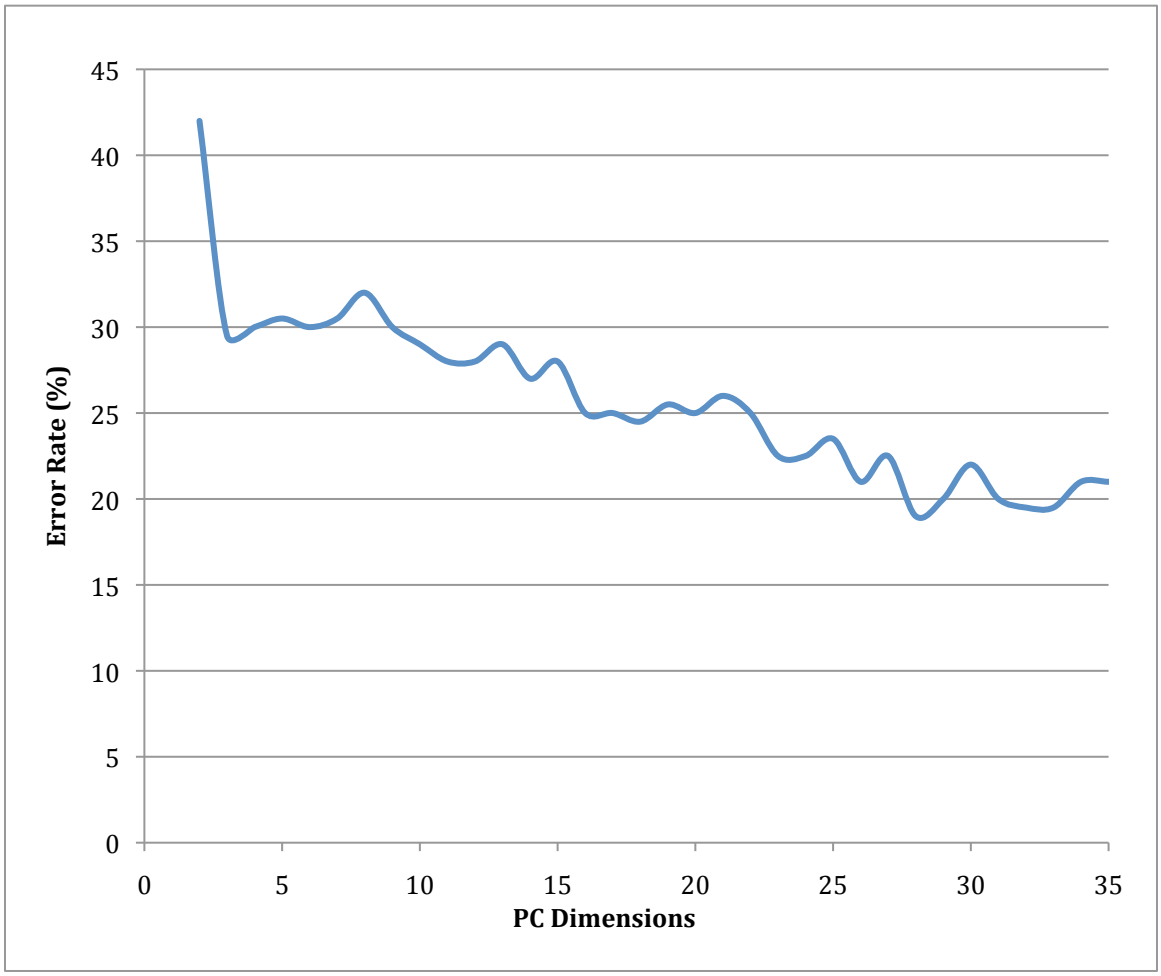


Figure 297: Graph of the tempered classification error rate versus PC dimensions for HOO-CV with PCA reduced CVA for the first set of 20 window glass first derivative (9-point smoothing) spectra (10 replicates), no data pretreatment.

Table 309: Tempered classification error rates for HOO-CV with PCA reduced CVA for the first set of 20 window glass first derivative (9-point smoothing) spectra (10 replicates), centered data. The smallest PC dimension with the minimum error rate is highlighted in yellow.

PCs	Error Rate (%)	PCs	Error Rate (%)	PCs	Error Rate (%)	PCs	Error Rate (%)	PCs	Error Rate (%)
2	41.50	9	30.00	16	24.50	23	22.00	30	20.00
3	29.50	10	29.00	17	24.50	24	23.00	31	19.00
4	30.50	11	27.50	18	24.00	25	23.00	32	19.00
5	30.50	12	28.00	19	25.50	26	22.50	33	18.50
6	30.00	13	28.50	20	25.50	27	23.50	34	21.50
7	30.50	14	27.00	21	26.00	28	21.00	35	21.00
8	31.50	15	28.00	22	26.00	29	19.00		

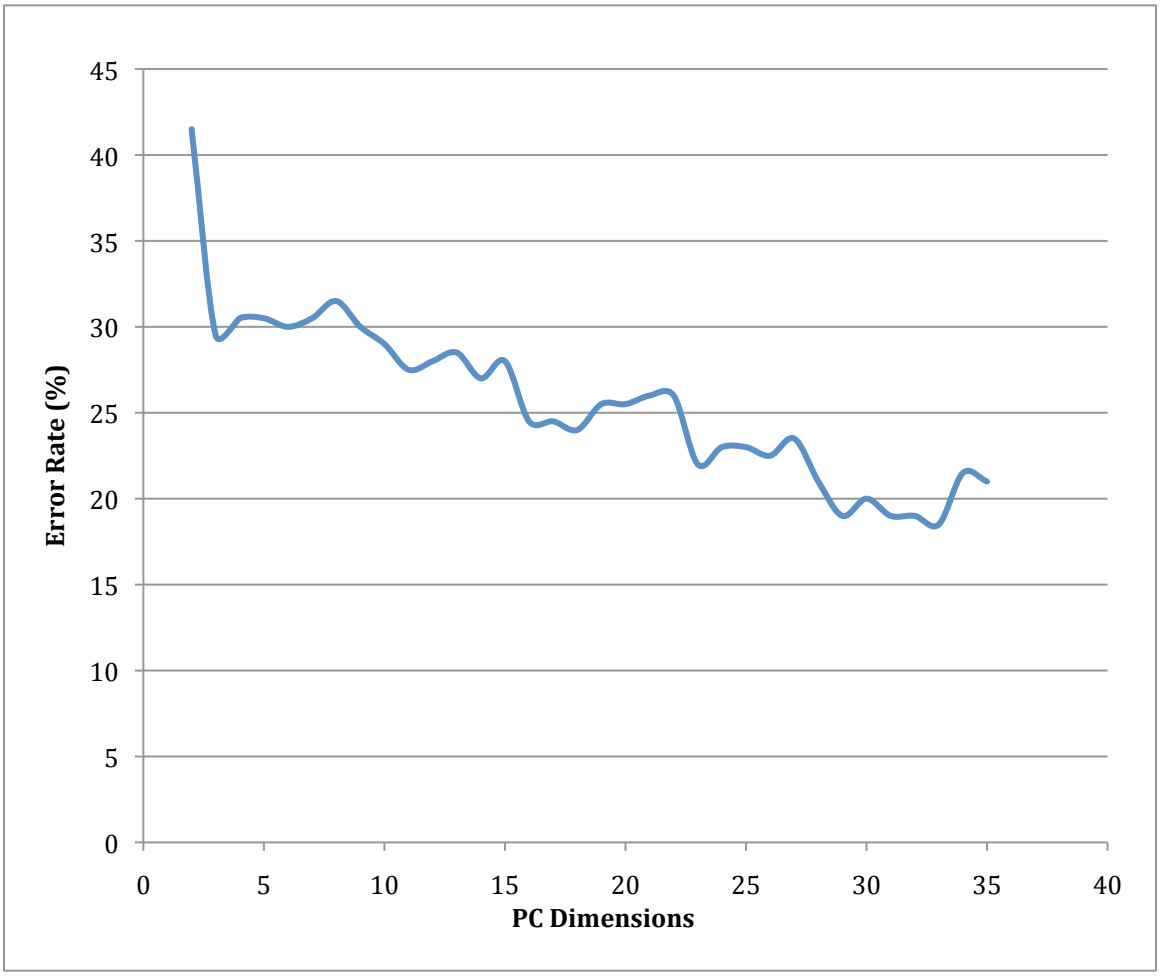


Figure 298: Graph of the tempered classification error rate versus PC dimensions for HOO-CV with PCA reduced CVA for the first set of 20 window glass first derivative (9-point smoothing) spectra (10 replicates), centered data.

Table 310: Tempered classification error rates for HOO-CV with PCA reduced CVA for the first set of 20 window glass first derivative (9-point smoothing) spectra (10 replicates), autoscaled data. The smallest PC dimension with the minimum error rate is highlighted in yellow.

PCs	Error Rate (%)	PCs	Error Rate (%)	PCs	Error Rate (%)	PCs	Error Rate (%)	PCs	Error Rate (%)
2	42.00	42	17.00	82	16.50	122	16.50	162	20.50
3	31.00	43	17.50	83	15.50	123	14.00	163	16.00
4	27.50	44	18.00	84	14.50	124	15.50	164	17.50
5	26.50	45	15.50	85	16.50	125	16.50	165	17.00
6	28.00	46	17.00	86	15.50	126	17.00	166	15.50
7	27.50	47	17.00	87	16.50	127	15.00	167	15.50
8	27.00	48	16.00	88	16.00	128	15.50	168	16.50
9	26.00	49	17.00	89	14.00	129	15.50	169	16.50
10	25.50	50	16.50	90	14.00	130	16.00	170	17.00
11	26.50	51	18.00	91	15.50	131	15.50	171	18.50
12	27.50	52	18.00	92	16.50	132	14.50	172	17.50
13	26.50	53	18.00	93	16.00	133	15.50	173	20.00
14	26.00	54	17.50	94	17.00	134	15.50	174	18.00
15	26.00	55	19.00	95	16.50	135	16.00	175	19.00
16	26.50	56	17.00	96	16.50	136	15.00	176	21.50
17	26.00	57	15.50	97	16.50	137	16.00	177	22.00
18	28.00	58	15.00	98	16.50	138	16.00	178	23.50
19	28.00	59	17.00	99	17.00	139	16.50	179	24.50
20	28.00	60	17.00	100	18.00	140	15.00	180	25.00
21	25.00	61	17.50	101	18.50	141	15.00	181	26.50
22	26.00	62	17.50	102	20.00	142	17.00	182	23.50
23	26.00	63	16.50	103	18.50	143	16.50	183	28.50
24	25.00	64	14.50	104	18.50	144	15.00	184	31.00
25	25.50	65	15.50	105	18.00	145	15.50	185	30.00
26	20.50	66	16.50	106	18.00	146	14.50	186	30.00
27	20.50	67	16.50	107	18.50	147	15.00	187	26.00
28	20.50	68	17.00	108	16.00	148	14.00	188	29.00
29	20.50	69	15.50	109	16.50	149	15.00	189	33.00
30	20.00	70	14.50	110	16.50	150	15.00	190	36.00
31	18.00	71	14.00	111	17.00	151	14.50	191	39.00
32	18.00	72	15.50	112	16.00	152	16.00	192	41.50
33	18.00	73	15.00	113	19.00	153	16.50	193	28.50
34	17.50	74	14.50	114	18.00	154	15.00	194	31.00
35	19.50	75	18.00	115	17.50	155	16.00	195	35.00
36	17.00	76	17.50	116	17.50	156	16.00	196	40.00

37	15.50	77	15.50	117	18.00	157	15.00	197	45.50
38	17.50	78	15.50	118	17.00	158	17.00	198	88.00
39	19.00	79	15.50	119	16.50	159	19.50	199	40.00
40	20.50	80	16.00	120	17.50	160	19.00		
41	20.50	81	15.00	121	17.00	161	19.00		

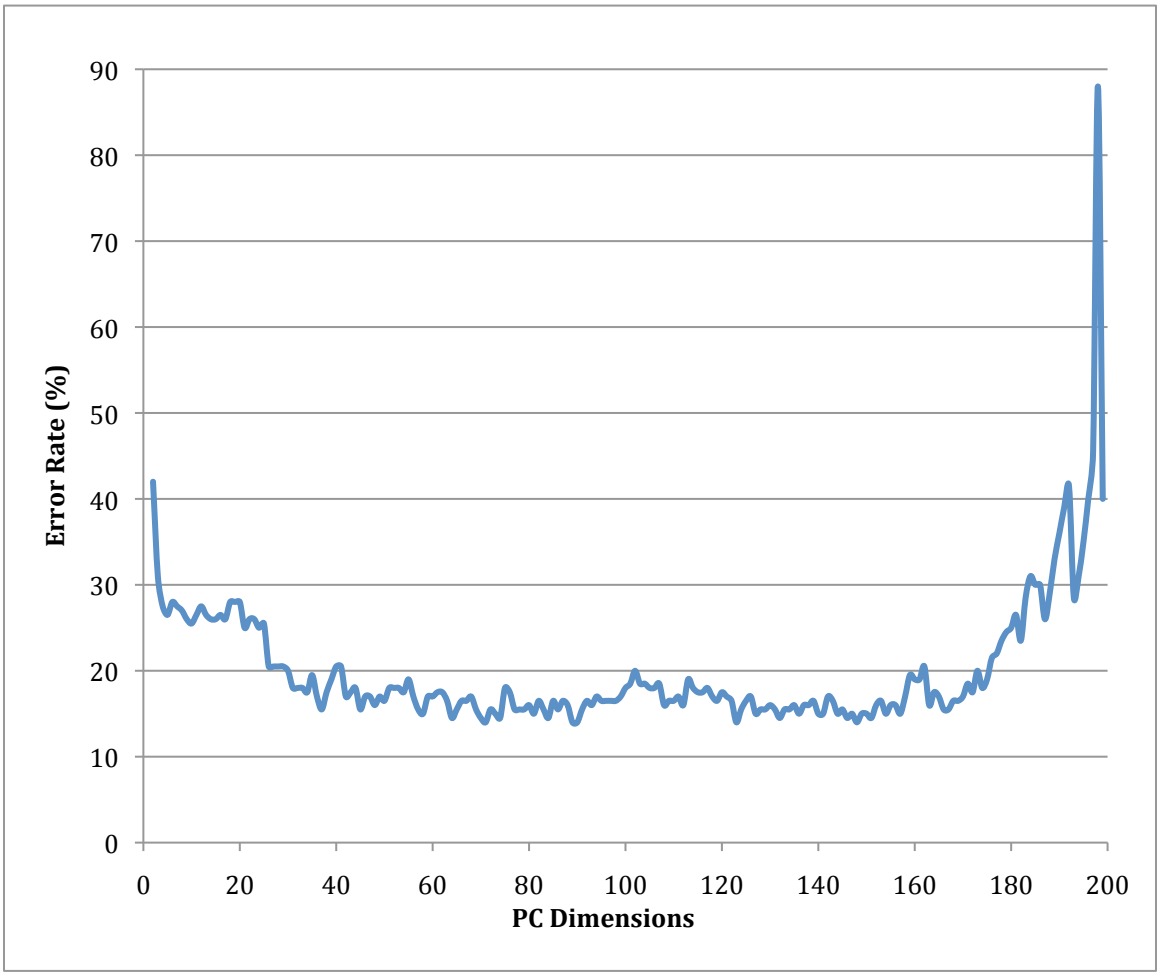


Figure 299: Graph of the tempered classification error rate versus PC dimensions for HOO-CV with PCA reduced CVA for the first set of 20 window glass first derivative (9-point smoothing) spectra (10 replicates), autoscaled data.

F. HOO-CV PCA-CVA Results for the Second Derivative Spectra (5-Point Smoothing)

First Set, Second Derivative (5-point smoothing) - Discrimination

Table 311: Discrimination error rates for HOO-CV with PCA reduced CVA for the first set of 30 glass second derivative (5-point smoothing) spectra (10 replicates), no data pretreatment. The smallest PC dimension with the minimum error rate is highlighted in yellow.

PCs	Error Rate (%)	PCs	Error Rate (%)	PCs	Error Rate (%)	PCs	Error Rate (%)	PCs	Error Rate (%)
2	98.00	18	71.33	34	56.33	50	47.67	66	40.33
3	96.67	19	71.67	35	54.00	51	45.00	67	37.33
4	95.67	20	71.67	36	53.00	52	45.00	68	39.00
5	93.67	21	69.33	37	53.00	53	44.33	69	38.00
6	88.00	22	69.33	38	53.00	54	44.00	70	36.00
7	84.67	23	70.00	39	52.00	55	44.00	71	36.33
8	83.33	24	68.67	40	54.67	56	41.67	72	36.67
9	85.00	25	66.33	41	53.33	57	42.33	73	36.00
10	83.00	26	66.00	42	50.00	58	40.33	74	35.00
11	81.67	27	64.00	43	49.67	59	41.67	75	34.00
12	80.00	28	64.00	44	47.00	60	42.33	76	33.67
13	80.33	29	63.33	45	46.33	61	40.00	77	32.67
14	77.67	30	63.67	46	45.00	62	39.33	78	32.33
15	76.33	31	61.00	47	46.33	63	39.33	79	30.00
16	71.00	32	59.33	48	45.67	64	38.00	80	32.33
17	72.00	33	55.00	49	48.33	65	38.33	81	30.00

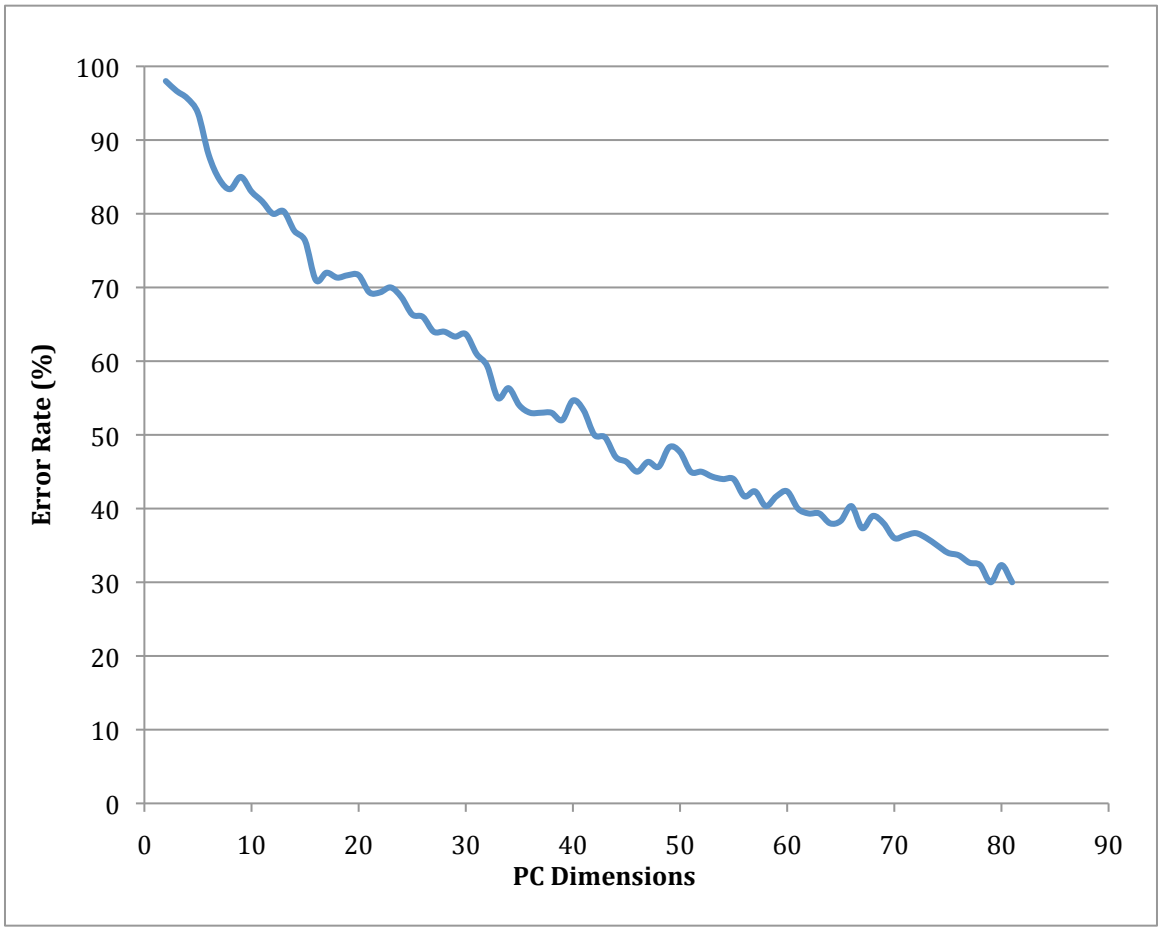


Figure 300: Graph of the discrimination error rate versus PC dimensions for HOO-CV with PCA reduced CVA for the first set of 30 glass second derivative (5-point smoothing) spectra (10 replicates), no data pretreatment.

Table 312: Discrimination error rates for HOO-CV with PCA reduced CVA for the first set of 30 glass second derivative (5-point smoothing) spectra (10 replicates), centered data. The smallest PC dimension with the minimum error rate is highlighted in yellow.

PCs	Error Rate (%)	PCs	Error Rate (%)	PCs	Error Rate (%)	PCs	Error Rate (%)	PCs	Error Rate (%)
2	97.00	19	69.67	36	52.33	53	43.67	70	34.67
3	96.33	20	70.00	37	51.67	54	42.67	71	36.33
4	96.33	21	70.33	38	50.67	55	44.67	72	36.33
5	92.00	22	70.67	39	52.67	56	43.00	73	34.67
6	88.33	23	69.33	40	52.00	57	42.00	74	35.67
7	86.67	24	67.33	41	53.00	58	40.00	75	35.33
8	84.33	25	65.67	42	48.67	59	41.00	76	33.00
9	85.67	26	64.67	43	47.33	60	39.33	77	31.67
10	83.00	27	63.67	44	48.33	61	40.00	78	30.00
11	81.33	28	61.00	45	46.67	62	39.33	79	33.33
12	80.33	29	63.33	46	48.67	63	39.00	80	30.00
13	77.00	30	61.67	47	47.67	64	39.67	81	29.00
14	79.00	31	58.33	48	44.67	65	41.33	82	30.33
15	75.00	32	57.00	49	45.33	66	39.67	83	30.67
16	75.33	33	56.33	50	44.33	67	36.00		
17	74.33	34	54.33	51	45.00	68	37.00		
18	70.67	35	53.33	52	44.00	69	36.33		

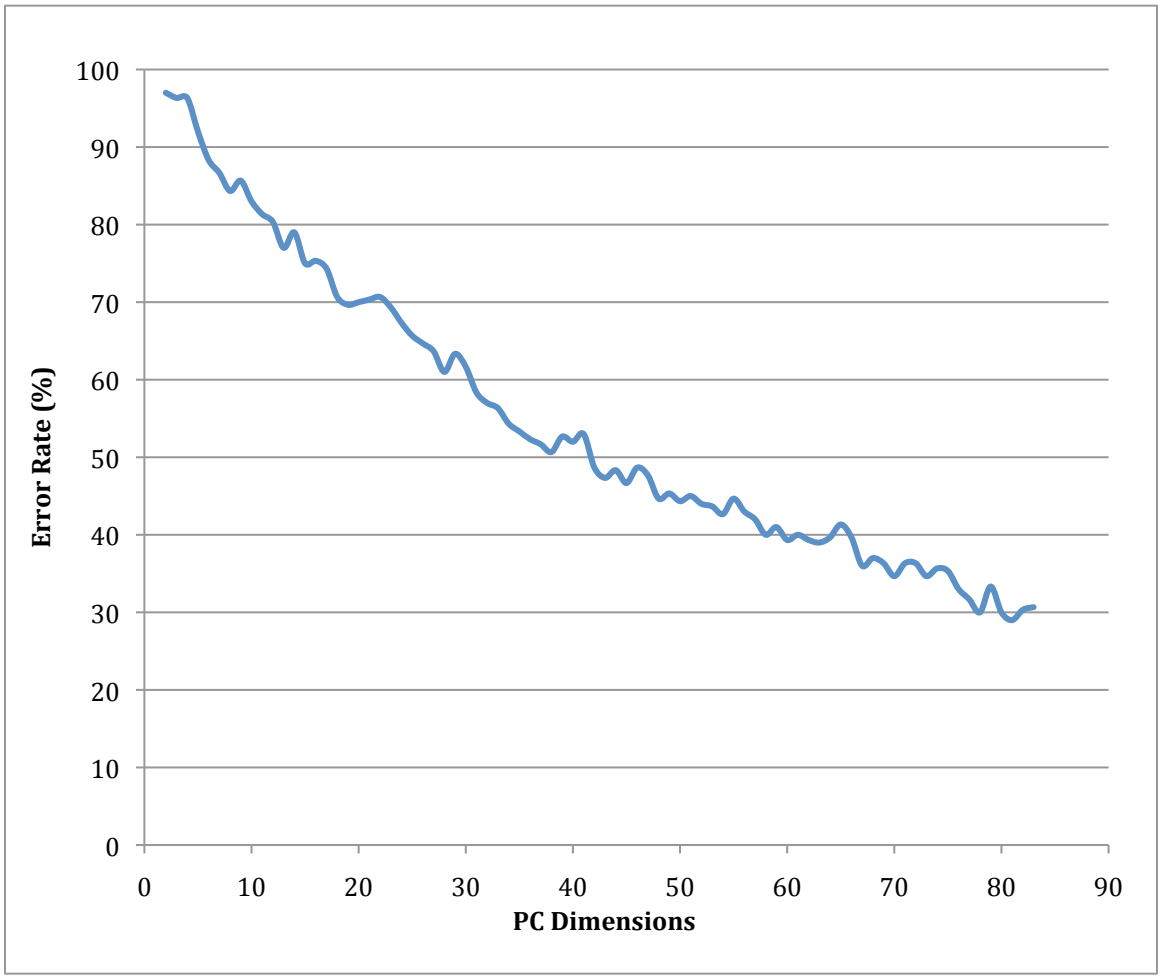


Figure 301: Graph of the discrimination error rate versus PC dimensions for HOO-CV with PCA reduced CVA for the first set of 30 glass second derivative (5-point smoothing) spectra (10 replicates), centered data.

Table 313: Discrimination error rates for HOO-CV with PCA reduced CVA for the first set of 30 glass second derivative (5-point smoothing) spectra (10 replicates), autoscaled data. The smallest PC dimension with the minimum error rate is highlighted in yellow.

PCs	Error Rate (%)	PCs	Error Rate (%)	PCs	Error Rate (%)	PCs	Error Rate (%)	PCs	Error Rate (%)
2	87.33	62	13.00	122	7.33	182	10.33	242	25.00
3	72.67	63	13.00	123	7.33	183	11.00	243	23.00
4	65.00	64	11.67	124	7.33	184	10.67	244	24.00
5	59.00	65	12.00	125	7.67	185	9.33	245	25.00
6	57.33	66	11.67	126	7.67	186	9.00	246	27.33
7	51.33	67	12.33	127	7.67	187	9.33	247	29.33
8	52.00	68	12.00	128	8.00	188	10.33	248	28.67
9	46.67	69	12.33	129	8.00	189	11.00	249	29.67
10	42.67	70	12.00	130	8.33	190	10.33	250	31.33
11	36.67	71	12.00	131	8.00	191	9.67	251	28.67
12	37.67	72	10.67	132	7.67	192	10.00	252	30.00
13	32.67	73	10.67	133	7.33	193	10.67	253	31.33
14	31.33	74	9.67	134	7.67	194	10.33	254	32.67
15	32.67	75	9.67	135	7.00	195	10.33	255	36.67
16	31.00	76	10.67	136	6.67	196	10.67	256	37.67
17	30.33	77	10.67	137	7.00	197	9.33	257	40.00
18	29.33	78	10.00	138	7.67	198	10.00	258	39.33
19	28.33	79	11.00	139	6.67	199	9.33	259	40.67
20	26.33	80	10.67	140	5.00	200	9.00	260	45.00
21	25.00	81	11.00	141	5.67	201	10.33	261	41.67
22	24.00	82	11.00	142	5.67	202	10.00	262	40.33
23	24.00	83	11.33	143	6.00	203	10.67	263	46.33
24	24.00	84	10.33	144	6.33	204	9.67	264	42.67
25	24.33	85	10.33	145	5.67	205	9.00	265	51.00
26	24.33	86	10.33	146	5.33	206	8.67	266	46.67
27	22.33	87	10.00	147	5.33	207	9.67	267	54.67
28	21.00	88	9.00	148	5.00	208	10.67	268	68.00
29	21.00	89	9.67	149	6.33	209	10.67	269	81.00
30	22.00	90	10.00	150	6.33	210	11.33	270	86.67
31	21.33	91	9.00	151	7.00	211	11.67	271	82.33
32	21.00	92	9.00	152	7.67	212	12.00	272	69.00
33	21.33	93	9.00	153	7.67	213	12.33	273	72.00
34	21.00	94	9.33	154	6.67	214	11.67	274	84.33
35	20.00	95	9.33	155	6.67	215	10.67	275	81.33
36	18.00	96	11.33	156	7.67	216	10.67	276	84.33
37	17.00	97	10.33	157	8.00	217	12.00	277	89.33
38	17.00	98	10.00	158	7.33	218	11.33	278	86.33

39	17.00	99	8.33	159	7.67	219	11.67	279	89.00
40	17.00	100	9.00	160	8.00	220	11.33	280	84.67
41	17.33	101	9.33	161	8.00	221	12.33	281	85.67
42	18.33	102	8.00	162	8.00	222	12.33	282	90.67
43	17.67	103	8.00	163	8.00	223	12.33	283	92.00
44	14.67	104	8.33	164	7.67	224	12.33	284	96.00
45	17.00	105	8.67	165	8.00	225	12.33	285	98.00
46	15.33	106	8.00	166	8.33	226	13.00	286	96.67
47	15.00	107	8.33	167	8.33	227	14.00	287	98.33
48	15.00	108	7.67	168	8.67	228	15.67	288	99.67
49	16.00	109	7.00	169	8.67	229	15.00	289	99.33
50	15.33	110	7.67	170	8.67	230	15.33	290	99.67
51	15.67	111	8.00	171	9.33	231	15.00	291	99.67
52	15.67	112	8.33	172	9.00	232	16.67	292	99.33
53	15.67	113	8.33	173	9.33	233	18.00	293	99.00
54	14.00	114	7.33	174	9.67	234	17.00	294	98.00
55	13.33	115	8.33	175	9.00	235	16.33	295	98.00
56	14.00	116	8.67	176	9.67	236	17.67	296	99.00
57	14.00	117	8.33	177	8.67	237	19.00	297	99.00
58	14.00	118	8.67	178	9.67	238	19.67	298	98.67
59	14.67	119	9.00	179	10.67	239	19.00	299	74.33
60	14.00	120	7.33	180	10.33	240	21.00		
61	12.67	121	7.00	181	10.33	241	22.00		

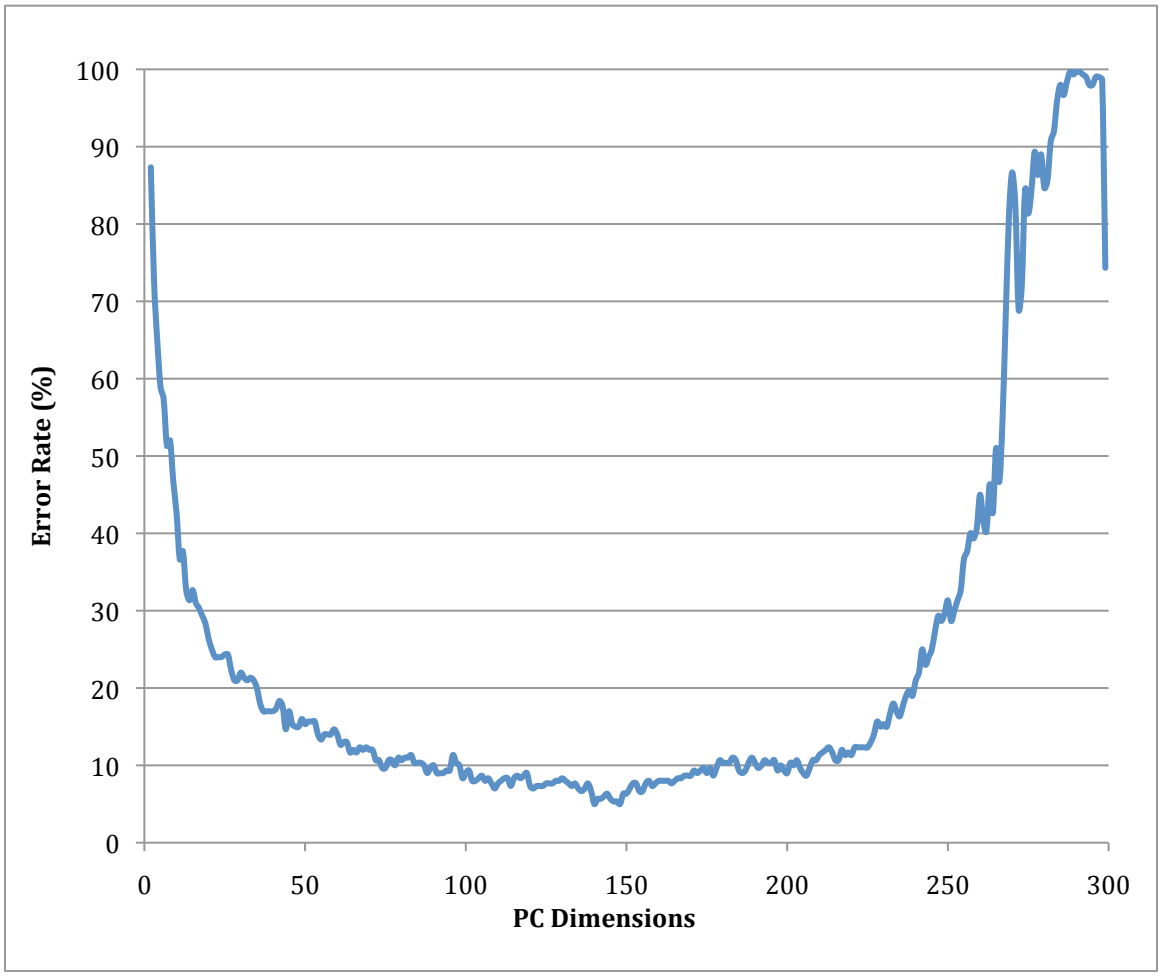


Figure 302: Graph of the discrimination error rate versus PC dimensions for HOO-CV with PCA reduced CVA for the first set of 30 glass second derivative (5-point smoothing) spectra (10 replicates), autoscaled data.

First Set, Second Derivative (5-point smoothing) – Classification (automotive, architectural or container)

Table 314: Classification (automotive, architectural or container) error rates for HOO-CV with PCA reduced CVA for the first set of 30 glass second derivative (5-point smoothing) spectra (10 replicates), no data pretreatment. The smallest PC dimension with the minimum error rate is highlighted in yellow.

PCs	Error Rate (%)	PCs	Error Rate (%)	PCs	Error Rate (%)	PCs	Error Rate (%)	PCs	Error Rate (%)
2	65.33	19	50.67	36	42.67	53	35.00	70	34.00
3	62.00	20	49.33	37	42.33	54	35.33	71	35.67
4	62.33	21	50.67	38	42.00	55	35.33	72	33.33
5	57.00	22	51.67	39	42.33	56	36.67	73	33.33
6	57.33	23	52.67	40	42.00	57	37.33	74	32.33
7	58.33	24	43.67	41	42.67	58	36.67	75	31.67
8	58.67	25	45.00	42	42.67	59	36.00	76	33.33
9	59.00	26	45.33	43	40.33	60	35.00	77	33.67
10	60.00	27	45.33	44	40.00	61	35.00	78	32.00
11	59.00	28	45.33	45	42.00	62	34.33	79	29.00
12	57.33	29	44.67	46	42.00	63	35.67	80	29.00
13	58.00	30	45.67	47	41.00	64	34.00	81	29.00
14	58.67	31	44.33	48	39.67	65	34.67	82	28.00
15	57.00	32	44.00	49	40.00	66	36.33	83	27.67
16	54.00	33	45.33	50	38.67	67	36.00	84	26.00
17	51.67	34	43.67	51	36.00	68	34.00	85	26.00
18	51.67	35	42.00	52	37.33	69	34.00		

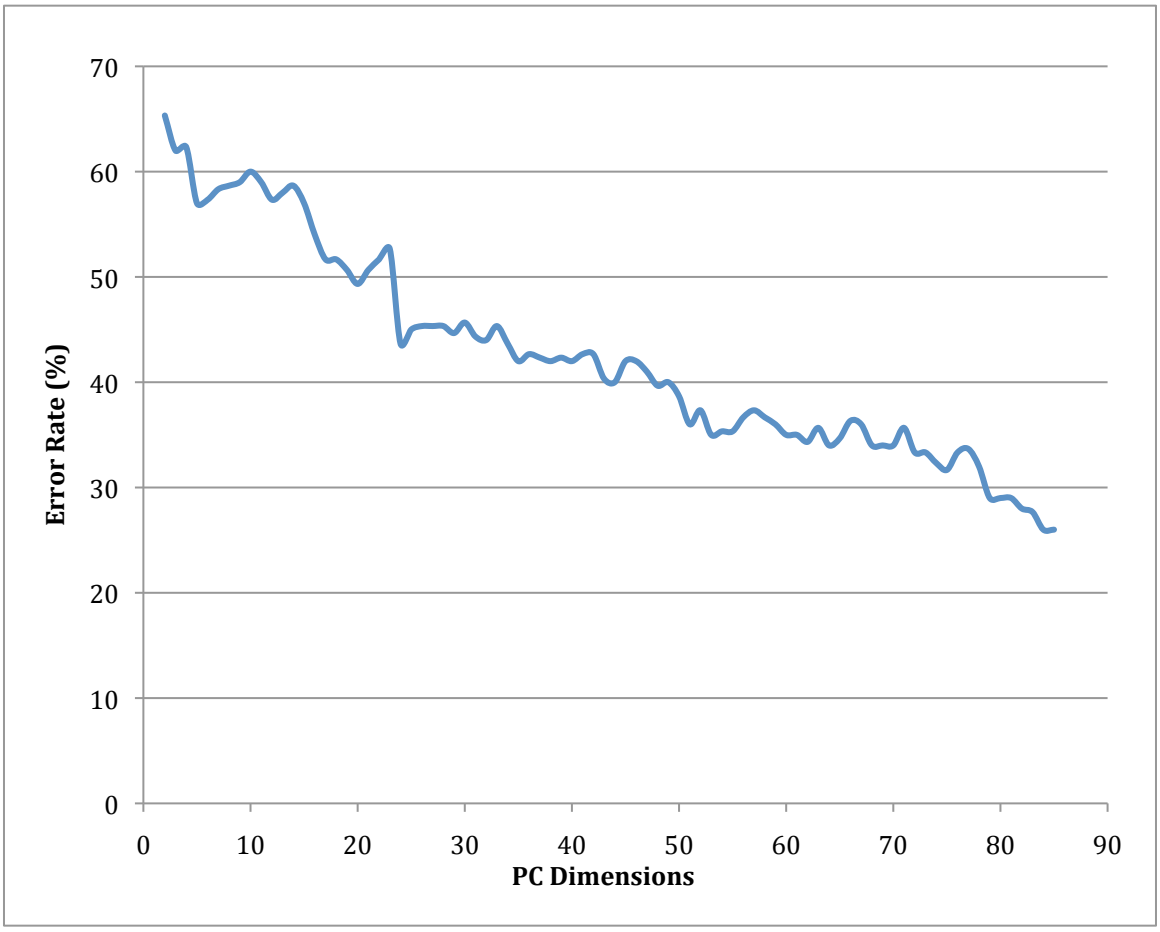


Figure 303: Graph of the classification (automotive, architectural or container) error rate versus PC dimensions for HOO-CV with PCA reduced CVA for the first set of 30 glass second derivative (5-point smoothing) spectra (10 replicates), no data pretreatment.

Table 315: Classification (automotive, architectural or container) error rates for HOO-CV with PCA reduced CVA for the first set of 30 glass second derivative (5-point smoothing) spectra (10 replicates), centered data. The smallest PC dimension with the minimum error rate is highlighted in yellow.

PCs	Error Rate (%)	PCs	Error Rate (%)	PCs	Error Rate (%)	PCs	Error Rate (%)	PCs	Error Rate (%)
2	64.33	19	51.67	36	42.00	53	35.00	70	34.00
3	63.00	20	49.00	37	43.67	54	34.33	71	33.33
4	59.33	21	51.00	38	41.67	55	35.33	72	33.67
5	58.33	22	52.67	39	42.67	56	36.67	73	33.00
6	57.67	23	51.00	40	43.33	57	36.33	74	32.67
7	58.33	24	44.67	41	43.33	58	34.67	75	31.33
8	59.33	25	45.00	42	43.00	59	34.67	76	32.33
9	59.33	26	46.67	43	41.33	60	34.33	77	31.00
10	60.00	27	47.33	44	41.67	61	36.33	78	30.67
11	57.33	28	46.33	45	42.67	62	32.33	79	30.33
12	57.33	29	46.33	46	39.67	63	34.33	80	29.00
13	57.33	30	44.67	47	40.00	64	35.00	81	28.00
14	56.33	31	45.00	48	39.67	65	35.33	82	28.00
15	53.67	32	43.67	49	37.00	66	37.00	83	26.33
16	52.33	33	45.00	50	36.67	67	35.00	84	27.67
17	51.00	34	44.00	51	37.00	68	34.00	85	26.67
18	52.00	35	41.67	52	37.33	69	34.33		

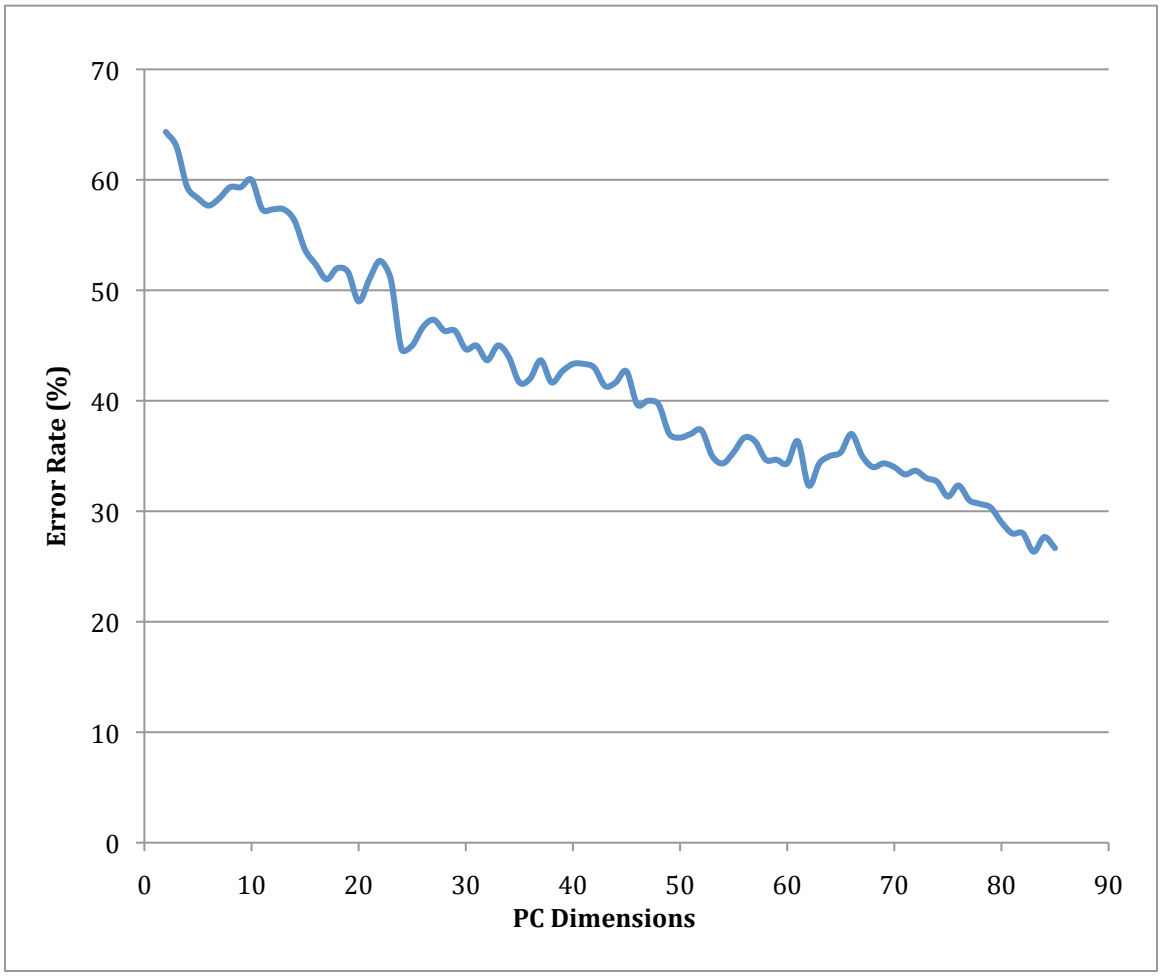


Figure 304: Graph of the classification (automotive, architectural or container) error rate versus PC dimensions for HOO-CV with PCA reduced CVA for the first set of 30 glass second derivative (5-point smoothing) spectra (10 replicates), centered data.

Table 316: Classification (automotive, architectural or container) error rates for HOO-CV with PCA reduced CVA for the first set of 30 glass second derivative (5-point smoothing) spectra (10 replicates), autoscaled data. The smallest PC dimension with the minimum error rate is highlighted in yellow.

PCs	Error Rate (%)	PCs	Error Rate (%)	PCs	Error Rate (%)	PCs	Error Rate (%)	PCs	Error Rate (%)
2	80.00	62	25.67	122	24.00	182	21.67	242	24.67
3	59.00	63	26.33	123	23.33	183	21.67	243	23.67
4	57.00	64	27.00	124	24.00	184	20.33	244	23.67
5	58.00	65	28.00	125	24.33	185	20.00	245	24.67
6	53.67	66	27.67	126	22.33	186	21.00	246	24.33
7	54.67	67	27.00	127	23.00	187	22.00	247	25.33
8	54.67	68	27.33	128	23.33	188	23.33	248	25.67
9	52.33	69	27.67	129	22.33	189	22.00	249	26.00
10	51.67	70	28.00	130	21.67	190	21.00	250	25.33
11	50.00	71	27.67	131	22.67	191	22.00	251	27.67
12	42.00	72	27.67	132	22.67	192	22.67	252	27.00
13	41.00	73	28.00	133	22.33	193	22.00	253	26.67
14	39.00	74	28.00	134	22.33	194	23.33	254	27.67
15	38.33	75	26.33	135	22.67	195	22.67	255	27.33
16	39.33	76	27.00	136	23.33	196	20.67	256	28.33
17	38.00	77	26.67	137	22.33	197	20.33	257	29.67
18	35.33	78	24.33	138	23.00	198	21.67	258	31.67
19	34.33	79	25.33	139	24.00	199	21.00	259	32.33
20	34.00	80	25.00	140	23.00	200	21.00	260	32.67
21	36.00	81	25.67	141	21.00	201	21.67	261	35.00
22	31.33	82	26.00	142	21.00	202	22.33	262	32.67
23	33.33	83	27.33	143	20.33	203	22.33	263	33.00
24	32.67	84	27.33	144	20.67	204	21.67	264	34.33
25	32.00	85	27.00	145	20.33	205	21.67	265	33.00
26	31.67	86	26.00	146	21.67	206	22.67	266	34.67
27	31.33	87	26.00	147	22.00	207	23.67	267	35.67
28	28.67	88	24.33	148	22.33	208	24.00	268	35.67
29	30.67	89	25.33	149	21.00	209	23.67	269	37.67
30	29.00	90	25.67	150	21.67	210	24.67	270	37.00
31	29.67	91	25.00	151	21.67	211	25.00	271	38.33
32	32.00	92	26.00	152	22.00	212	25.67	272	40.00
33	31.00	93	28.33	153	21.00	213	24.67	273	41.00
34	30.67	94	28.33	154	21.33	214	26.67	274	39.00
35	29.67	95	29.00	155	21.67	215	23.33	275	41.00
36	30.33	96	27.33	156	19.67	216	23.33	276	41.33
37	29.67	97	26.67	157	20.00	217	23.67	277	41.00

38	29.00	98	28.33	158	18.67	218	24.67	278	41.33
39	30.33	99	26.00	159	16.67	219	24.00	279	42.67
40	30.00	100	25.67	160	17.33	220	24.67	280	41.00
41	31.67	101	26.33	161	18.00	221	25.67	281	41.00
42	31.33	102	27.33	162	17.67	222	26.33	282	42.00
43	31.67	103	26.00	163	18.67	223	26.00	283	40.33
44	30.00	104	26.67	164	17.67	224	26.00	284	42.67
45	31.00	105	25.33	165	19.00	225	26.00	285	45.33
46	31.67	106	25.33	166	18.33	226	26.33	286	45.67
47	31.67	107	24.00	167	18.67	227	27.00	287	47.00
48	33.33	108	23.67	168	18.33	228	28.00	288	48.33
49	32.00	109	25.00	169	18.67	229	28.00	289	51.00
50	32.67	110	24.67	170	17.33	230	28.33	290	53.33
51	33.33	111	24.33	171	17.67	231	28.33	291	54.33
52	33.33	112	25.33	172	18.67	232	28.67	292	53.33
53	34.00	113	25.00	173	19.33	233	27.67	293	54.67
54	33.33	114	24.33	174	20.00	234	28.67	294	60.00
55	33.67	115	26.00	175	20.67	235	29.00	295	55.67
56	34.00	116	23.33	176	20.67	236	29.33	296	60.67
57	31.67	117	23.67	177	20.67	237	28.00	297	51.00
58	30.67	118	25.00	178	19.33	238	25.67	298	81.67
59	26.67	119	23.67	179	19.67	239	25.67	299	88.33
60	25.67	120	23.33	180	20.33	240	24.67		
61	26.33	121	23.67	181	21.00	241	24.33		

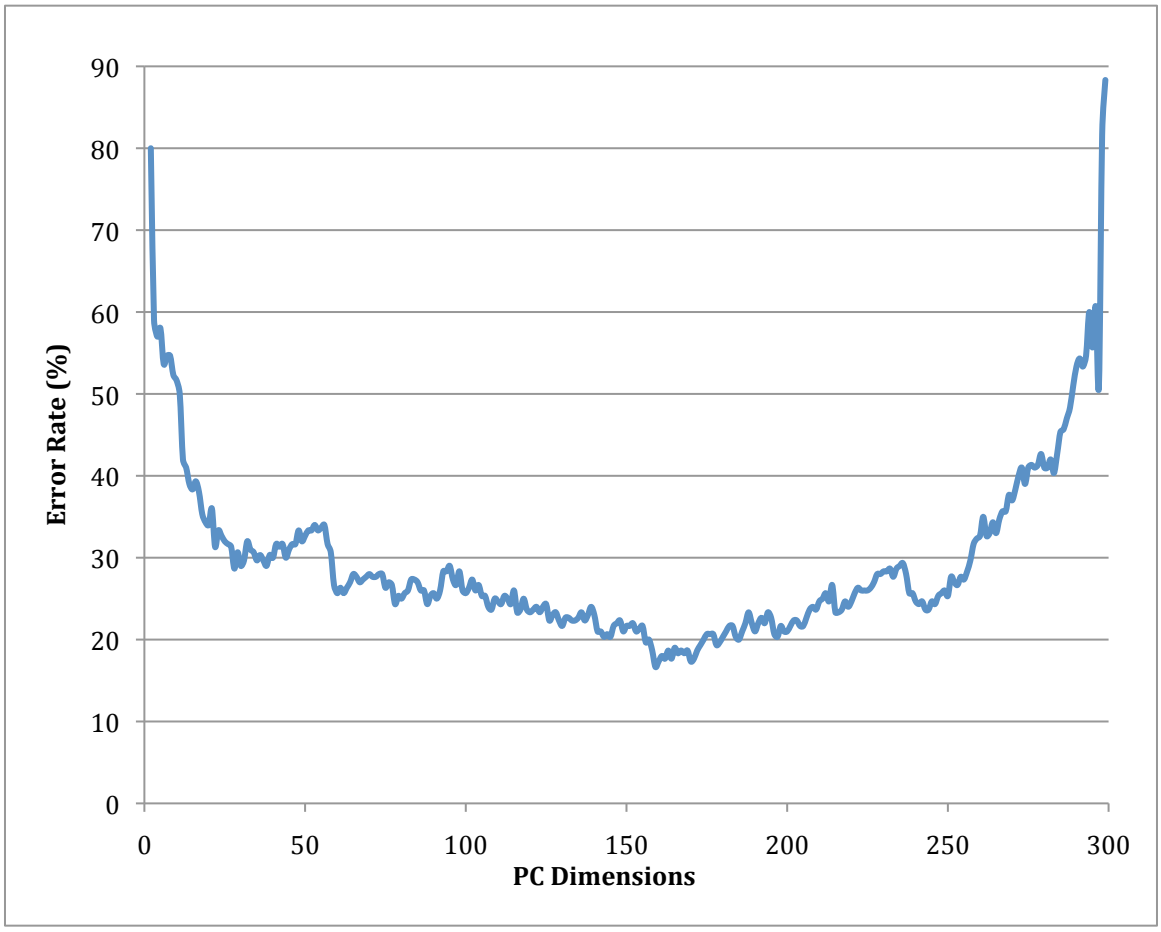


Figure 305: Graph of the classification (automotive, architectural or container) error rate versus PC dimensions for HOO-CV with PCA reduced CVA for the first set of 30 glass second derivative (5-point smoothing) spectra (10 replicates), autoscaled data.

First Set, Second Derivative (5-point smoothing) – Classification (window or container)

Table 317: Classification (window or container) error rates for HOO-CV with PCA reduced CVA for the first set of 30 glass second derivative (5-point smoothing) spectra (10 replicates), no data pretreatment. The smallest PC dimension with the minimum error rate is highlighted in yellow.

PCs	Error Rate (%)	PCs	Error Rate (%)	PCs	Error Rate (%)	PCs	Error Rate (%)	PCs	Error Rate (%)
2	33.33	19	32.00	36	21.67	53	10.00	70	7.00
3	32.00	20	29.00	37	22.00	54	9.67	71	6.33
4	33.00	21	29.67	38	21.67	55	8.67	72	6.67
5	34.00	22	29.67	39	22.67	56	8.33	73	6.67
6	31.67	23	29.00	40	22.67	57	8.33	74	5.33
7	32.33	24	26.33	41	22.67	58	8.67	75	5.33
8	33.67	25	28.00	42	23.00	59	8.33	76	6.67
9	33.67	26	27.67	43	19.33	60	9.00	77	6.67
10	34.00	27	28.00	44	17.67	61	6.33	78	5.67
11	34.00	28	26.67	45	17.00	62	7.00	79	5.67
12	32.67	29	26.00	46	19.00	63	7.33	80	6.00
13	32.67	30	26.00	47	16.00	64	7.67	81	5.67
14	30.33	31	22.00	48	16.00	65	7.33	82	6.00
15	31.33	32	22.67	49	16.33	66	7.00	83	6.00
16	31.00	33	22.33	50	16.33	67	7.33	84	5.67
17	29.33	34	21.67	51	13.00	68	6.33	85	5.67
18	30.33	35	21.67	52	13.33	69	7.00		

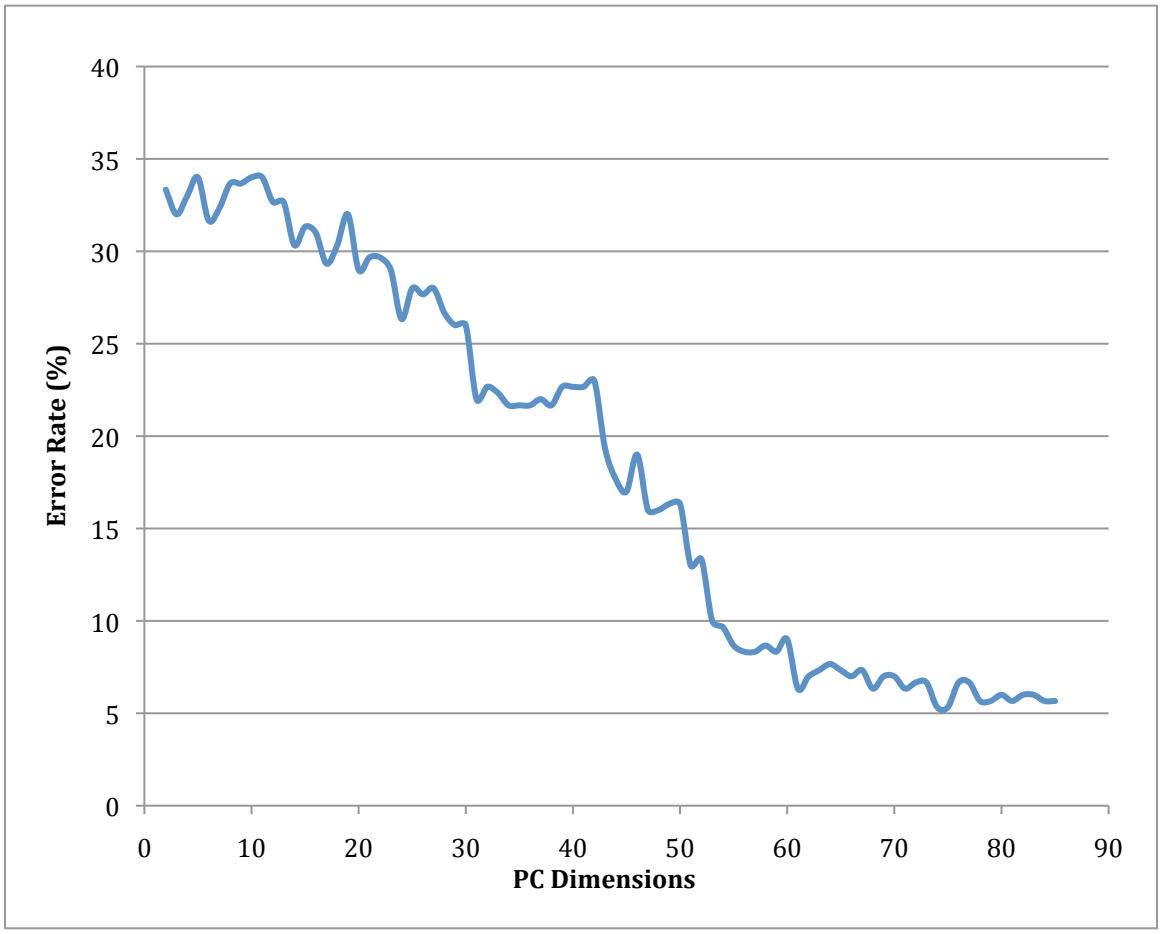


Figure 306: Graph of the classification (window or container) error rate versus PC dimensions for HOO-CV with PCA reduced CVA for the first set of 30 glass second derivative (5-point smoothing) spectra (10 replicates), no data pretreatment.

Table 318: Classification (window or container) error rates for HOO-CV with PCA reduced CVA for the first set of 30 glass second derivative (5-point smoothing) spectra (10 replicates), centered data. The smallest PC dimension with the minimum error rate is highlighted in yellow.

PCs	Error Rate (%)	PCs	Error Rate (%)	PCs	Error Rate (%)	PCs	Error Rate (%)	PCs	Error Rate (%)
2	33.33	19	30.00	36	21.00	53	9.33	70	7.00
3	33.00	20	30.00	37	22.00	54	9.33	71	6.67
4	33.67	21	30.00	38	22.67	55	9.00	72	7.00
5	31.67	22	28.00	39	22.67	56	9.00	73	6.00
6	32.00	23	30.00	40	22.67	57	9.00	74	5.67
7	32.67	24	26.67	41	22.00	58	8.33	75	5.67
8	33.00	25	27.33	42	21.00	59	8.00	76	5.67
9	33.00	26	28.00	43	20.67	60	8.33	77	6.00
10	32.67	27	26.00	44	19.67	61	7.67	78	5.67
11	31.33	28	25.67	45	19.00	62	7.33	79	5.67
12	31.00	29	25.67	46	15.33	63	7.33	80	5.67
13	30.67	30	21.67	47	16.33	64	7.33	81	6.00
14	31.00	31	23.00	48	14.00	65	7.00	82	6.00
15	31.33	32	22.00	49	14.67	66	7.67	83	5.33
16	30.33	33	20.67	50	12.67	67	6.67	84	6.00
17	30.67	34	20.33	51	13.00	68	7.00	85	6.00
18	31.00	35	21.00	52	12.67	69	7.33		

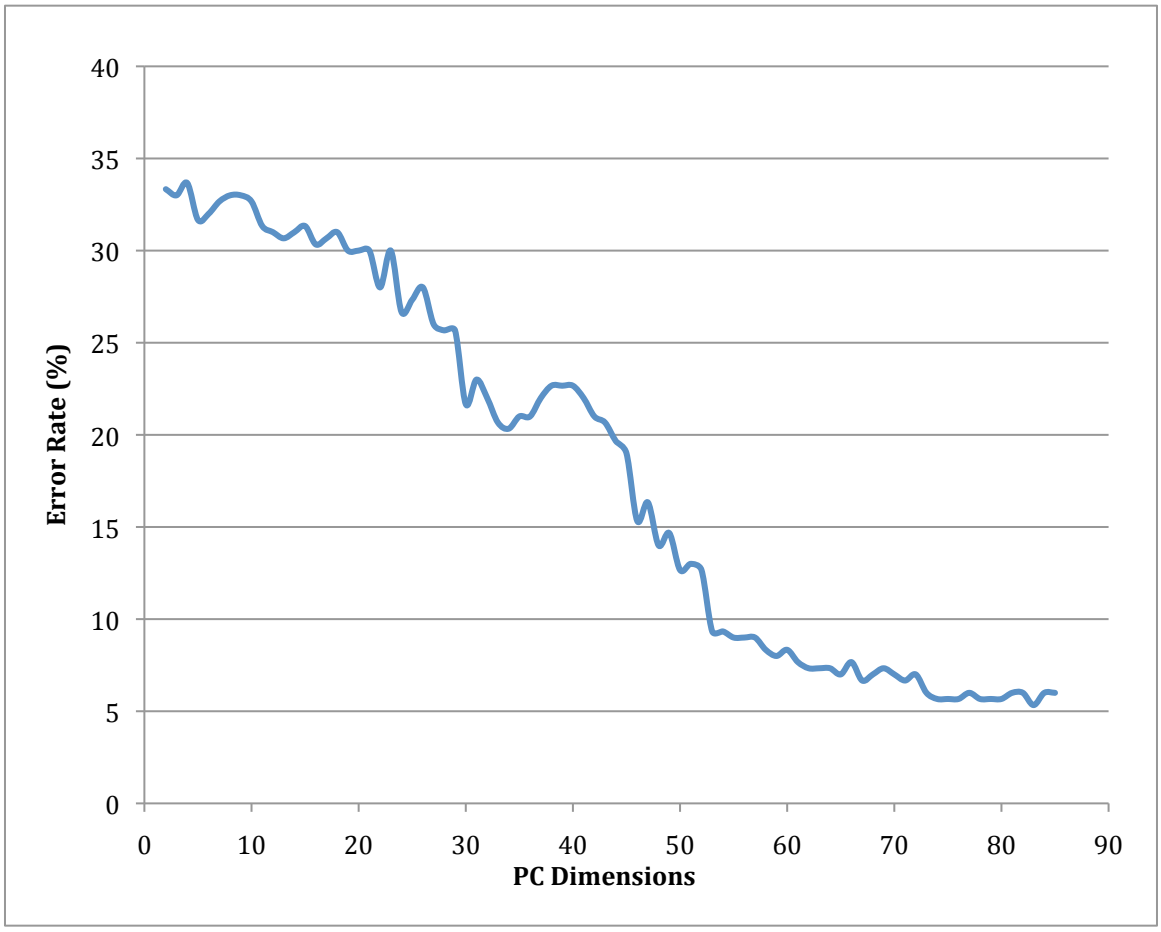


Figure 307: Graph of the classification (window or container) error rate versus PC dimensions for HOO-CV with PCA reduced CVA for the first set of 30 glass second derivative (5-point smoothing) spectra (10 replicates), centered data.

Table 319: Classification (window or container) error rates for HOO-CV with PCA reduced CVA for the first set of 30 glass second derivative (5-point smoothing) spectra (10 replicates), autoscaled data. The smallest PC dimension with the minimum error rate is highlighted in yellow.

PCs	Error Rate (%)	PCs	Error Rate (%)	PCs	Error Rate (%)	PCs	Error Rate (%)	PCs	Error Rate (%)
2	33.33	62	7.00	122	5.33	182	5.00	242	9.33
3	33.33	63	7.33	123	5.00	183	5.33	243	10.00
4	29.33	64	7.00	124	5.33	184	5.00	244	9.00
5	29.00	65	7.00	125	5.33	185	4.33	245	10.00
6	30.00	66	6.67	126	4.67	186	5.00	246	11.33
7	30.67	67	7.33	127	4.00	187	5.67	247	12.33
8	30.33	68	7.33	128	3.67	188	6.33	248	12.00
9	29.00	69	7.33	129	3.67	189	5.67	249	11.00
10	28.00	70	7.67	130	3.33	190	5.33	250	11.67
11	28.67	71	8.33	131	3.67	191	5.67	251	12.67
12	18.00	72	8.33	132	3.33	192	6.33	252	12.00
13	18.33	73	6.67	133	4.00	193	6.33	253	12.67
14	18.67	74	6.67	134	4.00	194	6.33	254	13.00
15	19.67	75	6.67	135	3.67	195	5.00	255	13.67
16	19.33	76	7.67	136	3.33	196	5.67	256	14.00
17	15.67	77	6.67	137	3.33	197	6.33	257	14.33
18	13.33	78	7.00	138	3.33	198	6.00	258	14.67
19	13.67	79	6.67	139	3.33	199	5.67	259	15.67
20	15.33	80	8.00	140	2.67	200	5.33	260	15.67
21	15.67	81	8.00	141	3.00	201	5.33	261	15.00
22	12.00	82	8.00	142	2.33	202	5.00	262	15.00
23	11.67	83	7.67	143	2.33	203	5.67	263	16.33
24	11.67	84	8.00	144	2.33	204	5.67	264	14.33
25	12.00	85	7.67	145	2.67	205	5.00	265	15.33
26	12.33	86	6.67	146	2.67	206	5.00	266	15.67
27	12.33	87	7.67	147	2.67	207	5.00	267	16.67
28	12.00	88	6.00	148	2.67	208	5.00	268	18.00
29	12.33	89	5.67	149	2.67	209	5.00	269	17.67
30	12.33	90	6.00	150	2.67	210	6.33	270	17.67
31	11.67	91	6.00	151	3.33	211	6.00	271	18.33
32	11.67	92	6.00	152	3.33	212	6.00	272	18.67
33	12.33	93	6.33	153	3.67	213	5.33	273	18.67
34	12.67	94	6.67	154	3.33	214	6.33	274	19.00
35	12.00	95	7.00	155	3.33	215	6.67	275	19.67
36	11.67	96	5.33	156	3.33	216	6.33	276	19.00
37	12.00	97	5.67	157	3.33	217	6.33	277	19.00

38	11.33	98	5.33	158	3.00	218	6.67	278	20.67
39	11.67	99	5.33	159	3.00	219	6.67	279	21.67
40	12.33	100	5.67	160	2.67	220	7.33	280	21.33
41	12.33	101	5.67	161	3.00	221	7.67	281	23.00
42	12.33	102	6.33	162	3.00	222	8.00	282	24.67
43	12.33	103	6.33	163	3.33	223	8.33	283	22.00
44	10.67	104	6.33	164	4.00	224	6.67	284	23.33
45	10.33	105	5.33	165	4.67	225	6.67	285	25.33
46	10.67	106	5.67	166	3.33	226	7.00	286	26.67
47	10.67	107	5.67	167	3.67	227	7.00	287	28.67
48	10.00	108	6.00	168	3.67	228	7.67	288	29.33
49	9.67	109	6.00	169	3.33	229	7.67	289	32.33
50	10.00	110	6.33	170	3.33	230	8.00	290	35.67
51	11.00	111	6.33	171	3.33	231	8.33	291	38.33
52	10.67	112	6.33	172	3.33	232	8.00	292	35.00
53	10.33	113	6.00	173	3.67	233	8.33	293	36.00
54	10.67	114	5.67	174	3.67	234	8.33	294	38.33
55	11.00	115	6.00	175	4.33	235	8.33	295	39.33
56	11.33	116	6.00	176	4.33	236	9.67	296	42.67
57	11.00	117	5.67	177	4.67	237	9.67	297	44.00
58	10.67	118	5.67	178	4.67	238	9.00	298	50.67
59	8.33	119	5.67	179	5.00	239	8.67	299	33.33
60	7.67	120	5.67	180	5.33	240	9.67		
61	7.00	121	5.33	181	5.00	241	9.33		

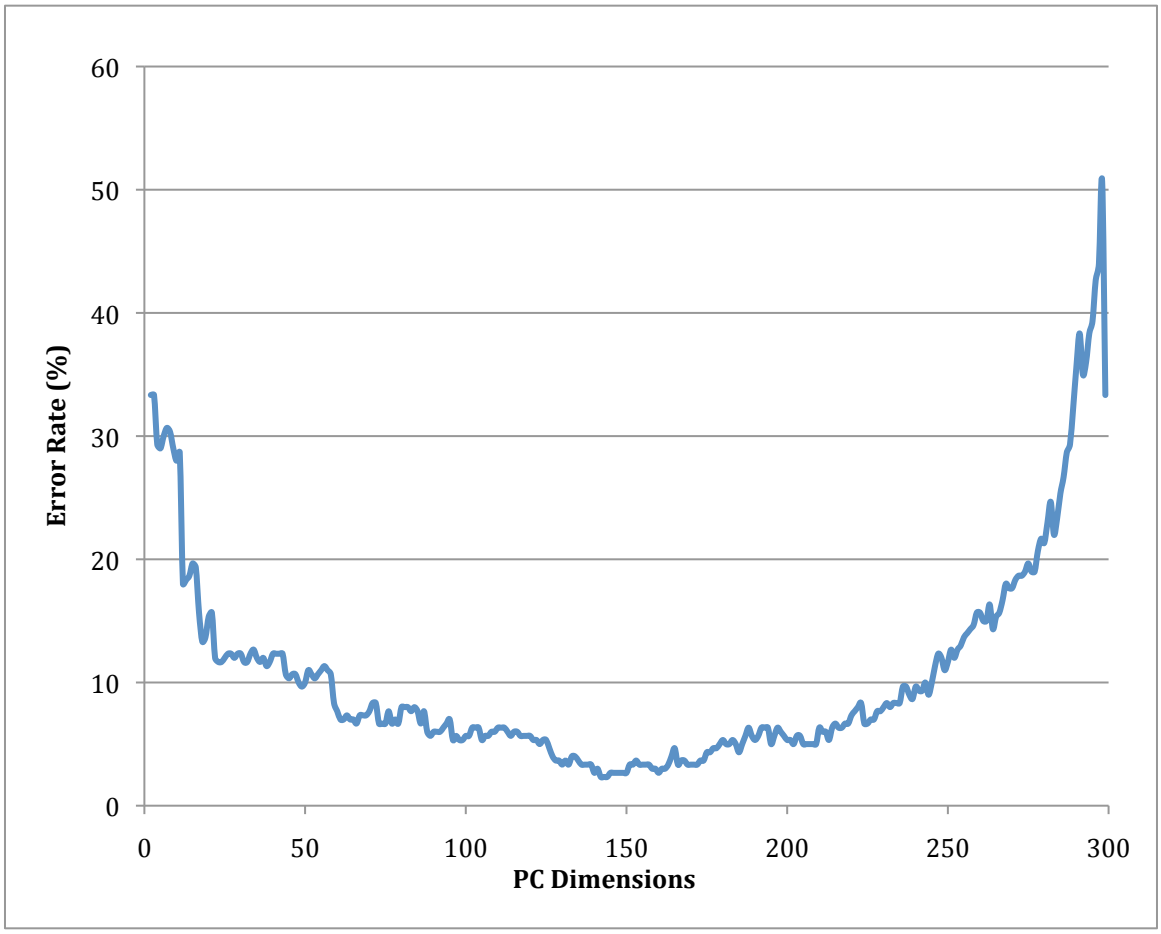


Figure 308: Graph of the classification (window or container) error rate versus PC dimensions for HOO-CV with PCA reduced CVA for the first set of 30 glass second derivative (5-point smoothing) spectra (10 replicates), autoscaled data.

First Set, Second Derivative (5-point smoothing) – Window Discrimination

Table 320: Discrimination error rates for HOO-CV with PCA reduced CVA for the first set of 20 window glass second derivative (5-point smoothing) spectra (10 replicates), no data pretreatment. The smallest PC dimension with the minimum error rate is highlighted in yellow.

PCs	Error Rate (%)	PCs	Error Rate (%)	PCs	Error Rate (%)	PCs	Error Rate (%)	PCs	Error Rate (%)
2	97.00	18	63.00	34	56.00	50	55.00	66	42.50
3	93.50	19	64.00	35	52.00	51	54.50	67	42.00
4	91.50	20	60.00	36	53.00	52	49.50	68	42.50
5	89.00	21	61.00	37	52.00	53	50.00	69	44.00
6	84.50	22	61.00	38	52.50	54	48.50	70	43.00
7	77.50	23	62.00	39	52.00	55	49.50	71	41.50
8	78.50	24	64.00	40	48.00	56	50.00	72	43.00
9	77.00	25	62.50	41	49.00	57	50.00	73	41.00
10	75.00	26	60.50	42	50.00	58	45.50	74	39.00
11	73.50	27	60.00	43	52.00	59	43.00	75	40.50
12	71.50	28	62.50	44	51.50	60	45.50	76	42.00
13	69.50	29	57.50	45	51.50	61	44.50	77	39.00
14	68.50	30	60.00	46	52.00	62	45.00	78	38.00
15	67.00	31	58.00	47	52.00	63	45.00		
16	65.00	32	57.00	48	51.00	64	46.00		
17	64.00	33	56.00	49	52.00	65	44.50		

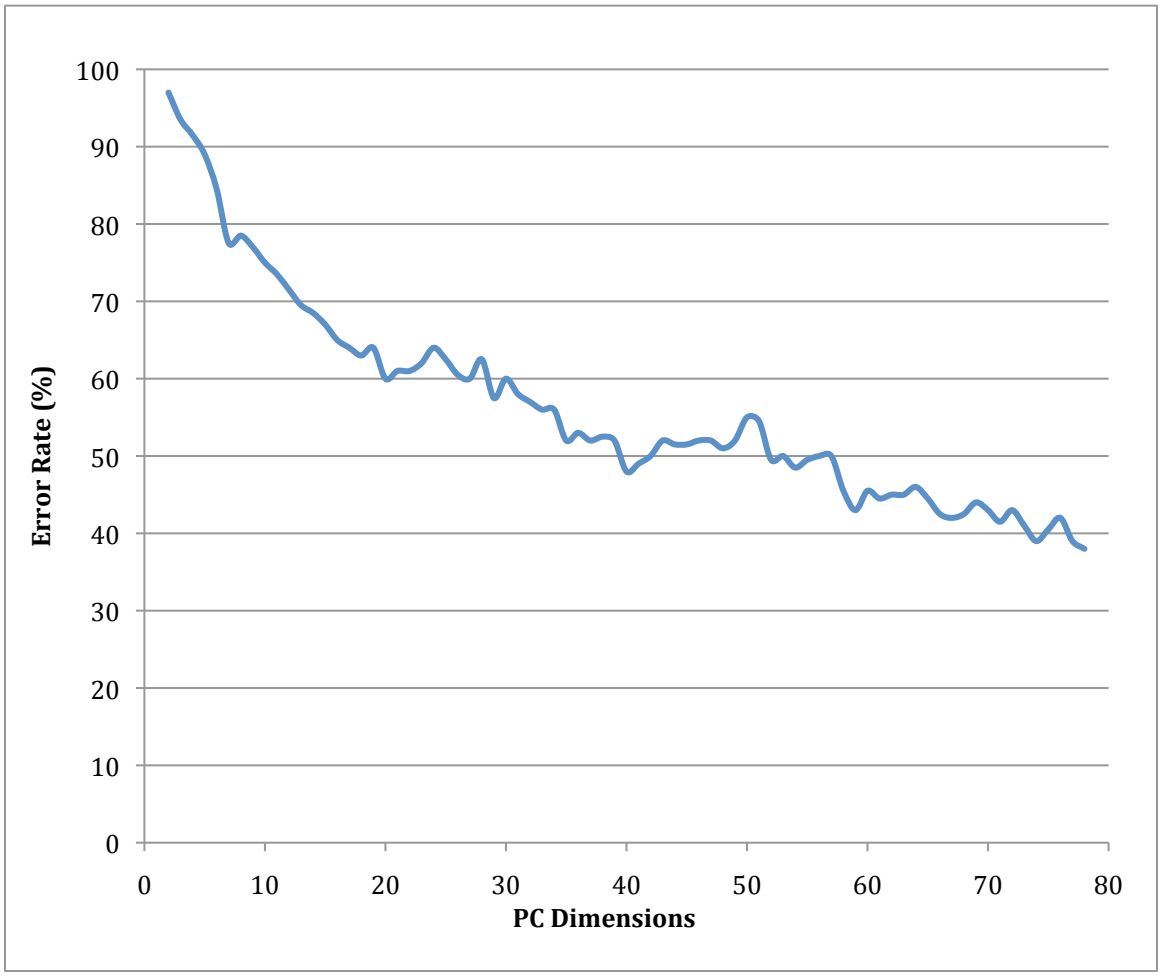


Figure 309: Graph of the discrimination error rate versus PC dimensions for HOO-CV with PCA reduced CVA for the first set of 20 window glass second derivative (5-point smoothing) spectra (10 replicates), no data pretreatment.

Table 321: Discrimination error rates for HOO-CV with PCA reduced CVA for the first set of 20 window glass second derivative (5-point smoothing) spectra (10 replicates), centered data. The smallest PC dimension with the minimum error rate is highlighted in yellow.

PCs	Error Rate (%)	PCs	Error Rate (%)	PCs	Error Rate (%)	PCs	Error Rate (%)	PCs	Error Rate (%)
2	97.00	18	66.50	34	54.00	50	54.00	66	45.00
3	95.50	19	62.00	35	54.50	51	53.00	67	44.50
4	92.50	20	61.00	36	53.50	52	48.00	68	44.00
5	90.50	21	63.00	37	53.50	53	50.50	69	42.50
6	86.50	22	63.50	38	54.00	54	48.50	70	44.00
7	79.50	23	64.50	39	52.00	55	50.50	71	42.50
8	82.00	24	63.50	40	47.50	56	48.00	72	42.50
9	77.50	25	62.00	41	48.00	57	47.00	73	40.00
10	73.00	26	61.00	42	49.50	58	46.50	74	39.50
11	72.00	27	61.00	43	50.00	59	46.00	75	40.00
12	68.00	28	58.50	44	53.50	60	45.00	76	38.00
13	70.00	29	60.00	45	52.50	61	43.50	77	39.00
14	71.50	30	57.50	46	53.00	62	44.00		
15	70.50	31	58.00	47	53.50	63	44.50		
16	70.00	32	55.00	48	54.00	64	46.50		
17	66.50	33	54.00	49	54.00	65	44.50		

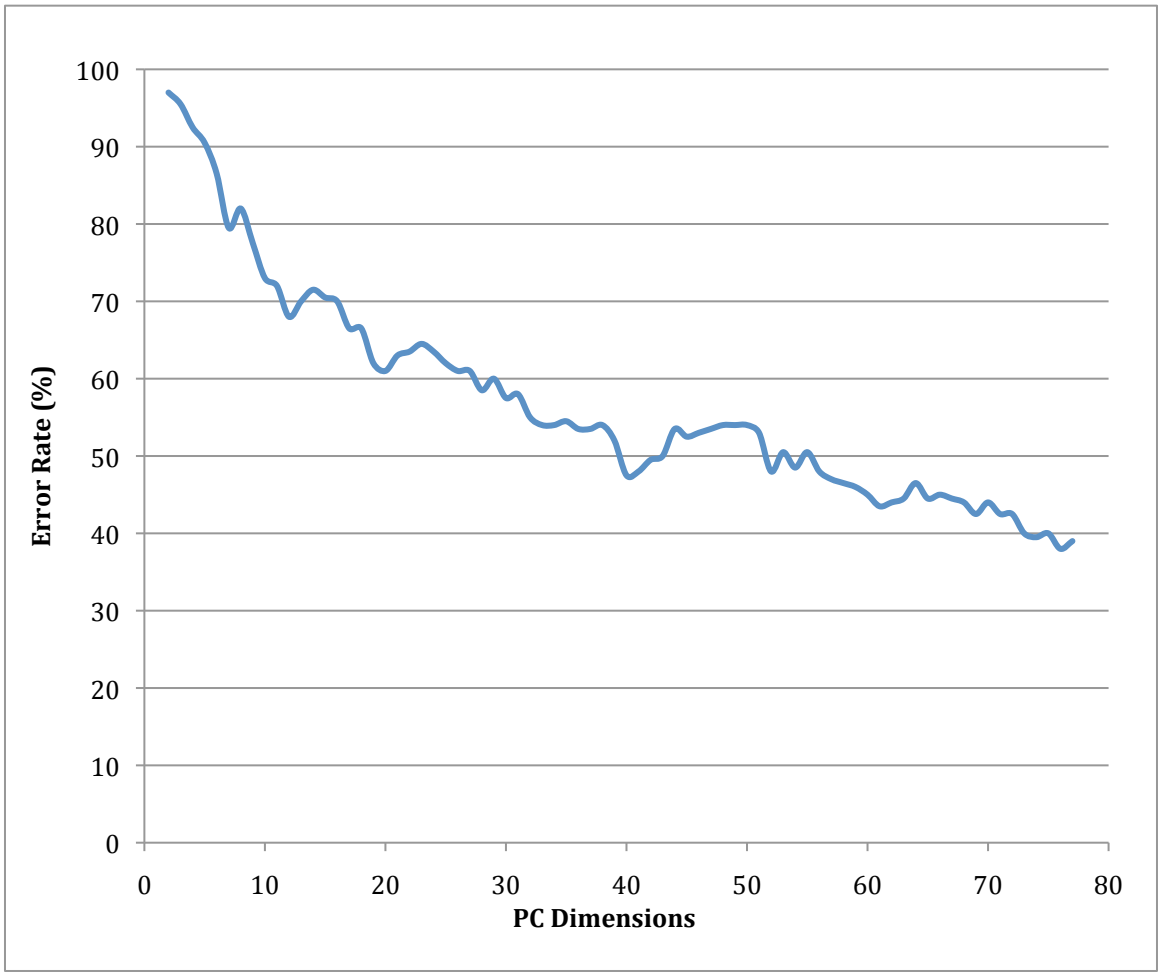


Figure 310: Graph of the discrimination error rate versus PC dimensions for HOO-CV with PCA reduced CVA for the first set of 20 window glass second derivative (5-point smoothing) spectra (10 replicates), centered data.

Table 322: Discrimination error rates for HOO-CV with PCA reduced CVA for the first set of 20 window glass second derivative (5-point smoothing) spectra (10 replicates), autoscaled data. The smallest PC dimension with the minimum error rate is highlighted in yellow.

PCs	Error Rate (%)	PCs	Error Rate (%)	PCs	Error Rate (%)	PCs	Error Rate (%)	PCs	Error Rate (%)
2	85.50	42	14.50	82	17.50	122	20.00	162	39.00
3	67.50	43	14.00	83	17.50	123	16.50	163	35.50
4	63.00	44	13.50	84	18.00	124	17.00	164	34.50
5	54.50	45	15.00	85	17.50	125	17.00	165	31.50
6	49.50	46	13.50	86	19.00	126	18.00	166	32.50
7	46.00	47	12.50	87	19.00	127	17.50	167	34.50
8	47.00	48	12.00	88	18.50	128	18.50	168	34.50
9	44.50	49	13.00	89	19.00	129	19.50	169	39.00
10	35.00	50	11.50	90	17.00	130	19.50	170	42.50
11	31.00	51	12.00	91	16.00	131	21.50	171	47.00
12	31.50	52	13.00	92	16.50	132	23.50	172	50.00
13	31.00	53	13.00	93	16.00	133	23.00	173	44.00
14	29.00	54	14.00	94	15.00	134	23.50	174	47.50
15	28.00	55	13.50	95	14.50	135	23.50	175	51.50
16	27.50	56	12.00	96	15.00	136	24.50	176	58.50
17	26.00	57	13.50	97	13.00	137	24.50	177	66.00
18	24.50	58	13.50	98	13.50	138	24.00	178	61.50
19	23.50	59	13.50	99	14.00	139	25.50	179	65.50
20	23.50	60	14.00	100	14.50	140	26.50	180	75.50
21	21.00	61	14.50	101	18.00	141	26.50	181	88.50
22	20.00	62	14.00	102	18.00	142	22.50	182	85.50
23	20.50	63	15.00	103	15.50	143	23.50	183	73.50
24	20.00	64	14.50	104	16.50	144	21.50	184	74.50
25	19.00	65	14.50	105	15.50	145	23.50	185	82.50
26	19.00	66	15.00	106	15.00	146	22.00	186	85.00
27	18.50	67	15.50	107	16.50	147	24.50	187	92.00
28	17.50	68	15.00	108	16.50	148	25.50	188	93.50
29	19.00	69	16.00	109	16.00	149	29.00	189	87.50
30	17.00	70	15.50	110	17.00	150	28.50	190	91.50
31	16.50	71	13.00	111	18.50	151	31.50	191	89.00
32	18.50	72	11.50	112	17.50	152	31.50	192	91.00
33	17.00	73	13.00	113	15.50	153	30.50	193	95.00
34	17.00	74	15.00	114	16.50	154	31.50	194	96.00
35	18.50	75	16.00	115	16.00	155	33.00	195	94.50
36	15.50	76	14.50	116	14.00	156	34.50	196	97.50
37	15.50	77	14.50	117	17.00	157	33.00	197	96.00
38	17.00	78	15.50	118	15.00	158	35.00	198	93.00

39	16.50	79	17.00	119	15.50	159	37.00	199	78.00
40	16.00	80	16.50	120	17.00	160	39.00		
41	15.00	81	17.00	121	19.50	161	37.00		

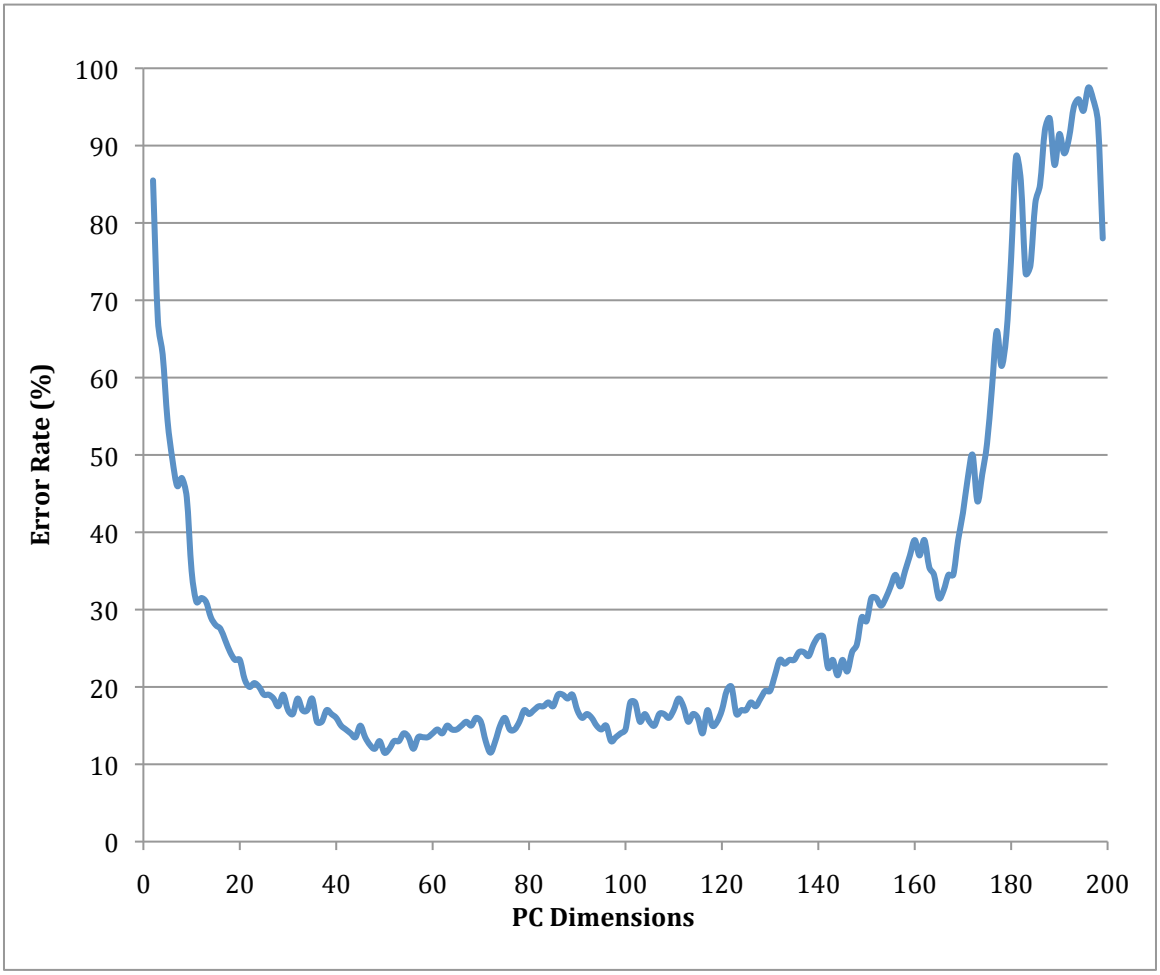


Figure 311: Graph of the discrimination error rate versus PC dimensions for HOO-CV with PCA reduced CVA for the first set of 20 window glass second derivative (5-point smoothing) spectra (10 replicates), autoscaled data.

First Set, Second Derivative (5-point smoothing) – Container Discrimination

Table 323: Discrimination error rates for HOO-CV with PCA reduced CVA for the first set of 10 container glass second derivative (5-point smoothing) spectra (10 replicates), no data pretreatment. The smallest PC dimension with the minimum error rate is highlighted in yellow.

PCs	Error Rate (%)	PCs	Error Rate (%)	PCs	Error Rate (%)	PCs	Error Rate (%)	PCs	Error Rate (%)
2	86.00	16	47.00	30	38.00	44	27.00	58	29.00
3	84.00	17	46.00	31	35.00	45	26.00	59	30.00
4	77.00	18	44.00	32	36.00	46	26.00	60	31.00
5	69.00	19	43.00	33	32.00	47	28.00	61	32.00
6	76.00	20	39.00	34	29.00	48	28.00	62	33.00
7	75.00	21	37.00	35	30.00	49	27.00	63	38.00
8	68.00	22	39.00	36	28.00	50	30.00	64	38.00
9	63.00	23	37.00	37	29.00	51	28.00	65	35.00
10	62.00	24	39.00	38	31.00	52	29.00	66	34.00
11	58.00	25	38.00	39	30.00	53	29.00	67	36.00
12	58.00	26	37.00	40	30.00	54	26.00		
13	56.00	27	37.00	41	29.00	55	28.00		
14	50.00	28	35.00	42	30.00	56	27.00		
15	46.00	29	36.00	43	28.00	57	27.00		

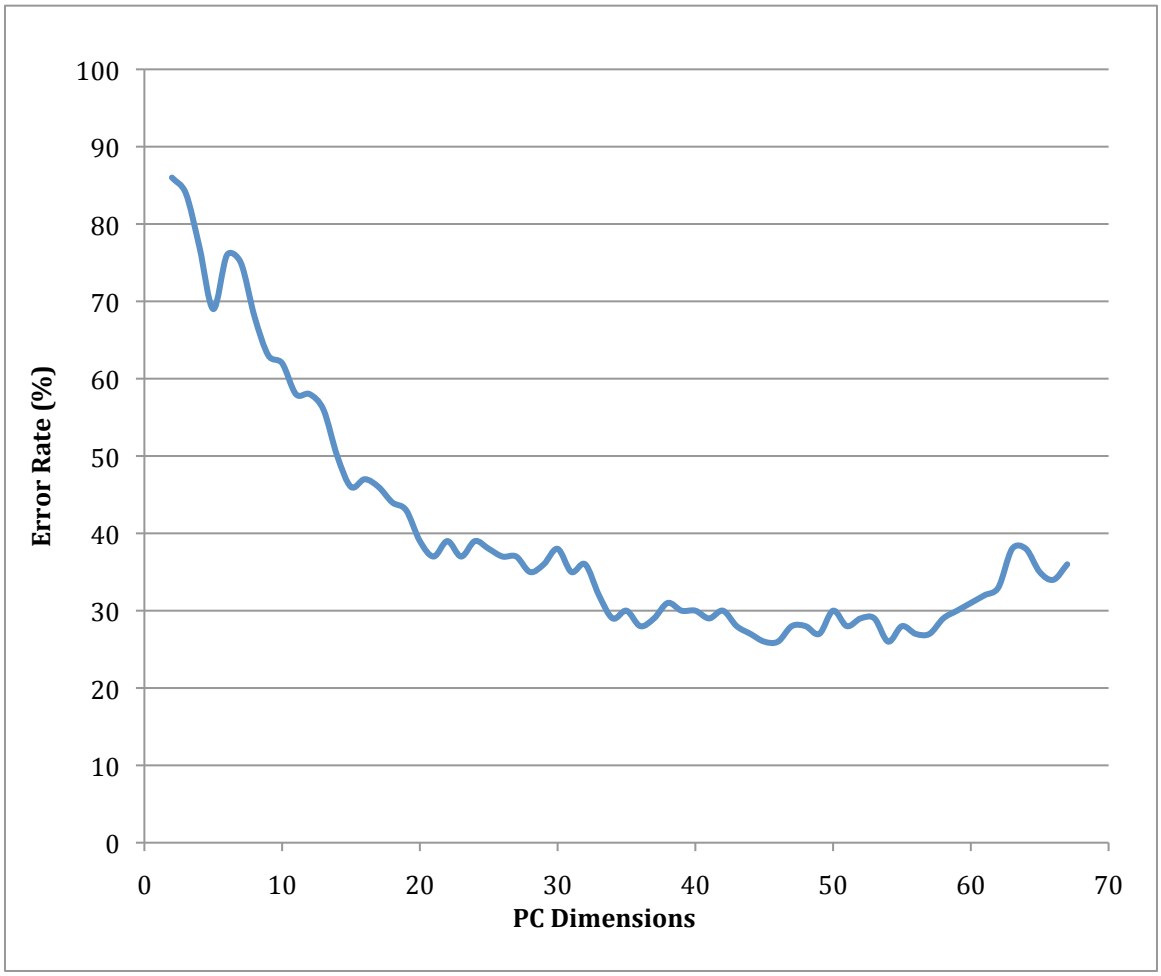


Figure 312: Graph of the discrimination error rate versus PC dimensions for HOO-CV with PCA reduced CVA for the first set of 10 container glass second derivative (5-point smoothing) spectra (10 replicates), no data pretreatment.

Table 324: Discrimination error rates for HOO-CV with PCA reduced CVA for the first set of 10 container glass second derivative (5-point smoothing) spectra (10 replicates), centered data. The smallest PC dimension with the minimum error rate is highlighted in yellow.

PCs	Error Rate (%)	PCs	Error Rate (%)	PCs	Error Rate (%)	PCs	Error Rate (%)	PCs	Error Rate (%)
2	84.00	15	48.00	28	33.00	41	29.00	54	28.00
3	83.00	16	44.00	29	35.00	42	28.00	55	27.00
4	75.00	17	42.00	30	35.00	43	29.00	56	28.00
5	73.00	18	43.00	31	36.00	44	27.00	57	28.00
6	77.00	19	44.00	32	36.00	45	27.00	58	27.00
7	76.00	20	42.00	33	32.00	46	31.00	59	31.00
8	70.00	21	41.00	34	32.00	47	30.00	60	28.00
9	67.00	22	44.00	35	25.00	48	32.00	61	29.00
10	59.00	23	40.00	36	28.00	49	28.00	62	33.00
11	60.00	24	42.00	37	29.00	50	27.00	63	33.00
12	58.00	25	40.00	38	27.00	51	27.00	64	32.00
13	57.00	26	37.00	39	29.00	52	27.00	65	30.00
14	45.00	27	36.00	40	29.00	53	31.00	66	31.00

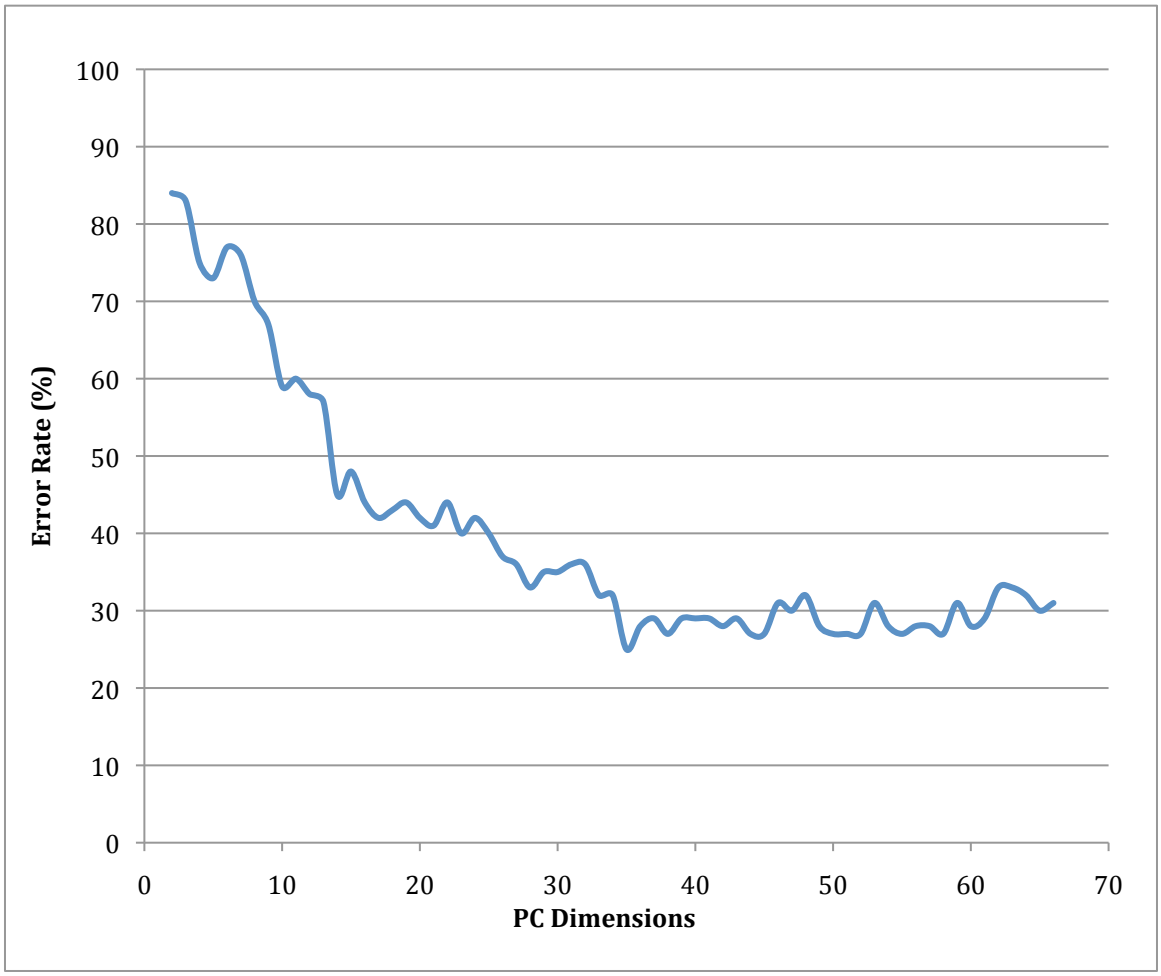


Figure 313: Graph of the discrimination error rate versus PC dimensions for HOO-CV with PCA reduced CVA for the first set of 10 container glass second derivative (5-point smoothing) spectra (10 replicates), centered data.

Table 325: Discrimination error rates for HOO-CV with PCA reduced CVA for the first set of 10 container glass second derivative (5-point smoothing) spectra (10 replicates), autoscaled data. The smallest PC dimension with the minimum error rate is highlighted in yellow.

PCs	Error Rate (%)	PCs	Error Rate (%)	PCs	Error Rate (%)	PCs	Error Rate (%)	PCs	Error Rate (%)
2	61.00	22	7.00	42	7.00	62	9.00	82	24.00
3	33.00	23	7.00	43	8.00	63	9.00	83	15.00
4	28.00	24	6.00	44	8.00	64	11.00	84	15.00
5	26.00	25	6.00	45	7.00	65	11.00	85	24.00
6	24.00	26	9.00	46	9.00	66	12.00	86	26.00
7	24.00	27	9.00	47	9.00	67	14.00	87	32.00
8	20.00	28	9.00	48	9.00	68	16.00	88	36.00
9	18.00	29	5.00	49	7.00	69	17.00	89	50.00
10	16.00	30	5.00	50	8.00	70	20.00	90	67.00
11	15.00	31	5.00	51	7.00	71	20.00	91	77.00
12	14.00	32	5.00	52	7.00	72	18.00	92	75.00
13	11.00	33	6.00	53	8.00	73	17.00	93	78.00
14	11.00	34	5.00	54	7.00	74	13.00	94	82.00
15	11.00	35	7.00	55	5.00	75	14.00	95	83.00
16	11.00	36	6.00	56	7.00	76	16.00	96	91.00
17	8.00	37	6.00	57	8.00	77	21.00	97	99.00
18	11.00	38	6.00	58	9.00	78	22.00	98	99.00
19	10.00	39	9.00	59	9.00	79	19.00	99	56.00
20	8.00	40	9.00	60	9.00	80	22.00		
21	8.00	41	8.00	61	10.00	81	22.00		

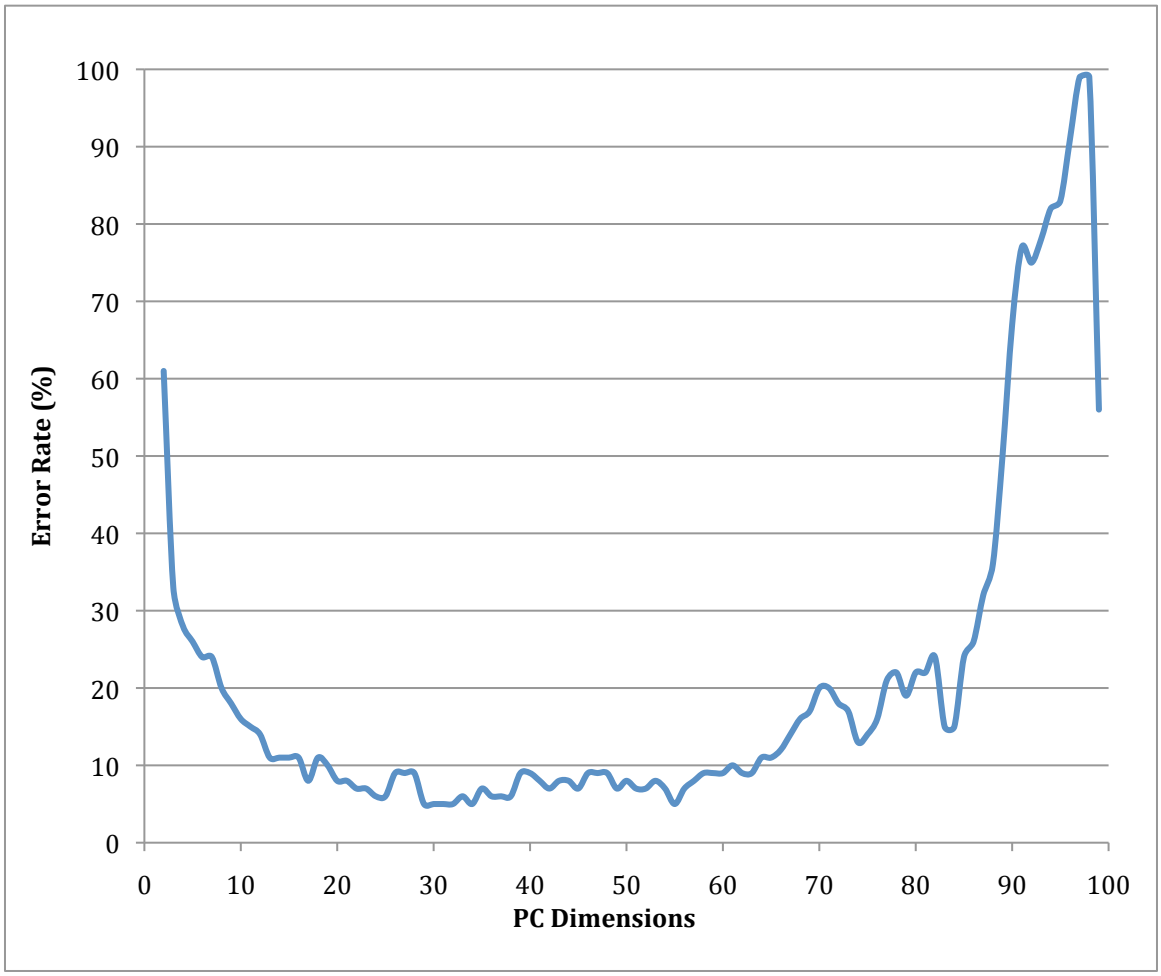


Figure 314: Graph of the discrimination error rate versus PC dimensions for HOO-CV with PCA reduced CVA for the first set of 10 container glass second derivative (5-point smoothing) spectra (10 replicates), autoscaled data.

First Set, Second Derivative (5-point smoothing) – Float Classification

Table 326: Float classification error rates for HOO-CV with PCA reduced CVA for the first set of 20 window glass second derivative (5-point smoothing) spectra (10 replicates), no data pretreatment. The smallest PC dimension with the minimum error rate is highlighted in yellow.

PCs	Error Rate (%)	PCs	Error Rate (%)	PCs	Error Rate (%)	PCs	Error Rate (%)	PCs	Error Rate (%)
2	41.50	18	32.00	34	27.00	50	28.50	66	29.50
3	34.50	19	32.00	35	27.50	51	30.50	67	29.00
4	38.50	20	28.50	36	29.50	52	30.50	68	30.00
5	36.00	21	29.50	37	30.50	53	30.00	69	30.50
6	37.00	22	29.50	38	30.50	54	30.50	70	31.50
7	33.00	23	30.00	39	31.00	55	29.00	71	32.00
8	33.00	24	30.50	40	30.50	56	29.00	72	31.00
9	32.50	25	31.50	41	30.50	57	29.50	73	32.00
10	33.50	26	33.00	42	31.50	58	30.50	74	33.00
11	33.00	27	29.50	43	33.00	59	31.00	75	33.50
12	33.00	28	30.50	44	30.00	60	29.00	76	33.50
13	32.50	29	25.00	45	25.50	61	29.50	77	33.00
14	33.00	30	26.50	46	27.00	62	29.50	78	33.50
15	33.50	31	24.50	47	27.00	63	28.50	79	33.50
16	29.50	32	25.00	48	28.50	64	29.50	80	35.50
17	31.50	33	25.00	49	28.50	65	29.00		

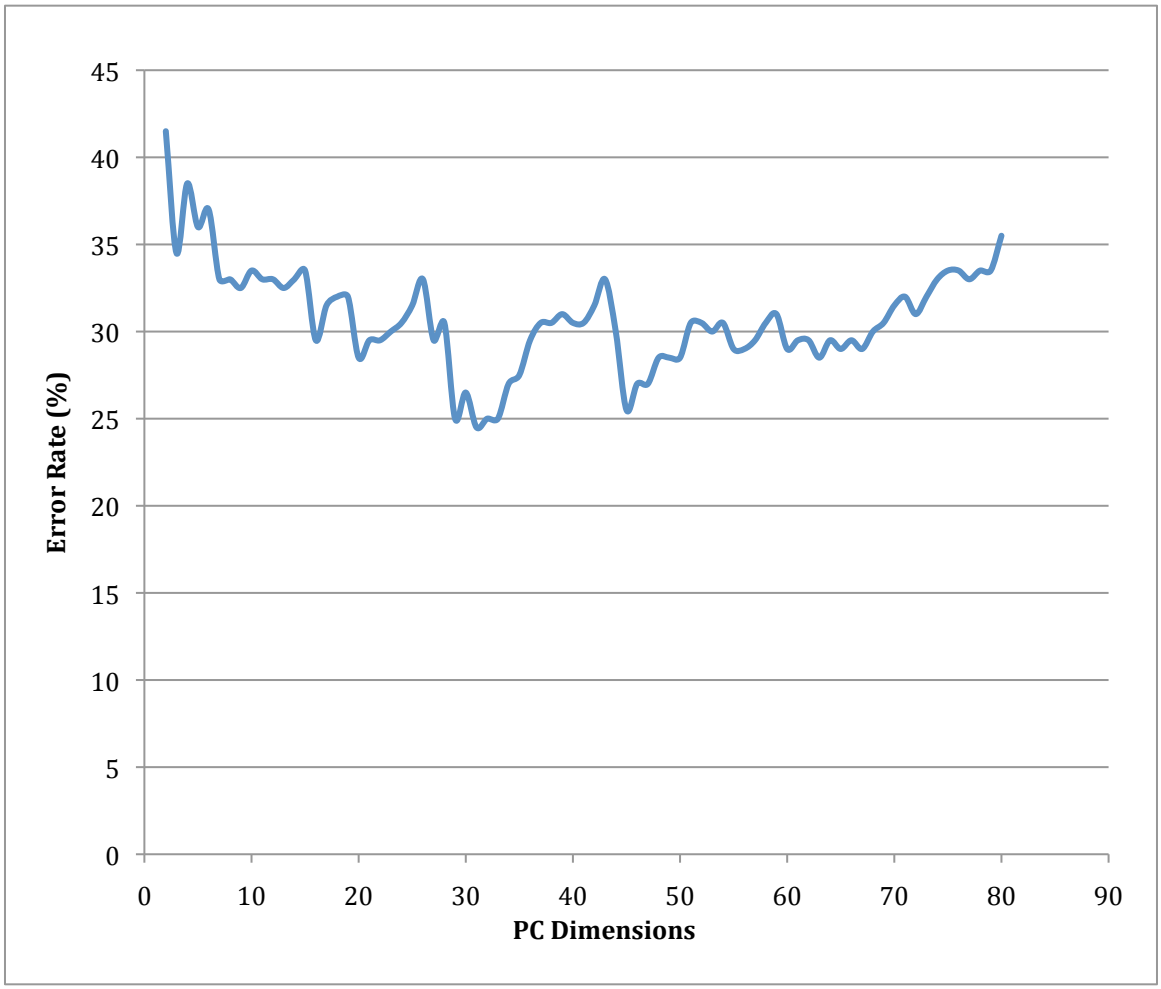


Figure 315: Graph of the float classification error rate versus PC dimensions for HOO-CV with PCA reduced CVA for the first set of 20 window glass second derivative (5-point smoothing) spectra (10 replicates), no data pretreatment.

Table 327: Float classification error rates for HOO-CV with PCA reduced CVA for the first set of 20 window glass second derivative (5-point smoothing) spectra (10 replicates), centered data. The smallest PC dimension with the minimum error rate is highlighted in yellow.

PCs	Error Rate (%)	PCs	Error Rate (%)	PCs	Error Rate (%)	PCs	Error Rate (%)	PCs	Error Rate (%)
2	40.00	18	31.50	34	26.50	50	30.00	66	30.00
3	37.00	19	31.00	35	28.50	51	29.50	67	29.50
4	40.00	20	31.00	36	28.00	52	31.00	68	31.50
5	40.50	21	29.00	37	28.00	53	30.50	69	32.00
6	36.00	22	29.50	38	28.50	54	30.00	70	32.50
7	31.50	23	30.50	39	30.00	55	30.00	71	31.00
8	32.00	24	31.50	40	30.50	56	28.50	72	31.50
9	32.50	25	32.50	41	31.00	57	29.00	73	32.00
10	31.50	26	29.50	42	31.50	58	30.00	74	35.00
11	31.00	27	29.50	43	30.00	59	30.00	75	35.50
12	31.00	28	27.00	44	26.00	60	30.00	76	35.50
13	33.50	29	27.50	45	26.50	61	29.00	77	35.00
14	32.50	30	25.50	46	27.50	62	30.50	78	34.50
15	32.50	31	25.50	47	28.00	63	29.00	79	35.50
16	31.50	32	25.50	48	28.00	64	29.00		
17	31.50	33	25.50	49	27.50	65	29.50		

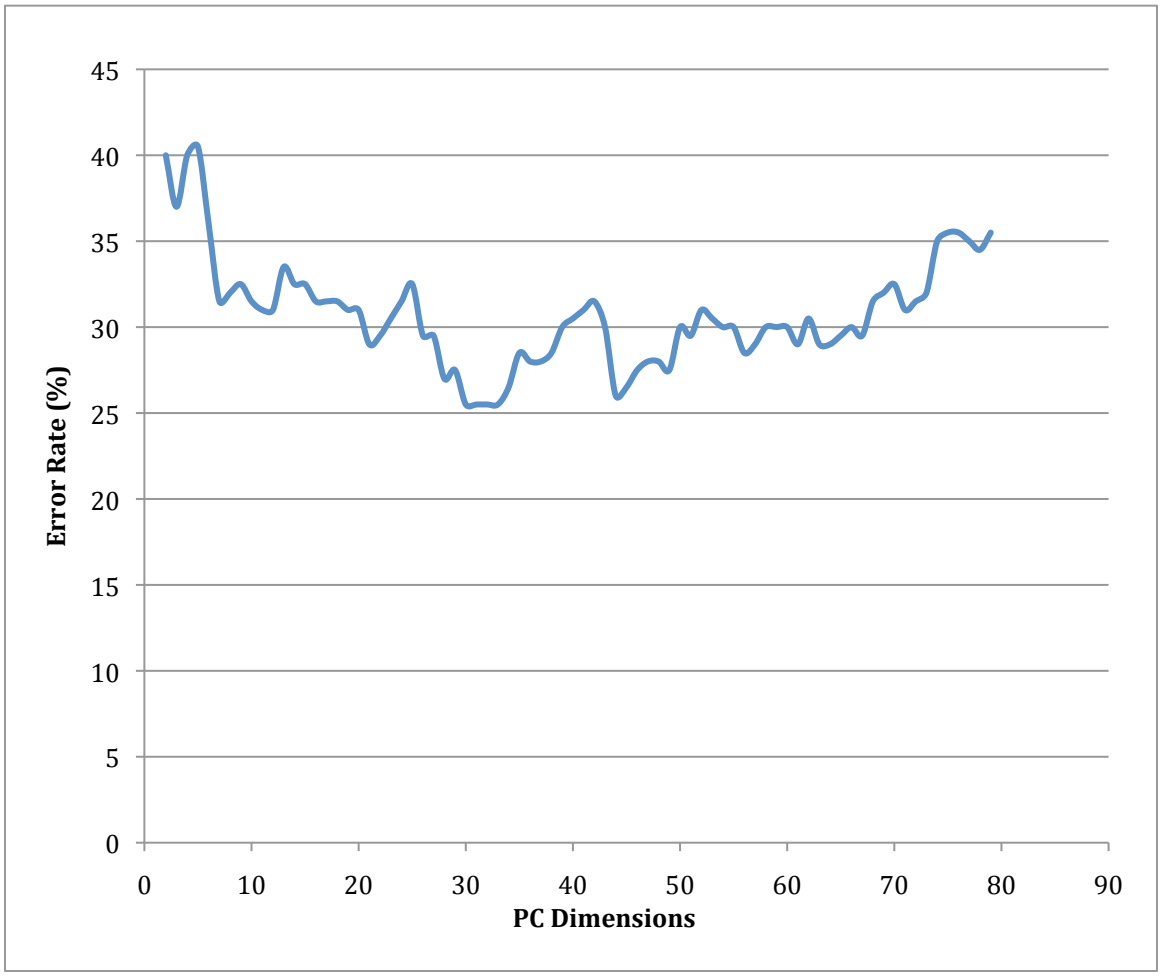


Figure 316: Graph of the float classification error rate versus PC dimensions for HOO-CV with PCA reduced CVA for the first set of 20 window glass second derivative (5-point smoothing) spectra (10 replicates), centered data.

Table 328: Float classification error rates for HOO-CV with PCA reduced CVA for the first set of 20 window glass second derivative (5-point smoothing) spectra (10 replicates), autoscaled data. The smallest PC dimension with the minimum error rate is highlighted in yellow.

PCs	Error Rate (%)	PCs	Error Rate (%)	PCs	Error Rate (%)	PCs	Error Rate (%)	PCs	Error Rate (%)
2	37.50	42	20.50	82	25.00	122	25.50	162	31.00
3	33.50	43	22.00	83	23.00	123	27.00	163	31.00
4	28.00	44	22.00	84	23.50	124	24.00	164	31.50
5	27.50	45	22.50	85	24.00	125	25.00	165	31.50
6	27.50	46	23.00	86	24.00	126	28.00	166	34.00
7	28.00	47	23.00	87	26.00	127	25.00	167	34.00
8	29.00	48	23.00	88	26.50	128	24.00	168	34.00
9	27.50	49	24.00	89	25.50	129	23.50	169	34.50
10	23.50	50	23.00	90	25.50	130	24.50	170	36.00
11	23.50	51	25.00	91	27.00	131	25.00	171	36.50
12	26.00	52	25.50	92	27.00	132	25.50	172	38.50
13	26.00	53	26.50	93	28.00	133	26.00	173	39.50
14	24.50	54	25.50	94	28.00	134	27.00	174	39.50
15	25.00	55	24.00	95	26.50	135	27.50	175	38.50
16	25.50	56	25.00	96	27.00	136	27.50	176	40.00
17	25.50	57	24.50	97	27.50	137	27.50	177	41.50
18	26.50	58	25.00	98	28.00	138	28.00	178	40.00
19	25.50	59	24.50	99	28.50	139	26.00	179	40.50
20	23.50	60	25.00	100	29.50	140	26.50	180	42.00
21	25.00	61	25.50	101	29.50	141	27.00	181	43.50
22	24.50	62	23.00	102	29.50	142	27.00	182	42.00
23	24.50	63	24.50	103	27.00	143	27.50	183	41.00
24	24.00	64	23.00	104	27.00	144	29.00	184	39.50
25	26.50	65	23.50	105	25.00	145	30.00	185	42.00
26	23.00	66	23.50	106	26.50	146	28.00	186	44.50
27	24.00	67	23.00	107	25.50	147	26.50	187	45.50
28	21.50	68	24.00	108	25.50	148	24.00	188	46.00
29	21.50	69	24.00	109	28.00	149	24.50	189	46.50
30	21.50	70	24.00	110	28.00	150	27.50	190	44.50
31	20.50	71	24.00	111	26.50	151	26.00	191	44.00
32	21.50	72	25.00	112	24.50	152	25.00	192	39.50
33	21.50	73	24.50	113	25.00	153	27.00	193	36.00
34	24.50	74	24.50	114	25.00	154	26.50	194	37.50
35	25.50	75	24.00	115	26.00	155	28.50	195	35.00
36	23.00	76	24.50	116	26.00	156	29.00	196	41.00
37	21.50	77	25.00	117	25.50	157	30.00	197	49.00
38	21.00	78	25.00	118	26.50	158	30.50	198	51.50

39	21.50	79	25.00	119	27.00	159	29.00	199	45.00
40	21.00	80	25.50	120	25.50	160	29.00		
41	21.50	81	25.00	121	25.00	161	31.00		

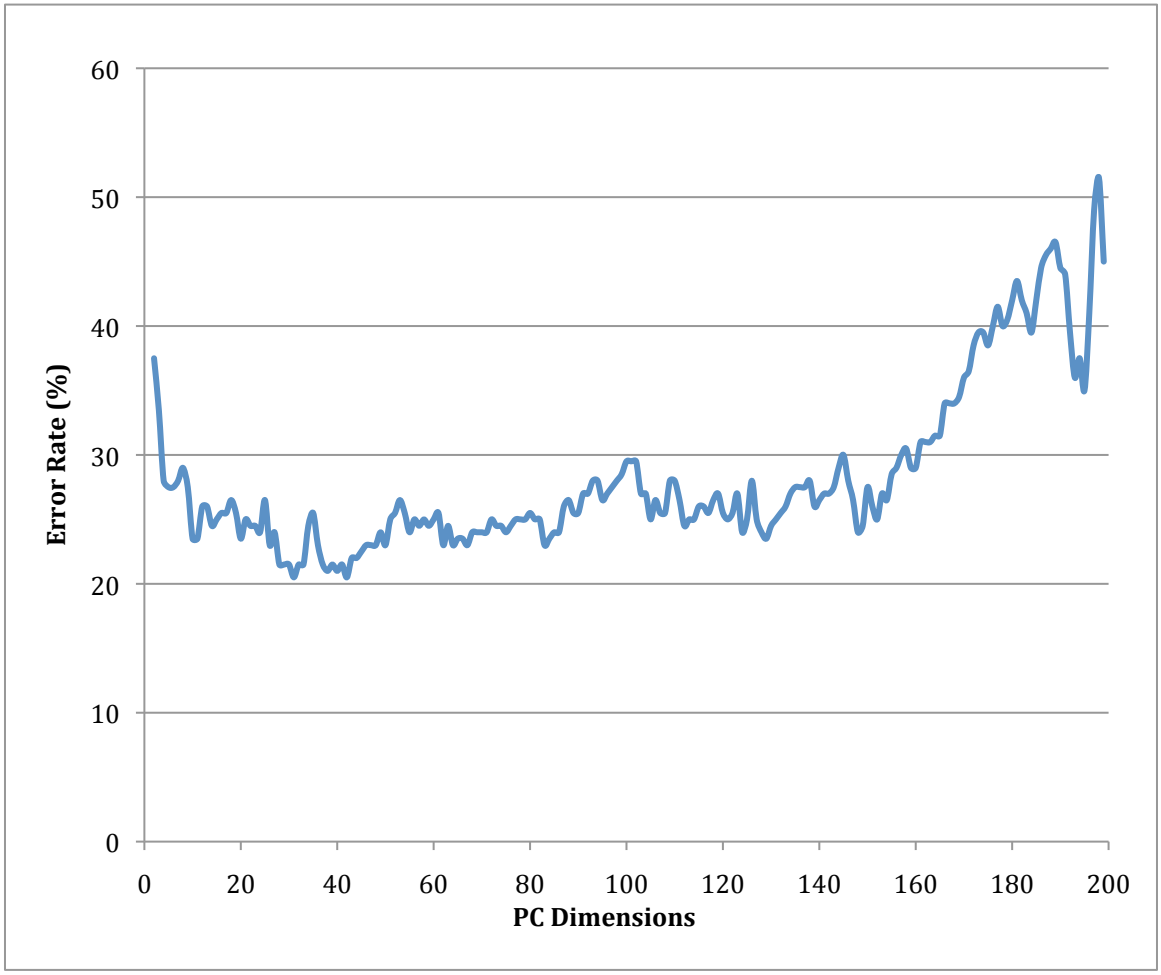


Figure 317: Graph of the float classification error rate versus PC dimensions for HOO-CV with PCA reduced CVA for the first set of 20 window glass second derivative (5-point smoothing) spectra (10 replicates), autoscaled data.

First Set, Second Derivative (5-point smoothing) – Tempered Classification

Table 329: Tempered classification error rates for HOO-CV with PCA reduced CVA for the first set of 20 window glass second derivative (5-point smoothing) spectra (10 replicates), no data pretreatment. The smallest PC dimension with the minimum error rate is highlighted in yellow.

PCs	Error Rate (%)	PCs	Error Rate (%)	PCs	Error Rate (%)	PCs	Error Rate (%)	PCs	Error Rate (%)
2	32.50	18	26.00	34	29.50	50	25.50	66	28.00
3	35.50	19	25.50	35	28.50	51	26.00	67	28.00
4	31.00	20	27.00	36	27.50	52	27.50	68	27.00
5	32.50	21	27.00	37	28.50	53	27.50	69	26.50
6	27.50	22	28.00	38	29.00	54	28.00	70	25.00
7	28.50	23	28.00	39	28.50	55	27.50	71	25.00
8	26.50	24	29.50	40	28.50	56	29.00	72	26.50
9	27.50	25	30.00	41	28.50	57	26.50	73	23.50
10	27.50	26	29.00	42	25.50	58	29.00	74	24.50
11	28.50	27	29.00	43	26.00	59	29.00	75	25.50
12	26.50	28	29.00	44	26.00	60	28.00	76	26.50
13	27.50	29	30.50	45	26.00	61	27.00	77	28.00
14	28.00	30	31.00	46	26.00	62	25.00	78	28.50
15	29.00	31	30.50	47	27.00	63	25.50	79	28.00
16	29.50	32	30.50	48	28.50	64	26.00	80	28.00
17	27.00	33	29.50	49	26.50	65	26.50		

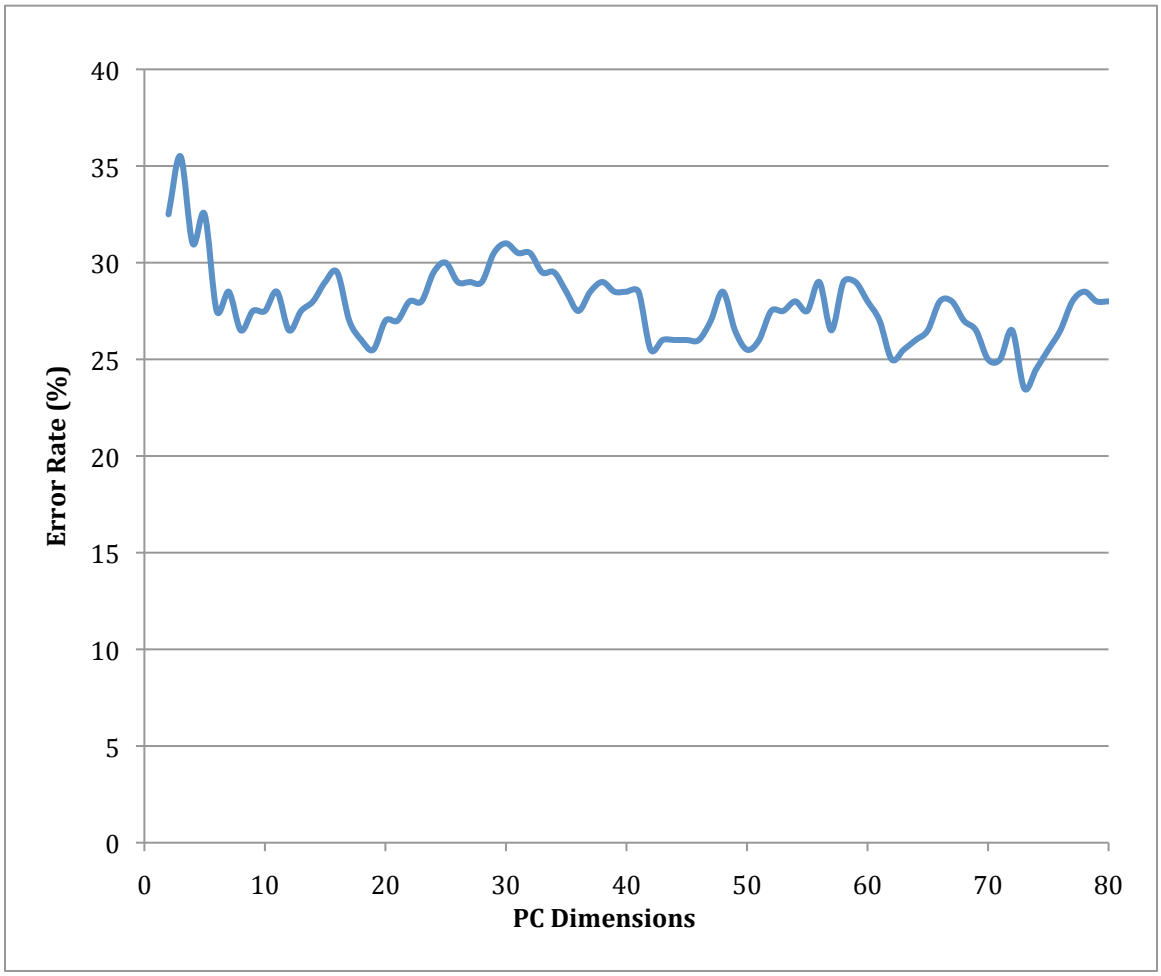


Figure 318: Graph of the tempered classification error rate versus PC dimensions for HOO-CV with PCA reduced CVA for the first set of 20 window glass second derivative (5-point smoothing) spectra (10 replicates), no data pretreatment.

Table 330: Tempered classification error rates for HOO-CV with PCA reduced CVA for the first set of 20 window glass second derivative (5-point smoothing) spectra (10 replicates), centered data. The smallest PC dimension with the minimum error rate is highlighted in yellow.

PCs	Error Rate (%)	PCs	Error Rate (%)	PCs	Error Rate (%)	PCs	Error Rate (%)	PCs	Error Rate (%)
2	32.50	18	28.50	34	30.50	50	27.50	66	26.00
3	40.00	19	28.00	35	31.00	51	27.50	67	25.50
4	36.00	20	27.00	36	31.50	52	27.50	68	25.50
5	34.00	21	26.00	37	32.50	53	27.50	69	26.50
6	26.50	22	27.00	38	32.00	54	27.50	70	27.00
7	26.50	23	27.50	39	33.00	55	28.00	71	28.00
8	28.00	24	29.50	40	32.50	56	28.00	72	27.00
9	27.00	25	29.00	41	27.00	57	27.00	73	25.50
10	28.50	26	29.50	42	25.50	58	28.00	74	26.00
11	25.50	27	29.00	43	25.50	59	27.00	75	26.00
12	26.50	28	29.50	44	27.00	60	28.00	76	27.50
13	26.50	29	30.50	45	27.50	61	26.00	77	28.00
14	26.50	30	29.50	46	29.50	62	25.00	78	28.00
15	28.00	31	30.50	47	28.50	63	25.00	79	28.50
16	28.50	32	31.00	48	29.50	64	25.50		
17	28.00	33	30.50	49	29.50	65	25.50		

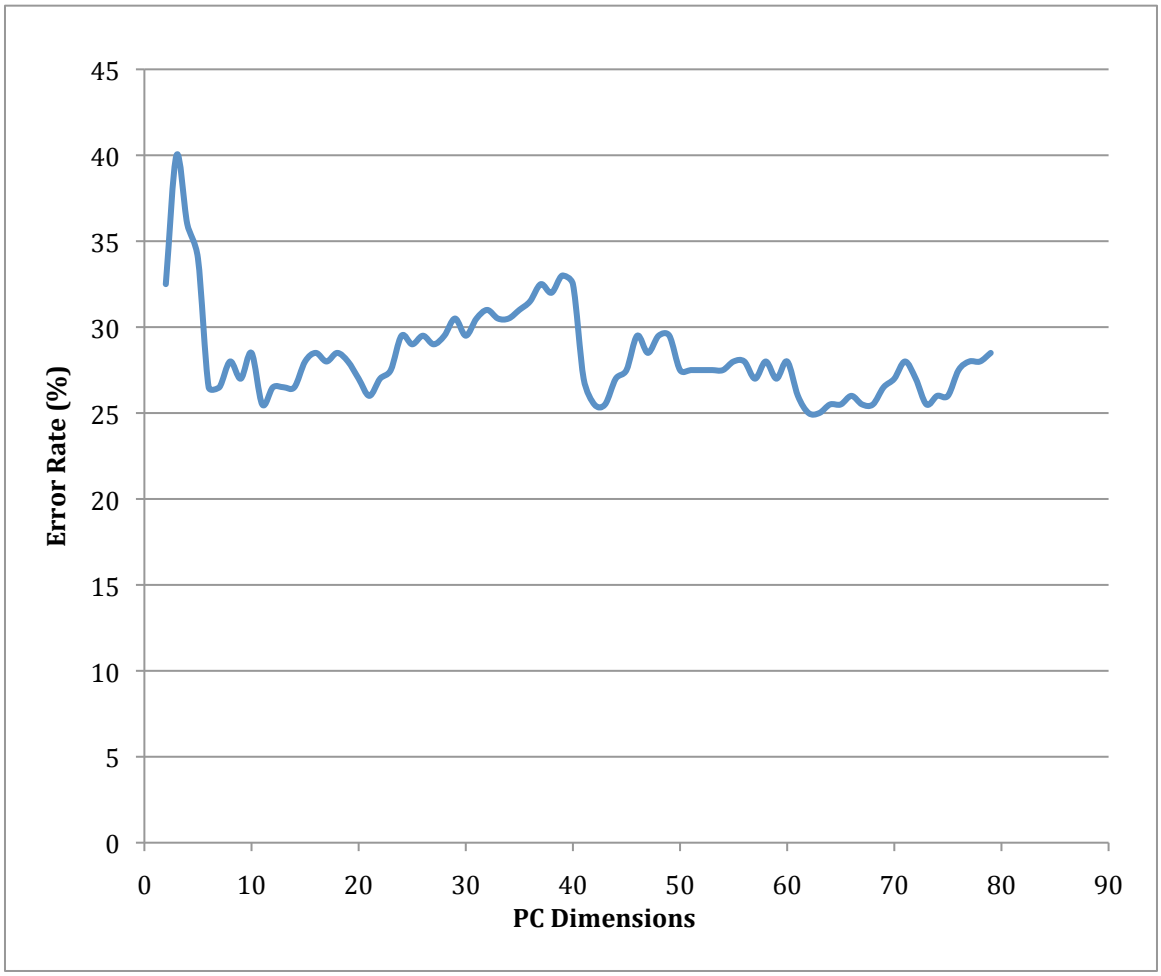


Figure 319: Graph of the tempered classification error rate versus PC dimensions for HOO-CV with PCA reduced CVA for the first set of 20 window glass second derivative (5-point smoothing) spectra (10 replicates), centered data.

Table 331: Tempered classification error rates for HOO-CV with PCA reduced CVA for the first set of 20 window glass second derivative (5-point smoothing) spectra (10 replicates), autoscaled data. The smallest PC dimension with the minimum error rate is highlighted in yellow.

PCs	Error Rate (%)	PCs	Error Rate (%)	PCs	Error Rate (%)	PCs	Error Rate (%)	PCs	Error Rate (%)
2	40.50	42	19.00	82	13.50	122	14.00	162	15.00
3	27.00	43	19.00	83	13.00	123	14.50	163	16.50
4	26.50	44	17.00	84	13.00	124	14.50	164	15.00
5	29.50	45	17.50	85	13.00	125	14.50	165	16.50
6	27.50	46	18.50	86	13.00	126	15.00	166	17.50
7	26.50	47	17.50	87	14.00	127	13.00	167	16.00
8	27.50	48	16.00	88	14.50	128	14.00	168	17.50
9	28.00	49	16.00	89	14.00	129	14.50	169	18.00
10	27.50	50	15.50	90	14.50	130	14.50	170	19.00
11	26.50	51	15.50	91	14.50	131	14.50	171	20.00
12	25.50	52	16.50	92	15.00	132	14.00	172	18.50
13	25.00	53	16.50	93	15.00	133	14.50	173	18.00
14	24.50	54	18.00	94	15.00	134	16.00	174	18.50
15	26.00	55	16.50	95	15.00	135	16.00	175	18.50
16	27.50	56	17.00	96	15.50	136	16.00	176	21.00
17	26.50	57	17.50	97	15.50	137	15.50	177	19.00
18	28.00	58	18.00	98	15.50	138	14.50	178	22.00
19	25.00	59	17.00	99	15.50	139	15.00	179	22.00
20	25.00	60	17.50	100	15.00	140	14.50	180	25.50
21	25.50	61	17.00	101	14.00	141	15.00	181	23.00
22	25.50	62	16.50	102	14.50	142	15.50	182	22.00
23	26.00	63	14.50	103	14.00	143	16.00	183	22.00
24	25.00	64	14.50	104	12.00	144	14.50	184	23.00
25	26.00	65	14.50	105	12.00	145	16.00	185	26.00
26	25.00	66	15.00	106	12.00	146	14.00	186	27.00
27	24.50	67	15.00	107	13.00	147	15.50	187	27.50
28	23.50	68	17.50	108	13.50	148	15.50	188	30.00
29	21.50	69	17.50	109	12.00	149	14.50	189	31.00
30	19.50	70	17.50	110	12.50	150	14.50	190	23.00
31	20.50	71	18.00	111	13.50	151	15.00	191	23.50
32	20.50	72	19.50	112	15.00	152	15.50	192	28.00
33	21.00	73	16.00	113	11.50	153	14.50	193	31.00
34	20.00	74	16.50	114	13.50	154	15.00	194	34.00
35	20.50	75	17.00	115	13.00	155	15.50	195	40.50
36	20.50	76	16.50	116	12.50	156	16.00	196	43.00
37	19.00	77	16.50	117	13.50	157	16.00	197	51.00

38	19.50	78	14.00	118	13.00	158	14.50	198	48.00
39	19.00	79	13.50	119	13.00	159	16.50	199	40.00
40	18.00	80	14.00	120	12.50	160	16.00		
41	19.50	81	14.50	121	14.00	161	16.50		

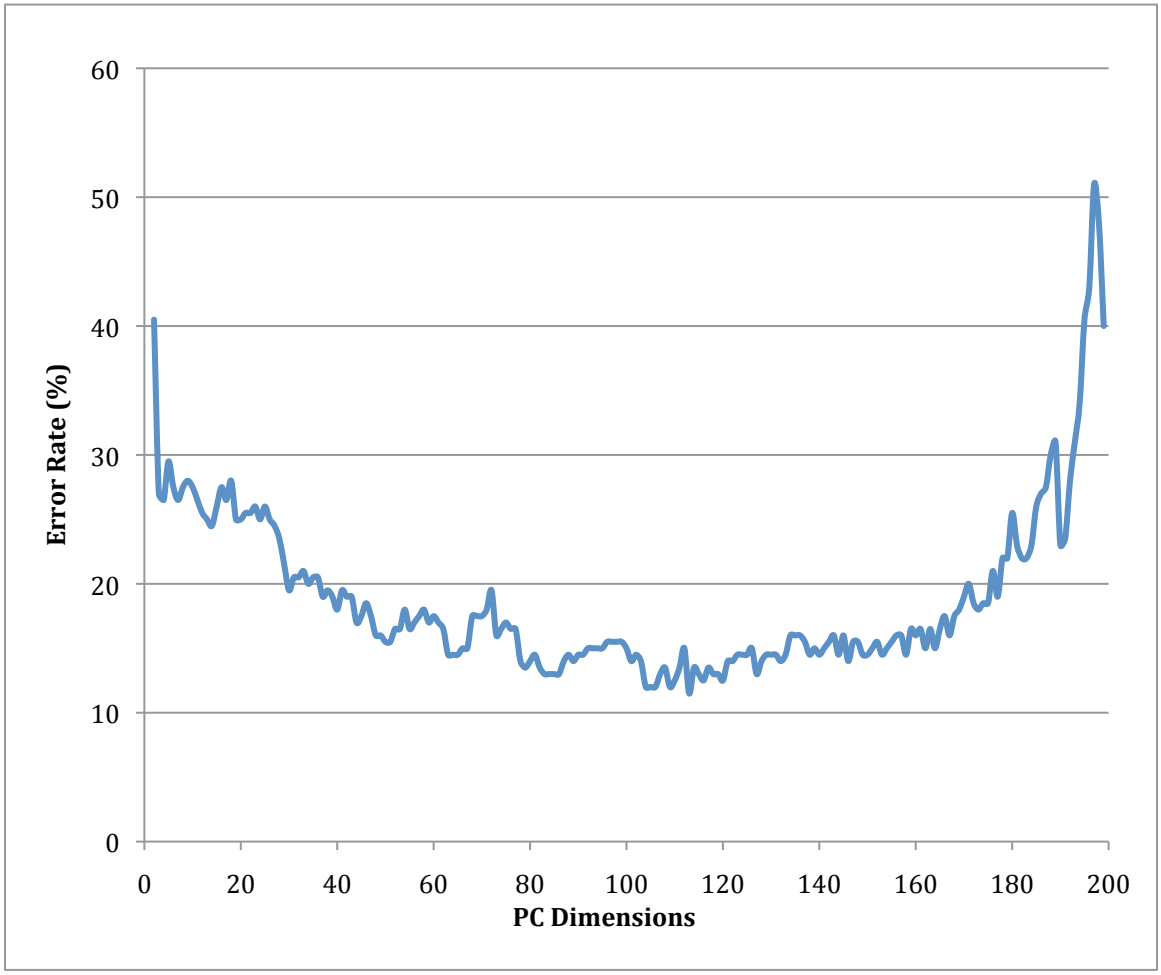


Figure 320: Graph of the tempered classification error rate versus PC dimensions for HOO-CV with PCA reduced CVA for the first set of 20 window glass second derivative (5-point smoothing) spectra (10 replicates), autoscaled data.

G. HOO-CV PCA-CVA Results for the Second Derivative Spectra (9-Point Smoothing)

First Set, Second Derivative (9-point smoothing) - Discrimination

Table 332: Discrimination error rates for HOO-CV with PCA reduced CVA for the first set of 30 glass second derivative (9-point smoothing) spectra (10 replicates), no data pretreatment. The smallest PC dimension with the minimum error rate is highlighted in yellow.

PCs	Error Rate (%)	PCs	Error Rate (%)	PCs	Error Rate (%)	PCs	Error Rate (%)	PCs	Error Rate (%)
2	97.33	7	95.00	12	69.67	17	55.67	22	51.33
3	96.67	8	88.33	13	63.33	18	55.33	23	46.67
4	94.67	9	85.67	14	62.67	19	55.33	24	47.33
5	92.33	10	78.33	15	64.00	20	52.67	25	47.00
6	93.67	11	74.33	16	58.67	21	53.33	26	47.67

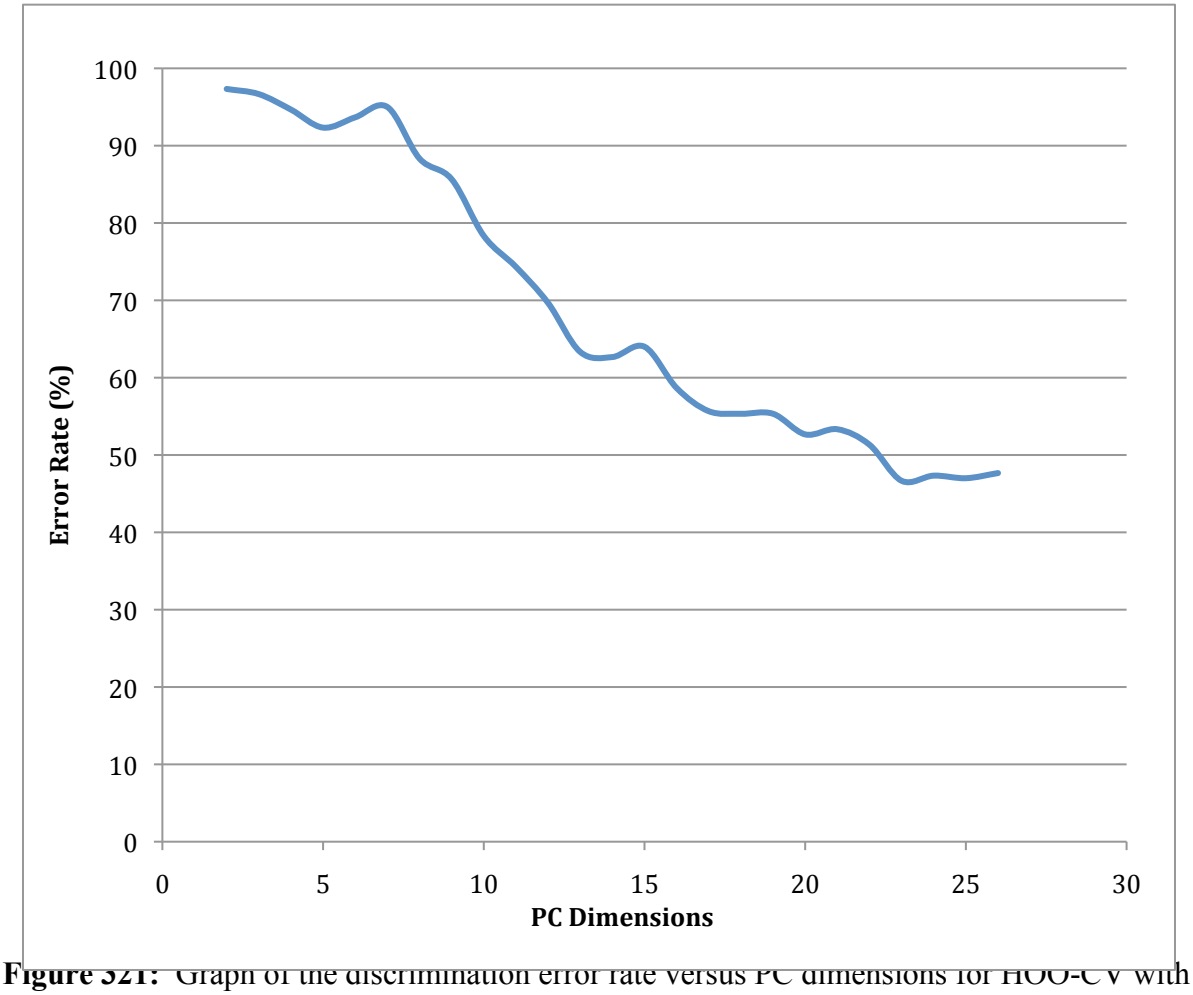


Figure 321: Graph of the discrimination error rate versus PC dimensions for HOO-CV with PCA reduced CVA for the first set of 30 glass second derivative (9-point smoothing) spectra (10 replicates), no data pretreatment.

Table 333: Discrimination error rates for HOO-CV with PCA reduced CVA for the first set of 30 glass second derivative (9-point smoothing) spectra (10 replicates), centered data. The smallest PC dimension with the minimum error rate is highlighted in yellow.

PCs	Error Rate (%)	PCs	Error Rate (%)	PCs	Error Rate (%)	PCs	Error Rate (%)	PCs	Error Rate (%)
2	95.33	7	90.67	12	70.33	17	56.67	22	51.00
3	96.67	8	87.67	13	64.33	18	54.33	23	47.33
4	95.33	9	81.33	14	62.33	19	55.67	24	48.00
5	93.67	10	76.33	15	63.67	20	53.00	25	46.00
6	95.33	11	73.33	16	58.00	21	51.00		

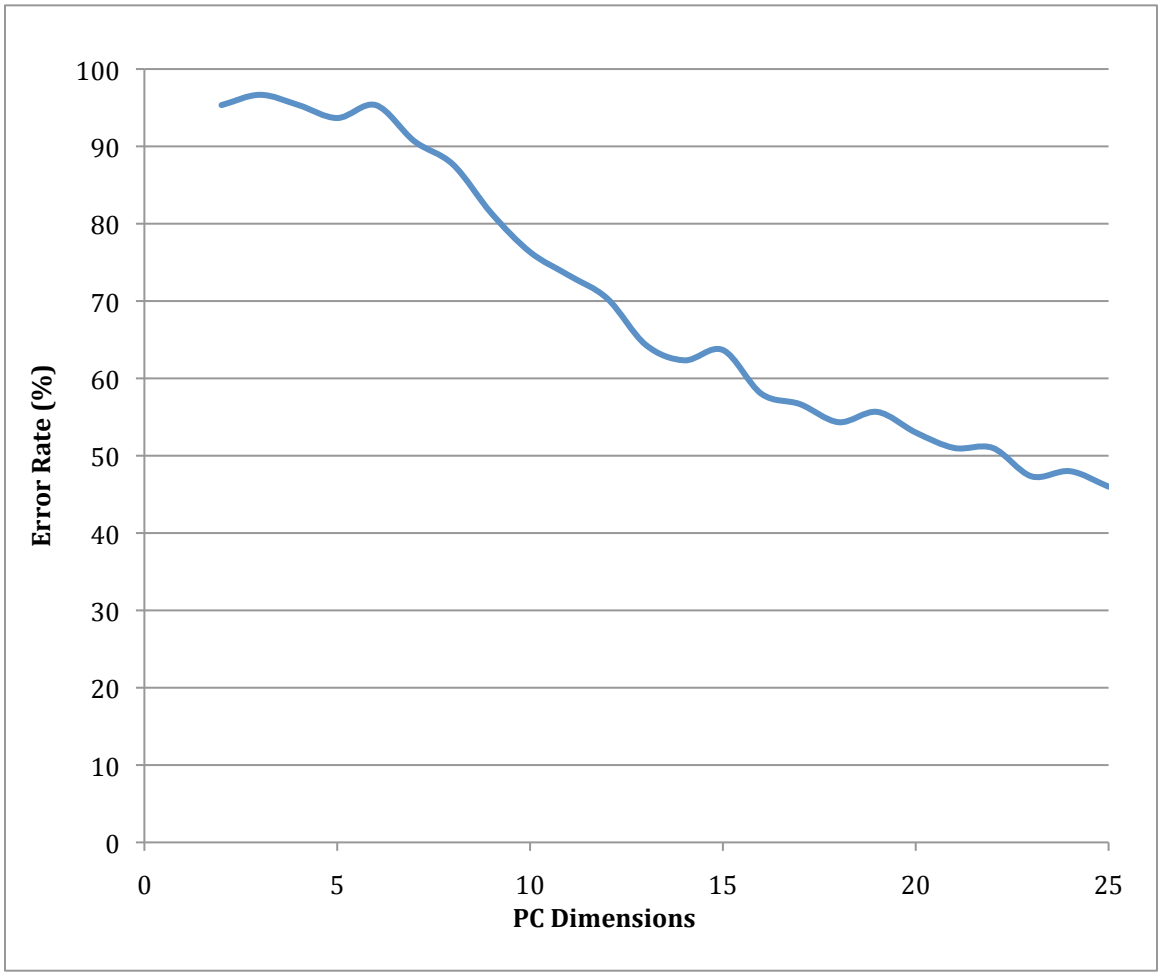


Figure 322: Graph of the discrimination error rate versus PC dimensions for HOO-CV with PCA reduced CVA for the first set of 30 glass second derivative (9-point smoothing) spectra (10 replicates), centered data.

Table 334: Discrimination error rates for HOO-CV with PCA reduced CVA for the first set of 30 glass second derivative (9-point smoothing) spectra (10 replicates), autoscaled data. The smallest PC dimension with the minimum error rate is highlighted in yellow.

PCs	Error Rate (%)	PCs	Error Rate (%)	PCs	Error Rate (%)	PCs	Error Rate (%)	PCs	Error Rate (%)
2	84.67	56	9.00	110	7.00	164	7.00	218	15.00
3	79.67	57	10.33	111	6.33	165	6.67	219	14.33
4	66.33	58	10.67	112	7.00	166	6.00	220	14.67
5	63.33	59	10.00	113	7.33	167	6.67	221	14.33
6	62.33	60	9.33	114	7.00	168	7.33	222	15.33
7	57.67	61	8.67	115	7.00	169	7.67	223	16.33
8	54.33	62	9.00	116	7.33	170	8.33	224	17.33
9	48.33	63	9.67	117	7.33	171	9.00	225	18.00
10	43.67	64	9.33	118	8.00	172	9.00	226	17.00
11	43.00	65	9.00	119	8.33	173	9.33	227	17.33
12	38.33	66	9.00	120	7.33	174	8.67	228	17.33
13	37.67	67	9.00	121	7.67	175	9.67	229	17.00
14	33.33	68	10.00	122	7.33	176	9.00	230	17.00
15	31.33	69	10.00	123	8.67	177	9.00	231	17.00
16	30.67	70	10.00	124	8.33	178	10.33	232	18.67
17	28.33	71	9.67	125	8.00	179	11.00	233	18.67
18	25.00	72	9.33	126	8.33	180	11.00	234	20.00
19	25.33	73	8.00	127	8.00	181	11.00	235	18.33
20	24.67	74	7.00	128	9.00	182	10.00	236	19.00
21	25.67	75	6.33	129	9.00	183	10.67	237	21.00
22	23.67	76	7.00	130	8.67	184	11.33	238	19.67
23	23.67	77	8.00	131	9.00	185	12.00	239	20.33
24	22.00	78	7.67	132	8.33	186	10.67	240	21.00
25	19.67	79	7.67	133	8.33	187	10.33	241	21.67
26	19.00	80	7.67	134	9.00	188	9.33	242	22.67
27	18.67	81	7.33	135	8.67	189	9.67	243	22.00
28	20.00	82	7.33	136	8.33	190	10.00	244	23.33
29	19.67	83	8.33	137	9.00	191	10.33	245	25.00
30	20.33	84	7.00	138	10.00	192	10.00	246	25.67
31	18.33	85	7.67	139	10.00	193	10.67	247	26.33
32	18.00	86	8.67	140	9.67	194	12.33	248	28.67
33	17.67	87	8.33	141	10.67	195	13.00	249	27.67
34	17.33	88	8.67	142	10.67	196	14.00	250	30.00
35	18.67	89	9.67	143	10.33	197	14.00	251	33.33
36	17.67	90	9.67	144	9.67	198	12.67	252	36.33
37	17.00	91	9.00	145	10.67	199	11.33	253	38.33
38	17.00	92	8.00	146	10.33	200	11.67	254	39.67

39	15.67	93	8.00	147	10.00	201	11.67	255	41.00
40	16.67	94	8.33	148	9.33	202	11.33	256	45.00
41	15.00	95	8.33	149	9.67	203	10.67	257	43.00
42	14.00	96	8.67	150	10.00	204	11.00	258	39.33
43	15.00	97	9.00	151	10.33	205	10.67	259	44.67
44	14.33	98	9.00	152	10.00	206	11.33	260	48.00
45	14.67	99	8.67	153	10.33	207	12.00	261	54.33
46	15.33	100	10.00	154	10.00	208	12.00	262	60.67
47	13.67	101	10.33	155	9.00	209	11.67	263	63.00
48	12.33	102	10.33	156	9.33	210	11.67	264	66.00
49	10.33	103	8.67	157	9.67	211	11.33	265	69.67
50	10.33	104	9.00	158	9.33	212	12.00	266	71.00
51	11.67	105	8.00	159	10.33	213	12.33	267	71.33
52	10.67	106	8.00	160	9.33	214	15.33	268	77.67
53	9.00	107	7.67	161	8.33	215	15.33	269	74.33
54	9.33	108	7.67	162	8.33	216	13.00	270	66.67
55	10.00	109	8.33	163	7.67	217	12.67	271	85.00

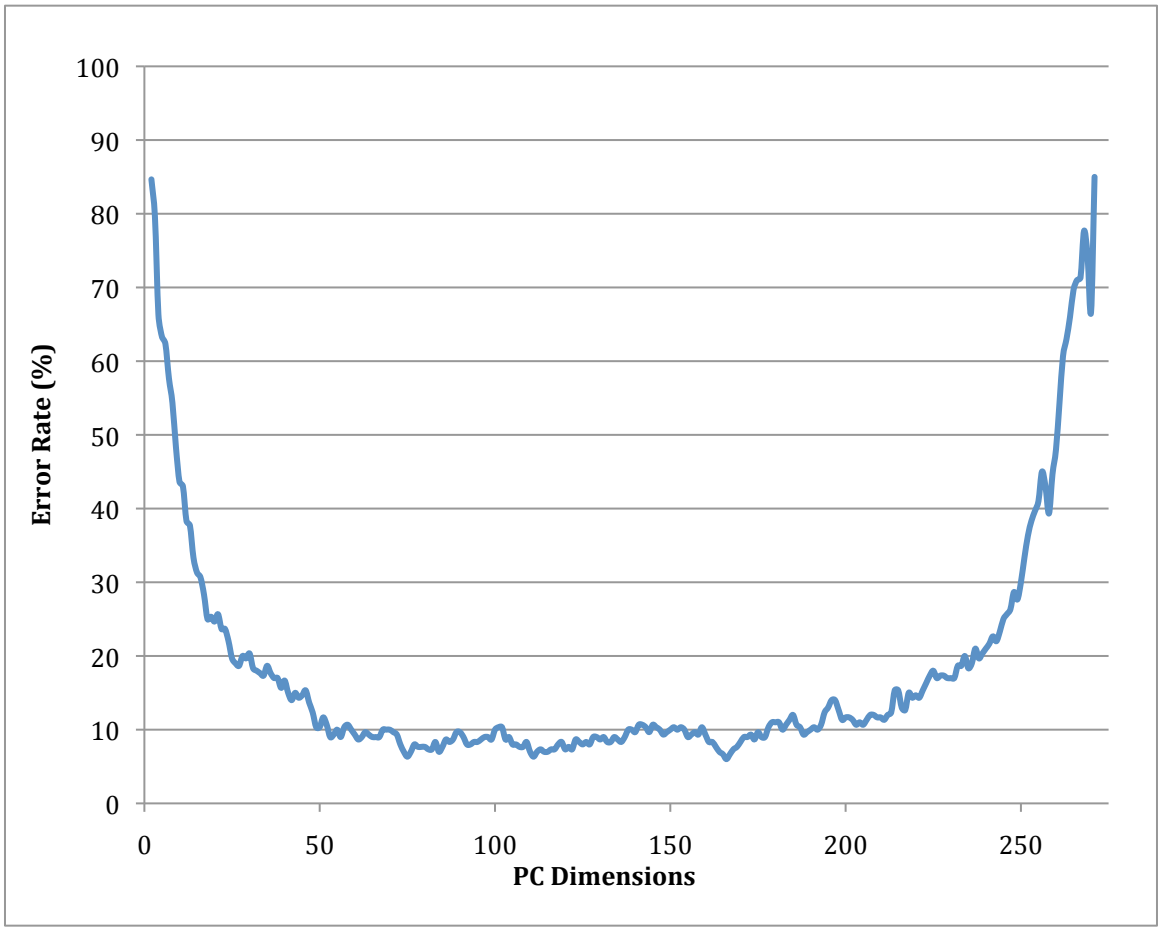


Figure 323: Graph of the discrimination error rate versus PC dimensions for HOO-CV with PCA reduced CVA for the first set of 30 glass second derivative (9-point smoothing) spectra (10 replicates), autoscaled data.

First Set, Second Derivative (9-point smoothing) – Classification (automotive, architectural or container)

Table 335: Classification (automotive, architectural or container) error rates for HOO-CV with PCA reduced CVA for the first set of 30 glass second derivative (9-point smoothing) spectra (10 replicates), no data pretreatment. The smallest PC dimension with the minimum error rate is highlighted in yellow.

PCs	Error Rate (%)	PCs	Error Rate (%)	PCs	Error Rate (%)	PCs	Error Rate (%)	PCs	Error Rate (%)
2	66.00	8	58.33	14	33.33	20	30.00	26	27.67
3	63.67	9	53.00	15	31.33	21	29.67	27	28.33
4	61.67	10	47.67	16	28.00	22	30.33	28	28.00
5	58.00	11	42.33	17	27.00	23	27.33	29	28.00
6	58.33	12	41.67	18	29.67	24	27.67		
7	59.00	13	32.33	19	30.33	25	27.33		

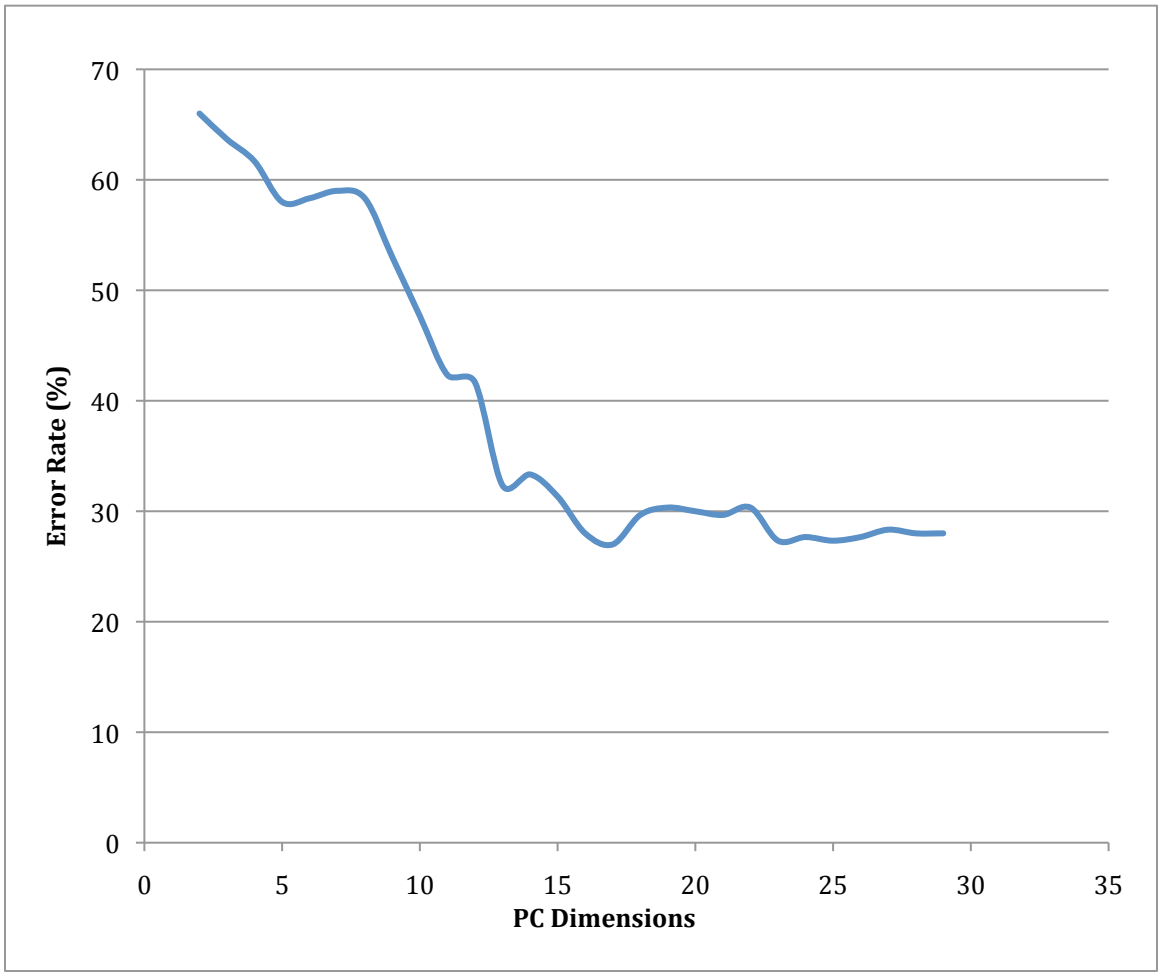


Figure 324: Graph of the classification (automotive, architectural or container) error rate versus PC dimensions for HOO-CV with PCA reduced CVA for the first set of 30 glass second derivative (9-point smoothing) spectra (10 replicates), no data pretreatment.

Table 336: Classification (automotive, architectural or container) error rates for HOO-CV with PCA reduced CVA for the first set of 30 glass second derivative (9-point smoothing) spectra (10 replicates), centered data. The smallest PC dimension with the minimum error rate is highlighted in yellow.

PCs	Error Rate (%)	PCs	Error Rate (%)	PCs	Error Rate (%)	PCs	Error Rate (%)	PCs	Error Rate (%)
2	64.67	8	53.67	14	33.00	20	30.33	26	27.00
3	64.33	9	47.33	15	31.00	21	29.67	27	27.67
4	59.33	10	44.33	16	28.33	22	29.00	28	28.00
5	59.33	11	41.00	17	28.33	23	28.00		
6	59.00	12	41.67	18	29.67	24	27.00		
7	58.33	13	32.33	19	31.00	25	27.33		

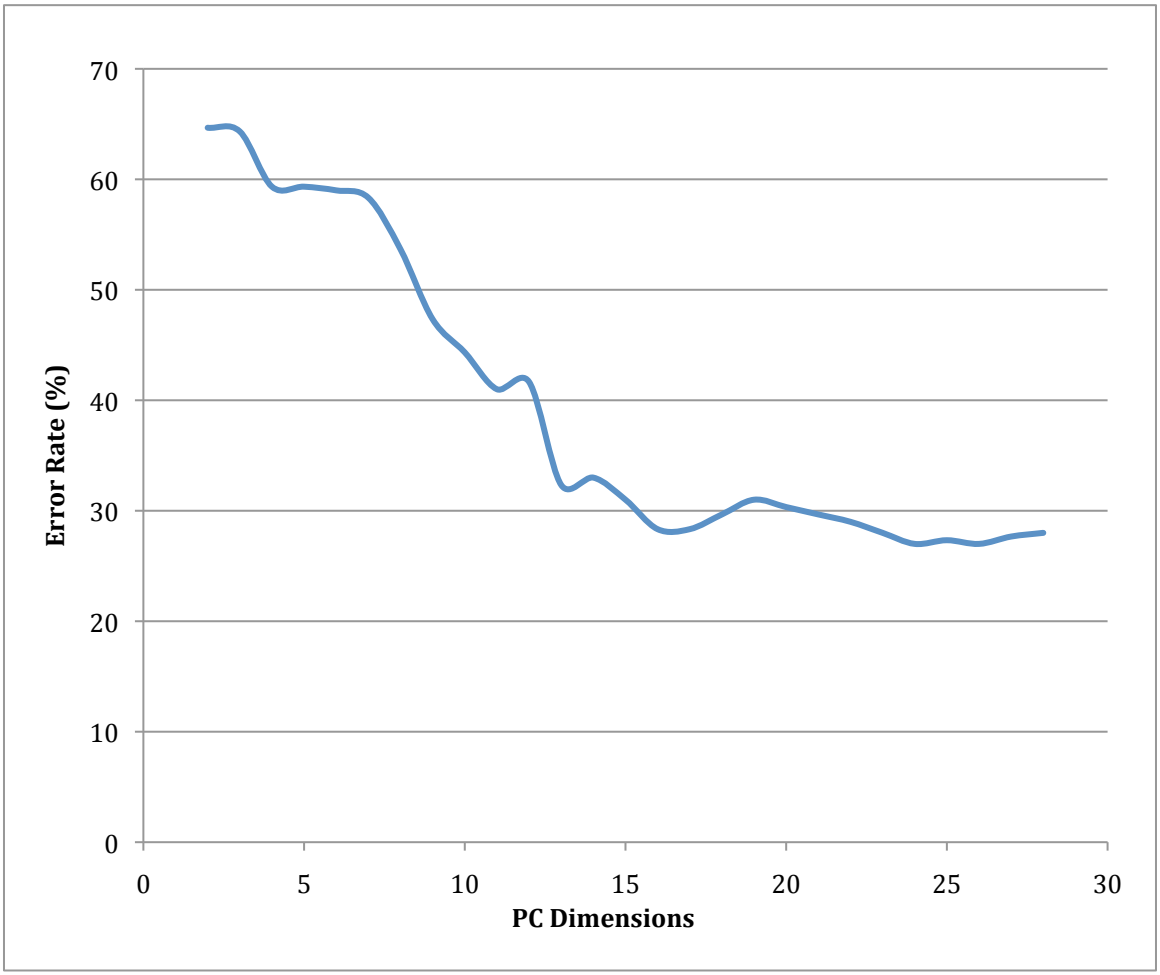


Figure 325: Graph of the classification (automotive, architectural or container) error rate versus PC dimensions for HOO-CV with PCA reduced CVA for the first set of 30 glass second derivative (9-point smoothing) spectra (10 replicates), centered data.

Table 337: Classification (automotive, architectural or container) error rates for HOO-CV with PCA reduced CVA for the first set of 30 glass second derivative (9-point smoothing) spectra (10 replicates), autoscaled data. The smallest PC dimension with the minimum error rate is highlighted in yellow.

PCs	Error Rate (%)	PCs	Error Rate (%)	PCs	Error Rate (%)	PCs	Error Rate (%)	PCs	Error Rate (%)
2	68.33	62	16.33	122	17.33	182	23.00	242	29.00
3	67.00	63	17.00	123	18.67	183	23.33	243	29.00
4	39.00	64	17.67	124	18.33	184	24.00	244	28.33
5	36.00	65	17.67	125	18.67	185	23.00	245	28.67
6	33.00	66	18.67	126	18.67	186	23.33	246	28.67
7	34.00	67	17.33	127	18.67	187	23.33	247	29.00
8	32.67	68	16.67	128	18.67	188	22.33	248	28.33
9	33.00	69	16.67	129	18.00	189	22.33	249	27.00
10	26.33	70	17.00	130	18.00	190	23.33	250	28.67
11	26.00	71	17.67	131	18.00	191	23.00	251	28.67
12	26.33	72	17.33	132	18.67	192	22.33	252	29.33
13	27.00	73	17.67	133	19.33	193	21.67	253	29.00
14	27.67	74	17.67	134	18.00	194	22.33	254	31.67
15	27.00	75	18.33	135	18.67	195	23.33	255	31.67
16	26.67	76	18.00	136	19.67	196	23.67	256	33.33
17	28.33	77	18.00	137	19.67	197	23.33	257	34.33
18	27.67	78	17.67	138	19.67	198	24.00	258	34.33
19	26.00	79	18.00	139	20.00	199	24.67	259	32.67
20	26.00	80	19.00	140	18.33	200	25.33	260	30.67
21	24.67	81	18.67	141	18.33	201	24.67	261	31.67
22	24.67	82	18.67	142	18.33	202	24.00	262	33.00
23	25.33	83	18.67	143	19.00	203	24.33	263	34.00
24	26.67	84	20.33	144	19.33	204	25.00	264	33.33
25	27.00	85	19.67	145	20.00	205	25.00	265	34.00
26	24.33	86	19.00	146	20.67	206	25.00	266	34.33
27	27.00	87	20.00	147	21.00	207	24.67	267	36.67
28	25.33	88	19.67	148	20.67	208	24.00	268	35.00
29	23.67	89	19.33	149	22.33	209	24.33	269	36.33
30	23.33	90	20.00	150	20.67	210	25.00	270	36.67
31	23.00	91	20.67	151	20.67	211	25.33	271	38.33
32	23.00	92	21.00	152	21.00	212	23.67	272	36.67
33	22.33	93	20.33	153	22.33	213	23.00	273	36.33
34	23.67	94	20.00	154	24.00	214	24.33	274	37.00
35	24.00	95	20.33	155	23.00	215	24.67	275	39.00
36	24.00	96	19.67	156	23.33	216	24.33	276	39.67
37	24.00	97	19.67	157	23.67	217	24.00	277	38.33

38	24.33	98	19.67	158	24.00	218	22.00	278	37.33
39	23.33	99	19.33	159	24.67	219	22.67	279	38.00
40	23.00	100	19.00	160	23.33	220	24.00	280	39.67
41	20.00	101	20.00	161	23.67	221	24.33	281	40.67
42	18.67	102	19.33	162	23.33	222	23.67	282	41.33
43	19.67	103	20.00	163	22.33	223	23.67	283	40.00
44	19.67	104	19.67	164	22.00	224	23.33	284	40.33
45	18.67	105	18.33	165	21.33	225	24.33	285	38.00
46	19.33	106	18.00	166	22.33	226	24.67	286	41.00
47	19.00	107	17.33	167	21.67	227	25.00	287	42.00
48	20.00	108	18.00	168	21.33	228	24.67	288	42.67
49	19.33	109	18.67	169	21.67	229	25.67	289	45.67
50	19.00	110	18.67	170	22.33	230	24.00	290	46.00
51	19.33	111	18.67	171	22.67	231	24.67	291	49.33
52	19.33	112	18.33	172	22.67	232	24.67	292	53.33
53	18.00	113	18.33	173	23.00	233	25.33	293	51.00
54	17.67	114	18.00	174	22.00	234	25.00	294	47.00
55	17.33	115	17.67	175	23.00	235	28.00	295	49.00
56	17.67	116	16.67	176	23.00	236	26.67	296	52.33
57	18.00	117	17.00	177	24.67	237	26.33	297	71.33
58	17.33	118	16.33	178	25.33	238	27.67	298	81.67
59	17.00	119	16.00	179	22.67	239	28.67	299	72.33
60	17.00	120	16.33	180	23.00	240	28.00		
61	16.00	121	16.67	181	23.00	241	27.67		

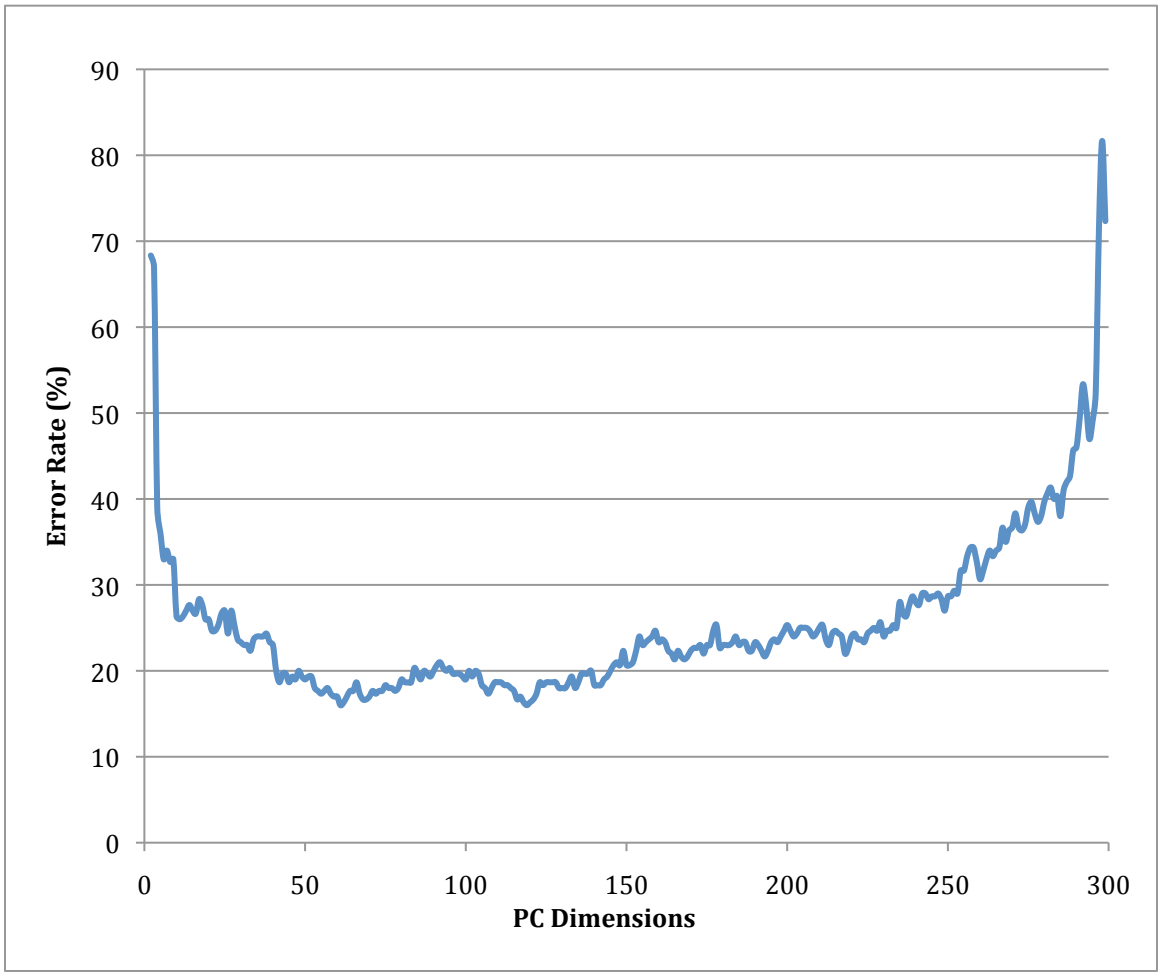


Figure 326: Graph of the classification (automotive, architectural or container) error rate versus PC dimensions for HOO-CV with PCA reduced CVA for the first set of 30 glass second derivative (9-point smoothing) spectra (10 replicates), autoscaled data.

First Set, Second Derivative (9-point smoothing) – Classification (window or container)

Table 338: Classification (window or container) error rates for HOO-CV with PCA reduced CVA for the first set of 30 glass second derivative (9-point smoothing) spectra (10 replicates), no data pretreatment. The smallest PC dimension with the minimum error rate is highlighted in yellow.

PCs	Error Rate (%)	PCs	Error Rate (%)	PCs	Error Rate (%)	PCs	Error Rate (%)	PCs	Error Rate (%)
2	33.33	8	28.33	14	9.00	20	5.00	26	6.00
3	32.33	9	24.67	15	9.00	21	5.33	27	5.33
4	32.33	10	22.67	16	5.00	22	5.33	28	5.33
5	31.00	11	19.33	17	5.00	23	6.00	29	5.67
6	32.00	12	19.00	18	5.00	24	6.00		
7	30.33	13	9.00	19	5.00	25	6.00		

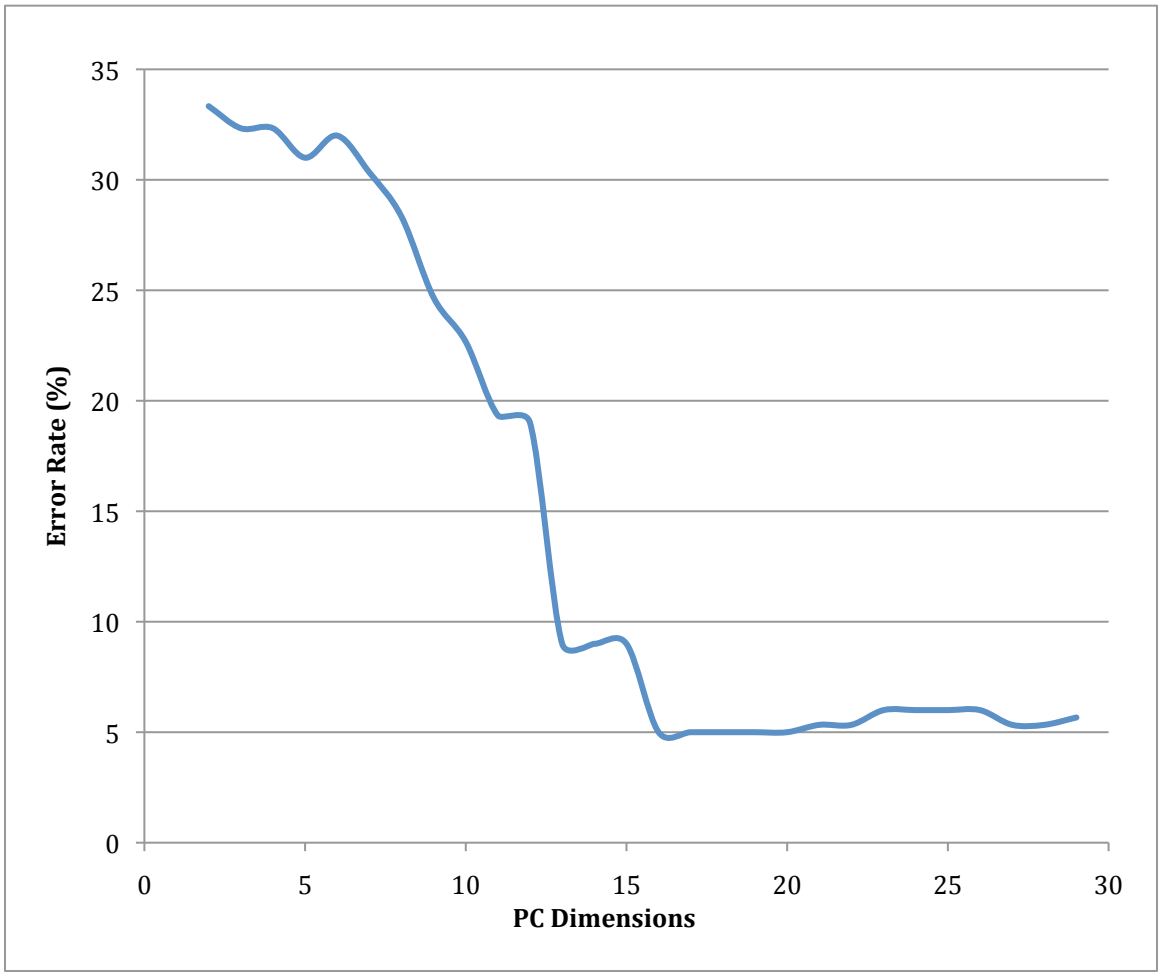


Figure 327: Graph of the classification (window or container) error rate versus PC dimensions for HOO-CV with PCA reduced CVA for the first set of 30 glass second derivative (9-point smoothing) spectra (10 replicates), no data pretreatment.

Table 339: Classification (window or container) error rates for HOO-CV with PCA reduced CVA for the first set of 30 glass second derivative (9-point smoothing) spectra (10 replicates), centered data. The smallest PC dimension with the minimum error rate is highlighted in yellow.

PCs	Error Rate (%)	PCs	Error Rate (%)	PCs	Error Rate (%)	PCs	Error Rate (%)	PCs	Error Rate (%)
2	33.00	8	28.00	14	9.00	20	5.33	26	5.67
3	33.33	9	24.67	15	8.67	21	5.33	27	5.33
4	34.67	10	19.33	16	5.00	22	5.33	28	5.33
5	33.00	11	19.33	17	5.33	23	6.00		
6	33.00	12	18.67	18	5.33	24	6.00		
7	28.67	13	9.00	19	5.33	25	6.00		

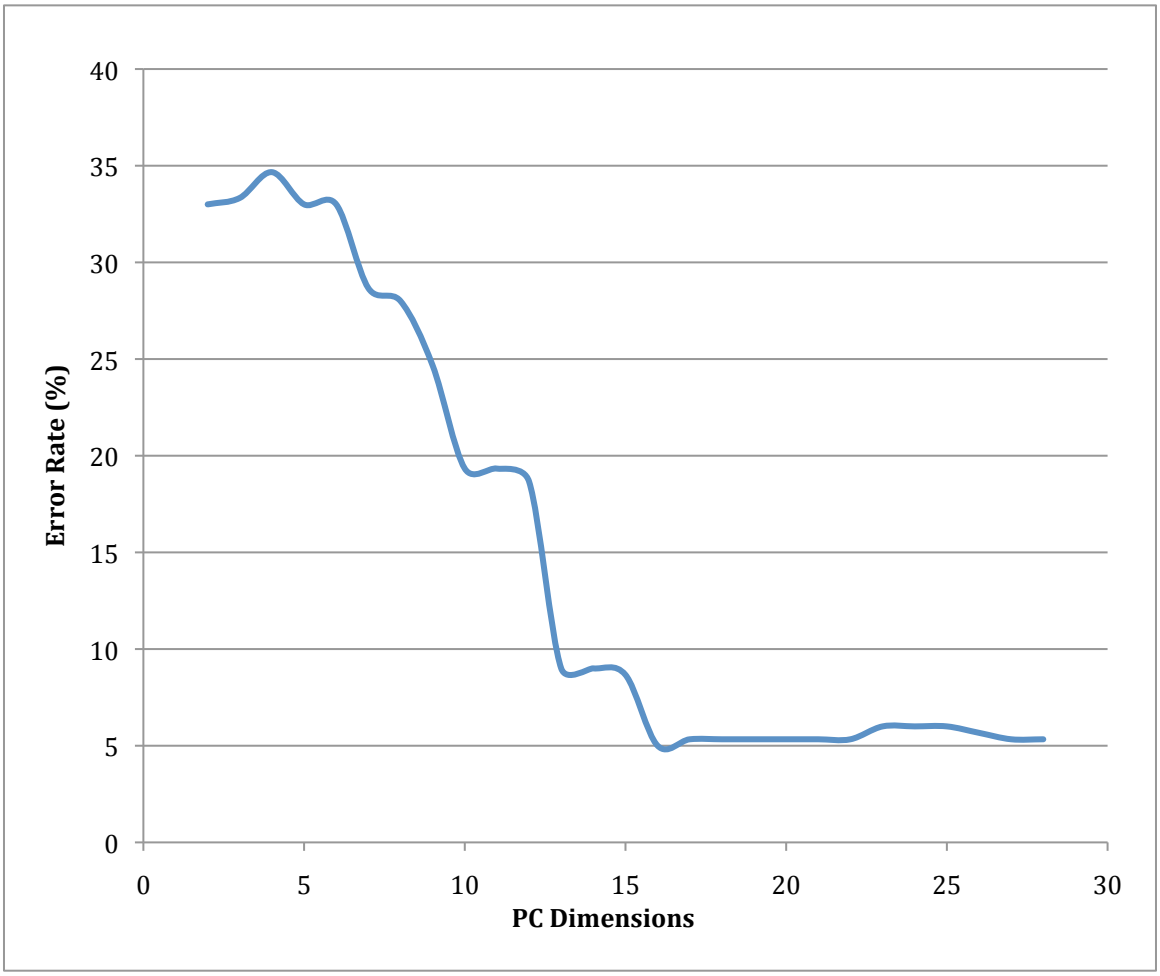


Figure 328: Graph of the classification (window or container) error rate versus PC dimensions for HOO-CV with PCA reduced CVA for the first set of 30 glass second derivative (9-point smoothing) spectra (10 replicates), centered data.

Table 340: Classification (window or container) error rates for HOO-CV with PCA reduced CVA for the first set of 30 glass second derivative (9-point smoothing) spectra (10 replicates), autoscaled data. The smallest PC dimension with the minimum error rate is highlighted in yellow.

PCs	Error Rate (%)	PCs	Error Rate (%)	PCs	Error Rate (%)	PCs	Error Rate (%)	PCs	Error Rate (%)
2	33.33	62	2.33	122	3.00	182	6.33	242	8.00
3	33.67	63	2.33	123	3.67	183	6.00	243	8.00
4	8.67	64	3.00	124	3.33	184	6.00	244	7.33
5	6.33	65	3.00	125	3.33	185	5.33	245	7.67
6	5.00	66	3.00	126	3.33	186	5.67	246	7.67
7	6.67	67	2.67	127	3.33	187	6.00	247	8.33
8	4.33	68	2.67	128	3.33	188	5.67	248	8.67
9	4.00	69	2.67	129	3.67	189	6.00	249	8.00
10	4.00	70	3.00	130	3.67	190	6.67	250	9.67
11	4.00	71	3.00	131	3.67	191	4.67	251	9.67
12	3.67	72	3.00	132	3.67	192	4.67	252	10.00
13	3.67	73	3.00	133	3.67	193	5.00	253	9.67
14	3.67	74	3.00	134	3.67	194	5.33	254	10.67
15	3.67	75	3.00	135	3.67	195	5.33	255	12.33
16	3.67	76	3.00	136	3.67	196	5.33	256	12.33
17	3.67	77	3.33	137	3.67	197	6.67	257	11.67
18	3.67	78	3.00	138	3.33	198	6.00	258	13.00
19	3.67	79	3.00	139	3.33	199	6.33	259	12.33
20	3.67	80	3.00	140	3.33	200	6.67	260	11.67
21	3.67	81	3.00	141	3.33	201	7.00	261	13.00
22	3.67	82	3.00	142	3.33	202	7.00	262	13.33
23	3.33	83	3.33	143	3.33	203	7.33	263	12.00
24	3.67	84	4.00	144	3.33	204	7.00	264	12.67
25	3.67	85	4.00	145	3.33	205	7.00	265	13.67
26	3.67	86	3.67	146	3.33	206	7.00	266	14.33
27	4.00	87	3.33	147	3.33	207	7.00	267	15.33
28	4.00	88	3.67	148	3.67	208	6.33	268	13.67
29	4.00	89	3.67	149	3.33	209	6.00	269	14.33
30	3.67	90	3.67	150	4.00	210	5.67	270	15.67
31	3.33	91	3.67	151	4.00	211	6.00	271	16.67
32	3.33	92	3.67	152	4.00	212	6.00	272	18.00
33	3.33	93	3.67	153	4.00	213	5.00	273	19.33
34	3.33	94	3.33	154	4.00	214	5.33	274	17.00
35	3.33	95	3.67	155	4.00	215	5.33	275	18.67
36	3.33	96	4.00	156	4.00	216	5.33	276	19.67
37	3.33	97	4.00	157	4.00	217	5.67	277	20.00

38	3.33	98	4.00	158	4.00	218	5.67	278	19.33
39	3.33	99	4.00	159	4.33	219	5.00	279	18.33
40	3.33	100	3.67	160	4.67	220	6.67	280	18.33
41	2.67	101	4.00	161	5.00	221	7.33	281	20.33
42	2.33	102	3.67	162	4.67	222	7.33	282	20.00
43	2.33	103	4.00	163	4.33	223	7.67	283	20.00
44	2.33	104	4.00	164	4.33	224	7.00	284	22.67
45	2.33	105	4.00	165	5.33	225	6.67	285	20.00
46	2.33	106	4.00	166	5.67	226	7.00	286	21.33
47	2.33	107	3.67	167	6.00	227	7.33	287	20.67
48	2.00	108	4.00	168	4.33	228	7.33	288	22.33
49	2.33	109	3.67	169	4.67	229	7.33	289	21.33
50	2.67	110	4.00	170	4.67	230	7.67	290	22.00
51	3.00	111	3.33	171	5.00	231	7.67	291	24.33
52	2.67	112	3.00	172	5.33	232	7.33	292	27.00
53	2.67	113	2.67	173	5.67	233	6.67	293	23.67
54	2.67	114	2.67	174	5.00	234	8.33	294	21.33
55	2.33	115	3.00	175	5.33	235	8.33	295	25.67
56	2.67	116	3.33	176	5.00	236	7.67	296	32.00
57	2.67	117	3.33	177	5.33	237	8.67	297	9.67
58	2.67	118	3.00	178	5.67	238	8.67	298	94.33
59	2.67	119	3.00	179	5.33	239	8.67	299	33.33
60	2.67	120	3.00	180	5.67	240	8.00		
61	2.33	121	3.00	181	6.00	241	7.67		

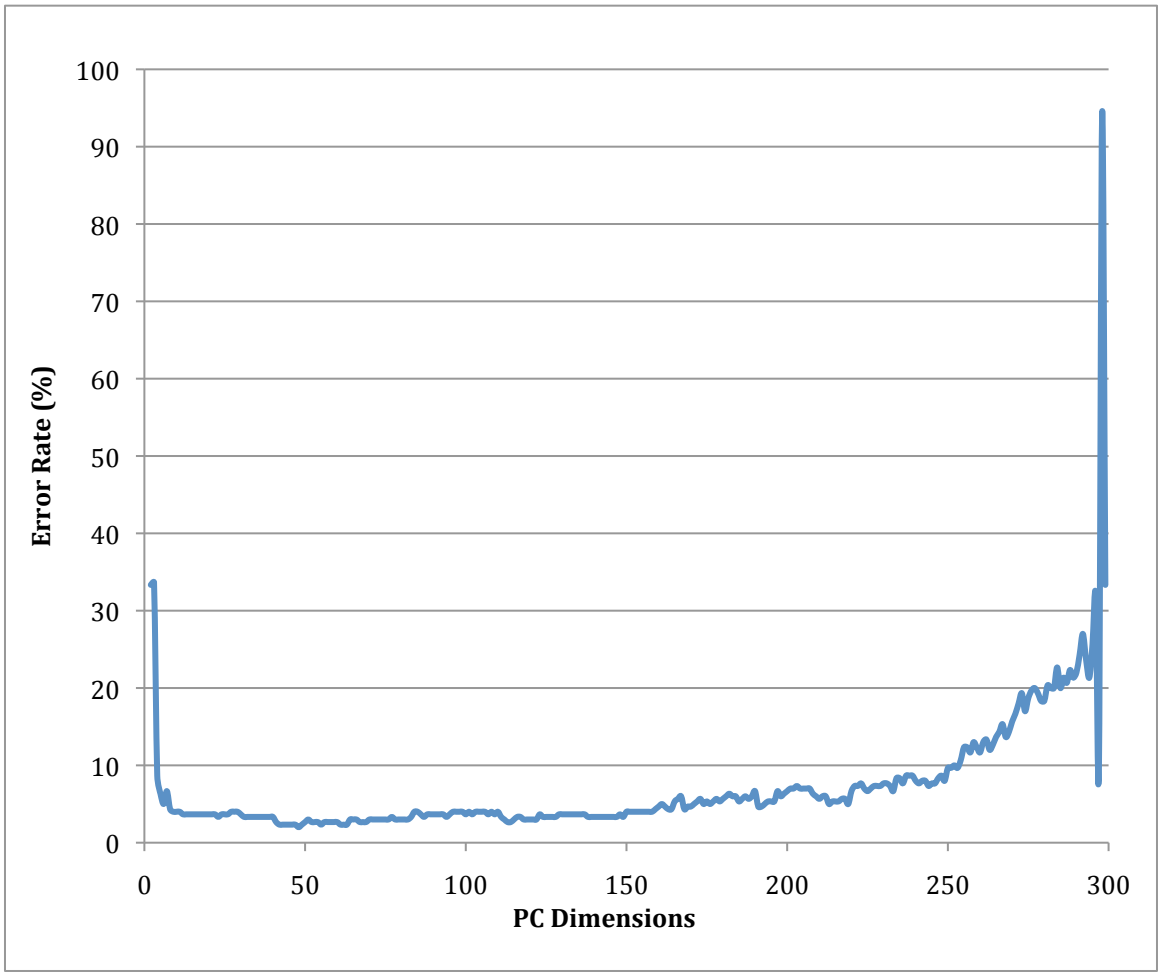


Figure 329: Graph of the classification (window or container) error rate versus PC dimensions for HOO-CV with PCA reduced CVA for the first set of 30 glass second derivative (9-point smoothing) spectra (10 replicates), autoscaled data.

First Set, Second Derivative (9-point smoothing) – Window Discrimination

Table 341: Discrimination error rates for HOO-CV with PCA reduced CVA for the first set of 20 window glass second derivative (9-point smoothing) spectra (10 replicates), no data pretreatment. The smallest PC dimension with the minimum error rate is highlighted in yellow.

PCs	Error Rate (%)	PCs	Error Rate (%)	PCs	Error Rate (%)	PCs	Error Rate (%)	PCs	Error Rate (%)
2	96.50	7	87.50	12	73.50	17	63.00	22	60.00
3	94.00	8	84.50	13	70.50	18	64.00	23	56.50
4	91.00	9	82.00	14	69.50	19	63.00	24	55.00
5	87.00	10	78.50	15	68.50	20	61.00	25	55.50
6	88.50	11	80.50	16	62.00	21	59.50		

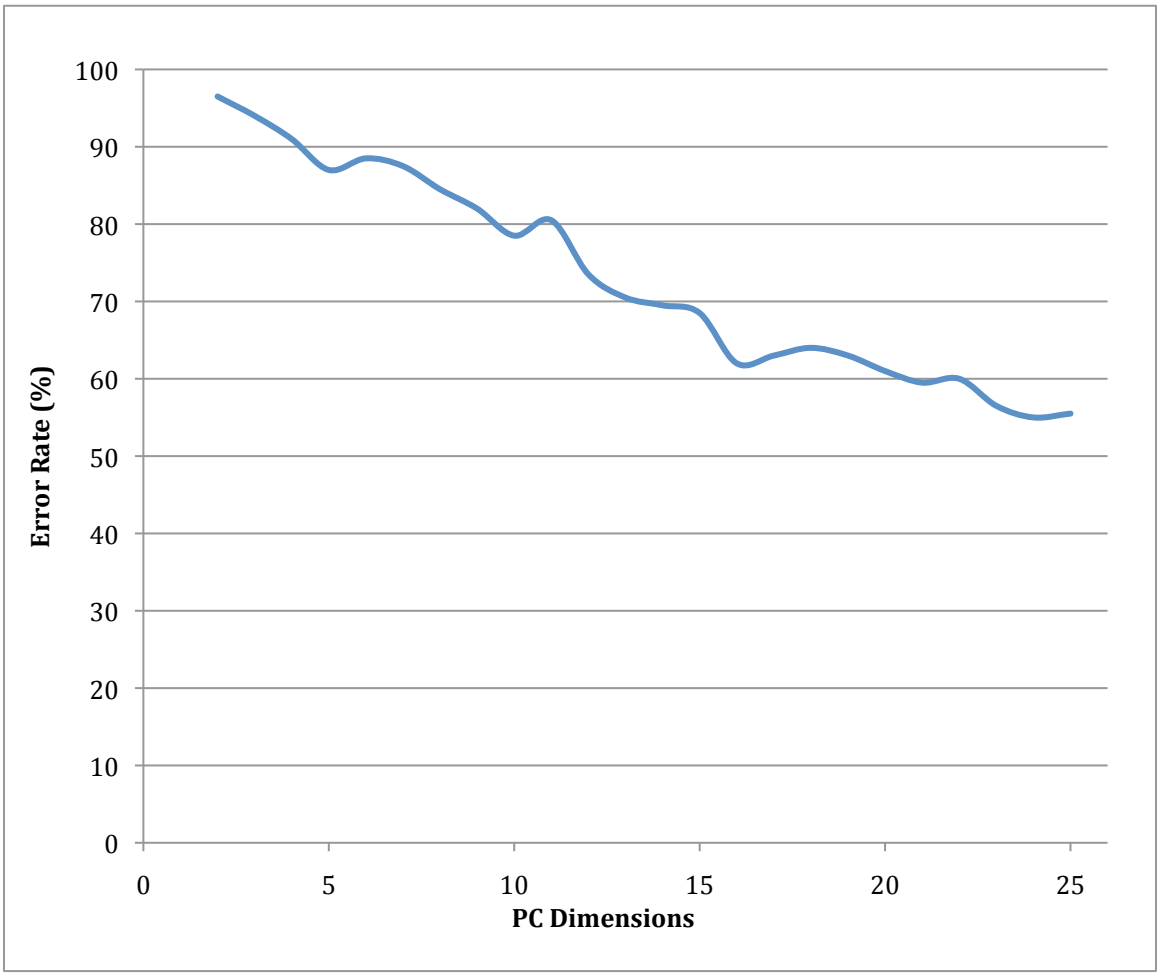


Figure 330: Graph of the discrimination error rate versus PC dimensions for HOO-CV with PCA reduced CVA for the first set of 20 window glass second derivative (9-point smoothing) spectra (10 replicates), no data pretreatment.

Table 342: Discrimination error rates for HOO-CV with PCA reduced CVA for the first set of 20 window glass second derivative (9-point smoothing) spectra (10 replicates), centered data. The smallest PC dimension with the minimum error rate is highlighted in yellow.

PCs	Error Rate (%)	PCs	Error Rate (%)	PCs	Error Rate (%)	PCs	Error Rate (%)	PCs	Error Rate (%)
2	96.00	7	86.50	12	75.50	17	63.50	22	58.50
3	96.00	8	84.50	13	71.00	18	63.50	23	58.00
4	93.00	9	82.00	14	68.00	19	65.50	24	55.50
5	92.00	10	81.00	15	65.00	20	62.00		
6	88.00	11	81.50	16	63.00	21	57.50		

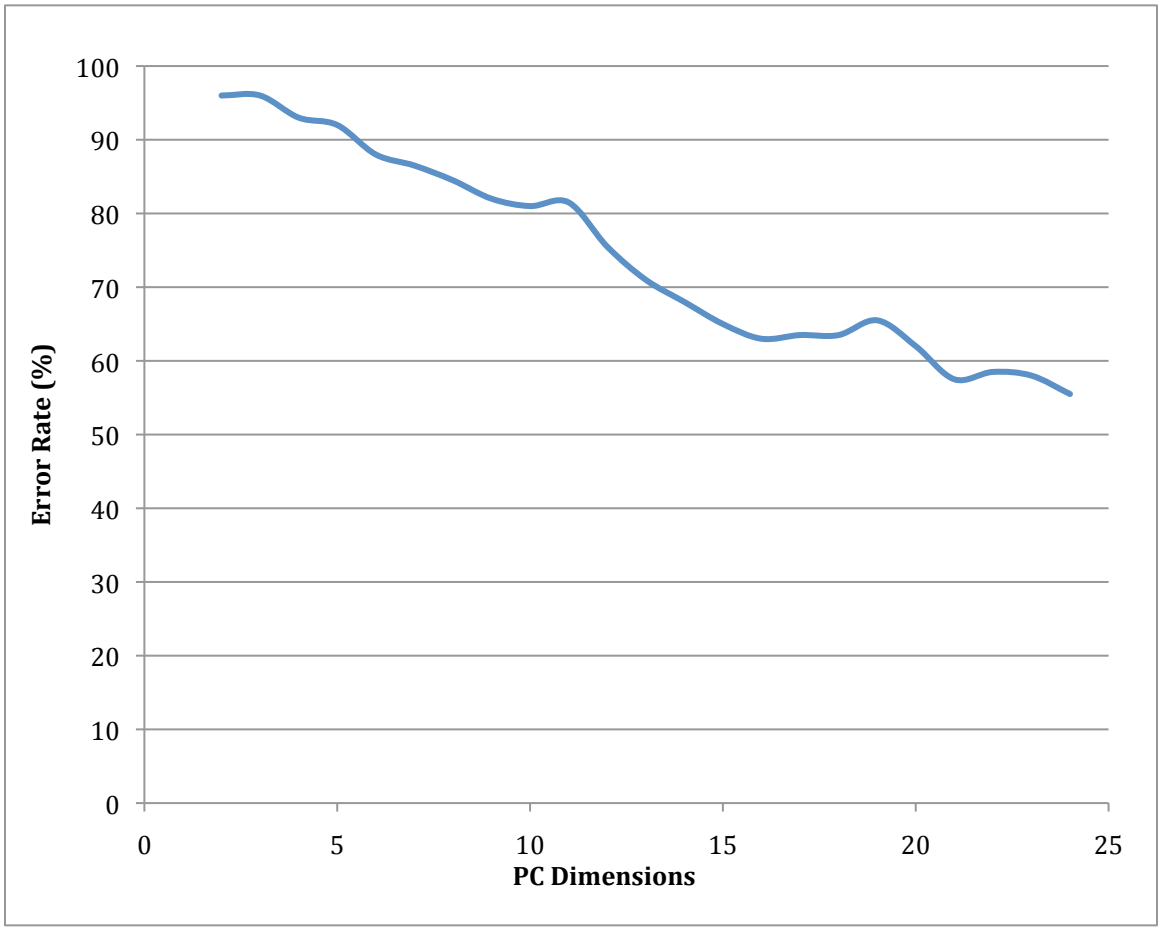


Figure 331: Graph of the discrimination error rate versus PC dimensions for HOO-CV with PCA reduced CVA for the first set of 20 window glass second derivative (9-point smoothing) spectra (10 replicates), centered data.

Table 343: Discrimination error rates for HOO-CV with PCA reduced CVA for the first set of 20 window glass second derivative (9-point smoothing) spectra (10 replicates), autoscaled data. The smallest PC dimension with the minimum error rate is highlighted in yellow.

PCs	Error Rate (%)	PCs	Error Rate (%)	PCs	Error Rate (%)	PCs	Error Rate (%)	PCs	Error Rate (%)
2	92.00	42	20.50	82	11.50	122	11.50	162	25.50
3	77.00	43	19.50	83	11.00	123	11.50	163	32.00
4	73.00	44	18.50	84	11.00	124	12.00	164	33.50
5	66.00	45	17.00	85	11.50	125	12.50	165	35.00
6	66.50	46	17.50	86	11.00	126	13.00	166	34.00
7	60.50	47	16.50	87	12.00	127	13.50	167	37.00
8	57.50	48	17.50	88	11.00	128	13.50	168	43.50
9	50.00	49	18.50	89	10.50	129	13.50	169	42.50
10	46.50	50	17.50	90	10.50	130	13.50	170	44.50
11	44.50	51	15.50	91	12.00	131	14.00	171	47.50
12	40.00	52	14.00	92	10.50	132	14.50	172	53.00
13	38.00	53	10.50	93	11.00	133	14.50	173	57.50
14	34.00	54	9.50	94	11.00	134	16.00	174	58.00
15	33.00	55	10.00	95	10.00	135	17.00	175	58.50
16	32.50	56	10.50	96	10.50	136	19.00	176	56.00
17	32.50	57	11.50	97	11.00	137	21.00	177	66.00
18	32.00	58	11.00	98	11.00	138	20.00	178	72.00
19	28.00	59	10.50	99	10.50	139	21.00	179	63.50
20	28.00	60	11.00	100	11.00	140	21.00	180	89.50
21	28.50	61	11.00	101	10.50	141	20.50	181	92.00
22	24.00	62	10.00	102	11.00	142	22.00	182	78.00
23	23.00	63	11.50	103	10.50	143	23.00	183	78.00
24	22.50	64	12.00	104	10.00	144	24.00	184	81.50
25	21.50	65	11.50	105	9.00	145	21.50	185	83.50
26	20.50	66	11.50	106	9.50	146	23.00	186	88.00
27	21.50	67	9.00	107	10.50	147	24.50	187	82.50
28	21.00	68	8.50	108	9.00	148	23.50	188	88.00
29	21.50	69	7.50	109	9.00	149	22.00	189	91.50
30	22.00	70	8.00	110	9.50	150	21.50	190	91.50
31	20.50	71	9.00	111	9.00	151	25.00	191	94.50
32	18.50	72	9.50	112	9.50	152	24.00	192	96.50
33	19.50	73	11.00	113	11.00	153	24.00	193	96.50
34	19.00	74	11.50	114	11.00	154	24.50	194	99.00
35	18.00	75	12.50	115	11.00	155	24.00	195	98.00
36	17.50	76	12.00	116	12.00	156	26.00	196	96.50
37	17.00	77	11.00	117	11.50	157	30.00	197	97.50
38	17.50	78	11.50	118	12.00	158	25.50	198	94.00

39	17.50	79	10.00	119	11.00	159	25.00	199	84.00
40	17.50	80	10.50	120	10.00	160	24.00		
41	19.00	81	11.00	121	11.00	161	26.50		

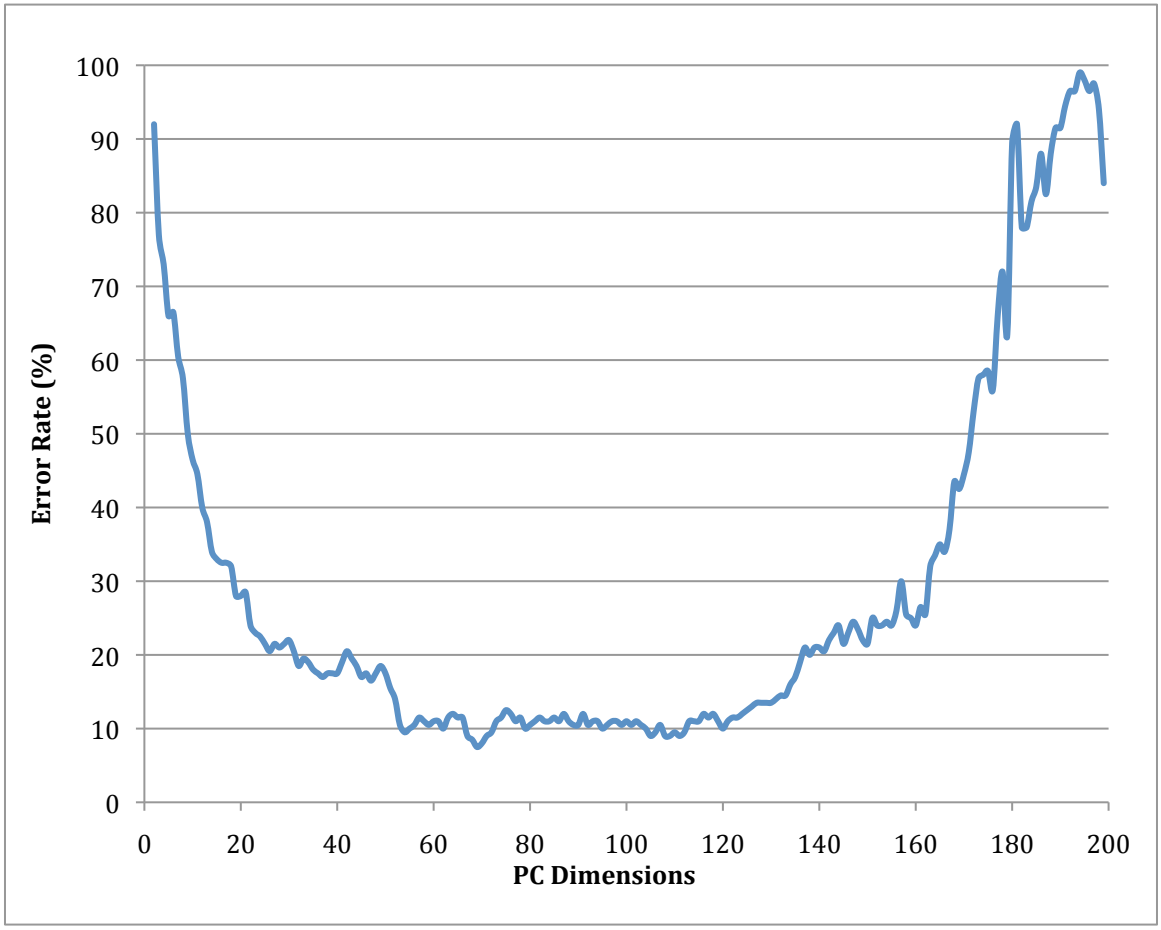


Figure 332: Graph of the discrimination error rate versus PC dimensions for HOO-CV with PCA reduced CVA for the first set of 20 window glass second derivative (9-point smoothing) spectra (10 replicates), autoscaled data.

First Set, Second Derivative (9-point smoothing) – Container Discrimination

Table 344: Discrimination error rates for HOO-CV with PCA reduced CVA for the first set of 10 container glass second derivative (9-point smoothing) spectra (10 replicates), no data pretreatment. The smallest PC dimension with the minimum error rate is highlighted in yellow.

PCs	Error Rate (%)	PCs	Error Rate (%)	PCs	Error Rate (%)	PCs	Error Rate (%)	PCs	Error Rate (%)
2	86.00	7	81.00	12	52.00	17	44.00	22	43.00
3	86.00	8	76.00	13	49.00	18	44.00	23	39.00
4	79.00	9	74.00	14	49.00	19	41.00	24	39.00
5	81.00	10	61.00	15	45.00	20	44.00		
6	84.00	11	54.00	16	45.00	21	42.00		

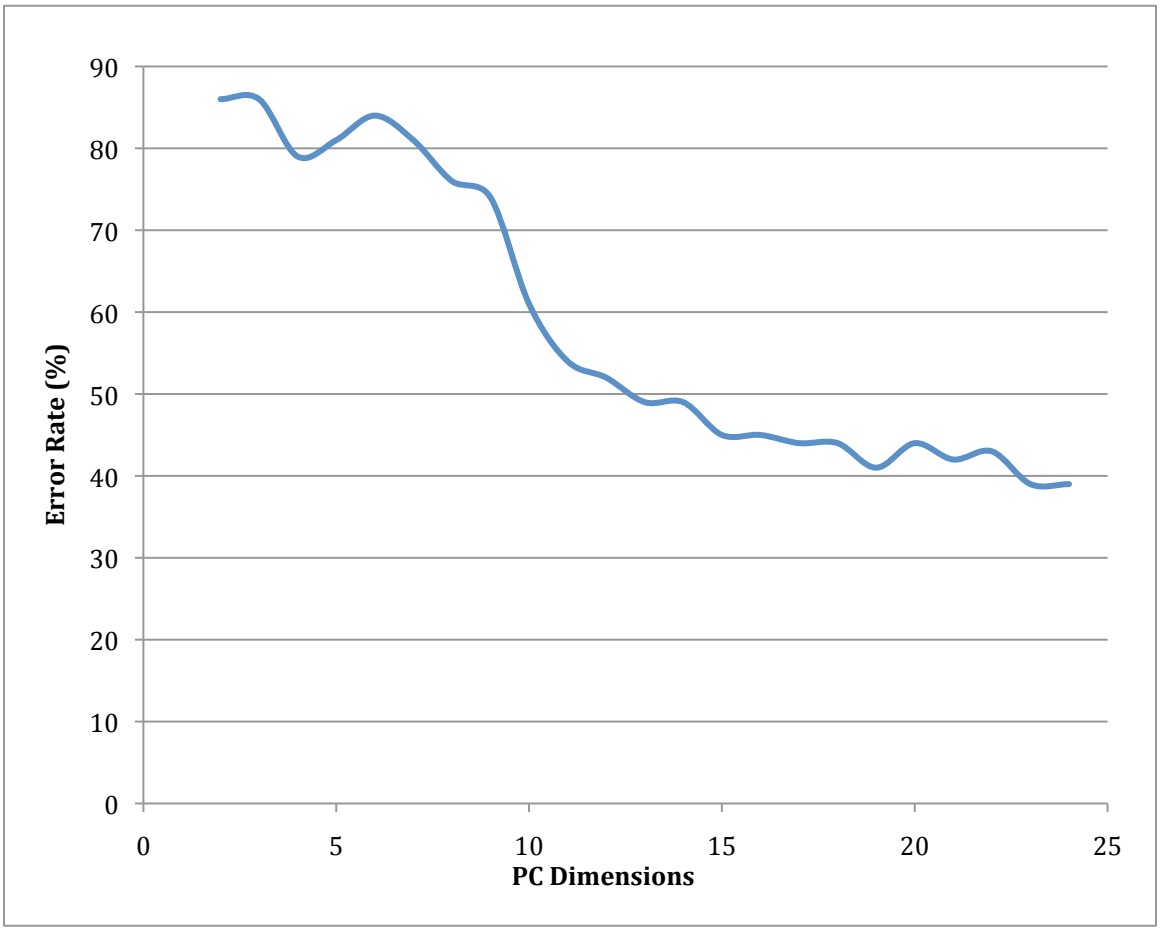


Figure 333: Graph of the discrimination error rate versus PC dimensions for HOO-CV with PCA reduced CVA for the first set of 10 container glass second derivative (9-point smoothing) spectra (10 replicates), no data pretreatment.

Table 345: Discrimination error rates for HOO-CV with PCA reduced CVA for the first set of 10 container glass second derivative (9-point smoothing) spectra (10 replicates), centered data. The smallest PC dimension with the minimum error rate is highlighted in yellow.

PCs	Error Rate (%)	PCs	Error Rate (%)	PCs	Error Rate (%)	PCs	Error Rate (%)	PCs	Error Rate (%)
2	84.00	7	75.00	12	50.00	17	45.00	22	42.00
3	82.00	8	77.00	13	45.00	18	45.00	23	41.00
4	83.00	9	61.00	14	46.00	19	42.00		
5	79.00	10	60.00	15	45.00	20	43.00		
6	81.00	11	53.00	16	49.00	21	45.00		

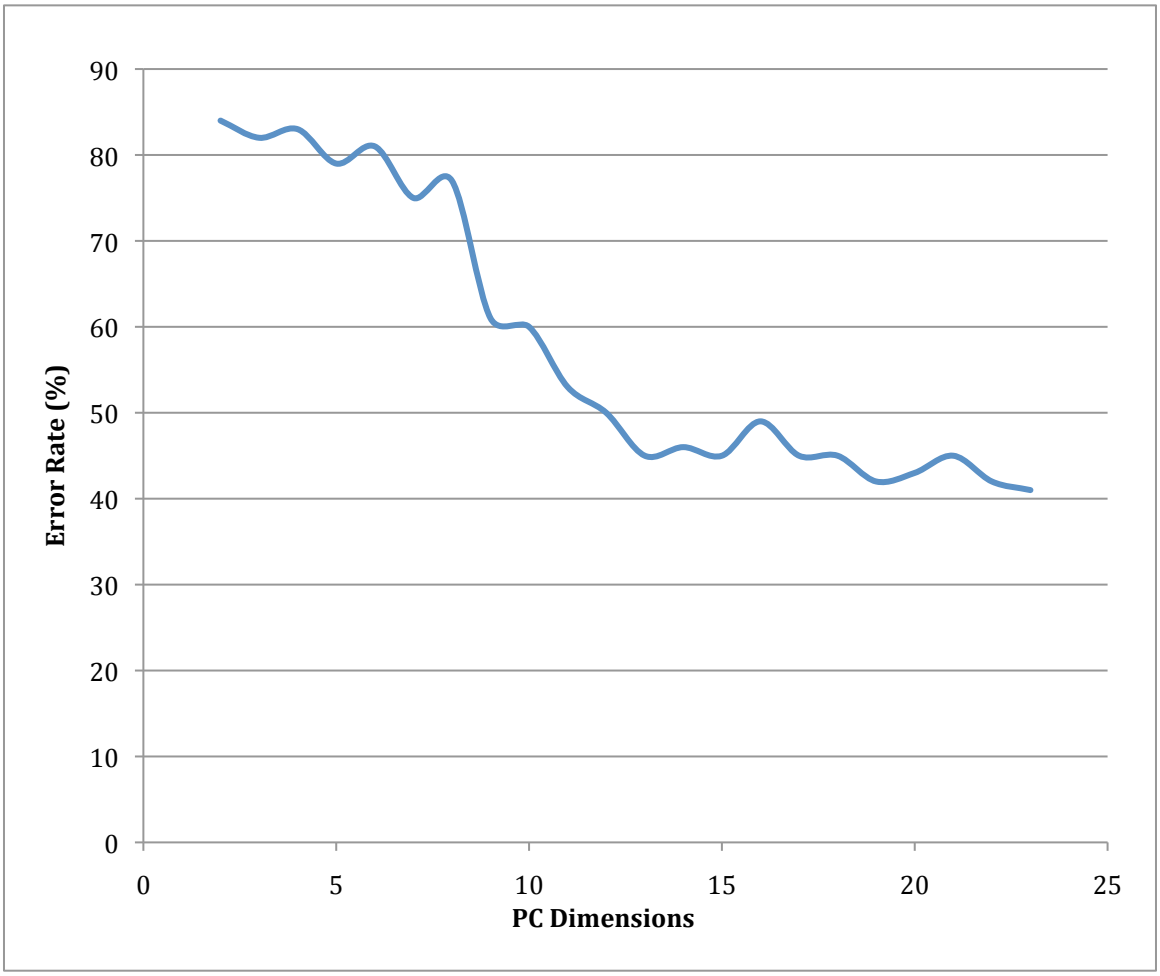


Figure 334: Graph of the discrimination error rate versus PC dimensions for HOO-CV with PCA reduced CVA for the first set of 10 container glass second derivative (9-point smoothing) spectra (10 replicates), centered data.

Table 346: Discrimination error rates for HOO-CV with PCA reduced CVA for the first set of 10 container glass second derivative (9-point smoothing) spectra (10 replicates), autoscaled data. The smallest PC dimension with the minimum error rate is highlighted in yellow.

PCs	Error Rate (%)	PCs	Error Rate (%)	PCs	Error Rate (%)	PCs	Error Rate (%)	PCs	Error Rate (%)
2	63.00	22	14.00	42	10.00	62	15.00	82	20.00
3	56.00	23	17.00	43	9.00	63	14.00	83	24.00
4	44.00	24	15.00	44	9.00	64	13.00	84	25.00
5	44.00	25	16.00	45	10.00	65	12.00	85	23.00
6	38.00	26	14.00	46	9.00	66	13.00	86	29.00
7	43.00	27	13.00	47	9.00	67	17.00	87	19.00
8	29.00	28	11.00	48	9.00	68	13.00	88	27.00
9	30.00	29	11.00	49	9.00	69	13.00	89	45.00
10	23.00	30	13.00	50	11.00	70	15.00	90	72.00
11	21.00	31	15.00	51	10.00	71	15.00	91	75.00
12	21.00	32	8.00	52	12.00	72	15.00	92	58.00
13	25.00	33	10.00	53	10.00	73	17.00	93	68.00
14	21.00	34	8.00	54	13.00	74	14.00	94	81.00
15	15.00	35	7.00	55	12.00	75	14.00	95	91.00
16	16.00	36	10.00	56	11.00	76	16.00	96	94.00
17	15.00	37	9.00	57	12.00	77	19.00	97	96.00
18	13.00	38	10.00	58	10.00	78	17.00	98	97.00
19	12.00	39	10.00	59	10.00	79	16.00	99	56.00
20	12.00	40	12.00	60	13.00	80	23.00		
21	12.00	41	12.00	61	14.00	81	17.00		

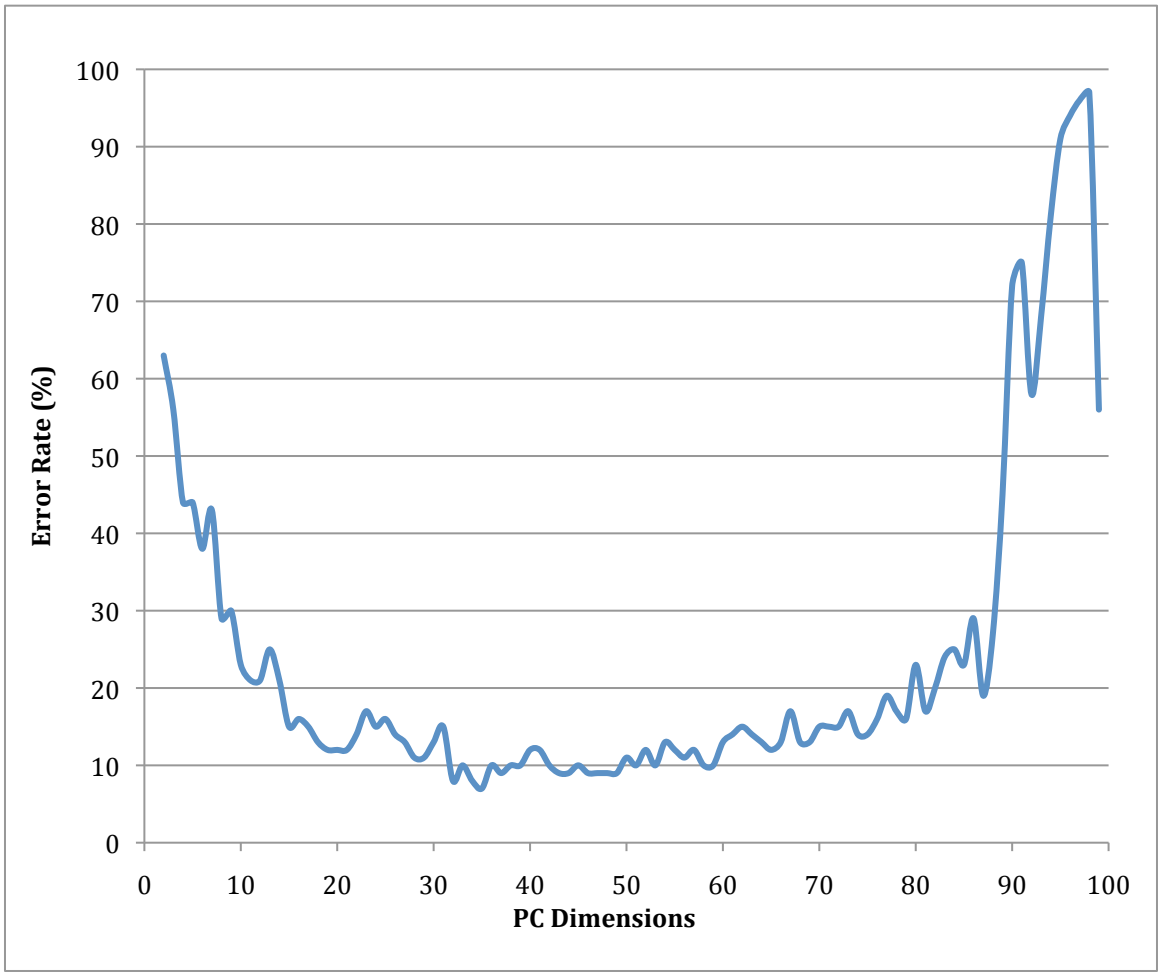


Figure 335: Graph of the discrimination error rate versus PC dimensions for HOO-CV with PCA reduced CVA for the first set of 10 container glass second derivative (9-point smoothing) spectra (10 replicates), autoscaled data.

First Set, Second Derivative (9-point smoothing) – Float Classification

Table 347: Float classification error rates for HOO-CV with PCA reduced CVA for the first set of 20 window glass second derivative (9-point smoothing) spectra (10 replicates), no data pretreatment. The smallest PC dimension with the minimum error rate is highlighted in yellow.

PCs	Error Rate (%)	PCs	Error Rate (%)	PCs	Error Rate (%)	PCs	Error Rate (%)	PCs	Error Rate (%)
2	39.00	8	31.00	14	33.50	20	31.00	26	27.00
3	34.00	9	31.50	15	33.50	21	27.00	27	28.50
4	39.50	10	30.00	16	33.00	22	27.00		
5	38.00	11	30.50	17	32.50	23	26.50		
6	31.00	12	29.50	18	29.50	24	27.50		
7	33.50	13	32.00	19	29.50	25	27.00		

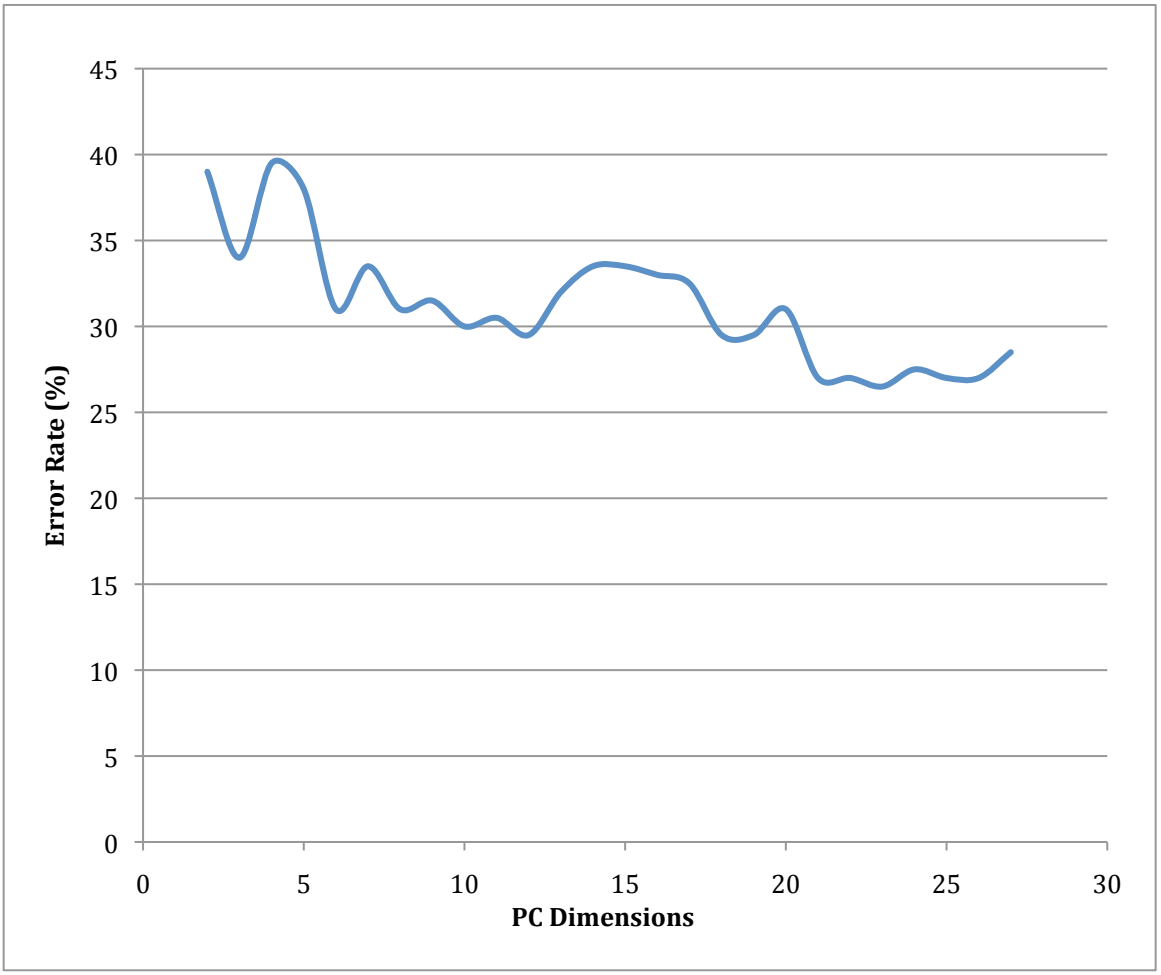


Figure 336: Graph of the float classification error rate versus PC dimensions for HOO-CV with PCA reduced CVA for the first set of 20 window glass second derivative (9-point smoothing) spectra (10 replicates), no data pretreatment.

Table 348: Float classification error rates for HOO-CV with PCA reduced CVA for the first set of 20 window glass second derivative (9-point smoothing) spectra (10 replicates), centered data. The smallest PC dimension with the minimum error rate is highlighted in yellow.

PCs	Error Rate (%)	PCs	Error Rate (%)	PCs	Error Rate (%)	PCs	Error Rate (%)	PCs	Error Rate (%)
2	41.00	7	29.50	12	30.50	17	32.50	22	28.00
3	36.50	8	29.00	13	30.50	18	29.50	23	26.50
4	40.50	9	28.50	14	33.50	19	31.00	24	28.00
5	38.00	10	30.00	15	33.50	20	30.50	25	27.50
6	30.00	11	30.00	16	32.00	21	28.00	26	27.50

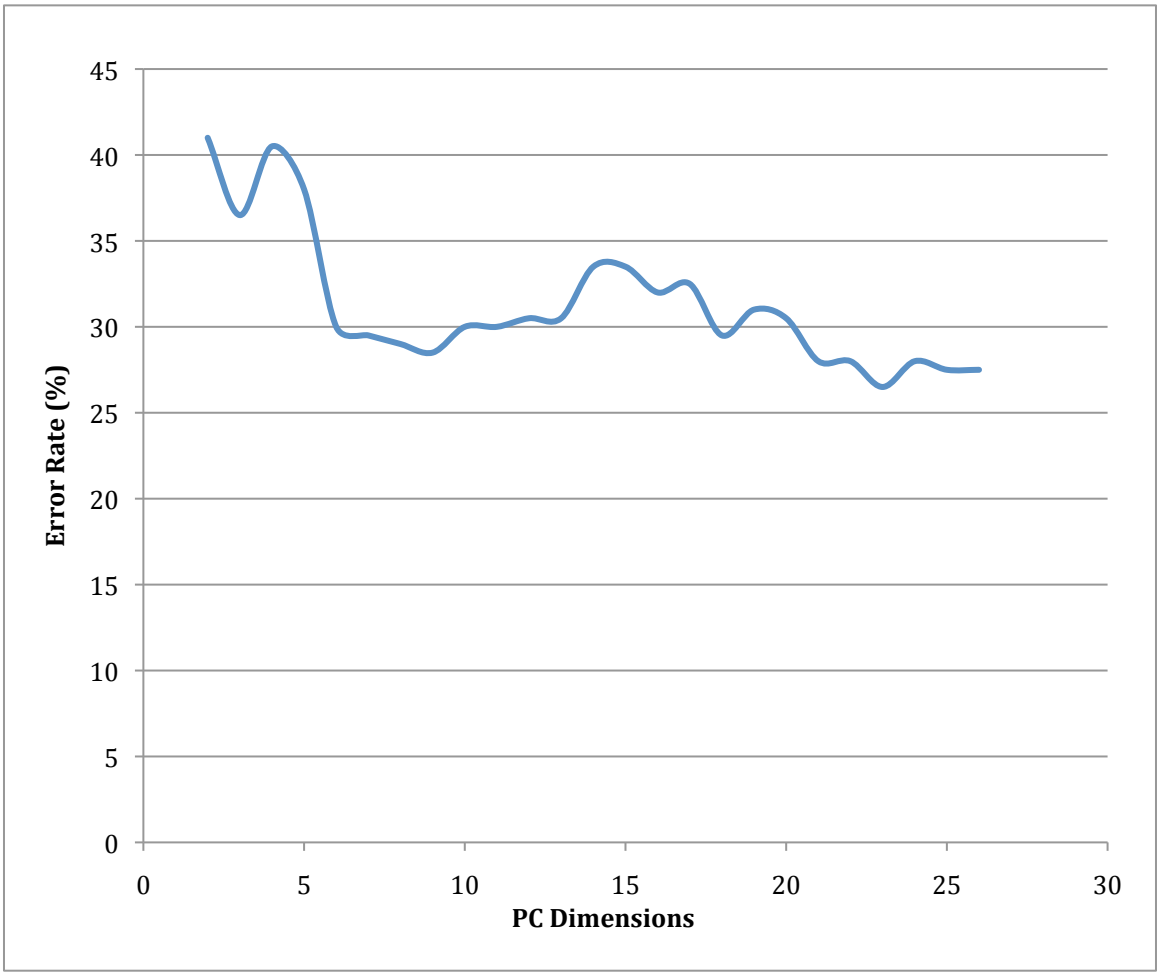


Figure 337: Graph of the float classification error rate versus PC dimensions for HOO-CV with PCA reduced CVA for the first set of 20 window glass second derivative (9-point smoothing) spectra (10 replicates), centered data.

Table 349: Float classification error rates for HOO-CV with PCA reduced CVA for the first set of 20 window glass second derivative (9-point smoothing) spectra (10 replicates), autoscaled data. The smallest PC dimension with the minimum error rate is highlighted in yellow.

PCs	Error Rate (%)	PCs	Error Rate (%)	PCs	Error Rate (%)	PCs	Error Rate (%)	PCs	Error Rate (%)
2	28.00	42	21.50	82	23.00	122	28.50	162	35.00
3	28.00	43	23.00	83	24.00	123	29.50	163	34.00
4	27.00	44	19.50	84	23.50	124	30.00	164	34.50
5	27.50	45	19.00	85	24.50	125	27.00	165	37.00
6	26.50	46	21.50	86	26.00	126	27.00	166	37.00
7	26.50	47	18.50	87	24.00	127	27.50	167	36.50
8	27.50	48	19.00	88	26.00	128	28.50	168	36.00
9	24.00	49	19.50	89	26.50	129	28.50	169	38.50
10	23.50	50	22.00	90	25.00	130	29.00	170	33.50
11	23.50	51	21.00	91	25.50	131	26.50	171	36.00
12	24.00	52	21.50	92	23.50	132	26.50	172	36.00
13	24.00	53	20.50	93	25.50	133	25.50	173	36.50
14	23.50	54	19.50	94	27.00	134	26.00	174	36.50
15	23.50	55	20.00	95	26.00	135	25.50	175	37.50
16	24.00	56	19.50	96	27.50	136	25.00	176	39.50
17	25.00	57	21.50	97	27.50	137	25.50	177	38.50
18	26.00	58	23.00	98	27.00	138	25.00	178	38.50
19	26.00	59	23.50	99	26.00	139	26.50	179	37.50
20	24.00	60	22.50	100	25.00	140	26.50	180	37.50
21	22.50	61	23.50	101	25.00	141	28.50	181	36.50
22	22.50	62	23.50	102	26.50	142	28.50	182	37.00
23	23.00	63	21.50	103	26.50	143	28.00	183	35.00
24	22.50	64	22.00	104	27.00	144	28.50	184	40.00
25	23.00	65	21.00	105	27.00	145	29.00	185	29.50
26	23.50	66	20.50	106	27.50	146	31.00	186	33.50
27	21.00	67	21.50	107	26.50	147	30.00	187	34.00
28	22.50	68	20.00	108	25.50	148	30.50	188	35.50
29	23.00	69	20.00	109	24.00	149	30.00	189	33.50
30	23.00	70	20.50	110	23.00	150	29.50	190	37.00
31	22.00	71	20.50	111	23.00	151	29.00	191	33.50
32	23.00	72	19.50	112	23.00	152	29.00	192	36.50
33	23.00	73	21.50	113	24.00	153	31.50	193	39.00
34	22.50	74	20.00	114	27.00	154	31.50	194	35.50
35	23.00	75	21.00	115	26.00	155	32.00	195	38.00
36	22.50	76	21.00	116	25.00	156	32.50	196	43.00
37	24.00	77	21.50	117	26.00	157	33.00	197	34.00
38	20.00	78	22.50	118	27.00	158	33.00	198	46.00

39	19.00	79	22.50	119	26.50	159	33.50	199	45.00
40	19.50	80	21.50	120	28.00	160	33.00		
41	22.50	81	21.50	121	28.00	161	33.00		

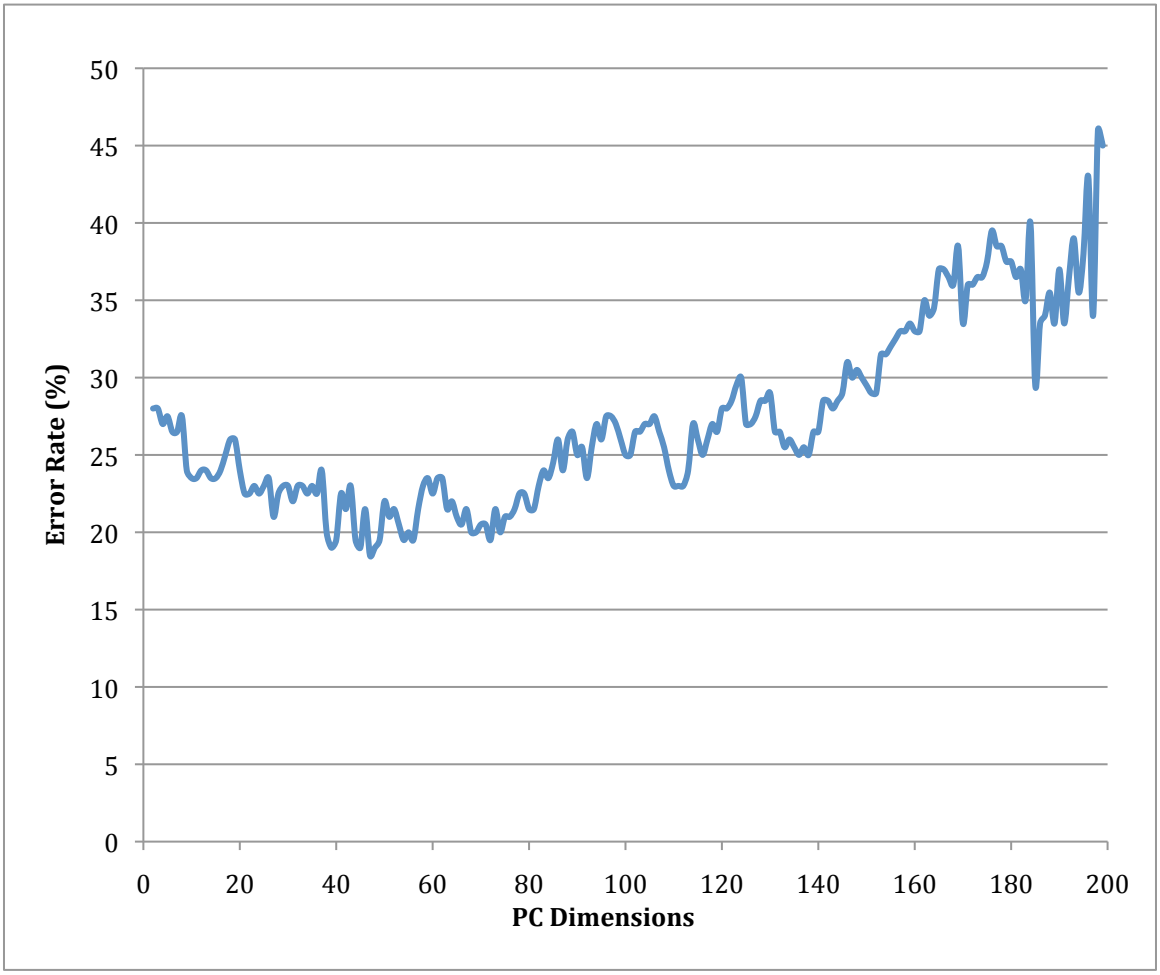


Figure 338: Graph of the float classification error rate versus PC dimensions for HOO-CV with PCA reduced CVA for the first set of 20 window glass second derivative (9-point smoothing) spectra (10 replicates), autoscaled data.

First Set, Second Derivative (9-point smoothing) – Tempered Classification

Table 350: Tempered classification error rates for HOO-CV with PCA reduced CVA for the first set of 20 window glass second derivative (9-point smoothing) spectra (10 replicates), no data pretreatment. The smallest PC dimension with the minimum error rate is highlighted in yellow.

PCs	Error Rate (%)	PCs	Error Rate (%)	PCs	Error Rate (%)	PCs	Error Rate (%)	PCs	Error Rate (%)
2	32.00	8	31.50	14	27.00	20	26.50	26	28.50
3	32.00	9	31.50	15	28.50	21	26.00	27	30.00
4	30.50	10	32.50	16	30.00	22	27.50		
5	32.50	11	30.50	17	29.00	23	28.00		
6	28.00	12	27.00	18	29.50	24	29.00		
7	28.00	13	27.00	19	27.00	25	28.50		

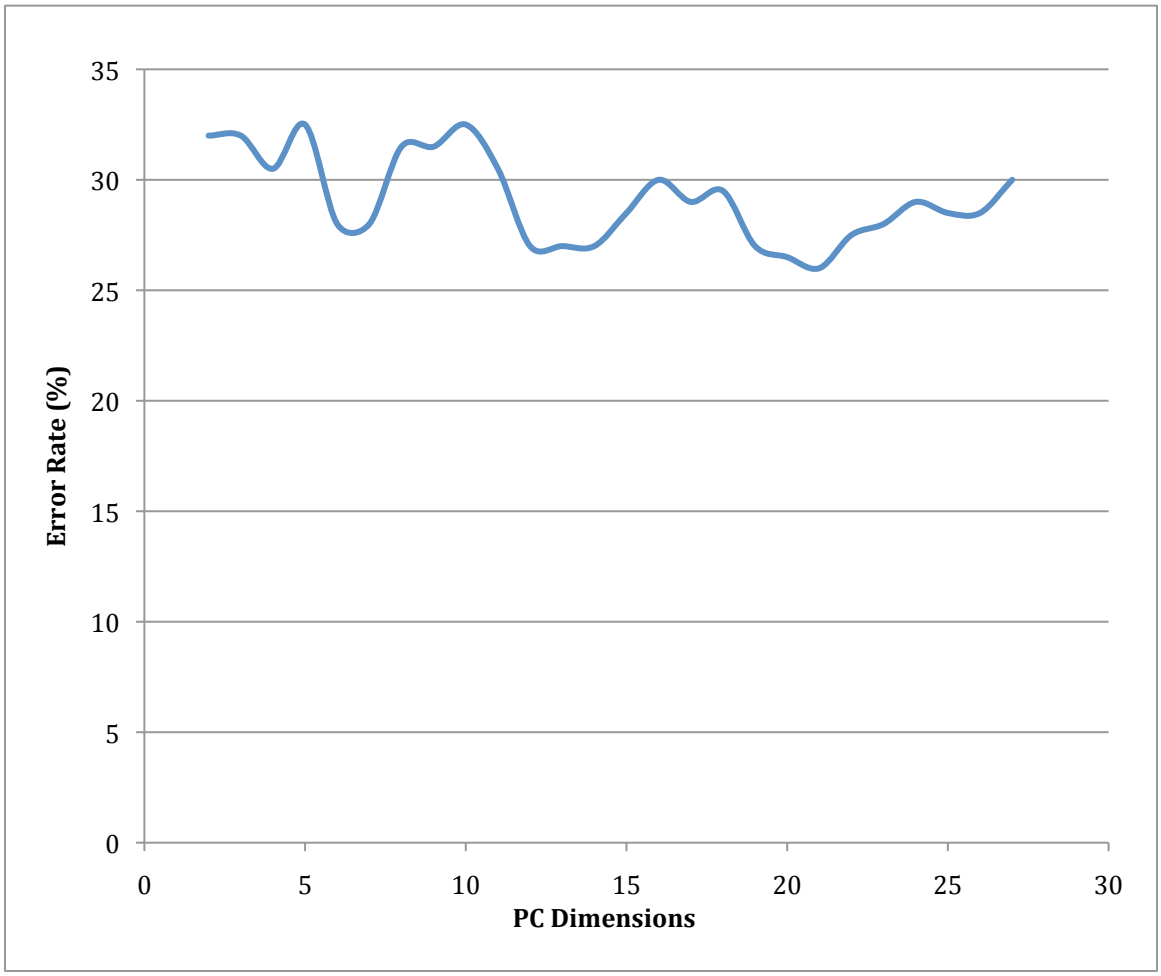


Figure 339: Graph of the tempered classification error rate versus PC dimensions for HOO-CV with PCA reduced CVA for the first set of 20 window glass second derivative (9-point smoothing) spectra (10 replicates), no data pretreatment.

Table 351: Tempered classification error rates for HOO-CV with PCA reduced CVA for the first set of 20 window glass second derivative (9-point smoothing) spectra (10 replicates), centered data. The smallest PC dimension with the minimum error rate is highlighted in yellow.

PCs	Error Rate (%)	PCs	Error Rate (%)	PCs	Error Rate (%)	PCs	Error Rate (%)	PCs	Error Rate (%)
2	29.50	7	31.00	12	30.50	17	28.50	22	28.00
3	34.00	8	32.00	13	28.50	18	29.00	23	29.00
4	30.50	9	32.50	14	27.50	19	27.50	24	29.50
5	29.00	10	32.50	15	27.00	20	26.50	25	29.00
6	31.00	11	31.50	16	28.00	21	28.00	26	28.00

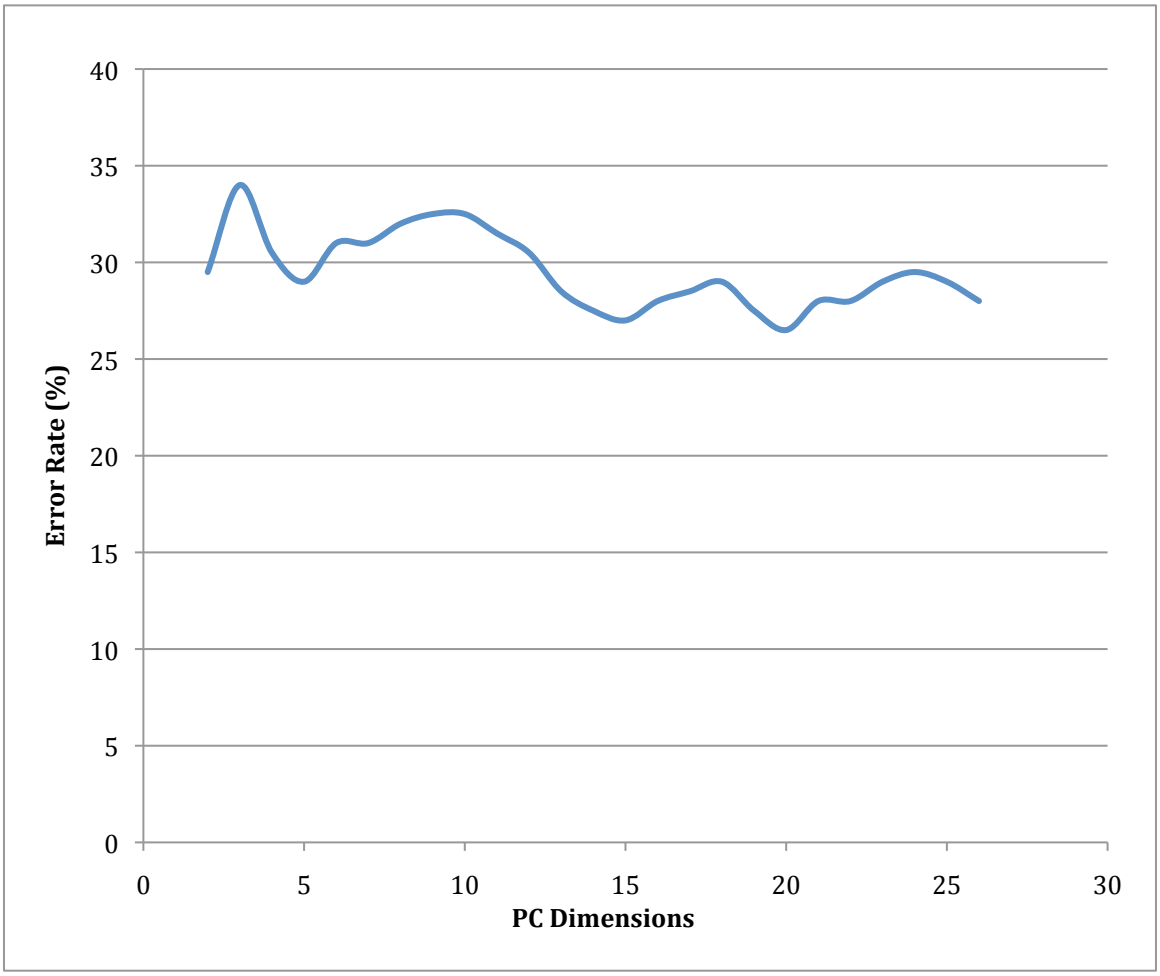


Figure 340: Graph of the tempered classification error rate versus PC dimensions for HOO-CV with PCA reduced CVA for the first set of 20 window glass second derivative (9-point smoothing) spectra (10 replicates), centered data.

Table 352: Tempered classification error rates for HOO-CV with PCA reduced CVA for the first set of 20 window glass second derivative (9-point smoothing) spectra (10 replicates), autoscaled data. The smallest PC dimension with the minimum error rate is highlighted in yellow.

PCs	Error Rate (%)	PCs	Error Rate (%)	PCs	Error Rate (%)	PCs	Error Rate (%)	PCs	Error Rate (%)
2	29.50	42	21.00	82	15.50	122	11.00	162	14.50
3	28.50	43	21.00	83	15.50	123	9.00	163	15.50
4	30.50	44	19.50	84	16.00	124	9.00	164	17.00
5	30.00	45	19.50	85	15.50	125	9.00	165	17.50
6	31.00	46	17.50	86	17.00	126	8.50	166	18.00
7	30.50	47	19.50	87	17.00	127	9.00	167	17.50
8	25.00	48	20.50	88	16.00	128	9.00	168	17.00
9	25.50	49	18.00	89	15.50	129	8.00	169	18.50
10	26.00	50	17.50	90	16.00	130	9.00	170	16.00
11	25.50	51	16.50	91	16.00	131	9.50	171	17.50
12	25.50	52	16.50	92	13.50	132	9.50	172	18.50
13	25.50	53	17.50	93	11.00	133	10.00	173	18.50
14	23.50	54	16.50	94	11.50	134	12.00	174	20.50
15	24.00	55	16.50	95	12.00	135	12.50	175	21.00
16	24.50	56	17.50	96	11.00	136	13.00	176	21.50
17	25.50	57	17.50	97	12.00	137	15.00	177	22.50
18	24.50	58	18.00	98	13.00	138	11.50	178	21.00
19	26.50	59	17.50	99	13.00	139	11.50	179	18.50
20	26.00	60	18.00	100	13.50	140	12.00	180	20.50
21	25.50	61	18.50	101	14.50	141	12.50	181	18.50
22	21.50	62	18.50	102	13.50	142	12.50	182	16.00
23	19.50	63	17.50	103	14.00	143	13.50	183	17.50
24	21.50	64	17.00	104	14.50	144	14.00	184	19.00
25	17.50	65	17.00	105	15.00	145	14.00	185	22.50
26	18.00	66	17.50	106	15.00	146	15.00	186	24.50
27	17.50	67	17.50	107	15.50	147	15.50	187	26.00
28	18.00	68	17.50	108	14.00	148	14.00	188	20.50
29	19.50	69	17.00	109	14.50	149	13.50	189	21.50
30	18.50	70	15.50	110	14.50	150	16.00	190	24.00
31	20.50	71	15.50	111	13.50	151	14.50	191	24.50
32	19.00	72	15.50	112	14.50	152	16.00	192	28.00
33	19.00	73	15.50	113	14.50	153	15.50	193	31.00
34	21.00	74	15.50	114	10.50	154	14.00	194	35.50
35	19.00	75	16.00	115	12.00	155	14.50	195	38.50
36	18.50	76	16.50	116	12.50	156	14.50	196	40.00
37	18.50	77	16.50	117	12.00	157	14.00	197	42.50

38	18.50	78	17.00	118	12.00	158	13.50	198	48.00
39	19.50	79	15.50	119	10.50	159	14.00	199	40.50
40	20.00	80	16.00	120	10.50	160	14.50		
41	20.50	81	15.50	121	10.50	161	15.00		

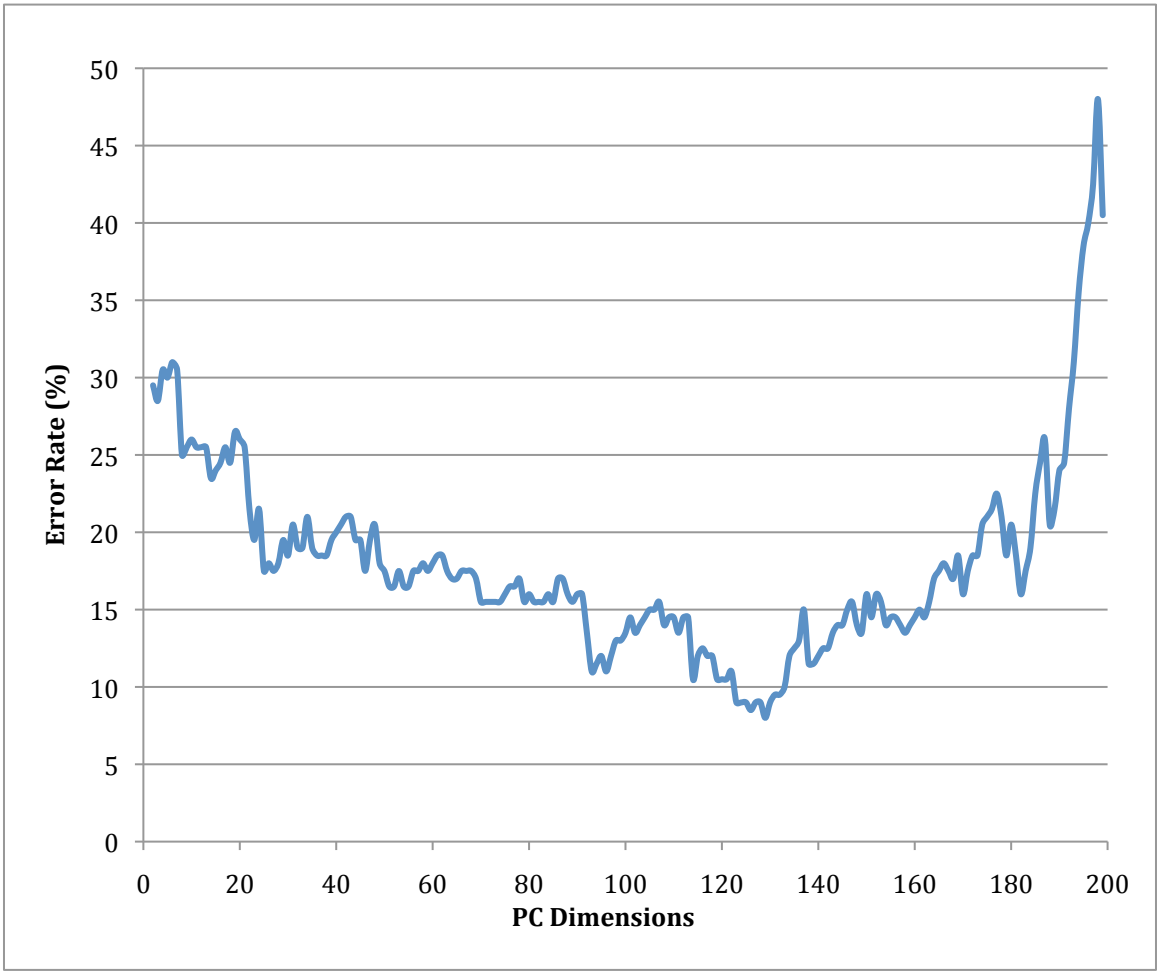


Figure 341: Graph of the tempered classification error rate versus PC dimensions for HOO-CV with PCA reduced CVA for the first set of 20 window glass second derivative (9-point smoothing) spectra (10 replicates), autoscaled data.

APPENDIX XII: PCA RESULTS FOR CHEMOMETRIC ANALYSIS OF 153 SODA-LIME SILICATE GLASSES

Table 353: PCA results for the set of 153 glass first derivative (5-point smoothing) spectra (10 replicates), autoscaled.

	PC1	PC2	PC3	PC4	PC5	PC6	PC7	PC8	PC9	PC10	PC11
Standard Deviation	12.4291	7.3856	5.6122	4.7126	3.6697	3.1129	3.1015	2.2741	1.9423	1.3816	1.3057
Proportion of Variance	0.4783	0.1689	0.0975	0.0688	0.0417	0.0300	0.0298	0.0160	0.0117	0.0059	0.0053
Cumulative Proportion	0.4783	0.6472	0.7447	0.8134	0.8551	0.8851	0.9149	0.9309	0.9426	0.9485	0.9538
	PC12	PC13	PC14	PC15	PC16	PC17	PC18	PC19	PC20	PC21	PC22
Standard Deviation	1.2480	0.9172	0.8752	0.8322	0.7612	0.7528	0.7126	0.6850	0.6625	0.6431	0.5900
Proportion of Variance	0.0048	0.0026	0.0024	0.0021	0.0018	0.0018	0.0016	0.0015	0.0014	0.0013	0.0011
Cumulative Proportion	0.9586	0.9612	0.9636	0.9657	0.9675	0.9693	0.9708	0.9723	0.9737	0.9749	0.9760
	PC23	PC24	PC25	PC26	PC27	PC28	PC29	PC30	PC31	PC32	PC33
Standard Deviation	0.5772	0.5581	0.5526	0.5374	0.5228	0.4878	0.4718	0.4617	0.4385	0.4266	0.4185
Proportion of Variance	0.0010	0.0010	0.0010	0.0009	0.0009	0.0007	0.0007	0.0007	0.0006	0.0006	0.0005
Cumulative Proportion	0.9770	0.9780	0.9790	0.9798	0.9807	0.9814	0.9821	0.9828	0.9834	0.9839	0.9845
	PC34	PC35	PC36	PC37	PC38	PC39	PC40	PC41	PC42	PC43	PC44
Standard Deviation	0.4050	0.3985	0.3943	0.3853	0.3793	0.3730	0.3655	0.3614	0.3504	0.3457	0.3398
Proportion of Variance	0.0005	0.0005	0.0005	0.0005	0.0005	0.0004	0.0004	0.0004	0.0004	0.0004	0.0004
Cumulative Proportion	0.9850	0.9855	0.9860	0.9864	0.9869	0.9873	0.9877	0.9881	0.9885	0.9889	0.9892
	PC45	PC46	PC47	PC48	PC49	PC50	PC51	PC52	PC53	PC54	PC55
Standard Deviation	0.3344	0.3302	0.3275	0.3185	0.3121	0.3080	0.3037	0.2976	0.2938	0.2855	0.2785
Proportion of Variance	0.0004	0.0003	0.0003	0.0003	0.0003	0.0003	0.0003	0.0003	0.0003	0.0003	0.0002
Cumulative Proportion	0.9896	0.9899	0.9902	0.9906	0.9909	0.9911	0.9914	0.9917	0.9920	0.9922	0.9925
	PC56	PC57	PC58	PC59	PC60	PC61	PC62	PC63	PC64	PC65	PC66
Standard Deviation	0.2772	0.2703	0.2644	0.2630	0.2604	0.2575	0.2443	0.2427	0.2396	0.2356	0.2323
Proportion of Variance	0.0002	0.0002	0.0002	0.0002	0.0002	0.0002	0.0002	0.0002	0.0002	0.0002	0.0002
Cumulative Proportion	0.9927	0.9929	0.9931	0.9934	0.9936	0.9938	0.9940	0.9941	0.9943	0.9945	0.9947
	PC67	PC68	PC69	PC70	PC71	PC72	PC73	PC74	PC75	PC76	PC77
Standard Deviation	0.2307	0.2249	0.2241	0.2206	0.2116	0.2094	0.2049	0.2024	0.2012	0.1970	0.1919
Proportion of Variance	0.0002	0.0002	0.0002	0.0002	0.0001	0.0001	0.0001	0.0001	0.0001	0.0001	0.0001
Cumulative Proportion	0.9948	0.9950	0.9951	0.9953	0.9954	0.9956	0.9957	0.9958	0.9959	0.9961	0.9962
	PC78	PC79	PC80	PC81	PC82	PC83	PC84	PC85	PC86	PC87	PC88

Standard Deviation	0.1866	0.1856	0.1840	0.1802	0.1791	0.1753	0.1728	0.1712	0.1675	0.1656	0.1647
Proportion of Variance	0.0001	0.0001	0.0001	0.0001	0.0001	0.0001	0.0001	0.0001	0.0001	0.0001	0.0001
Cumulative Proportion	0.9963	0.9964	0.9965	0.9966	0.9967	0.9968	0.9969	0.9970	0.9971	0.9971	0.9972
	PC89	PC90	PC91	PC92	PC93	PC94	PC95	PC96	PC97	PC98	PC99
Standard Deviation	0.1585	0.1574	0.1565	0.1552	0.1515	0.1502	0.1485	0.1446	0.1428	0.1413	0.1377
Proportion of Variance	0.0001	0.0001	0.0001	0.0001	0.0001	0.0001	0.0001	0.0001	0.0001	0.0001	0.0001
Cumulative Proportion	0.9973	0.9974	0.9975	0.9975	0.9976	0.9977	0.9977	0.9978	0.9979	0.9979	0.9980
	PC100	PC101	PC102	PC103	PC104	PC105	PC106	PC107	PC108	PC109	PC110
Standard Deviation	0.1369	0.1358	0.1355	0.1334	0.1317	0.1308	0.1286	0.1260	0.1238	0.1222	0.1219
Proportion of Variance	0.0001	0.0001	0.0001	0.0001	0.0001	0.0001	0.0001	0.0001	0.0001	0.0001	0.0001
Cumulative Proportion	0.9981	0.9981	0.9982	0.9982	0.9983	0.9983	0.9984	0.9984	0.9985	0.9985	0.9986
	PC111	PC112	PC113	PC114	PC115	PC116	PC117	PC118	PC119	PC120	PC121
Standard Deviation	0.1208	0.1162	0.1154	0.1143	0.1125	0.1122	0.1100	0.1094	0.1064	0.1059	0.1049
Proportion of Variance	0.0001	0.0000	0.0000	0.0000	0.0000	0.0000	0.0000	0.0000	0.0000	0.0000	0.0000
Cumulative Proportion	0.9986	0.9987	0.9987	0.9987	0.9988	0.9988	0.9989	0.9989	0.9989	0.9990	0.9990
	PC122	PC123	PC124	PC125	PC126	PC127	PC128	PC129	PC130	PC131	PC132
Standard Deviation	0.1045	0.1016	0.1002	0.0994	0.0979	0.0978	0.0959	0.0935	0.0919	0.0916	0.0904
Proportion of Variance	0.0000	0.0000	0.0000	0.0000	0.0000	0.0000	0.0000	0.0000	0.0000	0.0000	0.0000
Cumulative Proportion	0.9990	0.9991	0.9991	0.9991	0.9992	0.9992	0.9992	0.9992	0.9993	0.9993	0.9993
	PC133	PC134	PC135	PC136	PC137	PC138	PC139	PC140	PC141	PC142	PC143
Standard Deviation	0.0901	0.0898	0.0876	0.0857	0.0854	0.0828	0.0820	0.0808	0.0794	0.0781	0.0773
Proportion of Variance	0.0000	0.0000	0.0000	0.0000	0.0000	0.0000	0.0000	0.0000	0.0000	0.0000	0.0000
Cumulative Proportion	0.9993	0.9994	0.9994	0.9994	0.9994	0.9995	0.9995	0.9995	0.9995	0.9995	0.9996
	PC144	PC145	PC146	PC147	PC148	PC149	PC150	PC151	PC152	PC153	PC154
Standard Deviation	0.0760	0.0740	0.0737	0.0729	0.0695	0.0691	0.0674	0.0670	0.0660	0.0634	0.0608
Proportion of Variance	0.0000	0.0000	0.0000	0.0000	0.0000	0.0000	0.0000	0.0000	0.0000	0.0000	0.0000
Cumulative Proportion	0.9996	0.9996	0.9996	0.9996	0.9996	0.9996	0.9997	0.9997	0.9997	0.9997	0.9997
	PC155	PC156	PC157	PC158	PC159	PC160	PC161	PC162	PC163	PC164	PC165
Standard Deviation	0.0597	0.0593	0.0586	0.0585	0.0563	0.0542	0.0535	0.0518	0.0511	0.0497	0.0477
Proportion of Variance	0.0000	0.0000	0.0000	0.0000	0.0000	0.0000	0.0000	0.0000	0.0000	0.0000	0.0000
Cumulative Proportion	0.9997	0.9997	0.9997	0.9998	0.9998	0.9998	0.9998	0.9998	0.9998	0.9998	0.9998
	PC166	PC167	PC168	PC169	PC170	PC171	PC172	PC173	PC174	PC175	PC176
Standard Deviation	0.0474	0.0468	0.0462	0.0453	0.0442	0.0430	0.0423	0.0407	0.0405	0.0400	0.0387

Proportion of Variance	0.0000	0.0000	0.0000	0.0000	0.0000	0.0000	0.0000	0.0000	0.0000	0.0000	0.0000
Cumulative Proportion	0.9998	0.9998	0.9998	0.9998	0.9998	0.9999	0.9999	0.9999	0.9999	0.9999	0.9999
	PC177	PC178	PC179	PC180	PC181	PC182	PC183	PC184	PC185	PC186	PC187
Standard Deviation	0.0384	0.0381	0.0371	0.0367	0.0365	0.0351	0.0350	0.0347	0.0337	0.0333	0.0322
Proportion of Variance	0.0000	0.0000	0.0000	0.0000	0.0000	0.0000	0.0000	0.0000	0.0000	0.0000	0.0000
Cumulative Proportion	0.9999	0.9999	0.9999	0.9999	0.9999	0.9999	1.0000	0.9999	0.9999	0.9999	0.9999
	PC188	PC189	PC190	PC191	PC192	PC193	PC194	PC195	PC196	PC197	PC198
Standard Deviation	0.0320	0.0317	0.0310	0.0306	0.0297	0.0289	0.0283	0.0276	0.0269	0.0268	0.0258
Proportion of Variance	0.0000	0.0000	0.0000	0.0000	0.0000	0.0000	0.0000	0.0000	0.0000	0.0000	0.0000
Cumulative Proportion	0.9999	0.9999	0.9999	0.9999	0.9999	0.9999	0.9999	0.9999	0.9999	1.0000	1.0000
	PC199	PC200	PC201	PC202	PC203	PC204	PC205	PC206	PC207	PC208	PC209
Standard Deviation	0.0256	0.0248	0.0245	0.0238	0.0231	0.0228	0.0225	0.0223	0.0217	0.0206	0.0203
Proportion of Variance	0.0000	0.0000	0.0000	0.0000	0.0000	0.0000	0.0000	0.0000	0.0000	0.0000	0.0000
Cumulative Proportion	1.0000	1.0000	1.0000	1.0000	1.0000	1.0000	1.0000	1.0000	1.0000	1.0000	1.0000
	PC210	PC211	PC212	PC213	PC214	PC215	PC216	PC217	PC218	PC219	PC220
Standard Deviation	0.0199	0.0195	0.0189	0.0182	0.0181	0.0177	0.0173	0.0172	0.0170	0.0164	0.0162
Proportion of Variance	0.0000	0.0000	0.0000	0.0000	0.0000	0.0000	0.0000	0.0000	0.0000	0.0000	0.0000
Cumulative Proportion	1.0000	1.0000	1.0000	1.0000	1.0000	1.0000	1.0000	1.0000	1.0000	1.0000	1.0000
	PC221	PC222	PC223	PC224	PC225	PC226	PC227	PC228	PC229	PC230	PC231
Standard Deviation	0.0159	0.0157	0.0155	0.0154	0.0153	0.0149	0.0147	0.0145	0.0143	0.0142	0.0141
Proportion of Variance	0.0000	0.0000	0.0000	0.0000	0.0000	0.0000	0.0000	0.0000	0.0000	0.0000	0.0000
Cumulative Proportion	1.0000	1.0000	1.0000	1.0000	1.0000	1.0000	1.0000	1.0000	1.0000	1.0000	1.0000
	PC232	PC233	PC234	PC235	PC236	PC237	PC238	PC239	PC240	PC241	PC242
Standard Deviation	0.0139	0.0135	0.0131	0.0129	0.0128	0.0127	0.0124	0.0123	0.0122	0.0120	0.0117
Proportion of Variance	0.0000	0.0000	0.0000	0.0000	0.0000	0.0000	0.0000	0.0000	0.0000	0.0000	0.0000
Cumulative Proportion	1.0000	1.0000	1.0000	1.0000	1.0000	1.0000	1.0000	1.0000	1.0000	1.0000	1.0000
	PC243	PC244	PC245	PC246	PC247	PC248	PC249	PC250	PC251	PC252	PC253
Standard Deviation	0.0116	0.0115	0.0111	0.0111	0.0109	0.0106	0.0105	0.0104	0.0103	0.0100	0.0098
Proportion of Variance	0.0000	0.0000	0.0000	0.0000	0.0000	0.0000	0.0000	0.0000	0.0000	0.0000	0.0000
Cumulative Proportion	1.0000	1.0000	1.0000	1.0000	1.0000	1.0000	1.0000	1.0000	1.0000	1.0000	1.0000
	PC254	PC255	PC256	PC257	PC258	PC259	PC260	PC261	PC262	PC263	
Standard Deviation	0.0097	0.0095	0.0093	0.0091	0.0091	0.0089	0.0088	0.0086	0.0085	0.0083	
Proportion of Variance	0.0000	0.0000	0.0000	0.0000	0.0000	0.0000	0.0000	0.0000	0.0000	0.0000	

Cumulative Proportion	1.0000	1.0000	1.0000	1.0000	1.0000	1.0000	1.0000	1.0000	1.0000	1.0000	
	PC264	PC265	PC266	PC267	PC268	PC269	PC270	PC271	PC272	PC273	
Standard Deviation	0.0082	0.0081	0.0079	0.0075	0.0074	0.0073	0.0071	0.0069	0.0068	0.0067	
Proportion of Variance	0.0000	0.0000	0.0000	0.0000	0.0000	0.0000	0.0000	0.0000	0.0000	0.0000	
Cumulative Proportion	1.0000	1.0000	1.0000	1.0000	1.0000	1.0000	1.0000	1.0000	1.0000	1.0000	
	PC274	PC275	PC276	PC277	PC278	PC279	PC280	PC281	PC282	PC283	
Standard Deviation	0.0065	0.0064	0.0061	0.0060	0.0059	0.0058	0.0056	0.0054	0.0053	0.0051	
Proportion of Variance	0.0000	0.0000	0.0000	0.0000	0.0000	0.0000	0.0000	0.0000	0.0000	0.0000	
Cumulative Proportion	1.0000	1.0000	1.0000	1.0000	1.0000	1.0000	1.0000	1.0000	1.0000	1.0000	
	PC284	PC285	PC286	PC287	PC288	PC289	PC290	PC291	PC292	PC293	
Standard Deviation	0.0048	0.0047	0.0046	0.0045	0.0043	0.0043	0.0041	0.0040	0.0039	0.0039	
Proportion of Variance	0.0000	0.0000	0.0000	0.0000	0.0000	0.0000	0.0000	0.0000	0.0000	0.0000	
Cumulative Proportion	1.0000	1.0000	1.0000	1.0000	1.0000	1.0000	1.0000	1.0000	1.0000	1.0000	
	PC294	PC295	PC296	PC297	PC298	PC299	PC300	PC301	PC302		
Standard Deviation	0.0037	0.0036	0.0034	0.0033	0.0030	0.0026	0.0026	0.0025	0.0023		
Proportion of Variance	0.0000	0.0000	0.0000	0.0000	0.0000	0.0000	0.0000	0.0000	0.0000		
Cumulative Proportion	1.0000	1.0000	1.0000	1.0000	1.0000	1.0000	1.0000	1.0000	1.0000		
	PC303	PC304	PC305	PC306	PC307	PC308	PC309	PC310	PC311		
Standard Deviation	0.0022	0.0022	0.0019	0.0014	0.0009	0.0007	0.0005	0.0004	0.0003		
Proportion of Variance	0.0000	0.0000	0.0000	0.0000	0.0000	0.0000	0.0000	0.0000	0.0000		
Cumulative Proportion	1.0000	1.0000	1.0000	1.0000	1.0000	1.0000	1.0000	1.0000	1.0000		
	PC312	PC313	PC314	PC315	PC316	PC317	PC318	PC319			
Standard Deviation	0.0003	0.0003	0.0003	0.0002	0.0002	0.0002	0.0002	0.0001			
Proportion of Variance	0.0000	0.0000	0.0000	0.0000	0.0000	0.0000	0.0000	0.0000			
Cumulative Proportion	1.0000	1.0000	1.0000	1.0000	1.0000	1.0000	1.0000	1.0000			
	PC320	PC321	PC322	PC323							
Standard Deviation	0.0001	0.0001	0.0001	0.0000							
Proportion of Variance	0.0000	0.0000	0.0000	0.0000							
Cumulative Proportion	1.0000	1.0000	1.0000	1.0000							

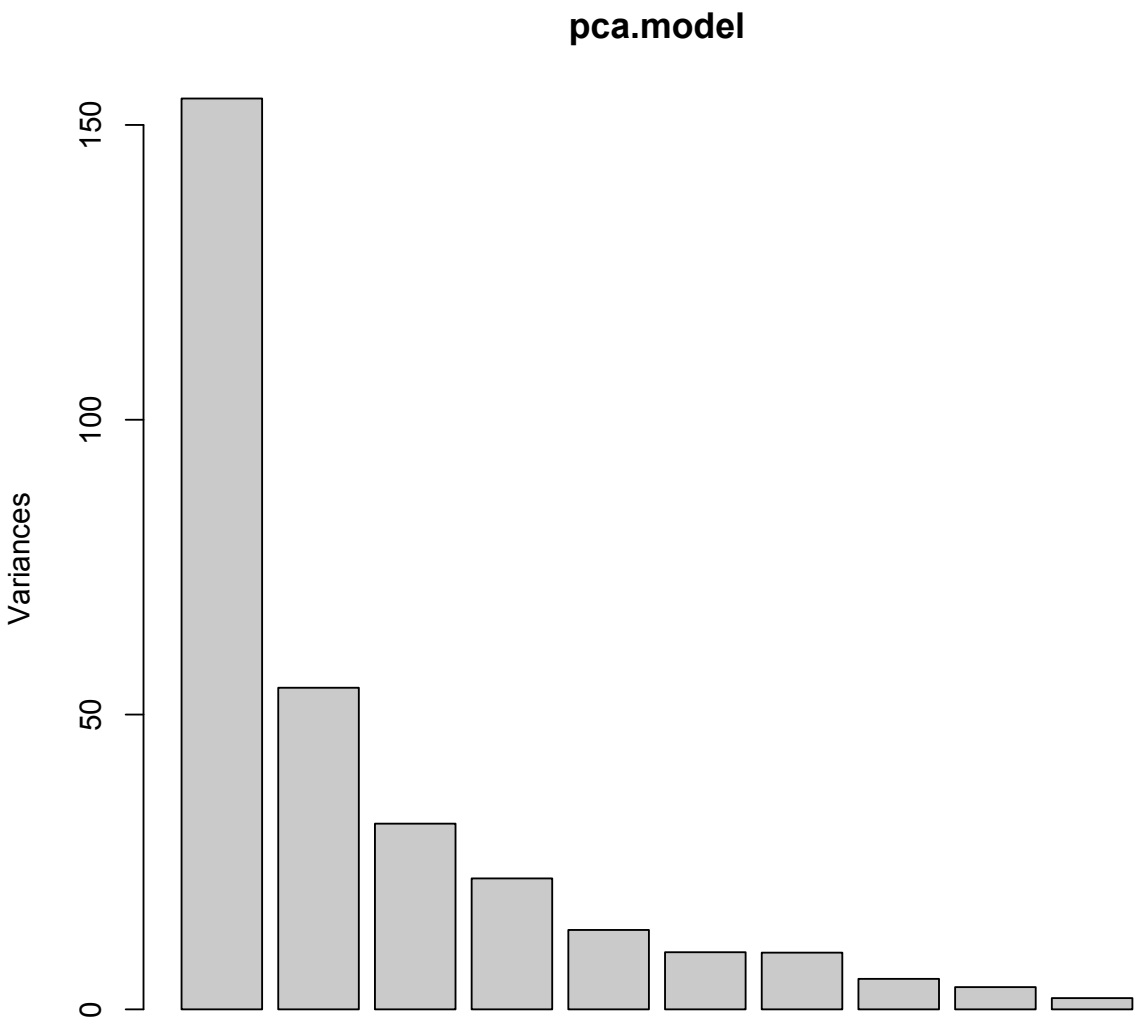


Figure 342: PCA scree plot for the set of 153 glass first derivative (5-point smoothing) spectra (10 replicates), autoscaled.

Table 354: PCA results for the set of 103 window glass first derivative (5-point smoothing) spectra (10 replicates), autoscaled.

	PC1	PC2	PC3	PC4	PC5	PC6	PC7	PC8	PC9	PC10	PC11
Standard Deviation	12.4910	8.0737	5.1968	4.3824	3.5581	3.1210	2.5247	2.4881	1.8793	1.2882	1.1677
Proportion of Variance	0.4830	0.2018	0.0836	0.0595	0.0392	0.0302	0.0197	0.0192	0.0109	0.0051	0.0042
Cumulative Proportion	0.4830	0.6848	0.7685	0.8279	0.8671	0.8973	0.9170	0.9362	0.9471	0.9522	0.9565
	PC12	PC13	PC14	PC15	PC16	PC17	PC18	PC19	PC20	PC21	PC22
Standard Deviation	1.1589	0.9714	0.9350	0.8616	0.7698	0.7229	0.6898	0.6825	0.6112	0.5856	0.5730
Proportion of Variance	0.0042	0.0029	0.0027	0.0023	0.0018	0.0016	0.0015	0.0014	0.0012	0.0011	0.0010
Cumulative Proportion	0.9606	0.9635	0.9663	0.9686	0.9704	0.9720	0.9735	0.9749	0.9761	0.9771	0.9782
	PC23	PC24	PC25	PC26	PC27	PC28	PC29	PC30	PC31	PC32	PC33
Standard Deviation	0.5604	0.5365	0.5316	0.4942	0.4827	0.4763	0.4731	0.4561	0.4356	0.4224	0.4161
Proportion of Variance	0.0010	0.0009	0.0009	0.0008	0.0007	0.0007	0.0007	0.0006	0.0006	0.0006	0.0005
Cumulative Proportion	0.9791	0.9800	0.9809	0.9816	0.9824	0.9831	0.9838	0.9844	0.9850	0.9855	0.9861
	PC34	PC35	PC36	PC37	PC38	PC39	PC40	PC41	PC42	PC43	PC44
Standard Deviation	0.4053	0.3968	0.3870	0.3793	0.3758	0.3669	0.3590	0.3581	0.3501	0.3495	0.3415
Proportion of Variance	0.0005	0.0005	0.0005	0.0005	0.0004	0.0004	0.0004	0.0004	0.0004	0.0004	0.0004
Cumulative Proportion	0.9866	0.9871	0.9875	0.9880	0.9884	0.9888	0.9892	0.9896	0.9900	0.9904	0.9908
	PC45	PC46	PC47	PC48	PC49	PC50	PC51	PC52	PC53	PC54	PC55
Standard Deviation	0.3353	0.3198	0.3136	0.3034	0.2992	0.2916	0.2889	0.2816	0.2785	0.2694	0.2662
Proportion of Variance	0.0004	0.0003	0.0003	0.0003	0.0003	0.0003	0.0003	0.0003	0.0002	0.0002	0.0002
Cumulative Proportion	0.9911	0.9914	0.9917	0.9920	0.9923	0.9926	0.9928	0.9931	0.9933	0.9935	0.9937
	PC56	PC57	PC58	PC59	PC60	PC61	PC62	PC63	PC64	PC65	PC66
Standard Deviation	0.2637	0.2554	0.2529	0.2488	0.2442	0.2393	0.2359	0.2337	0.2312	0.2230	0.2206
Proportion of Variance	0.0002	0.0002	0.0002	0.0002	0.0002	0.0002	0.0002	0.0002	0.0002	0.0002	0.0002
Cumulative Proportion	0.9940	0.9941	0.9943	0.9945	0.9947	0.9949	0.9951	0.9953	0.9954	0.9956	0.9957
	PC67	PC68	PC69	PC70	PC71	PC72	PC73	PC74	PC75	PC76	PC77
Standard Deviation	0.2159	0.2109	0.2043	0.2007	0.1992	0.1949	0.1917	0.1894	0.1842	0.1798	0.1778
Proportion of Variance	0.0001	0.0001	0.0001	0.0001	0.0001	0.0001	0.0001	0.0001	0.0001	0.0001	0.0001
Cumulative Proportion	0.9959	0.9960	0.9961	0.9963	0.9964	0.9965	0.9966	0.9967	0.9968	0.9969	0.9970
	PC78	PC79	PC80	PC81	PC82	PC83	PC84	PC85	PC86	PC87	PC88
Standard Deviation	0.1748	0.1746	0.1708	0.1674	0.1661	0.1639	0.1596	0.1563	0.1534	0.1498	0.1483
Proportion of Variance	0.0001	0.0001	0.0001	0.0001	0.0001	0.0001	0.0001	0.0001	0.0001	0.0001	0.0001
Cumulative Proportion	0.9971	0.9972	0.9973	0.9974	0.9975	0.9976	0.9976	0.9977	0.9978	0.9979	0.9979

	PC89	PC90	PC91	PC92	PC93	PC94	PC95	PC96	PC97	PC98	PC99
Standard Deviation	0.1474	0.1432	0.1422	0.1391	0.1378	0.1364	0.1336	0.1297	0.1289	0.1264	0.1234
Proportion of Variance	0.0001	0.0001	0.0001	0.0001	0.0001	0.0001	0.0001	0.0001	0.0001	0.0001	0.0001
Cumulative Proportion	0.9980	0.9981	0.9981	0.9982	0.9982	0.9983	0.9984	0.9984	0.9985	0.9985	0.9986
	PC100	PC101	PC102	PC103	PC104	PC105	PC106	PC107	PC108	PC109	PC110
Standard Deviation	0.1224	0.1206	0.1195	0.1167	0.1158	0.1130	0.1123	0.1116	0.1102	0.1072	0.1061
Proportion of Variance	0.0001	0.0001	0.0000	0.0000	0.0000	0.0000	0.0000	0.0000	0.0000	0.0000	0.0000
Cumulative Proportion	0.9986	0.9986	0.9987	0.9987	0.9988	0.9988	0.9988	0.9989	0.9989	0.9990	0.9990
	PC111	PC112	PC113	PC114	PC115	PC116	PC117	PC118	PC119	PC120	PC121
Standard Deviation	0.1054	0.1025	0.1016	0.1005	0.0983	0.0968	0.0953	0.0940	0.0920	0.0904	0.0896
Proportion of Variance	0.0000	0.0000	0.0000	0.0000	0.0000	0.0000	0.0000	0.0000	0.0000	0.0000	0.0000
Cumulative Proportion	0.9990	0.9991	0.9991	0.9991	0.9992	0.9992	0.9992	0.9992	0.9993	0.9993	0.9993
	PC122	PC123	PC124	PC125	PC126	PC127	PC128	PC129	PC130	PC131	PC132
Standard Deviation	0.0886	0.0869	0.0848	0.0843	0.0836	0.0819	0.0805	0.0800	0.0788	0.0783	0.0765
Proportion of Variance	0.0000	0.0000	0.0000	0.0000	0.0000	0.0000	0.0000	0.0000	0.0000	0.0000	0.0000
Cumulative Proportion	0.9993	0.9994	0.9994	0.9994	0.9994	0.9995	0.9995	0.9995	0.9995	0.9995	0.9995
	PC133	PC134	PC135	PC136	PC137	PC138	PC139	PC140	PC141	PC142	PC143
Standard Deviation	0.0751	0.0736	0.0724	0.0714	0.0697	0.0687	0.0681	0.0662	0.0646	0.0627	0.0622
Proportion of Variance	0.0000	0.0000	0.0000	0.0000	0.0000	0.0000	0.0000	0.0000	0.0000	0.0000	0.0000
Cumulative Proportion	0.9996	0.9996	0.9996	0.9996	0.9996	0.9996	0.9997	0.9997	0.9997	0.9997	0.9997
	PC144	PC145	PC146	PC147	PC148	PC149	PC150	PC151	PC152	PC153	PC154
Standard Deviation	0.0620	0.0605	0.0598	0.0577	0.0559	0.0553	0.0542	0.0537	0.0528	0.0516	0.0514
Proportion of Variance	0.0000	0.0000	0.0000	0.0000	0.0000	0.0000	0.0000	0.0000	0.0000	0.0000	0.0000
Cumulative Proportion	0.9997	0.9997	0.9997	0.9998	0.9998	0.9998	0.9998	0.9998	0.9998	0.9998	0.9998
	PC155	PC156	PC157	PC158	PC159	PC160	PC161	PC162	PC163	PC164	PC165
Standard Deviation	0.0493	0.0483	0.0472	0.0461	0.0456	0.0445	0.0441	0.0419	0.0415	0.0409	0.0407
Proportion of Variance	0.0000	0.0000	0.0000	0.0000	0.0000	0.0000	0.0000	0.0000	0.0000	0.0000	0.0000
Cumulative Proportion	0.9998	0.9998	0.9998	0.9998	0.9998	0.9999	0.9999	0.9999	0.9999	0.9999	0.9999
	PC166	PC167	PC168	PC169	PC170	PC171	PC172	PC173	PC174	PC175	PC176
Standard Deviation	0.0397	0.0389	0.0387	0.0374	0.0370	0.0357	0.0351	0.0346	0.0340	0.0335	0.0322
Proportion of Variance	0.0000	0.0000	0.0000	0.0000	0.0000	0.0000	0.0000	0.0000	0.0000	0.0000	0.0000
Cumulative Proportion	0.9999	0.9999	0.9999	0.9999	0.9999	0.9999	0.9999	0.9999	0.9999	0.9999	0.9999
	PC177	PC178	PC179	PC180	PC181	PC182	PC183	PC184	PC185	PC186	PC187
Standard Deviation	0.0318	0.0315	0.0312	0.0306	0.0300	0.0298	0.0288	0.0281	0.0276	0.0272	0.0266

Proportion of Variance	0.0000	0.0000	0.0000	0.0000	0.0000	0.0000	0.0000	0.0000	0.0000	0.0000	0.0000
Cumulative Proportion	0.9999	0.9999	0.9999	0.9999	0.9999	0.9999	0.9999	0.9999	1.0000	1.0000	1.0000
	PC188	PC189	PC190	PC191	PC192	PC193	PC194	PC195	PC196	PC197	PC198
Standard Deviation	0.0261	0.0255	0.0246	0.0235	0.0227	0.0224	0.0222	0.0217	0.0214	0.0211	0.0205
Proportion of Variance	0.0000	0.0000	0.0000	0.0000	0.0000	0.0000	0.0000	0.0000	0.0000	0.0000	0.0000
Cumulative Proportion	1.0000	1.0000	1.0000	1.0000	1.0000	1.0000	1.0000	1.0000	1.0000	1.0000	1.0000
	PC199	PC200	PC201	PC202	PC203	PC204	PC205	PC206	PC207	PC208	PC209
Standard Deviation	0.0203	0.0198	0.0193	0.0190	0.0189	0.0185	0.0179	0.0173	0.0170	0.0164	0.0162
Proportion of Variance	0.0000	0.0000	0.0000	0.0000	0.0000	0.0000	0.0000	0.0000	0.0000	0.0000	0.0000
Cumulative Proportion	1.0000	1.0000	1.0000	1.0000	1.0000	1.0000	1.0000	1.0000	1.0000	1.0000	1.0000
	PC210	PC211	PC212	PC213	PC214	PC215	PC216	PC217	PC218	PC219	PC220
Standard Deviation	0.0158	0.0155	0.0154	0.0149	0.0143	0.0141	0.0140	0.0137	0.0136	0.0131	0.0130
Proportion of Variance	0.0000	0.0000	0.0000	0.0000	0.0000	0.0000	0.0000	0.0000	0.0000	0.0000	0.0000
Cumulative Proportion	1.0000	1.0000	1.0000	1.0000	1.0000	1.0000	1.0000	1.0000	1.0000	1.0000	1.0000
	PC221	PC222	PC223	PC224	PC225	PC226	PC227	PC228	PC229	PC230	PC231
Standard Deviation	0.0129	0.0126	0.0123	0.0123	0.0119	0.0116	0.0115	0.0112	0.0110	0.0108	0.0105
Proportion of Variance	0.0000	0.0000	0.0000	0.0000	0.0000	0.0000	0.0000	0.0000	0.0000	0.0000	0.0000
Cumulative Proportion	1.0000	1.0000	1.0000	1.0000	1.0000	1.0000	1.0000	1.0000	1.0000	1.0000	1.0000
	PC232	PC233	PC234	PC235	PC236	PC237	PC238	PC239	PC240	PC241	
Standard Deviation	0.0105	0.0102	0.0100	0.0097	0.0096	0.0095	0.0094	0.0093	0.0090	0.0089	
Proportion of Variance	0.0000	0.0000	0.0000	0.0000	0.0000	0.0000	0.0000	0.0000	0.0000	0.0000	
Cumulative Proportion	1.0000	1.0000	1.0000	1.0000	1.0000	1.0000	1.0000	1.0000	1.0000	1.0000	
	PC242	PC243	PC244	PC245	PC246	PC247	PC248	PC249	PC250	PC251	
Standard Deviation	0.0087	0.0085	0.0083	0.0082	0.0080	0.0079	0.0077	0.0077	0.0075	0.0072	
Proportion of Variance	0.0000	0.0000	0.0000	0.0000	0.0000	0.0000	0.0000	0.0000	0.0000	0.0000	
Cumulative Proportion	1.0000	1.0000	1.0000	1.0000	1.0000	1.0000	1.0000	1.0000	1.0000	1.0000	
	PC252	PC253	PC254	PC255	PC256	PC257	PC258	PC259	PC260		
Standard Deviation	0.0072	0.0069	0.0067	0.0066	0.0066	0.0066	0.0064	0.0063	0.0061		
Proportion of Variance	0.0000	0.0000	0.0000	0.0000	0.0000	0.0000	0.0000	0.0000	0.0000		
Cumulative Proportion	1.0000	1.0000	1.0000	1.0000	1.0000	1.0000	1.0000	1.0000	1.0000		
	PC261	PC262	PC263	PC264	PC265	PC266	PC267	PC268	PC269		
Standard Deviation	0.0060	0.0059	0.0058	0.0056	0.0055	0.0054	0.0053	0.0052	0.0050		
Proportion of Variance	0.0000	0.0000	0.0000	0.0000	0.0000	0.0000	0.0000	0.0000	0.0000		

Cumulative Proportion	1.0000	1.0000	1.0000	1.0000	1.0000	1.0000	1.0000	1.0000	1.0000		
	PC270	PC271	PC272	PC273	PC274	PC275	PC276	PC277	PC278	PC279	
Standard Deviation	0.0049	0.0047	0.0047	0.0045	0.0044	0.0043	0.0042	0.0041	0.0039	0.0038	
Proportion of Variance	0.0000	0.0000	0.0000	0.0000	0.0000	0.0000	0.0000	0.0000	0.0000	0.0000	
Cumulative Proportion	1.0000	1.0000	1.0000	1.0000	1.0000	1.0000	1.0000	1.0000	1.0000	1.0000	
	PC280	PC281	PC282	PC283	PC284	PC285	PC286	PC287	PC288		
Standard Deviation	0.0036	0.0036	0.0034	0.0033	0.0033	0.0032	0.0030	0.0030	0.0028		
Proportion of Variance	0.0000	0.0000	0.0000	0.0000	0.0000	0.0000	0.0000	0.0000	0.0000		
Cumulative Proportion	1.0000	1.0000	1.0000	1.0000	1.0000	1.0000	1.0000	1.0000	1.0000		
	PC289	PC290	PC291	PC292	PC293	PC294	PC295	PC296	PC297		
Standard Deviation	0.0028	0.0028	0.0027	0.0025	0.0025	0.0023	0.0022	0.0021	0.0020		
Proportion of Variance	0.0000	0.0000	0.0000	0.0000	0.0000	0.0000	0.0000	0.0000	0.0000		
Cumulative Proportion	1.0000	1.0000	1.0000	1.0000	1.0000	1.0000	1.0000	1.0000	1.0000		
	PC298	PC299	PC300	PC301	PC302	PC303	PC304	PC305	PC306		
Standard Deviation	0.0018	0.0018	0.0016	0.0015	0.0014	0.0014	0.0013	0.0010	0.0008		
Proportion of Variance	0.0000	0.0000	0.0000	0.0000	0.0000	0.0000	0.0000	0.0000	0.0000		
Cumulative Proportion	1.0000	1.0000	1.0000	1.0000	1.0000	1.0000	1.0000	1.0000	1.0000		
	PC307	PC308	PC309	PC310	PC311	PC312	PC313	PC314	PC315		
Standard Deviation	0.0006	0.0004	0.0003	0.0003	0.0002	0.0002	0.0002	0.0002	0.0001		
Proportion of Variance	0.0000	0.0000	0.0000	0.0000	0.0000	0.0000	0.0000	0.0000	0.0000		
Cumulative Proportion	1.0000	1.0000	1.0000	1.0000	1.0000	1.0000	1.0000	1.0000	1.0000		
	PC316	PC317	PC318	PC319	PC320	PC321	PC322	PC323			
Standard Deviation	0.0001	0.0001	0.0001	0.0001	0.0001	0.0001	0.0001	0.0000			
Proportion of Variance	0.0000	0.0000	0.0000	0.0000	0.0000	0.0000	0.0000	0.0000			
Cumulative Proportion	1.0000	1.0000	1.0000	1.0000	1.0000	1.0000	1.0000	1.0000			

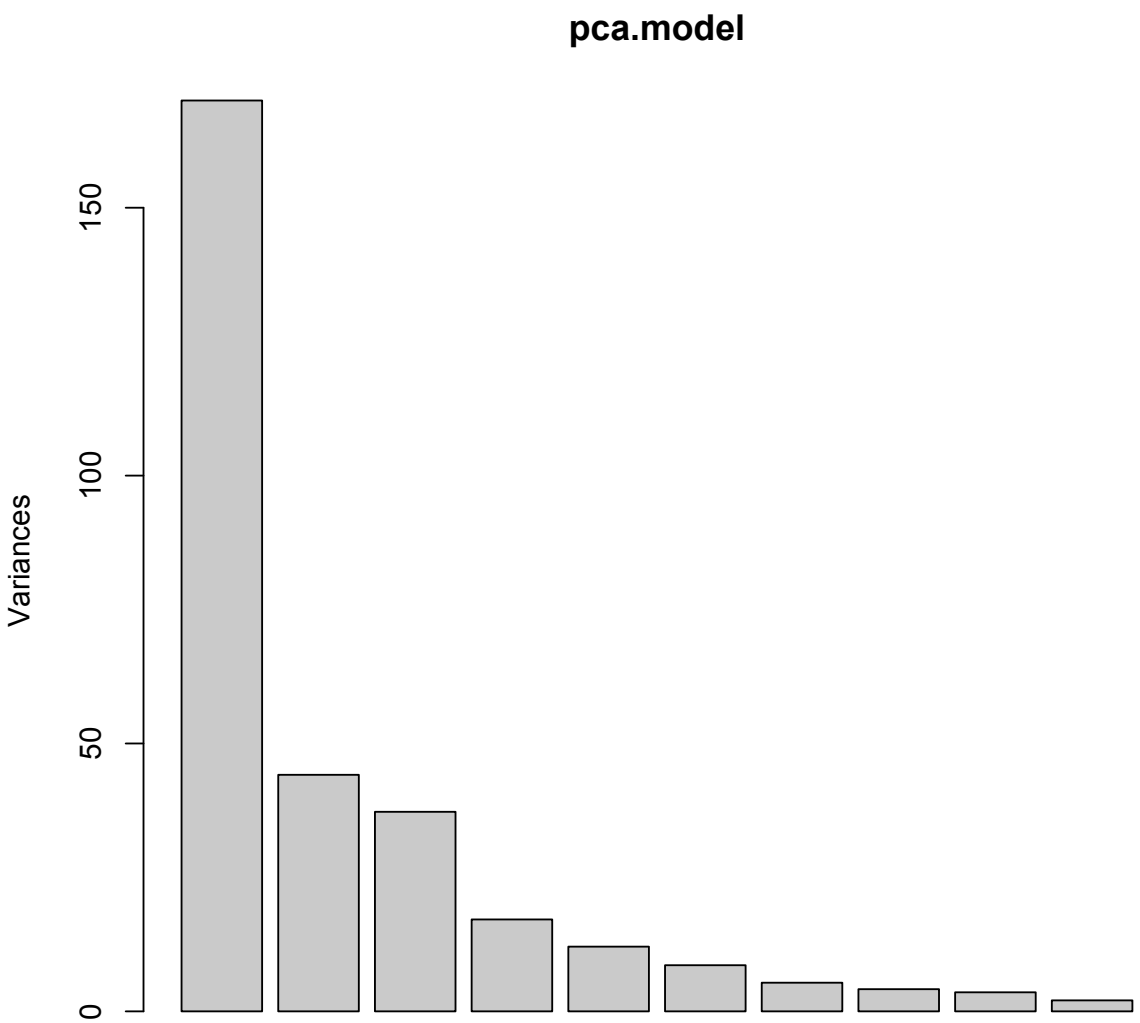


Figure 343: PCA scree plot for the set of 103 window glass first derivative (5-point smoothing) spectra (10 replicates), autoscaled.

Table 355: PCA results for the set of 50 container glass first derivative (5-point smoothing) spectra (10 replicates), autoscaled.

	PC1	PC2	PC3	PC4	PC5	PC6	PC7	PC8	PC9	PC10	PC11
Standard Deviation	13.0388	6.6446	6.1030	4.1417	3.4755	2.9345	2.3125	2.0347	1.8858	1.4316	1.3759
Proportion of Variance	0.5263	0.1367	0.1153	0.0531	0.0374	0.0267	0.0166	0.0128	0.0110	0.0064	0.0059
Cumulative Proportion	0.5263	0.6630	0.7783	0.8315	0.8689	0.8955	0.9121	0.9249	0.9359	0.9423	0.9481
	PC12	PC13	PC14	PC15	PC16	PC17	PC18	PC19	PC20	PC21	PC22
Standard Deviation	1.2647	0.9370	0.9101	0.8992	0.8428	0.7961	0.7894	0.7376	0.7171	0.6826	0.6502
Proportion of Variance	0.0050	0.0027	0.0026	0.0025	0.0022	0.0020	0.0019	0.0017	0.0016	0.0014	0.0013
Cumulative Proportion	0.9531	0.9558	0.9583	0.9608	0.9630	0.9650	0.9669	0.9686	0.9702	0.9717	0.9730
	PC23	PC24	PC25	PC26	PC27	PC28	PC29	PC30	PC31	PC32	PC33
Standard Deviation	0.6192	0.6037	0.5789	0.5719	0.5448	0.5307	0.4955	0.4861	0.4770	0.4555	0.4452
Proportion of Variance	0.0012	0.0011	0.0010	0.0010	0.0009	0.0009	0.0008	0.0007	0.0007	0.0006	0.0006
Cumulative Proportion	0.9742	0.9753	0.9763	0.9773	0.9783	0.9791	0.9799	0.9806	0.9813	0.9820	0.9826
	PC34	PC35	PC36	PC37	PC38	PC39	PC40	PC41	PC42	PC43	PC44
Standard Deviation	0.4368	0.4336	0.4156	0.4062	0.4035	0.3978	0.3919	0.3868	0.3823	0.3724	0.3666
Proportion of Variance	0.0006	0.0006	0.0005	0.0005	0.0005	0.0005	0.0005	0.0005	0.0005	0.0004	0.0004
Cumulative Proportion	0.9832	0.9838	0.9843	0.9848	0.9853	0.9858	0.9863	0.9867	0.9872	0.9876	0.9880
	PC45	PC46	PC47	PC48	PC49	PC50	PC51	PC52	PC53	PC54	PC55
Standard Deviation	0.3638	0.3509	0.3494	0.3371	0.3262	0.3217	0.3200	0.3112	0.3064	0.3051	0.2931
Proportion of Variance	0.0004	0.0004	0.0004	0.0004	0.0003	0.0003	0.0003	0.0003	0.0003	0.0003	0.0003
Cumulative Proportion	0.9884	0.9888	0.9892	0.9895	0.9899	0.9902	0.9905	0.9908	0.9911	0.9914	0.9917
	PC56	PC57	PC58	PC59	PC60	PC61	PC62	PC63	PC64	PC65	PC66
Standard Deviation	0.2892	0.2822	0.2742	0.2735	0.2648	0.2619	0.2584	0.2558	0.2501	0.2488	0.2446
Proportion of Variance	0.0003	0.0003	0.0002	0.0002	0.0002	0.0002	0.0002	0.0002	0.0002	0.0002	0.0002
Cumulative Proportion	0.9919	0.9922	0.9924	0.9926	0.9928	0.9931	0.9933	0.9935	0.9937	0.9939	0.9940
	PC67	PC68	PC69	PC70	PC71	PC72	PC73	PC74	PC75	PC76	PC77
Standard Deviation	0.2356	0.2323	0.2288	0.2275	0.2235	0.2199	0.2131	0.2127	0.2114	0.2050	0.2033
Proportion of Variance	0.0002	0.0002	0.0002	0.0002	0.0002	0.0002	0.0001	0.0001	0.0001	0.0001	0.0001
Cumulative Proportion	0.9942	0.9944	0.9945	0.9947	0.9949	0.9950	0.9951	0.9953	0.9954	0.9956	0.9957
	PC78	PC79	PC80	PC81	PC82	PC83	PC84	PC85	PC86	PC87	PC88
Standard Deviation	0.1986	0.1962	0.1927	0.1903	0.1893	0.1871	0.1845	0.1815	0.1810	0.1783	0.1753
Proportion of Variance	0.0001	0.0001	0.0001	0.0001	0.0001	0.0001	0.0001	0.0001	0.0001	0.0001	0.0001
Cumulative Proportion	0.9958	0.9959	0.9960	0.9962	0.9963	0.9964	0.9965	0.9966	0.9967	0.9968	0.9969

	PC89	PC90	PC91	PC92	PC93	PC94	PC95	PC96	PC97	PC98	PC99
Standard Deviation	0.1713	0.1695	0.1684	0.1671	0.1642	0.1619	0.1588	0.1577	0.1548	0.1520	0.1496
Proportion of Variance	0.0001	0.0001	0.0001	0.0001	0.0001	0.0001	0.0001	0.0001	0.0001	0.0001	0.0001
Cumulative Proportion	0.9970	0.9971	0.9971	0.9972	0.9973	0.9974	0.9975	0.9975	0.9976	0.9977	0.9978
	PC100	PC101	PC102	PC103	PC104	PC105	PC106	PC107	PC108	PC109	PC110
Standard Deviation	0.1474	0.1455	0.1447	0.1413	0.1391	0.1361	0.1353	0.1331	0.1318	0.1303	0.1289
Proportion of Variance	0.0001	0.0001	0.0001	0.0001	0.0001	0.0001	0.0001	0.0001	0.0001	0.0001	0.0001
Cumulative Proportion	0.9978	0.9979	0.9980	0.9980	0.9981	0.9981	0.9982	0.9982	0.9983	0.9984	0.9984
	PC111	PC112	PC113	PC114	PC115	PC116	PC117	PC118	PC119	PC120	PC121
Standard Deviation	0.1286	0.1258	0.1252	0.1220	0.1203	0.1168	0.1150	0.1140	0.1123	0.1120	0.1102
Proportion of Variance	0.0001	0.0001	0.0001	0.0001	0.0000	0.0000	0.0000	0.0000	0.0000	0.0000	0.0000
Cumulative Proportion	0.9985	0.9985	0.9986	0.9986	0.9986	0.9987	0.9987	0.9988	0.9988	0.9988	0.9989
	PC122	PC123	PC124	PC125	PC126	PC127	PC128	PC129	PC130	PC131	PC132
Standard Deviation	0.1099	0.1092	0.1072	0.1051	0.1047	0.1042	0.1018	0.1003	0.0983	0.0979	0.0954
Proportion of Variance	0.0000	0.0000	0.0000	0.0000	0.0000	0.0000	0.0000	0.0000	0.0000	0.0000	0.0000
Cumulative Proportion	0.9989	0.9990	0.9990	0.9990	0.9991	0.9991	0.9991	0.9992	0.9992	0.9992	0.9992
	PC133	PC134	PC135	PC136	PC137	PC138	PC139	PC140	PC141	PC142	PC143
Standard Deviation	0.0952	0.0938	0.0928	0.0904	0.0894	0.0883	0.0869	0.0861	0.0829	0.0816	0.0799
Proportion of Variance	0.0000	0.0000	0.0000	0.0000	0.0000	0.0000	0.0000	0.0000	0.0000	0.0000	0.0000
Cumulative Proportion	0.9993	0.9993	0.9993	0.9994	0.9994	0.9994	0.9994	0.9995	0.9995	0.9995	0.9995
	PC144	PC145	PC146	PC147	PC148	PC149	PC150	PC151	PC152	PC153	PC154
Standard Deviation	0.0796	0.0786	0.0759	0.0746	0.0735	0.0731	0.0723	0.0677	0.0670	0.0656	0.0639
Proportion of Variance	0.0000	0.0000	0.0000	0.0000	0.0000	0.0000	0.0000	0.0000	0.0000	0.0000	0.0000
Cumulative Proportion	0.9995	0.9996	0.9996	0.9996	0.9996	0.9996	0.9996	0.9996	0.9997	0.9997	0.9997
	PC155	PC156	PC157	PC158	PC159	PC160	PC161	PC162	PC163	PC164	PC165
Standard Deviation	0.0618	0.0611	0.0604	0.0592	0.0577	0.0566	0.0554	0.0542	0.0536	0.0524	0.0521
Proportion of Variance	0.0000	0.0000	0.0000	0.0000	0.0000	0.0000	0.0000	0.0000	0.0000	0.0000	0.0000
Cumulative Proportion	0.9997	0.9997	0.9997	0.9997	0.9997	0.9998	0.9998	0.9998	0.9998	0.9998	0.9998
	PC166	PC167	PC168	PC169	PC170	PC171	PC172	PC173	PC174	PC175	PC176
Standard Deviation	0.0505	0.0501	0.0490	0.0473	0.0468	0.0450	0.0443	0.0432	0.0419	0.0405	0.0404
Proportion of Variance	0.0000	0.0000	0.0000	0.0000	0.0000	0.0000	0.0000	0.0000	0.0000	0.0000	0.0000
Cumulative Proportion	0.9998	0.9998	0.9998	0.9998	0.9998	0.9998	0.9998	0.9999	0.9999	0.9999	0.9999
	PC177	PC178	PC179	PC180	PC181	PC182	PC183	PC184	PC185	PC186	PC187
Standard Deviation	0.0400	0.0398	0.0390	0.0383	0.0375	0.0372	0.0369	0.0363	0.0357	0.0348	0.0345

Proportion of Variance	0.0000	0.0000	0.0000	0.0000	0.0000	0.0000	0.0000	0.0000	0.0000	0.0000	0.0000
Cumulative Proportion	0.9999	0.9999	0.9999	0.9999	0.9999	0.9999	0.9999	0.9999	0.9999	0.9999	0.9999
	PC188	PC189	PC190	PC191	PC192	PC193	PC194	PC195	PC196	PC197	PC198
Standard Deviation	0.0337	0.0332	0.0322	0.0317	0.0308	0.0303	0.0291	0.0283	0.0281	0.0271	0.0267
Proportion of Variance	0.0000	0.0000	0.0000	0.0000	0.0000	0.0000	0.0000	0.0000	0.0000	0.0000	0.0000
Cumulative Proportion	0.9999	0.9999	0.9999	0.9999	0.9999	0.9999	0.9999	0.9999	0.9999	0.9999	0.9999
	PC199	PC200	PC201	PC202	PC203	PC204	PC205	PC206	PC207	PC208	PC209
Standard Deviation	0.0261	0.0259	0.0253	0.0251	0.0239	0.0236	0.0232	0.0230	0.0222	0.0216	0.0211
Proportion of Variance	0.0000	0.0000	0.0000	0.0000	0.0000	0.0000	0.0000	0.0000	0.0000	0.0000	0.0000
Cumulative Proportion	1.0000	1.0000	1.0000	1.0000	1.0000	1.0000	1.0000	1.0000	1.0000	1.0000	1.0000
	PC210	PC211	PC212	PC213	PC214	PC215	PC216	PC217	PC218	PC219	PC220
Standard Deviation	0.0207	0.0202	0.0197	0.0191	0.0187	0.0184	0.0183	0.0180	0.0178	0.0176	0.0171
Proportion of Variance	0.0000	0.0000	0.0000	0.0000	0.0000	0.0000	0.0000	0.0000	0.0000	0.0000	0.0000
Cumulative Proportion	1.0000	1.0000	1.0000	1.0000	1.0000	1.0000	1.0000	1.0000	1.0000	1.0000	1.0000
	PC221	PC222	PC223	PC224	PC225	PC226	PC227	PC228	PC229	PC230	PC231
Standard Deviation	0.0169	0.0167	0.0163	0.0161	0.0161	0.0159	0.0155	0.0153	0.0152	0.0150	0.0146
Proportion of Variance	0.0000	0.0000	0.0000	0.0000	0.0000	0.0000	0.0000	0.0000	0.0000	0.0000	0.0000
Cumulative Proportion	1.0000	1.0000	1.0000	1.0000	1.0000	1.0000	1.0000	1.0000	1.0000	1.0000	1.0000
	PC232	PC233	PC234	PC235	PC236	PC237	PC238	PC239	PC240	PC241	PC242
Standard Deviation	0.0144	0.0142	0.0141	0.0138	0.0136	0.0135	0.0132	0.0130	0.0129	0.0128	0.0126
Proportion of Variance	0.0000	0.0000	0.0000	0.0000	0.0000	0.0000	0.0000	0.0000	0.0000	0.0000	0.0000
Cumulative Proportion	1.0000	1.0000	1.0000	1.0000	1.0000	1.0000	1.0000	1.0000	1.0000	1.0000	1.0000
	PC243	PC244	PC245	PC246	PC247	PC248	PC249	PC250	PC251	PC252	PC253
Standard Deviation	0.0120	0.0119	0.0118	0.0114	0.0112	0.0111	0.0110	0.0106	0.0103	0.0102	0.0101
Proportion of Variance	0.0000	0.0000	0.0000	0.0000	0.0000	0.0000	0.0000	0.0000	0.0000	0.0000	0.0000
Cumulative Proportion	1.0000	1.0000	1.0000	1.0000	1.0000	1.0000	1.0000	1.0000	1.0000	1.0000	1.0000
	PC254	PC255	PC256	PC257	PC258	PC259	PC260	PC261	PC262	PC263	
Standard Deviation	0.0098	0.0097	0.0096	0.0095	0.0092	0.0090	0.0089	0.0088	0.0086	0.0085	
Proportion of Variance	0.0000	0.0000	0.0000	0.0000	0.0000	0.0000	0.0000	0.0000	0.0000	0.0000	
Cumulative Proportion	1.0000	1.0000	1.0000	1.0000	1.0000	1.0000	1.0000	1.0000	1.0000	1.0000	
	PC264	PC265	PC266	PC267	PC268	PC269	PC270	PC271	PC272		
Standard Deviation	0.0084	0.0082	0.0079	0.0078	0.0077	0.0076	0.0072	0.0070	0.0069		
Proportion of Variance	0.0000	0.0000	0.0000	0.0000	0.0000	0.0000	0.0000	0.0000	0.0000		

Cumulative Proportion	1.0000	1.0000	1.0000	1.0000	1.0000	1.0000	1.0000	1.0000	1.0000		
	PC273	PC274	PC275	PC276	PC277	PC278	PC279	PC280	PC281		
Standard Deviation	0.0067	0.0065	0.0063	0.0062	0.0060	0.0058	0.0057	0.0056	0.0054		
Proportion of Variance	0.0000	0.0000	0.0000	0.0000	0.0000	0.0000	0.0000	0.0000	0.0000		
Cumulative Proportion	1.0000	1.0000	1.0000	1.0000	1.0000	1.0000	1.0000	1.0000	1.0000		
	PC282	PC283	PC284	PC285	PC286	PC287	PC288	PC289	PC290		
Standard Deviation	0.0053	0.0052	0.0051	0.0049	0.0047	0.0046	0.0044	0.0042	0.0042		
Proportion of Variance	0.0000	0.0000	0.0000	0.0000	0.0000	0.0000	0.0000	0.0000	0.0000		
Cumulative Proportion	1.0000	1.0000	1.0000	1.0000	1.0000	1.0000	1.0000	1.0000	1.0000		
	PC291	PC292	PC293	PC294	PC295	PC296	PC297	PC298	PC299	PC300	
Standard Deviation	0.0041	0.0038	0.0038	0.0037	0.0035	0.0033	0.0032	0.0029	0.0027	0.0027	
Proportion of Variance	0.0000	0.0000	0.0000	0.0000	0.0000	0.0000	0.0000	0.0000	0.0000	0.0000	
Cumulative Proportion	1.0000	1.0000	1.0000	1.0000	1.0000	1.0000	1.0000	1.0000	1.0000	1.0000	
	PC301	PC302	PC303	PC304	PC305	PC306	PC307	PC308	PC309		
Standard Deviation	0.0024	0.0022	0.0022	0.0021	0.0019	0.0014	0.0008	0.0007	0.0005		
Proportion of Variance	0.0000	0.0000	0.0000	0.0000	0.0000	0.0000	0.0000	0.0000	0.0000		
Cumulative Proportion	1.0000	1.0000	1.0000	1.0000	1.0000	1.0000	1.0000	1.0000	1.0000		
	PC310	PC311	PC312	PC313	PC314	PC315	PC316	PC317			
Standard Deviation	0.0004	0.0003	0.0003	0.0003	0.0003	0.0002	0.0002	0.0002			
Proportion of Variance	0.0000	0.0000	0.0000	0.0000	0.0000	0.0000	0.0000	0.0000			
Cumulative Proportion	1.0000	1.0000	1.0000	1.0000	1.0000	1.0000	1.0000	1.0000			
	PC318	PC319	PC320	PC321	PC322	PC323					
Standard Deviation	0.0002	0.0001	0.0001	0.0001	0.0001	0.0000					
Proportion of Variance	0.0000	0.0000	0.0000	0.0000	0.0000	0.0000					
Cumulative Proportion	1.0000	1.0000	1.0000	1.0000	1.0000	1.0000					

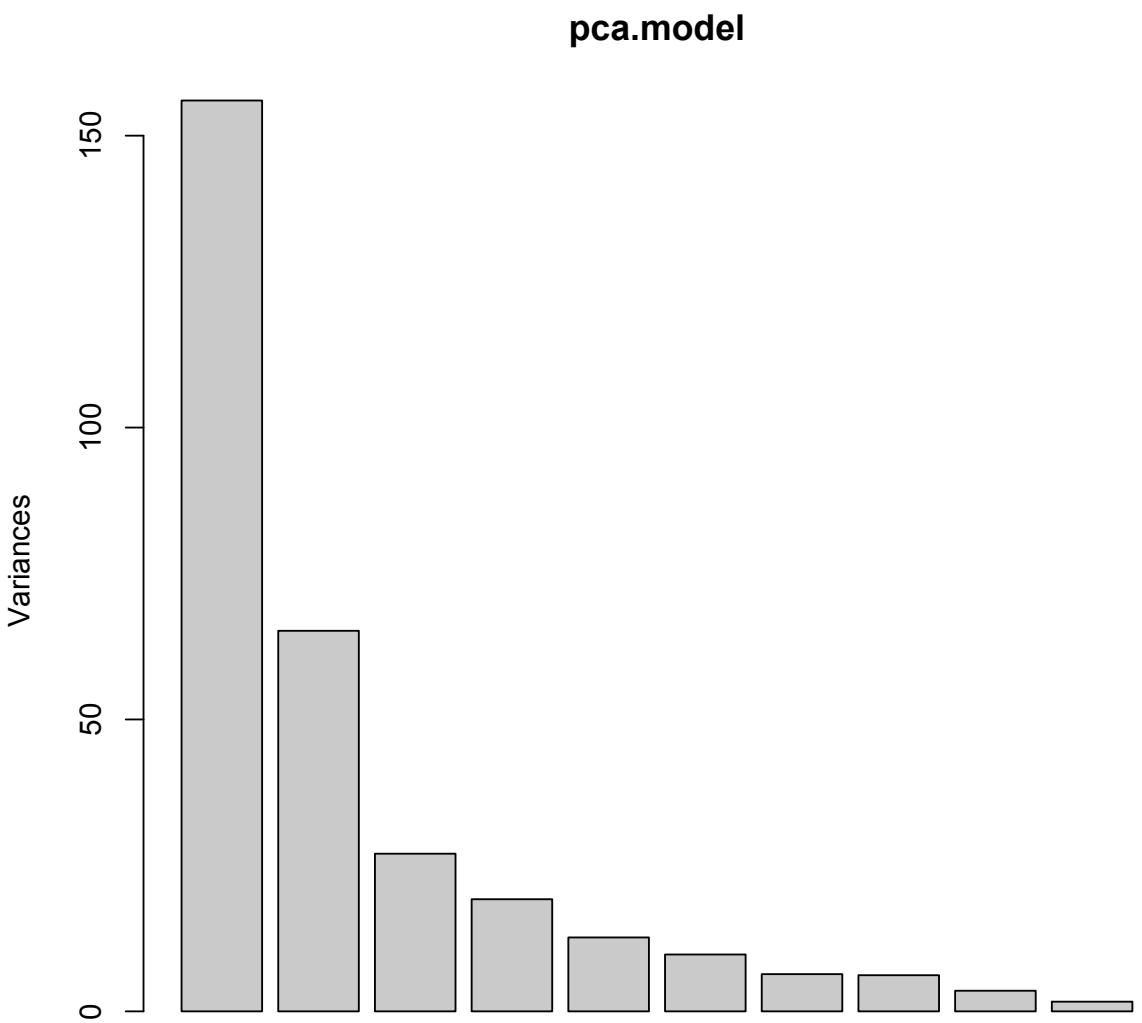


Figure 344: PCA scree plot for the set of 50 container glass first derivative (5-point smoothing) spectra (10 replicates), autoscaled.

Table 356: PCA results for the set of 153 glass first derivative (9-point smoothing) spectra (10 replicates), autoscaled.

	PC1	PC2	PC3	PC4	PC5	PC6	PC7	PC8	PC9	PC10	PC11
Standard Deviation	14.0498	6.3900	5.2293	4.1999	3.6038	2.7323	2.4152	1.9769	1.7183	1.1493	1.0688
Proportion of Variance	0.6111	0.1264	0.0847	0.0546	0.0402	0.0231	0.0181	0.0121	0.0091	0.0041	0.0035
Cumulative Proportion	0.6111	0.7376	0.8222	0.8768	0.9170	0.9401	0.9582	0.9703	0.9794	0.9835	0.9871
	PC12	PC13	PC14	PC15	PC16	PC17	PC18	PC19	PC20	PC21	PC22
Standard Deviation	0.8402	0.7686	0.5685	0.5629	0.4890	0.4647	0.4351	0.3819	0.3683	0.3374	0.3314
Proportion of Variance	0.0022	0.0018	0.0010	0.0010	0.0007	0.0007	0.0006	0.0005	0.0004	0.0004	0.0003
Cumulative Proportion	0.9893	0.9911	0.9921	0.9931	0.9938	0.9945	0.9951	0.9955	0.9959	0.9963	0.9966
	PC23	PC24	PC25	PC26	PC27	PC28	PC29	PC30	PC31	PC32	PC33
Standard Deviation	0.3087	0.2664	0.2648	0.2427	0.2354	0.2258	0.2122	0.2059	0.1995	0.1923	0.1835
Proportion of Variance	0.0003	0.0002	0.0002	0.0002	0.0002	0.0002	0.0001	0.0001	0.0001	0.0001	0.0001
Cumulative Proportion	0.9969	0.9971	0.9974	0.9975	0.9977	0.9979	0.9980	0.9981	0.9983	0.9984	0.9985
	PC34	PC35	PC36	PC37	PC38	PC39	PC40	PC41	PC42	PC43	PC44
Standard Deviation	0.1820	0.1732	0.1686	0.1571	0.1508	0.1396	0.1328	0.1302	0.1209	0.1189	0.1137
Proportion of Variance	0.0001	0.0001	0.0001	0.0001	0.0001	0.0001	0.0001	0.0001	0.0001	0.0000	0.0000
Cumulative Proportion	0.9986	0.9987	0.9988	0.9988	0.9989	0.9990	0.9990	0.9991	0.9991	0.9992	0.9992
	PC45	PC46	PC47	PC48	PC49	PC50	PC51	PC52	PC53	PC54	PC55
Standard Deviation	0.1055	0.1050	0.1024	0.0978	0.0954	0.0877	0.0859	0.0848	0.0824	0.0795	0.0751
Proportion of Variance	0.0000	0.0000	0.0000	0.0000	0.0000	0.0000	0.0000	0.0000	0.0000	0.0000	0.0000
Cumulative Proportion	0.9992	0.9993	0.9993	0.9993	0.9994	0.9994	0.9994	0.9994	0.9995	0.9995	0.9995
	PC56	PC57	PC58	PC59	PC60	PC61	PC62	PC63	PC64	PC65	PC66
Standard Deviation	0.0748	0.0738	0.0720	0.0710	0.0704	0.0696	0.0686	0.0678	0.0657	0.0647	0.0642
Proportion of Variance	0.0000	0.0000	0.0000	0.0000	0.0000	0.0000	0.0000	0.0000	0.0000	0.0000	0.0000
Cumulative Proportion	0.9995	0.9995	0.9995	0.9996	0.9996	0.9996	0.9996	0.9996	0.9996	0.9996	0.9997
	PC67	PC68	PC69	PC70	PC71	PC72	PC73	PC74	PC75	PC76	PC77
Standard Deviation	0.0631	0.0625	0.0604	0.0593	0.0590	0.0586	0.0572	0.0556	0.0550	0.0547	0.0537
Proportion of Variance	0.0000	0.0000	0.0000	0.0000	0.0000	0.0000	0.0000	0.0000	0.0000	0.0000	0.0000
Cumulative Proportion	0.9997	0.9997	0.9997	0.9997	0.9997	0.9997	0.9997	0.9998	0.9998	0.9998	0.9998
	PC78	PC79	PC80	PC81	PC82	PC83	PC84	PC85	PC86	PC87	PC88
Standard Deviation	0.0531	0.0525	0.0519	0.0509	0.0504	0.0494	0.0488	0.0480	0.0477	0.0470	0.0453
Proportion of Variance	0.0000	0.0000	0.0000	0.0000	0.0000	0.0000	0.0000	0.0000	0.0000	0.0000	0.0000
Cumulative Proportion	0.9998	0.9998	0.9998	0.9998	0.9998	0.9998	0.9998	0.9998	0.9998	0.9999	0.9999

	PC89	PC90	PC91	PC92	PC93	PC94	PC95	PC96	PC97	PC98	PC99
Standard Deviation	0.0444	0.0437	0.0432	0.0420	0.0413	0.0403	0.0397	0.0389	0.0378	0.0363	0.0357
Proportion of Variance	0.0000	0.0000	0.0000	0.0000	0.0000	0.0000	0.0000	0.0000	0.0000	0.0000	0.0000
Cumulative Proportion	0.9999	0.9999	0.9999	0.9999	0.9999	0.9999	0.9999	0.9999	0.9999	0.9999	0.9999
	PC100	PC101	PC102	PC103	PC104	PC105	PC106	PC107	PC108	PC109	PC110
Standard Deviation	0.0346	0.0336	0.0331	0.0322	0.0315	0.0309	0.0301	0.0288	0.0276	0.0268	0.0259
Proportion of Variance	0.0000	0.0000	0.0000	0.0000	0.0000	0.0000	0.0000	0.0000	0.0000	0.0000	0.0000
Cumulative Proportion	0.9999	0.9999	0.9999	0.9999	0.9999	0.9999	0.9999	0.9999	0.9999	0.9999	0.9999
	PC111	PC112	PC113	PC114	PC115	PC116	PC117	PC118	PC119	PC120	PC121
Standard Deviation	0.0249	0.0238	0.0234	0.0231	0.0229	0.0224	0.0219	0.0219	0.0215	0.0208	0.0203
Proportion of Variance	0.0000	0.0000	0.0000	0.0000	0.0000	0.0000	0.0000	0.0000	0.0000	0.0000	0.0000
Cumulative Proportion	1.0000	1.0000	1.0000	1.0000	1.0000	1.0000	1.0000	1.0000	1.0000	1.0000	1.0000
	PC122	PC123	PC124	PC125	PC126	PC127	PC128	PC129	PC130	PC131	PC132
Standard Deviation	0.0201	0.0200	0.0198	0.0194	0.0189	0.0187	0.0183	0.0182	0.0178	0.0178	0.0173
Proportion of Variance	0.0000	0.0000	0.0000	0.0000	0.0000	0.0000	0.0000	0.0000	0.0000	0.0000	0.0000
Cumulative Proportion	1.0000	1.0000	1.0000	1.0000	1.0000	1.0000	1.0000	1.0000	1.0000	1.0000	1.0000
	PC133	PC134	PC135	PC136	PC137	PC138	PC139	PC140	PC141	PC142	PC143
Standard Deviation	0.0170	0.0168	0.0167	0.0163	0.0162	0.0158	0.0155	0.0154	0.0152	0.0151	0.0148
Proportion of Variance	0.0000	0.0000	0.0000	0.0000	0.0000	0.0000	0.0000	0.0000	0.0000	0.0000	0.0000
Cumulative Proportion	1.0000	1.0000	1.0000	1.0000	1.0000	1.0000	1.0000	1.0000	1.0000	1.0000	1.0000
	PC144	PC145	PC146	PC147	PC148	PC149	PC150	PC151	PC152	PC153	PC154
Standard Deviation	0.0148	0.0145	0.0144	0.0141	0.0137	0.0134	0.0132	0.0128	0.0127	0.0126	0.0123
Proportion of Variance	0.0000	0.0000	0.0000	0.0000	0.0000	0.0000	0.0000	0.0000	0.0000	0.0000	0.0000
Cumulative Proportion	1.0000	1.0000	1.0000	1.0000	1.0000	1.0000	1.0000	1.0000	1.0000	1.0000	1.0000
	PC155	PC156	PC157	PC158	PC159	PC160	PC161	PC162	PC163	PC164	PC165
Standard Deviation	0.0122	0.0117	0.0117	0.0113	0.0112	0.0108	0.0106	0.0102	0.0101	0.0099	0.0099
Proportion of Variance	0.0000	0.0000	0.0000	0.0000	0.0000	0.0000	0.0000	0.0000	0.0000	0.0000	0.0000
Cumulative Proportion	1.0000	1.0000	1.0000	1.0000	1.0000	1.0000	1.0000	1.0000	1.0000	1.0000	1.0000
	PC166	PC167	PC168	PC169	PC170	PC171	PC172	PC173	PC174	PC175	
Standard Deviation	0.0095	0.0093	0.0092	0.0088	0.0087	0.0085	0.0084	0.0082	0.0080	0.0078	
Proportion of Variance	0.0000	0.0000	0.0000	0.0000	0.0000	0.0000	0.0000	0.0000	0.0000	0.0000	
Cumulative Proportion	1.0000	1.0000	1.0000	1.0000	1.0000	1.0000	1.0000	1.0000	1.0000	1.0000	
	PC176	PC177	PC178	PC179	PC180	PC181	PC182	PC183	PC184	PC185	
Standard Deviation	0.0078	0.0073	0.0072	0.0070	0.0068	0.0068	0.0067	0.0065	0.0065	0.0064	

Proportion of Variance	0.0000	0.0000	0.0000	0.0000	0.0000	0.0000	0.0000	0.0000	0.0000	0.0000	
Cumulative Proportion	1.0000	1.0000	1.0000	1.0000	1.0000	1.0000	1.0000	1.0000	1.0000	1.0000	
	PC186	PC187	PC188	PC189	PC190	PC191	PC192	PC193	PC194	PC195	
Standard Deviation	0.0063	0.0063	0.0062	0.0062	0.0060	0.0060	0.0059	0.0058	0.0058	0.0057	
Proportion of Variance	0.0000	0.0000	0.0000	0.0000	0.0000	0.0000	0.0000	0.0000	0.0000	0.0000	
Cumulative Proportion	1.0000	1.0000	1.0000	1.0000	1.0000	1.0000	1.0000	1.0000	1.0000	1.0000	
	PC196	PC197	PC198	PC199	PC200	PC201	PC202	PC203	PC204		
Standard Deviation	0.0055	0.0055	0.0055	0.0053	0.0052	0.0052	0.0051	0.0051	0.0050		
Proportion of Variance	0.0000	0.0000	0.0000	0.0000	0.0000	0.0000	0.0000	0.0000	0.0000		
Cumulative Proportion	1.0000	1.0000	1.0000	1.0000	1.0000	1.0000	1.0000	1.0000	1.0000		
	PC205	PC206	PC207	PC208	PC209	PC210	PC211	PC212	PC213		
Standard Deviation	0.0050	0.0049	0.0048	0.0047	0.0047	0.0046	0.0046	0.0045	0.0044		
Proportion of Variance	0.0000	0.0000	0.0000	0.0000	0.0000	0.0000	0.0000	0.0000	0.0000		
Cumulative Proportion	1.0000	1.0000	1.0000	1.0000	1.0000	1.0000	1.0000	1.0000	1.0000		
	PC214	PC215	PC216	PC217	PC218	PC219	PC220	PC221	PC222	PC223	
Standard Deviation	0.0044	0.0043	0.0042	0.0041	0.0041	0.0040	0.0040	0.0039	0.0038	0.0037	
Proportion of Variance	0.0000	0.0000	0.0000	0.0000	0.0000	0.0000	0.0000	0.0000	0.0000	0.0000	
Cumulative Proportion	1.0000	1.0000	1.0000	1.0000	1.0000	1.0000	1.0000	1.0000	1.0000	1.0000	
	PC224	PC225	PC226	PC227	PC228	PC229	PC230	PC231	PC232	PC233	
Standard Deviation	0.0037	0.0036	0.0036	0.0035	0.0033	0.0033	0.0033	0.0032	0.0031	0.0031	
Proportion of Variance	0.0000	0.0000	0.0000	0.0000	0.0000	0.0000	0.0000	0.0000	0.0000	0.0000	
Cumulative Proportion	1.0000	1.0000	1.0000	1.0000	1.0000	1.0000	1.0000	1.0000	1.0000	1.0000	
	PC234	PC235	PC236	PC237	PC238	PC239	PC240	PC241	PC242		
Standard Deviation	0.0031	0.0030	0.0029	0.0028	0.0028	0.0027	0.0027	0.0027	0.0026		
Proportion of Variance	0.0000	0.0000	0.0000	0.0000	0.0000	0.0000	0.0000	0.0000	0.0000		
Cumulative Proportion	1.0000	1.0000	1.0000	1.0000	1.0000	1.0000	1.0000	1.0000	1.0000		
	PC243	PC244	PC245	PC246	PC247	PC248	PC249	PC250	PC251		
Standard Deviation	0.0025	0.0024	0.0024	0.0023	0.0022	0.0022	0.0022	0.0021	0.0021		
Proportion of Variance	0.0000	0.0000	0.0000	0.0000	0.0000	0.0000	0.0000	0.0000	0.0000		
Cumulative Proportion	1.0000	1.0000	1.0000	1.0000	1.0000	1.0000	1.0000	1.0000	1.0000		
	PC252	PC253	PC254	PC255	PC256	PC257	PC258	PC259	PC260	PC261	
Standard Deviation	0.0020	0.0020	0.0019	0.0019	0.0018	0.0018	0.0018	0.0018	0.0017	0.0017	
Proportion of Variance	0.0000	0.0000	0.0000	0.0000	0.0000	0.0000	0.0000	0.0000	0.0000	0.0000	

Cumulative Proportion	1.0000	1.0000	1.0000	1.0000	1.0000	1.0000	1.0000	1.0000	1.0000	1.0000	
	PC262	PC263	PC264	PC265	PC266	PC267	PC268	PC269	PC270		
Standard Deviation	0.0017	0.0016	0.0016	0.0016	0.0015	0.0015	0.0015	0.0015	0.0015		
Proportion of Variance	0.0000	0.0000	0.0000	0.0000	0.0000	0.0000	0.0000	0.0000	0.0000		
Cumulative Proportion	1.0000	1.0000	1.0000	1.0000	1.0000	1.0000	1.0000	1.0000	1.0000		
	PC271	PC272	PC273	PC274	PC275	PC276	PC277	PC278	PC279		
Standard Deviation	0.0014	0.0014	0.0014	0.0014	0.0014	0.0013	0.0013	0.0013	0.0013		
Proportion of Variance	0.0000	0.0000	0.0000	0.0000	0.0000	0.0000	0.0000	0.0000	0.0000		
Cumulative Proportion	1.0000	1.0000	1.0000	1.0000	1.0000	1.0000	1.0000	1.0000	1.0000		
	PC280	PC281	PC282	PC283	PC284	PC285	PC286	PC287	PC288		
Standard Deviation	0.0012	0.0012	0.0012	0.0011	0.0011	0.0011	0.0011	0.0010	0.0010		
Proportion of Variance	0.0000	0.0000	0.0000	0.0000	0.0000	0.0000	0.0000	0.0000	0.0000		
Cumulative Proportion	1.0000	1.0000	1.0000	1.0000	1.0000	1.0000	1.0000	1.0000	1.0000		
	PC289	PC290	PC291	PC292	PC293	PC294	PC295	PC296	PC297		
Standard Deviation	0.0009	0.0009	0.0009	0.0008	0.0008	0.0007	0.0007	0.0006	0.0006		
Proportion of Variance	0.0000	0.0000	0.0000	0.0000	0.0000	0.0000	0.0000	0.0000	0.0000		
Cumulative Proportion	1.0000	1.0000	1.0000	1.0000	1.0000	1.0000	1.0000	1.0000	1.0000		
	PC298	PC299	PC300	PC301	PC302	PC303	PC304	PC305			
Standard Deviation	0.0006	0.0005	0.0005	0.0004	0.0004	0.0004	0.0003	0.0003			
Proportion of Variance	0.0000	0.0000	0.0000	0.0000	0.0000	0.0000	0.0000	0.0000			
Cumulative Proportion	1.0000	1.0000	1.0000	1.0000	1.0000	1.0000	1.0000	1.0000			
	PC306	PC307	PC308	PC309	PC310	PC311	PC312	PC313	PC314		
Standard Deviation	0.0003	0.0002	0.0002	0.0002	0.0002	0.0001	0.0001	0.0001	0.0001		
Proportion of Variance	0.0000	0.0000	0.0000	0.0000	0.0000	0.0000	0.0000	0.0000	0.0000		
Cumulative Proportion	1.0000	1.0000	1.0000	1.0000	1.0000	1.0000	1.0000	1.0000	1.0000		
	PC315	PC316	PC317	PC318	PC319	PC320	PC321	PC322	PC323		
Standard Deviation	0.0001	0.0001	0.0001	0.0001	0.0001	0.0001	0.0001	0.0001	0.0000		
Proportion of Variance	0.0000	0.0000	0.0000	0.0000	0.0000	0.0000	0.0000	0.0000	0.0000		
Cumulative Proportion	1.0000	1.0000	1.0000	1.0000	1.0000	1.0000	1.0000	1.0000	1.0000		

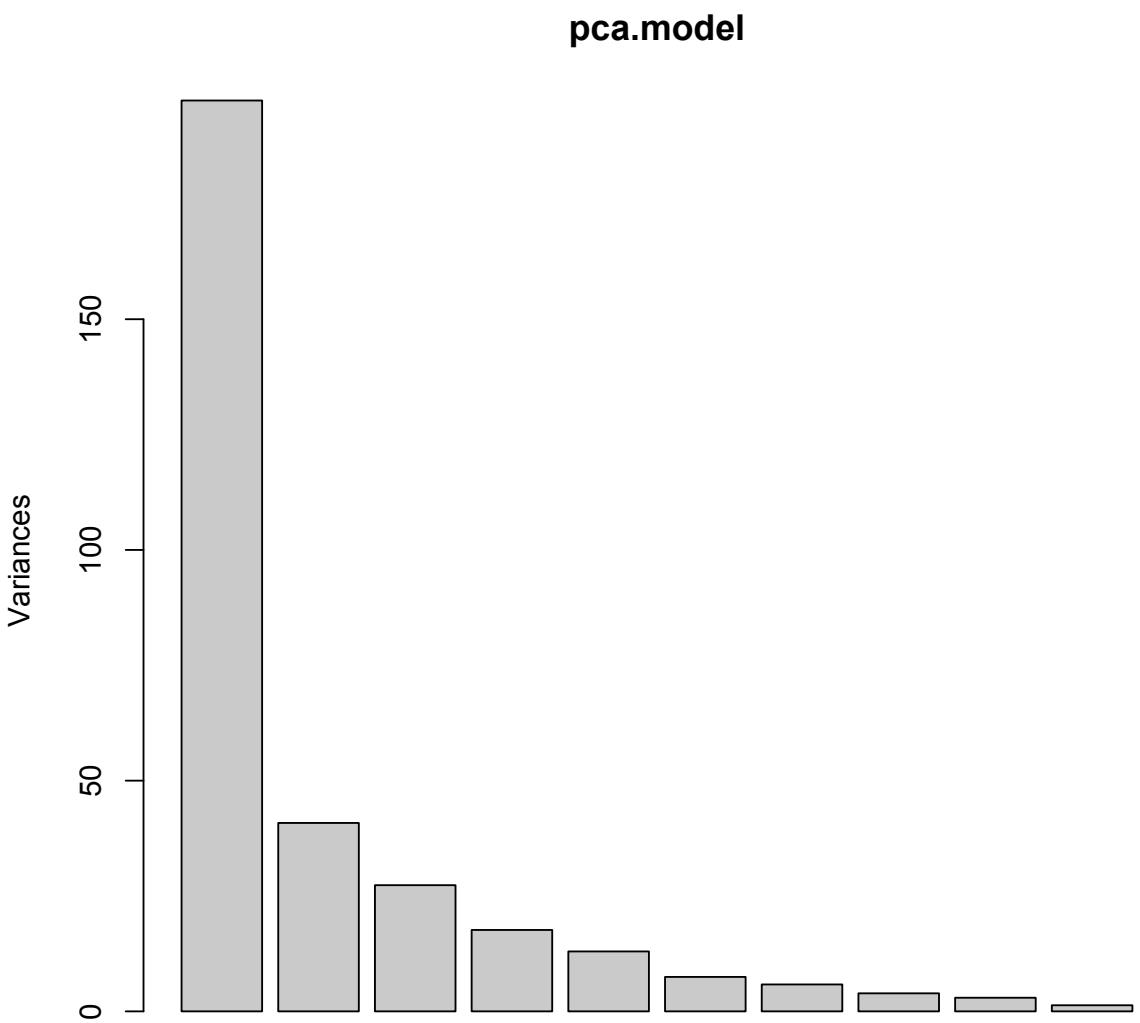


Figure 345: PCA scree plot for the set of 153 glass first derivative (9-point smoothing) spectra (10 replicates), autoscaled.

Table 357: PCA results for the set of 153 glass second derivative (9-point smoothing) spectra (10 replicates), autoscaled.

	PC1	PC2	PC3	PC4	PC5	PC6	PC7	PC8	PC9	PC10	PC11
Standard Deviation	8.4404	6.8280	4.6264	4.0905	3.3057	3.0919	2.7073	2.4809	2.3317	2.0749	2.0606
Proportion of Variance	0.2206	0.1443	0.0663	0.0518	0.0338	0.0296	0.0227	0.0191	0.0168	0.0133	0.0132
Cumulative Proportion	0.2206	0.3649	0.4312	0.4830	0.5168	0.5464	0.5691	0.5881	0.6050	0.6183	0.6314
	PC12	PC13	PC14	PC15	PC16	PC17	PC18	PC19	PC20	PC21	PC22
Standard Deviation	1.9704	1.9497	1.9134	1.8818	1.8516	1.8454	1.8091	1.7756	1.7382	1.7169	1.6889
Proportion of Variance	0.0120	0.0118	0.0113	0.0110	0.0106	0.0105	0.0101	0.0098	0.0094	0.0091	0.0088
Cumulative Proportion	0.6435	0.6552	0.6666	0.6775	0.6881	0.6987	0.7088	0.7186	0.7279	0.7371	0.7459
	PC23	PC24	PC25	PC26	PC27	PC28	PC29	PC30	PC31	PC32	PC33
Standard Deviation	1.6822	1.6361	1.6058	1.5967	1.5604	1.5169	1.4878	1.4482	1.4160	1.4022	1.3571
Proportion of Variance	0.0088	0.0083	0.0080	0.0079	0.0075	0.0071	0.0069	0.0065	0.0062	0.0061	0.0057
Cumulative Proportion	0.7547	0.7629	0.7709	0.7788	0.7864	0.7935	0.8003	0.8068	0.8130	0.8191	0.8248
	PC34	PC35	PC36	PC37	PC38	PC39	PC40	PC41	PC42	PC43	PC44
Standard Deviation	1.3202	1.3046	1.3025	1.2550	1.2381	1.2216	1.2080	1.2020	1.1570	1.1510	1.1146
Proportion of Variance	0.0054	0.0053	0.0053	0.0049	0.0048	0.0046	0.0045	0.0045	0.0041	0.0041	0.0039
Cumulative Proportion	0.8302	0.8355	0.8407	0.8456	0.8504	0.8550	0.8595	0.8640	0.8681	0.8722	0.8761
	PC45	PC46	PC47	PC48	PC49	PC50	PC51	PC52	PC53	PC54	PC55
Standard Deviation	1.0849	1.0691	1.0668	1.0444	1.0363	1.0230	1.0148	1.0037	0.9832	0.9660	0.9436
Proportion of Variance	0.0036	0.0035	0.0035	0.0034	0.0033	0.0032	0.0032	0.0031	0.0030	0.0029	0.0028
Cumulative Proportion	0.8797	0.8833	0.8868	0.8902	0.8935	0.8967	0.8999	0.9030	0.9060	0.9089	0.9117
	PC56	PC57	PC58	PC59	PC60	PC61	PC62	PC63	PC64	PC65	PC66
Standard Deviation	0.9251	0.9097	0.9032	0.8803	0.8657	0.8578	0.8481	0.8358	0.8313	0.8292	0.8007
Proportion of Variance	0.0027	0.0026	0.0025	0.0024	0.0023	0.0023	0.0022	0.0022	0.0021	0.0021	0.0020
Cumulative Proportion	0.9143	0.9169	0.9194	0.9218	0.9241	0.9264	0.9286	0.9308	0.9329	0.9351	0.9370
	PC67	PC68	PC69	PC70	PC71	PC72	PC73	PC74	PC75	PC76	PC77
Standard Deviation	0.7927	0.7804	0.7642	0.7594	0.7538	0.7383	0.7288	0.7168	0.7063	0.7012	0.6908
Proportion of Variance	0.0020	0.0019	0.0018	0.0018	0.0018	0.0017	0.0016	0.0016	0.0015	0.0015	0.0015
Cumulative Proportion	0.9390	0.9409	0.9427	0.9445	0.9462	0.9479	0.9496	0.9511	0.9527	0.9542	0.9557
	PC78	PC79	PC80	PC81	PC82	PC83	PC84	PC85	PC86	PC87	PC88
Standard Deviation	0.6777	0.6591	0.6502	0.6404	0.6248	0.6177	0.6004	0.5848	0.5711	0.5590	0.5474
Proportion of Variance	0.0014	0.0013	0.0013	0.0013	0.0012	0.0012	0.0011	0.0011	0.0010	0.0010	0.0009
Cumulative Proportion	0.9571	0.9585	0.9598	0.9610	0.9622	0.9634	0.9645	0.9656	0.9666	0.9676	0.9685

	PC89	PC90	PC91	PC92	PC93	PC94	PC95	PC96	PC97	PC98	PC99
Standard Deviation	0.5436	0.5340	0.5284	0.5119	0.5064	0.4940	0.4917	0.4875	0.4800	0.4694	0.4609
Proportion of Variance	0.0009	0.0009	0.0009	0.0008	0.0008	0.0008	0.0008	0.0007	0.0007	0.0007	0.0007
Cumulative Proportion	0.9694	0.9703	0.9712	0.9720	0.9728	0.9735	0.9743	0.9750	0.9757	0.9764	0.9771
	PC100	PC101	PC102	PC103	PC104	PC105	PC106	PC107	PC108	PC109	PC110
Standard Deviation	0.4584	0.4516	0.4426	0.4417	0.4378	0.4318	0.4284	0.4210	0.4125	0.4085	0.4054
Proportion of Variance	0.0007	0.0006	0.0006	0.0006	0.0006	0.0006	0.0006	0.0006	0.0005	0.0005	0.0005
Cumulative Proportion	0.9777	0.9783	0.9790	0.9796	0.9801	0.9807	0.9813	0.9818	0.9824	0.9829	0.9834
	PC111	PC112	PC113	PC114	PC115	PC116	PC117	PC118	PC119	PC120	PC121
Standard Deviation	0.4022	0.3944	0.3879	0.3830	0.3802	0.3723	0.3691	0.3573	0.3540	0.3494	0.3444
Proportion of Variance	0.0005	0.0005	0.0005	0.0005	0.0005	0.0004	0.0004	0.0004	0.0004	0.0004	0.0004
Cumulative Proportion	0.9839	0.9844	0.9848	0.9853	0.9857	0.9862	0.9866	0.9870	0.9874	0.9878	0.9881
	PC122	PC123	PC124	PC125	PC126	PC127	PC128	PC129	PC130	PC131	PC132
Standard Deviation	0.3376	0.3356	0.3278	0.3272	0.3180	0.3162	0.3141	0.3076	0.3051	0.2996	0.2941
Proportion of Variance	0.0004	0.0004	0.0003	0.0003	0.0003	0.0003	0.0003	0.0003	0.0003	0.0003	0.0003
Cumulative Proportion	0.9885	0.9888	0.9892	0.9895	0.9898	0.9901	0.9904	0.9907	0.9910	0.9913	0.9915
	PC133	PC134	PC135	PC136	PC137	PC138	PC139	PC140	PC141	PC142	PC143
Standard Deviation	0.2926	0.2862	0.2818	0.2806	0.2782	0.2750	0.2746	0.2730	0.2674	0.2592	0.2556
Proportion of Variance	0.0003	0.0003	0.0003	0.0002	0.0002	0.0002	0.0002	0.0002	0.0002	0.0002	0.0002
Cumulative Proportion	0.9918	0.9921	0.9923	0.9926	0.9928	0.9930	0.9933	0.9935	0.9937	0.9939	0.9941
	PC144	PC145	PC146	PC147	PC148	PC149	PC150	PC151	PC152	PC153	PC154
Standard Deviation	0.2537	0.2511	0.2479	0.2458	0.2366	0.2330	0.2310	0.2283	0.2222	0.2187	0.2140
Proportion of Variance	0.0002	0.0002	0.0002	0.0002	0.0002	0.0002	0.0002	0.0002	0.0002	0.0002	0.0001
Cumulative Proportion	0.9943	0.9945	0.9947	0.9949	0.9951	0.9952	0.9954	0.9956	0.9957	0.9959	0.9960
	PC155	PC156	PC157	PC158	PC159	PC160	PC161	PC162	PC163	PC164	PC165
Standard Deviation	0.2128	0.2107	0.2056	0.2041	0.2014	0.1998	0.1889	0.1856	0.1842	0.1816	0.1771
Proportion of Variance	0.0001	0.0001	0.0001	0.0001	0.0001	0.0001	0.0001	0.0001	0.0001	0.0001	0.0001
Cumulative Proportion	0.9961	0.9963	0.9964	0.9965	0.9967	0.9968	0.9969	0.9970	0.9971	0.9972	0.9973
	PC166	PC167	PC168	PC169	PC170	PC171	PC172	PC173	PC174	PC175	PC176
Standard Deviation	0.1733	0.1711	0.1672	0.1659	0.1604	0.1578	0.1573	0.1545	0.1518	0.1461	0.1436
Proportion of Variance	0.0001	0.0001	0.0001	0.0001	0.0001	0.0001	0.0001	0.0001	0.0001	0.0001	0.0001
Cumulative Proportion	0.9974	0.9975	0.9976	0.9977	0.9977	0.9978	0.9979	0.9980	0.9980	0.9981	0.9982
	PC177	PC178	PC179	PC180	PC181	PC182	PC183	PC184	PC185	PC186	PC187
Standard Deviation	0.1423	0.1401	0.1381	0.1368	0.1346	0.1299	0.1275	0.1256	0.1251	0.1225	0.1217

Proportion of Variance	0.0001	0.0001	0.0001	0.0001	0.0001	0.0001	0.0001	0.0001	0.0001	0.0001	0.0001
Cumulative Proportion	0.9982	0.9983	0.9984	0.9984	0.9985	0.9985	0.9986	0.9986	0.9987	0.9987	0.9988
	PC188	PC189	PC190	PC191	PC192	PC193	PC194	PC195	PC196	PC197	PC198
Standard Deviation	0.1203	0.1194	0.1166	0.1152	0.1141	0.1123	0.1102	0.1067	0.1056	0.1035	0.1018
Proportion of Variance	0.0000	0.0000	0.0000	0.0000	0.0000	0.0000	0.0000	0.0000	0.0000	0.0000	0.0000
Cumulative Proportion	0.9988	0.9989	0.9989	0.9989	0.9990	0.9990	0.9991	0.9991	0.9991	0.9992	0.9992
	PC199	PC200	PC201	PC202	PC203	PC204	PC205	PC206	PC207	PC208	PC209
Standard Deviation	0.1007	0.0993	0.0984	0.0967	0.0960	0.0935	0.0897	0.0892	0.0860	0.0851	0.0831
Proportion of Variance	0.0000	0.0000	0.0000	0.0000	0.0000	0.0000	0.0000	0.0000	0.0000	0.0000	0.0000
Cumulative Proportion	0.9992	0.9993	0.9993	0.9993	0.9993	0.9994	0.9994	0.9994	0.9994	0.9995	0.9995
	PC210	PC211	PC212	PC213	PC214	PC215	PC216	PC217	PC218	PC219	PC220
Standard Deviation	0.0826	0.0801	0.0796	0.0790	0.0777	0.0770	0.0768	0.0742	0.0734	0.0718	0.0711
Proportion of Variance	0.0000	0.0000	0.0000	0.0000	0.0000	0.0000	0.0000	0.0000	0.0000	0.0000	0.0000
Cumulative Proportion	0.9995	0.9995	0.9995	0.9996	0.9996	0.9996	0.9996	0.9996	0.9997	0.9997	0.9997
	PC221	PC222	PC223	PC224	PC225	PC226	PC227	PC228	PC229	PC230	PC231
Standard Deviation	0.0700	0.0696	0.0664	0.0659	0.0654	0.0651	0.0631	0.0606	0.0591	0.0588	0.0578
Proportion of Variance	0.0000	0.0000	0.0000	0.0000	0.0000	0.0000	0.0000	0.0000	0.0000	0.0000	0.0000
Cumulative Proportion	0.9997	0.9997	0.9997	0.9997	0.9998	0.9998	0.9998	0.9998	0.9998	0.9998	0.9998
	PC232	PC233	PC234	PC235	PC236	PC237	PC238	PC239	PC240	PC241	PC242
Standard Deviation	0.0557	0.0552	0.0544	0.0521	0.0513	0.0512	0.0495	0.0480	0.0472	0.0467	0.0451
Proportion of Variance	0.0000	0.0000	0.0000	0.0000	0.0000	0.0000	0.0000	0.0000	0.0000	0.0000	0.0000
Cumulative Proportion	0.9998	0.9998	0.9999	0.9999	0.9999	0.9999	0.9999	0.9999	0.9999	0.9999	0.9999
	PC243	PC244	PC245	PC246	PC247	PC248	PC249	PC250	PC251	PC252	PC253
Standard Deviation	0.0442	0.0414	0.0406	0.0397	0.0390	0.0356	0.0353	0.0346	0.0337	0.0328	0.0322
Proportion of Variance	0.0000	0.0000	0.0000	0.0000	0.0000	0.0000	0.0000	0.0000	0.0000	0.0000	0.0000
Cumulative Proportion	0.9999	0.9999	0.9999	0.9999	0.9999	0.9999	0.9999	0.9999	1.0000	1.0000	1.0000
	PC254	PC255	PC256	PC257	PC258	PC259	PC260	PC261	PC262	PC263	PC264
Standard Deviation	0.0311	0.0305	0.0289	0.0286	0.0275	0.0270	0.0264	0.0256	0.0245	0.0236	0.0229
Proportion of Variance	0.0000	0.0000	0.0000	0.0000	0.0000	0.0000	0.0000	0.0000	0.0000	0.0000	0.0000
Cumulative Proportion	1.0000	1.0000	1.0000	1.0000	1.0000	1.0000	1.0000	1.0000	1.0000	1.0000	1.0000
	PC265	PC266	PC267	PC268	PC269	PC270	PC271	PC272	PC273	PC274	PC275
Standard Deviation	0.0224	0.0216	0.0213	0.0204	0.0202	0.0199	0.0190	0.0189	0.0176	0.0175	0.0169
Proportion of Variance	0.0000	0.0000	0.0000	0.0000	0.0000	0.0000	0.0000	0.0000	0.0000	0.0000	0.0000

Cumulative Proportion	1.0000	1.0000	1.0000	1.0000	1.0000	1.0000	1.0000	1.0000	1.0000	1.0000	1.0000
	PC276	PC277	PC278	PC279	PC280	PC281	PC282	PC283	PC284	PC285	PC286
Standard Deviation	0.0162	0.0156	0.0148	0.0147	0.0141	0.0136	0.0134	0.0127	0.0121	0.0107	0.0106
Proportion of Variance	0.0000	0.0000	0.0000	0.0000	0.0000	0.0000	0.0000	0.0000	0.0000	0.0000	0.0000
Cumulative Proportion	1.0000	1.0000	1.0000	1.0000	1.0000	1.0000	1.0000	1.0000	1.0000	1.0000	1.0000
	PC287	PC288	PC289	PC290	PC291	PC292	PC293	PC294	PC295	PC296	
Standard Deviation	0.0098	0.0096	0.0093	0.0088	0.0082	0.0078	0.0073	0.0069	0.0068	0.0065	
Proportion of Variance	0.0000	0.0000	0.0000	0.0000	0.0000	0.0000	0.0000	0.0000	0.0000	0.0000	
Cumulative Proportion	1.0000	1.0000	1.0000	1.0000	1.0000	1.0000	1.0000	1.0000	1.0000	1.0000	
	PC297	PC298	PC299	PC300	PC301	PC302	PC303	PC304	PC305	PC306	
Standard Deviation	0.0063	0.0061	0.0058	0.0052	0.0048	0.0047	0.0043	0.0040	0.0035	0.0033	
Proportion of Variance	0.0000	0.0000	0.0000	0.0000	0.0000	0.0000	0.0000	0.0000	0.0000	0.0000	
Cumulative Proportion	1.0000	1.0000	1.0000	1.0000	1.0000	1.0000	1.0000	1.0000	1.0000	1.0000	
	PC307	PC308	PC309	PC310	PC311	PC312	PC313	PC314	PC315		
Standard Deviation	0.0029	0.0029	0.0026	0.0025	0.0024	0.0024	0.0021	0.0020	0.0015		
Proportion of Variance	0.0000	0.0000	0.0000	0.0000	0.0000	0.0000	0.0000	0.0000	0.0000		
Cumulative Proportion	1.0000	1.0000	1.0000	1.0000	1.0000	1.0000	1.0000	1.0000	1.0000		
	PC316	PC317	PC318	PC319	PC320	PC321	PC322	PC323			
Standard Deviation	0.0012	0.0011	0.0009	0.0008	0.0008	0.0007	0.0002	0.0002			
Proportion of Variance	0.0000	0.0000	0.0000	0.0000	0.0000	0.0000	0.0000	0.0000			
Cumulative Proportion	1.0000	1.0000	1.0000	1.0000	1.0000	1.0000	1.0000	1.0000			

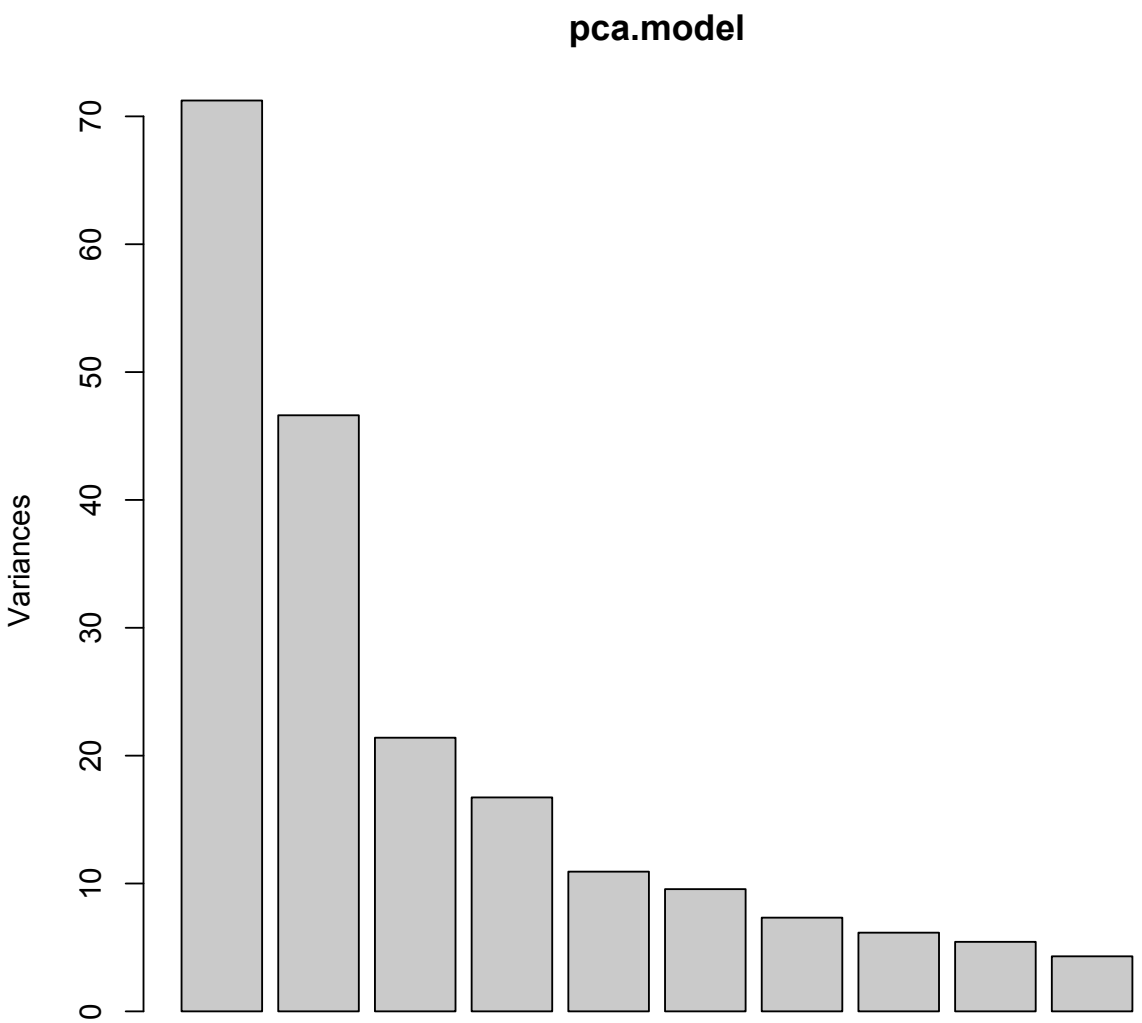


Figure 346: PCA scree plot for the set of 153 glass second derivative (9-point smoothing) spectra (10 replicates), autoscaled.

Table 358: PCA results for the set of 103 window glass second derivative (9-point smoothing) spectra (10 replicates), autoscaled.

	PC1	PC2	PC3	PC4	PC5	PC6	PC7	PC8	PC9	PC10	PC11
Standard Deviation	8.7847	5.9103	4.9484	3.4586	3.3161	2.9633	2.6738	2.5969	2.2314	2.1375	2.0909
Proportion of Variance	0.2389	0.1081	0.0758	0.0370	0.0341	0.0272	0.0221	0.0209	0.0154	0.0141	0.0135
Cumulative Proportion	0.2389	0.3471	0.4229	0.4599	0.4940	0.5211	0.5433	0.5642	0.5796	0.5937	0.6073
	PC12	PC13	PC14	PC15	PC16	PC17	PC18	PC19	PC20	PC21	PC22
Standard Deviation	2.0374	2.0252	2.0013	1.9587	1.9140	1.8876	1.8613	1.8289	1.7881	1.7634	1.7531
Proportion of Variance	0.0129	0.0127	0.0124	0.0119	0.0113	0.0110	0.0107	0.0104	0.0099	0.0096	0.0095
Cumulative Proportion	0.6201	0.6328	0.6452	0.6571	0.6684	0.6795	0.6902	0.7005	0.7104	0.7201	0.7296
	PC23	PC24	PC25	PC26	PC27	PC28	PC29	PC30	PC31	PC32	PC33
Standard Deviation	1.6966	1.6869	1.6460	1.6198	1.5830	1.5639	1.5388	1.4559	1.4281	1.4211	1.3958
Proportion of Variance	0.0089	0.0088	0.0084	0.0081	0.0078	0.0076	0.0073	0.0066	0.0063	0.0063	0.0060
Cumulative Proportion	0.7385	0.7473	0.7557	0.7638	0.7716	0.7791	0.7865	0.7930	0.7993	0.8056	0.8116
	PC34	PC35	PC36	PC37	PC38	PC39	PC40	PC41	PC42	PC43	PC44
Standard Deviation	1.3529	1.3447	1.3247	1.3207	1.3008	1.2953	1.2742	1.2435	1.2244	1.1770	1.1732
Proportion of Variance	0.0057	0.0056	0.0054	0.0054	0.0052	0.0052	0.0050	0.0048	0.0046	0.0043	0.0043
Cumulative Proportion	0.8173	0.8229	0.8283	0.8337	0.8390	0.8442	0.8492	0.8540	0.8586	0.8629	0.8672
	PC45	PC46	PC47	PC48	PC49	PC50	PC51	PC52	PC53	PC54	PC55
Standard Deviation	1.1522	1.1396	1.1190	1.0979	1.0780	1.0664	1.0643	1.0397	1.0235	1.0103	0.9963
Proportion of Variance	0.0041	0.0040	0.0039	0.0037	0.0036	0.0035	0.0035	0.0034	0.0032	0.0032	0.0031
Cumulative Proportion	0.8713	0.8753	0.8792	0.8829	0.8865	0.8900	0.8935	0.8969	0.9001	0.9033	0.9064
	PC56	PC57	PC58	PC59	PC60	PC61	PC62	PC63	PC64	PC65	PC66
Standard Deviation	0.9935	0.9808	0.9292	0.9165	0.9122	0.8780	0.8743	0.8674	0.8530	0.8465	0.8295
Proportion of Variance	0.0031	0.0030	0.0027	0.0026	0.0026	0.0024	0.0024	0.0023	0.0023	0.0022	0.0021
Cumulative Proportion	0.9094	0.9124	0.9151	0.9176	0.9202	0.9226	0.9250	0.9273	0.9296	0.9318	0.9339
	PC67	PC68	PC69	PC70	PC71	PC72	PC73	PC74	PC75	PC76	PC77
Standard Deviation	0.8273	0.8185	0.7942	0.7824	0.7776	0.7590	0.7503	0.7434	0.7217	0.7157	0.7003
Proportion of Variance	0.0021	0.0021	0.0020	0.0019	0.0019	0.0018	0.0017	0.0017	0.0016	0.0016	0.0015
Cumulative Proportion	0.9360	0.9381	0.9401	0.9419	0.9438	0.9456	0.9474	0.9491	0.9507	0.9523	0.9538
	PC78	PC79	PC80	PC81	PC82	PC83	PC84	PC85	PC86	PC87	PC88
Standard Deviation	0.6903	0.6770	0.6435	0.6434	0.6354	0.6142	0.5939	0.5890	0.5803	0.5750	0.5637
Proportion of Variance	0.0015	0.0014	0.0013	0.0013	0.0013	0.0012	0.0011	0.0011	0.0010	0.0010	0.0010
Cumulative Proportion	0.9553	0.9567	0.9580	0.9592	0.9605	0.9617	0.9628	0.9638	0.9649	0.9659	0.9669

	PC89	PC90	PC91	PC92	PC93	PC94	PC95	PC96	PC97	PC98	PC99
Standard Deviation	0.5545	0.5467	0.5341	0.5260	0.5193	0.5153	0.5091	0.5018	0.4954	0.4835	0.4741
Proportion of Variance	0.0010	0.0009	0.0009	0.0009	0.0008	0.0008	0.0008	0.0008	0.0008	0.0007	0.0007
Cumulative Proportion	0.9678	0.9688	0.9696	0.9705	0.9713	0.9722	0.9729	0.9737	0.9745	0.9752	0.9759
	PC100	PC101	PC102	PC103	PC104	PC105	PC106	PC107	PC108	PC109	PC110
Standard Deviation	0.4702	0.4626	0.4594	0.4570	0.4518	0.4477	0.4356	0.4290	0.4253	0.4196	0.4173
Proportion of Variance	0.0007	0.0007	0.0007	0.0007	0.0006	0.0006	0.0006	0.0006	0.0006	0.0005	0.0005
Cumulative Proportion	0.9766	0.9773	0.9779	0.9786	0.9792	0.9798	0.9804	0.9810	0.9815	0.9821	0.9826
	PC111	PC112	PC113	PC114	PC115	PC116	PC117	PC118	PC119	PC120	PC121
Standard Deviation	0.4060	0.3996	0.3956	0.3933	0.3884	0.3795	0.3779	0.3698	0.3655	0.3602	0.3541
Proportion of Variance	0.0005	0.0005	0.0005	0.0005	0.0005	0.0005	0.0004	0.0004	0.0004	0.0004	0.0004
Cumulative Proportion	0.9831	0.9836	0.9841	0.9846	0.9850	0.9855	0.9859	0.9864	0.9868	0.9872	0.9876
	PC122	PC123	PC124	PC125	PC126	PC127	PC128	PC129	PC130	PC131	PC132
Standard Deviation	0.3456	0.3448	0.3415	0.3317	0.3281	0.3225	0.3217	0.3160	0.3095	0.3063	0.3041
Proportion of Variance	0.0004	0.0004	0.0004	0.0003	0.0003	0.0003	0.0003	0.0003	0.0003	0.0003	0.0003
Cumulative Proportion	0.9879	0.9883	0.9887	0.9890	0.9893	0.9897	0.9900	0.9903	0.9906	0.9909	0.9912
	PC133	PC134	PC135	PC136	PC137	PC138	PC139	PC140	PC141	PC142	PC143
Standard Deviation	0.3013	0.2961	0.2920	0.2877	0.2847	0.2822	0.2792	0.2780	0.2736	0.2720	0.2637
Proportion of Variance	0.0003	0.0003	0.0003	0.0003	0.0003	0.0003	0.0002	0.0002	0.0002	0.0002	0.0002
Cumulative Proportion	0.9914	0.9917	0.9920	0.9922	0.9925	0.9927	0.9930	0.9932	0.9934	0.9937	0.9939
	PC144	PC145	PC146	PC147	PC148	PC149	PC150	PC151	PC152	PC153	PC154
Standard Deviation	0.2568	0.2563	0.2530	0.2458	0.2439	0.2383	0.2336	0.2315	0.2269	0.2217	0.2199
Proportion of Variance	0.0002	0.0002	0.0002	0.0002	0.0002	0.0002	0.0002	0.0002	0.0002	0.0002	0.0002
Cumulative Proportion	0.9941	0.9943	0.9945	0.9947	0.9949	0.9950	0.9952	0.9954	0.9955	0.9957	0.9958
	PC155	PC156	PC157	PC158	PC159	PC160	PC161	PC162	PC163	PC164	PC165
Standard Deviation	0.2172	0.2147	0.2101	0.2046	0.2044	0.2039	0.1994	0.1944	0.1919	0.1908	0.1841
Proportion of Variance	0.0002	0.0001	0.0001	0.0001	0.0001	0.0001	0.0001	0.0001	0.0001	0.0001	0.0001
Cumulative Proportion	0.9960	0.9961	0.9963	0.9964	0.9965	0.9966	0.9968	0.9969	0.9970	0.9971	0.9972
	PC166	PC167	PC168	PC169	PC170	PC171	PC172	PC173	PC174	PC175	PC176
Standard Deviation	0.1828	0.1783	0.1714	0.1695	0.1681	0.1609	0.1587	0.1544	0.1508	0.1497	0.1469
Proportion of Variance	0.0001	0.0001	0.0001	0.0001	0.0001	0.0001	0.0001	0.0001	0.0001	0.0001	0.0001
Cumulative Proportion	0.9973	0.9974	0.9975	0.9976	0.9977	0.9978	0.9978	0.9979	0.9980	0.9981	0.9981
	PC177	PC178	PC179	PC180	PC181	PC182	PC183	PC184	PC185	PC186	PC187
Standard Deviation	0.1442	0.1431	0.1408	0.1365	0.1348	0.1332	0.1296	0.1278	0.1259	0.1241	0.1226

Proportion of Variance	0.0001	0.0001	0.0001	0.0001	0.0001	0.0001	0.0001	0.0001	0.0001	0.0001	0.0001
Cumulative Proportion	0.9982	0.9983	0.9983	0.9984	0.9984	0.9985	0.9985	0.9986	0.9986	0.9987	0.9987
	PC188	PC189	PC190	PC191	PC192	PC193	PC194	PC195	PC196	PC197	PC198
Standard Deviation	0.1208	0.1195	0.1177	0.1171	0.1142	0.1118	0.1095	0.1078	0.1073	0.1056	0.1043
Proportion of Variance	0.0001	0.0000	0.0000	0.0000	0.0000	0.0000	0.0000	0.0000	0.0000	0.0000	0.0000
Cumulative Proportion	0.9988	0.9988	0.9989	0.9989	0.9989	0.9990	0.9990	0.9991	0.9991	0.9991	0.9992
	PC199	PC200	PC201	PC202	PC203	PC204	PC205	PC206	PC207	PC208	PC209
Standard Deviation	0.1012	0.0998	0.0993	0.0966	0.0951	0.0925	0.0921	0.0907	0.0886	0.0872	0.0860
Proportion of Variance	0.0000	0.0000	0.0000	0.0000	0.0000	0.0000	0.0000	0.0000	0.0000	0.0000	0.0000
Cumulative Proportion	0.9992	0.9992	0.9993	0.9993	0.9993	0.9993	0.9994	0.9994	0.9994	0.9994	0.9995
	PC210	PC211	PC212	PC213	PC214	PC215	PC216	PC217	PC218	PC219	PC220
Standard Deviation	0.0837	0.0832	0.0821	0.0811	0.0807	0.0787	0.0779	0.0762	0.0757	0.0739	0.0717
Proportion of Variance	0.0000	0.0000	0.0000	0.0000	0.0000	0.0000	0.0000	0.0000	0.0000	0.0000	0.0000
Cumulative Proportion	0.9995	0.9995	0.9995	0.9995	0.9996	0.9996	0.9996	0.9996	0.9996	0.9997	0.9997
	PC221	PC222	PC223	PC224	PC225	PC226	PC227	PC228	PC229	PC230	PC231
Standard Deviation	0.0699	0.0696	0.0693	0.0688	0.0667	0.0654	0.0647	0.0621	0.0600	0.0595	0.0584
Proportion of Variance	0.0000	0.0000	0.0000	0.0000	0.0000	0.0000	0.0000	0.0000	0.0000	0.0000	0.0000
Cumulative Proportion	0.9997	0.9997	0.9997	0.9997	0.9997	0.9998	0.9998	0.9998	0.9998	0.9998	0.9998
	PC232	PC233	PC234	PC235	PC236	PC237	PC238	PC239	PC240	PC241	PC242
Standard Deviation	0.0578	0.0567	0.0564	0.0537	0.0530	0.0514	0.0505	0.0501	0.0493	0.0479	0.0456
Proportion of Variance	0.0000	0.0000	0.0000	0.0000	0.0000	0.0000	0.0000	0.0000	0.0000	0.0000	0.0000
Cumulative Proportion	0.9998	0.9998	0.9998	0.9999	0.9999	0.9999	0.9999	0.9999	0.9999	0.9999	0.9999
	PC243	PC244	PC245	PC246	PC247	PC248	PC249	PC250	PC251	PC252	PC253
Standard Deviation	0.0445	0.0421	0.0416	0.0403	0.0393	0.0369	0.0360	0.0352	0.0341	0.0319	0.0311
Proportion of Variance	0.0000	0.0000	0.0000	0.0000	0.0000	0.0000	0.0000	0.0000	0.0000	0.0000	0.0000
Cumulative Proportion	0.9999	0.9999	0.9999	0.9999	0.9999	0.9999	0.9999	0.9999	1.0000	1.0000	1.0000
	PC254	PC255	PC256	PC257	PC258	PC259	PC260	PC261	PC262	PC263	PC264
Standard Deviation	0.0308	0.0302	0.0293	0.0286	0.0271	0.0267	0.0253	0.0251	0.0238	0.0235	0.0233
Proportion of Variance	0.0000	0.0000	0.0000	0.0000	0.0000	0.0000	0.0000	0.0000	0.0000	0.0000	0.0000
Cumulative Proportion	1.0000	1.0000	1.0000	1.0000	1.0000	1.0000	1.0000	1.0000	1.0000	1.0000	1.0000
	PC265	PC266	PC267	PC268	PC269	PC270	PC271	PC272	PC273	PC274	PC275
Standard Deviation	0.0226	0.0219	0.0210	0.0209	0.0204	0.0197	0.0196	0.0188	0.0182	0.0175	0.0170
Proportion of Variance	0.0000	0.0000	0.0000	0.0000	0.0000	0.0000	0.0000	0.0000	0.0000	0.0000	0.0000

Cumulative Proportion	1.0000	1.0000	1.0000	1.0000	1.0000	1.0000	1.0000	1.0000	1.0000	1.0000	1.0000
	PC276	PC277	PC278	PC279	PC280	PC281	PC282	PC283	PC284	PC285	PC286
Standard Deviation	0.0160	0.0157	0.0152	0.0149	0.0138	0.0134	0.0128	0.0125	0.0120	0.0107	0.0102
Proportion of Variance	0.0000	0.0000	0.0000	0.0000	0.0000	0.0000	0.0000	0.0000	0.0000	0.0000	0.0000
Cumulative Proportion	1.0000	1.0000	1.0000	1.0000	1.0000	1.0000	1.0000	1.0000	1.0000	1.0000	1.0000
	PC287	PC288	PC289	PC290	PC291	PC292	PC293	PC294	PC295	PC296	
Standard Deviation	0.0095	0.0094	0.0088	0.0083	0.0081	0.0072	0.0071	0.0068	0.0063	0.0061	
Proportion of Variance	0.0000	0.0000	0.0000	0.0000	0.0000	0.0000	0.0000	0.0000	0.0000	0.0000	
Cumulative Proportion	1.0000	1.0000	1.0000	1.0000	1.0000	1.0000	1.0000	1.0000	1.0000	1.0000	
	PC297	PC298	PC299	PC300	PC301	PC302	PC303	PC304	PC305		
Standard Deviation	0.0060	0.0058	0.0055	0.0052	0.0049	0.0044	0.0043	0.0034	0.0032		
Proportion of Variance	0.0000	0.0000	0.0000	0.0000	0.0000	0.0000	0.0000	0.0000	0.0000		
Cumulative Proportion	1.0000	1.0000	1.0000	1.0000	1.0000	1.0000	1.0000	1.0000	1.0000		
	PC306	PC307	PC308	PC309	PC310	PC311	PC312	PC313	PC314		
Standard Deviation	0.0030	0.0028	0.0027	0.0026	0.0025	0.0024	0.0023	0.0022	0.0018		
Proportion of Variance	0.0000	0.0000	0.0000	0.0000	0.0000	0.0000	0.0000	0.0000	0.0000		
Cumulative Proportion	1.0000	1.0000	1.0000	1.0000	1.0000	1.0000	1.0000	1.0000	1.0000		
	PC315	PC316	PC317	PC318	PC319	PC320	PC321	PC322	PC323		
Standard Deviation	0.0015	0.0012	0.0011	0.0008	0.0008	0.0008	0.0006	0.0002	0.0002		
Proportion of Variance	0.0000	0.0000	0.0000	0.0000	0.0000	0.0000	0.0000	0.0000	0.0000		
Cumulative Proportion	1.0000	1.0000	1.0000	1.0000	1.0000	1.0000	1.0000	1.0000	1.0000		

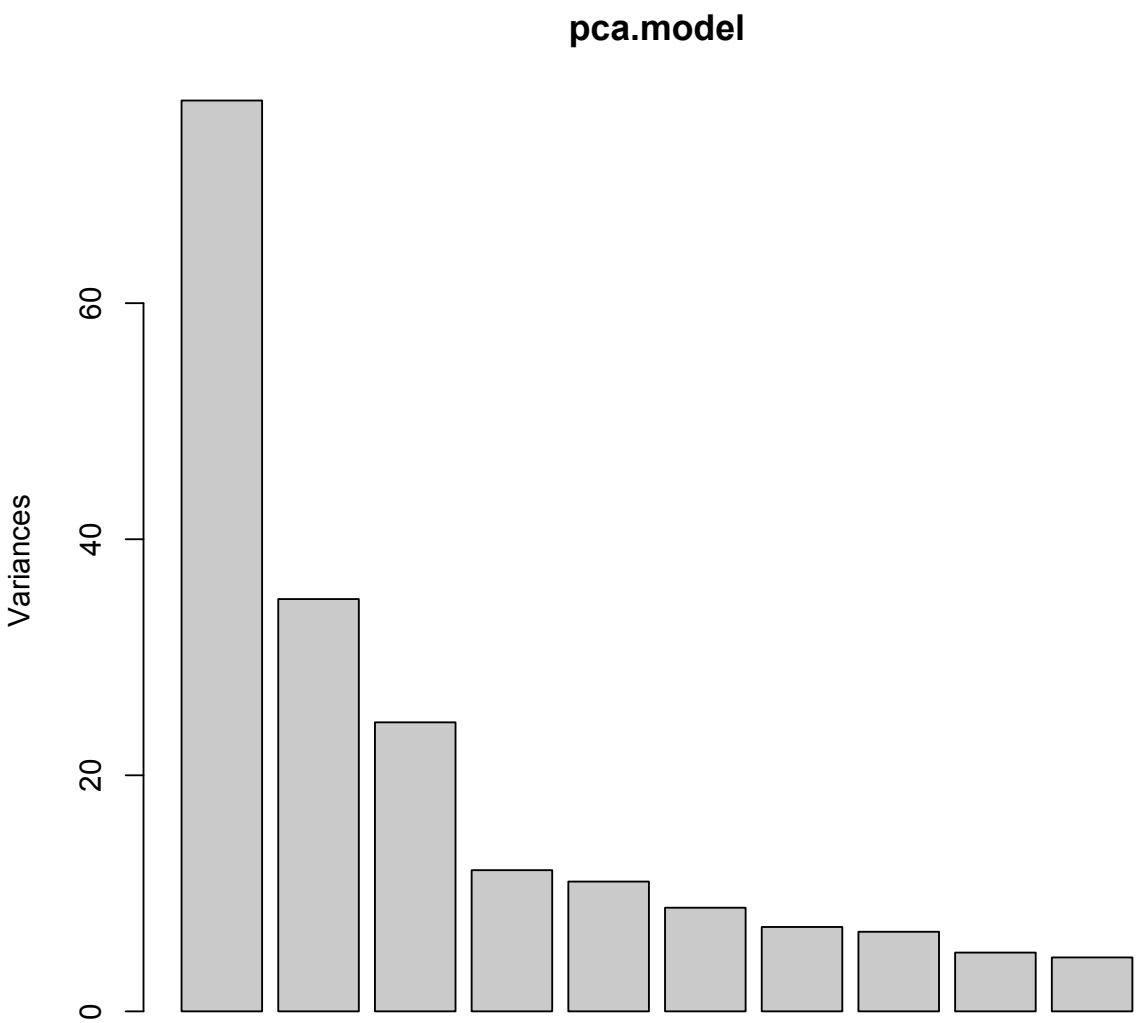


Figure 347: PCA scree plot for the set of 103 window glass second derivative (9-point smoothing) spectra (10 replicates), autoscaled.

APPENDIX XIII: HOO-CV PCA CVA RESULTS FOR CHEMOMETRIC ANALYSIS OF 153 SODA-LIME SILICATE GLASSES

Table 359: Discrimination error rates for HOO-CV with PCA reduced CVA for the set of 153 glass first derivative (5-point smoothing) spectra (10 replicates), autoscaled. The smallest PC dimension with the minimum error rate is highlighted in yellow.

PCs	Error Rate (%)	PCs	Error Rate (%)	PCs	Error Rate (%)	PCs	Error Rate (%)	PCs	Error Rate (%)
2	97.97	62	22.35	122	11.24	182	4.44	242	1.63
3	96.47	63	22.29	123	10.85	183	4.38	243	1.70
4	95.56	64	22.16	124	10.92	184	4.44	244	1.83
5	89.80	65	21.83	125	10.52	185	4.12	245	1.83
6	85.42	66	22.29	126	10.13	186	4.31	246	1.83
7	77.32	67	21.57	127	9.74	187	3.86	247	1.70
8	75.49	68	22.35	128	10.07	188	3.66	248	1.90
9	71.90	69	21.70	129	9.93	189	3.46	249	1.76
10	66.73	70	21.05	130	10.13	190	3.20	250	1.70
11	63.07	71	19.61	131	10.07	191	2.94	251	1.83
12	63.20	72	19.93	132	10.13	192	2.88	252	1.76
13	61.24	73	19.48	133	10.33	193	3.14	253	1.90
14	61.50	74	18.82	134	10.85	194	3.20	254	1.76
15	60.78	75	18.04	135	10.59	195	3.20	255	1.76
16	59.61	76	17.39	136	10.33	196	3.20	256	1.76
17	57.65	77	16.93	137	10.20	197	3.27	257	1.76
18	53.79	78	16.60	138	9.61	198	2.75	258	1.70
19	53.27	79	16.41	139	9.87	199	3.07	259	1.50
20	51.31	80	15.82	140	10.00	200	3.01	260	1.57
21	50.52	81	15.42	141	10.00	201	3.40	261	1.70
22	49.22	82	15.36	142	9.80	202	3.40	262	1.50
23	48.04	83	15.29	143	10.00	203	3.07	263	1.44
24	46.01	84	15.03	144	9.74	204	3.20	264	1.50
25	44.44	85	14.05	145	9.74	205	3.20	265	1.24
26	43.99	86	14.05	146	9.80	206	3.20	266	1.31
27	43.53	87	14.12	147	9.54	207	2.68	267	1.37
28	41.76	88	13.73	148	9.22	208	2.75	268	1.44
29	40.65	89	13.59	149	9.08	209	2.55	269	1.44
30	40.33	90	13.27	150	8.82	210	2.55	270	1.50
31	39.67	91	13.33	151	8.82	211	2.61	271	1.44
32	38.50	92	13.01	152	9.08	212	2.81	272	1.44
33	39.15	93	12.88	153	9.28	213	2.81	273	1.31
34	36.86	94	12.55	154	9.48	214	2.75	274	1.31

35	36.80	95	12.75	155	9.54	215	2.68	275	1.31
36	36.67	96	12.48	156	9.22	216	2.48	276	1.31
37	36.27	97	12.42	157	9.02	217	2.48	277	1.31
38	34.90	98	12.81	158	9.02	218	2.35	278	1.24
39	34.25	99	12.81	159	8.63	219	2.22	279	1.24
40	33.99	100	12.55	160	8.82	220	2.03	280	1.24
41	33.27	101	12.16	161	8.24	221	1.96	281	1.31
42	31.63	102	12.03	162	8.24	222	2.09	282	1.11
43	31.50	103	12.09	163	7.84	223	2.03	283	1.05
44	30.98	104	12.09	164	8.04	224	2.03	284	1.11
45	30.20	105	12.42	165	7.97	225	2.03	285	1.31
46	29.54	106	12.42	166	8.10	226	2.16	286	1.37
47	28.82	107	12.35	167	8.04	227	2.09	287	1.44
48	28.10	108	12.68	168	7.52	228	2.09	288	1.44
49	27.84	109	12.22	169	7.65	229	2.16	289	1.37
50	27.58	110	11.90	170	7.45	230	1.96	290	1.37
51	26.60	111	11.83	171	7.39	231	1.83	291	1.50
52	25.75	112	11.96	172	7.19	232	1.83	292	1.57
53	25.49	113	11.63	173	6.80	233	1.96	293	1.57
54	25.62	114	11.57	174	6.54	234	1.83	294	1.50
55	25.49	115	11.70	175	4.90	235	1.83	295	1.50
56	24.51	116	11.50	176	4.44	236	1.83	296	1.50
57	23.73	117	11.37	177	4.44	237	1.96	297	1.37
58	24.64	118	11.44	178	4.51	238	1.76	298	1.37
59	23.27	119	11.50	179	4.38	239	1.76	299	1.44
60	22.42	120	11.18	180	4.31	240	1.83	300	1.50
61	22.42	121	11.05	181	4.31	241	1.70	301	1.44

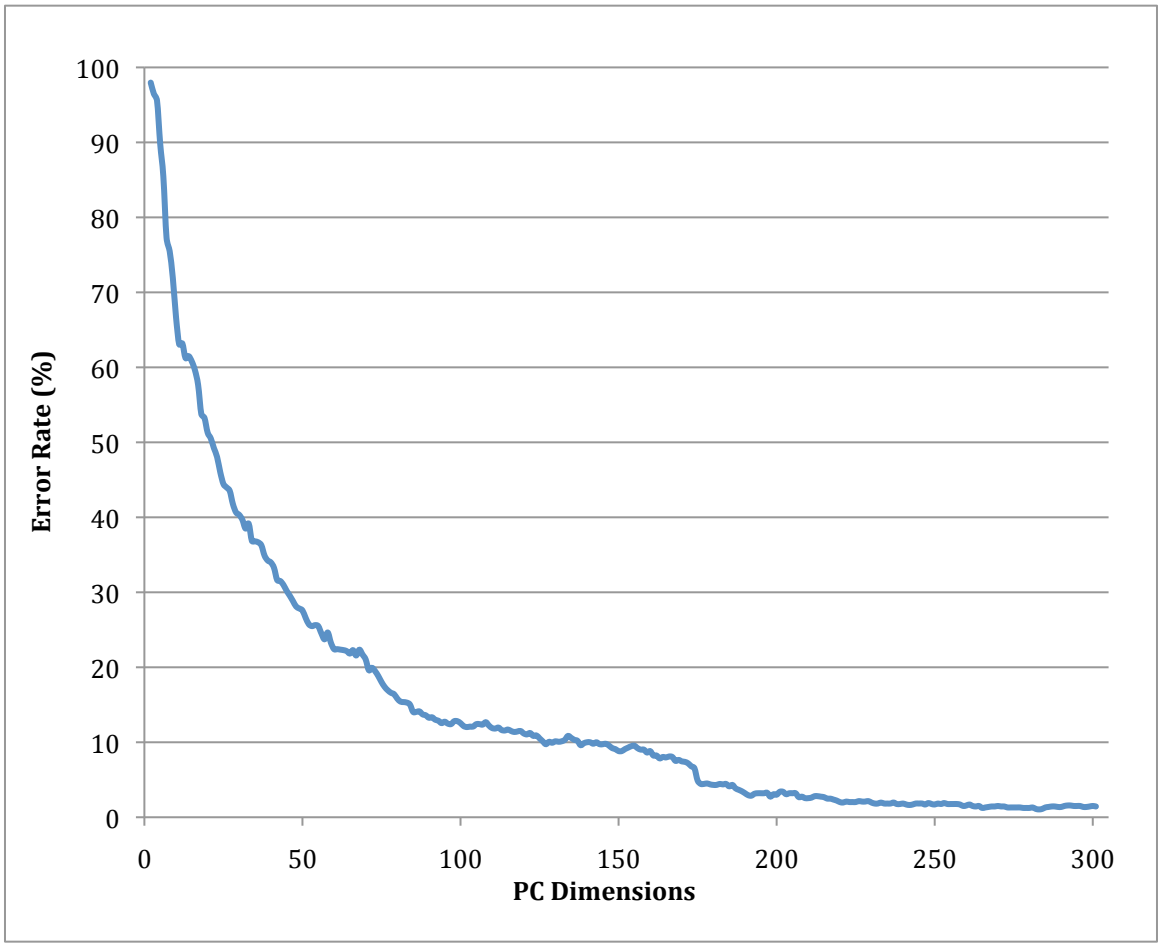


Figure 348: Graph of the discrimination error rate versus PC dimensions for HOO-CV with PCA reduced CVA for the set of 153 glass first derivative (5-point smoothing) spectra (10 replicates), autoscaled.

Table 360: Discrimination error rates for HOO-CV with PCA reduced CVA for the set of 103 window glass first derivative (5-point smoothing) spectra (10 replicates), autoscaled. The smallest PC dimension with the minimum error rate is highlighted in yellow.

PCs	Error Rate (%)	PCs	Error Rate (%)	PCs	Error Rate (%)	PCs	Error Rate (%)	PCs	Error Rate (%)
2	98.83	62	23.50	122	11.17	182	4.95	242	1.65
3	97.86	63	23.30	123	11.46	183	5.05	243	1.65
4	96.80	64	23.01	124	11.36	184	5.15	244	1.75
5	91.75	65	21.94	125	11.07	185	5.24	245	1.75
6	87.96	66	21.94	126	10.78	186	5.44	246	1.75
7	87.28	67	20.39	127	11.07	187	4.08	247	1.75
8	84.56	68	20.10	128	10.68	188	3.88	248	1.84
9	74.08	69	19.90	129	10.78	189	4.17	249	1.84
10	69.81	70	20.00	130	10.87	190	4.08	250	1.84
11	65.15	71	17.67	131	10.78	191	4.08	251	1.75
12	66.12	72	17.48	132	11.17	192	3.79	252	1.84
13	64.17	73	16.80	133	10.87	193	3.88	253	1.94
14	62.52	74	16.31	134	10.68	194	3.40	254	1.84
15	60.10	75	15.83	135	10.97	195	3.69	255	1.75
16	59.51	76	16.21	136	10.49	196	3.79	256	1.75
17	58.64	77	15.53	137	10.10	197	3.69	257	1.75
18	58.25	78	15.44	138	9.81	198	3.50	258	1.75
19	56.12	79	14.95	139	10.19	199	3.30	259	1.75
20	54.27	80	15.15	140	10.00	200	3.30	260	1.75
21	54.47	81	14.66	141	10.39	201	3.30	261	1.75
22	51.55	82	14.56	142	10.00	202	2.91	262	1.75
23	49.81	83	14.66	143	10.19	203	3.20	263	1.94
24	49.71	84	14.66	144	10.00	204	3.01	264	1.75
25	48.35	85	13.98	145	9.42	205	2.91	265	1.75
26	47.09	86	13.79	146	9.22	206	2.82	266	1.94
27	46.41	87	13.98	147	8.74	207	2.91	267	1.94
28	45.05	88	13.98	148	8.83	208	2.82	268	2.14
29	46.02	89	13.40	149	8.54	209	2.82	269	2.23
30	44.17	90	13.79	150	8.45	210	3.01	270	2.23
31	43.59	91	13.40	151	8.83	211	2.82	271	2.33
32	43.30	92	13.11	152	8.64	212	2.62	272	2.33
33	40.68	93	12.91	153	8.74	213	2.62	273	2.33
34	41.26	94	13.50	154	8.25	214	2.72	274	2.23
35	40.49	95	13.30	155	8.45	215	2.43	275	2.23
36	39.71	96	12.52	156	8.35	216	2.33	276	2.23
37	39.61	97	12.72	157	8.25	217	2.43	277	2.23
38	39.42	98	12.62	158	8.16	218	2.72	278	2.33

39	36.60	99	12.43	159	7.86	219	2.82	279	2.33
40	35.63	100	12.82	160	8.25	220	2.72	280	2.33
41	35.53	101	12.52	161	7.96	221	2.43	281	2.23
42	34.08	102	12.33	162	7.96	222	2.33	282	1.94
43	33.88	103	12.04	163	8.06	223	2.52	283	1.84
44	32.91	104	12.14	164	7.38	224	2.33	284	1.75
45	30.97	105	11.46	165	7.28	225	2.43	285	2.04
46	32.14	106	11.65	166	7.18	226	2.23	286	2.04
47	31.36	107	12.04	167	7.18	227	2.33	287	1.94
48	30.49	108	11.94	168	7.38	228	2.23	288	1.84
49	29.51	109	11.65	169	6.99	229	2.14	289	1.94
50	29.22	110	11.94	170	7.09	230	2.04	290	1.84
51	27.48	111	11.55	171	7.09	231	2.23	291	1.84
52	27.28	112	11.17	172	7.18	232	2.14	292	1.84
53	26.80	113	10.97	173	6.60	233	2.04	293	1.75
54	26.50	114	10.97	174	6.80	234	2.04	294	1.75
55	26.50	115	10.78	175	6.70	235	2.04	295	1.75
56	26.41	116	10.87	176	6.60	236	2.04	296	1.84
57	25.05	117	10.10	177	5.83	237	2.04	297	1.84
58	25.24	118	10.58	178	5.92	238	2.04	298	1.84
59	25.15	119	10.58	179	5.24	239	2.04	299	2.04
60	24.95	120	10.78	180	5.05	240	1.94	300	1.94
61	24.37	121	10.78	181	5.05	241	1.65		

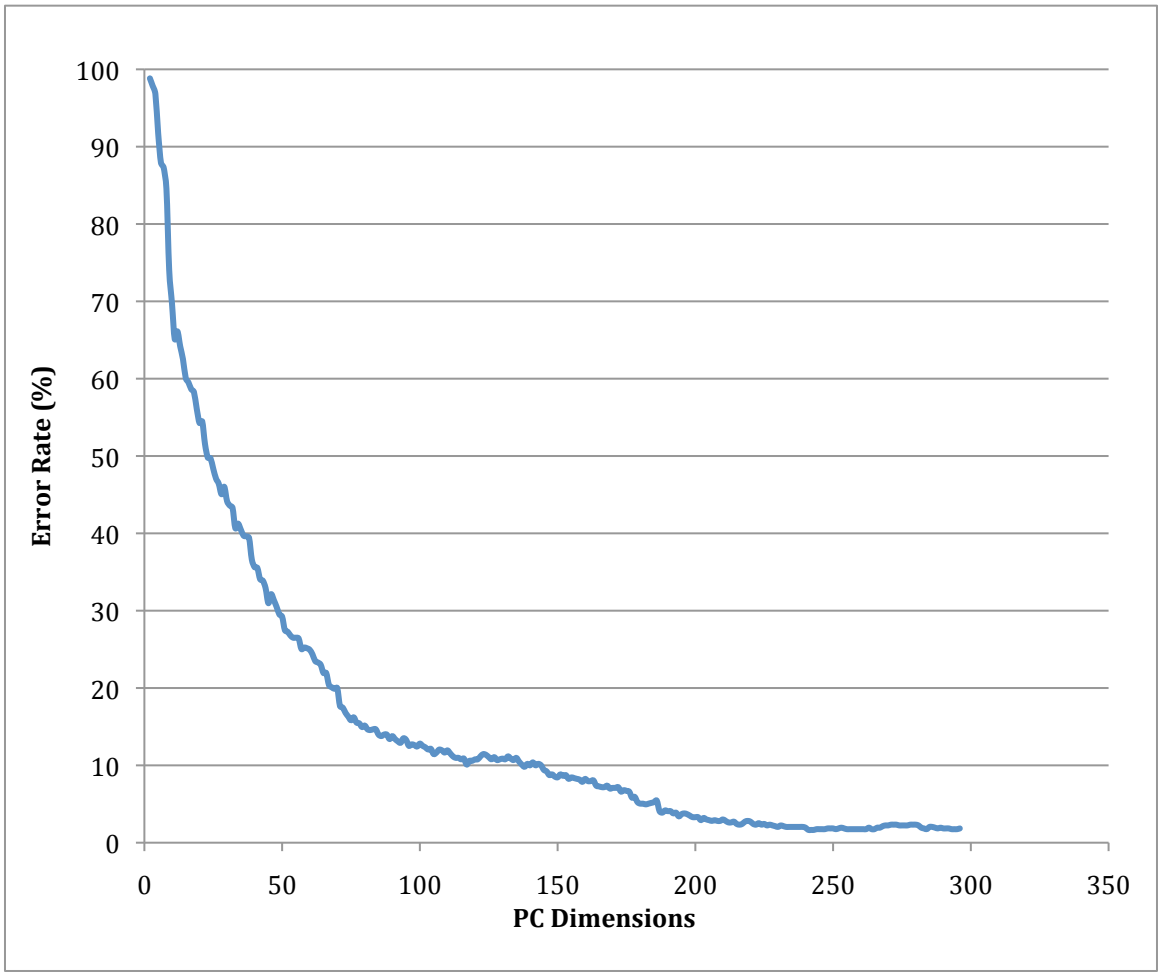


Figure 349: Graph of the discrimination error rate versus PC dimensions for HOO-CV with PCA reduced CVA for the set of 103 window glass first derivative (5-point smoothing) spectra (10 replicates), autoscaled.

Table 361: Discrimination error rates for HOO-CV with PCA reduced CVA for the set of 50 container glass first derivative (5-point smoothing) spectra (10 replicates), autoscaled. The smallest PC dimension with the minimum error rate is highlighted in yellow.

PCs	Error Rate (%)	PCs	Error Rate (%)	PCs	Error Rate (%)	PCs	Error Rate (%)	PCs	Error Rate (%)
2	92.00	66	14.00	130	7.80	194	3.40	258	2.00
3	90.40	67	13.40	131	7.60	195	3.20	259	2.00
4	90.00	68	13.20	132	7.80	196	3.00	260	2.20
5	80.40	69	12.20	133	8.00	197	3.00	261	2.20
6	75.20	70	12.40	134	7.40	198	3.20	262	2.40
7	73.80	71	12.20	135	7.60	199	3.20	263	2.40
8	66.40	72	12.20	136	7.00	200	3.00	264	2.60
9	61.80	73	11.80	137	7.00	201	3.60	265	2.40
10	58.40	74	11.40	138	7.20	202	3.60	266	2.20
11	57.00	75	11.80	139	7.00	203	3.60	267	2.00
12	51.00	76	11.40	140	7.00	204	3.20	268	1.60
13	50.80	77	11.80	141	6.80	205	3.20	269	1.60
14	50.20	78	11.40	142	6.80	206	3.40	270	2.00
15	48.40	79	11.80	143	6.80	207	3.40	271	2.20
16	48.40	80	11.60	144	7.40	208	3.20	272	2.20
17	47.80	81	9.80	145	7.20	209	2.80	273	2.20
18	43.00	82	9.00	146	6.80	210	3.80	274	2.20
19	43.20	83	8.80	147	6.20	211	3.60	275	2.20
20	40.60	84	8.80	148	6.20	212	3.20	276	2.20
21	39.40	85	9.00	149	6.80	213	3.20	277	1.80
22	37.40	86	8.80	150	6.60	214	2.60	278	1.80
23	34.00	87	8.60	151	6.40	215	2.60	279	1.60
24	32.80	88	7.40	152	6.20	216	2.40	280	1.60
25	31.40	89	8.20	153	6.00	217	2.20	281	1.80
26	29.60	90	8.60	154	5.80	218	2.60	282	1.80
27	29.40	91	8.40	155	6.20	219	2.80	283	1.80
28	28.60	92	8.00	156	6.60	220	2.40	284	2.20
29	27.40	93	7.80	157	6.80	221	2.60	285	2.00
30	27.00	94	7.80	158	6.80	222	2.20	286	2.20
31	25.80	95	7.00	159	6.00	223	2.40	287	2.20
32	25.40	96	7.40	160	5.60	224	2.20	288	2.80
33	23.40	97	7.80	161	5.80	225	1.80	289	2.60
34	23.00	98	7.20	162	5.60	226	2.20	290	2.80
35	21.40	99	7.60	163	5.60	227	1.80	291	2.80
36	20.00	100	6.80	164	5.00	228	1.80	292	2.80
37	19.20	101	7.60	165	5.40	229	2.00	293	2.40
38	19.80	102	9.00	166	5.40	230	1.80	294	3.00
39	18.80	103	9.00	167	5.40	231	2.20	295	3.00
40	18.60	104	9.80	168	5.40	232	2.00	296	3.20
41	18.20	105	9.80	169	5.80	233	2.00	297	3.40
42	17.80	106	9.60	170	6.00	234	1.80	298	3.40

43	17.80	107	9.60	171	6.00	235	1.80	299	3.40
44	18.20	108	9.40	172	5.60	236	1.80	300	3.00
45	17.20	109	9.20	173	5.00	237	1.80	301	3.20
46	16.80	110	8.40	174	4.80	238	1.80	302	3.20
47	16.20	111	8.80	175	4.60	239	1.60	303	3.60
48	15.40	112	8.80	176	4.80	240	1.80	304	3.40
49	15.00	113	8.60	177	4.60	241	1.60	305	3.80
50	14.20	114	8.40	178	4.40	242	1.60	306	3.40
51	14.40	115	8.00	179	4.00	243	2.00	307	3.00
52	13.40	116	7.80	180	3.80	244	1.80	308	2.80
53	13.60	117	7.80	181	3.80	245	1.20	309	2.60
54	13.20	118	7.80	182	3.60	246	1.40	310	2.40
55	13.00	119	8.00	183	3.40	247	1.40	311	2.40
56	12.40	120	7.80	184	3.80	248	1.60	312	2.40
57	13.40	121	7.80	185	3.20	249	1.60	313	2.40
58	13.80	122	8.00	186	3.20	250	1.80	314	2.40
59	13.80	123	8.60	187	3.20	251	2.00	315	2.40
60	13.80	124	8.40	188	3.20	252	2.00	316	2.60
61	13.60	125	8.40	189	3.60	253	1.80	317	2.60
62	14.00	126	8.20	190	3.60	254	2.00	318	2.40
63	13.40	127	8.60	191	3.80	255	2.20		
64	13.40	128	8.60	192	3.80	256	1.80		
65	13.00	129	7.60	193	3.80	257	2.00		

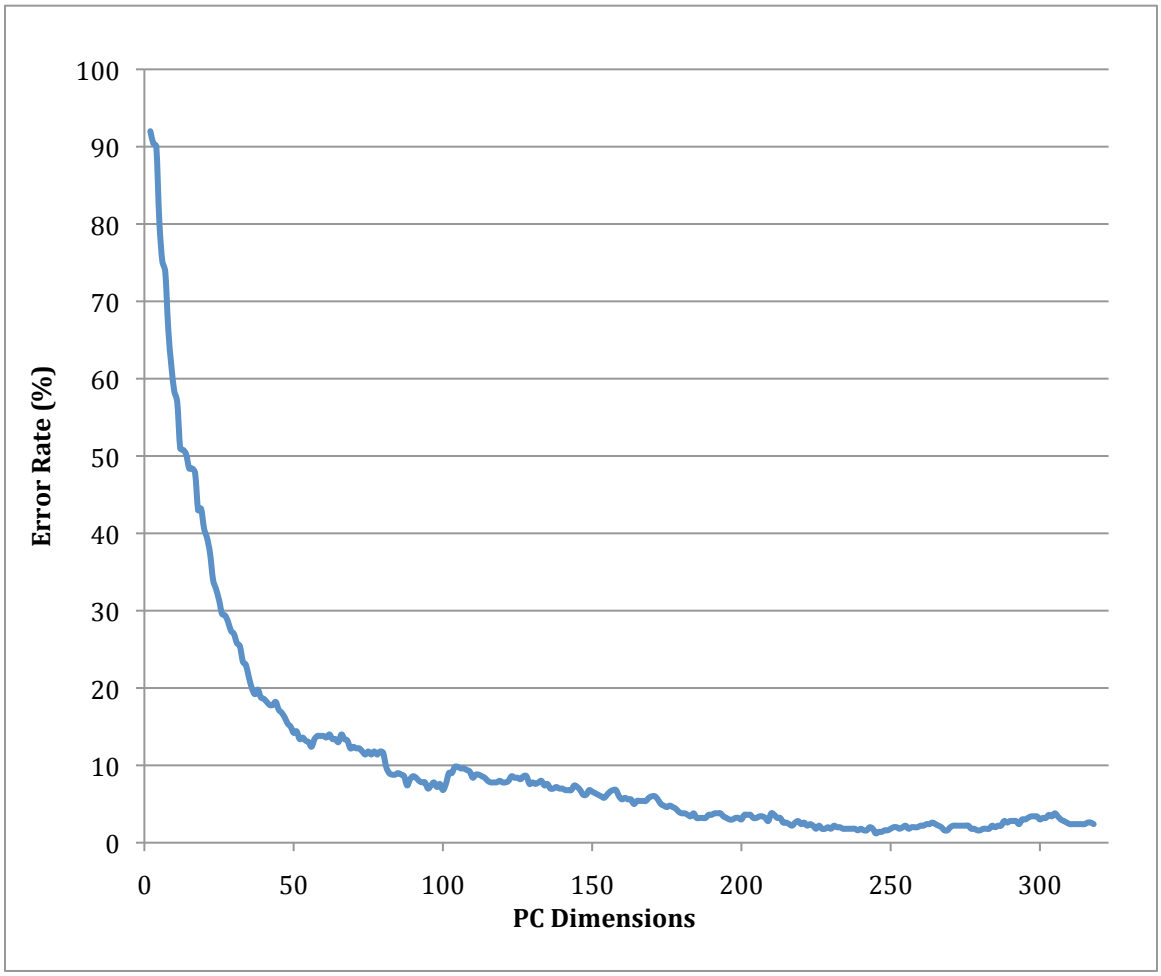


Figure 350: Graph of the discrimination error rate versus PC dimensions for HOO-CV with PCA reduced CVA for the set of 50 container glass first derivative (5-point smoothing) spectra (10 replicates), autoscaled.

Table 362: Discrimination error rates for HOO-CV with PCA reduced CVA for the set of 153 glass first derivative (9-point smoothing) spectra (10 replicates), autoscaled. The smallest PC dimension with the minimum error rate is highlighted in yellow.

PCs	Error Rate (%)	PCs	Error Rate (%)	PCs	Error Rate (%)	PCs	Error Rate (%)	PCs	Error Rate (%)
2	27.58	42	2.29	82	1.96	122	1.76	162	1.83
3	27.19	43	2.42	83	1.96	123	1.83	163	1.83
4	13.79	44	2.35	84	1.90	124	1.83	164	1.83
5	5.03	45	2.35	85	1.96	125	1.90	165	1.96
6	5.16	46	2.35	86	1.96	126	1.90	166	1.90
7	4.38	47	2.16	87	1.96	127	1.90	167	1.96
8	5.03	48	2.16	88	1.96	128	2.03	168	2.09
9	4.77	49	2.22	89	2.09	129	2.09	169	2.09
10	4.38	50	2.09	90	2.03	130	2.09	170	2.16
11	4.71	51	2.22	91	2.03	131	2.09	171	2.16
12	3.59	52	2.22	92	2.03	132	2.09	172	2.16
13	3.33	53	2.29	93	2.03	133	2.09	173	2.09
14	3.66	54	1.83	94	2.03	134	1.96	174	2.03
15	3.79	55	1.83	95	1.96	135	1.83	175	2.09
16	3.79	56	1.90	96	2.03	136	1.90	176	2.16
17	3.86	57	2.09	97	1.90	137	2.03	177	2.16
18	3.86	58	2.03	98	1.90	138	1.83	178	2.22
19	3.66	59	2.09	99	1.83	139	1.83	179	2.16
20	3.07	60	2.03	100	1.90	140	1.83	180	2.22
21	3.07	61	2.09	101	1.83	141	1.96	181	2.22
22	3.01	62	1.96	102	1.90	142	1.96	182	2.16
23	2.75	63	2.09	103	1.96	143	2.03	183	2.16
24	2.81	64	2.09	104	2.03	144	1.96	184	2.29
25	2.88	65	2.16	105	1.90	145	1.96	185	2.16
26	2.88	66	1.83	106	1.83	146	1.96	186	2.29
27	2.88	67	1.83	107	1.83	147	2.03	187	2.35
28	2.81	68	1.83	108	1.83	148	2.03	188	2.42
29	2.61	69	1.90	109	1.83	149	2.09	189	2.35
30	2.81	70	1.83	110	1.90	150	2.09	190	2.35
31	2.81	71	1.83	111	1.76	151	2.09	191	2.35
32	2.75	72	1.83	112	1.76	152	2.16	192	2.22
33	2.75	73	1.83	113	1.90	153	2.09	193	2.29
34	2.88	74	2.09	114	1.76	154	2.09	194	2.29
35	2.42	75	2.09	115	1.70	155	2.16	195	2.22
36	2.42	76	2.09	116	1.76	156	2.22	196	2.29
37	2.48	77	2.22	117	1.83	157	2.22	197	2.22
38	2.48	78	2.09	118	1.83	158	2.22	198	2.22

39	2.55	79	2.03	119	1.83	159	2.22	199	2.22
40	2.42	80	2.03	120	1.83	160	2.29	200	2.16
41	2.48	81	2.03	121	1.83	161	2.29		

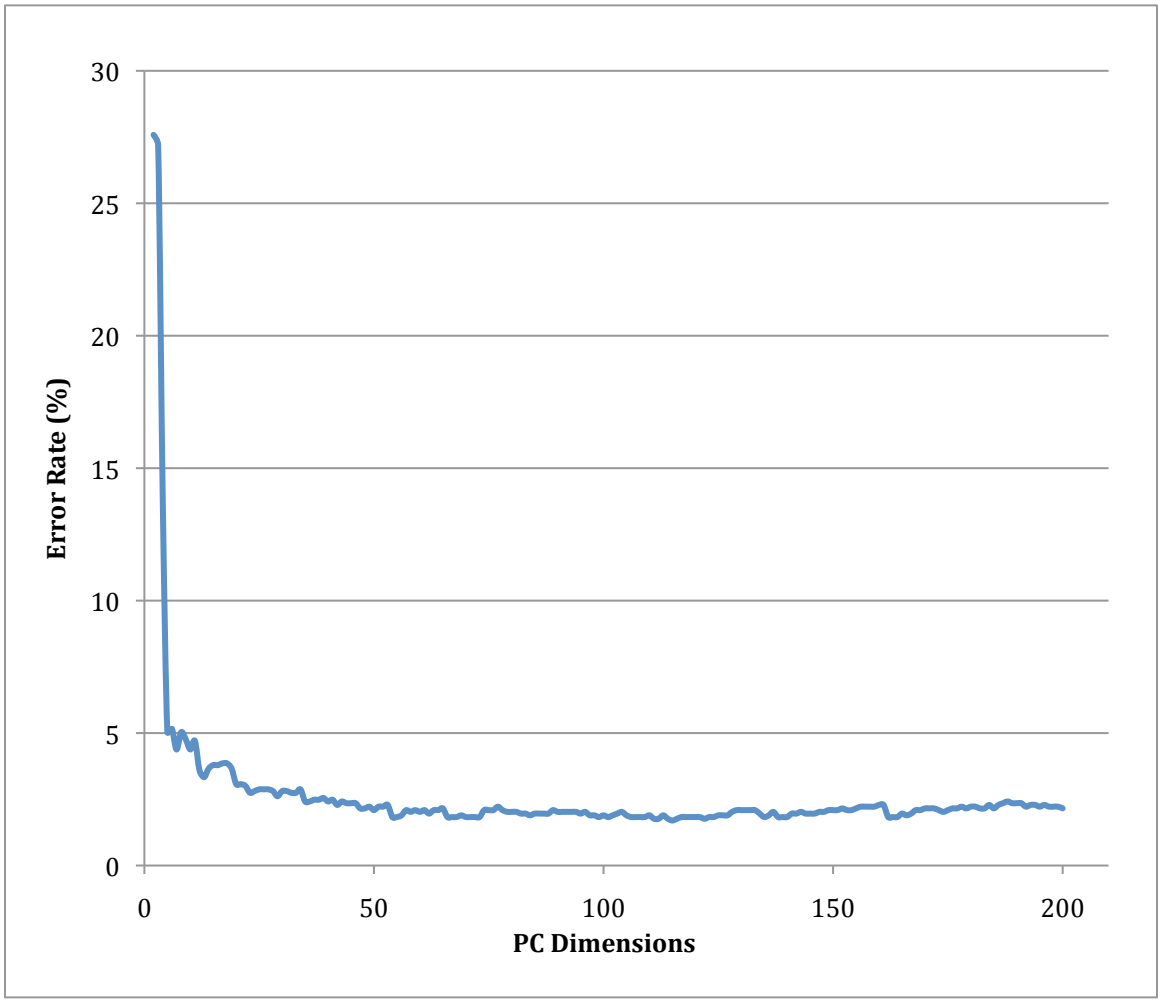


Figure 351: Graph of the discrimination error rate versus PC dimensions for HOO-CV with PCA reduced CVA for the set of 153 glass first derivative (9-point smoothing) spectra (10 replicates), autoscaled.

Table 363: Discrimination error rates for HOO-CV with PCA reduced CVA for the set of 153 glass second derivative (9-point smoothing) spectra (10 replicates), autoscaled. The smallest PC dimension with the minimum error rate is highlighted in yellow.

PCs	Error Rate (%)	PCs	Error Rate (%)	PCs	Error Rate (%)	PCs	Error Rate (%)	PCs	Error Rate (%)
2	20.20	43	2.61	84	2.29	125	2.09	166	2.35
3	18.50	44	2.61	85	2.29	126	2.16	167	2.35
4	9.22	45	2.61	86	2.22	127	2.16	168	2.35
5	9.74	46	2.61	87	2.16	128	2.03	169	2.35
6	8.56	47	2.61	88	2.29	129	2.03	170	2.29
7	5.03	48	2.61	89	2.09	130	2.22	171	2.22
8	4.38	49	2.55	90	2.09	131	2.22	172	2.22
9	4.51	50	2.68	91	2.22	132	2.29	173	2.22
10	4.31	51	2.48	92	2.22	133	2.22	174	2.22
11	3.99	52	2.75	93	2.22	134	2.22	175	2.29
12	3.99	53	2.55	94	2.09	135	2.22	176	2.22
13	4.05	54	2.42	95	2.22	136	2.29	177	2.22
14	4.18	55	2.42	96	2.16	137	2.35	178	2.22
15	4.18	56	2.55	97	2.16	138	2.35	179	2.29
16	3.86	57	2.48	98	2.09	139	2.42	180	2.29
17	3.86	58	2.48	99	2.16	140	2.42	181	2.29
18	4.05	59	2.22	100	1.96	141	2.16	182	2.29
19	3.99	60	2.22	101	2.03	142	2.16	183	2.16
20	3.99	61	2.29	102	1.96	143	2.22	184	2.16
21	3.92	62	2.29	103	1.96	144	2.22	185	2.03
22	3.99	63	2.29	104	1.96	145	2.29	186	2.09
23	3.92	64	2.29	105	2.03	146	2.29	187	2.22
24	3.92	65	2.29	106	1.96	147	2.29	188	2.16
25	3.86	66	2.22	107	1.96	148	2.29	189	2.16
26	3.79	67	2.22	108	2.03	149	2.22	190	2.09
27	3.46	68	2.42	109	2.03	150	2.29	191	2.03
28	3.46	69	2.42	110	2.03	151	2.29	192	2.16
29	3.46	70	2.35	111	2.16	152	2.35	193	2.16
30	3.46	71	2.42	112	2.16	153	2.35	194	2.22
31	3.46	72	2.35	113	2.03	154	2.35	195	2.03
32	3.46	73	2.35	114	2.09	155	2.35	196	2.09
33	3.01	74	2.55	115	2.22	156	2.35	197	2.09
34	3.20	75	2.48	116	2.09	157	2.35	198	2.09
35	2.94	76	2.48	117	2.09	158	2.35	199	2.09
36	2.88	77	2.48	118	2.09	159	2.35	200	2.22
37	2.94	78	2.48	119	2.03	160	2.35	201	2.16
38	2.88	79	2.55	120	1.90	161	2.48	202	2.22

39	2.55	80	2.55	121	1.96	162	2.48	203	2.22
40	2.48	81	2.48	122	2.03	163	2.42	204	2.22
41	2.48	82	2.42	123	2.03	164	2.42		
42	2.61	83	2.16	124	2.09	165	2.42		

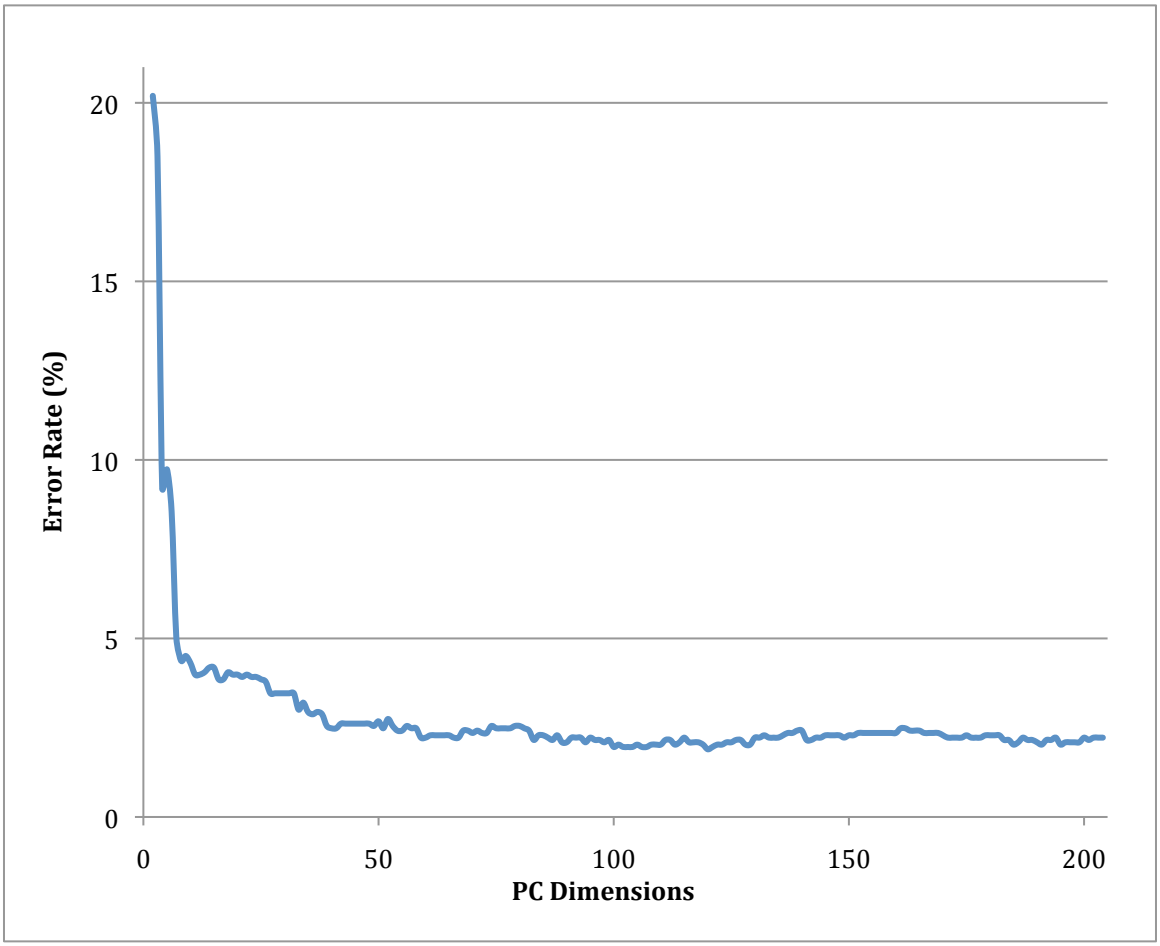


Figure 352: Graph of the discrimination error rate versus PC dimensions for HOO-CV with PCA reduced CVA for the set of 153 glass second derivative (9-point smoothing) spectra (10 replicates), autoscaled.

Table 364: Tempered classification error rates for HOO-CV with PCA reduced CVA for the set of 103 window glass second derivative (9-point smoothing) spectra (10 replicates), autoscaled. The smallest PC dimension with the minimum error rate is highlighted in yellow.

PCs	Error Rate (%)	PCs	Error Rate (%)	PCs	Error Rate (%)	PCs	Error Rate (%)	PCs	Error Rate (%)
2	34.27	43	29.03	84	27.67	125	24.47	166	20.19
3	33.01	44	28.74	85	27.67	126	23.59	167	20.68
4	33.59	45	28.54	86	27.86	127	24.37	168	20.58
5	33.79	46	28.64	87	27.86	128	23.69	169	20.68
6	32.14	47	28.16	88	27.57	129	23.88	170	20.68
7	30.97	48	27.67	89	27.28	130	24.08	171	20.68
8	30.19	49	27.67	90	28.16	131	23.98	172	20.78
9	30.19	50	27.57	91	27.38	132	23.69	173	20.87
10	30.39	51	27.77	92	27.48	133	24.08	174	20.00
11	31.17	52	27.67	93	27.57	134	24.17	175	20.39
12	30.87	53	27.67	94	26.12	135	24.76	176	20.68
13	30.87	54	27.96	95	26.41	136	24.66	177	20.97
14	30.87	55	27.38	96	26.02	137	23.69	178	20.97
15	31.36	56	27.48	97	26.12	138	23.40	179	21.17
16	29.90	57	27.57	98	26.60	139	23.59	180	20.49
17	30.39	58	27.86	99	26.50	140	23.30	181	20.58
18	30.10	59	27.86	100	26.31	141	22.82	182	20.29
19	30.00	60	27.57	101	26.60	142	23.01	183	20.68
20	29.81	61	27.48	102	26.50	143	22.04	184	20.00
21	29.81	62	27.48	103	26.80	144	22.82	185	19.81
22	29.71	63	27.38	104	26.70	145	22.43	186	19.61
23	30.10	64	27.48	105	26.31	146	22.43	187	19.90
24	29.61	65	27.38	106	26.12	147	22.33	188	19.32
25	29.90	66	27.96	107	26.02	148	22.33	189	19.51
26	29.22	67	28.16	108	25.53	149	21.94	190	19.13
27	29.61	68	27.09	109	25.63	150	21.84	191	19.03
28	28.93	69	28.25	110	25.63	151	21.94	192	18.83
29	29.51	70	28.35	111	24.56	152	22.04	193	18.83
30	30.00	71	27.96	112	24.17	153	22.33	194	19.13
31	30.10	72	27.96	113	24.56	154	22.43	195	19.51
32	30.19	73	27.96	114	24.66	155	22.23	196	19.81
33	30.19	74	28.06	115	25.44	156	21.46	197	20.00
34	30.39	75	28.83	116	25.63	157	21.65	198	20.19
35	30.49	76	27.86	117	25.24	158	21.55	199	19.90
36	30.10	77	28.35	118	25.15	159	21.36	200	20.00
37	30.00	78	28.54	119	25.24	160	21.75	201	20.19
38	29.22	79	28.16	120	25.24	161	21.75	202	20.19

39	29.42	80	28.16	121	25.24	162	20.29	203	20.49
40	29.42	81	28.16	122	24.17	163	20.10	204	20.58
41	29.71	82	28.35	123	24.27	164	20.39		
42	29.71	83	28.45	124	24.95	165	20.87		

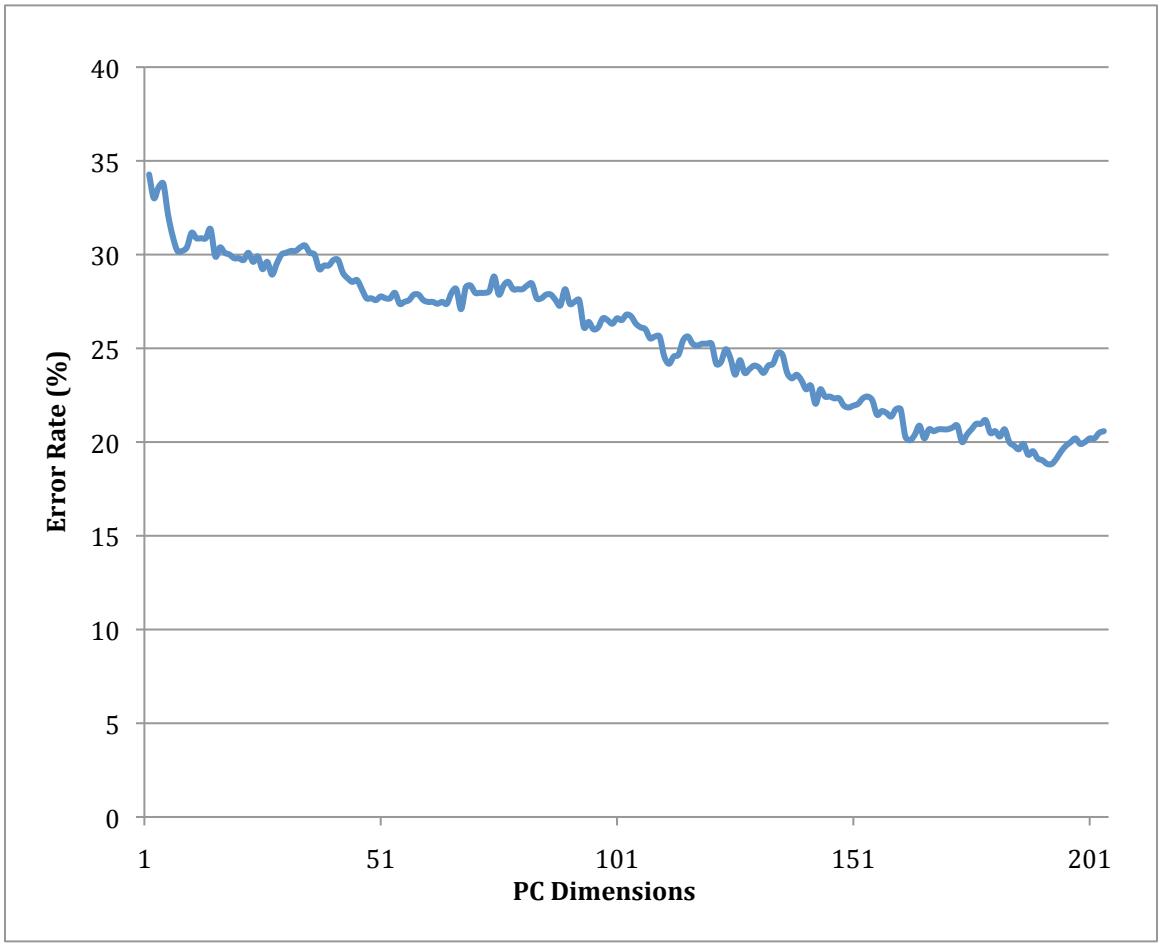


Figure 353: Graph of the tempered classification error rate versus PC dimensions for HOO-CV with PCA reduced CVA for the set of 103 window glass second derivative (9-point smoothing) spectra (10 replicates), autoscaled.

APPENDIX XIV: PCA RESULTS FOR CHEMOMETRIC ANALYSIS OF DECONVOLUTION DATA

Table 365: PCA results for the first set of 30 glass deconvolution data (10 replicates), no pretreatment.

Importance of components:						
	PC1	PC2	PC3	PC4	PC5	PC6
Standard deviation	2277.2045	50.27918	9.83936	8.59889	3.994	3.048
Proportion of Variance	0.9995	0.00049	0.00002	0.00001	0	0
Cumulative Proportion	0.9995	0.99996	0.99998	0.99999	1	1
	PC7	PC8	PC9	PC10	PC11	PC12
Standard deviation	2.579	2.111	1.328	1.249	0.9481	0.8865
Proportion of Variance	0	0	0	0	0	0
Cumulative Proportion	1	1	1	1	1	1

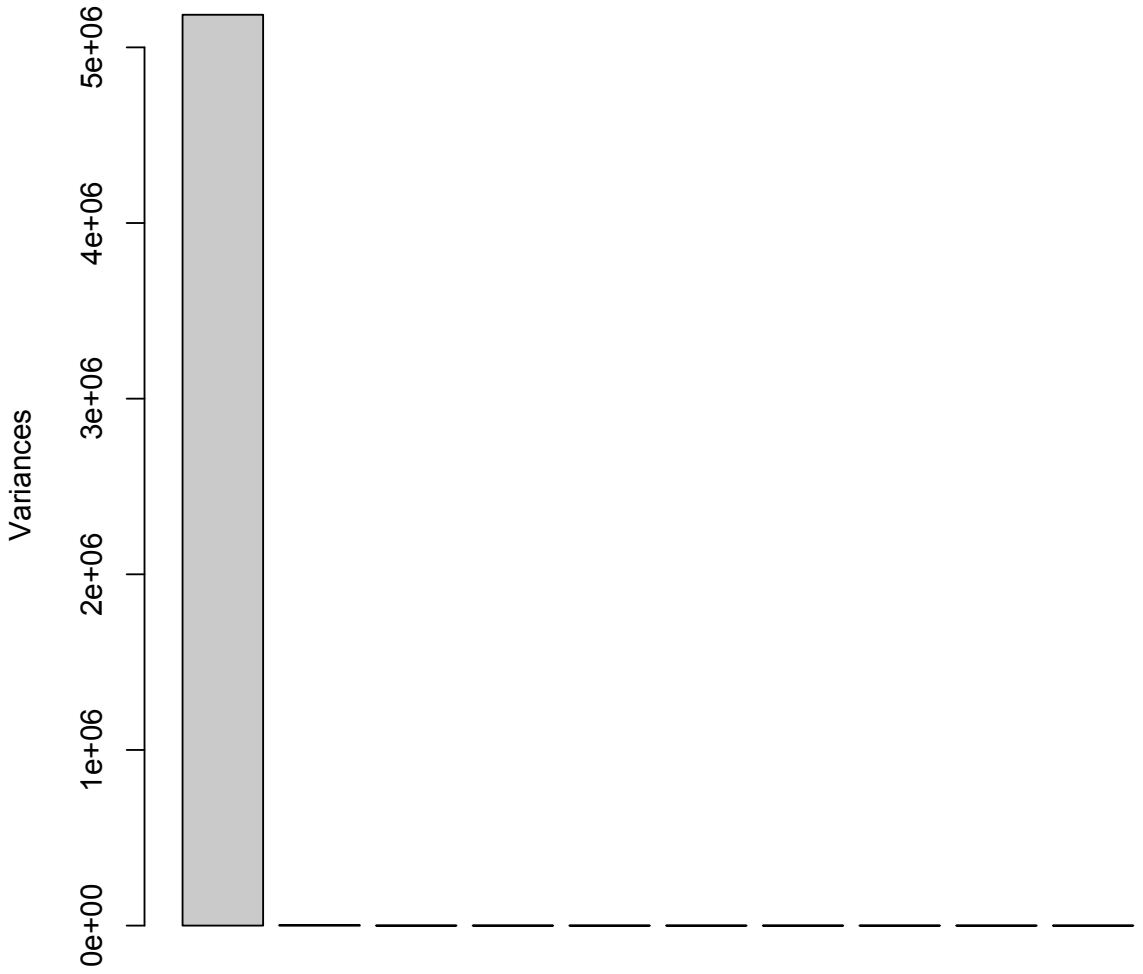


Figure 354: PCA scree plot for the first set of 30 glass deconvolution data (10 replicates), no pretreatment.

Table 366: PCA results for the first set of 30 glass deconvolution data (10 replicates), centered.

Importance of components:						
	PC1	PC2	PC3	PC4	PC5	PC6
Standard deviation	50.2913	9.84862	8.64732	4.9401	3.6771	2.9724
Proportion of Variance	0.9157	0.03512	0.02707	0.00884	0.0049	0.0032
Cumulative Proportion	0.9157	0.95085	0.97792	0.98676	0.9917	0.9949
	PC7	PC8	PC9	PC10	PC11	PC12
Standard deviation	2.3235	2.11068	1.29359	1.09252	0.9126	0.81988
Proportion of Variance	0.00195	0.00161	0.00061	0.00043	0.0003	0.00024
Cumulative Proportion	0.9968	0.99842	0.99902	0.99946	0.9998	1

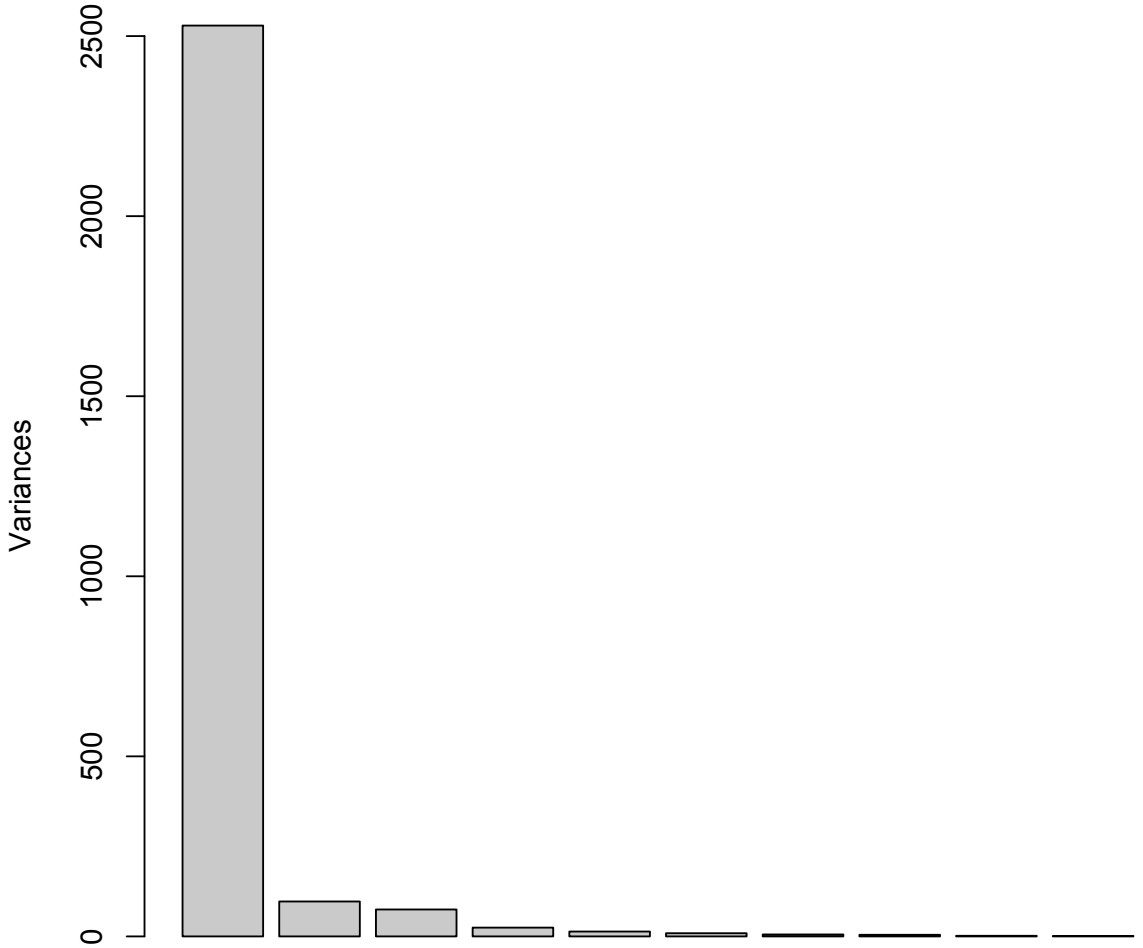


Figure 355: PCA scree plot for the first set of 30 glass deconvolution data (10 replicates), centered.

Table 367: PCA results for the first set of 30 glass deconvolution data (10 replicates), autoscaled.

Importance of components:						
	PC1	PC2	PC3	PC4	PC5	PC6
Standard deviation	2.0627	1.5696	1.2087	1.03584	0.91776	0.82297
Proportion of Variance	0.3545	0.2053	0.1218	0.08941	0.07019	0.05644
Cumulative Proportion	0.3545	0.5598	0.6816	0.77102	0.84121	0.89765
	PC7	PC8	PC9	PC10	PC11	PC12
Standard deviation	0.70641	0.5979	0.42818	0.31779	0.21964	0.19778
Proportion of Variance	0.04158	0.02979	0.01528	0.00842	0.00402	0.00326
Cumulative Proportion	0.93924	0.96903	0.9843	0.99272	0.99674	1

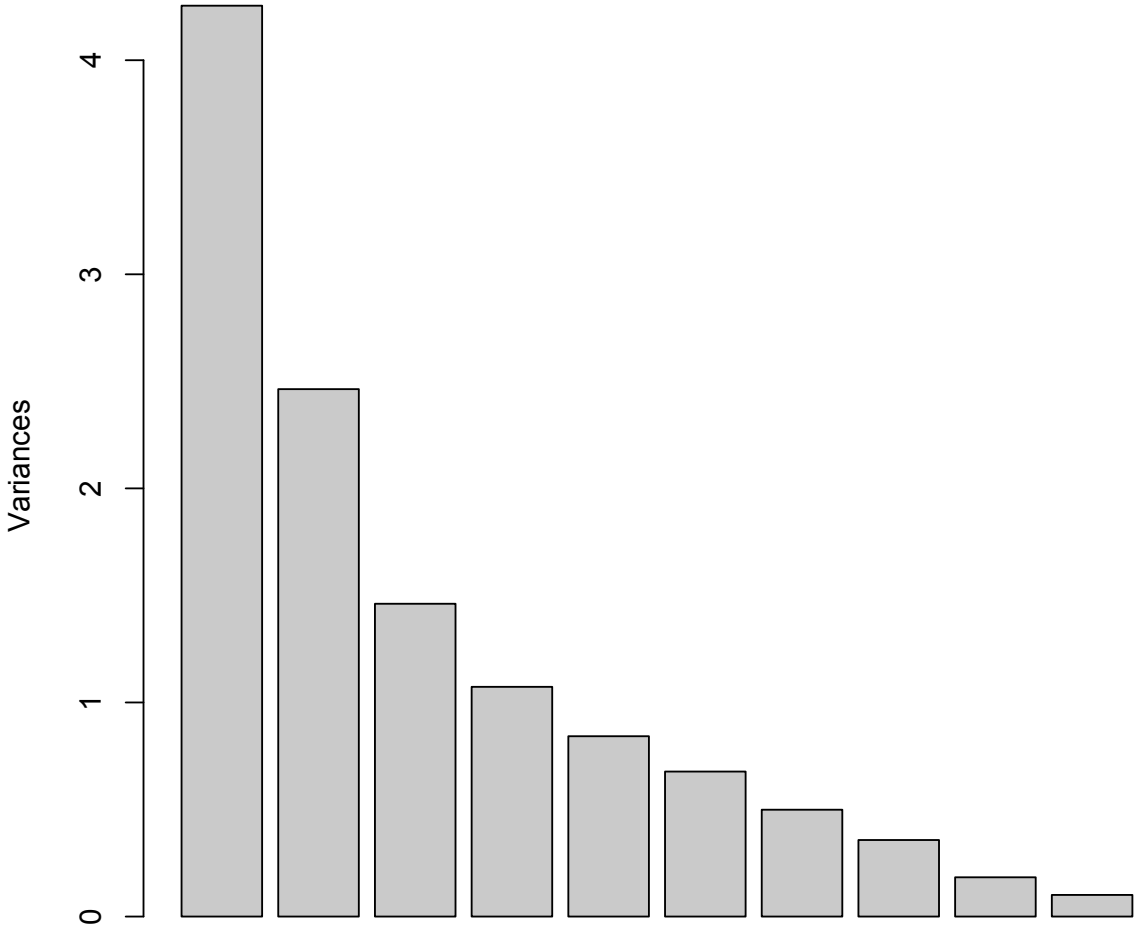


Figure 356: PCA scree plot for the first set of 30 glass deconvolution data (10 replicates), autoscaled.

Table 368: PCA results for the first set of 20 window glass deconvolution data (10 replicates), no pretreatment.

Importance of components:						
	PC1	PC2	PC3	PC4	PC5	PC6
Standard deviation	2280.0817	61.34357	9.15046	8.09719	3.368	2.571
Proportion of Variance	0.9992	0.00072	0.00002	0.00001	0	0
Cumulative Proportion	0.9992	0.99997	0.99998	0.99999	1	1
	PC7	PC8	PC9	PC10	PC11	PC12
Standard deviation	2.266	1.822	1.249	1.027	0.899	0.8335
Proportion of Variance	0	0	0	0	0	0
Cumulative Proportion	1	1	1	1	1	1

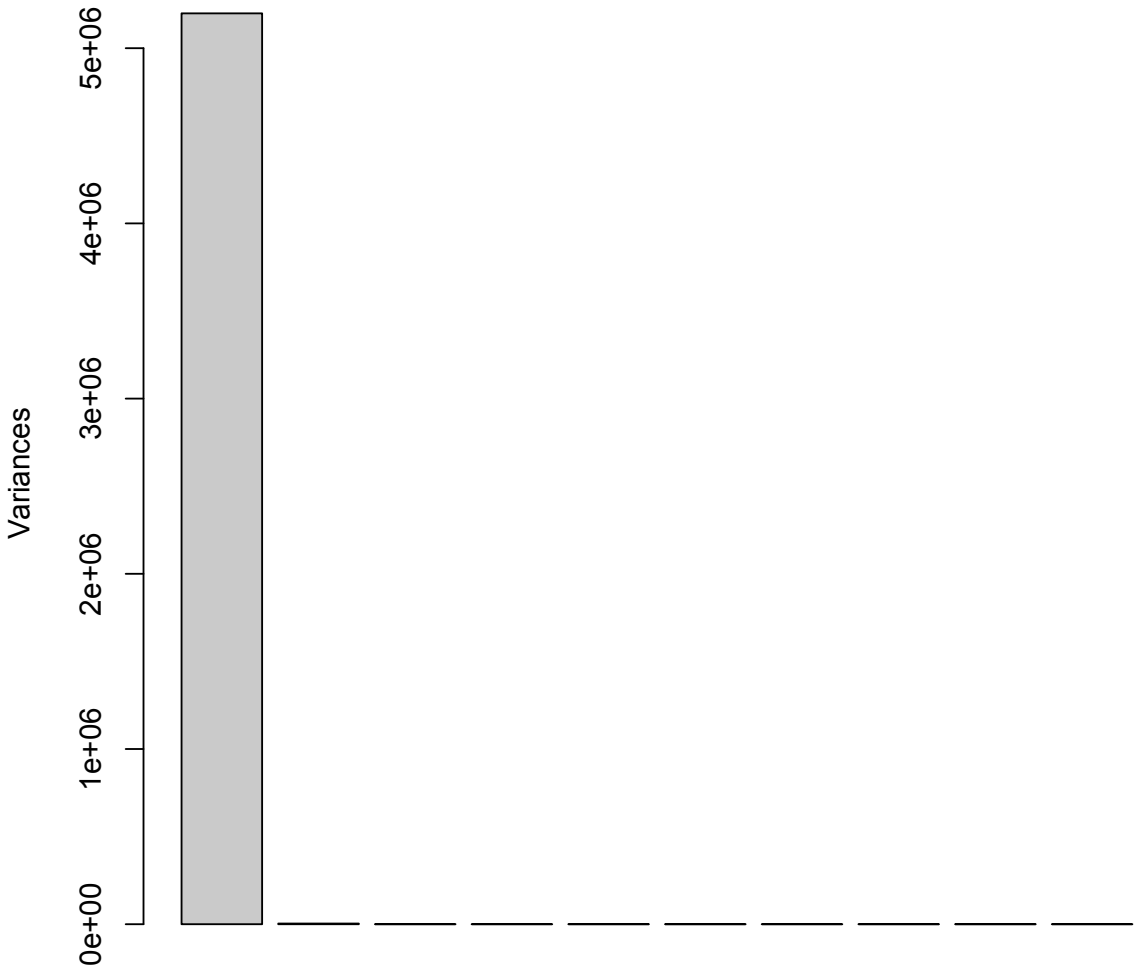


Figure 357: PCA scree plot for the first set of 20 window glass deconvolution data (10 replicates), no pretreatment.

Table 369: PCA results for the first set of 20 window glass deconvolution data (10 replicates), centered.

Importance of components:						
	PC1	PC2	PC3	PC4	PC5	PC6
Standard deviation	61.3566	9.33191	8.11767	3.94743	3.24675	2.3409
Proportion of Variance	0.9506	0.02199	0.01664	0.00393	0.00266	0.00138
Cumulative Proportion	0.9506	0.97255	0.98919	0.99312	0.99578	0.99717
	PC7	PC8	PC9	PC10	PC11	PC12
Standard deviation	2.20191	1.71958	1.13558	0.96762	0.83862	0.69699
Proportion of Variance	0.00122	0.00075	0.00033	0.00024	0.00018	0.00012
Cumulative Proportion	0.99839	0.99914	0.99946	0.9997	0.99988	1

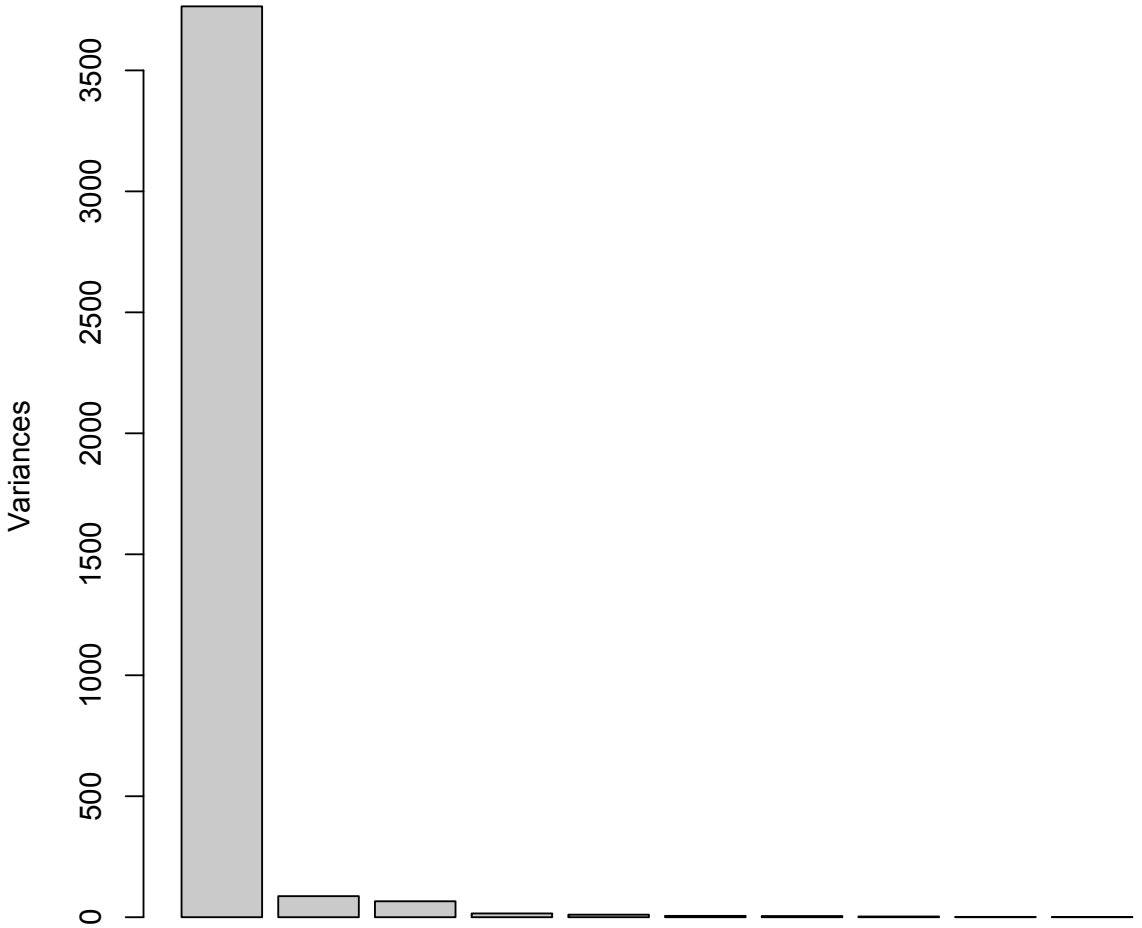


Figure 358: PCA scree plot for the first set of 20 window glass deconvolution data (10 replicates), centered.

Table 370: PCA results for the first set of 20 window glass deconvolution data (10 replicates), autoscaled.

Importance of components:						
	PC1	PC2	PC3	PC4	PC5	PC6
Standard deviation	2.0732	1.6123	1.1595	1.01257	0.86033	0.77482
Proportion of Variance	0.3582	0.2166	0.112	0.08544	0.06168	0.05003
Cumulative Proportion	0.3582	0.5748	0.6868	0.77227	0.83395	0.88398
	PC7	PC8	PC9	PC10	PC11	PC12
Standard deviation	0.73681	0.67109	0.4907	0.28394	0.20511	0.1885
Proportion of Variance	0.04524	0.03753	0.02007	0.00672	0.00351	0.00296
Cumulative Proportion	0.92922	0.96675	0.98681	0.99353	0.99704	1

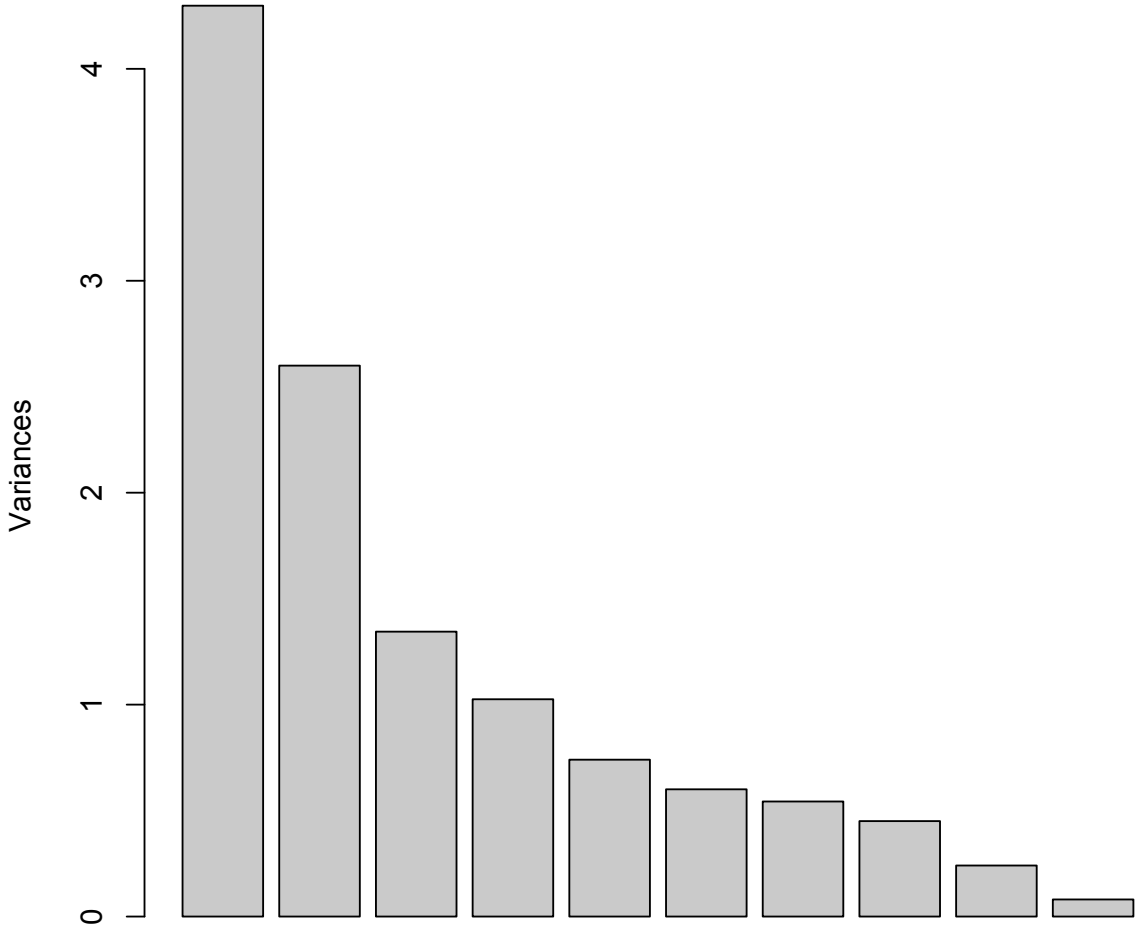


Figure 359: PCA scree plot for the first set of 20 window glass deconvolution data (10 replicates), autoscaled.

Table 371: PCA results for the first set of 10 container glass deconvolution data (10 replicates), no pretreatment.

Importance of components:						
	PC1	PC2	PC3	PC4	PC5	PC6
Standard deviation	2283	10.42569	8.20566	5.77064	3.458	3.402
Proportion of Variance	1	0.00002	0.00001	0.00001	0	0
Cumulative Proportion	1	0.99997	0.99999	0.99999	1	1
	PC7	PC8	PC9	PC10	PC11	PC12
Standard deviation	2.255	1.452	1.307	0.9025	0.7938	0.671
Proportion of Variance	0	0	0	0	0	0
Cumulative Proportion	1	1	1	1	1	1

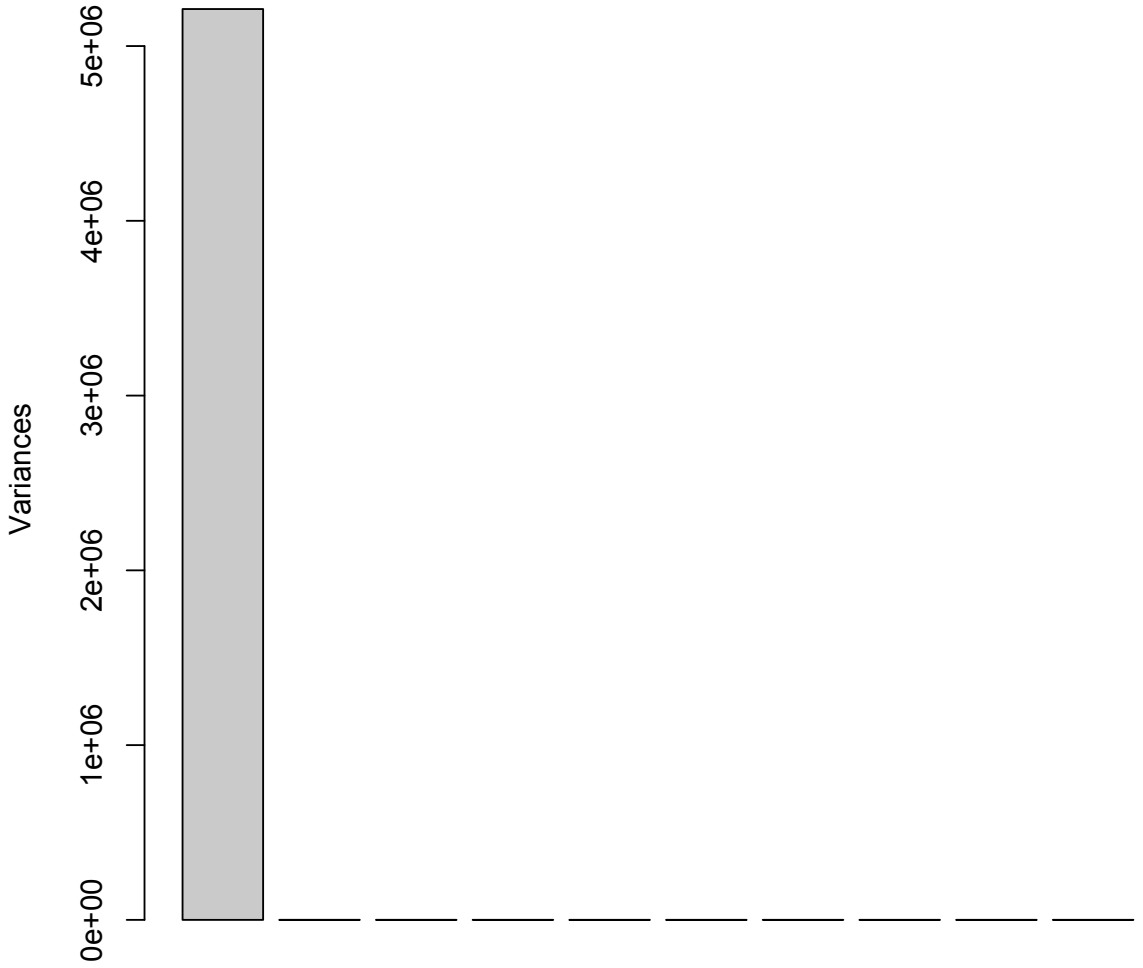


Figure 360: PCA scree plot for the first set of 10 container glass deconvolution data (10 replicates), no pretreatment.

Table 372: PCA results for the first set of 10 container glass deconvolution data (10 replicates), centered.

Importance of components:						
	PC1	PC2	PC3	PC4	PC5	PC6
Standard deviation	10.4559	8.2345	5.7987	5.6431	3.41765	2.34892
Proportion of Variance	0.4066	0.2521	0.125	0.1184	0.04343	0.02052
Cumulative Proportion	0.4066	0.6587	0.7837	0.9022	0.94558	0.9661
	PC7	PC8	PC9	PC10	PC11	PC12
Standard deviation	2.06541	1.42282	1.04536	0.85515	0.74404	0.6693
Proportion of Variance	0.01586	0.00753	0.00406	0.00272	0.00206	0.00167
Cumulative Proportion	0.98196	0.98949	0.99356	0.99628	0.99833	1

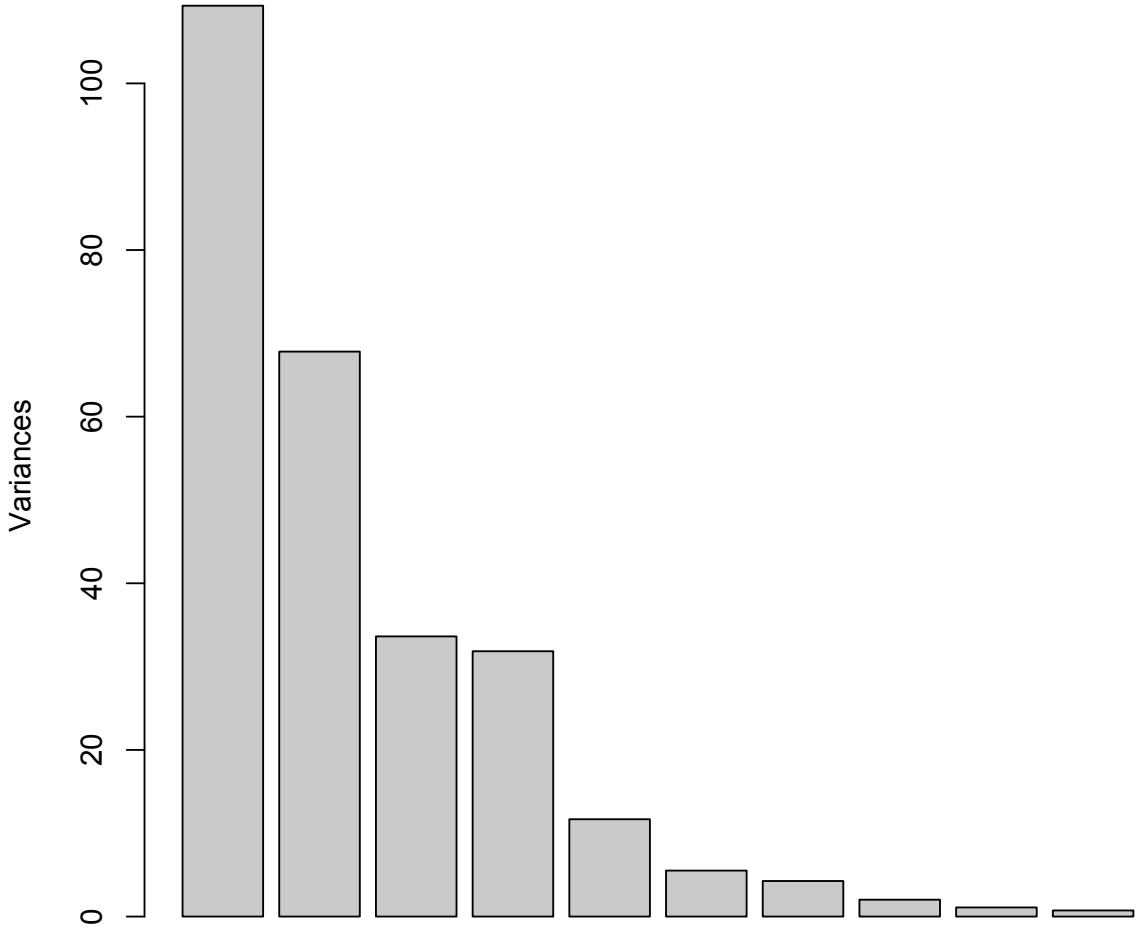


Figure 361: PCA scree plot for the first set of 10 container glass deconvolution data (10 replicates), centered.

Table 373: PCA results for the first set of 10 container glass deconvolution data (10 replicates), autoscaled.

Importance of components:						
	PC1	PC2	PC3	PC4	PC5	PC6
Standard deviation	2.0342	1.6092	1.5271	0.9637	0.95716	0.6444
Proportion of Variance	0.3448	0.2158	0.1943	0.0774	0.07635	0.0346
Cumulative Proportion	0.3448	0.5606	0.755	0.8324	0.90872	0.9433
	PC7	PC8	PC9	PC10	PC11	PC12
Standard deviation	0.54485	0.38356	0.29897	0.25032	0.22951	0.1772
Proportion of Variance	0.02474	0.01226	0.00745	0.00522	0.00439	0.00262
Cumulative Proportion	0.96806	0.98032	0.98777	0.99299	0.99738	1

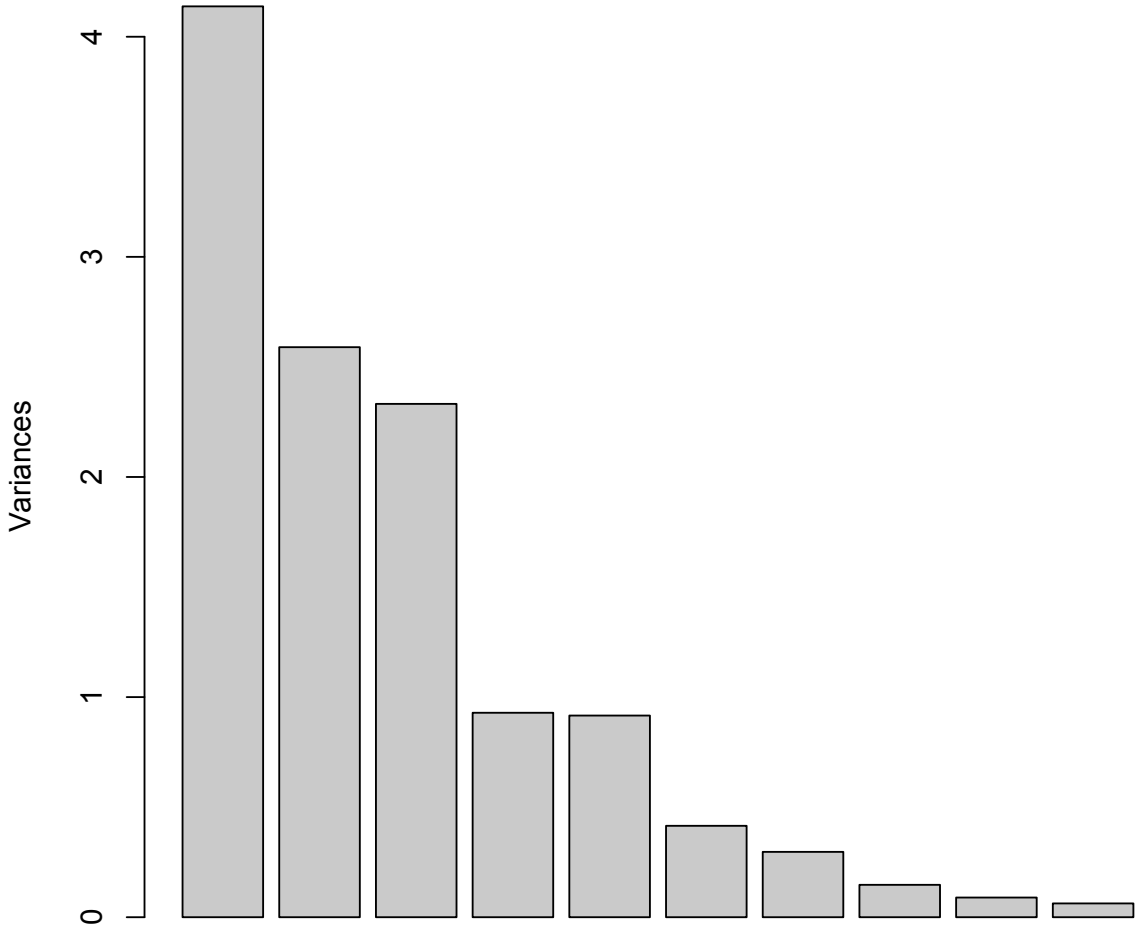


Figure 362: PCA scree plot for the first set of 10 container glass deconvolution data (10 replicates), autoscaled.

APPENDIX XV: PCA RESULTS FOR CHEMOMETRIC ANALYSIS OF GLASSES WITH THE SAME RI

Table 374: PCA results for the spectra of 21 glasses (10 replicates) with nominally similar RIs (same RI set 1), autoscaled.

	PC1	PC2	PC3	PC4	PC5	PC6	PC7	PC8	PC9	PC10	PC11
Standard Deviation	14.8953	9.1404	3.7643	1.3083	0.7501	0.6374	0.5086	0.4481	0.3373	0.2184	0.1941
Proportion of Variance	0.6869	0.2587	0.0439	0.0053	0.0017	0.0013	0.0008	0.0006	0.0004	0.0002	0.0001
Cumulative Proportion	0.6869	0.9456	0.9894	0.9947	0.9965	0.9977	0.9985	0.9992	0.9995	0.9997	0.9998
	PC12	PC13	PC14	PC15	PC16	PC17	PC18	PC19	PC20	PC21	PC22
Standard Deviation	0.1714	0.1324	0.0899	0.0773	0.0550	0.0367	0.0337	0.0302	0.0283	0.0237	0.0215
Proportion of Variance	0.0001	0.0001	0.0000	0.0000	0.0000	0.0000	0.0000	0.0000	0.0000	0.0000	0.0000
Cumulative Proportion	0.9999	0.9999	0.9999	1.0000	1.0000	1.0000	1.0000	1.0000	1.0000	1.0000	1.0000
	PC23	PC24	PC25	PC26	PC27	PC28	PC29	PC30	PC31	PC32	PC33
Standard Deviation	0.0187	0.0174	0.0143	0.0129	0.0123	0.0122	0.0119	0.0119	0.0114	0.0110	0.0108
Proportion of Variance	0.0000	0.0000	0.0000	0.0000	0.0000	0.0000	0.0000	0.0000	0.0000	0.0000	0.0000
Cumulative Proportion	1.0000	1.0000	1.0000	1.0000	1.0000	1.0000	1.0000	1.0000	1.0000	1.0000	1.0000
	PC34	PC35	PC36	PC37	PC38	PC39	PC40	PC41	PC42	PC43	
Standard Deviation	0.0107	0.0102	0.0101	0.0098	0.0097	0.0095	0.0092	0.0090	0.0089	0.0086	
Proportion of Variance	0.0000	0.0000	0.0000	0.0000	0.0000	0.0000	0.0000	0.0000	0.0000	0.0000	
Cumulative Proportion	1.0000	1.0000	1.0000	1.0000	1.0000	1.0000	1.0000	1.0000	1.0000	1.0000	
	PC44	PC45	PC46	PC47	PC48	PC49	PC50	PC51	PC52	PC53	
Standard Deviation	0.0086	0.0083	0.0081	0.0081	0.0080	0.0079	0.0077	0.0077	0.0075	0.0073	
Proportion of Variance	0.0000	0.0000	0.0000	0.0000	0.0000	0.0000	0.0000	0.0000	0.0000	0.0000	
Cumulative Proportion	1.0000	1.0000	1.0000	1.0000	1.0000	1.0000	1.0000	1.0000	1.0000	1.0000	
	PC54	PC55	PC56	PC57	PC58	PC59	PC60	PC61	PC62	PC63	
Standard Deviation	0.0070	0.0069	0.0068	0.0068	0.0066	0.0065	0.0065	0.0064	0.0061	0.0060	
Proportion of Variance	0.0000	0.0000	0.0000	0.0000	0.0000	0.0000	0.0000	0.0000	0.0000	0.0000	
Cumulative Proportion	1.0000	1.0000	1.0000	1.0000	1.0000	1.0000	1.0000	1.0000	1.0000	1.0000	
	PC64	PC65	PC66	PC67	PC68	PC69	PC70	PC71	PC72	PC73	
Standard Deviation	0.0060	0.0058	0.0058	0.0057	0.0057	0.0056	0.0054	0.0053	0.0052	0.0051	
Proportion of Variance	0.0000	0.0000	0.0000	0.0000	0.0000	0.0000	0.0000	0.0000	0.0000	0.0000	
Cumulative Proportion	1.0000	1.0000	1.0000	1.0000	1.0000	1.0000	1.0000	1.0000	1.0000	1.0000	
	PC74	PC75	PC76	PC77	PC78	PC79	PC80	PC81	PC82		
Standard Deviation	0.0051	0.0049	0.0048	0.0048	0.0046	0.0045	0.0045	0.0045	0.0043		

Proportion of Variance	0.0000	0.0000	0.0000	0.0000	0.0000	0.0000	0.0000	0.0000	0.0000		
Cumulative Proportion	1.0000	1.0000	1.0000	1.0000	1.0000	1.0000	1.0000	1.0000	1.0000		
	PC83	PC84	PC85	PC86	PC87	PC88	PC89	PC90	PC91		
Standard Deviation	0.0042	0.0041	0.0041	0.0040	0.0040	0.0040	0.0039	0.0038	0.0037		
Proportion of Variance	0.0000	0.0000	0.0000	0.0000	0.0000	0.0000	0.0000	0.0000	0.0000		
Cumulative Proportion	1.0000	1.0000	1.0000	1.0000	1.0000	1.0000	1.0000	1.0000	1.0000		
	PC92	PC93	PC94	PC95	PC96	PC97	PC98	PC99	PC100	PC101	
Standard Deviation	0.0036	0.0035	0.0035	0.0034	0.0034	0.0033	0.0033	0.0032	0.0032	0.0031	
Proportion of Variance	0.0000	0.0000	0.0000	0.0000	0.0000	0.0000	0.0000	0.0000	0.0000	0.0000	
Cumulative Proportion	1.0000	1.0000	1.0000	1.0000	1.0000	1.0000	1.0000	1.0000	1.0000	1.0000	
	PC102	PC103	PC104	PC105	PC106	PC107	PC108	PC109	PC110		
Standard Deviation	0.0031	0.0030	0.0030	0.0029	0.0029	0.0029	0.0028	0.0027	0.0027		
Proportion of Variance	0.0000	0.0000	0.0000	0.0000	0.0000	0.0000	0.0000	0.0000	0.0000		
Cumulative Proportion	1.0000	1.0000	1.0000	1.0000	1.0000	1.0000	1.0000	1.0000	1.0000		
	PC111	PC112	PC113	PC114	PC115	PC116	PC117	PC118	PC119	PC120	
Standard Deviation	0.0027	0.0026	0.0026	0.0025	0.0024	0.0024	0.0024	0.0024	0.0023	0.0023	
Proportion of Variance	0.0000	0.0000	0.0000	0.0000	0.0000	0.0000	0.0000	0.0000	0.0000	0.0000	
Cumulative Proportion	1.0000	1.0000	1.0000	1.0000	1.0000	1.0000	1.0000	1.0000	1.0000	1.0000	
	PC121	PC122	PC123	PC124	PC125	PC126	PC127	PC128	PC129		
Standard Deviation	0.0023	0.0022	0.0022	0.0022	0.0021	0.0021	0.0020	0.0020	0.0020		
Proportion of Variance	0.0000	0.0000	0.0000	0.0000	0.0000	0.0000	0.0000	0.0000	0.0000		
Cumulative Proportion	1.0000	1.0000	1.0000	1.0000	1.0000	1.0000	1.0000	1.0000	1.0000		
	PC130	PC131	PC132	PC133	PC134	PC135	PC136	PC137	PC138		
Standard Deviation	0.0019	0.0019	0.0019	0.0019	0.0018	0.0018	0.0018	0.0017	0.0017		
Proportion of Variance	0.0000	0.0000	0.0000	0.0000	0.0000	0.0000	0.0000	0.0000	0.0000		
Cumulative Proportion	1.0000	1.0000	1.0000	1.0000	1.0000	1.0000	1.0000	1.0000	1.0000		
	PC139	PC140	PC141	PC142	PC143	PC144	PC145	PC146	PC147		
Standard Deviation	0.0017	0.0017	0.0016	0.0016	0.0016	0.0016	0.0015	0.0015	0.0015		
Proportion of Variance	0.0000	0.0000	0.0000	0.0000	0.0000	0.0000	0.0000	0.0000	0.0000		
Cumulative Proportion	1.0000	1.0000	1.0000	1.0000	1.0000	1.0000	1.0000	1.0000	1.0000		
	PC148	PC149	PC150	PC151	PC152	PC153	PC154	PC155	PC156		
Standard Deviation	0.0014	0.0014	0.0014	0.0014	0.0013	0.0013	0.0013	0.0013	0.0013		
Proportion of Variance	0.0000	0.0000	0.0000	0.0000	0.0000	0.0000	0.0000	0.0000	0.0000		
Cumulative Proportion	1.0000	1.0000	1.0000	1.0000	1.0000	1.0000	1.0000	1.0000	1.0000		

	PC157	PC158	PC159	PC160	PC161	PC162	PC163	PC164	PC165		
Standard Deviation	0.0012	0.0012	0.0012	0.0012	0.0011	0.0011	0.0011	0.0011	0.0011		
Proportion of Variance	0.0000	0.0000	0.0000	0.0000	0.0000	0.0000	0.0000	0.0000	0.0000		
Cumulative Proportion	1.0000	1.0000	1.0000	1.0000	1.0000	1.0000	1.0000	1.0000	1.0000		
	PC166	PC167	PC168	PC169	PC170	PC171	PC172	PC173	PC174		
Standard Deviation	0.0010	0.0010	0.0010	0.0010	0.0010	0.0009	0.0009	0.0009	0.0009		
Proportion of Variance	0.0000	0.0000	0.0000	0.0000	0.0000	0.0000	0.0000	0.0000	0.0000		
Cumulative Proportion	1.0000	1.0000	1.0000	1.0000	1.0000	1.0000	1.0000	1.0000	1.0000		
	PC175	PC176	PC177	PC178	PC179	PC180	PC181	PC182	PC183		
Standard Deviation	0.0009	0.0009	0.0009	0.0008	0.0008	0.0008	0.0008	0.0007	0.0007		
Proportion of Variance	0.0000	0.0000	0.0000	0.0000	0.0000	0.0000	0.0000	0.0000	0.0000		
Cumulative Proportion	1.0000	1.0000	1.0000	1.0000	1.0000	1.0000	1.0000	1.0000	1.0000		
	PC184	PC185	PC186	PC187	PC188	PC189	PC190	PC191	PC192		
Standard Deviation	0.0007	0.0007	0.0007	0.0007	0.0007	0.0007	0.0006	0.0006	0.0006		
Proportion of Variance	0.0000	0.0000	0.0000	0.0000	0.0000	0.0000	0.0000	0.0000	0.0000		
Cumulative Proportion	1.0000	1.0000	1.0000	1.0000	1.0000	1.0000	1.0000	1.0000	1.0000		
	PC193	PC194	PC195	PC196	PC197	PC198	PC199	PC200	PC201		
Standard Deviation	0.0006	0.0006	0.0006	0.0005	0.0005	0.0005	0.0005	0.0005	0.0005		
Proportion of Variance	0.0000	0.0000	0.0000	0.0000	0.0000	0.0000	0.0000	0.0000	0.0000		
Cumulative Proportion	1.0000	1.0000	1.0000	1.0000	1.0000	1.0000	1.0000	1.0000	1.0000		
	PC202	PC203	PC204	PC205	PC206	PC207	PC208	PC209	PC210		
Standard Deviation	0.0004	0.0004	0.0004	0.0004	0.0003	0.0003	0.0003	0.0003	0.0000		
Proportion of Variance	0.0000	0.0000	0.0000	0.0000	0.0000	0.0000	0.0000	0.0000	0.0000		
Cumulative Proportion	1.0000	1.0000	1.0000	1.0000	1.0000	1.0000	1.0000	1.0000	1.0000		

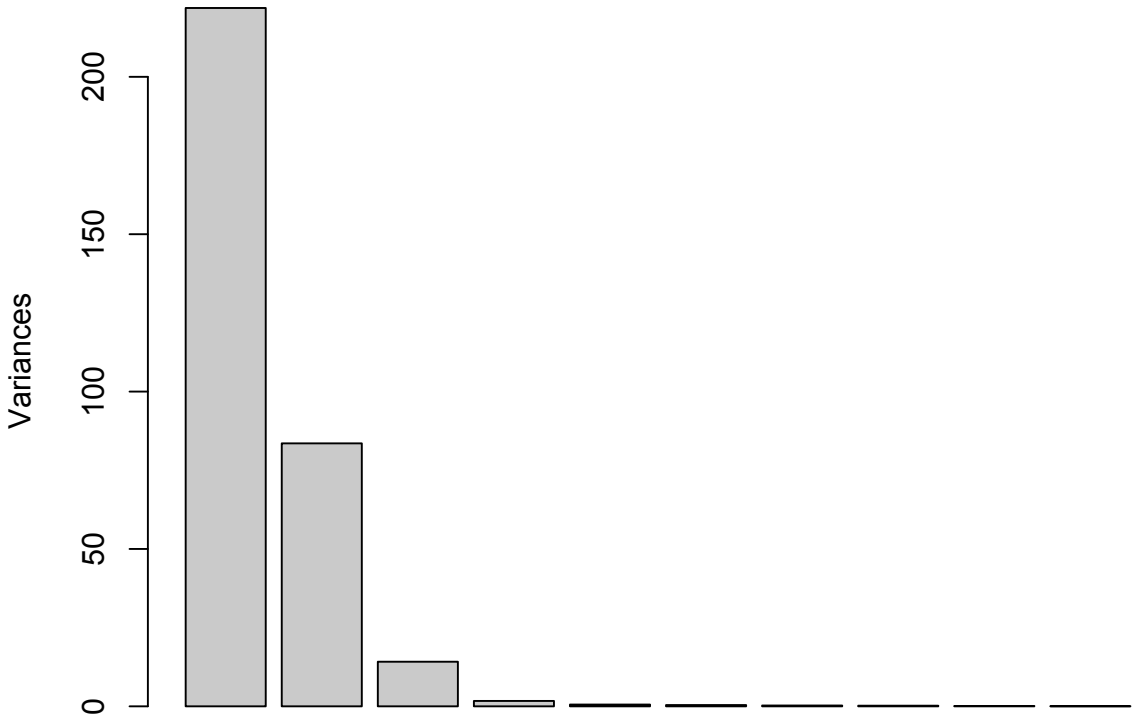


Figure 363: PCA scree plot for the spectra of 21 glasses (10 replicates) with nominally similar RIs (same RI set 1), autoscaled.

Table 375: PCA results for the first derivative spectra (5-point smoothing) of 21 glasses (10 replicates) with nominally similar RIs (same RI set 1), autoscaled.

	PC1	PC2	PC3	PC4	PC5	PC6	PC7	PC8	PC9	PC10	PC11
Standard Deviation	13.1700	7.3344	5.8701	3.6372	3.1786	2.6192	2.3392	2.0099	1.8199	1.5381	1.2482
Proportion of Variance	0.5370	0.1666	0.1067	0.0410	0.0313	0.0212	0.0169	0.0125	0.0103	0.0073	0.0048
Cumulative Proportion	0.5370	0.7036	0.8103	0.8512	0.8825	0.9037	0.9207	0.9332	0.9434	0.9508	0.9556
	PC12	PC13	PC14	PC15	PC16	PC17	PC18	PC19	PC20	PC21	PC22
Standard Deviation	1.1598	1.0341	0.9180	0.8413	0.8028	0.7437	0.7047	0.6962	0.6756	0.6473	0.5885
Proportion of Variance	0.0042	0.0033	0.0026	0.0022	0.0020	0.0017	0.0015	0.0015	0.0014	0.0013	0.0011
Cumulative Proportion	0.9597	0.9631	0.9657	0.9679	0.9698	0.9716	0.9731	0.9746	0.9760	0.9773	0.9784
	PC23	PC24	PC25	PC26	PC27	PC28	PC29	PC30	PC31	PC32	PC33
Standard Deviation	0.5850	0.5731	0.5627	0.5280	0.5189	0.5009	0.4881	0.4805	0.4567	0.4557	0.4428
Proportion of Variance	0.0011	0.0010	0.0010	0.0009	0.0008	0.0008	0.0007	0.0007	0.0007	0.0006	0.0006
Cumulative Proportion	0.9794	0.9805	0.9814	0.9823	0.9831	0.9839	0.9847	0.9854	0.9860	0.9867	0.9873
	PC34	PC35	PC36	PC37	PC38	PC39	PC40	PC41	PC42	PC43	PC44
Standard Deviation	0.4276	0.4204	0.4085	0.3998	0.3966	0.3845	0.3642	0.3437	0.3413	0.3305	0.3283
Proportion of Variance	0.0006	0.0006	0.0005	0.0005	0.0005	0.0005	0.0004	0.0004	0.0004	0.0003	0.0003
Cumulative Proportion	0.9878	0.9884	0.9889	0.9894	0.9899	0.9903	0.9907	0.9911	0.9915	0.9918	0.9921
	PC45	PC46	PC47	PC48	PC49	PC50	PC51	PC52	PC53	PC54	PC55
Standard Deviation	0.3222	0.3176	0.3062	0.3001	0.2948	0.2883	0.2783	0.2760	0.2637	0.2572	0.2530
Proportion of Variance	0.0003	0.0003	0.0003	0.0003	0.0003	0.0003	0.0002	0.0002	0.0002	0.0002	0.0002
Cumulative Proportion	0.9925	0.9928	0.9931	0.9933	0.9936	0.9939	0.9941	0.9943	0.9946	0.9948	0.9950
	PC56	PC57	PC58	PC59	PC60	PC61	PC62	PC63	PC64	PC65	PC66
Standard Deviation	0.2455	0.2428	0.2400	0.2370	0.2310	0.2261	0.2246	0.2151	0.2109	0.2098	0.2037
Proportion of Variance	0.0002	0.0002	0.0002	0.0002	0.0002	0.0002	0.0002	0.0001	0.0001	0.0001	0.0001
Cumulative Proportion	0.9952	0.9953	0.9955	0.9957	0.9959	0.9960	0.9962	0.9963	0.9964	0.9966	0.9967
	PC67	PC68	PC69	PC70	PC71	PC72	PC73	PC74	PC75	PC76	PC77
Standard Deviation	0.2017	0.1943	0.1918	0.1888	0.1860	0.1832	0.1798	0.1734	0.1691	0.1646	0.1636
Proportion of Variance	0.0001	0.0001	0.0001	0.0001	0.0001	0.0001	0.0001	0.0001	0.0001	0.0001	0.0001
Cumulative Proportion	0.9968	0.9970	0.9971	0.9972	0.9973	0.9974	0.9975	0.9976	0.9977	0.9978	0.9978
	PC78	PC79	PC80	PC81	PC82	PC83	PC84	PC85	PC86	PC87	PC88
Standard Deviation	0.1597	0.1567	0.1551	0.1542	0.1514	0.1460	0.1434	0.1414	0.1377	0.1372	0.1350
Proportion of Variance	0.0001	0.0001	0.0001	0.0001	0.0001	0.0001	0.0001	0.0001	0.0001	0.0001	0.0001
Cumulative Proportion	0.9979	0.9980	0.9981	0.9981	0.9982	0.9983	0.9983	0.9984	0.9985	0.9985	0.9986
	PC89	PC90	PC91	PC92	PC93	PC94	PC95	PC96	PC97	PC98	PC99

Standard Deviation	0.1333	0.1320	0.1278	0.1254	0.1228	0.1199	0.1189	0.1174	0.1136	0.1128	0.1106
Proportion of Variance	0.0001	0.0001	0.0001	0.0001	0.0001	0.0000	0.0000	0.0000	0.0000	0.0000	0.0000
Cumulative Proportion	0.9986	0.9987	0.9987	0.9988	0.9988	0.9989	0.9989	0.9990	0.9990	0.9990	0.9991
	PC100	PC101	PC102	PC103	PC104	PC105	PC106	PC107	PC108	PC109	PC110
Standard Deviation	0.1090	0.1060	0.1038	0.1036	0.0999	0.0996	0.0983	0.0959	0.0942	0.0917	0.0903
Proportion of Variance	0.0000	0.0000	0.0000	0.0000	0.0000	0.0000	0.0000	0.0000	0.0000	0.0000	0.0000
Cumulative Proportion	0.9991	0.9992	0.9992	0.9992	0.9992	0.9993	0.9993	0.9993	0.9994	0.9994	0.9994
	PC111	PC112	PC113	PC114	PC115	PC116	PC117	PC118	PC119	PC120	PC121
Standard Deviation	0.0894	0.0884	0.0866	0.0851	0.0830	0.0813	0.0804	0.0799	0.0782	0.0770	0.0753
Proportion of Variance	0.0000	0.0000	0.0000	0.0000	0.0000	0.0000	0.0000	0.0000	0.0000	0.0000	0.0000
Cumulative Proportion	0.9994	0.9995	0.9995	0.9995	0.9995	0.9996	0.9996	0.9996	0.9996	0.9996	0.9996
	PC122	PC123	PC124	PC125	PC126	PC127	PC128	PC129	PC130	PC131	PC132
Standard Deviation	0.0726	0.0700	0.0690	0.0686	0.0665	0.0660	0.0643	0.0619	0.0613	0.0602	0.0601
Proportion of Variance	0.0000	0.0000	0.0000	0.0000	0.0000	0.0000	0.0000	0.0000	0.0000	0.0000	0.0000
Cumulative Proportion	0.9997	0.9997	0.9997	0.9997	0.9997	0.9997	0.9997	0.9998	0.9998	0.9998	0.9998
	PC133	PC134	PC135	PC136	PC137	PC138	PC139	PC140	PC141	PC142	PC143
Standard Deviation	0.0591	0.0571	0.0547	0.0537	0.0523	0.0517	0.0502	0.0492	0.0490	0.0475	0.0470
Proportion of Variance	0.0000	0.0000	0.0000	0.0000	0.0000	0.0000	0.0000	0.0000	0.0000	0.0000	0.0000
Cumulative Proportion	0.9998	0.9998	0.9998	0.9998	0.9998	0.9998	0.9999	0.9999	0.9999	0.9999	0.9999
	PC144	PC145	PC146	PC147	PC148	PC149	PC150	PC151	PC152	PC153	PC154
Standard Deviation	0.0455	0.0438	0.0438	0.0424	0.0416	0.0409	0.0403	0.0386	0.0377	0.0366	0.0361
Proportion of Variance	0.0000	0.0000	0.0000	0.0000	0.0000	0.0000	0.0000	0.0000	0.0000	0.0000	0.0000
Cumulative Proportion	0.9999	0.9999	0.9999	0.9999	0.9999	0.9999	0.9999	0.9999	0.9999	0.9999	0.9999
	PC155	PC156	PC157	PC158	PC159	PC160	PC161	PC162	PC163	PC164	PC165
Standard Deviation	0.0337	0.0331	0.0329	0.0320	0.0310	0.0305	0.0295	0.0289	0.0273	0.0271	0.0259
Proportion of Variance	0.0000	0.0000	0.0000	0.0000	0.0000	0.0000	0.0000	0.0000	0.0000	0.0000	0.0000
Cumulative Proportion	0.9999	0.9999	1.0000	1.0000	1.0000	1.0000	1.0000	1.0000	1.0000	1.0000	1.0000
	PC166	PC167	PC168	PC169	PC170	PC171	PC172	PC173	PC174	PC175	PC176
Standard Deviation	0.0253	0.0244	0.0233	0.0230	0.0221	0.0216	0.0212	0.0204	0.0197	0.0196	0.0189
Proportion of Variance	0.0000	0.0000	0.0000	0.0000	0.0000	0.0000	0.0000	0.0000	0.0000	0.0000	0.0000
Cumulative Proportion	1.0000	1.0000	1.0000	1.0000	1.0000	1.0000	1.0000	1.0000	1.0000	1.0000	1.0000
	PC177	PC178	PC179	PC180	PC181	PC182	PC183	PC184	PC185	PC186	PC187
Standard Deviation	0.0182	0.0180	0.0171	0.0169	0.0162	0.0160	0.0156	0.0150	0.0144	0.0142	0.0138
Proportion of Variance	0.0000	0.0000	0.0000	0.0000	0.0000	0.0000	0.0000	0.0000	0.0000	0.0000	0.0000

Cumulative Proportion	1.0000	1.0000	1.0000	1.0000	1.0000	1.0000	1.0000	1.0000	1.0000	1.0000	1.0000
	PC188	PC189	PC190	PC191	PC192	PC193	PC194	PC195	PC196	PC197	
Standard Deviation	0.0133	0.0131	0.0125	0.0123	0.0117	0.0116	0.0109	0.0103	0.0101	0.0100	
Proportion of Variance	0.0000	0.0000	0.0000	0.0000	0.0000	0.0000	0.0000	0.0000	0.0000	0.0000	
Cumulative Proportion	1.0000	1.0000	1.0000	1.0000	1.0000	1.0000	1.0000	1.0000	1.0000	1.0000	
	PC198	PC199	PC200	PC201	PC202	PC203	PC204	PC205	PC206		
Standard Deviation	0.0096	0.0090	0.0084	0.0083	0.0080	0.0077	0.0074	0.0068	0.0063		
Proportion of Variance	0.0000	0.0000	0.0000	0.0000	0.0000	0.0000	0.0000	0.0000	0.0000		
Cumulative Proportion	1.0000	1.0000	1.0000	1.0000	1.0000	1.0000	1.0000	1.0000	1.0000		
	PC207	PC208	PC209	PC210							
Standard Deviation	0.0060	0.0057	0.0050	0.0000							
Proportion of Variance	0.0000	0.0000	0.0000	0.0000							
Cumulative Proportion	1.0000	1.0000	1.0000	1.0000							

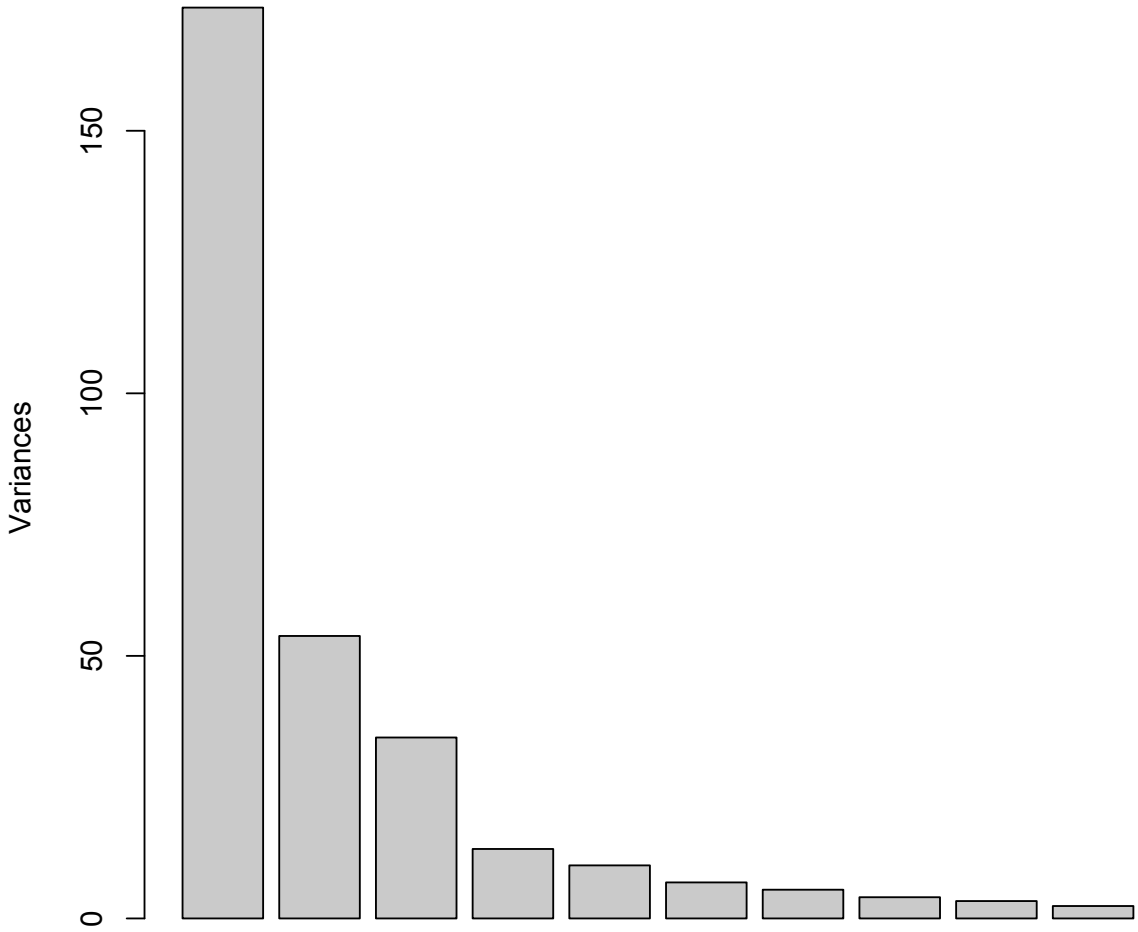


Figure 364: PCA scree plot for the first derivative spectra (5-point smoothing) of 21 glasses (10 replicates) with nominally similar RIs (same RI set 1), autoscaled.

Table 376: PCA results for the second derivative spectra (5-point smoothing) of 21 glasses (10 replicates) with nominally similar RIs (same RI set 1), autoscaled.

	PC1	PC2	PC3	PC4	PC5	PC6	PC7	PC8	PC9	PC10	PC11
Standard Deviation	5.9307	4.9785	4.6964	3.8999	3.4965	2.9680	2.8345	2.7955	2.5522	2.4228	2.3497
Proportion of Variance	0.1089	0.0767	0.0683	0.0471	0.0379	0.0273	0.0249	0.0242	0.0202	0.0182	0.0171
Cumulative Proportion	0.1089	0.1856	0.2539	0.3010	0.3389	0.3661	0.3910	0.4152	0.4354	0.4535	0.4706
	PC12	PC13	PC14	PC15	PC16	PC17	PC18	PC19	PC20	PC21	PC22
Standard Deviation	2.2989	2.2148	2.1898	2.1597	2.0952	2.0495	2.0089	1.9981	1.9611	1.9116	1.8658
Proportion of Variance	0.0164	0.0152	0.0149	0.0144	0.0136	0.0130	0.0125	0.0124	0.0119	0.0113	0.0108
Cumulative Proportion	0.4870	0.5022	0.5170	0.5315	0.5451	0.5581	0.5706	0.5829	0.5948	0.6061	0.6169
	PC23	PC24	PC25	PC26	PC27	PC28	PC29	PC30	PC31	PC32	PC33
Standard Deviation	1.8481	1.8201	1.8161	1.7812	1.7368	1.7279	1.6991	1.6570	1.6422	1.6222	1.5997
Proportion of Variance	0.0106	0.0103	0.0102	0.0098	0.0093	0.0092	0.0089	0.0085	0.0084	0.0082	0.0079
Cumulative Proportion	0.6275	0.6377	0.6480	0.6578	0.6671	0.6764	0.6853	0.6938	0.7021	0.7103	0.7182
	PC34	PC35	PC36	PC37	PC38	PC39	PC40	PC41	PC42	PC43	PC44
Standard Deviation	1.5943	1.5567	1.5429	1.5290	1.5163	1.4776	1.4405	1.4271	1.4044	1.3947	1.3727
Proportion of Variance	0.0079	0.0075	0.0074	0.0072	0.0071	0.0068	0.0064	0.0063	0.0061	0.0060	0.0058
Cumulative Proportion	0.7261	0.7336	0.7410	0.7482	0.7553	0.7621	0.7685	0.7748	0.7809	0.7869	0.7928
	PC45	PC46	PC47	PC48	PC49	PC50	PC51	PC52	PC53	PC54	PC55
Standard Deviation	1.3614	1.3569	1.3417	1.3217	1.3049	1.2906	1.2696	1.2368	1.2191	1.2085	1.2035
Proportion of Variance	0.0057	0.0057	0.0056	0.0054	0.0053	0.0052	0.0050	0.0047	0.0046	0.0045	0.0045
Cumulative Proportion	0.7985	0.8042	0.8098	0.8152	0.8205	0.8256	0.8306	0.8353	0.8399	0.8445	0.8489
	PC56	PC57	PC58	PC59	PC60	PC61	PC62	PC63	PC64	PC65	PC66
Standard Deviation	1.1958	1.1854	1.1670	1.1392	1.1230	1.1188	1.1073	1.1004	1.0953	1.0640	1.0568
Proportion of Variance	0.0044	0.0044	0.0042	0.0040	0.0039	0.0039	0.0038	0.0038	0.0037	0.0035	0.0035
Cumulative Proportion	0.8534	0.8577	0.8619	0.8660	0.8699	0.8737	0.8775	0.8813	0.8850	0.8885	0.8920
	PC67	PC68	PC69	PC70	PC71	PC72	PC73	PC74	PC75	PC76	PC77
Standard Deviation	1.0306	1.0135	1.0083	0.9976	0.9904	0.9701	0.9504	0.9424	0.9301	0.9082	0.8965
Proportion of Variance	0.0033	0.0032	0.0032	0.0031	0.0030	0.0029	0.0028	0.0028	0.0027	0.0026	0.0025
Cumulative Proportion	0.8952	0.8984	0.9016	0.9047	0.9077	0.9106	0.9134	0.9161	0.9188	0.9214	0.9239
	PC78	PC79	PC80	PC81	PC82	PC83	PC84	PC85	PC86	PC87	PC88
Standard Deviation	0.8839	0.8730	0.8583	0.8505	0.8417	0.8153	0.8117	0.7995	0.7867	0.7815	0.7756
Proportion of Variance	0.0024	0.0024	0.0023	0.0022	0.0022	0.0021	0.0020	0.0020	0.0019	0.0019	0.0019
Cumulative Proportion	0.9263	0.9286	0.9309	0.9332	0.9354	0.9374	0.9395	0.9414	0.9434	0.9452	0.9471
	PC89	PC90	PC91	PC92	PC93	PC94	PC95	PC96	PC97	PC98	PC99

Standard Deviation	0.7579	0.7499	0.7426	0.7257	0.7147	0.7033	0.6870	0.6779	0.6669	0.6541	0.6470
Proportion of Variance	0.0018	0.0017	0.0017	0.0016	0.0016	0.0015	0.0015	0.0014	0.0014	0.0013	0.0013
Cumulative Proportion	0.9489	0.9506	0.9523	0.9540	0.9555	0.9571	0.9585	0.9600	0.9613	0.9627	0.9639
	PC100	PC101	PC102	PC103	PC104	PC105	PC106	PC107	PC108	PC109	PC110
Standard Deviation	0.6429	0.6323	0.6175	0.6144	0.6023	0.5914	0.5853	0.5707	0.5649	0.5618	0.5582
Proportion of Variance	0.0013	0.0012	0.0012	0.0012	0.0011	0.0011	0.0011	0.0010	0.0010	0.0010	0.0010
Cumulative Proportion	0.9652	0.9665	0.9677	0.9688	0.9699	0.9710	0.9721	0.9731	0.9741	0.9751	0.9760
	PC111	PC112	PC113	PC114	PC115	PC116	PC117	PC118	PC119	PC120	PC121
Standard Deviation	0.5358	0.5283	0.5245	0.5040	0.5015	0.4887	0.4864	0.4722	0.4637	0.4620	0.4542
Proportion of Variance	0.0009	0.0009	0.0009	0.0008	0.0008	0.0007	0.0007	0.0007	0.0007	0.0007	0.0006
Cumulative Proportion	0.9769	0.9778	0.9786	0.9794	0.9802	0.9809	0.9817	0.9824	0.9830	0.9837	0.9843
	PC122	PC123	PC124	PC125	PC126	PC127	PC128	PC129	PC130	PC131	PC132
Standard Deviation	0.4427	0.4327	0.4281	0.4251	0.4144	0.4079	0.3966	0.3943	0.3894	0.3827	0.3806
Proportion of Variance	0.0006	0.0006	0.0006	0.0006	0.0005	0.0005	0.0005	0.0005	0.0005	0.0005	0.0005
Cumulative Proportion	0.9849	0.9855	0.9861	0.9866	0.9872	0.9877	0.9882	0.9887	0.9891	0.9896	0.9900
	PC133	PC134	PC135	PC136	PC137	PC138	PC139	PC140	PC141	PC142	PC143
Standard Deviation	0.3720	0.3637	0.3625	0.3553	0.3503	0.3426	0.3353	0.3312	0.3210	0.3138	0.3093
Proportion of Variance	0.0004	0.0004	0.0004	0.0004	0.0004	0.0004	0.0004	0.0003	0.0003	0.0003	0.0003
Cumulative Proportion	0.9905	0.9909	0.9913	0.9917	0.9920	0.9924	0.9928	0.9931	0.9934	0.9937	0.9940
	PC144	PC145	PC146	PC147	PC148	PC149	PC150	PC151	PC152	PC153	PC154
Standard Deviation	0.2976	0.2944	0.2893	0.2833	0.2820	0.2692	0.2662	0.2595	0.2555	0.2507	0.2462
Proportion of Variance	0.0003	0.0003	0.0003	0.0003	0.0003	0.0002	0.0002	0.0002	0.0002	0.0002	0.0002
Cumulative Proportion	0.9943	0.9946	0.9948	0.9951	0.9953	0.9955	0.9958	0.9960	0.9962	0.9964	0.9965
	PC155	PC156	PC157	PC158	PC159	PC160	PC161	PC162	PC163	PC164	PC165
Standard Deviation	0.2373	0.2339	0.2283	0.2242	0.2197	0.2168	0.2117	0.2082	0.2046	0.1969	0.1951
Proportion of Variance	0.0002	0.0002	0.0002	0.0002	0.0002	0.0002	0.0001	0.0001	0.0001	0.0001	0.0001
Cumulative Proportion	0.9967	0.9969	0.9970	0.9972	0.9974	0.9975	0.9976	0.9978	0.9979	0.9980	0.9981
	PC166	PC167	PC168	PC169	PC170	PC171	PC172	PC173	PC174	PC175	PC176
Standard Deviation	0.1921	0.1861	0.1801	0.1749	0.1701	0.1680	0.1635	0.1583	0.1556	0.1532	0.1503
Proportion of Variance	0.0001	0.0001	0.0001	0.0001	0.0001	0.0001	0.0001	0.0001	0.0001	0.0001	0.0001
Cumulative Proportion	0.9983	0.9984	0.9985	0.9986	0.9986	0.9987	0.9988	0.9989	0.9990	0.9990	0.9991
	PC177	PC178	PC179	PC180	PC181	PC182	PC183	PC184	PC185	PC186	PC187
Standard Deviation	0.1449	0.1401	0.1316	0.1275	0.1230	0.1203	0.1188	0.1160	0.1134	0.1084	0.1067
Proportion of Variance	0.0001	0.0001	0.0001	0.0001	0.0001	0.0000	0.0000	0.0000	0.0000	0.0000	0.0000

Cumulative Proportion	0.9992	0.9992	0.9993	0.9993	0.9994	0.9994	0.9995	0.9995	0.9996	0.9996	0.9996
	PC188	PC189	PC190	PC191	PC192	PC193	PC194	PC195	PC196	PC197	PC198
Standard Deviation	0.1021	0.0980	0.0961	0.0944	0.0882	0.0863	0.0839	0.0812	0.0785	0.0756	0.0726
Proportion of Variance	0.0000	0.0000	0.0000	0.0000	0.0000	0.0000	0.0000	0.0000	0.0000	0.0000	0.0000
Cumulative Proportion	0.9997	0.9997	0.9997	0.9997	0.9998	0.9998	0.9998	0.9998	0.9999	0.9999	0.9999
	PC199	PC200	PC201	PC202	PC203	PC204	PC205	PC206	PC207	PC208	PC209
Standard Deviation	0.0708	0.0691	0.0665	0.0612	0.0587	0.0563	0.0560	0.0522	0.0502	0.0463	0.0429
Proportion of Variance	0.0000	0.0000	0.0000	0.0000	0.0000	0.0000	0.0000	0.0000	0.0000	0.0000	0.0000
Cumulative Proportion	0.9999	0.9999	0.9999	0.9999	1.0000	1.0000	1.0000	1.0000	1.0000	1.0000	1.0000
	PC210										
Standard Deviation	0.0000										
Proportion of Variance	0.0000										
Cumulative Proportion	1.0000										

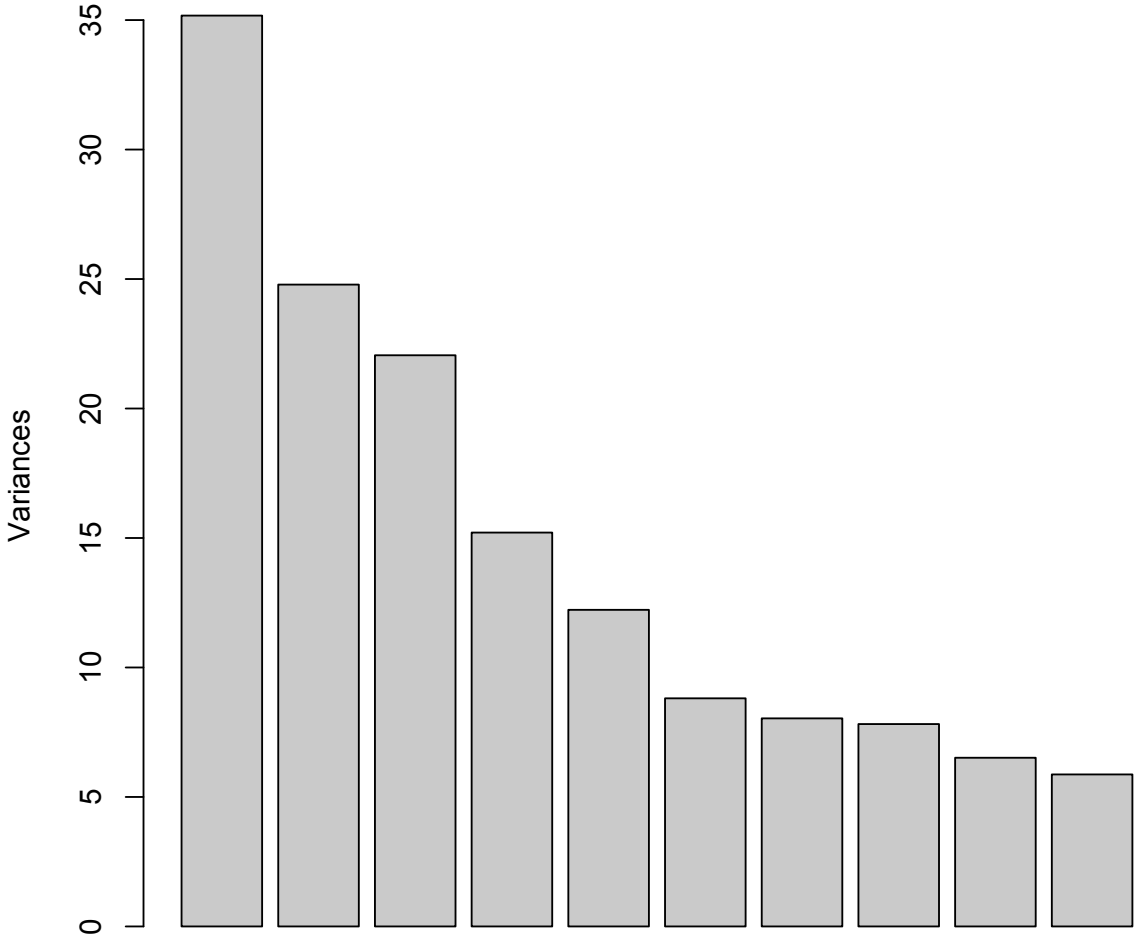


Figure 365: PCA scree plot for the second derivative spectra (5-point smoothing) of 21 glasses (10 replicates) with nominally similar RIs (same RI set 1), autoscaled.

Table 377: PCA results for the spectra of 30 glasses (10 replicates) with nominally similar RIs (same RI set 2), autoscaled.

	PC1	PC2	PC3	PC4	PC5	PC6	PC7	PC8	PC9	PC10	PC11
Standard Deviation	13.3796	10.9349	4.3629	1.7159	1.0248	0.7075	0.5350	0.4807	0.3598	0.2482	0.2277
Proportion of Variance	0.5542	0.3702	0.0589	0.0091	0.0033	0.0016	0.0009	0.0007	0.0004	0.0002	0.0002
Cumulative Proportion	0.5542	0.9244	0.9833	0.9925	0.9957	0.9973	0.9981	0.9989	0.9993	0.9995	0.9996
	PC12	PC13	PC14	PC15	PC16	PC17	PC18	PC19	PC20	PC21	PC22
Standard Deviation	0.1986	0.1674	0.1494	0.1084	0.0854	0.0516	0.0433	0.0401	0.0316	0.0300	0.0290
Proportion of Variance	0.0001	0.0001	0.0001	0.0000	0.0000	0.0000	0.0000	0.0000	0.0000	0.0000	0.0000
Cumulative Proportion	0.9997	0.9998	0.9999	0.9999	1.0000	1.0000	1.0000	1.0000	1.0000	1.0000	1.0000
	PC23	PC24	PC25	PC26	PC27	PC28	PC29	PC30	PC31	PC32	PC33
Standard Deviation	0.0230	0.0225	0.0220	0.0174	0.0163	0.0150	0.0146	0.0144	0.0137	0.0129	0.0127
Proportion of Variance	0.0000	0.0000	0.0000	0.0000	0.0000	0.0000	0.0000	0.0000	0.0000	0.0000	0.0000
Cumulative Proportion	1.0000	1.0000	1.0000	1.0000	1.0000	1.0000	1.0000	1.0000	1.0000	1.0000	1.0000
	PC34	PC35	PC36	PC37	PC38	PC39	PC40	PC41	PC42	PC43	PC44
Standard Deviation	0.0122	0.0120	0.0118	0.0113	0.0111	0.0106	0.0106	0.0105	0.0101	0.0100	0.0099
Proportion of Variance	0.0000	0.0000	0.0000	0.0000	0.0000	0.0000	0.0000	0.0000	0.0000	0.0000	0.0000
Cumulative Proportion	1.0000	1.0000	1.0000	1.0000	1.0000	1.0000	1.0000	1.0000	1.0000	1.0000	1.0000
	PC45	PC46	PC47	PC48	PC49	PC50	PC51	PC52	PC53		
Standard Deviation	0.0097	0.0097	0.0095	0.0094	0.0091	0.0091	0.0090	0.0088	0.0086		
Proportion of Variance	0.0000	0.0000	0.0000	0.0000	0.0000	0.0000	0.0000	0.0000	0.0000		
Cumulative Proportion	1.0000	1.0000	1.0000	1.0000	1.0000	1.0000	1.0000	1.0000	1.0000		
	PC54	PC55	PC56	PC57	PC58	PC59	PC60	PC61	PC62	PC63	
Standard Deviation	0.0083	0.0083	0.0082	0.0080	0.0079	0.0078	0.0076	0.0075	0.0074	0.0073	
Proportion of Variance	0.0000	0.0000	0.0000	0.0000	0.0000	0.0000	0.0000	0.0000	0.0000	0.0000	
Cumulative Proportion	1.0000	1.0000	1.0000	1.0000	1.0000	1.0000	1.0000	1.0000	1.0000	1.0000	
	PC64	PC65	PC66	PC67	PC68	PC69	PC70	PC71	PC72		
Standard Deviation	0.0073	0.0071	0.0071	0.0070	0.0068	0.0067	0.0065	0.0065	0.0064		
Proportion of Variance	0.0000	0.0000	0.0000	0.0000	0.0000	0.0000	0.0000	0.0000	0.0000		
Cumulative Proportion	1.0000	1.0000	1.0000	1.0000	1.0000	1.0000	1.0000	1.0000	1.0000		
	PC73	PC74	PC75	PC76	PC77	PC78	PC79	PC80	PC81		
Standard Deviation	0.0063	0.0062	0.0061	0.0060	0.0059	0.0058	0.0057	0.0056	0.0055		
Proportion of Variance	0.0000	0.0000	0.0000	0.0000	0.0000	0.0000	0.0000	0.0000	0.0000		
Cumulative Proportion	1.0000	1.0000	1.0000	1.0000	1.0000	1.0000	1.0000	1.0000	1.0000		
	PC82	PC83	PC84	PC85	PC86	PC87	PC88	PC89	PC90	PC91	

Standard Deviation	0.0054	0.0054	0.0054	0.0053	0.0052	0.0051	0.0051	0.0049	0.0049	0.0048	
Proportion of Variance	0.0000	0.0000	0.0000	0.0000	0.0000	0.0000	0.0000	0.0000	0.0000	0.0000	
Cumulative Proportion	1.0000	1.0000	1.0000	1.0000	1.0000	1.0000	1.0000	1.0000	1.0000	1.0000	
	PC92	PC93	PC94	PC95	PC96	PC97	PC98	PC99	PC100	PC101	
Standard Deviation	0.0048	0.0046	0.0045	0.0045	0.0044	0.0044	0.0044	0.0043	0.0043	0.0042	
Proportion of Variance	0.0000	0.0000	0.0000	0.0000	0.0000	0.0000	0.0000	0.0000	0.0000	0.0000	
Cumulative Proportion	1.0000	1.0000	1.0000	1.0000	1.0000	1.0000	1.0000	1.0000	1.0000	1.0000	
	PC102	PC103	PC104	PC105	PC106	PC107	PC108	PC109	PC110		
Standard Deviation	0.0041	0.0041	0.0040	0.0040	0.0039	0.0039	0.0038	0.0038	0.0037		
Proportion of Variance	0.0000	0.0000	0.0000	0.0000	0.0000	0.0000	0.0000	0.0000	0.0000		
Cumulative Proportion	1.0000	1.0000	1.0000	1.0000	1.0000	1.0000	1.0000	1.0000	1.0000		
	PC111	PC112	PC113	PC114	PC115	PC116	PC117	PC118	PC119	PC120	
Standard Deviation	0.0037	0.0036	0.0036	0.0035	0.0035	0.0034	0.0034	0.0033	0.0033	0.0033	
Proportion of Variance	0.0000	0.0000	0.0000	0.0000	0.0000	0.0000	0.0000	0.0000	0.0000	0.0000	
Cumulative Proportion	1.0000	1.0000	1.0000	1.0000	1.0000	1.0000	1.0000	1.0000	1.0000	1.0000	
	PC121	PC122	PC123	PC124	PC125	PC126	PC127	PC128	PC129		
Standard Deviation	0.0032	0.0032	0.0032	0.0031	0.0031	0.0031	0.0030	0.0030	0.0030		
Proportion of Variance	0.0000	0.0000	0.0000	0.0000	0.0000	0.0000	0.0000	0.0000	0.0000		
Cumulative Proportion	1.0000	1.0000	1.0000	1.0000	1.0000	1.0000	1.0000	1.0000	1.0000		
	PC130	PC131	PC132	PC133	PC134	PC135	PC136	PC137	PC138	PC139	
Standard Deviation	0.0029	0.0029	0.0028	0.0028	0.0028	0.0028	0.0027	0.0027	0.0026	0.0026	
Proportion of Variance	0.0000	0.0000	0.0000	0.0000	0.0000	0.0000	0.0000	0.0000	0.0000	0.0000	
Cumulative Proportion	1.0000	1.0000	1.0000	1.0000	1.0000	1.0000	1.0000	1.0000	1.0000	1.0000	
	PC140	PC141	PC142	PC143	PC144	PC145	PC146	PC147	PC148		
Standard Deviation	0.0026	0.0026	0.0025	0.0025	0.0024	0.0024	0.0024	0.0024	0.0023		
Proportion of Variance	0.0000	0.0000	0.0000	0.0000	0.0000	0.0000	0.0000	0.0000	0.0000		
Cumulative Proportion	1.0000	1.0000	1.0000	1.0000	1.0000	1.0000	1.0000	1.0000	1.0000		
	PC149	PC150	PC151	PC152	PC153	PC154	PC155	PC156	PC157	PC158	
Standard Deviation	0.0023	0.0023	0.0022	0.0022	0.0022	0.0021	0.0021	0.0021	0.0021	0.0021	
Proportion of Variance	0.0000	0.0000	0.0000	0.0000	0.0000	0.0000	0.0000	0.0000	0.0000	0.0000	
Cumulative Proportion	1.0000	1.0000	1.0000	1.0000	1.0000	1.0000	1.0000	1.0000	1.0000	1.0000	
	PC159	PC160	PC161	PC162	PC163	PC164	PC165	PC166	PC167		
Standard Deviation	0.0020	0.0020	0.0020	0.0019	0.0019	0.0019	0.0018	0.0018	0.0018		
Proportion of Variance	0.0000	0.0000	0.0000	0.0000	0.0000	0.0000	0.0000	0.0000	0.0000		

Cumulative Proportion	1.0000	1.0000	1.0000	1.0000	1.0000	1.0000	1.0000	1.0000	1.0000		
	PC168	PC169	PC170	PC171	PC172	PC173	PC174	PC175	PC176		
Standard Deviation	0.0018	0.0018	0.0017	0.0017	0.0017	0.0017	0.0016	0.0016	0.0016		
Proportion of Variance	0.0000	0.0000	0.0000	0.0000	0.0000	0.0000	0.0000	0.0000	0.0000		
Cumulative Proportion	1.0000	1.0000	1.0000	1.0000	1.0000	1.0000	1.0000	1.0000	1.0000		
	PC177	PC178	PC179	PC180	PC181	PC182	PC183	PC184	PC185		
Standard Deviation	0.0016	0.0016	0.0015	0.0015	0.0015	0.0015	0.0015	0.0014	0.0014		
Proportion of Variance	0.0000	0.0000	0.0000	0.0000	0.0000	0.0000	0.0000	0.0000	0.0000		
Cumulative Proportion	1.0000	1.0000	1.0000	1.0000	1.0000	1.0000	1.0000	1.0000	1.0000		
	PC186	PC187	PC188	PC189	PC190	PC191	PC192	PC193	PC194		
Standard Deviation	0.0014	0.0014	0.0014	0.0013	0.0013	0.0013	0.0013	0.0013	0.0012		
Proportion of Variance	0.0000	0.0000	0.0000	0.0000	0.0000	0.0000	0.0000	0.0000	0.0000		
Cumulative Proportion	1.0000	1.0000	1.0000	1.0000	1.0000	1.0000	1.0000	1.0000	1.0000		
	PC195	PC196	PC197	PC198	PC199	PC200	PC201	PC202	PC203		
Standard Deviation	0.0012	0.0012	0.0012	0.0012	0.0012	0.0011	0.0011	0.0011	0.0011		
Proportion of Variance	0.0000	0.0000	0.0000	0.0000	0.0000	0.0000	0.0000	0.0000	0.0000		
Cumulative Proportion	1.0000	1.0000	1.0000	1.0000	1.0000	1.0000	1.0000	1.0000	1.0000		
	PC204	PC205	PC206	PC207	PC208	PC209	PC210	PC211	PC212		
Standard Deviation	0.0011	0.0011	0.0010	0.0010	0.0010	0.0010	0.0010	0.0010	0.0009		
Proportion of Variance	0.0000	0.0000	0.0000	0.0000	0.0000	0.0000	0.0000	0.0000	0.0000		
Cumulative Proportion	1.0000	1.0000	1.0000	1.0000	1.0000	1.0000	1.0000	1.0000	1.0000		
	PC213	PC214	PC215	PC216	PC217	PC218	PC219	PC220	PC221		
Standard Deviation	0.0009	0.0009	0.0009	0.0009	0.0009	0.0008	0.0008	0.0008	0.0008		
Proportion of Variance	0.0000	0.0000	0.0000	0.0000	0.0000	0.0000	0.0000	0.0000	0.0000		
Cumulative Proportion	1.0000	1.0000	1.0000	1.0000	1.0000	1.0000	1.0000	1.0000	1.0000		
	PC222	PC223	PC224	PC225	PC226	PC227	PC228	PC229	PC230		
Standard Deviation	0.0008	0.0008	0.0007	0.0007	0.0007	0.0007	0.0007	0.0007	0.0007		
Proportion of Variance	0.0000	0.0000	0.0000	0.0000	0.0000	0.0000	0.0000	0.0000	0.0000		
Cumulative Proportion	1.0000	1.0000	1.0000	1.0000	1.0000	1.0000	1.0000	1.0000	1.0000		
	PC231	PC232	PC233	PC234	PC235	PC236	PC237	PC238	PC239		
Standard Deviation	0.0006	0.0006	0.0006	0.0006	0.0006	0.0006	0.0006	0.0006	0.0006		
Proportion of Variance	0.0000	0.0000	0.0000	0.0000	0.0000	0.0000	0.0000	0.0000	0.0000		
Cumulative Proportion	1.0000	1.0000	1.0000	1.0000	1.0000	1.0000	1.0000	1.0000	1.0000		
	PC240	PC241	PC242	PC243	PC244	PC245	PC246	PC247	PC248		

Standard Deviation	0.0005	0.0005	0.0005	0.0005	0.0005	0.0005	0.0005	0.0005	0.0004		
Proportion of Variance	0.0000	0.0000	0.0000	0.0000	0.0000	0.0000	0.0000	0.0000	0.0000		
Cumulative Proportion	1.0000	1.0000	1.0000	1.0000	1.0000	1.0000	1.0000	1.0000	1.0000		
	PC249	PC250	PC251	PC252	PC253	PC254	PC255	PC256	PC257		
Standard Deviation	0.0004	0.0004	0.0004	0.0004	0.0004	0.0004	0.0004	0.0004	0.0004		
Proportion of Variance	0.0000	0.0000	0.0000	0.0000	0.0000	0.0000	0.0000	0.0000	0.0000		
Cumulative Proportion	1.0000	1.0000	1.0000	1.0000	1.0000	1.0000	1.0000	1.0000	1.0000		
	PC258	PC259	PC260	PC261	PC262	PC263	PC264	PC265	PC266		
Standard Deviation	0.0003	0.0003	0.0003	0.0003	0.0003	0.0003	0.0003	0.0003	0.0003		
Proportion of Variance	0.0000	0.0000	0.0000	0.0000	0.0000	0.0000	0.0000	0.0000	0.0000		
Cumulative Proportion	1.0000	1.0000	1.0000	1.0000	1.0000	1.0000	1.0000	1.0000	1.0000		
	PC267	PC268	PC269	PC270	PC271	PC272	PC273	PC274	PC275		
Standard Deviation	0.0003	0.0002	0.0002	0.0002	0.0002	0.0002	0.0002	0.0002	0.0002		
Proportion of Variance	0.0000	0.0000	0.0000	0.0000	0.0000	0.0000	0.0000	0.0000	0.0000		
Cumulative Proportion	1.0000	1.0000	1.0000	1.0000	1.0000	1.0000	1.0000	1.0000	1.0000		
	PC276	PC277	PC278	PC279	PC280	PC281	PC282	PC283			
Standard Deviation	0.0002	0.0002	0.0002	0.0002	0.0002	0.0002	0.0001	0.0001			
Proportion of Variance	0.0000	0.0000	0.0000	0.0000	0.0000	0.0000	0.0000	0.0000			
Cumulative Proportion	1.0000	1.0000	1.0000	1.0000	1.0000	1.0000	1.0000	1.0000			
	PC284	PC285	PC286	PC287	PC288	PC289	PC290	PC291	PC292		
Standard Deviation	0.0001	0.0001	0.0001	0.0001	0.0001	0.0001	0.0001	0.0001	0.0001		
Proportion of Variance	0.0000	0.0000	0.0000	0.0000	0.0000	0.0000	0.0000	0.0000	0.0000		
Cumulative Proportion	1.0000	1.0000	1.0000	1.0000	1.0000	1.0000	1.0000	1.0000	1.0000		
	PC293	PC294	PC295	PC296	PC297	PC298	PC299	PC300			
Standard Deviation	0.0001	0.0001	0.0001	0.0001	0.0001	0.0000	0.0000	0.0000			
Proportion of Variance	0.0000	0.0000	0.0000	0.0000	0.0000	0.0000	0.0000	0.0000			
Cumulative Proportion	1.0000	1.0000	1.0000	1.0000	1.0000	1.0000	1.0000	1.0000			

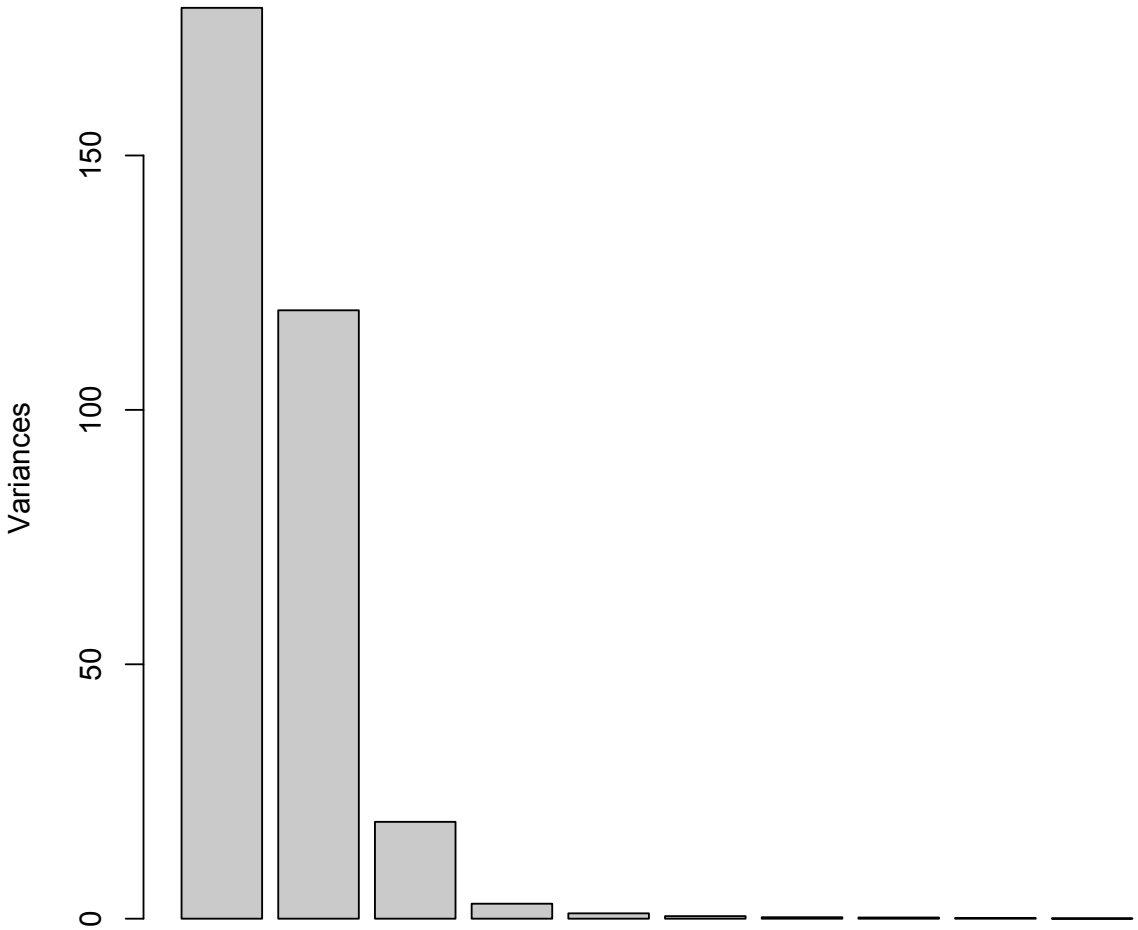


Figure 366: PCA scree plot for the spectra of 30 glasses (10 replicates) with nominally similar RIs (same RI set 2), autoscaled.

Table 378: PCA results for the first derivative spectra (5-point smoothing) of 30 glasses (10 replicates) with nominally similar RIs (same RI set 2), autoscaled.

	PC1	PC2	PC3	PC4	PC5	PC6	PC7	PC8	PC9	PC10	PC11
Standard Deviation	13.3097	6.8228	6.2980	3.9040	2.8936	2.6989	2.3551	1.6807	1.5679	1.2380	1.2235
Proportion of Variance	0.5484	0.1441	0.1228	0.0472	0.0259	0.0226	0.0172	0.0088	0.0076	0.0047	0.0046
Cumulative Proportion	0.5484	0.6926	0.8154	0.8626	0.8885	0.9110	0.9282	0.9370	0.9446	0.9493	0.9539
	PC12	PC13	PC14	PC15	PC16	PC17	PC18	PC19	PC20	PC21	PC22
Standard Deviation	1.0725	0.9716	0.8737	0.8587	0.7912	0.7770	0.7247	0.6759	0.6551	0.6282	0.6230
Proportion of Variance	0.0036	0.0029	0.0024	0.0023	0.0019	0.0019	0.0016	0.0014	0.0013	0.0012	0.0012
Cumulative Proportion	0.9575	0.9604	0.9628	0.9651	0.9670	0.9689	0.9705	0.9719	0.9733	0.9745	0.9757
	PC23	PC24	PC25	PC26	PC27	PC28	PC29	PC30	PC31	PC32	PC33
Standard Deviation	0.6016	0.5839	0.5693	0.5475	0.5339	0.5120	0.5076	0.4918	0.4835	0.4752	0.4680
Proportion of Variance	0.0011	0.0011	0.0010	0.0009	0.0009	0.0008	0.0008	0.0008	0.0007	0.0007	0.0007
Cumulative Proportion	0.9768	0.9779	0.9788	0.9798	0.9807	0.9815	0.9823	0.9830	0.9837	0.9844	0.9851
	PC34	PC35	PC36	PC37	PC38	PC39	PC40	PC41	PC42	PC43	PC44
Standard Deviation	0.4542	0.4391	0.4204	0.4192	0.4070	0.3961	0.3882	0.3736	0.3675	0.3632	0.3504
Proportion of Variance	0.0006	0.0006	0.0006	0.0005	0.0005	0.0005	0.0005	0.0004	0.0004	0.0004	0.0004
Cumulative Proportion	0.9858	0.9863	0.9869	0.9875	0.9880	0.9884	0.9889	0.9893	0.9898	0.9902	0.9906
	PC45	PC46	PC47	PC48	PC49	PC50	PC51	PC52	PC53	PC54	PC55
Standard Deviation	0.3442	0.3389	0.3315	0.3298	0.3119	0.2996	0.2959	0.2915	0.2874	0.2782	0.2728
Proportion of Variance	0.0004	0.0004	0.0003	0.0003	0.0003	0.0003	0.0003	0.0003	0.0003	0.0002	0.0002
Cumulative Proportion	0.9909	0.9913	0.9916	0.9920	0.9922	0.9925	0.9928	0.9931	0.9933	0.9936	0.9938
	PC56	PC57	PC58	PC59	PC60	PC61	PC62	PC63	PC64	PC65	PC66
Standard Deviation	0.2679	0.2654	0.2609	0.2520	0.2450	0.2410	0.2361	0.2321	0.2284	0.2253	0.2227
Proportion of Variance	0.0002	0.0002	0.0002	0.0002	0.0002	0.0002	0.0002	0.0002	0.0002	0.0002	0.0002
Cumulative Proportion	0.9940	0.9942	0.9944	0.9946	0.9948	0.9950	0.9952	0.9953	0.9955	0.9957	0.9958
	PC67	PC68	PC69	PC70	PC71	PC72	PC73	PC74	PC75	PC76	PC77
Standard Deviation	0.2162	0.2103	0.2091	0.2065	0.2035	0.2009	0.1948	0.1916	0.1856	0.1789	0.1776
Proportion of Variance	0.0001	0.0001	0.0001	0.0001	0.0001	0.0001	0.0001	0.0001	0.0001	0.0001	0.0001
Cumulative Proportion	0.9960	0.9961	0.9962	0.9964	0.9965	0.9966	0.9967	0.9969	0.9970	0.9970	0.9971
	PC78	PC79	PC80	PC81	PC82	PC83	PC84	PC85	PC86	PC87	PC88
Standard Deviation	0.1760	0.1729	0.1696	0.1689	0.1665	0.1637	0.1583	0.1569	0.1515	0.1487	0.1470
Proportion of Variance	0.0001	0.0001	0.0001	0.0001	0.0001	0.0001	0.0001	0.0001	0.0001	0.0001	0.0001
Cumulative Proportion	0.9972	0.9973	0.9974	0.9975	0.9976	0.9977	0.9978	0.9978	0.9979	0.9980	0.9980
	PC89	PC90	PC91	PC92	PC93	PC94	PC95	PC96	PC97	PC98	PC99

Standard Deviation	0.1470	0.1441	0.1421	0.1395	0.1388	0.1380	0.1339	0.1329	0.1298	0.1278	0.1249
Proportion of Variance	0.0001	0.0001	0.0001	0.0001	0.0001	0.0001	0.0001	0.0001	0.0001	0.0001	0.0001
Cumulative Proportion	0.9981	0.9982	0.9982	0.9983	0.9984	0.9984	0.9985	0.9985	0.9986	0.9986	0.9987
	PC100	PC101	PC102	PC103	PC104	PC105	PC106	PC107	PC108	PC109	PC110
Standard Deviation	0.1225	0.1213	0.1190	0.1179	0.1148	0.1145	0.1102	0.1084	0.1082	0.1061	0.1033
Proportion of Variance	0.0001	0.0001	0.0000	0.0000	0.0000	0.0000	0.0000	0.0000	0.0000	0.0000	0.0000
Cumulative Proportion	0.9987	0.9988	0.9988	0.9989	0.9989	0.9989	0.9990	0.9990	0.9991	0.9991	0.9991
	PC111	PC112	PC113	PC114	PC115	PC116	PC117	PC118	PC119	PC120	PC121
Standard Deviation	0.1004	0.1001	0.0986	0.0980	0.0968	0.0956	0.0931	0.0914	0.0904	0.0894	0.0865
Proportion of Variance	0.0000	0.0000	0.0000	0.0000	0.0000	0.0000	0.0000	0.0000	0.0000	0.0000	0.0000
Cumulative Proportion	0.9992	0.9992	0.9992	0.9992	0.9993	0.9993	0.9993	0.9994	0.9994	0.9994	0.9994
	PC122	PC123	PC124	PC125	PC126	PC127	PC128	PC129	PC130	PC131	PC132
Standard Deviation	0.0854	0.0838	0.0819	0.0809	0.0791	0.0786	0.0775	0.0741	0.0733	0.0721	0.0720
Proportion of Variance	0.0000	0.0000	0.0000	0.0000	0.0000	0.0000	0.0000	0.0000	0.0000	0.0000	0.0000
Cumulative Proportion	0.9994	0.9995	0.9995	0.9995	0.9995	0.9995	0.9996	0.9996	0.9996	0.9996	0.9996
	PC133	PC134	PC135	PC136	PC137	PC138	PC139	PC140	PC141	PC142	PC143
Standard Deviation	0.0702	0.0678	0.0661	0.0654	0.0637	0.0635	0.0610	0.0601	0.0599	0.0594	0.0579
Proportion of Variance	0.0000	0.0000	0.0000	0.0000	0.0000	0.0000	0.0000	0.0000	0.0000	0.0000	0.0000
Cumulative Proportion	0.9996	0.9997	0.9997	0.9997	0.9997	0.9997	0.9997	0.9997	0.9997	0.9998	0.9998
	PC144	PC145	PC146	PC147	PC148	PC149	PC150	PC151	PC152	PC153	PC154
Standard Deviation	0.0568	0.0558	0.0547	0.0537	0.0522	0.0508	0.0501	0.0492	0.0479	0.0469	0.0468
Proportion of Variance	0.0000	0.0000	0.0000	0.0000	0.0000	0.0000	0.0000	0.0000	0.0000	0.0000	0.0000
Cumulative Proportion	0.9998	0.9998	0.9998	0.9998	0.9998	0.9998	0.9998	0.9998	0.9998	0.9999	0.9999
	PC155	PC156	PC157	PC158	PC159	PC160	PC161	PC162	PC163	PC164	PC165
Standard Deviation	0.0455	0.0454	0.0430	0.0429	0.0418	0.0404	0.0394	0.0386	0.0381	0.0372	0.0366
Proportion of Variance	0.0000	0.0000	0.0000	0.0000	0.0000	0.0000	0.0000	0.0000	0.0000	0.0000	0.0000
Cumulative Proportion	0.9999	0.9999	0.9999	0.9999	0.9999	0.9999	0.9999	0.9999	0.9999	0.9999	0.9999
	PC166	PC167	PC168	PC169	PC170	PC171	PC172	PC173	PC174	PC175	PC176
Standard Deviation	0.0356	0.0347	0.0345	0.0334	0.0329	0.0320	0.0318	0.0307	0.0302	0.0297	0.0285
Proportion of Variance	0.0000	0.0000	0.0000	0.0000	0.0000	0.0000	0.0000	0.0000	0.0000	0.0000	0.0000
Cumulative Proportion	0.9999	0.9999	0.9999	0.9999	0.9999	1.0000	0.9999	0.9999	0.9999	1.0000	1.0000
	PC177	PC178	PC179	PC180	PC181	PC182	PC183	PC184	PC185	PC186	PC187
Standard Deviation	0.0279	0.0275	0.0269	0.0256	0.0254	0.0247	0.0243	0.0237	0.0233	0.0229	0.0225
Proportion of Variance	0.0000	0.0000	0.0000	0.0000	0.0000	0.0000	0.0000	0.0000	0.0000	0.0000	0.0000

Cumulative Proportion	1.0000	1.0000	1.0000	1.0000	1.0000	1.0000	1.0000	1.0000	1.0000	1.0000	1.0000
	PC188	PC189	PC190	PC191	PC192	PC193	PC194	PC195	PC196	PC197	PC198
Standard Deviation	0.0214	0.0211	0.0209	0.0200	0.0198	0.0194	0.0184	0.0181	0.0177	0.0176	0.0170
Proportion of Variance	0.0000	0.0000	0.0000	0.0000	0.0000	0.0000	0.0000	0.0000	0.0000	0.0000	0.0000
Cumulative Proportion	1.0000	1.0000	1.0000	1.0000	1.0000	1.0000	1.0000	1.0000	1.0000	1.0000	1.0000
	PC199	PC200	PC201	PC202	PC203	PC204	PC205	PC206	PC207	PC208	PC209
Standard Deviation	0.0169	0.0162	0.0158	0.0152	0.0148	0.0145	0.0142	0.0138	0.0136	0.0134	0.0132
Proportion of Variance	0.0000	0.0000	0.0000	0.0000	0.0000	0.0000	0.0000	0.0000	0.0000	0.0000	0.0000
Cumulative Proportion	1.0000	1.0000	1.0000	1.0000	1.0000	1.0000	1.0000	1.0000	1.0000	1.0000	1.0000
	PC210	PC211	PC212	PC213	PC214	PC215	PC216	PC217	PC218	PC219	PC220
Standard Deviation	0.0132	0.0127	0.0124	0.0122	0.0120	0.0117	0.0113	0.0110	0.0108	0.0104	0.0102
Proportion of Variance	0.0000	0.0000	0.0000	0.0000	0.0000	0.0000	0.0000	0.0000	0.0000	0.0000	0.0000
Cumulative Proportion	1.0000	1.0000	1.0000	1.0000	1.0000	1.0000	1.0000	1.0000	1.0000	1.0000	1.0000
	PC221	PC222	PC223	PC224	PC225	PC226	PC227	PC228	PC229	PC230	
Standard Deviation	0.0101	0.0100	0.0096	0.0092	0.0091	0.0088	0.0087	0.0083	0.0083	0.0081	
Proportion of Variance	0.0000	0.0000	0.0000	0.0000	0.0000	0.0000	0.0000	0.0000	0.0000	0.0000	
Cumulative Proportion	1.0000	1.0000	1.0000	1.0000	1.0000	1.0000	1.0000	1.0000	1.0000	1.0000	
	PC231	PC232	PC233	PC234	PC235	PC236	PC237	PC238	PC239		
Standard Deviation	0.0080	0.0079	0.0077	0.0076	0.0073	0.0071	0.0069	0.0067	0.0066		
Proportion of Variance	0.0000	0.0000	0.0000	0.0000	0.0000	0.0000	0.0000	0.0000	0.0000		
Cumulative Proportion	1.0000	1.0000	1.0000	1.0000	1.0000	1.0000	1.0000	1.0000	1.0000		
	PC240	PC241	PC242	PC243	PC244	PC245	PC246	PC247	PC248		
Standard Deviation	0.0064	0.0063	0.0062	0.0060	0.0059	0.0057	0.0055	0.0052	0.0051		
Proportion of Variance	0.0000	0.0000	0.0000	0.0000	0.0000	0.0000	0.0000	0.0000	0.0000		
Cumulative Proportion	1.0000	1.0000	1.0000	1.0000	1.0000	1.0000	1.0000	1.0000	1.0000		
	PC249	PC250	PC251	PC252	PC253	PC254	PC255	PC256	PC257		
Standard Deviation	0.0051	0.0049	0.0046	0.0046	0.0045	0.0044	0.0042	0.0041	0.0040		
Proportion of Variance	0.0000	0.0000	0.0000	0.0000	0.0000	0.0000	0.0000	0.0000	0.0000		
Cumulative Proportion	1.0000	1.0000	1.0000	1.0000	1.0000	1.0000	1.0000	1.0000	1.0000		
	PC258	PC259	PC260	PC261	PC262	PC263	PC264	PC265	PC266	PC267	
Standard Deviation	0.0038	0.0037	0.0035	0.0034	0.0033	0.0032	0.0031	0.0030	0.0029	0.0028	
Proportion of Variance	0.0000	0.0000	0.0000	0.0000	0.0000	0.0000	0.0000	0.0000	0.0000	0.0000	
Cumulative Proportion	1.0000	1.0000	1.0000	1.0000	1.0000	1.0000	1.0000	1.0000	1.0000	1.0000	
	PC268	PC269	PC270	PC271	PC272	PC273	PC274	PC275	PC276		

Standard Deviation	0.0027	0.0026	0.0026	0.0025	0.0024	0.0023	0.0022	0.0020	0.0019		
Proportion of Variance	0.0000	0.0000	0.0000	0.0000	0.0000	0.0000	0.0000	0.0000	0.0000		
Cumulative Proportion	1.0000	1.0000	1.0000	1.0000	1.0000	1.0000	1.0000	1.0000	1.0000		
	PC277	PC278	PC279	PC280	PC281	PC282	PC283	PC284	PC285		
Standard Deviation	0.0019	0.0018	0.0016	0.0016	0.0015	0.0014	0.0013	0.0013	0.0012		
Proportion of Variance	0.0000	0.0000	0.0000	0.0000	0.0000	0.0000	0.0000	0.0000	0.0000		
Cumulative Proportion	1.0000	1.0000	1.0000	1.0000	1.0000	1.0000	1.0000	1.0000	1.0000		
	PC286	PC287	PC288	PC289	PC290	PC291	PC292	PC293	PC294		
Standard Deviation	0.0011	0.0011	0.0009	0.0008	0.0008	0.0007	0.0006	0.0005	0.0005		
Proportion of Variance	0.0000	0.0000	0.0000	0.0000	0.0000	0.0000	0.0000	0.0000	0.0000		
Cumulative Proportion	1.0000	1.0000	1.0000	1.0000	1.0000	1.0000	1.0000	1.0000	1.0000		
	PC295	PC296	PC297	PC298	PC299	PC300					
Standard Deviation	0.0004	0.0004	0.0003	0.0002	0.0001	0.0000					
Proportion of Variance	0.0000	0.0000	0.0000	0.0000	0.0000	0.0000					
Cumulative Proportion	1.0000	1.0000	1.0000	1.0000	1.0000	1.0000					

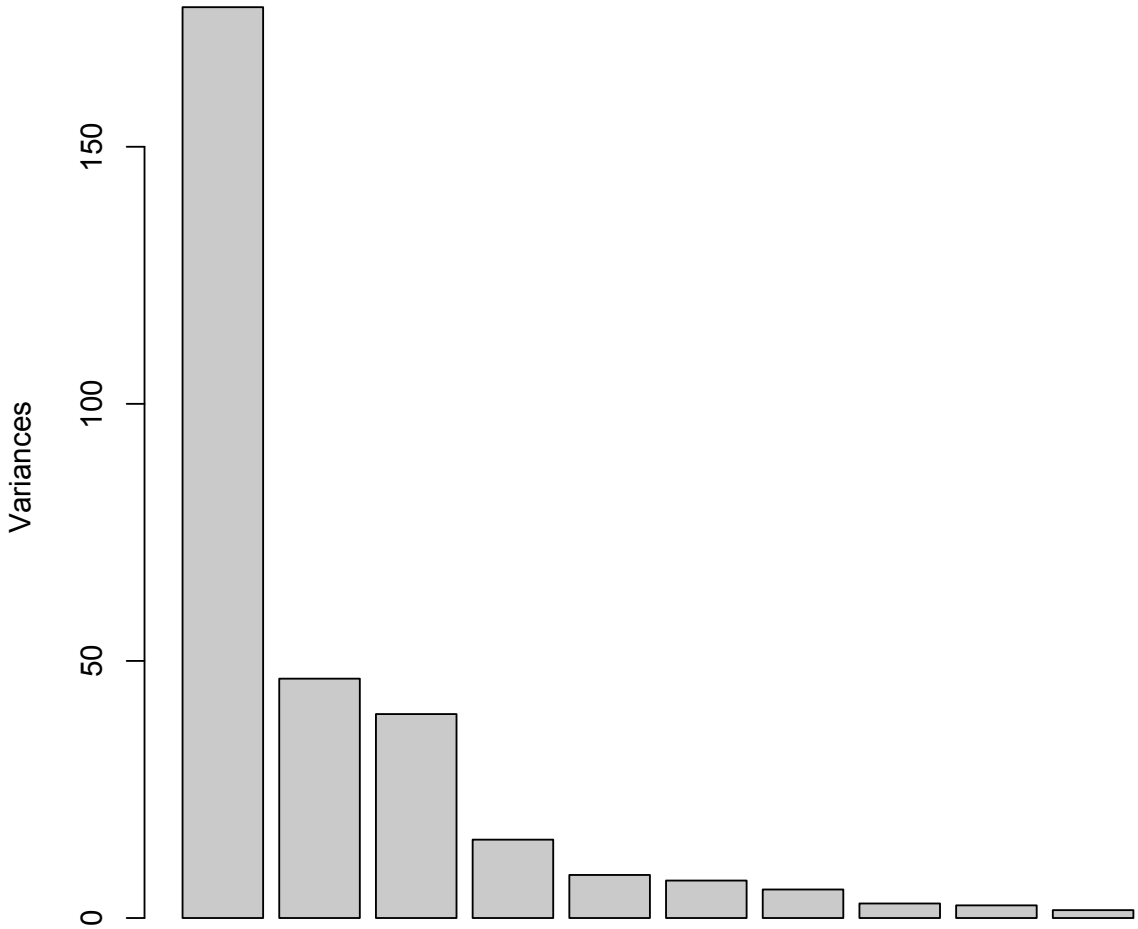


Figure 367: PCA scree plot for the first derivative spectra (5-point smoothing) of 30 glasses (10 replicates) with nominally similar RIs (same RI set 2), autoscaled.

Table 379: PCA results for the second derivative spectra (5-point smoothing) of 30 glasses (10 replicates) with nominally similar RIs (same RI set 2), autoscaled.

	PC1	PC2	PC3	PC4	PC5	PC6	PC7	PC8	PC9	PC10	PC11
Standard Deviation	5.5051	5.0580	4.0382	3.5719	3.2447	3.0640	2.7077	2.5525	2.5240	2.4191	2.3361
Proportion of Variance	0.0938	0.0792	0.0505	0.0395	0.0326	0.0291	0.0227	0.0202	0.0197	0.0181	0.0169
Cumulative Proportion	0.0938	0.1730	0.2235	0.2630	0.2956	0.3247	0.3474	0.3675	0.3873	0.4054	0.4223
	PC12	PC13	PC14	PC15	PC16	PC17	PC18	PC19	PC20	PC21	PC22
Standard Deviation	2.2685	2.2403	2.1677	2.1273	2.0741	2.0393	2.0064	1.9899	1.9329	1.9104	1.8723
Proportion of Variance	0.0159	0.0155	0.0146	0.0140	0.0133	0.0129	0.0125	0.0123	0.0116	0.0113	0.0109
Cumulative Proportion	0.4382	0.4538	0.4683	0.4823	0.4956	0.5085	0.5210	0.5332	0.5448	0.5561	0.5669
	PC23	PC24	PC25	PC26	PC27	PC28	PC29	PC30	PC31	PC32	PC33
Standard Deviation	1.8539	1.8242	1.8162	1.7889	1.7365	1.7175	1.7037	1.6999	1.6839	1.6566	1.6237
Proportion of Variance	0.0106	0.0103	0.0102	0.0099	0.0093	0.0091	0.0090	0.0090	0.0088	0.0085	0.0082
Cumulative Proportion	0.5776	0.5879	0.5981	0.6080	0.6173	0.6265	0.6355	0.6444	0.6532	0.6617	0.6698
	PC34	PC35	PC36	PC37	PC38	PC39	PC40	PC41	PC42	PC43	PC44
Standard Deviation	1.6090	1.5965	1.5914	1.5854	1.5747	1.5310	1.5062	1.4753	1.4640	1.4498	1.4314
Proportion of Variance	0.0080	0.0079	0.0078	0.0078	0.0077	0.0073	0.0070	0.0067	0.0066	0.0065	0.0063
Cumulative Proportion	0.6779	0.6858	0.6936	0.7014	0.7091	0.7163	0.7233	0.7301	0.7367	0.7432	0.7496
	PC45	PC46	PC47	PC48	PC49	PC50	PC51	PC52	PC53	PC54	PC55
Standard Deviation	1.4258	1.4170	1.3907	1.3849	1.3616	1.3526	1.3207	1.3111	1.3070	1.2857	1.2683
Proportion of Variance	0.0063	0.0062	0.0060	0.0059	0.0057	0.0057	0.0054	0.0053	0.0053	0.0051	0.0050
Cumulative Proportion	0.7559	0.7621	0.7681	0.7740	0.7797	0.7854	0.7908	0.7961	0.8014	0.8065	0.8115
	PC56	PC57	PC58	PC59	PC60	PC61	PC62	PC63	PC64	PC65	PC66
Standard Deviation	1.2502	1.2360	1.2225	1.2124	1.1982	1.1782	1.1603	1.1561	1.1339	1.1242	1.1094
Proportion of Variance	0.0048	0.0047	0.0046	0.0046	0.0044	0.0043	0.0042	0.0041	0.0040	0.0039	0.0038
Cumulative Proportion	0.8163	0.8211	0.8257	0.8303	0.8347	0.8390	0.8432	0.8473	0.8513	0.8552	0.8590
	PC67	PC68	PC69	PC70	PC71	PC72	PC73	PC74	PC75	PC76	PC77
Standard Deviation	1.0979	1.0859	1.0828	1.0661	1.0499	1.0335	1.0234	1.0109	1.0055	0.9914	0.9813
Proportion of Variance	0.0037	0.0037	0.0036	0.0035	0.0034	0.0033	0.0032	0.0032	0.0031	0.0030	0.0030
Cumulative Proportion	0.8627	0.8664	0.8700	0.8735	0.8769	0.8803	0.8835	0.8867	0.8898	0.8928	0.8958
	PC78	PC79	PC80	PC81	PC82	PC83	PC84	PC85	PC86	PC87	PC88
Standard Deviation	0.9666	0.9583	0.9361	0.9306	0.9284	0.9112	0.8926	0.8783	0.8734	0.8698	0.8615
Proportion of Variance	0.0029	0.0028	0.0027	0.0027	0.0027	0.0026	0.0025	0.0024	0.0024	0.0023	0.0023
Cumulative Proportion	0.8987	0.9015	0.9043	0.9069	0.9096	0.9122	0.9146	0.9170	0.9194	0.9217	0.9240
	PC89	PC90	PC91	PC92	PC93	PC94	PC95	PC96	PC97	PC98	PC99

Standard Deviation	0.8404	0.8374	0.8242	0.8206	0.8097	0.7902	0.7880	0.7764	0.7560	0.7539	0.7383
Proportion of Variance	0.0022	0.0022	0.0021	0.0021	0.0020	0.0019	0.0019	0.0019	0.0018	0.0018	0.0017
Cumulative Proportion	0.9262	0.9284	0.9305	0.9326	0.9346	0.9365	0.9385	0.9403	0.9421	0.9439	0.9456
	PC100	PC101	PC102	PC103	PC104	PC105	PC106	PC107	PC108	PC109	PC110
Standard Deviation	0.7279	0.7215	0.7030	0.6981	0.6920	0.6850	0.6719	0.6583	0.6526	0.6450	0.6333
Proportion of Variance	0.0016	0.0016	0.0015	0.0015	0.0015	0.0015	0.0014	0.0013	0.0013	0.0013	0.0012
Cumulative Proportion	0.9472	0.9488	0.9503	0.9518	0.9533	0.9548	0.9562	0.9575	0.9588	0.9601	0.9614
	PC111	PC112	PC113	PC114	PC115	PC116	PC117	PC118	PC119	PC120	PC121
Standard Deviation	0.6312	0.6144	0.6082	0.6014	0.5923	0.5875	0.5725	0.5614	0.5564	0.5530	0.5447
Proportion of Variance	0.0012	0.0012	0.0012	0.0011	0.0011	0.0011	0.0010	0.0010	0.0010	0.0010	0.0009
Cumulative Proportion	0.9626	0.9638	0.9649	0.9660	0.9671	0.9682	0.9692	0.9702	0.9711	0.9721	0.9730
	PC122	PC123	PC124	PC125	PC126	PC127	PC128	PC129	PC130	PC131	PC132
Standard Deviation	0.5331	0.5288	0.5228	0.5119	0.5083	0.5045	0.4964	0.4891	0.4827	0.4764	0.4622
Proportion of Variance	0.0009	0.0009	0.0009	0.0008	0.0008	0.0008	0.0008	0.0007	0.0007	0.0007	0.0007
Cumulative Proportion	0.9739	0.9747	0.9756	0.9764	0.9772	0.9780	0.9788	0.9795	0.9802	0.9809	0.9816
	PC133	PC134	PC135	PC136	PC137	PC138	PC139	PC140	PC141	PC142	PC143
Standard Deviation	0.4552	0.4446	0.4409	0.4314	0.4208	0.4184	0.4139	0.4021	0.4007	0.3947	0.3876
Proportion of Variance	0.0006	0.0006	0.0006	0.0006	0.0006	0.0005	0.0005	0.0005	0.0005	0.0005	0.0005
Cumulative Proportion	0.9822	0.9828	0.9834	0.9840	0.9846	0.9851	0.9856	0.9861	0.9866	0.9871	0.9876
	PC144	PC145	PC146	PC147	PC148	PC149	PC150	PC151	PC152	PC153	PC154
Standard Deviation	0.3824	0.3756	0.3684	0.3655	0.3610	0.3524	0.3418	0.3406	0.3361	0.3313	0.3246
Proportion of Variance	0.0005	0.0004	0.0004	0.0004	0.0004	0.0004	0.0004	0.0004	0.0004	0.0003	0.0003
Cumulative Proportion	0.9880	0.9885	0.9889	0.9893	0.9897	0.9901	0.9905	0.9908	0.9912	0.9915	0.9918
	PC155	PC156	PC157	PC158	PC159	PC160	PC161	PC162	PC163	PC164	PC165
Standard Deviation	0.3192	0.3123	0.3083	0.3046	0.2945	0.2875	0.2857	0.2792	0.2743	0.2721	0.2634
Proportion of Variance	0.0003	0.0003	0.0003	0.0003	0.0003	0.0003	0.0003	0.0002	0.0002	0.0002	0.0002
Cumulative Proportion	0.9921	0.9924	0.9927	0.9930	0.9933	0.9936	0.9938	0.9940	0.9943	0.9945	0.9947
	PC166	PC167	PC168	PC169	PC170	PC171	PC172	PC173	PC174	PC175	PC176
Standard Deviation	0.2624	0.2579	0.2486	0.2471	0.2452	0.2416	0.2333	0.2317	0.2242	0.2220	0.2173
Proportion of Variance	0.0002	0.0002	0.0002	0.0002	0.0002	0.0002	0.0002	0.0002	0.0002	0.0002	0.0002
Cumulative Proportion	0.9949	0.9951	0.9953	0.9955	0.9957	0.9959	0.9961	0.9962	0.9964	0.9965	0.9967
	PC177	PC178	PC179	PC180	PC181	PC182	PC183	PC184	PC185	PC186	PC187
Standard Deviation	0.2123	0.2083	0.2034	0.2009	0.1927	0.1898	0.1854	0.1848	0.1816	0.1788	0.1716
Proportion of Variance	0.0001	0.0001	0.0001	0.0001	0.0001	0.0001	0.0001	0.0001	0.0001	0.0001	0.0001

Cumulative Proportion	0.9968	0.9969	0.9971	0.9972	0.9973	0.9974	0.9975	0.9976	0.9977	0.9978	0.9979
	PC188	PC189	PC190	PC191	PC192	PC193	PC194	PC195	PC196	PC197	PC198
Standard Deviation	0.1661	0.1642	0.1600	0.1581	0.1563	0.1533	0.1522	0.1510	0.1457	0.1421	0.1381
Proportion of Variance	0.0001	0.0001	0.0001	0.0001	0.0001	0.0001	0.0001	0.0001	0.0001	0.0001	0.0001
Cumulative Proportion	0.9980	0.9981	0.9982	0.9983	0.9983	0.9984	0.9985	0.9985	0.9986	0.9987	0.9987
	PC199	PC200	PC201	PC202	PC203	PC204	PC205	PC206	PC207	PC208	PC209
Standard Deviation	0.1369	0.1331	0.1307	0.1266	0.1256	0.1235	0.1211	0.1203	0.1175	0.1132	0.1121
Proportion of Variance	0.0001	0.0001	0.0001	0.0001	0.0001	0.0001	0.0001	0.0000	0.0000	0.0000	0.0000
Cumulative Proportion	0.9988	0.9989	0.9989	0.9990	0.9990	0.9990	0.9991	0.9991	0.9992	0.9992	0.9993
	PC210	PC211	PC212	PC213	PC214	PC215	PC216	PC217	PC218	PC219	PC220
Standard Deviation	0.1090	0.1060	0.1040	0.1017	0.1003	0.0977	0.0946	0.0926	0.0898	0.0884	0.0857
Proportion of Variance	0.0000	0.0000	0.0000	0.0000	0.0000	0.0000	0.0000	0.0000	0.0000	0.0000	0.0000
Cumulative Proportion	0.9993	0.9993	0.9994	0.9994	0.9994	0.9995	0.9995	0.9995	0.9995	0.9996	0.9996
	PC221	PC222	PC223	PC224	PC225	PC226	PC227	PC228	PC229	PC230	PC231
Standard Deviation	0.0832	0.0826	0.0804	0.0789	0.0759	0.0746	0.0738	0.0722	0.0693	0.0668	0.0663
Proportion of Variance	0.0000	0.0000	0.0000	0.0000	0.0000	0.0000	0.0000	0.0000	0.0000	0.0000	0.0000
Cumulative Proportion	0.9996	0.9996	0.9996	0.9997	0.9997	0.9997	0.9997	0.9997	0.9997	0.9998	0.9998
	PC232	PC233	PC234	PC235	PC236	PC237	PC238	PC239	PC240	PC241	PC242
Standard Deviation	0.0636	0.0613	0.0608	0.0586	0.0577	0.0564	0.0551	0.0534	0.0528	0.0515	0.0498
Proportion of Variance	0.0000	0.0000	0.0000	0.0000	0.0000	0.0000	0.0000	0.0000	0.0000	0.0000	0.0000
Cumulative Proportion	0.9998	0.9998	0.9998	0.9998	0.9998	0.9998	0.9999	0.9999	0.9999	0.9999	0.9999
	PC243	PC244	PC245	PC246	PC247	PC248	PC249	PC250	PC251	PC252	PC253
Standard Deviation	0.0490	0.0477	0.0468	0.0458	0.0453	0.0437	0.0421	0.0405	0.0397	0.0390	0.0375
Proportion of Variance	0.0000	0.0000	0.0000	0.0000	0.0000	0.0000	0.0000	0.0000	0.0000	0.0000	0.0000
Cumulative Proportion	0.9999	0.9999	0.9999	0.9999	0.9999	0.9999	0.9999	0.9999	0.9999	0.9999	0.9999
	PC254	PC255	PC256	PC257	PC258	PC259	PC260	PC261	PC262	PC263	PC264
Standard Deviation	0.0365	0.0353	0.0342	0.0339	0.0332	0.0319	0.0305	0.0283	0.0282	0.0267	0.0265
Proportion of Variance	0.0000	0.0000	0.0000	0.0000	0.0000	0.0000	0.0000	0.0000	0.0000	0.0000	0.0000
Cumulative Proportion	1.0000	1.0000	1.0000	1.0000	1.0000	1.0000	1.0000	1.0000	1.0000	1.0000	1.0000
	PC265	PC266	PC267	PC268	PC269	PC270	PC271	PC272	PC273	PC274	PC275
Standard Deviation	0.0252	0.0239	0.0233	0.0216	0.0214	0.0211	0.0191	0.0190	0.0180	0.0175	0.0159
Proportion of Variance	0.0000	0.0000	0.0000	0.0000	0.0000	0.0000	0.0000	0.0000	0.0000	0.0000	0.0000
Cumulative Proportion	1.0000	1.0000	1.0000	1.0000	1.0000	1.0000	1.0000	1.0000	1.0000	1.0000	1.0000
	PC276	PC277	PC278	PC279	PC280	PC281	PC282	PC283	PC284	PC285	

Standard Deviation	0.0158	0.0150	0.0144	0.0141	0.0131	0.0127	0.0113	0.0108	0.0104	0.0095	
Proportion of Variance	0.0000	0.0000	0.0000	0.0000	0.0000	0.0000	0.0000	0.0000	0.0000	0.0000	
Cumulative Proportion	1.0000	1.0000	1.0000	1.0000	1.0000	1.0000	1.0000	1.0000	1.0000	1.0000	
	PC286	PC287	PC288	PC289	PC290	PC291	PC292	PC293	PC294	PC295	
Standard Deviation	0.0086	0.0081	0.0078	0.0075	0.0065	0.0059	0.0053	0.0047	0.0042	0.0032	
Proportion of Variance	0.0000	0.0000	0.0000	0.0000	0.0000	0.0000	0.0000	0.0000	0.0000	0.0000	
Cumulative Proportion	1.0000	1.0000	1.0000	1.0000	1.0000	1.0000	1.0000	1.0000	1.0000	1.0000	
	PC296	PC297	PC298	PC299	PC300						
Standard Deviation	0.0028	0.0026	0.0013	0.0012	0.0000						
Proportion of Variance	0.0000	0.0000	0.0000	0.0000	0.0000						
Cumulative Proportion	1.0000	1.0000	1.0000	1.0000	1.0000						

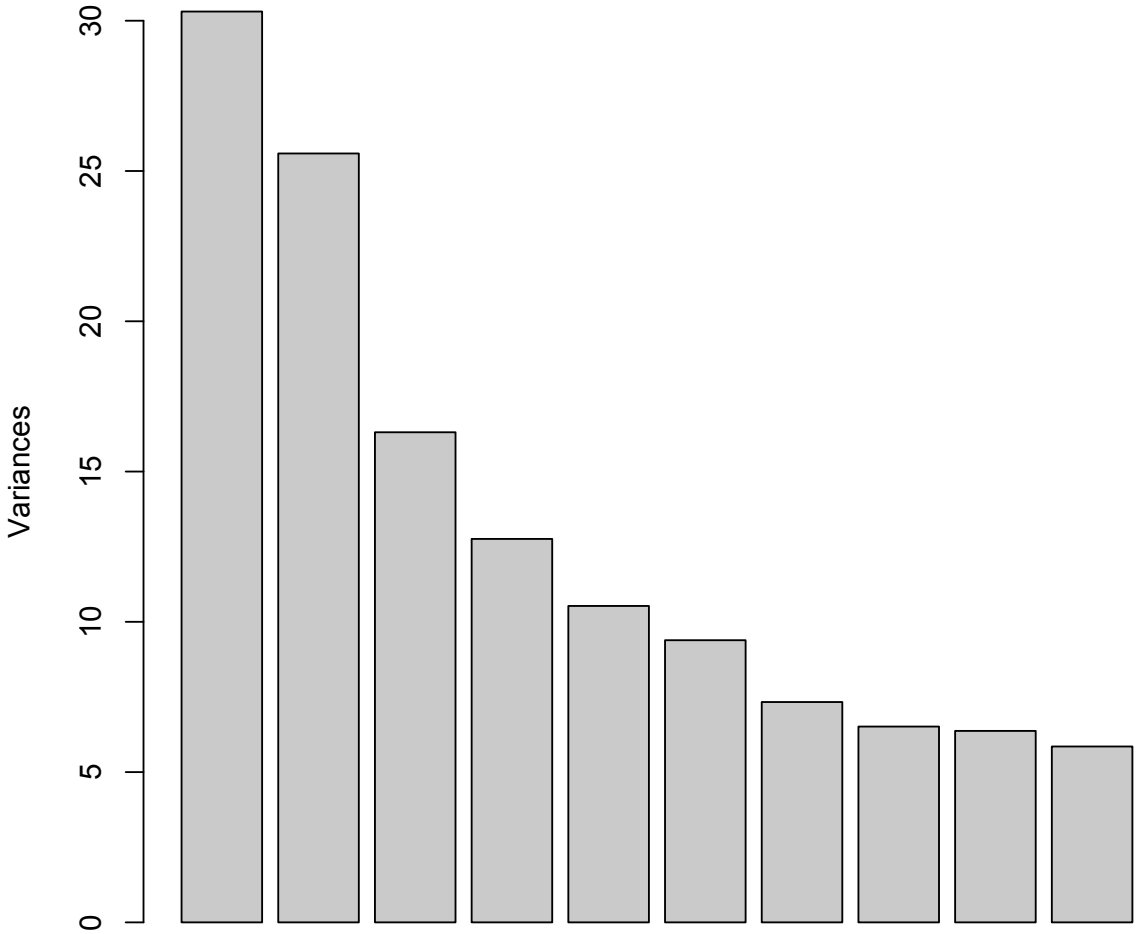


Figure 368: PCA scree plot for the second derivative spectra (5-point smoothing) of 30 glasses (10 replicates) with nominally similar RIs (same RI set 2), autoscaled.

APPENDIX XVI: HOO-CV PCA CVA RESULTS FOR CHEMOMETRIC ANALYSIS OF GLASSES WITH THE SAME RI

Table 380: Discrimination error rates for HOO-CV with PCA reduced CVA for the spectra of 21 glasses (10 replicates) with nominally similar RIs (same RI set 1), autoscaled. The smallest PC dimension with the minimum error rate is highlighted in yellow.

PCs	Error Rate (%)	PCs	Error Rate (%)	PCs	Error Rate (%)	PCs	Error Rate (%)	PCs	Error Rate (%)
2	94.29	44	27.62	86	26.67	128	24.76	170	37.14
3	88.10	45	29.05	87	25.24	129	23.33	171	39.52
4	85.24	46	27.14	88	26.67	130	24.29	172	40.48
5	82.86	47	27.62	89	26.19	131	24.29	173	42.86
6	77.62	48	29.05	90	26.19	132	23.81	174	44.29
7	77.62	49	29.05	91	26.67	133	24.76	175	48.57
8	79.05	50	30.00	92	26.19	134	24.29	176	50.95
9	71.43	51	29.05	93	25.24	135	27.14	177	50.48
10	67.62	52	29.52	94	26.19	136	28.57	178	52.86
11	64.29	53	29.52	95	27.14	137	28.10	179	55.24
12	63.81	54	28.57	96	24.76	138	29.05	180	61.43
13	64.76	55	28.10	97	21.90	139	30.00	181	64.76
14	62.38	56	29.52	98	24.29	140	29.05	182	64.76
15	61.90	57	27.62	99	23.33	141	27.62	183	71.90
16	63.33	58	27.62	100	21.90	142	28.57	184	76.19
17	60.95	59	30.00	101	23.81	143	28.57	185	82.86
18	56.19	60	29.05	102	23.33	144	28.57	186	82.38
19	53.33	61	29.52	103	23.81	145	29.52	187	87.62
20	51.43	62	29.05	104	24.29	146	29.05	188	90.48
21	51.43	63	30.00	105	25.24	147	30.95	189	87.14
22	41.90	64	29.52	106	23.81	148	30.48	190	88.10
23	38.57	65	27.62	107	23.81	149	31.43	191	64.76
24	37.14	66	28.10	108	24.29	150	30.48	192	79.52
25	33.81	67	27.14	109	24.29	151	31.90	193	89.52
26	31.90	68	26.67	110	24.29	152	31.90	194	87.14
27	30.95	69	27.14	111	22.38	153	32.38	195	89.52
28	31.90	70	29.05	112	23.81	154	30.00	196	87.14
29	31.43	71	29.52	113	25.24	155	32.86	197	89.05
30	30.00	72	29.52	114	24.76	156	33.81	198	90.48
31	32.38	73	27.62	115	24.76	157	33.33	199	90.95
32	28.57	74	28.10	116	23.33	158	35.24	200	93.33
33	28.10	75	27.62	117	25.24	159	35.24	201	94.76
34	30.00	76	27.62	118	22.86	160	35.71	202	95.24

35	28.57	77	27.62	119	23.33	161	36.67	203	96.19
36	28.57	78	27.14	120	24.76	162	33.81	204	95.71
37	28.57	79	30.00	121	24.29	163	31.90	205	95.24
38	28.57	80	27.14	122	24.76	164	33.81	206	95.71
39	29.05	81	28.57	123	25.71	165	35.71	207	97.14
40	29.05	82	28.10	124	22.38	166	34.76	208	97.62
41	27.62	83	22.38	125	24.29	167	36.67	209	87.62
42	27.62	84	25.71	126	25.71	168	37.14		
43	27.62	85	25.24	127	27.62	169	39.05		

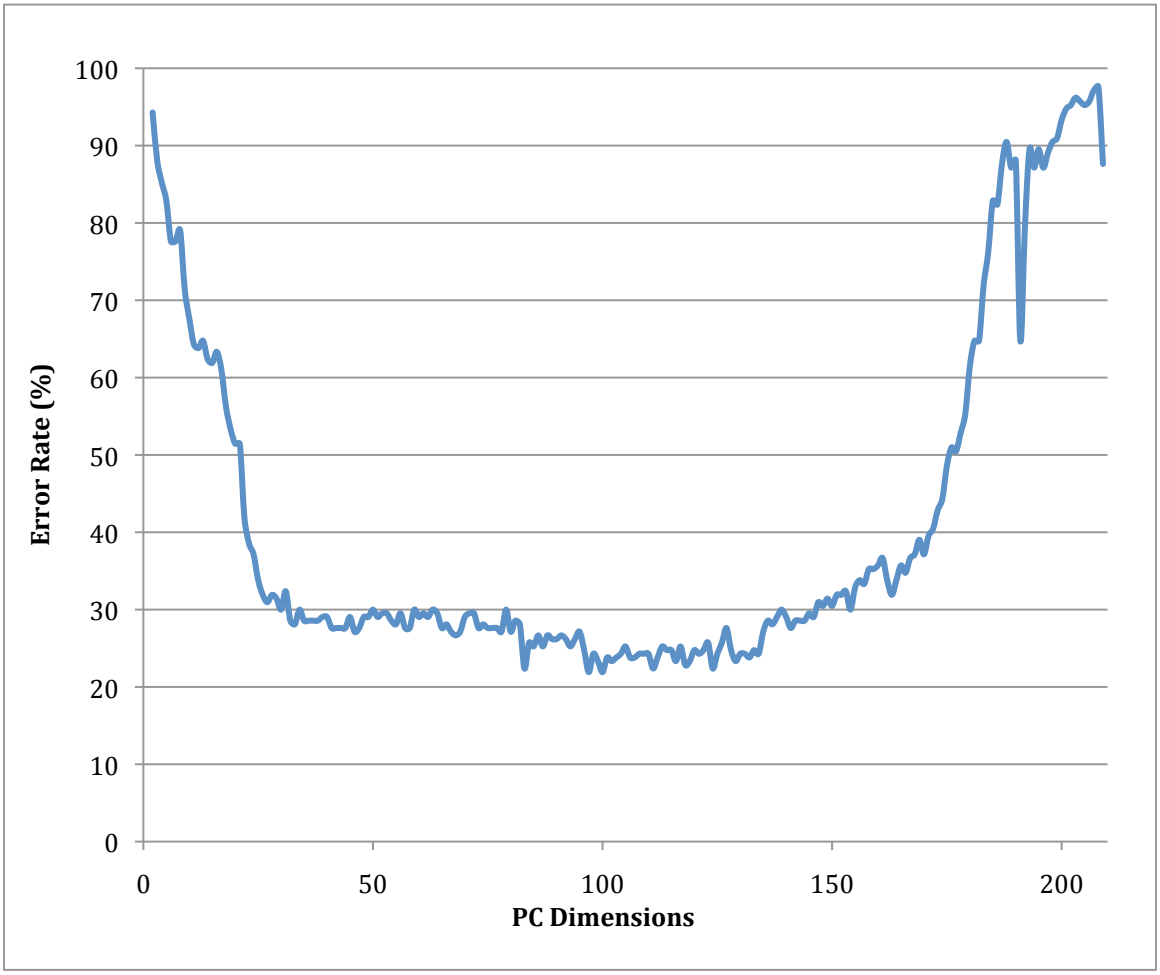


Figure 369: Graph of the discrimination error rate versus PC dimensions for HOO-CV with PCA reduced CVA for the spectra of 21 glasses (10 replicates) with nominally similar RIs (same RI set 1), autoscaled.

Table 381: Discrimination error rates for HOO-CV with PCA reduced CVA for the first derivative spectra (5-point smoothing) of 21 glasses (10 replicates) with nominally similar RIs (same RI set 1), autoscaled. The smallest PC dimension with the minimum error rate is highlighted in yellow.

PCs	Error Rate (%)	PCs	Error Rate (%)	PCs	Error Rate (%)	PCs	Error Rate (%)	PCs	Error Rate (%)
2	95.24	40	27.62	78	19.52	116	29.05	154	34.29
3	91.43	41	25.71	79	20.48	117	27.14	155	33.81
4	89.52	42	25.24	80	20.48	118	24.76	156	33.81
5	81.90	43	24.29	81	20.00	119	24.76	157	32.86
6	80.48	44	26.67	82	20.95	120	23.33	158	36.67
7	75.24	45	23.81	83	21.43	121	24.29	159	38.10
8	71.43	46	23.81	84	20.95	122	24.29	160	37.14
9	67.62	47	23.81	85	20.48	123	25.71	161	40.00
10	61.90	48	22.38	86	20.48	124	23.33	162	41.90
11	60.00	49	21.90	87	20.00	125	22.86	163	43.33
12	60.48	50	22.86	88	20.00	126	23.33	164	40.95
13	57.62	51	24.29	89	21.43	127	24.76	165	40.95
14	56.67	52	22.86	90	21.43	128	24.76	166	42.38
15	50.95	53	21.90	91	22.38	129	26.19	167	43.81
16	51.43	54	22.86	92	20.00	130	27.62	168	46.67
17	50.00	55	20.48	93	18.57	131	30.00	169	44.29
18	49.52	56	20.00	94	17.14	132	30.00	170	44.29
19	48.10	57	20.48	95	19.52	133	30.48	171	46.67
20	44.29	58	20.48	96	20.48	134	28.10	172	50.00
21	43.33	59	20.48	97	18.57	135	28.10	173	50.95
22	43.81	60	20.95	98	18.57	136	30.00	174	49.52
23	42.86	61	20.95	99	20.48	137	30.00	175	50.48
24	44.29	62	20.48	100	21.90	138	30.48	176	55.71
25	42.86	63	19.52	101	22.38	139	29.52	177	56.67
26	43.33	64	21.90	102	21.90	140	29.52	178	56.67
27	40.48	65	22.38	103	21.90	141	30.00	179	59.05
28	38.57	66	20.48	104	21.90	142	30.00	180	61.43
29	38.10	67	21.90	105	22.38	143	28.10	181	66.19
30	35.71	68	22.38	106	21.90	144	27.14	182	65.71
31	35.24	69	22.38	107	23.81	145	27.62	183	70.95
32	35.24	70	21.90	108	24.76	146	29.52	184	67.14
33	31.90	71	20.00	109	24.76	147	30.95	185	72.86
34	33.33	72	20.00	110	24.29	148	32.38	186	78.57
35	30.00	73	20.48	111	26.19	149	31.43	187	81.43
36	30.95	74	21.90	112	27.14	150	32.38	188	82.86
37	27.14	75	20.00	113	26.67	151	34.29	189	82.86

38	28.57	76	19.05	114	27.62	152	35.71	
39	28.10	77	20.00	115	28.10	153	36.67	

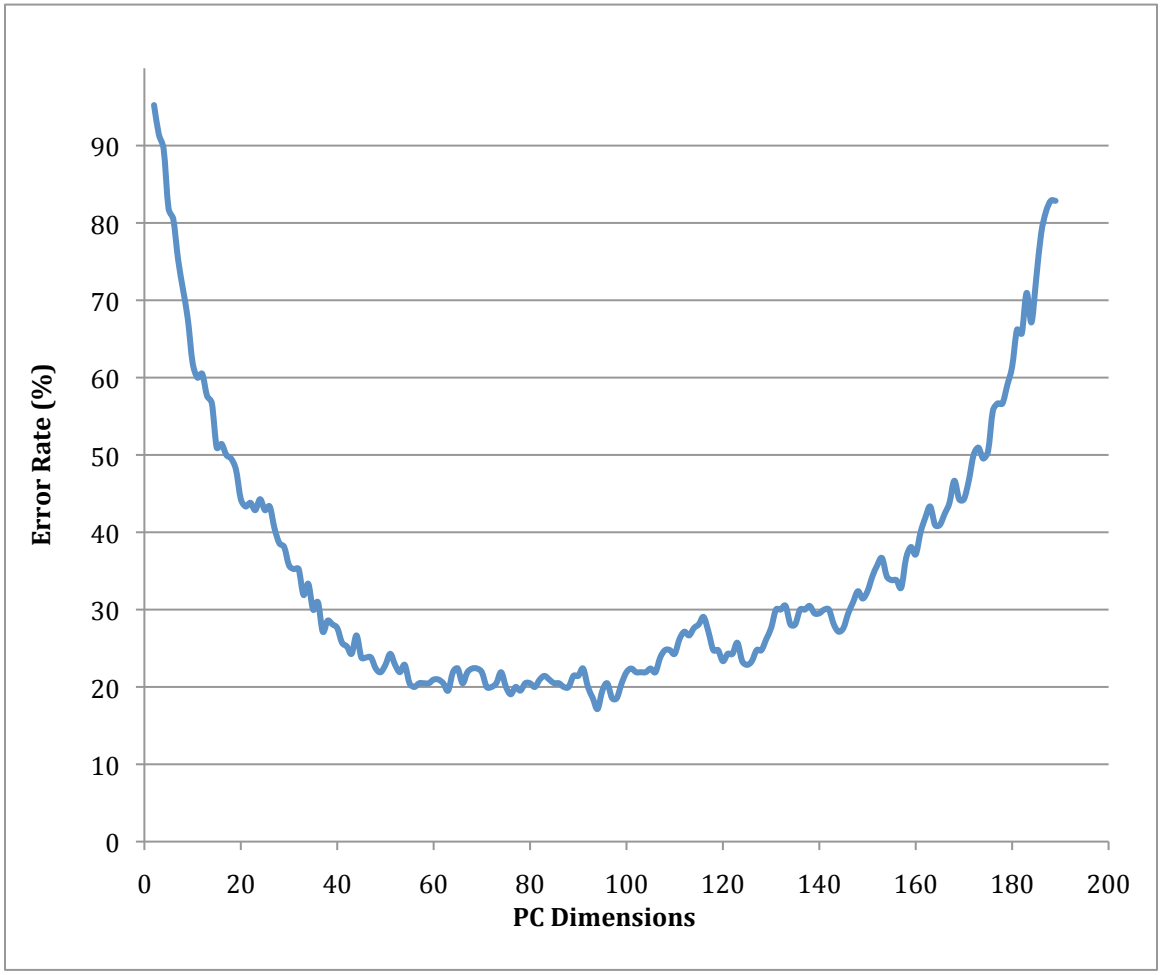


Figure 370: Graph of the discrimination error rate versus PC dimensions for HOO-CV with PCA reduced CVA for the first derivative spectra (5-point smoothing) of 21 glasses (10 replicates) with nominally similar RIs (same RI set 1), autoscaled.

Table 382: Discrimination error rates for HOO-CV with PCA reduced CVA for the second derivative spectra (5-point smoothing) of 21 glasses (10 replicates) with nominally similar RIs (same RI set 1), autoscaled. The smallest PC dimension with the minimum error rate is highlighted in yellow.

PCs	Error Rate (%)	PCs	Error Rate (%)	PCs	Error Rate (%)	PCs	Error Rate (%)	PCs	Error Rate (%)
2	80.95	40	27.62	78	15.71	117	26.67	155	32.86
3	74.76	41	26.67	79	16.19	118	27.62	156	36.19
4	72.86	42	25.24	80	14.76	119	25.71	157	32.38
5	70.95	43	25.24	81	15.24	120	25.71	158	33.33
6	61.90	44	25.71	82	14.29	121	25.24	159	33.33
7	61.43	45	25.71	83	13.33	122	27.62	160	34.29
8	61.90	46	26.19	84	12.86	123	25.71	161	33.33
9	60.48	47	26.19	85	12.38	124	26.67	162	35.71
10	56.67	48	25.71	86	12.86	125	27.14	163	36.67
11	57.62	49	25.71	87	14.29	126	28.10	164	35.71
12	55.24	50	26.19	88	17.14	127	24.76	165	36.67
13	53.33	51	25.71	89	16.19	128	25.71	166	34.29
14	51.90	52	25.71	90	15.24	129	23.33	167	36.67
15	46.67	53	25.71	91	18.57	130	24.76	168	39.05
16	46.19	54	26.67	92	17.62	131	26.19	169	41.90
17	45.71	55	24.29	93	18.10	132	25.71	170	38.10
18	43.81	56	24.76	94	18.57	133	25.71	171	37.62
19	43.33	57	24.76	95	20.48	134	24.76	172	39.52
20	40.00	58	22.38	96	18.57	135	25.71	173	42.38
21	38.57	59	22.38	97	19.05	136	25.24	174	46.67
22	38.57	60	25.24	98	19.05	137	26.67	175	44.76
23	39.52	61	23.81	99	19.52	138	28.57	176	46.67
24	35.71	62	23.81	100	19.05	139	27.62	177	46.67
25	35.24	63	21.43	101	19.05	140	26.67	178	50.00
26	31.43	64	20.00	102	20.00	141	25.24	179	51.90
27	33.33	65	20.48	103	20.00	142	25.71	180	54.29
28	33.33	66	20.95	104	21.43	143	25.24	181	51.43
29	31.43	67	19.05	105	21.90	144	24.76	182	50.48
30	32.38	68	18.57	106	20.48	145	23.33	183	58.57
31	30.48	69	18.57	107	20.48	146	25.24	184	60.95
32	30.95	70	17.62	108	21.90	147	29.05	185	63.81
33	31.43	71	17.62	109	20.95	148	29.05	186	69.05
34	32.38	72	18.57	110	21.90	149	29.52	187	70.95
35	32.86	73	20.00	111	22.86	150	30.48	188	80.48
36	31.43	74	19.52	112	22.86	151	30.95	189	66.67
37	28.57	75	20.95	113	24.29	152	33.33		

38	27.62	76	19.05	114	24.76	153	33.33	
39	27.14	77	18.10	115	25.71	154	33.33	

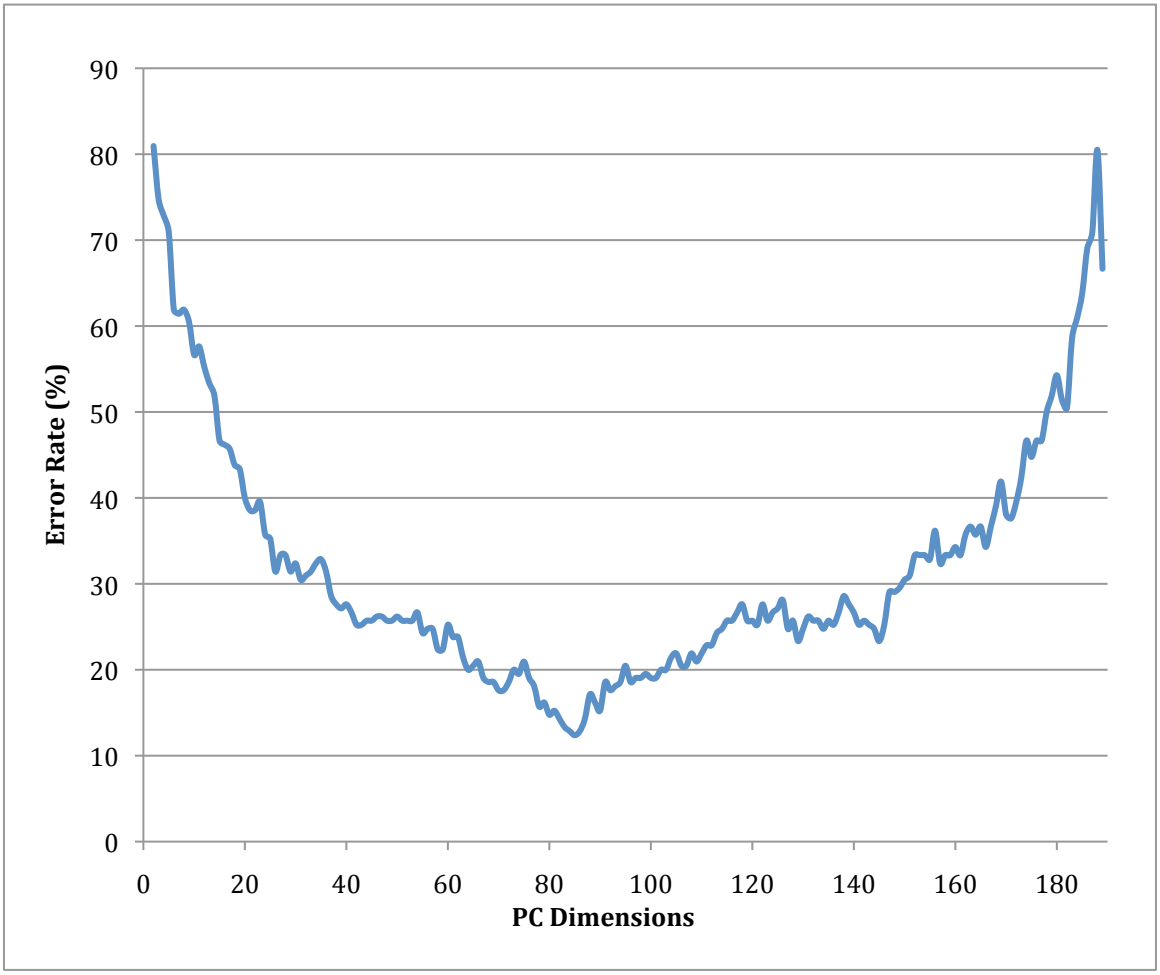


Figure 371: Graph of the discrimination error rate versus PC dimensions for HOO-CV with PCA reduced CVA for the second derivative spectra (5-point smoothing) of 21 glasses (10 replicates) with nominally similar RIs (same RI set 1), autoscaled.

Table 383: Discrimination error rates for HOO-CV with PCA reduced CVA for the spectra of 30 glasses (10 replicates) with nominally similar RIs (same RI set 2), autoscaled. The smallest PC dimension with the minimum error rate is highlighted in yellow.

PCs	Error Rate (%)	PCs	Error Rate (%)	PCs	Error Rate (%)	PCs	Error Rate (%)	PCs	Error Rate (%)
2	97.67	60	31.67	118	22.67	176	23.67	234	38.33
3	93.00	61	32.00	119	22.33	177	23.00	235	40.33
4	93.67	62	31.00	120	23.33	178	23.00	236	39.00
5	93.33	63	30.67	121	22.67	179	23.00	237	39.67
6	93.33	64	29.33	122	24.00	180	24.00	238	39.33
7	93.33	65	30.00	123	25.00	181	25.00	239	38.00
8	91.33	66	30.33	124	25.00	182	25.00	240	38.00
9	89.33	67	29.67	125	22.67	183	24.67	241	39.67
10	87.67	68	30.67	126	23.67	184	26.33	242	38.67
11	83.33	69	32.33	127	24.00	185	23.33	243	40.67
12	82.33	70	29.33	128	24.67	186	23.00	244	41.00
13	77.33	71	30.00	129	23.67	187	24.67	245	40.67
14	77.33	72	30.67	130	24.33	188	25.00	246	41.00
15	72.00	73	31.33	131	24.33	189	25.67	247	42.00
16	73.33	74	31.00	132	23.00	190	26.00	248	40.67
17	74.00	75	32.00	133	23.00	191	27.67	249	44.00
18	70.33	76	29.67	134	23.33	192	29.67	250	43.67
19	70.67	77	27.67	135	23.67	193	29.33	251	44.00
20	69.33	78	28.00	136	24.33	194	28.33	252	45.00
21	65.33	79	28.33	137	24.33	195	27.00	253	45.67
22	56.33	80	29.33	138	23.33	196	26.67	254	48.00
23	52.67	81	29.33	139	23.33	197	26.00	255	51.33
24	51.00	82	29.00	140	23.67	198	26.00	256	52.33
25	47.67	83	28.67	141	23.67	199	26.00	257	52.00
26	44.00	84	28.00	142	23.33	200	26.33	258	54.33
27	40.67	85	28.00	143	22.67	201	25.67	259	59.00
28	41.67	86	27.00	144	23.67	202	28.67	260	61.67
29	41.00	87	27.67	145	22.00	203	27.67	261	61.00
30	40.33	88	27.00	146	22.33	204	27.67	262	65.33
31	37.67	89	26.67	147	20.33	205	28.33	263	69.33
32	37.67	90	24.67	148	22.00	206	29.67	264	71.67
33	38.33	91	24.00	149	21.67	207	29.67	265	69.33
34	36.67	92	25.33	150	23.67	208	31.67	266	76.33
35	37.00	93	26.67	151	22.33	209	32.00	267	72.33
36	38.33	94	26.00	152	22.33	210	32.33	268	80.67
37	39.33	95	26.00	153	24.33	211	34.00	269	79.33
38	40.33	96	24.33	154	24.33	212	35.00	270	88.00

39	39.67	97	23.67	155	23.33	213	34.67	271	94.67
40	37.00	98	23.67	156	23.33	214	33.00	272	94.00
41	39.00	99	24.00	157	22.00	215	33.00	273	87.00
42	37.67	100	24.33	158	21.00	216	34.33	274	88.33
43	38.00	101	26.00	159	20.33	217	34.33	275	90.33
44	38.00	102	25.00	160	20.67	218	33.00	276	92.33
45	37.33	103	25.33	161	20.67	219	32.33	277	92.67
46	35.67	104	26.00	162	20.33	220	30.67	278	81.67
47	36.33	105	25.33	163	20.00	221	29.33	279	87.67
48	32.33	106	24.67	164	21.00	222	31.00	280	92.67
49	32.67	107	25.00	165	20.00	223	29.33	281	94.67
50	31.00	108	24.00	166	19.67	224	31.67	282	95.67
51	31.00	109	24.67	167	19.67	225	30.00	283	97.00
52	31.33	110	24.67	168	21.00	226	30.33	284	96.67
53	32.33	111	22.33	169	20.00	227	31.67	285	96.33
54	32.67	112	23.33	170	19.33	228	33.33	286	97.00
55	32.33	113	22.67	171	20.33	229	33.00	287	98.67
56	32.33	114	23.00	172	21.33	230	35.33	288	98.00
57	31.67	115	22.67	173	23.33	231	35.33		
58	29.33	116	22.33	174	24.00	232	38.00		
59	30.33	117	22.33	175	23.67	233	39.33		

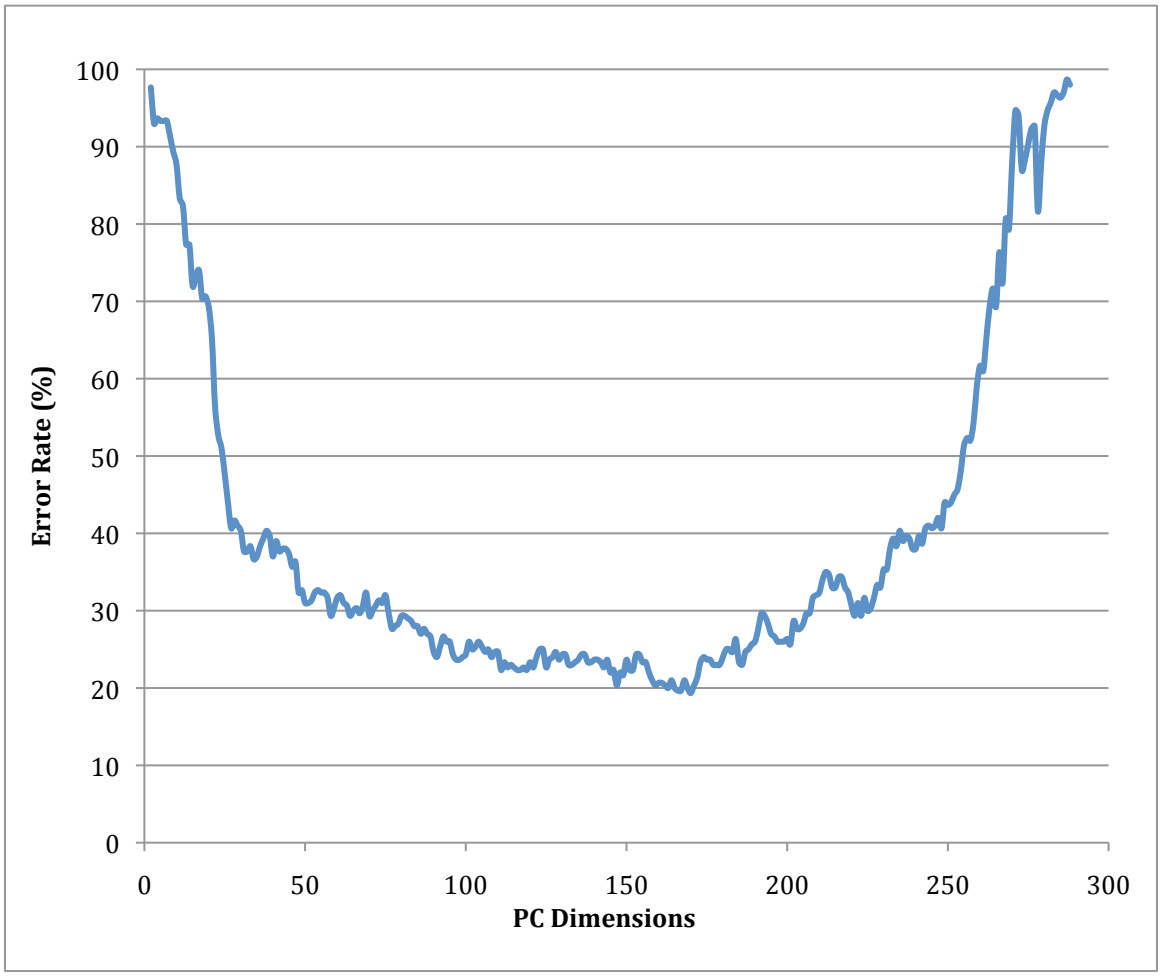


Figure 372: Graph of the discrimination error rate versus PC dimensions for HOO-CV with PCA reduced CVA for the spectra of 30 glasses (10 replicates) with nominally similar RIs (same RI set 2), autoscaled.

Table 384: Discrimination error rates for HOO-CV with PCA reduced CVA for the first derivative spectra (5-point smoothing) of 30 glasses (10 replicates) with nominally similar RIs (same RI set 2), autoscaled. The smallest PC dimension with the minimum error rate is highlighted in yellow.

PCs	Error Rate (%)	PCs	Error Rate (%)	PCs	Error Rate (%)	PCs	Error Rate (%)	PCs	Error Rate (%)
2	95.33	62	34.00	122	17.67	182	24.67	242	34.00
3	92.33	63	32.33	123	18.33	183	24.33	243	32.00
4	92.33	64	31.00	124	18.33	184	24.33	244	32.67
5	93.00	65	31.00	125	19.00	185	24.33	245	36.00
6	89.33	66	29.00	126	19.00	186	24.67	246	36.67
7	89.33	67	29.00	127	18.67	187	23.67	247	36.00
8	88.00	68	28.67	128	18.33	188	24.67	248	37.67
9	85.00	69	27.67	129	17.67	189	26.33	249	39.00
10	79.67	70	28.00	130	16.67	190	26.00	250	38.33
11	74.00	71	26.33	131	18.67	191	24.00	251	40.33
12	73.67	72	25.33	132	17.33	192	22.00	252	43.33
13	73.00	73	26.67	133	19.33	193	22.67	253	44.33
14	71.00	74	25.00	134	19.67	194	21.67	254	46.33
15	70.00	75	24.67	135	20.33	195	21.67	255	49.00
16	69.33	76	25.33	136	20.67	196	21.33	256	50.33
17	67.33	77	26.67	137	21.33	197	21.00	257	52.33
18	65.67	78	25.33	138	19.33	198	21.33	258	54.00
19	61.33	79	23.33	139	20.67	199	21.33	259	56.00
20	61.33	80	23.00	140	20.67	200	24.33	260	61.00
21	58.00	81	24.33	141	19.67	201	22.67	261	61.67
22	58.00	82	23.67	142	19.67	202	21.33	262	66.67
23	56.33	83	23.67	143	19.67	203	23.67	263	67.00
24	56.00	84	23.67	144	19.67	204	23.67	264	68.67
25	55.00	85	22.00	145	19.00	205	25.00	265	73.67
26	56.67	86	22.00	146	20.00	206	26.33	266	77.00
27	56.00	87	21.67	147	21.67	207	24.67	267	76.33
28	52.67	88	21.67	148	21.67	208	24.00	268	82.00
29	53.00	89	21.67	149	21.67	209	25.00	269	74.00
30	52.00	90	22.00	150	21.33	210	24.67	270	92.33
31	51.33	91	21.33	151	20.67	211	25.67	271	76.33
32	50.67	92	22.33	152	21.33	212	27.33	272	88.33
33	47.00	93	21.00	153	20.67	213	26.67	273	92.33
34	48.33	94	20.67	154	21.67	214	25.33	274	91.00
35	48.33	95	20.33	155	20.33	215	26.33	275	92.00
36	45.33	96	20.67	156	21.67	216	28.33	276	93.33
37	45.67	97	20.33	157	23.00	217	28.67	277	92.00

38	44.00	98	21.00	158	22.33	218	29.33	278	93.00
39	44.00	99	20.67	159	22.33	219	28.00	279	89.67
40	43.00	100	20.67	160	23.33	220	30.67	280	91.67
41	42.00	101	19.00	161	23.00	221	30.67	281	90.67
42	41.00	102	19.33	162	21.67	222	30.67	282	92.00
43	39.33	103	18.67	163	23.33	223	31.00	283	95.67
44	40.33	104	19.00	164	23.00	224	31.33	284	96.67
45	40.67	105	18.67	165	23.67	225	28.67	285	95.67
46	40.33	106	17.00	166	24.00	226	30.33	286	96.33
47	39.00	107	16.00	167	22.67	227	28.33	287	98.00
48	39.00	108	16.00	168	24.33	228	28.00	288	98.00
49	38.67	109	16.33	169	22.33	229	28.67	289	97.00
50	38.00	110	16.00	170	22.33	230	29.00	290	98.33
51	36.67	111	16.67	171	23.00	231	30.00	291	99.00
52	35.33	112	18.33	172	23.33	232	30.67	292	98.33
53	35.33	113	18.67	173	23.33	233	31.33	293	99.00
54	35.67	114	18.67	174	23.67	234	33.67	294	98.67
55	35.67	115	17.67	175	23.33	235	32.33	295	99.33
56	36.00	116	18.33	176	24.00	236	30.67	296	98.00
57	35.33	117	17.67	177	24.67	237	32.33	297	97.33
58	35.00	118	17.67	178	24.00	238	33.00	298	97.67
59	34.67	119	18.00	179	24.33	239	35.33	299	95.67
60	33.67	120	17.00	180	24.00	240	33.67		
61	35.00	121	18.33	181	24.00	241	34.33		

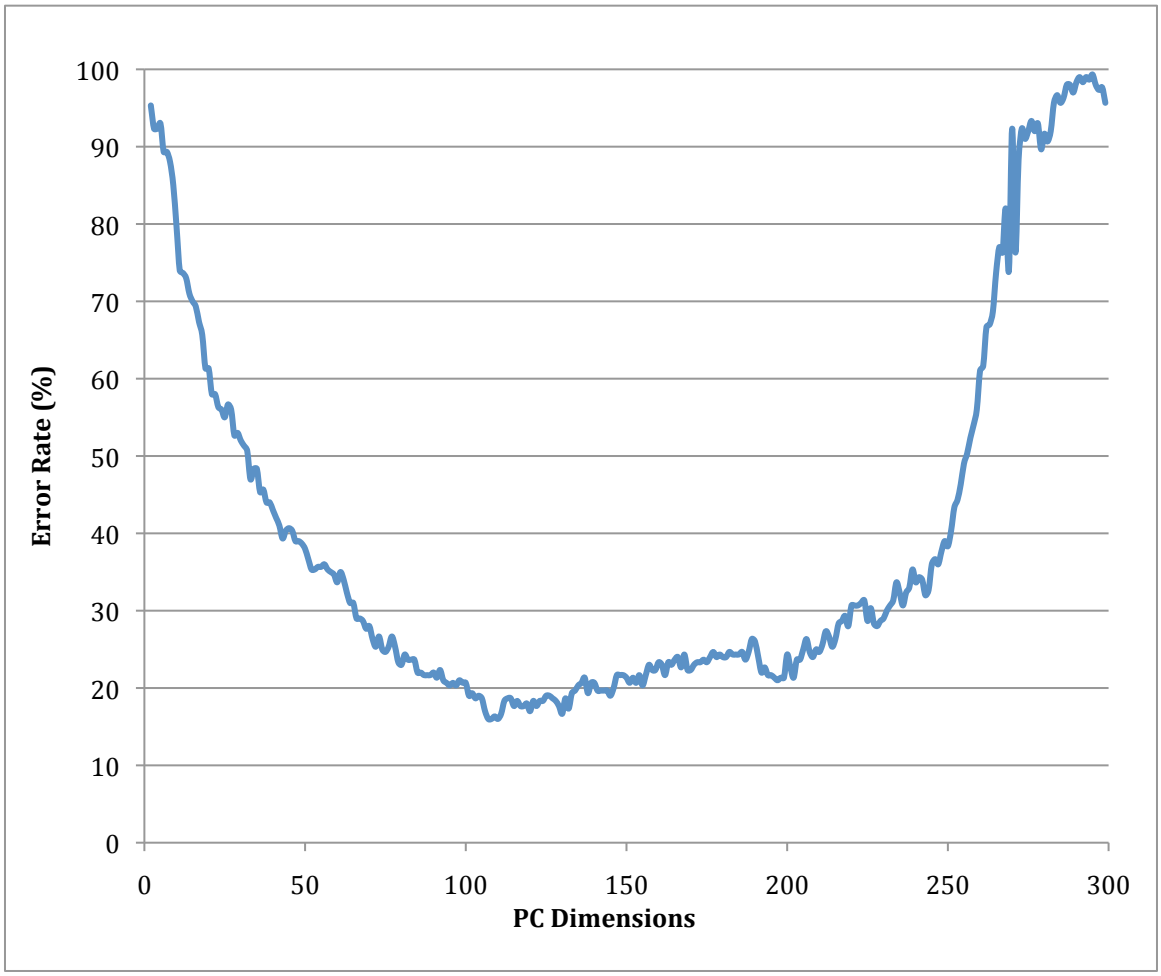


Figure 373: Graph of the discrimination error rate versus PC dimensions for HOO-CV with PCA reduced CVA for the first derivative spectra (5-point smoothing) of 30 glasses (10 replicates) with nominally similar RIs (same RI set 2), autoscaled.

Table 385: Discrimination error rates for HOO-CV with PCA reduced CVA for the second derivative spectra (5-point smoothing) of 30 glasses (10 replicates) with nominally similar RIs (same RI set 2), autoscaled. The smallest PC dimension with the minimum error rate is highlighted in yellow.

PCs	Error Rate (%)	PCs	Error Rate (%)	PCs	Error Rate (%)	PCs	Error Rate (%)	PCs	Error Rate (%)
2	88.67	62	24.33	122	22.33	182	24.33	242	31.67
3	85.67	63	23.67	123	22.33	183	25.00	243	32.00
4	84.00	64	24.00	124	22.67	184	24.67	244	30.33
5	79.67	65	25.00	125	22.00	185	24.67	245	34.00
6	75.00	66	24.33	126	24.00	186	22.00	246	32.33
7	70.67	67	23.67	127	25.00	187	22.67	247	35.00
8	69.67	68	23.33	128	25.00	188	23.33	248	36.00
9	68.33	69	23.67	129	24.00	189	21.00	249	38.00
10	62.33	70	23.67	130	23.33	190	20.67	250	38.33
11	62.00	71	24.00	131	22.00	191	21.00	251	40.67
12	59.00	72	24.00	132	21.67	192	20.67	252	41.67
13	55.00	73	23.67	133	22.00	193	22.33	253	42.33
14	50.67	74	24.00	134	22.67	194	22.00	254	45.33
15	50.67	75	24.00	135	22.67	195	22.33	255	43.67
16	51.33	76	23.00	136	23.00	196	22.33	256	47.67
17	48.00	77	22.67	137	21.00	197	24.00	257	51.33
18	48.67	78	23.33	138	22.00	198	20.67	258	53.00
19	44.00	79	23.67	139	21.00	199	20.33	259	56.00
20	42.67	80	23.00	140	21.67	200	20.33	260	58.33
21	39.33	81	25.67	141	21.33	201	22.67	261	53.00
22	37.67	82	26.00	142	21.67	202	23.33	262	57.00
23	37.33	83	25.00	143	21.67	203	22.33	263	60.67
24	36.33	84	24.00	144	23.00	204	23.33	264	64.33
25	35.00	85	24.00	145	23.00	205	23.00	265	69.33
26	33.33	86	24.00	146	22.33	206	24.00	266	73.67
27	34.33	87	24.00	147	23.00	207	25.33	267	77.33
28	33.33	88	24.00	148	22.33	208	23.00	268	74.00
29	36.00	89	23.33	149	21.00	209	24.33	269	80.00
30	34.67	90	23.00	150	23.00	210	23.00	270	80.67
31	34.00	91	24.33	151	21.00	211	24.00	271	80.33
32	34.33	92	24.67	152	21.00	212	25.67	272	78.33
33	33.33	93	22.33	153	20.67	213	27.33	273	85.67
34	32.33	94	23.00	154	22.67	214	26.67	274	86.33
35	33.67	95	20.67	155	23.33	215	26.33	275	86.00
36	33.67	96	21.00	156	23.00	216	27.33	276	86.33
37	34.00	97	20.67	157	23.33	217	26.00	277	84.33

38	33.00	98	19.33	158	24.33	218	25.33	278	88.00
39	32.67	99	20.33	159	23.00	219	24.67	279	91.33
40	34.33	100	20.67	160	22.67	220	24.67	280	90.00
41	31.00	101	21.00	161	24.67	221	26.67	281	93.67
42	30.33	102	20.00	162	24.67	222	26.00	282	95.33
43	29.33	103	20.00	163	26.00	223	26.33	283	96.33
44	29.00	104	19.33	164	25.33	224	27.67	284	96.33
45	30.33	105	20.00	165	24.67	225	27.00	285	96.00
46	30.00	106	20.67	166	25.67	226	28.00	286	96.00
47	28.33	107	20.33	167	24.33	227	28.67	287	96.33
48	29.00	108	19.67	168	23.00	228	25.00	288	97.00
49	27.33	109	20.33	169	23.33	229	24.67	289	97.33
50	28.33	110	20.67	170	21.67	230	25.67	290	96.67
51	29.00	111	22.33	171	21.67	231	26.33	291	99.00
52	28.33	112	21.33	172	20.00	232	26.00	292	99.33
53	28.00	113	21.33	173	21.00	233	28.33	293	98.00
54	26.67	114	21.00	174	21.33	234	30.33	294	98.67
55	28.00	115	20.33	175	20.67	235	29.00	295	99.33
56	28.67	116	21.67	176	22.33	236	29.67	296	99.00
57	27.00	117	23.33	177	23.00	237	29.67	297	97.33
58	25.33	118	22.00	178	22.67	238	29.33	298	95.67
59	24.33	119	21.67	179	22.67	239	29.33	299	84.67
60	24.00	120	21.00	180	23.00	240	31.67		
61	24.00	121	22.33	181	25.33	241	31.67		

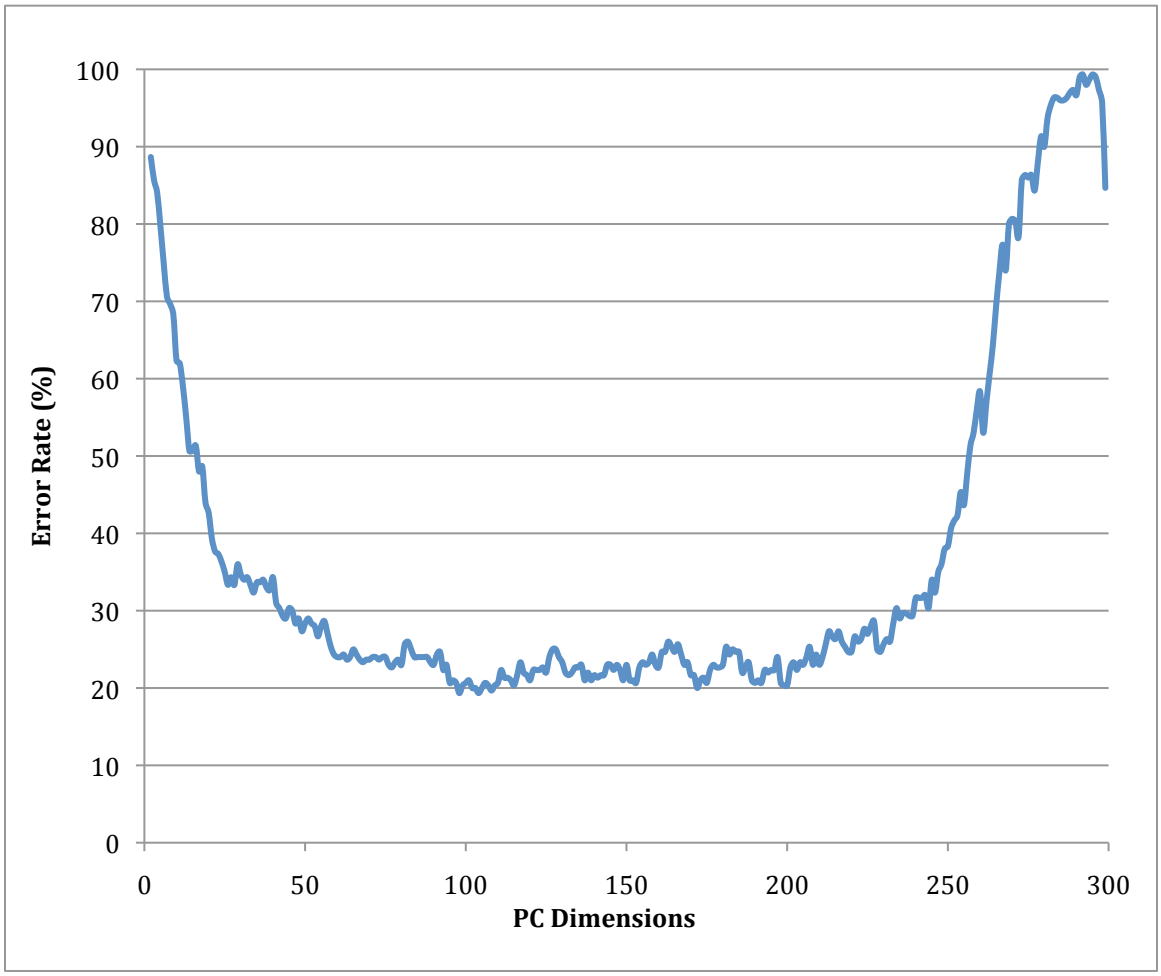


Figure 374: Graph of the discrimination error rate versus PC dimensions for HOO-CV with PCA reduced CVA for the second derivative spectra (5-point smoothing) of 30 glasses (10 replicates) with nominally similar RIs (same RI set 2), autoscaled.

CHAPTER 8: REFERENCES

Adhihetty, I.S., McGuire, J.A., & Haaland, D.M. (1991). Achieving transferable multivariate spectral calibration models: demonstration with infrared spectra of thin-film dielectrics on silicon. *Analytical Chemistry*, 63(20), 2329-2338.

Agarwal, A., Davis, K.M., & Tomozawa, M. (1995). A simple IR spectroscopic method for determining fictive temperature of silica glasses. *Journal of Non-Crystalline Solids*, 185, 191-198.

Almeida, R.M. (1992). Detection of LO modes in glass by infrared reflection spectroscopy at oblique incidence. *Physical Review B*, 45(1), 161-170.

Almirall, J.R. (2001). Elemental analysis of glass fragments. In B. Caddy (Ed.), *Forensic examination of glass and paint: analysis and interpretation* (pp. 65-83). New York: Taylor & Francis Inc.

Almirall, J.R., Cole, M.D., Gettinby, G., & Furton, K.G. (1998). Discrimination of glass sources using elemental composition and refractive index: development of predictive models. *Science and Justice*, 38, 93-100.

Andrasko, J., & Maehly, A.C. (1978). The discrimination between samples of window glass by combining physical and chemical techniques. *Journal of Forensic Sciences*, 23, 250–262.

ASTM International. (2003). ASTM E1967-98 Standard Test Method for the Automated Determinaton of Refractive Index of Glass Samples Using the Oil Immersion Method and a Phase Contrast Microscope. ASTM International, West Conshohocken, Pennsylvania.

ASTM International. (2006). ASTM C1036-06 Standard Specification for Flat Glass. ASTM International, West Conshohocken, Pennsylvania.

ASTM International. (2010). ASTM C162-05 Standard Terminology of Glass and Glass Products. ASTM International, West Conshohocken, Pennsylvania.

Bajic, S.J., Aeschiliman, D.B., Saetveit, N.J., Baldwin, D.P., & Houk, R.S. (2005). Analysis of glass fragments by laser ablation-inductively coupled plasma-mass spectrometry and principal component analysis. *Journal of Forensic Sciences*, 50(2), 1123-1127.

Barnett, C., Cahoon, E., & Almirall, J.R. (2008). Wavelength dependence on the elemental analysis of glass by laser induced breakdown spectroscopy. *Spectrochimica Acta Part B*, 63, 1016-1023.

Beeman, J. (1939). The effect of temperature variations on the determination of specific gravity of glass fragments. *Journal of Criminal Law and Criminology,* 36, 298-300.

Bell, R.J., Bird, N.F., & Dean, P. (1968). The vibrational spectra of vitreous silica, germania and beryllium fluoride. *Journal of Physics C: Solid State Physics*, 1(2), 299-303.

Bell, S.C., Nawrocki, H.D., & Morris, K.B. (2009). Forensic discrimination of glass using cathodoluminescence and CIE LAB color coordinates: A feasibility study. *Forensic Science International*, 189, 93-99.

Bennett, R.L., Kim, N.D., Curran, J.M., Coulson, S.A., & Newton, A.W.N. (2003). Spatial variation of refractive index in a pane of float glass. *Science and Justice-Journal of the Forensic Science Society*, 43, 71-76.

Bensch, W., & Bergholz, W. (1990). An FT-IR study of silicon dioxides for VLSI microelectronics. *Semiconductor Science and Technology*, 5(5), 421-428.

Berends-Montero, S., Wiarda, W., de Joode, P., & van der Peijl, G. (2006). Forensic analysis of float glass using laser ablation inductively coupled plasma mass spectrometry (LA-ICP-MS): validation of a method. *Journal of Analytical Atomic Spectrometry*, 21, 1185-1193.

Beveridge, A.D., & Semen, C. (1979). Glass density measurement using a calculating digital density meter. *Canadian Society of Forensic Science Journal*, 12(3), 113-116.

Blacklock, E.C., Rogers, A., Wall, C., & Wheals, B.B. (1976). The quantitative analysis of glass by emission spectrography: a six element survey. *Forensic Science*, 7(2), 121-130.

Bottrell, M.C. (2009). Forensic glass comparison: background information used in data interpretation. *Forensic Science Communications*, 11(2). Accessed on January 13, 2010 from http://www.fbi.gov/hq/lab/fsc/current/review/2009_04_review01.htm.

Boyd, I.W. (1987). Deconvolution of the infrared absorption peak of the vibrational stretching mode of silicon dioxide: Evidence for structural order. *Applied Physics Letters*, 51(6), 418-420.

Boyd, I.W., & Wilson, J.I.B. (1982). A study of thin silicon dioxide films using infrared absorption techniques. *Journal of Applied Physics*, 53(6), 4166-4172.

Boyd, I.W., & Wilson, J.I.B. (1987). Structure of ultrathin silicon dioxide films. *Applied Physics Letters,* 50(6), 320-322.

Bridge, C.M., Powell, J., Steele, K.L., & Sigman, M.E. (2007). Forensic comparative glass analysis by laser-induced breakdown spectroscopy. *Spectrochimica Acta Part B*, 62, 1419-1425.

Bridge, C.M., Powell, J., Steele, K.L., Williams, M., MacInnis, J.M., & Sigman, M.E. (2006). Characterization of automobile float glass with laser-induced breakdown spectroscopy and laser ablation inductively coupled plasma mass spectrometry. *Applied Spectroscopy*, 60(10), 1181-1187.

Buscaglia, J.A. (1994) Elemental analysis of small glass fragments in forensic science. *Analytica Chimica Acta*, 288, 17-24.

Bush, L. (2011). Lasers and Optics Interface: LIBS in Forensics. *Spectroscopy*, 26(4), 34-35.

Butterworth, A., German, B., Morgan, D., & Scaplehorn, A.W. (1974). A report on an investigation into the trace elements present in vehicle headlamp and auxillary lamp glasses. *Journal of the Forensic Science Society*. 14, 41–45.

Caldwell, R.J. (1972). Comparison of fragments of glass by neutron activation analysis. *Newsletter, NSW Branch, Australian Forensic Science Society*, 1, 5-6.

Calloway, A.R., & Jones, P.F. (1978). Enhanced discrimination of glass samples by phosphorescence analysis. *Journal of Forensic Sciences*, 23(2), 263-273.

Camo Software AS. (2010). *Chemometrics*. Retrieved from http://www.camo.com/rt/Resources/chemometrics.html.

Camo Software AS. (2010). *PLS-DA*. Retrieved from http://www.camo.com/resources/pls-da.html.

Cassista, A.R. & Sandercock, P.M.L. (1994a). Effects of annealing on toughened and non-toughened glass. *Canadian Society of Forensic Science Journal*, 27, 171–177.

Cassista, A.R., & Sandercock, P.M.L. (1994b). Precision of glass refractive index measurements: temperature variation and double variation methods, and the value of dispersion. *Canadian Society of Forensic Science Journal*, 27, 203–208.

Castro, W., Trejos, T., Naes, B., & Almirall, J.R. (2008). Comparison of high-resolution and dynamic reaction cell ICP-MS capabilities for forensic analysis of iron in glass. *Analytical and Bioanalytical Chemistry*. 392, 663-672.

Catterick, T. & Hickman, D.A. (1981). The quantitative analysis of glass by inductively coupled plasma-atomic emission spectrometry: A five element survey. *Forensic Science International*, 17, 253-263.

Collaborative Testing Services, Inc. (CTS) Forensic Testing Program. (2008). Glass Analysis Test No. 08-548 Summary Report. CTS, Inc.

Cobb, P.G.W. (1968). A survey of the variations in the physical properties of glass. *Journal of the Forensic Science Society*, 8, 29-31.

Coleman, R.F. & Goode, G.C. (1973). Comparison of glass fragments by neutron activation analysis. *Journal of Radioanalytical Chemistry*, 15, 367–388.

Copley, G.J. (2001). The composition and manufacture of glass and its domestic and industrial applications. In B. Caddy (Ed.), *Forensic examination of glass and paint: analysis and interpretation* (pp. 27-46). New York: Taylor & Francis Inc.

Curran, J.M., Buckleton, J.S., & Triggs, C.M. (1999). Commentary on Koons, R.D., Buscaglia, J. *Journal of Forensic Sciences*, 44(6), 1324-1325.

Dabbs, M.D.G., German, B., Pearson, E.F., & Scaplehorn, A.W. (1973). The use of spark source mass spectrometry for the analysis of glass fragments encountered in forensic applications, part 2, *Journal of the Forensic Science Society*. 13, 281–286.

Dabbs, M.D.G., & Pearson, E.F. (1970). The variation in refractive index and density across two sheets of window glass. *Journal of the Forensic Science Society*, 10, 139-148.

Dabbs, M.D.G., & Pearson, E.F. (1972). Some physical properties of a large number of window glass specimens. *Journal of Forensic Sciences*, 17(1), 70-78.

Dalby, K.N., & King P.L. (2006). A new approach to determine and quantify structural units in silicate glasses using micro-reflectance Fourier-Transform IR spectroscopy. *American Mineralogist,* 91, 1783–1793.

Daubert v. Merrell Dow Pharmaceuticals, Inc., 509 US 579 (1993)

Davies, M.M., Dudley, R.J., & Smalldon, K. (1980). An investigation of bulk and surface refractive indices for flat window glasses, patterned window glasses, and windscreen glasses. *Forensic Science International*, 16, 125–137.

Davis, J.E. (1956). Refractive index determinations of glass fragments—a simplified procedure. *The Journal of Criminal Law, Criminology, and Police Science*, 47(3), 380-386.

Davis, K.M., & Tomozawa, M. (1995a). Water diffusion into silica glass: Structural changes in silica glass and their effect on water solubility and diffusivity. *Journal of Non-Crystalline Solids*, 185, 203-220.

Davis, K.M., & Tomozawa, M. (1995b). An infrared spectroscopic study of water-related species in silica glasses. *Journal of Non-Crystalline Solids*, 201, 177-198.

Davis, K.M., Agarwal, A., Tomozawa, M., & Hirao, K. (1996). Quantitative infrared spectroscopic measurement of hydroxyl concentrations in silica glass. *Journal of Non-Crystalline Solids*, 203, 27-36.

Deer, W.A., Howie, R.A., Zussman, J. (1966). *An introduction to the rock forming minerals,* New York, NY: John Wiley and Sons Inc.

De Forest, P.R., Gaensslen, R.E., & Lee, H.C. (1983). *Forensic Science: An Introduction to Criminalistics*. New York: McGraw-Hill Book Company.

Devore, J.L. (2008). *Probability and Statistics For Engineering and the Sciences. 7th Ed*. California: Thomson Brooks/Cole.

Duckworth, D.C., Bayne, C.K., Morton, S.J., & Almirall, J.R. (2000). Analysis of variance in forensic glass analysis by ICP-MS: variance within the method. *Journal of Analytical Atomic Spectrometry*. 15, 821-828.

Duckworth, D.C., Morton, S.J., Bayne, C.K., Koons, R.D., Montero, S., & Almirall, J.R. (2002). Forensic glass analysis by ICP-MS: a multi-element assessment of discriminating power via analysis of variance and pairwise comparisons. *Journal of Analytical Atomic Spectrometry*. 17, 662-668.

Dudley, R.J., Howden, C.R., Taylor, T.J., & Smalldon, K.W. (1980). The discrimination and classification of small fragments of window and nonwindow glasses using energy-dispersive X-ray fluorescence spectrometry. *X-Ray Spectrometry*, 9, 119-122.

Efimov, A.M., & Pogareva, V.G. (2000). Water-related IR absorption spectra for some phosphate and silicate glasses. *Journal of Non-Crystalline Solids*, 275(3), 189-198.

Efimov, A.M., & Pogareva, V.G. (2006). IR absorption spectra of vitreous silica and silicate glasses: The nature of bands in the 1300 to 5000 cm-1 region. *Chemical Geology*, 229(1-3), 198-217.

Efimov, A.M., Pogareva, V.G., & Shashkin, A.V. (2003). Water-related bands in the IR absorption spectra of silicate glasses. *Journal of Non-Crystalline Solids*, 332(1-3), 93-114.

Efron, B., & Tibshirani, R.J. (1993). *An Introduction to the Bootstrap, 1st Ed.* Boca Raton, FL: Chapman & Hall/CRC.

Falcone, R., Sommariva, G., & Verita, M. (2006). WDXRF, EPMA and SEM/EDX Quantitative Chemical Analyses of Small Glass Samples. *Michrocimica Acta*, 155, 137-140.

Frye v. United States, 54 App. D.C. 46; 293 F. 1013 (D.C. Cir. 1923)

Fuller, C.W., & Whitehead, J. (1974). The determination of trace metals in high-purity sodium calcium silicate glass, sodium borosilicate glass, sodium carbonate and calcium carbonate by flameless absorption spectrometry. *Analytica Chimica Acta*, 68, 407-413.

Gamble, L., Burd, D.Q., & Kirk, P.L. (1943). Glass fragments as evidence: A comparative study of physical properties. *Journal of Criminal Law and Criminology,* 33(5), 416-421.

Garvin, E.J., & Koons, R.D. (2011). Evaluation of match criteria used for the comparaison of refractive index of glass fragments. *Journal of Forensic Sciences*, 56(2), 491-500.

Gemperline, P. J. (2006). Principal component analysis. In P. Gemperline (Ed.), *Practical guide to chemometrics* (pp. 69-104). Boca Raton, FL: Taylor & Francis.

German, B., & Scaplehorn, A.W. (1972). The use of spark source mass spectrometry for the analysis of glass. *Journal of the Forensic Science Society*. 12, 367–374.

Grams/AI Help Resource. (N.D.). [Computer Software]. Thermo Scientific.

Haaland, D.M. (1988). Quantitative infrared analysis of borophosphosilicate films using multivariate statistical methods. *Analytical Chemistry*, 60(11), 1208-1217.

Haaland, D.M., & Thomas, E.V. (1988). Partial least-squares methods for spectral analyses. 2. Application to simulated and glass spectral data. *Analytical Chemistry*, 60(11), 1202-1208.

Haken, U., Humbach, O., Ortner, S., & Fabian, H. (2000). Refractive index of silica glass: Influence of fictive temperature. *Journal of Non-Crystalline Solids,* 265, 9-18.

Harrick, N.J. (1987). *Internal Reflection Spectroscopy*. Ossining, New York: Harrick Scientific Corporation.

Heideman, D.H. (1975). Glass comparisons using a computerized refractive index data base. *Journal of Forensic Sciences*, 20(1), 103-108.

Hickman, D.A. (1981). A classification scheme for glass. *Forensic Science International*, 17, 265-281.

Hickman, D.A. (1983). Elemental analysis and the discrimination of sheet glass samples. *Forensic Science International*, 23, 213-223.

Hickman, D.A., Harbottle, G., & Sayre, E.V. (1983). The selection of the best elemental variables for the classification of glass samples. *Forensic Science International*, 23, 189-212.

Hicks, T., Sermier, F.M., Goldmann, T., Bunelle, A., Champod, C., & Margot, P. (2003). The classification and discrimination of glass fragments using non destructive energy dispersive X-ray μfluorescence. *Forensic Science International*, 137, 107-118.

Howden, C.R., German, B., & Smalldon, K.W. (1977). The determination of iron and magnesium in small glass fragments using flameless atomic absorption spectrophotometry, *Journal of the Forensic Science Society*, 17, 153-159.

Howden, C.R., Dudley, R.J., & Smalldon, K.W. (1978). The analysis of small glass fragments using energy dispersive X-ray fluorescence spectrometry. Journal of the Forensic Science Society, 18, 99-112.

Hughes, J.C., Catterick, T., & Southeard, G. (1976). The quantitative analysis of glass by atomic absorption spectroscopy, *Forensic Science*, 8, 217–227.

Humbach, O., Fabian, H., Grzesik, U., Haken, U., & Heitmann, W. (1996). Analysis of OH absorption bands in synthetic silica. *Journal of Non-Crystalline Solids*, 203, 19-26.

Ishikawa, K., Uchiyama, Y., Ogawa, H., & Fujimura, S. (1997). Dependence of TO and LO mode frequency of thermally grown silicon dioxide films on annealing temperature. *Applied Surface Science*, 117-118, 212-215.

Innocenzi, P. (2003). Infrared spectroscopy of sol-gel derived silica-based films: A spectra-microstructure overview. *Journal of Non-Crystalline Solids,* 316(2-3), 309-319.

Jackson, J.E. (2003). *A user's guide to principal components*. Hoboken, NJ: John Wiley & Sons, Inc.

Joliffe, I.T. (2002). *Principal component analysis, 2nd Ed*. New York, NY: Springer.

Keeley, R.H. & Christofides, S. (1979). Classification of small glass fragments by X-ray microanalyisis with the SEM and a small sample XRF spectrometer. *Proceedings of Scanning Electron Microscopy, SEM*, AMF O'Hare, Illinois, Part I, 459-464.

Kirk, C.T. (1988). Quantitative analysis of the effect of disorder-induced mode coupling on infrared absorption in silica. *Physical Review B*, 38(2), 1255-1273.

Kirk, P.L. (1951). Density and refractive index: their application in criminal identification. *American Lecture Series. Publication Number 112. A Monograph in American Lectures in Public Protection.* Snyder, L.M., Turner, R.F., Wilson, C.M. (Ed.) Charles C Thomas Publisher, Springfield, Illinois.

Kirk, P.L., & Dollar, A.M. (1949). Temperature variations with respect to the specific gravity of glass fragments: Comments on Donald F. McCall's paper. *Journal of Criminal Law and Criminology,* 39(5), 684-689.

Kirk, P.L., & Russel, R. (1941). Microdetermination of specific gravity in forensic chemistry. *Journal of Criminal Law and Criminology,* 32(1), 118-120.

Koller, K.B., Schmidt, W.A., & Butler, J.E. (1988). In situ infrared reflection absorption spectroscopic characterization of plasma enhanced chemical vapor deposited SiO2 films. *Journal of Applied Physics*, 64 (9), 4704-4710.

Koons, R.D. & Buscaglia, J. (1999a). The forensic significance of glass composition and refractive index measurements. *Journal of Forensic Sciences,* 44, 496-503.

Koons, R.D., & Buscaglia, J. (1999b). Authors' response on commentary on Koons, R.D., Buscaglia, J. *Journal of Forensic Sciences*, 44(6), 1326-1328

Koons, R., & Buscaglia, J. (2001). Distribution of refractive index values in sheet glass. Forensic Science Communications, 3(1). Accessed Jan 2010 from http://www.fbi.gov/hq/lab/fsc/backissu/jan2001/koons.htm

Koons, R.D., & Buscaglia, J. (2002). Interpretation of glass composition measurements: the effects of match criteria on discrimination capability. *Journal of Forensic Sciences*. 47(3), 505-512.

Koons, R.D., Buscaglia, J., Bottrell, M., & Miller, E.T. (2002). Forensic glass comparisons. In: *Forensic Science Handbook Volume 1, 2nd ed.* R. Saferstein, (Ed.). Prentice-Hall, Upper Saddle River, New Jersey, 161-213.

Koons, R.D., Fiedler, C., & Rawalt. R.C. (1988). Classification and discrimination of sheet and container glasses by inductively coupled plasma-atomic emission spectrometry and pattern recognition. *Journal of Forensic Sciences,* 33, 49-67.

Koons, R.D., Peters, C.A., & Rebbert, P.C. (1991). Comparison of refractive index, energy dispersive X-ray fluorescence and inductively coupled plasma atomic emission spectrometry for forensic characterization of sheet glass fragments. *Journal of Analytical Atomic Spectrometry*, 6, 451-456.

Kubic, T.A., Galgan, H., & Gillis, V. (1975). Use of pycnometer for determining glass density shown to be limited. *Crime Laboratory Digest*, 75(8), 6-9.

Kubic, T.A. (2002). Forensic applications of scanning electron microscopy with X-ray analysis. In Z.R. Li (Ed.), *Industrial Applications of Electron Microscopy* (pp. 279-329). New York: Marcel Dekker.

Lange, P. (1989). Evidence for disorder-induced vibrational mode coupling in thin amorphous SiO2 films. *Journal of Applied Physics*, 66(1), 201-204.

Lambert, J.A., & Evett, I.W. (1984). The refractive index distribution of control glass samples examined by the forensic science laboratories in the United Kingdom. Forensic Science International, 26, 1-23.

Latkoczy, C., Becker, S., Dücking, M., Günther, D., Hoogewerff, J.A., Almirall, J.R. et al. (2005). Development and evaluation of a standard method for the quantitative determination of elements in float glass samples by LA-ICP-MS. *Journal of Forensic Sciences,* 50, 1327–1341.

Lloyd, J.B.F. (1981). Fluorescence spectrometry in the identification and discrimination of float and other surfaces on window glasses. *Journal of Forensic Sciences*, 26, 325–342.

Locke, J., & Elliott, B.R. (1984). The examination of glass particles using the interference objective: part 2. a survey of flat and curved surfaces. *Forensic Science International*, 26, 53-66.

Locke, J., & Hayes, C.A. (1984). Refractive index variations across glass objects and influence of annealing. *Forensic Science International*, 26, 147-157.

Locke, J., Hayes, C.A., & Sanger, D.G. (1984) The design of equipment and thermal routines for annealing glass particles. *Forensic Science International*. 26, 139-146.

Locke, J., & Rocket, L.A. (1985). The application of annealing to improve the discrimination between glasses. *Forensic Science International*, 29, 237-245.

Locke, J., Sanger, D.G., & Roopnarine, G. (1982). The identification of toughened glass by annealing. *Forensic Science International*, 20, 295-301.

Locke, J., Underhill, M., Russel, P., Cox, P., & Perryman, A.C. (1986). The evidential value of dispersion in the examination of glass. *Forensic Science International*, 32, 474-483.

Locke, J., Winstanley, R., Rocket, L.A., & Rydeard, C. (1985). A comparison of long and short schedules for the annealing of glass particles. *Forensic Science International*, 29, 247-258.

Locke, J., & Zoro, J.A. (1983). The examination of glass particles using the interference objective: part 1. methods for rapid sample handling. *Forensic Science International*, 22, 221-230.

Long- and short-range order. (2010). *Encyclopedia Britannica*. Retrieved October 27, 2010, from http://www.britannica.com/EBchecked/topic/145105/crystal/51804/Long-and-short-range-order

Mackenzie, J.D. (1960). *Modern aspects of the vitreous state*. Washington: Butterworth & Co. Publishers Ltd.

Magdas, D.A., Cozar, O., Chis, V., Ardelean, I., & Vedeanu, N. (2008). The structural dual role of Fe2O3 in some lead-phosphate glasses. *Vibrational Spectroscopy*, 48, 251-254.

Marcouiller, J.M. (1990). A revised glass annealing method to distinguish glass types. *Journal of Forensic Sciences*, 35, 554-559.

Martinet, C., & Devine, R.A.B. (1995). Analysis of the vibrational mode spectra of amorphous SiO2 films. *Journal of Applied Physics*, 77(9), 4343-4348.

Martinez, V.L. (2008). Discrimination of glass samples by infrared microprobe analysis with diamond attenuated total reflection (Master's Thesis, John Jay College of Criminal Justice, 2008).

McCall, D.F. (1948). Temperature variations with respect to the specific gravity of glass fragments. *Journal of Criminal Law and Criminology,* 39(1), 113-117.

McCrone, W.C. (1974). Microscopical characterization of glass fragments. *Journal of the AOAC*, 57(3), 668-670.

Msimanga, H.Z. & Ollis, Jr., R.J. (2010). Discerning Some Tylenol Brands Using Attenuated Total Reflection Fourier Transform Infrared Data and Multivariate Analysis Techniques. *Applied Spectroscopy*, 64(6), 657-668.

Naes, B.E., Umpierrez, S., Ryland, S., Barnett, C., & Almirall, J.R. (2008). A comparison of laser ablation inductively coupled plasma mass spectrometry, micro X-ray fluorescence spectroscopy, and laser induced breakdown spectroscopy for the discrimination of automotive glass. *Spectrochimica Acta Part B*, 63, 1145-1150.

Nagai, N., & Hashimoto, H. (2001). FT-IR-ATR study of depth profile of SiO2 ultra-thin films. *Applied Surface Science*, 172(3-4), 307-311.

Nakanishi, T., Nishiwaki, Y., Miyamoto, N., Shimoda, O., Watanabe, S., Muratsu, S., Takatsu, M., Terada, Y., Suzuki, Y., Kasamatsu, M., & Suzuki, S. (2008). Lower limits of detection of synchotron radiation high-energy X-ray fluorescence spectrometry and its possibility for the forensic application for discrimination of glass fragments. *Forensic Science International*, 175, 227-234.

Newton, A.W.N., & Buckleton, J.S. (2008). An investigation into the relationship between edge counts and the variability of the refractive index of glass part I: edge morphology. *Forensic Science International*, 177, 24-31.

Newton, A., Curran, J., Trigs, C., & Buckleton, J. (2004). The consequences of potentially differing distributions of the refractive indices of glass fragments from control and recovered sources. *Forensic Science International*, 140, 185-193.

Newton, A.W.N., Kitto, L., & Buckleton, J.S. (2005). A study of the performance and utility of annealing in forensic glass analysis. *Forensic Science International*, 155, 119-125.

Niemczyk, T.M., Zhang, S., Franke, J.E., & Haaland, D.M. (1999) Quantitative determination of borophosphosilicate glass thin-film properties using infrared emission spectroscopy. *Applied Spectroscopy*, 53(7), 822-828.

Niemczyk, T.M., Zhang, S., & Haaland, D.M. (2001). Monitoring dielectric thin-film production on product wafers using infrared emission spectroscopy. *Applied Spectroscopy*, 55(8), 1053-1059.

O'Haver, T. (2008, October). *Differentiation*. Retrieved from http://terpconnect.umd.edu/~toh/spectrum/Differentiation.html

Ojena, S.M., & De Forest, P.R. (1972). Precise refractive index determination by the immersion method, using phase contrast microscopy and the Mettler hot stage. *Journal of the Forensic Science Society*, 12, 315-329.

Parke, S. (1974). Chapter 21: Glasses. In V.C. Farmer (Ed.), *The infrared spectra of minerals* (pp. 483-514). London, England: Mineralogical Society.

Parouchais, T., Warner, I.M., Palmer, L.T., & Kobus, H. (1996). The analysis of small glass fragments using inductively coupled plasma mass spectrometry. *Journal of Forensic Sciences*. 41, 351–360.

Pawluk-Kolc, M., Zieba-Palus, J., & Parczewski, A. (2008). The effect of re-annealing on the distribution of refractive index in a windscreen and a windowpane classification of glass samples. *Forensic Science International*, 174, 222-228.

Petraco, N. (2011). Chapter 8: How statistical pattern comparison methods can be applied to toolmarks. In *Color Atlas of Forensic Toolmark Identification* (pp. 85-107). New York, NY: Taylor & Francis Group.

Petraco, N.D.K. (2011, February-May). *Multivariate Analysis for Forensic Scientists*. Lectures conducted from the CUNY Graduate Center, New York, NY.

Popescu, M.A. (2005). Medium range order in non-crystalline materials. *Journal of Ovonic Research*. 1(1), 7-19.

Posener, D.W. (1959). The Shape of Spectral Lines: Tables of the Voigt Profile $\left(a/\pi\right)\int_{-\infty}^{\infty} e^{-y^2}\,dy\,/\left\{a^2+\left(v-y\right)^2\right\}$. *Australian Journal of Physics*. 12, 184-196.

Rada, S., Culea, E., Bosca, M., Culea, M., Muntean, R., & Pascuta, P. (2008). Spectroscopic and quantum mechanical investigation of boro-bismuthate glasses and glass ceramics structures. *Vibrational Spectroscopy*, 48, 285-288.

Reeve, V., Mathiesen, J., & Fong, W. (1976). Elemental analysis by energy dispersive X-ray: A significant factor in the forensic analysis of glass, *Journal of Forensic Sciences*, 21, 291-306.

Reffner J.A., Alexay C.C., & Hornlein R.W. (1991). Design of Grazing Incidence and ATR Objectives for FT-IR Microscopy. *8th International Conference on Fourier Transform Spectroscopy, SPIE Proceedings*, 1575, 301-302.

Reffner J.A. & Martoglio P.A. (1995). *Uniting Microscopy and Spectroscopy*. In H.J. Humecki (Ed.). Practical Guide to Infrared Microspectroscopy (pp. 41-84). New York: Marcel Dekkar, Inc.

Rencher, A.C. (2002). *Methods of Multivariate Analysis*. 2nd Ed. Canada: John Wiley & Sons, Inc.

Rochat, N., Chabli, A., Bertin, F., Vergnaud, C., Mur, P., Petitdidier, S., & Besson, P. (2003). Infrared analysis of thin layers by attenuated total reflection spectroscopy. *Materials Science and Engineering B: Solid-State Materials for Advanced Technology*, 102(1-3), 16-21.

Rodriguez-Celis, E.M., Gornushkin, I.B., Heitmann, U.M., Almirall, J.R., Smith, B.W., Winefordner, J.D., & Omenetto, N. (2008). Laser induced breakdown spectroscopy as a tool for discrimination of glass for forensic applications. *Analytical and Bioanalytical Chemistry*, 391, 1961-1968.

Rushton, K.P., Coulson, S.A., Newton, A.W.N., & Curran, J.M. (2011). The effect of annealing on the variation of glass refractive index. *Forensic Science International*, 209, 102-107.

Ryland, S.G. (1986). Sheet or container?—Forensic glass comparisons with an emphasis on source classification. *Journal of Forensic Sciences*, 31(4), 1314-1329.

Ryland, S.G. (1991). Discussion of 'a revised glass annealing method to distinguish glass types'. *Journal of Forensic Sciences*, 36(1), 14.

Ryland, S.G., & Koons, R.D. (1991). On the classification of small colorless glass fragments as to their sheet or container origin. *Journal of Forensic Sciences*, 36(2), 308-311.

Sandercock, P.M.L. (2000). Sample size considerations for control glass in casework. *Canadian Society of Forensic Science Journal,* 33, 173–185.

Schmitt, R. A. & Smith, V. (1970). Identification of origin of glass by neutron activation analysis in a forensic case, *Journal of Forensic Sciences*, 15, 252–260.

Scientific Working Group for Materials Analysis (SWGMAT). (2005a). Elemental Analysis of Glass. *Forensic Science Communications*, 7(1). Accessed January 2010 from http://www.fbi.gov/hq/lab/fsc/backissu/jan2005/standards/2005standards10.htm

Scientific Working Group for Materials Analysis (SWGMAT). (2005b). Glass Density Determination. *Forensic Science Communications*, 7(1). Accessed January 2010 from http://www.fbi.gov/hq/lab/fsc/backissu/jan2005/standards/2005standards8.htm

Scientific Working Group for Materials Analysis (SWGMAT). (2005c). Glass Fractures. Forensic Science Communications, 7(1). Accessed January 2010 from http://www.fbi.gov/hq/lab/fsc/backissu/jan2005/standards/2005standards7.htm

Scientific Working Group for Materials Analysis (SWGMAT). (2005d). Glass Refractive Index Determination. *Forensic Science Communications*, 7(1). Accessed January 2010 from http://www.fbi.gov/hq/lab/fsc/backissu/jan2005/standards/2005standards9.htm

Scientific Working Group for Materials Analysis (SWGMAT). (2005e). Initial Examinations of Glass. *Forensic Science Communications,* 7(1). Accessed January 2010 from http://www.fbi.gov/hq/lab/fsc/backissu/jan2005/standards/2005standards6.htm

Shelby, J.E. (2009). *Introduction to glass science and technology, 2nd Edition*. Cambridge, UK: The Royal Society of Chemistry.

Skoog, D.A., Holler, F.J., & Nieman, T.A. (1998). *Principles of Instrumental Analysis*, Fifth edition, Orlando, Florida: Harcourt Brace & Company.

Slater, D.P., & Fong, W. (1982). Density, refractive index, and dispersion in the examination of glass: their relative worth as proof. *Journal of Forensic Sciences*, 27(3), 474-483.

Stoecklein, W., & Gobel, R. (1992). Application of cathodoluminescence in paint analysis. *Scanning Microscopy International*, 6, 669-678.

Stolov, A.A., & Simoff, D.A. (2008). Micro attenuated total reflection spectra of bulk silica glass: effects of experimental conditions and glass thermal history on appearance of a surface polariton in the Si-O stretching region. *Applied Spectroscopy*, 62(6), 624-633.

Stoney, D.A., & Thornton, J.I. (1985). The forensic significance of the correlation of density and refractive index in glass evidence. *Forensic Science International*, 29, 147-157.

Palenik, C.S., & Buscaglia, J.A. (2007). Applications of cathodoluminescence in forensic science. In R.D. Blackledge (Ed.). *Forensic Analysis on the Cutting Edge: New Methods for Trace Evidence Analysis*. Hoboken, NJ: John Wiley and Sons, Inc., 141-173.

Tan, C.Z. (1998). Determination of refractive index of silica glass for infrared wavelengths by IR spectroscopy. *Journal of Non-Crystalline Solids*, 223(1-2), 158-163.

Tan, C.Z., & Arndt, J. (2000a). Interaction of longitudinal and transverse optic modes in silica glass. *Journal of Chemical Physics*, 112(13), 5970-5974.

Tan, C.Z., & Arndt, J. (2000b). Temperature dependence of refractive index of glassy SiO2 in the infrared wavelength range. *Journal of Physics and Chemistry of Solids*, 61, 1315-1320.

Tan, C.Z., & Arndt, J. (2001). Refractive index, optical dispersion, and group velocity of infrared waves in silica glass. *Journal of Physics and Chemistry of Solids*, 62(6), 1087-1092.

Terry, K.W., van Riessen, A., & Vowles, D.J. (1982). Elemental analysis of glasses in a SEM. *Micron*, 13, 293-294.

Tomozawa, M., Kim, D.L., Agarwal, A., & Davis, K.M. (2001). Water diffusion and surface structural relaxation of silica glasses. *Journal of Non-Crystalline Solids*, 288, 73-80.

Trejos, T., & Almirall, J.R. (2004). Effect of fractionation on the forensic elemental analysis of glass using laser ablation inductively coupled plasma mass spectrometry. *Analytical Chemistry*, 76(5), 1236-1242.

Trejos, T., & Almirall, J.R. (2005a). Sampling strategies for the analysis of glass fragments by LA-ICP-MS Part I. Micro-homogeneity study of glass and its application to the interpretation of forensic evidence. *Talanta*, 67, 388-395.

Trejos, T., & Almirall, J.R. (2005b). Sampling strategies for the analysis of glass fragments by LA-ICP-MS Part II. Sample size and sample shape considerations. *Talanta*, 67, 396-401.

Trejos, T., Montero, S., & Almirall, J.R. (2003). Analysis and comparison of glass fragments by laser ablation inductively coupled plasma mass spectrometry (LA-ICP-MS) and ICP-MS. *Analytical and Bioanalytical Chemistry*, 376, 1255-1264.

Tryhorn, F.G. (1939). The examination of glass. *Journal of Criminal Law and Criminology,* 30, 404-419.

Underhill, M. (1980). Multiple refractive index in float glass. *Journal of the Forensic Science Society*, 20, 169–176.

Verzani, J. (2002). *SimpleR – Using R for introductory statistics*. Retrieved January 26, 2012, from http://cran.r-project.org/doc/contrib/Verzani-SimpleR.pdf

Vogel, W. (1985). *Chemistry of glass*. Westerville, OH: The American Ceramic Society.

Vogel, W. (1994). *Glass chemistry: 2nd Edition*. New York: Springer-Verlag.

Wang, T.B., Liu, Z.G., & Tan, C.Z. (2003). Relationship between the frequency of the main LO mode of silica glass and angle of incidence. *Journal of Chemical Physics*, 119(1), 505-508.

Winstanley, R., & Rydeard, C. (1984). Observations on re-annealing very small particles of glass. *Glass International*, 54-56.

Winstanley, R., & Rydeard, C. (1985). Concepts of annealing applied to small glass fragments. *Forensic Science International*, 29, 1-10.

Wolnik, K.L., Gaston, C.M., & Fricke, F.L. (1989). Analysis of glass in product tampering investigations by inductively coupled plasma atomic emission spectrometry with a hydrofluoric acid resistant torch. *Journal of Analytical Atomic Spectrometry*, 4, 27-31.

Wong, J. (1973). Submicron thickness calibration of vapor-deposited SiO2 films by infrared spectroscopy. *Journal of Applied Physics,* 44(12), 5629-5630.

Wong, J., & Angell, C.A. (1976). *Glass structure by spectroscopy*. New York, NY: Marcel Dekker, Inc.

Yang, B., Townsend, P.D., & Holgate, S.A. (1994). Cathodoluminescence and depth profiles of tin in float glass. *Journal of Physics D: Applied Physics,* 27, 1757-1762.

Zachariasen, W.J. (1932). The Atomic Arrangement in Glass. *Journal of the American Chemical Society*, 54(10), 3841-3851.

Zadora, G. (2009). Classification of glass fragments based on elemental composition and refractive index. *Journal of Forensic Sciences*, 54(1), 49-59.

Zadora, G., Brozek-Mucha, Z., & Parczewski, A. (2001a). A classification of glass microtraces. *Problems of Forensic Sciences*, XLVII, 137-143.

Zadora, G., Brozek-Mucha, Z., & Parczewski, A. (2001b). A differentiation of glass microtraces of the same qualitative composition. *Problems of Forensic Sciences*, XLVII, 144-146.

Zhang, L., Franke, J.E., Niemczyk, T.M., & Haaland, D.M. (1997). Optimized external IR reflection spectroscopy for quantitative determination of borophosphosilicate glass parameters. *Applied Spectroscopy*, 51(2), 259-264.

Zoro, J.A., Locke, J., Day, R.S., Badmus, O., & Perryman, A.C. (1988). An investigation of refractive index anomalies at the surface of glass objects and windows. *Forensic Science International*, 39, 127-141.

Zurhaar, A. & Mullings, L. (1990). Characterisation of forensic glass samples using inductively coupled plasma mass spectrometry. *Journal of Analytical Atomic Spectrometry*, 5, 611–617.